Indexes
ENGINEERING-TRANSPORTATION
LIBRARY

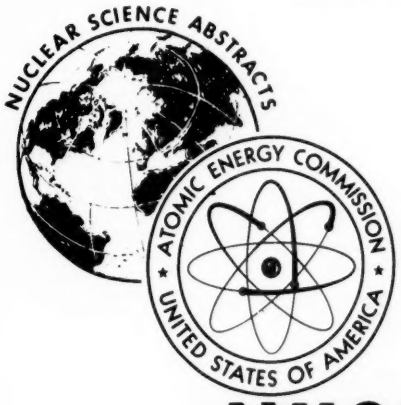

THE UNIVERSITY
OF MICHIGAN
MAR 25 1966
ENGINEERING
LIBRARY

NUCLEAR SCIENCE ABSTRACTS

Volume 20 Number 4

Abstracts 5228–6693

February 28, 1966

UNITED STATES ATOMIC ENERGY COMMISSION
Division of Technical Information

DEPOSITED BY THE
UNITED STATES OF AMERICA

USAEC DEPOSITORY LIBRARIES

Collections of USAEC reports are maintained in the libraries of the organizations listed below for reference use by the general public. Facilities for making photocopies are available. The USAEC also makes available through these libraries atomic energy reports of countries other than the U. S. that are abstracted in *Nuclear Science Abstracts*.

ALABAMA
Auburn, Auburn University
ALASKA
College, University of Alaska
ARIZONA
Tucson, University of Arizona
ARKANSAS
Fayetteville, University of Arkansas
CALIFORNIA
Berkeley, University of California
Davis, University of California
Los Angeles, University of California
San Diego, Public Library
Stanford, Stanford University
COLORADO
Boulder, University of Colorado
Denver, Public Library
CONNECTICUT
New Haven, Yale University
DELAWARE
Newark, University of Delaware
DISTRICT OF COLUMBIA
Washington, Library of Congress
FLORIDA
Coral Gables, University of Miami
Gainesville, University of Florida
Tallahassee, The Florida State University
GEORGIA
Atlanta, Georgia Institute of Technology
HAWAII
Honolulu, University of Hawaii
ILLINOIS
Chicago, John Crerar Library
Chicago, University of Chicago
Evanston, Northwestern University
Urbana, University of Illinois
INDIANA
Bloomington, Indiana University
Lafayette, Purdue University
IOWA
Ames, Iowa State University
KANSAS
Manhattan, Kansas State University
KENTUCKY
Lexington, University of Kentucky
Louisville, University of Louisville
LOUISIANA
Baton Rouge, Louisiana State University
New Orleans, Tulane University
MARYLAND
Baltimore, Johns Hopkins University
College Park, University of Maryland
MASSACHUSETTS
Cambridge, Harvard University
Cambridge, Massachusetts Institute of Technology
MICHIGAN
Ann Arbor, University of Michigan
Detroit, Public Library
East Lansing, Michigan State University
MINNESOTA
Minneapolis, University of Minnesota
MISSISSIPPI
State College, Mississippi State University
MISSOURI
Kansas City, Linda Hall Library
Rolla, University of Missouri School of Mines and Metallurgy
St. Louis, Washington University
MONTANA
Bozeman, Montana State College
NEVADA
Las Vegas, Nevada Southern University
Reno, University of Nevada
NEW JERSEY
Princeton, Princeton University
Teaneck, Fairleigh Dickinson University
NEW MEXICO
Albuquerque, University of New Mexico
NEW YORK
Albany, The University of the State of New York
Buffalo, State University of New York at Buffalo
Ithaca, Cornell University
New York, Atomic Industrial Forum, Inc.
New York, Columbia University
New York, New York University
Rochester, University of Rochester
Schenectady, Union College
Syracuse, Syracuse University
Troy, Rensselaer Polytechnic Institute
NORTH CAROLINA
Charlotte, Public Library of Charlotte and Mecklenburg County
Durham, Duke University
Raleigh, North Carolina State College
NORTH DAKOTA
Grand Forks, University of North Dakota
OHIO
Cincinnati, University of Cincinnati
Cleveland, Public Library
OHIO (CONT.)
Columbus, Ohio State University
Toledo, University of Toledo
Youngstown, Youngstown University
OKLAHOMA
Norman, University of Oklahoma
Stillwater, Oklahoma State University
OREGON
Corvallis, Oregon State University
Portland, Reed College
PENNSYLVANIA
Philadelphia, University of Pennsylvania
Pittsburgh, Carnegie Library
University Park, Pennsylvania State University
PUERTO RICO
Rio Piedras, University of Puerto Rico
RHODE ISLAND
Providence, Brown University
SOUTH CAROLINA
Columbia, University of South Carolina
TENNESSEE
Knoxville, University of Tennessee
Memphis, Public Library
Nashville, Joint University Libraries
Oak Ridge, Oak Ridge Associated Universities
TEXAS
Austin, University of Texas
College Station, Texas A & M University
Dallas, Southern Methodist University
Houston, Rice University
Lubbock, Texas Technological College
San Antonio, Public Library
UTAH
Salt Lake City, University of Utah
VIRGINIA
Blacksburg, Virginia Polytechnic Institute
Charlottesville, University of Virginia
Norfolk, Old Dominion College
WASHINGTON
Pullman, Washington State University
Seattle, University of Washington
WEST VIRGINIA
Morgantown, West Virginia University
WISCONSIN
Madison, University of Wisconsin
Milwaukee, Public Library
WYOMING
Laramie, University of Wyoming

DEPOSITED BY THE
UNITED STATES OF AMERICA

Volume 20, Number 4, February 28, 1966

NUCLEAR SCIENCE ABSTRACTS

A semimonthly publication of the USAEC Division of Technical Information, Edward J. Brunenkant, Director. Published by the USAEC Division of Technical Information Extension, Robert L. Shannon, Extension Manager.

Nuclear Science Abstracts covers the international literature on nuclear science and technology and provides the only comprehensive abstracting and indexing of this body of information. Published twice each month since 1947, *NSA* covers technical reports of the U. S. Atomic Energy Commission and its contractors, technical reports of U. S. Government agencies and other governments, universities, industrial and research organizations, as well as patents, books, and journal literature on a world-wide basis. Nearly 350,000 abstracts have appeared in *NSA* through Volume 19. The subject matter covered in *NSA* is described in issue Number 1 and in TID-4552, *Subject Scope of Nuclear Science Abstracts*, available free from the U. S. Atomic Energy Commission, Division of Technical Information Extension, P. O. Box 62, Oak Ridge, Tennessee 37830.

Abstracts are arranged according to a number of subject categories and subcategories. Definitions of categories appear in issues Number 1 and 13. If the language of the original item is not English, the language will be indicated. Translations are not abstracted where an abstract of the original item has appeared in *NSA*.

INDEXES TO NSA

Corporate author, personal author, subject, and report number indexes appear in each issue and are cumulated quarterly, semiannually, and annually. Multi-volume cumulations have been issued as indicated on the following page. Report number indexes for all volumes (1–18) were issued at the end of Vol. 18. At the end of Vol. 19, the indexes for Vols. 1–15 were reissued to include additional public availability information. This cumulation will be a permanent shelf item and will not be reissued. Report number indexes for Vol. 19 are included as a cumulation beginning with Vol. 16.

AVAILABILITY OF PUBLICATIONS ABSTRACTED

The public availability of all U. S. Atomic Energy Commission reports is indicated in the report number indexes. The availability of other reports, when known, is also indicated. The availability of some unnumbered reports is given in the abstract.

Dissertations abstracted in *Dissertation Abstracts* and included in *NSA* are available from University Microfilms, Inc., 315 N. First Street, Ann Arbor, Michigan 48103.

Most of the published literature abstracted in *NSA* is on deposit at the Library, Oak Ridge Associated Universities, Oak Ridge, Tennessee, (a USAEC depository library) and is available through interlibrary loan. When requesting papers from this source, it is important that *NSA* volume and abstract number be cited.

HOW TO OBTAIN NUCLEAR SCIENCE ABSTRACTS

NSA is available on an exchange basis to universities, research institutions, industrial firms, and publishers of scientific information. Inquiries should be directed to the U. S. Atomic Energy Commission, Division of Technical Information Extension, P. O. Box 62, Oak Ridge, Tennessee 37830.

Government agencies may obtain *NSA* free of charge.

NSA is available to the general public on a subscription basis from the Superintendent of Documents, U. S. Government Printing Office, Washington, D. C. 20402, as follows:

For the 24 regular issues, $30.00 domestic, $37.00 foreign. A single issue costs $1.75, plus 25 per cent for foreign mailing. Domestic rates apply to the United States, Canada, Mexico, and Central and South American countries except Argentina, Brazil, British and French Guiana, Surinam, and British Honduras. Foreign rates apply to the countries excepted above and to all other countries throughout the world.

For the quarterly, semiannual, and annual indexes, $22.00 domestic, $25.00 foreign.

Multivolume subject and author indexes are available as follows:

Vols. 1–4 (1948–1950) Johnson Reprint Corporation, 111 Fifth Avenue, New York, N. Y. 10003, $30.00.

Vols. 5–10 (1951–1956) Superintendent of Documents, U. S. Government Printing Office, Washington, D. C. 20402, $5.25.

Vols. 11–15, Subjects, Superintendent of Documents, U. S. Government Printing Office, Washington, D. C. 20402, $19.00.

Vols. 11–15, Personal Authors, Superintendent of Documents, U. S. Government Printing Office, Washington, D. C. 20402, $14.25.

Vols. 11–15, Corporate Authors, Superintendent of Documents, U. S. Government Printing Office, Washington, D. C. 20402, $2.50.

Cumulative Report Number Index, Vols. 1–15, Revised, is available from the Superintendent of Documents, U. S. Government Printing Office, Washington, D. C. 20402, $4.00.

Cumulative Report Number Index, Vols. 16–19, is available from the Superintendent of Documents, U. S. Government Printing Office, Washington, D. C. 20402, $2.50.

Annual Indexes are available separately from the U. S. Government Printing Office as follows:

Vol. 16, Subject and Authors, $9.75.
Vol. 17, Subject and Authors, $12.25.
Vol. 18, Subject and Authors, $12.50.
Vol. 19, Subject and Authors, $12.50.

ACKNOWLEDGMENTS

Agreements between the United States Atomic Energy Commission and the following organizations with regard to providing continuing services and specific literature coverage for *Nuclear Science Abstracts* are gratefully acknowledged:

American Institute of Physics; Atomic Energy of Canada Limited; Atomic Energy Research Establishment, United Kingdom; European Atomic Energy Community (EURATOM); Gmelin Institute; International Atomic Energy Agency; Japan Atomic Energy Bureau — Japan Atomic Energy Research Institute; Netherlands Patent Office; Reactor Centrum Nederland.

TABLE OF CONTENTS

Volume 20, Number 4, February 28, 1966

Category	*Page*
BIOLOGY AND MEDICINE	649
General	649
Ecology	651
Metabolism, Tissue Distribution, and Toxicology	651
Radiation Effects on Biochemicals	654
Radiation Effects on Tissues	656
Radiation Effects Therapy and Countermeasures	676
Radiation Hazards and Protection	679
Radiotherapy and Radiodiagnosis	681
CHEMISTRY	689
General	689
Analytical Procedures	689
Inorganic and Physical Chemistry	692
Organic Chemistry	697
Radiation Chemistry	698
Radiochemistry	701
Separation Processes and Procedures	702
ENGINEERING	704
General	704
Applications of Nuclear Explosions	704
Facilities and Equipment	704
Heat Transfer and Fluid Flow	705
Materials Testing	707
Protective Structures	707
Space Propulsion	707
Vacuum Engineering	708
GEOLOGY, METEOROLOGY, AND MINERALOGY	709
General	709
Meteorology	709
Natural Radioactivity and Fallout	709
Techniques and Equipment	710
Thorium and Uranium Minerals	711
HEALTH AND SAFETY	712
INSTRUMENTATION	715
General	715
Radiation Detection	718
Radiation Effects	728
ISOTOPE TECHNOLOGY	729
General	729
Industrial Applications	729
Power Application	730
Separation and Production	730
MATHEMATICS AND COMPUTERS	732
METALS, CERAMICS, AND OTHER MATERIALS	733
General	733
Corrosion	734
Fabrication	735
Properties and Structure	736
Radiation Effects	741
PHYSICS	744
General	744
Accelerators	744
Astrophysics and Cosmology	748
Atomic Physics	750
Cosmic Radiation	753
Direct Energy Conversion	755
Elementary Particles and Radiations	756
Field Theory, Scattering Theory, and Symmetries	763
Fluid Physics and Thermodynamics	769
Geophysics	771
Gravitation, Quantum Mechanics, and Relativity Theory	776
Low Temperature Physics	777
Neutron Physics	781
Nuclear Properties and Reactions	783
Plasma Physics and Thermonuclear Processes	803
Shielding	812
Solid State Physics	813
REACTOR TECHNOLOGY	817
General	817
Auxiliaries and Components	818
Criticality Studies	819
Design and Feasibility	821
Fuels	821
Power and Power-Breeder Reactors	822
Process Heat Reactors	828
Propulsion and Space	828
Research and Test Reactors	830
GENERAL AND MISCELLANEOUS	832
CORPORATE AUTHOR INDEX	INDEX-1
PERSONAL AUTHOR INDEX	INDEX-10
SUBJECT INDEX	INDEX-40
REPORT NUMBER INDEX	INDEX-112

STAFF OF NUCLEAR SCIENCE ABSTRACTS

MANAGING EDITOR

John W. Norris

ASSISTANT MANAGING EDITOR

Donald D. Davis

ASSOCIATE EDITORS

Lawrence T. Whitehead
David E. Bost
Robert C. Kelly
Lee M. Thompson

SUBJECT INDEX EDITOR

Everett J. Hoffman

EVALUATORS

William D. Matheny
John H. Mitchell
Mary H. Newman

ABSTRACTORS

F. S. Armstrong (AECL)
Jane G. Buchanan
D. Lamar Cason
Helen G. Donald
James R. Dulaney
Wells L. Green
Mary Catherine Grissom
Fernando J. Hamilton
Phyllis C. Hansen
Thomas F. Heagerty
Carolyn D. Houston
Rose V. Jermain
Betty L. McDowell
Jean F. Peckham
Mona H. Raridon
Julia Redford
Lila B. Smith
Charles E. Stuber
Martha J. Thomas
Anne G. Ward
David C. West
Milton O. Whitson

SUBJECT HEADING SPECIALIST

Robert E. Upchurch

CORPORATE AUTHOR SPECIALIST

Clara L. Fox

DESCRIPTIVE CATALOGING SPECIALIST

J. Paul Meredith

SCHEDULING AND PUBLISHING COORDINATOR

Brainard L. Patton

Communication concerning the editorial policy and content of *NSA* should be addressed to the Managing Editor, *Nuclear Science Abstracts*, AEC Division of Technical Information Extension, P. O. Box 62, Oak Ridge, Tennessee 37830.

Use of funds for printing this publication approved by the Director of the Bureau of the Budget, May 20, 1963

Volume 20, Number 4 February 28, 1966

NUCLEAR SCIENCE ABSTRACTS

BIOLOGY AND MEDICINE

General

5228 (AD-623599, pp 28-36) MODIFICATION OF A HYPERBARIC OXYGEN CHAMBER FOR USE IN HYPOBARIC OXYGEN EXPOSURE STUDIES. Doull, John; Simmons, Eric (USAF Radiation Lab., Univ. of Chicago, Ill.).

The design and performance of a hyperbaric oxygen exposure chamber used to chronically expose small groups of mice to enriched oxygen environments at decreased barometric pressure are described. (40 references.) (C. H.)

5229 (BNL-9407) GENETIC RECOMBINATION IN PNEUMOCOCCUS. Lacks, Sanford (Brookhaven National Lab., Upton, N. Y.). [1965]. Contract AT(30-2)-Gen-16. 6p. (CONF-650814-2). Dep. mn; CFSTI $1.00 cy, $0.50 mn.

From Symposium on Mutational Process, Prague.

The significance of differences in integration efficiencies of donor DNA strands in Pneumococcus is considered. Attempts are made to relate recombinant frequencies to the integration efficiencies of the markers involved and to the distance between them. (H.G.D.)

5230 (COO-119-232) RESEARCH IN RADIOBIOLOGY. Annual Report of Work in Progress on the Chronic Toxicity Program. Dougherty, Thomas F. (Utah Univ., Salt Lake City. Radiobiology Div.). Mar. 31, 1965. Contract AT(11-1)-119. 222p. Dep. mn; CFSTI, $6.00 cy, $1.25 mn.

Separate abstracts were prepared on 11 sections of this report. A list is included of 29 publications during the period covered. (C.H.)

For abstracts of individual sections see: 5231–5234, 5247–5249, and 5287–5290.

5231 (COO-119-232, pp 65-7) THE USE OF THERAPY IN EXPERIMENTAL ANIMALS. Taylor, G. N. (Utah Univ., Salt Lake City. Radiobiology Div.).

The use of prophylactic treatment and therapy in a large beagle colony is on much the same basis as would be expected in a human or veterinary practice and can be a significant factor in minimizing losses and variation from non-radiation induced factors. It is indispensable in achieving the maximum life span in a high percentage of animals. Also, it is a significant feature in providing the most humane care for the colony. (auth)

5232 (COO-119-232, pp 68-73) DENTAL ERUPTION PATTERN OF THE BEAGLE. Shabestari, L.; Taylor, G. N.; Angus, W. (Utah Univ., Salt Lake City. Radiobiology Div.).

The dental eruption pattern of beagles is described. Eruption of the deciduous teeth begins at about three weeks and is completed by the end of the fifth week. The canines appear first and are succeeded by the incisors and then the molars. Exfoliation of the temporary teeth begins at about 115 days and is invariably preceded by eruption of upper permanent premolar 1. The last tooth of the permanent dentition to appear is the third molar, which erupts at about 175 days. (auth)

5233 (COO-119-232, pp 99-121) STUDIES OF TRABECULAR BONE IN BEAGLES AND HUMANS. Jee, W. S. S.; Bromley, R. G.; Dockum, N. L.; Lowe, M.; Burggraaf, R.; Mical, R.; Dedekind, Kendra; Arnold, J. S. (Utah Univ., Salt Lake City. Radiobiology Div.).

The relationship between the percent of osteoid seams, the percent of osteoid seams in the central portion of the vertebral body, the percent of bone, and the total bone surface perimeter within the periosteal envelope of lumbar vertebral bodies with age was studied microscopically. Specimens included 72 human and 40 beagle lumbar vertebral bodies. In the human, the percent of centrally located osteoid seams was 12% at 2 years, 3% at ages 28 to 38, 2 to 14% at ages 40 to 50, and approximately 5% thereafter. In the beagle the distribution of osteoid seams with age resembled that for the human. The depression of osteoid seams occurred at 28 to 38 years in human and 4.1 to 5.4 years in beagles. The percent of osteoid seams in the entire vertebral body of humans paralleled that of the central portion, but was generally higher. In humans the percent of bone within the periosteal envelope decreased slower with age than it does in the dog (human slope = −0.0987 vs. dog slope = −0.810). In humans the total bone perimeter was small in the young, increased rapidly to age 40 years, then decreased gradually with age. In the dog the total bone surface perimeter remained almost constant over its life span. (auth)

5234 (COO-119-232, pp 122-52) BIOASSAY OF THE INFLUENCE OF CORTISOL IN BONES OF GROWING RABBITS. Jee, W. S. S.; Blackwood, E. L.; Tegge, Renate; Dockum, N. L.; Haslam, R.; Kincl, F. A. (Utah Univ., Salt Lake City. Radiobiology Div.).

Microradiographs of distal femurs, femoral shafts, and calvaria from growing rabbits fed a normal or rachitogenic diet plus 0, 1, 5, 15 mg cortisol/kg/day for 15 days were analyzed for epiphyseal plate thickness, presence of growth arrest plate, regression of metaphyseal trabeculae, thickness of metaphyseal trabeculae, and porosities of femoral shafts and calvaria (bone atrophy). Rabbits fed a normal diet plus 1, 5, 15 mg of cortisol exhibited epiphyseal plate of 0.73, 0.47, and 0.37 times as thick as their controls, while rabbits fed a deficient diet plus 1 and 5 mg of cortisol exhibited epiphyseal plate 0.76 times as thick as their controls. Growth arrest plates appeared in rabbits fed a normal or deficient diet plus 5 and 15 mg of cortisol. Regression of metaphyseal trabeculae occurred only in rabbits fed a normal diet and treated with 5 and 15 mg of cortisol. Porosity values of femoral cortices differed at all dose levels, while porosity values of calvaria differed only in animals fed normal diets plus 5 and 15 mg of cortisol. The dose response relationships between porosities of

femoral cortices and graded doses of cortisol exhibited slope values of 1.25 for rabbits fed normal diets and a value of 2.22 for rabbits on deficient diets. There was an advantage in using the rachitogenic diet in the femoral porosity analysis, but the use of the rachitogenic diet was a distinct disadvantage in the analyses of epiphyseal plate thickness, length of metaphysis, and calvarium porosity. (auth)

5235 (NP–15543, pp 83-90) UTILISATION DES RADIATIONS IONISANTES ET DES ISOTOPES RADIOACTIFS DANS LES RECHERCHES AGRICOLES ET FORESTRIERES EN ROUMANIE (1958–1964). (Utilization of Ionizing Radiation and Radioactive Isotopes in Agriculture and Forestry Investigations in Rumania, 1958–1964). Priadcencu, Al. (Rumanian Committee for Nuclear Energy, Bucharest).

The possibilities of obtaining, from the use of nuclear radiations, new plant forms with pre-established characteristics have been studied. In some cases seed irradiation has resulted in an improved harvest. Radioisotopes have been used in studies of soil-plant relations, growth and chemical composition of plants, and forest development. (J.S.R.)

5236 (UR–668) UNIVERSITY OF ROCHESTER, ATOMIC ENERGY PROJECT. BRIEF DESCRIPTION OF MOST OF THE RESEARCH PROGRAMS COMPLETED DURING 1964. Annual Report. (Rochester Univ., N. Y. Atomic Energy Project). Jan. 1, 1965. Contract W-7401-eng-49. 175p. Dep. mn; CFSTI $5.00 cy, $1.00 mn.

Research and development programs are described in seven sections. A separate abstract was prepared for each. (J.R.D.)

For abstracts of individual sections see: 5237, 5250, 5251, 5301, 5302, 5436, and 5745.

5237 (UR-668, pp 55-109) TOXICITY OF RADIOELEMENTS. (Rochester Univ., N. Y. Atomic Energy Project).

Results of research are summarized along with investigative procedures used in work on effects of inhaled alpha emitters; vitamin D relations with Ca metabolism; effects of Ca – P ratio on in vitro calcification; soft-tissue Ca analysis; equilibration between rat tissue Ca and injected radiocalcium; parathyroid extract effects on kidney metabolism of radiophosphate; dog blood and urine Ca specific activity; blood-bone exchange mechanisms; renal tissue Ca role in urinary Ca activity; fluoride, Mg, and phosphate effects on in vitro calcification; interactions of Y with physiological ligands; parathyroid hormone effects on HeLa cells; structures of octacalcium phosphate and hydroxylapatite; fluoridated water use in hemodialysis; ^{210}Po inhalation; phagocytosis mechanisms; body content of ^{232}Th daughters after thorotrast injection; Rn metabolism in man; ^{131}I uptake by man; antihypertensive effects of alpha-methyldopa and hydrochlorothiazide; skeletal metabolism; effects of inhaled Rn in rodents; ^{90}Sr retention and toxic effects in rats and rat embryos; Th determination in bone; reactions of uranyl ions with nucleotides; and effects of inhaled radioactive aerosols in man and animals. (J.R.D.)

5238 LINKAGE STUDIES IN PISUM. I. LINKAGE OF THE GENES Chl2, Chl3, AND Chl4, CAUSING CHLOROPHYLL DEFICIENCY. Blixt, Stig (Plant Breeding Inst., Weibullsholm, Sweden). Agri Hort. Genet., 23: 26-42 (1965).

Four mutant lines of peas, homozygous for a chlorophyll deficiency of the light green type (chlorotica), were studied. Crosses between these lines and test lines were carried out to develop gene maps. The mutant lines all originated from the variety Weitor following treatment with x radiation, ethylenimine, or ethylene oxide. Test lines with normal chromosome structures were used. Two of the four mutant lines were found to be mutated at the same loci. Three genes for chlorophyll deficiency were identified in the four mutant lines. Crosses with the test lines showed that one of the three genes had no certain linkage with any of the genes studied, whereas two of the three were linked with another gene. (TCO)

5239 MEDICAL PHYSICS IN EDINBURGH. Greening, J. R. (Royal Infirmary, Edinburgh). Amer. J. Med. Electron., 4: 45-7(Jan.-Mar. 1965).

Research in progress (including problems in electronics and instrumentation, application of radioactive materials, radiotherapy physics, radiation protection and fundamental radiation physics) in the Medical Physics Department at Edinburgh University is surveyed. (TCO)

5240 DISPERSAL STUDIES ON RADIOACTIVE-TAGGED CULEX QUINQUEFASCIATUS SAY. Fussell, E. M. (Navy Disease Vector Control Center, Jacksonville, Fla.). Mosquito News, 24: 422-6(Dec. 1964).

Procedures for labeling mosquitoes with ^{32}P, and use of this tracer in dispersal studies to determine the range and direction of flight of Culex quinquefasciatus from Waipio Peninsula (Hawaii) are described. Trays containing 4th instar (8-day) larvae in 1 in. of water, were filled to a total depth of 4 in. with radioactive solution. The resulting concentration of the ^{32}P was 0.074 mC/l of water. The larvae were allowed to remain in the radioactive solution throughout the remainder of their development. Pupae were present on the ninth day and were emerging by the tenth day. By the twelfth day pupation was complete. Emergence was 2 to 5%. Adults emerging on the twelfth day were predominantly males. By the end of the thirteenth day, emergence of the adults was complete. Monitoring of the adults was accomplished with a ratemeter and monitor equipped with a thin window G-M tube detector. Light traps were used in the recovery of the radioactive mosquitoes. These studies have shown that Waipio Peninsula is the primary source of C. quinquefasciatus for the Pearl Harbor area. From the release of 275,000 ^{32}P-tagged mosquitoes on the peninsula, 634 were recovered from distances up to 3.5 miles. Twenty specimens were recovered beyond the 0.5-mile radius of the release point. Wind influenced the flight of the tagged mosquitoes in a direction away from Pearl Harbor. It is concluded that from Waipio Peninsula this mosquito species is capable of flights of at least 3.5 miles. (BBB)

5241 ON SEVERAL CASES OF RADIATION INJURY. Mayer, E. G.; Zakovsky, J. (Univ., Vienna). Radiol. Austr., 14: 251-83(1963). (In German).

Four cases of radiation injuries and their legal implications are discussed. The responsibility of the physician toward the patient and to those who are engaged with him in radiological treatment of patients is considered. Medical liability insurance for irradiation injury indemnification is examined. The cases discussed include: a young x-ray technician who developed a cataract in the course of her employment, a young patient who underwent abdominal fluoroscopy before developing a typical chronic radiodermatitis with extensive central ulceration, a patient with mammary cancer who was irradiated preoperatively with an excessive irradiation dose because of defective equipment and as a result suffered severe complications after surgery, and a case of irradiation injury that resulted from treatment of a gynecological tumor. The cases discussed are reported in some detail and include descriptions of technical equipment and procedures, doses administered, and legal opinions. (BBB)

5242 REVERSION BY ERYTHROPOIETIN OF THE SUPPRESSION OF ERYTHROID CLONES CAUSED BY TRANSFUSION-INDUCED POLYCYTHEMIA. Bleiberg, Ilan; Liron, Meir; Feldman, Michael (Weizmann Inst. of Science, Rehovoth, Israel). Transplantation, 3: 706-10 (Nov. 1965).

The in vivo intrasplenic cloning method for bone marrow cells in mice was applied to studies on the regulation of erythropoiesis. Experiments were made to test whether erythropoietin would reverse the specific suppression of erythroid clones, caused by polycythemia. It was found that the injection of anemic plasma (erythropoietin) elicited the re-formation of erythroid clones. The kinetics of the

reversal is discussed in relation to the target cell for erythropoietin and its possible morphogenetic action. (auth)

Ecology

5243 (TID–13358(2nd Rev.)) OFFSITE ECOLOGICAL RESEARCH OF THE DIVISION OF BIOLOGY AND MEDICINE. Terrestrial and Freshwater. Schultz, Vincent (ed.) (Division of Biology and Medicine (AEC), Washington, D. C.). Mar. 1965. 134p. Dep. mn; CFSTI $2.50 cy, $1.00 mn.

Separate abstracts were prepared for two sections of this report. (C.H.)

For abstracts of individual sections see: 5244 and 5245.

5244 (TID–13358(2nd Rev.), pp 3-88) TERRESTRIAL RESEARCH. (Division of Biology and Medicine (AEC), Washington, D. C.).

Research programs on various aspects of terrestrial ecology conducted by colleges and universities and supported by the Division of Biology and Medicine, U. S. Atomic Energy Commission in 1965 are described. Information is summarized on the type of ecological research, objectives, justifications, and experimental procedures of 30 programs. Lists of publications, theses, and dissertations that report research results are included for each program. Emphasis was placed on studies of radioecological studies of selected sites; the effects of underground nuclear explosions on the distribution of native animal populations; food chain relationships of ^{131}I, ^{137}Cs, and ^{90}Sr; and the effects of radiation on various species, populations, and ecosystems. (C.H.)

5245 (TID–13358(2nd Rev.), pp 89-126) FRESHWATER RESEARCH. (Division of Biology and Medicine (AEC), Washington, D. C.).

Research programs on various aspects of freshwater ecology conducted by colleges and universities and supported by the Division of Biology and Medicine, U. S. Atomic Energy Commission in 1965 are described. Information is summarized on the type of ecological research, objectives, justifications, and experimental procedures of 13 programs. Lists of publications, theses, and dissertations that report research results are included for each program. Emphasis was placed on studies of the movement of Ca, Sr, and other radionuclides through aquatic ecosystems; productivity and mineral cycling in aquatic ecosystems; and the effects of γ and x radiation on the activities of fish. (C.H.)

5246 TAGGING THE ORIENTAL FRUIT MOTH, GRAPHOLITHA MOLESTA (BUSCK) WITH RADIOACTIVE PHOSPHORUS FOR FLIGHT AND DISPERSAL STUDIES. Dustan, G. G. (Canada Dept. of Agriculture, Ontario). Can. Entomol., 97: 810-16(Aug. 1965).

Procedures for labeling large numbers of the oriental fruit moth with ^{32}P are presented. Adults were successfully tagged (500 or more cpm) by holding them for 24 to 48 hr in cages provided with cotton wicks moistened with a water-solution of ^{32}P at 20 μC/ml. The addition of sugar to the tagging solution did not increase in effectiveness. Moths given ^{32}P (20 μC/ml) the day they emerged seldom attained much radioactivity during the first 24 hr but usually did so within 48 hr. Moths attained an average of 125 cpm per moth during the first 24 hr after emergence and 840 cpm within 48 hr. Extending the tagging period from 48 to 72 hr did not appreciably increase their radioactivity, possibly because the uptake of ^{32}P after 48 hr was about equalled by losses due to excretion and other causes. Attempts to tag large numbers of moths (400 to 1000 per cage) for release and recovery experiments were only partially successful as the radioactivities attained by individual moths varied widely at different times and from cage to cage, even under the same environmental conditions. This appeared to be partly due to differences in the feeding behavior of different batches of moths and it may have been influenced by the conditions under which they were reared. (BBB)

Metabolism, Tissue Distribution, and Toxicology

Refer also to abstract 5564.

5247 (COO-119-232, pp 188-99) PILOT STUDY OF THE EFFECT OF CORTISOL ON $Na_3CaDTPA$ ENHANCED EXCRETION OF ^{239}Pu IN THE BEAGLE. Atherton, D. R.; Dougherty, T. F.; Bruenger, F. W.; Taylor, G. N.; Stover, B. J. (Utah Univ., Salt Lake City. Radiobiology Div.).

Two massive doses of cortisol were given to mobilize ^{239}Pu to make it available for chelation by $Na_3CaDTPA$ and subsequent excretion. No practically significant increase in excretion was observed, and there was no significant removal of ^{239}Pu from the dog's liver. (auth)

5248 (COO–119-232, pp 200-2) EFFECT OF EDTA ON THE EXCRETION OF ^{90}Sr AND ^{90}Y. Atherton, D. R. (Utah Univ., Salt Lake City. Radiobiology Div.).

Administration of $CaNa_2EDTA$ to four dogs which had been injected with ^{90}Sr 0.7 years previously failed to enhance the excretion of ^{90}Sr, but did increase the urinary excretion of ^{90}Y by a factor of about 5. (auth)

5249 (COO–119-232, pp 203-18) THE DETERMINATION OF HALF-PERIODS OF DOG SERUM PROTEINS USING ^{35}S-L-METHIONINE. Bruenger, F. W.; Stevens, W.; Stover, B. J. (Utah Univ., Salt Lake City. Radiobiology Div.).

The measurement of the half-periods of serum proteins is of interest due to the relationships between turnover of these proteins and the binding of heavy radionuclides by them. These half-periods were measured using ^{35}S-L-methionine injected I.V. into a young healthy beagle dog. Blood samples were taken from 2 hours through 42 days after injection. Total ^{35}S activity of the serum and of the protein-bound ^{35}S was measured. The protein fractions were separated by electrophoresis and gel-filtration. The half-period of each protein fraction was then determined by measuring its ^{35}S activity over the period of 42 days. Single exponentials to describe the decrease of ^{35}S were computed using the method of least squares. (auth)

5250 (UR–668, pp 110-16) MOLECULAR AND CELLULAR LEVEL STUDIES. (Rochester Univ., N. Y. Atomic Energy Project).

Information is presented on development of staining techniques for electron microscopy and their application to biological problems. Results of research on bacteriophage nucleic acid metabolism are also presented. (J.R.D.)

5251 (UR–668, pp 123-49) CHEMICAL TOXICITY. (Rochester Univ., N. Y. Atomic Energy Project).

Investigation methods and results are summarized for work on cell surface role in radiation damage; inhalation and excretion of UO_2 aerosols by rats, monkeys, and dogs; biochemical and genetic behavior of cytochromes and related pigments in yeast; reactions of Na- and K-adenosine triphosphate; sensitive spectrochemical measurements; structural-functional relations in erythrocyte membranes; metabolism and excretion of Hg by rats; discrimination between alkali metal cations by yeast; factors affecting invertase distribution on yeast cells; animal metabolism of ^{203}Hg-labeled neohydrin; and kinetics of fluoride sorption by rats. (J.R.D.)

5252 SYNTHESIS AND METABOLISM OF GLUCOSE-3-^{3}H AND GLUCOSE-4-^{3}H. Rognstad, Robert; Katz, Joseph (Cedars-Sinai Medical Center, Los Angeles). Atomlight, No. 48, 1-6(Oct. 1965).

The synthesis of glucose-3-^{3}H and glucose-4-^{3}H was based on the stereospecific labeling of triose phosphates using the enzymes aldolase and triose phosphate isomerase in tritiated water. Slices of rat epididymal adipose tissue were incubated with glucoses labeled in the 1,6 and uniformly labeled positions with ^{14}C and in the 1, 6, 3, and 4 positions with tritium. Tritium from the 3 position of glucose was not found in the β position of glycerol or in

lactate indicating that triphosphopyridine nucleotide (TPNH) is not used in the reductive conversions of dihydroxyacetone-P (DHAP) to glycerol-P or pyruvate to lactate. The incorporation of tritium from glucose-3-^{3}H into fatty acids was nearly twice as great as the incorporation from glucose-1-^{3}H. The results obtained with glucose-4-^{3}H were not as clear. (P.C.H.)

5253 STUDIES OF INHIBITION OF INTESTINAL ABSORPTION OF RADIOACTIVE STRONTIUM. Skoryna, Stanley C.; Paul, T. M.; Waldron-Edward, D. Can. Med. Assoc. J., 93: 404-7(Aug. 1965).

A method is reported that permits selective suppression of absorption of radioactive strontium from ingested food material, allowing calcium to be available to the body. Studies were carried out on the inhibitory effect of various amounts of sodium alginate and the dose-response relationship of ^{89}Sr and bone uptake. The results obtained indicated that under laboratory conditions sodium alginate effectively reduces ^{89}Sr uptake in a constant proportion. This effect was observed at the three levels of administration of 1.4%, 12% and 24% of sodium alginate. The linear relationship between the dosage of the radioisotope and the bone uptake in the presence of sodium alginate suggests that the same proportion is maintained at the lower levels of intake of radioactive strontium. Previous studies with small constant doses of sodium alginate were extended in rats to a period corresponding approximately to three years of human life span. Low doses were sufficient to reduce appreciably bone uptake of radiostrontium. (auth)

5254 RADIOAUTOGRAPHIC DETECTION OF PROTEINS NEWLY SYNTHESIZED FROM LEUCINE-^{3}H IN THE MITOCHONDRIA OF THE LIVER AND KIDNEY OF THE RAT. Droz, Bernard; Bergeron, Michel (Commissariat a l'Energie Atomique, Saclay, France). Compt. Rend., 261: 2757-60(Oct. 4, 1965). (In French).

Radioautography combined with electron microscopy made it possible to show silver grains on the mitochondria at times varying from 10 min. to 6 hrs. after the injection of L-leucine-^{3}H. It was deduced that in the hepatic cells and in the cells of the kidney convoluted tubes, the mitochondria are the site of a probably continuous formation of proteins. (tr-auth)

5255 BEHAVIOR OF GLIOMAS IN TISSUE CULTURE. II. THE EFFECT OF X-RAY ON THE PHOSPHORUS METABOLISM OF GLIOMA CULTURES. Palyi, Iren; Toth, Geza; Csaky, Laszlo; Afra, Denes; Zoltan, Laszlo (Orvostudomanyi Egyetem Szoevet- es Fejloedestani Intezet, Budapest). Ideggyogy. Szemle, 16: 93-6(Mar. 1963). (In Hungarian).

To determine the effect of x irradiation on the phosphorus metabolism of glioma cultures, three human astrocytomas and three glioblastoma multiform tumors were used in cultures. Each tumor was explanted in 100 cultures, 50 of which served as controls and 50 were irradiated after 14 days at 6000 R with 230-kv x rays. The culture medium was removed prior to irradiation and replaced with a medium containing 6 μC/ml ^{32}P (carrier-free) after irradiation. After incubation for 6 to 22 hr the radioactivity of the cultures was measured, also the lipid-phosphorus fraction was removed and measured, as well as the RNA and DNA fractions. Results indicated that after 6 hr the inorganic phosphorus fraction in the irradiated samples had a higher sp act. than in the control group. The lipid and DNA fractions showed lower sp act. in the irradiated samples than the control group. The RNA fractions showed no significant changes. In subsequent tests various nontumorous tissue cultures were prepared and irradiated (brain cultures of human embryos, brain cultures of rat embryos, and liver, thymus, and heart muscle cultures of rat embryos); the results showed no significant changes in the phosphorus metabolism of irradiated and nonirradiated tissues. No definite conclusions are offered to explain the various changes. It is pointed out that the tests were made shortly after irradiation and it is not known whether these changes are reversible or irreversible. (BBB)

5256 STUDIES ON THE CRYSTALLINE LENS. XI. THE RELATIVE ROLE OF THE EPITHELIUM AND CAPSULE IN TRANSPORT. Kinsey, V. Everett; Reddy, D. V. N. (Kresge Eye Inst., Detroit). Invest. Ophthalmol., 4: 104-16(Feb. 1965).

Radioisotope experiments are reported in which the uptake of ^{86}Rb, ^{42}K, ^{14}C-labeled α-amino isobutyric acid (α-AIB), ^{22}Na, ^{36}Cl, and tritiated water (HTO) was studied in cultured rabbit lenses. Effect of ouabain or iodoacetate on transport of these isotopes is also reported. Ouabain significantly decreased the uptake of ^{42}K, whereas it increased the accumulation of ^{22}Na; it also decreased the uptake of ^{14}C-α-AIB, and increased that of ^{36}Cl, but only after a time delay. The effect of iodoacetate in reducing the uptake of ^{14}C-α-AIB was immediate. The turnover of HTO between the lens and its environment was extremely rapid ($t_{½}$ = 15 min); its movement was not appreciably altered by ouabain. The relative rate of appearance of ^{42}K and ^{22}Na in the medium from lenses which had accumulated these isotopes, as well as the effect of ouabain, was opposite in direction to that observed for influx of the same ions. Removal of surface membranes altered both the rate of accumulation and exit of all ions in a manner similar to that of the metabolic poisons. Penetration of ^{42}K, ^{14}C-α-AIB, and ^{86}Rb was greater across the anterior than posterior surface, a difference which was abolished by metabolic poisons, the removal of capsule and epithelium, and, in the case of α-AIB, by the addition of the nonlabeled amino acid to the medium. Penetration of ^{22}Na and ^{36}Cl was greater from the posterior side, and removal of the capsule and epithelium increased influx across both surfaces, as did iodoacetate and ouabain for ^{22}Na but not for ^{36}Cl. Decapsulation abolished the effect of inhibitors HTO and ^{14}C-urea accumulated at equal rates across both front and back surfaces. It is concluded that K, α-AIB, and Rb are actively transported into and Na out of the lens by carrier systems located in the epithelium, and that movement of water, Cl, and urea between lens and its environment occurs passively through diffusional exchange. (BBB)

5257 UPTAKE BY PLANTS OF RADIOSTRONTIUM FROM CONTAMINATED SOILS. Andersen, A. J. (Danish Atomic Energy Commission Research Establishment, Risoe, Roskilde). Nature, 208: 195-6(Oct. 9, 1965).

The influence of heat treatment and superphosphate application on the plant uptake of radiostrontium was examined in pot experiments. For comparison the effect of applying calcium carbonate to the contaminated soil surface was also determined. Spring barley was grown to maturity in pots. Two loamy and two sandy soils were used. Strontium-89, superphosphate, and calcium carbonate were added. Heating the contaminated soil to 800°C reduced the uptake of radiostrontium by plants from loamy soils by a factor of twenty. In the sandy soils only a fourfold decrease in the uptake was found. Addition of superphosphate caused a marked reduction in the plant uptake of radiostrontium. The largest amount resulted in a fourfold decrease in uptake from the sandy soils, in the loamy soils the reduction factor was three. The addition of calcium carbonate did not reduce the uptake of radiostrontium from these soils. In fact, the results indicate a slight increase in the uptake, even from the sandy soils of relatively low calcium saturation. These results are discussed. (J.F.P.)

5258 MECHANISM OF UPTAKE OF TRACE ELEMENTS BY PLANT ROOTS. Findenegg, G.; Broda, E. (Univ. of Vienna). Nature, 208: 196-7(Oct. 9, 1965).

The uptake of zinc-65 by roots of barley plants was studied. The uptake was computed from the remaining activity of the solutions, as measured with a Geiger counter after removal of the roots. For comparison analogous experiments were performed using potassium-42. In a few experiments the longer-lived rubidium-86 was substituted for potassium. The enrichment factor (defined as the ratio of the concentration in tissue (roots) to that in the supernatant) for zinc was high—about 10^{2} in the case of zinc concentrations of the order of 10^{-7} M

in the supernatant—and depended on experimental conditions. The mechanism of enrichment is clearly quite different from that for potassium. The results are given and discussed. It is suggested that the accumulation of zinc by plants is due to passive processes, not dependent on metabolism or the integrity of the cells, namely, to exchange absorption and compound formation. (J.F.P.)

5259 IODINE STORAGE IN THE THYROID GLAND OF THE HUMAN FETUS. **Lampe, Laszlo; Kertesz, Laszlo; Dzvonyar, Janos** (Orvostudomanyi Egyetem, Debrecen, Hungary). Orv. Hetilap, 105: 981-3(May 24, 1964). (In Hungarian).

Tests were conducted on human fetuses that were therapeutically aborted at the clinic for various reasons. The mothers were given 30 to 40 μC of carrier-free ^{131}I per os ~24 hr before abortion to facilitate measurements. The age of the 14 fetuses examined ranged from the 8th to 23rd weeks of pregnancy. Through the 12th week neither the thyroid nor the other organs examined contained any appreciable amount of iodine, the measured amounts barely reaching that of the background radiation. From the 13th week various minimal amounts of radioactivity were detected, mostly in liver, kidney, and stomach. From the 13th week the iodine contained in the thyroid equaled the amount contained in all other organs, and from that time on increased rapidly, until it reached 1 to 2% of the iodine administered between 16 and 23 weeks of gestation. The placenta in each instance contained more iodine than the fetal organs with the exception of the thyroid. This is due to its larger size and primary function in exchanging iodide. It is pointed out that radioiodine should not be administered for diagnostic or therapeutic purposes to women who are known to be pregnant because of possible hazards to the fetus. (TCO)

5260 FORMULATION AND TESTING OF A COMPARTMENTAL MODEL FOR CALCIUM METABOLISM IN MAN. **Cohn, S. H.; Bozzo, S. R.; Jesseph, J. E.; Constantinides, C.; Huene, D. R.; Gusmano, E. A.** (Brookhaven National Lab., Upton, N. Y.). Radiat. Res., 26: 319-33 (Nov. 1965). (BNL-8693).

A two-compartment model (corresponding to a first-order differential equation) was used to describe the kinetics of an injected tracer (^{47}Ca) in ten subjects. The solution of the equations of the above kinetic system was performed on a high-speed digital computer with the Berman (NIH-OMR-SAAM) program. This program determines the sizes of the compartments and the transfer constants between them. Further, the standard deviations of these values are calculated by an iterative least-squares fit of the data to provide a quantitative measure of the standard deviation of the measured parameters. When a standard set of data was analyzed, the calculated parameter values obtained correlated well with those reported by others. The solution obtained was shown to be consistent mathematically and compatible with stated physiological constants. In addition to plasma, urine, and feces data, whole-body counting and data from an externally counted bone compartment (knee) were utilized. The whole-body data and the knee data were utilized to obtain a more unique solution of the kinetic data, as measured by the standard deviation of the calculated parameter values. The primary advantage of the whole-body counter in these studies lies in its ability to measure retention of the tracer over long periods of time. With these long-term data, it is possible to modify the model appropriately in order to simulate resorption and long-term exchange, and thus to make a finer assessment of the kinetics of calcium metabolism. The digital computer analysis makes possible the objective and uniform handling of large amounts of data and thus a greatly increased scope of research. The result of such an approach should lead to a better understanding of calcium metabolism, and particularly pool sizes, rates of bone formation and turnover, and their physiological variation in health and disease. (auth)

5261 ENTRANCE OF ^{14}C INTO SPAWN AND GRUBS OF AUTUMN SPAWNING FISHES. **Fedorova, G. V.** (Leningrad State Univ.). Radiobiologiya, 5: 690-2(1965). (In Russian).

Roe of the flatfish Salvelinus lepechini were placed in a Petri dish, and covered with a thin layer of water containing ^{14}C in sodium acetate form at concentrations of 2×10^{-6}, 2×10^{-5}, and 2×10^{-4} curies/l, which exceeded the maximum allowable concentration of ^{14}C in water by factors of 10, 100 and 1000 respectively. The water was changed daily, but the activity was maintained constant. Samples of roe were dried, weighed, and counted on an end-window counter. Absolute counts were determined by comparison with a ^{14}C standard. It was found that the longer the roe or fish stayed in contact with the contaminated water, the greater was the buildup of radioactivity. The accumulation factors (ratio of activity in the roe to activity in the water) were found to be 3.5 at a concentration of 2×10^{-4} curies/l, and 10.8 at 2×10^{-5} curies of ^{14}C/l in the water. The activity of the flatfish Salvelinus lepechini was found to be 203 ± 2.3 μC/kg dry weight on the 50th day of observation which is a factor of 25 less than the 5229 ± 23.7 μC/kg dry weight found for the whitefish Coregonus peled under the same conditions. The average weight of one roe from the flatfish was found to be equal to 44.5 mg which is a factor of 17 less than the average weight of 2.6 mg for a single roe of the whitefish Coregonus peled. Hence, the smaller whitefish roe has a higher surface per unit weight and can absorb a larger amount of ^{14}C. It is concluded that the roe of similar fishes can absorb ^{14}C at different rates and amounts. (TTT)

5262 UTILIZATION OF INORGANIC RADIOSELENIUM FOR BIOSYNTHETIC LABELING OF TRACER PROTEINS. **Celander, D. R.; Celander, Evelyn** (Coll. of Osteopathic Medicine and Surgery, Des Moines). Tex. Rep. Biol. Med., 23: 589-99(Fall 1965).

Results are reported of experiments designed to determine the feasibility of using relatively large amounts of ^{75}Se for the biosynthesis of radioactive plasma proteins and subsequently employing these proteins, following purification, as radioactive protein tracer substances. Retention and distribution patterns of ^{75}Se, administered as sodium selenite to dogs in amounts from 0.03 to 0.5 mC/kg, are shown. Significant quantities of ^{75}Se are still present in the animal body as long as 75 days after injection. With time, an increasing proportion of the whole blood ^{75}Se is found in the erythrocytes. Plasma of such animals serves as a good source of ^{75}Se-labeled proteins, which in turn are used as tracer substances both in vivo and in vitro. Plasma samples from animals injected with $Na_2{}^{75}SeO_3$ were subjected to dialysis at three different pH values, to precipitation with such protein precipitants as tungstic acid, trichloroacetic acid, and lead nitrate in an alkaline medium, and to electrophoresis. The results of all these procedures indicate the firm association of ^{75}Se with protein. Canine fibrinogen, labeled in vivo with ^{75}Se, was used as a substrate for differentiating between fibrinolysin and an activator of the fibrinolytic enzyme system, urokinase. The radioselenium of an ^{75}Se-labeled fibrin clot is released only by proteolytic dissolution of the clot. A ^{75}Se-labeled fibrin-stabilizing factor (fibrinase) was isolated and used in vitro to demonstrate that fibrin-stabilizing factor is not adsorbed to fibrin during clot formation. A portion of the urinary ^{75}Se was associated with the small amounts of protein found in normal urine. Isolation of urokinase from the urine of ^{75}Se-treated animals gave a preparation containing about 1 μC/mg crude enzyme protein. Based on the data presented, it is suggested that proteins made radioactive through the biosynthetic incorporation of ^{75}Se constitute a valuable tool for use in the study of protein dynamics. (BBB)

5263 CALCIUM NUTRITION AND RADIOSTRONTIUM INJURY. **Pany, Johannes E.** (Univ., Wien). Z. Ernaehrungswiss., Suppl. 4, 171-4(1965). (In German).

Increased concentrations of radiostrontium in children's bones as a result of the resumption of nuclear weapons testing during 1961 to 1963 is discussed in relationship to methods for preventing human contamination. It is suggested that the most feasible approach would be to prevent

radiostrontium uptake from the gastrointestinal tract by dietary supplementation with Ca. The mechanism of Ca effect on radiostrontium is considered. Calcium and ^{90}Sr uptake by the Austrian population were determined to average 1030 mg/day and 27.1 pC/g Ca respectively. (TCO)

5264 THE DISSOCIATION OF RETICULOCYTE RIBOSOMES. Philipps, Georg R. (California Inst. of Tech., Pasadena). Z. Naturforsch., 20b: 930-2(Sept. 1965). (CALT-51-4).

Additional evidence is presented that ribosomes are the primary site of the amino acid polymerization during protein synthesis. The successful dissociation of mammalian reticulocyte ribosomes without chelating agents is described, and the influence of the growing peptide chain (peptidyl-sRNA) on dissociation are reported. Ribosomes dialyzed against tris buffer containing 0.1 M NaCl and 3×10^{-5} M Mg^{2+} showed the persistence of undissociated monosomes and two clearly separated subunits. The distribution of the radioactivity in peptidyl-sRNA of the dissociated ribosomes, prepared by incubation in vitro with radioactive leucine, is shown. The effect of variable NaCl concentrations on the growing peptide chain is discussed. An estimation of the length of the peptide chain was made by comparison of the radioactivity of the ^{3}H-labeled sRNA moiety with the ^{14}C-labeled peptidyl chain, on the assumption that 17 leucyl residues should be present in the complete chain. (J.S.R.)

Radiation Effects on Biochemicals

See also CHEMISTRY — Radiation Chemistry

5265 CHANGES IN THE CONCENTRATION OF UNSATURATED HIGHER FATTY ACIDS OF THE "FREE LIPID" FRACTION FROM LEAVES OF IRRADIATED PLANTS AND A STUDY OF ITS TOXIC PROPERTIES. Budnitskaya, E. V.; Borisova, I. G.; Aleksandrova, N. B. (Bakh Inst. of Biochemistry, Academy of Sciences, Moscow). Biochemistry (USSR) (Engl. Transl.), 29: 792-6 (Sept.-Oct. 1964).

Translated from Biokhimiya, 29: 930-5(Sept.-Oct. 1964).

It was shown that the irradiation of plants in doses of 10,000, 30,000, and 50,000 R leads to a substantial increase in the unsaturated higher fatty acid content in the free lipid fraction (by 30 to 80%). Irradiation in a dose of 1000 R produces a certain decrease in the amount of unsaturated higher fatty acids in the investigated fraction (by 20 to 40%). Irradiation of bean leaves subjected to preliminary influence of steam in order to inactivate the enzyme system does not lead to any increase or decrease in the content of the investigated acids (by 7 to 10%), which is evidence of the enzymatic character of the processes of accumulation of unsaturated higher fatty acids and their peroxides in the free lipid fraction, isolated from plants irradiated by x rays. In an investigation of the action of the free lipid fraction isolated from irradiated and nonirradiated bean sprouts on the growth and development of germinated wheat seeds, a strong toxic phenomenon was established, leading to a sharp suppression of the growth of the seeds and a free lipid fraction, containing a large amount of unsaturated higher fatty acids and lipid peroxides. (auth)

5266 THE RESISTANCE OF MICROCOCCUS RADIODURANS TO ULTRAVIOLET RADIATION. II. ACTION SPECTRA FOR KILLING, DELAY IN DNA SYNTHESIS, AND THYMINE DIMERIZATION. Setlow, Jane K.; Boling, M. E. (Oak Ridge National Lab., Tenn.). Biochim. Biophys. Acta, 108: 259-65(Oct. 11, 1965). (ORNL-P-992).

Micrococcus radiodurans cells were irradiated at different wavelengths of uv. The relative efficiencies of these radiations to kill the cells, delay DNA synthesis, and induce thymine dimers in the cellular DNA were determined. The shape of the action spectra indicated that: killing and delay in DNA synthesis must be at least in part the result of lesions other than the thymine dimer; and possibly deoxycytidine and protein damage are involved in these two effects of uv. (auth)

5267 A MICROFLUOROMETRIC EXAMINATION OF RADIATION INJURIES OF THE MACRONUCLEUS OF TETRAHYMENA PYRIFORMIS INFUSORIA. Zotikov, A. A. (Inst. of Radiation and Physico-Chemical Biology, Academy of Sciences, USSR). Dokl. Akad. Nauk SSSR, 162: 944-6(June 1, 1965). (In Russian).

Infusoria (Tetrahymena pyriformis) cells at 10°C were given a dose of x rays, and then diluted by a factor of 5 to 10 with fresh medium. Changes in the intensity of the secondary luminescence of the cells were followed by fixing cells with ethyl alcohol, washing with 0.1 M acetate buffer, staining for 10 minutes with a 0.001% solution of acridine orange, washing again with acetate buffer, and measuring the fluorescence on a specially built microscopic cytofluorometer. The results show that no radiation changes can be observed one hour after radiation up to a dose of 300 kR. The luminescence increases with increasing dose from 300 to 600 kR. Saturation of the effect is observed at 700 to 900 kR. The maximum increase in luminescent intensity is observed 3 hours after radiation at a dose as low as 100 kR. The effect decreases 4 hours after irradiation, but even 3 to 9 hours after irradiation the intensity is high at doses of 300 to 600 kR. These data show that radiation damage to nucleoproteins has an effect on the binding of acridine orange to the protein. (TTT)

5268 CROSS-LINKAGES AND LOCALLY DENATURED AREAS INDUCED IN DOUBLE-STRAND DNA BY ULTRAVIOLET LIGHT OF DIFFERENT WAVELENGTH. Savich, A. P.; Zavil'gel'skii, G. B. (Inst. of Radiation and Physico-Chemical Biology, Academy of Sciences, USSR). Dokl. Akad. Nauk SSSR, 162: 952-5(June 1, 1965). (In Russian).

DNA from T2 phage and from thymus was isolated by the phenol method, and stored at 4°C in a phosphate buffer at a pH of 7.2 (0.5 M NaCl + 0.01 M K-phosphate). Before irradiation the DNA content was adjusted to a concentration of 40 μg/ml in a 0.075 M buffer. The solution was irradiated with uv light from mercury vapor lamps at $\lambda = 240$, 265 and 280 mμ at intensities $I_{254} = 2900$, $I_{280} = 460$, $I_{265} = 530$, and $I_{240} = 20$ ergs/mm²-min. The number of cross-linkages and locally denatured areas in DNA were determined from the fluorescent characteristics of the basic dye acridine orange (AO) on reacting with DNA. From a study in the variation of the lifetime of the excited state of the dye it is concluded that cross-linking between complementary DNA strands is a result of the photodimerization of thymine residues from opposite strands. The efficiency of uv light with $\lambda = 265$ mμ significantly exceeds the efficiency of uv light with $\lambda = 254$ and 280 mμ in forming cross-linkages and locally denatured areas. Analogous results were obtained in measuring the ratio of AO fluorescent intensities in the red and green regions of the spectrum (I_{640}/I_{530}) as a function of uv dose. (TTT)

5269 THE INFLUENCE OF OCCUPATIONAL EXPOSURE TO CHEMICAL AGENTS AND X-RAYS ON THE LEUCOCYTE ALKALINE PHOSPHATASE ACTIVITY. Pawelski, S.; Wichrzycka, E.; Mdzewski, B.; Roszkowski, S. (Inst. of Hematology, Warsaw). Folia Haematol. (Leipzig), 83: 10-15(1965).

The activity of leucocyte alkaline phosphatase (LAP) was evaluated in persons exposed occupationally to known leukemogenic agents and in healthy blood donors. Cytochemical examinations, using a semiquantitative method, and counts of polymorphic neutrophils were performed in 30 blood donors (group I), in 77 assistants of radiological medical departments (group II), and in 62 workers employed in chemical factories. The latter were exposed to benzene (group III) and to various other agents, such as toluene, xylene, formaldehyde, aniline, and nitro dyes (group IV). The mean time of exposure in these groups was more than 10 years. Physical examinations were performed and additional examinations of red cell sedimentation rate and the blood morphology were made to exclude any other

pathologic state which could have influenced the LAP activity. The mean values of LAP activity in the control group and in the II and III groups were similar, and the differences observed were not statistically significant. In group IV the mean values were significantly lower than in the control group. No correlation between the LAP activity and duration of exposure to the noxious agents or the range of leucocytosis could be detected in any of the examined groups, particularly in the group IV. Thus, the LAP activity did not appear to be not changed by the exposure to x rays and the observed deviations are presumably not due to irradiation injury of the cells. However, the results obtained in group IV show that a long exposure to agents such as toluene, xylene, formaldehyde, aniline, and nitro dyes may cause a decrease of the LAP activity. (TCO)

5270 ENERGY TRANSFER IN RELATION TO WATER-CONTENT IN SOLID PROTEINS. Rosen, C.-G.; Ahnstroem, G. (Royal Univ. of Stockholm). Int. J. Radiat. Biol., 9: 435-47(1965).

Transfer of excitation energy from one chromophore to another in a protein molecule was measured in thin, transparent films of a protein with various amounts of hydration water. The decrease in transfer efficiency accompanying the adsorption of water was found to be of the same magnitude as that expected from the molecular expansion connected with the hydration. The influence of the water on the radiosensitivity of some biological materials is far more drastic than the decrease in transfer efficiency measured here. Although this decrease may be expected to be much greater in DNA than in the protein investigated, it is certainly not great enough to explain the total biological effect, as it has been assumed by a few authors. Other roles played by water in this connection are discussed in relation to possible effects of excitations on macromolecules. (auth)

5271 THE RADIOBIOLOGICAL ROLE OF THE HYDROGEN-PEROXIDE-CATALASE SYSTEM. Hernady, Tibor; Szlavy, Laszlo Pal (BOTE Radiologiai Klinika, Budapest). Magy. Radiol., 17: 246-9(Aug. 1965). (In Hungarian).

A summary is given of the research conducted to date in this field and the areas still to be explored are described. (BBB)

5272 EFFECT OF DIFFERENT pH LEVELS ON THE ACTIVITY OF THE PHOSPHOMONOESTERASES OF STYLONYCHIA PUSTULATA FOLLOWING ULTRAVIOLET IRRADIATION. Hunter, Norvell W. (Morgan State Coll., Baltimore). Physiol. Zool., 38: 343-8(Oct. 1965).

Spectrophotometric methods were used to study the activity between pH 3.1 and 12.4 of the phosphomonoesterases in homogenates of normal and uv-irradiated protozoa. Stylonychia pustulata were irradiated with intensities of 1860, 3720, or 7540 erg/mm^2. The enzymes were active at all pH levels; however, maximum activity occurred at a pH of 5.1 and 9.4. The enzymes from the normal animals liberated 2.6 μg more inorganic phosphate (Pi) per ml from glycerophosphate than those of the controls at a pH of 5.1, and 2.5 μg more Pi/ml at a pH of 9.4. At a pH of 5.1, the enzymes from animals irradiated with doses of 1860 erg/mm^2 liberated 1.8 μg more Pi/ml than the controls, those given doses of 3720 erg/mm^2 liberated 1.0 μg more Pi/ml than the controls, and those given doses of 7540 erg/mm^2, 0.9 μg more Pi/ml than the controls. At a pH of 9.4, the enzymes from animals irradiated with doses of 1860 erg/mm^2 liberated 0.4 μg more Pi/ml than the controls, those with doses of 3720 erg/mm^2 liberated 0.3 μg more Pi/ml than the controls, and those with doses of 7540 erg/mm^2 liberated 0.2 μg more Pi/ml than the controls. These data show that a constant diminution of activity of the enzymes occurred with the increasing intensity of irradiation of the animals. After an exposure of 7540 ergs/mm^2, the activity of the enzymes had almost disappeared except at pH 4.1, 5.1, and 6.1. This might indicate that the rate of inactivation of the enzyme can be measured over a longer period at acid pH than at alkaline pH. The response of the phosphomonoesterases of S. pustulata to uv radiation is similar to that of other hydrolases and other proteins, which are known to be inactivated by uv radiation. (BBB)

5273 ZERO-FIELD ELECTRON MAGNETIC RESONANCE OF IRRADIATED GLYCINE PEPTIDES. Mangiaracina, Richard S. (Roswell Park Memorial Inst., Buffalo). Radiat. Res., 26: 343-52(Nov. 1965).

The technique of zero-field magnetic resonance was employed to investigate the free radicals produced by x irradiation of some glycine peptides. The broad absorption lines in the ESR spectra of glycylglycine and acetylglycine are most probably the result of the presence of more than one radical rather than the effect of unresolved hyperfine interaction. Furthermore, evidence was presented to show that in glycylglycine the damage is localized on the α-carbon at the acid end of the molecule. The principal values of the hyperfine interaction tensor for the main radical in glycylglycine hydrochloride were established with high accuracy. The great similarity in the spectra of glycylglycine hydrochloride and glycylglycylglycine implies that irradiation gives rise to very similar free radicals in these compounds. Hence, it appears that in glycylglycine, acetylglycine, glycylglycine hydrochloride, and glycylglycylglycine the unpaired electron is located on the α-carbon at the acid end of the molecule. The x ray damage probably consists of the removal of one or the other of the nonequivalent methylene protons. The removal of one of these protons, however, is always favored. These results indicate a remarkable degree of specificity in the x ray damage of these glycine peptides. (auth)

5274 IRRADIATION OF ESTRONE AND DERIVATIVES IN ACETIC ACID. Wheeler, Owen H.; Montalvo, Rafael (Puerto Rico Nuclear Center, Mayaguez). Radiat. Res., 26: 353-62(Nov. 1965).

The x irradiation of estrone in acetic acid gave 2-hydroxyestrone monoacetate and diacetate. Estradiol afforded 2-hydroxyestradiol 2,17β-diacetate. Estradiol 3-methyl ether was also acetoxylated in position 2 and acetylated at the 17-hydroxyl group; estrone acetate gave 2-hydroxyestrone diacetate and also apparently 4-hydroxyestrone diacetate and a trace of estrolactone acetate. The apparent $G_{(-m)}$ values were estrone 0.93, estrone acetate 2.47, estradiol 2.11, and estradiol 3-methyl ether 1.69. (auth)

5275 RADIATION INACTIVATION OF POTATO PHOSPHORYLASE. Phillips, G. O.; Griffiths, W. (University Coll., Cardiff, Wales). Radiat. Res., 26: 363-77(Nov. 1965).

The inactivation of potato phosphorylase by γ-radiation was studied in aqueous solution and in the solid state. The kinetics of enzyme inactivation were examined. (C.H.)

5276 RADIATION INDICATION OF SUBUNIT OF LACTIC DEHYDROGENASE. Fluke, Donald J.; Hochachka, Peter W. (Duke Univ., Durham, N. C.). Radiat. Res., 26: 395-402(Nov. 1965).

Lactic dehydrogenases extracted from various tissues of rat and goldfish were irradiated in dry films in vacuum with fast electrons. The material was redissolved, assayed for enzymatic activity remaining, and the results interpreted according to single-hit theory. For all sources tested the target mass is 30,000 to 45,000 gm/mole, suggesting that enzyme subunits demonstrable electrophoretically in this size range can bind and catalyze independently within the tetrameric complexes of the holoenzyme. (auth)

5277 ON THE METHOD FOR DETERMINING INACTIVATION OF ALKALINE PHOSPHATASE SOLUTIONS UNDER THE INFLUENCE OF IONIZING RADIATION. Nikolskaya, E. B. Radiobiologiya, 5: 757-9(1965). (In Russian).

Alkaline phosphatase isolated from the small intestine of the dog was prepared as an aqueous solution of 0.004 mg/ml, and was irradiated with ^{60}Co gamma radiation at doses varying from 0.3 to 33 kR. Unirradiated solutions of enzyme served as controls. Hydrolysis of sodium phenylphosphate

by the irradiated and unirradiated alkaline phosphatase was carried out in a carbonate buffer at a pH of 10 and at a temperature of 37°C with a substrate concentration of 5 μmols/ml in the reaction mixture. Two parallel samples were taken at 2, 5, 10, 15, 20 and 30 minute intervals. One sample was analyzed for phenol, and the other for phosphate. The enzyme activity decreased with increasing time after the start of the hydrolysis. Values of K were calculated for the equation $\ln A/A_0 = KD$, which relates the inactivation of the enzyme (A/A_0) to the irradiation dose D. K is a constant depending on the nature of the enzyme, source strength, and concentration of enzyme. (TTT)

5278 EFFECT OF GAMMA IRRADIATION ON THE CONTENT OF FREE AMINO ACIDS IN MEAT. Niewiarowicz, A.; Palmin, W. W. (Coll of Agriculture, Poznan, Poland). Rocz. Technol. Chem. Zywnosci, 10: 89-99 (1964). (In Polish).

Beef muscle (gracilis and sartorius) was irradiated with ^{60}Co at a dose rate of 60 rep/sec to give total doses of 1.5 or 3.0 MR. Some samples were stored for four months at 17 to 22°C. Ethanolic extracts of irradiated meat were examined by paper chromatography to detect changes in free amino acid concentration. In beef irradiated with doses of 1.5 and 3.0 MR, cystine and aspartic acid contents decreased, while the level of other amino acids, such as alanine, glycine, threonine, serine, tyrosine, and glutamic acid, increased. In samples of meat for which the pH had been adjusted to 7.2 before irradiation, decomposition of aspartic acid and cystine occurred but the release of tyrosine and threonine was not observed as in the samples irradiated at the normal pH (5.6) of beef. After storage of γ-irradiated meat for 4 months the contents of all free amino acids except cystine increased markedly. It was observed that the higher dose of irradiation (3.0 MR) inhibited proteolysis more effectively in comparison with the 1.5-MR dose. A higher pH value of beef did not inhibit the course of proteolysis but only changed its character. A significant inhibition of the release of hydroxy amino acids (threonine, serine, tyrosine) was observed, however, at the higher pH. (BBB)

5279 INDUCTION OF THE SYNTHESIS OF PHAGE AND COLICIN IN A CULTURE MEDIUM IRRADIATED BY UV RAYS. Smarda, J.; Cermak, V. (Univ., Brno). Zentralbl. Allgem. Mikrobiol., 4: 358-66(1964).

Strain 18 of Escherichia coli, which is both lysogenic and colicinogenic, was used to study induction of bacteriophage and colicin by growth of cultures in a nutritive medium that had previously been exposed to high doses of uv rays. Production of phage showed a 4-fold increase after irradiation of the broth or after irradiation of the water prior to preparing the broth. Production of colicin was increased twofold. Optimum exposure of the broth to irradiation under the given conditions was 26 min for the induction of phage and 20 min for the induction of colicin. The inducing effect of the irradiated medium appeared to be caused mainly by the hydrogen peroxide formed. It is suggested that inductive agents have no direct effect upon prophage or the colicinogenic factor, but interfere primarily with cell metabolism, probably with the metabolism of nucleic acids. By all methods of induction used, the optimum dose for the induction of colicin was lower than the dose required for the induction of phage in the same strain. The effective dose for uv induction of phage in a lysogenic culture is considerably higher than that for induction of colicin in a colicinogenic culture. Chronological analysis of the production of phage and colicin showed that both these factors are not produced at the same time within the induced cells; in an induced culture certain cells produce only phage and others, only colicin. This is analogous to the production of two unrelative phages by a polylysogenic strain where each of the phages is produced independently of the other, and it indicates that the population of a certain lysogenic and colicinogenic culture is not altogether homogenic concerning the effect of inductive agents upon cells. (BBB)

5280 THE INFLUENCE OF IONIZING RADIATION FROM RADIOACTIVE COBALT ON CERTAIN BIOCHEMICAL PROCESSES IN PEAS. Ore, V. (Inst. of Biology, Academy of Sciences, Latvian SSR). pp 191-5 of Tautsaimnieciba Derigie Augi. II. Riga, Latvijas PSR Zinatnu Akademijas Izdevnieciba, 1963. (In Latvian).

A series of investigations on the effect of radiation on the growth, development, and change of the qualitative composition of different agricultural plants was carried out. Annual data of the effects of the exposure of seeds of two varieties of peas to ^{60}Co at doses of 200, 1000, and 8000 R were reported. The doses studied produced changes in the rate of development of the plants and of the time of onset of the phenophase. The analysis of the concentration of the total sugar before flowering showed that in leaves of plants from exposed peas (doses of 200 and 1000 R) increased the amount of total sugar. Doses of 8000 R showed a depressing effect. Doses of 1000 R appeared to give the optimum effect. In this case the quantity of total sugar in the leaves was 69 and 43% greater in the two varieties than in the controls. (tr-auth)

Radiation Effects on Tissues

Refer also to abstract 5815.

5281 (AD-623599) QUARTERLY PROGRESS REPORT NO. 57 [ON RADIOBIOLOGY]. (USAF Radiation Lab., Univ. of Chicago, Ill.). Oct. 15, 1965. Contract AF 41(609)-1693. 44p.

Separate abstracts were prepared on four sections of this report. (C. H.)

For abstracts of individual sections see: 5228, 5282, 5283, and 5407.

5282 (AD-623599, pp 1-15) THE INFLUENCE OF SUBLETHAL DOSES OF X-RADIATION ON THE SYNTHESIS OF HEPATIC MICROSOMAL ENZYMES. DuBois, Kenneth P.; Kinoshita, Florence (USAF Radiation Lab., Univ. of Chicago, Ill.).

Measurements of the influence of sublethal doses of x radiation on the synthesis of phosphorothioate oxidase activity of the livers of young male rats demonstrated that doses of 200 R and 400 R produce marked inhibition of the rate of development of the enzyme activity while 100 R produces partial inhibition of the enzyme development. Reversal of the effect was observed with 100 R and 200 R, with the rate of reversal being dependent upon the dose of x ray. Information on the approximate site of action of radiation was obtained by partial body shielding experiments. Shielding the liver and testes did not prevent the effect, thus demonstrating that the inhibition of enzyme synthesis in the liver was due to an abscopal effect. Shielding the head markedly reduced the inhibitory effects, and irradiation of only the head with the rest of the body shielded produced the same effect as whole-body irradiation. Measurements of the effect of radiation on the development of the detoxification system for (o-ethyl o-[4-nitrophenyl] phenylphosphonate (EPN) and the N-demethylation system indicated that radiation inhibited the rate of synthesis of both of these systems. O-Demethylase activity of the livers of weanling rats approached the adult level at 23 days of age and radiation had no effect on this enzyme system. (14 references.) (auth)

5283 (AD-623599, pp 16-27) STUDIES ON THE EFFECT OF X-RADIATION ON THE HEXOBARBITAL METABOLIZING ENZYME SYSTEM OF LIVER MICROSOMES. Yam, Kei-Ming; DuBois, Kenneth P. (USAF Radiation Lab., Univ. of Chicago, Ill.).

Studies on the hexobarbital oxidizing system of liver microsomes have indicated that there is a marked age difference in enzyme activity in young male rats. Rapid development of the enzyme system to the adult level took place between 30 and 45 days of age which corresponds to the age of puberty in the rat. Hypophysectomy of immature rats arrested the normal development of enzyme activity in young male rats. Exposure of 23-day old male

rats to 400 R of total-body x irradiation markedly retarded the development of the hexobarbital metabolizing enzyme system. This dose of radiation also retarded the resynthesis of the enzyme system in the regenerating liver of partially hepatectomized adult male rats. MEA was shown to afford no protection in vivo against inhibition of development of the hexobarbital metabolizing system. Studies on the influence of magnesium ion on the in vitro inhibitory effect of MEA on the metabolism of hexobarbital revealed that the addition of magnesium does not relieve the inhibition. Thus the in vitro inhibition of hexobarbital metabolism by MEA is not mediated through chelation between MEA and magnesium. (23 references.) (auth)

5284 (AED-C-04-21) RADIATION EFFECTS ON LIVING TISSUES AND ORGANISMS. Series C: Bibliographies. Section 4, No. 21. Stahlhofen, W. (comp.) (Max-Planck-Institut fuer Biophysik, Frankfurt am Main (West Germany)). Apr. 1965. 92p. Dep. mn.

Approximately 330 references are given to reports and journals published during 1964. Separate author and subject indexes are included. (P.C.H.)

5285 (BNWL-SA-172) GAMMA RADIATION DOSIMETRY OF ^{137}Cs IN SHEEP EVALUATED WITH THERMOLUMINESCENT DOSIMETERS. Watson, C. R.; McClellan, R. O. (Battelle-Northwest, Richland, Wash. Pacific Northwest Lab.). Nov. 2, 1965. Contract AT(45-1)-1830. 16p. Dep. mn; CFSTI $1.00 cy, $0.50 mn.

Lithium fluoride thermoluminescence dosimetry (TLD) was used to measure gamma doses in vivo in male sheep ingesting ^{137}Cs. Two commercial TLD systems were found satisfactory for measurements of 500 to 800 mR after a nitrogen purge of the readout chamber was added. Specially fabricated teflon capsules (4mm wall thickness) shielded the LiF from the beta radiation of ^{137}Cs without appreciably attenuating the gamma radiation. Dosimeters were surgically implanted and exposed in vivo for 15 days to measure gamma radiation dose rates of 20-60 mrad/day (total dose less than 1 rad) in sheep with body burdens of approximately 300 μC ^{137}Cs. Dosimeters were implanted in another group of sheep prior to feeding of 50 μC ^{137}Cs per day. These animals were killed at intervals to study the accumulation of gamma dose at various organs during a month of ^{137}Cs feeding. Tissue acceptance of the dosimeters was excellent, and dose distribution patterns were similar to those reported earlier. These measurements support NCRP recommendations which assume that designation of the whole body as critical organ will adequately consider the dose to the gonads in the case of a relatively uniformly distributed gamma emitting radionuclide. (auth)

5286 (CONF-650616-16) MOUSE PHANTOM DEPTH DOSE STUDIES AT THE HEALTH PHYSICS RESEARCH REACTOR OF THE OAK RIDGE NATIONAL LABORATORY. Goodman, L. J.; Pearlman, M. (Columbia Univ., New York. Radiological Research Lab.). [nd]. Contract AT(30-1)-2740. 25p. Dep. mn; CFSTI $1.00 cy, $0.50 mn.

From Health Physics Society, Annual Meeting, Los Angeles.

Fission neutrons and gamma rays from the Health Physics Research Reactor were used in an investigation into the shielding and scattering effects produced when several unrestrained mice sharing the same cage are simultaneously irradiated. Measurements in mouse phantoms were made for various phantom configurations to determine the distribution of dose along the axis and through the cross section of a mouse. Scattering from one or two adjacent mice was found to be small but attenuation produced significant variations in absorbed dose. The attenuation along the axis of a mouse was found to be almost two-thirds and even the shielding produced by one mouse was observed to reduce the dose to the shielded mouse by more than 30 percent. In addition, the tissue Kerma rate in free air at various reactor power levels was measured and the ratio of gamma ray Kerma to neutron Kerma was estimated. (auth)

5287 (COO-119-232, pp 5-64) INJECTION TABLES. (Utah Univ., Salt Lake City. Radiobiology Div.).

The dosimetry of ^{226}Ra, ^{228}Ra, and ^{90}Sr in dogs maintained until death after injection is discussed. Data are presented on the radioisotope dose and cause of death of dogs that died during the report period, some of whom were injected as early as 1952. (C.H.)

5288 (COO-119-232, pp 74-87) ^{228}Th INDUCED FRACTURES IN BEAGLES. Taylor, G. N.; Jee, W. S. S.; Christensen, W. R.; Rehfeld, C. E.; Nebeker, N. (Utah Univ., Salt Lake City. Radiobiology Div.).

Significant numbers of pathological fractures were induced in beagles by a single intravenous injection of ~0.3 μc/kg or ~0.9 μc/kg ^{228}Th. Fractures were not observed at the next higher level, 2.7 μc/kg because of early death from radiation induced nephritis and/or blood dyscrasia. Only one fracture occurred at the ~0.1 μc/kg level in nine dogs observed and no fractures were observed below this dose. This lowest level at which a fracture occurred was approximately 6 times higher than the dose which has induced osteosarcomas, thus far. (auth)

5289 (COO-119-232, pp 88-98) THE CORRELATION OF BONE STRENGTH WITH RADIATION DOSE FROM INTERNAL EMITTERS AND BONE RESORPTION. Taysum, David H.; Jee, Webster S. S.; Clarke, David O. (Utah Univ., Salt Lake City. Radiobiology Div.).

A previous study of the strength of samples of tibial compacta of beagles burdened with radionuclides (^{226}Ra, ^{228}Ra, or ^{90}Sr) indicated a relationship between resorption area and bone strength that was of greater magnitude than the relationship between strength and radiation dose or strength and age. This indicated relationship was investigated by radiography, using 10 kvp x rays, of sites closely adjoining the break and calculating the actual area gravimetrically. The correlation of strength and as a function of bone actually present was made. (auth)

5290 (COO-119-232, pp 165-89) A COMPARISON OF TWO METHODS OF ANALYZING THE HEMATOLOGICAL DATA FROM ^{90}Sr INJECTED BEAGLES. Dougherty, Jean H.; Rosenblatt, Leon S.; Mikolaj, Peter J. (Utah Univ., Salt Lake City. Radiobiology Div.).

Selected hematological data from strontium-90 injected beagles were subjected to two methods of statistical analysis, a randomized block and a one-way analysis of variance. The experimental dogs were compared both to strontium 0-level dogs and to pooled 0-level dogs from all radionuclides. Comparable results were obtained with either control group in terms of significant differences. The randomized block design analysis of variance was found to be the more sensitive type of analysis and is considered the method of choice for subsequent analyses of hematological changes following internal irradiation. (auth)

5291 (COO-205-55) PROGRESS REPORT [ON RADIOBIOLOGY]. Wilson, Raphael (Notre Dame Univ., Ind. Dept. of Biology). 1965. Contract AT(11-1)-205. 158p. Dep. mn; CFSTI $5.00 cy, $1.00 mn.

Separate abstracts were prepared for three papers included in this report. (C. H.)

For abstracts of individual papers see: 5292–5294.

5292 (COO-205-55, Paper 1) GAMMA-RAY EFFECTS ON MECHANICAL ACTIVITY OF A MAMMALIAN MUSCLE PREPARATION. Pierson, Mary Brendan (Notre Dame Univ., Ind. Dept. of Biology). 115p.

The effects of γ radiation on the mechanical activity of preparations of rat diaphragm muscle maintained in standard or modified Tyrode's solution or preparations of frog (Rana pipiens) muscle in standard or modified Ringer's solution were studied. Stimuli were provided by a Gross stimulator, an instrument was developed to control the tension applied during the experiments, and results were recorded on a transducer. The modifications induced by nitrate ion, D-tubocurarine, and AET were recorded. Results are reported on alterations in contraction tension,

rate of contraction, and rate of relaxation as a function of γ dose. Results indicate that the events occurring at the neuromuscular junction during γ irradiation are mediated by either the release of acetylcholine from the presynaptic nerve endings or the permeability of the muscle end plates. (41 references.) (C. H.)

5293 (COO–205-55, Paper 2) EFFECTS OF GAMMA RADIATION ON ELECTRICAL PROPERTIES OF MUSCLE. Crump, M. Dominique (Notre Dame Univ., Ind. Dept. of Biology). 24p.

The effects of γ radiation on the electrical potential of muscle membranes were studied in muscles excised from frog (Rana pipiens) legs and maintained in normal or K-free Ringer solutions. Microelectrodes were developed for use in the studies. Data are presented on alterations in electrical potential induced by 150 to 450 k R radiation doses and the effects of nitrate, thiocyanate, iodide, and bromide ions, known to affect the mechanical properties of muscles, and the radioprotective compound, AET, on the radiation response of muscle membranes. (130 references.) (C. H.)

5294 (COO–205-55, Paper 3) THE INFLUENCE OF ENVIRONMENTAL CONDITIONS ON THE RADIATION SENSITIVITY OF NITELLA FLEXILIS. Esch, Harald E. (Notre Dame Univ., Ind. Dept. of Biology). 17p.

Results are reported from studies of the effects of γ radiation on the electrical properties of internodal cells of the aquatic plant Nitella flexilis grown in normal or K-free Findley solution (artificial pond water) on a north window ledge or grown in Findley solution and illuminated with a 15-watt light night and day. Changes induced by doses of γ radiation ranging from 1.5 k R to 30 k R were followed with glass microelectrodes. Low doses of radiation caused a change in the permeability of the cell membrane, especially for K. The different reactions of cells in different bath solutions indicate possible sites of radiation action in plant cells at doses below 30 k R. (C. H.)

5295 (NP–15559) LES EFFETS DES DOSES NON-LETHALES DE RAYONS X SUR LE COMPORTEMENT EXPLORATEUR ET ALIMENTAIRE DE LA LARVE DE DROSOPHILA MELANOGASTER MEIG [These]. (Effects of Non-Lethal Doses of X Rays on the Exploring and Feeding Behavior of the Larvae of Drosophila Melanogaster Meig [Thesis]). Kapil, Rajendra (Lyon Univ. (France). Faculte des Sciences). 1964. 48p. Dep. mn.

The effects of non-lethal doses of x rays on the exploring and feeding behavior was investigated on the larvae of two varieties of Drosophila–sauvage and vestigial. The larvae were exposed to whole-body doses from 200 to 2500 R. The projections of the head and the synchronized vertical movement of the mandibles was chosen as the standard behavior pattern for measurement of the radiation effects. The results showed that this behavior pattern connected to the taking of nourishment can be measured and is suitable as a norm. The function evolves in a comparable fashion during the larval period for the two varieties. The function depends on the age and varies rapidly up to the age of 12 hr. After 24 hr, it becomes linear and changes are slight until the larvae become pupae. Experiments on the x-ray effects showed that the response of the two varieties are different. Maximum inhibition of the function was observed at 500 and 1500 R for sauvage and vestigial larvae, respectively. Inhibition at low doses was replaced by an excitation effect at higher doses. Response of the function remained the same in sauvage whether larvae aged 2 hr or embryos aged 10 hr were irradiated. Delayed effects in the behavior studied were not detected at the doses studied. (J.S.R.)

5296 (NP–15585) FIFTH REPORT FROM NORSK HYDRO'S INSTITUTE FOR CANCER RESEARCH FOR 1963–1964. (Norsk Hydro's Inst. for Cancer Research, Oslo). 1965. 68p. Dep. mn.

Data are summarized from analytical studies of clinical cancer specimens and the value of different prognostic factors, such as macroscopic and microscopic examinations of material, tumor size and location, grade of malignancy, and Duke's classification of tumors is discussed. The possibility of isolating cancer cells in the blood or lymph stream is discussed. Data are included from a number of studies related to the etiology of cancer. These include the effect of ^{90}Sr injected intraperitoneally on the bone marrow of rats; the repopulation of x irradiated lymph nodes by lymphocytes; the effects of cyclophosphamide, a nitrogen mustard derivative, on the hematopoietic system of rats, and the effects of various treatments such as hypoxia, whole-body irradiation, and nitrogen mustard on this response; the induction of bone sarcomas in rats by exposure to β particles from a $^{90}Sr-^{90}Y$ source; the effects of injected ^{91}Y on reproduction in Drosophila; the x-ray sensitivity of Drosophila spermatogonia; the effects of various cytotoxic compounds and steroids on the growth of tumor cells in culture; the radioprotective effects of H_2S on tumor cells in culture; the mechanisms of action of radioprotective sulfur compounds; the radiation chemistry of p-aminobenzoic acid in neutral and acid solutions; reaction mechanisms involved in the radioprotective effect of N_2O in biological systems; and the radioprotective effect of radical scavengers in biological systems. A list is included of 72 publications that report results of these, and related, studies. (C.H.)

5297 (ORNL-P–1734) EXPERIMENT S-4, RADIATION OF BLOOD. Bender, Michael A.; Gooch, P. Carolyn; Kondo, Sohei (Oak Ridge National Lab., Tenn.). [1964]. Contract W-7405-eng-26. 32p. (CONF-651042–1). Dep. mn; CFSTI $2.00 cy, $0.50 mn.

From Manned Space Flight Experiments Symposium, Gemini Missions 3 and 4, Washington, D. C.

Studies were made on the synergistic effect of zero-G and radiation on white blood cells during the GT-3 manned space flight. The experiment consisted of the simultaneous irradiation of a series of samples of whole, human blood with ^{32}P beta rays during the orbital phase of the mission. Irradiation was accomplished by duplicate experimental devices, one located on the right-hand hatch of the spacecraft and the other on the ground at the launch site. The results showed that while there was no significant difference between the yields of multiple-break aberrations, the frequency of single-break aberrations was significantly higher in the flight samples. A synergism between radiation and some space flight parameter thus appears to exist for human chromosome aberration production. (P.C.H.)

5298 (RLO–353-4) A STUDY OF FACTORS THAT GOVERN RADIOSENSITIVITY OF PLANTS. Research Report No. 15, November 1, 1964–October 31, 1965. Nilan, Robert A.; Konzak, C. F. (Washington State Univ., Pullman). Nov. 1, 1965. Contract AT(45-1)-353. 13p. Dep. mn; CFSTI $1.00 cy, $0.50 mn.

Studies were made on the oxygen effect in dry (2 to 10% water content) and moist (11 to 14% water content) irradiated barley seeds and of the mutagenic action of oxygen in barley seeds of different water contents. The effects of nitric oxide and dimethyl sulfoxide on the oxygen effects were also investigated. The results suggest that in dry seeds oxygen availability is a limiting factor in reaching maximum damage, presumably induced through oxygen-radical interaction, and that possibly oxygen-radical interactions do occur even in moist seeds when oxygen is available. It was also found that oxygen may be more effective in moist seeds at a lower than a higher pH. (P.C.H.)

5299 (TID–22187) REACTIONS OF BACTERIAL CELLS TO FOREIGN NUCLEIC ACIDS. Summary Report, November 1, 1962–October 31, 1965. Ginoza, William (Pennsylvania State Univ., University Park. Dept. of Biophysics). July 1965. Contract AT(30-1)-3116. 15p. Dep. mn; CFSTI $1.00 cy, $0.50 mn.

Simple target theory was examined in tobacco mosaic virus and coliphages R17 and ϕX174 using γ and x irradiation. It was concluded that: target analysis yields sufficiently accurate estimates of the molecular weights of single-stranded nucleic acids; successful application of the theory depends on the recognition and avoidance of

agents in the medium during irradiation; radiosensitivity (target size) remains invariant over the temperature range of −180° to 30°; radiosensitive molecular weights of the viruses are the same as their nucleic acids; and target analysis is simple to perform. When φX174-DNA was compared with its double-stranded counterpart RF-DNA and with T-4, it was shown that: killing efficiency (α) for RF-DNA is 5 fold greater than that for T-4, an argument against the idea that α is an expression of the probability that the occurrence of a certain physicochemical lesion is the cause of lethality; α is likely a measure of the molecular dimension of some critically sensitive target within the phage genome; and when only non-critical targets are hit, the virus can still restitute normal phage progeny. In studies on the kinetics of thermal inactivation of single-stranded viral RNA, it was found trace contamination by RNAase is not the cause of RNA instability. Progress on studies of the fate of coliphage R17 coat protein during injection is reported. (H.G.D.)

5300 (UCLA-12-573) A FORTRAN IV PROGRAM FOR THE EVALUATION OF POST-IRRADIATION SURVIVAL TIMES. Leitch, James L.; Hagen, Nancy S. (California Univ., Los Angeles. Lab. of Nuclear Medicine and Radiation Biology). Nov. 1965. Contract AT-04-1-GEN-12. 39p. Dep. mn; CFSTI $2.00 cy, $0.50 mn.

A Fortran IV computer program was developed for the rapid evaluation of post-irradiation survival times in animals. It takes into account the cage effect between cages within the same experiment, a factor not covered by the Litchfield time-percent effect method of analysis. The program may also be modified for evaluating drug and toxicity studies and for extended (life span) studies on both experimental (treated) and normal (untreated) animals. The terms protection ratio and protection value are defined. A new standardization procedure to allow comparison of results from different experiments is outlined and designated survival ratio. Four appendices give the list of the program, flow diagrams for the program and the subprogram, preparation of the data deck, and an output from a single experiment. (auth)

5301 (UR-668, pp 1-54) RADIATION EFFECTS—GENERAL. (Rochester Univ., N. Y. Atomic Energy Project).

Results of research are summarized along with investigative procedures used in work on whole- and partial-exposure x radiation effects on dogs and rats; radioinduced myocardial necrosis; radiation effects on thyroid gland; radioinduced hemolytic changes; radioinduced intestinal syndromes; cold-stress effects on postirradiation responses; effects and therapy of acutely irradiated animals; x radiation effects on cell sensitivity; x radiation effects on rat sclerosis, hypertension, and reproduction; metabolism in diseased and normal irradiated animals; x radiation effects on dog and Drosophila spermatozoa; x radiation effects on chromosomes and cell mitoxic indices; blood cell morphology of nuclear excursion casualties; x radiation effects on dog renal functions; erythropoietic changes in normal and acutely bled dogs; use of tanned erythrocytes in cell volume determinations; and membrane filter techniques for counting megakaryocytes. (J.R.D.)

5302 (UR-668, pp 161-6) WORK FOR OTHER AGENCIES. (Rochester Univ., N. Y. Atomic Energy Project).

Information is presented on the physiologic effects of partial body irradiation and on the combined effects of injury in animals. Work on the effects of microwaves on animals is summarized. (J.R.D.)

5303 (USNRDL-TR-925) THE HUMORAL FACTOR IN RADIATION-INDUCED MOTIVATION. Hunt, E. L.; Kimeldorf, D. J. (Naval Radiological Defense Lab., San Francisco, Calif.). Oct. 15, 1965. 35p. CFSTI $2.00 cy, $0.50 mn.

According to the evidence now available, the motivational effect of irradiation, exhibited in various conditioned avoidance responses, has general characteristics whereby it can be differentiated from the prompt stimulatory effects of irradiation. In one experiment, it was found that in rats temporarily deeply anesthetized during x irradiation with 90 R (60 R/min), a conditioned aversion to saccharin-flavored fluid could be produced by providing a taste experience with saccharin in the postanesthesia-postexposure period. The preliminary findings in another study, still in progress, indicates that in rat pairs joined by a vascular, non-neural anastomosis, a saccharin aversion can be conditioned in the sham-irradiated member following exposure of its partner to 360 R of x rays (24 R/min). This constitutes positive evidence for a systemic humoral factor which can mediate radioinduced motivation. (P.C.H.)

5304 (JPRS-32985, pp 45-50) COMPARISON OF THE RADIATION SENSITIVITY OF CHROMOSOME IN WHITE BLOOD CELLS OF HUMAN BEINGS, MONKEYS, AND RABBITS. Wang, An-chu; Chou, Hsien-ting; Chen, I-feng. Translated from K'o Hsueh T'ung Pao, No. 10, 917-18(Oct. 1965).

Blood from veins in men and monkeys and from hearts of rabbits was x irradiated with a dosage of 25, 50, 100, 200, and 300 Rads at a rate of 25 Rads/min. A comparison of the results revealed that there was no great or distinctive difference in mutation values of chromosomes between men and monkeys with respect to the dosage, but that there was quite a difference between men and rabbits, and between monkeys and rabbits. It was concluded that it is better to use monkeys as experimental material for cellular genetic studies than any other animal. (P.C.H.)

5305 RESPONSE OF HYBRID AND INBRED MAIZE TO RADIATION OF RADIOACTIVE $^{32}PO_4$. Benedek-Lazar, Magda. Acta Botan. Acad. Sci. Hung., 10: 1-12(1964).

The effect of ^{32}P β radiation on corn seedlings was studied by growing them in soil containing various levels of $Na_2H^{32}PO_4$ (200, 400, 600, 800 μC per pot containing 10 plants—weight of soil not stated). Yellow dent C/5 corn and a hybrid (C/5 × 18T) were used. A 200-μC dose did not affect germination percentage, but compared with untreated seedlings, germinative activity of treated samples was lower by 40 to 45% in C/5 and by 20 to 30% in the hybrid, especially in the first two days of germination. No radiation effect on the growth of above-ground parts could be observed. Application of 200 μC per pot to seedlings at the 2- to 3-leaf stage caused only small difference in their growth, but at the stage of 3 to 4 leaves growth differences became clearly visible. The uptake of ^{32}P by the roots and shoots of hybrid maize surpassed by three times that of the corresponding parts of inbred seedlings. Moderate doses did not change the mass of maize roots, only treatments with 800 μC caused some decrease in comparison to untreated seedlings. After doses of 400 and 600 μC the green matter of foliaged shoots increased by 26% in hybrid and by 15 to 19% in C/5. In cultures with inadequate levels of nitrogen, phosphorus, and potassium the radiophosphate exerted a harmful effect in nearly all treatments. The dry matter, P_2O_5, and total nitrogen content both of hybrid and inbred corn increased after treatments with 400 and 600 μC, while 800-μC doses caused a slight drop. In comparison to untreated seedlings, doses of 200 μC did not depress respiration in the hybrid. The max effect of treatment on respiration (an increase of 58.9%) was caused by 400 μC, whereas 600 μC stimulated respiration by 46.3% and 800 μC by 19.1%. Hybrid corn reacted more intensively to radiation than the inbred variety. Identical doses of ^{32}P exerted a stimulative effect on the growth and metabolism of seedlings under favorable nutritional conditions but inhibited them under adverse conditions. (BBB)

5306 HISTOCHEMICAL STUDIES IN IRRADIATED CHICK EMBRYOS. Bose, Asoke (Univ. of Kalyani, Nadia, India). Acta Histochem., 20: 136-42(1965).

Results are reported from an investigation of the localization of alkaline phosphatase, nucleic acids, and glycogen in irradiated chick embryos, with special reference to their changes during differentiation. White Leghorn eggs, collected immediately after laying were irradiated by a 1-

Mev x ray unit; the range of dose was 300 to 2000 R, including 14% back scattering. The eggs were transferred to an incubator at 38°C and fixed after 24 and 48 hr of incubation. At radiation doses up to 1000 R the embryos showed some retardation in development when examined after 24 hours of incubation, but the 48-hr embryos showed normal ontogeny. Basophilic substances and DNA in the cells of 24-hr embryos showed weaker reactions than the controls, but in no cases were totally depleted. The localization of alkaline phosphatase followed the same pattern as the basophilic granules. The reaction for the enzyme was more intense in the neural region than the epiblast and the hypoblast. In the irradiated embryos, the hypoblast layer showed the least reaction and the highest activity was in the neural area. Glycogen deposits in the experimental and control embryos showed the same intensity. There was a progressive retardation in the morphogenesis at doses above 1000 R, and at 1500 R the organization was practically disrupted. Both at 24 and 48 hr of incubation, the regulative property of the cells seemed to be practically lost. (TCO)

5307 STATISTICAL STUDIES IN THE ETIOLOGY OF MALIGNANT NEOPLASMS. I. REVIEW AND RESULTS. SUPPLEMENT 174. I. Clemmesen, J. (Finsen Inst., Copenhagen). Acta Pathol. Microbiol. Scand., 1-543(1965).

Extensive data were compiled from the literature relating to the significance of possible etiologic agents in human malignancy. Reports referring to radioinduced malignancies are comprehensively reviewed. By the end of 1957 a total of 88 cases of leukemia had been detected in residents of Hiroshima and Nagasaki who had been exposed under 2000 m of the hypocenter, as against an expected number of about 12. The general incidence of leukemia in the nonirradiated population of Hiroshima and Nagasaki, 20 to 30 cases per million per year, was the same as in all of Japan. The peak incidence seems to have been reached in 1951–1952, six to seven years after the bombing, but the incidence afterwards remained higher than normal. In the late 1950's various attempts were made to determine the risk of neoplasia in exposure to ionizing radiation from therapy and diagnostic tests. It is likely that a decrease in the uncritical use of x irradiation may have taken place before conclusive evidence had been provided. From 1950 to 1958 mortality rates for leukemia in Israel rose from 3.9 to 6.1 per 100,000, and although the rise affected persons of all ages and of all ethnic groups, it was most marked among immigrants from Afro-Asian countries below the age of 15. Therefore, it was ascribed to widely applied x-ray treatment for ringworm of the scalp caused by Trichophyton violaceum. This therapy was initiated with x-ray epilation of the scalp, with a total of 450 R given as divided doses over a period of 2-5 days. In one survey of the possible induction of leukemia by in utero diagnostic irradiation, among the mothers of leukemia, 692 reported at least one diagnostic x-ray exposure, compared with only 593 mothers of controls, which gives a case/control ratio of 1.17. The ratio was, however, higher for abdominal (1.38) than for other types of examination (1.16), and higher for all examinations during the relevant pregnancy (1.48) than during earlier periods (1.22 and 1.07). The ratio for abdominal x-ray examination during the relevant pregnancy was outstandingly high (1.91). These results suggested that abdominal roentgen examination during pregnancy may contribute to the etiology of malignant disease in children. The finding of a leukemia excess for fetal irradiation, although it did not account for the increase in malignant disease in childhood, did underline the need for the use of minimum doses for essential medical x-ray examinations and treatments. Criticisms are advanced against such studies which depend on mothers' memories as a source of data, which are likely to result in an overestimate of relative risk, while the reliance on hospital records as in other studies tend to underestimate the relative risk if records are incomplete. (BBB)

5308 NEW METABOLIC AND HEMATOLOGIC ASPECTS IN PATHOPHYSIOLOGY OF POSTIRRADIATION CHANGES. Dienstbier, Zdenek (Charles Univ., Prague). Acta Univ. Carolinae Med., 11: 3-37(1965).

Data are reviewed from studies of postirradiation changes in blood cells and enzyme systems. Peripheral blood changes are the most sensitive criteria of the damage of the organism after acute irradiation, especially from external sources of radiation. Attempts were made to elucidate the casual relation between the reactions in the peripheral blood cells to metabolic effects caused by irradiation. The hematopoietic system is a useful model for investigation of the dynamics of postirradiation damage. The simultaneous reactions of neuroendocrine systems and their participation in these changes cannot be neglected but it is assumed that the crucial lesion deciding the fate of an irradiated individual is primarily dependent on metabolic disturbances. The relatively early irradiation damage which presumably takes place at the level of the synthesis of the DNA and the disturbance of energy metabolism are also considered. The author has demonstrated an increased excretion of deoxycytidine in urine in irradiated rats and an increased excretion of ^{32}P, and its decreased incorporation especially in radiosensitive organs of irradiated animals. The findings of a decreased incorporation of ^{32}P in the bone marrow was correlated well with the quantitative cellular depletion. A block in hemopoiesis occurs and other mechanisms may also account for the decreased incorporation of radiophosphorus, e.g., as the disturbance of the oxidative phosphorylation. Reticulocytosis, occurring after the internal contamination by radioisotopes, has been described as a secondary finding, while reticulocytopenia is a constant symptom occurring after external irradiation. It reflects functional damage of blood cells after whole-body irradiation, which can be demonstrated in thrombocytes by coagulation tests. (82 references.) (BBB)

5309 ETIOLOGY AND PATHOGENESIS OF MOUSE LEUKEMIA. Miller, J. F. A. P. (Royal Cancer Hospital, London). Advance. Cancer Res., 6: 291-368 (1961).

The role of ionizing radiation and other physical agents, as well as chemical and biological agents in induction of mouse leukemia is reviewed. Many strains of mice develop leukemia in response to ionizing radiations. Thymic lymphomas are the commonest type of leukemia induced, and myeloid or other types of reticular neoplasms are encountered less often. All types of ionizing radiations tested, electromagnetic and corpuscular, have proved to be leukemogenic, and there appears to be no basic qualitative differences in the leukemogenic ability of the different types of radiations. (TCO)

5310 INACTIVATION AND DENATURATION OF PLANT VIRUSES. Price, W. C. (Univ. of Florida, Gainesville). Advance. Virus Res., 10: 171-217(1963).

The effects of α particles, deuterons, and γ radiation as inactivating agents of plant viruses are reviewed. The use of inactivation by radiation as a means of determining the size of tobacco mosaic virus is discussed. The target volume for irradiation agrees with the nucleic acid volume for all but the largest viruses. Evidence so far obtained is convincing that ionizing irradiation of TMV is not lethal unless a hit is obtained in the RNA fraction of the particle and, furthermore, that without a hit the particle is not rendered more susceptible to denaturation by heat. There are, however, other changes that can take place in the particle when ionization occurs in the protein fraction. Whereas irradiation of TMV by deuterons leads to inactivation in a logarithmic fashion, the same is not true for their serological activity. Loss of serological activity occurs at a much slower rate than loss of infectivity and the target cross section is much smaller for the latter than for the former. (TCO)

5311 NEOPLASMS OF THE LIVER FOLLOWING INJECTION OF THOROTRAST. Nettleship, Anderson; Fink, William J. (Veterans Administration Hospital, Fayetteville, Ark.). Amer. J. Clin. Pathol., 35: 422-6 (May 1961).

A patient who was diagnosed as having a malignant

hemangioma of the liver 16 yr after intravenous injection of Thorotrast (ThO_2) is described. Thorotrast (75 ml) was used in radiography of the liver and spleen. The finding of a hemangio-endothelioma in this patient represents the eighth tumor of this type to be reported following thorium dioxide administration. (TCO)

5312 HISTOPATHOLOGY OF THE DEVELOPMENT OF THE AXIAL SKELETON AND SPINAL CORD IN THE IRRADIATED TAIL OF THE YOUNG AXOLOTL (SIREDON MEXICANUM). **Brunst, V. V. (Roswell Park Memorial Inst., Buffalo). Amer. J. Roentgenol., 95: 992-1012 (Dec. 1965).**

The tails of axolotls (Siredon mexicanum) were irradiated locally in five groups of 25 animals each, receiving 500, 1,000, 2,000, 3,000 and 6,000 R, respectively, 1 month after hatching, and in one group of 20 animals, receiving 3,000 R 38 days after hatching; 35 animals served as untreated controls. Axial skeleton development in normal and irradiated animal is discussed histologically. Changes in development following irradiation were much rarer and were ordinarily observed much later in the spinal cord than in the axial skeleton. No distinct zone of stimulation was observed, but irradiation did occasionally stimulate the development of portions of the axial skeleton or spinal cord. An instance of unusual development of neural outgrowths from the distal portion of the spinal cord and another of unusually early development of the cartilaginous trunk were considered examples or x-ray stimulation. (H.G.D.)

5313 THE FATE OF GAMMA-IRRADIATED SCHISTOSOMA MANSONI CERCARIAE IN MICE. **Erickson, Duane G. (Walter Reed Army Inst. of Research, Washington, D. C.). Amer. J. Trop. Med. Hyg., 14: 574-8 (July 1965).**

Experiments on the effects of γ radiation on cercariae of S. mansoni and on their immunogenic ability demonstrated that cercariae exposed to 5000 R or more do not mature and are not recoverable from mice when perfused by normal techniques eight weeks after exposure. The time and site of death and destruction of irradiated schistosomes was determined by location of schistosomes in the mouse host by histological and perfusion techniques. (TCO)

5314 OXYGEN UPTAKE OF THREE LIFE STAGES OF TENEBRIO MOLITOR PRIOR AND SUBSEQUENT TO MASSIVE DOSES OF LOW ENERGY X-RAYS. **Neidinger, J. W.; Baratz, R. A.; Moos, W. S. (Univ. of Illinois, Chicago). Atompraxis, 11: 564-8 (Sept.-Oct. 1965).**

The pre and post irradiation oxygen uptake of Tenebrio Molitor, larva, pupa, and adults was measured. 45 kv x rays at doses of 4.6×10^4 to 1.4×10^5 r and a dose rate of 760 r/sec were employed to irradiate the beetles. Comparison of experimental animals and controls showed a trend to reduced O_2 consumption at lower doses and enhanced O_2 consumption at the higher dose rates. (auth)

5315 THE EFFECT OF ENDOTOXIN UPON SUSCEPTIBILITY TO INFECTION: THE ROLE OF THE GRANULOCYTE. **Mulholland, John H.; Cluff, Leighton E. (Johns Hopkins Univ., Baltimore). Bacterial Endotoxins, Proc. Symp., Inst. of Microbiology, Rutgers, The State Univ., New Brunswick, N. J. 1963., 211-29 (1964).**

Leukopenia induced by endotoxin, nitrogen mustard, benzene, or x irradiation was found to be associated with increased pathogenicity of staphylococci in rabbit skin. Increased pathogenicity was not demonstrated in rabbits treated with benzene and nitrogen mustard which had not developed leukopenia. For induction of leukopenia, nitrogen mustard (Mustargen) was injected into rabbits in 7.5–10 mg doses, rabbits were exposed to 600-R whole-body ^{60}Co irradiation, or benzene (1 ml/kg) in olive oil was injected into rabbits subcutaneously. Inhibition of leukocyte migration into the peritoneal cavity of rabbits with staphylococcal peritonitis was demonstrated by pretreatment with endotoxin or the induction of leukopenia with nitrogen mustard. Endotoxin also inhibited the response to chemical peritonitis. When corrections were made for leukocyte count, blood from endotoxin-treated rabbits had the same phagocytic capacity as did blood from normal rabbits. The increased susceptibility to staphylococcal skin infection could be transferred to normal recipients with whole blood but not plasma from endotoxin-treated donors, and therefore the factor responsible for the transfer must be associated with cells. That endotoxin may be transferred with cells is suggested by failure of transfer to endotoxin-tolerant rabbits. Increased leukocytic sticking, increased migratory activity, and in some instances diapedesis noted in blood vessels in rabbit ear chambers within the 3 to 4 hr period following endotoxin injection seemed inadequate to explain the increased susceptibility to infection. The results indicate that an important effect of endotoxin responsible for transiently increasing susceptibility to infection is granulocytopenia with a consequent reduction in the number of phagocytes migrating into areas of microbial injection. This event is confined to a critical few hours following endotoxin injection. (BBB)

5316 THE SIGNIFICANCE OF EXPERIMENTAL MALFORMATIONS OF THE HEAD REGION FOR EARLY ONTOGENETIC DEVELOPMENT. **Degenhardt, K. H. (Univ., Frankfurt am Main). Ber. Deut. Ophthalmol. Ges., 65: 160-8 (1964). (In German).**

Experimentally produced malformations of the head in amphibians and the results obtained from studies of intrauterine head development in mammals definitely show relations between a rather narrowly limited phase in the second stage of primitive development and the normal or defective differentiation of particular areas of the head region. Whole-body x irradiation of mice with 140 R showed four types of regionally specific effects on the head region of the fetus during the seventh and eighth day of pregnancy. The frequency of chin defects produced ranged from 1.9 to 38%. The frequency of eye malformations ranged from 0.5 to 70%. The relative numbers of resorbed fetuses was used as a measure of effects in a group of mice that received 130 R of whole-body x irradiation. In addition, inspection of remaining fetuses showed defects consisting of aprosopia, cyclops, and several nonviable frontal head defects. Studies of the skeleton revealed failure of lower jaw development, fusion of the jaw in the region of the ear, dysplasia of the upper jaw with distal lower jaw fusion and dental aplasia, and severe cranio-facial dysplasia with absence of the cranial roof. All animals had anophthalmia or microphthalmia. The extensive range and the severity of the head region malformations indicated that the critical time for irradiation injury for mice was during the 7th and 8th day of pregnancy. In humans this critical phase would correspond to the second half of the third week of pregnancy. (BBB)

5317 EFFECT OF D_2O ON THE VITAL STAINING AND HEAT STABILITY OF THE SKELETAL MUSCLES OF THE FROG. **Deshcherevskii, V. I.; Korniyenko, I. A. (Moscow State Univ. Inst. of Biological Physics, Moscow). Biophysics, 9: 338-45 (1964).**

Dissected sartorius muscles of Rana temporaria were kept in Ringer solution for about 1 hr and were then stained at 18 to 19° in 0.02% solution of neutral red diluted in Ringer solution containing 50 or 99% D_2O (test) and ordinary Ringer solution (control). Sorption of the dyes in heavy water was reduced, showing that heavy water does not produce paranecrotic changes in muscle tissue. However, it was suggested that the reduction in dye sorption may be connected with increase in stability of the intracellular structures on replacing H_2O by D_2O. The minimum temperature at which heat contraction of the muscle began was determined in order to measure heat stability of contractile tissues, a good indicator of the stability of intracellular structures. Thermal contraction of the muscles kept in 95% heavy water did not differ appreciably from the controls but occurred at higher temperatures. The time necessary for manifestation of the heavy water effect, measured by the time required to arrest contraction, was 60 ± 9 sec. Reversal of the heavy water effect occurred 90 ± 9 sec after replacing the heavy-water Ringer solution by ordinary solution. (H.G.D.)

5318 ULTRA-VIOLET FLUORESCENCE OF FROG BLOOD CELLS ON COOLING. Brumberg, I. Ye. (Inst. of Biological Physics, Moscow). Biophysics, 9: 411-12 (1964).

Ultraviolet fluorescence of the neutrophils and lymphocytes was determined in the peripheral blood of Rana temporaria at different temperatures. The intensity of uv fluorescence of the segmented nuclear leukocytes fell appreciably when the frog was cooled from room temperature to +4°. However, no regular change with changing body temperature was noted in the intensity of uv fluorescence of lymphocytes and erythrocytes. (H.G.D.)

5319 ADAPTIVE RESPONSES TO IONIZING RADIATION. Garcia, John; Buchwald, Nathaniel A.; Hull, C. D.; Koelling, R. A. (Univ. of California, Los Angeles). Bol. Inst. Estud. Med. Biol. (Mex.), 22: 101-13(Apr. 1964).

Evidence is presented indicating that mammals perceive and respond adaptively to radiation exposures at doses equivalent to those received by people during diagnostic x-ray examination. These studies demonstrate a greater radiosensitivity in organisms than previously supposed and may indicate the existence of specialized radiation receptors or profound acute effects of radiation upon functions of the central nervous system. In the experiments described, rats were conditioned to avoid drinking sweetened water during exposure to 250-kv x rays at a rate of 0.05 R/sec, with a total exposure time of 0.2 sec (10-mR dose). Data collected in an instrumental conditioning situation which required the animal to inhibit bar pressing during exposure demonstrated that, in the threshold range (20 to 200 mR/sec), probability of detection is a function of the log of the dose rate, a relation that is markedly similar to the action of stimuli operating via known receptors. In another series of experiments the effect of partial-body exposures was tested with an instrumental conditioning technique. X rays proved to be an effective perceptual stimulus when directed towards the head but were completely ineffective when the head was shielded and the rest of the body was exposed to the beam. The results indicated that the anterior head region was most sensitive. Exposures of less than one R will produce immediate arousal in sleepy animals and have been used as signals in discrimination tests. The probability of the animal perceiving radiation is a function of the log of the intensity (dose rate). The response habituates rapidly in the absence of reinforcement. This resembles the action of a peripheral receptor. The olfactory system is the locus of maximum sensitivity for the response. Radiation also acts as a noxious stimulus to produce avoidance reactions toward any stimulus associated with exposure. The effect is not immediate and it is a function of the total dose received by the animal. Avoidance effects resemble the action of internal receptors responding to toxic products produced by the radiation. The abdomen is the locus of maximum sensitivity for avoidance reactions. Adaptive responses to radiation fields are discussed within the framework of this dual-receptor model which is proposed. (BBB)

5320 THE LONG TERM EFFECTS OF 2000 R OF X RAYS ON THE BONE MARROW OF THE MOUSE TIBIA. Sams, Alice (Westminster Hospital, London). Brit. J. Radiol., 38: 914-19(Dec. 1965).

The changes in the bone marrow of the tibiae of mice after a dose of 2,000 R of 200 kvp x rays are described. After an initial phase of cell depletion, there was uniformly good recovery until about six to nine weeks after irradiation. After this period recovery was not always maintained and in some mice a second phase of degeneration of the irradiated bone marrow occurred. These degenerative changes were not consistent throughout a given tibia and also showed much individual variation. It is considered that impairment of the associated vascular system as a result of irradiation was responsible for this second phase of degeneration. The extent to which this occurred was probably due to variation in the siting of the original lesions in the irradiated vessels and to the hemodynamics of the vascular system. This would influence the rate at which such lesions underwent further pathological changes, causing in some cases a progressive loss of function leading to atrophy of the bone marrow, while in others only a minimal reduction in flow rate so that the bone marrow maintained its recovery. (auth)

5321 THE CARCINOGENIC EFFECTS OF ^{241}Am AND ^{239}Pu IN THE RAT. Bensted, J. P. M.; Chir, B.; Taylor, D. M.; Sowby, F. D. (Inst. of Cancer Res., Surrey, Eng.). Brit. J. Radiol., 38: 920-5(Dec. 1965).

A comparison was made of the relative radiotoxicities of ^{239}Pu and ^{241}Am in terms of tumor production and, in particular, of bone tumor production. For approximately equivalent microcurie doses of the two nuclides, ^{241}Am is far less effective in producing bone tumors than ^{239}Pu. Fractionation of a single dose of ^{239}Pu did not increase the number of tumors though there was a slight increase in the number of leukemias. The fact that fewer bone tumors appear for equivalent microcurie doses of the two nuclides suggests that maximum permissible levels for ^{241}Am might well be reconsidered. (auth)

5322 THE "MELANOSEBACEOUS FORMATION" OF THE GOLDEN HAMSTER: IV. LONG-TERM REACTION AFTER LOCAL IRRADIATION WITH X RAYS. Oberman, B.; Riviere, M. R. (Institut de Recherches Scientifiques sur la Cancer, Villejuif, France). Bull. Ass. Franc. Etude Cancer, 51: 535-40(Oct.-Dec. 1964). (In French).

One of the two cheek pouches (so-called melanosebaceous formation) of two- to four-month-old male golden hamsters was x irradiated. Four groups of ten animals each were exposed to 600, 1200, 2400, and 4800 R, respectively. After 16 months the animals were sacrificed. Macroscopically, the alterations observed became more pronounced as the radiation dose increased. Sixteen months after receiving 600 R, there was no appreciable difference between the irradiated and nonirradiated tissues. At 1200 R, there was a decrease, by half, of the normal surface of the tissue. At 2400 and 4800 R, the melanosebaceous formation measured only one to two mm, while the controls measured eight to nine. The irradiated zone was totally depigmented. Microscopically, there was no significant difference between the nonirradiated organ and the one exposed to 600 R. After 1200 R, the sebaceous glands were less numerous and atrophied. The epidermis was practically unchanged, but the quantity of melanin had decreased. At 2400 R, the hair follicles and associated sebaceous glands had almost disappeared. The quantity of melanin was reduced. In the dermis the volume of connective tissue increased. The epidermis retained its normal morphology. After 4800 R, the effects resembled those after 2400 R, but were more pronounced. (BBB)

5323 RADIOMIMETIC EFFECTS OF NITROGEN MUSTARD ON THE MULTIPLICATION OF MAMMALIAN CELLS CULTURED IN VITRO. Spanio, Luigi; Levis, Angelo Gino (Univ., Padua). Caryologia, 15: 551-63 (Sept.-Dec. 1962). (In Italian).

The inhibitory effects of nitrogen mustard (NM) were compared with those of x rays on the RCP strain of cells originally obtained from guinea pig liver. The growth curves indicated inhibition of cell multiplication due to NM, which increased with increasing doses. With 0.08 μg/ml and 0.50 μg/ml the increase in cell number was reduced, and the doubling time extended when compared with the controls. With 0.75 μg/ml no significant increase in cell number was noted until the fourth day after treatment; then there seemed to be complete inhibition of cell division. These results were confirmed by a drop in the mitotic index which was observed in cultures treated with the same doses of NM. With the lowest dose, a transitory inhibition of mitotic division occurred; mitotic activity was reduced but not completely suppressed. Recovery followed, characterized by a peak resulting from increasing metaphasic alterations. Among cytological alterations which followed NM treatment, nuclear damage and giant cell formation in particular were studied. The giant cells formed in response to NM resembled those seen after x irradiation of the same strain of cells. As

with x-irradiated cells, cellular metabolism is not immediately blocked by NM, and synthesis of RNA and protein continues. Both NM and x rays appeared to act directly on some process controlling cell division and only secondarily on metabolic processes. (BBB)

5324 THE EARLY DESTRUCTION OF THE GONADS OF THE VIVIPAROUS LIZARD EMBRYO BY IRRADIATION (X RAYS) AND ITS EFFECT ON THE DEVELOPMENT OF GENITAL TUBERCULES. Dufaure, Jean-Pierre (Univ. Paris, Clermont-Ferrand, France). Compt. Rend., 231: 1735-7(Aug. 18, 1965). (In French).

The total, subtotal, or partial destruction of the genital glands of the viviparous lizard embryo by means of localized x irradiation is followed by the formation of male-type genital tubercules, confirming the anhormonal character of the orientation of these rudiments in this sex. (tr-auth)

5325 FIBRINOLYSIS IN WHOLE-BODY IRRADIATION OF RABBITS. Zografov, D. (Inst. for Radiobiological Research, Sofia). Compt. Rend. Acad. Bulg. Sci., 15: 783-5(1962). (In German).

Adult rabbits were irradiated with either 400 or 700 R of 200-kv x irradiation at a dose rate of 40.8 R/min. The animals that received 400 R survived, but those that were irradiated with 700 R died within 8 to 14 days. Fibrinolysis reached its maximum delay during the third and fifth day after irradiation, whereas normally it ends by the first 24 hr. It was accelerated after the fifth day, disappearing after the 20th day. These effects varied with the irradiation dose. Fibrinolysis decreased earlier and to a greater extent when 700 R was given. It amounted to 75 hr by the first day after irradiation. Although it began to decrease again in all of the animal groups at the same time it never reached its original value in the 700-R groups even after 15 days. The fact that irradiation inhibited fibrinolysis suggested that there may have been some inactivation of profibrinolysin or an increase in the antifibrinolysins. It is also indicated injury of the blood cell-forming organs, increasing tissue activators and the thrombocyte count. Thrombocytes have an antifibrinolytic effect, but in the presence of streptokinase a marked fibrinolysis is produced. The period when the thrombocyte count was least coincided with the recovery period of the altered fibrinolysis, while the smallest decrease in thrombocytes took place on the first day when the fibrinolysis time was most delayed. The thrombocyte count was reduced the most in the animal group that received a dose of 700 R, where fibrinolysis also was markedly delayed. The results suggested that fibrinolysis was not closely related to the pathogenesis of the hemorrhagic syndrome resulting from whole-body irradiation. (BBB)

5326 ON THE DEVELOPMENT OF THE SECONDARY PALATE. Ritter, W. (Univ. Muenster, Ger.). Deut. Zahnaerztl., 18: 167-76(1964). (In German).

Pregnant mice were irradiated in a single exposure of 130-R whole-body x irradiation on the seventh day of pregnancy. At this time the fetuses were considered to be most sensitive to induction of cranio-facial dysplasias by the irradiation. Pregnancy was terminated by surgery at term and three of the fetus were studied for evidence of teratogenic injuries. Typical hypoplasia of the lower mandible and tongue were observed histologically. These varied in severity. In two of the fetuses the palate was closed normally but in the third the palatine cleft had failed to close. The observations indicated that in the mouse it is possible to have development of the secondary palate with almost total hypoplasia of the tongue, and it suggested that the role of the tongue was passive as far as it related to the capacity of the palatine process to develop. The tongue did not have any supportive function for the horizontally surrounded palatine process, as previous authors have reported. (BBB)

5327 DENTAL FUSIONS INDUCED IN THE MOUSE BY X IRRADIATION. II. HISTOLOGICAL FINDINGS. Ritter, W. (Univ. Muenster, Ger.). Deut. Zahnaerztl. Z., 18: 1063-8(1963). (In German).

Pregnant mice were x irradiated with a single whole-body dose of 130 R during the seventh to eighth day of pregnancy. The young were removed on the 19th day of pregnancy and examined for histological evidence of cranio-facial dysplasia. Fusions of the gnawing teeth were directly associated with the degree to which the anterior jaw parts were micrognathic. Generally, the cranio-facial dysplasias were represented by two groups of malformations. These were injuries of the upper mandibular-brain region, and malformations that affected the lower jaw and ear region. It is believed that the head region of higher vertebrates includes two different primordial areas. One is the apical prosencephalic region and the other the rhombencephalic region. Developmental derangements may be induced by irradiation injury of these regions. The displacement of the dental anomalies observed from the region of gnawing teeth to the molar regions with increasing evidence of low jaw micrognathy suggested that the epithelial ridge was forced to accommodate itself to the altered conditions of growth of the dental arch. Thus the degree of dental fusion and the mandibular micrognathy observed may have been related to the lack of space available for development. (BBB)

5328 DECREASE IN THE RESISTANCE OF MICE TO BLASTOMOGENETIC EFFECT OF URETHAN AFTER THEIR GENERALIZED TREATMENT WITH SMALL DOSES OF γ-RAYS. Lukash, N. I. Dokl. Akad. Nauk SSSR, 62: 947-9(June 1, 1956). (In Russian).

One group of mice (70 animals) was given a single, whole-body, ^{60}Co dose of 20 R. Another group of 30 mice was given a dose of 2 R each 10 days until a total dose of 20 R had been administered. The third group of mice serving as controls were not irradiated. The irradiations were arranged so that all the irradiations were completed on the same day. Then, 0.1 ml of a 10% urethan solution was given to all the mice. Each mouse received a total of 50 mg of urethan in five injections at 3 day intervals. Seven months after the last injection the mice were killed, and the lungs were fixed in a 10% formalin solution. The adenomas were counted under a microscope, cut out, and weighed. The average number of adenomas was 7.5 ± 0.8 for the mice given a single dose of 20 R, 4.3 ± 0.5 for the mice given a fractionated dose of 20 R, and 5.2 ± 0.26 for the unirradiated controls. The average weights of the adenoma were 0.86 mg for the mice given a single dose of 20 R and 0.75 mg for the other two groups of mice. It is concluded that a single dose of 20 R decreases the ability of the organism to resist the formation of adenoma induced by urethan. (TTT)

5329 EFFECT OF WHOLE BRAIN ^{60}Co GAMMA IRRADIATION ON CORTICAL AROUSAL IN THE BURRO. Naitoh, P. (Univ. of California, Los Angeles); Spurrell, F. A.; Heistad, G. T. Electroencephalogr. Clin. Neurophysiol., 19: 172-81(Aug. 1965).

Acute effects of single, whole-brain γ irradiation on cortical arousal was studied in the burro. The burros were conditioned, and the conditioned stimulus (CS) was used as the means of producing cortical arousal. A defensive motor conditioned response, heart rate, respiration rate, rectal temperature, leukocytic patterns, and behavioral manifestations of CNS disorders were examined before and after irradiation in an attempt to determine whether the changes in cortical arousal were due to direct CNS damage, or to radiation sickness without CNS disorders. Cortical arousal to the CS was examined in male adult burros up to 7 days following 200, 400, and 600 R. A 200 R dose of radiation did not affect either the resting patterns of electrocorticograms or the CS-induced cortical arousal. Degradation and rapid loss of the CS-induced cortical arousal were observed only if the subjects were irradiated with 400 or 600 R. Since the 600 R exposed subjects suffered from significant physiological changes and died early of radiogenic neuropathic death, a facilitated extinction of the cortical arousal observed in this group might merely reflect effects of radiation sickness. Collateral data indicated that facilitation of extinction of the CS-induced cortical arousal would not be caused by radio-

genic changes in the unconditioned stimulus (US) efficacy and in attention, but by difficulties in getting emotion activation in response to learned cues. The subjects experienced significant changes in their autonomic, leukocytic, and neurological functions following 600 R: fever (up to 103°F), lasting tachycardia (up to 110 beats/min), neutrophilic leukocytosis, profound eosinopenia, lymphopenia, and difficulties in equilibrium and locomotion. The mortality for this group was 86%. Whole-brain irradiation with 400 R did not produce significant systemic changes. (BBB)

5330 LIFE SPAN AND SOLUBLE/INSOLUBLE COLLAGEN (HYDROXYPROLINE) RATIOS IN NORMAL AND IRRADIATED HAMSTERS. Walford, Roy L.; Sjaarda, John R.; Anderson, Robert E. (Univ. of California, Los Angeles). Exp. Gerontol., 1: 117-25(July 1965).

Results are reported from experiments performed to determine whether the life span of the Syrian hamster (Benzanson strain) is alterable by x irradiation in a fashion analogous to that with rats and mice, including changes in age-specific incidence of disease, and to ascertain whether there are age-correlated changes in soluble/insoluble collagen ratios in the skin of normal and irradiated hamsters. Measurements of collagen were used as a biochemical estimate of physiologic age. Whole-body x irradiation (250 kv, 60 R/min) was given in a single dose of 425 R at the age of three months. This corresponded to the LD_{20} for this species. Collagen studies were conducted in survivors at 29.5 months of age by determinations of the ratios of soluble to insoluble collagen (as hydroxyproline) in skin of normal and irradiated groups. Comparison of control and irradiated animals of the same chronologic age revealed no statistically significant difference in this small series of animals studies. Insofar as collagen changes reflect physiologic aging, these experiments do not support the concept that reduced life span following x irradiation is due to acceleration of the normal process of aging. (BBB)

5331 X-IRRADIATION OF PUPAE OF THE HOUSE FLY MUSCA DOMESTICA L. AND ADULT SURVIVAL. Bhatnagar, Prem Lata; Rockstein, M.; Dauer, M. (Univ. of Miami School of Medicine, Coral Gables, Fla.). Exp. Gerontol., 1: 149-59(July 1965).

Longevity data were obtained to determine the nature of the structural and functional derangements induced in the normally aging house fly adults, following x irradiation of the pupae. At 36 to 48 hr following pupation, the pupae were exposed to x rays in single doses at the rate of 2000 rad per min, at 250 kvp. It was found that the ratio of male to female is almost 1:1 in the control flies, whereas the ratio shifts in favor of the males as radiation dosage is increased (the ratio was 1.35:1 after 20,000 rad). The adults which emerged from the x-irradiated pupae did not show any structural abnormalities and appeared to be otherwise normal. Abrasion of wings, a normal aging concomitant in male house flies especially, was observed only in the flies emerging from the pupae previously exposed to doses of 20,000 rad or lower. At 30,000 rad, no wing loss was observed. Moreover, all flies emerging from previously irradiated pupae failed to lay any eggs. The median life span of the males emerged from the pupae exposed to 10,000 rad was 15 days and that of the females was 18 days. Thus, in comparison to the control, the life span of the male increases by 3 days and that of the female shortens by 3 days, so that the negative skewedness of the female survival curve is equal to the positive skewedness of the male survival curve. Comparison of the mean survival periods of each revealed that the differences were highly significant. However, x irradiation of 10,000 rad did not alter the value of the total life span of the flies significantly. (BBB)

5332 RENAL CARCINOMA AS A THOROTRAST INJURY. Krueckemeyer, K.; Lessmann, H. D.; Pudwitz, K. R. (Staedtische Krankenhaus, Berlin). Fortschr. Geb. Roentgenstr. Nuklearmed., 93(3): 313-21(Sept. 1960). (In German).

A 45-yr-old female patient who had been subjected to a retrograde pyelogram with Thorotrast 23 yr previously developed a carcinoma in the region of the left renal pelvis. Concentrations of Thorotrast were detected by scintigraphic measurements. The carcinoma had infiltrated the renal pelvis extensively, producing a secondary hydronephrosis, and had grown into the perirenal fatty and connective tissue. On removal of the diseased kidney the Thorotrast particles were found to be deposited directly in or under the epithelia of the renal tissue. Some of the Thorotrast deposits were so concentrated that they produced the appearance of stones when viewed with x ray. Histologically the deposition could be considered to be massive, particularly in the portions of the tissue that had become hyalinized. There was a definite positive relation between the spatial location of the Thorotrast deposits and the appearance of tumor tissue. In contrast to many animal experiments and a few reports from human cases where the connective tissue portions of the kidney have been reported to develop malignant growths when exposed to Thorotrast for extended periods of time, in the case reported here the epithelial structure was the region affected. The case reported here again emphasizes the danger of using Thorotrast or other radioactive substances that remain deposited in tissue for long periods of time as contrast media or diagnostic materials. (BBB)

5333 EXPERIMENTAL CONTRIBUTION TO THE EFFECT OF X IRRADIATION ON METABOLIC ACTIVITY OF THE LENS AS RELATED TO AGE. Hockwin, Otto (Univ., Bonn). Fortschr. Med., 80: 659-66(1962). (In German).

The lens exhibits a pronounced age-dependent reaction to irradiation. Guinea pig and calf lens were exposed in vitro to 100 kR of x irradiation. In young lenses, aerobic glycolytic metabolism was markedly reduced by irradiation. In older lenses, where the metabolism rate is similar to that of resting tissue, glycolysis was also reduced after irradiation, but this effect seemed to be compensated for by other metabolic processes in the lens. This was illustrated in reference to studies of frog muscle metabolism. The O utilization and amount of energy-rich phosphate in irradiated muscle was directly related to the changes in membrane potentials and K concentration gradients observed. These were similar to those observed after muscular activity. In the lenses exposed to 100 kR of x irradiation, concentration changes of several metabolites were studied. Hexosemonophosphate (HMP) concentration was increased as a result of impaired breakdown. Triose phosphates incorporated less ^{32}P than normal, probably as a result of the impaired HMP metabolism. In addition, their concentrations were increased above normal. Concentrations of adenosine triphosphate were unchanged after irradiation, but its turnover rate was slightly reduced after irradiation. The concentration of adenosine diphosphate was slightly reduced, but its turnover rate was increased. The concentration of creatine phosphate was reduced after irradiation, but its ^{32}P sp act. was increased. The inorganic P concentration was transiently reduced after irradiation. These changes suggested that glycolytic activity was decreased after irradiation. (BBB)

5334 EXPERIMENTAL OSTEOGENIC SARCOMA: HISTOGENESIS OF OSTEOGENIC SARCOMA. Horie, Kenya; Makita, Motoo; Sato, Kazuto (Tachikawa Hospital, Japan). Gann, 51: 399-407(Dec. 1960).

Using ^{32}P, alone or in combination with methylcholanthrene (Mc), benzpyrene (Bp) or croton oil (Cr), it was possible to produce osteogenic sarcomas in Wistar rats. Differences in carcinogenic action of these substances were studied and a hypothesis regarding the histogenesis of osteogenic sarcoma thus produced, based on histological studies, is presented. The ^{32}P was given intraperitoneally in doses of 1 mC/kg of body weight once monthly. Mc was administered into the bone marrow in single doses of 15 mg. Equal amounts of Bp and 0.25-ml doses of Cr were given similarly. In the combined groups, after ^{32}P was given 3 times at monthly intervals, Mc, Bp, and Cr were given once, after which ^{32}P was continued monthly until sarcomas developed. In the singly

treated groups, ^{32}P was given monthly, while Mc, Bp, and Cr were given just once at the start of the experiment. Thirty out of 74 rats developed sarcomas. In general, the carcinogenesis rate was higher in the combined group than in the singly administered groups. The ^{32}P + Mc and ^{32}P + Bp groups showed high rates, 8 out of 14 rats in ^{32}P + Mc group developing sarcomas. The average time required for the appearance of tumor in the ^{32}P + Mc group was 9 months, the average of the other groups being 10 months. In the combined treatment groups pulmonary metastases were observed in 7 out of 22 rats. Among the singly treated groups, only one case of pulmonary metastasis in the ^{32}P group was seen. Tumors developed in most cases in the combined groups at the site of the injection of Mc, Bp, and Cr into the bone. The shortest time between the appearance of the tumor as seen grossly or radiographically and the death of the animal was 15 days, the longest 53 days, and the average 24 days. The average total dose of ^{32}P used in the animals which developed sarcoma was 2.1 mC in the combined groups. Cr, said to have promoting action in carcinogenesis, when used in combination with ^{32}P, did not enhance the carcinogenic action of ^{32}P. In 18 out of 30 instances the tumors produced were osteogenic sarcomas and 7 were fibrosarcomas. Chondrosarcoma was not seen. In studying histologically the process of development of immature osteogenic sarcoma cells into mature sarcoma cells, it was noted that the immature cells were frequently arranged in lobules or funiculi. The closely packed immature cells gradually hypertrophied and became more basophilic and atypical, and at the same time the intercellular spaces increased and hyaline substance formed. This was finally transformed to osteoid tissue and then bone. With completion of ossification, the cells atrophied and some became embedded in the bone matrix. (BBB)

5335 INFLUENCE OF X RAYS ON THE TAKE OF SKIN HOMOGRAFTS. Bruzzese, E.; Favuzzi, E.; Patriarca, G.; Greco, G. (Centro Studi e Ricerche della Sanita Militare, Rome). Giorn. Med. Mil., 114: 41-50(Jan.-Feb. 1964). (In Italian).

The effect of x irradiation of both donor and recipient on skin homografting was studied in Wistar rats. Donor rats received a lethal dose of 700 R immediately before, or 5 or 10 days before skin was removed for grafting. Recipient rats of the same strain received a sublethal dose of 500 R on days 0, 5, or 15 before grafting. In control (nonirradiated) rats the nonirradiated skin graft became necrotic after an average of 4.5 days and the graft sloughed after 10.7 days. The average values for the grafts obtained from 700-R irradiated donors were 6.7 and 13.8 days for grafts taken immediately after irradiation, 5.8 and 13.3 days for grafts removed at 5 days, and 7.3 and 15.1 days for grafts taken 15 days post-irradiation. The corresponding values for 500-R irradiated recipients were: 7.1, 17.6; 5.2, 20.2; and 6.1, 14.5 days. Thus, for irradiated donors, the 15-day post-irradiation period was most effective for prolonging homograft survival. However, the earlier periods (0 and 5 days) were more effective in terms of recipient irradiation, which is in accord with the known period of inhibition of the immune response by ionizing irradiation. The results show that duration of survival of the grafts can be doubled by 500 R x irradiation of recipient rats 5 days before grafting. (BBB)

5336 RADIOSENSITIVITY, CIRCADIAN RHYTHMICITY, AND RADIOBIOLOGY. Spalding, J. F.; McWilliams, Paul (Los Alamos Scientific Lab., N. Mex.). Health Phys., 11: 647-51(1965). (LA-DC-6404(Rev.)).

Two methods were used to study the influence of circadian rhythmicity on x radiosensitivity in mice as a factor in acute radiation effects studies. The results suggested the presence of diurnal differences in radiosensitivity; however, these slight differences were neither consistent nor significant. It was concluded that circadian rhythmicity is not a primary factor in studying whole-body effects from acute radiation exposure. (auth)

5337 CLEFTS OF THE LIPS, JAWS AND PALATE INDUCED IN MICE BY MEANS OF X-RAYS. Ritter, W. (Univ. Munster, Ger.); Degenhardt, K. H. Int. Dent. J., 13: 489-94(Sept. 1963).

Pregnant female mice were subjected to a single dose of 130 R x rays. The irradiation began with embryos six days and eight hr old, and continued in a systematic series, at intervals of 12 hr, to embryo ten days and 20 hr old. The newborn mice were killed post partum, inspected externally, and subjected to a post mortem examination. In the controls, no clefts of the upper jaw were found. Of the irradiated series, detailed results are described of 74 cleft formations of the upper jaw in the 1095 animals examined. (TCO)

5338 THE EFFECT OF POST-TREATMENT WITH N_2 OR O_2 ON THE FREQUENCIES OF RECESSIVE LETHALS AND TRANSLOCATIONS PRODUCED BY IRRADIATION IN N_2 OR O_2. Sobels, F. H. (Univ. of Leyden, Netherlands). Int. J. Radiat. Biol., 6: 492(May 1963).

The effect of post-treatment with N_2 and O_2 on the repair of premutational damage and the realization of chromosome breaks, induced by x irradiation in either N_2 or O_2, was studied. Male flies (Drosophila) carrying a ring-shaped X-chromosome ($X^{C^2}yB/sc^8Y$), were pretreated for 25 min in either N_2 or O_2 and exposed to x rays in the gases (3000 R in N_2 and 1000 R in O_2). Subsequently they were post-treated with either N_2 or O_2 for 25 min. The males were mated to females for five successive two-day broods so that the induction of sex-linked recessive lethal mutations and translocations between the second and third chromosomes could be followed simultaneously through the successive stages of spermatogenesis with different sensitivities to the mutagenic action of x rays. The results showed that with 3000 R given under anoxic conditions, post-treatment with O_2 significantly reduces the mutation frequency in spermatids, in comparison with that found after post-treatment with N_2. It is assumed that post-treatment with O_2 activates a repair system, which had been effectively inhibited by anoxia preceding and during radiation exposure. A similar result was obtained if, after radiation in N_2, the flies were held anoxic for 25 min and then transferred to O_2. Fixation of premutational damage in N_2 thus does not occur within 25 min after irradiation. After exposure to 1000 R in O_2, however, the effect of post-treatment with O_2 equalled that with N_2. The same mutation frequencies were then observed as after exposure to 3000 R in N_2, followed by post-treatment with N_2. In contrast to these data for induced mutations, post-treatment with O_2 did not affect the frequency of translocations induced by radiation in N_2, but modified the translocation frequency after irradiation in O_2. Thus the process responsible for repair of premutational damage differs from that involved in the restitution of chromosome breaks or in the conversion of potential breaks to real breaks. (BBB)

5339 ANTIOXIDANTS AND LIPOPEROXIDES IN THE ORGANS OF IRRADIATED RATS. Glavind, Johs. (Polytechnic Inst., Copenhagen); Hansen, Lis; Faber, Mogens. Int. J. Radiat. Biol., 9: 409-20(1965).

Antioxidants in organs of normal and irradiated rats were determined by means of the stable free-radical α,α-diphenyl-β-picrylhydrazyl. High doses of γ radiation reduced the level of water-soluble antioxidants; the fat-soluble antioxidants were unaffected, and the ability of the proteins to react with the stable free radical was unchanged or slightly elevated. It is concluded that the water-soluble non-protein antioxidants act as free radical scavengers in radiation. No great amounts of lipoperoxides were found in the irradiated animals. The basic analogy, but at the same time the great dissimilarities, between free radical processes in radiation and in autoxidation is discussed. (auth)

5340 THE EFFECTS OF X-RADIATION AND NICOTINAMIDE ON THE RESPIRATION OF RAT THYMOCYTES. Whitfield, J. F.; Brohee, H.; Youdale, T. (EURATOM, C. C. R., Ispra, Italy). Int. J. Radiat. Biol., 9: 421-7 (1965).

The respiration rate of thymocyte suspension cultures x irradiated with 1.5 kR remains normal until the process of nuclear structural homogenization is well under way. Reduction of respiration rate by cyanide, nicotinamide, and a very high dose of x radiation (30 kR) is associated with a strong retardation of nuclear changes. It is proposed that the inhibition of respiration is, in fact, responsible for the inhibition of nuclear structural changes by these agents. A possible mechanism for this effect of respiratory inhibition is discussed. (auth)

5341 BIOCHEMICAL AND MORPHOLOGICAL CHANGES IN LYMPHATIC TISSUES AFTER PARTIAL-BODY IRRADIATION. van Bekkum, D. W.; de Vries, M. J.; Klouwen, H. M. (TNO, Rijswijk, Netherlands). Int. J. Radiat. Biol., 9: 449-59(1965).

The oxidative phosphorylation of nuclei isolated from the thymus and of mitochondria isolated from the spleen and the morphological changes in these organs were studied after partial and whole-body x irradiation of rats. Early inhibition of oxidative phosphorylation and cellular destruction was observed only after whole-body irradiation with or without shielding of the head. Irradiation of the head alone had no such effects. The results seem to exclude the possibility that abscopal factors may be involved in the production of radiation-induced changes of oxidative phosphorylation in the spleen and thymus. (auth)

5342 EFFECTS OF X RADIATION AND DIFFERENT SUBSTANCES ON THE PERMEABILITY CHARACTERISTICS OF RED CELLS. Koever, G.; Schoffeniels, E. (Univ., Liege). Int. J. Radiat. Biol., 9: 461-76(1965). (In French).

The effects of cysteamine and NaCN applied alone or together with x radiation, on the permeability characteristics of erythrocytes of man, dogs, chickens, and pigeons were studied. Results indicate that the shift in intracellular cationic balance induced by x radiation is related to the inhibition of the K−Na−activated ATPase. Cysteamine had a slight protective effect against radioinduced hemolysis of the erythrocytes but CN ions had no protective effect. (C.H.)

5343 CHROMOSOME ABERRATIONS AND THE THEORY OF RBE. 1. GENERAL CONSIDERATIONS. Neary, G. J. (Medical Research Council Radiobiological Research Unit, Harwell, England). Int. J. Radiat. Biol., 9: 477-502(1965).

It is suggested that primary radiation damage to a macromolecule in a cell which may lead to observable biological effect is normally the direct effect of a single energy-loss event in the macromolecule. This concept is applied to the production of (radioinduced) chromosome aberrations, regarding a local region of a chromosome as a molecule of DNA, and assuming that an aberration results from an exchange between two damaged regions. The model is consistent with the observed dependence of aberration yield on dose, LET and modifying agents. Over a considerable range of LET, effectiveness per unit dose is proportional to dose-average LET. Similar basic concepts appear to be applicable to cell killing. (auth)

5344 TRANSPLANTATION SITE PRERADIATION AND REJECTION PATTERNS. Banks, D. E.; Auburn, R. P.; Persky, Lester; Hubay, Charles (Western Reserve Univ., Cleveland). Invest. Urol., 2: 338-41(Jan. 1965).

Attention was focused on destroying the regional lymphatics and lymph nodes, thus blocking the local transfer of antigen through these channels and production of cellular antibodies in the regional nodes in twenty dogs receiving homologous renal transplants from separate unrelated donor animals. Ten of these first received 1000 R of x radiation to the graft site one to two days prior to operation, and 10 were used as control animals. The average survival time of the experimental transplants was 11.1 days and that of the control group was 9.3 days; this difference was not statistically significant. Grossly and microscopically, the kidneys of both groups were similar. The data did not show a significant change in the rejection picture after the destruction of the regional lymphatic system. The radiation-induced fibrosis and inflammation surrounding the areas of regional nodes and the lack of regional lymph node tissue indicated their functional inactivation. The importance of hematogenous spread of antigen, and activation of distant components of the diffuse reticuloendothelial system, is suggested. It seems likely that the regional lymphatics play a minor role in the rejection of a homologous organ supplied by a vascular pedicle. (TCO)

5345 EFFECTS OF ULTRAVIOLET MICROBEAM IRRADIATION ON MORPHOGENESIS IN EUPLOTES. Wise, Benjamin N. (Yale Univ., New Haven). J. Exp. Zool., 159: 241-68(July 1965).

Alteration of developmental mechanisms in Euplotes plumipes in response to damage produced by a uv microbeam was examined. Animals, representing all stages of the morphogenetic cycle, were irradiated at a variety of cortical sites, including bases of mature cirri and membranelles, primordial structures, and nonciliated regions; they were then observed and fixed for silver staining. Immediate uv damage was restricted to cortical and ciliary structures directly irradiated. Irradiated cirri and membranelles, including their associated basal structures (infraciliature), were effectively destroyed after about two-minute exposure to the uv microbeam. No regeneration response ensued following uv-induced damage in these animals. Damage to cirri persisted until these organelles were replaced during normal predivision morphogenesis; damage to adoral membranelles, which are not normally replaced at division, persisted indefinitely through succeeding generations of proters. It is conclused that destruction of infraciliary structures does not, in itself, provide a sufficient stimulus to regeneration in Euplotes. Ultraviolet irradiation of either mature or primordial cortical organelles was effective, however, in causing the temporary arrest of normal predivision morphogenesis, including resorption of all primordial structures, and arrest or disappearance of macronuclear replication bands. Results are discussed in terms of the functional relation between infraciliary structures and the mechanisms controlling development. (TCO)

5346 PHYSIOLOGICAL CHANGES INDUCED BY GAMMA IRRADIATION OF BACTERIA FROM SHRIMP. Liuzzo, Joseph A.; Novak, Arthur F.; Ortego, Jesse R. (Louisiana State Univ., Baton Rouge). J.Food Sci., 30: 710-13(July-Aug. 1965).

A study was undertaken to isolate and identify bacteria from Gulf shrimp that are resistant to radiopasteurization doses, and to ascertain if physiological changes are induced in the bacteria by γ irradiation. Seven radioresistant bacteria were isolated and identified from fresh Gulf shrimp. These bacteria were classed as follows: Brevibacterium minutiferula, Gaffkya homari, Sarcina flava, Bacillus megaterium, Achromobacter eurydice, Bacillus firmus, and Bacillus pumilus. Irradiation of the cultures affected the optimum incubation temperature of three organisms, the temperature required for best growth being lowered 12 to 15°C. Since shellfish are usually preserved under refrigeration, the ability of the organisms to grow more rapidly at lower temperatures could become a problem in extension of the storage life of irradiated shrimp. Changes in chromogenesis, due to alterations in metabolism as a result of radiation, were seen in two species. The only changes in carbohydrate utilization resulting from radiation were experienced by B. firmus and B. pumilus; in each case the irradiated culture failed to ferment glucose as the unirradiated counterpart. Three bacteria were affected in the utilization of B vitamins by irradiation: B. minutiferula lost its ability to utilize niacin and pantothenic acid by irradiation; Gaffkya homari did not use thiamine after treatment; and B. megaterium's use of the vitamin was enhanced by low-dose radiation. Results that the metabolic roles of NAD, coenzyme A, and thiamine pyrophosphate have been changed for the respective bacteria. Irradiation did not alter the organisms' metabolism of nitrate, hydrolysis of gelatin, motility, or production of hydrogen sulfide. Hence, it is suggested that the pattern of

metabolism in radioresistant bacteria can be altered by low-dose radiation, presumably by mutation. (BBB)

5347 EVIDENCE THAT INITIAL ULTRAVIOLET LETHAL DAMAGE IN ESCHERCHIA COLI STRAIN 15 IS INDEPENDENT OF GROWTH PHASE. Ginsberg, D. M. (Walter Reed Army Inst. of Research, Washington, D. C.); Jagger, J. J. Gen. Microbiol., 40: 171-84(Aug. 1965).

Results are reported from a study of the kinetics of killing by uv radiation (2537 Å) and subsequent photoreactivation (with black light) of Escherichia coli strain $15_{T^-A^-U^-}$ (requires thymine, arginine, uracil) by using logarithmic-phase, early-stationary-phase, or logarithmic-phase cultures after 90-min incubation in the absence of arginine and uracil (–AU cultures). The stationary and –AU cultures showed the same enhanced resistance to uv killing. In all three cultures the photoreactivable sectors were the same, the rate of photoreactivation was the same function of uv dose, and the amount of light required for max photoreactivation was a linear function of the uv dose. It is concluded that the initial lethal lesions produced by a given uv dose were qualitatively and quantitatively the same in all three cultures, despite differences in uv survival. This implies that the stationary-phase cultures and the –AU cultures were more radiation resistant solely because they were better able to cope with the initial lethal damage. The survival curves can be satisfactorily described mathematically in terms of this model. (TCO)

5348 RADIATION SENSITIVITY AND GROWTH CHARACTERISTICS OF AN ARGININE- AND URACIL-STARVED CULTURE OF ESCHERICHIA COLI STRAIN 15. Ginsberg, D. M. (Walter Reed Army Inst. of Research, Washington, D. C.); Jagger, J. J. Gen. Microbiol., 40: 185-90(Aug. 1965).

It was shown earlier that both the uv survival and photoreactivation curves were the same for –AU and early stationary cultures of Escherichia coli strain $15_{T^-A^-U^-}$. Further confirmation of their photobiological similarity was obtained. Bacteria from each of the two cultures were inoculated into fresh growth media (+T +AU) and grown at 37° for 30 min to mid-lag phase. The uv sensitivity of the lag-phase culture was the same whether grown from –AU or from early stationary-phase bacteria and the photoreactivable sectors were the same. The photoreactivable sectors in these experiments had the same values as for logarithmic-phase, –AU and early stationary-phase cultures. This shows that the photoreactivable sector and, consequently, the spectrum of uv damage produced, did not change during transition from the uv-resistant (stationary-phase or –AU) to the uv-sensitive (logarithmic-phase) state. It also appeared that the lag-phase survival curves had the same final slopes as the curves for logarithmic-phase, –AU, and stationary-phase cultures, suggesting that the nature of the initial lesions did not change during lag-phase transition, at least for the higher doses. To study the effects of ionizing radiation, bacterial suspensions in phosphate buffer were exposed to ^{60}Co γ rays, and survivors were assayed by colony formation. The survival curve was the same for γ-ray inactivation of either early stationary-phase or –AU cultures. The dose-reduction factor for early stationary-phase and –AU cultures compared to the logarithmic culture was constant (about 0.50) in the survival range studied. The constant dose-reduction factor over the survival range tested suggests that a situation analogous to that for uv killing could exist, namely, that the initial damage by a given γ-ray exposure is independent of growth phase or metabolic state, and, therefore, the difference in survival is the result of differences in ability to cope with the damage. This is consistent with the earlier experimental findings which showed that a given x-ray dose produces the same initial damage in mammalian cells in logarithmic and in stationary-phase, even though the stationary-phase cells show a higher survival. (BBB)

5349 REORIENTATION OF CHROMOSOME REPLICATION AFTER EXPOSURE TO ULTRAVIOLET LIGHT OF ESCHERICHIA COLI. Hewitt, R.; Billen, D. (Univ. of Texas, Houston). J. Mol. Biol., 13: 40-53(Aug. 1965).

Radioisotopic and density labeling methods were used to examine the location of the site at which chromosome replication is resumed after the restoration of net DNA-synthesizing activity in uv-irradiated cells. Results showed that postirradiation chromosome replication commences from a site other than the site that was active prior to exposure. The extent of postirradiation replication of the total DNA or of a chromosome region which was pulse-labeled immediately prior to exposure is limited to about 50%. The earlier observation of a requirement for protein synthesis in the restoration of DNA-synthesizing activity was extended to show that inhibition of protein synthesis prevents the appearance of the new replication site. It is concluded that chromosome regions at, or nearest, the origin have the highest probability of being replicated following the restoration of DNA-synthetic capacity. (TCO)

5350 EVIDENCE FOR A MUTAGENIC LOCAL EFFECT ACCOMPANYING THE DECAY OF INCORPORATED TRITIUM IN ESCHERICHIA COLI. Person, S.; Bockrath, R. C. Jr. (Pennsylvania State Univ., University Park). J. Mol. Biol., 13: 600-2(Sept. 1965).

The decay of incorporated tritium compounds produces loss of colony-forming capacity in bacteria. The loss of colony-forming capacity seems explicable mainly on the basis of radiation dose to the nuclear region of the bacterium. Thus the existence of a local effect, e.g., a molecular rearrangement at the site of decay, has never been substantiated. The mutagenic efficiencies of the precursors for RNA (^{3}H-uridine, ^{3}H-uracil), DNA (^{3}H-thymidine), or protein (^{3}H-labeled amino acids) have relative values of 6.6, 2.4 and 1.0, respectively. A theoretical study of the distribution of radiation dose within a bacterium as a function of various simulated positions within a bacterium for the incorporated tritium showed no regions receiving differential doses which vary by a factor nearly as great as 6.6, except the central core of the nuclear region should give a radiation dose to the center of this region ten times that from tritium restricted to an extreme peripheral region of the cell. Since it is unlikely that incorporated ^{3}H-uracil or ^{3}H-uridine occupies predominantly the nuclear region, generalized differential irradiation seems an unlikely explanation for the pronounced effect of the RNA precursor. The ^{3}H-uracil and ^{3}H-uridine carry the tritium isotope primarily in the 5-position of the pyrimidine ring, but 6-^{3}H-uridine has recently become available so it was used to study mutagenesis resulting from decay, in the manner previously reported for 5-^{3}H-uracil and -^{3}H-uridine. Results showed a large difference in the mutative power of the 5- and the 6-position uracil compounds. On a per decay basis, cultures labeled with 6-^{3}H-uridine were reverted no more efficiently than if labeled by a protein precursor. Studies of the distribution of incorporated 5-^{3}H-uracil, 6-^{3}H-uridine, and ^{3}H-thymidine, as determined by separation of bacterial nucleic acids, showed no appreciable difference between the metabolic distribution of 5-position labeled pyrimidine and that of the 6-position labeled pyrimidine. These results indicate a local alteration at the site of the tritium transmutation when the tritium nuclide occupies the 5-position. When the 6-position is labeled, this local alteration becomes much less likely. (BBB)

5351 PERSISTING CLONE OF CELLS WITH AN ABNORMAL CHROMOSOME IN A WOMAN PREVIOUSLY IRRADIATED. Dekaban, Anatole (National Inst. of Health, Bethesda, Md.). J. Nucl. Med., 6: 740-6(Oct. 1965).

Chromosome studies performed on the mother who gave birth to a dystrophic and malformed child showed two types of abnormality. The first abnormality consisted of a clone of cells characterized by frequent breaks in the same general region of long arms in the presumed chromosome No. 9. Since this was observed in the repeated blood cultures but not in the skin culture, the clone is probably confined to the blood forming tissue. The second abnormality consisted of a moderately increased rate of chromosome-

type aberrations occurring at random in all chromosomes. The woman received 1550 rads x radiation to the skin for treatment of eczematous dermatitis during the preceding 16 years, resulting in an estimated dose of 242 rads to portions of the bone marrow and lymph nodes. The type of random chromosome abnormality observed in her blood cultures was reported previously to be associated with exposure to radiation. The aberrant cell clone may also have been induced by the same etiological factor. (auth)

5352 A STUDY OF THE ACTION OF X RAYS ON CELLULAR METABOLISM, USING THE WARBURG TECHNIQUE. Tanniou, J. (Faculte de Medecine, Paris). J. Radiol. Electrol. Med. Nucl., 45: 23-30(Mar.-Apr. 1964). (In French).

Tissue sections of the renal cortices of adult male white rats were exposed, in vitro, to x-ray doses of 100, 600, and 1500 R at 30 R/min. Oxygen consumption was measured, using the Warburg method. In the two series of ten sections each exposed to 100 R, there was average respiratory inhibition of 18 to 20%. The inhibition decreased rapidly, falling from 21 to 15% and 26 to 15% over the two-hr observation period. After 600 R the respiration values of ten tissue sections averaged 96.9% of normal rates. It did not seem that this dose had any significant effect on cellular respiration. In ten sections which received 1500 R, average respiratory inhibition was 14%. However, the values obtained each hr varied greatly. In a series of eight sections of kidneys exposed to 1500 R, the average respiratory inhibition was 16%. Here again there was a great variability in values from hr to hr (e.g. 65 to 119%). By measuring respiration every half-hr, it was determined that the average inhibition was the sum of phases of inhibition and stimulation through which the cells passed. (BBB)

5353 SEQUELAE OF THOROTRAST. Lancet, 1: 771-2(Oct. 2, 1965).

Late effects of Thorotrast are discussed. A report concerning 2377 patients in Portugal in whom Thorotrast was used between 1930 and 1952 is reviewed. Causes of death included liver tumors, liver fibrosis, leukemia, asplastic anemia, and granulomas at the site of injection. Latent periods between Thorotrast administration and development of each of these conditions are identified. It is suggested that Thorotrast should not be given to patients with a life expectancy of more than two years. (H.G.D.)

5354 THE EFFECT OF IONIZING RADIATION ON THE IRON METABOLISM OF THE BODY. Adam, Geza; Miltenyi, Laszlo; Mucsi, Otto (Orvostudomanyi Egyetem, Debrecen, Hung.). Magy. Radiol., 17: 234-6(Aug. 1965). (In Hungarian).

Attempts were made to determine the ability of the body to retain iron after ionizing irradiation, if that iron is introduced as ferritin rather than an electrolyte. Tests were also conducted simultaneously to determine the rate of elimination of iron when ferritin is given. The tests were conducted on rats which received 2 mC $^{59}FeCl_3$ parenterally, and after four days the ferritin was isolated from their liver and spleen by the Keiderling method. Another group of rats received a single whole-body dose of 250 rad, and 4 hr later each was injected with 1 μC of prepared ferritin. The control group received no irradiation, but the same amount of ferritin. Results were analyzed after 1, 3, 4, and 10 days. Data indicate that the ferritin activity in the liver rose steadily for four days and then leveled off and remained stable for the next six days in the control group; the irradiated group reached max height after 3 days at the same level as the control, and then declined, reaching lower than the original level after 10 days. Data for spleen indicate that activity in the control group rose considerably for three days, dropped to the original level on the fourth day, and then showed a slight decrease until the 10th day; the curve for the irradiated group was similar to the control group, but the ability to bind ferritin was moderately larger. Levels on the 10th day were identical. Ferritin absorption in the blood remained steady for the first three days, then rose rapidly reaching five times the original level in the control group; the irradiated group showed a slight decrease in values in the first four days, then a slow rise in iron levels was noted which surpassed the original level by a small amount. In earlier experiments, $^{59}FeCl_3$ injection produced no rise in iron levels in the blood in the irradiated animals. A study of the kidneys showed that activity on the 3rd day was almost double that of the control group and was still slightly higher on the 4th day. It normalized by the 10th day. It is contended that the protein-iron complex which is apparently damaged by irradiation may be successfully supplemented by ferritin. This substance can be stored by the spleen and its iron used for formation of red blood cells. The data indicate that protein-bound iron produced favorable results as opposed to electrolytic iron. (BBB)

5355 THOROTRAST DISEASE. APROPOS OF VARIOUS CASES OF SPLENIC CALCIFICATION. Vilar Bonet, J. (Facultad de Medicina, Barcelona). Med. Clin. (Barcelona), 42: 342-6(May 1964).

The case histories of five patients with pathologic changes attributable to previous injection of Thorotrast (ThO_2) as a contrast agent are described, one of them in detail. In four cases the Thorotrast had been administered 10, 16, 17, and 19 yr previously. Thoracic and pelvic radiographs are illustrated for the fifth case which was detected from nodular opaque regions corresponding to the spleen and liver in x-ray photographs. Thorotrast had been injected in this case 30 yr earlier for phlebography during examination for varicosities. This was the only fatal case among the five reported here. No pathologic data are available for these cases, only clinical and radiographic findings. Thorotrast deposition in the spleen may be confused with splenic calcification, so a history of Thorotrast angiography should be sought. Some radiographic differences between the two conditions are discussed. (BBB)

5356 RADIORESISTANCE INDUCED BY TOTAL-BODY GRID IRRADIATION IN SMALL DOSES AND THE BEHAVIOR OF GUINEA PIGS AFTER A SUBSEQUENT LETHAL DOSE OF X-RAYS. Bianchi, E. (Instituto di Radiologia dell'Ospedale Civile, Monfalcone, Italy). Minerva Radiol., Fisiotherap. Radiobiol., 8: 500-6(Nov. 1963). (In Italian).

The ability of small, repeated doses of x rays, given through a grid, to protect guinea pigs against a subsequent lethal dose was investigated. Five groups of animals were exposed to 180-kv x rays with or without a lead grid giving 50% transmission. The first group received a single whole-body 700-R dose through the grid, death occurring in all animals by the 12th day. The second group received 25 R (no grid) daily for eight days, and 20 days from the first irradiation day were exposed to 700 R (no grid). Only 50% of these animals were dead by the 12th day and 15% survived for 30 days or more. The third group was exposed to 50 R (no grid) daily doses for 8 days, followed by a 700 R (no grid) dose on the 20th day. These animals all died by the 12th day but early survival rate (up to the 10th day) was improved over the controls not given preliminary doses. The fourth group was exposed through the grid to 50 R daily doses for 8 days, then to 700 R (no grid) on the 20th day. Only 8% of these animals died by the 12th day and 80% survived for 30 days more. When the same experiment was repeated with 100 R (through the grid) rather than 50 R doses, 30-day survival was 40%. The results show that conditioning by preirradiation through the grid protects against subsequent lethal doses. Histologic examination of the spleen suggests that regenerating germinal centers seen in preirradiated mice may enable them to withstand a later lethal dose because of more active lymphatic tissue. (BBB)

5357 ON THE TIME PERIOD OF MUTATION INDUCTION AFTER TREATING SOAKED SEEDS OF ARABIDOPSIS WITH N-NITROSO-N-METHYLUREA. Mueller, Andreas J. (Inst. fuer Kulturpflanzenforschung, Deutsche Akademie der Wissenschaften, Berlin). Mutat. Res., 2: 426-37(Oct. 1965).

The frequency of recessive lethals (embryonic lethals

and chlorophyll mutations) induced by N-nitroso-N-methylurea and x-rays in soaked seeds of Arabidopsis thaliana during various treatments was determined. The effectiveness of each mutagen was found to be dependent on the duration of presoaking of the seeds in water under partially anaerobic conditions. With presoaking at 36°, maximum sensitivity was reached after about two hrs. Prolongation of soaking, certainly up to 3 days, did not significantly increase the degree of sensitivity. There was no germination of the seeds during the anaerobic soaking period and probably also no DNA replication. The mutation frequency was not changed by delaying the start of germination (and, probably, DNA replication as well) up to 4 days after treatment of the seeds with nitrosomethylurea or x-rays. The conclusion is that mutation induction by nitrosomethylurea or its reaction products is not associated with the replication process of DNA. Chromosome aberrations becoming manifest as recessive or haplophasic lethals are thus viewed as consequences of the induction of primary lesions (potential breaks) in non-replicating chromosomes. By modifying the treatment time, and by different post-treatments, it was shown that nitrosomethylurea penetrated into the meristem cells within a few minutes and that its mutagenic activity was mainly associated with the time of treatment. Maximum effectiveness was reached within 15 min treatment time. (auth)

5358 VIABILITY OF HETEROZYGOTES FOR INDUCED MUTATIONS IN DROSOPHILA MELANOGASTER. I. IRRADIATED X-CHROMOSOME. **Falk, Raphael; Rahat, Ana; Ben-Zeev, Nehama (Hebrew Univ., Jerusalem). Mutat. Res., 2: 438-51(Oct. 1965).**

The mean viability of Drosophila flies carrying a wild type and a marked irradiated X-chromosome was studied. The viability of hemizygotes as well as that of heterozygotes for each irradiated chromosome was calculated. Irradiation of nearly 3000 R induced about as many severe detrimentals (semi-lethals and sub-vitals) as lethals. The viability of heterozygotes for the severe detrimentals was even worse than that of the heterozygotes for lethals. The dominance of lethals and severe detrimentals was 5% and 15% respectively. Within the normal range the viability of hemizygotes for irradiated chromosomes was reduced by about 2%, and a similar reduction was observed in the heterozygotes for these chromosomes. Complete dominance for the slight deleterious effects is suggested. The significance of the study in relation to fitness and population structure is discussed. (auth)

5359 RADIOSENSITIVITY OF DIFFERENT MEIOTIC STAGES OF OOCYTES IN PARTHENOGENETIC DIPLOID ARTEMIA SALINA LEACH. **Cervini, A.; Giavelli, S. (Univ. of Milan). Mutat. Res., 2: 452-6(Oct. 1965).**

Adults of Artemia were irradiated when their oocytes were at different stages of the first meiotic prophase (corresponding respectively to pachytene, and to early and late diakinesis) or in the first meiotic metaphase. The criterion of damage induced by x radiation was hatchability. It was found that, either with 500 R or with 1000 R, the oocytes were more sensitive in prophase than in metaphase, and that there was a progressive decrease in sensitivity during the course of the prophase. (auth)

5360 INDUCTION BY PHYSICAL AND CHEMICAL AGENTS OF MUTATIONS FOR RADIORESISTANCE IN SACCHAROMYCES CEREVISIAE. **Moustacchi, E. (Institut du Radium, Paris). Mutat. Res., 2: 403-12(Nov. 5, 1965).**

Phosphorus-32 decay, x-rays, and ultraviolet irradiation induce a mutation to resistance to ionizing radiations (xr mutation) in haploid Saccharomyces cerevisiae. Nitrous acid and nitrogen mustard are also efficient in inducing this mutation. Compared with the frequency of induced characters the percentage of induced radioresistant cells is high (~ 1000 times higher). Acriflavine and 5-fluorouracil, powerful mutagens for the cytoplasmic character petite colonie, do not induce the xr mutation. The xr determinants are most probably located on the chromosomes. (auth)

5361 INCREASED SENSITIVITY OF IN VITRO MURINE LEUKAEMIA CELLS TO FRACTIONATED X-RAYS AND FAST NEUTRONS. **Caldwell, William L. (Inst. of Cancer Research, Sutton, Surrey, Eng.); Lamerton, Leonard F.; Bewley, David K. Nature, 208: 168-70(Oct. 9, 1965).**

Investigations are reported using a mammalian cell suspension in which it was found that the radiosensitivity increases above normal following an initial dose of radiation. The data are described and discussed in relation to possible mechanisms operating. Murine leukemia cells growing in vitro in suspension were used for the investigation. The dose-survival curves were obtained by backward extrapolation of growth curves, following varying doses of radiation. The two features of particular interest in these results are that the sensitivity after an initial conditioning dose is actually increased above normal, and that with an interval of 5 hr between exposures, the effect of a total dose of 200 rads is greater when the smaller fraction is given first. The maximum effect on survival is achieved with an initial dose of 20 rads. These results are discussed. (J.F.P.)

5362 EVALUATION OF RADIOSENSITIVITY IN THE CYCLIC PHASES OF MOUSE FIBROSARCOMA CELLS IN VITRO. **Bose, S.; Ranade, S. S.; Ranadive, K. J. (Indian Cancer Research Centre, Bombay). Naturwissenschaften, 52: 497(1965).**

Establishment of the life cycle of mouse fibrosarcoma cell line (MFS_8) and evaluation of the order of radiosensitivity of the phases of the life cycle was investigated. MFS_8 cells were exposed to 1000 rads of ^{60}Co γ radiation after 24 hrs of growth. The radiation was evaluated on the basis of the percent of labeled nuclei, mitotic index, and grain count in the interphase nuclei. The differences in the percent labeled nuclei in the normal and irradiated series showed an increase with time. There was a lower grain count, which revealed damage to preexistent DNA in (G_1) in priming DNA synthesis in the S phase. No mitotic cells were seen one hr after irradiation. The absence of recovery during 6 hrs of observation indicated the total blockade of transition of cells from G_2 to M. The order of radiosensitivity in the cyclic process of MFS_8 is G_2, G_1, S, and M. (J.S.R.)

5363 THE DIFFERENT EFFECT OF BROMOURACILDESOXYRIBOSIDE AND IODOURACILDESOXYRIBOSIDE IN THE IRRADIATION OF HERPES SIMPLEX-VIRUS WITH UV LIGHT. **Wacker, A.; Reinhardt, D.; Cramer, J. (Univ., Frankfurt am Main). Naturwissenschaften, 52: 502-3(1965). (In German).**

The uv sensitivity of HeLa cell cultures of Herpes simplex virus treated with bromouracildesoxyriboside (BUDR) or Iodouracildesoxyriboside (IUDR) was investigated. The results showed that the HeLa cells infected with the Herpes simplex virus were completely destroyed; those cells however containing BUDR or IUDR were destroyed to only 64 or 54%, respectively. If the cells are irradiated with uv light at a wave length of 254 mμ, the virulence of the virus decreased as a function of the radiation dose. Viruses in a BUDR medium were more sensitive to uv light than the control solutions. The viruses containing IUDR had a higher death rate than those in the control solutions. The significance of these results is discussed. (J.S.R.)

5364 ADAPTATION OF THE ORGANISM DURING FRACTIONATED X-RAY TREATMENT. A CONTRIBUTION TO THE PROBLEM. **Pradac, J.; Hlavaty, V. (Charles Univ., Prague). Neoplasma, 12: 187-91(1965).**

Previous studies comparing the effect of a single lethal dose of x radiation with that of the same total dose divided in two equal portions applied at various intervals have demonstrated an adaptation of biological systems to irradiation. Graphical and mathematical expressions of the functional relations of the observed adaptation phenomenon have been developed to relate the dose and time distribution of irradiation in attempts to explain the mechanism of the process. Equations were derived to describe the adaptation of the hematopoietic system following irradiation of the whole

organism with repeated doses of radiation. The necessary experimental data were obtained by determining leukocyte counts in the blood of rabbits x irradiated every other day with 50 or 100 R, at a dose rate of 7.2 R/min. Each animal was irradiated with 8 doses, receiving an over-all dose of 400 to 800 R. In each instance, prior to subsequent irradiation, a blood sample was taken and the leukocyte count was determined. Thus two series of values were obtained, showing the relation between a decrease in the number of leukocytes and the dose. On repeated irradiation with a dose of 50 R, the correlation coefficient showing the relation between the experimental values and the 2nd equation was −0.856; on repeated irradiation with a dose of 100 R, it was −0.87. This indicates a fairly good agreement between experimental values and the theoretical curve. (BBB)

5365 THE EFFECT OF X-RAYS ON THE RETRACTION OF THROMBOCYTE CONTAINING CLOTTED BLOOD PLASMA. Brilla, G.; Kuhnke, E. (Universitaet, Bonn). Nucl. Energy, 233-34(July 1965). (In German).

The effects of x rays on the isolated thrombocytes, on the cell-free plasma, and on thrombocyte-plasma mixtures were investigated. After the irradiation, the completed retraction mixture was clotted with $CaCl_2$ solution. The irradiation dose was between 2 and 360 kR. The comparison of the results was possible by calculation of the retraction extent in terms of retraction degree in % of the respective control values. A measureable inhibition of the retraction occurred after irradiation of thrombocyte-containing plasma first at 20 kR. At a dose of 320 kR, the retraction was 13% of the control value. The clots obtained from irradiated plasma were transparent and had better retraction properties than the unirradiated control clots as long as the x-ray dose did not exceed 80 kR. First at irradiation of the plasma with doses over 160, a retraction decrease was observed that attains 34% at 320 kR. The thrombocytes suspended in physiological NaCl solution were the most sensitive to x radiation. At 320 kR, no variation with respect to the thrombocytes irradiated in plasma was observed. The number of thrombocytes was not altered by the irradiation up to 320 kR. The thrombocyte drop observed shortly after whole-body irradiation could not be attributed to a direct modification of the thrombocytes. Irradiated retraction mixtures clotted more slowly when the retraction event was delayed. An exception was delayed. An exception was noted in those mixtures in which a retraction acceleration occurred. For the results of a clot retraction, the structure of the fibrin clot is important in addition to the number of thrombocytes and their vitality. (tr-auth)

5366 ON RESISTANCE TO PHYSICAL AND CHEMICAL AGENTS OF ENDAMOEBA HISTOLYTICA IN RELATION TO ITS PRESENCE IN DRINKING WATER AND WASTE WATER. Molinari, Vincenzo (Univ., Naples). Nuovi Ann. Ig. Microbiol., 15: 455-62(Sept.-Oct. 1964). (In Italian).

Experiments with various agents indicate that, among other agents tested, ionizing irradiation in doses of 100,000 R or more inhibits growth of Endamoeba histolytica. (BBB)

5367 STUDIES ON THE LEUKEMOGENESIS OF MOUSE LEUKEMIA BY X IRRADIATION. PART II. CLASSIFICATION OF LEUKEMIA AND VARIOUS FACTORS INVOLVED IN LEUKEMOGENESIS. Sota, Susumu (Okayama Univ. Medical School, Japan). Okayama Igakkai Zasshi, 77: 25-48(Jan. 1965). (In Japanese).

For the elucidation of leukemogenesis of mouse leukemia induced by x rays, a study was carried out on various factors influencing the development of leukemia. Thus, an effort was made to correlate the age of mice receiving x irradiation, dose and method of irradiation, and strain and sex of mice with the rate of leukemia induction. Also, a comparative study was made of the types of mouse leukemia elicited by x rays. For C57BL and C3Hf mice given four whole-body irradiations of 160 R each at an interval of 4 days to a total dose of 600 R, the rate of leukemia induction was 77.3, 88, and 20% in the respective groups. It was demonstrated that the rate of leukemia induction was highest in mice of the RF strain 30 to 40 days old, and this rate decreased with advance in age of the mice. No significant difference in sex incidence of leukemia was shown. The rate of leukemia induction increased with reaching a maximum at the dose of 350 R. Two types of lymphocytic leukemia were induced in RF strain mice by x irradiation, thymoma and nonthymoma. Distinct differences in the peripheral blood pictures and in the patterns of leukemic cell infiltration into the liver were observed between these two types. (TCO)

5368 STUDIES ON THE LEUKEMOGENESIS OF MOUSE LEUKEMIA BY X IRRADIATION. PART III. OBSERVATIONS OF HEMATOPOIETIC ORGANS BY FLUORESCENT STUDIES OF CULTURES AND MORPHOLOGICAL STUDY OF LEUKEMIC CELLS. Sota, Susumu (Okayama Univ. Medical School, Japan). Okayama Igakkai Zasshi, 77: 49-57(Jan. 1965). (In Japanese).

By phase-contrast microscopy, vital staining, and fluorescent studies of cell cultures, cytologic and tissue culture observations were carried out with the leukemic cells of RF strain mice after x irradiation. The characteristics of lymphoblasts and myeloblasts were delineated, and from the growth patterns of the cells from various organs of the leukemic mice, it was possible to differentiate the two classifications, namely the thymoma type and the nonthymoma type of lymphocytic leukemias, as described in previous reports. The results of the study support earlier views on the mechanism of induction of leukemia in RF mice by x irradiation. In the thymoma type of lymphocytic leukemia, leukemic changes originate in the thymus, whereas in nonthymoma type of lymphocytic leukemia, the leukemic changes originate in the spleen or in lymph nodes. (BBB)

5369 EFFECT OF RADIATION ON AUDITION AND CONDITIONED RESPONSES IN THE SPANISH GOAT. Casey, Albert; Krise, George M. (Texas A and M Univ., College Station). Percept. Mot. Skills, 20: 871-2(Feb. 1965).

Russian investigators have reported that the auditory mechanism is radiosensitive; degenerative changes and functional losses were found following doses below the midlethal level. Western researchers, on the other hand, have found no changes, or only transitory increases, in auditory acuity following irradiation. A parallel discrepancy exists with respect to the radiosensitivity of conditioned responses. The present study was undertaken in response to these areas of contradictory findings. Eight male Spanish goats were overtrained to avoid shocks by foreleg flexion during a 5-sec tone. Generalization was promoted by varying the quality and intensity of the tone throughout training. These procedures were carried out with subjects constrained in a remote sound-deadened chamber. Frequency and intensity thresholds were determined by the method of limits, with the occurrence of the conditioned flexion response indicating the audibility of the tone being presented. The usual controls for anticipation and habituation were employed. Additionally, standard conditioned response trials using a 900-cps and 57-db stimulus were interspersed throughout training and threshold testing to study radiation effects on various indices of conditioned response. Radiation and testing were carried out weekly for 5 weeks; irradiation preceded testing by 24 hr in each case. Every week 4 goats received an integrated whole-body dose of 104 rad of γ rays delivered in 2.2 min to a total 5-week dose of 520 rad. Four goats were nonirradiated controls. Analysis of variance revealed no significant differences between irradiated and control animals with respect to frequency thresholds, intensity thresholds, latency of a conditioned response, or probability of a conditioned response. Thus, the Russian findings were not supported. (BBB)

5370 GENERALIZED RESPONSE OF CALCIFIED MAMMALIAN TISSUES TO LOCAL INJURY. Babicky, A.; Kolar, J. (Czechoslovak Academy of Sciences, Prague). Physiol. Bohemoslov., 14: 173-85(1965).

Several experiments were performed on male Wistar

rats, aged 11 weeks, to investigate the influence of various injurious physical agents (heat, cold, mechanical force, electrical current, ultrasound, and x rays) on bone metabolism of ^{45}Ca and ^{35}S. To investigate the effect of ionizing radiation on bone metabolism, one hind leg of the rat was given 750, 2000, or 3000 R doses of 50-kv x rays over a 4-cm diameter area. Following exposure of the animals to the various injurious physical agents, they received a dose of 20 μC $^{45}CaCl_2$ or 200 μC $Na_2{}^{35}SO_4$ intraperitoneally. The x-irradiated bones were shorter, deformed, and fragile as early as 5 to 6 weeks following this irradiation. Depilation and sometimes skin ulcers appeared in the irradiated skin. After irradiation with 750 R, depression of ^{45}Ca uptake of tibia was more pronounced than after administration of 3000 R. In another study the effect of denervation on the course of the mineral uptake, a dose of 2000 R was used. On the denervated and irradiated side, the depression of ^{45}Ca uptake was seen as in the case of radiation damage only, but the maximum depression was observed later in the former case, i.e. on day 42, instead of on day 28 as seen in animals irradiated only. The depression was even more pronounced; an elevation was seen in the denervated leg only on day 61. Thus, this elevation occurred around the same day as in the denervated leg without irradiation and the uptake into the irradiated tibial shafts paralleled the curve for the proximal tibial epiphysis. The uptake of radiosulfur investigated in the same way in separate sets of animals showed that curves of the ^{35}S uptake in the proximal tibial epiphysis of healthy animals and animals with denervated right hind limb run essentially the same course, whereas the uptake in the bone of the denervated extremity was decreased from day 8. The uptake in both the irradiated and non-irradiated extremity in rats without denervation was different. Some depression of ^{35}S uptake in the irradiated proximal epiphysis could already be seen from day 8, being accentuated on day 16, and lasting until the end of this period, as seen with ^{45}Ca uptake. Although the same dose (2000 R) was used, the depressions and elevations of ^{35}S uptake was less pronounced than those of ^{45}Ca uptake. The harmful effects of irradiation could be seen at an earlier stage in the organic than inorganic components of bone. Similar inhibition of bone metabolism was observed with the other physical agents, when adequate intensities were used. In addition to local bone mineral changes, generalized shifts of mineral metabolism in bones and teeth were encountered even in the case of local injury. An explanation of this reaction is given, considering it to be a part of regulative and restoratory mechanisms and mediated by neurohumoral pathways. (BBB)

5371 EFFECT OF SPORE POPULATION AND AGE OF INFECTION ON THE RESPONSE OF BOTRYTIS CINEREA TO GAMMA RADIATION. Couey, H. Melvin; Bramlage, William J. (Dept. of Agriculture, Fresno, Calif.). Phytopathology, 55: 1013-15(Sept. 1965).

Responses of B. cinerea infections to γ radiation at different stages of development on grapes (Vitis vinifera) of the Emperor variety were studied. When the fruit was inoculated and irradiated immediately, the effectiveness of a given radiation dose depended on the relative number of spores on the grapes. The greater the number of spores, the greater was the dose required to reduce decay to a given level. When the fruit was inoculated, incubated for 16 hr, fumigated, and then irradiated, decay reductions by increasing radiation doses were statistically significant. When comparable, nonfumigated samples were irradiated, decay reductions resulting from irradiation were greater than on grapes that had been fumigated, but the amounts of decay following given radiation doses were usually greater than on the fumigated samples. When time between inoculation and fumigation was increased from 12 to 24 hr, the percentage of decayed grapes increased in both nonirradiated and irradiated samples. The increasing resistance of developing Botrytis infections to radiation appeared to be caused by the increasing number of cells that must be inactivated to halt the infection. It is concluded that if radiation is used commercially to control post-harvest decay of fresh fruits and vegetables, it should be considered an adjunct to, not as a substitute for, such traditional decay-control measures as sanitation, refrigeration, careful handling, and perhaps chemical protectants. (TCO)

5372 SPLEEN WEIGHT AS A MEASURE OF MARROW CELL GROWTH IN IRRADIATED MICE. Popp, Raymond A.; Congdon, C. C.; Goodman, Joan Wright (Oak Ridge National Lab., Tenn.). Proc. Soc. Exp. Biol. Med., 120: 395-8(Nov. 1965). (ORNL-P-1288).

C57BL, C3H, C57BL/6, and DBA/2 parental marrow cells were injected at varying doses into lethally irradiated $BC3F_1$ and $B6D2F_1$ mice. Spleen weight in recipients was compared to spleen colony formation and ^{59}Fe uptake. Results showed that increased spleen weight was proportional to formation of increased numbers of splenic nodules and percentage of ^{59}Fe uptake. Data suggest that spleen weight, spleen colony formation, and ^{59}Fe uptake are equally suitable assays, within appropriate limits, for studies on proliferation of marrow cell transplants in irradiated mice. Spleen weight is a useful index of growth for doses of transplanted marrow cells which promote recovery of hematopoietic injury in lethally irradiated mice. (auth)

5373 SUPPRESSION OF ^{90}Sr-INDUCED DEVELOPMENT OF BONE TUMORS BY INFECTION WITH BACILLUS CALMETTE-GUERIN (BCG). Nilsson, Agnar (Research Inst. of National Defence, Sundbyberg, Sweden); Revesz, Laszlo; Stjernswaerd, Jan. Radiat. Res., 26: 378-82(Nov. 1965).

Infection of ^{90}Sr-treated mice by BCG at a time close to the expected appearance of the first bone tumors resulted in a delay of the development and a significant decrease of the total incidence of such tumors. Neither the osteogenic or osteolytic character of the tumors, nor their distribution in the skeleton, nor the survival time of the animals was affected by BCG. On the other hand, an increase of leukemia incidence was noted in the infected animals. (auth)

5374 DEVELOPMENT OF INTESTINAL DAMAGE AFTER X-IRRADIATION AND ^3H-THYMIDINE INCORPORATION INTO INTESTINAL EPITHELIAL CELLS OF IRRADIATED GOLDFISH, CARASSIUS AURATUS, AT DIFFERENT TEMPERATURES. Hyodo, Yasuko (National Inst. of Radiological Sciences, Chiba, Japan). Radiat. Res., 26: 383-94(Nov. 1965).

When goldfish irradiated with 8 kR of x rays were kept at 4°C, a majority of the fish survived for more than 110 days. However, between 150 and 200 days after irradiation, about three-fourths of them died. In the cool thermal surroundings, the development of characteristic histological damage of the intestine seldom took place during a period of 100 days after irradiation, but in fish examined at 181 or 201 days marked histological damage had occurred in the intestine, the epithelial cells being increased in size but reduced in number. Autoradiographic studies of intestinal epithelium of fish given an intraperitoneal injection of ^3H-thymidine showed that, at 22°C, the number of labeled cells and of grains per labeled cell reached the maximum within 3 hours after injection of ^3H-thymidine, whereas at 4°C the values remained low even at 24 hours. All mitotic figures were labeled at 3 hours after injection at 22°C, whereas 20 to 80% were labeled at 44 hours at 4°C. Even at 4°C, ^3H-thymidine was incorporated into intestinal epithelial cells in both irradiated and nonirradiated fish. However, at 44 hours after injection, the ratio of labeled mitotic figures was definitely smaller in irradiated fish than in nonirradiated fish. (auth)

5375 ALTERATIONS IN MUSCLE ACTIVITY DURING GAMMA-IRRADIATION. Pierson, Mary B.; Bachofer, C. S. (Univ. of Notre Dame, Ind.). Radiat. Res., 26: 403-12(Nov. 1965).

Increases in contraction tension, rate of contraction, and rate of relaxation of isometric responses of the rat diaphragm were recorded during γ irradiation when neuromuscular transmission was not blocked. The enhancement occurred in both maximal and submaximal

responses. Since no enhancement of activity occurred when neuromuscular transmission was blocked with d-tubocurarine, the radiation effect appears to arise either in the efferent nerve fibers or at the neuromuscular junctions. (auth)

5376 THE EFFECTS OF IONIZING RADIATION ON GROWTH AND REGENERATION OF INTRARENAL THYMUS GRAFTS IN MICE. Haran-Ghera, Nechama (Weizmann Inst. of Science, Rehovoth, Israel). Radiat. Res., 26: 442-9(Nov. 1965).

Observations were made on growth and regeneration of intrarenal isologous thymus grafts in normal and x irradiated C57BL mice. The growth of intrarenal thymus graft was found to be determined by the age of the donor thymus. No sex effect on thymus growth was demonstrated except for a partial male histoincompatibility effect. The autonomy of the thymus graft growth was demonstrated by refractoriness to environmental changes, due to irradiation in the host. Irradiation of newborn thymus graft reduced its growth rate. An adult intrarenal thymic graft, when irradiated, showed the same typical regeneration pattern established for the thymus in situ. Similarly, thigh shielding during irradiation and bone marrow injection after irradiation were also effective, enhancing intrarenal thymic graft regeneration. The rate of full recovery from radiation injury differed in the thymus in situ and in the intrarenal graft. (auth)

5377 BEHAVIOR OF ENTEROCHROMAFFIN CELLS OF THE INTESTINE OF THE HEDGEHOG IRRADIATED DURING HIBERNATION. Cavina Pratesi, A.; Ghiringhelli, F. (Univ., Pavia, Italy). Radiobiol. Radioterap. Fis. Med., 19: 133-43(Mar.-Apr. 1964). (In Italian).

Histologic studies were conducted on the enterochromaffin cells in the duodenum and colon of male hedgehogs (Erinaceus europaeus), weighing 340 to 370 g, exposed to high local doses of x rays. Animals, either in the waking state or after about 60 days of spontaneously induced hibernation, were given a single abdominal dose of 2000 R of 180-kv x rays. Half of the animals in each group were sacrificed 36 hr postirradiation and the other half at 96 hr. The argentaffin histologic reaction was used to examine changes in the enterochromaffin cells in duodenum and colon. The results showed that in waking animals the number of enterochromaffin cells increased 110% at 36 hr and decreased 92% at 96 hr postirradiation in duodenum. In colon the increase was 31% at 36 hr and the decrease 85% at 96 hr. In hibernating animals the number of cells was decreased both at 36 hr (4% below controls) and at 96 hr (24%) in duodenum; in colon the decrements were 28% and 64% respectively. In both waking and hibernating state the number of granules per enterochromaffin was decreased at 96 hr postirradiation in both duodenum and colon, but no changes in cell granularity was noted at 36 hr. The results confirm the lower radiosensitivity of cells in the hibernating mammal. They also suggest that diarrhea in the acute radiation syndrome may have its origin in smooth-muscle active biogenic amines released from the intestinal enterochromaffin cells by irradiation. To test this hypothesis it would be useful to measure urinary excretion of 5-hydroxyindoleacetic acid at various intervals postirradiation. (BBB)

5378 CHANGES OF SERUM PROTEIN FRACTIONS IN THE BLOOD OF RATS IRRADIATED WITH 660-Mev PROTONS. Govorun, R. D.; Orlyanskaya, R. L. (Inst. of Industrial Hygiene and Occupational Diseases, Academy of Sciences, USSR). Radiobiologiya, 5: 656-8(1965). (In Russian).

Rats were irradiated with 660 Mev protons at doses of 500, 800, 1000 and 1350 rads. Analyses were run for six serum protein fractions by paper electrophoresis: A-albumins, α_1-, α_2-, β_1-, β_2- and γ-globulins. The most characteristic changes in the serum protein fractions were observed in the first 10 days after irradiation at a dose of 800 to 1350 rads, as noted by a significant decrease in albumin content and by an increase in the content of α- and β-globulins. The deviations in the protein values increased with increasing radiation dose. Recuperation was not complete at the end of a 30-day observation period. These changes are qualitatively similar to the changes in serum protein fractions induced by other forms of radiation such as gamma irradiation. (TTT)

5379 INFLUENCE OF IRRADIATION ON LIPIDS OF MITOCHONDRIA OF LIVER CELLS. Blokhina, V. D.; Martynova, T. T. Radiobiologiya, 5: 659-61(1965). (In Russian).

Rabbits 2.5 to 3.5 kg in weight were given an absolutely minimum lethal dose of 800 R with ^{60}Co gamma irradiation. The animals were killed; the liver was removed, washed with a 0.9% NaCl solution, and homogenized with a 0.88 M sugar solution. A fraction of mitochondria was isolated, and the protein content was determined by titration. The lipids extracted by the method of Folch were arbitrarily designated as weakly bound lipids. The contents of cholesterol and of phospholipids were determined in the weakly bound lipid fraction. Then the mitochondria residue was subjected to alkaline hydrolysis in 1.0 M KOH for 18 hours at 37°C in order to determine the tightly bound lipids. The normal content of total lipids was found to be 26% on the average, calculated with respect to the protein content of the mitochondria sample. The weakly bound fraction was 11%, and the tightly bound fraction was 15%. The tightly bound lipid fraction increased to 21% at a period 24 hours after the irradiation with an increase in the amount of triglycerides. With the onset of severe radiation sickness 72 hours after irradiation, the total lipid content in the mitochondria decreased to 18%, and the tightly bound lipid content fell to 6%. These results show that the binding of the lipid to the lipoprotein complex has been weakened as a result of the irradiation. (TTT)

5380 ACTIVITY OF DEAMINATION OF ADENOSINE AND ADENYLIC ACID IN THE TISSUES OF IRRADIATED RABBITS. Elkina, N. I.; Libinson, R. E. Radiobiologiya, 5: 662-6(1965). (In Russian).

Rabbits 2 to 2.5 kg in weight were given a 1000 R dose of ^{60}Co gamma radiation. The rabbits were killed by an air embolism at 15 minutes, 5, 12, and 24 hr after irradiation, and a 2% aqueous homogenate was made of various tissues. The enzyme activity was determined by adding adenylic acid to the homogenate. The deamination of adenylic acid was measured on a spectrophotometer from the drop in absorption at 265 mμ and the increase in absorption at 240 mμ. The enzyme activity was expressed as the amount of deaminated substrate per mg of nitrogen in the homogenate per minute. The activity of adenosinedeaminase was 0.370 in the mucous membrane of the small intestine, 0.206 in the spleen, 0.140 in the lymphoid tissue of the appendix, 0.093 in the bone marrow, and 0.012 μmol of adenosine per 1 mg of nitrogen in the liver homogenate of the unirradiated control animals. The activity of the adenylic acid deaminase was 0.325 in the skeletal muscles, 0.028 in the spleen, 0.026 in the mucous membrane of the small intestine, and 0.010 μmols per 1 mg of homogenate nitrogen in the lymphoid tissue of the appendix. Irradiation with a dose of 1000 R gave increases of 55 and 65%, respectively, in adenosinedeaminase activity 15 minutes and 4 hr after the irradiation. Smaller increases in enzyme activity were noted in the bone marrow and in the mucous membrane of the small intestine. The activity of the adenylic acid deaminase was lowered by 30% in the muscles of the irradiated rabbits a few days after the irradiation. (TTT)

5381 INFLUENCE OF LOW DOSES OF INTERNAL IRRADIATION ON SOME ASPECTS OF WATER, MINERAL, AND NITROUS METABOLISM IN ANIMALS. 2. CONTENTS IN BLOOD AND EXCRETION WITH URINE OF ELECTROLYTES AND PRODUCTS OF NITROUS METABOLISM UNDER THE INFLUENCE OF LOW DOSES OF ^{24}Na. Azhipa, Ya. I.; Filyashina, G. A. (Inst. of The Higher Nervous Activity and Neurophysiology, Moscow). Radiobiologiya, 5: 667-74(1965). (In Russian).

A total of 50 μC of ^{24}Na per kg of body weight was given to three dogs via the stomach. The sodium content of the blood increased from 311 ± 12 mg % to 404 ± 15 mg % on the average, and the Ca content increased from 10.5 ± 0.2 mg % in

the controls to 12 ± 0.4 mg % at 2 to 2.5 months. The concentration of inorganic phosphate in the blood was decreased for a period of two months. The changes in content of K, Cl, urea, and creatinine in the blood were insignificant and only temporary. However, the irradiation did result in a sustained increase in secretion of Na, K, Ca, Cl, inorganic phosphate, urea, and creatinine by the kidneys. These increased secretions were due to a decrease in reabsorption, or to a decrease in reabsorption with a simultaneous increase in filtration. It is possible that irradiation stimulates the secretory activity of the nephrons, and activates canal ion exchange processes. The irradiation had a diuretic effect. (TTT)

5382 URINARY SECRETION OF THYMIDINE FOLLOWING WHOLE-BODY EXPOSURE OF RATS TO VARIOUS DOSES OF X RADIATION. Zharkov, Yu. A.; Fedorova, T. T.; Mikhailova, L. F. Radiobiologiya, 5: 675-80 (1965). (In Russian).

The amount of thymidine excreted in the urine of rats was found to increase in direct proportion to the x-ray dose. The thymidine in the urine was separated chromatographically with a isopropanol-n-butanol-ammonia mixture, and determined colorimetrically. The results showed the amount of excreted thymidine increased on the first day after irradiation by a factor of 8 at a dose of 650 R, by a factor of 4 to 4.5 at 500 R, and by a factor of 2.5 at 200 R. On the 3rd to 4th day after irradiation at 650 R, the thymidine level in the urine was decreased by 80 to 90% as compared to the normal value, and on the 7th day the thymidine values returned to normal. On irradiating the rats at a sublethal dose of 200 R, the thymidine excretion in the urine remained significantly above the normal value during the entire period of study (24 days). With a dose of 50 R the thymidine excretion was higher than normal on the 3rd, 10th, and 24th days after irradiation, but lower than normal on the 8th and 14th days after irradiation. The thymidine level in the urine reflects the DNA catabolism of dead cells and the intensity of recuperative processes. (TTT)

5383 FLUORIMETRIC INVESTIGATION OF SECOND LUMINESCENCE OF LYMPHOCYTES OF LYMPHATIC GLANDS IN IRRADIATED RATS. Manteifel', V. M.; Golenko, O. D. (Inst. of Molecular Biology, Moscow). Radiobiologiya, 5: 685-9(1965). (In Russian).

By microfluorimetry it is possible to detect small differences in fluorescence intensity in lymphocyte nucleoli of normal cells from the lymphatic nodes that reflect natural aging processes and cell degeneration. After irradiating white rats with a whole-body x ray dose of 500 R, an increased luminescence intensity in lymphocytes could be detected by staining with acridine orange. The relative radiation effect, which was defined as the ratio of the difference in average luminescence intensity of the irradiated and control animals to the average luminescence of the control nucleoli, was found to be 0.49 at 10 minutes, 1.56 at 2 hours, 2.22 at 3 hours, and 1.15 at 12 hours after the irradiation. These changes are due to the development of pyknotic processes in the cell as a result of the irradiation. (TTT)

5384 DYNAMICS OF GASTRIC SECRETION AND RIBOFLAVIN IN BLOOD DURING RADIATION SICKNESS. Perepelkin, S R. (Moscow Medical Inst.). Radiobiologiya, 5: 693-9(1965). (In Russian).

Dogs were given a whole-body, x ray dose of 400 R. The amount of gastric secretion per hour, and the enzyme activity of the gastric juice were determined on the isolated stomach with a normal diet and with a strong stimulant (200 g raw meat) or a weak stimulant (300 ml of milk). With the onset of severe radiation sickness an increase in gastric secretion was observed. With the occurrence of a subacute form of radiation sickness, periodic changes in stomach secretion were observed. With the vagus nerve cut, hypersecretion was noted the first few days after irradiation followed by hyposecretion at later periods. This behavior is in contrast to normal behavior. The disturbances in gastric secretion were greater with the use of a strong stimulant (meat) than with the use of a weak stimulant (milk). With severe radiation sickness the riboflavin content of blood fell from a normal value of 5.3 to 6.3 γ % to a low value of 0.18 to 0.52 γ %. Hypersecretion was accompanied by a decrease in blood riboflavin, and hyposecretion of gastric juices was accompanied by an increase in blood riboflavin. (TTT)

5385 ABSENCE OF "OXYGEN AFTER-EFFECTS" IN CALANDRA GRANARIA DURING HIBERNATION INDUCED WITH LOW TEMPERATURE. Bychkovskaya, I. B.; Ochinskaya, G. K. (Central Scientific-Research Inst. of Roentgen-Radiology, Leningrad). Radiobiologiya, 5: 700-2(1965). (In Russian).

The insects Calandra granaria were irradiated in special vacuum tubes at x ray doses of 5, 6, 7, 8, 9, and 10 kR at a temperature of 1 to 5°C. The insects were held at a lowered temperature after irradiation for periods varying from 30 minutes to 12 days. The oxygen concentration was varied from 20 to 2% during and after irradiation. The survival at 60 days and the average lifetime of the irradiated insects were taken as criteria of radiation damage. On maintaining conditions of hypoxia during and after irradiation, a definite protective effect was observed. On creating conditions of hypoxia from the moment that the weevils had been warmed up to room temperature, no protective effect could be observed. Thus, no oxygen aftereffect could be detected by maintaining the weevils at low temperatures. (TTT)

5386 INFLUENCE OF SHORT-WAVE UV-LIGHT ON SENSITIVITY OF INFUSORIA TO INHIBITORS OF BREATHING AND GLYCOLYSIS. Samoilova, K. A. (Inst. of Cytology, Leningrad). Radiobiologiya, 5: 703-6(1965). (In Russian).

Clones of Paramecium caudatum were cultured, and infusoria cultures 4 to 5 days in age were irradiated with monochromatic UV-light (2537 Å) at doses of 570, 2280, 5700, and 9120 ergs/mm^2. A total of 100 irradiated Paramecia were placed in a microaquarium containing an inhibitor solution of 2×10^{-3} M KCN, 2 to 4×10^{-4} M malonic acid as respiratory inhibitor, or of 10^{-5} M monoiodoacetate (MIA) for the suppression of glycolysis. The number of survivors were counted at definite intervals. The irradiated cells were more resistant to KCN than the unirradiated cells. The resistance to KCN increases with increasing UV-dose, and is maintained over the entire period of survival. The irradiated cells were also more resistant to the monoiodoacetate inhibitor but only at moderate doses of 570 and 2280 ergs/mm^2, (30 and 35% survival after 48 hours contact with the inhibitor) and not at the high dose of 9120 ergs/mm^2 (4% survival after 48 hours contact with the inhibitor). At the higher concentration of malonic acid (4×10^{-4} M) the irradiated cells died off faster than the control cells. The resistance to KCN is probably related to disturbances in the respiratory system of the irradiated cells. (TTT)

5387 ON THE ACTION OF LOW IRRADIATION DOSES AND INCORPORATED NATURAL RADIOACTIVE ELEMENTS ON SPERMATOGENESIS OF MICROTUS OECONOMUS UNDER NATURAL CONDITIONS. Verkhovskaya, I. N.; Maslov, V. I.; Maslova, K. I. (Komi Division, Academy of Sciences, Syktyvkar, USSR; Bakha Inst. of Biochemistry, Moscow). Radiobiologiya, 5: 720-9(1965). (In Russian).

Field mice living on radium-bearing soil of average activity obtain a dose of 17 R in 6 months (a factor of 400 higher than normal), and mice living on a uranium-radium soil of comparatively high activity obtain a dose of about 35 R in 6 months (a factor of 800 above normal). Male mice were trapped in regions of varying activity levels, and a cytological study of the gonads was carried out. The results showed that many degenerative changes took place in the gonads under the long-term chronic irradiation. With a radiation dose of 8×10^{-3} R/hr, the average testicle weight decreased a factor of four from a normal value of 2.19% to 0.58% of the body weight. Vacuolization of the canal parenchyma was observed. The diameter of the seminal channels is significantly constricted. The destructive changes were more obvious in the younger mice than in the older mice in whom recuperative changes may be taking place. A total of 58.3% of the sexually mature young males were sterile. (TTT)

5388 SOME REGULARITIES OF CHANGES IN PLANTS AFTER γ IRRADIATION. Mamedov, T. G.; Khalisi, Feisal (Moscow State Univ.). Radiobiologiya, 5: 730-1(1965). (In Russian).

The Black Russian bean and the Pioneer pea were irradiated at various stages of growth with ^{60}Co gamma radiation. The LD_{50} values were determined for seedling shoots. The LD_{50} values were higher for the bean than for the pea. The effective dose varied with the extent of the postradiation period due to recuperative processes. The effective dose was a minimum at 10 to 20 days, and increased thereafter. The dose required for complete suppression of recuperative growth (SRG) was significantly larger than the dose for the initial suppression of growth (ISG). Thus, with 5-day pea shoots the SRG dose was 4500 R compared to 1100 R for the ISG dose. With 10 day pea shoots the SRG and ISG doses were 9450 and 2050 R respectively. With 5-day bean shoots the SRG and ISG doses were 3900 and 860 R respectively. With 10-day bean shoots the SRG and ISG doses were 7650 and 1470 R respectively. (TTT)

5389 INFLUENCE OF ^{60}Co γ IRRADIATION ON THE GROWTH OF CHLORELLA CULTURES. Gileva, E. A.; Timofeeva, N. A.; Timofeev-Resovskii, N. V. (Inst. of Biology, Academy of Sciences, Sverdlovsk, USSR). Radiobiologiya, 5: 732-4(1965). (In Russian).

Cultures of Chlorella vulgaris Beyer were given a single ^{60}Co gamma dose varying from 0.5 to 50 kR. Samples of the culture were taken on the 1st, 7th, 10th, 14th, and 18th day, and the number of cells per ml was determined. On the 18th day a dose of 0.5 to 1.0 kR had a stimulating effect on cell growth. A further increase in irradiation dose had a depressing effect on the growth of the culture. A dose of 25 kR was lethal. It is not possible to grow cultures of Chlorella with an irradiation dose higher than 25 kR. (TTT)

5390 CHANGES IN THE PROCESS OF CELL DIVISION AND NUCLEUS STRUCTURE UNDER THE INFLUENCE OF IRRADIATION AND RADIOTOXINS. Breslavets, L. P.; Kasymov, A.; Filippova, H. F. (Inst. of Biological Physics, Moscow). Radiobiologiya, 5: 735-7(1965). (In Russian).

Potato tubers were exposed to a ^{137}Cs gamma dose of 50 kR, and 24 hours later the pulp (40 g) was extracted with 200 ml of ethyl alcohol. After driving off the alcohol, the residue was taken up in water, and pea seeds were steeped in this extract. A count of the dividing cells in the root of seedlings showed that the mitotic index had decreased to 1.3 compared to a value of 15.4 for plants grown in an extract of unirradiated plants. It was found that a ^{60}Co gamma dose of 250 R caused an increase in pyknotic cells from a normal value of 0.17% to 1.2%. Detailed cytological studies showed that in pea roots growing in the radiotoxin extract the number of bridge aberrations increased from a normal value of 1.83% to 7.1%. It can be concluded that changes brought about by direct irradiation such as a slow-down in cell division, chromosome aberrations, and pyknosis can also take place under the effect of radiotoxins. (TTT)

5391 THE INFLUENCE OF CONTINUOUS IRRADIATION UPON THE NON-SPECIFIC RESISTANCE AGAINST EXPERIMENTAL DIPHTHERIAL INTOXICATION IN RATS. Vasku, J.; Praslicka, M.; Urbanek, E. (Purkinje Univ., Brno). Rev. Can. Biol., 24: 75-82(June 1965).

Pretreatment by gamma rays greatly reduced nonspecific resistance of rats against a small dose of diphtheria toxin, with a resulting high mortality. This was caused mainly by an exhaustive stimulation of the adrenal cortex, which induced acute disintegration of the thymic and lymphatic tissues. The effects may be ascribed to the action of glycocorticoids from the adrenal cortex, which presented a marked lipid depletion. Non-irradiated rats treated with a massive dose of toxin showed a similar picture. On the other hand, all non-irradiated rats treated with a small dose of toxin, and rats treated with irradiation only, survived and did not show any essential deviation from normal picture. Thus, the picture of acute stress which was observed in the irradiated rats with diphtherial intoxication was due to the intoxication rather than to the irradiation. A marked lipid depletion in the interscapular brown fat (hibernating gland) was observed only in non-irradiated rats after the massive dose of toxin. (auth)

5392 INJURY OF THE SMALL INTESTINE FOLLOWING IRRADIATION FOR GYNECOLOGIC CANCER. Kaplan, Alan L.; Hudgins, Philip T.; Wall, John A. (Baylor Univ. Coll. of Medicine, Houston, Tex.). S. Med. J., 58: 1109-14(Sept. 1965).

Two cases are presented in which injury to the small intestine followed irradiation for gynecologic malignancy. The complication has occurred twice among 264 patients with gynecologic carcinoma treated with radiation. Following Ra application, both patients were treated over a 3-week period with the 2-Mev Van de Graaff machine. The pathogenesis of radiation injury to the small intestine is discussed, and medical management is considered. (TCO)

5393 INDUCED PARTIAL MALE-STERILE AND MULTIPISTILLATE DWARF PLANT IN TETRAPLOID RICE BY X-RAY TREATMENT. Richharia, A. K. (Central Rice Research Inst., Cuttack, India). Sci. Cult. Calcutta), 31: 375-6(July 1965).

The induction of mutations in rice by exposure of dried seeds to x radiation is discussed. A dwarf plant with longer flowering duration, partial or complete male sterility, and multipistillate condition was obtained by x irradiation of an auto-tetraploid (2n = 48) of O. sativa. The quantitative characters of treated and normal plants are compared. (C.H.)

5394 ENHANCEMENT OF FUNCTIONAL ACTIVITY OF PARS INTERMEDIA FOLLOWING ^{60}Co IRRADIATION IN THE TOAD. Chang, Chi-ye; Tsuang, Ling-tsu (Inst. of Zoology, Peking). Shih Yen Sheng Wu Hsueh Pao, 10: 33-8(Mar. 1965). (In Chinese).

To investigate the effect of large doses of radiation on the functional activity of pars intermedia in the toad (Bufo bufo), hibernating adult females received 10,000, 50,000, and 100,000 R doses of ^{60}Co γ rays (at 300 R/min and 5°C) and were killed at two to three days later. The hormone content of the irradiated and the nonirradiated (control) glands was assayed semiquantitatively by injection of an extract of the gland into the hypothalectomized tadpoles (Rana nigromaculata). It is known that removal of hypothalamus anlage during the neurula stage of anuran embryos results in contraction of melanophores and leads to the development of albino tadpoles. Injection of extract of pars intermedia of the nonirradiated (control) toads into such albino tadpoles caused resumption of near normal pigmentation, while injection of same amount of extract of irradiated glands at 10,000 R induced further darkening of the skin. With glands of toad receiving radiation doses of 50,000 or 100,000 R, a greater or even full expansion of melanophores was observed. No destructive effect on the secretory activity of pars intermedia was detected within the range of the radiation doses employed. These results demonstrate that irradiation of the animals with heavy doses of γ radiation can enhance hormonal release and production in the pars intermedia. The effect increased linearly with the increase in radiation dose. (BBB)

5395 MEDIAN JAW AND TOOTH FUSION INDUCED BY X IRRADIATION IN THE MOUSE. Ritter, W.; Degenhardt, K. H. (Univ., Muenster, Ger.). Stoma, 4: 227-40(1962). (In German).

Pregnant mice were x irradiated with 130 R at a rate of 60 R/min during the sixth, seventh, eighth, and tenth day of pregnancy. The skeletons of the newborn mice were examined for injuries and malformations. Morphogenesis of the spine was disturbed in all irradiated animals. Animals that had been irradiated during the seventh day of fetal development showed the highest incidence of cranio-facial dysplasias. Median jaw and tooth fusion was prominent in all but one of the strains of mice. Basically the lower jaw was more resistant to teratogenic effects of x irradiation than was the upper jaw. According to these studies the anterior jaw area was the most sensitive to x irradiation during the

sixth day of fetal development. The experimental findings showed that there was a close relation between a narrowly bounded phase of organogenesis and the normal or aberrant differentiation of particular areas of the cranial anlage. In the mouse it was restricted to the advanced second stage of primitive development before beginning of neurulation. For humans this phase corresponds approximately to the second half of the third week of pregnancy. This indicates that the normal or abnormal genesis of the human fetus will be determined at a point in time when many mothers will still not be aware of their pregnancy. (BBB)

5396 POSITIVE AND NEGATIVE CHEMOTAXIS AS OBSERVED AFTER THE DESTRUCTION OF A CELL BY U. V. OR LASER MICROBEAMS. Bessis, M.; Burte, B. (Centre National de la Transfusion Sanguine, Paris). Tex. Rep. Biol. Med., 23: Suppl.1, 204-12(June 1965).

In the course of experiments on the effects of uv and laser microbeam irradiation on living cells, the effect of the cells' death upon the surrounding leukocytes was observed. Necrotaxis was noted in leukocytes and erythrocytes. Negative chemotaxis, the repulsion of granulocytes by certain substances, was not observed. It was also shown in studies with Euglenae (Euglena viridis) that there is an immediate but momentary necrophobia or departure of all the animals from the vicinity where one of them has just been destroyed. However, after 3 to 4 min, the animals returned to the field but did not appear to notice the dead cell. Positive necrotaxis was the same whether the cell destroyed was a polymorph, a lymphocyte, or a red blood cell. About one second after the destruction of one of these cells, a pronounced movement of certain leukocytes toward the damaged cell was seen. In general, the neutrophils move more rapidly than the eosinophils which in turn are more rapid than the monocytes. Observations of time-lapse films show that after the irradiated cell has shown signs of incipient death, neighboring healthy cells begin to move toward the corpse from all directions. In a few minutes the so-called foreign body rosette of classical pathology was formed. These cells literally tear the corpse apart. Phagocytosis was almost immediate. Granulocytes were attracted only as a cellular death agony took place. (TCO)

5397 HOST-GRAFT AGGLUTININ ACTIVITY BY SPLEEN CELLS OF HETEROLOGOUS RADIATION CHIMERAS CULTIVATED IN DIFFUSION CHAMBERS. Urso, Paul (Seton Hall Univ., South Orange, N. J.); Gengozian, Nazareth. Transplantation, 3: 762-4(Nov. 1965).

Spleen cells obtained from lethally x irradiated mice during the second month after treatment with rat bone marrow were cultivated in diffusion chambers implanted into untreated rats and mice. Rat anti-mouse and mouse anti-rat RBC agglutinins were detected in the chamber fluids, suggesting that immunologically competent cells of graft and host type exist simultaneously in the spleens of heterologous radiation chimeras. (auth)

5398 ON THE THOROTRAST PROBLEM. Bluemel, G.; Lehner, R.; Zaunbauer, W. (Univ., Vienna). Wien. Med. Wochensch., 114: 345-8(May 16, 1964). (In German).

Circulatory disturbances were observed in the lower extremities of 5 patients who had been injected about 20 yr previously with Thorotrast. Extensive deposits of Thorotrast were found in the inguinal regions of the patients, as well as in adjacent lymph nodes, liver, and spleen. The patients had been injected either unilaterally or bilaterally in the inguinal region by intra- or extravasal routes. One patient had an ulcerated inguinal Thorotrast granuloma, but there was no evidence of malignant growth in any of the patients. Radiological measurements were made. The results of these measurements when compared with those in the literature suggested that the dosage values estimated to be received by whole organs from deposited Thorotrast may be too high. However, in the immediate proximity of deposited Thorotrast particles the dose may be underestimated. Pulse height analysis measurements made with the patients indicated the presence of ^{232}Th, ^{224}Ra, and ^{228}Ac in the areas where Thorotrast deposits were observed. It was not possible to remove any of the radioactive materials by surgical procedures. (BBB)

5399 CONCLUDING WORD TO THE CURRENT REMARKS OF P. KOEPPE. Bluemel, G.; Lehner, R.; Zaunbauer, W. (Univ., Vienna). Wien. Med. Wochensch., 115: 223-4(1965). (In German).

The radioactive material deposited as Thorotrast in lymph nodes was identified in ashed nodes using relatively simple measurement apparatus. The characteristics of Th decay products are tabulated. It was concluded that the decay products of ^{232}Th and ^{228}Th do not play an important role in the irradiation effect produced after injection of Thorotrast because of their relatively selective excretion. For this reason they do not attain radioactive equilibrium with ^{228}Th in the body. The number of α particles alone, without consideration of particle energy, is insufficient for estimation of dose. (BBB)

5400 REMARKS ON THE WORK "ON THE THOROTRAST PROBLEM" OF G. BLUEMEL, R. LEHNER, AND W. ZAUNBAUER. Koeppe, P. (Univ., Berlin). Wien. Med. Wochensch., 115: 222-3(Mar. 13, 1965). (In German).

Although freshly prepared Th essentially contains only ^{232}Th and ^{228}Th, the decay products of ^{228}Th form so rapidly that within four days after separation they reach 50% of their equilibrium value. The full equilibrium value between ^{228}Th and its decay products is reached within a month. Since there is usually several days delay before the processed Thorotrast is injected, there is a considerable buildup of ^{228}Th decay products. The author points out that the number of α particles is more significant for the irradiation received than the number of α emitters that may be present. (BBB)

5401 PHOTOSYNTHETIC REACTIONS IN UV-IRRADIATED CHLOROPLASTS. Trebst, Achim; Pistorius, Elfriede (Univ., Goettingen, Ger.). Z. Naturforsch., 20b: 885-9(Sept. 1965). (In German).

Photosynthetic reactions in isolated chloroplast fragments were investigated after they had been exposed to UV-light of 254 mμ, which is found to destroy the endogenous plastoquinone. The oxygen evolution is the most UV sensitive photosynthetic reaction. The ATP formation in the noncyclic and in the cyclic system with vitamin K_5 as cofactor is less sensitive; the inactivation goes parallel to the destruction of the plastoquinone of the chloroplasts. Cyclic photophosphorylation with PMS as cofactor is diminished only after longer UV-irradiation. Photosynthetic reduction of NADP at the expense of an artificial electron donor system like DAD/ascorbate is not inactivated even after prolonged UV-exposure of the chloroplasts and therefore requires no plastoquinone. This indicates again, that the site of function of plastoquinone is close to the second light-reaction of photosynthesis. (tr-auth)

5402 EFFECT OF X RAYS ON CHLOROPLAST REACTIONS AND THE PROTECTIVE EFFECT OF ASCORBATE. Jacobi, Guenter (Tieraerztliche Hochschule, Hanover). Z. Naturforsch., 20b: 911-14(Sept. 1965). (In German).

Intact isolated chloroplasts were irradiated with x rays and tested for the inactivation of oxygen evolution, ATP-formation, and photoreduction of NADP. In accordance with results published previously, phosphorylation is the most sensitive process influenced by x rays. In the presence of ascorbate, phosphorylation is partly protected, presumably at the site of ascorbate induced phosphorylation. (tr-auth)

5403 STUDIES ON THE RELATION BETWEEN RADIATION SENSITIVITY, MUTATION FREQUENCY, AND DEGREE OF POLYPLOIDY IN THE GENUS TRITICUM. Gottschalk, W.; Imam, M. (Univ., Bonn). Z. Pflanzenzuecht., 53: 344-70(Aug. 1965). (In German).

The seeds of two diploid, nine tetraploid, and two hexaploid species or varieties of wheat were irradiated with

doses of 10 to 32.5 kR of x rays. The X_1 and X_2 generations were examined. On the basis of germination, the material tested could be divided into two groups differing in radiation sensitivity. There was no direct relation between the degree of radiosensitivity and the degree of polyploidy. The variety rufinigrum of the diploid species T. boeoticum was particularly sensitive whereas varieties valenciae of T. durum (=4 n) and lutescens of T. aestivum (=6 n) were considerably more resistant. The low radiation sensitivity of the tetraploid variety valenciae and the hexaploid variety lutescens was expressed in an analogous manner in classification for degree of tillering, length of stem, and fertility relation of the X_1 generation. On the basis of germination of the irradiated seeds and plant height, a negative correlation with dose was demonstrated and for number of tillers per plant a positive correlation. The curves for degree of fertility of the X_1 plants initially showed a fall and then a rapid rise. The behavior of these curves indicated a correlation between the negative effect of irradiation, on the one hand, and the positive influence, on the other, of the improved spacing relations in the plots with the high irradiation doses. In the X_2 generation, 242 different mutation types, mainly forms with chlorophyll defects, were detected. A high deficit of recessives was observed in their segregation ratios and this was confirmed in a further series of experiments. In terms of mutation frequency, no fundamental difference could be established between the diploid and tetraploid material tested. The mutation rate for the hexaploid forms was, however, considerably lower; it was of the order of $^1/_{40}$ of the value for the other two polyploid levels. Wide variations were observed within the tetraploid group. It is concluded that the degree of radiation sensitivity of an organism is dependent not only on the number of genomes present but on the composition of the genome. (BBB)

5404 RADIOBIOLOGICAL EFFECTS OF GAMMA RAYS ON POTATOES. Roze, K. K. (Inst. of Biology, Academy of Sciences, Latvain SSR). pp 137-49 of Tautsaimnieciba Derigie Augi. II. Riga, Lajvijas PSR Zinatnu Akademijas Izdevnieciba, 1963. (In Latvian).

The irradiation of early potatoes with small doses (200 to 400 R) of γ rays increases the number of tubers in the clusters and under favorable growing conditions can give in a later harvest some increase in yields. Protracted irradiation of growing plants of early potatoes with small doses (of the order of 200 to 300 R in all periods of vegetation) gives similar results. From the effect of γ rays (2000 to 4000 R) on intergrown tubers of red tuber hybrids, recessive-type mutations were obtained. The economic nature and the cytology of the individual plants were studied. Irradiation with γ rays of two types of potatoes for the purpose of lengthening the storage term showed that in unrefrigerated storage (temperature from 10 to 16°C) the samples irradiated with 300 R do not give seedlings during 8 months of storage. From preliminary data it appears that the irradiation dose can be reduced to 6000 to 7000 R. (tr-auth)

5405 MAMMALIAN RADIATION LETHALITY. A DISTURBANCE IN CELLULAR KINETICS. Bond, Victor P.; Fliedner, Theodor M.; Archambeau, John O. An American Inst. of Biological Sciences and United States Atomic Energy Commission Monograph. New York, Academic Press, 1965. 211p. $9.50.

A comprehensive treatment of the short-term effects of a single exposure to large doses of ionizing radiation in the mammal is presented. While it deals in detail with what is known about the pathogenesis and manifestations of radiation injury, it is oriented throughout to the underlying cellular changes. The book deals initially with the normal cell cycle and the cell kinetics of the principal organs responsible for the observed radiation syndromes. Principles of cellular radiobiology and the extent to which the manifestations of single-large-dose exposure of mammals can be explained in terms of time and dose dependency and on the basis of the responsible cell and cell population changes that lead to the depletion of mature functional cells necessary for well-being and for survival are discussed. The manifestations of single high-dose exposure in man are explained. The differences between the exposure conditions and effects seen in accidents vs controlled laboratory conditions are pointed out. A chapter on the therapy of radiation illness in relation to the therapeutic measure providing an understanding of the basic mechanisms involved in the initial injury is included. (H.G.D.)

5406 RECURRENT INTERCROSSING COUPLED WITH NEUTRON IRRADIATION AS A MEANS OF INCREASING GENETIC VARIABILITY IN NAVY BEANS (PHASEOLUS VULGARIS L.) [Thesis]. Pinchinat, Antonio Michael. East Lansing, Mich., Michigan State Univ., 1964. 64p.

The hypothesis was proposed that a combination of irradiated and recurrent intercrossing would generate more variability in a complex trait than would either method alone. To test it, 10 homozygous lines of navy beans were crossed in all possible combinations. Each of the resulting 45 first cycle intercrosses was simultaneously selfed for seed increase and out-crossed to 4 unrelated hybrids. These second cycle intercrosses were also selfed afterwards to produce enough seed for the subsequent treatments. Then each group, including the original parents, was split into two lots: one to be neutron-irradiated and the other kept as control. They were grown in bulk for two years and as single plant progenies the third year. The statistical analysis of the recorded data indicated that the combination of recurrent intercrossing and irradiation increased both variances and coefficients of variability of yield and its components more than did either alone. Intercrossing alone rated better than the radiation treatment per se. But only a few isolated significant changes in treatment means emerged. Apparently the neutron dosage applied was not high enough to produce drastic effects. (TCO)

Radiation Effects Therapy and Countermeasures

5407 (AD-623599, pp 37-44) FURTHER STUDIES ON THE DOSE REDUCTION FACTOR FOR RADIATION LETHALITY IN MICE AS A FUNCTION OF THE DOSE OF MERCAPTOETHYLAMINE. Hasegawa, A. T.; Landahl, H. D. (USAF Radiation Lab., Univ. of Chicago, Ill.).

The radioprotective effect of mercaptoethylamine (MEA) when given in doses of 750 and 900 mgm/kgm to mice exposed to 450 R, 510 R, or 570 R x radiation was investigated. The effect of these doses on the oxygen tension and sulfhydryl levels in the spleens of mice were also studied. The mortality up through the third day after MEA injection and x ray exposure was 7%, 24.8%, and 45% for 600, 750, and 900 mgm/kgm respectively. The mortality was 9%, 17.3%, and 23.2% for intravenous doses of 500, 550, and 600 mgm/kgm. Of the total 3-day mortality, 60.7% occurred shortly after irradiation, 30.1% on the next day, 5.0% on the second, and 4.2% on the third day. The 3-day mortality did not appear to be related to the amount of x ray dose administered. Polarographic measurements of the oxygen tension in the spleen showed a tendency for the oxygen tension level to rise slightly during the 30-minute period following the injection of 300, 600, 750, and 900 mgm/kgm of MEA. Polarographic measurements of the sulfhydryl level in the spleen following the injection of 750 and 900 mgm/kgm of MEA showed the levels to rise to about 4 and 5 times original values in 7 to 11 minutes. (auth)

5408 (USNRDL-TR-920) HOMOGRAFT RESPONSE AND HEMAGGLUTININ PRODUCTION BY SENSITIZED THYMECTOMIZED IRRADIATED ADULT MICE. Tyan, M. L.; Cole, L. J. (Naval Radiological Defense Lab., San Francisco, Calif.). Oct. 13, 1965. 25p. CFSTI $1.00 cy, $0.50 mn.

Thymectomized and nonoperated male B6D2F_1 mice were sensitized by the following means: an allogeneic (A/HeJ) skin graft; three subcutaneous injections of A/HeJ spleen cells in Freund's complete adjuvant; and three intraperi-

toneal injections of A/HeJ spleen cells. One week after the last injection, thymectomized and nonoperated mice from each group received 870 rad whole-body x radiation. The mice were grafted with A/HeJ and rat skin 102, 143, 184, 205, and 225 days after irradiation. Sera were obtained frequently for anti-A/HeJ and anti-rat hemagglutinins. The results indicated that although both hemagglutinin production and the homograft response were initially greatly impaired by thymectomy and lethal irradiation, repeated antigenic challenge resulted in return of the specific homograft response to near normal reactivity while antibody production became progressively more impaired. The results suggested that: antibody production and homograft sensitivity are manifestations of immunologic responses by associated but distinct cell populations; antibody production is more thymus-dependent than is the homograft response; and the method of sensitization employed determines both the relative and absolute number of sensitized cells produced within each cell population. (auth)

5409 BACKGROUND RADIATIONS AND THEIR ORIGINS. Mayneord, M. V. (Inst. of Cancer Research, London). Advance. Sci., 21: 127-31(July 1964).

Some data relating to human exposure to natural and artificial radioactivity in the environment are reviewed. Data on natural radioactivity in soil and drinking water in various regions of England are reported. Surface water in regions of high radioactive soil content are often relatively low in activity, the material evidently being relatively insoluble or absorbed on its way to or during storage. Some spa waters are very active and contain, besides radium, relatively large amounts of radon, far in excess of that to be expected from their radium contents. How this high gaseous activity arises is unknown. Very variable amounts of natural radioactivity are found in foods. High values are found particularly in cereals and about 70% of the α radioactivity normally eaten per day by the population of England comes from this source. In spite of the large variations from food the mean amount of radioactivity taken in per day is surprisingly independent of economic circumstances or geographical region, although it is difficult to make reliable estimates even with relatively good statistical data. Little is known of what amount of natural radiation is received by the world's population or what amount of radioactivity is ingested per day. The mean daily intake of radium per day estimated in England is 2.5 $\mu\mu$C, but much the largest absolute amount of radioactivity taken in per day is as ^{40}K. The largest man-made contribution to the irradiation of the population is that of diagnostic radiology, the doses contributed by radiotherapy or internally administered isotopes being very small. In diagnostic radiology, however, the doses are relatively high, even averaged over the population, being in England 15% of the natural background. Moreover, the doses are given at high dose rates sometimes to a most sensitive fraction of the population, namely unborn children. There is growing recognition of the problem and by good technique the doses may be substantially reduced. (BBB)

5410 STUDIES ON CHEMICAL PROTECTORS AGAINST RADIATION INJURY. I. RADIOPROTECTIVE EFFECT OF 2-AMINOTHIAZOLINE SALTS AGAINST LETHAL DOSES OF GAMMA IRRADIATION. Taira, Kazumasa; Katsuhara, Ryo; Kubota, Masayuki. Boei Eisei, 12: 99-105(1965). (In Japanese).

Twenty organic and inorganic salts of 2-aminothiazoline (2-AT) were synthesized as potential protective agents against radiation injury. The LD_{50} values of the compounds in the dd strain of mice were determined. Their radioprotective effect was tested in mice of the same strain by injection before γ irradiation with whole-body doses of 1090 R. The 30-day mortality rates of the various compounds were compared with that for AET, which gave 33% 30-day survivors. The corresponding values for the various salts of 2-AT were: hydrobromide 21% 30-day survivors, sulfate 0%, acetate 12%, succinate 28%, glutamate 24%, fumarate 27%, adipate 15%, benzoate 25%, p-aminobenzoate 12%, mandelate 0%, formate 0%, malonate 10%, cinnamate 0%, and nicotinate 0%. Of these salts, on a molar basis, 2-AT acetate and malenate were found to be most effective, and 2-AT glutamate, fumarate, succinate, benzoate gave effects similar to those of 2-AT hydrobromide. Some of the organic salts tested, such as 2-AT adipate, succinate, cinnamate, nicotinate were less toxic than the inorganic salts, such as 2-AT hydrobromide or hydrochloride. (BBB)

5411 SUPPRESSION OF THE DIARRHEA PROVOKED IN THE RAT BY A FATAL DOSE OF X RAYS. Loiseleur, Jean; Catinot, Liliane; de Vomecourt, Annick (Institut Pasteur, Paris). Compt. Rend., 261: 2415-16(Sept. 20, 1965). (In French).

The serum of a rabbit that had received two successive irradiations on the intestinal region prevents the appearance of diarrhea in a rat that has received 1000 R in whole-body irradiation. The treatment is efficacious for 39% of the animals. (tr-auth)

5412 THE INFLUENCE PRODUCED BY HOMOGENATES OF DIFFERENT TISSUES ON THE RADIOPROTECTIVE ACTIVITY OF CYSTAMINE IN THE PROCESS OF IRRADIATION OF CELLS OF EHRLICH'S ASCITIC CARCINOMA IN VITRO. Nekrasova, I. V. (Severtsov Inst. of Animal Morphology, Academy of Sciences, USSR). Dokl. Akad. Nauk SSSR, 162: 950-1(June 1, 1965). (In Russian).

Ehrlich ascitic cancer cells and tissue homogenates containing 100 mg of muscle, thymus, spleen, liver, or ascitic cell homogenate were mixed in a ratio of 1:5 (0.2 ml of homogenate containing 100 mg of tissue per 1 ml of ascitic cells). A total of 0.6 mg of cystamine was added, and the samples were held for 20 minutes at 37°C. Then an x ray dose of 700 R was given to the samples. Immediately after irradiation 1 ml of sample was given intraperitoneally to intact mice, and 24 hours later the mice were killed and smears were prepared from the ascitic liquid. The number of cells with chromosome bridges and acentric fragments at anaphase or early telophase was taken as a criterion of radiation damage. The results show that the homogenates of muscle tissue and ascitic cells were ineffective. On the other hand, homogenates of liver, spleen, and thymus tissue enhanced the radioprotective activity of the cystamine outside of the organism. Apparently liver, spleen, and thymus contain a reducing agent that can convert cystamine to cysteine. (TTT)

5413 INFLUENCE OF CYSTAMINE ON THE IMMUNIZATION PHENOMENA AFTER WHOLE-BODY IRRADIATION. Booz, G.; Simar, L. J.; Betz, E. H. (Univ., Liege). Int. J. Radiat. Biol., 9: 429-34(1965). (In French).

Whole-body x irradiation (450 R) inhibited the development of hemagglutinins against sheep erythrocytes in mice when the cells were injected 24 hr after irradiation. Seven days after irradiation there was an incomplete recovery of antibody production. The injection of cystamine had only a slight protective effect on the antibody synthesis when immunization was started 24 hr after irradiation. The protective effect was more marked when the erythrocytes were injected 7 days after the x-ray exposure. Whole-body x irradiation also inhibited the development of transplantation immunity induced by a sarcoma graft. The administration of cystamine had a protective effect. The number of spontaneous regressions was much higher in the irradiated and protected mice than in irradiated controls. (C.H.)

5414 THE EFFECTS OF FREEZING ON THE RADIATION SENSITIVITY OF RAT THYMOCYTES. Tanaka, Y.; Rixon, R. H. (Atomic Energy of Canada Ltd., Chalk River, Ontario). Inst. J. Radiat. Biol., 9: 503-7(1965).

Isolated rat thymocytes were found to survive short periods in the frozen state and to display a marked reduction in radiosensitivity when frozen and exposed to 100 to 900 R γ radiation in the presence of oxygen. This decrease in radiosensitivity was not apparent when the cells were frozen in the absence of oxygen or in the presence of cysteamine. (C.H.)

5415 A REVIEW OF THE LITERATURE ON BURNS AND TRAUMA, SEPTEMBER 1963 TO AUGUST 1964.

Kernahan, D. A. (Univ. of Manitoba, Winnipeg, Can.). Med. Serv. J. Can., 21: 117-50(Feb. 1965).

An extensive review of the literature is given, including reports on injury from radiation. Reports from both Canada and the United Kingdom indicate that radioactive fallout is still being closely watched. Any causal relation between fallout and ill effects, particularly upon infants, is unlikely to be demonstrated at the present time, providing nuclear weapon testing is not resumed. Radiological practice is at present the largest single contribution to the average annual radiation dose the population receives. The 1962 ^{90}Sr levels in the bones of British children were still less than 5% of the permissible levels even in the most heavily contaminated children. The United Kingdom Agricultural Research Council's Radiological Laboratory found that, in the six-to-12-month age group, the 1962 values are less than three-quarters of the 1958 levels. Following resumption of nuclear testing in September 1962, fallout over England increased, but even in areas of heavy rainfall did not reach anywhere near the cautionary level. Radiation protection in Canada is described in two articles giving an account of the role of the Radiation Protection Division of the Department of National Health and Welfare. (426 references.) (BBB)

5416 MEANS OF PROTECTION FROM FALLOUT OF NUCLEAR AND THERMONUCLEAR EXPLOSIONS. Gennarelli, L. (Centro Oncologico, Ancona, Italy). Minerva Med., 55: 355-6(Feb. 10, 1964). (In Italian).

The effects of explosions of thermonuclear weapons are discussed with reference to protective measures for human populations. The discussion is based on postulated destruction, immediate radiation, and fallout from detonation of a 20-Mt weapon in a populated area. For such a weapon the destructive and thermal effects would extend for 40 km, and radioactivity from fallout would be appreciable up to 300 km. Problems associated with protection from early and late fallout are considered, along with meteorologic factors that would affect the intensity of fallout in various situations. Requirements for protective shelters against fallout are outlined. It is estimated that seven hr after a detonation the ambient radioactivity would fall to $1/10$ the initial level and by 49 hr to $1/100$ that present initially. The β emission of ^{14}C would be one of the most serious consequences in humans in the postattack phase; ^{137}Cs, ^{90}Sr, and ^{131}I would also be highly hazardous although their half lives are much shorter than that of ^{14}C. Various methods whereby the body burden of these radionuclides could be reduced in the postattack phase, such as by giving Lugol's solution (containing ^{127}I-iodide) to infants to lower ^{131}I uptake by the thyroid, are presented. (BBB)

5417 THE INDUCTION OF REPARABLE PERMUTATIONAL DAMAGE IN PARAMECIUM AURELIA BY THE ALKYLATING AGENT TRIETHYLENE MELAMINE. Kimball, R. F. (Oak Ridge National Lab., Tenn.). Mutat. Res., 2: 413-25(Nov. 5, 1965). (ORNL-P-1214).

Triethylene melamine (TEM) induces lethal and slow-growth mutations in Paramecium aurelia at doses well below those that affect survival or the duration of the cell cycle. The pattern of mutation induction during the cell cycle is much like that found for x rays, with the maximum yield just before DNA synthesis as expected if most of the mutations arise by errors in replication. It differs from that for x rays in having an appreciable yield in G_2, though the yield is smaller than in G_1. Posttreatment with streptomycin reduces the yield of mutations induced in either G_1 or G_2, showing that both must come from initially reversible steps. When the mutagenic treatment is given in the G_1 period, the yield can be decreased by subsequent treatment with streptomycin only if it is begun within the same period. When the mutagenic treatment is given in G_2, the yield can be decreased by streptomycin treatment in the remaining part of the same cell cycle and also in the G_1 period of the next cell cycle. It is concluded that TEM, like x rays, induces initially reparable premutational damage that is converted to final mutation at DNA synthesis. Most of the TEM mutations affect only a half or a quarter of the progeny by cell division from the initial cell in which a mutation was induced, whereas most x-ray-induced mutations affect all progeny of such cells. The pattern of distribution shows that at least part of the mutations involve an effect on the old as well as the new strands, but it also shows that the initial damage produced by TEM differs basically from that produced by x rays. Consequently it may be concluded that P. aurelia is capable of repairing at least two, quite possibly more, initially different kinds of premutational damage. (auth)

5418 STUDIES ON CHEMICAL PROTECTION AGAINST RADIATION INJURIES IN CULTURED L-STRAIN CELLS IN VITRO. 1. PROTECTIVE EFFECTS OF CYSTEINE AND 2-MERCAPTOETHYLAMINE (MEA) IN CULTURED L-STRAIN CELLS AGAINST X IRRADIATION. Ando, Norio (Okayama Univ., Japan). Okayama Igakkai Zasshi, 77: 181-200(Jan. 1965). (In Japanese).

The protective effects of cysteine and MEA against x irradiation were investigated in vitro by comparing the population of cultured L-strain cells of the treated groups with that of the control groups two days and four days after 400 or 800 R irradiation. The protective effect of 10^{-4} M cysteine was observed to be significant at two days after 800 R irradiation. Cysteine (10^{-5} M) was significantly effective at two and four days after 800 R irradiation. MEA seemed to be more effective than cystine. (131 references.) (BBB)

5419 STUDIES ON CHEMICAL PROTECTION AGAINST RADIATION INJURIES IN CULTURED L-STRAIN CELLS IN VITRO. 2. PROTECTIVE EFFECTS OF S-2-AMINOETHYLISOTHIURONIUM Br–HBr (AET), CYSTAMINE, AND HOMOCYSTEINETHIOLACTONE (HCT) IN CULTURED L-STRAIN CELLS AGAINST X IRRADIATION. Ando, Norio (Okayama Univ., Japan). Okayama Igakkai Zasshi, 77: 201-14(Jan. 1965). (In Japanese).

The protective effects of AET, cystamine, and HCT against radiation injuries in cultured L-strain cells were studied by comparing the cell population of the treated groups with that of the irradiated control groups two and four days after 400 or 800 R x irradiation. The protective effect of 10^{-4} M AET was observed to be significant in both 400 and 800 R irradiated groups. The protective effect of 10^{-3} M AET was observed both two and four days after irradiation. Protective effects were not observed in cystamine and HCT treated cells. (BBB)

5420 HEMATOPOIETIC CELL GRAFTS AND THEIR APPLICATIONS. Mathe, Georges (Hopital Paul-Brousse, Villejuif, France). Presse Med., 72: 2391-4(Oct. 3, 1964). (In French).

Successful grafts of isogenic blood-forming cells are not difficult to achieve. They are utilized when the bone marrow has been destroyed, as after total-body irradiation. It is probable that the isogenic grafts provide transitory function and the recipient's own bone marrow function is restored over a period of time. Chromosome anomalies, known to be induced by irradiation, have been observed after restoration by grafts. The author's clinical studies included 23 patients, divided into three groups: (1) eight leukemic patients who were exposed to 200 to 400 R by x rays or the betatron, (2) five patients who were accidentally exposed to γ rays or neutrons to an LD_{75} for four and LD_{30} for the fifth case, and (3) ten leukemic patients who were irradiated in toto by an 800-R dose of ^{60}Co γ radiation. In group one, allogenic bone marrow was transplanted, but no grafts took. In group two, transplantation was followed by restoration of the blood-forming tissues. Autologous bone-marrow cell production was restored, and no secondary syndrome appeared because of the transitory nature of the graft. The third group received allogenic marrow transfusions. Four died, but one other was restored by an isogenic transfusion. All the others underwent restoration of marrow function, although some exhibited severe secondary syndromes. (47 references.) (BBB)

5421 ON THE ROLE OF THE VEGETATIVE NERVOUS SYSTEM IN TRANSFERRING REMOTE RADIATION

EFFECTS. Domareva, O. P. (Inst. of Genetics, Moscow). Radiobiologiya, 5: 707-12(1965). (In Russian).

Male mice 2 to 3 months old whose heads were covered with a lead shield were given an x ray dose of 600 R. Redergam and hexonium, which were nerve blocking agents, were administered subcutaneously to the mice or by dripping directly on the cornea before irradiation. Controls were irradiated mice who were given a 1% physiological solution in place of the nerve blocking agent. Unirradiated mice who were given the nerve blocking agent served as a second control. Intact mice served as the third control. The cornea was fixed two hours after irradiation, and the mitotic activity was determined microscopically. The results showed that the number of mitoses per 100 fields was 379 for the unirradiated mice given the nerve blocking agent redergam compared to a value of 339 for the unirradiated controls given physiological solution. The values were 319 and 295 respectively for the irradiated mice. The values were 490 and 348 respectively when the nerve blocking agent was put directly in the eye of the unirradiated mice. The values were 367 and 284 respectively for the irradiated mice with the nerve blocking agent put directly in the eye. Similar results were obtained with the use of the nerve blocking agent, hexonium. It is assumed that cell division in the cornea epithelium is regulated by means of adrenaline secreted by the adrenal glands. By blocking the nerve endings or nerve ganglions, the secretion of excess adrenaline is suppressed, and a decrease in mitotic activity does not take place. (TTT)

5422 MODEL STUDY OF PROTECTIVE CHARACTERISTICS OF SOME RADIOPROTECTORS. Pisarevskii, A. N.; Selesnev, A. F.; Pashek, G. M. (Belorussian State Univ., Minsk). Radiobiologiya, 5: 768-70(1965). (In Russian).

A liquid scintillator system was used as a model for studying the radioprotective properties of certain chemical compounds. Changes in the scintillating ability of dioxane as a result of admixtures was used as a measure of the changes in the protective action of the material studied, using a scintillation counter and an analyzer system for the determinations. The 661-kev γ line of ^{137}Cs was used as the excitation source for obtaining absorption and luminescence spectra. The material under study was introduced into the dioxane as an acid aqueous solution with a concentration of 20 g/l; the results were compared with those obtained using a water scintillator of the same acidity. The results indicated that S-β-aminoethylisothiuronium bromide, β-mercaptopropylamine, and 5-methoxytryptamine have nearly identical protective action while serotonin did not appear to possess any radioprotective ability. Comparison of the characteristics obtained by means of this model with the known protective properties of these materials indicated that the discharge of the excitation energy is of great importance for the determination of the radioprotective mechanism. (TTT)

5423 A STUDY OF THE ACTION OF RADIOMIMETIC COMPOUNDS (NITROGEN MUSTARD) ON PROTEIN MACROMOLECULES. Furnica, Gheorghe; Dimitriu, Aurora (Inst. of Hygiene and Occupational Safety, Bucharest). Rev. Roum. Biochim., 1: 31-40(1964). (In French).

These experiments were conducted with several chemical agents with actions resembling those of ionizing radiation, and with radioprotective compounds, to investigate the mechanism by which radiation and these agents damage macromolecules and how they are protected by substances such as AET [S-(2-aminoethyl)isothiuronium bromide hydrobromide]. Using chromatography, a study was made of the modifications of several amino acids in aqueous solutions (pH 5.6, 7.2, or 8.6; 37°C) after incubation with sarcolysine or Degranol for three or 24 hr. Using the same method, the modifications were studied of serum albumin hydrolyzates incubated with sarcolysine or Degranol (pH 7.5, 8.6, or 9.6) for one or eight hr. A third series was carried out similar to the above, but 15 min before adding nitrogen mustard, AET was added. In the presence of sarcolysine, cystine, lysine, arginine, taurine, serine, glycine, glutamic acid, threonine, valine, and leucine formed intermolecular complexes; phenylalanine and alanine did not. The speed of the reactions was modified by length of time and pH. Sarcolysine showed the greatest affinity for threonine. Degranol showed a great affinity for serine, arginine, and alanine. The greater intensity of the chromatographic spots of taurine, glycine, glutamic acid, tyrosine, and methionine indicated a new intramolecular arrangement of the peptide chain, caused by the breaking of certain bonds and freeing of the amino acids. This phenomenon was explained by the bond between AET and the polypeptide chain. It appeared that sarcolysine attached itself to cystine, lysine, histidine, and, probably, the glycine of the polypeptide chain when the pH was 8.6 and to arginine when the pH was 7.6. AET, in the serum albumin solution, was able to ameliorate certain modifications caused by sarcolysine. (BBB)

5424 BIBLIOGRAPHY OF HEMATOPOIETIC TISSUE TRANSPLANTATION. Addendum No. 2. Sekiguchi, Morimasa (comp.). Transplantation, 3: 769-801(Nov. 1965).

A list is presented of 815 references to literature on the transplantation of hematopoietic tissues, the effects of radiation on immune reactions to hematopoietic transplants, and the use of hematopoietic transplants in the treatment of radiation injuries. (C.H.)

Radiation Hazards and Protection

See also HEALTH AND SAFETY

5425 (NP-15543, pp 77-82) RECHERCHES ET APPLICATIONS PRATIQUES DE RADIOPROTECTION EN ROUMANIE (1958-1964). (Investigations and Practical Applications of Radioprotection in Rumania, 1958-1964). Costachel, O. (Rumanian Committee for Nuclear Energy, Bucharest).

Because of the continuous increase in the number of workers involved with radioactivity (from 352 in 1957 to 1023 in 1963), the Committee for Nuclear Energy of the Council of Ministers, the Ministry of Health and of Social Welfare, and the Commission of Radiology of the Academy of the R.P.R. have legislated radioprotection, introduced individual dosimetry and dosimetry of radiation fields, and created 15 laboratories for radiation hygiene and 10 for radiation medicine. The existence and major importance of the indirect biological effect in the realization of biological radioprotection (graft of bone marrow), especially after the experimental application of dangerous or lethal doses, are discussed. The effects of radiations on synthetic macromolecules, variations of nucleic acids of the tissues and organs after irradiation, indirect radiobiological effect on the hemocytopoietic tissue, and effects of narcosis and neuroplegy on the radiobiological effect are considered. (tr-auth)

5426 SYSTEMATIC ARC CALIBRATION METHOD FOR BODY RADIOACTIVITY MEASUREMENT. Lillegraven, A. L.; Rundo, J. (Atomic Energy Research Establishment, Harwell, England). Acta Radiol. Therapy, Phys., Biol. (N.S.), 3: 369-83(Oct. 1965).

In the arc technique for calibrating whole-body counting arrangements, the radiation emitted by the body is simulated by that from a point source in a phantom. A procedure is described in which phantom spectrum information is extracted systematically and then used for preparing a calibration chart which can be employed in all subsequent body activity measurements of the same nuclide. Its application is illustrated by the results of measurements on five human subjects after their intake of strontium-85. (auth)

5427 USAF WHOLE BODY GAMMA SPECTROMETRY. Burner, Alvin M.; Benson, Richard E.; Thomas, Robert G. (Wright-Patterson Air Force Base, Ohio). Aerospace Med., 36: 864-8(Sept. 1965).

The design and initial operation of the whole-body γ-spectrometry facility established in the USAF Radiological Health Laboratory at Wright–Patterson AFB are described. In particular, experience concerning background activity, which has been observed to vary by as much as 40% during an eight-hr period, is discussed. Such variation poses a serious problem for accurate calibration and measurement of in vivo radioactivity. Studies undertaken to identify the sources of the variation in background activity and actions taken to limit the magnitude of the variation are reported. Techniques employed for calibration of the whole body counter are emphasized. Studies involving human subjects and phantoms to demonstrate the influence of factors such as body size and changing distribution of nuclides within the body upon in vivo counting efficiency are described. The importance and application of whole-body γ spectrometry in support of Air Force aerospace missions are discussed. Astronauts, whose missions take them far beyond the earth's atmosphere, will be exposed to the hazards of cosmic radiation, solar flares, and Van Allen zones of trapped particles, and secondary radiations. Because of the uncertainties and unknowns concerning the existence, magnitude, and extent of these biological hazards, whole-body γ-spectrometric evaluation of individuals participating in these missions may prove to be a valuable aid to the total effort directed toward assessment and documentation of the environmental hazards involved. (BBB)

5428 RADIATION PROTECTION OF PERSONNEL DURING URANIUM ORE MINING. Bykhovskii, A. V.; Chesnokov, N. I.; Shalaev, I. L. At. Energ. (USSR), 19: 161-8(Aug. 1965). (In Russian).

Radiation injuries to respiratory organs in personnel working in uranium mines were estimated and complex protective measures are discussed. Descriptions are given of measures for decontamination of the mine atmosphere and protection of miners against radioactive contamination of skin tissues in uranium mines. (R.V.J.)

5429 BIOLOGICAL DOSE OF ^{90}Sr INTERNAL IRRADIATION OF MAN. Malyhin, V. M.; Moiseev, A. A.; Shamov, V. P. At. Energ. (USSR), 19: 401-3(Oct. 1965). (In Russian).

Results of calculations of the levels of accumulation of ^{90}Sr in bone tissue of man as functions of time for an initial activity of 1 pC are presented for the step model using two different sets of parameters and for the exponential model. Formulas are developed for the internal absorbed dose accumulated in a given time for an initial burden of 1 pC of ^{90}Sr and for the biological dose as a function of the quantity of ^{90}Sr in the organism at the moment of observation. Results of calculations are presented of the factors giving absorbed dose to the skeleton as functions of time for an initial body burden of 10 nC of ^{90}Sr and for a body burden of 1 nC at the moment of observation, for the step and exponential models. (M.J.T.)

5430 SOURCES OF X RADIATION IN THE DENTAL OFFICE. Richards, Albert G. (Univ. of Michigan, Ann Arbor). Dent. Radiol. Phot., 37: 51-7, 64-8(1964).

The amounts of x radiation to which dentists are exposed occupationally were measured by the use of lead-walled pinhole cameras and x-ray film. Eight series of radiographs were made to record the relative intensities of the sources of secondary radiation to which the dentist would be exposed. The phantom head was composed of plastic shaped like a human head and contained a skull surrounded by water. The x-ray apparatus was operated at 90 kvp and 1.25 ma continuously for 12 hr to produce each series of radiographs. These measurements and those made with a roentgen rate meter showed the exposure dose rate to be lowest at positions on either side of the patient's head at an angle of 45° to the central ray. Positions at 90° to the central ray were next in order of safety. The radiographs indicated that when the tongue of the patient is irradiated, it becomes a potent source of secondary radiation, which can produce recognizable images of the teeth and jaws. Methods for protection from exposure to radiation leakage and secondary radiation are discussed. (TCO)

5431 RADIONUCLIDES IN FOOD. Lafontaine, A. (Institut d'Hygiene et d'Epidemiologie, Brussels). Food Cosmet. Toxicol., 2: 663-6(Dec. 1964). (In French).

The isotopes found in food which contribute to the natural background are ^{226}Ra, ^{40}K, ^{14}C, and ^{3}H; the first may deposit in the bones, but the next two are the most important sources of activity in food which may affect the body. Other isotopes resulting from nuclear explosions are also considered. Supplementary irradiation probably does not exceed 10% of the natural amount, but more than 100% of the natural background dose may be absorbed in medical diagnostic studies. One other source which might contribute eventually to the natural level in food is the activity induced by irradiation for sterilization purposes; if low energy sources are used, this danger is insignificant. Nevertheless certain risks are introduced by irradiation: alteration or destruction of essential items (amino acids, vitamins), formation of toxic substances, mutagenic or carcinogenic agent introduction, and selections and mutations in the microbiological population or in radioresistant virus populations. Further research is needed in these areas. (BBB)

5432 DEVELOPMENT OF A METHOD FOR LOW-LEVEL GAMMA RADIOACTIVITY MEASUREMENT WITH A STUDY OF SHORT-TERM VARIATIONS. Folsom, T. R.; (Scripps Inst. of Oceanography, La Jolla, Calif.); Mohanrao, G. J.; Betz, J. M.; Garber, W. F. J. Water Pollut. Contr. Federation, 37: 25-59(Jan. 1965).

The short-term variation of γ-emitting radionuclides was determined in the Los Angeles Hyperion Sewage Treatment Plant, its upstream system, and the downstream environment. Through use of γ radioassays, information was sought concerning lag properties, partition of the nuclides between solids and liquids, and short-term budgets equating input and output flows in portions of the plant. These measurements were made under actual working conditions with normal plant practices, and as much use as possible was made of sampling procedures already well developed. No use was made of deliberate tagging by introducing known amounts of nuclides. Actual radioactive load was identified and followed through the plant with radioactivity techniques, covering a wide range of fluctuation. Serious limitations were presented by the moderate value of the actual concentration load when studies of continuous γ monitoring were undertaken. Nevertheless, some measurements could be made to show what problems would be involved if early-warning continuous γ-radiation monitors were to be installed in a plant of this sort. This objective stems from interest in the load that is likely to come from a city in the future and means for preparing for this load and possibly policing it. This report is limited to the low fallout period preceding the renewal of nuclear weapons test in October 1961. During this period, short-lived fallout fission products became greatly attenuated by decay, making it possible to follow relatively small concentrations of the relatively long-lived nuclides such as ^{137}Cs and ^{60}Co, as well as ^{131}I. Data are given for the fluctuations of levels of these nuclides in raw sewage and dried sludge. Concentrations of radioactivity observed were well below what is considered acceptable in drinking water. (BBB)

5433 ON HEALTH PROTECTION AGAINST THE DANGERS OF IONIZING RADIATION IN THE HOSPITAL AREA. Buzzi, G.; Franco, L.; Veronesi, G. (Ospedale dei Santi Antonio e Biagio, Alessandria, Italy). Minerva Med., 56: 113-8(Jan. 12, 1965). (In Italian).

The directive of the Italian government on radioprotection measures to be instituted as part of the program for the peaceful uses of nuclear energy, published on February 13, 1964, is outlined and explained. The implication of this directive on radioprotective practices required in hospitals is considered. In situations where occupational exposure occurs, no person under the age of 18 should be permitted, and persons over the age of 18 should not receive a whole-body dose of more than 5 rem/yr or an accumulated dose of 40 rem. For the population in general, the annual dose should not exceed 1.5 rem. Radiologists and their assistants should not be subjected

to levels beyond 100 mR/hr in using 120-kv diagnostic x rays or 1 R/hr in using 250-kv therapeutic x rays. These doses should be kept minimal by use of diaphragms to narrow the beam, maintenance of a proper distance from the patient, and wearing radio-opaque materials or remaining behind shields. The need for dosimetric studies in radiologic departments to assess personnel exposure is discussed. The radiation sources in operation at the authors' hospital, and the protective measures that are taken are described. Results of personnel monitoring are given. (BBB)

5434 MEDICAL X-RAY TECHNIQUE: PRINCIPLES AND APPLICATIONS. Van Der Plaats, G. J. Springfield, Ill., Charles C Thomas, 1961. 484p. $14.50.

The use of x rays in medical diagnosis and treatment and radiation hazards to patients and radiologic personnel are reviewed. Recommendations for reducing the hazards are made. The maximum permissible doses for radiological personnel are explained, and specific measures whereby they can minimize exposure are outlined. Differences in exposure and safety attitudes of diagnostic and therapy-department personnel are indicated, and it is pointed out that doses in excess of the permissible dosage occur less often in therapy departments than in diagnostic departments. Supervisory steps to insure that radioprotective measures are maintained are outlined, and various procedures for monitoring are considered. (H.G.D.)

Radiotherapy and Radiodiagnosis

5435 (NP–15543, pp 59-75) SYNTHESE DES RECHERCHES A L'AIDE DES ISOTOPES RADIOACTIFS EN MEDECINE EFFECTUEES EN ROUMANIE PENDANT LA PERIODE 1958–1964. (Summary of Investigations in Medicine Carried Out in Rumania with the Aid of Radioisotopes, 1958–1964). Milcu, S. M. (Rumanian Committee for Nuclear Energy, Bucharest).

The results of clinical and experimental studies are analyzed briefly for the following: endocrine illnesses, gastroenterology, hematology, oncology, and metabolism. The importance of methods using radioactive isotopes, applied to the study of the etiological and pathogenic mechanisms in illnesses of the thyroid gland, neuroendocrine correlations, and illnesses of the liver, are emphasized. (tr-auth)

5436 (UR–668, pp 149-60) UNIQUE APPLICATIONS OF RADIOISOTOPES. (Rochester Univ., N. Y. Atomic Energy Project).

A study of tissue specific antibodies as possible therapeutic agents for cancer treatment is described. (J.R.D.)

5437 CLINICAL TRIAL OF RADIOSENSITIZERS, INCLUDING SYNKAVIT AND OXYGEN INHALED AT ATMOSPHERIC PRESSURE. Mitchell, J. S.; Brinkley, Diana; Haybittle, J. L. (Cambridge Univ., England. Addenbrooke's Hospital, Cambridge, England). Acta Radiol. Therapy, Phys., Biol. (N.S.), 3: 329-41(Oct. 1965).

Results are reported from a clinical trial of the radiosensitizers Synkavite, oxygen inhaled at atmospheric pressure, and a compound closely related to Synkavite, in palliative radiotherapy of inoperable cases of carcinoma of the bronchus. The only conclusion which emerges from the statistical assessment of the results is that intravenous Synkavit has a small, probably significant, radiosensitizing effect. (auth)

5438 DOSE PLANNING FOR IRRADIATION OF THORAX WITH ^{60}Co IN FIXED-BEAM TELETHERAPY. Sundbom, Lennart (Institute of Radiophysics, Stockholm). Acta Radiol. Therapy, Phys., Biol. (N.S.), 3: 342-52(Oct. 1965).

The problem of accurate dose planning in irradiation of tumors of the thorax is discussed. A short survey is given of the published methods for the solution of this problem. An additional method is described for ^{60}Co fixed beam teletherapy. The method gave a relatively high accuracy and at the same time was very easy to use in manual dose planning. (auth)

5439 TRANSFER OF IMAGES FROM ROENTGENOGRAMS TO TRANSVERSAL BODY-CONTOUR EQUIVALENTS FOR DOSE PLANNING IN RADIOTHERAPY. Setaelae, Kai (Univ. of Helsinki). Acta Radiol. Therapy, Phys., Biol. (N.S.), 3: 361-8(Oct. 1965).

A simple and accurate technique employing a special device for dose planning in x ray therapy of tumors is described. (auth)

5440 INTEGRAL ABSORBED DOSES IN ROENTGEN DIAGNOSTIC PROCEDURES. II. MEASUREMENT OF INTEGRAL DOSES IN TWO ROENTGEN DIAGNOSTIC DEPARTMENTS. Carlsson, Carl (Univ. of Lund). Acta Radiol. Therapy, Phys., Biol. (N.S.), 3: 384-408(Oct. 1965).

With large plane-parallel ionization chambers (monitors), placed between the adjustable diaphragms of the roentgen tube and the patient, measurements of integral absorbed dose in some roentgendiagnostic examinations have been performed. The monitors were mounted on 23 roentgen tubes in two hospitals. Tables with the results of about 2,000 integral dose measurements are given. Twenty-five physicians performed the roentgen examinations. How the integral dose is distributed at different moments during the examination is effectively revealed by the records, of which several examples are given. The records also show the diagnostic methods used at these departments. Finally, the integral dose measurements are compared with those of other authors. (auth)

5441 IRRADIATION IN THE MANAGEMENT OF TUMOURS OF THE HEAD AND NECK. Watson, T. A. Amer. J. Surg., 110: 542-8(Oct. 1965).

Specific applications of γ and x radiation to the treatment of head and neck tumors are explained, with particular attention to preventing complications. (TCO)

5442 RADIOTHERAPY OF CANCER. Diethelm, L. (Univ., Mainz, Ger.). Anglo-Ger. Med. Rev., 2: 496-518(Sept. 1964).

Application of radiobiologic principles to tumor radiotherapy is discussed, in terms of tissue-sparing effects of high-energy radiation, tumor cell sensitization with drugs, dose measurements with phantoms, dose distribution, and treatment planning. The problem of protection of healthy tissues while delivering a cancericidal dose is examined. (TCO)

5443 BETA THERAPY OF HEMANGIOMAS WITH ARTIFICIAL RADIOISOTOPES. Pierquin, B. (Institut Gustave-Roussy, Villejuif, France). Ann. Chir. Plast. Sem. Hop., 9: 285-9(Dec. 1964). (In French).

Considerable discussion still marks the question of whether juvenile hemangiomas should be irradiated, because of the morphological and genetic hazards that this type of treatment poses for the child. If the hemangioma develops slowly, it is probably best to continue to observe it without irradiation treatment. Treatment with Ra is inadvisable because of the radiation protection problem. Beta emitters, such as ^{32}P, ^{90}Sr, or ^{90}Y are preferable because they can be applied directly to the lesion in the form of plastic or metal applicators. Planar hemangiomas require a β dose of about 3000 rad at the surface. This produces a dose of about 1500 rad at a depth of 0.7 mm. The usual dose rate from a ^{32}P applicator is about 1200 rad/hr. If necessary, 6000 to 9000 rad may be administered over a period of 6 to 10 months. For treatment of flat hemangiomas a ^{32}P applicator is necessary for lesions of 10 to 12 mm dia, while ^{90}Sr is satisfactory for smaller lesions. The first treatment should amount to 3000 rad, but this can be repeated over a period of 3 months for a total of 8000 to 9000 rad. Tuberous hemangiomas can be treated by insertion of metal tubules containing ^{90}Y grains. Tubules of this type have dimensions of 0.1 × 1 mm. The doses administered by these amount to 1500 to 2000 rad

for each treatment, which varies from one to 6 hr. This treatment is still subject to considerable testing and consideration before it will become a standard procedure for use with tuberous hemangiomas. (BBB)

5444 HORMONAL AND ISOTOPE MEASURES IN THYROID CARCINOMA. Thomas, Colin G. Jr.; Jenkins, Samuel G. Jr. (Univ. of North Carolina, Chapel Hill). Ann. Surg., 157: 960-73(June 1963).

Methods, clinical results, and hazards of radioiodine treatment of thyroid cancer are reviewed. Problems and complications associated with the treatment of thyroid metastases with ^{131}I are classified and discussed. (TCO)

5445 THE GENETIC IRRADIATION BURDEN OF PATIENTS IN DERMATOLOGICAL X RAY THERAPY. Schirren, C. G. (Dermatologische Universitaetsklinik, Munich). Arch. Clin. Exp. Dermatol., 213: 32-68(1961). (In German).

The most important factors to consider in dermatological irradiation therapy are that the magnitude of the gonadal dose increases with the size of the skin field irradiated, the hardness of the irradiation, the direction of the radiation beam, the distance of the irradiation field from the gonads, and the use of a Pb irradiation shield. A Pb shield should be used for the gonad whenever male or female patients are irradiated in the region of the head, upper extremities, or distal portions of the lower extremities. It is extremely important to keep the gonadal irradiation burden as low as possible because so little is known about its effects. (40 references). (TCO)

5446 THE DIAGNOSIS AND TREATMENT OF OVARIAN MALIGNANCIES. Kottmeier, H. L. (Radiumhemmet, Stockholm). Arq. Patol. (Lisbon), 37: 51-64(Apr. 1965).

The use of various types of radiation for therapy of ovarian cancer, is evaluated. Ovarian radiotherapy is usually accompanied by surgery. A five-year cure rate of 81.9% was reached in 226 cases in which a combination of intracavitary Ra and external radiation were used. The value of radiotherapy in the management of ovarian carcinomas removed surgically is demonstrated by the fact that the 5-year recovery rate is 66.7% compared with 16.7% in surgery-only cases. (TCO)

5447 CROSSED SWEEPING: A SIMPLE PROCEDURE FOR IMPROVING GAMMA SCINTILLOGRAPHY. Hill, Walter S.; Traibel, Jorge (Facultad de Ingenieria y Agrimensura, Montevideo, Uruguay). Bol. Fac. Ing. Agri-Mens. Montevideo, 8: 431-4(Dec. 1964). (In Spanish).

The new technique of crossed sweeping in diagnosis is applicable to all conventional apparatus, but is particularly useful when equipment with great refinement is not available. It improves the image of the organ, particularly when electromagnetic recording is used. Single-direction scanning produces intense darkening only in one direction; if, however, the scan over the same area is repeated at an angle of 90° to the original and recorded on the same trace, the visual inhomogeneity of the unidirectional first recording is greatly diminished, and a well-defined cross hatching produces an improved picture of the affected area. Several scintillograms of thyroid glands before and after operation obtained by the conventional technique and crossed sweeping are compared. In order to attain the same illustration density by the conventional technique, it is necessary to quadruple the usual exposure time, while crossed sweeping requires only two normal exposures to obtain the same density. (BBB)

5448 CANCER OF THE MIDDLE EAR; TECHNIQUE OF RADIATION TREATMENT. Lederman, M.; Jones, C. H.; Mould, R. F. (Royal Marsden Hospital, London). Brit. J. Radiol., 38: 895-905(Dec. 1965).

The techniques used to treat patients with tumors of the middle ear are described, as well as more recent developments. A stationary wedge absorber used with an arcing technique was devised to provide a convenient and accurate means of obtaining uniform doses throughout the three treatment volumes without irradiating surrounding structures to unnecessarily high levels. (auth)

5449 AUTOMATION OF RADIATION TREATMENT PLANNING. V. CALCULATION AND VISUALISATION OF THE TOTAL TREATMENT VOLUME. Sterling, Theodor D.; Perry, Harold; Weinkam, James J. (Univ. of Cincinnati). Brit. J. Radiol., 38: 906-13(Dec. 1965).

The method for calculating per cent depth doses for all points in the major plane of a ^{60}Co beam was extended to all points in the treatment volume. An outline for rapid calculation of volumes of co- or multiplanar treatment plans is presented and an application of the system demonstrated. (auth)

5450 CANCER DIAGNOSIS BY RADIOISOTOPIC SCANNING. Galambos, John T.; Izenstark, Joseph L. (Emory Univ. School of Medicine, Atlanta). CA Med. J., 15: 98-104(May-June 1965).

A review is given of numerous techniques and radioisotope used to detect cancer in various organs. A table lists the particular isotope, radiopharmaceutical preparation, physical half-life of the radioisotope, amount of radioactivity usually administered, and length of time that the patient must wait after administration of the radioisotope before the scan can be performed. (TCO)

5451 RADIOTHERAPY FOR CANCER. Kaplan, Henry S. (Stanford Univ., Palo Alto, Calif.). CA Med. J., 15: 128-33(May-June 1965).

Use of supervoltage and megavoltage radiation therapy in cancer, and advantages of this type of therapy over kilovoltage therapy is discussed with particular reference to therapy of cervical carcinomas and bladder cancer. Survival figures for carcinoma of several primary sites and of comparable extent, treated by kilovoltage compared with supervoltage, indicate clearly the advantage of the latter, both in greater patient comfort during treatment and in significantly improved long-term survival rates. (TCO)

5452 OBSERVATIONS ON THE COMBINED USE OF 5-FLUOROURACIL AND 2-Mev RADIATION IN ADVANCED SOLID TUMORS IN MAN. Crews, Quintous E. Jr. (Los Angeles Tumor Inst.). Cancer Chemotherapy, Rep., No. 14, 45-7(1961).

Attempts were made to detect a synergistic effect when supervoltage (2-Mev) radiation and 5-fluorouracil (FU) were used in combination in the treatment of 33 patients with advanced solid malignancies. The severity of the toxic manifestations varied according to the method of FU administration. Undiluted intravenous administration resulted in severe symptoms, while a slow infusion in 5% dextrose and water produced mild symptoms. Good palliation was noted in one-third, poor palliation in one-third, and no effect in one-third of the patients. One drug-induced death occurred. Some degree of alopecia was noted in 50% of the patients; five developed complete alopecia. Dermatitis occurred in five patients and ranged from a generalized maculo-papular rash, which was moderately pruritic, to a mild localized urticarial rash on the face and forearms. Stomatitis was seen frequently, usually appearing on the 5–7th day and lasting up to a week. While usually mild, it was severe and painful in several patients who showed marked and severe toxic symptoms. With this combined therapy, the depth dose level of radiation to the various tumors was not decreased nor was the fractionation period prolonged. No definite radiomimetic potentiating effect was noted with respect to tumor shrinkage, either primary or metastatic; yet nausea was present in 100% of the patients and appeared somewhat earlier and was more severe than would be expected with radiation alone. There was definite potentiation of radiation with respect to the gastrointestinal tract, and severe diarrhea occurred in several patients who received radiation over the abdomen and pelvis. Except for a more rapid drop in the leukocyte counts, particularly in the latter cases, the blood studies followed closely that expected in advanced malignancies. No increase in the skin reaction was noted when supervoltage radiation was used, and the skin-sparing effects of this quality of radiation remain valid. (BBB)

5453 MEGAVOLTAGE THERAPY. Holsti, L. R.; Taskinen, P. J. (Univ. Central Hospital, Helsinki). Duodecim, 81: 548-55(1965). (In Finnish).

The physical and biological characteristics of betatron and ^{60}Co γ radiations are discussed. The principles of treatment planning are presented and the importance of accurate localization of tumors is stressed. Isodose patterns are illustrated for various types of radiations. Complication rates with conventional and super- and ultravoltage techniques are discussed. The clinical use of megavoltage therapy is described and the comparative results of orthovoltage and megavoltage radiotherapy are discussed on the basis of the literature and 721 cases treated at this hospital. The results offered no unequivocal evidence of the superiority of megavoltage therapy as regards the end results; much larger comparative material is necessary for a conclusive evaluation. It was demonstrated that patients tolerate megavoltage therapy better, also that it gives better palliative results. Technical-physical developments have not solved the problems of radiotherapy, which are mainly biological in nature. Radiobiological research has brought into prominence the fundamental problems of radiotherapy of which solution may lead to better therapeutic results. They are: (1) the presence of anoxic cells in tumors and (2) dose fractionation, i.e., the possibility of giving treatments by other regimes than daily treatment. The importance of radiobiology for radiotherapists is discussed. (BBB)

5454 OLD AND NEW METHODS OF RADIATION THERAPY OF CARCINOMA OF THE BLADDER. Voci, Vincenzo (Univ., Bologna). Fracastoro, 55: 162-88 (May-June 1962). (In Italian).

Various types of radiation used in treating bladder cancer are reviewed, including implantation of radioisotopes and modes of external radiation (250-kv x rays, ^{60}Co, and high-energy electrons). Interstitial irradiation with Ra, Rn, and ^{60}Co is explained and illustrated, showing instruments and technics for inserting these sources in bladder tissue. Doses used in various radiotherapy centers and reported results are presented. Intracavitary irradiation with applicators bearing Ra, ^{60}Co, ^{24}Na (as NaCl), ^{82}Br (as $CaBr_2$), ^{76}As, ^{90}Y, and ^{198}Au is also described, with attention to the various forms and means of insertion of these sources. Forms of transcutaneous irradiation are considered in terms of their modifications in use in various treatment centers and means that may be taken to protect normal tissues, such as with rotation technics and lead shielding. Combined internal and external irradiation methods are also examined. It is concluded that the latest methods which seem to be most effective are those using implanted radioisotopes and high-energy moving-beam external irradiation methods. (200 references.) (BBB)

5455 RADIATION PROBLEMS IN CHILDREN WITH HEART DISEASE. Spach, Madison S.; Capp, M. Paul (Duke Univ., Durham, N. C.). Heart Bull., 13: 101-4 (Nov.-Dec. 1964).

A general quantitative appraisal of radiation exposure from diagnostic radiography in children with congenital heart disease is attempted after a review of the historical background leading to the present concern over potential radiation hazards. (TCO)

5456 ^{99m}Tc COMPOUNDS FOR VISUALIZATION OF BODY ORGANS. Loken, Merle K.; Telander, Gerald T.; Salmon, Robert J. (Univ. of Minnesota Hospitals, Minneapolis). J. Amer. Med. Ass., 194: 152-6(Oct. 11, 1965).

The preparation and use of small colloid particles (500 μ) and large aggregates (50 μ) of serum albumin labeled with ^{99m}Tc as agents for obtaining scintigrams of liver and lung respectively, and the use of pertechnetate for visualization of brain pathology are described. Reference is also made to the use of albumin labeled with radiotechnetium for placental localization. (TCO)

5457 IS REIRRADIATION OF RECURRENT CERVICAL CARCINOMA OF ANY VALUE? Murphy, Walter. J. Amer. Med. Ass., 94: 276(Oct. 18, 1965).

The value of a second course of irradiation for recurring cervical carcinoma is considered, with emphasis on the hazards and avoidance of severe radiation reactions from the cumulative dose. This discussion is based on the premise that the patient initially had received a complete therapeutic radiation regimen and presents, four or more months later, persistent or recurrent carcinoma, histologically proven. Reirradiation in such a patient would depend upon the site and degree of recurrent disease and general health. Successful results have followed reirradiation of carcinoma limited to the uterus or vagina or both, as well as for well-delineated pelvic masses. Intracavitary radium and teletherapy technics can be used, alone or combined. Tissue changes resulting from the original irradiation may not contraindicate retreatment if the radiation therapist feels that the planned technique might be successful. This decision can only be made by an experienced radiotherapist who can weigh the salvage probability against complication rate. (TCO)

5458 TREATMENT OF ANTRAL CARCINOMA WITH RADIOACTIVE IRIDIUM. Alexander, Leslie L.; Beneventano, Thomas C. (State Univ. of New York, Brooklyn). J. Nat. Med. Ass., 56: 139-42(Mar. 1964).

The use of multiple radioiridium sources for treatment of carcinoma of the antrum is recommended. The iridium seeds are 3 mm in length and are covered with sufficient stainless steel that the β irradiation is absorbed. These seeds are encased in flexible, inert Nylon tubing for relatively easy and accurate interstitial implantation into tumors and almost effortless removal. The radioactive seeds are spaced 1 cm apart. An illustrative case is presented in which 25 strands of Nylon tubing containing 300 radioiridium seeds were threaded through plain gauze nasal packing. This was equivalent to 150 mg of radium. The ^{192}Ir and packing were then placed into the antral-ethmoid-sphenoid cavity for a total of 50 hr. This delivered 5000 γ R to a depth of 1.5 cm along the walls of the cavity. Because insufficient iridium extended into the ethmoid area, three 27-mm one-mg radium needles with 0.5 mm of platinum filtration were placed percutaneously into the left ethmoid region for a total of 123 hr. This procedure delivered 3500 γ R to the lower ethmoid area and 3700 R to the upper ethmoid area. The procedure is relatively painless, requires no anesthesia, and is simple. Because there is no embedding of radiation sources into bone and tissues, bone necrosis, compromise of blood supply, and devitalization of entire regions are minimal. (TCO)

5459 SAFETY FACTORS IN URETHROGRAPHY. Becker, L. E. (Veterans Administration Center, Wadsworth, Kans.). J. Nat. Med. Ass., 56: 143-7(Mar. 1964).

The radiation hazards to patient and personnel in urethrography are discussed. Most urethrographic techniques attempt to prevent or minimize exposure of the hands or body of the operator to radiation. Such techniques may involve use of special shields, or, more commonly, wearing of special gloves and aprons. With an unshielded x-ray source, a urologist doing an average of 7.4 retrograde pyelograms a week receives 278 mR (maximum permissible dose is 300 R) but, 18 in. away from the source of x rays, only 64 mR may be received by the operator under the same conditions. The modern x-ray apparatus with small-cone aperture, diaphragms, and effective (2 mm) filters has reduced the secondary or scatter radiation and almost completely eliminated leaks and peripheral or dispersed beams. Latent damage to hands, nails, and gonads of the operator can be further prevented or reduced by careful attention to distance from the patient and primary source, to minimize scattered radiation. (BBB)

5460 RADIOACTIVE IODINE TREATMENT OF INTRACTABLE ANGINA PECTORIS. Burke, Gerald; Feldman, Jerome M. (Michael Reese Hospital and Medical Center, Chicago). J. Nucl. Med., 6: 699-704(Oct. 1965).

The effectiveness of ^{131}I ablative therapy in a series of 80 patients with intractable angina pectoris is evaluated. Meaningful follow-up information was available in 48 pa-

tients who constituted the actual study group. Thirty of 39 patients (76%) rendered hypothyroid showed significant improvement. However, six of nine patients remaining euthyroid also showed significant improvement. The study also affords a comparison of the single and multiple dose forms of ^{131}I therapy and, aside from an apparent decrease in the incidence of radiation thyroiditis, no significant difference between these two forms of ^{131}I therapy was noted. No attempt was made to compare the evolution of the anginal syndrome in a similar control group, and no allowance was made for the possible contributory role of other forms of medical therapy after the administration of radioactive iodine. No estimate of the effect of ^{131}I therapy on survival was attempted. Although the results achieved in the study are entirely comparable to those previously reported, the virtually identical improvement rate obtained in the smaller group of patients remaining euthyroid would seem to preclude meaningful assessment of the efficacy of this form of therapy. (auth)

5461 THE SPINTHARICON: A NEW APPROACH TO RADIATION IMAGING. Horwitz, Norman H.; Lofstrom, James E.; Forsaith, Ann L. (William Beaumont Hospital, Royal Oak, Mich.). J. Nucl. Med., 6: 724-39(Oct. 1965).

An imaging device is described based on the principle that a gamma ray photon may be made to trigger a spark discharge that is accompanied by sufficient luminosity to be photographed. The spark discharge method of imaging was found to be a simple and relatively inexpensive method of obtaining radioisotope distribution patterns. The images are of high resolution and are obtained in about one-half the time required for a conventional scintillation scan. (H.G.D.)

5462 A TECHNIQUE FOR SCANNING THE POSTERIOR FOSSA. Witcofski, Richard L.; Roper, T. J. (Bowman Gray School of Medicine, Winston-Salem, N. C.). J. Nucl. Med., 6: 754-61(Oct. 1965).

A technique for brain scanning of the posterior fossa with an angled detector probe is presented. Normal and abnormal scans with pathologic diagnoses are shown to illustrate the value of the angled posterior projection. (auth)

5463 SURGERY OF THE LARYNX AND HYPOPHARYNX AFTER RADIOTHERAPY. Cachin, Y.; Richard, J.; Lalanne, C. M. (Institut Gustave-Roussy, Villejuif, France). J. Radiol. Electrol. Med. Nucl., 45: 861-3(Dec. 1964). (In French).

Compared to conventional 200-kv x irradiation, the use of high-energy irradiation such as telecobalt therapy does not solve the difficulties of pharyngo-laryngeal postirradiation surgery. In a series of 228 cases it was accompanied by a frequency of 7.5% of carotid hemorrhage. In addition, in 6% of the cases where total laryngectomy or pharyngolaryngectomy was carried out corrective surgery was subsequently required. There was a definite correlation between the frequency of hemorrhage and the appearance of lateral laryngeal fistulas intersecting the carotid axis. The presurgical tumor doses ranged from 4000 to 7000 R. These difficulties may be explained by the characteristics of high-energy irradiations. By necessity, the depth dose at the level of the tumor induces extensive necrotic changes of the tissues from the tumor outward to the cutaneous layers. However, despite its disadvantages, high-energy radiotherapy is valuable as a pretreatment before pharyngo-laryngeal surgery. Irradiation techniques are discussed. (TCO)

5464 A NEW APPARATUS FOR INCREASED PROTECTION IN TELEVISED RADIOSCOPY. Manchette, M. (Compagnie Generale de Radiologie, Paris). J. Radiol. Electrol. Med. Nucl., 45: 891-2(Dec. 1964). (In French).

An apparatus for use in televised radioscopy is described that permits radiological studies of the body to be carried out at currents of 0.3 ma and only facilitates kinetic studies of heart movements and studies of pulmonary ventilation where the broncho-vascular image produced is much better than can be obtained by classic fluoroscopy methods. (TCO)

5465 THE USE OF TOMOGRAPHY FOLLOWING THORIUM DIOXIDE INFUSIONS TO DEMONSTRATE MALIGNANT LESIONS IN THE LIVER. Hahn, Richard G.; Hodgson, John R.; Moertel, Charles G.; Reitemeier, Richard J. (Mayo Clinic, Rochester, Minn.). Mayo Clin. Proc., 40: 456-61(June 1965).

Twenty-five patients with recurrent and inoperable gastrointestinal carcinoma were given stabilized ThO_2 suspensions intravenously after which tomograms were made to outline the areas of metastatic disease and to observe the response to chemotherapy. Eighty per cent of the initial tomograms were interpreted as being fair to excellent in their demonstration of hepatic involvement; 87% of the patients available for follow-up tomograms had roentgenograms that were interpreted as being fair to excellent in their demonstration of hepatic involvement. Improved visualization relative to the initial examination occurred in three instances, whereas lessened visualization was present in one case. No follow-up tomograms were possible in nine of the original group. Two instances of sensitivity reactions to ThO_2 (one requiring the discontinuation of the infusion) occurred. Changes in liver function could not be ascribable to the use of the medium during the relatively short periods of observation. The use of ThO_2 infusions as a means of establishing an indicator lesion in hepatic cancer verified by biopsy seems reasonable but applicable on a limited basis. (TCO)

5466 RADIOTHERAPY. Tudway, Robert C. Med. Ann., 83: 366-72(1965).

Progress in radiotherapeutic technics over the last year is reviewed in relation to parallel developments in radiobiologic research. Possible carcinogenic effect of radiation, as revealed by a study of the incidence of malignant tumors of the stomach, lung, thyroid, and uterus in the populations of Hiroshima and Nagasaki exposed to the atomic bombs, with a range of 1400 m from the hypocenter are discussed. In the case of the stomach, lung, and uterus, there was no significant increase in the incidence of neoplasms. In the case of thyroid cancer there may be a significant increase, and an increase in the incidence of myelofibrosis was also found. Experience with various schemes of fractionation of radiation is considered, as well as recent data on hyperbaric oxygen technics. One report on the results of replacing the daily treatment of patients with treatment on alternate days indicates that a total dose of about 10% less was required than with usual fractionation. Another report on the use of still larger fractions of 1000 rad or over given once or twice weekly two or three times, usually to total doses of a little over 3000 rad in 2 weeks, indicated that this fractionation may not be so successful as the smaller fractions. In a study on dogs to estimate changes of radiosensitivity of the normal kidney due to the use of hyperbaric oxygen, comparisons were made between the effects of doses of 1900, 2500, and 3100 rad, all given over 13 days at normal atmospheric pressure in air to some groups of animals and at 45 lb/in^2 pressure of pure oxygen to other groups (three atm). Kidney function tests before and at intervals after irradiation, and histological examination of the kidneys showed no significant additional renal damage was found after the hyperbaric oxygen treatment. Studies on the synergistic effects of chemotherapy and radiotherapy are also surveyed. In several studies of radiation combined with 5-fluorouracil, there was no synergistic effect between the two treatments and their effects were purely additive. Among the other topics considered are ^{60}Co treatment technics and use of ^{137}Cs in interstitial locations. (BBB)

5467 CLINICAL STUDIES WITH THE GAMMA CAMERA. Thomson, John A.; Boyle, James A.; McGirr, Edward M. (Royal Infirmary, Glasgow). Med. Biol. Illus., 15: 188-92(July 1965).

The gamma camera is described and illustrated, and some of its clinical applications, especially in thyroid scanning, are discussed. The system uses a modified pinhole camera in which the screen or film is replaced

by a large scintillation crystal, upon which a fraction of the γ radiation emitted from the patient falls. Results in 107 patients with a variety of thyroid disorders are reported. (TCO)

5468 PITUITARY ABLATION IN THE TREATMENT OF DIABETIC RETINOPATHY. Bradley, Robert F.; Rees, Searle B.; Fager, Charles A. (New England Deaconess Hospital, Boston). Med. Clin. N. Amer., 49: 1105-24(July 1965).

The partial or complete destruction of the pituitary by surgery or irradiation in 387 patients is reviewed. The irradiation techniques, which included implantation of isotopes or use of heavy particle beams, are described. Yttrium-90 appears to be the best material for pituitary implantation because of its intense but localized β radiation, which will deliver over 100,000 rad to the whole pituitary gland, while sparing the diaphragm and nearby cranial nerves and optic chiasm. The use of heavy-particle-induced tissue ionization (proton) associated with mineral scatter and great depth dose due to the Bragg-Peak effect is also of value to achieve partial or complete hypophysectomy with minimal radiation of intervening tissues. With the Harvard Cyclotron, 26 patients were irradiated usually in doses between 10,000 and 14,000 rad stereotactically directed to the contents of the sella turcica. A single treatment session under local anesthesia was considered to be low in risk and inconvenience to the patient. Use of the more dense ionization at the end of range of the beam, the so-called Bragg Peak, aids in relative sparing of brain substance along all the paths of the 14 separate portals over which the radiation beam is directed so that the entry dose is usually under 500 rad. The time of onset of hypopituitarism varied widely. A technical change was made which improved the reliability and regularity of the onset of hypopituitarism. More precise dosimetry permitted the beam to be centered in such a fashion that the zero percentile course of the optic nerves receives 2000 rad or less and the anterior wall of the sella receives 10,000 rad. Three patients developed transient oculomotor disturbance related to the fact that the converging beams become confluent in the cavernous sinus exposing the oculomotor nerves to higher doses of radiation than other nontarget structures. The rate at which hypopituitarism developed following proton beam pituitary irradiation was both gradual and variable. Those receiving higher doses of radiation developed clinical evidences of hypopituitarism much more rapidly, as early as two to eight weeks. At lower doses, some patients showed little if any evidence of hypopituitarism as late as six months after irradiation. The management of pituitary-irradiated patients is described. (BBB)

5469 LATE COMPLICATIONS IN SUBJECTS TREATED WITH RADIOACTIVE IODINE. Ciabotti, Arnaldo (Casa di Cura Villa Adria, Ancona, Italy). Minerva Med., 54: 2229-33(Aug. 4, 1963). (In Italian).

Since 1956 the author has observed 10 patients who developed severe late side-effects among persons treated with radioiodine. These 10 patients were all women aged 20 to 65 who at various intervals (one patient at 1½ yr, five at 2 yr, and three at four yr later) developed hypothyroidism associated with hypoplastic anemia. All 10 patients presented the typical picture of adult myxedema, with the usual psychic, cutaneous, electrocardiographic, hematologic, and serum protein alterations. In five cases, hemoglobin and red cell and white cell counts were low; in six cases total serum cholesterol exceeded 500 mg %. The case histories of each of these patients are described and the literature relating to this late complication of ^{131}I treatment of hyperthyroidism is reviewed (showing that the incidence of myxedema has varied from 8% to 20% in different studies). Consideration of dose factors indicates that an effective dose of ^{131}I should deliver 25,000 R to the thyroid; studies with x rays indicate that external irradiation of the thyroid with 6000 R does not alter its function. About 90% of the dose of ^{131}I is eliminated from the body in one month and 99.5% by two months. More accurate calculation of the ^{131}I dose is considered. Treatment of these 10 patients made myxedematous with ^{131}I consisted of daily injections of thyroglobulin (600 to 800 mg), which resulted in improvement in their condition. (BBB)

5470 HYPERTHYROIDISM DURING PREGNANCY. Herbst, Arthur L.; Selenkow, Herbert A. (Peter Bent Brigham Hospital, Boston). New Engl. J. Med., 273: 627-33(Sept. 16, 1965).

Management of pregnant hyperthyroid patients is considered. It is recommended the use of radioiodine in diagnosis or treatment of the condition be avoided during pregnancy. (TCO)

5471 INCIDENCE OF LEUKEMIA IN PATIENTS WITH BREAST CANCER TREATED BY RADIOTHERAPY. Sakka, Masatoshi (Tohoku Univ., Sendai). Nippon Igaku Hoshasen Gakkai Zasshi, 24: 466-7(Aug. 1964). (In Japanese).

Six cases of leukemia are reported as occurring in patients with breast cancer treated by radiation. The observed incidence was significantly higher than the expected incidence for the same period of time. The statistical treatment of the data is discussed. (TCO)

5472 STUDIES ON THE INFLUENCES OF ESTROGEN ON THE RADIOSENSITIVITY OF CERVICAL CANCER. Koga, Kohachiro; Yamada, Mamoru; Sugimori, Hajime; Takiguchi, Yoji; Tanaka, Hisao (Kyushu Univ., Fukuoka, Japan). Nippon Sanka Fujinka Gakkai Zasshi, 11: 181-8 (July 1964).

The effect of estrogen combined with radiation treatment was studied in 43 patients with cervical carcinoma from clinical, cytological, histological, and enzymological aspects. Administration of estrogen started three days before the beginning of radiation treatment; 1-4 mg of estradiol benzoate was injected daily or every other day and 10-20 mg of estradiol valerianate every 10 days. Radiation therapy consisted of ^{60}Co irradiation (400 R daily through 6 portals) and transvaginal x irradiation (42.5 kv, 1000 R daily) followed by several radium insertions (for an average total dose of 6000 mg-hr). Macroscopic changes of tumor after irradiation were classified and serial vaginal smears taken during the course of radiation treatment were examined for sensitization response and radiation response. Results suggest that estrogen enhances the radiosensitivity of cervical cancers. (BBB)

5473 THE GYNECOLOGISTS' RETREAT FROM CANCER THERAPY. Lewis, George C. Jr. Obstet. Gynecol., 26: 143-5(July 1965).

The role of gynecologist in radiotherapy of cancer is discussed, with emphasis on the necessity of the gynecologist having a close knowledge of radiation technics and hazards. More and more gynecologists are turning over to radiologists the intracavitary or interstitial placement of radioactive sources, mainly because of a reluctance to keep informed as to the technical details of various radiation therapy technics. Also, in a growing number of instances the radioactive sources are purchased and maintained by another hospital department, the members of which feel that the ownership entitles them to their exclusive use, and qualifies them to do implantations. When radiation therapy is selected, the gynecologist should collaborate closely with the radiologist. The gynecologist who undertakes intracavitary or interstitial applications of radium or other radioisotopes is obliged to be thoroughly familiar with the various types of sources available. For each he should know the loading, active length, filtration, and dose distribution. He should have a working knowledge of external radiation so that he can effectively collaborate in dose planning with the radiologist. The hazards and disadvantages of radiation should also be as well known. The actual insertion of radioactive containers can best be handled as a procedure shared by the radiologist and gynecologist, both being present in the operating room. This definitely can reduce the exposure of both physicians. (BBB)

5474 RADIATION THERAPY IN RELATION TO MALIGNANT TUMORS OF THE TEMPORAL BONE. Dalley, V. M. (Royal Marsden Hospital, London). Progr. Radiat. Therapy, 3: 92-117(1965).

Treatment of tumors of the ear with various forms of radiation is considered, with a discussion on prevention of injury to the bone and brain. Whether surgery or radiotherapy alone, or in combination, should be used is still a matter of controversy. A policy of combined treatment is generally used, surgery being performed first in order to find out the extent of the disease and also to relieve the severe pain. This procedure may, however, cut through the tumor and also interfere with the blood supply, thus decreasing its radiosensitivity. Surgery combined with a γ or x radiation dose of 5000 to 6000 R in 6 to 7 weeks has been given in most of the cases which have survived. The use of Ra applicators following surgery is used infrequently now, since it has the disadvantage of giving a very high localized dose which may easily cause bone necrosis while grossly underexposing the peripheral parts of the tumor. Conventional (250-kv) x radiation is inadequate because the amount absorbed in the bone makes it difficult to treat the deep-seated part of the tumor, and the severe skin reaction may result. A ^{60}Co source activity large enough for a source-skin-distance of 30 cm is practicable with the resultant advantage of increased depth dose. Both the ^{60}Co unit and 2-Mev Van de Graaff accelerator are potentially dangerous because of their large depth dose and the proximity of both orbits and the brain to the tumor region. Thus, irradiation of more than 5 cm of brain to above 5500 R often gives rise to severe damage, and subsequent death. Injudicious use of these units may also heavily irradiate not only one but both orbits. Two possible techniques using these units are shown, in which two wedged fields are employed in the one case, and a technique involving two wedged and one open field in the other. Care in technique can avoid these complications. Whether irradiation has a direct effect on the tumor or only on the blood vessels is discussed. Although it is usually agreed that the patient benefits from radiotherapy, histologic examination of the tumors after treatment rarely shows much change, and it therefore seems possible that radiation affects vessels rather than tumor cells, probably the feeding vessels of the tumor. Only the temporal bone itself need be treated unless lymph node metastases are known to be present. Whatever the mode of action of radiotherapy may be, an adequate dosage is needed, and most patients have received a dose of at least 4500 R. It is important that the brain and orbit are not damaged by irradiation, since many patients may live long enough to show the results of injudicious radiotherapy. (BBB)

5475 THE RANGE OF PROTONS IN HUMAN SKULL-BONE. Koehler, A. M.; Dickinson, J. G.; Preston, W. M. (Harvard Univ., Cambridge, Mass.). Radiat. Res., 26: 334-42(Nov. 1965).

The use of proton beams in the energy range from 100 to 1000 Mev for intracranial irradiations is reviewed. Results are reported from studies that show that if the thickness of skullbone to be penetrated by a beam of protons can be estimated to ±0.5 mm, the range correction required by the presence of bone can be predicted within ±0.5 mm in about two-thirds of the cases. Accuracy can be improved substantially only if the local density of bone as well as its thickness is determined. An empirical relationship between the average density and thickness for bone is given, and the stopping power of bone relative to water was determined. Good agreement was found between theoretical and experimental values of the mass stopping power of bone. (auth)

5476 THE CHANGING PATTERN OF OBSTETRIC RADIOLOGY. Robinson, A. W. (Dudley Road Hospital, Birmingham, Eng.). Radiography, 31: 83-8(Apr. 1965).

New technics for radiologic procedures in pregnant patients are reviewed, with comments on present concepts of radiation protection in such patients. In view of new assessments of the radiation hazard, changes have occurred in obstetric radiology and radiography. Although it had long been known that x rays can do harm, this was not considered an overriding factor in the early days of obstetric radiology. Not until relatively recently, with increasing evidence that fetal irradiation might sometimes induce a later malignancy, was the problem fully accepted and considered. Realizing the risk to fetus, obstetricians became more cautious in their requests for radiography, and radiology departments tightened and improved protection methods and initiated new radiographic techniques to diminish the fetal dose. Now, years later, under better perspective, it is evident that as little radiation as possible should be given but that in the second half of pregnancy the risk to the fetus is slightly less than was originally thought and less, it is suggested, than is generally realized. Obstetricians requesting x rays now know of this small risk and judge that the patient will be at greater risk if he does not acquire the information which radiography will provide. (BBB)

5477 CYTOLOGICAL ASPECTS OF RADIOTHERAPY. Hug, Otto (Univ., Munich). Radiol. Austr., 15: 146-59 (1964). (In German).

The effectiveness of presurgical irradiation of tumors depends on the level of the total dose, type of fractionation, and interval between irradiation and operation. The author discusses results of a wide variety of studies on radiosensitivity of many types of cells, both in vivo and in vitro. The effects of irradiation on single tumor cells are to inhibit or prevent their reproduction, kill them, or alter them qualitatively. Irradiation may alter the tumor tissue in part or as a whole, and produce changes in tumor-host relations. These changes may be morphological, metabolic, or immunological. Irradiation may or may not have favorable effects on tumor metastasis. Presurgical tumor irradiation has several possible effects. It reduces the danger of dispersing live cells during a surgical procedure, even though the dose administered may be far below an effective curative dose. This effect increases almost directly with dose administered. The absolute number of surviving cells or the cells capable of growth or metastasizing varies directly with the dose, the initial number of cells, and the size of the active tumor. The time interval between irradiation and surgery when the preirradiation effect is greatest is brief because the surviving cells quickly resume growth. (BBB)

5478 DOSIMETRY IN RADIOTHERAPEUTIC PRACTICE. Wachsmann, F.; Adam, W. E. (Univ., Erlangen-Nuernberg). Radiologe, 4: 246-55(Aug. 1964). (In German).

Problems encountered in radiation dosimetry for radiotherapy are discussed. The most important of these is the estimation of the dose magnitude in R and rad, and the conversion from one unit to the other. Methods of dose measurement and problems of relating dose measurements to patient care are discussed. Problems of measurement of radiation quality, filtration of x-ray tubes, definition of the term "focus," the effects of irradiation of tissues that are not water-equivalent, and the integral or space dose and its calculation are discussed. Biological problems, such as the effect of fractionated or protracted irradiation, relative biological effect, and the magnitude of irradiated volumes are considered. The fact that quantitative dosimetry is the basis of radiotherapy does not alter the need for the physician to assume the clinical responsibility for deciding how much radiation to administer to the patient. (BBB)

5479 SOLID BODY DOSIMETRY IN RADIOTHERAPY. Drexler, Guenter; Scharmann, Artur (Univ., Erlangen-Nuernberg). Radiologe, 4: 262-7(Aug. 1964). (In German).

The physical principles of the thermoluminescence dosimeter, the radiophotoluminescence dosimeter, and the semiconductor dosimeter are described. The suitability of these types of dosimeters for use in clinical dosimetry is discussed. Doses within the range of 1 to 1000 R can be

measured with thermoluminescent dosimeters. One disadvantage of thermoluminescent methods is their varying sensitivity and the energy dependence of the LiF crystals, and the shift of the "glow peaks." The crystals are easy to purify. For in vivo studies the crystals can be sterilized. CaF_2 with Mn is sometimes used as a substitute for LiF. However, this is 10 times as energy dependent, although it has greater sensitivity. Photoluminescent dosimeters, or fluorods, are suitable for measurement of 2 R or more of hard or ultrahard irradiation, and should be in or near to the beam. Measurements can be made with ±2% accuracy at doses of about 200 R. The glass rods must be heat treated before use. The energy dependence of CdS crystals limits their accurate use to measurements of irradiation of known energy. Comparison of isodose measurements made with CdS crystals, Ag phosphate glass, and LiF with ionization chamber measurements indicate that hard radiation measurements are in close agreement. However, for conventional irradiation thermoluminescence dosimetry with LiF is the only one that should be used. (BBB)

5480 FILM DOSIMETRY IN RADIOTHERAPY. Keller, H. L. (Univ., Erlangen, Ger.). Radiologe, 4: 272-5(Aug. 1964). (In German).

The advantages and disadvantages of film dosimetry are compared. Film blackening is not proportional to the exposure time or the irradiation intensity, but it is related exponentially to the product of these factors. Fading is an important factor when the interval between film exposure and development is long. Long storage times increase the film background and reduce film sensitivity. The range of dose differences that can be measured with film extend over a range of 100-fold. The degrees of blackening detectable must be carefully calibrated photometrically. Film blackening varies with the direction of the incident irradiation and with the radiation energy. The greatest blackening capacity is obtained with a normal irradiation between 60 and 70 kv, and the more the irradiation varies from this value the larger is the dose that is required to produce equivalent blackening. Since the average radiation energy at various depths in tissue is altered very much compared to the primary radiation the correction factor required must be adjusted to conform with the tissue depth and field size. This is particularly true for monochromatic radiations from ^{137}Cs or ^{60}Co. Graphical estimates of the correction factors for these and other radiations are presented. Uses of film dosimetry in radiotherapy are discussed for various radiation energies and for fast electrons. These are compared with dose determinations made with ionometric devices. (BBB)

5481 PHANTOMS FOR RADIOTHERAPEUTIC MEASUREMENTS. Herve, A. (Clinic of Our Lady of Hope, Liege). Radiologe, 4: 291-2(Aug. 1964). (In German).

Phantoms constructed from materials that contain C, H, O, and N are best suited for x or γ irradiation measurements. Tissue absorption results from the photoelectric effect, the Compton effect, pair formation, and nuclear processes or activation. The photoelectric effect is almost proportional to the third power of the atomic number, decreases with increasing photon energy, and for the light elements is almost proportional to the third power of the wavelength. At 100 kv and 200 kv about 15 and 1.5% of absorption is due to the photoelectric effect. The Compton effect is related to the total number of electrons per mass unit, and decreases slowly with increasing irradiation quality. It is greater than the photoelectric effect at low energies. The mass scatter coefficient is about 85% at 100 kv and about 98.5% at 200 kv. Pair formation is proportional to the fourth power of the at. wt. of the absorbing medium, and increases with energy of the irradiation. Nuclear processes are important only above energies of 15 Mev. In the energy region of conventional irradiation where absorption is related to atomic number, water and Plexiglas are best for phantoms. In the region of hard irradiation where the Compton effect is important, water, Plexiglas, and polystyrene are suitable. Water phantoms are generally suitable, but they do not provide for measurements of radiation dose in denser tissue. For this purpose other materials, such as paraffin, beeswax, wood, bone, rice, etc. must be built into the phantom. These types of phantoms are very expensive to construct or buy. (BBB)

5482 ^{131}Cs SEEDS FOR PERMANENT IMPLANTS. Henschke, U. K.; Lawrence, D. C. (Memorial Sloan-Kettering Cancer Center, New York). Radiology, 85: 1117-19(Dec. 1965).

The therapeutic use of encapsulated seeds of low-energy ^{131}Cs was studied. In comparison with seeds of ^{222}Rn and ^{198}Au, a significant absorption of the Cs by the metal planchets was demonstrated. Advantages of using ^{131}Cs are indicated. (H.G.D.)

5483 RADIOTHERAPY OF POLYCYTHEMIA. Benassi, Enrico; Toretta, Alessandro (Univ., Turin). Rass. Clin., 40: 209-11(July-Aug. 1964). (In Italian).

Use of various types of radiotherapy in the treatment of polycythemia is discussed, along with hematologic effects and late complications. Transcutaneous x ray treatment (400 to 600 rad) of the spleen and bone marrow sites has been effective and the use of 200-kv x rays to deliver 50 to 100 rad single doses is described. Single doses can be increased to 250 rad and total doses to a localized field of as high as 1500 rad can be given over a month. Treatment is stopped when the red cell count falls to 5 million/mm^3. Whole-body ^{60}Co irradiation has been used with success in some cases. Daily doses of 5 to 7 R have been used for as many as 40 sessions. Long remissions have been obtained with such treatment. Often ^{32}P treatment is preferred because of its predilection for hematopoietic tissue and its convenient half life (14.3 days) and energetic β emission (1.7-Mev) with short tissue path (2 mm). An initial dose of 0.9 mC/10 kg body weight is recommended; the oral dose should be 25% higher than the intravenous dose. The usual intravenous dose is 3 to 7 mC initially, which may be repeated up to three times if necessary to lower the red cell count. In general, the interval between doses should exceed two months. Remissions after ^{32}P therapy average one to two yr, and 80–85% of cases showed improvement in symptoms as well as reduced erythrocyte production. Side effects of radiotherapy include leukemia, thrombocytopenia, and even anemia. In a few cases, marrow aplasia may ensue, with fatal results. There is a tendency for elevated incidence of leukemia in radiation-treated polycythemia patients, but whether it can be attributed to radiation or an inherent predilection in such patients to develop leukemia is not yet clear. (BBB)

5484 EXPERIENCE WITH VITAMIN B_{12} IN A CASE OF ALOPECIA FOLLOWING DEEP RADIOTHERAPY (X-RAYS). (USED AS A SURGICAL COMPLEMENT IN A CASE OF TUMOR OF THE RIGHT CEREBELLAR HEMISPHERE WITH EPENDYMOMA). Antunes, Caio Antonio (IAPB, Rio de Janeiro, Brazil). Rev. Brasil. Med., 20: 171-2(Mar. 1963). (In Portuguese).

The case history of a 5-yr-old girl is described who underwent deep x-ray therapy of the cranium. This resulted in persistent baldness which was successfully treated by large doses of vitamin B_{12}. The child was observed to have severe occipital headaches, aggravated by movements of the head, with severe episodes of vomiting. Radiologic studies were negative, but ventriculography revealed evidence of a cerebellar tumor. An ependymoma was surgically removed from the right cerebellar hemisphere. Because it was found to be highly malignant, deep x-ray therapy was given to the cranium in 25 doses (individual or total doses not stated). Complete, and persistent, loss of hair on the back of the head resulted. Repeated injections (1000 μg) of vitamin B_{12} were given for the alopecia, and complete regrowth of hair ensued. (BBB)

5485 LYMPHOSARCOMA: CHOICE OF TREATMENT AND END-RESULTS IN 567 PATIENTS: ROLE OF SURGICAL TREATMENT FOR CURE AND PALLIATION. Molander, David W.; Pack, George T. (Pack Medical Foundation, New York). Rev. Surg., 20: 3-31(Jan.-Feb. 1963).

The use of x radiation, as well as surgery and chemotherapy, in the treatment of lymphosarcoma is described, with attention to doses for specific sites, prevention of complications, and their treatment when they do occur. Adequate surgical extirpation in selected patients is useful for unicentric lymphosarcoma, but patients should also receive a tumor dose of at least 3000 to 3600 R to the involved region with 250-kv x rays. Patients with regional lymphosarcoma should receive 2400 to 3000 R to the diseased sites. Constitutional symptoms are controlled with chemotherapeutic agents. Patients with generalized lymphosarcoma should receive 1200 to 1800 R to the involved sites, if tolerated. Radiation therapy may have to be limited or used intermittently when the patient's platelet count is depressed below 75,000 per mm^3. Following a radiation dosage of 2500 to 3000 R to the lung, radiation fibrosis may ensue. The late sequelae of pulmonary and mediastinal radiation fibrosis may be distressing and disabling. Diminished vital capacity constitutes a physical handicap of variable degree owing to lessened aeration of the fibrotic lung. The mediastinal retraction toward the side of the fibrosis may add to the discomfort of the patient. Mediastinal fibrosis may cast a broad radiographic shadow simulating residual lymphosarcoma, thus promoting additional and hazardous radiation therapy if erroneous interpretation is made. (BBB)

5486 IRRADIATION THERAPY OF THE LARYNX. Winborn, Claude D.; Collier, Richard E.; Mallams, John T. (Baylor Univ. Medical Center, Dallas). S. Med. J., 58: 1296-7(Oct. 1965).

The use of ^{60}Co irradiation for carcinoma of the larynx is described, showing the lower incidence of deleterious side effects that can be obtained if certain dose schedules and precautions are taken. The lower complication rate when supervoltage therapy is used is compared with that seen with conventional x ray therapy. (TCO)

5487 RADIOISOTOPE PHOTOSCANS IN NUCLEAR MEDICINE. Haynie, Thomas P.; Otte, William K. Jr. (Univ. of Texas Medical Branch, Galveston). Tex. State J. Med., 61: 304-13(Apr. 1965).

Recent advances in radioisotope applications in medical diagnosis are reviewed, with emphasis on advantages of one procedure or isotope over another. Instrumentation is described and some illustrative scans are reproduced. (TCO)

5488 RESULTS OF RADIOIODINE TREATMENT OF THYROID CANCER. Emrich, D. (Univ., Freiburg i. Breisgau). Verhandl. Deut. Ges. Inn. Med., 70: 870-9 (1964). (In German).

The results of radioiodine treatment of thyroidal cancer have been less favorable than was expected for this procedure, but this treatment is still beneficial. Several factors limit the effectiveness of this treatment. The tumor tissue concentrates radioiodine poorly and does not retain it. Tumor radiosensitivity differs considerably, and the possibility of excessive irradiation of extrathyroidal tissue, such as bone marrow, is a hazard. The tumor ^{131}I uptake is limited by three factors, including its histology, its function, and by the amount of healthy thyroid tissue still remaining. Undifferentiated tumors cannot be treated as readily as differentiated tumors, although high concentration of ^{131}I is not a sure indication for success of radioiodine therapy. Uptake of ^{131}I can be increased by surgical thyroidectomy or administration of thyrotropic hormone or thyrostatic agents. The irradiation burden of extrathyroidal tissues depends largely on two factors: the amount of ^{131}I administered and the degree of function of the tumor. At least 5000 R are necessary to destroy the tumor, and usually ^{131}I is given in 100- to 200-mC doses at intervals of 6 to 12 weeks until it is no longer taken up. If diffuse lung or marrow metastases are present, the dose should be kept to 80 to 125 mC to prevent pancytopenia or lung fibrosis. Results of ^{131}I treatment show that 30 to 50% of treated cases are benefited. Almost 50% of the treated cases have a survival time of more than 3 yr, and about 13% have a survival time of more than 5 yr after ^{131}I treatment. (95 references.) (BBB)

5489 A TEXTBOOK OF ELEMENTARY RADIOGRAPHY FOR STUDENTS AND TECHNICIANS. Bauer, Donald deForest. Springfield, Charles C Thomas, 1965. 242p. $8.50.

This textbook includes a chapter on radioprotection practices to be employed in radiodiagnosis, with extensive data on radiation hazards to patients and personnel, and radiation protection procedures. Four main rules of radioprotection in diagnosis emphasized include adequate distance of personnel from the x-ray beam, collimation and filtration of the beam, and use of shielding devices. (TCO)

5490 RADIOTHERAPY OF BENIGN DISEASE. Dewing, Stephen B. Springfield, Charles C Thomas, 1965. 311p. $9.75.

This monograph deals with the use of various types of radiation in the treatment of nonmalignant conditions with attention to possible hazards seen as late sequelae, technical factors used, doses required for various diseases, and shielding technics for healthy tissues. Radiobiologic effects are discussed in terms of both beneficial and detrimental effects of radiotherapy in benign diseases. (TCO)

5491 THE INHERITANCE OF LEAF MARKING AND THE EFFECTS OF X-RAYS AND ETHYL METHANESULFONATE TREATMENT AS MEASURED BY M_1—GENERATION RESPONSE IN RED CLOVER (TRIFOLIUM PRATENSE L.) [Thesis]. Liang, George Hsueh-Lee. Madison, Wis., Univ. of Wisconsin, 1964. 59p.

Two studies relating to the leaf-mark locus in red clover were made. The genetic basis for the various leaf markings was clarified, and the effects of x rays and ethyl methanesulfonate as mutagens in red clover were analyzed. Red clover was found to have considerable resistance to x rays. Seed set was obtained when blooming heads were subjected to a dosage as high as 7 kR, but was not reduced significantly at dosages of 1.5 kR and lower. Differential effects of x irradiation on sexes were observed in terms of seed setting. The female part seems to be more resistant than the male counterpart. Different genotypes also appear to respond differently to x irradiation. The proportion of shrivelled seeds increased substantially when blooming heads were irradiated at doses of 2.5 kR and higher. The proportion of shrivelled seeds obtained from treated plants pollinated with normal pollen was consistently lower than that obtained from untreated plants with treated pollen. Seed weight was not affected by pollen irradiation, but was affected when ovules were irradiated. Higher dosages resulted in a lighter seed weight. Variability in seedling vigor was increased when pollen was irradiated at appropriate dosages. Differences among variances were tested. When moist seeds were x rayed at 20 kR, seedling emergence, seedling vigor, fertility, amount of bloom, plant size, and seed yield were reduced, and maturity delayed. Treatment with ethyl methanesulfonate (EMS) at three concentrations did not show any sign of adversely affecting those characters. Seed weight was not affected by treatment with x rays and EMS on moist seeds. Fertility did not contribute significantly to the genetic variability manifested in seed weight in the mutagen-treated populations. Increase of variability was observed in the progeny derived from mutagen-treated seeds. There was no consistency for the induced variances among the characters examined. There appears to be a differential response to mutagens among those quantitative characters. The correlations between characters in EMS-treated populations were low suggesting that mutations from this source are predominantly genic. The correlations between the characters in x-rayed populations are greater than those in EMS-treated populations indicating that mutations induced by x rays are predominantly of the gross deletion and/or duplication type. (TCO)

CHEMISTRY

General

5492 (ANL–6925) CHEMICAL ENGINEERING DIVISION SEMIANNUAL REPORT, JULY–DECEMBER 1964. (Argonne National Lab., Ill.). May 1965. Contract W-31-109-eng-38. 260p. Dep. mn; CFSTI $6.00 cy, $1.25 mn.

Research and development are reported in nine sections. A separate abstract was prepared for each section. (J.R.D.)

For abstracts of individual sections see: 5493, 5523, 5594, 5595, 5875, 6024, 6280, 6552, and 6553.

5493 (ANL–6925, pp 253–4) ANALYTICAL RESEARCH AND DEVELOPMENT. Larsen, R. P.; Meyer, R. J. (Argonne National Lab., Ill.).

Activities in a program to develop methods for determining burnup of fast reactor fuels and for measurement of fission yields are summarized. Data and information are included on ^{235}U fast fission yields of ^{95}Mo, ^{97}Mo, ^{98}Mo, and ^{100}Mo. Data and information are also included on ^{235}U fast fission yields of ^{101}Ru, ^{102}Ru, and ^{104}Ru. (J.R.D.)

Analytical Procedures

See also Separation Processes and Procedures

Refer also to abstracts 5727 and 6258.

5494 (AEET–217) ACTIVATION ANALYSIS THROUGH ADDITION OF "STANDARD" AND SOLVENT EXTRACTION. PRINCIPLE OF THE METHOD. Alian, A. (Atomic Energy Establishment, Trombay (India). Analytical Div.). 1965. 5p. Dep. mn.

. A method is proposed for the determination of trace amounts of metals. The analytical procedure consists of a single stage extraction and then measuring the radioactivity of the extract obtained. In this way, no carrier is added and determination of the chemical yield is avoided. (P.C.H.)

5495 (DP–972) ISOLATING AMERICIUM AND CURIUM FROM $Al(NO_3)_3$–$NaNO_3$–HNO_3 SOLUTIONS BY BATCH EXTRACTION WITH TRIBUTYL PHOSPHATE. Henry, Hugh E. (Du Pont de Nemours (E. I.) and Co., Aiken, S. C. Savannah River Lab.). Aug. 1965. Contract AT(07-2)-1. 23p. Dep. mn; CFSTI $1.00 cy, $0.50 mn.

Batch solvent extraction was used to isolate ^{243}Am and ^{244}Cm from the aqueous solution remaining after dissolution of an irradiated Pu–Al alloy in nitric acid and recovery of the Pu by anion exchange. The solution was adjusted to 6.5–6.8M inextractable nitrate and 0.10–0.35M HNO_3 before extracting the Am–Cm with an equal volume of 50 volume percent tri-n-butyl phosphate in a hydrocarbon diluent and then back-extracting into 0.2M HNO_3. Recovery was greater than 95% with up to one-liter batches in laboratory tests and with 1500-gallon batches on a plant scale. Factors affecting the degree of extraction were measured in the laboratory. (auth)

5496 (DP–985) AUTOMATED ANALYSIS OF LITHIUM SOLUTIONS. Gaddy, Rufus H. (Du Pont de Nemours (E. I.) and Co., Aiken, S. C. Savannah River Lab.). Oct. 1965. Contract AT(07-2)-1. 12p. Dep. mn; CFSTI $1.00 cy, $0.50 mn.

An automated flame photometric method was developed for the precise determination of lithium in highly radioactive process solutions containing curium, americium, and fission product radionuclides. (auth)

5497 (KFK–339) DIE RADIOCHEMISCHE ERMITTLUNG DER HAEUFIGKEIT DER PLUTONIUM-ISOTOPE SOWIE DIE QUANTITATIVE BESTIMMUNG VON PLUTONIUM IN MIKROGRAMM-MENGEN. (The Radiochemical Determination of the Frequency of Plutonium Isotopes as well as the Quantitative Determination of Plutonium in Microgram Amounts). Wolf, Peter; Reinhardt, Johann (Kernforschungszentrum, Karlsruhe (West Germany). Institut fuer Radiochemie). July 1965. 20p. Dep. mn.

A method is described for the radiochemical determination of the isotope frequency in plutonium samples of known plutonium content when a sample of at least 50 μg of plutonium was available. If the isotopic frequency is radiochemically determined, then the plutonium content of each additional sample (of the same charge) can be determined radiochemically in the microgram scale with an accuracy of ±1.5%. For this determination a plutonium mass of at least 2 μg is necessary in the analysis sample. (tr-auth)

5498 (NP–15636) BORON INTERFERENCE IN FAST-NEUTRON ACTIVATION ANALYSIS FOR OXYGEN. Technical Note 105. Wood, D. E. (Kaman Nuclear, Colorado Springs, Colo.). June 10, 1965. 3p.

The irradiation of materials containing boron or oxygen, and the subsequent analysis of the energy spectrum and time decay of the induced activities are discussed. Results showed that oxygen can be measured in the presence of boron if the oxygen content is 1% or more of the boron content. A Lucite beta-shield is desirable on the counter to minimize interference from the high-energy betas emitted by irradiated boron. (P.C.H.)

5499 (NP–15637) SELECTED REFERENCES FOR NEUTRON ACTIVATION ANALYSIS. Technical Bulletin No. 108. Wood, Donald E. (Kaman Nuclear, Colorado Springs, Colo.). [1965]. 11p.

Fifty-eight references are given to books, bibliographies, conferences, reports, and journals published 1955 through June 1965. Neutron cross sections, radioisotope data, crystal efficiencies are included through large tabulations and a few primary articles. (P.C.H.)

5500 (ORNL–3876) ACID LEACHING OF PRODUCTS FROM THE FLUIDIZED-BED COMBUSTION OF GRAPHITE-BASE REACTOR FUELS AND THE HF–O_2 DISINTEGRATION OF STAINLESS STEEL- AND ZIRCONIUM-CLAD OXIDE FUELS. Ferris, L. M. (Oak Ridge National Lab., Tenn.). Nov. 1965. Contract W-7405-eng-26. 31p. Dep. mn; CFSTI $2.00 cy, $0.50 mn.

A summary of laboratory-scale leaching studies conducted with typical products from unirradiated fuel samples is reported. Graphite-base fuels containing carbon-coated Th–U carbide or oxide fuel particles were easily burned in oxygen at 700 to 750°C in a fluidized bed of alumina. The product beds were dispersions of Th–U oxides in alumina. Leaching for 3 to 6 hr of typical product beds with boiling 4 to 13 M HNO_3 solutions that were also 0.05 M in HF resulted in thorium and uranium recoveries of 99.7% or higher. Less than 2% of the alumina (Norton RR) was dissolved. Reaction in a fluidized bed of alumina of stainless steel- or zirconium-clad UO_2 fuel with HF–O_2 mixtures at 600 to 650°C resulted in conversion of the claddings to their respective powdered oxides and the UO_2 to U_3O_8 powder. The product beds (dispersions of U_3O_8 and stainless steel or zirconium oxides in alumina) usually contained 5 to 10% fluorine. Removal of this fluorine prior to leaching was desirable to avoid excessive fluoride concentrations in the leach solution and subsequent solvent extraction streams. More than 90% of the fluorine can be removed by pyrohydrolysis (steam, 1 atm pressure) for about 4 hr at 600°C. Leaching of the pyrohydrolyzed beds with 2 to 15 M HNO_3 for about 5 hr resulted in the recovery of greater than 99.8% of the uranium. Less than 2% of the alumina was dissolved under all conditions tested, whereas the amounts of zirconium and stainless steel components dissolved varied with leaching conditions. (auth)

5501 HIGH-RADIATION-LEVEL ANALYTICAL LABORATORIES. Anal. Chem., 37: 83A–5A (Dec. 1965).

The ORNL high-radiation-level analytical laboratory is described. It was designed especially for use in the treatment and analysis of highly radioactive beta- and gamma-emitting materials. The hot-cell block has six work cells, a sample-carrier unloading cell, and a sample storage cell. Exterior walls of high-density concrete in the sample storage cell and of normal concrete in the work cells provide shielding for 25000 and 1400 C of ^{60}Co, respectively; the level of radiation at the outer surface is <1 mr/hr. The equipment used to handle the radioactive materials is described. Remotely controlled equipment of special design is used for amperometry, coulometry, potentiometry, and spectrometry. The irradiated materials frequently analyzed are thorium oxide, uranium dicarbide, and uranium oxide. The radioactive gas samples are analyzed on a gas chromatograph and discharged into the cell-exhaust system. (F.J.H.)

5502 CONTINUOUS BACK-TITRATIONS WITH DIRECT READOUT. Blaedel, W. J.; Laessig, R. H. (Univ. of Wisconsin, Madison). Anal. Chem., 37: 1650-3(Dec. 1965).

A continuous automated potentiometric titrator with direct readout was adapted to the back-titration of metal ions with EDTA. The metals studied were those that are commonly back-titrated because of slow reaction with the chelate. After calibration of the titrator with standard samples, readout of sample concentration is both digital and direct, requiring no computation to obtain the analytical result. The average standard deviation for a typical series of samples was 0.0001 mole per liter with sample concentrations ranging from 0 to 0.035M. The precision of the titrator was obtained for the following titrations at pH 9.7 or 4.8: Zn(II), Ce(III), La(III), Pr(III), Cu(II), Th(IV), In(III), Zr(IV), Cr(III), and Al(III). For Zr(IV), Cr(III), and Al(III), 1 minute on stream at 98°C was used to promote reaction. (auth)

5503 ELECTROCHEMICAL PREPARATION OF THIN METAL FILMS AS STANDARDS ON PYROLYTIC GRAPHITE. Vassos, Basil H.; Berlandi, Francis J.; Neal, Thomas E.; Mark, Harry B. Jr. (Univ. of Michigan, Ann Arbor). Anal. Chem., 37: 1653-6(Dec. 1965).

Gold, silver, copper, and cobalt were deposited quantitatively in microgram to milligram amounts on disks of pyrolytic graphite. Electrochemical plating conditions and the electrode pretreatment procedures that provided for the most uniform and strongly adhering metal film deposit are described. The procedures employed make use of both potentiometric and amperostatic electrochemical deposition techniques. The linearity of plating deposits, as a function of time, concentration, and current, is discussed together with other parameters affecting the deposition. With the use of operational amplifiers in the control circuits, the film deposits prepared showed an internal precision that was within ±2% when checked by a number of independent methods, including activation analysis. Potential application of such quantitatively prepared disks to neutron flux monitoring and to other analytical methods is discussed. (auth)

5504 DIRECT RADIOCHEMICAL DETERMINATION OF ^{210}Pb IN BONE. Petrow, Henry G.; Cover, Arthur (New York Univ. Medical Center, New York). Anal. Chem., 37: 1659-60(Dec. 1965).

A procedure for the radiochemical determination of ^{210}Pb in bone ash is based on the solvent extraction of a lead bromide complex into a quaternary amine. ^{210}Pb is detected, after a suitable ingrowth period, by beta-counting its ^{210}Bi daughter. Ash samples up to 30 can be routinely analyzed, and as little as 2×10^{-12} C of ^{210}Pb can be determined. Interference from other elements, both stable and radioactive, is slight. The procedure is applicable to materials other than bone ash. (auth)

5505 RADIOCHEMICAL DETERMINATION OF ^{210}Pb IN MILL PRODUCTS AND BIOLOGICAL MATERIALS. Sill, Claude W.; Willis, Conrad P. (Atomic Energy Commission, Idaho Falls, Idaho). Anal. Chem., 37: 1661-71 (Dec. 1965).

The determination of ^{210}Pb through its ^{210}Bi daughter was re-examined for application to complex inorganic systems in addition to biological materials. Special emphasis was placed on complete recovery of both lead and bismuth, so that either element can be used in the determination. In the large number of cases in which secular equilibrium is known to exist, the bismuth fraction can be counted and results obtained within a few hours, eliminating the lengthy delays common to many other procedures. Extraction with a solution of diethylammonium diethyldithiocarbamate in chloroform separates lead and bismuth quantitatively from large quantities of other metals in strongly acid solution. Dithizone then eliminates the remaining interferences and separates the two elements from each other prior to beta counting. High activities of gamma-emitting ^{212}Pb and ^{207}Bi tracers were used to detect and identify any source of error larger than about 0.05%. Recovery of both elements through the entire procedure was over 99% from 500 ml of river water or liquid mill effluents, 1 g of ores or mill tailings, 100 g of blood, tissue, feces, or grain, 1500 ml of urine, or large samples of air dusts. Overall recovery was still about 98% even from 100 g of soil or bone ash. Separation of lead and bismuth from each other was better than 99.9%. Several sources of error are discussed. (auth)

5506 ARSENATE METHOD FOR IODOMETRIC DETERMINATION OF YTTRIUM IN PRESENCE OF ALUMINUM. Shakhtakhtinskii, G. B.; Veliev, B. S.; Aslanov, G. A. Azerbaidzh. Khim. Zh., No. 6, 85-90 (1964). (In Russian).

The arsenate-iodometric method for the determination of Y in the presence of Al was described. The proposed method makes it possible to determine Y ions in the presence of Al in a wide concentration range with an error of ±0.1 to 0.2%. (tr-auth)

5507 IRON DETERMINATION IN ANTIMONY BY ACTIVATION ANALYSIS. Simkova, M.; Kukula, F.; Stejskal, R. (Inst. for Nuclear Research, Czechoslovak Academy of Sciences, Rez). Collect. Czech. Chem. Commun., 30: 3193-7(Sept. 1965). (In German).

The method of neutron activation for determination of iron in antimony, purified by zone fusion, is described. The iron was separated from irradiated antimony in the form of FeS. After peroxidation of the antimony sulfide, it was separated on Aberlit IR 120 that was eluted first with tartaric acid and then with 6N HCl. The chemical yield of the iron was 75 to 80%. Iron could be determined in antimony at 5×10^{-7} g. The time required for the analysis was 10 to 12 hr. (tr-auth)

5508 OPTIMUM OPERATION OF RECORDING COUNT RATE METERS FOR RADIOACTIVE PAPER CHROMATOGRAMS. Johnson, Marvin J. (Univ. of Wisconsin, Madison). J. Chromatog., 20: 100-6(Oct. 1965).

Operating variables in the use of recording ratemeters for scanning radioactive paper chromatographic strips are discussed. Best sensitivity, and least statistical error in estimation of peak area, was obtained with a wide slit. However, wide slits gave poor fidelity, that is, the shape of the record was not an accurate representation of the shape of the actual peak. Short time constants gave a record showing undesirable fluctuations due to statistical count rate variations, while long time constants gave poor fidelity. Slow strip speed was required for strips of low activity. Optimal selection of operating conditions was considered from a quantitative standpoint. (auth)

5509 THE SEPARATION OF SOME FISSION PRODUCTS AND ACTINIDES ON PAPER TREATED WITH LIQUID ANION EXCHANGER. Knoch, W.; Muju, B.; Lahr, H. (Technische Hochschule, Brunswick). J. Chromatog., 20: 122-30(Oct. 1965).

After treatment of paper with a liquid anion exchanger (tri-n-octylamine) the differences in the stability of the metal complexes may be used to improve the analytical separation of some important fission products and actinides by paper chromatography. The R_F values of Y, La, Ce, Zr, Ru, Th, Pa, U, Np, Pu, and Am with nitric acid

and nitrates as eluents are given. Quantitative determination by scanning the radioactive nuclides is possible and some methods are proposed. The oxidation states of Np and Pu were identified by their different R_F values. The composition of mixtures with different valency states of the metals may be determined quantitatively. (auth)

5510 INFLUENCE OF SAMPLE VOLUME ON WEAK β-COUNTING EFFICIENCY IN LIQUID SCINTILLATION COUNTING. Quazi, A. H. (Technische Hochschule, Munich). Naturwissenschaften, 52: 490-1(1965).

The effect of volume of different samples in different scintillator solutions on the counting efficiency at 0°C was investigated in order to determine the optimum sample volume. The dependence of this counting efficiency on the sample volume was measured on tritiated toluene, ^{14}C-toluene, tritiated water, and ^{35}S-labeled urine. The results showed that the counting weight was not constant with the increase of sample volume with fixed specific activity. The maximum counting efficiency in all cases was obtained with samples between 7 and 15 ml and was independent of the type of scintillator solution. (J.S.R.)

5511 A DEVICE FOR PRECISE MEASUREMENTS OF ^{14}C RADIOACTIVITY IN ORGANIC COMPOUNDS. Forys, Mechislav; Zlotowski, Iznaii. Nukleonika, 10: 427-31(1965). (In Russian).

The construction and operation of a self-quenching G-M counter for measuring radioactivity of ^{14}C in organic compounds, converted to CO_2, is described. The statistical error involved in measuring specific activities of the order of 5×10^{-5} μc/mg was less than 1%. (auth)

5512 SEPARATION OF SOME INORGANIC AND PHENYL PHOSPHORUS COMPOUNDS BY PAPER CHROMATOGRAPHY AND PAPER ELECTROPHORESIS. Siuda, Andrzej (Inst. of Nuclear Research, Warsaw). Nukleonika, 10: 459-61(1965).

Paper chromatographic and paper electrophoresis methods for the separation and identification of inorganic and phenyl derivatives of phosphorus were developed. Triphenylphosphine, diphenylphosphonic acid, phenylphosphonous acid, phenylphosphonic acid, ammonium orthophosphate, sodium hypophosphate, potassium pyrophosphate, sodium orthophosphite, and sodium hypophosphite were studied. Paper chromatography was carried out with the ascending technique on paper pretreated with 2% versene. The solvent used was n-propanol and 25% ammonia. Paper electrophoresis was carried out using paper soaked in ammonium oxalate at pH 5.5 and pressed between silicon-treated glass plates. Results are shown in figures. (M.C.G.)

5513 A TRIAL METHOD OF DETERMINING URANIUM AND THORIUM CONTENT IN ROCKS BY RADIOACTIVE MEASUREMENTS. [PART] I. Hatuda, Zin'itiro; Nishimura, Susumu (Univ., Kyoto. Univ., Osaka). Radioisotopes (Tokyo), 14: 445-50(Nov. 1965). (In Japanese).

Determination of uranium, thorium, and potassium in rocks is discussed. The usual method, using a gamma pulse height analyzer, requires relatively expensive apparatus and considerable time. This is especially true when the samples have a low radioactivity, such as in rocks. A method for determining the content of uranium and thorium by means of the parallel measurements with an alpha scintillation counter and a radioscope is described. Variations in the content of uranium and thorium across igneous contacts were traced with continuous samples by the use of this method. (auth)

5514 A METHOD OF ACTIVATION ANALYSIS FOR COMPETING REACTIONS BY USING REACTOR NEUTRON SPECTRA (ACTIVATION ANALYSIS OF MANGANESE IN IRON). Kato, Hidemasa; Seino, Hideaki (Tokyo Atomic Industrial Research Lab., Ltd.). Radioisotopes (Tokyo), 14: 468-74(Nov. 1965). (In Japanese).

In activation analysis using a reactor the interference of competing reactions often becomes troublesome. For example, in the determination of manganese in iron, in which the $^{55}Mn(n,\gamma)^{56}Mn$ reaction is used, another reaction, $^{56}Fe(n,p)^{56}Mn$, also produces ^{56}Mn. Therefore, it is necessary to know the production ratio of both reactions. These quantities depend on the neutron spectrum in the reactor. A method of activation analysis for competing reactions was developed and the practical usefulness of this method was checked. Activation analysis accompanied with competing reaction is practicable by use of this method. The technique is simple, because it is necessary only to measure cadmium ratio. Since competing products can accurately be measured by this method, high neutron density near the reactor core can be used for activation analysis. (auth)

5515 STUDIES ON THE QUALITY AND TEST METHOD OF RADIOPHARMACEUTICALS. I. PAPER CHROMATOGRAPHY OF PREPARATIONS LABELED WITH ^{131}I AND ^{125}I. Urakubo, Goro; Kido, Yasumasa; Hasegawa, Akira (National Inst. of Hygienic Sciences, Japan). Radioisotopes (Tokyo), 14: 504-7(Nov. 1965). (In Japanese).

Paper chromatographic methods for purity tests on some kinds of radiopharmaceuticals labeled with ^{131}I and ^{125}I, using various kinds of developing solvents, were developed. Among the solvents tested, the following were regarded as the most suitable for purity tests: for labeled sodium iodide, ethanol : water : benzene (65 : 35 : 1) and methanol : water (75 : 25); for radioactive triiodothyronine, n-butanol : dioxane (4 : 1) saturated with 2N ammonium carbonate; and for radioactive sodium o-iodohippurate, n-butanol : ethanol (4 : 1) saturated with 2N ammonium carbonate. (auth)

5516 DETERMINATION OF URANIUM IN TRIBUTYLPHOSPHATE, KEROSENE, AND SYNTHOL IN FORM OF THIOCYANATE. Deberdeeva, R. Yu.; Nemodruk, A. A.; Pale, P. N. Radiokhimiya, 7: 271-3(1965). (In Russian).

It was found that solutions of tributyl phosphate in kerosene, synthol, or aliphatic hydrocarbons are not well suited for the determination of U by methods requiring the addition of a solution of NH_4CNS in acetone because the system separates into two layers, one of which consists of TPB in acetone, the other containing TPB in kerosene or synthol and nearly all of the uranium. Tests were therefore carried out to find solvents that form a homogeneous solution under the above conditions. It was found that a solution of TBP itself in the same diluent used for the sample to be analyzed yields the best results. Addition of ascorbic acid, needed to remove the interfering Fe(III) ions caused a yellow coloration that disturbed the analysis. This coloration could be suppressed by adding one drop of 1.5M nitric acid per 5 ml of the 10% solution of NH_4CNS in TBP, containing 0.2% ascorbic acid. Instead of the acid itself, NH_4NO_3 could be used. The optical density of the solution did not change under these conditions for 30 minutes. Temperature variations within 15 to 35°C did not affect the photometric measurements. The method was found to work with an error of ±1.6% for 10 and 20% solutions of TBP containing 0.75 to 1.25 mg/ml of uranium. (TTT)

5517 DETERMINATION OF NATURAL TRITIUM. Bainbridge, A. E. (La Jolla Natural Tritium Lab., Calif.). Rev. Sci. Instrum., 36: 1779-82(Dec. 1965).

The experimental methods employed at the La Jolla Natural Tritium Laboratory, for the determination of natural tritium are briefly described. The method is to assay the electrolytically enriched sample as ethane gas in a proportional counter. An error of less than 4% is obtained for samples enriched by reducing the sample volume from 2 liters to 10 ml. It is found that the previous methods of calculating the electrolytic enrichment are not necessary nor are large volume reductions necessary for most applications. In the method adapted at La Jolla, the enrichment in five electrolyzed samples is determined by using a sixth spiked sample. In this way it is shown that the enrichment in the sixth sample is within 4% of the enrichment in the other five and can be quickly determined. (auth)

5518 DETERMINATION OF URANIUM AND FREE ACID IN ORGANIC SOLUTIONS OF LONG-CHAIN AMMO-

NIUM NITRATES. Koch, Guenter (Kernforschungszentrum, Karlsruhe). Z. Anal. Chem., 214: 99-105(1965). (In German).

Uranium and free acid may be determined by potentiometric titration with alkali. The applicability of this method to solutions of long-chain tertiary and quaternary ammonium nitrates in organic solvents containing uranium and nitric acid was studied. In solutions of quaternary ammonium nitrates, uranium and free acid may be determined by direct titration in a two-phase mixture, while in the case of tertiary ammonium nitrates they may be determined only after back-extraction by dilute aqueous sodium nitrate and removal of the organic phase. (auth)

5519 POTENTIOMETRIC DETERMINATION OF RARE EARTHS (e.g. ERBIUM). Wawrzyczek, Wiktor; Benedict, Andrzej; Jagosz, Ryszard (Landwirtschaftliche Hochschule, Olsztyn, Poland). Z. Anal. Chem., 214: 258-61(1965). (In German).

A method for the potentiometric titration of erbium by means of ammonium oxalate solution in a water-acetone medium (1:1) was developed. The system Pt | $ErCl_3$ | Hg_2Cl_2 + KCl | Hg was used. The potential jump at the neutral point was distinct, even if only one drop of the reagent was added. The error of the measurement was not greater than ±0.5%. Metal ions forming insoluble precipitates with ammonium oxalate interfered with this method. (auth)

5520 ON THE TITRATION OF FLUORIDE WITH URANIUM(IV). Harzdorf, C. (Anorganisch Analytisches Laboratorium der Farbenfabriken Bayer AG, Leverkusen, Ger.). Z. Anal. Chem., 214: 345-50(1965). (In German).

Possibilities for the titration of fluoride with U^{IV} were investigated. In the presence of potassium ions 4 to 50 mg of fluoride in 100 ml could be determined by turbidimetric or visual titration. Xylenol orange or methylthymol blue were used as indicators. Electrochemical methods of indication of the end-point were unsatisfactory. X-ray diffraction and chemical analysis proved the precipitate to be 7 KF · 6 UF_4. The methods described are equally applicable after separation of fluoride by distillation. (auth)

5521 A SURVEY OF SYSTEMS FOR CONCENTRATION AND LOW BACKGROUND COUNTING OF TRITIUM IN WATER. Cameron, J. F. (International Atomic Energy Agency, Vienna). 28p. (CONF-650652-3). Gmelin, AED-CONF-65-158-7.

From International ^{14}C and ^{3}H Dating Conference, Pullman, Wash.

Systems used for concentrating and counting tritium activities in the range from 0.1 to 5000 T. U. are reviewed. The tritium-measuring systems should be capable of measuring large numbers of samples rapidly with an accuracy of about ±10% or better. The speed of measurement is determined by the tritium content of the sample, the amount of sample in the counter, and the counter background. Gas counters and liquid scintillation counters are discussed and compared. The concentration systems described employ electrolysis and thermal diffusion. Standardization and accuracy of tritium measurements are based on combined data from several laboratories. Absolute tritium values are obtained by calibrating with a standard of known disintegration rate. The backgrounds are determined using water of zero tritium content or the lowest tritium content available or a tritium-free sample of the counting gas. As a check on the overall accuracy of different systems a number of samples of unknown content were circulated by the IAEA. (72 references) (F.J.H.)

5522 APPARATUS FOR X-RAY DETERMINATION OF METAL IN HYDROCARBON FUEL. Cropper, Wendell P.; Thourson, Thomas L. (to Standard Oil Co.). U. S. Patent 3,210,541. Oct. 5, 1965. Filed Oct. 7, 1960.

An apparatus for determining the concentration of lead in a hydrocarbon fuel includes a radioactive beta source, an absorber, a molybdenum target for receiving beta rays and emitting x rays, a hydrocarbon sample cell, and an x-ray detecting means. The source is placed between the reflecting target and the absorber, which is shaped and arranged to substantially completely absorb all energy receivable upon the reflecting target. The sample cell is arranged to receive x rays emitted from the target, and those x rays that pass through the sample are received by the detector. (B.L.M.)

Inorganic and Physical Chemistry

Refer also to abstracts 5823, 5839, and 6159.

5523 (ANL-6925, pp 175-85) CALORIMETRY. Hubbard, W. N.; Feder, H. M. (Argonne National Lab., Ill.).

Data and information are presented concerning combustion of P, S, SiC, US, graphite, Mg, Al, Y, La, Gd, Ho, and TaB_2 in F_2. The design and operation of 1500°C and 2500°C drop colorimeters are described. (J.R.D.)

5524 (ANL-7076) PICTORIAL STUDIES OF MOLECULES. I. MOLECULAR ORBITAL DENSITY COMPARISONS OF H_2, Li_2, B_2, C_2, N_2, O_2, AND F_2. Wahl, Arnold C. (Argonne National Lab., Ill.). July 1965. Contract W-31-109-eng-38. 58p. Dep. mn; CFSTI $3.00 cy, $0.75 mn.

Contour diagrams of the molecular orbital and total electron densities of the homonuclear diatomic molecules H_2, Li_2, B_2, C_2, N_2, O_2, and F_2 are presented on a consistent basis convenient for comparison. These diagrams are calculated and drawn automatically by programs written for the CDC-3600 computer. The molecular orbitals used are the result of recent self-consistent field calculations and are thought to be very near the Hartree-Fock orbitals. The importance of such visual presentations is stressed, and further use in studies of chemical bond formation and molecular ionization indicated. (auth)

5525 (IA-1041) REACTIONS OF THE HYDRATED ELECTRON. Anbar, M. (Israel Atomic Energy Commission, Yavne. Soreq Nuclear Research Center). May 1965. 45p. Dep. mn.

The reactions of hydrated electrons with inorganic and organic compounds are reviewed. The rates of these reactions as well as the reaction products are discussed. It is shown that the reactivity of a compound toward e^-_{aq} is a function of the availability of a vacant orbital which is capable of accommodating an additional electron. The products of these reactions, which contain an additional electron, always have a finite lifetime, even if they are only short-lived intermediates. 126 references are cited. (auth)

5526 (KFK-250) PHOTOMETERPROG 4—EIN IBM 7070-PROGRAMM ZUR BERECHNUNG VON STABILITAETSKONSTANTEN AUS SPEKTRALPHOTOMETRISCHEN MESSUNGEN. (PHOTOMETERPROG 4—An IBM-7070 Program for Calculation of Stability Constants From Spectrophotometric Measurements). Eberle, Siegfried Helmut (Kernforschungszentrum, Karlsruhe (West Germany). Institut fuer Radiochemie). May 1965. 28p. Dep. mn.

A program for the calculation of the stability constants at successive formation of the complexes MA and MA_2, where M = metal and A = anion of the ligands H_2A, is described for the IBM-7070. The extinctions measured at three wave lengths and the pH value of the aqueous solutions of the components were used as the measurement data. For evaluation it was assumed that only the metal-containing species contribute to the absorption and that the extinction modulus for M and MA_2 are known. The program looks for the stability constants K_1 and K_2 and the extinction modulus for MA which yields a minimum of a suitable selected error size. The FORTRAN list of the program statements and an example are given. (tr-auth)

5527 (NP-15646) BIBLIOGRAPHY ON THE HIGH TEMPERATURE CHEMISTRY AND PHYSICS OF MATERIALS IN THE CONDENSED STATE. Volume 1965,

Number 3, July–September 1965. Diamond, J. J. (ed.) (National Bureau of Standards, Washington, D. C.). 105p.

References (1110) on properties of materials in the condensed state and devices for measuring the properties are given to U. S. and foreign journals published during 1964 and 1965. (P.C.H.)

5528 (ORNL-TM-1292) PURIFICATION OF ZIRCONIUM TETRAFLUORIDE. Yeatts, L. B. Jr.; Rainey, W. T. Jr. (Oak Ridge National Lab., Tenn.). Nov. 1965. Contract W-7405-eng-26. 24p. Dep. mn; CFSTI $1.00 cy, $0.50 mn.

The factors which were studied, during the purification of ZrF_4 by sublimation, for their effect upon the product purity level were the: rate of sublimation; rate of condensation of sublimate; successive or multistage sublimations; number and arrangement of baffles; and pre-treatment of the starting material. A single stage vacuum sublimation at 700 to 800°C with one baffle present was sufficient to lower the impurity level of iron to less than 100 ppM. Pretreatment of the starting material with NH_4HF_2 and use of a more elaborate baffling system gave a product with an oxygen level of 250 ppM. The application of a vapor-zone sublimation technique seems potentially useful for ZrF_4 purification. (auth)

5529 (SC-DC-65-1706) THE ELECTROCHEMISTRY OF SOME TRANSITION METALS AND LANTHANIDES DISSOLVED IN MOLTEN ALKALI METAPHOSPHATE. Final Report, July 1, 1964–June 30, 1965. Caton, Roy D. Jr. (New Mexico Univ., Albuquerque. Dept. of Chemistry). Contract AT(29-1)-789. 9p. (CONF-651027-1). Dep. mn; CFSTI $1.00 cy, $0.50 mn.

From New Mexico Academy of Science, Albuquerque, N. Mex.

A reference electrode ($Ag-AgPO_3$) for use in the metaphosphate melts was found and tested. The electrode is quite stable, attains its potential within 15 min, and is of rugged construction. Corning 1720 glass was found to possess the desirable properties of a salt bridge material, and is now being used in all the emf studies. An inert atmosphere container was designed and fabricated and an illustration is given. Preliminary studies that have been initiated but not completed are described. These include: use of chronopotentiometry as means of analyzing the melt for electroactive species; emf studies of transition metal Redox couples; and chemical reactions in the melt. (P.C.H.)

5530 (SC-RR-65-625) ABSORPTIVITIES OF COMPLEXES FROM THE VARIATION AND THE MOLE RATIO METHODS FOR COMPLEX DETERMINATIONS. Wear, James O. (Sandia Corp., Albuquerque, N. Mex.). Nov. 1965. Contract AT(29-1)-789. 15p. Dep. mn; CFSTI $1.00 cy, $0.50 mn.

Studies showed that the absorptivities of complexes can be determined from the slopes of the lines in the standard plots of the variational and the mole ratio methods for complex determination. The mathematics of the mole ratio method were developed and are presented. The variational method was used to determine the complexes of phenolphthalein with Np(VI). Two complexes, $(NpO_2)_3\ Y^{\underline{n}}$ and $(NpO_2)_4\ Y^{\underline{m}}$, where $\underline{n}$ and $\underline{m}$ are the charges and Y is phenolphthalein or some ionic form of it. The absorptivities of the different complexes at various wavelengths were determined by using the techniques developed. The mole ratio method was used to determine two complexes of Np(V) with oxalate ion, $(NpO_2)_2C_2O_4$ and $NpO_2(C_2O_4)_3^{3-}$. The absorptivities of these complexes were also determined by using techniques developed for this purpose. (auth)

5531 (UJV-1382/65) AKTIVEROVANNYI SERNOKISLYI BARII KAK SORBENT NEBOLSHIKH KOLICHESTV STRONTSIYA. III. IZUCHENIYA SKOROSTI ZAKHVATA STRONTSIYA NA SERNOKISLOM BARII AKTIVIROVANNOM PUTEM SPEKANIYA S SERNOKISLIM KALTSIEM. (Calcium-Activated Barium Sulfate as Sorbent of Radiostrontium. III. The Sorption Rate of Strontium upon the Heat Treated Barium Sulfate). Berak, L.; Muenich, J. (Ustav Jaderneho Vyzkumu, Ceskoslovenska Akademie Ved, Rez). 1965. 50p. Dep. mn.

The process limiting the sorption efficiency of the calcium-activated, heat treated barium sulfate for radiostrontium was determined. (P.C.H.)

5532 (K-Trans-10) THERMIONIC EMISSION OF THE HEXABORIDES OF SAMARIUM AND GADOLINIUM. Ermakov, S. V.; Tsarev, B. M. Translated for Oak Ridge Gaseous Diffusion Plant, Tenn., from Radiotekhn. Elektron., 10: 972-5(1965). 7p. Dep. mn; CFSTI $1.00 cy, $0.50 mn; JCL $1.10 fs, $0.80 mf.

The thermionic emission of SmB_6, EuB_6, and GdB_6 on W and Ir substrates is measured at 1000 to 2000°K. The results are compared with previous results on LaB_6, TmB_6, and WB_x. (T.F.H.)

5533 ELECTRON SPIN RESONANCE OF COPPER(II) AND MANGANESE(II) IONS IN POLYCRYSTALLINE SUBSTANCES. Nicula, Al (Univ., Cluj). Acad. Repub. Pop. Rom. Stud. Cercet. Fiz., 17: 257-321(1965). (In Rumanian).

The energy levels of a paramagnetic ion in a magnetic field and their dependence on the field are calculated by the spin Hamiltonian; the wave function describes the spin state. This was illustrated in two stages: assuming that the nuclear moment I = 0, using the $Ni^{2+}(3d^8)$ ion as an example and considering the case of the $Cu^{2+}(3d^9)$ ion with $S = \frac{1}{2}$, $I = \frac{3}{2}$. The Cu^{2+} and Mn^{2+} ions were introduced in synthetic zeolites, which are able to absorb and desorb water molecules in the cavities without disrupting the crystal structure. The unit cell of the X and Y type zeolites had the composition $Na_{88}[(AlO_2)_{88}(SiO_2)_{104}]$ and $Na_{56}[(AlO_2)_{56}(SiO_2)_{136}]$, respectively. It was found that the Cu(II) ion exhibited an anisotropic spectrum with a group of 4 hyperfine structure lines in a band parallel with the magnetic lines. The spin Hamiltonian constants, which define the state of Cu(II), were also determined. The effect of the absorbed water molecules on the electron spin resonance signals was also examined; it was found that the hyperfine structure that appears at high paramagnetic ion concentrations depended on the activation energy threshold of spin–spin and spin–lattice interactions. Similar results were obtained with the compound $Cu^{2+}(NH_3)_4$ at various concentrations in a glycerine solution at liquid-nitrogen temperature. In the case of Mn(II), the constants of the Hamiltonian were determined and the fine and hyperfine structures were established. It was found that gaseous oxygen reduces the intensity of the spin electron resonance signal and the width of the absorption line of Mn(II) ions in zeolites. (Thesis, 60 references). (TTT)

5534 STUDY OF SOME OF THE PHYSICAL PROPERTIES OF THE NICKEL–CHROMIUM TRIOXIDE CATALYST FOR THE HYDROGEN–DEUTERIUM ISOTOPIC EXCHANGE REACTION. Barb, Danila (Inst. of Atomic Physics, Rumanian Academy of Sciences. Univ., Cluj). Acad. Repub. Pop. Rom. Stud. Cercet. Fiz., 17: 383-445 (1965). (In Rumanian).

Structural, magnetic, catalytic, and electric properties of the $Ni-CrO_3$ system were studied, in order to understand its action for the H–D isotopic exchange reaction between gaseous hydrogen and water vapor. The contact surface between Ni and CrO_3 is largest in the concentration range from 90 to 98% Ni because in that case the grain size of the components lies within the same order of magnitude. Because of the presence of Ni, the mixtures exhibit ferromagnetic properties; for a given field, the magnetic permeability increases with increasing Ni content. Mixtures with Ni concentration between 10 and 90% behave like semiconductors; their conductivity increases by one-half order of magnitude in helium, one order of magnitude in hydrogen, and four to five order of magnitude in oxygen. In hydrogen atmosphere the n-type and in oxygen the p-type conductivity predominates. A complex equilibrium is established on the catalyst's surface between the H_2, HD, D_2, H_2O, HDO, and D_2O molecules; the ratio of D in the gaseous and liquid phases depends primarily on the temperature of the catalyst but the distribution of D between the various molecular species is only slightly affected by the temperature. With

certain limitations due to capillary condensations, the isotopic exchange reaction follows the Arrhenius law. The CrO_3 plays the role of promoter in the reaction. The transfer constant changes from $K = 1.2 \times 10^{-6}$ to 1.35×10^{-4} mole D_2/g sec when 4 atomic % of Cr are added to Ni. The action of CrO_3 is due to the reduction of the dimensions of the Ni crystals, thus increasing their surface and their catalytic activity. Chemosorption of oxygen modifies the surface properties of the catalysts. (Thesis, 93 references) (TTT)

5535 ON THE INTERACTION BETWEEN HAFNIUM TETRAFLUORIDE AND AMMONIUM FLUORIDE IN AQUEOUS SOLUTION. Sazhin, N. P.; Shchepochkin, B. V.; Yagodin, G. A. (Mendeleev Inst. of Chemical Engineering, Moscow). Izv. Akad. Nauk SSSR, Ser. Khim., No. 7: 1127-30(1965). (In Russian).

By methods of separate potentiometric and conductometric titrations, microscopic observations, and x-ray structure analysis, the reaction between hafnium tetrafluoride and ammonium fluoride in aqueous solution was studied. Under the experimental conditions the formation of two compounds, $NH_4HfF_5 \cdot \frac{2}{3}H_2O$ and $(NH_4)_2HfF_6$, was detected. By differential thermal analysis and thermogravimetric methods, the thermal stability of the compounds was investigated. $NH_4HfF_5 \cdot \frac{2}{3}H_2O$ loses water at 110°C and at 386°C ammonium fluoride separates. $(NH_4)_2HfF_6$ loses the first molecule of ammonium fluoride at 336°C and the second at 386°C. (tr-auth)

5536 POLYMORPHISM OF RARE-EARTH SESQUIOXIDES. Glushkova, V. B.; Boganov, A. G. (Grebenshchikov Inst. of Chemistry of Silicates, Academy of Sciences, USSR). Izv. Akad. Nauk SSSR, Ser. Khim., No. 7, 1131-8 (1965). (In Russian).

As a result of high-temperature x-ray and thermal analysis, the absence of reversible polymorphic transformations in the temperature range from 50 to 1500°C was established for oxides Y_2O_3, La_2O_3, Nd_2O_3, Sm_2O_3, Eu_2O_3, Gd_2O_3, Dy_2O_3, Ho_2O_3, Er_2O_3, Tm_2O_3, and Yb_2O_3. By means of x-ray analysis the presence of irreversible transitions was confirmed in the oxides Nd_2O_3, Sm_2O_3, Eu_2O_3, and Gd_2O_3 and their absence, in the temperature range from 100 to 1500°C, confirmed in the oxides Y_2O_3, Dy_2O_3, Ho_2O_3, Er_2O_3, Tb_2O_3, and Tm_2O_3. The impossibility of producing low-temperature C forms of lanthanum oxides was shown by the decomposition of the oxide and the hydroxide during annealing in air at pressures from 760 to 1 mm. The C form of Nd_2O_3 was produced both by decomposition of the nitrate and by decomposition of the carbonate, oxalate, and oxide hydrate. The irreversible transitions C → A for Nd_2O_3 and C → B for Sm_2O_3 were accompanied by intense gas evolution (1.5 to 2 wt. %). The hypothesis showed that the low-temperature forms of the oxides of Nd, Sm, Gd, and Eu appear with the metastable formation and possess thermodynamic stability in their temperature interval of existence only because of inclusions of foreign ions in the oxide lattice. (tr-auth)

5537 STABILITY OF ZIRCON IN THE TEMPERATURE RANGE 1180 deg TO 1366 deg C. Rosen, Erik (Pennsylvania State Univ., University Park); Muan, Arnulf. J. Amer. Ceram. Soc., 48: 603-4(Nov. 21, 1965).

A method was developed for determining the standard Gibbs free energy of reaction between ZrO_2 and SiO_2 to form zircon ($ZrSiO_4$). The method consists of equilibrating cobalt, a gas phase of known oxygen pressures, and chosen phases in the systems $CoO-ZrO_2-SiO_2$ and $CoO-SiO_2$. Results of equilibrium runs are presented in tabular form. Data indicated decomposition of $ZrSiO_4$ into ZrO_2 and SiO_2 at ~1600 to 1650°C. (M.C.G.)

5538 CHELATE CHEMISTRY. III. CHELATES OF HIGH COORDINATION NUMBER. Muetterties, E. L.; Wright, C. M. (E. I. duPont de Nemours and Company, Wilmington, Del.). J. Amer. Chem. Soc., 87: 4706-17 (Nov. 5, 1965).

Synthesis, properties, and structural interpretations are presented for seven- and eight-coordinate structures based on the tropolone anion and the following elements: scandium, yttrium, titanium, zirconium, hafnium, thorium, vanadium, niobium, tantalum, rare earth metals, indium, tin, and lead. Oxygen atoms in the chelated tropolone anion apparently are three-coordinate in the tris-chelates of some rare earth metals and yttrium but not in scandium, titanium, iron, and rhodium. (auth)

5539 THERMODYNAMICS OF IODINE SOLUBILITY AND TRIIODIDE ION FORMATION IN WATER AND IN DEUTERIUM OXIDE. Ramette, R. W.; Sandford, R. W. Jr. (Carleton Coll., Northfield, Minn.). J. Amer. Chem. Soc., 87: 5001-5(Nov. 20, 1965).

The solubility of iodine in water and in deuterium oxide was determined in the range from 5 to 50°C using packed-column techniques, and the thermodynamic results were compared for the two solvents. The solubility of iodine in very dilute potassium iodide solutions led inherently to apparent values of the triiodide formation constant that were higher than those obtained by precise spectrophotometric work at exceedingly low concentrations. The difference is explained in terms of the species I_5^-. For the reaction, $I_3^- + I_2 \rightleftharpoons I_5^-$, the formation constant was about 9 at 25°C. (auth)

5540 MASS-SPECTROMETRIC STUDY OF THE YTTRIUM–CARBON SYSTEM. De Maria, G.; Guido, M.; Malaspina, L.; Pesce, B. (Univ., Rome). J. Chem. Phys., 43: 4449-52(Dec. 15, 1965).

A high-temperature investigation of the vapor in thermodynamic equilibrium with the Y – C condensed system was carried out in the temperature range from 2075 to 2340°K. Y and YC_2 are shown to be important species in the vapor phase. Utilizing the pressure-independent reaction $Y_{(g)} + 2C_{(s)} \rightarrow YC_{2(g)}$ second- and third-law methods yielded $D_0^0 = 155 \pm 6$ and $D_0^0 = 156 \pm 5$ kcal mole^{-1}, respectively, for the Y – C_2 bond energy. An estimated heat of formation $\Delta H_{f\,298}^0 = -27 \pm 6$ kcal mole^{-1} for solid dicarbide was also obtained. Comparison between Me – C_2 and Me – O bond strengths was made for Group IIIA elements and for the first two elements of the lanthanide series. (auth)

5541 DIFFERENCES IN THE SPHERICAL INTERMOLECULAR POTENTIALS OF HYDROGEN AND DEUTERIUM. Mason, E. A. (Univ. of Maryland, College Park); Amdur, I.; Oppenheim, I. J. Chem. Phys., 43: 4458-63 (Dec. 15, 1965).

The differences in the Lennard-Jones parameters of hydrogen and deuterium were determined from a reanalysis of the second-virial-coefficient data of Michels et al. and an analysis of the diffusion data of Amdur and Beatty and of Mason, Annis, and Islam. The effects of higher Chapman-Enskog approximations, spherical quantum corrections, inelastic collisions, and the anisotropy of the intermolecular potentials on the transport coefficients were found to be very small, and the experimental differences can be ascribed unambiguously to differences in the isotropic intermolecular potentials. Reanalysis of the second-virial-coefficient data indicated that $(\epsilon_{H_2} - \epsilon_{D_2})/\epsilon_{H_2} = 0.06$ and $(\sigma_{H_2} - \sigma_{D_2})/\sigma_{H_2} = 0.008$; these results are consistent with the transport-coefficient data. (auth)

5542 ENERGY LOSSES OF FAST ELECTRONS IN NITROGEN. Geiger, J.; Stickel, W. (Technische Univ., Berlin). J. Chem. Phys., 43: 4535-6(Dec. 15, 1965).

Marked differences were found between experimental light-absorption coefficients and experimental electron-impact excitation cross sections in nitrogen. The absorption spectra showed striking deviations in the region 12.4 to 14.5 ev (wavelength range 970–855Å) where the intensity of the energy losses was much higher. Only about 30% of the intensity of the energy loss peak at 12.936 ev was ascribed to the levels $\underline{v}^1 = 4$ and 5 of $\underline{b}'\Pi_u$. It was concluded that the remainder was due to the excitation of the states $\underline{c}'\Pi_u$ and $\underline{P}''\Sigma_u^+$ lying closely together. (M.C.G.)

5543 ELECTROCHEMICAL STUDIES ON ZIRCONIUM AND HAFNIUM IN MOLTEN LiCl–KCl EUTECTIC. Baboian, R.; Hill, D. L.; Bailey, R. A. (Rensselaer Polytechnic Inst., Troy, N. Y.). J. Electrochem. Soc., 112: 1221-4(Dec. 1965).

Electrode potential and polarographic studies were made

on solutions of zirconium and hafnium ions in molten LiCl-KCl eutectic at 450 to 550°C. Anodic dissolution of Zr at 450°C yielded Zr(IV), but at 550°C, chiefly Zr(II). Only Hf (IV) was observed over this range. Apparent standard electrode potentials were (mole fraction scale, Pt(II)/Pt(0) reference): Zr(II)/Zr(0), −1.77v at 550°C; Zr(IV)/Zr(0), −1.86v at 450°C; and Hf(IV)/Hf(0), −1.88v at 450°C, −1.92v at 550°C. (auth)

5544 INVESTIGATIONS ON AgI CATALYST SURFACE STRUCTURE BY ISOTOPE EXCHANGE REACTIONS. Galiba, I.; Latzkovits, L.; Gal, D. (Jozsef Attila Univ., Szeged). J. Inorg. Nucl. Chem., 27: 2279-89(Nov. 1965).

The isotopic exchange reaction between solid AgI precipitates and $CH_3\ ^{131}I$ vapor was investigated and the dependence of the exchange reaction on the preparation and surface structure of the solid catalyst was determined. Precipitates were prepared in a well defined way so that Ag^+ and I^- in excess as well as neutral surfaces were obtained. It appeared that on positively charged surfaces the exchange goes further and more rapidly compared to negatively charged surfaces. The mechanism of the exchange also varied with the surface structure. It was found that the exchange is preceded by an adsorption equilibrium and takes place between the adsorbed intermediate and the solid surface. This is followed by desorption. On the basis of a mathematical analysis of the kinetic curves it is shown that the AgI crystals took part in the reaction as a uniformly heterogeneous surface. On surfaces with a Ag^+ excess exchange occurred as an S_N1-type nucleophyllic substitution and the first step of this was a slow heterolysis, while on surfaces with an I^- excess the exchange process took place as a pseudo-S_N2-type reaction by an electron transfer. (auth)

5545 SOLID-SOLID INTERACTIONS. II. URANYL NITRATE-UREA COMPLEXES. Gentile, P. S.; Campisi, L. S. (Fordham Univ., New York). J. Inorg. Nucl. Chem., 27: 2291-2300(Nov. 1965). (TID-22035).

The usefulness of solid−solid interactions as a technique for the formation of complexes was demonstrated by the isolation of isomers of dinitratobis(urea)dioxouranium (VI) (designated as the α- and β-forms), nitratotris (urea)dioxouranium (VI) nitrate, and pentakis(urea) dioxouranium (VI) nitrate. Based on these results, various solutions were examined for the presence of these complexes, from which they were ultimately isolated. The evidence suggested the α-isomer is a monomer, whereas the β-modification may be a dimer although polymorphism cannot be excluded. The complexes $[UO_2(NO_3)(urea)_3]NO_3$ and $[UO_2(urea)_5](NO_3)_2$ appeared to be polymeric in nature also. Although $[UO_2(NO_3)(H_2O)(urea)_4]NO_3$ was a discrete polymeric compound, heating it at 110°C did not yield the anhydrous complex; instead, a mixture of the tris(urea) and pentakis(urea) complexes were formed. The infrared spectra indicated in all cases that the ligand, urea, was bound to the metal via the carbonyl group. Nitrato coordination was evident, but the tendency for this group to co-ordinate decreased until only nitrate groups were present in the pentakis complex. The deleterious effects of the KBr matrix upon the infrared spectra are discussed. (auth)

5546 SOLID STATE STUDIES ON AMMONIUM URANYL PEROXY OXALATES. Prasad, N. S. Krishna (Atomic Energy Establishment, Trombay, India). J. Inorg. Nucl. Chem., 27: 2311-16(Nov. 1965).

Infrared absorption spectra, x-ray-powder diffraction data, and differential thermal analysis curves for the ammonium uranyl peroxy oxalates $(NH_4)_2U_2O_8(C_2O_4)_2 \cdot 2H_2O$, $(NH_4)_2UO_4C_2O_4 \cdot 3H_2O$, $(NH_4)_2U_2O_8C_2O_4 \cdot 4H_2O$, and ammonium pyroperuranate $(NH_4)_2U_2O_9 \cdot 6H_2O$ are recorded. The peroxy oxalates are characterized as ionic from their infrared spectra. The infrared spectra do not show any vibrations for the −O−O− group. (auth)

5547 STUDIES OF THE FORMATION OF URANYL(VI) FROM URANIUM DIOXIDE AND CHLORINE IN MOLTEN ALKALI CHLORIDES. E.m.f. MEASUREMENTS AND THERMODYNAMIC VALUES. Stromatt, R. W. (Battelle-Northwest, Richland, Wash.). J. Inorg. Nucl. Chem., 27: 2331-9(Nov. 1965).

Emf measurements were used to calculate thermodynamic properties of the reaction of uranium dioxide with chlorine forming uranyl chloride in several molten salt solutions. The thermodynamic data are given for this reaction in eutectic NaCl−LiCl, eutectic KCl−LiCl, 1:1 KCl−LiCl, and 1:1 KCl−NaCl; and emf data are given for the reaction in NaCl−LiCl, KCl−LiCl, and KCl−NaCl solvent systems of systematically varied composition. The variations of these data with solvent composition showed an increasing stability of UO_2(VI) with the decreasing effective charge density of the solvent cations. This was attributed to an increasing efficacy, or activity, of the chloride resulting from the decreasing polarizing power of the solvent cations. (auth)

5548 OXIDATION REDUCTION POTENTIAL OF THE U(IV)–U(VI) SYSTEM. III. PHOTOELECTROCHEMICAL PROPERTIES OF THE U(V) ION. Sobkowski, J. (Univ. of Warsaw). J. Inorg. Nucl. Chem., 27: 2351-9(Nov. 1965).

The influence of light on the redox potential was investigated in U(IV) and U(VI) ion solutions in relation to temperature, hydrogen ion concentration, and complex-forming agents. It was established that the action of these factors is due to a change in the equilibrium of the reaction, U(IV) + U(VI) ⇌ 2U(V). The effects of the platinum electrode surface and of chloride ions on the kinetics of U(V) ion disproportionation were also examined. (auth)

5549 SPECTROPHOTOMETRIC AND POTENTIOMETRIC STUDIES OF THE SYSTEM CONTAINING UO_2^{2+}, $C_2O_4^{2-}$ AND H_2O_2. Prasad, N. S. Krishna; Abubacker, K. M. (Atomic Energy Establishment, Trombay, India). J. Inorg. Nucl. Chem., 27: 2391-5(Nov. 1965).

The reaction of uranyl ions with hydrogen peroxide in the presence of oxalate ions gave rise to complex species $[(UO_2)_2OO(C_2O_4)_2]^{2-}$ and $[UO_2OO\ C_2O_4]^{2-}$ in the pH ranges from 1 to 4.5 and 4.5 to 7.5, respectively, as indicated by potentiometric and spectrophotometric data. This was supported by the isolation of the corresponding ammonium salts in the solid state from solutions in these pH ranges. The stability constants of the two complexes calculated from potentiometric data are 2×10^7 and 5.1×10^5, respectively. (auth)

5550 HIGH RESOLUTION MEASUREMENTS ON THE INFRARED ABSORPTION SPECTRUM OF HBr. Rank, D. H.; Fink, Uwe; Wiggins, T. A. (Pennsylvania State Univ., University Park). J. Mol. Spectros., 18: 170-83 (Oct. 1965).

Wavelengths of 39 lines in the 1 to 0 band, 43 lines in the 2 to 0 band, and 27 lines in the 3 to 1 band of $H^{81}Br$ were precisely measured. From these lines and Gordy's microwave data very accurate molecular constants for $H^{81}Br$ were obtained. Isotope differences of $H^{79}Br - H^{81}Br$ for the same three bands were also measured and shown to agree with the values calculated from mass spectroscopic data. (auth)

5551 SAMARIUM BORIDES. THE TETRABORIDE–HEXABORIDE CONVERSION. Sturgeon, George D.; Eick, Harry A. (Michigan State Univ., East Lansing). J. Phys. Chem., 69: 3705-8(Nov. 1965).

The high-temperature conversion of solid samarium tetraboride into solid hexaboride and elemental samarium vapor was studied by the Knudsen effusion technique. The partial pressure of samarium was determined by neutron activation assays of the effusate, which was condensed onto silica collectors. From the pressure vs temperature data, values for the standard enthalpy and entropy of the reaction were obtained. The heat of formation of the hexaboride was calculated to be −50 kcal/mole. (auth)

5552 A NEAR-INFRARED STUDY OF HYDROGEN BONDING IN WATER AND DEUTERIUM OXIDE. Thomas, Mary R. (Cornell Univ., Ithaca, N. Y.); Scheraga, Harold A.; Schrier, Eugene E. J. Phys. Chem., 69: 3722-6(Nov. 1965).

The spectra of liquid H_2O, liquid D_2O, H_2O ice, and D_2O ice were obtained in the region from 1.16 to 1.25μ for H_2O and the region from 1.56 to 1.69μ for D_2O. The temperature dependence of the liquid spectra and the extinction coefficients for the solids were utilized to calculate the concentrations of the unbonded, singly hydrogen-bonded, and doubly hydrogen-bonded water molecules as a function of temperature for liquid H_2O and for liquid D_2O. The fraction of possible hydrogen bonds remaining intact at various temperatures for H_2O compared well with previous experimental and theoretical results. The results for D_2O were consistent with the calculations of Némethy and Scheraga. (auth)

5553 A SMALL ANGLE X-RAY SCATTERING STUDY OF COLLOIDAL THORIUM OXIDE. Schmidt, Paul W. (Univ. of Missouri, Columbia). J. Phys. Chem., 69: 3849-57(Nov. 1965). (ORNL-P-261).

Small-angle x-ray scattering data were obtained from four dilute polydisperse colloidal thorium oxide sols and from two gels prepared by drying the sols. From the complete small-angle x-ray scattering curve for a dilute polydisperse sol, the quantities $\overline{S}/\overline{V}$, $\overline{V}^2/\overline{V}$, and $\overline{R}^2$ were obtained, where S, V, and R represent, respectively, the surface area, volume, and radius of gyration of a single colloidal particle, and bars over a quantity indicate that the quantity is averaged over the polydisperse sample. For each value of $\overline{S}/\overline{V}$, $\overline{V}^2/\overline{V}$, and $\overline{R}^2$, which could be obtained for a sol an average particle dimension could be computed. By comparison of the different average particle dimensions for a sol with each other and with other measurements by different techniques, qualitative information was obtained about the distribution of particle diameters in the sols. For dried gels, two different small-angle x-ray scattering procedures can be used to find the specific surface $\overline{S}/\overline{V}$. To test the reliability of these determinations of the specific surface in gels, the two methods of measuring specific surface were used on a thoria gel with comparatively well-understood properties. The results obtained by the two methods agreed within the expected experimental error of ±15%. The small-angle x-ray scattering data for the specific surface of a second gel helped to explain the large discrepancy between the average particle dimensions obtained for this gel by BET nitrogen adsorption and x-ray diffraction line widths. (auth)

5554 THE THERMODYNAMIC AND PHYSICAL PROPERTIES OF BERYLLIUM COMPOUNDS. VIII. HEAT OF FUSION AND HIGH-TEMPERATURE HEAT CAPACITY OF BERYLLIUM OXIDE. Greenbaum, Michael A.; Weiher, Justine; Farber, Milton (Maremont Corp., Pasadena, Calif.). J. Phys. Chem., 69: 4035-7(Nov. 1965).

A study was made of the high-temperature thermodynamic properties of $BeO_{(c)}$. An electron bombardment furnace-drop calorimeter combination was employed. It was determined that rhenium was completely unattacked by solid, liquid, or gaseous BeO at temperatures as high as 3000°K and under vacuum (10^{-4} to 10^{-6} mm). The sensible enthalpy of $BeO_{(c)}$ was measured between 2270 and 2525°K. The heat of fusion of BeO was found to be 19.3 ± 0.8 kcal/mole. (F.J.H.)

5555 CONDUCTOMETRIC AND POTENTIOMETRIC STUDY OF THE INTERACTION BETWEEN SODIUM SUCCINATE AND THORIUM CHLORIDE. Upadhya, Y. D.; Mushran, S. P. (Univ. of Allahabad, India). J. Prakt. Chem., 20: 233-6(June 1963).

Thorium succinate gels can be obtained by the interaction of sodium succinate and thorium chloride solutions of suitable concentrations in presence of stabilizing glucose solutions. A quantitative assessment was made of the nature of the insoluble substance separating out in the gelling region as a result of metathesis of the interacting solutions. The interaction was investigated by conductometric and potentiometric titration methods. The formation of the normal disuccinate, $Th(C_4H_4O_4)_2$, was observed near the point of equivalence, where the ratio of metal : succinate was nearly 1 : 2. In the absence of glucose solutions a highly unstable colloidal solution was obtained. Addition of peptizer, such as glucose, increased the stability, and the rapid precipitation of the dispersed phase was controlled in a manner as to give stable and transparent gels. The conductometric and potentiometric titration curves were interpreted in terms of a reaction scheme. The maximum hydrogen ion concentration recorded corresponded to pH 2.7. When the ratio of thorium : succinate attains a value of 1 : 2, complete precipitation of thorium succinate takes place. Here a break in the conductivity curve is observed, after which the conductivity rises due to the presence of excess of sodium succinate. (BBB)

5556 RADIOMETRIC MEASUREMENTS OF THE DIFFUSION RATE OF FERRIC IONS IN SOLUTIONS. Dorabialska, Alicja; Chyzewski, Adam. Nukleonika, 10: 411-19(1965). (In Polish).

An apparatus consisting of two glass chambers connected by means of a sintered glass plate was devised. In one of the chambers acidified solutions of $FeCl_3$ labeled with ^{59}Fe was introduced, in the other one the dilute solution of hydrochloric acid was placed. Aliquots of solutions from both chambers were taken in the course of an experiment. Logarithms of concentrations versus time gave the straight lines. From the slopes of these lines some conclusions regarding forms of ferric ions were drawn. Solutions of $FeCl_3$ at concentrations from 0.06 to 0.3 m and for pH values from 1.0 to 3.85 were studied. (auth)

5557 KINETICS OF METHANE-DEUTERIUM EXCHANGE OVER NOBLE METAL ALLOYS. McKee, D. W. (General Electric Research Lab., Schenectady, N. Y.). Trans. Faraday Soc., 61: 2273-83(Oct. 1965).

The kinetics of the exchange reaction between methane and deuterium were studied between 90 and 170°C over a series of palladium–ruthenium catalysts. The preparations were homogeneous alloy powders up to a composition of 21 wt % ruthenium. Ruthenium showed a greater tendency to promote multiple exchange than palladium and stepwise exchange was predominant over the binary catalysts at lower temperatures. The specific activity of the catalysts showed a pronounced maximum at a composition of about 40 wt % Ru–Pd and the activation energy fell to a minimum value at this point. The rates of exchange of CD_4 and H_2 were also studied and a marked kinetic isotope effect was observed. Maximum catalytic activity for several similar alloy systems was found at alloy compositions corresponding to one unpaired d electron per metal atom. (auth)

5558 LITHIUM, CESIUM, AND LANTHANUM FLUORIDE SYSTEMS. Bukhalova, G. A.; Babaeva, E. P. (Rostov Construction Inst., USSR). Zh. Neorgan. Khim., 10: 1883-5(Aug. 1965). (In Russian).

The phase diagram of the ternary system consisting of the fluorides of Li, Cs, and La was investigated by means of the visual thermal method. The melts were prepared in Pt containers using Pt stirrers. The temperatures were determined by means of Pt–Pt/Rh thermocouples. The LiF–LaF_3 system possesses a eutectic at 750°C and 14 mole % LaF_3; the LiF–CsF system has a congruently-melting compound, CsF · LiF, at 492°C and eutectics at 474°C and 40% LiF and at 487°C and 52% LiF. The CsF–LaF_3 system forms a congruently-melting, cryolite-like compound, Cs_3LaF_6 at 798°C and eutectics at 600°C and 11.5% LaF_3 and at 724°C and 33% LaF_3. The ternary system was studied at 15 internal sections. The results indicated an absence of complex formation between LiF and LaF_3. This may be explained by the fact that the Li ion, in view of its small radius of 0.78 Å has a large field of force; the radius of the La ion is also small, 1.28 Å. These two ions, which possess a large field, are also probably highly polarized and thus unable to form a compound. On the other hand, the Cs ion, which has a relatively large radius of 1.65 Å, forms the compounds $3CsF \cdot LaF_3$ or Cs_3LaF_6. The compounds CsF · LiF and Cs_3LaF_6, congruently melting in the binary systems, conserve this property in the ternary system. The Li^+, Cs^+, La^{3+} II F^- system is divided in three secondary triangular diagrams: CsF–Cs_3LaF_6–CsF · LiF; LiF–Cs_3LaF_6–CsF · LiF; and LiF–Cs_3LaF_6–LaF_3. (TTT)

5559 ENTHALPY OF FORMATION OF LANTHANUM AND PRASEODYMIUM FLUORIDES. Polyachenok, O. G. Zh. Neorgan. Khim., 10: 1939-40(Aug. 1965). (In Russian).

An indirect method, study of high-temperature equilibria of the $LaCl_{3\ liq} + AlF_{3\ liq} \rightleftharpoons LaF_{3\ liq} + AlCl_{3\ gas}$ type, was used to determine the approximate value of the enthalpy of formation of La and Pr fluorides. The anhydrous fluorides were melted in a Pt crucible within a quartz tube at 930°C; the upper portion of the tube was kept at a temperature of only 200°C. The equilibrium constant of the reaction was calculated from the amount of $AlCl_3$ sublimed and the concentrations of LaF_3, $LaCl_3$, and AlF_3. In order to derive the value for $\Delta H_{1200°C}$ of the reaction, the temperature dependence of the entropy of $AlF_{3\ solid}$ and $AlCl_{3gas}$ and the entropy values of the La and Pr chlorides and fluorides, calculated by the additive law, were used. A value of 54 kcal was obtained for $\Delta H_{1200°C}$ of La and Pr. The approximate values of the enthalpies of formation of LaF_3 and PrF_3, derived from the experimental data and literature values, were found to be −405 and −401 kcal/mole, respectively, with an error of 5 to 7 kcal/mole. (TTT)

5560 PRODUCTION OF UNUSUAL RARE EARTH PHTHALOCYANINES. Kirin, I. S.; Moskalev, P. N.; Makashev, Yu. A. (Ioffe Inst. of Physics and Tech., Leningrad). Zh. Neorgan. Khim., 10: 1951-3(Aug. 1965). (In Russian).

The synthesis of Nd, Pr, Er and Lu phthalocyanines was carried out by reacting rare earth acetates with o-phthalonitrile at a temperature between 280 and 290°C. The brittle, crystalline product formed upon cooling was identified spectrophotometrically, using dimethyl formamide as solvent. The spectra of these compounds contained 2 absorption bands of nearly equal intensity at 635 and 672, 634 and 672, 621 and 672, and 616 and 673 mμ for Pr, Nd, Er, and Lu, respectively. Similar results were also obtained with solutions in ethanol, methanol, and pyridine. Chromatographic separation of these compounds in dimethyl formamide resulted in the formation of a green zone and a blue zone. The more intensive maxima of these compounds coincided with those of the original materials; both fractions were found to contain the rare earth element. The spectra indicated that the green modification contains one and the blue modification two phthalocyanine ligands. In electrochromatographic separation experiments the green modification was found to migrate to the cathode, the blue one to the anode, corresponding to the number of negatively charged ligands. (TTT)

5561 METHOD FOR THE OXIDATION OF Pu(III) TO Pu(IV) IN A BASIC SOLUTION. Bouzou, Monique; Deroite, Andre (to Commissariat a l'Energie Atomique). German Patent 1,201,321. Sept. 23, 1965. Priority date Apr. 9, 1963, France.

The oxidation is effected by means of nitrous gases. The solution contains preferably a reducing agent. (Gmelin Inst.)

5562 THORIUM OXIDES AND MIXED THORIUM OXIDES AND METHOD. Rombau, Paul; Peltier, Marcel (to Pechiney, Compagnie de Produits Chimiques et Electrometallurgiques). U. S. Patent 3,214,238. Oct. 26, 1965. Priority date June 28, 1961, France.

A process for the preparation of thorium oxide or mixtures of oxides containing at least 90% thorium oxide having large specific surface area is patented. The process comprises the following steps: adding freshly precipitated thorium oxalate to a concentrated solution of aqueous ammonia, heating the solution to about 65°C for ½ to 2 hours to convert the thorium oxalate to thorium hydroxy-oxalate, recovering the thorium hydroxy-oxalate from solution, acidifying the hydroxy-oxalate in aqueous suspension to a pH of less than 5, heating the suspension to a temperature of 80–100°C for about 10 min to produce flat crystals, adjusting the pH of the acidified aqueous suspension to between 6 and 9 with stirring to precipitate the thorium hydroxy-oxalate, separating the precipitate, and heating the separated precipitate to calcination temperatures to convert it to thorium oxide. (B.L.M.)

Organic Chemistry

Refer also to abstract 5612.

5563 (EUR–2482.f) ETUDE PAR SPECTROMETRIE DE MASSE, DE LA PYROLYSE DU BYPHENYLE. (Mass Spectrometry Study of Diphenyl Pyrolysis). Collin, J. E. (Liege Univ. (Belgium). Institut de Chimie). Sept. 1965. Contract 049-61-12 ORGB. 32p. Dep. mn.

The thermal behavior of biphenyl and perdeuterated biphenyl in a quartz furnace, between 375 and 1375°K, was studied with a Bendix time-of-flight mass spectrometer. At pressures of about 20 microns the biphenyl undergoes substantial decomposition at temperatures of 500°C and over, the reaction products detected being carbon, acetylene, propyne, vinylacetylene, benzene, a substance with probable formula C_6H_4, and hydrogen. No methane, ethylene, ethane or propane were found. Small quantities of free radicals C_3H_3 and C_6H_5 were revealed by the low potentials method, apparently chiefly above 1,000°K. The decay activation energy was calculated to be 81 ± 8 kcal/mole. The overall reaction, apparently homogeneous, is of first order. The principal characteristics of the mass spectra of biphenyl and perdeuterated biphenyl were compared, more especially from the standpoint of isotopic effects on fragmentation processes. (auth)

5564 ON THE METABOLISM OF NOVERIL: ^{14}C LABELING AND SYNTHESIS OF METABOLITES. Hunziker, F.; Schindler, O. Helv. Chim. Acta, 48: 1590-7 (Oct. 30, 1965). (In German).

5-Methyl-10-β-dimethylamino-ethyl-10, 11-dihydro-11-oxo-5H-dibenzo[b,e]-1,4-diazepine (I; base of Noveril) was labeled with ^{14}C in the basic side chain for the purpose of metabolism studies. The synthesis of several postulated metabolites is also described. The desmethyl compounds containing secondary amine moieties were obtained by hydrogenolysis of N-benzyl-N-methyl derivatives. A ring-hydrogenated product was also isolated and assigned the structure based on the infrared spectrum. Some primary amines were obtained by hydrogenation of the cyanomethyl compounds. Dehydration products were formed easily from these amines. Contrary to the literature the monobromination product obtained from m-nitrophenol was 4-bromo-3-nitrophenol and not 2-bromo-3-nitrophenol. A compound hydroxylated in the 8-position was also obtained. (auth)

5565 CATALYSIS OF α-HYDROGEN EXCHANGE. I. THE REACTION OF ISOBUTYRALDEHYDE-2-d WITH TERTIARY AMINES AND OXYGEN BASES. Hine, Jack; Houston, James G.; Jensen, James H.; Mulders, Julien (Georgia Inst. of Tech., Atlanta). J. Amer. Chem. Soc., 87: 5050-9 (Nov. 20, 1965).

Isobutyraldehyde-2-d was prepared by the reaction of isobutenyl acetate with heavy water in the presence of an acid catalyst, and the kinetics of its deuterium exchange in the presence of tertiary amines, oxygen bases, and strong acid were studied, using NMR measurements to follow the reaction. Only the basic components of the buffers used catalyzed the reaction significantly. The catalysis constants for three unhindered pyridines and for seven phenoxide ions fit the Bronsted catalysis equation satisfactorily with β values around 0.5. Pyridines with 2- and 6-substituents were less reactive than predicted by the Bronsted equation, by more than 100-fold in the cases of 2,6-lutidine and 2,4,6-collidine. These decreases in reactivity and analogous decreases observed in the reactions of pyridine and its methyl derivatives with acetone, methyl isopropyl ketone, and pinacolone are explained in terms of the commonly accepted transition state for the formation of carbanions from aldehydes and ketones, in which the broken carbon–hydrogen bond is held almost parallel to the π orbitals of the carbonyl group. The most reactive catalysts for their basicity were the saturated tertiary amines trimethylamine and 1,4-diazabicyclo[2.2.2]-

octane. Other amines of this type were less reactive, probably because of steric hindrance, and, in the case of β-hydroxyamines, internal hydrogen bonds. The magnitude of the decrease in reactivity due to these effects appeared to be the largest, among the amines studied, in the case of tris-2-hydroxypropylamine, whose reactivity was smaller by about 3000-fold than would be expected for an unhindered amine. The decreased reactivity of N-methylimidazole, relative to that of unhindered pyridines of similar basicity, was attributed to the fact that the molecular geometry of an imidazole changes much more on protonation than does that of a pyridine. (auth)

5566 ELECTRON SPIN RESONANCE STUDIES OF DEUTERIUM ISOTOPE EFFECTS. A NOVEL RESONANCE-INTEGRAL PERTURBATION. Karplus, Martin; Lawler, Ronald G.; Fraenkel, George K. (Columbia Univ., New York). J. Amer. Chem. Soc., 87: 5260-1(Nov. 20, 1965).

Electron spin resonance (ESR) studies of aromatic radicals previously demonstrated that the replacement of a hydrogen atom by deuterium can produce significant modifications in the proton hyperfine splitting constants (a^H) for ring positions other than the one of substitution. It is proposed that a consistent explanation of these data is provided by a vibrational perturbation of the Hückel resonance-integral parameter B. If the carbon-atom $2p\pi$ orbitals follow the out-of-plane bending motion of the C−H or C−D bonds, the integral B depends on the deuterium or hydrogen position. An equation is given for the energy shift of the Hückel molecular orbital for a deuterated species. Application of the equation to benzene-1-d and cyclooctatetraene-d is discussed. It was found that for both compounds the antisymmetric orbital is unaffected while the symmetric orbital is destabilized, and the magnitude of the effect for $C_6H_5D^-$ indicated that there would be an observable perturbation for $C_8H_7D^-$, in disagreement with experiment. The resonance-integral perturbation model can be applied to other radicals. (F.J.H.)

5567 KINETIC PARAMETERS OF DEHYDROGENIZATION AND DEHYDRATION OF ISOPROPYL ALCOHOL AND DEHYDROGENIZATION OF TETRALIN ON PRASEODYMIUM OXIDE. Tolstopyatova, A. A.; Balandin, A. A.; Yu, Chi-chuan (Zelinskii Inst. of Organic Chemistry, Academy of Sciences, USSR). Kinet. Kataliz, 6: 682-7 (July-Aug. 1965). (In Russian).

The actual activation energies of the dehydrogenation and dehydration of isopropyl alcohol on praseodymium oxide approached the apparent energies. The comparative adsorption coefficients of the reaction products of the dehydrogenation and dehydration of isopropyl alcohol and the dehydration of tetraline depended on the temperature; the reaction products were adsorbed more strongly than the original substances (except for propylene). The most inhibiting effects were shown by acetone and water. (tr-auth)

Radiation Chemistry

See also BIOLOGY AND MEDICINE — Radiation Effects on Biochemicals Radiation Effects on Tissues

Refer also to abstracts 5670, 6298, and 6638.

5568 (BNL-9664) THE POSSIBILITY OF CHEMO-NUCLEAR REACTORS PRODUCING OZONE FOR WATER TREATMENT. Beller, Morris; Steinberg, Meyer (Brookhaven National Lab., Upton, N. Y.). Oct. 1965. Contract AT(30-2)-Gen-16. 9p. Dep. mn; CFSTI $1.00 cy, $0.50 mn.

The potential usage of ozone in the New York area where problems of water shortage and pollution exist is discussed. Three cases are considered. The first is the New York State proposed Riverhead dual-purpose reactor, in which 1 mgpd of water and 2500 kW(e) of power are to be produced. Case II involves the use of ozone to purify the New York City water consumption of 1×10^9 gpd. The third case considers the abatement of pollution in the Hudson River. (P.C.H.)

5569 (CONF-650217, pp 108-10) RADIATION DAMAGE. Blewitt, T. H. (Argonne National Lab., Ill.).

The feasibility of use of reactors operating in the liquid nitrogen and liquid-helium temperature ranges for fundamental studies of radiation damage in materials is discussed. (T.F.H.)

5570 (JUL-228-RC) ZUR CHEMIE NUKLEOGENER KOHLENSTOFFATOME. (On the Chemistry of Nucleogenic Carbon Atoms). Stoecklin, Gerhard (Kernforschungsanlage, Juelich (West Germany). Institut fuer Radiochemie). July 1965. 102p. Dep. mn.

The reactions of ^{11}C recoil atoms with simple aliphatic and alicyclic hydrocarbons, with oxygen, and with methylamine were investigated both in the gaseous and liquid phase. The basic mechanisms of these reactions were studied, and the carrier-free ^{11}C-labeled reaction products were identified and quantitatively determined by radiogaschromatographic methods. The origin of hot reaction products in hydrocarbons can be explained by insertion reactions of ^{11}C atoms and their secondary species ^{11}CH and $^{11}CH_2$ in C−H compounds. A highly excited intermediate compound arising first can either decay (formation of fragmentation products) or be stabilized (formation of stabilization products). A decrease of the fragmentation products or an increase of the stabilization products (phase effect) was observed in the condensed phase. The insertion reactions were not discriminatory in any of the cases studied, i.e., the energetic radicals cannot distinguish between the various C−H compounds. A principal product in all the hydrocarbons investigated was acetylene-^{11}C, that was proved to be a fragmentation product by a significant phase effect. The yield of this compound showed a marked dependence on the structure of the substrate. The effective cross section for the acetylene products is proportional to the relative number of primary C atoms in the substrate molecule. On the basis of the observed structure and deuterium isotope effects, it was concluded that acetylene-^{11}C was formed exclusively from naked ^{11}C atoms. The second most frequently occurring product in all alicyclic hydrocarbon was ethylene-^{11}C. 113 references are cited. (P.C.H.)

5571 (ORNL-TM-1283) THE EFFECT OF IONIZING RADIATION ON COALESCENCE RATES IN LIQUID-LIQUID SYSTEMS [Thesis]. Chester, Conrad V. (Oak Ridge National Lab., Tenn.). Dec. 1965. Contract W-7405-eng-26. 105p. Dep. mn; CFSTI $4.00 cy, $0.75 mn.

Submitted to Univ. of Tennessee, Knoxville.

An investigation of the effect of irradiation by alpha particles and fission fragments on the coalescence times of aqueous drops with a planar liquid-liquid interface was carried out. It was found that, on impact of the drop on the interface, coalescence probability was roughly proportional to the particles flux at the drop surface; as flux increased to 240 fission fragments or 570 alpha particles crossing the drop surface per second (extrapolated), the coalescence probability approached unity. The effect of irradiation was manifested only at the moment of impact, and was not affected by temperature, pressure, or composition of the organic phase, whether n-hexane, n-heptane, or n-decane. The systems studied were very pure, as very minute traces of surface-active contaminants stopped the effect of irradiation. A mechanism which is not at variance with any of the experimental observations is proposed. In this mechanism, it is postulated that free radicals produced in the wake of a particle crossing the interface at a very low grazing angle (less than 1°) can react with nearby molecules of the other phase to produce molecules which have high surface activity, e.g., hexyl alcohol. The local decrease of interfacial tension can start a ripple in the interface which can be amplified by the shear forces at impact to initiate coalescence. (auth)

5572 (USNRDL-TR-909) RESPONSE OF LiF TO NEUTRONS AND CHARGED PARTICLES. Wingate, C. L.;

Tochilin, E.; Goldstein, N. (Naval Radiological Defense Lab., San Francisco, Calif.). Sept. 28, 1965. 34p. CFSTI $2.00 cy, $0.50 mn.

The thermoluminescent response of LiF was investigated with thermal neutrons and fast neutrons at energies extending from 0.26 to 14 Mev. The results indicated that thermal neutron fluence may be conveniently measured with normal LiF but a higher readout temperature is required than for gamma dose measurements. Studies of fast neutron response with ^{7}LiF (to minimize thermal effects) showed a low neutron sensitivity which was strongly dependent on energy. Fast neutron response was also investigated for a dosimeter in which the powder was suspended in alcohol. The LET response of LiF was studied using alpha particles with energies from 900 down to 2 Mev. (auth)

5573 THE IONOLUMINESCENCE OF MgO AND Zn_2SiO_4:Mn. Van Wijngaarden, A.; Bradley, D. J.; Finney, N. M. A. (Univ. of Windsor, Ont.). Can. J. Phys., 43: 2180-91(Dec. 1965).

The luminescence response of MgO and Zn_2SiO_4 : Mn phosphors to bombardment with various ions was determined as a function of ion energy, for energies smaller than 100 kev. The light output of MgO was found to be proportional to the total energy transferred from the projectile to the electrons in the phosphor lattice. The light output of Zn_2SiO_4 : Mn under ion excitation was found to be independent of the population of the electron traps immediately below the conduction band. This suggests that the ionoluminescence was caused by the excitation of the electrons in the host lattice. (auth)

5574 REDUCTION OF CARBON DIOXIDE BY HYDROGEN UNDER THE EFFECT OF FAST ELECTRONS. Mikhailov, B. M.; Bogdanov, V. S.; Kiselev, V. G. (Zelinskii Inst. of Organic Chemistry, Academy of Sciences, USSR). Izv. Akad. Nauk SSSR, Ser. Khim., No. 7, 1271-3 (1965). (In Russian).

Under the effects of fast electrons, mixtures of carbon dioxide with hydrogen were converted into carbon monoxide, glyoxal, and other products. The mechanism of the radiolysis consisted in the decomposition of CO_2 to CO and O, dependent on the participation of molecular hydrogen in the reaction. (tr-auth)

5575 THE EFFECT OF ELECTRIC FIELD ON RADIOLYSIS OF LIQUID HYDROCARBONS. Cusynin, V. I.; Tal'rose, V. L. (Inst. of Chemical Physics, Academy of Sciences, USSR). Izv. Akad. Nauk SSSR, Ser. Khim., No. 7, 1313(1965). (In Russian).

During the irradiation of liquid saturated hydrocarbons with electrons at 1.6 Mev at room temperature, installed in an ampule between metal electrodes, an abrupt increase in the speed of the hydrogen formation was observed by mass spectrometry at the moment when stationary voltage was introduced to the electrodes. This increase remained for approximately 10 to 30 sec after which it decreased, but remained at a higher level in comparison with its values in the absence of an electric field. The shutdown of the electric field led to the previous values for the speed of formation of H_2. The magnitude of the effect did not depend on the polarity of the applied voltage, but it increased with increased voltage and decreased with increased irradiation dose. (J.S.R.)

5576 RADICAL YIELDS IN THE RADIOLYSIS OF HYDROCARBONS. II. NEOPENTANE, ISOPENTANE, AND CYCLOPENTANE. Holroyd, Richard A.; Klein, George W. (Mellon Inst., Pittsburgh. Atomics International, Canoga Park, Calif.). J. Amer. Chem. Soc., 87: 4983-8(Nov. 20, 1965). (RRL-2310-157).

Individual radical yields from neopentane, isopentane, and cyclopentane were determined using the $^{14}C_2H_5$-radical-sampling method. In neopentane only four alkyl radicals were present whereas in isopentane nine were observed. Fragment alkyl radicals, arising from the scission of carbon–carbon bonds, accounted for 79 and 41%, in neopentane and isopentane, respectively, of the alkyl radicals formed in primary processes. The relative probability (per bond) of rupture of primary, secondary, and tertiary carbon–hydrogen bonds in isopentane was found to be 1 : 3 : 9. The observations that $G(CH_3)$ exceeds $G(C_4H_9)$ in both neopentane and isopentane and that fragmentation is more probable for branched structures were attributed to the fact that decomposition of molecular ions is more probable for highly branched structures. In cyclopentane 90% of the radicals were cyclopentyl though small amounts of three additional C_5 radicals were observed. In neopentane a small yield of isobutyl radicals (G = 0.16) was observed, which was believed to result from ionic isomerization. Evidence is cited, which suggested that considerable combination of radicals occurs in tracks for low LET radiolysis. The fraction of methyl radicals that escape the track, $N(CH_3)/N(CH_3)_0$, was estimated to be ≤0.66 for neopentane. (auth)

5577 PRODUCTION OF TRAPPED RADICALS FROM ALKYL HALIDES IN ORGANIC GLASSES BY DISSOCIATIVE ELECTRON ATTACHMENT AND BY PHOTODISSOCIATION. Claridge, R. F. C.; Willard, J. E. (Univ. of Wisconsin, Madison). J. Amer. Chem. Soc., 87: 4992-7 (Nov. 20, 1965). (COO-32-108).

The production of free radicals from alkyl halides by the dissociative electron attachment reaction ($RX + e^- \rightarrow R + X^-$) was demonstrated, using electrons from the photoionization of N,N,N′,N′-tetramethyl-p-phenylenediamine (TMPD) in 3-methylpentane (3-MP) glass at 77°K. The radicals were detected by electron spin resonance. The relative yields for the same amount of light absorbed by TMPD were approximately: CH_3Cl, 100; CH_3Br, 30; CH_3I, 10; C_2H_5Cl, 40; C_2H_5Br, 25; C_2H_5I, ≤5; i-C_3H_7Cl, 20; n-C_3H_7Cl, 10; i-C_4H_9Cl, 20; and n-C_4H_9Cl, 10. The methyl radicals produced from different parent species and at different concentrations all decayed at a first-order rate with the same half-life (16 min.). This seemed to require that decay is by combination with the parent partner and within the solvent cage where bond rupture occurred. Irradiation of solutions of CH_3I or C_2H_5I in 3-MP glass at 77°K with 2537-Å radiation absorbed by the iodide produced alkyl radical spectra attributable to rupture of the C–I bond and to abstraction of H from 3-MP by hot CH_3 or C_2H_5 radicals. A sharp ESR line, tentatively attributed to trapped electrons, was observed in both pure 3-MP radiolyzed with γ rays at 77°K and in TMPD solutions in 3-MP at 77°K exposed to ultraviolet radiation absorbed by the TMPD, in accordance with reports from other laboratories. (auth)

5578 CATALYTIC ACTIVATION OF VYCOR GLASS FOR THE H_2–D_2 EXCHANGE REACTION BY BETA IRRADIATION. Fulkerson, William; Leland, Thomas W. Jr. (Rice Univ., Houston, Tex.). J. Catalysis, 2: 87-92(Apr. 1963).

The H_2–D_2 exchange reaction was studied in small-volume Vycor reaction vessels consisting of two concentric Vycor tubes. The reaction gas volume was the annular space between the tubes plus the space in a side-arm filler tube for a total of less than 10 cm^3. A 50 to 50 mole % mixture of H_2 and D_2 was used. Two different types of β sources were used, one containing ^{90}Sr and its ^{90}Y decay product, and the other ^{35}S. The catalytic activity of the Vycor vessels was measured before and during irradiation. Activation energy for the vessels ranged from 8.3 to 9.4 kcal/mole, which compared closely to the 9 kcal/mole for unirradiated silica gel. At 98°C the catalytic activity of the vessel irradiated by ^{90}Y β rays from the ^{90}Sr source increased gradually in 9 days to a steady-state value, which was greater than the preirradiated activity by a factor of about 7. The activation energy after reaching this steady value was 8.3 kcal/mole, not appreciably different from that of the unirradiated glass. Catalytic activity of the vessels containing $Cd^{35}S$ films measured at 98°C also increased gradually with time to a steady value. For a tube containing an 8-mC $Cd^{35}S$ film, catalytic activity increased by a factor of about 9 in 6 days. The activation energy measured after achieving this steady value was 8.4 kcal/mole compared to a value of 8.3 kcal/mole for

the blank unirradiated tube. A value of 9.4 kcal/mole was obtained for the tube containing a nonradioactive CdS film. Since there was little change in activation energy, the gradual increase in activity to a steady value after a few days of irradiation is explained by assuming that the enhanced activity is due to the production of new active sites on the Vycor surface accompanied by the annealing of these sites at some rate that is proportional to the number of sites. Because of the similarity in the behavior of the Vycor tube irradiated by the $^{90}S-^{90}Y$ source and the tubes containing radioactive CdS films, it is likely that in both cases the same type of active site is responsible for the enhanced activity. (BBB)

5579 DISSOCIATION OF MOLECULAR HYDROGEN BY ELECTRON IMPACT. Corrigan, S. J. B. (Univ. of Oklahoma, Norman). J. Chem. Phys., 43: 4381-6(Dec. 15, 1965).

The dissociation of molecular hydrogen by electron impact was studied by observing the rate of pressure decrease in a closed system when the dissociation fragments were trapped on molybdenum trioxide. An onset potential of 8.8 (±0.2) ev was obtained, indicating that a large part of the dissociation must proceed through direct excitation of the repulsive $b\ ^3\Sigma_u^+$ state of the molecule. From the onset potential to 95 ev, the upper energy limit of the observations, the dissociation rate increased rapidly at first, then more slowly above 14 ev, passing through a flat maximum at 40 ev, and then slowly decreasing up to the highest energy investigated. Reasons are given for supposing that the observed cleanup of hydrogen at high electron energies contains an effect due to dissociative neutralization of molecular ions. With this assumption the cross section for excitation of the molecule to triplet states was derived by subtracting the molecular ionization cross section from the observed total dissociation cross section. In this way a cross section for dissociation into neutral atoms was obtained which has a maximum of 9×10^{-17} cm^2 at an energy of 16.5 ev, followed by a rapid decrease with increasing electron energy. (auth)

5580 STEP ANNEALING IN RADIATION DAMAGE IN SOLIDS. Lal, M. (Atomic Energy Establishment, Trombay, India). J. Inorg. Nucl. Chem., 27: 2449-50 (Nov. 1965).

The kinetics of two stage annealing of radioinduced damage in various solids were studied. Mathematical analysis showed that the difference between single-stage and double-stage annealing is to be expected irrespective of the mechanism of annealing. It was found that the measured value of a property at any time will always be higher in double-stage annealing at the higher temperature. (F.J.H.)

5581 THE RADIOLYSIS OF METHANOL AND METHANOLIC SOLUTIONS. IV. THE EFFECT OF WATER ON PEROXIDE YIELDS. Lichtin, Norman N.; Wilson, Judith W. (Univ., Boston). J. Phys. Chem., 69: 3673-76(Nov. 1965).

Radiolytically generated or added approximately 10^{-4} to 10^{-3}M H_2O_2 is unstable in dry, aerated methanolic solution and decays by a first-order process. As little as 0.1 wt. % of H_2O inhibits the decay significantly. The nature of the protective action of water is obscure. $G(CH_3OOH)$ appears to be approximately 0.2, in agreement with a previously assigned value of G_{CH_3}. (auth)

5582 γ-RADIOLYSIS OF ETHYLENE SENSITIZED BY "INERT" GASES. Site, A. Delle; Mele, A. (Univ., Rome). J. Phys. Chem., 69: 4033-5(Nov. 1965).

Radiolysis of ethylene in the presence of He, Ne, Ar, Kr, Xe, and N_2 was studied. Irradiation was carried out with a ^{60}Co source of 6000 C at a dose rate of 4.17×10^5 r/hr. The radiolysis of pure ethylene was studied in the range of pressures from 123 to 593 mm. The $G(-C_2H_4)$ values, measured at four different pressures, are given. Mixtures of ethylene and inert gases of various composition were irradiated and, after irradiation, the samples were analyzed by gas chromatography. The crude effect of the addition of inert gases to ethylene was to increase its rate of consumption. Data indicated $G(-C_2H_4)$ does not depend on the nature of the inert gas, but on the fraction of energy absorbed by the inert gas itself and transferred to the ethylene molecules. (F.J.H.)

5583 EFFECT OF ADDITIVES ON CERTAIN PHYSICO-CHEMICAL PROPERTIES OF SILVER OXALATE. V. PHOTOLYSIS, RADIOLYSIS, AND THERMAL DECOMPOSITION OF SILVER OXALATE. Zakharov, Yu. A.; Savel'ev, G. G. (Tomsk Polytechnic Inst., USSR). Kinet. Kataliz, 6: 611-18(July-Aug. 1965). (In Russian).

The effect of Cd^{2+} and Pb^{2+} ions on the speed of photolysis and radiolysis of silver oxalate was studied. It was established that in the process series, thermolysis, photolysis, and radiolysis, tendencies to a transition from delayed processes to accelerated processes were observed in the presence of additives. In a quantitative relation, this transition to an accelerated process was stronger for Pb^{2+} additives than for Cd^{2+} additives. The results obtained were considered from the viewpoint of the effect of additives on the course of separate elementary stages of the dissociation process of $Ag_2C_2O_4$ and with a consideration of the data obtained earlier on the electrical and optical properties of silver oxalate containing Cd^{2+} and Pb^{2+}. The reasons cited for the existence of the effects observed were confirmed by data on the EPR spectrum during the exposure of solid solutions. (tr-auth)

5584 ON THE NATURE OF SURFACE RADIATION-INDUCED DEFECTS IN IRRADIATED SILICAGEL. I. MECHANISM OF HYDROGEN ADSORPTION. Pariiskii, G. B.; Mishchenko, Yu. A.; Kazanskii, V. B. (Inst. of Chemical Physics, Academy of Sciences, USSR). Kinet. Kataliz, 6: 625-33(July-Aug. 1965). (In Russian).

According to the optical spectrum and the EPR spectrum of irradiated silica gel, the structure formed, under the action of irradiation, by the surface color centers, connected with additives in Al samples, was established. Irradiation caused positively charged holes, stabilized on the oxygen atoms and adjacent to atoms of Al. This defect appeared with centers of irreversibly adsorbed hydrogen. (tr-auth)

5585 NEW GLASSES FOR LOW BACKGROUND COUNTING. Sakurai, Junji (Toshiba Electric Co., Japan); Shibata, Shinkichi; Yamakoshi, Kazuo. Radioisotopes (Tokyo), 14: 457-62(Nov. 1965). (In Japanese).

The following characteristics of glass materials suitable for liquid-scintillator containers and shell tubes of external cathode G-M counters are discussed: natural radioactivities in glass materials, optical transmittance and index, phosphorescence emitted from glass materials excited by visible light, chemical resistance of glass materials to scintillator solvents, and suitability for shell tubes of G-M counters. Correlations between counting rates in the ^{14}C energy region and potassium contents in various glasses were experimentally determined. Phosphorescence was emitted from one glass with a decay constant of ~30 sec. Higher counting rates were obtained for a uranium glass than a quartz, but no decaying component was observed. The alkaline component of a glass dissolved into hot toluene was not detected within errors of the measurement. A glass (LB-47) for container vials of liquid scintillators was produced with a potassium oxide content of 0.0116 (1 ± 0.07) wt %. In the case of 200 cc vials made of LB-47 the background counting rate caused from ^{40}K in the glass was estimated to be ~0.4 cpm in the quarter of ^{14}C energy region. For shell tubes of external cathode G-M counters a glass (LB-96) was also developed. It contains potassium oxide of 0.014 to 0.020 wt % and has a specific resistance of 7.5 to 15×10^{11} (ohm-cm) at 10°C. (auth)

5586 DEVELOPMENT OF HOT SYNTHESIS METHODS FOR ^{35}S LABELED BIOLOGICALLY ACTIVE SUBSTANCES. III. PREPARATION OF TRIETHYLENIMINE-THIOPHOSPHORAMIDE WITH BINARY LABELING WITH ^{35}S AND ^{32}P. Dzantiev, B. G.; Kiseleva, N. N.; Shishkov, A. V. Radiokhimiya, 7: 366-8(1965). (In Russian).

An attempt was made to use the hot synthesis method, which takes advantage of the energy of recoil atoms, for

preparation of biologically-active, twice-labeled compounds, such as the strong anticancer agent triethylenemine thiophosphoramide (thioTEP). Solutions of this substance dissolved in CCl_4 were exposed in a quartz ampoule to a fast-thermal neutron flux of the IRT-1000 reactor. The thermal flux amounted to 1 to 2×10^{11} n/cm^2 sec; the fast flux was about 1% of this value while the γ dose was 0.5×10^{14} ev/cm^3. The temperature during irradiation was kept at 50°C. The CCl_4 was the source of hot atoms formed by the $^{35}Cl(n,p)^{35}S$ and $^{35}Cl(n,\alpha)^{32}P$ reactions. Some of the hot atoms were also obtained from the S and P of the thioTEP by the $^{34}S(n,\gamma)^{35}S$, $^{32}S(n,p)^{32}P$, and $^{31}P(n,\gamma)^{32}P$ reactions. The relatively large nuclear reaction cross sections and half lives made it possible to obtain high S and P activities in short irradiation periods, not exceeding 15 hours, thus preventing radiolysis of the the thioTEP. The mixture was analyzed and the thioTEP was purified by paper and radiochromatography; further purification steps were carried out by subsequent extraction and precipitation of the PO_4 and SO_4 ions. The material was used for biological studies. (TTT)

5587 STUDIES ON X-AGENT. XXIV. SPECIAL ATTITUDE OF KAOLIN SUSPENSION TOWARD X-AGENT. Moriyama, Hideo (Shonan Hygiene Inst., Kamakura, Japan). Yokohama Med. Bull., 13: 355-62(Oct. 1962).

The action of a hypothetical cosmic radiation (X-agent) on a suspension of kaolin particles was investigated by attempting to detect secondary radiation, produced by X-agent acting on this colloidal solution, in surrounding solutions of protein and dye. Test tubes containing egg albumin or methyl red solution were arranged around a kaolin suspension. Changes in the transmittances of the protein solution were analyzed according to the directions in which test tubes containing the solution were placed in relation to the kaolin tube. The directional patterns around the kaolin suspension were different from those around a tube of water, in terms of the turbidity of the protein solutions. Transmittances around the kaolin suspension were high as compared with those around water. The kaolin particles suspended in water affected the turbidity of protein solutions placed close to it, but did not affect the magnitude of the directional pattern. The patterns varied strikingly from day to day, indicating that the X-agent was changing greatly from day to day in its quality or quantity. It is suggested that a secondary X-agent is emitted from a substance, especially when the substance is in a colloidal state, and that the emission takes place as a result of the Tyndall effect. This effect of colloidal kaolin particles is unsystematic and irregular, and varies with the time and place when and where the observations were performed. The effect, even though unsystematic and irregular, could be demonstrated when the protein solution was employed, but not when the methyl red solution was used, indicating that X-agent does not exhibit an identical action on different materials. (BBB)

5588 PREPARATION OF RADIATION-CURED ELASTOMERIC ROCKET PROPELLANTS. Colichman, Eugene L.; Cramer, Frank B. (to North American Aviation, Inc.). U. S. Patent 3,214,306. Oct. 26, 1965. Filed May 28, 1956.

A method of preparing a hydrocarbon elastomeric rocket composition comprises forming a liquid mixture containing a hydrocarbon fuel-binder, an inorganic oxidant, and a metallic oxide combustion catalyst; and then subjecting the resulting mixture to high energy radiation to a total radiation dose of approximately 5×10^7 to 5×10^9 roentgen. (B.L.M.)

5589 ISOBUTYLENE-DIENE COPOLYMERIZATION BY LOW TEMPERATURE IRRADIATION. D'Alelio, Gaetano (to Dal Mon Research Co.). U. S. Patent 3,214,358. Oct. 26, 1965. Filed Jan. 29, 1960.

A process for the preparation of isobutylene–diene copolymers consists of treating a monomeric mixture made up of 99.5–80 wt % isobutylene and 0.5–20 wt % of at least one diene, based on the combined weight of monomers, with at least 0.1 Mrep of irradiation at a temperature below –40°C in the presence of at least one aliphatic saturated cyclic hydrocarbon. (B.L.M.)

Radiochemistry

See also Separation Processes and Procedures

Refer also to abstract 5813.

5590 (NP–15543, pp 5-26) UTILIZATION OF TRACERS AND OF INTENSE RADIATION SOURCES IN CHEMICAL RESEARCH. Ripan, R. (Babes-Bolyai Univ., Cluj (Romania)).

A general account is given of research activities in Rumania concerning the use of radioactive tracers and of nuclear radiations in chemistry. After a description of the original procedures developed for the preparation of radioactive isotopes and of labeled compounds, the utilization of radioactive tracers in various branches of chemistry is discussed: in inorganic chemistry, the structure of complex compounds of W, Th, Pa, and U was elucidated; in organic chemistry, the mechanism of aliphatic acylation and the structure of chlorophenothiazines were studied; in analytical chemistry various methods were employed, among which radiometric titrations deserve a special mention; in physical chemistry, radioisotopes were employed for determining transport numbers in molten salts and for studying interfacial as well as ionic exchange processes. The application of intense radiation sources in chemical research enables Rumanian research workers to study the chemical effects of nuclear transformations, and to perform radiolytic oxidations of paraffins and of xylene. The action of ionizing radiations on solid oxidic catalysts was also studied. (119 references.) (auth)

5591 (SGAE-CH–18/1965) ^{99m}Tc GENERATOR USING Fe_2O_3 AS SORBENT FOR ^{99}Mo. Bulbulian, S.; Bauer, B.; Sorantin, H. (Oesterreichische Studiengesellschaft fuer Atomenergie G.m.b.H., Seibersdorf. Institut fuer Chemie). June 1965. 12p. Dep. mn.

Carrier free ^{99m}Tc was obtained using a generator, which was filled with Fe_2O_3 and then loaded with ^{99}Mo. Elutions were made with 0.1 N HNO_3 at different intervals of time getting a high specific activity of ^{99m}Tc. The overall yield was 55–70%. The results of laboratory and hospital scale tests are reported. (auth)

5592 A METHOD FOR THE PRODUCTION OF RADIOACTIVE CHROMIUM PREPARATIONS. (to Institutt fuer Atomenergi). British Patent 1,009,236. Nov. 10, 1965. Priority date Oct. 24, 1961, Norway.

A process is described for the production of radioactive chromium compounds having a high specific activity, particularly ^{51}Cr. After neutron irradiation of a hexavalent Cr target, the trivalent ^{51}Cr is isolated by dissolving it and passing it through a pretreated anion exchange resin. Hexavalent Cr is absorbed, while the trivalent Cr in solution passes through and is led to an evaporating bottle. After evaporation, the pH is adjusted with NaOH, and the trivalent Cr is oxidized by the addition of a suitable amount of 30% H_2O_2. The excess H_2O_2 is boiled off, and the final product is dissolved sodium chromate. (B.L.M.)

5593 METHOD FOR PREPARING RADIOACTIVE HYDROCARBONS. Doyle, William P.; Child, Edward T. (to Texaco Inc.). U. S. Patent 3,214,486. Oct. 26, 1965. Filed June 21, 1961.

A method for preparing a tritium-containing hydrocarbon consists of reacting a saturated or unsaturated hydrocarbon having from about 3 to 30 carbon atoms with tritiated water having an activity in the range of 0.001 to 1 million μC/g in the presence of BF_3 as a catalyst. (B.L.M.)

Separation Processes and Procedures

See *also* Analytical Procedures
ISOTOPE TECHNOLOGY — Separation and Production

Refer also to abstracts 6553, 6558, and 6600.

5594 (ANL-6925, pp 21-106) COMPACT PYROCHEMICAL PROCESSES. (Argonne National Lab., Ill.).

Work on melt refining is reported and developmental efforts on processes using liquid metal solvents are summarized. Research and development work on fuel processing facilities for EBR-II is discussed. Startup and preliminary performance testing of the fuel cycle facility are reported. Work on the chemistry and thermodynamic properties of liquid metals is in progress. Data and information are included on Na, binary alkali metal solutions, and rare earth–Cd solutions. Methods are being developed for preparation of refractory fuels. Data and information are included on preparation of UC by liquid–metal processes and fluid-bed processes. Work on homogeneous precipitation of UC and (U–Pu)C from fused salts is described along with studies of mobile blanket fuels for fast reactors. (J.R.D.)

5595 (ANL-6925, pp 107-64) FUEL CYCLE APPLICATIONS OF VOLATILITY AND FLUIDIZATION TECHNIQUES. Jonke, A. A. (Argonne National Lab., Ill.).

Results of laboratory investigations are reported on fluid-bed fluorination of U_3O_8–PuO_2 mixtures, fluid-bed fluorination of UO_2–PuO_2 mixtures, phase studies of UF_6–PuF_6, reactions of PuF_6, alpha-induced decomposition of PuF_6, corrosion of fluoride volatility process container materials, fluorination of Rocky Flats waste for Pu recovery, NP chemistry, behavior of molybdenum oxides and SnF_4 under fluorination. Engineering-scale investigations are reported on fluid-bed fluoride volatility processes for recovery of Pu and U from UO_2 fuels, recovery of U from enriched U-alloy fuels, corrosion of Ni-200 in fluoride volatility process environments, and gas-fluidized bed behavior. (J.R.D.)

5596 PLUTONIUM PRODUCTION AT MARCOULE. Comit. Naz. Energia Nucl., Notiz., 11: 46-51(July 1965). (In Italian).

The installation at Marcoule for the processing of irradiated fuel elements and the production of Pu is described. A simplified flow diagram of the extraction method used is given. (J.S.R.)

5597 ION EXCHANGE PROCEDURES. VII. SEPARATION OF ALKALI METAL IONS. Nelson, Frederick; Michelson, Donna C.; Phillips, Harold O.; Kraus, Kurt A. (Oak Ridge National Lab., Tenn.). J. Chromatog., 20: 107-21(Oct. 1965). (ORNL-P-1138).

A comparative study of the adsorbability of alkali metals, lithium to francium, in HCl-water and HCl–methanol–water solutions was carried out with sulfonic acid cation exchangers of the polystyrene–divinylbenzene and phenol–formaldehyde types. Separation of potassium, rubidium, and cesium was also studied using a zirconium phosphate cation exchanger. Procedures for separating the alkali elements from each other are described. (auth)

5598 ELECTROPHORETIC SEPARATION OF SOME ACTINIDE AND LANTHANIDE ELEMENTS. Kraak, W.; Wals, G. D. (Reactor Centrum Nederland, Petten, Netherlands). J. Chromatog., 20: 197-201(Oct. 1965).

The potentialities of the electrophoretic method for separation of actinide and lanthanide elements were studied. All the elements studied were radioactive and were used in tracer concentration. They were: ^{241}Am, ^{244}Cu, ^{144}Ce, $^{152}Eu + ^{154}Eu$, ^{153}Gd, ^{160}Tb, and ^{170}Tm. After completion of electrophoresis, the paper strips were cut into sections of 0.5-cm and counted for relative activities. (M.C.G.)

5599 ELECTROTRANSPORT OF INTERSTITIAL ATOMS IN YTTRIUM. Carlson, O. N.; Schmidt, F. A.; Peterson, D. T. (Ames Lab., Ames, Iowa). J. Less-Common Metals, 10: 1-11(Jan. 1966). (IS-1210).

The electrotransport velocities of carbon, oxygen, and nitrogen in yttrium were determined in the temperature range from 1235 to 1460°C. Diffusion coefficients and effective charges were calculated for these elements for the same temperatures. Yttrium metal purified by the electrotransport method showed a decrease in oxygen content from 780 to 90 ppm and an increase in the resistance ratio from 12 to 45. (auth)

5600 SYNERGIC AND ANTAGONISTIC EFFECTS IN THE SOLVENT EXTRACTION OF INORGANIC COMPOUNDS WITH MIXTURES OF AMINE AND ALKYLPHOSPHORIC ACIDS. THE SYSTEM. TRI-N-OCTYLAMINE + ALKYLPHOSPHOSPHORIC ACID + DILUENT – H_2SO_4 + H_2O. Deptula, Czeslaw; Minc, Stefan. Nukleonika, 10: 421-6 (1965). (In Polish).

The influence of the concentration of sulfuric acid on its extraction with mixtures of tri-n-octylamine and alkyl esters of phosphoric acids (HDBP, HD2EHPA, H_2MBP, H_2DDPA) was investigated. It was found that addition of alkyl esters of phosphoric acids to the solutions of tri-n-octylamine causes antagonistic effects that result from reaction of the amine with the corresponding ester. (auth)

5601 ON THE EXTRACTION OF FRANCIUM BY ORGANIC SOLVENTS. Adloff, J. P. (Centre de Recherches Nucleaires, Strasbourg). Radiochim. Acta, 4: 169-70(Aug. 1965). (In French).

The extraction of francium from NaOH solutions with 4-sec-butyl-2-(α-methylbenzyl) phenol (BAMP) was investigated. The extraction by BAMP in cyclohexane was investigated as a function of the NaOH concentration and the results showed that in 3M NaOH 100% Fr is extracted. Fr could be extracted from ^{227}Ac in a pure form using BAMP. The use of this organic solvent in the final phase of the separation of ^{223}Fr from Ac by tungstosilicic acid was also considered. Fr was easily returned to aqueous solution by agitation of the organic phase with diluted acid. (J.S.R.)

5602 EXTRACTION OF CARRIER-FREE ^{57}Co FROM IRRADIATED TARGETS. Gilbert, E. N.; Pronin, V. A.; Artyukhin, P. I.; Valov, P. V. Radiokhimiya, 7: 358-9 (1965). (In Russian).

^{57}Co, used for the study of the states of Fe by the Mössbauer effect, was prepared by the irradiation of an Fe target with high-energy neutrons. The simultaneously formed ^{54}Mn, ^{52}Mn, and ^{58}Co must be removed from the system. The Fe was removed by β,β'-dichloroethyl ether. It was found that at starting HCl concentrations higher than 10M, the partition coefficient of Fe is higher than 100. Co and Mn were only slightly extracted because they had coefficients of 5.9×10^{-2} and 2.6×10^{-2}, respectively. Two or three extraction steps were sufficient to remove practically all of the Fe. The Fe must be reduced and subsequently reoxidized with H_2O_2. The Co was separated from the Mn by extracting it with a solution of trioctylamine in benzene. About 75 to 90% of the ^{57}Co may be thus extracted from the starting solution; the yield may be improved by using a countercurrent extraction method. (TTT)

5603 RAPID SEPARATION OF BARIUM FROM A MIXTURE OF FISSION PRODUCTS. Vobecky, Miloslav; Benes, Jaroslav (Akademie der Wissenschaften, Prague). Z. Anal. Chem., 213: 404-8(1965). (In German).

A method was developed for the rapid and selective isolation of barium from a mixture of fission products, based on precipitating barium sulfate in EDTA medium. The selectivity was checked by measuring γ spectra and by decay curve analysis. The rapidity of the method is illustrated by the isolation of the ^{137m}Ba isomer from an equilibrium mixture of $^{137}Cs + ^{137m}Ba$. The method is convenient for preparing radiochemically pure barium, for quantitative evaluation of decontamination, and for determining the age of fallout. (auth)

5604 METHOD AND MEANS FOR THE PRODUCTION OF PURE Ti AND Zr BY ELECTROLYSIS. Opie, William Robert; Svanstrom, Kjell Ake (to Titanium Metals Corp. of America). German Patent 1,201,567. Sept. 23, 1965. Priority date Nov. 6, 1953, United States.

For the continuous electrolytic production of pure Ti and Zr according to patent 1,103,600 the cathode basket is arranged and constructed in such a way in the electrolytic cell that a concentration gradient of the reducing Ti and Zr halides is maintained in the molten halide electrolyte during the reducing process. (Gmelin Inst.)

5605 RECOVERY OF METAL VALUES FROM AQUEOUS SOLUTION BY SOLVENT EXTRACTION WITH AN ORGANO PHOSPHORUS EXTRACTANT. Hazen, Wayne C.; Henrickson, Angus V. (to Kerr-McGee Oil Industries, Inc.). U. S. Patent 3,214,239. Oct. 26, 1965. Filed July 2, 1962.

A process is described for the recovery of U and/or V values from aqueous solutions by solvent extraction with an organo-phosphorus extractant in an inert water immiscible solvent with special precautions to prevent the oxidation of ferrous ions to ferric, which are readily extracted by the organo-phosphorus extractant. A vapor space filled with a non-oxidizing atmosphere is provided above the aqueous solution to be extracted and above the loaded extractant during separation and stripping to prevent the ferrous oxidation. (B.L.M.)

ENGINEERING

General

Refer also to abstracts 5633 and 5834.

5606 (GAMD–6675) STMGEN—A COMPUTER CODE FOR THE DESIGN OF A STEAM GENERATOR. Schultz, G. M.; Doering, D. A. (General Atomic, San Diego, Calif. John Jay Hopkins Lab. for Pure and Applied Science). Aug. 27, 1965. Contract AT(04-3)-167. 149p. Dep. mn; CFSTI $4.00 cy, $1.00 mn.

STMGEN is a Computer Code written for the IBM-7044 Digital Computer. It is the first of a series of programs that will be used in a plant optimization program. The code will compute the geometry of each section of a steam generator required to satisfy the design conditions. (auth)

5607 (GAMD–6675(Suppl.)) STMGEN. A COMPUTER CODE FOR THE DESIGN OF A STEAM GENERATOR. Schultz, G. M. (General Atomic, San Diego, Calif. John Jay Hopkins Lab. for Pure and Applied Science). 1965. Contract AT(04-3)-167. 35p. Dep. mn; CFSTI $2.00 cy, $0.50 mn.

This report is a supplement to GAMD-6675, entitled "A Computer Code for the Design of a Steam Generator." The design and cost additions that were made to facilitate the use of the code as a sub-program in the optimization code currently under development at General Atomic are discussed. (auth)

5608 (TID–4102(1st Rev.)) ENGINEERING MATERIALS LIST. Cumulative Indexes. Duthie, Richard E. C. (ed.) (Division of Technical Information Extension (AEC), Oak Ridge, Tenn.). Nov. 1965. 150p. Dep.; DTI Extension Free.

The availability of engineering materials developed in conjunction with nuclear and related engineering projects of the AEC is announced. A complete list of titles of CAPE packages of engineering materials is included, along with a cumulation of the Subject, Engineering Category, and Corporate Author Indexes. Codes identifying the originating organizations are listed under the Identification of Codes. The cumulative Title List supersedes all previous title lists, and the cumulative Subject and Corporate Author Indexes supersede TID-4102, issued March 1964. (P.C.H.)

Applications of Nuclear Explosions

5609 (LA–3403) THERMAL NEUTRON SPECTRA FROM AN UNDERGROUND NUCLEAR EXPLOSION WITH SPECIAL CONSIDERATION OF SPECTRAL MODIFICATION DUE TO BOMB DEBRIS MOTION. Sandmeier, Henry A.; Hansen, Gordon E. (Los Alamos Scientific Lab., Univ. of California, N. Mex.). Aug. 1965. Contract W-7405-eng-36. 46p. Dep. mn; CFSTI $3.00 cy, $0.50 mn.

The following problem was solved: given a spherical ball of bomb debris moving radially outwards with material velocity $\vec{v}_0$ and containing neutrons in local thermal equilibria, then what is the neutron spectrum on top of a long narrow pipe of length R and radius η. It is assumed that the debris density has become so small that no further neutron collisions will occur; in other words, the neutrons do not find a diffusive medium anymore. The neutrons are therefore liberated from a moving source containing "bottled up" neutrons with local Maxwell Boltzmann distributions. The spectrum on top of the pipe will depend on how much one "sees" of the bomb debris sphere looking down the long narrow pipe. This problem was discussed previously by Nordheim, as well as Bell. The problem was investigated in a more general way, and the case treated by Nordheim and Bell becomes here a special case where the observer looking down the pipe sees only a "pencil" of the bomb debris sphere. The general case where the observer sees a general portion of the debris sphere is investigated. Two special cases called the "pencil" model and the "spherical" model are investigated. As the name implies, one sees the whole sphere in the "spherical" model, and in the "pencil" model one sees only a small pencil-like section of the debris sphere. The numerical bomb parameters relevant to this investigation are given. The theoretical predictions of the neutron spectrum on top of the pipe are compared with the experimental data from the "Parrot" shot. The effect of the finite bomb debris sphere on measurements is investigated. (M.O.W.)

5610 PROBING THE EARTH WITH NUCLEAR EXPLOSIONS. Griggs, D. T. (Univ. of California, Los Angeles); Press, Frank. J. Geophys. Res., 66: 237-58(Jan. 1961).

Progress in seismology is reviewed with emphasis on the usefulness of past nuclear weapon tests in determining the internal structure of the earth. Shot times and locations are tabulated for 169 U. S. atomic explosions, with seismic data recorded at Pasadena, California. The advantages of using large chemical explosions and future nuclear explosions detonated under the Plowshare program as controlled energy sources for carefully instrumented seismological experiments are discussed. An international program of explosions for seismological research is proposed, and specific suggestions are made for attacking several outstanding problems in seismology by means of chemical and nuclear explosions and the instrumentation network proposed at Geneva for nuclear test detection. Deep oceanic seismometer lines are proposed as a means for making important improvements in seismic knowledge of the world and possible improvements in the detection of atomic explosions. It was concluded that these programs will constitute a very important aspect of the use of nuclear explosions for peaceful purposes. (TCO)

Facilities and Equipment

Refer also to abstracts 5670, 5837, and 6178.

5611 (BNWL–137) A HIGH TEMPERATURE CREEP MACHINE FOR IN-CELL OPERATION. Nyman, D. H.; Keegan, M. R.; Williams, J. A. (Battelle-Northwest, Richland, Wash. Pacific Northwest Lab.). Sept. 1965. Contract AT(45-1)-1830. 8p. Dep. mn; CFSTI $1.00 cy, $0.50 mn.

A high temperature creep machine capable of conducting creep and stress-rupture tests to 1300°C by remote operation was developed. Evaluation tests demonstrated that the apparatus meets the requirements of ASTM Recommended Practice E 139-58T. (auth)

5612 (ORNL-TM–1326) URETHANE MANIPULATOR GAUNTLETS. Dice, D. T.; Wicker, C. D. (Oak Ridge National Lab., Tenn.). Nov. 9. 1965. Contract W-7405-eng-26. 10p. Dep. mn; CFSTI $1.00 cy, $0.50 mn.

A method for fabricating manipulator gauntlets from liquid urethane monomer was developed. In most hot cells the service life expectancy of these gauntlets is approximately five times that of the neoprene gauntlets previously used. However, it is necessary to add a coating of neoprene to maintain this life expectancy in areas where oxidizing acids are encountered. As an additional benefit, special urethane boots, bellows and other objects are easily fabricated by this method. (auth)

5613 (SWRI–1228-8-16) FUNDAMENTAL INVESTIGATION OF LIQUID-METAL LUBRICATED JOURNAL

BEARINGS. Quarterly Technical Report No. 5, August 1, 1965–October 31, 1965. Burton, R. A.; Hsu, Y. C.; Carper, H. J. (Southwest Research Inst., San Antonio, Tex.). Nov. 1, 1965. Contract AT(11-1)-1228. 63p. (RS–471). Dep. mn; CFSTI $3.00 cy, $0.75 mn.

An analytical approach to continuous turbulent films, described in previous reports, is exploited to provide estimates of performance of very short, full bearings operating in the turbulent regime. Similarly, the analysis is applied to tilted pads without end leakage, and shown to check with experimental measurements. Computer techniques are described whereby the analysis technique can be applied to finite bearings, of arbitrary film thickness variation. Experimental data are reported for leading edge pressure rise under tilted pads, and for the pressure distribution under stepped pads. Further analysis is given for steady and fluctuational velocity profiles near a blockage in the bearing clearance. (auth)

5614 A SUPERCONDUCTING MAGNET USING DOUBLE HELMHOLTZ COILS. Maentysalo, E.; Laiho, R. (Univ. of Turku, Finland). J. Sci. Instrum., 42: 766-7 (Oct. 1965).

A superconducting Nb–Zr magnet using a double Helmholtz coil arrangement is constructed. The design of the magnet is based on Franzen's extension of Garrett's theory of axially symmetric magnetic fields. In this way it is possible to achieve a theoretical field homogeneity of 1 in 10^4 over a sphere of radius 0.5 cm. A magnetic field up to 7 kOe has been generated using this magnet. (auth)

5615 IMPROVEMENTS RELATING TO HANDLING EQUIPMENT FOR RADIOACTIVE CHARGES. Webb, John (to United Kingdom Atomic Energy Authority). British Patent 1,009,333. Nov. 10, 1965. Filed Feb. 17, 1961.

Handling equipment for radioactive charges is described in which a receptacle and a linearly movable grasping means are carried in common by a single support means through respective elongated supports. Angular movement of the elongated supports effects a relative movement of the grasping means and the receptacle laterally of the line of movement of the grasping means to enable the receptacle to be adjusted to a postion beneath the grasping means for receiving the charge. (B.L.M.)

5616 IMPROVEMENTS IN OR RELATING TO MASTER-SLAVE MANIPULATORS. Waelischmiller, Hans. British Patent 1,009,637. Nov. 10, 1965. Priority date Aug. 21, 1963, Germany.

The master-slave manipulator is patented in which rotary shafts are provided for the transmission of the working movements from a master arm to a slave arm. The shafts extend in a tube through a protective wall and are connected with the movement elements of the manipulator arms by plug connections housed in a connecting head. An axially displaceable mounting for the connection head of the slave arm is arranged at the end of the tube. The mounting is provided with a shifting arrangement operable on the cold side and mounted approximately in the axis of the tube, and the axial shifting path of the arrangement is adequate for the coupling and uncoupling of the plug connections. The shifting arrangement provides an automatic blocking arrangement against rotation for the connection shafts in the connection head. (B.L.M.)

5617 PACKAGE IRRADIATION SYSTEMS. Jefferson, Sidney (to United Kingdom Atomic Energy Authority). U. S. Patent 3,214,582. Oct. 26, 1965. Priority date Dec. 30, 1960, Great Britain.

A package irradiation system is patented in which trolleys suspended on an overhead railway are used to convey packages past a radiation source. Lift means for the trolley comprises a movable section of the railway that alternately aligns with fixed portions of the railway within and without the shield. Each end of the lift means forms a radiation shielding plug for the aperture in the biological shield. (B.L.M.)

Heat Transfer and Fluid Flow

See also PHYSICS — Fluid Physics and Thermodynamics

Refer also to abstracts 5681 and 5879.

5618 (AD–619511) SURVEY AND EVALUATION OF TECHNIQUES TO AUGMENT CONVECTIVE HEAT TRANSFER. Technical Report No. 5382-34. Bergles, Arthur E.; Morton, Harmon L. (Massachusetts Inst. of Tech., Cambridge. Dept. of Mechanical Engineering). Feb. 1965. Contract AF49(638)-1468. 143p. CFSTI $4.00 cy, $1.00 mn.

A survey and evaluation of the numerous techniques which have been shown to augment convective heat transfer is presented. These techniques are: surface promoters, including roughness and treatment; displaced promoters, such as flow disturbers located away from the heat-transfer surface; vortex flows, including twisted-tape swirl generators; vibration of the heated surface or the fluid near the surface; electrostatic fields; and various types of fluid additives. Natural and forced convection situations for nonboiling, boiling, and condensation heat transfer are included. The conditions under which heat transfer is improved are summarized, and the efficiency of each technique is presented in terms of a performance criterion where possible. (auth)

5619 (AE–199) MIXED CONVECTION HEAT TRANSFER ON THE OUTSIDE OF A VERTICAL CYLINDER. Bhattacharyya, A. (Aktiebolaget Atomenergi, Stockholm (Sweden)). Oct. 1965. 52p. Dep. mn.

An experimental study was made of turbulent heat transfer from a vertical cylinder placed in a square channel. The flow medium was water flowing upwards. Basic differential equations governing the mixed flow heat transfer phenomena in a vertical annulus are presented. A dimensional analysis is done to find the dimensionless variables affecting the relative magnitude of the effect of buoyancy on forced convection heat transfer. Dimensionless equations correlating the experimental data and incorporating a buoyancy parameter of the form (Gr/Re^2) are presented. Reynolds number range covered is 690 to 129,500 and the Rayleigh number range covered is 10^9 to 4.2×10^{13}. Effects of different length parameters, like hydraulic diameter and distance of the measuring point from the inlet of the test section, on dimensionless equations were studied. (auth)

5620 (AE–200) AN EXPERIMENTAL STUDY OF NATURAL CIRCULATION IN A LOOP WITH PARALLEL FLOW TEST SECTIONS. Mathisen, R. P.; Eklind, O. (Aktiebolaget Atomenergi, Stockholm (Sweden)). Oct. 1965. 48p. Dep. mn.

The dynamic behavior of a natural circulation loop with two parallel round duct channels was studied. The test sections were both electrically heated and the power distribution was uniform along the 4300 mm heated length of the 20 mm dia channels. The interchannel interference and the threshold of flow instability were obtained by using a dynamically calibrated flowmeter in each channel. The pressure was 50 bars and the sub-cooling 6°C. The main parameters varied, were the flow restrictions in the one-phase and two-phase sections. The instability data were correlated to the resistance coefficients due to these restrictions. Theoretical calculations for parallel channels in natural circulation were compared with the experimental results. For the conditions determined by the above mentioned magnitudes, the steady-state computations are in excellent agreement with experiment. The transients are also nearly similar, except for the resonance frequency which for the theoretical case is higher by an amount between 0.3 and 0.5 cps. (auth)

5621 (AEEW-R-416) THE STABILITY OF LAMINAR FLOW OF A LIQUID BETWEEN PARALLEL PLANES.

Barnett, P. G. (Atomic Energy Establishment, Winfrith (England)). Jan. 1965. 34p. Dep. mn.

The stability of laminar flow of an incompressible viscous liquid moving between two fixed parallel planes when the laminar motion is subjected to a particular kind of infinitesimally small disturbance was examined. A new numerical method was developed for solving the resulting eigenvalue problem; this method was used to obtain some seventy results. These results enable the curve of neutral stability to be plotted accurately. They were also compared with results from two other sources. The magnitudes of the various forms of instability which arise suggest that infinitesimally small disturbances of the type considered are unlikely to provide a complete explanation of the transition from laminar to turbulent flow. (auth)

5622 (ANL–7032) AN INVESTIGATION OF INSTABILITIES ENCOUNTERED DURING HEAT TRANSFER TO A SUPERCRITICAL FLUID. Cornelius, Archie Junior (Argonne National Lab., Ill.). Apr. 1965. Contract W-31-109-eng-38. 93p. Dep. mn; CFSTI $3.00 cy, $0.75 mn.

The unstable behavior of heat transfer in loops operating at supercritical pressures is investigated. The mechanisms that trigger and maintain the observed pressure and flow oscillations are postulated. (T.F.H.)

5623 (EURAEC–1325) LARGE SCALE EXPERIMENTS ON HEAT TRANSFER AND HYDRODYNAMICS WITH STEAM-WATER MIXTURES. FURTHER CRITICAL POWER AND PRESSURE DROP MEASUREMENTS IN ROUND VERTICAL TUBES WITH AND WITHOUT INTERNAL OBSTACLES. Topical Report No. 5. Peterlongo, G.; Ravetta, R.; Riva, V.; Rubiera, L.; Tacconi, F. A. (Centro Informazioni Studi Esperienze, Milan (Italy)). Nov. 1964. Contract 056-62-1-RDI. 75p. (EUR–2307; CISE-R–122). Dep. mn; CFSTI $3.00 cy, $0.75 mn.

Work Performed under United States–Euratom Joint Research and Development Program.

Heat transfer crisis and pressure drop data for upward flow of steam-water mixtures in round vertical tubes with and without internal obstacles are presented. The range of variables is test element heated length, inner diameter, obstacles, pins, filling rods in the upstream region, pressure, specific mass flowrate, and inlet steam quality. The test elements are preceded by a valve, and followed by a separator. A description of results is given, putting in evidence the influence of different types of obstacles. (M.O.W.)

5624 (MIT–3496-1) THE MOMENTUM FLUX IN TWO-PHASE FLOW. Technical Report No. 4547-38. Andeen, Gerry B.; Griffith, Peter (Massachusetts Inst. of Tech., Cambridge. Div. of Sponsored Research). Oct. 1965. Contract AT(30-1)-3496. 141p. Dep. mn; CFSTI $4.00 cy, $1.00 mn.

The average momentum flux at a section of a pipe with two-phase upflow was measured by the impulse technique. Steam-water and air-water mixtures were tested in one-inch and one-half inch nominal pipes. Homogeneous velocities ranging from 150 to 1200 ft/sec and qualities from 5 to 85% were tested. The results were compared to the results of models currently in practice for predicting pressure drop and critical flow. The influence of the void fraction, the velocity profile, phase distribution, and fluctuations upon the momentum flux are discussed. (auth)

5625 (TRG-Report–1013) THERMAL RESISTANCE OF PRESSED CONTACTS. Thomas, T. R.; Probert, S. D. (Reactor Group, United Kingdom Atomic Energy Authority, Risley (England)). June 18, 1965. 30p. Dep.; BIS $0.90; HMSO 4s. 6d.

A review of theoretical results and experimental data is presented. It is concluded that the most promising line of attack on problems concerning thermal contact conductances is the use of surface analyzers with data-processing equipment to record surface parameters in great detail. Experimentally, there are very large differences between the results of different workers using apparently very similar specimens. There is a need for a standard specimen to be circulated among workers in the field. (auth)

5626 (NP-tr–1300) HEAT TRANSFER AND FRICTIONAL RESISTANCE OF A HIGH-TEMPERATURE GAS FLOW. Ter-Oganes'yants, A. A.; Shorin, S. N. Translated from Teploenergetika, No. 2, 83-6(1965). 15p. Dep. mn; CFSTI $1.00 cy, $0.50 mn; JCL $1.60 fs, $0.80 mf.

On the basis of a study of measurements of the heat transfer and frictional resistance of a high-temperature gas flow and comparison with the measurement results of others, an attempt was made to derive formulas corresponding to the analogy between the transfer of heat and transfer of momentum. The heat transfer and frictional resistance were measured in separate sections of a tube at comparatively high numbers $\Psi \equiv T/T_W$ (up to 3.9), and the effects of the state of the surface on the heat transfer and resistance were studied. It was concluded that in the case of complex convective-conductive-radiant heat transfer, and because of the simplification of the calculation formulas of the Stenton number, the Nusselt number is to be preferred. (P.C.H.)

5627 ALKALI METALS BOILING HEAT TRANSFER. Borishanskii, V. M.; Zhokhov, K. A.; Andreevskii, A. A.; Putilin, M. A.; Kozyrev, A. P.; Shneiderman, L. L. At. Energ. (USSR), 19: 191-3(Aug. 1965). (In Russian).

Sodium and potassium boiling heat transfer was measured in the heat load range from (14 to 125) $\times 10^3$ kcal/$m^2 \cdot hr$. The pressure and saturation temperature varied from 0.15 to 1.25 atm. and 697 to 905°C. The results showed that as free convection the heat transfer coefficient is a function of the heat load as close as 0.7, while absolute pressure has a very small effect on the heat transfer. An empirical formula $\alpha = Ap^{0.15}q^{0.7}$, kcal/$m^2 \cdot$ hr °C (where for sodium A = 7.0 and for potassium A = 3.0) was suggested for computing the heat transfer in sodium and potassium large volume bubbling boiling, at first approximation. The same formula may be used for computing the heat transfer in developed potassium and sodium bubble boiling in tubes and spherical gaps not affected by the vapor content. (R.V.J.)

5628 CORRELATION OF SOUND GENERATION AND HEAT TRANSFER IN BOILING. Schwartz, F. L. (Univ. of Florida, Gainesville); Siler, L. G. J. Heat Transfer, 87: 436-8(Nov. 1965).

The generation of sound accompanying boiling heat transfer is known. The intensity of the sound varies with the rate of heat transfer. A study was made to determine whether a correlation existed between intensity and frequency with the rate of heat transfer. It was concluded that a measurement of sound level could be used to predict the approach to maximum heat-transfer rate and control heat input to prevent burnout of a nuclear reactor. (M.C.G.)

5629 AVERAGE VOLUMETRIC CONCENTRATION IN TWO-PHASE FLOW SYSTEMS. Zuber, N.; Findlay, J. A. (General Electric Co., Schenectady, N. Y.). J. Heat Transfer, 87: 453-68(Nov. 1965).

A general expression that can be used either for predicting the average volumetric concentration or for analyzing and interpreting experimental data is derived. The analysis takes into account both the effect of nonuniform flow and concentration profiles as well as the effect of the local relative velocity between the phases. The first effect is taken into account by a distribution parameter, whereas the latter is accounted for by the weighted average drift velocity. Both effects are analyzed and evaluated. The results predicted by the analysis are compared with experimental data obtained for various two-phase flow regimes, with various liquid-gas mixtures in adiabatic, vertical flow over a wide pressure range. Good agreement with experimental data is shown. (auth)

Materials Testing

Refer also to abstract 6632.

5630 (NAA-SR-Memo-11562) EVALUATION OF INCLUSIONS FOUND BY RADIOGRAPHIC INSPECTION IN SAP TUBING. Vandervort, P. S. (Atomics International, Canoga Park, Calif.). Aug. 12, 1965. Contract AT(11-1)-Gen-8. 15p. Dep. mn; CFSTI $1.00 cy, $0.50 mn.

Radiography is a reliable NDT method for examining SAP tubing for dense type inclusions located in the tubing wall. Cross-sectional areas of this type of inclusion as small as 0.002 in. can be detected in 0.030 in. thick tube walls with this inspection method. The size of these inclusions as indicated by radiography was verified by metallographic examination and the type, iron, was determined by electron microprobe analysis. The longest dimension of any inclusion found during this examination measured 0.030 in. on the radiograph and this was subsequently verified by metallographic examination. (auth)

5631 UNDERWATER RADIOGRAPHIC EXPOSURE DEVICE. Graham, Gene P. (to General Motors Corp.). U. S. Patent 3,214,586. Oct. 26, 1965. Filed Oct. 29, 1962.

An underwater radiographic exposure device is described that is particularly applicable to the inspection of underwater piling used to support off-shore platforms for oil drilling rigs. A radiation shield contains a radioactive source and is positioned within the hollow object to be inspected, and any liquid is displaced from the portion of the object to be inspected. A photographic film is placed around the outer wall of the object, and the source is projected from the shield into the portion to be inspected so that the interior walls of the object will be irradiated to produce a radiogram on the photographic film. (B.L.M.)

Protective Structures

5632 FOLDABLE FALLOUT SHELTER. Forbes, Robert S. (to U. S. Atomic Energy Commission). U. S. Patent 3,213,868. Oct. 26, 1965. Filed Feb. 26, 1962.

A portable, easily erectable, and collapsible frame is patented for supporting a special cover material that is substantially impervious to fallout dust and associated radioactivity in a tent-like fashion. The support includes an erecting mechanism that is either mechanical or hydraulic operated and that is independent of external power sources. (B.L.M.)

Space Propulsion

See also ISOTOPE TECHNOLOGY — Power Application
REACTOR TECHNOLOGY — Propulsion and Space

Refer also to abstracts 6025 and 6470.

5633 (NASA-SP-5033) PLASMA JET TECHNOLOGY. Dennis, P. R.; Smith, C. R.; Gates, D. W.; Bond, J. B. (comps. and eds.) (National Aeronautics and Space Administration, Washington, D. C.). Oct. 1965. 200p. GPO $1.00.

A survey of some of the present industrial applications of plasma-arc devices and NASA work in this field is presented. NASA work with such devices has resulted largely from the need to simulate the environments into which space vehicles are sent and from efforts to develop propulsion units for satellite attitude and position control. Equipment manufacturers have been more concerned with welding, cutting, chemical synthesis, particle preparation, melting, and other such operations, and their views are presented to indicate ways in which NASA research and development may prove helpful here on earth as well as in space. NASA work in the plasma-arc field is summarized briefly and a bibliography with selected abstracts is included. Both arc heater and propulsion work are noted because both are of industrial interest. Work done on small thruster units may prove valuable in cutting, welding, etc., and that done on larger units may be adaptable to chemical and other processes. (M.O.W.)

5634 RADIOISOTOPE PROPULSION. Romero, Jacob B. (Boeing Co., Seattle). J. Spacecraft Rockets, 1: 532-8(Sept.-Oct. 1964).

Propulsion devices, powered with isotopes for which large-scale production is anticipated, are evaluated from the point of view of design concepts and performance limitations. Direct-heating devices, in which the propellant is heated in a radioisotope core, and direct-momentum devices, in which escaping particles impart thrust, are considered. Since direct-heating devices must reject excess heat during "off" periods, self-cooled designs or designs integrated with power units are suggested. These devices are limited in thrust by isotope availability. The maximum operating temperature for long-period operation must be maintained below 4000°F (I_{sp} = 800–1000 sec) to avoid excessive fuel clad evaporation. Component weights (radiation shields, structures, and isotope investment), thrust, and operating temperature limit engine thrust-to-weight ratio to 10^{-2} to 10^{-4}. Probable applications may be in orbit changes and satellite control. Direct momentum devices are limited to low thrusts and low thrust-to-weight ratios by particle self-absorption, particle isotropy, radiation hazards, and charge neutralization. Their application to propulsion is very limited. (auth)

5635 NUCLEAR-THERMAL VS CHEMICAL DRIVES FOR SUPER-ORBITAL VELOCITIES. Sandri, R. (National Research Council of Canada, Ottawa). J. Spacecraft Rockets, 1: 568-9(Sept.-Oct. 1964).

A brief analysis of the merits of chemical and nuclear-thermal propulsion units for rockets operating above orbital velocity is presented. (D.C.W.)

5636 ROCKET MOTOR WITH ELECTRIC ACCELERATION IN THE THROAT. Rosciszewski, Jan (General Dynamics/Astronautics, San Diego, Calif.). J. Spacecraft Rockets, 2: 278-80(Mar.-Apr. 1965).

The combination of a rocket motor and electric propulsion for obtaining intermediate specific impulses around 1000 to 2000 sec is described. The working gas is accelerated to the sonic speed in a convergent nozzle after the combustion chamber, accelerated to supersonic speed in a straight channel with segmented electrodes and normal magnetic and applied electric fields, and is allowed to expand in a divergent nozzle. The flow characteristics of the gas along the $j \times B$ accelerator were calculated numerically for various accelerator parameters, and the results are presented. (M.J.T.)

5637 ION PROPULSION SYSTEMS FOR SPACECRAFT. Reader, Paul D.; Mickelsen, William R. (Lewis Research Center, Cleveland). J. Spacecraft Rockets, 2: 577-83(July-Aug. 1965).

Performance characteristics and power requirements of existing electron-bombardment thrustors are presented in a form useful to electric-propulsion-system analysis and design. This information is based on experimental operation of laboratory thrustor modules of 5 to 50 cm in dia and module and array power levels up to 30 kw. Static and dynamic control characteristics of electron-bombardment thrustors are summarized. From these data, it is evident that no serious problems should arise in control-system design. A thrustor circuit design is described which suppresses electric breakdowns to a magnitude sufficiently small to eliminate damaging interaction between the thrustor and the power-conversion system. This circuit design is based on data obtained in operation of single thrustor modules and large thrustor arrays. It is shown that power-conversion and thrustor weights and performance penalties

could reduce the payload of a 500-kw, 28,500-lb Mars-orbiter vehicle by 5000 to 9000 lb. (auth)

5638 DESIGN AND PERFORMANCE OF ION-ENGINE SYSTEMS FOR CONTROL OF EARTH SATELLITES. Molitor, J. H. (Hughes Research Labs., Malibu, Calif.); Kaplan, M. H. J. Spacecraft Rockets, 2: 712-18(Sept.-Oct. 1965).

The application and optimization of ion-propulsion systems for orbit control of earth satellites was studied. These studies consisted of an evaluation of control requirements of various satellite systems and a design analysis of optimized ion engine systems that satisfy these requirements. A computer program was developed to determine the motion of earth satellites under the influence of perturbing forces such as the asphericity of the earth, the gravitational attraction of the sun and moon, atmospheric drag, solar pressure, and corrective thrust. From these data conceptual designs of ion engine control systems were performed. The applications considered were synchronous satellites, nonsynchronous medium altitude satellites, and manned space stations. (auth)

5639 ELECTRIC PROPULSION POSSIBILITIES USING STEAM SPACE POWER. Kroeger, Henry R.; Coneybear, J. Frank (Astra, Inc., Raleigh, N. C.). J. Spacecraft Rockets, 2: 830-2(Sept.-Oct. 1965).

A preliminary examination of systems consisting of electric thrusters and advanced steam space power plants is presented. Power ranges of interest for electric propulsion are considered. Performance characteristics for the combined system—lifetime, temperature, properties of water-steam systems, and waste-heat disposal—are discussed. Pressure, temperature, and weight characteristics of the steam power subsystem are surveyed. Possible arrangements and regimes for cooling thruster and power-conditioning components are discussed. (M.J.T.)

5640 IMPROVEMENTS IN METHODS AND DEVICES FOR PRODUCING A STRONGLY IONIZED GASEOUS STREAM. (to Electricite de France). British Patent 1,009,563. Nov. 10, 1965. Priority date Apr. 1, 1963, France.

A method and device are described for producing a strongly ionized gaseous stream from a gaseous stream flowing through a conduit. A series of pairs of ionization electrodes are carried by the walls of the conduit and are arranged with the discharge ends of every pair located opposite each other in the path of the gaseous stream. Means are provided for applying to the feed ends of every pair voltage pulses of a sufficient amplitude to start discharge or arcs between the corresponding discharge ends. The conduit is located in a magnetic field whose direction is substantially transverse to the direction of flow of the gaseous stream, and the electrodes are so disposed that the line joining the discharge ends of each pair is substantially parallel to the field. (B.L.M.)

Vacuum Engineering

Refer also to abstract 6513.

5641 TOTAL PRESSURE MEASUREMENTS BELOW 10^{-10} TORR WITH NON-MAGNETIC IONIZATION GAUGES. Redhead, P. A.; Hobson, J. P. (National Research Council, Ottawa). Brit. J. Appl. Phys., 16: 1555-66(Oct. 1965).

The modulation method has been applied to the Bayard–Alpert gauge and the suppressor gauge to reduce their lower pressure limits and measurements made with these two gauges to pressures as low as 10^{-14} torr. It is shown that the modulated Bayard–Alpert gauge can measure pressure to 3×10^{-11} torr (10% error) without correction for the residual-current modulation effect, and measurements can be extended to 3×10^{-13} torr if corrections for the residual-current modulation are made. The residual limit of the suppressor gauge has been measured (approximately 2×10^{-13} torr). With modulation applied to the suppressor gauge the lowest measurable pressure, set by amplifier noise, is about 10^{-13} torr for a 10:1 signal-to-noise ratio. Electronic desorption of chemisorbed material from the grid of a gauge and/or a molecular flux in the gauge are shown to cause a limitation to the lowest measurable pressure; these limits may be higher than the x-ray limit under certain conditions. (auth)

5642 BAKEABLE, PULSED GAS VALVE FOR PLASMA PHYSICS EXPERIMENTS. Birdsall, D. H.; Ping, D. E. (Univ. of California, Livermore). Rev. Sci. Instrum., 36: 1777-8(Dec. 1965). (UCRL-14150).

A magnetically actuated gas valve is described with which reproducible gas pulses of 1 to 150 μ liter can be obtained. (D.C.W.)

GEOLOGY, METEOROLOGY, AND MINERALOGY

General

5643 (TEI–862) PERCHED GROUND WATER IN ZEOLITIZED-BEDDED TUFF, RANIER MESA AND VICINITY, NEVADA TEST SITE, NEVADA. Thordarson, William (Geological Survey, Washington, D. C.). 1965. 95p. Dep. mn; CFSTI $3.00 cy, $0.75 mn.

The occurrence, movement, and discharge of perched groundwater in tuffaceous rocks that cap and underlie Rainier Mesa, which is the site of the first series of underground nuclear detonations made by the AEC at the Nevada Test Site, are described. The occurrence of groundwater in other rock types adjacent to and beneath Rainier Mesa is also described. Measured declines in head with depth in test wells suggests that the movement of the perched water is slowly downward along steeply dipping fractures to discharge points within the underlying more permeable Paleozoic strata. The head measurements made at different depths in two wells suggest vertical hydraulic gradients ranging from 0.3 to 1.0 ft per ft. A marked difference in the salinity of the interstitial and fracture water was indicated by study of electric logs and by chemical analyses of the fracture water. (P.C.H.)

Meteorology

See also Site Survey and Selection

Refer also to abstracts 5649, 5650, and 5667.

5644 (COO–1340-2, pp 110-21) THE BEHAVIOR OF JET STREAMS IN POTENTIAL FALLOUT SITUATIONS. Reiter, Elmar R. (Colorado State Univ., Fort Collins).

It is shown from a case study that the splitting of jet streams into several branches, which is frequently observed over the United States on the leading edges of intense jet maxima, may be explained by conservation of potential vorticity within an atmospheric layer moving over an obstacle. Such an obstacle may be a large mountain barrier, such as the Rocky Mountains, or a slow-moving dome of cold air in the lower troposphere, as is typical for cold outbreaks associated with strong jet streams. (11 references.) (auth)

5645 (COO–1340-2, pp 122-45) DEVELOPMENT OF COMPUTER PROGRAMS FOR COMPUTATION OF MONTGOMERY STREAM FUNCTIONS AND PLOTTING OF THERMODYNAMIC DIAGRAMS. Mahlman, J. D.; Kamm, W. (Colorado State Univ., Fort Collins).

Machine procedures are developed for computation of isentropic analysis parameters and for plotting of tephigrams, both in terms of derived basic equations. Computation flow charts and program copies are included from both programs. (auth)

5646 CORRELATION BETWEEN THE RADON CONCENTRATION AT GROUND LEVEL AND CERTAIN METEOROLOGICAL PARAMETERS. Mageru, Victor; Rezlescu, Nicolae (Lab. of Environmental Radioactivity, Rumanian Academy of Sciences, Iasi). Acad. Repub. Pop. Rom. Stud. Cercet. Fiz., 17: 245-56(1965). (In Rumanian).

It was previously reported that the Rn concentration of the air layer at the surface of the earth undergoes wide daily variations within 10^{-18} to 10^{-6} C/cm^2. As the atmospheric Rn originates from diffusion of the gas contained in the soil, an attempt was made to correlate these changes with variations of atmospheric pressure, wind velocity, precipitation, and the duration of sunlight. The Rn content of the air was determined on the basis of a counting of deposits on filter paper through which a large known volume of air has passed. The results indicated that the correlation between the Rn concentration and the various meteorological factors is not always direct because many factors affect the concentration of radioactive materials at the surface of the earth. The temperature, pressure, and wind velocity were found to be most important. An increase of the temperature and a decrease of the air pressure caused an enhanced diffusion of the Rn from the soil capillaries into the atmosphere. Increasing wind velocities caused a transfer of the Rn into the upper layers and a decrease of its concentration at the surface. The duration of the sunlight and humidity exerted only an indirect effect. (TTT)

Natural Radioactivity and Fallout

See also HEALTH AND SAFETY

Refer also to abstract 5644.

5647 (COO–1340-2) FURTHER STUDIES ON RADIOACTIVE FALLOUT. Progress Report No. 2. Technical Paper No. 70. (Colorado State Univ., Fort Collins). Sept. 1965. Contract AT(11-1)-1340. 149p. Dep. mn; CFSTI $4.00 cy, $1.00 mn.

Separate abstracts were prepared for five sections of this report. (C.H.)

For abstracts of individual sections see: 5644, 5645, and 5648–5650.

5648 (COO–1340-2, pp 1-53) HEAVY ^{131}I FALLOUT OVER THE MIDWESTERN UNITED STATES, MAY 1962. Reiter, E. R.; Mahlman, J. D. (Colorado State Univ., Fort Collins).

Heavy I-131 fallout observed in milk from the Wichita milkshed on 13 May 1962 raised a controversy on whether the debris originated from a vented underground test in Nevada or from the U. S. atmospheric test series over Christmas Island. Careful meteorological analysis excludes the 8 May 1962 Nevada Paca shot as a debris source for this Wichita fallout case. There is a possibility, however, that some fractionated radioactive material from this Paca shot may have drifted into the Colorado region, causing slight increases in radioactivity and significant debris age shifts on 11 May 1962. (47 references). (auth)

5649 (COO–1340-2, pp 54-83) A CASE STUDY OF MASS TRANSPORT FROM STRATOSPHERE TO TROPOSPHERE, NOT ASSOCIATED WITH SURFACE FALLOUT. Reiter, E. R.; Mahlman, J. D. (Colorado State Univ., Fort Collins).

On 18 and 19 April 1963 an intrusion of stratospheric air, descending into the troposphere within a stable layer, was observed east of the Rocky Mountains. No significant increases of radioactive fallout at the ground were measured in connection with this intrusion. Differences between this and earlier case studies, therefore, help to establish and confirm meteorological criteria for rapid transport of nuclear debris from the stratosphere to the low troposphere under quasi-adiabatic conditions. (19 references.) (auth)

5650 (COO–1340-2, pp 84-109) RELATION OF TROPOPAUSE–LEVEL INDEX CHANGES TO RADIOACTIVE FALLOUT FLUCTUATIONS. Mahlman, J. D. (Colorado State Univ., Fort Collins).

The downward transport of radioactive debris from the stratosphere, in association with tropopause-level cyclogenesis, offers a possible physical explanation for seasonal and shorter-period fallout peaks. In order to examine these possibilities an index designed to measure the relative amount of cyclonic activity in the atmosphere is derived and then compared with seasonal and short-term variations in mean fallout intensity. It is shown from the analyses that the spring fallout peak cannot be explained

adequately by an increase of cyclonic activity at this time of year. Shorter-period fallout increases, however, are statistically related to occurrences of cyclogenesis in the upper troposphere. Seasonal stratospheric-tropospheric mass exchange calculations, determined independently from the fallout and index data, indicate a mean stratospheric residence half-time of one year. Therefore, the proposed cyclogenetic process appears to provide the predominant transport mechanism. (34 references.) (auth)

5651 (RISO-107) ENVIRONMENTAL RADIOACTIVITY IN DENMARK IN 1964. Aarkrog, A.; Lippert, J. (Atomenergikommissionen, Risoe (Denmark). Forsoegsinstitut). June 1965. 98p. Dep. mn.

Results are reported from measurement of fallout radioactivity in Denmark in 1964. Sr-90 was determined in samples of precipitation, soil, ground water, sea water, grass, dried milk, fresh milk, grain, bread, potatoes, vegetables, fruit, meat, total diet, and human bone collected throughout the country. Sr-90 was also determined in local samples of air, rain water, grass, sea plants, animal bone, and human milk. Cs-137 was determined in milk, grain products, potatoes, vegetables, fruit, total diet, pork, beef, and human milk samples, and Cs-137 was measured by whole-body counting in persons from different parts of the country. Estimates of the mean content of radiostrontium and radiocaesium in the human diet in Denmark in 1964 are given. Data are included from regular surveys of environmental samples from the Risö area. (auth)

5652 γ-SPECTROMETRIC ANALYSES OF THE 1963 ATMOSPHERIC FALLOUT SAMPLES. Iorgulescu, Adriana (Inst. of Atomic Physics, Bucharest). Acad. Repub. Pop. Rom. Stud. Cercet. Fiz., 17: 359-67(1965). (In Rumanian).

A method previously developed (Stud. Cercet. Fiz., 14: 769(1963)) was used to determine the γ spectra of samples collected during 1963. The measurements were carried out by means of a single-channel analyzer, a NaI(Tl)-type scintillation counter, and a photomultiplier. In view of the low intensity of the sources, four weekly samples were used jointly, increasing the operating time and shielding out the background. The linearity of the analyzer was determined by a series of radioisotopes; its resolution for the 662-kev line was 11%. Analysis of the 1963 monthly specimens' spectra revealed the presence of the short-lived isotopes, as it is characteristic for samples with an age of less than two years. All of the monthly samples contained $^{95}Zr + ^{95}Nb$; ten of the samples did not contain any ^{137}Cs. In the September and December samples the 662-kev line could be noted as a weak photopeak. The 724-kev or a combination of the 756 and 765-kev lines are attributed to $^{95}Zr + ^{95}Nb$. The absence of the ^{137}Cs line in most of the samples is explained by the loss of its photopeak in the Compton continuum of the ^{95}Zr spectrum. (TTT)

5653 GAMMA RADIATION SPECTRUM FROM ARTIFICIAL MODEL OF RADIOACTIVE FALLOUT. Izrael', Yu. A.; Nekozyrev, A. F.; Nikolaev, P. V.; Stukin, E. D. At. Energ. (USSR), 19: 199-200(Aug. 1965). (In Russian).

Studies were made of fallout γ radiation simulated with a hundred ^{60}Co sources 96 mg equiv. Ra units. Each source was placed at 10 to 15 cm over the 40 × 40 mm wooden support placed over a 500 m diameter area. The surface density was 3.8×10^{-2} mC/m^2[3.5×10^2 Mev/cm^2 sec]. At 1 m over the earth the γ dose was 1.75 mR/hr and 200 m near 0.12 mR/hr. The γ radiation spectrum was monitored by a helicopter at 20 to 200 m at a speed of 50 to 60 km/hr. The correlated theoretical and experimental data were in good agreement. (R.V.J.)

5654 TRITIUM CONCENTRATION OF GERMAN RIVER WATERS MEASURED WITH THE PROPORTIONAL-COUNTING TECHNIQUE. Buttlar, H. v.; Farzine, K.; Wohlfahrt, H. -D. (Technische Hochschule, Darmstadt, Ger.). Nucl. Instrum. Methods, 37: 288-92(Nov. 1965).

Sample water is converted to hydrogen gas and then reacted with ethene to yield ethane. The tritium radioactivity is counted in an Oeschger-type counter in the limited proportional region. A transistorized electronic circuit allows simultaneous registration of tritium counts plus background below, and mainly background above, about 15 kev. With a geometric volume of the central tritium counter of 2.9 l the anticoincidence background is 2.74 ± 0.03 cpm in the tritium channel; a sample of 100 TU has a sample counting rate of 1.32 cpm when the ethane pressure is 750 mm Hg. Details about background, tritium spectrum, efficiency, reliability, and long-time stability are given. The tritium concentrations of water samples from the Rhine and Main rivers taken between 1961 and 1964 show pronounced maxima in the summer, about two months later than the rain maxima. (auth)

5655 DETERMINATION OF ^{90}Sr IN DECIDUOUS TEETH. Del Vecchio, V.; Lanzola, E.; Alasia, A. M. (Univ., Rome). Nuovi Ann. Ig. Microbiol., 15: 193-9 (May-June 1964). (In Italian).

Results of determination of ^{90}Sr in 1088 deciduous teeth of children aged 3 to 11 yr are reported. The teeth were collected at a dental clinic in Rome from spring to autumn of 1962, and consisted of incisors 32%, canines 6%, first molars 17%, and second molars 5%. The mean values for teeth of children of various ages, in pC ^{90}Sr/g Ca, were as follows: age 3 yr, 5.2; 4 yr, 3.7; 5 yr, 2.75; 6 yr, 2.4; 7 yr, 1.5; 8 yr, 1.3; 9 yr, 0.8; 10 yr, 0.45; and 11 yr, 0.33 (the ash contained ~ 38% Ca). This shows a progressive rise in ^{90}Sr content of teeth of children born between 1951 and 1959. When figures for the ^{90}Sr content of milk are compared with the concentrations in teeth, a parallel increase is noted. Milk ^{90}Sr content tended to decline after 1959. The values found for ^{90}Sr in teeth of Italian children are slightly higher than those reported for teeth of children in St. Louis, Missouri, by Rosenthal et al. (Science, 140: 176(1963)). It is pointed out that the ready availability of deciduous teeth and their low rate of mineral turnover offer a very useful material for estimating ^{90}Sr burden of children. (BBB)

5656 STRONTIUM ISOTOPES: GLOBAL CIRCULATION AFTER THE CHINESE NUCLEAR EXPLOSION OF 14 MAY 1965. Kuroda, P. K. (Univ. of Arkansas, Fayetteville); Miyake, Y.; Nemoto, J. Science, 150: 1289-90 (Dec. 3, 1965).

Strontium-89 and strontium-90, released into the atmosphere by the Chinese nuclear device on 14 May 1965, circled the world in less than a month and caused a sharp peak in the $^{89}Sr/^{90}Sr$ ratio in rain at Tokyo on 12 June. (auth)

Techniques and Equipment

Refer also to abstracts 5610 and 6651.

5657 (NP–15543, pp 47-58) USE OF RADIOACTIVE TRACERS IN HYDROLOGY IN RUMANIA. Gaspar, E.; Oncescu, M. (Institutul de Fizica Atomica, Academia R. P. R., Bucharest).

The scope of the investigations carried out in Rumania in the field of hydrology by means of radioactive tracers has been to establish the direction and the flow speed of underground waters; subinfiltrations currents in dams; water exchange between depression zones; and perimeter of sanitary protection required by underground resources for the supply of water works. Interesting conclusions based on the interdependence of concentration of the radioactive solutions (C) at the point of measurement and the phenomena investigated, have been derived from the various measurements effected. (auth)

5658 RADIOACTIVITY WELL LOGGING APPARATUS UTILIZING A SCINTILLATION DETECTOR. Monaghan, Ralph (to Dresser Industries, Inc.). U. S. Patent 3,214,587. Oct. 26, 1965. Filed May 12, 1961.

An apparatus for investigating the nature of the subsurface substances comprises a scintillation means emitting in response to incident radiation functionally related light pulses having decay characteristics related to the charac-

ter of the incident radiation. Means are optically connected to the scintillation means for producing a first electrical signal composed of pulses having widths related to the decay characteristics of the light pulses. Sorting means receive the first signal and produce simultaneously in response to it a second signal and a third signal both composed of pulses related to those of the first signal. The pulses of the second signal have widths greater than a pre-determined width and the pulses of the third signal have widths less than the pre-determined pulse width. Means are provided for receiving and sorting the second and third signals. The method for using the apparatus is described in detail. (B.L.M.)

Thorium and Uranium Minerals

5659 (RME-4545(Rev.)) RECONNAISSANCE FOR URANIUM IN NORTHEAST COASTAL BRAZIL. Gabelman, John W. (Division of Raw Materials (AEC), Washington, D. C. Comissao Nacional de Energia Nuclear de Brasil, Rio de Janeiro). Jan. 1964. 33p. Dep. mn; CFSTI $2.00 cy, $0.50 mn.

The uraniferous gold deposits of the Jacobina district, Bahia, Brazil, occur in conglomerate reefs within the Jacobina quartzite of Precambrian age and resemble the Witwatersrand and Blind River ores in South Africa and Canada. The ores are mined for gold but are not economical for uranium alone or thus far as a by-product. Their origin has not yet been established. The known uranium and other minerals seem to be weak and of low temperature, but the presence of even small quantities of uranium in a strongly oxidized and leached surface containing other mineralization products suggests that northeast coastal Brazil may contain more important uranium deposits than those presently known. The most favorable area for economic uranium deposits probably would be in and near the Tucano basin where uranium could have been derived by lateral secretion or from hydrothermal solutions. (P.C.H.)

5660 ABOUT USE OF $^{234}U/^{238}U$ ISOTOPIC RATIO FOR INTERPRETATION OF URANIUM ANOMALY. Syromyatnikov, N. G. At. Energ. (USSR), 19: 169-74(Aug. 1965). (In Russian).

The ratio of $^{234}U/^{238}U$ in two exogenic uranium accumulations in arid zones were analyzed in order to determine their genetic origin. The mechanism of uranium deposition on the surface of porous formations and cementation zones is discussed. The time of sooty uranite formation was set for ~3 million years. An isotopic-uranium criterion was suggested for the uranium anomalies. (R.V.J.)

HEALTH AND SAFETY

See also BIOLOGY AND MEDICINE — Radiation Hazards and Protection
GEOLOGY, METEOROLOGY, AND MINERALOGY — Natural Radioactivity and Fallout

Refer also to abstracts 5878, 5966, 6552, 6584, and 6670.

5661 (AEET–215) MEASUREMENTS OF RADIOACTIVE FALLOUT IN INDIVIDUAL RAIN SHOWERS AT BOMBAY. Bhatnagar, V. S.; Sadasivan, S. (Atomic Energy Establishment, Trombay (India). Health Physics Div.). 1965. 35p. Dep. mn.

A few individual rain showers were collected at Bombay during the 1963 monsoon with the object of studying the variation of fallout radioactivity of rain water during the course of a single rain shower. The fallout radioactivity of rain water due to ^{137}Cs, ^{106}Ru, and ^{95}Zr was determined using a gamma scintillation spectrometer. Relevant meteorological observations, e.g., rainfall intensity, wind, and lowest cloud base heights, were also obtained, and efforts made to relate the variation in specific radioactivity to these parameters. Generally, the trends in radioactivity concentration of rain water, as a rain shower progressed with time, were found to be independent of precipitation rate, cloud base height, and the existing meteorological conditions. Also considering the mean specific radioactivity of a whole shower, the variations from shower to shower were found to be unaffected by general meteorological conditions. On the basis of these observations it is surmised that the trends in the specific radioactivity of rain water during the course of a rain shower, are determined primarily by the cloud processes, such as the coagulation of fallout particles with cloud particles, the condensation of water vapor on the fallout particles serving as condensation nuclei, etc. (P.C.H.)

5662 (NLCO–962) THORIUM AND ITS MPC'S. Heatherton, R. C.; Boback, M. W. (National Lead Co. of Ohio, Cincinnati). Sept. 1, 1965. Contract AT(30-1)-1156. 15p. (CONF-651008–3). Dep. mn; CFSTI $1.00 cy, $0.50 mn.

From Annual Bio-Assay Meeting, Albuquerque, N. Mex.

Maximum permissible concentration (MPC) values for thorium are discussed from the viewpoint of an AEC contractor. Inconsistencies presently found in the official publications of the International Commission on Radiological Protection (ICRP), the National Committee on Radiation Protection (NCRP), and the USAEC are confusing and require clarification. In addition, it has been reported unofficially that the ICRP, in the next revision of its tables, will probably exclude or make more restrictive the provisional statement regarding the maximum permissible concentration in air $(MPC)_a$ for long-lived thorium isotopes. It is felt that, in view of available information, such action by the ICRP is questionable and should be reconsidered. (auth)

5663 (NP–15451) L'APPLICATION DES NORMES SANITAIRES EN MATIERE DE PROTECTION RADIOLOGIQUE. (Application of Sanitary Standards in the Matter of Radiological Protection). Jammet, Henri (Paris Univ. (France). Institut de Droit Compare). 1965. 33p. Dep. mn.

The standards for radiological protection set up by the ICRP and their implementation by signatory nations, particularly France, are indicated. The classification of radiations and the reference doses are given. The regions of application and health standards for each are summarized. The administrative control for the enforcement of regulations enacted is considered. In conclusion, the problems of transport, wastes, and fallout are discussed. (P.C.H.)

5664 (NP–15639) FALLOUT IN NEW ZEALAND. Quarterly Report, April–June 1965. (National Radiation Lab., Christchurch (New Zealand)). 20p. (NRL–F17). Dep. mn.

Data are given for measurements of total beta and total gamma activity in atmosphere and deposition on ground and strontium-90 in milk and rain and cesium-137 in milk. Method of measurement and sample collection are discussed. (P.C.H.)

5665 (ORNL-TM–1304) A STANDARD SURFACE FOR FISSION PRODUCT DEPOSITION EXPERIMENTS. Browning, W. E. Jr.; Davis, M. E. (Oak Ridge National Lab., Tenn.). Oct. 29, 1965. Contract W-7405-eng-26. 20p. Dep. mn; CFSTI $1.00 cy, $0.50 mn.

A standard surface is recommended for use in the USAEC Nuclear Safety Program to provide a basis for comparison of fission product deposition between different experiments and by different experimenters. Precautions are discussed relative to the use of such a standard and to the interpretation of results. Type 304 stainless steel strip with number 1 finish (cold rolled, and annealed, and pickled) produced according to ASTM Specification A-240 should be used. This material should be cut into coupons, degreased, pickled one hour with occasional stirring in an aqueous solution of 3 wt % HF and 20 wt % HNO_3 at room temperature, rinsed with distilled water, and heated for one hour at 600°C in a slowly moving air stream. Extreme care should be taken to see that the coupons are not contacted by bare hands after beginning this surface preparation. (auth)

5666 (TID–21995) THE NUCLEAR ASPECTS OF THE ACCIDENTAL CRITICALITY AT WOOD RIVER JUNCTION, RHODE ISLAND, JULY 24, 1964. Supplemental Report. Nakache, F. R.; Shapiro, Mathew M. (United Nuclear Corp., New Haven, Conn. Fuels Div.). Nov. 12, 1964. Contract AT(30-1)-2303. 152p. Dep. mn; CFSTI $5.00 cy, $1.00 mn.

The results of various investigations on the nuclear physics aspects of the accidental criticality which occurred on July 24, 1964, at Wood River Junction, R. I. are reported. Total fissions which occurred are estimated to be 1.3×10^{17}. Evidence that a second excursion took place is described and the possible mechanisms are evaluated. Estimates of doses received by personnel are given and the methods of calculation are described. The postulated events leading to the criticality and the statement in the earlier report that the criticality occurred due to the accidental pouring of a concentrated solution of uranyl nitrate from safe to non-safe geometry are verified by the results of these subsequent investigations. (auth)

5667 (VUF–1020) WEATHER AND SURFACE RADIATION PREDICTION ACTIVITIES FOR THE SALMON EVENT—PROJECT DRIBBLE. Final Report. (Weather Bureau Research Station, Las Vegas, Nev.). Aug. 1965. 41p. Dep. mn; CFSTI $2.00 cy, $0.50 mn.

The Weather Bureau provided weather planning and prediction for the radiological safety program of the Salmon event, Project Dribble. Observations of winds and weather conditions at the site began 20 months prior to the event. Wind and temperature soundings and weather and radioactivity forecasting facilities were added during the detonation and post-event drilling phases. The winds during the 4 weeks following the Ready date were sufficiently abnormal in direction and speed that the planned firing criteria were not met, resulting in delays and changes in criteria to accept a wider range of conditions. (auth)

5668 (WASH–1061) NATURAL ENVIRONMENTAL RADIOACTIVITY. An Annotated Bibliography. Klement,

Alfred W. Jr. (Division of Biology and Medicine (AEC), Washington, D. C. Fallout Studies Branch). July 1965. 129p. Dep. mn; CFSTI $4.00 cy, $1.00 mn.

Approximately 2000 annotated references are presented to literature on natural environmental radioactivity in the atmosphere, biological materials, soils, and waters. (C.H.)

5669 REMOTE OPENING OF METAL CONTAINERS WITH A LASER BEAM. Horrocks, Donald L.; Studier, Martin H. (Argonne National Lab., Ill.). Anal. Chem., 37: 1782(Dec. 1965).

The method involves focusing a beam of light from a laser through a lens onto the metal container in a closed system, i.e., a glass vacuum line or behind a protective wall. A laser with a 0.05% chromium-doped ruby rod cooled to liquid nitrogen temperature was employed. Bending the laser beam and remote opening operations are discussed. Any number of holes can be put in the metal container. The laser is outside the closed system and can be moved, repaired, or altered without disturbing the closed system. It is applicable to any type of remote operation provided the light beam from the laser can be focused, directly or indirectly, by mirrors or prisms, onto the metal containers (for different depths of penetration, lenses with different focal length are used). Small holes are produced in the metal container. They decrease the chances of vaporizing large amounts of the metal container or possibly the sample itself. (F.J.H.)

5670 ABOUT AIR-EXCHANGE CALCULATION IN ROOMS FOR HIGH-POWER GAMMA UNITS. Sobol', N. V.; Petushkov, A. A.; Breger, A. Kh. At. Energ. (USSR), 19: 201(Aug. 1965). (In Russian).

Correlations were made of various data on radiochemical yields and permissible doses of nitrogen oxides and ozone formation and toxicity. The possibility of explosive gas accumulations in case of mixed shielding and water shielding of the source was analyzed, and it is suggested that regular ventilation of the room excludes the danger of explosive gas accumulations. (R.V.J.)

5671 ^{137}Cs BODY BURDENS IN TORONTO. McNeill, K. G.; Harrison, J. E.; Grimshaw, J. D. C. (Univ. of Toronto). Can. J. Phys., 43: 2380-3(Dec. 1965).

Over the last seven years, measurements were made of the ^{137}Cs body burden of persons in Toronto who had no history of radioactive contamination apart from that present in the normal population. Some results for ^{137}Cs in milk are also given. The average whole-body ^{137}Cs measurement increased from 4.2 to 21.2 nanocuries from the summer of 1962 to winter of 1963-64. (F.S.A.)

5672 RADIATION CONTROL AT THE NATIONAL INSTITUTE OF RADIOLOGICAL SCIENCES. Ishikawa, Tomokiyo (National Inst. Radiol. Sci., Chiba, Japan). Genshiryoku Kogyo, 10: 58, 68-71(Dec. 1964). (In Japanese).

The radiation control at the institute is described in the following sections: organization for the radiation control; objects for radiation control; radiation control systems; control areas; personal radiation control; medical checks; radiation control for the facilities and equipment; equipment for radiation control and storage of radioisotopes; radioactive waste disposal; countermeasures for accidents; and development of radiation control technology. (auth)

5673 RADIATION SHIELDING REQUIREMENTS FOR MANNED SATELLITES. French, Francis W.; Hansen, Kent F. (Mitre Corp., Bedford, Mass.). J. Spacecraft Rockets, 2: 931-7(Nov.-Dec. 1965).

The radiation shielding requirements for the protection of the crews of manned satellites are investigated. Two diverse types of missions are studied: a long-duration, high-altitude mission above the Van Allen Belt, and a short-duration, low-altitude, polar mission below it. Radiobiological tolerance criteria are considered, and a criterion based on partial recovery of sustained somatic damage is examined for the long-duration mission. Model solar flare, cosmic, and Van Allen Belt radiation environments are postulated. Radiation transport calculations are carried out to obtain the biological doses due to the various environmental components. Curves of dose vs shielding thickness, together with the model environments and the postulated radiobiological tolerance criteria, are used to calculate minimum amounts of shielding. For the high-altitude mission, results show that considerable savings in shielding weight are obtained if a radiation recovery criterion, rather than a straight cumulative-dose criterion, is used. For the low-altitude mission, the effects of different geomagnetic field models in modifying the free-space dose and the results of using different target models are illustrated. (auth)

5674 ENVIRONMENT AND LEUKEMIA MORBIDITY. III. DISTRIBUTION OF LEUKEMIA MORBIDITY AND BACKGROUND IONIZING RADIATIONS OF THE ENVIRONMENT. Plewa, Stanislaw; Aleksandrowicz, Julian; Janicki, Kazimierz (Geophysical Inst., Krakow. Third Clinic of Internal Diseases, Krakow). Pol. Arch. Med. Wewn., 32: 844-9(1962). (In Polish).

Evidence is reviewed which implicates exposure to ionizing radiation in the causation of leukemia, particularly as pertains to environmental sources of radiation. Several reports are cited relating certain geologic substrata to increased incidence of leukemia in populations living in the vicinity of them. The importance of taking into account all environmental sources of the population at risk is emphasized, including water supplies and atmospheric radioactivity, as well as that in geologic structures. An attempt was made to relate incidence of leukemia in certain districts of Poland with geologic radiometric data obtained by air surveys. In two districts a correlation was found. A particularly high incidence of leukemia was noted in a region that had one of the highest measurements of ambient radioactivity. In a region of very low radioactivity (Limanowa), a lower than normal occurrence of leukemia was noted. Granite outcrops were found to be closely related to increased terrestrial radiation levels. (BBB)

5675 DESORPTION OF CARRIER-FREE ^{60}Co, ^{144}Ce, AND ^{147}Pm FROM CHARCOAL SURFACES BY WATER AND SODIUM DODECYL SULFATE SOLUTION. Wadachi, Yoshiki; Muarmatsu, Mitsuo (Japan Atomic Energy Research Inst., Tokyo. Tokyo Metropolitan Univ.). Radioisotopes (Tokyo), 14: 475-9(Nov. 1965).

Experimental conditions suitable for preparing radioactive dust samples, which consist of charcoal powders and radioactive isotopes adsorbed on them for experiments on contamination of solid surfaces and its removal were studied. Carrier-free radioisotopes including ^{144}Ce, ^{147}Pm, and ^{60}Co were tested as the adsorbing species that can be retained on washing with water and solutions of sodium dodecyl sulfate (SDS) above and below its critical micelle concentration (CMC). It was found that ^{144}Ce and ^{147}Pm are more suited than ^{60}Co for labeling charcoal powders for soiling solid surfaces to be washed with water. For washing with SDS (below its CMC) ^{60}Co was better suited than ^{144}Ce and ^{147}Pm. None of the radioisotopes examined proved to be reliable for labeling charcoal for contaminating solid surfaces to be washed with SDS above its CMC. It was concluded that the radioisotope best suited for labeling pulverous samples should reasonably depend on what conditions would be adopted for washing the solid surfaces to be soiled with the labeled sample. (auth)

5676 REMOVAL OF RADIOACTIVE ISOTOPES FROM COTTON CLOTHS CONTAMINATED WITH IONIC RADIOISOTOPES ACCOMPANYING OILY SOILS. Takada, Kazuo (Japan Atomic Energy Research Inst., Tokyo); Wadachi, Yoshiki; Yamaoka, Yoshito; Noguchi, Shun; Muramatsu, Mitsuo. Radioisotopes (Tokyo), 14: 487-92(Nov. 1965).

Various decontaminants were compared for cleaning cotton cloth soiled with ionic radioisotopes, including ^{60}Co, ^{32}P, and ^{131}I, in the presence of oily materials. It was found that the ^{60}Co contamination is removed more easily when it occurs after soiling the cloth with non-polar hydrocarbon than when it occurs before. However, a larger decontamination effect was observed when the cloth was soiled first

by the radioisotope followed by soiling with a polar oil, such as octadecanol-1 or tripalmitin, than when the cloth was soiled in the reverse order. The mechanism of ^{60}Co contamination seemed to involve ionic processes. The contaminant was removed easily by replacing it with simple cations or by combining it with sequestering agents. The best way to remove ^{60}Co was found to be by isotopic exchange with nonradioactive cobaltous ion or by the treatment of soiled cloth with EDTA solution. Little effects on decontamination were found with detergent solutions of below CMC (critical micelle concentration), while above CMC the contaminant was removed. Addition of inorganic salts to detergent solutions caused an increased decontamination due possibly to the enhanced micelle formation and to the ion-exchanging character of the salts. Such anionic contaminants as ^{32}P or ^{131}I exhibited weak attractive force to cellulose and, accordingly, were removed easily even with water. Small or negligible effects on decontamination were found with addition of various detergents to water, suggesting the unlikelihood of special interaction, which was considered for explaining ^{60}Co contamination and its removal. (auth)

5677 THE GAMMA-RAY EVALUATION OF DIAGNOSTIC SHIELDING BARRIERS. Witcofski, R. L.; Watts, F. C.; Engstrom, L. L.; Blackwell, C. E. Radiology, 85: 1123(Dec. 1965).

A gamma source was sought for use in the evaluation of shielding barriers in diagnostic x-ray facilities. Criteria of choice were: a gamma-emitter comparable in energy to diagnostic x rays; availability; half life; and cost. The radioisotope that appeared to best meet the specifications was $^{144}Ce-^{144}Pr$. (H.G.D.)

5678 MANDAN MILK MYSTERY. Pfeiffer, E. W. Sci. Citizen, 7: No. 10, 1-5(Sept. 1965).

The Minot-Mandan region, which includes several counties of central North Dakota, lies in an area in which radiation from fallout is 2 to 3 times higher than in adjacent areas. In 1958 the ^{90}Sr content in milk from Mandan had reached 33 Sr units, the highest level recorded at any of the AEC's 39 sampling stations located throughout the world. Other stations in the U. S. had levels of about 5 Sr units (1 pC of Sr/Ca g). In May 1959 Mandan milk had 48 Sr units and in the spring of 1963 105 Sr units were recorded, and in 1964 the average content in milk was over 70 Sr units. The prairie provinces of Canada to the north of North Dakota had levels of ^{90}Sr in milk higher than the U. S. average, but not as high as the North Dakota average. Data are presented on the ^{90}Sr content in bones collected from the area but the small population has resulted in a small sample size. Data are presented from measurements of the ^{90}Sr content in samples of rain water, forage plants, and soil from the area. The possible influence of geography, meteorological conditions, farming practices, and fallout from nuclear weapons tests at the Nevada Test Site are discussed. It appears that special meteorological factors may be responsible for the high ^{90}Sr content in milk of this region. (C.H.)

5679 MANUFACTURE OF MOTOR VEHICLES FOR ADDITIONAL PROTECTION FROM RADIATION HAZARDS. Johnston, Herbert Charles. U. S. Patent 3,212,809. Oct. 19, 1965. Filed Oct. 12, 1961.

A self-propelled land vehicle, such as a station wagon, is provided with special features that make it applicable for use by civilian defense personnel during early radiation fallout from a nuclear attack. The body portion of the vehicle includes a sheath of lead of not less than $\frac{1}{16}$ in. thickness, and the windows and windshield are fabricated of lead glass. The outside of the body is painted with a highly reflective lead paint or one coat of a lead paint and one coat of a highly reflective paint. (B.L.M.)

INSTRUMENTATION

General

Refer also to abstracts 5929 and 6180.

5680 (ELI–91) GENERAL PURPOSE SUB-ASSEMBLIES. (Atomic Energy of Canada Ltd., Chalk River (Ontario)). June 1965. 40p. (AECL–2294). Dep.; AECL $1.00.

Circuit diagrams and electric characteristics are presented for several electronic devices having wide applicability. These devices include amplifiers, discriminators, ratemeter pumps, a BF_3 counter and preamplifier, a 5-Mc gated oscillator, fast and slow scalers, and bistable and monostable circuits. (T.F.H.)

5681 (MLM–1288) A GENERAL METHOD OF DETERMINING THE TOTAL TIME INTEGRAL OF TRANSIENTS IN LINEAR SYSTEMS. Jordan, K. C. (Mound Lab., Miamisburg, Ohio). Feb. 1, 1965. Contract AT-33-1-GEN-53. 17p. Dep. mn; CFSTI $1.00 cy, $0.50 mn.

A general method is derived whereby the total time integral of the current through any branch, or the voltage between any two modes, of an electrical circuit, which has been subjected to a driving force of finite duration or to a unit-step driving force, may be calculated by analyses involving only steady-state direct-current circuit theories. In cases where the equation of the transient is known, the exactness of the equation may be checked by taking the total time integral of the transient terms and comparing with the exact integral obtained by the method presented. In an example, a relationship of parameters is derived that will result in zero deflection of a ballistic galvanometer in a circuit used to measure mutual inductances. Another example demonstrates the application of this method to transient heat-flow problems with distributed parameters. The exact equation is presented and checked by the total time integral, which is then used to fabricate an approximate solution that is in good agreement with the exact solution. The application of the method to heat capacity measurement is described. (auth)

5682 (MURA–716) HIGH SPEED DIGITAL DYNAMIC FIELD MEASURING SYSTEM. Bush, G. E. (Midwestern Universities Research Assn., Stoughton, Wis.). Aug. 31, 1965. Contract W-31-109-38-1707. 19p. Dep. mn; CFSTI $1.00 cy, $0.50 mn.

A facility for measuring high gradient time variant magnetic fields was developed. The system consists of pickup coils, integrators, a multiplexer, one analog-to-digital converter, and an IBM 1401 computer. There are nine precision-wound dipole pickup coils that are placed in the unknown field. The induced coil voltages are fed into nine precision integrating amplifiers whose outputs are proportional to the ΔB that is seen by the nine coils. These outputs plus the signal from a current shunt placed in the magnet excitation line are then sequentially scanned by a ten-channel multiplexer. The multiplexer feeds a high speed analog-to-digital converter which feeds the computer through a parallel to serial converter. This measuring system was designed to be fast enough so that interpolation to any point in time is possible. The coils were designed to be insensitive to the second and third spatial field harmonics and thereby effectively measure fields at a point instead of over the whole coil area. The direct link to the computer is a two-way tie, with data flowing to the computer and control signals flowing to the measuring system. (auth)

5683 (UCRL–14438) EFFECT OF A RADIALLY INHOMOGENEOUS PLASMA ON MICROWAVE INTERFEROMETER MEASUREMENTS. Schneider, Herman (Lawrence Radiation Lab., Univ. of California, Livermore). Sept. 27, 1965. Contract W-7405-eng-48. 18p. Dep. mn; CFSTI $1.00 cy, $0.50 mn.

The phase shift and attenuation in the plasma path of a "single-pass" microwave interferometer was calculated for a variety of radial electron density profiles. The radiators were circular waveguides operating in the TE_{11} mode and had apertures of several wavelengths. Polarization was parallel to the axis of a cylindrical plasma whose radius was much greater than a wavelength. As expected, the phase shift for peak densities well below cut-off was proportional to the member of electrons along the path, while at higher densities the actual shape of the profile became important. It was found that at the higher densities the attenuation was quite sensitive to the shape of the radial gradient; for instance, a Gaussian distribution although containing fewer electrons than a trapezoidal distribution of the same peak density produces a larger attenuation. (auth)

5684 (WAPD-T–1770) COMPUTER CONTROL AND DATA PROCESSING FOR ISOTOPIC MASS SPECTROMETERS. Cook, H. D.; Barker, F. B.; Hudgens, J, E. (Bettis Atomic Power Lab., Pittsburgh, Pa.). Apr. 1965. Contract AT(11-1)-Gen-14. 13p. (CONF-650519–7). Dep. mn; CFSTI $1.00 cy, $0.50 mn.

From 13th Annual Conference of American Society of Testing Materials, St. Louis.

A system is described that provides both flexible instrument control and accurate data evaluation. One of the most valuable characteristics of the system is the immediate display of isotopic abundances obtained at the completion of a scan of the mass spectrum and of the average of all scans at the end of a sample run. It permits the instrument operator to observe trends that might tend to bias results and to determine readily whether sufficient data has been obtained before removing the sample from the mass spectrometer. This advantage has improved reliability of data and reduced the number of reruns necessary because of insufficient data. (auth)

5685 (K-Trans–5) EQUIPMENT FOR INDICATING, RECORDING AND CONTROLLING OSCILLATIONS OF THE AXIS OF ROTATION AND THE SPEED OF THE ROTOR OF A GAS CENTRIFUGE. Paap, W.; Mitscherlich, H.; Gunschmann, K. Translation of German Patent 1,144,195, Mar. 17, 1960. 7p. Dep. mn; JCL $1.10 fs, $0.80 mf.

Equipment is described for indicating, recording, and controlling oscillations of the axis of rotation and the speed of the rotor of a centrifuge rotating on a pin like a top and held in a vertical position by magnets. The device consists of at least one coil which surrounds a section of the stray field of the magnets and which is connected by an amplifier to a signaling, indicating, or recording instrument or to a correction device. (M.O.W.)

5686 (NP-tr–1313) THE STUDY OF CHARGED PARTICLE BEAMS BY MEANS OF PICK-UP ELECTRODES. Gol'din, L. L. (Gosudarstvennyi Komitet po Ispol'zovaniyu Atomnoi Energii SSSR, Moscow. Institut Teoreticheskoi i Eksperimental'noi Fiziki). Translated by J. Rice and Revised by N. Mouravieff (European Organization for Nuclear Research, Geneva (Switzerland)), from report ITEF–363. 1965. 11p. Dep. mn; CFSTI $1.00 cy, $0.50 mn; JCL $1.60 fs, $0.80 mf.

The design of probes consisting of pick-up electrodes for determining the characteristics of charged-particle beams is discussed. Some characteristics (viz. beam charge, beam displacement, and moments) that can be measured by these types of probes are noted. (T.F.H.)

5687 (UCRL-Trans–1237(L)) SYSTEMATIC INVESTIGATIONS INTO ELECTROSTATIC IMMERSION OBJECTIVES. Soa, E. A. Translated for Univ. of California Lawrence Radiation Lab., Livermore, from pp 115-53 of Jenaer Jahrbuch, 1959. 73p. Dep. mn; JCL $7.60 fs, $2.39 mf.

A systematic investigation was made of the image properties of a three-electrode apertured system as an immersion objective. The focal lengths and Wehnelt potentials necessary for focusing are measured. The geometrical parameters (distances, thickness, bore) are successively varied. Besides the systematic investigation of plane electrodes, it was suggested that other electrode shapes with good imaging properties be looked for, which permit ion bombardment or irradiation of the object with photons or electrons, in order to produce an image by the resulting secondary electrons. The measurements necessitated, among other things, the construction of a laminar-shaped oxide cathode with very small filament power. An improvement of the immersion objective was attempted by different electrode shapes in one and the same arrangement, by eliminating cathode surface roughness and by increasing the field strength in front of the cathode by voltage pulses. Since in electron optics lens errors with the usual electrostatic unipotential lenses now pass through a minimum in the vicinity of the refractive power maximum of the image, this was also assumed for the immersion objective and the investigation was made on this assumption. (M.O.W.)

5688 (UCRL-Trans-1273(L)) LOW-INDUCTANCE CAPACITORS. Konotop, V. V.; Linetskii, V. Ya.; Fertik, S. M. Translated for Lawrence Radiation Lab., Univ. of California, Livermore, from Elektrotekhnika, 36: No. 1, 23-6(Jan. 1965). 15p. Dep. mn; CFSTI $1.00 cy, $0.50 mn; JCL $1.60 fs, $0.80 mf.

Possible means of reducing the self-inductance of high-voltage capacitors are considered, and a description is given of eight types of capacitors having a low self-inductance. A "self-inductance quality factor" is proposed to allow comparison of the capacitors. (auth)

5689 ELECTROSTATIC PROBE PERFORMANCE AS INFLUENCED BY ITS MAGNETOGASDYNAMIC BOUNDARY LAYER. Yen, J. T. (Aerospace Corp., San Bernardino, Calif.). AIAA (Amer. Inst. Aeron. Astronaut.) J., 3: 2146-7(Nov. 1965).

An investigation to determine the performance of a particular electrostatic probe by taking into account its MGD boundary layer is presented. It is shown that the resistance against drawing of currents from the sheath and the ambipolar regions is increased by the applied magnetic field, whereas that from the mobility region may be approximately the same as that of the nonmagnetic case. (M.O.W.)

5690 LIGHT PENCIL. Kurashov, A. A.; Paramonov, V. V. At. Energ. (USSR), 19: 400-1(Oct. 1965). (In Russian).

The principle of operation of a storage device, programmed using a light pencil together with a cathode-ray tube, is described. The light pencil is directed onto the desired point of a photosensitive point raster on the cathode-ray tube; each point on the raster corresponds to a memory cell in the storage apparatus. The motion of the beam in the cathode-ray tube occurs synchronously with the operation of the address register of the storage apparatus. The light pencil produces an electric pulse when the electron-beam position corresponds to the raster point indicated by the pencil; the pulse actuates the corresponding cell in the storage apparatus. (M.J.T.)

5691 SOME RESULTS OF EXPERIMENTAL INVESTIGATION OF ELECTROSTATIC CHARGED PARTICLE ENERGY ANALYZER PROPERTIES. Shapovalov, A. S.; Kozlov, I. G. (Saratov State Univ., USSR). Izv. Vyssh. Ucheb. Zaved., Radiofiz., 8: 775-83(1965). (In Russian).

The main characteristics of charged-particle energy analyzer with a dispersive element in the form of a cylindrical capacitor were investigated. The charged particle beam is injected at an acute angle to the axis. (auth)

5692 A SIMPLE METHOD FOR PREPARING X-RAY FILTERS OF STRONTIUM METAL. Becherer, G.; Herms, G.; Motzfeld, V. (Univ., Rostock, Ger.). J. Sci. Instrum., 42: 754(Oct. 1965).

The production of a sandwich-like filter consisting of Sr-foil between two sheets of mica is described. The additional absorption caused by the mica amounts to only a few per cent for the Mo Kα line. The filters are suitable for the Ross balanced filter technique, i.e. optimum thickness and plane parallelism are attainable. (auth)

5693 A COMPREHENSIVE SAFETY SHUTTER AND COLLIMATOR COUPLING FOR THE PHILIPS X-RAY TUBE SHIELD PW 1016. Hallewell, V. A.; Murphy, R. J.; Pauling, P. J.; Robertson, G. B. (University Coll., London). J. Sci. Instrum., 42: 763-5(Oct. 1965).

A set of safety shutters and collimator couplings for the Philips x-ray tube shield PW 1016 have been designed and made for use with (i) the Enraf–Nonius Weissenberg camera, (ii) the Charles Supper precession camera, (iii) the Philips Debye–Scherrer powder camera, (iv) the Nonius Guinier powder camera and (v) unused tube windows. The shutter couplings provide (i) a scatter shield around the filter disk, (ii) a scatter shield around the collimator face, (iii) a gravity and spring-loaded safety shutter over the direct beam, (iv) an electrical interlock to the shutter solenoid by camera movement, (v) a readily visible shutter knob, (vi) a fail-safe green lamp for indication that the electromagnetic shutter is closed and (vii) easy movement of the filter disk. (auth)

5694 FAST AMPLITUDE DISCRIMINATOR. Sojka, Bohumil; Dana, Jiri (Inst. of Nuclear Studies, Czechoslovak Academy of Sciences, Rez). Jaderna Energie, 11: 267-9(July 1965). (In Czech).

A fast-amplitude discriminator is described, which uses high-frequency transistors extended into the region of avalanche action. Several circuits were examined, which make use of the negative resistance arising in the avalanche ionization of transistors. The chief problem lies in the selection of a suitable transistor, since even among those of the same type there are considerable differences in their action in an amplitude discriminator. It is possible to use avalanche-effect transistors to make a simple circuit with the capability of amplitude discrimination, suitable for a fast-amplitude discriminator and a fast-coincidence circuit. (TTT)

5695 THEORETICAL STUDY OF THE EXTRACTION OF A PERIODIC SIGNAL IN A NOISE BY ACCUMULATION OF DATA. Bonnet, Georges (Centre d'Etudes Nucleaires, Grenoble, France). Nucl. Instrum. Methods, 37: 217-30 (Nov. 1965). (In French).

A method applied usually to nuclear magnetic resonance is used to describe a process of extraction of a periodic signal from noise, by means of a multichannel selector working as a data integrator. A possible improvement, consisting in an additional sequential smoothing is studied and the amelioration thus obtained in the signal-to-noise ratio is defined for measurements performed either during a predetermined time or for a duration limited by the memory saturation. After the lay-out of an equivalent analog pattern, an optimal system in which storage and sequential smoothing are combined with pre-filtering is proposed. (auth)

5696 SPHERICAL ABERRATION OF COMPOUND QUADRUPOLE LENSES AND SYSTEMS. Dymnikov, A. D.; Fishova, T. Ya.; Yavor, S. Ya. (Ioffe Inst. of Physics and Tech., Leningrad). Nucl. Instrum. Methods, 37: 268-75 (Nov. 1965).

Equations of third-order trajectories are given for a compound quadrupole lens. These equations are used to deduce expressions for the spherical aberration in the form of integrals. Coefficients of spherical aberration are given in the thin-lens approximation. Analytical expressions are obtained for the coefficients of spherical aberration for a bell-shaped field distribution. In the case of a doublet consisting of two compound lenses with a bell-shaped field distribution it is possible to compensate the spherical aberration of the width of a linear image over all its length. (auth)

5697 CONSIDERATIONS ON THE NOISE OF AN INPUT STAGE OF A PULSE AMPLIFIER. Balland, J. C.; Pigneret, J.; Samueli, J. -J.; Sarazin, A. (Univ., Lyon). Nucl. Instrum. Methods, 37: 276-80(Nov. 1965). (In French).

The noise of an input stage of the bootstrapped cascade type is studied in view of designing a low noise pulse amplifier providing a low input impedance and good qualities of stability and linearity. An amplifying stage with a 20 dB gain is described. The value of the noise is about 10 μv rms with a 10-Mc bandwidth and a 50 Ω input and output impedance. (auth)

5698 A MULTICHANNEL SPECTROMETER FOR THE ANALYSIS OF PULSED ION SOURCES. Ruby, L.; Kramasz, J. G. Jr.; Pon, W. G.; Vuletich, T. (Univ. of California, Berkeley). Nucl. Instrum. Methods, 37: 293-6(Nov. 1965). (UCRL-16167).

A 180° mass spectrometer has been constructed for the analysis of pulsed ion sources, chiefly of the occluded-gas type. A complete ion spectrum can be obtained in five pulses of the source. The ions are collected in 94 equally spaced cups. Each of these cups is supported by a ceramic feedthrough insulator. Outside the vacuum tank each insulator is connected to a capacitor, one side of which is grounded. An electrical pick-up progressively samples the potentials across the 94 capacitors. The pick-up is connected to an electrometer whose output is fed into a recorder. (auth)

5699 A TUNNEL DIODE CASCADE CIRCUIT. Verweij, H. (CERN, Geneva). Nucl. Instrum. Methods, 37: 309-12(Nov. 1965).

A method is described to combine the input sensitivity and stability of a low-peak-current tunnel diode with the high power output of a high-peak-current tunnel diode, by connecting tunnel diodes and back diodes in cascade. (auth)

5700 OPERATIVE DEFINITION OF THE THRESHOLD OF TUNNEL DIODE SWITCHING CIRCUITS. Abbattista, N. (Univ., Bari, Italy); Plantamura, V. L.; Coli, M. Nucl. Instrum. Methods, 37: 323-6(Nov. 1965).

The variation of the threshold of a tunnel-diode circuit with input-pulse rise time is determined. An operative definition of the threshold is suggested that can be used for input-pulse rise times from zero to infinity. (T.F.H.)

5701 AN IMPEDANCE MATCHED DELAY-LINE CLIP. Zlock, K. (Univ. of Virginia, Charlottesville). Nucl. Instrum. Methods, 37: 353(Nov. 1965).

A simple delay-line clipping circuit is described that incorporates means for termination of signals reflected to the source. (T.F.H.)

5702 GERMANIUM COMPENSATION BY Li-DRIFT IN BOILING LIQUIDS FOR p-i-n-DIODE CONSTRUCTION. Cappellani, F.; Fumagalli, W.; Restelli, G. (C.C.R., Euratom, Ispra, Italy). Nucl. Instrum. Methods, 37: 354-6 (Nov. 1965).

The fabrication of lithium-drifted germanium p-i-n diodes having compensated volumes as high as 4 cc is reported. The lithium drifting process is carried out in boiling liquids in order to provide temperature control and heat removal. The liquids studied include pentane, hexane, o-xylene, chloroform, methanol, acetone, and petroleum spirits. (T.F.H.)

5703 AN INSTRUMENTED PROBE FOR FAST CLEARANCE MEASUREMENT. Kaercher, Gerald C. (Detroit Edison Co.). Nucleonics, 23: No. 11, 58-9(Nov. 1965).

A strain-gage-instrumented probe for measuring small and inaccessible clearances was developed. Such probes were used in the Fermi program to determine the extent of fuel pin warpage that accompanies any phase transformation of the uranium alloy and to determine the general dimensional stability of the assembled units. The probes can be made in various lengths and for various ranges of measurement. Incorporated within the head of the probe are three deflection-sensing cantilever elements arranged so that they can be easily pushed into the spacings between rows of pins. The strain induced by the deformation of the middle sensing element of the probe when recorded on a direct-writing oscillograph, indicates the clearance into which the probe was inserted. The construction and results are given. (J.F.P.)

5704 A FAST UNIVERSAL DIODE-TRANSISTOR LOGIC CIRCUIT AND SOME OF ITS USES. Sawicki, Aleksander. Nukleonika, 10: 493-502(1965). (In Polish).

The performance of an universal logic circuit is discussed and the principle of its design is given. This circuit has many advantages of direct-current transistor logic circuits and enables the use of transistors unsuitable for the direct coupling technique. Some uses of this circuit are also given. (auth)

5705 GENERATION AND DETECTION OF SUBNANOSECOND LIGHT PULSES: APPLICATION TO LUMINESCENCE STUDIES. Yguerabide, Juan (Sandia Lab., Albuquerque, N. Mex.). Rev. Sci. Instrum., 36: 1734-42(Dec. 1965).

Some techniques developed to study the kinetics of very fast luminescent systems are described. Included are lamps that generate subnanosecond light pulses and an instrument, using an image-converter tube, that measures the shape of subnanosecond light pulses of low intensity. The factors that determine the time resolution of an image-converter tube are discussed theoretically. (D.C.W.)

5706 BASIC PROPERTIES OF ELECTRON MULTIPLIER ION DETECTION AND PULSE COUNTING METHODS IN MASS SPECTROMETRY. Dietz, Leonard A. (Knolls Atomic Power Lab., Schenectady, N. Y.). Rev. Sci. Instrum., 36: 1763-70(Dec. 1965).

The critical role played by first-stage gain in shaping the output-pulse-height distribution and detection efficiency of an electron multiplier used as an ion detector is studied theoretically and experimentally. In a well-focused electron multiplier, it is found that anode pulse height distributions observed for different ion species agree well with distributions calculated by using compound Poisson statistics. Models are developed to explain measurement bias in an electron multiplier which is used in either the d-c or pulse counting modes, and it is shown how these results can be applied to isotope ratio measurements. Design and operating characteristics are described for a 20-stage electron multiplier which was developed for high-speed pulse counting and high-detection efficiency. The surface of the first dynode is coated with a thin film of Al_2O_3 to provide a stable first stage yield of 7–9 secondary electrons/incident ion for monatomic alkali ions with 20-kv impact energy. The polyatomic ion $Na_2BO_2^+$ yields about 16 secondary electrons/incident ion at 20-kv impact energy. Resolving time of the entire detector system is reduced to 10 nsec by using a specially designed solid state discriminator and pulse shaper. Also, a technique is described for the simultaneous detection and pulse counting of two ion beams. (auth)

5707 ELIMINATION OF UNDESIRABLE UNDERSHOOT IN THE OPERATION AND TESTING OF NUCLEAR PULSE AMPLIFIERS. Nowlin, C. H.; Blankenship, J. L. (Oak Ridge National Lab., Tenn.). Rev. Sci. Instrum., 36: 1830-9(Dec. 1965). (ORNL-P-1585).

The techniques of modern network theory were applied to some of the problems of pulse shaping in nuclear pulse amplifiers. A technique referred to as pole-zero cancellation was evolved which permits a system designer to specify the pulse decay time at the amplitude-limiting section of the system and the pulse shape at the final output as completely independent parameters. The deadtime of the amplifier system can be reduced by orders of magnitude without degrading the signal-to-noise ratio. In addition, the usual charge-injection system was examined; and a simple, linear lumped-element network was evolved which makes possible an improved evaluation of the amplifier response to detector charge pulses. (auth)

5708 REMOTE OPERATING GAS PYCNOMETER. Guon, J.; Bodine, J. E. (Atomics International, Canoga Park, Calif.). Rev. Sci. Instrum., 36: 1885(Dec. 1965).

A gas pycnometer developed for remote volume measurements on highly irradiated uranium dioxide pellets is described. (D.C.W.)

5709 SPLIT BEAM COMPARATOR (Engineering Materials). (Los Alamos Scientific Lab., Univ of California, N. Mex.). (CAPE–1314).

2 drawings.

The split beam comparator is an optical instrument used for measuring thermal and other expansions of large specimens. It is convenient to use, easy to keep in adjustment, and relatively inexpensive. A 1 × 1 × 1 in. beam splitting prism, a 286-mm fl × 30-mm dia achromatic lens, and a B and L filar eyepiece are employed in the apparatus. (For details, see TID-4100). (L.B.S.)

5710 RAMP PULSE GENERATOR (Engineering Materials). (Lawrence Radiation Lab., Univ. of California, Berkeley). (CAPE–1315).

61 drawings.

An instrument is described for setting up and testing complex electronic pulse-handling systems. It provides pulses ranging to ±10 v into a 125-Ω line at regular or random rates to as high as 10^6 pps. The pulse amplitude can be electronically swept through the whole amplitude range in a timewise linear fashion, with periods from 0.5 msec to 20 sec. Rise times of 0.05 to 1 μsec can be obtained. Pulses can be flat-topped or have exponential tails from 5 μsec to 100 μsec. A d-c coupled output is provided for reliable measurements of rate-sensitive effects in pulse amplifiers and analyzers. The instrument is also used as a time-to-amplitude converter for times greater than 5 μsec. The components include: tail-pulse generator, linear output driver, linear pulse driver, sampled ramp generator, reference source rate meter circuit and gate, capacitors, pulse generator, oscillators, and a noise generator. (For details, see TID-4100). (L.B.S.)

5711 GLOVE BOX FOR THE DECONTAMINATION AND DISMANTLING OF RADIOACTIVELY CONTAMINATED CONTAINERS. Simon, Albert (to Commissariat a l'Energie Atomique). German Patent 1,197,560. July 29, 1965. Priority date Nov. 29, 1961, France.

For the cleaning of the inner surface of a radioactively contaminated container a glove box is provided with an attachment flange to which the container is attached from the outside, and with pulley arrangments for the removal of the cover of the container and the washing of the cover and the inner surface of the container. (Gmelin Inst.)

5712 METHOD OF COMPENSATING A RADIATION GAUGE FOR UNWANTED CHANGES IN MEASURED MATERIAL. Barnett, Glenroy W. (to Industrial Nucleonics Corp.). U. S. Patent 3,210,545. Oct. 5, 1965. Filed July 24, 1961.

A method is described for compensating a mass per unit area or thickness measurement gage for changes in composition of the material being measured. Penetrating radiation is passed through the material and is detected to yield a first signal component representing the mass per unit area or thickness of the material and a record component to represent the composition. The backscattered radiation is detected to develop a second signal also having a component representing the mass per unit area or thickness and a component representing the composition of the material. The first and second signals are combined in a predetermined relation to produce a corrected signal representative of the mass per unit area or thickness of the material. (B.L.M.)

Radiation Detection

Refer also to abstracts 5285, 5510, 5585, 5807, 5944, 6006, 6014, 6260, 6268, 6289, 6307, and 6567.

5713 (AD–623384) NUCLEAR TRACK REGISTRATION IN DOSIMETER GLASSES FOR NEUTRON DOSIMETRY IN MIXED RADIATION FIELDS. Becker, K. (Naval Radiological Defense Lab., San Francisco, Calif.). Aug. 5, 1965. 43p. (USNRDL-TR–904).

The properties of combinations of some dosimeter glasses with several fissionable materials for thermal and fast neutron dosimetry in mixed radiation fields, using Fleischer, Price and Walker's etching technique for the visualization of the fission fragment tracks, were investigated. The effect of the glass composition, different etching chemicals (NaOH, EDTA and HF), their concentration and temperature on etching kinetics, and the fading and "over-etching" stability of the tracks were studied. The neutron sensitivity is given for natural U and Th, ^{235}U, ^{233}U, and ^{237}Np with and without additional thermal neutron absorbers for several neutron energies (thermal, TRIGA and HPRR fission, 2.7 Mev, Pu/Be and 14 Mev.) For thick foils of fissionable metals, the sensitivity is 1.3×10^{-5} track/neutron/barn ± 10%. For higher neutron energies (2 – >20 Mev), ^{238}U is of particular interest because of its rem-equivalent response. The detection limits are discussed. Different techniques for the automatic optical (microscopic and macroscopic) evaluation of the fission track density in glasses are described. The effects of the foil radioactivity and the neutron induced fission fragments on the radiophotoluminescence in the glass were studied. Most of the results given are also valid for ordinary glasses. The possible applications of the system in personnel dosimetry and for special applications were investigated. (auth)

5714 (AD–623722) NEUTRON DETECTION AND SPECTROSCOPY WITH SEMICONDUCTOR DETECTORS. Zatzick, M. R.; Zimmerman, E. L. (Solid State Radiations, Inc., Los Angeles, Calif.). Revised Apr. 1965. Contract DA18-108-405-Cml-1012. 114p. (NDL-TR–54). CFSTI $4.00 cy, $0.75 mn.

Results are presented of a study of methods for utilizing diffused-junction semiconductor detectors in neutron detection and spectroscopy. Various neutron-sensitive coated detectors, and the ^6Li epithermal-neutron spectrometer system, which consists of a ^6Li-sandwich detector and a complete, integrated electronic system, are described. (auth)

5715 (AEET–227) NUCLEAR DATA MEASURING FACILITIES IN INDIA. (Atomic Energy Establishment, Trombay (India). Nuclear Physics Div.). May 1965. 44p. Dep. mn.

Nuclear data measuring facilities (including beta spectrometers, crystal spectrometers, mass separators and mass spectrometers, nuclear orientation devices, particle accelerators, and pile oscillators) in India are cataloged. The characteristics of the instrumentation available at these facilities are given. (T.F.H.)

5716 (AEEW-M–470) THE NEUTRON ACTIVATION OF TITANIUM AND ITS INFLUENCE ON IONISATION CHAMBER DESIGN. Goodings, A.; Paull, P. R. (Atomic Energy Establishment, Winfrith (England)). Oct. 1964. 34p. (JNPC/RPWP/NFISG/P35). Dep. mn.

The neutron activation aspect of commercially available titanium was examined experimentally and it is concluded that the metal is, in some ways, superior to aluminum for wide range ionization chamber construction. Similar tests on a titanium/aluminum/tin alloy and on low manganese content stainless steel are also reported. (auth)

5717 (AEEW-M–508) THE RESULTS OF THE RCIO IONISATION CHAMBER DEVELOPMENT. Goodings, A. (Atomic Energy Establishment, Winfrith (England)). Mar. 1965. 10p. Dep. mn.

The design characteristics of a ^{10}B-coated, He-filled ionization chamber capable of operating in reactor environments at temperatures up to 400°C are tabulated. The sensitivities of the chamber to neutrons and gamma radiation are shown. (T.F.H.)

5718 (BNL–9634) USE OF VIDICONS IN ON-LINE MEASURING MACHINES AT BNL. Rosenblum, M. (Brook-

haven National Lab., Upton, N. Y.). [nd]. Contract AT (30-2)-Gen-16. 14p. (CONF-651039-1). Dep. mn; CFSTI $1.00 cy, $0.50 mn.

From Conference on Programming for Flying Spot Devices, Columbia, N. Y.

The use of vidicons in micro-scanning systems for digitized stages is described. The assembled apparatus is used for on-line analysis of particle-track photographs. (T.F.H.)

5719 (CEA-R-2846) SUR QUELQUES UTILISATIONS DE L'ENREGISTREMENT DES FRAGMENTS DE FISSION DANS LES ISOLANTS. (On Some Uses of the Recording of Fission Fragments Occurring in Insulators). Mory, Jean (Commissariat a l'Energie Atomique, Fontenay-aux-Roses (France). Centre d'Etudes Nucleaires). Sept. 1965. 60p. Dep. mn.

After briefly recalling the interaction processes between charged particles and matter, and giving a quantitative study of the relationships connecting the various parameters, some of the following applications are considered; thermal neutron dosimetry, fast neutron dosimetry, dosage of very low fissile impurity concentrations, and study of fissile elements occurring in atmospheric dusts. Results are then briefly given of an automated counting test for traces effected by measuring the electrical resistivity of the irradiated membrane. Finally, the advantages and disadvantages of these solid detectors are discussed, especially with respect to nuclear emulsions whose uses are approximately identical. (M.O.W.)

5720 (CERN-65-33) A SONIC SPARK CHAMBER SYSTEM. Bellettini, G.; Cocconi, G.; Diddens, A. N.; (and others) (European Organization for Nuclear Research, Geneva (Switzerland)). Oct. 25, 1965. 66p. Dep. mn.

A sonic spark-chamber system used for measurements of proton scattering, in the angular region of 2 to 20 mrad and at energies around 20 Bev at the CERN Proton Synchrotron, is described. Up to 12 events per machine cycle can be recorded, the relevant parameters of each event being written on magnetic tape after having been checked by a small computer on-line. All subsequent calculations were done on a large computer off-line. (auth)

5721 (CLOR/IBJ-II-37/D) SILICON SURFACE-BARRIER DETECTORS FOR ALPHA RADIATION DOSIMETRY. Roman, J.; Bukowiecki (Centraline Laboratorium Ochrony Radiologicznej, Warsaw (Poland)); Chwaszczewska, J. (Institute of Nuclear Research, Warsaw (Poland)). 1965. 29p. Dep.

Applications of gold–silicon surface-barrier detectors to routine alpha radiation dosimetry are discussed. The performance of the detectors is discussed. (M.O.W.)

5722 (CONF-640919, pp I2-43) MAGNETIC CLOUD CHAMBER SYSTEM TO STUDY INTERACTIONS UP TO 10^{12} eV. Thompson, R. W. (Chicago Univ., Ill.).

Advantages and limitations of high-energy physics experiments using cosmic rays as sources are discussed, including the very high energies available and the relatively low nucleon and pion fluxes. The facility being constructed at the University of Chicago is described, including the theoretical determination of the optimum target thickness and the selection and design of the magnetic cloud chamber, the photon chamber, and the ionization calorimeter. The choice of the target material is considered. Experiments to be done before installation of the ionization calorimeter are discussed, including intercomparison of secondary interactions in light nuclei, study of the total charge distribution of the secondaries of high energy jets to determine the degree of secondary interactions in the target nucleus, discovery of new long-lived hyperons and mesons, search for high-lying isobaric states with short lifetime, search for the neutral intermediate boson, search for massive fundamental triplets, and investigation of the fireball mechanism for pion production. Experiments proposed subsequent to the installation of the ionization calorimeter are briefly mentioned, including especially the determination of energy variations of cross sections. (M.J.T.)

5723 (CONF-640919, pp I55-65) PROPOSED 600 m^3 DETECTOR FOR MUONS AND NEUTRINOS. Keuffel, Jack.

The two types of detecting elements to be used in the large detection instrument are described. A spark counter was developed, based on operation of a G-M counter at increased pressure and quenching-vapor concentration in a corona-spike model; the corona discharge is detected audibly. A directional Cherenkov counter, using a wave-shifter reflector on one surface of the water, is described. The overall detector configuration is shown. Possible observation of the W intermediate boson, produced in neutrino reactions with nuclei and antineutrino(e) resonant scattering by electrons, is discussed. The use of the apparatus to study muon interactions at high energy is also mentioned. (M.J.T.)

5724 (CONF-640919, pp II13-23) PROPOSED BALLOON BORNE SYSTEM FOR INTERACTIONS ABOVE 10^{11} ev. Alvarez, L.; Humphrey, W. (California Univ., Berkeley).

The beam-defining and interaction-detector sections of the payload for the balloon experiment are described, including the Cherenkov trigger, the spark chambers and nuclear emulsions, the wide-gap spark chambers, the superconducting magnets and the liquid hydrogen target. The apparatus is intended for the study of particle interactions at 100 to 1000 Bev. A detailed formal proposal for the experiment is included, as well as the paper presented at the conference. (M.J.T.)

5725 (CONF-640919, pp II27-30) PROPOSED SYSTEM TO STUDY INTERACTIONS AT 300 Gev. Jones, L.

The design of a mountain-top system consisting of a liquid hydrogen target and large-gap spark chambers for studying strong interactions at about 300 Bev is discussed. The economics of the proposed experiment are considered. Detailed paramenters are given for the incoming beam magnet, the reaction products magnet, acceptance and rates, resolution of incoming and outgoing particles, and photography. (M.J.T.)

5726 (CONF-650217, pp 102-7) SOME ASPECTS OF NEUTRON DIFFRACTION AND ELASTIC SCATTERING USING PULSED AND STEADY NEUTRON SOURCES. Shull, C. G. (Massachusetts Inst. of Tech., Cambridge).

The relative merits of steady-state-operation and pulsed-operation sources for neutron spectrometers are compared, as regards data collection rates, resolution, background intensity, and usefulness in specialized applications. (T.F.H.)

5727 (CONF-651101-46) NUMERICAL METHODS FOR SOLUTION OF COMPLEX GAMMA SPECTRA. Schunicht, B. F. (Knolls Atomic Power Lab., Schenectady, N. Y.). Oct. 26, 1965. Contract W-31-109-eng-52. 34p. Dep. mn; CFSTI $2.00 cy, $0.50 mn.

From 13th Conference on Remote Systems Technology, Washington, D. C.

A least-squares regression method designed for analysis of complex gamma spectra of mixtures of radioisotopes is described. The method incorporates a method for correcting detection-instrument errors and nonlinearities, criteria for eliminating from the analysis those radionuclides known to be absent from the unknown, and constraints involving combinatory characteristics of gamma spectra of given nuclides. The method is incorporated in a computer program written in FORTRAN IV. (T.F.H.)

5728 (IBM-65-825-1487) NEUTRON AND GAMMA SENSITIVITIES OF DYNAMIC DETECTORS. Kloepper, R. M.; Martin, J. A.; Shatzkes, M. (International Business Machines Corp., Owego, N. Y. FSD Space Guidance Center). July 1965. 13p.

The neutron and gamma sensitivities of nine detectors were studied in experiments performed at the Sandia

Pulsed Reactor (SPR). Of the detectors tested, six are predominantly gamma detectors and three produce a significant fraction of their total current as a result of the neutron flux during a normal SPR burst. None of the detectors studied were found to be predominantly sensitive to the neutron flux during a normal SPR burst. Tests performed at pure gamma sources on a PIN diode detector are also described. The neutron-induced current in the silicon detectors is treated theoretically. (auth)

5729 (INR–617/XIX/D) PRZY POMIARACH AKTYWNOSCI PREPARATOW β-PROMIENIOTWORCZYCH METODA STALEJ GEOMETRII. (Reduction Possibilities of Some Errors in the β-Activity Measurements by the Solid Angle Method). Zharnovetski, K. I. (Institute of Nuclear Research, Warsaw (Poland)). 1965. 22p Dep.

The influence of some factors on the diminution of accuracy in β–activity measurements by the solid angle method is examined. Special attention is paid to the accurate assessment of the solid angle value and to the effects of scattering and absorption of particles in the shield and in air. Practical advice is given on methods for gaining an accuracy that is only little less than that offered by other special methods that are time consuming and require complex equipment. (auth)

5730 (JINR-E–2366) ANALOGUE WIRE SPARK CHAMBER SYSTEM FOR MEASUREMENTS OF PARTICLE MOMENTA AND ANGLES. Golutvin, L. A.; Zanevsky, Yu. V.; Kulakov, B. A.; Tsyganov, E. N. (Joint Inst. of Nuclear Research, Dubna (USSR). Lab. of High Energy). 1965. 18p. Dep. mn.

A four-spark-chamber array, for rapid measurements of particle momenta, is constructed and tested. The system has ferrite cores and provides an analog recording of information. The time during which information can be obtained is less than 1 μsec. The output signal is the value of the angle of the particle deflection in the magnetic field. The accuracy of measurement of the particle deflection angle at a distance of 1 m between a pair of the chambers is ±2 mrad. Systems of similar types can be applied to solving various physical problems, e.g., elastic scattering, search for new resonances, etc. They can also be used for triggering more complicated spark chamber arrays. (auth)

5731 (JINR-P–2394) O POGRESHNOSTYAKH AMPLITUDNO-VREMENNYKH PREOBRAZOVATELEI. (On Inaccuracies of Amplitude-to-Time Converters). Prikhod'ko, V. I.; Tishin, V. G. (Joint Inst. for Nuclear Research, Dubna (USSR). Lab. of Neutron Physics). 1965. 12p. Dep. mn.

The influence of the following factors is estimated: nonlinear capacitance of the charging diode and current-stabilization transistor resistances shunting the storage capacitance, and reverse resistance of the charging diode. Theoretical and experimental curves of the differential non-linearity for the amplitude-to-time converter are constructed with account of the factors considered. (M.O.W.)

5732 (KFK–335) IMPULSFORMDISKRIMINIERUNG BEI HALBLEITERZAEHLERN ZUR UNTERSUCHUNG VON (γ,α)-REAKTIONEN. (Pulse Shape Discrimination in Half-Life Determination for a Study of (γ,α) Reactions). Gehm, Helmut; Ullrich, Horst (Kernforschungszentrum, Karlsruhe (West Germany). Institut fuer Experimentelle Kernphysik). June 1965. 30p. Dep. mn.

A method for pulse-form discrimination for semiconductor counters is developed and tested. The method makes possible the discrimination of α particles and protons, and thereby the measurement of photoalpha particles in the presence of an interfering proton and electron background. The efficiency of the method is discussed and illustrated on the reaction $^{27}Al(\gamma,\alpha)^{23}Na$. For this reaction the yield ratio $Y(\gamma,\alpha)/(\gamma,p)$ can be measured. The experimental α spectrum is compared with the α spectrum calculated by the statistical theory. (tr-auth)

5733 (LA-DC–6790) AREA RADIATION MONITOR SYSTEM WITH LOGARITHMIC INDICATION AND AUDIO-VISUAL WARNING. Engelke, M. J.; Henkel, R. L.; Hiebert, R. D.; Jennings, H. K.; Lang, H. J. (Los Alamos Scientific Lab., Univ. of California, N. Mex.). [nd]. Contract W-7405-eng-46. 13p. (CONF-650306–63). Dep. mn; CFSTI $1.00 cy, $0.50 mn.

From Particle Accelerator Conference, Washington, D. C.

An improved neutron and gamma detection system for use with the Los Alamos large Van de Graaff accelerator was developed. The indicating system was expanded to give rapid visual information at the control room and other locations as well as audio alarms in the experimental area. By transistorizing all the electronic circuits and using only low voltages, both reliability and safety is improved. A gamma system, utilizing ionization chambers and an electrometer tube, is an integral part of the radiation system. It energizes the same alarm system as the neutron detectors. (M.O.W.)

5734 (LFEN–NI–19) CONSTRUCAO E UTILIZACAO DE CAMARAS DE CISAO DE PEQUENAS DIMENSOES. (Construction and Utilization of Small-Dimension Fission Chambers). Brunson, Glenn S.; Afonso, Luis Amaral; Salgado, Jose Francisco (Laboratorio de Fisica e Engenharia Nucleares, Junta de Energia Nuclear, Sacavem (Portugal)). 1964. 12p. (CONF-640711–4). Dep. mn.

From 27th Portugo-Spanish Conference on Progress in Sciences, Bilbao, Spain.

The construction of a small fission counter using Al was described. The characteristics of the counter using filling gases of nitrogen, carbon dioxide, or commercial propane were determined. (J.S.R.)

5735 (LYCEN–6523) CHAMBRES A ETINCELLES CIRCULAIRES A LOCALISATION ELECTRIQUE EN BASSES ENERGIES [THESES]. (Circular Spark Chambers with Electric Localization at Low Energies [Thesis]). Gouanere, Michel (Lyon Univ. (France). Institut de Physique Nucleaire). July 15, 1965. 57p. Dep. mn.

Circular spark chambers with electric localization of the spark were investigated. The spark chamber used is described with a survey of its development, principal characteristics, construction, and methods used for the automatic localization of the spark. The studies made on the detection efficiency and the chamber calibration show that the spark formed on the particle trajectory is localized by an electrical procedure and the scattering angle is obtained with a precision of 3°. The particle energy is measured by the number of plates traversed with a precision that can attain 1%. The apparatus can register approximately 1 event per second. The visualization of the trajectories makes possible a constant verification of the operation of the apparatus. Measurements of the efficiency show that the selection of the event by the associated electronics gives information without background. The electric localization leads to a signal proportional to the scattering angle which facilitates the use of the multichannel recorder. There exist several possibilities of transformation such as the utilization of plates of greater thickness, the increase of the number of plates, and the use of two locations for the same semisector. Spark chambers used as polarimeters lead to a time economy for accelerator utilization and makes it possible to use low-intensity beams. With these chambers nuclear reactions with a low cross section can also be studied. (J.S.R.)

5736 (NP–15597) BOL'SHIE STSINTILLYATSIONNYE SCHETCHIKI I SCHETCHIKI DLYA RABOTY V MAGNITNYKH POLYAKH. (Large Scintillation Counters and Counters for Operation in Magnetic Fields). Bayatyan, G. L.; Galaktionov, Yu. V.; Zel'dovich, O. Ya.; Landsberg, L. G. (Gosudarstvennyi Komitet po Ispol'zovaniyu Atomnoi Energii SSSR, Moscow. Institut Teoreticheskoi i Eksperimental'noi Fiziki). 1965. 16p. Dep. mn.

The results of investigations of large scintillation counters, 700 × 350 × 150 mm, using a single photomultiplier as well as of counters with long lightpipes and with magnetic field compensation, for work in strong magnetic fields, are given. (auth)

5737 (ORNL–3858(Vol.1), pp 59–64) RADIATION DETECTOR STUDIES. [PART] I. (Oak Ridge National Lab., Tenn.).

Summaries of 8 papers on radiation detector development and research are presented. (M.O.W.)

5738 (ORNL–3858(Vol.2), pp 91–3) RADIATION DETECTOR STUDIES. [PART] II. (Oak Ridge National Lab., Tenn.).

Summaries of 6 papers dealing primarily with the performance of various radiation detectors are presented. (M.O.W.)

5739 (SLAC-PUB–140) STREAMER CHAMBER DEVELOPMENT. Bulos, F.; Boyarski, A.; Diebold, R.; Odian, A.; Richter, B.; Villa, F. (Stanford Linear Accelerator Center, Stanford Univ., Calif.). Sept. 1965. Contract AT(04-3)-400. 36p. (CONF-650923–25). Dep. mn; CFSTI $2.00 cy, $0.50 mn.

From 5th International Conference on High Energy Accelerators, Frascati, Italy.

Some properties of the streamer chamber are presented. Special attention is given to the practical use of large-volume chambers as particle detectors. In particular, the following problems are discussed: pulsing large-volume chambers; reducing the rather long memory of the chamber by suitable quenching; amplification of the light output by the use of image intensifiers with large photocathode area. All measurements are made on straight tracks from particles of various energy. Scatter and curvature fitting as well as ionization measurement (using gap length technique) are presented. (auth)

5740 (TID–22407) NEW METHOD FOR OXIDE PASSIVATION OF SEMICONDUCTOR DETECTORS. Final Report. (Solid State Radiations, Inc., Los Angeles, Calif.). July 30, 1965. Contract AT(04-3)-574. 17p. Dep. mn; CFSTI $1.00 cy, $0.50 mn.

The production of silica surface layers on Si semiconductor detectors by immersion in oxygen plasma is reported. The properties of the protective surface layers thus formed under controlled conditions are studied. The results obtained using this method are compared with those obtained using film-deposition and thermal-oxidation processes. (T.F.H.)

5741 (UCRL–14263) AMBIENT STORAGE EFFECTS AND MOUNTING PROBLEMS OF VERY LARGE VOLUME Ge LID DETECTORS. Armantrout, Guy (Lawrence Radiation Lab., Univ. of California, Livermore). Oct. 8, 1965. Contract W-7405-eng-48. 34p. (CONF-651001–11). Dep. mn; CFSTI $2.00 cy, $0.50 mn.

From IEEE Nuclear Science Symposium, San Francisco.

A study was undertaken of the surface-setting procedure before mounting and the effect of diode storage for varying periods of time at the ambient temperature was investigated. The diode surface potential, diode capacitance, and diode V-I characteristics were taken as a function of different surface treatments before mounting. The results were correlated using an inversion layer model for the diode. Leakage currents less than 0.5 nA at 3 kv were obtained. The compensated region of Ge LID diodes is slightly supersaturated with lithium at room temperature. These diodes tend to revert back to the original P-type material because of lithium precipitation. The rate of precipitation was found for several diodes and was found to be a function of the effective lithium mobility. (auth)

5742 (UCRL–14351) HAZARDS CONTROL QUARTERLY REPORT NO. 21, APRIL–JUNE 1965. (Lawrence Radiation Lab., Univ. of California, Livermore). Contract W-7405-eng-48. 39p. Dep. mn; CFSTI $2.00 cy, $0.50 mn.

Papers are included on a portable continuous air monitor for field or laboratory use, transistorized solid-state plutonium-alpha air monitor, sensitivity of Eastman NTA personnel-monitoring film to 14-Mev neutrons, stimulated-emission radiation dosimetry, improved cleaning technique for silver metaphosphate glass dosimeters, preparation of high-density grass samples for radioactivity measurements, ventilation improvements for standard LRL fume hoods, fire-hose friction losses and nozzle flows in LRL stock equipment, and condensation of high expansion foam using a cyclone separator. (M.O.W.)

5743 (UCRL–14405) RESPONSE FUNCTION AND SENSITIVITY OF DOUBLE-DIFFUSED SILICON DETECTORS IN HIGH γ-DOSE RATE FIELDS. Kuckuck, R. W.; Bernescut, R.; Zatzick, M. R.; Jupiter, C. (Lawrence Radiation Lab., Univ. of California, Livermore). Oct. 12, 1965. Contract W-7405-eng–48. 29p. (CONF-651001–12). Dep. mn; CFSTI $2.00 cy, $0.50 mn.

From IEEE Nuclear Science Symposium, San Francisco.

A number of double-diffused (PIN) silicon detectors were exposed to peak γ-dose rates of 10^{19} γ-Mev/cm^2-sec generated by a flash x-ray machine. Detailed examination of the rate-of-rise and linearity was accomplished by superposition of 200-Mc Rossi signal on the oscilloscope traces of the test detector, as well as that of the non-saturable monitor detector. At detector bias voltages of 3000 v, and load impedances of 25 ohms, peak linear currents of approximately 48 amp were observed with rise times less than 10 nanoseconds. Sensitivity measurements of the detectors were obtained at lower dose rates of about 10^{16} γ-Mev/cm^2-sec by exposure to a thick target bremsstrahlung source, using a 10-Mev linac beam. The current-time integral of a detector signal provided a measure of the charge per pulse and a thimble ionization chamber was used to measure the average dose per pulse. (auth)

5744 (UCRL–16227) AN AMPLITUDE-INDEPENDENT NANOSECOND TIMING DISCRIMINATOR FOR FAST PHOTOMULTIPLIERS. Wieber, Donald L.; Lefevre, Harlan W. (Lawrence Radiation Lab., Univ. of California, Berkeley). Oct. 12, 1965. Contract W-7405-eng-48. 16p. (CONF-651001–14). Dep. mn; CFSTI $1.00 cy, $0.50 mn.

From IEEE Nuclear Science Symposium, San Francisco.

A circuit was developed which reduces amplitude-dependent timing errors to less than 0.2 nsec over a dynamic amplitude range of more than 100 to 1. The anode signal is clipped, and a pedestal added, allowing adjustment of the discriminator to the true "zero-crossing" point. Tunnel diodes are used as threshold devices and pulse shapers. A version of this circuit adapted to RCA-2067 photomultipliers is described which features a pulse-recognition threshold variable from <1 to 10 mA and a pulse-pair resolution of <15 nsec. In tests performed with a mercury-light pulser and in coincidence experiments with plastic scintillation counters, the time delay through this discriminator was found to be essentially independent of the signal amplitude over the linear range of the photomultipliers. (auth)

5745 (UR–668, pp 117–23) RADIATION INSTRUMENTS. (Rochester Univ., N. Y. Atomic Energy Project).

Information is presented on measurement of x and gamma radiation absorption by means of glass rod dosimetry and on methods for mapping spatial distribution of radionuclides in vivo. (J.R.D.)

5746 (ZFK-RN–18) UNTERSUCHUNGEN AN EINEM FLUESSIGEN SZINTILLATOR FUER LANGSAME NEUTRONEN. (Studies on a Liquid Scintillator for Slow Neutrons). Andreeff, Alexander; Manfrass, Peter (Zentralinstitut fuer Kernphysik, Rossendorf bei Dresden (East Germany)). Apr. 1963. 11p. Dep. mn.

The properties of a liquid neutron scintillator and some measurements necessary for the construction of such a detector were described. The results obtained agree in essence with the values reported in the literature. (tr-auth)

5747 (NP-tr–1302) POSITION FINDING COUNTER FOR THE BUECHNER MAGNET. Melzer, W.; Puehlhofer, F. (Max-Planck-Institut fuer Kernphysik, Heidelberg (West Germany)). Translated by L. J. Herbst (U.K.A.E.A. Atomic Energy Research Establishment, Harwell, Eng.), from report 1965/V/2. 21p. Dep. mn; JCL $2.60 fs, $0.83 mf.

Silicon surface barrier detectors for determining

simultaneously the energy of the incident particle and the position of impact are described. The counters are used for arranging the focal plane of the Buechner magnetic spectrograph. The principle of the counter and a calculation of position resolving power are given. Experiments are described which illustrate the testing and application of position finding counters. The arrangement of the Buechner spectrograph is discussed. (auth)

5748 (UCRL-Trans-1266(L)) DEVELOPMENT AND INVESTIGATION OF A PHOTON COUNTER AND MEASUREMENT OF THE OPTICAL EXCITATION FUNCTIONS OF HELIUM [Thesis]. Smit, Christiaan (Utrecht Rijksuniversiteit (Netherlands)). Translated by R. A. Waldron (Univ. of California Lawrence Radiation Lab., Livermore), from Ontwikkeling en Onderzock van een Fotonentelmethode on Meting van Optische Aanalagfuncties van Helium. 189p. Dep. mn; JCL $13.00 fs, $5.87 mf.

Various aspects of an investigation to determine the optical excitation functions of a number of helium lines are presented. Separate sections are discussed in terms of a literary survey of the problem, discussion of the experimental apparatus, properties of the photon counter (determined by the upper limit of the range where this can be used with advantage), fluctuation phenomena which determine the lower limit of detection for the photon counter, properties of the excitation tube, measurement of the excitation functions of helium, discussion of the excitation functions, and an investigation of the feasibility of using an excitation tube and a photon counter for the analysis of gases. (M.O.W.)

5749 CONTINUOUS CENTRALIZED CONTROL OF INDIVIDUAL RADIATION DOSES. Zhernov, V. S.; Ryzhov, N. V.; Skatkin, V. M.; Starovoitov, V. S. At. Energ. (USSR), 19: 157-60(Aug. 1965). (In Russian).

Construction of a continuous centralized control system for recording individual personnel radiation doses is discussed considering modern nuclear radioelectronics, radiotechniques, and computing methods. Correlations were made of various control systems using dosimeters equipped with transmitters, and stationary detectors for ionizing radiation. Problems of recording individual radiation doses, at various time intervals, for individual dosimeters and continuous control are analyzed. (tr-auth)

5750 METHOD FOR COMPUTING EFFICIENCY COEFFICIENT OF RADIATION APPARATUS WITH PLANE GAMMA SOURCES. Makhlis, F. A.; Breger, A. H. At. Energ. (USSR), 19: 193-6(Aug. 1965). (In Russian).

A method is described for computing the efficiency of the radiation detector (i.e., the ratio of the energy absorbed by γ-irradiated object to the energy generated at the same time by the source) at various plane dimensions of the source and object. The method utilized the γ method, used for computing problems in radiation protection physics and radio-chemical devices, and the Monte-Carlo method for estimating the energy distribution from ^{60}Co point source in water. In addition a ferrosulfate dosimeter was used for measuring the absorbed doses inside rectangular vessels filled with water and aluminum and iron blocks. A monoenergetic point source of γ quanta coinciding with one of the vertices of a rectangular object and a linear source erected so that two points coincide with two vertices of the irradiated rectangular object are analyzed. (R.V.J.)

5751 ABOUT ABSORPTION OF GAMMA RAY ENERGY BY POINT SOURCES IN MACROSYSTEMS. Terent'ev, B. M.; El'tekov, V. A.; Breger, A. Kh. At. Energ. (USSR), 19: 196-9(Aug. 1965). (In Russian).

The efficiency of radiochemical devices was analyzed considering η the ratio of gamma radiation absorbed in the reactive volume of the device to the γ energy emitted by radiation source. The η value for two radiochemical devices was computed by the volume integration method and by the Monte Carlo method. Calculations for the first model consisted of a sphere R filled with a water-equivalent substance and ^{60}Co and ^{137}Cs point sources. Data derived by Monte Carlo method coincided with 1 to 2%, indicating negligible reverse scattering from the medium. The macrosystem of cylindrical configuration with a point γ source was taken as the second model. The results of the Monte Carlo calculations of the γ-radiation efficiency of a water-equivalent finite dimension cylinder (5 to 60 cm in radius and 5 to 200 cm in height) was plotted for various source distributions. The results of the calculations for finite cylinders made by the method of integration and Monte Carlo method were in good agreement at the quantum energy $E_0 = 1.25$ Mev. Tabulated data are given also for the efficiency of macrosystems (cylinder-point source) calculated by various methods at 0.65 Mev energy. The results showed that the derived integration and asymptotic formulas can be used for practical computations. (R.V.J.)

5752 APPLICATION OF POLYETHYLENE PIPES IN DOSIMETRIC LINES FOR AIR CONTROL. Konovalov, E. A.; Ploshchanskii, L. M.; Solov'ev, V. A. At. Energ. (USSR), 19: 201-3(Aug. 1965). (In Russian).

Experimental tests made with (20 mm in diameter and 4 mm thick) polyethylene tubes prepared by extrusion showed no signs of deformation at temperatures up to 60°C, and up to 3 kg/cm^2 pressure. Operations of VVR-M reactor dosimetric control lines, equipped with 3000 m of polyethylene tubes since the year of 1961, proved the efficiency of the tube material. (R.V.J.)

5753 USE OF GAMMA-GAMMA COINCIDENCE SPECTROMETER WITH SUMMATION OF PULSE AMPLITUDES FOR ANALYSIS OF A MIXTURE OF RADIOACTIVE ISOTOPES. Blinov, V. A.; Dmitriev, V. N.; Kuznetsov, M. I. At. Energ. (USSR), 19: 342-6(Oct. 1965). (In Russian).

The method of γ-γ coincidences with summation is used for the selective detection of radioactive isotopes emitting cascade γ quanta. This method allows the quantitative content of those isotopes whose γ emission is 3 to 4% of the γ emission of the mixture and the quantitative content of radioisotopes whose decay is accompanied by the emission of a positron with the subsequent emission of a γ quantum to be determined. (tr-auth)

5754 METHODS FOR THE ACTIVITY MEASUREMENTS OF SOFT β-RAYS. Kiefer, H. (Gesellschaft fuer Kernforschung mbH, Karlsruhe, Ger.). Chem.-Ing.-Tech., 37: 1020-8(Oct. 1965). (In German).

Soft betas are measured by instruments in which autoabsorption by the substance being investigated and extraneous absorption in the detector are as low as possible. Solid specimens require internal counters that can be operated in the Geiger-Mueller-zone or in the proportional range, and in which the substances can flow directly into the counting chamber. Liquid scintillators are employed for liquid specimens; here, the specimen and the scintillator are in solution together. Gaseous substances can be investigated in gas-filled tube counters, ionization, and scintillation chambers. (auth)

5755 COMPARISON OF THE REGISTRATION OF TRACKS OF HEAVY IONS IN IONOGRAPHIC EMULSIONS AND IN VARIOUS SOLID MATERIALS. Pfohl, Raymond; Monnin, Micheal; Debeauvais, Monique (Centre de Recherches Nucleaires, Strasbourg; Univ. Paris, Clermont, France). Compt. Rend., 261: 2216-18(Sept. 13, 1965). (In French).

The registration of tracks of heavy ions in ionographic emulsions and various solid materials was compared from the viewpoint of their length and the intrinsic sensitivity of the detecting material. A mechanism for the formation of tracks in these two types of detectors based on the emission of δ rays was proposed. (tr-auth)

5756 SOME PRELIMINARY RESULTS OF THE DETECTION OF PRODUCTS OF FISSION AND OF FRAGMENTATION OF DIFFERENT AVERAGE AND HEAVY METALS UNDER THE EFFECT OF 3-Gev PROTONS BY DETECTION IN NEW SOLID DETECTORS. Debeauvais, Monique; Cueer, Pierre (CRN, Strasbourg). Compt. Rend., 261: 2633-6(Oct. 4, 1965). (In French).

The forward-backward ratio of heavy ion tracks produced by the action of protons on targets of natural U, Pb, Au, Ag and Cr were compared for the ion tracks recorded in micas and Makrofol. This ratio was higher than 1 in all cases except in Makrofol in the case of elements with low Z where it is <1. (tr-auth)

5757 DETECTION OF SECONDARY-ELECTRON CURRENTS BY SCINTILLATION COUNTER IN THE STUDY OF SECONDARY ION-ELECTRON EMISSIONS (BY THE PULSE-COUNTING METHOD). Arifov, U. A.; Kogan, V. I.; Khalikov, A. Kh. (Inst. of Physics and Tech., Academy of Sciences, USSR). Izv. Akad. Nauk Uz. SSR, Ser. Fiz.-Mat. Nauk, No. 2, 16-22(1965). (In Russian).

The applicability of a method of electron detection by scintillation counters in studies of secondary ion-electron emission is discussed. The device used is described, and its performance under various conditions is analyzed. It is found that for low values of photometer supply voltage and low amplifier gain, the recording efficiency is low. However, the ratio of the number of pulses per second produced by the incidence of secondary electrons on the scintillator to the number of pulses produced in the absence of an ion beam is large. When the supply voltage and the gain are increased, the recording efficiency increases. Recording efficiency also increases with increasing energy of the electrons incident on the scintillator. Weak currents can be detected by means of pulse amplitude discrimination. Currents as low as 7×10^{-17} amp can be measured. However, the method has several drawbacks, such as the need for a super high vacuum and the fact that when the period of incidence on the scintillator is less than 10^{-6} sec, two electrons are counted as one. (ATD)

5758 CONTRIBUTION TO THE THEORY OF SEMICONDUCTOR COUNTERS FOR IONIZING PARTICLES. Lenchenko, V. M.; Iminov, I. (Inst. of Nuclear Physics, Academy of Sciences, USSR). Izv. Akad. Nauk Uz. SSR, Ser. Fiz.-Mat. Nauk, No. 2, 54-9(1965). (In Russian).

A surface-barrier n-p counter with a broad space-charge region which encloses the entire track of the ionizing particle is considered. To obtain information on the effect of the semiconductor properties (carrier lifetime, mobility, etc.) on its counting ability, the track length, and the ionizing ability of the particle, it is necessary to calculate the waveform of the current and voltage pulses produced by the ionizing particle in the counter. Calculations were made neglecting the deviation of the semiconductor space-charge field from homogeneity, neglecting the dependence of the carrier lifetime on their density, and assuming the width of the space-charge region to be much larger than the track length. Typical current and voltage pulses obtained for such a counter are shown and are in good agreement with experimental data. Calculation of the amplitude of the voltage pulse and its growth time as functions of the parameters and of the particle are also in satisfactory agreement with experiment. (ATD)

5759 AN INVESTIGATION OF THE SUITABILITY OF THE PROPORTIONAL COUNTER AS CHARGED PARTICLE SPECTROMETER AND THE STUDY OF THE REACTION $^{10}B(d,p)^{11}B$. Chohan, A. S.; Hussain, S. A. (Government Coll., Lahore). J. Nat. Sci. Math., 5: 7-14 (Apr. 1965).

The suitability of the proportional counter as a broad range charged particle spectrometer for the study of nuclear reactions was investigated and is reported. An energy resolution of 1.6 per cent with 8 Mev protons was achieved. The energy range available was 6 Mev at one atmosphere filling. The ground and the first excited states of ^{11}B from the reaction $^{10}B(d,p)^{11}B$ was studied. Absolute differential cross sections at 5.1 and 6.07 Mev deuteron energies were obtained. (auth)

5760 SCINTILLATION SPECTRA FROM POINT SOURCES IN A SCATTERING MEDIUM. Mohindra, V. K.; McNeill, K. G. (Univ. of Toronto). J. Nucl. Med., 6: 747-53(Oct. 1965).

Results pertinent to the estimation of the depths of point sources of γ radiation in a human body using only a single NaI crystal are reported. In order to obtain differential energy spectra of a source immersed in water, NaI(Tl) crystals and a hundred channel pulse height analyzer were used. Three separate crystals were employed to test the consistency of the results obtained. The results indicated that a first approximation to the source depth can be obtained by the method; but the spread in results suggests that individual variations, such as relative sizes of lung cavities, make determinations with an accuracy better than 10 to 15% unlikely in any individual case. (H.G.D.)

5761 THE USE OF A PLASTIC SCINTILLATOR AS AN AIRBORNE GAMMA RADIATION DETECTOR. Duggelby, J. C. (Australian Atomic Energy Commission Research Establishment, Sutherland, New South Wales). J. Sci. Instrum., 42: 772-3(Oct. 1965).

An instrument is described which uses a large plastic scintillator instead of the more expensive NaI(Tl) crystal scintillator for airborne monitoring of ground radioactivity. (auth)

5762 RADIATION PROTECTION MEASURING DEVICES OF THE VEB VAKUTRONIK WIB DRESDEN. Kernenergie, 8: 439-43(July 1965). (In German).

The characteristics of the radiation detection instruments available commercially are described. The counting devices, scintillation counters, and ionization chambers available are considered. (J.S.R.)

5763 SEMICONDUCTOR-TYPE NUCLEAR RADIATION DETECTORS AND SPECTROMETERS. PART I. Deme, Sandor; Csakany, Antal (Central Inst. for Physics Research, Budapest). Magyar Fiz. Foly., 13: 273-307 (1965). (In Hungarian).

Semiconductor detectors have excellent energy resolution, linearity, and small size. The thickness of the barrier layer can be easily adjusted, allowing discrimination between radiations of different penetrating power. The sensitive surface is smaller than that of scintillation counters; this defect can be overcome by using several detectors in parallel. The principle of operation involves production of electron-vacancy pairs by charged particles. Fabrication methods are described, reviewing detectors with surface-barrier layers, diffusion-barrier layers, and Li-ion drifting. The magnitude, shape, and duration of the signal are examined in detail. Factors affecting the operation of the instruments, such as radiation damage, environment, and high vacuum, are studied; high magnetic fields have only a slight effect. Applications are discussed. 66 references. (TCO)

5764 ANALYSIS OF GAMMA-RAY CIRCULAR POLARIZATION WITH TRANSMISSION MAGNETS. Chesler, R. B. (California Inst. of Tech., Pasadena). Nucl. Instrum. Methods, 37: 185-93(Nov. 1965).

The results of Monte Carlo type calculations of multiple scattering in iron transmission magnets used to measure γ-ray circular polarization are presented. These calculations show that the effects of multiple scattering (differential cross section) are of the same order as those of pure transmission (integral cross section), and thus can appreciably alter the interpretation of polarization measurement data. Several experiments were performed using polarizer and analyzer magnets, and their results are compared with the calculations. (auth)

5765 ENERGY DEPENDENCE OF A QUANTAMETER. I. THEORY. Tomimasu, T.; Sugiyama, H.; Ibaraki, Y. (Electrotechnical Lab., Tokyo). Nucl. Instrum. Methods, 37: 194-200(Nov. 1965).

The energy dependence of a free air quantameter has been studied theoretically. The energy and spatial dependence of the mean mass stopping power ratio for bremsstrahlung is calculated by the use of the Spencer and Attix method to take account of the cavity size effect, and an approximation method to simplify complex calculations for secondary Compton scattered photons and annihilation photons. A correction factor is introduced to

take account of an underestimation in the automatic integration of the shower curve for low-energy x rays. The calculated calibration of a free air quantameter with 5 mm thick copper plates decreases gradually by 3% with the increase of x-ray energy from 6 to 20 Mev and has a constant value from 20 to 30 Mev. In the higher energy region, it decreases again very slowly by about 2% with the increase of x-ray energy. (auth)

5766 ENERGY DEPENDENCE OF A QUANTAMETER. II. EXPERIMENT. Tomimasu, T.; Sugiyama, H.; Sugiyama, S. (Electrotechnical Lab., Tokyo). Nucl. Instrum. Methods, 37: 201-3(Nov. 1965).

The energy dependence of a free air quantameter is shown by comparison with a replica chamber of the NBS P2 chamber. It is also shown that the NBS P2 should have a more smoothly varying calibration than that given by NBS at energies below 18 Mev. (auth)

5767 STABILIZATION OF LITHIUM-DRIFTED SILICON SURFACE-BARRIER DETECTORS. Tuzzolino, A. J.; Perkins, M. A.; Kristoff, J. (Univ. of Chicago). Nucl. Instrum. Methods, 37: 204-16(Nov. 1965).

A simple fabrication technique is found that yields lithium-drifted silicon surface-barrier detectors that have a low leakage current, and that exhibit stable electrical and α-particle characteristics under conditions of prolonged aging and repeated exposure to thermal-vacuum environments. The detectors operate at a temperature of 65°C and high vacuum for several days with no evidence of noise instability. The operating characteristics of such detectors are studied over a period of several months. These studies include measurements of the electrical and α-particle characteristics taken before, during, and after thermal-vacuum testing at 65°C and additional testing at 50°C. Degradation in electrical and α-particle characteristics resulting from such testing and aging is found to be negligible over a period of approximately four months. The measurements at 50 and 65°C indicate that the fractional change in the mean energy per ion pair is approximately -1.3×10^{-4}/°C over the temperature range from room temperature to 65°C. The results of these studies are reported. (auth)

5768 COMPUTER ANALYSIS OF BETA-RAY AND CONVERSION-ELECTRON SPECTRA OBSERVED WITH LOW-RESOLUTION DETECTORS. Rogers, P. C.; Gordon, G. E. (Massachusetts Inst. of Tech., Cambridge). Nucl. Instrum. Methods, 37: 259-64(Nov. 1965). (MIT-905-36).

A computer program that permits one to resolve β and conversion-electron energy spectra into their various components, taking into account experimental distortions, is written. The program is designed to treat spectra taken with low-resolution detectors, in which distortions of the true energy spectra are quite serious. Effects of the distortions upon the continuous β spectra are handled by an iterative least-squares fitting technique. An initial set of endpoint energies E_{0i} for the various components is assumed, the true energy spectrum corresponding to the set E_{0i} is computed from the Fermi treatment of β decay, the spectrum is distorted with the use of response functions appropriate to the detection system and the resulting calculated spectrum is compared with the observed spectrum. Adjustments of the intensities and endpoint energies are made and a new iteration is performed. The process is continued until termination requirements are met. Output information includes the final values of the intensities and endpoint energies of the various components and uncertainties in their values, as well as statistical goodness-of-fit data. One of the main advantages of this treatment is that it retains all of the statistical information present in the observed spectrum. As written, the calculation of response functions is designed for plastic scintillators used under conditions in which scattering is a serious problem. However, the calculation of response functions is entirely contained within one subroutine, which can be easily modified for use with other detection systems. (auth)

5769 A VERSATILE ROUTING SYSTEM FOR MULTICHANNEL ANALYZERS. Kantele, J. (Univ., Helsinki); Kohonen, T. Nucl. Instrum. Methods, 37: 265-7(Nov. 1965).

A versatile routing system for multichannel analyzers is described. The system can be used in simultaneous storing of four independent spectra, any number of which may be singles or coincidence spectra. Also, the unit is capable of performing many logic functions, in conjunction with multigroup storing, which are useful in various coincidence experiments involving the use of several detectors. (auth)

5770 A FAST COINCIDENCE SYSTEM FOR LOW ENERGY γ-RAY SPECTROSCOPY. Bertolaccini, M.; Cova, S.; Bussolati, C. (Istituto di Fisica del Politecnico, Milan). Nucl. Instrum. Methods, 37: 297-304 (Nov. 1965).

A reliable triple coincidence system for low energy γ rays with good time and energy resolution, high detection efficiency, and high singles counting rate cabability was required for a 3-quantum positron decay experiment. NaI(Tl) detector–153 AVP photomultiplier integral-lines were selected. A general description is given of the complete coincidence system, which includes a fast coincidence-anticoincidence circuit, delay-line differentiating amplifiers, single-channel analyzers, linear gates, and a supervisory coincidence to combine energy and time requirements. The system tested with 511 kev γ-rays allows better than 10 nsec resolution at 100% coincidence efficiency, and better than 6 nsec at 95% efficiency, with about 10% energy resolution and good counting rate capability. A 3-quantum positron measurement is described, which shows the accuracy of the instrument. (auth)

5771 ON THE BACKGROUND CURRENT IN THE DIELECTRIC LIQUID IONIZATION CHAMBERS. Ladu, M.; Pelliccioni, M.; Roccella, M. (CNEN, Frascati, Italy). Nucl. Instrum. Methods, 37: 318-22(Nov. 1965).

The background current in a dielectric-liquid ionization chamber was studied. The contribution of the ionic impurities inside the liquids, and of the intrinsic conductivity to this current was shown. (auth)

5772 A PREAMPLIFIER WITH 0.7 kev RESOLUTION FOR SEMICONDUCTOR RADIATION DETECTORS. Elad, E. (Univ. of California, Berkeley). Nucl. Instrum. Methods, 37: 327-9(Nov. 1965). (UCRL-16390).

A low-noise preamplifier, utilizing a field-effect transistor in its input stage, is described. The preamplifier (pulse generator resolution 0.7 kev fwhm) is designed from the viewpoint of optimization of the signal-to-noise ratio. In use with a semiconductor radiation detector, the preamplifier yields 1.1 kev resolution. (T.F.H.)

5773 THE ELECTRON-PHOTON BEAM MONITORING WITH THE IMAGE AMPLIFYING PLATE. Kajikawa, R.; Kikuchi, K.; Masaika, A.; Murata, Y. (Nagoya Univ., Japan). Nucl. Instrum. Methods, 37: 332-3(Nov. 1965).

Low-intensity (about 10^7 photons/cm^2·sec or 10^7 electrons/cm^2·sec) gamma and electron beams at 600 Mev are observed by means of image-intensifying plates. These plates consist of sandwiches of the form glass–phosphor–photoconductive layer containing fine tungsten wires–opaque layer-reflector–electroluminescent layer–transparent electrode-glass plate. By suitable choices of the above layers, and of the alternating potential applied to the tungsten-wire grid and the transparent electrode, a luminescent image of the beam is produced whose decay time is 3 sec to 10 min. Thus the sandwich can be used for the study of the variable features of the beam, or of the characteristics of the beam after cutoff, for fairly low-intensity electron and gamma beams. (T.F.H.)

5774 THE CALIBRATION OF RADIOACTIVE GAS MONITORS. Caplan, H. S.; Walsh, M. L. (Univ. of Toronto). Nucl. Instrum. Methods, 37: 334-5(Nov. 1965).

Liquid N_2 is irradiated by 22-Mev bremsstrahlung to produce ^{13}N by the (γ,n) reaction. In the liquid state, the

^{13}N activity can be readily determined and compared with standard sources. The liquid nitrogen is then dumped into a full-scale model of the system (in this case, a laboratory ventilation duct system) in which airborne ^{13}N activity must eventually be monitored. The known ^{13}N activity is mixed thoroughly with the air in the test area, and the activity is measured by the monitors that will eventually be used in the routine monitoring. The response of the monitor to this known ^{13}N concentration gives the desired monitor calibration. (T.F.H.)

5775 SINGLE CRYSTAL COMPTON SPECTROSCOPIC TECHNIQUES. Grissom, J. T.; Koehler, D. R. (U. S. Army Missile Command, Redstone Arsenal, Ala.). Nucl. Instrum. Methods, 37: 336-9(Nov. 1965).

The behavior of Compton distributions in scintillation detectors as a function of experimental resolution is investigated, and data differentiation techniques are discussed. The purpose of the study is the use of the Compton distributions for gamma spectroscopy, using a single detector. (T.F.H.)

5776 ETCHING CELL FOR SEMICONDUCTOR COUNTERS. Muggleton, A. H. F. (Atomic Weapons Research Establishment, Aldermaston, Eng.). Nucl. Instrum. Methods, 37: 345(Nov. 1965).

A cell is designed in which semiconductors (and, in particular, lithium-drifted semiconductors) can be etched under controlled conditions with ease. The cell may be constructed of polythene or Teflon. (T.F.H.)

5777 AN INDIRECT METHOD FOR MONITORING 2.5 Mev NEUTRONS, PRODUCED BY A 150 kv ACCELERATOR. Mangialajo, M. (CISE, Milan). Nucl. Instrum. Methods, 37: 346-7(Nov. 1965).

Neutron beams produced in the $D(d,n)^3He$ reaction by deuterons up to 150 kev are monitored indirectly, by monitoring the simultaneous production of protons on the same deuterium target via the D(d,p)T reaction at a set angle. A comparison of the cross sections for n and p production then yields the neutron production yield. (T.F.H.)

5778 A DIFFERENTIAL ION CHAMBER FOR BEAM ENERGY MEASUREMENT. Hanna, R. C.; Hodges, T. A. (Rutherford High Energy Lab., Chilton, Eng.). Nucl. Instrum. Methods, 37: 348-9(Nov. 1965).

A device is designed for measuring the energy of 10- to 200-Mev proton beams. The device consists of an energy degrader of variable superficial mass, followed by a differential ionization chamber. When the degrader thickness is equal to the proton range, the current in the ionization chamber is zero. If the thickness is greater or less than the range, the chamber current is negative or positive respectively. Thus a measurement of the chamber current as a function of thickness yields the range, and hence the beam energy. (T.F.H.)

5779 SIMULTANEOUS GAS-PROPORTIONAL COUNTING OF ^3H AND ^{14}C. Jordan, Pierre (Swiss Federal Inst. of Tech., Zurich). Nucleonics, 23: No. 11, 46-9(Nov. 1965).

Attention is given to the question of the strong dependence of proportional-counter amplification on the gas filling so that the counters become useful as proportional devices only after proper calibration. The measurement procedure with such counting devices is described. This permits separate determinations of tritium or carbon-14 with an ultimate precision of about 0.2% for active preparations as well as simultaneous determinations of both elements. Gas proportional counting of carbon-14 and tritium is found to be more precise, more sensitive and less expensive than the more usual liquid-scintillation counting technique. Topics discussed include counting precision, simultaneous measurements, sample preparation, and the performing of the measurements. (J.F.P.)

5780 NUCLEAR PULSE AMPLIFIERS—FUNDAMENTALS AND DESIGN PRACTICE. PART 3. Fairstein, E. (Tennelec Instrument Co., Inc., Oak Ridge, Tenn.); Hahn, J. Nucleonics, 23: No. 11, 50-5(Nov. 1965).

Several characteristics of nuclear pulse amplifiers are discussed. These include overload recovery, since the scintillation counter can perform under conditions of high amplitude overload. Noise is also discussed. System noise appears as a random fluctuation of the instantaneous baseline, and modulates the desired signals. The main amplifier input stage and amplification control are considered. Pulse-shaping networks are described including pulse shaping, frequency response, noise, and the effect of pulse shape on pulse-height analyzer response. Timing is considered. Leading edge timing and crossover timing or zero-crossing timing are described. Finally, practical pulse shaping networks are discussed including the cusp, triangle, delay-line differentiator, and RC integrator, and the Gaussian. (J.F.P.)

5781 THE DETECTION OF LOW β-ACTIVITY WITH G-M DETECTOR. Wojtowicz, Stefan. Nukleonika, 10: 397-404(1965). (In Polish).

Methods of eliminating the influence of outer cosmic radiation on the background counting rate of the G-M tubes are described. Practical solutions to this problem are discussed and results are given that allow comparison of the methods. (auth)

5782 THE ELECTRONIC COLLIMATION OF α PARTICLES IN GRIDDED IONIZATION CHAMBER. Pawlowski, Zdzislaw; Bienkowski, Andrzej (Polytechnic Inst., Warsaw). Nukleonika, 10: 433-41 (1965). (In Polish).

Electronic collimation in a conventional gridded ionization chamber is described. This method, based on the evaluation of pulse rise time at the collector, allows direct information on the angle formed by the tracks of the particles with the electric field to be obtained. The energy resolution was improved about 30%, when the electronic collimation of α particles was used. Results of an investigation are presented for gas mixtures Ar + 2% N_2 and Ar + 0.8% C_2H_2. (auth)

5783 A LOW-BACKGROUND BETA SCINTILLATION COUNTING METHOD WITH THIN PLASTIC SANDWICH PHOSPHORS. Dimchev, Teodor (Inst. of Physics, Bulgarian Academy of Sciences, Sofia). Nukleonika, 10: 477-83(1965).

A beta scintillation sandwich counting method for measuring low activities with plastic phosphors of 0.254 mm thickness is described. Simple radiometrical instruments were applied, without using anticoincidence or special shielding of the counter. With a background of 0.87 cpm without cooling of the photomultiplier the efficiencies obtained were 39% for $^{90}Sr + {}^{90}Y$, 19.5% for ^{204}Tl, and 1.25% for ^{147}Pm. The background may be lowered further and the efficiency of counting increased by cooling the photomultiplier and by using optical coupling between the plastic phosphors and photocathode. (auth)

5784 AVERAGE ENERGY EXPENDED PER IONIZED ELECTRON-HOLE PAIR IN SILICON AND GERMANIUM AS A FUNCTION OF TEMPERATURE. Emery, F. E.; Rabson, T. A. (Rice Univ., Houston, Tex.). Phys. Rev., 140: A2089-93(Dec. 13, 1965).

Measurements were made over a range of temperature of the amount of ionization produced by the passage of ionizing radiation through the junctions of Ge and Si Li-drifted solid-state detectors. These data are presented in the form of the average energy per hole-electron pair. A simple model for the value of ϵ, the average energy per hole-electron pair, was proposed by Shockley in 1960. This model was extended to predict temperature effects upon ϵ. Silicon and Ge Li-drifted counters were designed for detecting 1-Mev electrons and/or 5.5-Mev alphas over a temperature range of 4 to 300°K. The techniques and necessary equipment were designed to enable the measurement of the charge detected from a single incident ionizing particle with a probable error less than 0.4%. Data were taken on Si and Ge detectors for temperatures ranging from 20 to 200°K. The data only qualitatively agree with the simple model. The evidence points to additional effects besides those considered by Shockley. The room temperature values of ϵ for the Si Li-drifted counters agree with those for silicon surface barriers which were recently published. (auth)

5785 A METHOD FOR PREPARATION OF LIQUID SCINTILLATOR IN VACUUM. Mitani, Shichiro (Osaka City Univ.). Radioisotopes (Tokyo), 14: 463-7(Nov. 1965). (In Japanese).

A method was developed by which liquid scintillators of high and uniform scintillation efficiency can be prepared. The total amount of solutes required for the number of liquid scintillators to be prepared is weighed and dissolved in an adequate solvent at a slightly greater concentration than normal. The required volume of this solution is measured and poured into each scintillator vessel. The solvent is then distilled from these vessels under high vacuum; solutes corresponding to the scintillator volume of each vessel thus remain in it. The required volume of scintillator solvent is then distilled into each vessel under high vacuum, and after tip-off vacuum-sealed liquid scintillators are obtained. These liquid scintillators are very uniform in solute concentration and have negligibly small amounts of dissolved air. Therefore, they have higher and more uniform scintillation efficiency than those obtained by other methods. (auth)

5786 OPTICAL METHOD FOR ABSOLUTE VELOCITY CALIBRATION OF MOESSBAUER SPECTROMETERS. de Waard, H. (Univ., Groningen, Netherlands). Rev. Sci. Instrum., 36: 1728-33(Dec. 1965).

The variable "moiré pattern," formed when a 1 : 1 image of an 8 μ grating connected to a Mössbauer drive is reflected back onto itself, is used to measure the instantaneous velocity of the drive. A photodiode converts the intensity modulated light from the pattern into an electrical signal. From this signal pulses are derived that correspond to shifts of the grating by multiples of 2 μ. These pulses can be applied to a multichannel analyzer used as a part of the Mössbauer spectrometer and thus yield a velocity calibration spectrum. Instantaneous velocities can be measured with accuracies down to about 1 μ/sec. (auth)

5787 VACUUM SEALING TECHNIQUE FOR PHOTOMULTIPLIER TUBES. Nyman, J. C. (Defence Chemical, Biological, and Radiation Labs., Ottawa). Rev. Sci. Instrum., 36: 1887-8(Dec. 1965).

Some vacuum sealing techniques for photomultiplier tubes are briefly discussed. The Garlock Klozure greatly simplifies the vacuum sealing of photomultiplier tubes. (D.C.W.)

5788 THEORY OF AN IONIZATION CALORIMETER. Rylov, Yu. A.; Skuridin, G. A. Yadern. Fiz., 2: 691-704 (Oct. 1965). (In Russian).

The accuracy with which the energy of primary superhigh energy cosmic particles can be determined using an ionization calorimeter is investigated. An expression is obtained for the energy of the primary particle as a function of the reading of the ionization calorimeter detectors. It is shown that the problem reduces to the solution of a system of linear integro-differential equations for the mean numbers of various types of particles. The accuracy of the ionization calorimeter is estimated. (auth)

5789 ON THE SPREAD TIMES OF DISCHARGES IN SELF-QUENCHING COUNTERS. [PART] V. Franke, H. G. (Univ., Muenster, Ger.). Z. Phys., 188: 339-51 (1965). (In German).

The statistical distribution of spread times of discharges in self quenching Gieger-Müller counters shows, except for very high counting rages, that the photoelectric effect in the gas (wire component) determines the process of the discharge. Although there are many long range photons which make photoelectric effect at the cathode (cathode component), only in a few cases they can contribute to the discharge process because the speed of the wire component exceeds in most cases the speed of the cathode component. The ratio of both components was measured as follows: The wire component can be decelerated or even suppressed by a zone of smaller electric field. On the other hand the cathode component can be almost suppressed by using a cathode with very small masking degree. The drift-time of photoelectrons from the cathode to the wire was measured. (auth)

5790 STUDY OF SEMICONDUCTOR SURFACE BARRIER DETECTORS AT 4.2 deg K. Fabjan, C. W.; Kenawy, M.; Rauch, H. (Oesterreichische Hochschule, Vienna). Z. Phys., 188: 378-84(1965). (In German).

The behavior of semiconductor surface barrier detectors was studied in the temperature range from 300 to 4.2°K. Measurements of the resolution for α and β particles are given. The mean energy E required for producing an electron-hole-pair in Si is found to be 3.54 ± 0.10 ev at 279°K, and 3.72 ± 0.11 ev at 78°K and 4.2°K respectively. Measured rise time of detector impulses is compared with theoretical values. (auth)

5791 ABSORPTION AND SCATTERING IN β ACTIVITY MEASUREMENT OF SAMPLES OF ARBITRARY THICKNESS USING END WINDOW COUNTERS AND SMALL ANGLE GEOMETRY [Thesis]. Richter, P. Hanover, Tech. Univ., 1964. 74p. $2.00 Gmelin, AED-DISS. 64-481.

The influence of scattering and absorption on end window counter β-activity measurements is studied. An approximative formula valid for sample thicknesses up to several 100 mg/cm^2 is given. (Gmelin Inst.)

5792 EXPERIMENTAL STUDIES OF ČERENKOV RADIATION IN OPTICALLY SINGLE AXIS CRYSTALS [Thesis]. Gfoeller, D. Goettingen, Ger., Univ., 1964. 45p., $2.00 Gmelin, AED-DISS. 64-747.

An arrangement for coincidence detection of Cherenkov radiation produced in a single axis $NaNO_3$ plate by ^{32}P β-radiation is described. Anisotropy factor is 1.15. This value is in good agreement with theoretical data. (Gmelin Inst.)

5793 PARTICLE COUNTING BY CASCADE PRODUCTION IN SOLIDS ESPECIALLY IN Si p-n LAYERS [Thesis]. Ruge, I. Munich, Tech. Univ., 1964. 138p. $2.00 Gmelin, AED-DISS. 64-581.

The application of charge multiplication in plasma channels in solids for particle counting is studied. Methods for production of microchannels in Si p-n layers are discussed. The effective volume of the counter is estimated. A probe operating by charge transport in plasma channels can also be used as an infrared detector. (Gmelin Inst.)

5794 THE DETERMINATION OF THE NUCLEAR QUADRUPOLE MOMENT OF THE 482 kev LEVEL OF ^{181}Ta BY MEANS OF $\gamma-\gamma$ ANGULAR CORRELATIONS [Thesis]. Pandey, R. C. Berlin, Humboldt Univ., 1964. 64p. $2.00 Gmelin, AED-DISS. 64-475.

Design and construction of a coincidence apparatus for nuclear quadrupole moment studies are described. Anisotropies as a function of magnetic field strength are given. Results indicate that the first rotation level of ^{181}Ta has the same quadrupole moment as the ground level (6×10^{-24} cm^2). (Gmelin Inst.)

5795 DIE PHYSIKALISCHEN GRUNDLAGEN DER KERNSTRAHLUNGSMESSUNGEN. (The Physical Fundamentals of Nuclear Radiation Measurements). Fenyves, E.; Haiman, O. Budapest, Publishing House of the Hungarian Academy of Sciences, 1965. 727p.

After an introductory review of the development of nuclear radiation measurements and the development tendencies in the forseeable future, the interactions of nuclear radiation with matter and its penetration through matter is described. The physical operational principles and the construction of particle counters and particle track detectors are then considered. The most important measurements in which these counter and detectors are used are evaluated. The methods for the measurement of individual particles, beams, and sources are analyzed, and bases for comparing the different methods and for evaluating the results obtained are reported. In an appendix the application of particle counters and detectors to the discovery of elementary particles, the statistical evaluation of measurement results,

and electronic amplification, discrimination, and counting are discussed. (J.S.R.)

5796 WALK CORRECTION CIRCUIT (Engineering Materials). (Oak Ridge National Lab., Tenn.). (CAPE–1264).

1 drawing.

A circuit is designed for use with a neutron time-of-flight spectrometer to correct timing errors caused by different types of pulses such as time shifts. The shifts are caused by variations in signal amplitudes in the start and stop channels of a time-to-pulse-height converter. The walk circuit corrects the output of a time-to-pulse-height converter by adding a signal to the output that is dependent on the amplitude of the start pulse. It has been successfully used to stop the converter by a constant-amplitude signal derived from the pulsed beam of a Van de Graaff accelerator, so that the "amplitude effect" or "walk" occurs only in the start channel. This circuit makes it possible to obtain excellent time resolution while using almost the total Compton spectrum to start the converter. (For details, see TID-4100). (L.B.S.)

5797 A METHOD OF AND APPARATUS FOR RECORDING PULSE SPECTRA. Boclet, Daniel; Ducros, Georges; Goupil, Jean (to Commissariat a l'Energie Atomique). British Patent 1,009,465. Nov. 10, 1965. Priority date May 10, 1962, France.

A method is provided of recording pulses produced by Geiger counters, photomultipliers, or other detectors associated with sources of particles or sources of radiation usually studied using multi-channel analyzers in such a way that the recording may be very rapidly read off by a selector. The train of pulses may have any amplitude and any desired repetition rate, and each of the of the pulses is transformed into a train of identical signals of a stable frequency. Each train has a duration that is a function of the amplitude of the pulse it represents. When a train is being recorded on a flexible recording support, a newly incident pulse is prevented from being transformed as long as the train of signals representing the last pulse admitted to undergo the transformation is not recorded. (B.L.M.)

5798 SCINTILLATION COUNTER FOR THE MEASUREMENT OF BETA RADIOACTIVITY OF LOW CONCENTRATION IN LIQUIDS. Ralkova, Jarmila (to Ceskolovenska Akademie Ved.). German Patent 1,200,963. Sept. 16, 1965. Priority date Apr. 26, 1960, Czechoslovakia.

The sample container consisting of clear-glass artificial material is disposed between two coaxially arranged multipliers. Thin plates of scintillating material are disposed within the container parallel to the axis of the multipliers. (Gmelin Inst.)

5799 READING AND CHARGING INSTRUMENT FOR DOSIMETERS WITHOUT AN INSTALLED ELECTROMETER. Weiss, Rene (to Landis and Gyr AG). German Patent 1,201,921. Sept. 30, 1965. Priority date Sept. 18, 1962, Switzerland.

In order to prevent the charging of the dosimeter prior to the reading, the reading and charging instrument is provided with a two-stepped push-button switch in which the resistance of sliding friction between the first and the second position of the button is essentially higher than in any other position. A detailed description of the push-button switch is given. (Gmelin Inst.)

5800 PULSE COUNTING FISSION IONIZATION CHAMBER. Peschke, Fritz (to VEB Vakutronik). German Patent 1,201,922. Sept. 30, 1965. Filed June 29, 1961.

The chamber contains two independently operated measuring systems (electrode systems) connected alternatively to a common measuring channel. The amount of fissionable material on the different electrode systems differs in such a way that an over-all coverage of the neutron flux range is obtained. The ratio of the two quantities of fissionable material may be varied between 2 : 1 and 10^7 : 1. (Gmelin Inst.)

5801 CIRCUIT ARRANGEMENT FOR A GEIGER-MUELLER COUNTING TUBE. Moehrung, Rolf (to VEB Vakutronik). German Patent 1,201,923. Sept. 30, 1965. Filed Mar. 24, 1964.

The circuit arrangement comprises an auxiliary voltage source connected via a rectifying tube to an intermediate position of a voltage divider through which the tube current flows and which connects the tube to the voltage source of the tube. By this means it is achieved that only part of the current flowing through the tube is measured by the measuring instrument switched between the voltage source of the tube and the voltage divider whereby an integrating condenser is switched in parallel with the measuring instrument. (Gmelin Inst.)

5802 DISCRIMINATING RADIATION DETECTOR FOR DETERMINING A GIVEN RADIATION IN THE PRESENCE OF OTHER RADIATIONS. Sun, Kuan H. (to Westinghouse Electric Corp.). U. S. Patent 3,201,590. Aug. 17, 1965. Filed Dec. 4, 1958.

A radiation detector is patented that includes means sensitive to a given type of radiation and also an arrangement for cancelling out the effects of other radiations in order to render the detector insensitive to any other than the given radiation, e.g., a neutron flux meter that is completely insensitive to gamma and fast neutron radiation. The detector includes opposed semiconductor devices, each having p- and n-type regions with a junction between them. The outputs of the semiconductor devices are connected in opposition. A quantity of neutron-reactive material is supported by one of the devices in proximity to its output region, and a neutron insensitive material is supported by the other device in proximity to its output region with means provided for measuring the differential output of the devices. (B.L.M.)

5803 ION CHAMBER DOSIMETER FOR NUCLEAR RADIATIONS. Cooke-Yarborough, Edmund Harry (to United Kingdom Atomic Energy Authority). U. S. Patent 3,214,588. Oct. 26, 1965. Priority date May 21, 1962, Great Britain.

An ion chamber type dosimeter is described that has a momentary aural warning when the measured radiation reaches a certain level. The ion chamber includes a polarizing electrode and collector electrode. The ion chamber is charged initially so that a potential difference is set up between these two electrodes. The potential difference decreases slowly when the chamber is subjected to radiation that causes an ionization current to flow between the electrodes. Means are provided for causing the potential of the polarizing electrode to rise progressively until the potential of the collector electrode reaches a threshold value, and the momentary aural warning sounds each time the threshold potential is reached. Means are included for returning the potential of the polarizing electrode to its initial value to recommence its rise each time the potential of the collector electrode reaches the threshold value. (B.L.M.)

5804 SOLID STATE RADIATION DETECTION SYSTEM WITH LOW NOISE AMPLIFICATION. Graham, R. H. (to U. S. Atomic Energy Commission). U. S. Patent 3,219,825. Nov. 23, 1965.

A radiation detection system is designed using solid-state detectors of the type which respond to incident radiation by the issuance of current pulses in combination with a parametric amplifier to facilitate low noise amplification of the output signals of the solid state detector. The pulse output, which is comprised of a plurality of radio-frequency components proportional to the magnitude of the pulse, is directed through an electronic filter which selects a predetermined frequency component and directs it to a pumped parametric amplifier to energize the amplifier to produce an amplified output signal including the selected radio-frequency component. By combining the solid-state radiation detector with a selected electronic filter, a parametric amplifier may be employed to amplify electrical signals representative of information contained in pulse type elec-

trical signals and thereby gain outstanding signal-to-noise ratio amplification. (AEC)

Radiation Effects

5805 (AD-617782) ENERGY TRANSFER DURING TRANSIENT NUCLEAR PULSES. Semiannual Report No. 1, May 1-October 31, 1964. Kallmann, Hartmut P. (New York Univ., N. Y. Radiation and Solid State Lab.). Nov. 1964. Contract DA28043AMC00129E. 28p. CFSTI $2.00 cy, $0.50 mn.

A method is proposed for reduction of the radiation response in cables or capacitors. This proposal is based on the charge accumulation near interfaces. It emphasizes the design of an insulator composed of various thin layers of material. Each layer should have a thickness less than the observed width of the charge layers (.25 to .5 mm). The layers should eventually be separated by thin films of mylar or similar material, or they should be firmly pressed together. It is believed that a radiation-insensitive coaxial cable could be designed along the lines of this suggestion. (TAB)

5806 (AD-619387) ANALYSIS OF RADIATION EFFECTS IN TELEMETRY CIRCUITS. Report No. 1965-20. Stanley, A. G. (Lincoln Lab., Massachusetts Inst. of Tech., Lexington). July 21, 1965. Contract AF19(628)-5167. 31p. (ESD-TDR-65-310). CFSTI $2.00 cy, $0.50 mn.

The effects of nuclear radiation on the telemetry circuits in the LES satellites were analyzed by direct irradiation and by simulating the effects on individual components on a breadboarded circuit. The simulation method is described in detail. It requires a precise knowledge of the behavior of each component operating under specified bias condttions in a radiation environment, but may be applied to circuits of considerable complexity. The analysis confirmed that circuits such as the flip-flop, which operate at 50% duty cycle, are insensitive to moderate leakage currents and have low gain requirements, and are extremely radiation resistant. The converse holds for circuits that operate at low duty cycles, that are sensitive to leakage currents and that have more stringent gain requirements. (auth)

5807 (AEEW-M-493) A NOTE ON THE IRRADIATION TESTING OF A PULSE FISSION CHAMBER DESIGN. Goodings, A. (Atomic Energy Establishment, Winfrith England)). 1964. 36p. Dep. mn.

Three models of a 1 in.-diameter pulse fission chamber design are tested using a low-noise matched-input head amplifier, and the results are discussed in comparison with predicted values. The effect of gamma flux on discriminator bias plateaus is examined, and experiments on chamber activation following neutron irradiation are described. (auth)

5808 (N65-35081) COMPONENTS IRRADIATION TEST NO. 13. 2N2501 TRANSISTORS, TI 551 DIODES, AND VARIOUS TYPES OF THERMISTORS. (Lockheed-Georgia Co., Marietta). Apr. 1965. 38p. (ER-7899; NASA-CR-64433). CFSTI $3.00 cy, $0.50 mn.

Twenty (20) specimens of the type 2N2501, General Instrument, transistor and 20 specimens of the type TI 551, Texas Instruments, diode were subjected to a nuclear radiation environment at 30°C. Radiation exposure was a combination of neutrons and gamma rays. Also subjected to the same radiation environment at 0°C were the following thermistors; Types A0610P-13; A1406P-13; R172; GB31L1; GB41L1; RL13M1; RL20E1; RL4M1; and RL7E1. Measurements were made to determine the effect of the radiation on the h_{FE}, h_{ie} and I_{CBO} parameters of the transistors, the V_F and I_R parameters of the transistors, the V_F and I_R parameters of the diodes, and the resistance (temperature indication) of the thermistors. (auth)

5809 ELECTRODE PROTRUSIONS PRODUCED BY ELECTRON BEAM BOMBARDMENT AND THEIR ROLE IN VACUUM BREAKDOWN. Maitland, A.; Hawley, R. (International Research and Development Co. Ltd., Newcastle-upon-Tyne, Eng.; C. A. Parsons and Co. Ltd., Newcastle-upon-Tyne, Eng.). Brit. J. Appl. Phys., 16: 1591-2(Oct. 1965).

It was found that bombardment of copper samples by an electron beam in a vacuum chamber produced the formation of minute metallic projections on the copper surface. The possible bearing of such a process on the mechanism of electrical breakdown in high vacuum is considered. (auth)

ISOTOPE TECHNOLOGY

General

5810 (NP–15543) PEACEFUL USES OF RADIOISOTOPES IN THE RUMANIAN PEOPLE'S REPUBLIC, 1958–1964. (Rumanian Committee for Nuclear Energy, Bucharest). 1964. 91p. Dep. mn.

Six articles describing uses of radioisotopes in Rumania are compiled. Each article was abstracted separately. (J.S.R.)

For abstracts of individual papers see: 5235, 5425, 5435, 5590, 5657, and 5814.

5811 (PAEC(A)IN–653) ^{198}Au. A Literature Search. (Philippine Atomic Energy Commission, Manila). Feb. 1965. 58p. Dep. mn.

References (316) on the uses and study of gold-198 are given to journals, books, and reports published from August 1948 to May 1963 inclusive. The references are listed under the following subject headings: biology and medicine; chemistry; engineering and equipment; geology and mineralogy; health and safety; instrumentation; isotope technology; metals, ceramics, and other materials; and physics. Separate author and corporate author indexes are included. (P.C.H.)

5812 (PAEC(A)IN–654) RADIOISOTOPES IN PHARMACY. A Literature Search. (Philippine Atomic Energy Commission, Manila). Mar. 1965. 14p. Dep. mn.

Sixty-one references are given to reports, conferences, journals, and books published from Oct. 1952 through July 1963. The references are listed under the following subject headings: biology and medicine; chemistry; health and safety; industrial applications of isotopes and radiations; and physics. Separate author and corporate author indexes are included. (P.C.H.)

5813 (JPRS–32260) RADIOACTIVE SOURCE PRODUCTION AT BORIS KIDRIC INSTITUTE. Nemoda, Djordje; Bircanin, Ljubisa. Translated from Teknika (Belgrade), 20: 1458-63(Aug. 1965). 13p. (TT–65–32750). CFSTI $1.00 cy, $0.50 mn.

The preparation of radioactive sources of ^{60}Co and ^{192}Ir are discussed along with methods for the calculation of activation time, packaging of samples in reactor channels, and measurement of activity. (P.C.H.)

Industrial Applications

Refer also to abstract 5810.

5814 (NP–15543, pp 27-45) USE OF TRACERS AND OF INTENSE RADIATION SOURCES IN INDUSTRIAL PROCESSES. Diaconescu, A.; Ioanid, G. (Rumanian Committee for Nuclear Energy, Bucharest).

The applications of radioactive isotopes and intense sources of radiations in Rumania are reviewed. New and highly efficient methods have been devised for the locations of slush loss zones in drilling, the checking of oil well cementing, the circulation between pay beds and bore holes, and the various procedures for increasing the oil flow to the bore hole. Details are given on the checking of the multiple stage selective hydraulic fracturing, the water injection into the deposit in the flooding patterns, the behavior at retention-elution in the conditions of the well, which may be considered as methods specifically adequate to local conditions and which are widely used in Rumanian oil fields. Paraffine oxidation on an industrial scale has been achieved through the use of intense sources of gamma radiations. The use of radioactive tracers has extended the methods for finding out the best working parameters in various industrial processes such as: superphosphate manufacture, electrolysis of NaCl with Hg electrodes, carbide manufacture, and gold extraction from gold ores. The benefits derived from the use of radioactive tracers in the chemical industry of Rumania are emphasized. (17 references.) (auth)

5815 (STI/DOC/10/44) ADVANCES IN INSECT POPULATION CONTROL BY THE STERILE-MALE TECHNIQUE. Report of a Panel Held in Vienna, July 20-24, 1964. Technical Reports Series No. 44. LaBrecque, G. C.; Keller, J. C. (eds.) (International Atomic Energy Agency, Vienna (Austria)). June 1965. 81p. IAEA US $2.00; S 42,-; 12/-stg; F.Fr. 8,-; DM 6,40.

Prior to 1962 only the screw worm in the southeastern United States had been successfully eradicated by the sterile-male technique. Since then, this technique has been successfully used in the control or eradication of at least eight species of insect in either experimental or field trials. This method of insect population control is unique in that it utilizes an inherent mating instinct to the detriment of a species without harm to any other species in the environment, with perhaps the exception of obligatory parasites of the species under attack. Recent progress made in inducing sexual sterility in insects by means of irradiation, chemosterilants, or mutagens is reviewed. Emphasis is placed on fruit flies and tsetse flies but data are included on 39 species of economic or medical significance. The utilization of radioisotopes to label insects for use in ecological studies is also discussed. (52 references.) (C.H.)

5816 THE INTERNATIONAL PROJECT ON IRRADIATION OF FRUITS AND FRUIT JUICES. Kaindl, K. (Reaktorzentrum, Seibersdorf, Austria). Atompraxis, 11: 517-20(Sept.-Oct. 1965). (In German).

An International Project on Irradiation of Fruits and Fruit Juices was begun. The program includes three different areas of research: basic research in the field of radiosensitivation of microorganisms, technological studies on radiopreservation of fruit juices, and wholesomeness tests on irradiated fruits and fruit juices by animal feeding. The status of the project is described. (auth)

5817 SOME EXAMPLES OF RECENT DEVELOPMENTS IN THE USE OF RADIOACTIVE ISOTOPES IN BRITISH INDUSTRY. Clayton, C. G. (Wantage Res. Lab., Eng.). Ind. Chim. Belg., 28: 833-43(Aug. 1963).

Some industrial applications of radioisotopes are described. Isotope velocity and dilution methods for flow measurement in closed conduits are used for measurement of the efficiency of pumps in cooling water systems and in providing on-site calibration of orifice plates, venturi flumes, and other hydraulic structures. Valves are used, through which radiation detectors can be inserted into the flow and through which the tracer can be injected and samples removed. The amount of radiotracer required for the velocity method is much less (~1/100th) than for the dilution method so that many more measurements can be made for the same amount of radioactivity. The measurement time is also shorter and the method can be operated as a direct reading system. For flow measurement in open streams and rivers the continuous sample method has many advantages; a single injection of the radiotracer is made and a sample is withdrawn at a constant rate from some point beyond the mixing distance. Measurement of gas flow with isotopes in the chemical engineering, petroleum, steel, and power industries is considered. The application of radioisotopes to leak detection and location in single pipes is discussed. The use of ^{85}Kr to detect leaks in small hermetically sealed components such as bellows, valves, transistors, and fuel elements is described. In one method, mainly applicable to small components, each unit is subjected to a high pressure of ^{85}Kr so that the radio-

active gas is forced through any cracks which are present. With larger components, such as pressure switches and fuel elements, ^{85}Kr may be introduced during manufacture and its presence detected subsequently using a scintillation counter in close contact. Allowing one hr for gas to leak out from a pressure switch containing 830 μC ^{85}Kr, it was possible to check a leak rate of 4×10^{-2} ml/sec under test conditions of 0.04 atm above vacuum. Bulk flow studies using radioisotopes are described. Beta and γ transmission thickness and density gages and level detectors are now in widespread use, and this type of radioisotope application is mainly confined to the energy range from 1 to 200 kev. Three techniques are described, which are being developed for analysis in the low-energy x-ray region. (BBB)

5818 LOCKWOOD—THE WOOD OF THE FUTURE. Burford, A. O.; Roberts, P. J. Lockheed Ga. Quart., 2: No. 3, 2-6(1965).

Radioinduced polymerization of woods impregnated with plastics in the production of Lockwood is discussed. The final material has properties characteristic of both the wood and the plastic so that, by proper choice of monomer system and wood species, Lockwood can be tailored to produce a composite with specific properties. Tests at the 10-Mw Lockwood Radiation Effects Reactor showed that the polymerization process in Lockwood production can be effectively reduced or stopped by control of radiation intensity. It was found that wood of any thickness of commercial interest may be processed. The production process and physical properties of the product are discussed. (F.J.H.)

5819 INVESTIGATION OF THE NEUTRON SURFACE MOISTURE GAGE FOR DETERMINING MOISTURE CONTENTS OF BUILDING MATERIALS, PLANE, THIN, AND HOMOGENEOUS. Okajima, Nobuo; Yamamoto, Moriyuki; Mizushina, Tomoyuki (Taisei Construction Co., Ltd., Japan). Radioisotopes (Tokyo), 14: 493-7(Nov. 1965). (In Japanese).

Problems in determining surface moisture contents (10 to 15 cm depth) of plane and homogeneous building materials by use of neutron surface moisture gage were studied. Fast neutrons emitted by the 5mC Ra–Be source were moderated by paraffin wax and directed into the medium in which the moisture content was to be measured. Since the fast neutrons were moderated to some extent before being directed into the medium, the effective measuring volume of medium was reduced. Relations between moisture contents and thickness of samples were checked by changing the thickness of paraffin wax moderators. Samples consisted of aluminum molds containing sugar and standard sand mixed to keep desired moisture contents and some concrete samples. The mixing ratio was determined by calculations based on moisture contents in one molecule of sugar. In our determination of moisture contents in the samples 15-cm thick and with a 10% moisture content, accuracy was kept within ±1.5% with a count time of 5 minutes in one measurement. (auth)

Power Application

See also ENGINEERING — Space Propulsion

Refer also to abstract 5634.

5820 (NASA-CR-316) THERMAL INTEGRATION OF ELECTRICAL POWER AND LIFE SUPPORT SYSTEMS FOR MANNED SPACE STATIONS. Hanson, K. L. (General Electric Co., Philadelphia, Pa. Missile and Space Div.). Nov. 1965. Contract NAS 3-2799. 315p. CFSTI $7.00 cy, $1.50 mn.

The effects of thermal integration of the life-support and electric-power systems of a six-man space station are evaluated. The thermal power and temperature requirements of specified life-support systems are analyzed, and possible sources of thermal power from selected electric-power systems are investigated. The goal of the evaluation is the achievement of maximum utilization of waste energy from the electric-power system. Preliminary designs of thermally integrated systems are presented and evaluated. The power systems studied include Stirling-cycle, Brayton-cycle, and Mercury-cycle solar and radioisotope systems, and solar photovoltaic systems. (T.F.H.)

5821 POWER FROM RADIOISOTOPES. Perret, R. P.; Haeussermann, W. (European Nuclear Energy Agency, Paris). Atompraxis, 11: 508-16(Sept.-Oct. 1965).

Electrical power generators using heat from radioisotopes as their primary energy source have advantages for certain applications in remote areas and in space. Investigations are being made of these applications as well as the possibility of creating a European industry for the production of such generators and the necessary isotope sources. (auth)

Separation and Production

See also CHEMISTRY — Separation Processes and Procedures

5822 (DP-1000) PRODUCTION OF TRANSPLUTONIUM ELEMENTS AT SAVANNAH RIVER. Overbeck, W. P.; Ice, C. H.; Dessauer, G. (Du Pont de Nemours (E. I.) and Co., Aiken, S. C. Savannah River Lab.). Nov. 1965. Contract AT(07-2)-1. 16p. (CONF-651101-42). Dep. mn; CFSTI $1.00 cy, $0.50 mn.

From 13th Conference on Remote Systems Technology, Washington, D. C.

The Savannah River Plant has been engaged in two programs for production of transplutonium elements. The first, a research effort, involved the irradiation of plutonium to produce target material for the Oak Ridge HFIR. The second is a production effort to produce 3 kg of ^{244}Cm. These programs have recently been combined in a manner that enhances both, through the use of a new mode of high-flux operation for the Savannah River reactors. Extended irradiation of the HFIR target material was accomplished in a high-flux test at 5.4×10^{15} neutrons/(cm^2)(sec), and the high-flux mode will be used to accelerate the production of ^{244}Cm. (auth)

5823 (ORNL-tr-892) THE PRODUCTION OF ^{242}Pu AND ^{242}Cm BY IRRADIATING ^{241}Am WITH NEUTRONS. Dedov, V. B.; Volkov, V. V.; Gvozdev, B. A.; Ermakov, V. A.; Lebedev, I. A.; Razbitnoi, V. M.; Trukhlyaev, P. S.; Chuburkov, Yu. T.; Yakovlev, G. N. Translated by S. J. Rimshaw and J. J. Pinajian (Oak Ridge National Lab., Tenn.), from Radiokhimiya, 7: 453-61(1965). 21p. Dep. mn; CFSTI $1.00 cy, $0.50 mn; JCL $2.60 fs, $0.83 mf.

^{242}Pu and ^{242}Cm are isolated from neutron-irradiated ^{241}Am by means of solvent extraction and chromatographic operations. In a second study, the properties of a number of solid curium compounds (oxalate, oxide, double sulfate of curium and potassium, hydroxide, and carbonate) are described. (auth)

5824 IMPROVED SEPARATION OF ISOTOPIC HYDROGENS BY GAS CHROMATOGRAPHY. Gersh, Michael E. (Yale Univ., New Haven). Anal. Chem., 37: 1786(Dec. 1965).

A method for separating the isotopic hydrogens, H_2, HD, HT, D_2, DT, and T_2, by gas chromatography, based on adsorption on solid substrates such as Al_2O_3, Al_2O_3 + Fe_2O_3, Al_2O_3 + Cr_2O_3, molecular sieves, and silica gel was modified. It was found that addition of a small amount of H_2 to the He carrier gas obviates the problem of tailing and improves the separation factors when used in conjunction with very highly activated columns. (F.J.H.)

5825 ON THE CASCADE THEORY FOR MULTICOMPONENT ISOTOPE SEPARATION. Kucherov, R. Ya.; Minenko, V. P. At. Energ. (USSR), 19: 360-7(Oct. 1965). (In Russian).

A stationary process for the separation of multicomponent isotope mixtures in cascades of arbitrary profile is considered. The limiting cases of zero and infinite relative rate of isotope exchange are studied theoretically. The solution of the system of transfer equations for a square stepped cascade is obtained, and a method for solving these cascades is developed. (tr-auth)

5826 ELECTROMAGNETIC ISOTOPE SEPARATOR AT LUBLIN. **Zuk, W.; Maczka, D.; Pomorski, J. (Maria Curie-Sklodowska Univ., Lublin). Nucl. Instrum. Methods, 37: 249-58(Nov. 1965).**

A description of an electromagnetic isotope separator of laboratory type is given. The separator has a 90° magnetic lens with the symmetrical image of an object. The ion beam radius in the magnetic field is equal to 160 cm, and ensures for heavy elements dispersion of the order of 8 mm per mass unit and a resolving power above 1000. Special attention is concentrated upon new construction systems. The construction of the electromagnet coils and ion source coil as well as the cooling systems of both coils are described. An arrangement of the optics system especially of the ion accelerating lens and a construction of the high temperature source are given. The arrangement of the electronic systems, the high voltage for accelerating the ion beam, the electromagnet current stabilizer, and the ion beam position stabilizer are described. (auth)

5827 METHOD FOR THE BITHERMAL ISOTOPIC ENRICHMENT OF AMMONIA WITH DEUTERIUM. **Lazard, Bertrand; Lerat, Jean-Marie (to Houilleres du Bassin du Nord et du Pas-de-Calais, Commissariat a l'Energie Atomique). U. S. Patent 3,214,243. Oct. 26, 1965. Priority date Aug. 28, 1959, France.**

A method is described for the bithermal isotopic enrichment of ammonia with deuterium that comprises establishing a countercurrent flow of a gas phase containing hydrogen and a liquid ammonia phase charged with an alkali metal amide as a non-volatile adjuvant in a system including at least two stages. Isotopic deuterium exchange is effected in the first stage, and heat exchange is effected between the gas and liquid streams in the second stage while simultaneously the hydrogen gas stream is saturated with vapors of ammonia. (B.L.M.)

MATHEMATICS AND COMPUTERS

Refer also to abstract 5645.

5828 (AAEC/TM–293) THE EXPANSION OF A FUNCTION IN TERMS OF CHEBYSHEV POLYNOMIALS USING THE I.B.M. 7040. Hawker, P. A. E.; Ridgway, N. W. (Australian Atomic Energy Commission Research Establishment, Lucas Heights). June 1965. 27p. Dep. mn.

A digital computer program for expanding a function in terms of Chebyshev polynomials is described. The functions considered are assumed to be continuous and known at only a finite number of points. The coefficients of the Chebyshev polynomial expansion and those of the corresponding power polynomial are determined. (auth)

5829 (CEA-R–2824) CALCUL DE ψ, φ ET DE LEURS DERIVEES. (Calculations of ψ, φ, and of Their Derivatives). Dandeu, Yves; Gautier, Lucienne; Guillermin, Jean; Olivie, Ginette; Roche, Franck (Commissariat a l'Energie Atomique, Saclay (France). Centre d'Etudes Nucleaires). June 1965. 76p. Dep. mn.

The functions $\psi(x,\beta) = (1/\beta\sqrt{\pi}) \int_{-\infty}^{+\infty} [e^{-(y-x/\beta)^2}/1 + y^2]\, dx$ and $\varphi(x,\beta) = (1/\beta\sqrt{\pi}) \int_{-\infty}^{+\infty} [y\, e^{-(y-x/\beta)^2}/1 + y^2]\, dy$, as well as their primary and secondary derivatives with respect to x and β, were calculated for the whole of the (x,β) plane using a certain number of different method series: development, asymptotic development, Hermites polynomials, and approximating formulas. These methods have made it possible to conserve a constant relative accuracy, except in the neighborhood of the regions where the derivatives disappear. (auth)

5830 (CERN–65–38) LE THEOREME DE LIOUVILLE ET LE PROBLEME GENERAL DE LA STABILITE. (The Liouville Theorem and the General Problem of Stability). Fronteaur, J. (European Organization for Nuclear Research, Geneva (Switzerland)). Nov. 12, 1965. 36p. Dep. mn.

The Liouville theorem, of which the theorem of conservation of volumes in phase space is a specific case, is studied. The relations of the Liouville theorem to the general stability problem are shown. It is also shown that the theorem links the behavior of systems in relativistic frames of reference with that in nonrelativistic reference frames. (T.F.H.)

5831 (EUR–1919.f) INEGALITES LINEAIRES SUR UN ANNEAU D'INTEGRITE TOTALEMENT ORDONNE (APPLICATIONS A LA PROGRAMMATION LINEAIRE ET A LA THEORIE DES GRAPHES). (Linear Inequalities on a Total Ordered Linear Integer Ring (Applications to the Linear Programmation and to the Graphs Theory)). Camion, P. (European Atomic Energy Community, Ispra (Italy). Joint Nuclear Research Center. European Atomic Energy Community, Ispra (Italy). European Scientific Data Processing Center). 1965. 32p. Dep. mn.

A theory of linear programming available on linear ordered integer rings is discussed. It only uses the notion of interval, and not the notion of convexity. By this means, one improves the known results on feasibility of systems of linear inequalities. New algorithms are given in linear programming and it is shown how a whole chapter in graph theory belongs to this theory. (auth)

5832 (ORNL–3858(Vol.1), pp 47–58) MATHEMATICS AND COMPUTER PROGRAMS. (Oak Ridge National Lab., Tenn.).

Summaries of 21 papers on mathematics and computer programs are presented. The summaries give a brief description of the programs written at ORNL during the past 2 years. (M.O.W.)

5833 (ORNL–3866) FOURIER ANALYSIS OF UNIFORM RANDOM NUMBER GENERATORS. Coveyou, R. R.; MacPherson, R. D. (Oak Ridge National Lab., Tenn.). Nov. 1965. Contract W-7405-eng-26. 65p. Dep. mn; CFSTI $3.00 cy, $0.75 mn.

A method of analysis of uniform random number generators is developed, applicable to almost all practical methods of generation. The method is that of Fourier analysis of the output sequences of such generators. With this tool it is possible to understand and predict relevant statistical properties of such generators and compare and evaluate such methods. Many such analyses and comparisons were carried out. (M.O.W.)

5834 (ORNL–TM–1323) THE EFFECTS OF TIME DELAY SIMULATION METHODS UPON THE STABILITY AND TIME RESPONSE OF SIMULATED SYSTEMS [Thesis]. Wright, Wister Cordell (Oak Ridge National Lab., Tenn.). Dec. 1965. Contract W-7405-eng-26. 147p. Dep. mn; CFSTI $4.00 cy, $1.00 mn.

Submitted to Univ. of Tennessee, Knoxville.

Problems involved in the analog-computer simulation of time delays are studied, including those simulations utilizing conventional mathematical approximations and computer components, and those utilizing the capacitor wheel (an electromechanical delay simulator). A theoretical and experimental study of the phase and magnitude errors induced by these simulations on the stability of simulated closed-loop systems is presented. (T.F.H.)

5835 GENERAL PURPOSE ANALOG PULSE HEIGHT COMPUTER. Strauss, M. G.; Brenner, R. (Argonne National Lab., Ill.). Rev. Sci. Instrum., 36: 1857-76(Dec. 1965).

An instrument capable of pulse-height multiplication, division, exponentiation, as well as pulse-height addition and subtraction is described. These operations are performed in about 0.5 μsec with a precision of $\pm 0.1\%$ of full scale over a pulse height range of 20 : 1. At room temperature, the computer exhibits a drift of about 0.05%/C° or $\pm 0.3\%$/day. With an input rate of 10,000 counts/sec, the pulse-height distribution shifts 0.2%, and with 25,000 counts/sec it shifts 1%. Multiplication, division, and exponentiation are performed by using logarithms and antilogarithms. The log and antilog function generators are based on the fact that the emitter-base voltage of a silicon planar transistor is proportional to the logarithm of its collector current. Addition and subtraction are performed by using linear operational amplifiers. Results of experiments are shown in which the computer was used for identification of charged particles, pulse shape discrimination, measurement of mass yield distributions in fission, as well as for other on-line data reduction techniques. (auth)

METALS, CERAMICS, AND OTHER MATERIALS

General

Refer also to abstracts 6556, 6558, 6559, 6596, 6600, and 6601.

5836 (NASA-SP-5035) TUNGSTEN POWDER METALLURGY. Barth, V. D.; McIntire, H. O. (Battelle Memorial Inst., Columbus, Ohio). Nov. 1965. 39p. GPO $0.35.

Recent developments in tungsten powder metullurgy technology as related to space vehicles and the less traditional applications are summarized. Information is given on properties of W, mineral reserves, powder production, consolidation, and structures. 252 references are cited. (P.C.H.)

5837 (NLCO-966) THE PLASMA SPRAYING OF PROTECTIVE COATINGS. Elston, D. L. (National Lead Co. of Ohio, Cincinnati). Sept. 29, 1965. Contract AT(30-1)-1156. 18p. (CONF-651029-2). Dep. mn; CFSTI $1.00 cy, $0.50 mn.

From 15th Annual National Lead Co. Analytical and Physical Testing Symposium, Highstown, N. J.

Direct-current, arc-generated plasma equipment was developed that makes possible the melting and deposition of refractory materials of even the highest melting points. The resulting coatings have little porosity, bond well, and are ready for immediate use. The plasma-spraying system was installed for the primary purpose of developing protective coatings for the graphite crucible and other graphite components used in melting and casting uranium. The equipment and auxiliary components are described, along with the procedure used. (P.C.H.)

5838 (RISO-110) METALLURGY DEPARTMENT ANNUAL PROGRESS REPORT FOR THE PERIOD ENDING MARCH 31, 1965. (Atomenergikommissionen, Risoe (Denmark). Forsoegsinstitut). July 1965. 53p. Dep. mn.

Progress in the various research activities is described and results of investigations on the mechanical and physical properties of sintered aluminum products made in order to determine their suitability as structural materials in organic-cooled reactors are presented. (W.L.G.)

5839 (RL-SEP-244(Del.)) CONTINUOUS ELECTROWINNING OF PLUTONIUM METAL. SCALEUP STUDIES: PROGRESS REPORT. Soine, T. S. (General Electric Co., Richland, Wash. Hanford Atomic Products Operation). Apr. 1965. Contract AT(34-1)-1350. 41p. Dep. mn; CFSTI $2.00 cy, $0.50 mn.

Conditions necessary for a cell capable of electrowinning plutonium metal from plutonium trichloride were established. The cell was operated once at 600 g/hr for short periods of time with a total average throughput of 410 g/hr. Several runs were made at lower throughputs. The majority of the runs were of one-shift duration. Large runs attempted during the later stages of the work lasted for about two shifts (12 to 16 hr). The process is capable of handling $PuCl_3$ containing 10 to 20% unchlorinated material (oxide). The upper limit was not determined, but may be as high as 50%. Plutonium metal was electrowon from PuO_2 at 65% electrical efficiency and at a rate of about 65 g/hr. The electrowon product was substantially good. Densities ranged up to 19.4, and the impurity level was about the same as in the feed. Because of the high decomposition potential of $PuCl_3$, little or no purification was observed. Cell life is the essential unsolved problem. The best results pointed to extrapolated lifetimes of 10 to 15 kg throughput (ceramic cells). The plutonium content of the cell at the end of a run, regardless of length of the run, consists of about 200 g of metal and 200 g of slag ($PuCl_3$). This is solubilized fairly easily by hydrochloric acid for subsequent aqueous processing. Several methods for criticality hazards control are suggested. (P.C.H.)

5840 (SB-413(Suppl.1)) BERYLLIUM. Selective Bibliography of Government Research Reports and Translations. (Clearinghouse for Federal Scientific and Technical Information, Springfield, Va.). 1965. 35p. CFSTI Free.

Approximately 550 references on beryllium metals, alloys, compounds, carbides, isotopes, and toxicity and safe handling are given to reports and translations published from approximately 1949 to 1965. (P.C.H.)

5841 (JPRS-32341) ZIRCONIUM AND ITS ALLOYS. Translation of four articles on zirconium and its alloys in the Soviet Union. 32p. (TT-65-32831). CFSTI $2.00 cy, $0.50 mn.

Separate abstracts are included for 3 of 4 papers. The remaining paper was previously abstracted in NSA as 19: 37121. (P.C.H.)

For abstracts of individual papers see: 5854, 5855, and 5899.

5842 REACTOR MATERIALS. Volume 8, Number 1. Dayton, R. W.; Simons, E. M.; Endebrock, R. W. (eds.). Contract W-7405-eng-92. One of the five Quarterly Technical Progress Reviews published for the Division of Technical Information, USAEC. Battelle Memorial Inst., Columbus, Ohio, Spring 1965. 56p. GPO $0.70 Domestic, $0.90 Foreign.

Separate abstracts were prepared for 5 of the 6 sections included. Materials presented at the Third International Conference on the Peaceful Uses of Atomic Energy are listed by session, number, author, and title in the remaining section. These papers were abstracted and indexed in NSA Vol. 18, Nos. 18 and 21. (W.L.G.)

For abstracts of individual sections see: 5843–5846, and 5866.

5843 FUEL AND FERTILE MATERIALS. Reactor Mater., 8: 1-17(Spring 1965).

A summary of recent research developments is presented. (88 references). (W.L.G.)

5844 MODERATOR MATERIALS. Reactor Mater., 8: 18-23(Spring 1965).

A summary of recent research developments is presented. (28 references). (W.L.G.)

5845 NUCLEAR POISONS. Reactor Mater., 8: 24-6(Spring 1965).

A summary of recent research developments is presented. (17 references). (W.L.G.)

5846 CLADDING AND STRUCTURAL MATERIALS. Reactor Mater., 8: 27-44(Spring 1965).

A summary of recent research developments is presented. (85 references). (W.L.G.)

5847 REACTOR MATERIALS. Volume 8, Number 3. Dayton, R. W.; Simons, E. M.; Endebrock, R. W. (eds.). Contract W-7405-eng-92. One of the five Quarterly Technical Progress Reviews published for the Division of Technical Information, USAEC. Battelle Memorial Inst., Columbus, Ohio, Fall 1965. 58p. GPO $0.70 Domestic, $0.90 Foreign.

Separate abstracts were prepared for the 5 sections of the report. (W.L.G.)

For abstracts of individual sections see: 5848–5851, and 5867.

5848 FUEL AND FERTILE MATERIALS. Reactor Mater., 8: 119-34(Fall 1965).

A summary of recent research developments is presented. (70 references). (W.L.G.)

5849 MODERATOR MATERIALS. Reactor Mater., 8: 135-8(Fall 1965).

A summary of recent research developments is presented. (16 references). (W.L.G.)

5850 NUCLEAR POISONS. Reactor Mater., 8: 139-41(Fall 1965).

A summary of recent research developments is presented. (10 references). (W.L.G.)

5851 CLADDING AND STRUCTURAL MATERIALS. Reactor Mater., 8: 142-62(Fall 1965).

A summary of recent research developments is presented. (81 references). (W.L.G.)

Corrosion

Refer also to abstracts 5595, 6024, 6566, and 6666.

5852 (EURAEC-1522) IN-PILE CORROSION OF NUCLEAR MATERIALS. Final Report, March 1, 1962-March 31, 1964. (Centre d'Etude de l'Energie Nucleaire, Brussels (Belgium). Centre d'Etude de l'Energie Nucleaire, Mol (Belgium)). Contract 084-62-3 RDB. 43p. (EUR-2674). Dep. mn; CFSTI $2.00 cy, $0.50 mn.

Work Performed under United States-Euratom Joint Research and Development Program.

Corrosion experiments on aluminum, stainless steel, zirconium, titanium, niobium, zircaloy-2 and platinum were carried out in-pile and after pile irradiation, and the results were compared with those obtained out-of-pile under identical conditions. Two horizontal channels and one vertical channel of the BR1 reactor were used in which the thermal neutron flux was 1.38×10^{12} n/cm^2/sec and the fast neutron flux was 1.4×10^{12} n/cm^2/sec (2.8 Mev). The gamma flux during operation of the reactor was 7.3×10^5 R/hr for energies between 1 and 5 Mev. After shut-down the gamma flux was 2.6×10^5 R/hr for energies from 0.4 to 2.8 Mev. Electrochemical techniques were applied as testing method. It was confirmed that passivation of aluminum is improved by pile irradiation, as indicated by decreased anodic currents and increased oxygen overvoltages. Potential-current curves on 18/8 chrome nickel steels showed that the anodic currents increased with irradiation when the solution was nitrogen, oxygen, or argon saturated and in all acidities. In-pile potential-current measurements on a ferritic steel (CSX) showed large anodic currents and current peaks. These electric currents indicated a strong general corrosion. The post irradiation examination of zirconium, Zircaloy-2, titanium, and niobium showed that the thickness of the initial oxide films on those metals increased with increasing irradiation dose. Gamma rays had a similar, but smaller effect as pile irradiation. It was concluded that the effects of pile irradiation on the corrosion process are mainly solution effects and not so much metal effects. However, the mechanism of the reactions is not well understood. (P.C.H.)

5853 (TIM-898) COLUMBIUM-1 ZIRCONIUM ALLOY FORCED CONVECTION LITHIUM SLAVE LOOP TEST LCCDB-1. Bourdon, P. A.; Bleckerman, S. S.; Schenck, G. F. (Pratt and Whitney Aircraft, Middletown, Conn. Connecticut Advanced Nuclear Engineering Lab.). Oct. 1965. Contract AT(30-1)-2789. 38p. Dep. mn; CFSTI $2.00 cy, $0.50 mn.

Tube specimens of refractory alloys PWC-11 (Nb-1Zr-0.1C), PWC-33 (Nb-3Zr-0.3C), T-111 (Ta-8W-2Hf), FS-85 (Nb-28Ta-10W-1Zr), and W-25 Re were tested for 200 and 1000 hours in the surge tank of Nb-1 Zr alloy forced circulation lithium slave loop LCCDB-1. Specimens were subjected to 2200°F lithium at velocities of 0.45 and 0.88 fps. The slave loop which operated for 6228 hours in an inert atmosphere chamber contained lithium flowing at 250 lb/hr in the maximum velocity regions at a maximum temperature of 2200°F and with a 400°F thermal gradient. Operation of the loop and testing of additional specimens was terminated when the helium to water heat exchanger which cooled the slave loop developed a leak. Lithium attack was not observed in any of the specimens tested. Depletion of both carbide phase and zirconium, attributed to lithium, was observed in PWC-11 and PWC-33 alloys. Single phase surface regions were also observed in T-111 (Ta-8W-2Hf) and FS-85 (Nb-28Ta-10W-1Zr) alloys but could not be attributed to lithium because thermal control specimens heated in argon exhibited the same effect after 1000 hours at 2200°F. Thermally induced grain boundary precipitation of sigma phase occurred in the W-25Re alloy. Although all alloys except the T-111 alloy were softened by both argon and lithium exposure, no decrease in rupture strength was observed except for an expected 10 to 15% decrease in the PWC-11. (auth)

5854 (JPRS-32341, pp 8-16) OXIDATION OF BINARY ALLOYS. Frantsevich, I. N.; Voytovich, R. F. Translated from Mekh. Vzaimodeistviya Metal. s Gaz., Akad. Nauk SSSR, Inst. Fiz. Khim., 135-42(1964).

Studies were made on the oxidation kinetics of a number of high-melting alloys of metals W, Ta, Nb, Ti, Zr, Fe, Co, Ni, and Cu in the temperature range from 500 to 900°C and concentrations of 5, 10, 30, 50, 70, 90, and 95% by weight of the second component. The alloys were melted in an arc furnace and subsequently subjected to homogenizing annealing at 1200°C for 30 hr. Oxidation kinetics were studied by the continuous weighing method for 10 hr at each temperature. The results are presented in the form of graphs characterizing the dependence of the oxidation intensity on the content of the alloying element at various temperatures. (P.C.H.)

5855 (JPRS-32341, pp 24-31) CORROSION OF ZIRCONIUM IN THE ALKALINE METAL CHLORIDE MELT. Volodin, V. P.; Ozeryanaya, I. N.; Smirnov, M. V. Translation from Tr. Inst. Elektrokhim., Akad. Nauk SSSR, Ural. Filial, No. 6, 87-91(1965).

Studies were made on the corrosion of Zr in the molten equimolar mixture of potassium and sodium chlorides, which had been thoroughly freed of all traces of oxygen and moisture, under the atmosphere of argon. Three methods were used: direct determination of the corrosion rate of Zr according to the loss of weight of the sample and the data of the chemical analysis of the melt; computation of the corrosion current from the values of the equilibrium potential; and changes of anodic polarization. The results showed that within the limits of possible errors, the corrosion rate determined by the direct method conforms well with the corrosion rate computed from the values of equilibrium potentials and according to the anodic polarization curves. (P.C.H.)

5856 CORROSION OF AUSTENITIC STAINLESS STEEL DURING EVAPORATION OF RADIOACTIVE SOLUTION. Kurtepov, M. M. At. Energ. (USSR), 19: 153-7 (Aug. 1965). (In Russian).

Descriptions are given of corrosion of austenitic type 18-8 stainless steel vessels used for evaporating radioactive wastes in the form of nitrates. The effects of concentration and temperature of HNO_3 solutions and corrosion products on corrosion of the stainless steel apparatus are discussed and corrosion-protection measures are suggested. (R.V.J.)

5857 ELECTROCHEMICAL ASPECTS OF THE HYDROLYSIS OF UC-10 percent Fe. Antill, J. E.; Peakall, K. A. (Atomic Energy Research Establishment, Harwell, Eng.). Corros. Sci., 5: 739-44(Nov. 1965).

Experiments with sintered compacts of uranium monocarbide showed that anodic conditions and coupling of the carbide to iron reduces the corrosion rate of the carbide in aqueous environments. The results are discussed in relation to the resistance of uranium carbide cemented with iron towards steam and water at elevated temperatures. (auth)

5858 AN ELECTROCHEMICAL MODEL FOR THE OXIDATION OF ZIRCONIUM. Bradhurst, D. H.; Draley, J. E.; Van Drunen, C. J. (Argonne National Lab., Ill.). J. Electrochem. Soc., 112: 1171-7(Dec. 1965).

A simple electrochemical model for gaseous oxidation was derived and applied to the oxidation of zirconium at 700°C. It was concluded that the part of reaction involving electron transport is rate-controlling. The factor determining the difficulty of ion transport was not identified; passage through the oxide film did not seem to be limiting. Half-cell potentials for oxidation and reduction were calculated to be approximately equal. Some variation in the oxide film defect structure with oxidation time was deduced. (auth)

5859 DIFFUSION-CONTROLLED OXIDATION OF SEVERAL LANTHANIDES. Brett, J.; Seigle, L. (General Telephone and Electronics Labs., Bayside, N. Y.). J. Less-Common Metals, 10: 22-8(Jan. 1966).

The high-temperature oxidation of liquid yttrium, lanthanum, neodymium, samarium, gadolinium, terbium, ytterbium, and dysprosium and liquid alloys of these elements with gold was studied to obtain parabolic, diffusion-controlled oxidation-rate constants. The diffusion-controlled oxidation of the heavier lanthanides proceeded at a lower rate. The structure of the sesquioxide that forms is not always that expected from equilibrium studies, which introduces a complexity in the interpretation of the results on a fundamental basis. (auth)

5860 ZIRCONIUM–COPPER ALLOYS RESISTANT TO OXIDATION BY CARBON DIOXIDE AT HIGH TEMPERATURE. Darras, R.; Loriers, H.; Baque, P. (Commissariat a l'Energie Atomique, Gif-sur-Yvette, France; CEN, Saclay, Gif-sur-Yvette, France). J. Nucl. Mater., 17: 79-82(Aug.-Sept. 1965). (In French).

The oxidation kinetics and microhardness of 4 Zr–Cu alloys, a Zr–Cu–Mo alloy, and unalloyed Zr were measured in CO_2 under pressure at temperatures of 600 and 700°C. The results showed that the Zr–2.5% Cu alloy had the best oxidation resistance. The diffusion tests showed that at 600°C the addition of Cu decreases significantly the diffusion coefficient of oxygen in the zirconia, but has little effect on the diffusion coefficient in the metallic phase. At 700°C the values of these two coefficients are lowered by the addition of Cu. (J.S.R.)

5861 CAVITATION DAMAGE RESISTANCE OF MATERIALS IN LIQUID SODIUM. Thiruvengadam, A.; Couchman III, C.; Preiser, H. S. (Hydronautics, Inc., Laurel, Md.). J. Spacecraft Rockets, 2: 267-9(Mar.-Apr. 1965).

Five metals were studied—pure iron, nickel 201, inconel 600, 316 stainless steel, and titanium 100A. The relation between the rate of cavitation damage and the test duration is discussed. The effects of variations in the displacement amplitude of the specimen and in the liquid sodium temperature up to 1000°F on the rate of weight loss are considered. The correlation of the strain energy of the metal with volume loss rate is described. The intensity of cavitation damage is defined and is calculated for the steady-state zone. (M.J.T.)

Fabrication

Refer also to abstracts 5874 and 6624.

5862 (EURAEC–1481) THE STAINLESS STEEL PLATING OF VERY THICK STEELS. Quarterly Report No. 4, April 1–June 30, 1965. (Neratoom, N. V., The Hague (Netherlands). Ghent Rijksuniversiteit (Belgium). Soudometal, S. A., Brussels (Belgium)). Contract 008-63-12 TEEB. 43p. Dep. mn; CFSTI $2.00 cy, $0.50 mn.

Work Performed under United States–Euratom Joint Research and Development Program.

The composition and microstructures of the transition zone between the 18/10 stainless steel plating and the 1.2 MD07 A or Soudotenax 56 low alloy steel base were investigated. Variations in the Cr and Ni contents in the transition zone were attributed to structural irregularities. Metallography revealed intergranular precipitates of unknown composition in the bonding area and a bainite structure in the heat-affected zone of the base metal. (W.L.G.)

5863 (NLCO–945) THE EFFECTS OF VARIOUS FABRICATION VARIABLES ON TEXTURE GRADIENTS IN URANIUM FUEL CORES. Henry, P. E. (National Lead Co. of Ohio, Cincinnati). May 4, 1965. Contract AT(30-1)-1156. 16p. (CONF-650210–4). Dep. mn; CFSTI $1.00 cy, $0.50 mn.

From Application of X-Ray Diffraction in the Atomic Energy Field Meeting, Richland, Wash.

Uranium fuel cores produced by various fabrication processes and having different heat treatments were evaluated by x-ray diffraction to determine the effect of geometry, heat-treatment quenching media, and certain fabrication characteristics on theoretical growth indexes. These indexes were used to predict the anisotropic growth tendencies of the cores under irradiation by thermal neutrons. A shorter method of investigating texture gradients in the longitudinal, circumferential, and radial direction by examination of only three points across the core wall is discussed. (auth)

5864 (ORNL–3879) LABORATORY PREPARATION OF URANIUM NITRIDE MICROSPHERES BY A SOL-GEL TECHNIQUE. Gens, T. A.; Helton, D. M.; Clinton, S. D. (Oak Ridge National Lab., Tenn.). Nov. 1965. Contract W-7405-eng-26. 26p. Dep. mn; CFSTI $2.00 cy, $0.50 mn.

Methods were successfully developed for preparing urania-carbon sols and converting these sols into gel microspheres. Two methods were investigated for converting the gel microspheres into UN microspheres: heating the gel microspheres in nitrogen to produce uranium nitride directly; and heating in argon to produce uranium carbide, then in nitrogen to produce uranium nitride from the carbide. Both methods appear promising. The second method always yields a product containing carbon. (auth)

5865 (WCAP–3269-37) A NEW ZIRCALOY END CLOSURE WELD JOINT CONFIGURATION. Duncan, R. (Westinghouse Electric Corp., Pittsburgh, Pa. Atomic Power Div.). Sept. 1965. Contract AT(30-1)-3269. 14p. Dep. mn; CFSTI $1.00 cy, $0.50 mn.

A new welded closure offering increased reliability at reduced processing cost was developed. Combining the attachment of the end plug to the Zircaloy-4 cladding with closure of the gas vent hole reduces the number of welding operations per element from 3 to 2. In order to assure that the new closures would not exhibit unusual corrosion effects and thus complicate final evaluation of loop test results, it was decided to make them under normal weld box conditions. The design is illustrated. (P.C.H.)

5866 SPECIAL FABRICATION TECHNIQUES. Reactor Mater., 8: 45-51(Spring 1965).

A summary of recent research developments is presented. (49 references). (W.L.G.)

5867 SPECIAL FABRICATION TECHNIQUES. Reactor Mater., 8: 163-73(Fall 1965).

A summary of recent research developments is presented. (29 references). (W.L.G.)

5868 METHOD OF WELDING TOGETHER THE SHEATHING TUBES OF NUCLEAR FUEL OR BREEDER ELEMENTS WITH THEIR END CLOSURES. Blomeyer, Walter (to Nuklear-Chemie und -Metallurgie GmbH). German Patent 1,200,966. Sept. 16, 1965. Filed July 26, 1963.

The inside of the sheathing tube is kept under reduced pressure (1 torr) in relation to the outside (760 torr). The welding chamber is filled with an inert gas atmosphere (Ar). (Gmelin Inst.)

5869 METHOD FOR THE FABRICATION OF COMPACT URANIUM DIOXIDE PARTICLES OF A PREDETERMINED GRAIN SIZE. Mueller, Norbert; Ruprecht, Manfred; Meyer, Wolfgang (to Nuklear-Chemie und -Metallurgie GmbH). German Patent 1,201,320. Sept. 9, 1965. Filed Mar. 5, 1964.

Compact uranium dioxide particles are fabricated by the

steps of mixing uranium dioxide powder with an organic binding agent, heating the mixture, compacting the mixture by rolling or pressing, grinding the mass obtained to a predetermined grain size, rounding off the particles, separating undesired fractions, and sintering the remaining particles. (Gmelin Inst.)

5870 METHOD FOR THE PRODUCTION OF URANIUM. Cacciari, Alberto; de Leone, Ruggero; Ferrari, Sergio; Cogliati, Guido (to Comitato Nazionale per l'Energia Nucleare). German Patent 1,202,505. Oct. 7, 1965. Priority date Dec. 5, 1961, Italy.

The method consists of reducing uranyl nitrate solutions containing at least 0.5 moles of free nitric acid per mole of uranium catalytically with gaseous hydrogen at ambient temperatures. Double uranium fluoride is precipitated by adding 5.5 moles of hydrofluoric acid and 1.2 moles alkaline salt. The fluoride is dried and mixed with magnesium. The mixture is pressed using a pressure of more than 0.5 t/cm^2. The pressed body is thermally reduced to uranium metal. (Gmelin Inst.)

5871 MANUFACTURE OF NUCLEAR REACTOR FUEL ELEMENTS. Fairhurst, William (to United Kingdom Atomic Energy Authority). U. S. Patent 3,210,255. Oct. 5, 1965. Priority date Dec. 8, 1960, Great Britain.

A process for the manufacture of a reactor fuel element from a fuel member of either U or a U-base alloy and a Mg-base alloy sheath of the grain size includes the steps of pressurizing the sheath at a temperature, such that uncontrolled grain growth of the material of the sheath doses not occur, into keying contact with the grooves in the fuel member to prevent longitudinal movement between the element and the sheath, and allowing the assembly to cool. After cooling, the assembly is annealed at a temperature substantially above the range of 350–470°C at which the fuel element is intended to operate to effect recrystallization of the material of the sheath to a structure that is relatively stable in grain size in the temperature range in order to discourage the formation of large grain structure favorable to leak paths. (B.L.M.)

5872 MANUFACTURE OF NUCLEAR REACTOR FUEL ELEMENTS. Heal, Thomas John; Morrison, Ian Hugh (to United Kingdom Atomic Energy Authority). U. S. Patent 3,210,526. Oct. 5, 1965. Priority date Dec. 8, 1960, Great Britain.

The process described in U. S. Pat. 3,210,255 for the fabrication of U and U-base alloy fuel elements sheathed with a Mg-base alloy of fine grain size is applied particularly to the fabrication of fuel elements for operation in the temperature range of 140–350°C. The process provides a sheath with sufficient ductility to discourage cavitation failures on subjecting the element to prolonged straining at the operating temperature since there is little tendency to grain growth within that temperature range. (B.L.M.)

5873 PROCESS FOR MAKING NUCLEAR FUEL ELEMENT. Burnham, John B. Jr.; Darrah, James G. (to General Motors Corp.). U. S. Patent 3,214,499. Oct. 26, 1965. Filed Nov. 29, 1962.

A process for making a nuclear reactor fuel element consists of forming a uniform pulverized mixture of from 5 to 90 wt % graphite bonded with UC having a grain size of from 40 to 200 mesh; from 0 to 90 wt % SiC, and from 5 to 15 wt % organic resin binder; forming the mixture into a briquette; and then immersing the briquette into molten Si maintained at a temperature of from 3200 to 3600°F. (B.L.M.)

Properties and Structure

See *also* CHEMISTRY — Inorganic and Physical Chemistry

Refer also to abstracts 5611, 5726, 6023, 6565, and 6602.

5874 (AGARDograph-94) HANDBOOK ON THE PROPERTIES OF NIOBIUM, MOLYBDENUM, TANTALUM, TUNGSTEN AND SOME OF THEIR ALLOYS. Syre, R. (Advisory Group for Aeronautical Research and Development, Paris (France)). May 1965. 302p. Dep. mn. In English and French.

The latest data on the physical, mechanical (at low or elevated temperatures), chemical, welding, fabrication, and miscellaneous properties for the four refractory metals (Nb–Ta–Mo–W) and their alloys (commercial or under development) are reported. Protective coatings are also discussed, and properties of the main protective coatings are given. 269 references are cited. (auth)

5875 (ANL-6925, pp 165-74) HIGH TEMPERATURE REACTOR MATERIALS DEVELOPMENT. Edwards, R. K.; Feder, H. M. (Argonne National Lab., Ill.).

The status of work on high-temperature phase relations and thermodynamics of U–uranium oxide systems is reviewed. Data and information on vapor pressures and effusion of U–uranium oxide systems are included along with results of transpiration studies of vaporization, U–uranium oxide phase studies, and U–US phase studies. (J.R.D.)

5876 (ANL-6974) PHASE STUDIES ON U–20w/o Pu–Fs ALLOYS. Kruger, Owen L. (Argonne National Lab., Ill.). May 1965. Contract W-31-109-eng-38. 44p. Dep. mn; CFSTI $2.00 cy, $0.50 mn.

The phase transformations, microstructures, and melting points of alloys containing U-20 wt. % Pu–Fs were investigated as part of a broad program to evaluate plutonium-containing fuel materials of interest for the second loading of Experimental Breeder Reactor-II. The term fissium denotes the elements Ru, Mo, Pd, Te, Rh, Zr, and Nb in the proportions that are left in the fuel after pyrometallurgical refining. Crystallographic data are presented for the alpha and gamma uranium phases and other intermediate phases that occur in these alloys. A primary phase termed theta was present in all the alloys to their melting points. Transformations of the matrix phases appear to be somewhat similar to those in the U–Pu–Mo system. The gamma uranium phase was stable down to 555°C, and at high fissium contents, the beta transformation was entirely suppressed. All alloys contained matrix phases of alpha uranium, gamma-prime, and zeta at 400°C, and these phases appeared to be in equilibrium to room temperature. Analysis of the transformations that occur in the matrix phases showed that the phase relationships of the fissium alloys can be schematically represented by a pseudoternary system in which U, Pu, and Fs are the components. The microstructures of an injection-cast fuel pin were also examined. (auth)

5877 (ANL-7048) A THERMODYNAMIC STUDY OF THE URANIA–URANIUM SYSTEM. Ackermann, R. J.; Rauh, E. G.; Chandrasekharaiah, M. S. (Argonne National Lab., Ill.). July 1965. Contract W-31-109-eng-38. 34p. Dep. mn; CFSTI $2.00 cy, $0.50 mn.

The phase diagram for the uranium-oxygen system from 1600 to 2500°K for the composition range of the bivariant urania phase was investigated in three steps. The composition of the urania phase in equilibrium with liquid uranium was determined by an isopiestic method. This phase dissolves uranium up to a composition given by the ratio O/U = 1.82 at 2500°K. The total volatility rates for urania-liquid uranium mixtures were measured by means of the effusion method from 1580 to 2400°K. An effective vapor pressure p_e was calculated from the measured effusion rates, assuming the vapor to be UO(g). The least-squares treatment of the data resulted in the expression $\log p_e$ (atm) = (7.25 ± 0.14) – (27,024 + 255)/T. A mass-spectrometric investigation of the same system showed the vapor to be predominantly UO(g) with smaller amounts of U(g) and UO_3(g). The thermodynamic data for UO(g), UO_2(g), and UO_3(g) were examined for internal consistency. (P.C.H.)

5878 (BNL-9667) CHEMICAL CONSIDERATIONS IN FAST REACTOR SAFETY. Castleman, A. W. Jr.; Tang,

I, N. (Brookhaven National Lab., Upton, N. Y.). Oct. 1965. Contract AT(30-2)-Gen-16. 24p. (CONF-651009-6). Dep. mn; CFSTI $1.00 cy, $0.50 mn.

From Conference on Safety, Fuels and Core Design in Large Fast Power Reactors, Argonne, Ill.

The results of studies on the chemical states of iodine released from U and UC into helium between 1200 and 2500°C are summarized. The iodine chemical states formed upon release from these fuels into air and steam are given, and calculations are included that predict the behavior of iodine in sodium based on thermodynamic considerations. It was concluded that the relative quantities of each species is primarily a function of fuel temperature. The two iodides are tenaciously held on surfaces at temperatures of ~275 and 200°C in an inert atmosphere, but readily evolve elemental iodine into an oxidizing environment. Where iodine is released during a metal-water reaction, conversion to HI can be validly estimated from thermodynamic considerations. (P.C.H.)

5879 (D-910092-6) EXPERIMENTAL REFRACTIVE INDICES AND THEORETICAL SMALL-PARTICLE SPECTRAL PROPERTIES OF SELECTED METALS. Marteney, P. J.; Krascella, N. L.; Burwell, W. G. (United Aircraft Corp., East Hartford, Conn. Research Labs.). Sept, 1965. Contract NASw-847. 62p.

An applied research program was conducted to determine the absorption, scattering, and extinction parameters of small spherical metal particles which might be employed as seeding agents to control radiant heat transfer in gaseous nuclear rocket engines. Under the experimental phase of the program, measurements were made using an ellipsometric technique to determine the complex refractive indices of hafnium, molybdenum, nickel, and tungsten in the wavelength range between 0.2 and 0.7 micron. Under the theoretical phase of the program, calculations were made using the Mie theory to determine spectral absorption, scattering, and extinction parameters of small spherical particles made from nine different metals. These calculations were made using values of the complex refractive indices of the four metals investigated in the experimental phase of the program and the complex refractive indices for cobalt, iron, titanium, vanadium, and zirconium determined from the current literature. Calculations were also made of the Rosseland mean opacity parameter of 0.05μ-radius tungsten particles using spectral absorption parameters determined from the Mie theory. (auth)

5880 (EURAEC-1310) RESEARCH TO DETERMINE THE LONG-TERM MECHANICAL PROPERTIES OF METALS SUBJECTED TO MECHANICAL STRESS AT ELEVATED TEMPERATURES AND NEUTRON IRRADIATION. Eighth Quarterly Report. Siegfried, W.; Zimering, S. (Battelle Memorial Inst., Geneva (Switzerland)). Mar. 1965. Contract 100-62-12 RDS. 63p. Dep. mn; CFSTI $3.00 cy, $0.75 mn.

Work Performed under United States–Euratom Joint Research and Development Program.

A description is given of a system of mathematical criteria that verifies if a given set of experimental data can be represented by an exponential function of real order and if the data is complete enough and without too much scatter to be so. The results of extrapolations of isothermal, isobaric, and isothermal-isobaric data are presented as a verification of the method. The physical meaning of the mathematical parameters of the exponential function are illustrated. (W.L.G.)

5881 (EURAEC-1441) A STUDY ON EMBRITTLEMENT BY PLASTIC FATIGUE IN REACTOR VESSELS. Quarterly Report No. 6, April 1–June 30, 1965. (Centre National de Recherches Metallurgiques, Liege (Belgium)). July 1965. Contract 005-63-12-TEEB. 18p. Dep. mn; CFSTI $1.00 cy, $0.50 mn.

Work Performed under United States–Euratom Joint Research and Development Program.

Charpy-V-notch-impact bending tests on fatigue samples damaged under tensile stress and compression were continued on three types of steel (ZD, ZS, and ZA). Fatigue processing consisted in a number of comparatively small cycles of alternate plastic deformations at ambient temperature. The behavior of the steels under study was found to be rather different according to the importance of the damage to which they were subjected. However, it was possible to trace a general tendency in which impact energies corresponding to crystalline ruptures increase in relation to the number of cycles of the damage applied. Finally, Charpy V transition temperatures tend to increase in a significant manner; however, the importance of this increase does not seem to be related with the initial values of the transition temperature of the materials under study. Additional Side Bend Embrittlement Tests after fatigue under alternate biaxial bending at ambient temperature and at 300°C were also carried out. These tests confirmed the general impression that an embrittlement of the steel occurs already with the first cycles of plastic fatigue. (auth)

5882 (EURAEC-1454) PHYSICAL PROPERTIES OF UO_2 SINGLE CRYSTALS. Quarterly Report No. 12, November 1, 1964–March 31, 1965. (Centre d'Etude de l'Energie Nucleaire, Mol (Belgium)). Contract 056-64-3 TEEB. 26p. (EUR-2384; R-2354). Dep. mn; CFSTI $2.00 cy, $0.50 mn.

Work Performed under United States–Euratom Joint Research and Development Program.

Two independent methods were developed allowing the determination of oxygen self-diffusion in UO_2. The reprecipitation of U_4O_9 after heating in the electron microscope until complete disappearance was studied in further detail. Generally, a much denser set of precipitates was detained after cooling than before heating. Exceptionally the precipitates were observed to precipitate apparently in the same sites as before dissolution. Pulse annealing experiments were performed on quenched UO_{2+x} crystals with compositions slightly exceeding the excess oxygen solubility limit at room temperature. Upon heating at temperatures above 110°C, the oxygen interstitials start migrating and form U_4O_9 precipitates. The activation energy for this migration process was found to be about 0.9 ± 0.1 ev. Several measurements of the thermoelectric power of as-grown and reduced crystals indicate an activation energy for the number of charge carriers of about 0.05–0.08 ev in the temperature range 140–350°K. The magnetic susceptibility of two single crystals of composition $UO_{2.056}$ was measured between 7 and 17 kOe at temperatures between 90 and 300°K. The results are discussed. The thermal conductivity of a second well reduced single crystal was determined in the temperature range 4 to 300°K. Again a maximum in the thermal conductivity (187 mw|°K|cm) is found at 6.2°K. The elastic constants of UO_2 were determined in two different crystallographic directions using a single crystal prepared at Nukem. Combining these results with earlier measurements, a complete set of elastic constants of UO_2 was obtained. (P.C.H.)

5883 (IS-1268) MEASUREMENT OF PIEZORESISTANCE IN SEMICONDUCTORS. Temple, Paul Arthur; Danielson, G. C. (Ames Lab., Iowa State Univ. of Science and Tech.). Nov. 1965. Contract W-7405-eng-82. 46p. Dep. mn; CFSTI $2.00 cy, $0.50 mn.

Apparatus for the measurement of piezoresistance in semiconductors was designed and constructed. A method of stressing the sample using gas pressure applied across a bellows was incorporated. This method of stressing made it possible to vary the stress applied to the sample without disturbing the sample temperature. The linear combination of the piezoresistance tensor components of n-type germanium was measured over the temperature range from 50 to 300°K. (auth)

5884 (LA-2312) BEHAVIOR OF SOME DELTA-STABILIZED PLUTONIUM-GALLIUM ALLOYS AT HIGH PRESSURES. Elliott, R. O.; Gschneidner, K. A. Jr. (Los Alamos Scientific Lab., Univ. of California, N. Mex.). Apr. 1, 1959. Contract W-7405-eng-36. 20p. Dep. mn; CFSTI $1.00 cy, $0.50 mn.

A number of delta-stabilized plutonium-gallium alloys were subjected to pressures as high as 11,000 atm at 24°C. Transformation pressures and volumes, compressibilities, densities, and hardnesses of these alloys were determined as a function of composition, and the effect of gallium content on the stability of delta plutonium was studied and related to the plutonium-gallium phase diagram. (auth)

5885 (NAS-CR-54773) GENERATION OF LONG TIME CREEP DATA OF REFRACTORY ALLOYS AT ELEVATED TEMPERATURES. Ninth Quarterly Report, June 26, 1965–September 26, 1965. Sawyer, J. C.; Steigerwald, E. A. (TRW Equipment Labs., Thompson Ramo Wooldridge Inc., Cleveland, Ohio). Oct. 8, 1965. Contract NAS-3-2545. 107p. CFSTI $4.00 cy, $0.75 mn.

A summary of creep data obtained to date on W, W-25% Re, Sylvania A, Mo base alloys TZC and TZM, Nb base alloys Nb 132M and As-30, and the Ta alloy T-222 is presented. A review of the processing history of all the alloys is appended. Considering the high-strength refractory alloys on a stress-to-weight basis, the TZC material was found to have creep resistance that was significantly superior to the other alloys. The data obtained on T-222 indicate that it has creep resistance that is substantially inferior to the Mo-base alloys. Preliminary results indicated that no consistent variation in chemical composition had occurred in any of the materials as a result of creep test exposure. (P.C.H.)

5886 (NASA-TN-D-3120) SUMMARY OF THERMOPHYSICAL PROPERTIES OF POTASSIUM. Coe, Harold H. (National Aeronautics and Space Administration, Cleveland, Ohio. Lewis Research Center). Dec. 1965. 39p. CFSTI $2.00 cy, $0.50 mn.

Recently reported thermodynamic and physical property data on the alkali metal potassium are compiled and the results of the various sources are compared with previously existing data. Data for the liquid properties of specific heat, thermal conductivity, enthalpy, entropy, viscosity, electrical resistivity, density, and surface tension are presented over the temperature range from 200 to 2200°F when possible. Data for the saturated vapor properties of specific heat, thermal conductivity, vapor pressure, heat of vaporization, entropy of vaporization, viscosity, and density are presented over the temperature range from 800 to 2200°F. The results from the several sources agree very well for most of the properties in the lower temperature range up to about 1400°F. However, significant differences are apparent for some of the properties at temperatures above 1400°F. (auth)

5887 (NLCO-953) A STUDY OF AS-CAST AND HEAT-TREATED URANIUM-BASE DILUTE-CARBON ALLOYS BY OPTICAL AND ELECTRON MICROSCOPY. Althaus, William A.; Cook, Marlin M.; Bieker, Richard J. (National Lead Co. of Ohio, Cincinnati). May 5, 1965. Contract AT(30-1)-1156. 10p. (CONF-650602-79). Dep. mn; CFSTI $1.00 cy, $0.50 mn.

From American Nuclear Society 11th Annual Meeting, Gatlinburg, Tenn.

Optical and electron microscopy techniques were used to study the additive effects of carbon on uranium. Observation of uranium samples with carbon contents of 40, 140, and 270 ppM showed a progressive increase in network particle density. A tentative peritectic phase diagram is proposed to explain data on the C–U system. Carbon effects on hardness are also described. It was concluded that reactor fuel cores alloyed with carbon are not suitable for gamma heat treatments. (P.C.H.)

5888 (NP-15592) LOW TEMPERATURE RESISTIVITY OF YTTRIUM-BASED ALLOYS CONTAINING SMALL AMOUNTS OF RARE EARTH METALS. Series A, No. 171. Sugawara, Tadashi (Tokyo Univ. (Japan). Inst. for Solid State Physics). Sept. 1965. 33p. Dep. mn.

The resistivity of the dilute alloys of rare earth metals with yttrium was measured at low temperatures. The result is in qualitative agreement with the recent theories due to Kondo and others on the s-d or s-f scattering. The effective s-f exchange integrals for various rare-earth solutes were derived from the analysis of the resistivity data and compared with the reported values in other matrices. The integral for Ce is negative, leading to a resistance minimum, while those for heavier rare earths are positive. The sign of the integral is discussed in terms of the mixing of conduction electrons with localized 4f electrons. The increase of the residual resistivity due to added rare earths depends upon the number of 4f electrons of the solute in a complicated way and is anomalously large for lighter rare earths such as La, Ce, and Pr. (auth)

5889 (NUMEC-2389-8) EFFECT OF PuO_2 CONTENT ON SINTERING BEHAVIOR OF MECHANICALLY MIXED UO_2–PuO_2. Houston, M. D. (Nuclear Materials and Equipment Corp., Apollo, Pa.). [1964]. Contract AT(30-1)-2389. 21p. Dep. mn; CFSTI $1.00 cy, $0.50 mn.

Studies indicated that physical densities in excess of 90% of theoretical can be readily achieved with the use of mechanical-blended feed powders in the practical composition range of UO_2 to UO_2–40% PuO_2. The results further show that solid solution is difficult to achieve by the blending and sintering techniques used and hence that there may be differences in in-pile behavior between pellets prepared from coprecipitated feed and those prepared by the mechanical blending of component powders. This indicates that further effort is warranted to improve blending procedures and to ascertain sintering conditions that are more amenable to solid solution formation. The data further indicate some interesting effects in the UO_2–PuO_2 system and, in addition, verify some effects previously reported by others. The data should be useful for the ultimate preparation of the U–Pu–O phase diagram and indicate areas where further work can be fruitfully performed. (auth)

5890 (NUMEC-2389-9) THERMAL EXPANSION OF COPRECIPITATED (U, Pu)O_2 POWDERS BY X-RAY DIFFRACTION TECHNIQUES. Roth, J.; Halteman, E. K. (Nuclear Materials and Equipment Corp., Apollo, Pa.). Oct. 1965. Contract AT(30-1)-2389. 67p. Dep. mn; CFSTI $3.00 cy, $0.75 mn.

A high temperature x-ray powder diffraction study was made of the (U,Pu)O_2 system over the entire composition range using a Materials Research Corporation high temperature, high vacuum diffractometer. An internal standard, thoria, was used for temperature determination. The polynomial expansions giving the lattice parameter as a function of temperature in °C to 1200°C for the compositions studied are given along with polynomial expansions for coefficient of thermal expansion as function of composition in weight percent at various temperatures and as function of temperature to 1200°C for compositions studied. The results showed that there is no simple relation between temperature, thermal expansion coefficient, and composition. Data are tabulated. (P.C.H.)

5891 (NYO-2159-1) METALLURGICAL STUDIES OF ZIRCONIUM AND THORIUM AND OF THE ALLOYING BEHAVIOR OF RARE EARTH-TRANSITION METAL SYSTEMS. Final Report. Clough, W. R. (Rensselaer Polytechnic Inst., Troy, N. Y. Dept. of Materials Engineering). Nov. 1, 1965. Contract AT(30-1)-2159. 99p. Dep. mn; CFSTI $3.00 cy, $0.75 mn.

The effects of rare earth elements on the allotropic transformation of zirconium was studied in terms of its thermodynamic and electronic nature. In addition to the partial phase diagrams, the complete zirconium-yttrium equilibrium diagram was experimentally determined. The recrystallization kinetics of Zr-rich Zr-rare earth alloys was determined and explained. Heat of solution and heat of formation calorimetry experiments were done with the same materials, and thermodynamic explanations of observed behavior were developed. The effect of rare earth solutes on the liquid surface tension of zirconium and thorium solvents were measured by the drop method. Thorium-rare earth allotropic phase boundaries were experimentally determined

under equilibrium conditions, and the effect of valence on Q_b was determined for Zr and Th solvents. Amplitude dependent internal friction measurements were performed on dilute solid solutions of Zr-rare earth binary alloys, and interactions between solute atoms and dislocations were studied. Work-hardening and fracture behavior of Zr and Zr-rare earth alloys were studied by tensile tests, optical metallography, and electron microscope means. (auth)

5892 (PWAC–476) FISSION GAS MIGRATION STUDIES IN URANIUM CARBIDE. DeCrescente, M. A.; Selleck, E. G. (Pratt and Whitney Aircraft, Middletown, Conn. Connecticut Advanced Nuclear Engineering Lab.). Oct. 1965. Contract AT(30-1)-2789. 16p. Dep. mn; CFSTI $1.00 cy, $0.50 mn.

A technique is described for studying migration of inert gases in nuclear fuels using ion bombardment and replication electron microscopy. Helium atoms were agglomerated into 100–5000 Å bubbles which moved up an indicating temperature gradient. The velocity, which was found to be inversely proportional to bubble size, indicated a surface diffusion controlled mechanism. (auth)

5893 (PWAC–480) THERMAL CONDUCTIVITY AND ELECTRICAL RESISTIVITY OF URANIUM MONOCARBIDE. Hayes, B. A.; DeCrescente, M. A. (Pratt and Whitney Aircraft, Middletown, Conn. Connecticut Advanced Nuclear Engineering Lab.). Oct. 1965. Contract AT(30-1)-2789. 24p. Dep. mn; CFSTI $1.00 cy, $0.50 mn.

The thermal conductivity of 95% dense uranium carbide with 860 ppM oxygen and 520 ppM nitrogen was found to be 0.175 ± 0.005 watts/cm-C in the temperature range 1100 to 1600°C. The effect of increasing the combined oxygen and nitrogen impurity level from 1380 to 2180 ppM was minor; however, a general lowering of the thermal conductivity was observed when the impurity level increased from 1380 to 4000 ppM. The portion of the thermal conductivity due to electrons, estimated from electric resistivity data and the Weidemann-Franz relationship, was found to be almost 100% at temperatures above 1000°C. Considerable agreement with previous results was found. A study of all the data indicates that the thermal conductivity of uranium carbide does not vary significantly with temperature in the range 1000 to 2000°C. (auth)

5894 (SWRI–1228-3-3) NONDESTRUCTIVE TESTING OF PLASTIC FATIGUE PRESSURE VESSELS. Final Report. Lautzenheiser, Clarence E.; Whiting, Allen R. (Southwest Research Inst., San Antonio, Tex.). Nov. 5, 1965. Contract AT(11-1)-1228. 112p. Dep. mn; CFSTI $4.00 cy, $1.00 mn.

Nondestructive testing techniques were utilized to improve knowledge and inspection procedures necessary for the determination of crack initiation and propagation rate in pressure vessel materials subjected to low cycle plastic fatigue conditions. Pressure vessels were nondestructively inspected using radiographic, ultrasonic, magnetic particle and penetrant techniques at discreet intervals in the vessel's cyclic life. The results of these inspections were plotted against the cyclic life of the pressure vessels and curves representing defect magnitude (length, depth, cross-sectional area, etc.) were produced. Also from the curves, fatigue crack propagation rates can be determined for each of the test conditions. These curves can be used to indicate possible life expectancy, on a fatigue basis, for pressure vessels in service under similar conditions. (auth)

5895 (TID–22271) INTERACTION OF SOLID METAL AND LIQUID ALLOYS. Final Report. Chalmers, Bruce (Gordon McKay Lab. of Applied Science, Harvard Univ., Cambridge, Mass.). Sept. 1965. Contract AT(30-1)-1956. 16p. Dep. mn; CFSTI $1.00 cy, $0.50 mn.

Developments in the understanding of solidification are discussed. Studies were made primarily on: atomic processes that take place at the interface between a crystalline solid and liquid; and influence of crystallography, heat flow, and diffusion on the morphology of the growing crystals. (P.C.H.)

5896 (TID–22388) STUDY OF ALLOYS IN THE COLUMBIUM–ALUMINUM–TITANIUM SYSTEM. Final Report. Rhines, Frederick N. (Florida Univ., Gainesville. Engineering and Industrial Experiment Station). June 30, 1961. Contract AT(11-1)-171; Subcontract AT-153. 130p. Dep. mn; CFSTI $4.00 cy, $1.00 mn.

For General Electric Co., Cincinnati, Ohio. Aircraft Nuclear Propulsion Dept.

The constitution diagram and oxidation behavior of eleven binary and nine ternary alloys in the Al–Nb–Ti ternary system were studied. X-ray diffraction studies are reported on the binary alloys and the Nb–Al–Ti (CAT) alloys. The x-ray method was also used for identifying the phases present in oxidized layers produced during oxidation treatments. Metallographic techniques were developed and applied to the examination of both binary and ternary cast alloys. Oxidation runs were made on a total of ten binary alloys and nine CAT alloys using an apparatus that permitted measurement of the amount of oxygen that reacted with the specimen as a function of time. The experimental data were plotted logarithmically to obtain the constants n and k that enter into the general expression for rate of oxidation. Irregularities in oxidation behavior were tentatively explained in terms of excess surface area associated with cracks and porosity and also as a result of gas evolution from the specimen during oxidation. From the x-ray and metallographic data a tentative isothermal section at 850°C is proposed for the Nb–Al–Ti system. Isomorphism was found between $NbAl_3$ and $TiAl_3$, with two-phase fields involving Al and TiAl, respectively, on the Al- and Ti-sides of this single phase region. The AlTi phase extends far into the ternary diagram but appears to experience a solid state reaction below 850°C. (P.C.H.)

5897 (TID–22420) EFFECTS OF NEUTRON DAMAGE ON THE MECHANICAL PROPERTIES OF PYROLYTIC AND SINGLE CRYSTAL GRAPHITE. Semiannual Progress Report, January 1–June 30, 1965. Meers, J. T. (Union Carbide Corp., Parma, Ohio. Carbon Products Div.). Nov. 5, 1965. Contract AT(40-1)-3237. 63p. Dep. mn; CFSTI $3.00 cy, $0.75 mn.

Pre-irradiation testing of compression-annealed pyrolytic graphite was completed. A set of elastic compliance and stiffness constants was obtained for compression-annealed pyrolytic graphite. In addition, the behavior of this material when subjected to shear is described and the stress-strain curve for shear is given. Values for shear strength of single-crystal graphite are also given. Work has continued on the problem of measuring the tensile strength of single-crystal graphites. (auth)

5898 (WAPD-TM–519) ANGULAR VALUES BETWEEN CRYSTALLOGRAPHIC PLANES IN ZIRCONIUM AS USED IN TRANSMISSION ELECTRON MICROSCOPY. Katz, O. M. (Bettis Atomic Power Lab., Pittsburgh, Pa.). Nov. 1965. Contract AT-11-1-GEN-14. 20p. Dep. mn; CFSTI $1.00 cy, $0.50 mn.

The angular values between crystallographic planes in zirconium, as used in transmission electron microscopical studies, are presented for utilization in diffraction pattern analyses due to a recently devised computer program. (auth)

5899 (JPRS–32341, pp 1-7) VISCOSITY OF LIQUID ZIRCONIUM. Elyutin, V. P.; Maurakh, M. A.; Pen'kov, I. A. Translated from Izv. Vyssh. Ucheb. Zaved., Chern. Met., 8: No. 7, 128-32 (July 1965).

The viscosity of liquid zirconium was measured at temperatures up to 2400°K using the method of torsional oscillations of the crucible filled with liquid metal. The results showed that near the melting point, the kinematic viscosity of Zr is high (1.2 to 1.4 centistokes). However, with an increase in temperature the kinematic viscosity of Zr decreases evenly to 0.25 centistokes at about 2,400°K. Determination of the dynamic viscosity of Zr is also discussed. (P.C.H.)

5900 BERYLLIUM AGING. Papirov, I. I. At. Energ. (USSR), 19: 144-53 (Aug. 1965). (In Russian).

A review is given of the data on improving beryllium

plasticity at 400 to 600°C. Thermal treatment of beryllium results in separation of impurities from the saturated solution which in turn changes metal properties, specifically plasticity, hardness, creep, and electric resistance. Descriptions are given of the mechanism of beryllium aging and means for increasing beryllium plasticity at high temperatures. (tr-auth)

5901 DEPENDENCE OF HEAT CONDUCTIVITY OF SODIUM ON CONCENTRATION OF OXIDES. Kozlov, F. A.; Antonov, I. N. At. Energ. (USSR), 19: 391-2(Oct. 1965). (In Russian).

The thermal conductivity of sodium with various concentrations of Na_2O was determined by measuring the temperature distribution along the length of a pipe filled with a Na-Na_2O mixture and heated at one end. Results of the dependence of the thermal conductivity on the average oxide concentration at 328°K are presented. Errors in the results are within ±25%. The results show that for a 50 to 60% increase in the oxide concentration the thermal conductivity decreases to less than half its original value. (M.J.T.)

5902 BRITTLE AND PLASTIC BEHAVIOR OF HOT-PRESSED BeO. Bentle, G. G.; Kniefel, R. M. (Atomics International, Canoga Park, Calif.). J. Amer. Ceram. Soc., 48: 570-7(Nov. 21, 1965).

The flow and fracture mechanisms of hot-pressed polycrystalline BeO were studied. Modulus of rupture tests were made from −196 to 1800°C on specimens of constant density and varying grain size. The fracture surfaces were studied with fractography and x-ray rocking curves. Compression tests were performed both below and above the phase transformation temperature for BeO (2050°C). A model was developed for fracture below 1000°C, involving propagation of existing surface cracks through dissimilar barriers to form a crack front of irregular shape, which generates dislocations near the tip. Above 1000°C a model of grain boundary sliding to open cracks at grain boundary junctions was indicated. Permanent deformation under compression was attributed to grain separation and void formation. (auth)

5903 PETCH RELATION IN SINGLE-PHASE OXIDE CERAMICS. Carniglia, S. C. (Atomics International, Canoga Park, Calif.). J. Amer. Ceram. Soc., 48: 80-3 (Nov. 21, 1965).

Detailed examination of recent strength-grain size data for MgO, Al_2O_3, and BeO ceramics showed that for large grain sizes behavior was of the form of the Knudsen equation: $\bar{\sigma}_f = k_b(\bar{D})^{-\frac{1}{2}}$. For small grain sizes, behavior fitted the form of the Petch equation, $\bar{\sigma}_f = \sigma_y + k_y(\bar{D})^{-\frac{1}{2}}$, or appeared similar but with negative slope. Three characteristic fracture-initiation modes were inferred, all based on the principles of the Griffith criterion and on a critical crack length $c \simeq D$: true brittle or elastic failure, initiation by plastic yield, and initiation by viscous sliding of grain boundaries. Fracture initiation was viewed as the restart of crack growth that was previously interrupted at a grain boundary. (auth)

5904 COMPRESSIVE CREEP OF BERYLLIUM OXIDE–URANIUM DIOXIDE MIXTURES. Vandervoort, Richard R.; Barmore, Willis L. (Univ. of California, Livermore). J. Amer. Ceram. Soc., 48: 587-90(Nov. 21, 1965).

Beryllium oxide-uranium dioxide mixtures were deformed in compression in the region from 1375 to 1540°C. The average apparent activation energy for creep of the oxide mixtures containing up to 10 wt % uranium dioxide was 95.1 kcal/mole. The activation energy was not sensitive to the applied stress and did not vary with urania additions. Creep rate was linearly dependent on the applied stress to 6000 psi. At constant stress and temperature, creep rate dependence on grain size for BeO−10 wt % UO_2 specimens can be described by the relation $\dot{\epsilon} \approx 1/d^2$. The creep rate dependence on the applied stress and grain size is consistent with the Nabarro-Herring mechanism. Creep behavior of the oxide mixtures is ascribed to the deformation of the beryllium oxide matrix. (auth)

5905 SOME OBSERVATIONS ON THE FRACTURE CHARACTERISTICS OF HYDRIDED α-ZIRCONIUM. Coleman, C. E.; Hardie, D. (University, Newcastle-upon-Tyne, England). J. Less-Common Metals, 10: 12-21 (Jan. 1966).

A comprehensive examination of the polished surfaces of deformed Charpy impact specimens and the fracture surfaces of slow-bend specimens of hydrided zirconium indicated that fracture originated at broken hydrides resulting largely from dislocation pile-ups. The characteristics of the fracture surface suggested that propagation occurred in a similar manner in ductile and brittle samples and that microcracks linked up by ductile failure of the intervening matrix. (auth)

5906 THE TUNGSTEN-RICH END OF THE TUNGSTEN–BERYLLIUM SYSTEM. Goldschmidt, H. J.; Ham, W. M. (B.S.A. Group Research Center, Birmingham, England). J. Less-Common Metals, 10: 57-65(Jan. 1966).

The solid solubility of beryllium in tungsten and the nature of the associated tungsten-richest beryllide were investigated. The system showed the solubility of Be to be approximately 5 at. % at the eutectic temperature (≈2100°C). The solubility limit did not vary appreciably down to 1800°C and decreased to about 3 at. % Be in the 1000 to 1300°C range. The solid solution was substitutional and lattice spacing variations are described. The equilibrating phase is WBe_2 (of hexagonal Laves structure), which precipitates from the primary (W, Be) solution; the compound is shown to have a significant homogeneity range, with lattice expansion on increasing Be content, as opposed to the contraction within the primary solution. (auth)

5907 GROWTH OF LARGE GRAINS IN A GALLIUM-STABILIZED DELTA-PLUTONIUM ALLOY. Berndt, A. F. (Argonne National Lab., Ill.). J. Less-Common Metals, 10: 71-2(Jan. 1966).

The feasibility of applying the strain-anneal technique for growing large-grained specimens of a Ga-stabilized δ−Pu alloy was examined. A Pu-3 at. % Ga alloy was prepared by induction melting, in vacuo, Ga (99.99+% pure with high-purity Pu. The ingot was annealed at 490°C for 168 hr, round rolled to 6.7 mm dia, machined into tensile specimens, and homogenized at 500°C for 288 hr. Metallographic examination showed the alloy to be single phase. A tapered tensile specimen was pulled to fracture and was then annealed at 500°C for 73 hr. Metallographic examination of a longitudinal section showed three large grains. The dimensions of each of these grains were about 2.5 mm in the direction parallel to the axis of the specimen and about 1 mm in the direction perpendicular to the axis. Medium sized grains were observed adjacent to these large grains toward the direction of greater strain. The remainder of the grains were similar to those observed before straining. The stresses between which the large grains developed were calculated from measurements made on the photomicrograph to be ~950 kg/cm² and 1200 kg/cm². (F.J.H.)

5908 VISCOSITY OF NaK 78 AT LOW TEMPERATURES. Macur, George; Grove, E. L.; Gaynor, Allan J.; Hersh, Charles K. (Illinois Inst. of Tech., Chicago). J. Phys. Chem., 69: 3782-5(Nov. 1965).

The viscosities of sodium−potassium alloys containing 79.2 to 77.3 wt % potassium were determined in the temperature range from −10 to 148.9°C. The oxygen content of the alloys ranged from 32.3 to 238 ppm. The viscosities of the alloys increased rapidly at low temperatures but were not abnormally high even at temperatures a few degrees above the point when the alloy began to solidify. A plot of the data according to the second equation of Andrade was reasonably linear. (auth)

5909 THE SCANDIUM–YTTRIUM–HYDROGEN SYSTEM. Lieberman, M. L.; Wahlbeck, P. G. (Illinois Inst. of Tech., Chicago). J. Phys. Chem., 69: 3973-80(Nov. 1965). (COO-1029-7).

Equilibrium hydrogen pressures up to 1 atm were mea-

sured for the scandium–yttrium–hydrogen system at 700, 800, and 900°C. These data indicated a large primary solid solution region of hydrogen in scandium–yttrium alloys and a three-condensed-phase region. The latter region indicated limited miscibility of the two metal dihydrides which was confirmed by x-ray diffraction analysis. The phase diagram at 700°C was constructed, and the relative partial molal and differential thermodynamic properties of hydrogen were calculated. For scandium–yttrium alloys with at least 60 at. % yttrium, evidence for a trihydride phase was found at 242°C. Hysteresis was observed in the hydrogenation reaction to produce the trihydride phase. (auth)

5910 STATUS OF COATED REFRACTORY METALS. Perkins, Roger A. (Lockheed Missiles and Space Co., Palo Alto, Calif.). J. Spacecraft Rockets, 2: 520-3(July-Aug. 1965).

An objective analysis of the capabilities and limitations of coated refractory metals is presented. In particular, experimental results for silicide-coated Mo alloys (and some Nb alloys) are discussed. It is shown that useful coating life can be predicted on the basis of the time required to complete the diffusion of silicon into the substrate to form intermediate and lower silicides (e.g., to form Mo_5Si_3). For $MoSi_2$ on Mo, the Arrhenius-type relation $t = [S_0/1140 \exp(-33{,}400/RT)]^2$ was found for coating failure, where t = time (minutes), S_0 = coating thickness (mils), and T = temperature (degrees Kelvin). Thus doubling S_0 gives a fourfold increase in coating life, and a ±100°F temperature variation from a nominal 2600°F also makes a fourfold change in life. Performance limitations due to temperature, pressure (maximum degradation occurs between 0.1 and 10 mm Hg), defect tolerance limit (cracks are self-healing up to a point), and structural stability are discussed. Problems are particularly severe on thin sheet. (auth)

5911 PHONONS IN DISORDERED NIOBIUM–MOLYBDENUM ALLOYS. Woods, A. D. B.; Powell, B. M. (Chalk River Nuclear Labs., Ontario). Phys. Rev. Lett., 15: 778-80(Nov. 15, 1965).

Inelastic neutron-scattering studies of the disordered niobium-molybdenum alloys are reported. These studies indicate that, contrary to expectation, they do possess an ordered electronic structure, enabling phonons to propagate as in a pure metal. The alloys form a complete series of disordered solid solutions, all having a body-centered cubic structure. The neutron scattering measurements were made at room temperature on a triple-axis spectrometer for two alloys, $Nb_{0.65}-Mo_{0.35}$ and $Nb_{0.25}-Mo_{0.75}$. A series of the neutron groups were obtained on the branch, both for the alloy $Nb_{0.65}-Mo_{0.35}$ and for pure Mo. The observed groups from both alloys showed no marked increase in width. The absence of any observed broadening of the neutron groups indicates that although the alloys are crystallographically disordered systems, each has a well-defined electronic structure which allows phonons to propagate in a similar manner to those in a pure metal. The measured dispersion curves of the alloys and metals are also shown. Anomalies appear in both Mo and Nb. An interpretation of the neutron results indicates the possibility of correlation of the behavior of the dispersion curves of the complete Nb–Mo system in terms of a rigid-band structure. (J.F.P.)

5912 NEUTRON DIFFRACTION OF ORDERED $PtMn_3$. Wuttig, Manfred (Univ. of Illinois, Urbana). Z. Angew. Math. Phys., 16: 535-6(1965).

Two neutron diffraction patterns of an ordered $PtMn_3$ powder sample were taken at room temperature and 250°C, to check the hypothesis that a change in spin ordering causes the abrupt change in the susceptibility of ordered $PtMn_3$ at 180°C. The differences in the diffraction patterns are interpreted as due to variations in the amount of magnetic scattering; this interpretation agrees with the hypothesis of spin-ordering change. (M.J.T.)

Radiation Effects

See also CHEMISTRY — Radiation Chemistry

Refer also to abstracts 5569 and 6602.

5913 (EURAEC–1488) RESEARCH TO DETERMINE THE LONG-TERM MECHANICAL PROPERTIES OF METALS SUBJECTED TO MECHANICAL STRESS AT ELEVATED TEMPERATURES AND NEUTRON IRRADIATION. Tenth Quarterly Report. Siegfried, W.; Zimering, S. (Battelle Memorial Inst., Geneva (Switzerland)). Oct. 1965. Contracts 100-62-12-RDS; 057-64-7-TEES(RD). 10p. (EUR–2655). Dep. mn; CFSTI $1.00 cy, $0.50 mn.

Work Performed under United States–Euratom Joint Research and Development Program.

The method of thermodynamics of irreversible processes was used for time-to-rupture tests on heat-resistant, ferritic, and austenitic steels. Also the dependence of stress and temperature of the rheological parameters was determined, and it was possible to describe these values by a number of simple rate-processes which can be very easily explained physically. The application of the results to studies on scattering involved in experiments on rupture time for industrial alloys is discussed. (P.C.H.)

5914 (GEAP–3771-17) HIGH PERFORMANCE UO_2 PROGRAM. Quarterly Progress Report No. 17, April–June 1965. Lyons, M. F. (ed.) (General Electric Co., San Jose, Calif. Atomic Power Equipment Dept.). July 15, 1965. Contract AT(04-3)-189. 95p. (EURAEC–1512). Dep. mn; CFSTI $3.00 cy, $0.50 mn.

Work Performed under United States–Euratom Joint Research and Development Program.

Post-irradiation examination of the maximum thermal performance, high burnup assembly, EX-12A, was essentially completed. The EX-12A fuel rods appeared capable of continued, satisfactory operation with no evidence of any significant deterioration. The measured fission gas release fraction varied from slightly greater than 50% for Rod 12KCF to greater than 100% for powder Rod 12GV. Examination of the fuel microstructures indicates evidence of considerably greater melting than expected based on end-of-life thermal performance values. No evidence of UO_2-Zircaloy-2 interaction was detected in any of the rods. Some UO_2-Incoloy interaction was evident in Rod 12KCF where the Incoloy foil overlapped. A capsule containing hypostoichiometric pellets was irradiated and indicated slightly lower thermal conductivity than stoichiometric pellets under the same conditions. However, the interpretation of the results is clouded by the probability that pellet-cladding interface conductivity was low during the irradiation. Two isothermal fission gas release capsule irradiations were operated with a UO_2 sample temperature of 1530 and 1680°C. The measured fission gas release up to 1680°C was 2% or less. The retention of Kr in molten and solidified UO_2 was less than 7×10^{-4} cm^3/gm-atm after heat treatment of the UO_2 at 2900°C for 15 minutes under an approximate pressure of 16 kg/cm^2. Although some bonding between individual small particles occurs at 1900°C, the disappearance of the concrete-like structure in vibratory compacted, arc-fused UO_2 seems to start at about 2000°C for 500 hours at temperature. The molten boundary in partially molten powder samples was indicated by the disappearance of porosity, i.e., the same boundary observed in pellet UO_2. Further experiments with W markers incorporated at UO_2 confirmed earlier results that the appearance of the original solid-liquid interface is altered by subsequent heat treatment below the melting point. Results of out-of-pile studies of Zr and Zircaloy-2 interaction with I_2 are summarized. Two types of I_2 attack were observed: gross pitting with extensive metal removal, and cracking with little or no metal removal. The pitting attack appears to be related to imperfections in the ZrO_2 film and proceeds in the absence of stress on both wire and tube samples. Cracking requires both I_2 and stress and occurred in tubular samples only. The correspondence of the out-of-pile,

iodine-induced cracks to the pinhole failures experienced in-pile remains tenuous. The only established similarities are their common transgranular character and the presence of I_2 in each case. Fission product distribution data from a rod operated with gross central melting during irradiation shows that the concentration of most fission products is homogenized both radially and axially within the molten core. Exceptions to this rule are some of the more volatile elements such as Cs. The homogenization indicates mixing from convection in the molten zone and confirms earlier, heat-transfer-derived evidence of molten fuel convection. Fission products were axially distributed in the unmelted shell of UO_2 about in proportion to the integrated average axial neutron flux profile. There is a general correspondence between the alpha autoradiograph characteristics and variations, and analytical measurements of the heavy element concentrations and distributions. The interaction between Zircaloy-2, Incoloy, and UO_2, and between Zircaloy-2 and UO_2, was studied out-of-pile at temperatures to 1300°C for 200 hours. The limiting step in the UO_2-Zircaloy-2 interaction appears to be oxygen diffusion through the oxygen-enriched layer in the Zircaloy adjacent to the reaction interface. Linear extrapolation of the test results indicates a 0.01-cm-thick oxygen rich layer will form in 2 years at 970°K. An Incoloy foil between the Zircaloy-2 and UO_2 prevents their interaction, but the Zircaloy-2 and Incoloy react instead with about the same time and temperature characteristics as UO_2-Zircaloy-2. (W.L.G.)

5915 (ORNL-P-1724) PROPERTIES AND PROSPECTS OF THORIA-BASE NUCLEAR FUELS. Olsen, A. R.; Douglas, D. A.; Hirose, Y.; Scott, J. L.; Ullmann, J. W. (Oak Ridge National Lab., Tenn.). [1965]. Contract W-7405-eng-26. 40p. (CONF-651041-1). Dep. mn; CFSTI $2.00 cy, $0.50 mn.

From Nuclear and Engineering Ceramics Conference, Harwell, Eng.

The results of irradiation tests and complementary supportihg research and development that is being done to establish the performance characteristics of vibratorily compacted sol-gel derived ThO_2-UO_2 fuels are presented. The program includes a comparison of such material with ThO_2-UO_2 derived from other processes. Irradiation tests with vibratorily compacted thoria-base fuels at linear heat ratings up to 1000 w/cm and burnups in excess of 100,000 Mwd/t showed that this material must be considered as a unique fuel and not just as a UO_2 substitute. Semitheoretical calculations of the minimum possible swelling in UO_2 and ThO_2-UO_2 match closely the experimental evidence and indicate at least a 20% lower swelling rate for bred ^{233}U fissions than for bred ^{239}Pu fissions. The structural stability and higher thermal capability of thoria-base fuels, when compared with UO_2, indicate potential savings in inventory and fabrication costs provided the reactor design is based on these fuel limitations. (P.C.H.)

5916 TEMPERATURE AND NEUTRON IRRADIATION EFFECTS ON PLASTIC DEFORMATION OF ALPHA URANIUM SINGLE CRYSTALS. Butra, F. P.; Evkina, Z. F.; Fufaeva, O. L.; Korobeinikov, I. A.; Lebedev, L. M. At. Energ. (USSR), 19: 372-80(Oct. 1965). (In Russian).

The plastic deformation of alpha-uranium monocrystals was studied at various crystallographic orientations and various temperatures. An explanation for the shape of the stress-strain curves as a function of the action of the basic systems of plastic deformation is given. The monocrystals were irradiated by neutrons in a reactor at temperatures up to 100°C with integral fluxes up to 5.5×10^{17} n/cm and a flux of 4×10^{20} n/cm^2. It was shown that irradiation increases 3 to 5 times the critical shearing stress in the (010) plane and decreases the relative linear expansion and the region of light slip. Annealing of monocrystals irradiated with fluxes up to 5.5×10^{17} n/cm^2 leads to recovery of the mechanical properties. (tr-auth)

5917 NEUTRON-IRRADIATION EFFECTS ON A Nb-MODIFIED 80 Ni-20 Cr ALLOY. Robertshaw, F. C. (General Electric Co., Cincinnati). Nucleonics, 23: No. 11, 60 (Nov. 1965).

The influence of pile ambient-temperature irradiation and postirradiation annealing on the stress-rupture properties at 1,200 and 1,500°F of a Nb-modified 80 Ne-20 Cr alloy was investigated. This alloy is a reactor structural material. Results at both test temperatures show a substantial radiation-induced decrease in ductility, which is partially recovered by annealing. Rupture life at 1,200°F is reduced by irradiation while it is increased at 1,500°F, at lower stresses. Annealing appears to remove radiation effects on rupture life. The radiation induced defects, which are initially produced at pile ambient temperature, thermally and under the influence of strain evolve at 1,200°F into a form that is weakening, and at 1,500°F into a form that is strengthening. These defects appear to be of the lattice type, since they can apparently be removed by relatively low-temperature annealing. (J.F.P.)

5918 RECOVERY OF PURE AND ALLOYED ALUMINUM IN STAGES I AND II AFTER 2-Mev ELECTRON IRRADIATION. Snead, C. J. Jr.; Shearin, P. E. (Univ. of North Carolina, Chapel Hill). Phys. Rev., 140: A1781-7 (Nov. 29, 1965). (TID-21961).

Pure (99.9999%) aluminum and dilute alloys of aluminum were irradiated near helium temperature with 2-Mev electrons and the annealing of stages I and II studied. Five recovery substages are resolved in stage I with the lowest two ascribed to ⟨110⟩ close-pairs and I-C to ⟨110⟩ migration. The addition of 0.3 at. % of Zn, Cu, and Ge suppresses recovery as measured by percent of total recovery throughout stage I. Stage II is quite impurity-sensitive but is present in the pure aluminum, as evidenced by two annealing peaks. The results fit the framework of the two-interstitial model with few reservations. (auth)

5919 THERMAL CONDUCTIVITY OF ELECTRON-IRRADIATED SILICON. Vook, Frederick L. (Sandia Lab., Albuquerque, N. Mex.). Phys. Rev., 140: A2014-19(Dec. 13, 1965).

Changes in the low-temperature thermal conductivity of single-crystal Si were investigated upon 2-Mev electron irradiation and annealing. The additive thermal resistivity of high-purity p-type Si irradiated below 60°K to maximum time-integrated fluxes Φ of 8.0×10^{18} 2-Mev e/cm^2 increases as $1/K - 1/K_0 = 3.75 \times 10^{-13}\ \Phi^{0.61}$ cm-deg/W at 47°K. The $\Phi^{0.61}$ dependence of the additive thermal resistivity of Si on bombardment is very similar to the $\Phi^{0.58}$ dependence previously observed for Ge. The magnitude of the increase is, however, much smaller than previously observed for either Ge, InSb, or GaAs. The linear concentration dependence of GaAs has been related to mass-difference strain-field scattering, whereas the nonlinear concentration dependencies of InSb, Ge, and Si suggest phonon-electron scattering. For the high-purity Si, annealing begins near 80°K, and exhibits a single dominant annealing stage near 140°K corresponding to the annealing temperature of vacancies of p-type Si. Measurements of the temperature dependence of the thermal conductivity indicate that the defects anneal primarily as point defects, although evidence exists for a small amount of precipitation of point defects in the annealing-temperature interval between 80 and 135°K. Sharp minima observed in the temperature dependence of the thermal conductivity of Si are similar to those previously observed in Ge and attributed to resonant scattering. (auth)

5920 RECOVERY OF ELECTRICAL PROPERTIES IN 45-Mev-ELECTRON-IRRADIATED n-TYPE Si FROM 80 TO 350 deg K. Cheng, L. J.; Corelli, J. C. (Rensselaer Polytechnic Inst., Troy, N. Y.). Phys. Rev., 140: A2130-5(Dec. 13, 1965).

Isochronal annealing from 80 to 360°K of defects induced by 45-Mev electrons in floating-zone and pulled n-type silicon was studied using electrical properties, namely, conductivity and carrier concentration. The results indicate that the annealing behavior in this temperature range depends on the imperfections present in the samples before irradiation. In particular, oxygen impurities are found to have a pronounced effect on the defect production and annealing process. The total numbers of silicon A centers produced after irradiation at 80°K and measured after an-

neal to 350°K yield production rates of 0.2 to 0.3 cm^{-1} which depend only slightly on the impurity concentration of the samples studied (3×10^{13} to 3×10^{15} phosphorus atoms/cm^3). The production rate of A centers by 45-Mev electrons is comparable for 80 and 300°K irradiations; this is different from results found in 1-Mev electron irradiation. The production of A centers in 15°K irradiation is found to be about one-half the value measured in 80°K irradiations. A comparison of the characteristics of defects induced by 45- and 1–4.5-Mev electrons in silicon is given. (auth)

5921 INFLUENCE OF IRRADIATION BY FAST NEUTRONS ON THE MECHANICAL PROPERTIES OF SOME CARBON OR LOW-ALLOY STEELS. Lemaire, J.; Cibois, E. (Centre d'Etudes Nucleaires, Saclay, France). Rev. Met. (Paris), 62: 785-90(Sept. 1965). (In French).

Hardening and embrittlement of carbon steels by irradiation were investigated. The effects of grain size, structure prior to work-hardening, and irradiation temperature were determined. Recovery was found to be produced in two stages with retardation at ~300°C. (auth))

PHYSICS

General

Refer also to abstracts 5239 and 5830.

5922 (AD–618689) DIFFRACTION AND SCATTERING OF ELECTROMAGNETIC WAVES IN ANISOTROPIC MEDIA. Rulf, Benjamin (Polytechnic Inst. of Brooklyn, N. Y. Microwave Research Inst.). Apr. 26, 1965. Contract AF19(628)-2357. 137p. (PIBMRI–1262-65). CFSTI $4.00 cy, $1.00 mn.

Two-dimensional scattering and diffraction problems in anisotropic media are considered. The intent is twofold: first, to generalize mathematical methods applicable in isotropic regions to a certain class of anisotropic problems; and second, to study the solutions of the anisotropic problems in such a manner as to high-light certain common properties which point the way toward the construction of approximate solutions for configurations with more general structural shape of anisotropy. In the low-frequency range, the method of multipole expansion is used. It is demonstrated that the rigorous solution for the problem of scattering of a plane or cylindrical wave by an obstacle which is small compared to the wavelength may be expanded in a series whose terms correspond to multipole radiation in the anisotropic medium. As an illustration, the excitation coefficients of the first few terms arising from scattering by a narrow conducting ribbon are calculated. In the high frequency range, geometrical optics, the first-order asymptotic solution of Maxwell's equations is considered first. The ray refractive index is calculated, and the laws of propagation and reflection of rays, which define the trajectories of energy transport, are derived from Fermat's principle. To obtain an insight into diffraction phenomena, two types of representative problems — diffraction by a straight edge, and diffraction by a smoothly curved object — are discussed. (TAB)

5923 (BNWL–149) PHYSICS RESEARCH QUARTERLY REPORT, APRIL–JUNE 1965. (Battelle-Northwest, Richland, Wash. Pacific Northwest Lab.). July 15, 1965. Contract AT(45-1)-1830. 71p. Dep. mn; CFSTI $3.00 cy, $0.75 mn.

Separate abstracts were prepared for the 5 included sections. (M.O.W.)

For abstracts of individual sections see: 6577–6579, 6668, and 6669.

5924 (ISS–65/19) ATTIVITA E COMPITI DEI LABORATORI DI FISICA DELL'ISTITUTO SUPERIORE DI SANITA. (The Activities and Duties of the Physics Laboratory of the Istituto Superiore di Sanita). Ageno, M. (Istituto Superiore di Sanita, Rome (Italy). Laboratori di Fisica). July 2, 1965. 39p. Dep. mn.

The research-work in progress at this Laboratory is briefly described, giving evidence of the strict correlations between these activities and the control tests carried out by law in the Laboratory. Given at the same time is a brief account of the internal organization of the Laboratory and of its way of functioning. (auth)

5925 (ORNL–3858(Vol.1)) NEUTRON PHYSICS DIVISION ANNUAL PROGRESS REPORT FOR PERIOD ENDING AUGUST 1, 1965. (Oak Ridge National Lab., Tenn.). Nov. 1965. Contract W-7405-eng-26. 79p. Dep. mn; CFSTI $3.00 cy, $0.75 mn.

Separate abstracts were prepared for the 6 included sections. (M.O.W.)

For abstracts of individual sections see: 5737, 5832, 6296, 6519, 6520, and 6588.

5926 (ORNL–3858(Vol.2)) NEUTRON PHYSICS DIVISION ANNUAL PROGRESS REPORT FOR PERIOD ENDING AUGUST 1, 1965. (Oak Ridge National Lab., Tenn.). Nov. 1965. Contract W-7405-eng-26. 26p. Dep. mn; CFSTI $2.00 cy, $0.50 mn.

Separate abstracts were prepared for the 3 included sections. (M.O.W.)

For abstracts of individual sections see: 5738, 6297, and 6521.

5927 (ORNL-P–1733) CALCULATION OF THE NUCLEON-MESON CASCADE IN IRON INITIATED BY 1- AND 3-Gev PROTONS AND COMPARISON WITH EXPERIMENT. Alsmiller, R. G. Jr. (Oak Ridge National Lab., Tenn.); Barish, J. (Oak Ridge Gaseous Diffusion Plant, Tenn.). [1965]. Contract W-7405-eng-26. 13p. (CONF-651101–38). Dep. mn; CFSTI $1.00 cy, $0.50 mn.

From 13th Conference on Remote Systems Technology, Washington, D. C.

One-dimensional nucleon-meson cascade calculations have been carried out for the cases of 1- and 3-Bev protons incident on steel. The thick target cross sections are calculated and compared with experimental values. The calculated values are generally larger than the experimental values for large depths. (auth)

5928 (PR-P–66) PHYSICS DIVISION PROGRESS REPORT, APRIL 1–JUNE 30, 1965. (Atomic Energy of Canada Ltd., Chalk River (Ontario)). 59p. (AECL–2501). Dep.; AECL $1.50.

Work accomplished in the areas of nuclear physics, space physics, solid state studies, and solid state radiation detectors is summarized. (M.O.W.)

5929 THE USE OF IMPULSE MAGNETIC FIELDS IN DEVICES WITH TROCHOIDAL ELECTRON BEAMS. Antakov, I. I.; Klimov, V. G.; Lin'kov, R. V. (Gor'kii State Univ., USSR). Izv. Vyssh. Ucheb. Zaved., Radiofiz., 8: 948-54(1965). (In Russian).

The possibilities are investigated of using pulsed magnetic fields in oscillators with resonant interaction of trochoidal electron beams and traveling electromagnetic waves at electron cyclotron frequency. An estimation is given for distortions of impulse magnetic field by metallic electrodes of the tube. The conditions are found under which the distortions are negligible. The peak power of about 30 w was detected in a 8 mm pulse oscillator device. (auth)

5930 ELECTROMAGNETIC FIELD INSIDE A CURRENT-CARRYING REGION. Fikioris, John G. (Avco Corp., Wilmington, Mass.). J. Math. Phys. (N. Y.), 6: 1617-20(Nov. 1965).

The improper integrals appearing in the course of evaluating the vector potential A and the electric field E inside a current-carrying region are carefully examined. It is found that the integrals exist and have a well-defined meaning only when the current density function satisfies a Hölder condition. A definite and precise way of evaluating them is derived, and A, E are shown to satisfy the usual inhomogeneous equations. (auth)

Accelerators

Refer also to abstracts 5715, 5733, and 6276.

5931 (BNL–9352) MULTITURN BEAM EXTRACTION IN AG SYNCHROTRONS. Robertson, D. S. (Brookhaven National Lab., Upton, N. Y.). June 10, 1965. Contract AT-30-2-GEN-16. 21p. Dep. mn; CFSTI $1.00 cy, $0.50 mn.

One method of extracting particles from a synchrotron is to turn on a magnetic discontinuity, or bump. The bump induces oscillation of the beam, which can then be extracted by an appropriately positioned septum magnet. A theoretical analysis of the problem is given. (M.O.W.)

5932 (BNL–9662) ALTERNATING GRADIENT SYNCHROTRON CONVERSION SUMMARY. Distenfeld, Carl; Colvett, Robert (Brookhaven National Lab., Upton, N. Y.).

[1965]. Contract AT(30-2)-Gen-16. 19p. (CONF-651109-9). Dep. mn; CFSTI $1.00 cy, $0.50 mn.

From 1st Symposium on Accelerator Radiation Dosimetry and Experience, Upton, N. Y.

Some of the past and present high energy physics experiments and relating AGS facilities are outlined and compared to the programs that justify the AGS conversion to higher intensity. Years of maintenance experience illuminate basic changes that will improve operations of the machine. Present experimental magnets, modular components, and remoting of operational equipment outside of the radiation environment are a few of the changes that will decrease down time and increase maintainability. Comprehensive measurements of skyshine and direct radiation to neighboring facilities, ring air and magnet water activations, and experimental floor radiation were studied during different targeting conditions. Health physics aspects of the AGS conversion are summarized along with some of the more important general interest information. Emphasis is placed on the radiation safety problems. (auth)

5933 (CERN-65-34) ESTIMATE OF INDUCED RADIOACTIVITY IN ACCELERATORS. Barbier, M.; Cooper, A. (European Organization for Nuclear Research, Geneva (Switzerland)). Oct. 25, 1965. 143p. Dep. mn.

The results of extensive calculations of the radioactivity induced in accelerators are presented. Separate discussions and results are presented for the activity induced by electrons, nucleons, and pions. (M.O.W.)

5934 (CERN-65-37) DISC-LOADED DEFLECTING WAVEGUIDE-COMPUTATIONS. Bell, M.; Hereward, H. G. (European Organization for Nuclear Research, Geneva (Switzerland)). Nov. 4, 1965. 48p. Dep. mn.

The results of computations on waveguides operating in the deflecting mode used in the r-f particle separator are described. The theory of the calculations, done on the CERN Mercury computer, was described in an earlier report. The programs calculate the dimensions of the guide, and for phase velocity equal to that of light, stored energy, losses, power flow, and group velocity are also found. The calculations are described in detail and the results are presented in the form of graphs. (M.O.W.)

5935 (CONF-650217, pp 73-6) A THERMAL NEUTRON FACILITY FOR LAMPF. Motz, Henry T. (Los Alamos Scientific Lab., Univ. of California, N. Mex.).

The use of the beam-stop area of LAMPF accelerator as a neutron source is discussed. Considering the 1-ma beam of 700-Mev protons to be stopped by a Bi target, it is found that 10^{17} neutrons/sec are produced. If the neutrons from this source are moderated by D_2O, a time-averaged flux of 4×10^{14} n/cm^2 · sec results. The costs and uses of such a neutron source are outlined. (T.F.H.)

5936 (CONF-650217, pp 77-81) PHERMEX—A HIGH CURRENT LINAC. Motz, Henry T. (Los Alamos Scientific Lab., Univ. of California, N. Mex.).

PHERMEX is a three-cavity standing-wave electron linac, used to generate high-intensity bremsstrahlung. PHERMEX operates at 20 Mev. The possibility of upgrading the energy and intensity of the PHERMEX beam to the extent that it could be used as a high-intensity photoneutron source is discussed. (T.F.H.)

5937 (KFK-346) ZWISCHENBERICHT UEBER UNTERSUCHUNGEN AN HOCHFREQUENZ-STRUKTUREN FUER PROTONEN-LINEARBESCHLEUNIGER. (Intermediate Report on a Study of the High-Frequency Structure for Proton Linear Accelerator). Bauer, W.; Eschelbacher, H.; Kuntze, M. (Kernforschungszentrum, Karlsruhe (West Germany). Institut fuer Experimentelle Kernphysik). July 1965. 44p. Dep. mn.

The acceleration of charged particles was effected in a linear accelerator by a high-frequency field E(z,t) produced along its axis. This electric field was excited in hollow conductors or hollow cavity resonators that show in their interior a certain structure. Since these structures affect the construction of the suitable acceleration field, it is significant to begin considerations on the construction of a linear accelerator with investigations on possible structures. The requirements that must be given to the high-frequency structures are enumerated. A compilation of the facts important in this relation are deduced from the hollow-conductor theory, and a brief description is given of the structures taken into consideration. The results measured on these structures up to now are reported. (tr-auth)

5938 (LA-3372) ANALYSIS OF A PROTON LINEAR ACCELERATOR RF SYSTEM AND APPLICATION TO RF PHASE CONTROL. Jameson, Robert A. (Los Alamos Scientific Lab., Univ. of California, N. Mex.). June 1965. Contract W-7405-eng-36. 293p. Dep. mn; CFSTI $7.00 cy, $1.50 mn.

The general transient behavior of the accelerating structure is derived using an equivalent circuit, and functions describing r-f field phase and amplitude envelope responses are obtained for control system design. Experimental verification of the theory is presented. The combination of the accelerator structure and the r-f amplifier which drives it through a long waveguide feed is analyzed. The magnitude of beam loading effects in the accelerator is discussed. The problem of providing a phase reference is examined, and the properties of direct comparison r-f phase detectors and various microwave phase shifters are analyzed. The characteristics of these individual elements are combined in a study of the phase control system. Design criteria are established, and an example meeting these criteria is developed in detail. Digital computer programs were used in various parts of the work. (auth)

5939 (LA-DC-7267) THE LASL TANDEM ACCELERATOR FACILITY DATA SYSTEM. Gardiner, T.; Levin, J. (Los Alamos Scientific Lab., Univ. of California, N. Mex.). [1964]. Contract W-7405-eng-36. 24p. (CONF-651001-15). Dep. mn; CFSTI $1.00 cy, $0.50 mn.

From IEEE Nuclear Science Symposium, San Francisco.

An on-line data processing system was recently placed in operation in conjunction with two electrostatic accelerators at LASA. The system consists of a Scientific Data Systems Model 930 computer and an experiment-computer interface unit designed and fabricated at LASL. The system provides for time-shared operation of three separate experiments. Up to nine fast analog-to-digital converters may be utilized by these three experiments. These ADCs may be connected and fanned-in to the computer in a variety of ways ranging from nine simultaneously operating separate devices to a combination for a nine parameter coincidence experiment. The system design places considerable emphasis upon rapid setup to facilitate change from one experiment to another. Provision was made for computer control of experimental apparatus, and for data input to the computer from other sources such as scalers, clocks and voltmeters. The interface portion of the system was implemented entirely with integrated circuits and is modular to the extent that future expansion can easily be accomplished. (auth)

5940 (LA-DC-7522) THE RADIATION AND SHIELDING DESIGN FACTORS FOR THE LOS ALAMOS MESON PHYSICS FACILITY. Cochran, D. R. F.; Israel, H. I.; Mueller, D. W. (Los Alamos Scientific Lab., Univ. of California, N. Mex.). Oct. 20, 1965. Contract W-7405-eng-36. 15p. (CONF-651109-13). Dep. mn; CFSTI $1.00 cy, $0.50 mn.

From 1st Symposium on Accelerator Radiation Dosimetry and Experience, Upton, N. Y.

The proposed advancements of accelerator performance to higher energy and higher intensity have provided a great stimulus to the careful consideration of the associated shielding and radiation problems. For each energy, intensity, and kind of accelerator, the ultimate designs for the handling of the shielding and radiation problems are correlated closely to factors of economy, maintenance, safety, allowable accelerator performance, and the environment which the accelerator occupies or is intended to occupy. The relative importance of the various factors can be decided within the scope of an operational philosophy devel-

oped to optimize the usefulness of the accelerator. The results of the above considerations with particular reference to special problems are presented as they pertain to the proposed Los Alamos Meson Physics Facility (LAMPF). (auth)

5941 (NP-15598) IZMERENIE ZAVISIMOSTI IMPUL'SA PROTONOV SINKHROTRONA ITEP OT VREMENI USKORENIYA. (Measurement of the Relationship of a Proton Pulse in the ITEP). Birger, N. G.; Borisov, V. S.; Bysheva, G. K.; Gol'din, L. L.; Korotkov, M. M.; Martusov, E. T.; Sidorenko, Z. S.; Tumanov, G. K. (Gosudarstvennyi Komitet po Ispol'zovaniyu Atomnoi Energii SSSR, Moscow. Institut Teoreticheskoi i Eksperimental'noi Fiziki). 1965. 12p. Dep. mn.

Internal polyethylene target measurements of proton beam momentum of ITEP synchrotron were made. The momentum values were determined by energy of the elastically scattered protons. Measurements were made at 4 different time intervals from the beginning of the acceleration cycle. The empirical relation between the proton momentum and the acceleration time was obtained. (auth)

5942 (NP-15615) SYNCHROTRON RESONATOR FOR THE ILLINOIS 300-Mev BETATRON. Harlan, James R. (Illinois Univ., Champaign. Physics Research Lab.). May 10, 1965. Contract ONR 1834 (05). 48p.

The fabrication and testing of a quarter-wavelength synchrotron resonator and the incorporation of this resonator in a 60° porcelain vacuum tube assembly which was installed in the University of Illinois 300-Mev betatron are described. Radio-frequency energy developed by the resonator-oscillator system is used to give post-betatron acceleration to the electron beam of the betatron. X-ray energies of 335 Mev (±2%) were reached using radio-frequency post-betatron acceleration. (auth)

5943 (SLAC-48) TWO-MILE ACCELERATOR PROJECT. Quarterly Status Report, April 1-June 30, 1965. (Stanford Linear Accelerator Center, Stanford Univ., Calif.). Aug. 1965. Contracts AT(04-3)-400; AT(04-3)-515. 112p. Dep. mn; CFSTI $4.00 cy, $0.75 mn.

Development progress in the two-mile linear accelerator is reported. Separate sections are presented for work on plant engineering, systems engineering and installations, accelerator physics, instrumentation and control, heavy electronics, mechanical design and fabrication, klystron studies, sector tests, beam switchyard, target area development, and pre-operations research and development. (M.O.W.)

5944 (SLAC-PUB-132) A GENERAL FIRST- AND SECOND-ORDER THEORY OF BEAM TRANSPORT OPTICS AND ITS APPLICATION TO THE DESIGN OF HIGH-ENERGY PARTICLE SPECTROMETERS. Brown, Karl L. (Stanford Linear Accelerator Center, Stanford Univ., Calif.). Aug. 1965. Contract AT(04-3)-400. 24p. (CONF-650923-24). Dep. mn; CFSTI $1.00 cy, $0.50 mn.

From 5th International Conference on High Energy Accelerators, Frascati, Italy.

A general first and second order theory of beam transport optics was developed. From this the first and second order matrix elements of bending magnets, quadrupoles, and sextupoles were derived. Utilizing this theory, very general first and second order theorems of beam transport optics were formulated which were extremely useful for designing single and multiple element magnetic optical systems. The theorems are expressed as functions of five characteristic first order trajectories of a system. In fact, all of the first and second order optical properties of a system may be expressed in terms of these five trajectories. A general discussion of the theory is presented along with specific applications of the theory to the design of high energy particle spectrometers. (auth)

5945 (UCRL-16464) NEW RADIATION PROBLEMS ASSOCIATED WITH THE 200-Bev ACCELERATOR. Gilbert, William S. (Lawrence Radiation Lab., Univ. of California, Berkeley). Oct. 14, 1965. Contract W-7405-eng-48. 15p. (CONF-651109-10). Dep. mn; CFSTI $1.00 cy, $0.50 mn.

From 1st Symposium on Accelerator Radiation Dosimetry and Experience, Upton, N. Y.

The 200-Bev proton accelerator studied by the Lawrence Radiation Laboratory is described, with special attention given to those aspects of the design relating to radiation problems. Various radiation problems are compared with those already encountered at presently operating accelerators. The primary use of external beams greatly facilitates machine maintenance and operation. Muon shielding is discussed in some detail. (auth)

5946 (UJV-1408/65) INITIAL TRAJECTORIES OF IONS LEAVING AN OPEN CYCLOTRON ION SOURCE AT NON ZERO INITIAL CONDITIONS. Hrda, A.; Kult, K.; Kuzmiak, M. (Ustav Jaderneho Vyzkumu, Ceskoslovenska, Akademie Ved, Rez). 1965. 24p. Dep. mn.

Under simplifying conditions, initial trajectories are studied of ions that emerge from an open cyclotron source with nonzero initial energies within the plane angle of 2π. This problem is solved in connection with the problem of accelerating polarized ions. (auth)

5947 (ANL-Trans-241) METHOD FOR THE EXTRACTION OF A HEAVY ION BEAM FROM A CYCLOTRON WITH AZIMUTHAL VARIATION OF THE MAGNETIC FIELD. Vyalov, G. N.; Oganesyan, Yu. Ts.; Flerov, G. N. Translated by Elmar K. Wilip (Argonne National Lab., Ill.), from report JINR-P-1884. 1964. 20p. Dep. mn; CFSTI $1.00 cy, $0.50 mn; JCL $1.60 fs, $0.80 mf.

A method is proposed for the extraction of heavy ions from a cyclotron with azimuthal variation of the magnetic field. It is based on the utilization of the radial instability of charged particles in the azimuthal heterogenous magnetic field which occurs at the prompt change of their charge. (auth)

5948 (ANL-Trans-246) EFFECT OF THE GEOMETRY OF THE CYCLOTRON CENTER UPON THE STARTING MOTION OF HEAVY IONS (MEDIAN PLANE). Indreash, G.; Shelaev, I. A. (Joint Inst. for Nuclear Research, Dubna (USSR). Lab. of Nuclear Reactions). Translated by Elmar K. Wilip (Argonne National Lab., Ill.), from report JINR-P-2164. 1965. 57p. Dep. mn; CFSTI $3.00 cy, $0.50 mn; JCL $5.60 fs, $1.91 mf.

The singularities of the starting motion of heavy ions at different geometries of the cyclotron center are discussed and the distributions of the electric field in the center are given for the relevant variants determined on a 1:1-scale model in an electrolytic tank. The trajectories were calculated on an electronic computer. It is shown that in the case of a starting optics with a puller electrode ("bow") a sharp phase grouping is observed in the vicinity of a small positive phase and a high scattering of the revolution centers of ions with different initial phases. In the case of a slit optics the phase grouping is insignificant and the scattering of the revolution centers considerably smaller, which facilitates the adjustment of the beam to its finite radius and its extraction. (auth)

5949 LEAKAGE OF PARTICLES FROM STORAGE RINGS DUE TO RANDOM VARIATIONS IN AMPLITUDE AND FREQUENCY OF THE COMPENSATING FIELD. Bakai, A. S. At. Energ. (USSR), 19: 386-8(Oct. 1965). (In Russian).

The amount of leakage of particles from a storage ring, caused by instability of the amplitude and frequency of the potential difference between the dees, which compensates the radiative energy losses of the particles, is calculated. It is assumed that the amplitude and frequency of the compensating field are random variables and that their perturbations occur by fast random processes. Equations are written for the radial and phase motion of an electron in the storage ring. A general formula for the leakage is derived, and the limiting cases of no perturbation in the amplitude and in the frequency of the potential are considered. Numerical calculations for the example of an electron-positron storage ring with strong focusing are carried out. (M.J.T.)

5950 ON LIMITATIONS IN DENSITY OF INTERACTING CURRENTS IN COLLIDING ULTRARELATIVISTIC BEAMS. Khiefets, M. I.; Shapiro, V. D. At. Energ., (USSR), 19: 388-9(Oct. 1965). (In Russian).

Collective instabilities in a system of two colliding relativistic beams are investigated. It is assumed that beam-density nonhomogeneities due to electrostatic interaction of charges are small because of compensation of the repulsive forces by the intrinsic magnetic fields of the beams. The beam dispersion equation is obtained using the Maxwell equations and the equation for the dielectric tensor in the hydrodynamic approximation. The dispersion equation is solved for the case of growing wave amplitude, and an expression for the maximum increament of growth is found. The maximum particle density is determined assuming instability due to collective interactions is insignificant. The maximum density for electron or electron-positron beams is found. (M.J.T.)

5951 ION SOURCE WITH LONGITUDINAL MAGNETIC FIELD. Starodubtsev, S. V.; Muminov, V. A. (Inst. of Nuclear Physics, Academy of Sciences, USSR). Izv. Akad. Nauk Uz. SSR, Ser. Fiz.-Mat. Nauk, No. 1, 57-9(1965). (In Russian).

The source is based on the fact that a larger fast-electron current density can be produced in an oscillating discharge in a longitudinal magnetic field, which causes the electrons to travel along helical trajectories and thereby increases the average distance traveled between electrodes and the ionization probability. The source was intended for the production of hydrogen ions. The discharge current reached 0.5 amp and the field 750 Oe. The voltage was adjustable between 0 and 1000 v. The working pressure was 2×10^{-4} mm Hg. Discharge could be produced when the field reached 180 Oe, and saturation set in above 500 Oe. The drawing voltage could be adjusted from 2 to 1000 kv. The maximum ion current reached 17 mamp. (ATD)

5952 POLE FACE WINDINGS IN THE TODAI AG ELECTRON SYNCHROTRON. Huke, Kazuo; Kawasaki, Sunao (Tokyo Univ.). Jap. J. Appl. Phys., 4: 915-20 (Nov. 1965).

Pole face windings were applied to the Todai AG electron synchrotron to avoid an integral resonance line of betatron oscillations and to increase the energy of accelerated electrons that would be lost at 98 Mev. Magnetic fields produced by the pole face windings were calculated by the use of a linear transformation and an image method, and were compared with the value measured. Good agreement was obtained. The locus of the frequency of the betatron oscillations in the stability pattern was also analyzed, when the pole face windings were applied, and was compared with experiments. With a rather small power supply, an electron energy of 135 Mev was obtained. (auth)

5953 DATA LOGGING USED ON A PROTON LINEAR ACCELERATOR AND A DESCRIPTION OF THE ANALOGUE TO DIGITAL CONVERTER USED. Kracht, U. (CERN, Geneva). Nucl. Instrum. Methods, 37: 231-9(Nov. 1965).

Data logging from pulsed particle accelerators requires many analog-to-digital converters to sample the information at precise moments. The simple transistorized converter described uses the principle of fast charging of a capacitor and subsequent discharge with constant current. Thus the discharge time, which is converted to a burst of pulses (100 kc), is proportional to the capacitor charge amplitude. The converter circuit designed has an output of 255 pulses for a 10 v input pulse. The circuit for the necessary 8 bit store with reset and overflow circuits is also given. Two varieties of the converter circuit together with a simple digital to analog converter for connection to a pen recorder, are added. (auth)

5954 STABILIZATION OF THE ACCELERATION INTENSITY OF THE U-120 CYCLOTRON. Teodoru, V. (Inst. of Physics, Bucharest). Prib. Tekh. Eksp., No. 5, 21-6(Sept.-Oct. 1965). (In Russian).

Four methods used for the stabilization of the voltage of the U-120 cyclotron were reported with brief indications of the advantages and deficiencies of each method. Emphasis was placed on voltage stabilization with control of the thyratron grid phase of the rectifier with an efficiency comparable to that attainable at the present. (tr-auth)

5955 RESONANCE METHOD FOR ADJUSTING CIRCULAR IRIS WAVEGUIDES IN LINEAR ACCELERATORS. Zverev, B. V.; Sobenin, N. P. (Inst. of Engineering Physics, Moscow). Prib. Tekh. Eksp., No. 5, 26-9(Sept.-Oct. 1965). (In Russian).

The accuracy of the measurement of the frequency in resonance-type segments of circular iris waveguides was evaluated. The method, that makes it possible to adjust the waveguides with plane variable dimensions even at tolerances ±50 mcoulomb, was described. The band characteristics of the waveguide after adjustment were satisfactory from the viewpoint of steady operation of high frequency generators. The validity of the correction of the phase velocity was retained with an error <1%. (tr-auth)

5956 MEASUREMENTS OF THE ION BEAM PHASE VOLUME IN A LINEAR ACCELERATOR INJECTOR. Ivanov, N. F.; Sivkov, Yu. P.; Solnyshkov, A. I. (Scientific-Research Inst. of Electrophysical Apparatuses, Leningrad). Prib. Tekh. Eksp., No. 5, 30-4(Sept.-Oct. 1965). (In Russian).

The results of the measurement of the phase volume of the axial-symmetrical beam of protons at energies from 500 to 600 kev with currents of the order of 100 mamp were reported. The density distribution of the beam in the phase space was recorded on a photofilm. The determination of the parameters of the beam in the phase space (xx'yy'), determining the possibility of further acceleration of the particles in channels of finite cross section, led to the cylindrical coordinates $(R,R',\theta,R\theta)$, which makes it possible to analyze the experimental results graphically and simply. (tr-auth)

5957 AUTOFOCUSING ION SOURCE FOR ELECTROSTATIC ACCELERATORS. Romanov, V. A.; Serbinov, A. N. (Inst. of Physics and Power Engineering, Obninsk, USSR). Prib. Tekh. Eksp., No. 5, 34-7(Sept.-Oct. 1965). (In Russian).

On the basis of the method for the calculation of the focusing beam in accelerating tubes on the conditions that N = const., the construction of an autofocusing ion source was selected. The change of the voltage on the accelerating tube from 0.5 to 5 Mv does not affect the focusing of the ion beam. (tr-auth)

5958 RECORDING OF SHORT PULSES OF ELECTRON CURRENT FROM A BETATRON INJECTOR. Kolotov, O. S.; Lobanov, Yu. N.; Tulinova, N. I. (Moscow State Univ.). Prib. Tekh. Eksp., No. 5, 37-9(Sept.-Oct. 1965). (In Russian).

The injection of electrons, working in a regime of short pulses (up to 6 nsec), and the method for the recording of the form and duration of the pulses of the electron current from the injector in the betatron chamber were described. (tr-auth)

5959 MEASUREMENTS OF INDEX OF MAGNETIC FIELD LOSS IN CHARGED PARTICLE ACCELERATOR. Papadichev, V. A. (Inst. of Nuclear Physics, Novosibirsk, USSR). Prib. Tekh. Eksp., No. 5, 213-16(Sept.-Oct. 1965). (In Russian).

The method and the device for the determination of the index of magnetic field loss in charged particle accelerators are described. The device is based on the measurement of the gradients of radial components of the magnetic field. The construction of the device is given and with it the index of the magnetic field loss can be measured with a precision of 2 to 3%. (tr-auth)

5960 DESIGN OF THE DEFLECTOR FOR THE rf BEAM SEPARATOR AT THE BROOKHAVEN AGS. Hahn, H.; Halama, H. J. (Brookhaven National Lab., Upton, N. Y.). Rev. Sci. Instrum., 36: 1788-96(Dec. 1965). (BNL-9306).

The iris-loaded deflector for the Panofsky/type r-f beam

separator now under construction at the AGS is described. General expressions for the transverse momentum acquired by an ultrarelativistic particle traversing the deflector are derived from the field equations. Useful figures of merit (shunt impedance R, series impedance Z, quality factor Q, R/Q, etc.) are defined. Computational results for the aperture radius a, the guide radius b, Q, R/Q, and R as functions of group velocity v_g, the number of irises per wave-length N, and iris thickness d/w are presented for structures with the phase velocity $v_p = c$. They are compared with experimental results reported from deflection tests. The design procedure of a deflector is developed for the realistic case that the shunt impedance varies with group velocity. Optimization of operating frequency $f_{\pi/2}$ deflector length l, v_g, d/w, and N is carried out. Higher-order modes in iris-loaded waveguides are investigated, and methods for the suppression of mode degeneracies are outlined. The effect of the mechanical tolerances on the phase shift per cell Φ is considered. The chosen deflector structure has $\lambda_0 = 10.495$ cm, N = 4, $\Phi = \frac{1}{2}\pi$, d/w = 0.8, 2a = 48.13 mm, 2b = 116.71 mm, l = 3.07 m, rounded iris edges, and lateral rods as mode stabilizers. "Cold" measurements on cavities and waveguides are described, and a precise R/Q perturbation method is detailed. Pertinent results are $f_{\pi/2} = 2856.35$ Mc, Q = 8700, phase error per cell $\Delta\Phi = 2.7°$ rms, R/Q = 1.41 kΩ/m, $v_g/c = -0.0204$, $\alpha l \approx 0.5$. It is concluded that a klystron pulse of ≥ 14 MW is sufficient to give a 1 mrad peak deflection of 18 Bev/c particles. (auth)

5961 HIGH FIELD AIR-CORED BETATRON USED TO INVESTIGATE INTENSE RUNAWAY ELECTRON STREAMS. Skarsgard, H. M.; Gore, J. V. (Univ. of Saskatchewan, Saskatoon). Rev. Sci. Instrum., 36: 1807-12(Dec. 1965).

An air-cored betatron was constructed whose coil is effectively a single turn made up from four circular turns connected in parallel. The design was facilitated by choosing independently the positions of the four parallel turns and the current distribution through them. The desired current distribution was obtained by making two of the turns in the form of toroidal coils whose inductance could be adjusted. The betatron was used in combination with an azimuthal magnetic field for the production of an intense stream of runaway electrons, consisting of essentially all the electrons of a plasma. After a short interval (~0.1 μsec) of normal acceleration, the electrons experience less-than-normal acceleration followed by deceleration and disruption of the stream. Intense bursts of microwave radiation occur during the current pulse. The observed stream behavior is reasonably well explained by the theory of the two-stream instability. (auth)

5962 LONGITUDINAL SPACE-CHARGE EFFECTS IN STANDING WAVE LINACS. Morton, P. L. (Midwestern Universities Research Assn., Stoughton, Wis.). Rev. Sci. Instrum., 36: 1826-30(Dec. 1965).

The techniques used in Nielsen and Sessler's treatment of the longitudinal space-charge problem in circular accelerators are applied to the longitudinal space-charge problem in linear accelerators. A method for determining the dependence of the available longitudinal phase-space area on the beam current is outlined. An example is worked out using the parameters of a linac designed at MURA for various values of stable phase angle, drift-tube hole radius, and beam radius. Numerical results show that there is a significant decrease in stable longitudinal phase-space area for instantaneous beam currents larger than about 100 to 200 mamp. (auth)

5963 DOUBLE PULSER (Engineering Materials). (Lawrence Radiation Lab., Univ. of California, Livermore). (CAPE-1215).

14 drawings.

The double pulser described is used in a system that supplies 1500 v d-c "bias" to a pair of deflecting plates, which control a beam of accelerated particles to or away from a target. The double pulser has inputs terminated in 125 ohms and is followed by differentiators. The positive outputs from two dynodes are combined. Normally only one input is connected except for output repetition rates between 1.25 and 2.5 Mp/s. Two shaper stages suppress ringing introduced by the variable delay line. Power amplifiers that are used must always be terminated in 125 ohms external to the chassis. (For details, see TID-4100). (M.C.G.)

5964 LINEAR ELECTRON ACCELERATOR. Jarvis, Timothy Robert (to Associated Electrical Industries Ltd.). German Patent 1,200,972. Sept. 16, 1965. Priority date July 26, 1962, Great Britain.

In order to obtain electron bunches of a duration of 10^{-11} seconds an iris loaded wave guide is disposed in front of the exit of the accelerator and in coaxial alignment with it in which the electrons are deflected. (Gmelin Inst.)

5965 MICROWAVE LINEAR ACCELERATOR. Kelliher, Maurice Grodon (to High Voltage Engineering Corp.). German Patent 1,201,929. Sept. 30, 1965. Filed Dec. 14, 1959.

The accelerator comprises in axially alignment with each other an injector, an accelerating and bunching iris loaded wave guide, and a main accelerating iris loaded wave guide. The bunching wave guide is provided with phase shifting means in the feed back circuit which induce a negative feedback. (Gmelin inst.)

Astrophysics and Cosmology

Refer also to abstract 6206.

5966 (AD-618905) SOLAR FLARE HAZARDS: PREDICTABILITY. Good, R. C. Jr. (General Electric Co., Philadelphia, Pa. Missile and Space Div.). July 1965. 45p. (R65SD31). CFSTI $2.00 cy, $0.50 mn.

The hazards of solar flares are discussed in some detail to show the need for prediction. Hazards are noted as protons, x rays, ultraviolet, and radio interference. Since the first is potentially the most dangerous, some data on dosage during flares are presented to evaluate the hazards. Since flares occur at or near sunspots and since there seems to be a direct correlation with the characteristics of sunspots, some discussion is given of the dimensions and characteristics of sunspots. One prediction scheme is presented which involves the statistics of flares, and a scheme is described that is presently being used for flare studies at the Space Sciences Laboratory. (auth)

5967 (AD-619740) DEVELOPING A SYSTEM OF SOLAR FLARE PREDICTION. Semiannual Report No. 2, January 1-June 30, 1965. Billings, Donald E. (Colorado Univ., Boulder). Contract Nonr114713. 5p. CFSTI $1.00 cy, $0.50 mn.

Evidence was sought bearing on the understanding of flare mechanisms necessary for a successful system of flare prediction. Intervals between flares in a given region were studied. The distribution peaked sharply at 80 to 100 min for simple sunspot configurations, with shorter intervals for more complex groups. The hypothesis that flare energy is supplied into a flaring region at a steady rate, but that the flare occurs when it has built up to an unstable level, was favored. Manifestations of flare energy were also studied regarding the question as to whether all of the flare energy discharges during the flash phase of a flare or whether the input continues at a decreasing rate throughout the duration of the flare. Two instances of x-ray curves covering the entire lifetime of flares were found having good rapid-sequence flare hydrogen alpha photographs. (TAB)

5968 (NP-15626) X-RAY ASTRONOMY. Final Report. Ziock, Klaus (Virginia Univ., Charlottesville. Dept. of Physics). [1964]. 59p.

The recent discovery of extra-solar x-ray sources has created an intense interest in the field of x-ray astronomy. The present state of the field is reviewed and instruments and experiments to further the exploration of the sky in the x-ray region are proposed. The literature is surveyed for: experimental evidence of extra solar x-ray sources, theoretical attempts to explain the observations, and reports of

proposed and actually used x-ray telescopes. An array of small paraboloidal telescopes is proposed that is significantly smaller in volume and total length than other proposed designs. A collimator spectroscope combination is proposed that promises sufficient spectral resolution and sensitivity to distinguish between various theoretical models for discrete x-ray sources. Detailed calculations of optimum design parameters for the proper instruments are given in an appendix. (auth)

5969 ON THE ENERGY SPECTRUM OF PROTONS AND α PARTICLES OF COSMIC RAY FLARES ON THE SUN. Charakhchyan, A. N.; Charakhchyan, T. N. (Moscow State Univ. and Lebedev Inst. of Physics, Moscow). Geomagnetizm i Aeronomiya, 5: 220-5(1965). (In Russian).

The differential energy spectrum of primary solar protons with energies of 100 to 170 Mev has the exponent $\gamma \sim 6$. A comparison of data obtained on the ground with those obtained in the stratosphere during a low-energy flare showed that the exponent could be about 3. Further measurements indicated that cosmic rays with energies of hundreds of Mev may be associated with a spectral exponent $\gamma \sim 3.0$ if they are measured in the stratosphere. The same cosmic rays measured on the ground may be associated with the exponent $\gamma \sim 6$. This proton spectrum is connected with a supplementary proton flow carried by the magnetic field and captured from the solar wind in interplanetary space. The spectra of cosmic rays with energies of hundreds of Mev generated in various flares coincide with one another. Energy spectra of solar α particles and nuclei are obtained by nuclear photoemulsions carried by balloons and rockets. Measurements in the stratosphere yielded α-particle energies of 320 to 800 Mev, and measurements taken at great heights by means of rockets yielded 120 to 480 Mev. Spectra from both types of measurements are represented graphically. (ATD)

5970 ON THE COEFFICIENT OF DIFFUSION OF SOLAR COSMIC RAY PROTONS IN THE INTERPLANETARY SPACE. Charakhchyan, A. N.; Charakhchyan, T. N. (Moscow State Univ.). Geomagnetizm i Aeronomiya, 5: 226-9(1965). (In Russian).

Two types of dependence in time of flare emissions on the electromagnetic state of the interplanetary medium are discussed. The first type includes cosmic rays which are generated on the western side of the solar disk and propagate freely in space between the sun and the earth, independently of other chromospheric flares. The second type consists of temporary radiation from the flare with particles that penetrate into the regular stream of a previous chromospheric flare. Four cases of flares related to the first type are discussed. The propagation of cosmic rays occurred freely without corpuscular streams in space. The results obtained are represented graphically. Graphs of observation data obtained on the ground resemble the curve obtained in the stratosphere. Three cases of flares of the second type are discussed. Cosmic rays generated in an active solar region reached the earth when the latter was surrounded by the corpuscular stream of a previous flare. The motion of solar cosmic rays is considered as motion within a magnetic shell of corpuscles ejected during a previous flare. (ATD)

5971 IMPULSIVE EMISSION OF ~40-kev ELECTRONS FROM THE SUN. Van Allen, J. A.; Krimigis, S. M. (Univ. of Iowa, Iowa City). J. Geophys. Res., 70: 5737-51 (Dec. 1, 1965).

Using data from a system of three thin-window Geiger tubes and one thin silicon surface barrier detector on the Mars-bound spacecraft Mariner 4, three interplanetary particle events were observed, on May 25–28, June 5–7, and June 13–14, 1965. The particles are identified conclusively as electrons of energy $E_e \gtrsim 40$ kev with steeply falling energy spectrums and with approximately isotropic angular distributions. The maximum unidirectional intensities are 80, 58, and 5 cm^{-2} sec^{-1} $ster^{-1}$, respectively. The time profiles of intensity exhibit abrupt onsets, increases to maximum values in times of the order of several hours, and gradual declines over periods of the order of the day. It appears that these bursts of interplanetary electrons are emitted impulsively from the sun at approximately the same time as bursts of radio noise and x rays observed by others with terrestrial equipment. The interplanetary diffusion of electrons is discussed, and it is estimated that about 10^{34} electrons $E_e > 40$ kev were emitted on May 25 and on June 5 and about 10^{33} on June 13. The solar emission of nonthermal electrons was suggested previously but not observed so clearly. Such electrons constitute a new tool for study of the structure of the interplanetary magnetic field and for discussion of the physics of solar flares. (auth)

5972 QUASI-STATIONARY COROTATING STRUCTURE IN THE INTERPLANETARY MEDIUM. Wilcox, John M. (Univ. of California, Berkeley); Ness, Norman F. J. Geophys. Res., 70: 5793-5805(Dec. 1, 1965).

A quasi-stationary corotating structure in the interplanetary magnetic field was observed with the Imp 1 satellite during 3 solar rotations. The interplanetary field is directed predominantly away from the sun for $2/7$ of a rotation, then toward the sun for $2/7$ of a rotation, then away from the sun for $2/7$ of a rotation, and finally toward the sun for $1/7$ of a rotation. The interplanetary magnetic field magnitude and the solar wind velocity, density, and flux are discussed with regard to this sector structure. As the structure rotates past the earth once every 27 days it influences geomagnetic activity and cosmic-ray density. A recurring stream of protons of a few Mev energy is almost entirely contained within one sector. The solar source of the recurring geomagnetic storm of December 2, 1963, is associated with a ghost unipolar magnetic region in the solar photosphere. (auth)

5973 SECONDARY PROTONS FROM COSMIC-RAY COLLISIONS IN SPACE. Feit, J. (Adelphi Univ., Garden City, N. Y.); Milford, S. N. J. Geophys. Res., 70: 5957-60(Dec. 1, 1965).

The existence in interstellar space of an appreciable intensity of low-energy protons arising from collisions of the primary cosmic ray beam with interstellar matter is suggested. To estimate the production of secondary protons Webber's calculated unmodulated beam at solar minimum is used as a reasonable estimate of the primary galactic cosmic-ray intensity. The interactions of the cosmic ray proton beam with interstellar helium and the cosmic ray alpha beam with interstellar hydrogen were not included in these estimates. (J.F.P.)

5974 VARIATIONAL PRINCIPLE FOR THE HYDROSTATIC EQUILIBRIUM OF A RELATIVISTIC, ROTATING FLUID. Hartle, James B.; Sharp, David H. (Princeton Univ., N. J.). Phys. Rev. Lett., 15: 909-11(Dec. 13, 1965).

A variational principle is given which supplies a general approach to rotating configurations of equilibrium in general relativity. It is appropriate either to solve the elliptic system of partial differential equations which the problem presents, or to solve a variational problem which is equivalent to this set of equations. Such a variational principle is given. For clarity it is presented in parallel with the Newtonian variational principle. (J.F.P.)

5975 ON THE ISOTOPIC COMPOSITION AND ON THE SITE OF THE LIGHT PRIMORDIAL RARE GASES IN STONE METEORITES. Hintenberger, H.; Vilcsek, E.; Waenke, H. (Max-Planck-Institut fuer Chemie, Mainz). Z. Naturforsch., 20a: 939-45(July 1965). (In German).

Using newly developed techniques for the separate measurements of rare gases in different mineral components of stone meteorites, comprehensive investigations were carried out on meteorites containing primordial rare gases. For the bronzite chondrites Breitscheid and Pantar, it was proven that all main mineral components contain light primordial gases, probably this is also true for the carbonaceous chondrite Murray and for the achondrite Kapoeta. The light primordial gases are highly concentrated in the outmost layers of the single mineral grains. The ratios for $^4He/^3He$ and $^{20}Ne/^{22}Ne$ vary for different meteorites and also for different mineral components within a single meteorite. Both ratios show a correlation with the diffusion coefficients of the minerals involved;

the lighter isotope being always more depleted in those minerals with the higher diffusion losses. According to the observed diffusion losses, the original primordial helium content of Pantar comes out to be at least about two orders of magnitude higher than at present. For the true and original elemental and isotopic ratios of 13.8 and 14.0 for $^{20}Ne/^{22}Ne$, 2200 for $^{4}He/^{3}He$ and 800 for $^{4}He/^{20}Ne$ were obtained. These ratios have been altered considerably on account of gas losses by diffusion. (auth)

5976 THE SOLAR WIND AS THE SOURCE OF PRIMORDIAL RARE GASES IN STONE METEORITES. Waenke, H. (Max-Planck-Institut fuer Chemie, Mainz). Z. Naturforsch., 20a: 946-9(July 1965). (In German).

The solar wind proves to be the main, if not the only source for the large amounts of the so-called primordial gases, which are found in various meteorites especially in the bronzite-chondrites. The presence of the primordial gases in all main mineral components of the meteorites, including the metal phase, and their high concentration in the surface layers of the individual meteoritic grains, indicate a source in form of corpuscular radiation. The measured element ratios of the true original meteoritic primordial gases—especially the He/Ne ratio of 750—prove their correlation to the sun; the solar wind therefore remains the only possible source. The rather high concentration of ^{3}He in the primordial gases—$^{4}He/^{3}He$ = 2200—and therefore also in the solar wind, seems of principal importance for the conditions in the solar atmosphere. (auth)

5977 RARE GAS MEASUREMENTS ON IRON METEORITES AND THEIR INCLUSIONS. Begemann, F. (Univ., Bern; Max-Planck-Institut fuer Chemie, Mainz). Z. Naturforsch., 20a: 950-60(July 1965). (In German).

The isotopes of He, Ne, and Ar were measured in a number of iron meteorites and their troilite and schreibersite inclusions using a statically operated omegatron-type mass spectrometer. In the metal samples the isotopic ratios are in general agreement with expectations based on the curves given by Signer and Nier. An excess of $(13 \pm 2) \cdot 10^{-8}$ cc STP $^{4}He/g$—which might be of radiogenic origin—is indicated, however, in the case of Cranbourne, a large meteorite with a radiation age $27 \cdot 10^{6}$ a $< T_g <$ $70 \cdot 10^{6}$ a. Similar amounts appear to be present in several other iron meteorites as well. Variations in the $^{38}Ar/^{21}Ne$-ratios due to different effective energy spectra are not paralleled by similar changes in the $^{38}Ar/^{36}Ar$-ratios. The data, combined with those of Signer and Nier and Heymann, Lipschutz, Nielsen, and Anders show the reason to be a simultaneous shift of the yield curve along the isobar M = 36, the trend being in agreement with results from target experiments. For the He and Ne produced on S the ratios $^{3}He/^{4}He \geq 0.112$ and $^{20}Ne : {}^{21}Ne : {}^{22}Ne = 1.12 : 1.00 : 1.21$ were obtained while the production rates of ^{3}He, ^{4}He, ^{20}Ne, ^{21}Ne, and ^{22}Ne on S relative to iron were found to be 0.75 ± 0.2, ≤ 1.79, 7.8 ± 1.3, 7.35 ± 1.2, and 8.3 ± 1.4, resp. Possible reasons for the unexpectedly high production rate of ^{20}Ne are being discussed. (auth)

5978 THE ORIGIN OF ANOMALOUS ^{129}Xe IN METEORITES. Merrihue, Craig (Smithsonian Astrophysical Observatory, Cambridge, Mass.; Harvard Coll. Observatory, Cambridge, Mass.); Turner, Grenville. Z. Naturforsch., 20a: 961-2(July 1965). (In German).

Evidence is presented showing that the presence of xenon-129 in meteorites originated from the decay of iodine-129 within the meteorite itself. Four lines of evidence are invoked: variations in the $^{129}Xe/^{132}Xe$ ratio among meteorites and in different phases of the same meteorite; variations in the $^{129}Xe/^{132}Xe$ ratio in whole meteorites or meteorite minerals with temperature during gas release; correlation of radiogenic ^{129}Xe release with ^{128}Xe produced artificially from ^{127}I in meteorites by neutron irradiation; and close agreement between these correlations for several different meteorites manifested by a similarity in calculated formation intervals. It is concluded that the evidence available strongly supports an in situ decay origin of the special ^{129}Xe anomaly in meteorites. (J.F.P.)

5979 POTASSIUM ANALYSIS OF AMPHOTERITE CHONDRITES AND THEIR K–Ar AGE. Kaiser, W.; Zaehringer, J. (Max-Planck-Institut fuer Kernphysik, Heidelberg). Z. Naturforsch., 20a: 963-5(July 1965). (In German).

The K-content of 18 amphoterite chondrites was determined by isotope dilution technique. In contrast to hypersthene- and bronzite-chondrites the K-content of which is around 800 ppm, the amphoterites show large variations from 200 to 2180 ppm. It has also been found that K is not homogeneously distributed within the same specimen. The K-A-ages lie in the narrow range of $(4 \pm 0.5) \times 10^{9}$ years. Only two out of 18 specimens partially lost radiogenic and cosmic ray produced rare gases. An origin from a common source material seems likely. (auth)

Atomic Physics

Refer also to abstract 5748.

5980 (AD–617522) QUANTUM MECHANICS OF THE $(p\text{-}Mu\text{-}p)^{+}$ MOLECULAR ION. Phillipson, Paul (Colorado Univ., Boulder. Dept. of Physics); Wessel, W. Roy (Michigan Univ., Ann Arbor. Dept. of Physics). 1963. 7p. (U-COL–64-16). CFSTI $1.00 cy, $0.50 mn.

Wave functions and energies are computed using the exact hamiltonian of $(p\text{-}\mu\text{-}p)^{+}$. (TAB)

5981 (AD–620002) DESIGN AND CONSTRUCTION OF A BAKEABLE SPUTTERING APPARATUS. Technical Documentary Report, November 1960–December 1963. Laubert, Roman (Radiation Dynamics, Inc., Westbury, N. Y.). Feb. 1965. Contract AF33(616)-8063. 63p. (AL-TDR-64-58). CFSTI $3.00 cy, $0.75 mn.

The construction and testing of an apparatus for studying sputtering is described. The apparatus consists of a duoplasmatron ion source, analyzing magnet, deceleration system, and target chamber. Temperature cycling of the entire system to 400°C can be tolerated. The operations of the ion source, analyzing magnet, and deceleration system are described individually, and as a system. A target holder bakeable to 400°C with two degrees of rotational freedom is described. A short feasibility study was made of an ultraviolet ionization source capable of ionizing sputtered atoms. (auth)

5982 (AERE-R-5061) n = 4 LEVELS OF N^{V} BY ELECTRON IMPACT, COMPUTED WITH THE COULOMB-BORN APPROXIMATION. Taylor, A. Joanna; Lewis, B. A. (Atomic Energy Research Establishment, Harwell (England)). Oct. 1965. 16p. Dep.; BIS $0.50; HMSO 2s. 6d.

Cross sections for the excitation of the N(V) ion by electron impact are calculated in the Coulomb-Born approximation. The transitions considered are those from the n = 2 and 3 states to any of the n = 4 states for the energy range between threshold and 435.36 ev. (auth)

5983 (D–910099-2) THEORETICAL INVESTIGATION OF THE LOWEST FIVE IONIZATION POTENTIALS OF URANIUM. Williamson, H. A.; Michels, H. H.; Schneiderman, S. B. (United Aircraft Corp., East Hartford, Conn. Research Labs.). Sept. 1965. Contract NASw-847. 59p.

Ionization potentials were calculated for uranium and its first four positive ions using approximate quantum mechanical methods. A range of values was obtained for each ionization potential, with the individual values depending upon the approximations entering into the calculations. The final suggested values are: U(I)–6.11 ev; U(II)–17.5 ev; U(III)–37.5 ev; U(IV)–61 ev; and U(V)–118 ev. Ionization potentials for U(I) through U(III), differing only slightly from these final suggested values, were employed in an evaluation of the following properties of equilibrium mixtures of hydrogen and uranium: species concentration, coefficients of viscosity and diffusion, and effective Schmidt number. The calculations were performed at pressures of 100, 500, and 1000 atm, temperatures of 20,000, 60,000, and 100,000°K, and fuel partial pressure fractions of 0.09, 0.1, 0.233, 0.367, 0.5,

0.633, 0.767, and 0.9. The results of these calculations indicate that the uranium ions of lower valency play an important role in the determination of the properties of the mixture up to temperatures higher than had been indicated in preceding studies. (auth)

5984 (NYO-2543-1) ATOMIC ENERGY LEVELS. Final Report. Bearden, J. A.; Burr, A. F. (Johns Hopkins Univ., Baltimore, Md.). 1965. Contract AT(30-1)-2543. 249p. Dep.; CFSTI $6.00 cy, $1.25 mn.

Two sets of tables are presented. The first set presents the calculated energy levels and their errors. The second and the largest set gives for each element energy levels and their differences. Both sets of tables are given in terms of various commonly used units. Three appendices were added, all of which refer to the primary source of x-ray data, representing additional data and changes in interpretation. (M.O.W.)

5985 (ORNL-TM-1262) INTERACTION OF THERMAL ELECTRONS WITH POLARIZABLE AND POLAR MOLECULES [Thesis]. Christophorou, L. G.; Hadjiantoniou, A.; Hurst, G. S. (Oak Ridge National Lab., Tenn.). Nov. 1965. Contract W-7405-eng-26. 79p. Dep. mn; CFSTI $3.00 cy, $0.75 mn.

Submitted by A. Hadjiantoniou to Vanderbilt Univ., Nashville, Tenn.

The electron swarm technique was used to study electron transport in several gases of both the polar and polarizable classes. Measurements were made of free electron drift velocities, W, the ratio W/D where D is the diffusion coefficient, and the attachment coefficient. From the measurement of W or D the cross section for momentum transfer was deduced. Ethylene was used as a carrier gas to provide a swarm of thermal electrons (low E/P). The nonpolar gases N_2, CO_2, C_2H_4, C_3H_8, C_4H_{10}, C_5H_{12}, and C_6H_6 were studied without carrier gas. Other nonpolar molecules, such as propane, pentane, hexane, heptane, octane, nonane, decane, benzene, cyclohexane, p-xylene, and p-dichlorobenzene, and polar molecules, such as m-xylene, o-xylene, o-bromotoluene, m-dichlorobenzene, bromobenzene, chlorobenzene, and o-dichlorobenzene were studied with carrier gas. It was found that the Altshuler theory and experimental results are in relative agreement, which becomes better for small molecules with large permanent dipole moments. (P.C.H.)

5986 (UCRL-14402-T) PLANE WAVE—A COMPUTER PROGRAM TO FIND IONIZATION CROSS SECTIONS. Lawrence, J. Dennis (Lawrence Radiation Lab., Univ. of California, Livermore). Sept. 14, 1965. Contract W-7405-eng-48. 57p. Dep. mn; CFSTI $3.00 cy, $0.75 mn.

In connection with the bombardment of elements by particles, it was desired to compute ionization cross sections of the various electronic shells. A numerical method for doing this was developed, with error terms, and programmed for the Remington-Rand Univac Larc computer. (auth)

5987 (ANL-Trans-248) GROUND-STATE ENERGY OF He. Demkov, Yu. N.; Neigauz, M. G.; Senyukov, R. V. Translated by Elmar K. Wilip (Argonne National Lab., Ill.), from Opt. Spektros., 4: 709-11(1958). 10p. Dep. mn; CFSTI $1.00 cy, $0.50 mn; JCL $1.10 fs, $0.80 mf.

The upper and lower limits of the ground-state energy of the He atom in non-relativistic approximation were calculated from the stationary function. All coefficients (n = 30) were determined. (auth)

5988 (JPRS-32421) REPORTS PRESENTED AT THE THIRD ALL-UNION CONFERENCE OF THE PHYSICS OF ELECTRON AND ATOM COLLISIONS, JUNE 21–28, 1965. Translated from pp 3-87 of Tret'ya Vsesoyuznaya Konferentsiya po Fizike Elektronnykh i Atomnykh Stolknoveniy, Iunya 21–28, 1965, Tezicy Dokladov. 86p. (TT-65-32910; CONF-650662). CFSTI $3.00 cy, $0.75 mn.

Summaries of papers presented at the above conference are presented. The subject areas of the papers include collision of heavy particles, electron collisions with atoms and molecules, excitation of noble gases during electron-atom collisions, electron-molecule collisions and ionic molecular processes, experiment and experimental procedures, low temperature plasma, photoionization, photodissociation, and second order collisions, and a theoretical section. (M.O.W.)

5989 IONIZATION CROSS-SECTIONS OF ATOMS AND MOLECULES BY ELECTRON IMPACT. Batabyal, A. K.; Barua, A. K.; Srivastava, B. N. (Indian Assoc. for the Cultivation of Science, Calcutta). Indian J. Phys., 39: 219-26(May 1965).

Apparent ionization cross sections of several atoms and molecules for 70-ev electrons were measured with the help of a mass spectrometer. By introducing a simple correction an attempt was made to improve the method of Otvos and Stevenson for the calculation of the ionization cross sections of atoms and molecules. With this correction, the additivity postulate for the molecular ionization cross sections appears to hold better. (auth)

5990 PHOTOELECTRIC CROSS SECTIONS OF GAMMA RAYS FOR HEAVY ELEMENTS. Ghose, A. M. (Bose Inst., Calcutta). Nucl. Phys., 75: 539-48(1966).

Measurements of photoelectric cross sections of heavy elements by the sphere transmission method are presented. By using a constant spectral sensitivity photon counter and a rotation arrangement for averaging the photon intensities, total photoelectric cross sections σ_a of Pb and Hg were measured for ^{60}Co photons as 4.43 ± 0.20 b/atom and 4.01 ± 0.25 b/atom, respectively. For ^{137}Cs, the value of total σ_a for Pb was found as 14.1 ± 0.7 b/atom. These results are compared with the measurements of previous workers and with the theories of photoelectric effect. It is found that the experimental results obtained by different workers for ^{60}Co γ rays show mutual agreement, if the ratios of K shell to total photoabsorption are assumed to have the values given by Hultberg. However for ^{137}Cs photons, different values of these ratios must be used to restore agreement between the results obtained by different workers. There is general agreement between the sphere transmission and beta spectroscopic methods. (auth)

5991 ABSOLUTE MEASUREMENT OF THE COMPTON SCATTERING CROSS SECTION IN LEAD. Quivy, R. (Centre de la Faculte Polytechnique, Mons, Belg.). Nucl. Phys., 76: 362-8(1966). (In French).

An experimental method for an absolute measurement of Compton effect differential cross section is proposed. An experiment was carried out with 662 kev γ rays scattered by lead for angles from 20° to 160°. Results are in good agreement with the Klein-Nishina formula for scattering angles above 30° and with the Heisenberg-Bewilogua theory for smaller scattering angles, showing the decreasing effect of electron scatterer binding energy upon the cross section of Compton scattering. (auth)

5992 ON THE MOTT POLARIZATION EFFECT IN SCATTERING OF FAST ELECTRONS ON THOMAS-FERMI AND HARTREE-FOCK ATOMS. Tietz, T. (Univ. of Lodz, Poland). Nuovo Cimento (10), 36: 1365-71(Apr. 16, 1965). (In German).

The effect of the electron shell of the scattering atom on the asymmetry effect in the intensity distribution was investigated. The Sauter representation of the Born-Dirac collision method was used. The potential pattern in the core of the atom was treated by the Thomas-Fermi and Hartree-Fock methods. The application of these potential patterns gave no significant difficulties. Numerical values were tabulated for the γ_4 constants for various Z values. The asymmetry of the Hartree-Fock and of the Coulomb field was evaluated as a function of the angle and energy. These results are tabulated. (J.S.R.)

5993 CALCULATIONS OF THE ENERGY AND ANGULAR DISTRIBUTION OF ELECTRONS EJECTED FROM HELIUM BY PROTONS. Oldham, William J. B. Jr. (Manned Spacecraft Center, Houston, Tex.). Phys. Rev., 140: A1477-81(Nov. 29, 1965).

Doubly differential cross sections (ddcs), for ejection of secondary electrons of various energies at various angles for helium bombarded by 50-, 100-, and 150-kev protons, were calculated and compared with the recent experimental results of Rudd and Jorgensen. Differential cross sections obtained by integrating the ddcs over all ejection angles are compared with similar results obtained from the experimental ddcs. The wave functions employed by Mapleton to calculate ionization cross sections are used in the Born approximation. General agreement between theory and experiment for the ddcs is found, but discrepancies are noted in the forward and backward directions. The integrated cross sections show good agreement over a large range of ejection energies. (auth)

5994 ION-ELECTRON RECOMBINATION. D'Angelo, Nicola (Princeton Univ., N. J.). Phys. Rev., 140: A1488 (Nov. 29, 1965).

It is shown that the rate of ion-electron recombination by collisions of two electrons in the field of an ion can be obtained by an elementary calculation based on a formula given by J. J. Thomson in 1924. A comparison is made with the results obtained by Hinnov and Hirschberg and by Bates et al. (auth)

5995 ENERGY-LEVEL SHIFT FOR ATOMS WITH POINT NUCLEI DUE TO HIGHER ORDER VACUUM POLARIZATION. Nigam, B. P. (Arizona State Univ., Tempe). Phys. Rev., 140: B1693-?(Dec. 20, 1965).

The energy-level shifts for hydrogen and mesonic hydrogen due to higher order vacuum polarization effects were calculated using Schwinger's result for the Lagrangian density which takes into account the effect of vacuum polarization so as to include Feynman diagrams involved in photon-photon scattering and similar higher order diagrams. The calculations are carried out by defining a field-dependent dielectric constant. The values of the level shifts for hydrogen and mesonic hydrogen are estimated, respectively, to be about 10^{-4} times and 10^{-2} times that obtained for the lowest order diagram. Results for Z = 2 and 3 are also given. (auth)

5996 PERTURBATION INDUCED IN ELASTIC SCATTERING BY CROSSING OF MOLECULAR STATES. Smith, F. T.; Lorents, D. C.; Aberth, W.; Marchi, R. P. (Stanford Research Inst., Menlo Park, Calif.). Phys. Rev. Lett., 15: 742-6(Nov. 8, 1965).

It was previously noted that the regularity of simple oscillations was marred by reproducible perturbations at certain points possibly due to the crossing or pseudocrossing of two molecular electronic curves of the same symmetry. An identification of one of these features with a particular crossing is reported. The use of such a perturbation for estimating both the location of a crossing and the magnitude of the interaction energy is described. Curves with these features are given representing the scattering spectrum of $He^+ + He$ at $E_{lab} = 100$ ev, and also those of $He^+ + Ne$, and $He^+ + Ar$. These curves show clearly that the first perturbation structure is followed by other features of the same type at larger angles. A discussion of the theory explaining this phenomenon is given. The curve-crossing perturbation represents a coupling of electronic states induced primarily by the radial motion of the nuclei. It should be clearly distinguished from the rotation-inversion coupling that induces a phase-shift of π in the odd scattering amplitude in the limit of high energy and small impact parameter. (J.F.P.)

5997 POSITRON LIFETIMES IN LOW-TEMPERATURE HELIUM GAS. Roellig, L. O.; Kelly, T. M. (Wayne State Univ., Detroit). Phys. Rev. Lett., 15: 746-8(Nov. 8, 1965).

The results of a series of positron lifetime measurements in helium gas at 4.2°K are presented. A shoulder was observed in the lifetime spectrum which exhibited an exponential decay, in contrast to the results reported in argon, followed by a hump and then another exponential decay. The shape of the annihilation spectrum reported is the basis for a re-examination of the decay process of positrons in helium. Typical delayed coincidence spectra at various helium-gas pressures are shown. The values for various lifetimes and the shoulder width for helium gas at various pressures between one-half and one atmosphere are given. The existence of the hump at the inflection point of the shoulder indicates that the annihilation rate changes very rapidly after a fixed time interval from the birth of the positron. The variation of the density-shoulder width product with density for helium gas at 4.2°K is also given. It is suggested that the annihilation process which yields a certain lifetime in low-temperature gaseous helium is the same process which produces the intermediate component in liquid helium. (J.F.P.)

5998 SPIN POLARIZATION OF SLOW ELECTRONS BY ELASTIC RESONANCE SCATTERING FROM NEON. Franzen, W.; Gupta, R. (Boston Univ.). Phys. Rev. Lett., 15: 819-22(Nov. 22, 1965).

It is pointed out that a more powerful method for the production of intense beams of polarized electrons is a direct consequence of the recent discovery of a doublet structure in the resonance for elastic scattering of electrons by neon atoms at 16 ev. The observed resonance consists of a small decrease in cross section, followed by two successive peaks, which are interpreted as corresponding to the formation of metastable compound states. Under these circumstances, interference between resonance and potential scattering in the presence of fine-structure splitting will give rise to almost complete polarization of electrons scattered through 90° at certain energies, as in the polarization of neutrons and protons by scattering from helium. This is demonstrated. The electron polarization averaged over three different solid angles is shown as a function of electron energy for electrons scattered by neon in the vicinity of the scattering resonance at $E_0 = 16.079$ ev. (J.F.P.)

5999 ELECTRON–H-ATOM ELASTIC-SCATTERING RESONANCES. McGowan, J. William; Clarke, E. M.; Curley, E. K. (General Atomic Div., General Dynamics Corp., San Diego, Calif.). Phys. Rev. Lett., 15: 917-20 (Dec. 13, 1965).

Resonances are reported in the e-H scattering signal observed essentially at 90° to the plane of intersection between a modulated beam of H atoms and a beam of energy-analyzed electrons. The experimental arrangement is shown. Two resonances are found which are defined below 10 ev. If the center of a resonance is defined as half-way between the maximum and the minimum, the first is centered near 9.45 and the second near 9.68 ev. Above 10 ev there is a complex structure which is probably associated with a number of resonances just below the first excitation threshold of the H atom and, at 10.20 ev, the threshold itself. The existence and placement of resonances in the e-H system were first predicted theoretically, and followed by two experimental reports of such structure prior to the present work. These are each discussed, and the present experiment is also discussed further. (J.F.P.)

6000 BEAM SOURCE FOR MOLECULAR AND ATOMIC HYDROGEN. Eisenstadt, Melvin M. (Univ. of Arizona, Tucson). Rev. Sci. Instrum., 36: 1878-9(Dec. 1965).

A beam source is described from which atomic beams are obtained by dissociation of molecular hydrogen through heating of the source to a high temperature. (D.C.W.)

6001 ANISOTROPIC HYPERFINE INTERACTION OF SHALLOW DONOR ELECTRON WITH ^{29}Si NUCLEUS. Chang, Yi-hsiang. Wu Li Hsueh Pao, 21: 1139-61(June 1965). (In Chinese).

The spin hamiltonian of the hyperfine interaction between a shallow donor and the ^{29}Si nuclei was derived on the basis of the effective mass wave function. The interference effect between the Bloch functions of different valleys is shown to be largely responsible for the anisotropy of the electron-nuclear hyperfine interaction. An expression for the resonance frequency was derived in the high field approximation. The theory is shown to account for the experimental observations of Feher on the anisotropic hyperfine interaction

quantitatively. The coefficient of the 2p core function in the OPW conduction band edge Bloch functions was determined by comparison with Feher's results to be 0.20 approximately. It is pointed out that on the basis of the theory given, the positions of the conduction band minima and the anisotropy of the donor effective mass wave function can be precisely determined by the method of ENDOR and its pressure effects. (auth)

6002 QUANTUM NOISE OPERATORS FOR THE N-LEVEL SYSTEM. Haken, H.; Weidlich, W. (Technische Hochschule, Stuttgart). Z. Physik, 189: 1-9 (1965).

An N-level system of one electron subject to a heatbath or fluctuating forces as well as to classical or quantum mechanical driving forces is considered. It is assumed that the equation of the density matrix averaged over the heatbath is already determined with all damping constants and transition probabilities. By this procedure the electron transition operators $a_i^\dagger(t)a_k(t)$ lose their property to form an algebraic ring with the relation $a_i^\dagger a_k a_l^\dagger a_m = \delta_{kl} a_i^\dagger a_m$. Fluctuating forces are reintroduced into the density matrix equation, and it is required that the above equation be averaged over the heatbath. It is shown that this requirement determines uniquely all second order correlation functions of the fluctuating forces, which are assumed to be markoffian. An explicit formula is given by which these correlation functions can be calculated by a simple sum over averaged density matrix elements multiplied with the coefficients of the averaged density matrix equation. Usually the fluctuating forces stem from many statistically independent subsystems of the heatbath, so that they are to a very good approximation gaussian. In this case the treatment fixes also all higher correlation functions. (auth)

6003 PRODUCTION OF METASTABLE Hg ATOMS BY CHARGE EXCHANGE [Thesis]. Rostron, Robert Walther. Tucson, Ariz., Univ. of Arizona, 1964. 70p.

Mercury ions were extracted from the plasma of a mercury arc discharge through the small aperture in a probe at high negative potential. By means of suitable electrodes, the ions were brought to any desired energy in the range 100 to 4000 ev. The ions then passed through a field-free region containing mercury vapor where part of them became neutralized by charge-transfer collisions. The remaining ions were stopped by a retarding potential. The beam of neutral atoms then struck a metal target within a suitable cage for collecting ejected secondary electrons. The yield of secondary electrons was so large that it seemed unlikely that neutral atoms of mercury in their ground state could be responsible. Values of γ as high as 0.40 were noted. The only reasonable alternative seemed to be that the neutral atoms were in a metastable state. Two methods were used to test this hypothesis. The first consisted of increasing the distance of flight of the metastables giving them more time to decay in flight. The second method was to introduce small amounts of foreign gases to quench the metastables in flight. In both cases the resulting large decreases in secondary electron current at the target confirmed the metastable hypothesis. By plotting the energy spectrum of the secondary electrons and noting their maximum energy, the most energetic state of the metastable atoms was found to be 8.95 ev. A pertinent side light of the experiment was the observation of Hg^- ion formation. (Dissertation Abstr.)

Cosmic Radiation

See also Elementary Particles and Radiations
Nuclear Properties and Reactions

Refer also to abstract 5722.

6004 (AD-619508) A STUDY OF THE ATMOSPHERIC EFFECTS ON COSMIC RAY RECORDS FROM PLASTIC SCINTILLATION MONITORS AT UPPSALA. Ekstroem, L. (Uppsala Univ. (Sweden)). Apr. 15, 1965. Contract AF-EOAR64-64. 17p. (SR-2; AFCRL-65-587). CFSTI $1.00 cy, $0.50 mn.

Atmospheric effects on cosmic ray records from the plastic scintillation monitors at Uppsala are studied according to modified Duperier and Dorman models. Pressure coefficients were found for the vertical as well as the inclined directions. The two models were investigated partly by an "ordinary" or "direct" method and partly by a "successive difference" method. A significant difference between the results from the two methods was found especially in the Dorman case. The serial correlation of the residuals was tested with a statistic difference introduced by Durban and Watson, 1951. This test seemed to point out that the "difference" method is more favorable and gives more reliable results from a statistical point of view. (auth)

6005 (AD-623632) A STUDY OF VERTICALLY INCIDENT COSMIC-RAY TRAJECTORIES USING SIXTH-DEGREE SIMULATIONS OF THE GEOMAGNETIC FIELD. Environmental Research Papers, No. 141. Shea, M. A.; Smart, D. F.; McCracken, K. G. (Air Force Cambridge Research Labs., L. G. Hanscom Field, Mass.). Sept. 1965. 395p. (AFCRL-65-705). CFSTI $7.00 cy, $1.75 mn.

A study was made of vertically incident cosmic-ray trajectories at more than 400 positions on the earth's surface using sixth-degree simulations of the quiescent geomagnetic field. Twenty-six of these positions are near the South African magnetic anomaly, and six other points are in a region of the North Atlantic where Pomerantz and Agarwal have reported anomalous results. The trajectories were calculated for rigidities separated by intervals as small as 0.01 Bv to allow for the effects of the penumbra. When these trajectories are used to determine cosmic-ray cutoff rigidities, differences greater than 15 percent from the Quenby and Wenk threshold values are found in the vicinity of South Africa, the South Atlantic, and the Canary Islands. Various latitude surveys are shown to exhibit consistency when plotted against the cutoff rigidities determined by this computational method. It is concluded that although currently available simulations of the geomagnetic field are not completely adequate over some portions of the earth to describe the cosmic-ray effects in their entirety, there is essentially no difference in the cutoff rigidities determined using two currently accepted field models, even though different penumbral structures are obtained. Asymptotic directions of approach and cutoff ridigities for a number of locations are listed. (auth)

6006 (CONF-640919) PROCEEDINGS OF CONFERENCE ON THE INTERACTION BETWEEN COSMIC RAYS AND HIGH ENERGY PHYSICS HELD AT CASE INSTITUTE OF TECHNOLOGY, CLEVELAND, OHIO, SEPTEMBER 25-26, 1964. (Case Inst. of Tech., Cleveland, Ohio). Contract AT(11-1)-818. 240p. (AD-613611). Dep. mn; CFSTI $6.00 cy, $1.25 mn.

Discussions are given of high-energy physics experiments carried out using cosmic radiation. Coordination of future research, possible space-environment experiments, and construction of facilities for joint use are discussed. Separate abstracts were prepared for eleven papers. Two papers were previously abstracted for NSA; see abstracts 19: 16595 and 34983. (M.J.T.)

For abstracts of individual papers see: 5722-5725, and 6007-6013.

6007 (CONF-640919, pp I43-8) COSMIC RAY MUON INTERACTIONS AT 5-50 Gev. Neddermeyer, Seth (Washington Univ., Seattle).

Cloud chamber studies of interactions of cosmic-ray muons with electrons and nuclei at 5 to 50 Bev are described. Evidence for a possible asymmetry in the behavior of positive and negative muons in hard collisions with electrons is discussed. (M.J.T.)

6008 (CONF-640919, pp I48-54) NEUTRINO AND MUON MEASUREMENTS 10,000 FT. UNDERGROUND. Reines, F. (Case Inst. of Tech., Cleveland, Ohio).

An experiment is described to investigate the interactions of high-energy neutrinos produced in the atmosphere by high-energy cosmic rays and to detect muons conceivably produced by extragalactic energetic neutrinos origi-

nating, e.g., in the Crab Nebula. The detection system, consisting of scintillators in a rail geometry, is located 10,500 ft underground in a South African gold mine. It is hoped to obtain crude angular distributions, with an expected count rate as low as 10/yr from atmospheric neutrinos; if only atmospheric sources are found, information on the neutrino cross sections to several Bev can be found. The possibility of detecting the W resonance in the interaction $\nu_e + e^- \rightarrow W \rightarrow \nu_\mu + \mu^-$ is mentioned. (M.J.T.)

6009 (CONF-640919, pp II1-13) COSMIC RAY FLUXES AND POSSIBLE EXPERIMENTS. Pal, Y.

Experiments using cosmic rays as providing particle beams and experiments using the atmosphere itself as a laboratory are discussed. The fluxes of cosmic nucleons, pions, muons, and kaons and the resulting neutrino fluxes at various energies are summarized. The advantages of mountain-based and of balloon or satellite experiments are described. Experiment design for study of isobar production and of fireballs is considered. Implications of these experiments for astrophysics and for very-high-energy behavior of elementary particles are discussed briefly. (M.J.T.)

6010 (CONF-640919, pp II23-7) EXPERIMENT TO DETECT BASIC TRIPLETS. Schwartz, M. (Columbia Univ., New York).

A version of the basic triplet scheme based on sets of three baryons and three bosons is discussed. The questions of the mass and stability of these particles are mentioned. The experimental set-up, consisting of plastic scintillators and spark chambers, to detect the basic triplets either in the primary cosmic-ray flux or in production interactions in the atmosphere is described. (M.J.T.)

6011 (CONF-640919, pp II30-3) THEORIST'S COMMENTS. Jackson, J.

Cosmic-ray physics experiments are considered to be in one of two groups: those involving accelerator physics at higher energies than available in machines and those involving specialized tests of theoretical conjectures. Problems in the experiments using cosmic rays as a higher energy source are discussed, including flux limitations, ambiguity in the primary-ray identity, high multiplicities, and high backgrounds. (M.J.T.)

6012 (CONF-640919, pp III1-23) RELEVANCE OF COSMIC RAY EXPERIMENTS TO ASTROPHYSICS. Cameron, A.

It is commented that any measurement of the cosmic neutrino fluxes will give strong evidence about the mechanisms occurring in the Crab Nebula. Another question of interest to astrophysics is the composition of cosmic rays as a function of energy. Possible experiments in space—in manned satellite or on the moon—are discussed. (M.J.T.)

6013 (CONF-640919, pp IV17-33) GAMMA-RAY INDUCED SHOWERS. Clark, George.

The detector arrangement of scintillation counters in a large concrete and lead structure is described. Electromagnetic showers, having 0.01 the average concentration of electrons, were observed. The possible gamma-ray origin of these muon-less showers is discussed in view of the apparent isotropy of arrival directions. Energy spectra of the ordinary primaries at 10^{14} to 10^{16} ev were also measured. The nature of the burst observed at the center of 10^{14}-ev showers is considered. (M.J.T.)

6014 (NP-15380) CONTRIBUTION A LA REALISATION ET A LA MISE AU POINT D'UN TELESCOPE CERENKOV POUR L'ETUDE DU RAYONNEMENT COSMIQUE MESURES AU NIVEAU DU SOL [THESES]. (Contribution to the Design and Construction of a Cherenkov Telescope for the Study of Cosmic Radiation Measurements at Ground Level [Thesis]). Durand, Pierre (Clermont-Ferrand Univ. (France). Faculte des Sciences). 1962. 75p. Dep. mn.

Cosmic radiation was analyzed and its time variations studied in order to determine the corrections necessary for different measurements. The theory, application, and utilization of the Cherenkov effect are studied as a function of its adaptation to the measurement and detection of cosmic radiation. The construction of the telescope and the various associated electronic circuits are described. The complexity of the apparatus and the number of electronic circuits necessitate precise control and calibration in order to utilize the apparatus to the maximum of its performance. These are given. The aperture of the telescope is calculated and the results obtained at ground level are reported. (J.S.R.)

6015 THE SECOND MAXIMUM OF COSMIC-RAY STAR FREQUENCY UNDER LEAD. Forbes, V. M.; McPherson, A. I. (McGill Univ., Montreal). Can. J. Phys., 43: 2150-5(Dec. 1965).

The transmission of cosmic radiation at 3392 meters through lead was studied over a range of thicknesses between 10 and 20 cm with intensities measured in terms of star frequency in photographic emulsions. A second maximum was observed between 16 and 17 cm of lead, the transmitted radiation being equal in intensity to the incident radiation. (auth)

6016 DAILY VARIATIONS OF THE HARD COMPONENT INTENSITY OF COSMIC RADIATIONS FOR 1960-1963 BY THE DATA OF NARROW-ANGLE CROSSED TELESCOPES. Akhababyan, N.; Betev, B.; Kavlakov, Sht.; Popova, L. (Inst. of Physics, Bulgarian Academy of Sciences, Sofia). Geomagnetizm i Aeronomiya, 5: 230-3(1965). (In Russian).

The solar-diurnal variation of the intensity of the meson component of cosmic rays, recorded in the south and north directions at mountain level, is examined. It is shown that the characteristics of the diural variation are the same at sea and mountain levels. (tr-auth)

6017 INVESTIGATION OF THE FRACTION OF THE ENERGY TRANSFERRED TO THE SOFT COMPONENT BY PARTICLES INTERACTING WITH CARBON NUCLEI. Azimov, S. A.; Polyak, Yu. V.; Abdullaev, R. S. (Inst. of Nuclear Physics, Academy of Sciences, USSR). Izv. Akad. Nauk Uz. SSR, Ser. Fiz.-Mat. Nauk, No. 1, 38-40(1965). (In Russian).

Experimental results are presented of the measurement of the soft-component graphite obtained using a large number of ionization chambers placed between layers of a dense absorber. The particle energy was obtained by a calorimetric method. The thickness of the absorber in which the electron-nuclear shower took place exceeded 5 t-units for the nuclear interaction, so that the energy of the primary particles could be determined with sufficient reliability. For 75 selected cases in which particles with energy larger than 100 Bev interacted in the graphite, the average coefficient of the soft component was 0.30 ± 0.04. This large value shows that when particles interact with light nuclei the processes accompanied by considerable transfer of energy to the electron-photon (soft) component are quite appreciable. (ATD)

6018 ON OPTIMUM WAVELENGTH AND SPECTRAL INTERVAL MEASUREMENTS OF DISTRIBUTED COSMIC RADIATION POLARIZATION. Razin, V. A.; Khrulev, V. V. (Gor'kii State Univ., USSR). Izv. Vyssh. Ucheb. Zaved., Radiofiz., 8: 857-61(1965). (In Russian).

The optimum conditions for the polarization measurements of cosmic-ray distributions are determined. The expressions are obtained for evaluation of the wavelength and bandwidth of the receiver providing maximum of signal to noise ratio. If the measurements of the cosmic radiation polarization are made by antennas of moderate sizes, the waves of dm band are most suitable. (auth)

6019 STRUCTURAL CHARACTERISTICS OF FIELDS OF OUTGOING RADIATION ACCORDING TO DATA OF THE ARTIFICIAL SATELLITES TIROS II AND TIROS III AND THEIR INTERPRETATION. Borisenkov, E. P.; Doronin, P.; Dondrat'ev, K. Ya. Kosm. Issled., 3: 433-43(May-June 1965). (In Russian).

The structure of the radiation field leaving the earth's atmosphere was studied on the basis of radiation data catalogs of the satellites Tiros II and Tiros III, which characterize the winter and summer radiation fields. A special coefficient was introduced for comparing the radiation measured by the two satellites. Structural functions of integral radiation obtained from measurements made by the two satellites differ from one another, and the difference increases with distance. The shortwave radiation measured by these satellites depends upon the reflectivity of the clouds and ground of the regions over which they flew. Structural functions of radiation fields obtained from satellite measurements also differ. It is more convenient to use correlation functions and compute the spectral density since it is independent of the filter transmission. The analysis of data obtained by Tiros III led to the conclusion that the radiation field is isotropic in a space from 1000 to 2000 km. Reliable results about upwelling radiation may be obtained by performing measurements at points close to each other. (ATD)

6020 EXPECTED ANISOTROPY OF NONTHERMAL COSMIC RADIO EMISSION AT LOW FREQUENCIES. Getmantsev, G. G. Kosm. Issled., 3: 495-6(May-June 1965). (In Russian).

It is hypothesized that the reason for the bend in the frequency spectrum of nonthermal cosmic radio emission at frequencies less than 5 Mc is an increase in absorption in the interstellar ionized gas near the galactic plane. If this is true, a very strong anisotropy should be observed at frequencies less than about 5 Mc in the angular distribution of the nonthermal cosmic radio emission, due to the angular dependence of the synchrotron radio emission intensity. Measurements of this effect would yield information on the degree of homogeneity of the interstellar magnetic field near the solar system and on the nature of the relativistic-electron energy spectrum. Methods for the measurements are discussed briefly. (M.J.T.)

6021 THE SPECTRUM OF MUONS, PROTONS, AND ELECTRONS AT 5200 m ALTITUDE. Allkofer, O. C.; Kraft, E. (Univ., Kiel). Nuovo Cimento (10), 39: 1051-6 (Oct. 16, 1965). (In German).

A magnetic spectrograph was used at 5200 m above sea level to measure the differential momentum spectrum of the cosmic particles. Two measurements taken without and with a lead absorber of 3 cm have allowed the separation of the spectrum of electrons, protons, and muons. The spectra were measured in the range (0.2 to 20) Bev/c. (auth)

6022 ELECTRON COMPONENT OF THE PRIMARY COSMIC RADIATION AT ENERGIES $\gtrsim$15 Gev. Daniel, R. R.; Stephens, S. A. (Tata Inst. of Fundamental Research, Bombay). Phys. Rev. Lett., 15: 769-72(Nov. 15, 1965).

An experiment was carried out to study the electron component of the primary cosmic radiation at energies $\gtrsim$15 Bev using a nuclear-emulsion stack flown under 10.2 g/cm^2 of residual atmosphere. The emulsion stack consisted of 265 hypersensitive Ilford G-5 emulsions. From observations made on the electron events, they are conclusively identified as due to electrons. Scanning was carried out on a total length of 334 cm along the scan line, and 24 electrons of energy >1 Bev were obtained. A plot of electron energies at the top of the atmosphere against their arrival directions in the east-west plane is shown. The flux and energy spectrum of electrons of atmospheric origin are given in which the magnitudes of the contribution through the decay of atmospheric mesons (π) was calculated and shown separately. Also the integral energy spectrum of primary electrons in the energy region 10 to 100 Bev, and the calculated spectrum for electrons arising from collisions of cosmic rays in 3 g/cm^2 of interstellar matter are shown. It is emphasized that using nuclear emulsions and the techniques now available it is possible to obtain decisive information concerning the primary cosmic-ray electron component at very high energies. (J.F.P.)

Direct Energy Conversion

Refer also to abstract 6657.

6023 (AD-619379) RESEARCH AND DEVELOPMENT OF THERMIONIC CONVERSION OF HEAT TO ELECTRICITY. Quarterly Letter Report No. 4, March 30, 1964-June 29, 1965. (General Electric Co., Pleasanton, Calif. Special Purpose Nuclear Systems Operation). Contract NObs90496. 7p. CFSTI $1.00 cy, $0.50 mn.

Progress is reported on the development of a nuclear thermionic electrical generating system for the Department of the Navy. Work is being performed to develop the materials capabilities which are essential for this nuclear thermionic system. This consists of three major tasks: UO_2-refractory metal reaction kinetics; insulator materials development; and ceramic-to-metal seal development. (TAB)

6024 (ANL-6925, pp 235-47) ENERGY CONVERSION. Crouthamel, C. E.; Hesson, J. C.; Tevebaugh, A. D. (Argonne National Lab., Ill.).

Progress on development of emf cells is reviewed. Data and information are included from studies on LiH cells, electrode kinetics, Na-Bi solubility, alkali metal tellurides, alkali metal bismuthides, and liquid-vapor relations in Na-Bi cell regeneration. Results are reported from studies of an experimental Na-Bi cell, design and testing of frozen electrolyte-silicon rubber insulation seals, and corrosion of emf cell materials. (J.R.D.)

6025 EXPERIMENTS ON A FARADAY-TYPE MHD ACCELERATOR WITH SERIES-CONNECTED ELECTRODES. Tempelmeyer, K. E.; Rittenhouse, L. E.; Wilson, D. R. (ARO, Inc., Arnold Air Force Station, Tenn.). AIAA (Amer. Inst. Aeron. Astronaut.) J., 3: 2160-2(Nov. 1965).

The advantages and disadvantages of series-connected electrodes in MHD accelerators are discussed. Experiments were conducted on a Faraday-type MHD accelerator with series-connected electrodes to evaluate the performance of this setup. The results are discussed. (M.O.W.)

6026 AN ALTERNATING CURRENT MAGNETOHYDRODYNAMIC GENERATOR. Yano, Syukuro; Matsunanga, Sakuro (to Nihon Genshiryoku Kenkyu Sho). British Patent 1,009,714. Nov. 10, 1965. Filed Jan. 23, 1964.

In a MHD generator the plasma is introduced perpendicular to a magnetic field rotating at a constant rate to generate alternating current at electrodes. The magnetic field is produced by a multi-coil field winding in which the coils are energized by multi-phase currents of predetermined frequency and phase. The electrodes of the generator collect two groups of multi-phase electric currents spaced apart from one another by a predetermined phase angle. The currents in one group all pass through the windings of the generator. (B.L.M.)

6027 A MAGNETOHYDRODYNAMIC GENERATOR HAVING HELICAL GAS FLOW. (to Westinghouse Electric Corp.). British Patent 1,009,766. Nov. 10, 1965. Priority date July 17, 1962, United States.

A MHD generator includes two elongated electrodes, the second one disposed coaxially within the first hollow one, defining an elongated duct having a generally annular and uniform cross section throughout its length. Means are provided for establishing in the duct a magnetic field extending axially throughout the length of the duct. Fluid supply means communicate with the duct near one end for introducing an ionized fluid into the duct with a tangential velocity such as to cause the fluid to flow along a helical path toward the other end of the duct. (B.L.M.)

6028 HIGH-EFFICIENCY A.C. MHD APPARATUS. Maeder, Paul F. (to Paul Levinger). U. S. Patent 3,214,614. Oct. 26, 1965. Filed Apr. 24, 1961.

In the magnetohydrodynamic apparatus for translating energy through a stream of electrically conductive fluid, a number of electrical windings are provided for develop-

ing a periodically varying magnetic flux field having an intensity distribution along a predetermined elongated path. Means are provided for guiding the flow of the fluid through the magnetic field along the predetermined path and form substantially unobstructed paths at the sites of the electrical windings for net electrical currents induced in the fluid to circulate transversely in relation to the direction of the intensity distribution and of the flow. Electrical end winding means are positioned in adjoining relationship to at least the downstream end of the electrical windings. Nonmagnetic and electrically non-conductive baffles means underlie and are spaced from the electrical windings. The baffle means divide the flow guide means into flow passageways extending in the direction of the flow and substantially prevent flow of electrical current transversely in relation to the path at the site of the end winding means. (B.L.M.)

6029 MAGNETOHYDRODYNAMIC GENERATOR APPARATUS. Way, Stewart (to Westinghouse Electric Corp.). U. S. Patent 3,214,615. Oct. 26, 1965. Filed June 15, 1962.

A conventional MHD generating system made up of a number of generator stages is provided with reheat means between successive generator stages. The reheat means provides for the injection of a combustion agent into a combustion chamber of the associated generator stage so as to supply additional heat of combustion to the working fluid and to maintain it in an efficient operating temperature range for the generation of electric current between the electrode means of the generating system. (B.L.M.)

6030 MAGNETOHYDRODYNAMIC GENERATOR. Way, Stewart; Hunstad, Richard L. (to Westinghouse Electric Corp.). U. S. Patent 3,214,616. Oct. 26, 1965. Filed July 13, 1962.

A MHD generator is described in which a cesium mineral, particularly pollucite, is used as a seeding material in conjunction with combustion product gases. The reaction products are removed from the gas stream at the duct end opposite the point of seeding and have a higher Cs content than the seeding material. The recovered reaction products may be recycled for use as a seeding material. (B.L.M.)

Elementary Particles and Radiations

See *also* Field Theory, Scattering Theory, and Symmetries

Refer also to abstracts 6006, 6277, 6282, 6283, and 6304.

6031 (BNL-9613) $K_2^0 \rightarrow \pi^+\pi^-\pi^0$ DECAY. Guidoni, P.; Barnes, V. (Brookhaven National Lab., Upton, N. Y.); Ferbel, T.; (and others) (Yale Univ., New Haven, Conn.). Oct. 18, 1965. Contract AT(30-2)-Gen-16. 13p. (CONF-651043-1). Dep. mn; CFSTI $1.00 cy, $0.50 mn.

From Weak Interactions Conference, Argonne, Ill.

Various aspects of the $K_2^0 \rightarrow \pi^+\pi^-\pi^0$ decay are discussed. The branching ratio for the charged three-pion decay is discussed. To investigate the T_0 (kinetic energy of the π^0 in cms) dependence of the matrix element squared, a division by a phase-space factor and a correction for resolution broadening especially for the extreme bins was made. (M.O.W.)

6032 (BNL–9666) HYPERON NON-LEPTONIC DECAYS. Samios, N. P. (Brookhaven National Lab., Upton, N. Y.). Oct. 1965. Contract AT(30-2)-Gen-16. 26p. (CONF-651043–2). Dep. mn; CFSTI $2.00 cy, $0.50 mn.

From Weak Interactions Conference, Argonne, Ill.

A review of non-leptonic decay of hyperons Λ^0, Σ^+, Σ^-, Σ^0, Ξ^-, Ξ^0, and Ω^- is presented. In particular, the $\Delta I = 1/2$ rule and $|\Delta S| \leq 1$ theories are discussed. (M.O.W)

6033 (CEA-R–2798) ETUDE DE LA PRODUCTION D'HYPERON ET D'ANTIHYPERON DANS LES COLLISIONS ANTIPROTON-PROTON A 4 Gev/c [Theses]. (Study of Hyperon-Antihyperon Production in Antiproton-Proton Collision at 4 Gev/c [Thesis]). Revel, Daniel (Commissariat a l'Energie Atomique, Saclay (France). Centre d'Etudes Nucleaires). 1965. 78p. Dep. mn.

Submitted to Paris Univ., Orsay (France). Faculte des Sciences.

The results on hyperon-antihyperon production by 4 Bev/c antiprotons in hydrogen are presented. The aim of this work was the study, through the cross sections and the angular distributions, of production mechanisms of hyperon-antihyperon pairs and excited hyperons (or antihyperons). For most of the channels, these angular distributions show a strong forward peaking of the antihyperon in the center of mass of the interaction. This suggests that a peripheral-type mechanism is predominant in these processes. The results of some cross sections are compared with theoretical predictions according to SU_3 unitary symmetry. (M.O.W.)

6034 (CERN–64-13(Vol.4)) PROCEEDINGS OF THE 1964 EASTER SCHOOL FOR PHYSICISTS USING THE CERN PROTON SYNCHROTRON AND SYNCHRO-CYCLOTRON, HERCEG-NOVI, MAY 18–31, 1964. (European Organization for Nuclear Research, Geneva (Switzerland)). Jan. 25, 1965. 278p. Dep. mn.

Separate abstracts were prepared for the 4 included papers. (M.O.W.)

For abstracts of individual papers see: 6035, 6036, 6282, and 6283.

6035 (CERN–64-13(Vol.4), pp 1-49) THE WEAK INTERACTIONS OF STRANGE PARTICLES. Van Hove, L. (European Organization for Nuclear Research, Geneva (Switzerland)).

A discussion of the whole field of weak interactions is presented. Separate discussions are presented for non-strange weak interactions, weak interactions of strange particles, leptonic interactions, selection rules, the matrix element for $K \rightarrow \pi + l + \nu_l$, universality of weak interactions, and nonleptonic decays of strange particles. (M.O.W.)

6036 (CERN–64-13(Vol.4), pp 51-95) HIGH-ENERGY NEUTRINO INTERACTIONS. Franzinetti, C. (European Organization for Nuclear Research, Geneva (Switzerland)).

Some of the neutrino research carried out at CERN is discussed. Physical problems such as the intermediate vector boson, the existence of two neutrinos, elastic form factors, and inelastic neutrino interactions are discussed. The results of these studies are included. (M.O.W.)

6037 (DESY–65/11) PHOTOPRODUCTION OF PION AND NUCLEON RESONANCES AT ENERGIES UP TO 5.5 Gev. Brall, U.; Reimann, G.; Bothin, W.; (and others) (Deutsches Elektronen-Synchrotron, Hamburg (West Germany)). Sept. 1965. 23p. Dep. mn.

The photoproduction of N^*, π, ω, ρ, and η on protons at 0.3 to 5.5 Bev is observed, using data from 5339 bremsstrahlung reactions in a hydrogen bubble chamber. The production of $N^*(1238)$ is verified. (T.F.H.)

6038 (INR-646/VI/PH) A GENERAL CHARACTERISTIC OF THE π^--PROTON INELASTIC COLLISIONS AT 10 Gev/c. Bartke, Jerzy (Institute of Nuclear Research, Warsaw (Poland)). July 1965. 16p. Dep.

The experimental data on the π^--proton interactions at 10 Bev/c are used for a discussion of the two problems: the applicability of the statistical model and the existence of "central" collisions. It is shown that a simple version of the statistical model can be used in order to predict the relative probabilities for different reaction channels. A method is proposed for the estimation of the fraction of "central" collisions. It is based on the symmetry of the angular distribution of baryons in the cms and seems justified from the experimentalist's point of view. The cross-section for "central" collisions evaluated according to this definition turns out to be 25 to 30% of the total inelastic cross-section. This is consistent with the estimate

of Fast and Hagedorn, obtained from the analysis of the large-angle elastic scattering. (auth)

6039 (INSJ–90) REMARK ON 30 Gev JET SHOWERS. [PART] A. Hasegawa, S.; Kawamura, T.; Yajima, N.; Dake, S.; Ohata, I.; Yokoi, K.; Teranaka, M. (Institute for Nuclear Study, Tokyo Univ. (Japan)). Oct. 1, 1965. 13p. Dep. mn.

Proton-nucleon and quasi-(proton-nucleon) interactions in emulsion are studied for a primary proton momentum of 30.5 Bev/c. Data from the jets produced by these interactions suggest that: some of the jets may have an essentially asymmetric angular distribution in the CMS; and the intermediate-particle or fireball model may be applicable to the interactions. The similarities of the investigated 30-Bev jets to those having primary energies above several hundred Bev are discussed. (T.F.H.)

6040 (NP–15602) NEKOTORYE ZAPRETY DLYA ANNIGILYATSII POLYARIZOVANNYKH FERMIONOV. (Some Selection Rules for the Annihilation of Polarized Fermions). Khriplovich, I. B. (Akademiya Nauk SSSR, Novosibirsk. Institut Yadernoi Fiziki). 1965. 6p. Dep. mn.

Some selection rules are given for pseudoscalar meson production in the annihilation of transversely polarized electrons and positrons. The invariance under the reflection of a space axis and the chirality conservation are used. (auth)

6041 (UCRL-11942) INELASTIC π^-p INTERACTIONS AT 3.3 Bev/c AND 3.9 Bev/c [Thesis]. Schumann, Thomas G. (Lawrence Radiation Lab., Univ. of California, Berkeley). July 1965. Contract W-7405-eng-48. 113p. Dep. mn; CFSTI $4.00 cy, $0.75 mn.

The results of an investigation of final states with four or more particles, at 3.3 Bev/c and 3.9 Bev/c in liquid hydrogen, are presented. Several well-known multipion and pion-nucleon resonances are produced in the final state. In addition, evidence is presented for the existence of two new π-nucleon resonances. One has a mass of 2.65 Bev, charge +1 and decays into several channels with a nucleon and two or three pions; the other has a mass of 1.71 Bev, charge +2 and decays into $\pi^+\pi^0$p. Comparison of these enhancements with structure in the π^-p (with mass of 2.65 Bev) and π^+p (with mass of 1.7 Bev) total cross-sections is made. (auth)

6042 (UCRL–16189) MEASUREMENT OF THE N^{*-}–N^{*++} MASS DIFFERENCE [Thesis]. Kim, Sedong (Lawrence Radiation Lab., Univ. of California, Berkeley). July 1965. Contract W-7405-eng-48. 66p. Dep. mn; CFSTI $3.00 cy, $0.75 mn.

A measurement of the mass and width difference between N^{*-} ($I_Z = -3/2$) and N^{*++} ($I_Z = +3/2$) is described, where N* is the pion-nucleon p-wave resonance of spin and isotopic spin $3/2$ and mass approximately 1240 Mev. The resonances were produced in the inelastic reactions $n\,n \rightarrow p\,n\,\pi^-$ and $p\,p \rightarrow n\,p\,\pi^+$, which are known to proceed almost entirely via N^{*-} and N^{*++} production, respectively, in the observed energy region of a few Bev. The masses and widths of N^{*-} and N^{*++} were obtained from their respective effective mass distributions. In fitting the data for the masses two different formulas were used; (a) the OPE (one-pion-exchange) formula and (b) the resonance formula, with constant matrix element, which goes according to the phase space. Because the above inelastic reactions are known to be dominated by OPE, the values obtained with the OPE formula are taken to the best estimate of the resonance parameters. This gives a mass difference of $\delta\omega_0 = N^{*-} - N^{*++} = 7.9 \pm 6.8$ Mev and a width difference of $\delta\Gamma_0 = 25 \pm 23$ Mev. This result agrees with the predictions based on the SU(3) and SU(6) symmetry schemes and various dynamical theories. (auth)

6043 TRANSIENT RADIATION AT ANISOTROPIC CONDUCTIVE PLANE. Barsukov, K. A.; Naryshkina, L. G. (Moscow State Pedagogical Inst.). Izv. Vyssh. Ucheb. Zaved., Radiofiz., 8: 936-41(1965). (In Russian).

The radiation of a charged particle incident upon an anisotropic conductive plane is considered, the latter may be realized as an array with $l \ll \lambda$, where l is array period and λ is the wavelength. The radiation field, the radiation energy and its angular distribution are found. The peculiarities of slow surface-wave excitation by the charge are considered. (auth)

6044 ON THE COMPLETE UNITARITY EQUATIONS FOR PION-PION SCATTERING. Broido, Michael M. (Cambridge Univ., Eng. Trinity Coll., Cambridge, Eng.). J. Math. Phys. (N. Y.), 6: 1702-8(Nov. 1965).

The off-the-mass-shell equations for pion-pion scattering in the lowest approximation of the complete unitarity formalism of Taylor are discussed. It is shown that if the vertex-function renormalization constant is taken to be zero, the equations have no (nonzero) solution. These equations are equivalent to certain bootstrap equations, which thus also have no solution. Both systems are discussed in the case where the renormalization constant is not put equal to zero. (auth)

6045 SHADOW UNIVERSE AND THE NEUTRINO EXPERIMENT. Okun', L. B.; Pomeranchuk, I. Ya. (Inst. of Nuclear Physics, Academy of Sciences, USSR). JETP Lett. (USSR) (Engl. Transl.), 1: 167-9(June 15, 1965).

It is pointed out that the shadow universe hypothesis is in contradiction with the results of the neutrino experiment. The number of mesons (K^0) produced in the target of the neutrino experiment is of the order of 10^{15}. Assuming a detector located approximately 50 meters from the target and with an effective dimension of about 10 meters, the number of θ decays in the detector would amount to about 10^{11}–10^{12}. This number remains practically unchanged if account is taken of the presence of an iron shield 25 meters thick. Thus the iron wall is transparent to the mesons (K_3). Since the number of possible θ decays did not exceed 10^2 in the neutrino experiment, the discrepancy between experiment and the model of the shadow universe amounts to ten orders of magnitude. These considerations do not apply to the hypothesis according to which the long-lived θ_L meson can have strong interactions. It is noted that if there exist two CP-even mesons (K), namely K_1 and K_3, then two CP-odd mesons (K), K_2 and K_4 should exist. (J.F.P.)

6046 PROTON-PROTON BREMSSTRAHLUNG AT 158 Mev. Gottschalk, B.; Shlaer, W. J.; Wang, K. H. (Harvard Univ., Cambridge, Mass.). Nucl. Phys., 75: 549-60(1966).

The reaction $p + p \rightarrow p + p + \gamma$ was investigated for coplanar protons with symmetric angles of 30, 32.5, 35, 37.5, and 40°. The cross sections integrated over all γ-ray angles are respectively 7.8, 10.1, 12.4, 13.3, and 23.8 μb/sterad^2 ± 20%. For each proton angle, the angular distribution of the emitted γ ray was inferred and was found to be almost uniform with a slight tendency to forward peaking. (auth)

6047 THE GENERAL FORM OF THE TIME-REVERSAL NON-INVARIANT INTERNUCLEON POTENTIAL. Herczeg, P. (Univ., Copenhagen). Nucl. Phys., 75: 655-8(1966).

The most general internucleon potential which violates time-reversal invariance is given. The possible one-particle potentials are also discussed, and the presence of a tensor force in the general time-reversal invariant pseudoscalar one-particle potential is stressed. (auth)

6048 DETERMINATION OF THE COUPLING CONSTANTS IN MUON DECAY FROM EXPERIMENTS. Jarlskog, Cecilia (Lund Univ., Sweden). Nucl. Phys., 75: 659-68(1966).

From experiments on the muon decay $\mu \rightarrow e + \nu + \bar{\nu}$, five different parameters (functions of the coupling constants) are known. The measured values of these parameters are in accord with the predictions of the V–A theory, so that the theoretical V–A values can be used to obtain various relationships among the coupling constants. When all the available information is used, the S, P, and T terms vanish for the particular ordering chosen in the interaction hamiltonian. However, only the sum of the absolute values

of the two remaining coupling constants, i.e., $|g_V|^2+|g_A|^2$, can be determined. Future experiments which can test the validity of the universal V–A interaction in the above decay are discussed. Further, the effect of the present-day experimental uncertainties on the coupling constants is briefly examined. (auth)

6049 CALCULATION OF s-WAVE NUCLEON-NUCLEON SCATTERING PARAMETERS IN THE I = 0, S = 1 STATE BY THE N/D METHOD. Bose, Sudesh (Univ., Delhi). Nucl. Phys., 75: 682-6(1966).

Balázs' method of approximating the N function by two poles is applied to calculate the scattering length and effective range for s-wave nucleon-nucleon scattering in the I = 0, S = 1 state. The residue of the poles is determined by matching the scattering amplitude and its derivative with those obtained from the fixed s dispersion relation. Only the contributions of π, η, ρ, and ω poles are retained in the fixed s dispersion relation. The agreement between the calculated and the experimental values is found to be reasonably good. (auth)

6050 PROPOSAL OF AN EXPERIMENT WITH ARTIFICIAL NEUTRINO SOURCE. Kuchowicz, Bronislaw (Univ. of Warsaw). Nukleonika, 10: 523-5(1965).

The possibility of producing artificial neutrino sources in a reactor is discussed. ^{63}Cu, which, after neutron capture, decays by neutrino emission, was proposed for use as a neutrino source. It is shown that difficulties with background could be reduced by locating the detecting apparatus about 500 m underground and transporting the irradiated copper from the reactor to a position surrounded on all sides by the detector tanks. (M.C.G.)

6051 A FURTHER SEARCH FOR $Y_0^*(1405)$ PRODUCTION BY K⁻ AT REST IN EMULSION. Drieschner, M. (Univ., Munich. Max-Planck-Institut fuer Physik und Astrophysik, Munich). Nuovo Cimento (10), 39: 1032-6 (Oct. 16, 1965).

Mass and momentum of the (Σ,π) system were measured for 197 K⁻ captures in nuclear emulsion in which a $\Sigma^\pm$, a $\pi^\mp$, and at most one additional charged particle with a range ≤ 5 mμ were emitted. The mass distribution shows a maximum at 1405 Mev with a width of (25 to 30) Mev. A "world statistics" of all 941 events of the same type published to date was also compiled. Comparison with theoretical calculations by Block and Adair shows that the distributions may be explained without assuming a resonance. (auth)

6052 THE LOCATION AND ANALYSIS OF NEUTRINO INTERACTIONS IN PHOTOGRAPHIC EMULSION. Burhop, E. H. S. (University Coll., London); Busza, W.; Davis, D. H. (and others). Nuovo Cimento (10), 39: 1037-44(Oct. 16, 1965).

A stack of nuclear emulsion pellicles of total volume 10 liters was placed, together with two spark chambers in the neutrino beam of the CERN proton synchrotron. The tracks of secondary particles from neutrino interactions in the emulsion were observed in the spark chamber. The spark chamber tracks were used to locate the tracks produced by the same particles in the emulsion. These tracks were then followed back in the emulsion to the neutrino interaction in which they originate. Of a total of seven neutrino interactions expected to be produced in the emulsion stack during this exposure four were located in this way and their characteristics studied. (auth)

6053 ON A BREMSSTRAHLUNG THEORY FOR THE MULTIPLE PRODUCTION OF MESONS. Bialas, A.; Ruijgrok, T. (CERN, Geneva). Nuovo Cimento (10), 39: 1061-81(Oct. 16, 1965).

The bremsstrahlung theory of multiple meson production in very-high-energy nucleon-nucleon collisions is considered. The motion of the nucleons is represented by an orbit, chosen in such a way that the energy and momentum loss are in rough agreement with the observed values of the inelasticity K and the transverse momentum q. The field equation for the meson field is then solved in the natural scalar meson approximation. Assuming that there is no other mechanism for the production of mesons it is then possible to calculate for the final state the average number of mesons for each momentum value. From this, the following quantities were computed; the average multiplicity, the width of the diffraction peak for elastic scattering, the distributions of longitudinal and transverse momentum, and the distributions of log ctg $\theta/2$ and of the azimuthal angle. Where possible a comparison with the experimental results was made. Qualitatively the comparison is quite encouraging. The conclusion is that a more realistic version of the bremsstrahlung theory is likely to explain many features of multiple meson production at very high energies. (auth)

6054 VIRTUAL NUCLEON EFFECTS. Selleri, F. (Cornell Univ., Ithaca, N. Y.). Nuovo Cimento (10), 39: 1122-39(Oct. 16, 1965).

The effects of the virtuality of the nucleon on the pion-nucleon vertex, on the nucleon propagator and on the matrix element for low-energy pion-nucleon scattering were investigated. The vertex and propagator can be expressed in terms of the empirical $T = 1/2$, $S_{1/2}$ and $P_{1/2}$ πN phase-shifts. The influence of a resonance in the latter state is discussed. Pion scattering off a virtual nucleon is studied with the help of one-dimensional dispersion relations. The dependence of the $T = J = 3/2$ partial-wave amplitude on the squared four-momentum of the virtual nucleon is so determined. (auth)

6055 SU_6, SU_6W AND THE MESON PHOTOPRODUCTION. Jengo, R.; Odorico, R. (Univ., Bologna). Nuovo Cimento (10), 39: 1178-82(Oct. 16, 1965).

Some predictions of SU(6) and SU(6)W on the photoproduction processes on nucleons are discussed. The performance of these techniques is discussed in terms of comparisons of experimental and predicted meson data. (M.O.W.)

6056 MEASUREMENT OF PROTON-PROTON TRIPLE SCATTERING AT 430 Mev. Roth, R. (Princeton Univ., N. J.); Engels, E. Jr.; Wright, S. C.; Kloeppel, P.; Handler, R.; Pondrom, Lee G. Phys. Rev., 140: B1533-40(Dec. 20, 1965). (COO–881-53).

The polarization parameters P, D, R, A, and A' were measured at seven scattering angles between 30 and 120° in the center-of-mass system with an incident energy of 430 Mev. A 56% polarized beam was prepared by scattering on an internal beryllium target. A liquid-hydrogen target was used for the p-p scattering, and the outgoing polarization was analyzed with a third scattering in the carbon plates of a spark chamber. The scattering asymmetry ϵ was determined by fitting the data to a distribution $1 + \epsilon \cos\theta$ by the maximum-likelihood method. The analyzing power of the spark chamber as a function of energy was measured in beams of known polarization. The beam polarization before and after the p-p scattering was manipulated with a solenoid and two bending magnets. The measurements are compared with the extrapolations of several phase-shift and resonance analyses of experimental data at higher and lower energies. (auth)

6057 S-MATRIX THEORY AND HIGHER ORDER CORRECTIONS TO THE WEAK INTERACTIONS. Halpern, M. B. (CERN, Geneva. Harvard Univ., Cambridge, Mass.). Phys. Rev., 140: B1570-8(Dec. 20, 1965).

The use of dispersive and unitary methods to calculate higher-order corrections to the weak interactions was studied, with emphasis on the W meson theory. (D.C.W.)

6058 KINETIC SUPERMULTIPLETS OF $\tilde{U}(12)$. Gatto, R. (Univ., Florence. Istituto Nazionale di Fisica Nucleare, Florence); Maiani, L.; Preparata, G. Phys. Rev., 140: B1579-83(Dec. 20, 1965).

A further extension of the multiplet structure of broken $\tilde{U}(12)$ is proposed. The "kinetic supermultiplets" are represented by reducible tensors and group together separate nondegenerate multiplets. The example of the lowest kinetic boson supermultiplet is treated in detail. Such a supermultiplet has already been shown by Borchi and Gatto to provide for a classification of the higher boson reso-

nances. The mass relations are derived including first-order SU_3 breaking. Comparison with the data shows a remarkable accuracy. The predicted equidistance relation $\frac{1}{2}[m^2(A_2) + m^2(A_1)] = m^2(B)$ between the squared masses of the resonances A_1, A_2, and B is satisfied to $\lesssim$1.5%. A T = 1, $J^{PC} = 0^{++}$ meson at (970 ± 50) Mev and a T = 0, $J^{PC} = 1^{+-}$ meson at (1215 ± 15) Mev are directly predicted. If K*(1430), κ(725), and f^0(1253) are included in the supermultiplet, as suggested by their quantum numbers, and the assumption is made that f^0 has a maximal mixing with another particle of the same T and J^{PC}, one can predict in addition the following resonant masses: (1560 ± 50) Mev with T = 0, $J^{PC} = 2^{++}$; (1270 ± 30) Mev with T = 0, $J^{PC} = 1^{+-}$; (1180 ± 190) Mev and (990 ± 200) Mev both with T = 0, $J^{PC} = 1^{++}$. The supermultiplet also includes two mixed K resonances K′ and K″ with $J^P = 1^+$. One of them could be K*(1175) or C (1215), the other resonance being then predicted at (1100 ± 40) Mev or (1050 ± 40) Mev, respectively. (auth)

6059 T VIOLATION AND ELECTROMAGNETIC INTERACTIONS. Mani, H. S.; Mohan, Gyan; Pande, L. K. (National Physical Lab., New Delhi, India). Phys. Rev., 140: B1584-5(Dec. 20, 1965).

Compton scattering on protons and related processes are discussed with a view to detecting any T violation in the electromagnetic interaction of strongly interacting particles. (auth)

6060 BOOTSTRAP ALGEBRA FOR MESONS. Hwa, Rudolph C.; Patil, Sharashchandra H. (Inst. for Advanced Study, Princeton, N. J.). Phys. Rev., 140: B1586-91 (Dec. 20, 1965).

The bootstrap of vector and pseudoscalar mesons is considered. The self-supporting dynamics for an arbitrary finite number of these particles is formulated in the analytic S-matrix approach, leading to a set of bootstrap equations. From these, a set of algebraic relations is obtained for the coupling coefficients, called bootstrap algebra. This algebra includes the Lie algebra, whose structure constants are the coefficients of the trilinear coupling of the vector mesons. It is also shown that the pseudoscalar mesons belong to some representation of the associated Lie group. Restrictions on the dimension of this representation are derived; in particular, the pseudoscalar mesons must be in the adjoint representation if there exists a singlet vector meson in addition to the multiplet in the adjoint representation. Physical consequences of the bootstrap algebra, regarding the conservation of G and A parities, are discussed. (auth)

6061 THEORETICAL AND EXPERIMENTAL COMMENTS ON THE MOMENTUM DEPENDENCE OF THE S MATRIX FOR MANY-PARTICLE PROCESSES. Goldberg, M. (Syracuse Univ., N. Y.); Rohrlich, F.; Leitner, J. Phys. Rev., 140: B1592-4(Dec. 20, 1965).

Reactions including five or more particles require quadrilinear momentum invariants for their complete kinematical specification, in contrast to those involving less than five particles, where bilinear invariants suffice. This raises the possibility that the structure of the S matrix may be different in the two cases, and even leads one to consider the remote possibility that different conservation laws might operate. Both the linear and quadratic dependence of the S matrix on the quadrilinear invariants were investigated for the five- and six-particle reactions $K^- + p \to \Lambda + \pi^+ + \pi^-$ ($+\pi^0$). No significant linear or quadratic dependence, the former implying that parity or time-reversal invariance holds for the above reactions, was observed. (auth)

6062 MODIFICATION OF A REGGE-POLE REPRESENTATION. Abbe, W. J.; Kaus, P.; Nath, P.; Srivastava, Y. N. (Univ. of California, Riverside). Phys. Rev., 140: B1595-8(Dec. 20, 1965).

A recent representation by Cheng of the partial-wave scattering amplitude was modified to display the large-energy behavior explicitly in order to improve convergence in terms of Regge poles. The resulting representation has the following properties regardless of the number of trajectories included: it is unitary for all l and $s > 0$; it gives the correct threshold behavior as $s \to 0$ for the real and imaginary parts of the amplitude; it reproduces the appropriate analytic properties for the total amplitude in the $\cos\theta$ plane; and it converges rapidly. (auth)

6063 APPROXIMATE SOLUTION TO THE MULTI-CHANNEL ND^{-1} EQUATIONS. Pagels, Heinz (Stanford Univ., Calif.). Phys. Rev., 140: B1599-1604(Dec. 20, 1965).

By making a pole approximation to the spectral integral over the kinematical factor $\rho_l(z)$ it is shown that the partial-wave matrix ND^{-1} integral equations are reduced to algebra. The approximation depends only on the particular partial wave and not the dynamics of the reaction, and it admits of systematic improvement. The resulting scattering amplitude $T_l(z)$ is symmetric, is independent of the subtraction point for the D function, has the correct discontinuities on the right- and left-hand cuts, and can moreover be explicitly expressed as an algebraic function of the driving term $B_l(z)$. This last feature enables us to directly inspect the relation between the driving force and the scattering amplitude and establishes the general usefulness of the method. It is found for example, that the solution imposes general conditions on $B_l(z)$ for the existence of bound states, resonances, or possible ghosts. The self-consistency property of bootstrap calculations imposes additional explicit restrictions on acceptable $B_l(z)$ for the existence of the bootstrap. (auth)

6064 DETERMINATION OF THE UPPER LIMIT TO THE ELECTRIC DIPOLE MOMENT OF THE ELECTRON AT HIGH MOMENTUM TRANSFER. Rand, R. E. (Stanford Univ., Calif.). Phys. Rev., 140: B1605-10(Dec. 20, 1965).

A new limit on the electron's electric dipole moment at high momentum transfer was determined by scattering 100-Mev electrons at 180° from ^{12}C nuclei. A full discussion of the theory involved and the experimental corrections due to multiple scattering, etc. is given. Assuming that the electron possesses no spurious magnetic moment, apart from the well-established Dirac and anomalous moments, its electric dipole moment is $\lesssim 2.3 \times 10^{-16}$ e cm at a momentum transfer of 1.0 fermi^{-1}. The result is consistent with time-reversal invariance in quantum electrodynamics. (auth)

6065 BARYON RESONANCE PRODUCTION BY NEUTRINOS AND THE RELATIVISTIC GENERALIZATIONS OF SU(6). Albright, C. H.; Liu, L. S. (Northwestern Univ., Evanston, Ill.). Phys. Rev., 140: B1611-17(Dec. 20, 1965).

An extension of our phenomenological study of baryon resonance production by neutrinos is carried out to include the relativistic generalizations of SU(6). The semileptonic weak-interaction Lagrangian invariant under the group SL(6,c) is constructed for the 364-to-364 supermultiplet transitions. Two special cases are considered for this interaction Lagrangian: One invokes invariance under the larger group M(12), while the other includes a simple M(12) symmetry-breaking term. Detailed comparisons with the present experimental information on weak N* production and with the SU(6) theory are made for each of these relativistic symmetry schemes. (auth)

6066 EXPERIMENTAL TESTS OF BROKEN $\tilde{U}(12)$ AND APPROXIMATE U(6) × U(6). Harari, H. (Israel Atomic Energy Commission, Yavne); Lipkin, H. J. Phys. Rev., 140: B1617-19(Dec. 20, 1965).

Broken $\tilde{U}(12)$ and the Dashen-Gell-Mann nonchiral U(6) × U(6) symmetry are shown to lead to equivalent predictions for a large number of processes. Predictions based on invariance under certain subgroups of $\tilde{U}(12)$ are shown to be valid in $\tilde{U}(12)$ calculations which include symmetry breaking to all orders by momentum spurions. New predictions from the W-spin collinear group include M1 dominance for N* photoproduction and electroproduction and justify the Stodolsky-Sakurai assumption of M1 dominance in vector-meson-exchange peripheral reactions. (auth)

6067 RADIATIVE τ DECAYS AND THE σ MESON. Lapidus, I. Richard; Tausner, Menasha J. (Stevens Inst.

of Tech., Hoboken, N. J.). Phys. Rev., 140: B1620-5 (Dec. 20, 1965).

The rate for radiative τ decay $\tau^{\pm} \rightarrow \pi^{\pm} + \pi^{+} + \pi^{-} + \gamma$ was calculated using a linearized form of the Brown-Singer meson (σ) model. The corrections to the leading term, which was obtained previously by Dalitz, are of the order of a few percent. The validity of the linear approximation for nonradiative τ decay is discussed. (auth)

6068 THEORY OF LOW-ENERGY $\pi\omega$ SCATTERING. Kang, Kyungsik (Brown Univ., Providence). Phys. Rev., 140: B1626-42(Dec. 20, 1965). (NYO-2262-99).

The $\pi\omega$ problem, as the simplest case of the pseudoscalar-meson and vector-meson system, is discussed from the standpoint of the S-matrix approach. A general procedure of constructing invariant amplitudes in spin and isospin space of the pseudoscalar-vector system is given, and for $\pi\omega$ scattering, a set of invariant amplitudes are conveniently chosen and their crossing properties are discussed. These amplitudes are expressed by one-dimensional representations which are derived from the Mandelstam representations by the Cini-Fubini technique. Partial-wave expansions as well as projections are done by the use of the Jacob-Wick helicity amplitudes. A prescription for calculating the driving forces from the exchange of particles is presented and is applied to the exchange of the ρ and β mesons in states of the two possible quantum numbers $J^P = 1^+$ and 2^-. The procedure consists of a zero-width approximation to the transition amplitudes in states of given J and L, crossing-symmetric relations, and the one-dimensional dispersion representations of the invariant amplitudes. The relation between the invariant amplitudes and the helicity amplitudes greatly facilitates this procedure. The t-channel reaction is also analyzed. A method of solution of the partial-wave dispersion relations is discussed based on a recently developed formalism, and is extended further to avoid the difficulty associated with the zeros of the driving forces. A systematic program to understand the quantum numbers of the β meson are a $\pi\omega$ resonance is also discussed. The qualitative nature of the forces due to the β exchange in states of each possible quantum number is briefly sketched. A model calculation which favors a 2^- state of the β meson is presented. (auth)

6069 SINGLE-RESONANCE PRODUCTIONS AND DOUBLE-RESONANCE PRODUCTIONS. Hara, Yasuo (Univ. of Chicago). Phys. Rev., 140: B1649-53(Dec. 20, 1965).

Single-resonance productions ($\pi^{\pm}N \rightarrow \rho^0 N$, $K^{\pm}N \rightarrow K^{*0}N$, and $\pi N \rightarrow \omega N$) and double-resonance productions ($\pi N \rightarrow \rho\Delta$, $KN \rightarrow K^*\Delta$, and $\pi N \rightarrow \omega\Delta$) are studied by making use of the assumption that Δ is a bound state of N and π (the Chew-Low model). The following relations among vector-meson spin density matrix elements of the single-resonance productions ($P^{\pm}N \rightarrow V^0N$) and those of the double-resonance productions ($PN \rightarrow V\Delta$) are found: $\gamma_V^{-1}\rho_{0,0}(PN \rightarrow VN) = \rho_{0,0}(PN \rightarrow V\Delta) \geq \rho_{0,0}(PN \rightarrow VN)$, $\gamma_V^{-1}\,\mathrm{Re}\rho_{1,0}(PN \rightarrow VN) = \mathrm{Re}\rho_{1,0}(PN \rightarrow V\Delta)$, and $\gamma_V\rho_{1,-1}(PN \rightarrow V\Delta) = \rho_{1,-1}(PN \rightarrow VN) - \frac{1}{2}(1 - \gamma_V)$, where $1 \geq \gamma_V \geq 0$. These relations are compared with experimental results. For productions with large momentum transfer [$t \approx -1(\mathrm{Bev/c})^2$] at high energy, values of spin density matrix elements are predicted by making use of the Regge-pole model. (auth)

6070 TWO TYPES OF BARYONS IN BROKEN $(SU_3)_L \otimes (SU_3)_R$ SYMMETRY. Riazuddin (Univ. of Rochester, N. Y.); Fayyazuddin; Rashid, M. A. Phys. Rev., 140: B1653-4(Dec. 20, 1965).

Physical baryons belonging to a mixture of representations (8,1), (1,8), (3,3*), and (3*,3) are considered in broken $(SU_3)_L \otimes (SU_3)_R$ symmetry. In this way an F-type vector current and both F- and D-type axial-vector currents for the $\frac{1}{2}^+$ baryon octet are obtained such that $G_A = G_V$ and $G_A^F/G_A^D = 0.58$. In addition to the $\frac{1}{2}^+$ baryon octet, another baryon octet $\frac{1}{2}^-$ and a singlet $\frac{1}{2}^+$ are predicted at about 1700 and 1400 Mev, respectively. (auth)

6071 POLARIZATION OF THE Λ^0 PARTICLE PRODUCED FROM PROTONS IN CARBON NUCLEI BY 1.17-Bev/c NEGATIVE PIONS. Kim, Young S. (Ohio State Univ., Columbus); Burleson, G. R.; Kalmus, P. I. P.; Roberts, A.; Romanowski, T. A. Phys. Rev., 140: B1655-60(Dec. 20, 1965). (COO-1261-17).

The angular distribution of the direction and polarization of the Λ^0 particles produced from the protons in carbon nuclei by 1.17-Bev/c π^- were measured in a magnetic spark chamber system. From a total of 794 observed Λ^0's, the mean polarization was found to be -0.68 ± 0.10. Both the direction and polarization distributions show close similarity to those produced in hydrogen at this momentum. (auth)

6072 RADIATIVE CORRECTIONS. I. HIGH-ENERGY BREMSSTRAHLUNG AND PAIR PRODUCTION. Mork, Kjell; Olsen, Haakon (National Bureau of Standards, Washington, D. C. Norges Tekniske Hogskole, Trondheim, Norway). Phys. Rev., 140: B1661-74(Dec. 20, 1965).

The radiative corrections to the high-energy bremsstrahlung and pair-production spectra are calculated in the Weizsäcker-Williams approximation. Results for the soft-photon radiative correction to the spectra are given, and for the case of pair production the soft-plus-hard-photon radiative correction is also obtained. The radiative correction to the total pair-production cross section is found to be practically independent of the photon energy and of the atomic number of the target material. Comparison with available experimental data shows essential agreement within the relatively wide experimental limits. (auth)

6073 CROSS SECTION FOR THE PRODUCTION OF A POSSIBLE BOUND CASCADE-NUCLEON SYSTEM. Ebel, M. E.; Goble, R. L. (Univ. of Wisconsin, Madison). Phys. Rev., 140: B1675-80(Dec. 20, 1965). (COO-30-102).

A theoretical prediction is made of the cross section for the production of a conjectured Ξ^--n bound state in K^--deuteron scattering. The calculation assumes that the anomalous threshold of the triangle diagram is the dominant singularity, and uses the experimental Ξ^- production amplitude. At incident K^- momenta of 1.3 and 2.0 Bev/c, the cross sections are computed to be 30 and 6 μb. The former value is a maximum in the cross section caused by the maximum in the cascade production amplitude. It is shown that the calculation is not materially modified if the Ξ^--n is not bound, but forms a low-lying resonance. (auth)

6074 HIGHER SYMMETRIES AND THE NEUTRON-PROTON MAGNETIC-MOMENT RATIO. Moffat, J. W. (Univ. of Toronto). Phys. Rev., 140: B1681-5(Dec. 20, 1965).

A quark model of SU(4) is developed in which the quarks possess charge $\frac{2}{3}$ and $-\frac{1}{3}$ and baryon number $N = \frac{1}{3}$. The new particles predicted are characterized by a quantum number $W \neq 0$ (superstrangeness); they possess integer charge but fractional hypercharge $\frac{1}{3}$ or $\frac{2}{3}$, and are called hyperquarks. A spin extension of SU(4) is formulated and leads to the study of the group SU(8) and the subalgebra SU(4) $\otimes$ SU(2). The baryons and isobars are grouped in the representation 120 and the mesons in the adjoint representation 63. It is found that the F/D ratio in SU(8) is uniquely specified by the scheme. The ratio of the magnetic moments of the neutron and proton is uniquely determined by assuming that the magnetic-moment operator transforms as the adjoint representation of SU(8), and by specifying the extended Gell-Mann–Nishijima relation for the quarks. The value $-\frac{2}{3}$ is found for the neutron-proton magnetic-moment ratio in agreement with the result found in SU(6). The selection rules forbidding processes like $\phi \rightarrow \rho\pi$ and $\pi + N \rightarrow \pi + N + \phi$ are obtained from the conservation of the four quark spins. These results strongly indicate that the physical predictions of a symmetry scheme like SU(6) are not unique and that there exists a hierarchy of symmetries all possessing equally good (or bad) physical predictions, but with new quantum numbers associated with superstrange particles. (auth)

6075 LONGITUDINAL POLARIZATION OF LOW-ENERGY MUONS FROM $K_{\mu 3}^+$ DECAY. Borreani, G. (Istituto Nazionale di Fisica Nucleare, Turin); Gidal, G.; Ri-

naudo, G.; Werbrouck, A. E.; Caforio, A.; Garelli, C. M.; Natali, S.; Villani, M. Phys. Rev., 140: B1686-8(Dec. 20, 1965).

The longitudinal polarization of the muon from $K^+_{\mu 3}$ decay was studied in the muon energy interval from 6 to 27 Mev using a hydrogen bubble chamber. The muon polarization is determined from a measurement of the angular and momentum distribution of the decay positrons. The result is $\langle P_\mu \rangle = +0.33 \pm 0.19$ and yields a value for the form factor ratio $\xi \equiv f_-/f_+ = 1.2^{+2.4}_{-1.8}$. Combining this with previous experiment to resolve the various ambiguities gives a best value of ξ based on polarization measurements alone of $\xi = +0.2 \pm 0.8$. (auth)

6076 SPIN CORRELATIONS IN THE PHOTOPRODUCTION OF VECTOR MESONS. McClure, J. A.; Weaver, D. L. (Tufts Univ., Medford, Mass.). Phys. Rev., 140: B1688-92(Dec. 20, 1965).

Spin correlations are analyzed for the photoproduction of 1^- resonances by polarized photons on unpolarized nucleons. The spin of the vector meson can be studied through its decay. Aside from an overall phase, there are twenty-three real numbers which comprise the twelve amplitudes specifying the production process. It is found that all but one of these can be determined from measurements with an unpolarized target. (auth)

6077 CURRENT COMMUTATION RELATIONS AND MESON-MESON SCATTERING. Kawarabayashi, K. (Argonne National Lab., Ill.); McGlinn, W. D.; Wada, W. W. Phys. Rev. Lett., 15: 897-900(Dec. 6, 1965). (COO-1261-21).

A further test is given for partially conserved axial-vector current (PCAC) by calculating different matrix elements by the same technique developed by Adler and Weisberger. The results are presented from an application to the pseudoscalar mesons under the assumption that the operator equation of PCAC for $\Delta y = 0$ transitions holds when applied to pseudoscalar meson states as it apparently does for nucleon states. It is concluded from the calculations that it is possible that the sum rule is satisfied for the case $\pi\pi$ scattering. There are both theoretical and experimental indications for strong low-energy $\pi^-\pi^+$ scattering, and as indicated this is apparently required for the sum rule. In the case of πK scattering, the situation is much less clear. (J.F.P.)

6078 SEARCH FOR A HEAVY ELECTRON BY ELECTRON-PROTON COINCIDENCE MEASUREMENTS. Behrend, H. J. (Deutsches Elektronen Synchrotron, Hamburg); Brasse, F. W.; Engler, J.; Ganssauge, E.; Hultschig, H.; Galster, S.; Hartwig, G.; Schopper, H. Phys. Rev. Lett., 15: 900-2(Dec. 6, 1965).

A search for a heavy electron was extended to electron masses of 0.5 to 1.0 Bev. No evidence for a heavy electron was found. For these investigations electron-proton coincidences were observed by means of an apparatus which was set up for investigating elastic electron-proton scattering. The e-p coincidence rate per quantameter charge as a function of the proton angle is shown. From the observed counting rates upper limits of the cross sections for the production of heavy electrons can be deduced and given. If these experimental results are compared to theoretical cross sections computed with the coupling suggested by Low (Phys. Rev. Letters 14, 238 (1965)) upper limits can be inferred for the coupling constant λ. The results are compatible with $\lambda^2 \leq 4\ (10^{-4})$ whereas $\lambda^2 \sim 1$ could be expected theoretically. Hence a heavy electron with a mass between 0.2 and 1 Bev does not exist. The limits on λ also imply that the pair production results must be explained in a different way. (J.F.P.)

6079 SEARCH FOR A NEUTRAL SCALAR MESON. Cohn, H. O. (Oak Ridge National Lab., Tenn.); Bugg, W. M.; Condo, G. T.; McCulloch, R. D.; Luetjens, G.; Gelfand, N. Phys. Rev. Lett., 15: 906-8(Dec. 6, 1965). (ORNL-P-1665).

A search was made for the existence of a $J = 0^+$, $T = 0$ meson (π)-meson (π) resonance (ϵ^0) as an explanation for the symmetry observed in ρ^0 decay. The experimental missing-mass spectrum for events with two identifiable protons from an exposure of a deuterium chamber to 3.29 Bev/c mesons (π^+) is shown. No evidence was found for decay into neutrals of any other particle in the mass region of 700 Mev, the region in which previous evidence was found. An analysis was made of the reaction $\pi^+ + d \rightarrow p + p + \pi^+ + \pi^- + \pi^0$ in the same exposure, and also the entire sample of about 2,800 $pp\pi^+\pi^-$ events, including those without a visible spectator proton, was examined for evidence of the decay mode $\epsilon^0 \rightarrow \pi^+\pi^-$. It was concluded that in π^+d interactions at 3.29 Bev/c, the neutral mass spectrum shows no evidence for the production of a $J = 0$, $T = 0$ meson with mass near 700 Mev and intensity sufficient to explain the ρ^0 decay asymmetry. Also the data on the above reaction show none of the indications reported for a neutral scalar resonance with mass 720 Mev. (J.F.P.)

6080 K_{e3} DECAY AND UNIVERSALITY IN CABIBBO'S THEORY OF LEPTONIC DECAYS. Oneda, S.; Sucher, J. (Univ. of Maryland, College Park). Phys. Rev. Lett., 15: 927-9(Dec. 13, 1965).

Within the framework of Cabibbo's theory of leptonic decays (Phys. Rev. Letters, 10: 531(1963)) the bare coupling constant for beta decay is G $\cos\theta$ and that for $|\Delta S| = 1$ decay is G $\sin\theta$, where G is the coupling constant for muon (μ) decay. It is pointed out that the use of $|C^2-1| \lesssim 1-5\%$ and the most recent best value of the K_{e3} decay rate together with the inclusion of hitherto neglected form-factor effects in the determination of G $\sin\theta$ from this rate, may yield a value of $\cos\theta$ which is in quite close agreement with that determined from beta decay. It is noted that the present experimental situation seems to be quite compatible with Cabibbo's version of universality and with $C^2 = 1$ to within a few percent. (J.F.P.)

6081 RELATION BETWEEN πp, pp, AND $\overline{pp}$ SCATTERING AT HIGH ENERGIES. Freund, Peter G. O. (Univ. of California, Los Angeles. Univ. of Chicago). Phys. Rev. Lett., 15: 929-30(Dec. 13, 1965).

It is pointed out that the Johnson-Treiman relation for the scattering of mesons on baryons under M(12) invariance can be derived assuming the odd charge-conjugation amplitude in the crossed (t) channel to be dominated by F-type coupled vector mesons as suggested by universality. Universality and M(12) invariance further relate the zero momentum-transfer (q) coupling of the nonet of vector mesons to the eight $\frac{1}{2}^+$ baryons and eight 0^- mesons. An equation is found in this way which agrees with experiment with the same accuracy as that of the Johnson-Treiman relation. It thus substantiates the M(12) relation between the F-type coupling of baryons to the vector-meson octet and their coupling to the vector-meson singlet, as well as the universality principle. It is further observed that another relation is implied by the Johnson-Treiman relation. This last equation also agrees with existing experimental data. (J.F.P.)

6082 ANALYSIS OF TOTAL CROSS-SECTION DIFFERENCES AT HIGH ENERGY. Barger, V.; Olsson, M. (Univ. of Wisconsin, Madison). Phys. Rev. Lett., 15: 930-4(Dec. 13, 1965). (COO-881-55).

An analysis is made of the total cross section differences Δ_{MN} and the Δ_{NN}, which are the meson-nucleon and nucleon-nucleon scattering respectively, in terms of the Regge trajectories of the vector-meson nonet. The ratio of the meson (ρ) couplings to the conserved $\pi\pi$ and $\overline{K}K$ meson currents is determined, and it agrees within one standard deviation with the SU(3)-invariant coupling prediction. From a statistical fit to the data, the f/d ratio of the $V\overline{B}B$ charge coupling, the ratio of the $V\overline{N}N$ to the VMM coupling at zero momentum transfer, and the trajectory intercepts are evaluated. (J.F.P.)

6083 NEW DETERMINATION OF THE PION-NUCLEON COUPLING CONSTANT AND s-WAVE SCATTERING LENGTHS. Samaranayake, V. K.; Woolcock, W. S. (University Coll., London). Phys. Rev. Lett., 15: 936-8(Dec. 13, 1965).

A re-evaluation is made of the dispersion relations for the $\pi^\pm$p elastic-scattering amplitudes in the forward di-

rection, taking account of experimental data available. The calculation also yields the s-wave scattering lengths. A brief account is given of the method used, and of the values obtained for the constants. Instead of writing the dispersion relations in the usual form, advantage is taken of the sum rule to eliminate one of the scattering-length combinations. A good fit to the data was found. The values of the real parts of the π^+p forward-scattering amplitudes in the laboratory system were calculated by two methods, and in the final fit the goodness of the fit was not significantly different for the sets of these values obtained by the two methods. But the scattering-length combinations were found to be in bad agreement with those given previously. Reasons for this are considered. (J.F.P.)

6084 RELATIVISTIC CORRECTIONS TO THE TRITON BINDING ENERGY. Gupta, V. K.; Bhakar, B. S.; Mitra, A. N. (Univ., Delhi). Phys. Rev. Lett., 15: 974-6(Dec. 20, 1965).

Results are presented on the relativistic corrections to the triton binding energy using the three-body technique developed recently. The present method, which uses separable two-body potentials leads to an exact expression for the three-body wave function, and is therefore ideally suited for the calculation of relativistic and similar effects in a perturbative manner. The results not only confirm that a perturbative procedure is justified, but that the magnitude of the total relativistic correction is small. The second-order relativistic correction is +0.473 Mev, and the kinetic-energy correction is −0.995 Mev. Thus the total correction to the energy amounts to −0.522 Mev. This correction increases the binding energy of the triton, which had a previous value of −8.85 Mev. (J.F.P.)

6085 SELECTION RULES IN NONLEPTONIC DECAYS OF STRANGE PARTICLES. Lo, Liau-fu (Inner Mongolian Univ., China). Wu Li Hsueh Pao, 21: 1132-8 (June 1965). (In Chinese).

The SU_3 and G_2 transformation properties of the weak interactions are discussed. By assuming selection rules for certain operators in SU_3 different from isospin, a series of relations between the amplitudes of the nonleptonic decays of the strange particles are obtained, which include some results obtained in previous works. Assuming the G_2 symmetry of the strong interactions, the selection rules in these processes are discussed in a similar manner and it is shown that the weak interactions cannot transform according the representations 7 or 14 of G_2. (auth)

6086 INFLUENCE OF STRONG INTERACTIONS BETWEEN FINAL STATE π-MESONS ON THE PROBABILITY RATIO OF $K \to 3\pi$ DECAYS. Anisovich, V. V.; Dakhno, L. G. (Joint Inst. for Nuclear Research, Dubna, USSR). Yadern. Fiz., 710-15(Oct. 1965). (In Russian).

The influence of strong interactions between π mesons on the probability ratio of $K \to 3\pi$ decays is considered. It is shown that the violation of isotopic invariance in the strong interactions, connected with the π-meson mass difference, can lead to a significant contribution of transitions with $\Delta T \neq \frac{1}{2}$, even if the rule $\Delta T = \frac{1}{2}$ holds exactly in the nonrenormalized weak interactions. The ratio of the induced $\Delta T = \frac{5}{2}$ transition amplitudes to the amplitude with $T = \frac{1}{2}$ can be of the order of 10%. (auth)

6087 CP-PARITY VIOLATION IN THE DECAY OF POLARIZED NEUTRONS. Lobov, G. A. (Inst. of Theoretical and Experimental Physics, Moscow). Yadern. Fiz., 2: 716-19(Oct. 1965). (In Russian).

An effective hamiltonian containing baryon currents of the 1st and 2nd type (six form factors) is used to calculate the spin correlation $s[p_p \times p_e]$ (s is the neutron spin vector, p_p, p_e—the proton and electron momenta) in the decay of a polarized neutron. Models are discussed in which the nonconservation of CP-parity is due to currents of the second type and to the existence of an imaginary part of the axial-vector interaction constant. The appearance of the spin correlation, $s[p_p \times p_e]$, due to the Coulomb interaction of the proton and electron in the final state is investigated. (auth)

6088 ON THE THEORY OF LEPTONIC BARYON DECAYS. Tsukerman, I. S. (Inst. of Theoretical and Experimental Physic, Moscow). Yadern. Fiz., 2: 720-7 (Oct. 1965). (In Russian).

The angular, energy, and polarization correlations for the muon and baryon produced in the β decay of a hyperon are calculated, taking all six complex form factors into account, keeping terms up to the order $(m/M)^2$, where m and M are the muon and baryon masses respectively. Explicit expressions are obtained for the angular $e\nu$ correlation, spectrum, emission asymmetry of the electrons, their polarization and the total probability for the β decay of a polarized neutron, in a linear approximation with respect to the electron-nucleon mass ratio, taking six real form factors into account. (auth)

6089 THE CREATION OF MUONS BY ELECTRONS IN THE COULOMB FIELD OF A NUCLEUS. Viblyi, N. I.; Sannikov, S. S. Yadern. Fiz., 2: 728-9(Oct. 1965). (In Russian).

The creation of μ mesons by electrons in the field of a nucleus is calculated in the first nonvanishing approximation of perturbation theory, for large energies of the initial electrons and created μ mesons. The differential cross section with respect to the energy and μ-meson angular variables is found. The total cross section is estimated. (auth)

6090 ON THE MAGNETIC POLARIZABILITY OF π AND K MESONS. Lebedev, A. I.; Petrunkin, V. A. Yadern. Fiz., 2: 730-2(Oct. 1965). (In Russian).

The magnetic polarizability of π and K mesons is estimated on the basis of the resonance approximation for processes of meson photoproduction on mesons. (auth)

6091 THE RESONANCE Ξ_{1820} AND UNITARY SYMMETRY. Belov, V. P.; Shekhter, V. M. (Ioffe Inst. of Physics and Tech., Leningrad). Yadern. Fiz., 2: 757-61 (Oct. 1965). (In Russian).

The identification of the resonance Ξ_{1820} in a unitary multiplet model is discussed. Unitary relations for the partial widths of two-particle decays are found, and, when possible, the results are compared with experimental data. (auth)

6092 BOUND STATES IN A SYSTEM OF TWO VECTOR MESONS [Thesis]. Saffouri, Mohammad Hussein. Urbana, Ill., Univ. of Illinois, 1965. 44p.

It is proposed that ρ-exchange gives the major contribution to the forces between two ρ-mesons. Dispersion relations techniques are used to look for s-wave bound states between two such particles. Three bound states are found in the 1.2 Bev region. These have the IJ^{PG} assignments 0^{2++}, 1^{1++}, and 0^{0++}. The f and the B-resonances are identified with the first and the second of these states. There are no known resonances corresponding to the third state. Next, the above mechanism is extended to the octet of vector mesons. Invariance is required under SU_3 and G, the charge parity operator. Again there are bound states in the energy region cited above. These have the following quantum numbers: 2^+(8 or 1), 1^+(8′), and 0^+(8 or 1). The numbers in parenthesis refer to the dimension of the corresponding irreducible representation of SU_3. The f and the A_2 are assigned to the 2^+ octet, the B and the K_c to the 1^+ octet. For the rest, there is no experimental evidence yet. (Dissertation Abstr.)

6093 RADIATIVE CORRECTIONS FOR COINCIDENCE ELECTRON SCATTERING [Thesis]. Atkinson III, Reilly. Stanford, Calif., Stanford Univ., 1965. 119p.

Radiative corrections are calculated for coincidence detection, high energy electron scattering experiments. Radiative correction formulas that may be used by experimentalists in their data analysis are presented, and the experimental circumstances for which this work is valid are explained. Calculations for the following cases are made: 1) coincidence detection elastic electron proton scattering, in which both final particles are detected with well defined energies and angles; 2) inelastic electron-deuteron scattering, in which the final electron is de-

tected in coincidence with a final nucleon, again with well defined energies and angles; and 3) coincidence detection elastic electron proton scattering, in which the final electron is detected with essentially no energy resolution at all. The calculation for 1) is, with minor modifications, applicable to elastic electron nucleus scattering. Only quasi-elastic scattering is treated in case 2); the calculation for this case is, with minor modifications, applicable to any coincidence inelastic electron scattering experiment with a three-body final state, in which the energy required to break up the target is small compared to the individual masses of the daughter particles, and in which the electron is one of the two detected particles. In the calculation for case 3), only the part of the radiative correction that is linear in the proton charge is considered. The radiative corrections are calculated to order α with standard techniques of quantum electrodynamics, and particular attention is paid to experimental conditions in calculation of the radiative cross sections. In the case of the inelastic scattering calculation, the effect of deuteron structure on real photon emission is considered as this effect can be important for high energy experiments. (Dissertation Abstr.)

6094 DEUTERON COMPTON EFFECT [Thesis]. Fox, John Dana. St. Louis, Washington Univ., 1964. 195p.

Cross sections for elastic scattering of photons by deuterium were measured at cms scattering angles of 137° and 88° in the range 180 to 290 Mev incident photon energy. Spark chambers were used to determine the trajectories of the recoil deuteron and the scattered photon. Separation of elastic-scattering events from π^0 photoproduction was accomplished by analysis of the kinematics; elastic scattering events appear as a peak in the distribution in angular and vertical correlation functions over a background of uncorrelated π^0 production events. Cross sections in units of 10^{-32} cm^2/sr are for the 137° scattering angle 2.02 ± 0.4 at 188 Mev, 2.64 ± 0.6 at 217 Mev and 3.12 ± 0.5 at 251 Mev; for the 88° scattering angle, 4.6 ± 0.6 at 271 Mev. The results supplement those of a previous counter experiment at this laboratory and agree with the predictions of dispersion-theory calculations. The cross sections for π^0 photoproduction were also measured in this experiment. (Dissertation Abstr.)

6095 AN EXPERIMENTAL INVESTIGATION OF K^0_{e3} DECAY [Thesis]. Fisher, George Phillip. Urbana, Ill., Univ. of Illinois, 1965. 118p.

An experiment to study the leptonic decays of the K^0_2 meson was done in a 30° neutral beam at the AGS of the Brookhaven National Laboratory. The results of the K^0_{e3} ($K^0_2 \rightarrow \pi^\pm + e^\mp + \nu$) part of the experiment are presented. The K^0_{e3} decays are observed in an evacuated region that is 2 feet long and 67 feet from the internal AGS target where the neutral K mesons are produced. The detection system consists of two parts: the first part is used to observe the paths of the charged K^0_2 decay products and to measure their angles at decay and momenta; the second part is used to identify the charged particles from each observed K^0_2 decay. The data are inconsistent with a scalar or tensor interaction and are in good agreement with a pure vector interaction. There are two vector form factors f_+ and f_-. However, in K^0_{e3} decay only f_+ is of consequence. Of 1046 identified K^0_{e3} decay events, 577 are useful in studying the energy dependence of the form factors. An attempt was made to fit form factors having the following energy dependence: $f_+(q^2) = \alpha(1 + \lambda q^2/m_\pi^2)$ and $f_+(q^2) = \beta/(M^2 - q^2)$ where q^2 is the four-momentum transfer in the Kπ system ($q^2 = m_K^2 + m_\pi^2 - 2m_K E_\pi$), α and β are normalization constants, and λ and M are the parameters which are of interest. A reasonable fit to the data was found with $\lambda = 0.25^{+0.13}_{-0.00}$ and $M = 440^{+80}_{-30}$ (Mev). The energy dependence of the form factor $f_+(q^2)$ is assumed to be due to either an intermediate weak vector boson or to intermediate states in the Kπ system. The parameter M = 440 (Mev) may be interpreted as the mass of an intermediate vector boson or a bound state in the Kπ system. The energy dependence of $f_+(q^2)$ is more likely to be due to interfering resonant states in the Kπ system. (A.G.W.)

6096 CALCULATION OF THE ENERGIES OF THE HIGHER RESONANCES IN PION-NUCLEON SCATTERING [Thesis]. Teplitz, Vigdor Louis. College Park, Md., Univ. of Maryland, 1962. 147p.

The model of Cook and Lee for the coupled processes $\pi + N \rightarrow \pi + N$, $\pi + N \rightarrow \pi + \pi + N$, and $\pi + \pi + N \rightarrow \pi + \pi + N$ is used to calculate the positions of the $D_{\frac{3}{2}}$ and $F_{\frac{5}{2}}$ resonances. The three-body state is considered as a nucleon plus a two-pion system at the T = 1, J = 1 pion-pion resonance energy. For the left hand cuts, only the one-pion exchange contribution to the production amplitude is retained. The branch cut in the helicity amplitudes for this diagram is found by requiring that the exchanged pion be on the mass shell. The one pole approximation is made and resonance energies in fair agreement with the observed energies are found. No $T = \frac{3}{2}$, $F_{\frac{5}{2}}$ resonance is predicted at any energy, while for $T = \frac{1}{2}$, $D_{\frac{3}{2}}$ state, the result is ambiguous. The neglect of the $T = \frac{3}{2}$, $P_{\frac{3}{2}}$ final state pion-nucleon interaction in the production amplitude is considered; and it is shown that, although this interaction is essential for understanding the production cross section at the resonances, it has negligible effect on the location of the resonance energies. (Dissertation Abstr.)

6097 INELASTIC MULTIPLE PION PRODUCTION IN ANTIPROTON—PROTON INTERACTIONS FOR 3.6 Bev/c [Thesis]. Dehne, H. -C. Hamburg, Univ., 1964. 65p. $2.00 Gmelin, AED-DISS. 64-761.

Reaction cross sections for various reaction channels were determined from bubble chamber photographs using the CERN antiproton beam. The production of an ω meson with a cross section of 56 μb was observed. The importance of the peripheral interaction mechanism with an intermediate pion is emphasized. (Gmelin Inst.)

6098 MEASUREMENT OF THE PION ELECTRON SCATTERING CROSS SECTION FOR 16 Bev/c PIONS [Thesis]. Fischer, K. Aachen, Tech. Univ., 1964. 69p. $2.00 Gmelin, AED-DISS. 64-741.

The pion-electron cross section was determined for 16 Bev/c pions by means of a hydrogen bubble chamber. Results agree with theoretical data for small energy transfer. For high energy transfer experimental cross sections are lower. (Gmelin Inst.)

6099 THE PROPERTIES OF Ξ HYPERONS [Thesis]. Schneider, H. Hamburg, Univ., 1964. 58p. $2.00 Gmelin, AED-DISS. 64-762.

Production of Ξ hyperons in the CERN Kaon beam is studied by means of a hydrogen bubble chamber. Computer programs for the analysis of bubble chamber films are described. A value of Ξ hyperon mass of 1321.1 ± 0.65 Mev/c^2 was found. The lifetime is $1.5 \pm 0.3 \times 10^{-10}$ sec. (Gmelin Inst.)

6100 π^-p INTERACTIONS AT 4 Bev/c [Thesis]. Wolf, G. Hamburg, Univ., 1964. 144p. $2.00 Gmelin, AED-DISS. 64-485.

Results of bubble chamber measurements obtained at the CERN proton synchrotron are reported. Total π^-p cross section is 33.2 ± 0.7 mb. Elastic scattering, which is nearly pure diffraction scattering, contributes 20.5%. Single and multiple pion production are investigated. Results are in satisfactory agreement with theoretical data obtained from the statistical model. (Gmelin Inst.)

Field Theory, Scattering Theory, and Symmetries

See also **Elementary Particles and Radiations**

6101 (BNL–9652) STRONG INTERACTIONS AT HIGH ENERGY. Lindenbaum, S. J. (Brookhaven National Lab., Upton, N. Y.). [1965]. Contract AT(30-2)-Gen-16. 71p. (CONF-650945–3). Dep. mn; CFSTI $3.00 cy, $0.75 mn.

From International Conference on Elementary Particles, Oxford.

A review is presented of attempts at interpretation of high-energy strong-interaction data, in terms of axiomatic field theory and the forward dispersion relations that follow therefrom. (T.F.H.)

6102 (IC/65/79) ON THE COUPLING OF NON-COMPACT GROUP REPRESENTATIONS. Salam, Abdus; Strathdee, J. (International Centre for Theoretical Physics, Trieste (Italy)). Nov. 10, 1965. 16p. Dep. mn.

Elementary particle "tower" representations in $U(\nu,\nu)$ and $GL(\nu,C)$ are shown, and the decomposition of several particular $U(\nu,\nu)$ representations is carried out. The trilinear coupling of representations is investigated. Coefficients are computed for the example of trilinear coupling of two baryon-like towers to a meson-like tower. (T.F.H.)

6103 (IC/65/80) DEGENERATE REPRESENTATIONS OF COMPACT AND NON-COMPACT UNITARY GROUPS. Raczka, R. (International Centre for Theoretical Physics, Trieste (Italy)). Nov. 1965. 14p. Dep. mn.

Degenerate representations of compact groups U(n) on domains of rank one are considered. Degenerate representations of non-compact groups U(p,q) acting in a Hilbert space of discrete basis is studied. The problem of maximal reduction of a number of commuting operators for a given higher symmetry group is solved. (T.F.H.)

6104 (IC/65/81) ON THE SPIN EXTENSION OF UNITARY GROUPS. Santhanam, T. S. (International Centre for Theoretical Physics, Trieste (Italy)). Nov. 11, 1965. 6p. Dep. mn.

It is shown that since the spin extension of unitary groups puts a restriction in addition to the one usually faced with baryonic number, the SU(4) group would be interesting only if particles with fractional quantum numbers would be observed, using a simple model in which the basic objects are fermions. (auth)

6105 (ISS-65/14) THE TWO CHANNEL PROBLEM AND THE INELASTIC UNITARITY CONDITION IN EIGENSTATES OF THE TOTAL ANGULAR MOMENTUM. Amaldi, U. Jr.; Biancastelli, R.; Francaviglia, S. (Istituto Superiore di Sanita, Rome (Italy). Laboratori di Fisica). May 10, 1965. 24p. Dep. mn.

Relations coming from the unitarity of the S-matrix in the inelastic two channel problem are written. If the inelastic contributions are known, the moduli of the elastic amplitudes are obtained, starting from the unitarity relations only. A careful study is made of the conditions implied in the inelastic "absorption" and in the (real) phases of the elastic amplitudes. Finally, the feasibility of the random-phases hypothesis is briefly discussed. (auth)

6106 (JINR-P-2369) METOD POSTROENIYA NEKOTORYKH KLASSOV RESHENII URAVNENII TIPA URAVNEMII CHU-LOU. (A Method of Constructing Certain Classes of Solutions for Chew-Low Type Equations). Meshcheryakov, V. A. (Joint Inst. for Nuclear Research, Dubna (USSR). Lab. of Theoretical Physics). 1965. 32p. Dep. mn.

A method is suggested to construct certain solutions of equations of the Chew-Low type. The solutions have a finite number of poles. The extent to which general solutions of these equations are not unique is clarified. It is shown that by using the non-uniqueness of the solutions it is possible to construct a whole class of solutions for the Chew-Low equations. (auth)

6107 (JINR-P-2401) NARYSHENNAYA SIMMETRIYA SU(6) I ELEKTROMAGNITNYE SVOISTVA BARIONOV. (Broken Symmetry SU(6) and Electromagnetic Properties of Baryons). Babaev, Z. R.; Zamiralov, V. S. (Joint Inst. for Nuclear Research, Dubna (USSR). Lab. of Theoretical Physics). 1965. 8p. Dep. mn.

The relations between magnetic moments and the amplitudes of magnetic transitions in the SU(6) symmetry are found, the corrections owing to the introduction of the medium-strong interaction being taken into account. The formulas obtained are compared with experimental data. (auth)

6108 (NP-15600) NA KAKIKH RASTOYANIAKH PROISKHODIT VZAIMODEISTVIE PRI VYSOKIKH ENERGIYAKH? (At What Distances Does Interaction at High Energies Occur?). Gribov, V. N.; Ioffe, B. L.; Pomeranchuk, I. Ya. (Gosudarstvennyi Komitet po Ispol'zovaniyu Atomnoi Energii SSSR, Moscow. Institut Teoreticheskoi i Eksperimental'noi Fiziki). 1965. 18p. Dep. mn.

The question of what distances are essential for elastic and inelastic scattering at high energies may be resolved by investigating experimentally the radiation of soft quanta accompanying the given scattering process. In this case if the region of applicability of usual formulas of accompanying radiation proves to decrease with the growth of the energy of incident particle ϵ, it means that the effective longitudinal distances, essential for interaction at high energies, grow with the growth of ϵ. (auth)

6109 (NP-15638) MASS SUM RULES, SYMMETRIES AND DISPERSION RELATIONS. Seminar Lecture 20. Venkatesan, K. (Institute of Mathematical Science, Madras (India)). [1964]. 10p. Dep. mn.

Currents involving fields corresponding to strongly interacting particles are considered, for cases in which these currents appear in weak interaction processes. Within the framework of SU(3) symmetry, these considerations are used to derive mass sum rules and dispersion relations. (T.F.H.)

6110 SPIN AND UNITARY SPIN INDEPENDENCE IN SU(8) SYMMETRY. Iwao, S. (Univ., Bern). Ann. Phys. (N. Y.), 35: 1-17(Oct. 1965).

Theory of SU(8) symmetry model in the spin and unitary spin independence for elementary particles is developed. The classification of the meson and baryon states in the subgroup SU(4) ⊗ SU(2) is discussed and a possible assignment to the observed states is given. The assignment given will be verified when the doubly charged mesons and triply charged baryon etc., are observed. The mass differences and various decay rates of mesons with both odd and even parity are calculated and compared with the available information. The sizes of the anomalous magnetic moments of quartets must be identical. The result of the theory is compared with SU(4) and SU(6) predictions. The detailed measurement of the suggested radiative decay rates of known mesons will distinguish the validity between SU(6) and SU(8) theory. The "charm-changing" weak current is introduced into the weak interaction in conformity with the Cabibbo current. The strength of the additional weak current thus introduced can be determined as to explain the apparent discrepancy between the muon and the neutron beta-decay coupling constant. (auth)

6111 VERTEX THEORY OF MANY-FERMION SYSTEMS. Layzer, Arthur (Stevens Inst. of Tech., Hoboken, N. J.). Ann. Phys. (N. Y.), 35: 67-95(Oct. 1965).

A general theory of the weak-response of many-fermion systems is formulated in terms of the longitudinal vertex function, Γ. By including effects of exchange the vertex theory embeds the conventional dielectric theory, as expressed by the momentum-energy space factorization $\Gamma = \epsilon^{-1}\tilde{\Gamma}$. Here $\tilde{\Gamma}$ is the proper vertex function and ϵ^{-1} is the generalized dielectric constant. The integral equation for Γ is rederived via weak-response theory, then factored into separate equations for Γ and ϵ^{-1}. Basic properties of Γ, particularly gauge-invariance, are discussed. A nonperturbative approximation, called the v′ approximation, is introduced in which the interaction kernel of the integral equation for $\tilde{\Gamma}$ is replaced by a suitably chosen energy-independent effective interaction v′. The v′ approximation is shown to be a generalization of the time dependent Hartree-Fock approximation. By using the v′ approximation as an input to a more exact theory expressions are obtained for the quasi-particle lifetime and the coupling of the quasi particle to the collective mode. Some new physical consequences of the theory are (a) the momentum dependence of the quasi-particle scattering amplitude in a weak external potential, (b) the existence of an intrinsic

longitudinal coupling constant renormalization associated with the static two wavelength limit of $\tilde{\Gamma}$, and (c) the formal occurrence of a "spurious" pole of $\tilde{\Gamma}$ coupled with a zero of ϵ^{-1} for a sufficiently strong repulsive interaction v'. The last bears a resemblance to a phenomenon recently noted in elementary-particle theory. (auth)

6112 FUNDAMENTALS OF DYNAMICS IN NON-LINEAR SPIN THEORY OF ELEMENTARY PARTICLES. Rampacher, H.; Stumpf, H.; Wagner, F. (Max-Planck-Institut fuer Physik und Astrophysik, Munich). Fortschr. Phys., 13: 385-480(1965). (In German).

The fundamentals of dynamics in the non-linear theory of elementary particles are developed through a consideration of the non-relativistic quantum field theory, the coupling theory, non-canonical quantization, relativistic quantum field theory, and S-matrix theory. A systematic representation of the experimental results that have lead to the theoretical developments is not given but only such experimental results as are necessary for the orientation of the developed theory of elementary particles. (J.S.R.)

6113 RELATIVISTIC THREE-PARTICLE SU_3 STATES. Dragt, A. J. (Inst. for Advanced Study, Princeton, N. J.). J. Math. Phys. (N. Y.), 6: 1621-5 (Nov. 1965).

The scheme for classifying three-particle states according to SU_3 is extended to the relativistic domain. A discussion is also given of the basic group theory lying behind the scheme. (auth)

6114 ANALYTIC PROPERTIES OF THE ELASTIC UNITARITY INTEGRAL. Aks, S. O.; Gilbert, R. P.; Howard, H. C. (Univ. of Maryland, College Park). J. Math. Phys. (N. Y.), 6: 1626-34(Nov. 1965).

Certain results concerning the singularities of holomorphic functions with integral representations are used to investigate the analytic properties of the elastic unitarity integral of the quantum theory of fields. In particular, it is shown that each of the Landau singularities of the scattering amplitude is an actual singularity. It is also shown that, if the scattering amplitude is not identically zero, it must have a natural boundary on the unphysical sheet. (auth)

6115 CROSSING SYMMETRIC REGGE REPRESENTATION FOR THE INVARIANT SCATTERING AMPLITUDE. Rothe, Heinz, J. (Univ. of California, Berkeley). J. Math. Phys. (N. Y.), 6: 1635-42(Nov. 1965). (UCRL-11790).

A crossing symmetric Regge representation for the invariant scattering amplitude is constructed which simultaneously exhibits all Regge poles in the three channels. It is assumed that the amplitude satisfies the Mandelstam representation and that the usual Mandelstam-Sommerfeld-Watson transform exists. To achieve explicit crossing symmetry it is found necessary to work with the Legendre function of the second kind. Except for neglecting the influence of possible angular momentum cuts, the representation is exact for all s, t, and u, with no restriction on the location of the Regge poles. As an illustration of how it might be used in practice, the Chew-Jones formula for the amplitude of definite signature is derived in the strip approximation. (auth)

6116 ALTERNATIVE FORMULATIONS OF SCATTERING IN MODEL FIELD THEORIES. Gelman, Harry (Sandia Corp., Albuquerque, N. Mex.); Haller, Kurt. J. Math. Phys. (N. Y.), 6: 1653-63(Nov. 1965).

A comparison is made between the expression for the boson-fermion scattering amplitude in a model theory obtained by renormalizing Feynman diagrams, and the one that originates from the dressed-particle picture. A proof is given of a surmise, previously verified to sixth order, that the two expressions for the transition amplitude are identical, although the former stems from a theory that leads to paradoxes from which the latter is exempt. The proof of the identity of the two representations is extended to transition amplitudes in which a weak interaction, considered to first order, is modified by a strong one considered to all orders. It is shown how the operations in the dressed-particle picture directly lead to iterations in terms of the physical mass and coupling constant, whereas the expressions obtained from the Feynman diagrams require renormalization before they have this form. (auth)

6117 ROTATIONALLY-SYMMETRIC MODEL FIELD THEORIES. Klauder, John R. (Bell Telephone Labs., Inc., Murray Hill, N. J.). J. Math. Phys. (N. Y.), 6: 1666-79(Nov. 1965).

A class of highly symmetric, nonrelativistic, Euclidean invariant, model scalar field theories is examined assuming the existence of field and momentum operators that satisfy the canonical commutation relations (CCR). The high degree of symmetry assumed permits explicit determination of every relevant CCR representation. These consist of a two-parameter family of unitarily inequivalent representations, some of which are irreducible while the others are reducible. It is demonstrated that only those models that are analogs of the free field can be encompassed within the irreducible representations. Hence every model with interaction — including an analog of the relativistic $\lambda\varphi^4$ theory — requires a reducible CCR representation. For the reducible representations, every relevant hamiltonian operator possessing the required high degree of symmetry is determined. These hamiltonians, as well as the generators of space translations, can not be expressed (solely) as functions of the field and momentum operators, a property which is characteristic of any system with a unique ground state and reducible CCR representation. Nevertheless, it is demonstrated that these hamiltonians, as well as the generators of space translations, fulfill the weak correspondence principle, in which the expectation value of a quantum generator, such as the hamiltonian operator, in a suitably labeled overcomplete family of states is identified with the associated classical generator, such as the classical hamiltonian. The principal results depend on the existence and make extensive use of the countably infinite number of degrees of freedom existing in a field theory. Entirely analogous results apply to related models defined in a finite spatial volume since they still have an infinite number of degrees of freedom. (auth)

6118 THRESHOLD REGGE POLES FOR COUPLED CHANNELS. Carnahan, W. H. (Indiana Univ., Bloomington). J. Math. Phys. (N. Y.), 6: 1709-19(Nov. 1965).

The threshold Regge poles are investigated in a variety of many-channel problems. The cases considered are a simple j-independent interaction between two spin-zero channels, the tensor force problem for two spin-$\frac{1}{2}$ particles, and a truncated interaction between a particle and a bound system of two particles. (auth)

6119 ON THE BOUND-STATE WAVEFUNCTIONS OF A NONLOCAL SOLVABLE POTENTIAL. Catara, F.; Di Toro, M. (Univ., Catania, Italy). J. Math. Phys. (N. Y.), 6: 1720-2(Nov. 1965).

The Schrödinger equation is solved in the momentum representation with a nonlocal factorable potential, with at most two point eigenvalues. When the potential is a bilinear form in the Bessel transforms of Yukawa functions, it is proved that it is impossible to have two bound states whose asymptotic behavior is determined by the binding energy. (auth)

6120 ON A SET OF COUPLED SECOND-ORDER DIFFERENTIAL EQUATIONS. Chen, Joseph C. Y. (Brookhaven National Lab., Upton, N. Y.). J. Math. Phys. (N. Y.), 6: 1723-9(Nov. 1965). (BNL-8707).

An alternative method for solving a set of coupled second-order differential equations, which often appears in theoretical treatments of many-body problems, is proposed. This method makes use of both mathematical relations derived in matrix theory and physical properties of the potentials provided by the set of equations to be solved. (auth)

6121 SINGULAR LOGARITHMIC POTENTIALS IN COORDINATE SPACE. Cornille, Henri (CERN, Geneva); Predazzi, Enrico. J. Math. Phys. (N. Y.), 6: 1730-40 (Nov. 1965). (COO-264-225).

The problem of the determinations of the Jost function for singular repulsive potentials behaving near the origin like inverse powers was studied previously. The key was to define new Jost solutions which, still being asymptotically ingoing (or outgoing) waves, tend to constant (Jost functions) near the origin. It was shown from the perturbation expansion in coordinate space of these new Jost solutions that the Jost functions can be constructed by connecting the radial coordinate r and the order of the perturbation expansion p. More precisely, if an r(p) dependence is introduced, the Jost function is the limit of convergent sequences provided r(p) goes to zero less rapidly than a given limiting dependence $r_L(p)$. The same method is extended for two other families of singular potentials, working in coordinate space. The case in which the most singular part of the potentials behaves like $G^2(\log r^{-1})^{\beta} r^{-2n}$, ($n \geq 1$, β arbitrary) near the origin is considered, and exponentially singular repulsive potentials of finite range are studied. It is found that the more singular is supposed to be the potential, the higher becomes the available limiting dependence. (auth)

6122 ONE-PARTICLE SINGULARITIES OF THE S-MATRIX IN QUANTUM FIELD THEORY. Hepp, Klaus (Inst. for Advanced Study, Princeton, N. J.). J. Math. Phys. (N. Y.), 6: 1762-7(Nov. 1965).

In the framework of the Haag-Ruelle collision theory one-particle singularities are proved to exist in the physical region of any connected scattering amplitude. They occur with the causal propagator $(p^2 - m^2 + i\epsilon)^{-1}$ in the dominant term and have a residue, which factors into the product of two connected amplitudes for subprocesses. The remainder of the amplitude is infinitely often differentiable in the critical variable. These results rely essentially on short-range forces and the one-particle spectrum, but neither depends on analyticity or on unitarity. (auth)

6123 SOLUTION OF AN INTEGRAL EQUATION IN V – θ SCATTERING. Kazes, E. (Pennsylvania State Univ., University Park). J. Math. Phys. (N. Y.), 6: 1772-3(Nov. 1965).

The Muskhelishvili method is used to obtain the off-the-mass-shell V – θ scattering amplitude. (auth)

6124 ON THE UNITARY REPRESENTATIONS OF THE GALILEI GROUP. II. TWO-PARTICLE SYSTEMS. Voisin, J. (Syracuse Univ., N. Y.). J. Math. Phys. (N. Y.), 6: 1822-32(Nov. 1965). (NYO–3399-22).

Mackey's theory is used to study the kinematics of a nonrelativistic two-particle system. The helicity coupling and the l – S coupling are considered, and a Jacob-Wick's formula relating these two couplings (Clebsch-Gordan coefficients) is derived. (auth)

6125 CASIMIR OPERATORS FOR THE UNITARY GROUP. Perelomov, A. M.; Popov, V. M. JETP Lett. (USSR) (Engl. Transl.), 1: 160-2(June 15, 1965).

A solution to the problem of determining all the invariant operators that can be formed from the generators of a group is presented. (J.F.P.)

6126 INTEGRAL EXPRESSIONS FOR THE DIFFERENCE BETWEEN CONTIGUOUS DIRAC PHASE SHIFTS. Calogero, F. (Univ., Rome); Fradkin, D. M. Nucl. Phys., 75: 470-4(1965).

The extensions to the Dirac case of a formula by Tietz are presented. This formula relates phase shifts differing by one unit of angular momentum to an appropriate average of the radial rate of change of the potential. (auth)

6127 INTEGRAL EXPRESSIONS FOR ARBITRARY PHASE SHIFT DIFFERENCES. Fradkin, D. M. (Univ., Rome); Calogero, F. Nucl. Phys., 75: 475-80(1965).

General methods are presented to obtain integral expressions for the difference between phase shifts. In particular, formulas which relate scattering phase shifts with different angular momenta are presented for both the Schrödinger and Dirac cases. The same technique, when applied to Schrödinger bound states, yields a formula which is just the quantal analog of the classical balance between centrifugal and external radial force. (auth)

6128 THE GREEN FUNCTIONS OF THE THIRRING MODEL. Fried, H. M. (Brown Univ., Providence). Nucl. Phys., 75: 691-4(1966).

Gauge transformations of the third kind are defined and used to provide a connection between solutions of the Thirring model obtained by Johnson, Sommerfield, and Birula et al. There exists a Yennie-type gauge in which the Green functions are the corresponding free-field ones, as well as a class of gauges for which the Green functions are finite. (auth)

6129 TEST OF THE N/D METHOD IN POTENTIAL SCATTERING. Aly, H. H. (Max-Planck-Institut fuer Physik and Astrophysik, Munich); Mueller, H. J. W. Nucl. Phys., 76: 241-7(1966).

The potential $V(r) = \lambda \sinh^{-2} \alpha r$ is used to test the applicability of the N/D method for effective range calculations. It is shown that the first pole approximation leads to good agreement with the results obtained from the exact solution. The physical interest of this potential is discussed. (auth)

6130 SOLUTION OF SINGULAR N/D EQUATIONS. I. FORMAL DERIVATION AND PROPERTIES. Atkinson, D.; Contogouris, A. P. (CERN, Geneva). Nuovo Cimento (10), 39: 1082-1101(Oct. 16, 1965).

The N/D equations are derived for a partial-wave amplitude which increases as rapidly as is allowed by unitarity. The resulting marginally singular integral equation is split into a system of two coupled integral equations: one with a singular and one with a Fredholm kernel. The explicit resolvent kernel of the singular equation is constructed. This is done first in the approximation of neglecting the gap between the left- and right-hand cuts, when Mellin transforms yield an explicit resolvent; and then the resolvent is set up as a quadrature in the realistic case, without this approximation. In both cases the analytic properties in an appropriate eigenparameter λ are studied. The asymptotics in λ and in energy are also investigated. The properties of the solution of the complete equation, including the Fredholm part, are then deduced. Finally, explicit expressions for the N and D functions are given in certain simple cases. (auth)

6131 SOLUTIONS OF SINGULAR N/D EQUATIONS. II. APPLICATIONS. Contogouris, A. P.; Atkinson, D. (CERN, Geneva). Nuovo Cimento (10), 39: 1102-21(Oct. 16, 1965).

The exact solutions of the singular N/D equations that arise from the assumption of saturated unitarity are applied to three problems of current interest in the physics of strong interactions. In the first, related to the bootstrap calculation of the parameters of a vector meson, an exact solution for the undamped vector exchange between scalars is given. This solution contains an arbitrary parameter implying that, in general, either the vector-scalar mass ratio or coupling constant must be given a priori. However, with an extra requirement (which is supported by a field-theoretic argument) a solution completely free of arbitrary parameters is singled out. In the second, the basic equations and conclusions of the new strip approximation of Chew are rederived by means of the authors' formalism: this gives the resolvent of the basic singular integral equation in the form of a single contour integral which allows a direct study of certain of its analytic and asymptotic properties. A physical assumption on the phase shift is shown to specify a unique solution. The third problem is the investigation of the Gribov-Pomeranchuk singularity. The continuation of a scattering amplitude to J = –1 is defined by an N/D equation and it is shown that at this point there is an energy-dependent power branch point and an accumulation of poles in every Riemann sheet of the complex J plane. (auth)

6132 $\tilde{U}_{12}$, ITS 143 MOMENTA, ITS LITTLE GROUP $U_6 \times U_6$ AND ITS IRREGULAR COUPLINGS. Bell, J. S.; Ruegg, H. (CERN, Geneva). Nuovo Cimento (10), 39: 1166-73(Oct. 16, 1965).

The $\tilde{U}(12)$ symmetry is developed along lines used for SL(6,C) by Rühl and by Katz. There are 143 components of momentum. The Wigner-Bargmann equations are

formally invariant. The little group is U(6) × U(6), rather than SU(6), which explains the increased dimensions of multiplets. New irregular couplings are permitted. Charge conjugation and the substitution rule are briefly explained. (auth)

6133 BARYON-ANTIBARYON PAIR PRODUCTION IN SU_8 SYMMETRY. Badier, S.; Bouchiat, C. (Faculte des Sciences, Orsay, France). Nuovo Cimento (10), 39: 1183-91(Oct. 16, 1965).

As an experimental test of SU(6) symmetry, the cross sections for baryon-antibaryon pair production in proton-antiproton interactions were studied. A rough agreement between the theoretical predictions and the experimental results of the baryon-antibaryon pairs belonging to representatives 56 and $\overline{56}$ of SU(6) was found. The data comparisons are presented. (M.O.W.)

6134 CLASSIFICATION OF HIGHER BOSON RESONANCES. Gatto, R. (Univ., Florence. Istituto Nazionale di Fisica Nucleare, Florence); Maiani, L.; Preparata, G. Nuovo Cimento (10), 39: 1192-6(Oct. 16, 1965)

A further discussion of a boson supermultiplet proposed by Borchi and Gatto (Phys. Lett., 14: 352(1965)) is presented. Classification of higher boson resonances based on the proposed supermultiplet is discussed. (M.O.W.)

6135 EVIDENCE FOR QUARKS FROM BARYON RESONANCES? Hill, R. D. (Univ. of Illinois, Urbana). Nuovo Cimento (10), 39: 1197-1200(Oct. 16, 1965).

Data on baryon resonances appear to indicate a systematic ordering of the states. It is shown that when the states are regarded entirely in terms of their assigned angular momenta and parities, there is a strong suggestion of an arrangment similar to the levels of a potential well system. Some consequences of interpreting the nucleon (Y = +1) states in terms of a 3-quark system of interacting particles in a simple potential well is discussed. (M.O.W.)

6136 HERMITIAN MASS OPERATORS IN CERTAIN COMBINED INVARIANCE THEORIES. Mirman, R. (Long Island Univ., Brooklyn). Nuovo Cimento (10), 39: 1208-10(Oct. 16, 1965).

From operators obeying certain conditions, which are obeyed by the translation operators, it is shown to be impossible to form a Hermitian operator that is of second order in the operators. It is shown that if one has an operator p such that p = [M,q], [p,q] = 0, then it cannot commute with the Hermitian conjugate. Furthermore, it is proven that it is impossible to form a Hermitian second order operator from operators which obey the above relation and which are mutually commutating. (M.O.W.)

6137 VARIATION GROUND-STATE ENERGY OF A BOSE SYSTEM. Sawada, K. (Univ. of California, San Diego, La Jolla). Phys. Rev., 140: A1564-7(Nov. 29, 1965).

An upper bound of the variational ground-state energy of a Bose system, for purely repulsive interactions and for a certain class of mainly repulsive interactions, is given using the Jastrow-type variational wave function. The upper bound obtained for a hard-sphere interaction is slightly lower than the bound obtained previously by Dyson. (auth)

6138 VERTEX-FUNCTION POLES AND THE BOOTSTRAP CONDITION IN FIELD THEORY. Gerstein, I. S.; Deshpande, N. G. (Univ. of Pennsylvania, Philadelphia). Phys. Rev., 140: B1643-8(Dec. 20, 1965).

The implications are discussed of maintaining finite mass renormalization when the wave-function renormalization constant Z_3 of an elementary particle is set equal to zero, making only the approximations of two-particle unitarity. It is shown that this defines a field-theory bootstrap for the elementary particle which is completely equivalent to the usual type of bootstrap based on the N/D method. As Z_3 goes to zero, the vertex function and inverse propagator develop poles which move to μ^2, the elementary-particle mass, in the limit. For nonzero Z_3, this pole does not contribute to the scattering amplitude; but at $Z_3 = 0$, it cancels the elementary-particle pole in the single-particle reducible part, leaving the dynamical pole in the irreducible part. It is also suggested that in this limit the bootstrapped state is a Regge pole. (auth)

6139 OFF-SHELL EQUATIONS FOR TWO-PARTICLE SCATTERING. Kowalski, K. L. (Case Inst. of Tech., Cleveland). Phys. Rev. Lett., 15: 798-800(Nov. 15, 1965).

The equivalence of the results for the two-particle partial-wave scattering amplitudes, both off and on the energy shell, which was described in terms of a solution of a manifestly nonsingular integral equation (Phys. Rev. Letters 15: 538(1965)) are established as equivalent to those of a previous, apparently different, analysis (J. Math. Phys. 4: 507(1963)). This may reveal the mathematical implications of this representation. Then using the methods of the latter analysis, an explicit general form for the nonseparable part of the off-shell amplitude, which should be useful in estimating the magnitude of this term, is determined. Some comments on off-shell unitarity are also made. (J.F.P.)

6140 RENORMALIZATION EFFECTS AND THE CABIBBO ANGLE. Nieh, H. T. (Harvard Univ., Cambridge, Mass.). Phys. Rev. Lett., 15: 902-5(Dec. 6, 1965).

Calculations of the renormalization of the semileptonic weak coupling constants by the U(3) symmetry-breaking interactions are reported. The consideration is based on a phenomenological field-theoretical model of U(3) symmetry breakdown, which is an extension of the idea that the symmetry breakdown is dominated by the nonvanishing expectation value of the scalar field S_{33}. The conclusions depend essentially on meson-pole dominance approximations. (J.F.P.)

6141 EXTENSION OF A THEOREM OF STREATER. Fuchs, N. (Univ. of Pennsylvania, Philadelphia). Phys. Rev. Lett., 15: 911-12(Dec. 13, 1965).

The proof of a theorem on broken symmetry by Streater (Phys. Rev. Letters 15: 475(1965)) which states that if a conserved current generates a transformation $\phi_1(x) \rightarrow \phi_2(x)$ between fields corresponding to particles of different mass, then there must be states in the theory degenerate with the vacuum (in the absence of states of negative norm), makes use of certain assumptions on the Lehmann weights for the two fields. It is shown that by dropping these assumptions a result is obtained which essentially is the same as that obtained by Streater. (J.F.P.)

6142 REMARKS ON THE CONNECTION BETWEEN EXTERNAL AND INTERNAL SYMMETRIES. Flato, M.; Sternheimer, D. (Institut Henri Poincare, Paris). Phys. Rev. Lett., 15: 934-6(Dec. 13, 1965).

A series of articles (Phys. Rev. 139: B1052(1965); Phys. Rev. Letters 14: 332(1965) and 14: 575(1965)) concerning the impossibility of explaining mass splitting within the context of finite-order Lie algebras, containing the Poincaré (inhomogeneous Lorentz) Lie algebra are discussed. It is shown that the proofs given were not sufficient. (J.F.P.)

6143 NONCOLLINEAR DIAGRAMS AND THE JOHNSON-TREIMAN RELATIONS. Harari, H. (Stanford Univ., Calif.); Lipkin, H. J. Phys. Rev. Lett., 15: 983-6(Dec. 20, 1965).

Some aspects of symmetry-breaking mechanisms are discussed. In particular, it is shown that the contribution of the two-meson exchange mechanism and the exchange of a two-meson ladder satisfy the Johnson-Treiman relations, provided that all the involved three-point functions are invariant under their own $SU(6)_W$ groups, respectively. SU(3) and its breaking and the noncollinear terms which break SU(6) are considered. It is shown that the contributions of the two-meson exchange diagrams also satisfy the Johnson-Treiman relations if the constituent three-point vertex functions are invariant under $SU(6)_W$. Similar arguments can be applied to a larger class of diagrams, and in particular to the exchange of a two-meson ladder. (J.F.P.)

6144 COMPARISON OF SOME $SU(6)_W$ PREDICTIONS ON COLLINEAR PROCESSES WITH EXPERIMENT. Jack-

son, J. D. (Univ. of Illinois, Urbana). Phys. Rev. Lett., 15: 990-6(Dec. 20, 1965).

Some of the predictions of Carter (Phys. Rev. Letters 15: 373(1965)) for collinear processes on the basis of a relativistic generalization of SU(6) are compared with existing experimental data. Gross disagreement is found. Some arguments are given to show that the failures of the predictions are to be expected, and that the symmetry schemes are probably valid only for vertices and perhaps for nonperipheral contributions to reaction amplitudes. The most important feature omitted in such attempts is the modifications introduced by the existence of competing channels and the resultant inelasticities of the low partial waves. (J.F.P.)

6145 THE INHOMOGENEOUS GROUP $P(SU_6)$ IN ELEMENTARY PARTICLES THEORY. Novozhilov, Yu. V.; Terent'ev, I. A. Vestn. Leningr. Univ., No. 10, Ser. Fiz. Khim., No. 1, 5-12(1965). (In Russian).

Nontrivial extension of Poincaré group is considered. The group $P(SU_6)$ is suggested as the group of elementary particles symmetry. The group $P(SU_6)$ has SU_6 group in nonrelativistic limit. Its little group is also SU_6. There are 35 space-like rotations M_a, 35 Lorentz transformations N_a and 36 moments P_α in $P(SU_6)$. Commutation relations are given, but in the group $P(SU_6)$ an invariant Hermitian form cannot be constructed. Therefore the group with reflections $P(SU_6)$ is considered. In this case the number of all representations is doubled. For example, a vector G_α transformed as the momentum in $P(SU_6)$ be taken in $P(SU_6)$ together with 36 axial components $\tilde{G}_\alpha$, the form $G_0^2 - G_a^2 - \tilde{G}_0^2 + \tilde{G}_a^2$ being preserved. The states, which are the objects of SU_6 in this theory, are the superpositions of states transforming like as irreducible representations of the Poincaré group. The most attractive feature of such presentation is the mass relations, specific for the SU_6-group. Proposed symmetry includes broken symmetry effects as well. (auth)

6146 HYPERVIRIAL RELATIONS FOR THE DISTORTED COULOMB FIELD. Rudakov, V. S. Vestn. Leningr. Univ., No. 10, Ser. Fiz. Khim., No. 1, 13-17(1965). (In Russian).

A method of deriving the hypervirial relations for the case of stationary scattering on the Coulomb potential distorted by a spherically symmetric short-range potential is considered. Several examples illustrating the method are given. (auth)

6147 THE DENSITY MATRIX FOR THE SYSTEM OF NONINTERACTING FERMIONS. Demkov, Yu. N.; Komarov, I. V. Vestn. Leningr. Univ., No. 10, Ser. Fiz. Khim., No. 1, 18-28(1965). (In Russian).

Exact expressions for the density matrix (DM) for the system consisting of non-interacting fermions in some fields were investigated. One- and three-dimensional problems were solved. For the first time the DM for the three-dimensional isotropic oscillator and the DM for the Coulomb shell in the coordinate representation were obtained in closed form. Semi-classical asymptotics of the DM is discussed. (auth)

6148 THE ADEMOLLO-GATTO THEOREM FOR AN ARBITRARY SU(3) REPRESENTATION. Zakharov, V. I.; Tyutin, I. V. (Inst. of Theoretical and Experimental Physics, Moscow). Yadern. Fiz., 2: 705-9(Oct. 1965). (In Russian).

The renormalization of the vector interaction couplings of the hadron leptonic decays due to the SU(3) symmetry breaking interaction L_{MS} is considered. It is shown that to the first order in L_{MS} these constants are not renormalized for an arbitrary SU(3) representation (p,q). In the second order in L_{MS} the renormalization of vector constants takes place in every SU(3) representation. In the order $p + q + 1$ in L_{MS} there are no relations between different decay constants. (auth)

6149 ON THE POSSIBLE USE OF GROUPS B_3, C_3 AND D_3 FOR THE CLASSIFICATION OF ELEMENTARY PARTICLES. Manko, V. I. (Lebedev Inst. of Physics, Moscow). Yadern. Fiz., 2: 733-7(Oct. 1965). (In Russian).

Young patterns are used to formulate a simple rule, according to which all weights belonging to irreducible representations of the groups B_3, C_3, and D_3 can be found, starting from the highest weight. The lowest representations of these groups and their isotopical contents are discussed. (auth)

6150 A GEOMETRICAL METHOD FOR REDUCING THE GROUPS SU(4) AND SU(3) WITH RESPECT TO THE SUBGROUPS $SU(2) \otimes SU(2)$ AND O(3). Perelomov, A. M.; Popov, V. S. (Inst. of Theoretical and Experimental Physics, Moscow). Yadern. Fiz., 2: 738-47(Oct. 1965). (In Russian).

A simple geometrical method is suggested to find the isotopical and spin content of Wigner supermultiplets and also the isotopical structure of N pion systems. From the mathematical point of view the considered problems mean the reduction of the SU(4) and SU(3) groups with respect to their subgroups $SU(2) \otimes SU(2)$ (or O(4) and O(3) respectively). (auth)

6151 ON THE CLASSIFICATIONS OF MESON RESONANCES WITH HIGHER SPINS IN THE SU(6) SYMMETRY THEORY. Duc, Dao-wong; Tu, Pham Qui (Joint Inst. for Nuclear Research, Dubna, USSR). Yadern. Fiz., 2: 748-51 (Oct. 1965). (In Russian).

The 189-dimensional SU(6) meson multiplet, the lowest multiplet containing mesons with spin 2, is considered. The mixing parameters between states belonging to different unitary multiplets and having the same quantum numbers are obtained. The mass splitting of particles in the given multiplet is discussed. (auth)

6152 HADRONIC DECAYS OF BARYONS IN BROKEN SU(6)-SYMMETRY. Matinyan, S. G. (Inst. of Physics, Academy of Sciences, Georgian SSR). Yadern. Fiz., 2: 752-6(Oct. 1965). (In Russian).

The influence of moderately strong interactions on the relations between the amplitudes of s-waves in the hadronic decays of baryons is considered on the basis of SU(6) symmetry. It is shown that the moderately strong interactions imply a possible admixture of the s-wave in the decay $\Sigma^+ \to n\pi^+$. Other relations obtained from the SU(6)-symmetry broken only by weak interactions must also be modified. (auth)

6153 WHAT IS THE RANGE OF HIGH ENERGY INTERACTIONS? Gribov, V. N.; Ioffe, B. L.; Pomeranchuk, I. Ya. (Ioffe Inst. of Physics and Tech., Leningrad. Inst. of Theoretical and Experimental Physics, Moscow). Yadern. Fiz., 2: 768-76(Oct. 1965). (In Russian).

It is possible to determine at what distances high-energy elastic and inelastic scattering occurs by investigating experimentally the emission of soft photons accompanying the given scattering process. If it proves that the region in which the usual formula for the accompanying radiation can be applied decreases as the energy of the incident particles increases, this will mean that the effective longitudinal distances at which the interaction occurs at high energies increase as the energy increases. (auth)

6154 REMARK ON THE UNCERTAINTY BETWEEN ANGLE AND ANGULAR MOMENTUM. Kraus, K. (Univ., Marburg, Ger.). Z. Phys., 188: 374-7(1965).

It was previously shown that the uncertainty relation (with $h = 1$) $\Delta L \cdot \Delta\varphi \geq \frac{1}{2}$ between angle φ and the corresponding angular momentum L to be incorrect. The derivation of a new uncertainty relation is presented ($\Delta L \cdot \Delta\varphi \geq \frac{1}{2}|1 - 2\pi|f(\pi)|^2|$). A discussion of this uncertainty relation with respect to L and φ is presented. (M.O.W.)

6155 INVARIANT LAGRANGE FORMALISM AND CONSERVATION PRINCIPLES [Thesis]. Demmig, F. Hamburg, Univ., 1964. 72p. $2.00 Gmelin, AED-DISS. 64-763.

An invariant Lagrange formalism for the description of quantized fields is studied. Transformation formulas for a scalar Lagrange density are given. Results indicate that in the general case divergence equations cannot be identified with conservation principles. The existence of a symmetric energy-momentum tensor is demonstrated. (Gmelin Inst.)

Fluid Physics and Thermodynamics

See also Plasma Physics and Thermonuclear Processes

6156 (AD-617562) FUNDAMENTALS OF MHD FLOW. Final Report. Sherman, Arthur (General Electric Co., Philadelphia, Pa. Missile and Space Div.). June 1964. Contract AF49(638)-914. 12p. (AFOSR-64-1425). CFSTI $1.00 cy, $0.50 mn.

Magnetohydrodynamic phenomena associated with crossed field devices were investigated. The working medium was assumed to be a partially ionized plasma at relatively low temperatures (1500-3000°K), so that Magnetic Reynolds numbers were assumed to be much less than one. As a result, it was typically assumed that the applied magnetic field was not distorted by currents flowing in the plasma, although for some problems this simplification was not necessary. Several studies were made of the properties of the low temperature plasmas of interest. Then a large number of channel flow problems were analyzed and reported upon. Some magnetohydrodynamic boundary layer phenomena were next reviewed, and following this a broad review was made of the propulsion and power generation application areas. New concepts were developed for the macroscopic description of the non-equilibrium ionization idea. (TAB)

6157 (AD-617898) MHD CHARACTERISTICS AND DISPERSION RELATION FOR FINITE ELECTRICAL CONDUCTIVITY. Friedel, Helmut (Innsbruck Univ. (Austria)). Mar. 13, 1965. Contract AF61(052)-675. 15p. (SR-23; AFOSR-65-1313). CFSTI $1.00 cy, $0.50 mn.

MHD characteristics were investigated for the case of finite electrical conductivity in connection with dispersion relations of linear waves. The basic equations are no longer total hyperbolic, but parabolically or elliptically degenerated. The nature of the characteristic directions for the degenerated MHD basic equations are explained. (auth)

6158 (AD-619999) A STUDY OF HYDROMAGNETIC SHOCKS AND ALLIED PROBLEMS. Final Report, April 5, 1960-October 31, 1964. (Case Inst. of Tech., Cleveland, Ohio). June 1, 1965. Contract AF19(604)-7287. 14p. (AFCRL-65-426). CFSTI $1.00 cy, $0.50 mn.

Theoretical and experimental investigations on the onset mechanism of an electromagnetically driven shock wave, on the dynamics of current sheets, and on the propagation of waves in nonuniform magnetic fields are discussed. Brief descriptions of a number of separate investigations undertaken in these areas are presented and references given. (auth)

6159 (AERE-M-1597) LOW-VOLTAGE DIFFUSE DISCHARGE IN ATMOSPHERIC-PRESSURE HELIUM WITH SMALL ADDITIONS OF POTASSIUM. Ellington, H. I. (Atomic Energy Research Establishment, Harwell (England)). July 1965. 25p. Dep. mn.

A description is given of the properties of a low-voltage, high-current electric discharge in atmospheric-pressure helium containing a small quantity of potassium vapor as seed. The results for helium are compared with those for argon. The dependence of the properties of the discharge on total current, temperature, and potassium pressure is discussed. The reasons for the difference between the helium and argon results are given, and these differences are shown to be consistent with the theory of non-equilibrium conductivity. As in the case of argon, a theoretical explanation of the variation of positive column field with current is given, and the existence of an optimum seed pressure demonstrated. The dependence of the breakdown voltage of the gas on electrode spacing, temperature, and potassium pressure is discussed. (auth)

6160 (NP-15604) USLOVIYA EVOLYUTSIONNOSTI KOSYKH I KONICHESKIKH UDARNYKH VOLN I TRANSZVUKOVYKH TECHENII. (Evolutionary Conditions of Oblique and Conical Shock Waves and of Transonic Flows). Polovin, R. V. (Akademiya Nauk Ukrainskoi SSR, Kharkov. Fiziko-Tekhnicheskii Institut). 1964. 26p. Dep. mn.

A review of papers which deal with transonic flow around bodies and with attached oblique and conical shock waves is presented. It is shown that the continuous transition through the sound speed in one-dimensional ordinary-hydrodynamics is possible only with increase of Mach number. The starting point in this proof is the evolutionary condition. Then this theorem is extended on two-dimensional flow if sonic line joins the wall in the point where the velocity vector has definite direction. Other demonstrations of this theorem are reviewed. It is then generalized in magnetohydrodynamics. Oblique shock waves attached to the corner are next. Possible bending of the discontinuity line and the impossibility of oblique shock waves, belonging to the strong family, are discussed. It is proven that downstream of the oblique shock wave attached to the corner, the flow is supersonic, the starting point being again the evolutionary condition. It is also proven that oblique detonation waves may exist only in Chapman-Jouget regime, the duct being supposed to have constant cross section. (M.O.W.)

6161 (NP-15630) MAGNETOHYDRODYNAMICS OF AN OSCILLATING DIELECTRIC SPHERE. Plasma Research Laboratory Report No. 21. Motz, Robin O. (Columbia Univ., New York. Plasma Lab.). Aug. 1965. 97p.

A dielectric sphere executing rapid small amplitude oscillations in an incompressible, electrically conducting fluid with a uniform magnetic field aligned along the axis of oscillation is studied. For large Hartmann and Reynolds numbers, the magneto-hydrodynamic equations are linearized for an inviscid fluid by an expansion in the magnetic Reynolds number of all quantities of interest. Solutions correct to $O(R_m)$ are obtained for the velocity, pressure, and current in the fluid, and for the electric and magnetic field both outside and inside the sphere. The MHD contribution to the sphere is found to be derivable from the Joule loss in the fluid. Experiments were performed with an oscillating sphere in mercury with applied magnetic field strengths to 8 kilogauss. The measured MHD drag agrees well with the theory. The angular dependence of the induced electric field was also measured and verifies the use of the inviscid velocity field to determine the induced current. Measurements also showed the presence of damped Alfven waves. (auth)

6162 (UCRL-12238-T) ONE-DIMENSIONAL EULERIAN HYDRODYNAMICS DIFFERENCE EQUATIONS. De Bar, Roger (Lawrence Radiation Lab., Univ. of California, Livermore). Oct. 1965. Contract W-7405-eng-48. 16p. Dep. mn; CFSTI $1.00 cy, $0.50 mn.

A set of Eulerian hydrodynamics difference equations are developed. The approach used is that of alternating steps; that is, the essentially Lagrangian parts of the Eulerian difference equations are treated first, and the transport of these (Lagrangian) advanced quantities is treated second. (M.O.W.)

6163 INVESTIGATIONS ON ELECTRIC ARCS IN THE GRAVITATIONLESS STATE. Ebert, Wilhelm (Institut fuer Magnetohydrodynamik, Berlin). Beitr. Plasmaphys., 5: 371-6(1965). (In German).

Experiments were carried out on long (up to 75 mm) free-burning arcs in the gravitationless state. Direct-current arcs, alternating-current arcs, and disconnected arcs were investigated in air, nitrogen, argon, and carbon dioxide. The results of the studies made on the arcs in the stationary and nonstationary state are reported. The most important properties of long, free-burning, and convectionless arcs were determined. (J.S.R.)

6164 THE SPACE POTENTIAL DETERMINATION USING GLOW PROBES. Arndt, Rudolf (Institut fuer Gasentladungsphysik, Deutsche Akademie der Wissenschaften, Greifswald, Ger.). Beitr. Plasmaphys., 5: 381-93(1965). (In German).

Measurements on low current Ne discharges showed that the glow probes should be built in a hairpin shape because of the reaction of the glow discharge and should have a feed

wire as thin as possible with ∞-shaped cross section. A relatively simple method for the preparation of such probes is described. The parallel displacement or divergence between the characteristic lines of the hot and cold probe in the electron input range was traced back to contact potential variations and thermally limited surface growth. The glow probe is usable as the counter probe in double probe circuits because of its constant output work and the sharp decay of the characteristic line. (J.S.R.)

6165 THE THEORY OF A GLOW LIGHT OF A LOW-PRESSURE DISCHARGE. Wilhelm, Johannes; Kind, Wolfgang (Institut fuer Gasentladungsphysik, Deutsche Akademie der Wissenschaften, Greifswald, Ger.). Beitr. Plasmaphys., 5: 395-403(1965). (In German).

The proposal of Weizel et al. was expanded to the decay of the beam in the passage of the glow light and to a consideration of the radio leakage. The first comparison of the equation obtained with results of measurements of a He discharge show better than qualitative agreement. (tr-auth)

6166 LIGHT FROM THE FALL SPACE. Hantzsche, E.; Wieczorek, L. W. (Physikalisch-Technisches Institut, Berlin). Beitr. Plasmaphys., 5: 425-34(1965). (In German).

The excitation light density in the cathode drop of glow discharges was calculated for four fall space voltages (normal up to highly abnormal drop) using distribution functions from the statistical fall space theory. The "moved light" of the fast neutral atoms, which damages the similarity law, was considered in particular. The light density distributions calculated as a function of the distance from the cathode were in satisfactory agreement with measured values. (tr-auth)

6167 BREAKDOWN IN THE LOW PRESSURE REGION. Gladitz, B. (Physikalisch-Technisches Institut, Berlin). Beitr. Plasmaphys., 5: 435-45(1965). (In German).

An integral equation for the first Townsend ionization coefficients α was formulated. The discussion of this equation yields data on the capture mechanism of the discharge in the low-pressure region. (tr-auth)

6168 MULTI-CATHODE DISCHARGES IN A XENON–HYDROGEN MIXTURE. Schulz, Paul; Spiegelhalter, Fritz (Technische Hochschule, Karlsruhe, Ger.). Beitr. Plasmaphys., 5: 447-54(1965). (In German).

A discharge through a Xe–H mixture was operated with two cathodes, one of which surrounded the arc in a ring and was heated up during operation by the plasma of the column. The dimensioning of the electrodes and charge of the discharge are so selected that the recombination zone of the H dissociated in the hot arc gas is found near the inner surface of the ring cathode. Because of the introduction of the dissociation energy, the electrode at this place was so strongly heated that the arc even at low charge produced no cathode spot. The conditions under which the discharge burns with or without cathode spots are discussed in dependence on the contraction theory of Ecker. With the addition of H the arc can also be sharply contracted on the anode. The conditions under which the anodic on-set would result almost without contraction are given. (tr-auth)

6169 THE NATURE OF THE PRE-BREAKDOWN CURRENT IN HIGH VACUUM. Juettner, B. (Physikalisch-Technisches Institut, Berlin). Beitr. Plasmaphys., 5: 461-78(1965). (In German).

The current in the range from 10^{-12} to 10^{-4} amp was investigated with various measurement methods in the preliminary stages of high vacuum breakdown. The main current was shown to be voltage dependent with inconstant fields. For the frequently occurring characteristic current oscillations, various elementary mechanisms are discussed on the basis of a field emission hypothesis. (tr-auth)

6170 PROPAGATION OF WEAK DISTURBANCES IN MAGNETOHYDRODYNAMICS. Dubrovskii, V. A.; Skuridin, G. A. Geomagnetizm i Aeromomiya, 5: 234-50(1965). (In Russian).

Newton's iteration method is applied to equations of magnetohydrodynamics. This method leads to a sequence of linearized equations, the first of which describes small disturbances of the main current. The linearized equations are solved by the asymptotic method. The common factor in the exact solution is the exponential, which, in the first step of iteration, for example, depends on the parameters of the main flow. This makes it possible, in principle, to formulate the problem of the stability of this flow. It is shown how to obtain an asymptotic solution in the form of an expansion in negative powers of conductivity in the case of finite conductivity. Its relation to the case of infinite conductivity is discussed. (tr-auth)

6171 MOTION OF A MEDIUM WITH A FINITE CONDUCTIVITY IN THE PRESENCE OF MASS FORCES AND A PLANAR MAGNETIC FIELD. Khantadze, A. G. (Inst. of Geophysics, Academy of Sciences, Georgian SSR). Geomagnetizm i Aeronomiya, 5: 342-5(1965). (In Russian).

The unidimensional nonstationary flow of an ideal compressible medium of finite conductivity in the presence of mass forces and a planar magnetic field is considered. The equations of magnetohydrodynamic flow are developed and analyzed, and expressions are obtained for the altitude-dependent density and the total pressure of the medium. (M.J.T.)

6172 ABOUT ONE OF N. E. KOCHIN'S PROBLEMS IN MAGNETOHYDRODYNAMICS. Khantadze, A. G. (Inst. of Geophysics, Academy of Sciences, Georgian SSR). Geomagnetizm i Aeronomiya, 5: 345-6(1965). (In Russian).

The magnetohydrodynamic equations are written for the case of nonuniform rotational motion in a medium in the presence of gravity and a planar magnetic field, and expressions are obtained for the magnetic-field components and the density and the total pressure. The formation and breakdown of vortices can be seen to occur in this case. The results agree with those of Kochin for adiabatic motion in a compressible baroclinic fluid under the influence of conservative forces. (M.J.T.)

6173 FLOW MODES IN ELECTRIC SHOCK TUBES. Barach, J. P.; Vermillion, R. E. (Vanderbilt Univ., Nashville). Phys. Fluids, 8: 1976-84(Nov. 1965).

Electric shock tube flow was studied at low pressures, after cessation of the powering discharge, in a 4-in.-diam tube. Three modes of plasma flow down the tube are found: a diffusion type of flow below 10 μ, flow with a single luminous front, and flow with a separated shock front and contact surface. The criterion for the appearance of flow with a separated shock wave appears to be Taylor stability of the contact surface. Since electric shock tube flow is always decelerating strongly, this occurs when the driver density becomes less than that of the shocked gas layer immediately ahead. As a result separated shock flow is more likely the weaker the powering discharge, the higher the ambient pressure, the less the erosion of the electrodes, and the further downstream one observes. These considerations are also found to be consistent with the observed behavior of a medium and a high-pressure shock tube. (auth)

6174 STABILITY DIAGRAMS FOR MAGNETOGAS-DYNAMIC CHANNEL FLOW. Hains, F. D. (Boeing Co., Seattle). Phys. Fluids, 8: 2014-19(Nov. 1965).

A study is made of the influence of a coplanar magnetic field on the stability of a conducting fluid flowing between parallel planes. After derivation of the general stability equations for small magnetic Reynolds number, numerical results are obtained for the case where initial perturbations of the magnetic field vanish. This must occur if the channel walls have zero or infinite conductivity. Four sets of stability diagrams are presented so that each stability curve will represent the effect of a given applied magnetic field as only one of the four quantities in the Reynolds number is changed. The flow is always stable for initial disturbances of the field produced by passage of a pulsating current through walls of finite conductivity. (auth)

6175 LAMINAR AND TURBULENT MAGNETOHYDRODYNAMIC FREE JET. Smith, David C.; Cambel, Ali

Bulent (Northwestern Univ., Evanston, Ill.). Phys. Fluids, 8: 2107-9(Nov. 1965).

An analytical perturbation solution to the incompressible, electrically conducting free jet problem subject to a transverse magnetic field is presented. The same notation and analysis is used as that given by Peskin (Phys. Fluids 6: 643(1963)). The stream function is expanded in terms of the magnetic interaction parameter which is the ratio of the magnetic body force to the inertia force. The centerline velocity of the nonmagnetic jet solution and the axial coordinate are taken as the characteristic values in determining the interaction parameter. The basic results of the analytical solution are identical with Peskin's results. But rather than identifying the perturbation parameter in the same way, the magnetic interaction parameter is pointed out as the ratio of the magnetic force to the inertia force of the jet, giving a more physical meaning to the expansion parameter. (J.F.P.)

6176 TRANSIENT MAGNETOHYDRODYNAMIC FLOW AND HEAT TRANSFER. Singer, Ralph M. (Argonne National Lab., Ill.). Z. Angew. Math. Phys., 16: 483-94 (1965).

The effects of combined forced and free convection, a transverse magnetic field, internal energy generation, and fluid diffusive properties upon the unsteady, fully-developed, laminar flow of an electrically conducting fluid through a vertical parallel-plate channel are studied analytically. It is found that an oscillatory approach to steady state occurs whenever the Hartmann or Rayleigh numbers are large, or the thermal Prandtl number is near unity. Conversely, the oscillations are largely damped by the diffusive character of the fluid, i.e., for very small or very large thermal or magnetic Prandtl numbers. Also, if a sufficiently large magnetic field is allowed to become established prior to putting the fluid in motion, little, if any, oscillation is observed. Unsteady fluid temperatures are found to be significantly different from the steady-state values for certain ranges of the parameters, so that any design of a MHD device must take cognizance of the start-up phenomena. (auth)

6177 INVESTIGATIONS ON THE STATISTICAL OSCILLATIONS OF THE INFRARED RADIATION OF A HIGH-PRESSURE, HIGH-CURRENT ARGON DISCHARGE. PART II. PROPERTIES OF THE HIGH-PRESSURE, HIGH-CURRENT ARGON ARC AND CALCULATION AND MEASUREMENT OF THE STATISTICAL RADIATION OSCILLATIONS. Gubler, W.; Strutt, M. J. O. (Technische Hochschule, Zurich). Z. Naturforsch., 20a: 1156-69(Sept. 1965). (In German).

An argon discharge at high pressure (up to 20 atmos.) and large d-c current is described. The discharge is used in the investigation of spontaneous fluctuations of photon radiation. Electron and ion densities are calculated as functions of pressure and temperature from which the continuous emission and absorption coefficients are determined. By comparing the calculated emission with the measured distribution of the infrared spectral radiation intensity in a disk of plasma, which is 0.2 mm in front of the cathode, the radial temperature distribution in the disk is determined. The temperature in the arc axis was found to be independent of the gas pressure and must be higher than 28,000°K. Investigations on electrical conductivity confirm the temperature distributions. Finally, the statistical radiation fluctuations can be calculated by means of the equations previously given and are compared with the experimental results. A satisfactory coincidence between calculated and measured values was found. (auth)

6178 FLUID TRANSPIRATION PLASMA JET. Sheer, Charles (to Sheer-Korman Associates, Inc.). U. S. Patent 3,214,623. Oct. 26, 1965. Filed Feb. 12, 1962.

An apparatus for transferring electric energy from an electric arc to a stream of fluid includes a solid cylindrical cathode with a tubular insulator fitted over the cathode with both parts terminating in a common conical surface providing a protruding cathode point and a cylindrical anode fitted over the insulator. The anode has a circumferentially disposed conical channel having its inner surface in substantial alignment with the conical surface of the cathode and insulation. When gaseous material is discharged through the conical channel while the parts are energized, it will be directed to pass over the conical surface of the cathode and insulator and over the point of them. (B.L.M.)

Geophysics

6179 (AD-618911) A THREE FLUID MODEL IONOSPHERE. Comstock, Craig (Harvard Univ., Cambridge, Mass. Div. of Engineering and Applied Physics). June 1965. Contract Nonr186620. 150p. CFSTI $4.00 cy, $1.00 mn.

Discussion is presented on understanding the distribution of particles in a planetary atmosphere and the mechanisms responsible for maintaining that distribution. Model atmospheres are considered which have relatively simple chemical compositions and which are ionized to some degree. The distribution of particles throughout the atmosphere, the associated electric fields, and the boundary conditions which are necessary to maintain the distributions are discussed. The problem considered is to obtain some further insight into the mechanism which controls the distribution of particles in an ionosphere. The roles played by diffusion, the electric field, and the boundary conditions are of interest. A more general set of equations is derived for the distribution of particles than has been previously published. This set of equations is applied to a series of simple models, one of which is a reasonable model for the F layer of the Earth's ionosphere. Some conclusions are drawn on the various mechanisms involved in maintaining the structure of planetary atmospheres. (auth)

6180 (AD-619250) STUDY OF VLF RADIATION BY USE OF A NIKE-CAJUN ROCKET. Renard, Claude; Fayard, Christian (Centre National d'Etudes des Telecommunications (France)). Apr. 15, 1965. Contract AF61 (052)-571. 63p. CFSTI $3.00 cy, $0.75 mn.

The payload of a NIKE-CAJUN rocket consisted of equipment developed to measure the magnetic field in the ionosphere of a vlf wave radiated by the Annapolis transmitter (NSS) on 22.3 kc/s. After the measurement principles are exposed, a detailed description of the equipment is given and the telemetry results are analyzed. In spite of an antenna effect on the loops, an approximate measure of the vlf field in the whistler mode between the D and e layers is given. An analysis of the propagation above Wallops-Island is carried out, which allows the development of the processing of the Doppler effect observed on the vlf wave received in the ionosphere. The electron density profile obtained between 70 and 100 km was analyzed and showed two layers at 78 and 87 km. (auth)

6181 (AD-619288) X-RAY EXCITATION OF THE SECOND POSITIVE AND FIRST BANDS OF NITROGEN. Low, W. (Hebrew Univ., Jerusalem (Israel). Dept. of Physics, Massachusetts Inst. of Tech., Cambridge). 1964. Contract N62558. 7p. CFSTI $1.00 cy, $0.50 mn.

It is shown that x-rays can produce emission of light in air and can excite the second positive and first negative bands of nitrogen, found prominently in aurorae. (TAB)

6182 (AD-619447) PROJECT AURORA III. PART I. SOME EVIDENCE FOR THE OCCURRENCE OF HIGH ELECTRON DENSITIES IN THE AURORAL D AND E REGION. PART II. AN ANALYSIS OF THE STATISTICS OF SIMULTANEOUS AURORAL ECHOES. Final Report, February 12, 1962–June 15, 1965. Flood, Walter A. (Cornell Aeronautical Lab., Inc., Buffalo, N. Y.). Contract AF19 (628)-380. 38p. (CAL-CM-1677-P-1; AFCRL-65-451). CFSTI $2.00 cy, $0.50 mn.

A-scope photographs of simultaneous auroral echoes at 49.7, 143.5, and 226 Mcs using scaled antenna systems with five degree beamwidths are presented and discussed. The photographs showed that on occasion the 49.7 and

143.5 Mcs echoes can arise at disparate ranges. These photographs are interpreted as indicating the presence of local electron densities (occupying regions that subtend angles smaller than the five degree system beamwidth) in excess of $2 \times 10{,}000{,}000$ electrons/cu cm. Consequently single scatter theory cannot always be applied to the analysis of auroral echoes at frequencies as low as 50 Mcs. The amplitude distribution and wavelength dependence of the simultaneous auroral echoes at 49.7, 143.5, and 226 Mcs were studied. Amplitude distributions were very closely Rayleigh distributed. The data were interpreted as indicating a wavelength dependence that varied as lambda to 3.5 power for frequencies between 50 and 143.5 Mcs and lambda to 6.5 power for frequencies between 143.5 and 226 Mcs. During conditions of strong auroral activity, auroral absorption may tend to mask the wavelength dependence at the two lower frequencies. (auth)

6183 (AD–619821) POWER SERIES SOLUTION OF THE F2 LAYER DIFFUSION EQUATION. Baxter, R. G.; Kendall, P. C.; Windle, D. W. (Sheffield Univ. (England). Dept. of Applied Mathematics). Mar. 1, 1965. Contract AF-EOAR54-74). 25p. (SR–2; AFCRL–65-563). CFSTI $1.00 cy, $0.50 mn.

If the equatorial electron density profile in the region is known, the equilibrium electron density everywhere else can in theory be computed. A method is given for carrying out this process for regions within 30 degrees of latitude of the dip equator for an exponential atmosphere of constant scale height and for symmetry about the dip equator. This was achieved by simplifying the diffusion equation for an isothermal atmosphere, then expanding in a power series, convergent at great height and whose coefficients are functions of latitude. The method was applied to a study of the distributions of electron density expected from an equatorial profile with a single maximum, similar to a Chapman profile. Attention was confined to the case of no production and loss, with an upward electrodynamic drift at right angles to the magnetic field lines and uniform at the dip equator. (auth)

6184 (AD–619977) PROPOSED ELECTRONIC SYSTEMS FOR THE LES RADIATION EXPERIMENT (SEPTEMBER 1964). Binsack, Joseph H. (Lincoln Lab., Massachusetts Inst. of Tech., Lexington). July 2, 1965. Contract AF19(628)-5167. 90p. (TN–1965-5; ESD-TDR–65-54). CFSTI $3.00 cy, $0.75 mn.

To study the electron radiation environment of the Lincoln Experimental Satellite (LES), an electron detecting telescope was proposed by C. Mack, et al. The proposed electronic system for this radiation experiment is described. The design of the electronic system is based on the use of a "hybrid counter" as the scaler. The "hybrid counter" employs the best features of both the "fixed time" and the "fixed count" scalers and can operate over a wide range of counting rates. Coincidence logic is programmed within the experiment so that the telescope can monitor the electron flux for energies from 60 kev to 10 Mev with counting rates from 100,000 down to 0.1 count/sec. The design of a charge sensitive solid state preamplifier and measurement chain is described. The integrating and differentiating time constant is set at 0.5 μsec, and a noise line width of 27 kev is achieved at 30°C with a simulated input capacitance of 100 pf. (auth)

6185 (AFCRL–65-620) ELECTRON DENSITIES IN THE D REGION OF THE IONOSPHERE FROM LOW FREQUENCY SIGNAL STRENGTH MEASUREMENTS IN ROCKETS. Scientific Report No. 254. Seliga, T. A. (Pennsylvania State Univ., University Park. Ionosphere Research Lab.). Nov. 1, 1965. Contract AF19(628)-4050. 143p. CFSTI $4.00 cy, $1.00 mn.

Techniques of determining electron densities in the D region of the ionosphere from rocket measurements of field quantities of a c-w radio wave transmitted from the ground are described. Iterative methods which are based on a full wave solution of the generalized form of the differential equations governing radio wave propagation in the ionosphere are used to analyze data from two rocket flights at Ft. Churchill, Manitoba, Canada. The results of one flight (July 20, 1963) during a solar eclipse are compared with electron density profiles obtained from an impedance probe flown on the same rocket and from Langmuir probes flown in other rockets about the same time. The data from the second flight (July 26, 1963) were used to qualitatively verify the results of an impedance probe in the same rocket. The methods of analysis were also applied to data obtained in the nighttime D region by Mechtly (1962), and the electron density profiles obtained by this analysis are presented. (auth)

6186 (UCRL-Trans-1269(L)) THE SCINTILLATION OF TERRESTRIAL RADIATION. Siedentopf, H.; Wisshak, F. Translated for Univ. of California Lawrence Radiation Lab., Livermore), from Optik, 3: 430-43(1948). 25p. Dep. mn; JCL $2.60 fs, $0.95 mf.

Atmospheric disturbances near the ground produce an intensity modulation in the radiation of distant light sources and this modulation can be measured by an oscillograph. Under radiating conditions, the diurnal variation of the modulation factor shows two minima (one shortly after sunrise, the other shortly before sunset) and two maxima (a steep one at midday and a flat one in the evening). Various experiments were carried out with a view to determining scintillation with the aid of an oscillograph. The results of these experiments are discussed. (M.O.W.)

6187 OSCILLATION OF IONIZATION IN THE IONOSPHERE IN MEDIAN LATITUDES AND VARIATION OF THE MAXIMUM USABLE FREQUENCY FOR SHORT-WAVE LONG-DISTANCE-PROPAGATION WITH A 27-DAY PERIOD CAUSED BY SOLAR WAVE RADIATION. Lange-Hesse, G.; Schott, E. (Max-Planck-Institut fuer Aeronomie, Lindau, Ger.). Arch. Elek. Uebertr., 19: 59-65 (1965). (In German).

Periodic variations in ionization frequency in the F_2, F_1, and E_1 layers of the ionosphere (as recorded at Slough, England and Lindau, Germany) were analyzed in relation to sunspot activity (as recorded at Zurich, Switzerland), after eliminating the particle-radiation component. The resulting solar wave radiation responsible for the production of the ionization in the ionosphere was shown to vary in its intensity in close correlation with the period of the 11-yr sunspot cycle. Furthermore, intensity variations with a quasipersistent 27-day period could occur in instances where sunspots were unsymmetrically distributed in heliographic longitude and where the sun, in the course of its rotation in about 27 days, exhibited alternatively discs with many spots and with few spots. It was shown that such intensity variations produce considerable 27-day variations with the same phase in the critical frequencies of the F_1, F_2, and E_1 layers as well as in the MUF 3000 (max usable frequency for the 3000-km distance), but 27-day variations with reversed phase in the M 3000 factor (conversion factor from vertical to oblique-incidence critical frequency for the 3000-km distance). The 27-day quasipersistent variations in the average temperature of the F layer may be responsible for the production of these M 3000 variations. Numerical data are given for magnitude and seasonal variations of the average relative amplitude of the 27-day variations of the ionospheric data presented. (BBB)

6188 GEOMAGNETIC MICROPULSATION RESULTS FROM BYRD STATION AND GREAT WHALE RIVER. Jacobs, J. A.; Wright, C. S. (Univ. of British Columbia, Vancouver). Can. J. Phys., 43: 2099-122(Dec. 1965).

A report from the near-conjugate stations at Great Whale River and Byrd Station is given, in which the chief emphasis is on the time-agreement of the abrupt commencements of the numerous examples of Birkeland's "Polar Elementary Storms." Passing reference only is made to the associations at Byrd between vlf hiss and other ionospheric phenomena that are being reported by Stanford University. In the auroral zones, the magnetic activity is usually so great, even during the IQSY, that magnetograms can be employed usefully to supplement the micropulsation records. By using selected nighttime occasions, when the change in H

is so sudden that a reasonable accuracy in the timing of the micropulsations can be achieved, it is found that the time differences between the two conjugate stations average ±1 minute, although there is clear evidence that the two stations are not conjugate at all times, as evidenced by the lack of similarity of records. It is confirmed that the more abrupt changes in the magnetic field are associated with high-frequency riders of the order of 1 cps, and that these events are often seen with the same riders at the same time at the midlatitude stations. The return currents that show up in these lower latitudes must be taken into consideration when the areas of conjugate station agreement are considered. The daytime regime of regular (Pc) variations did not lend itself to accurate time comparison, except for very long-period oscillations at the two stations, when the maximum excursions were so far apart in time that it could reasonably be assumed that the indicated phase differences on the records at the two stations were correct. On this assumption, the long-period oscillations are nearly coincident at the two stations. This may usually be true for the shorter-period oscillations also, but, in many cases, considerable phase differences do exist. These, however, may be due partly to differences in the electronic equipment. The general course of the geomagnetic diurnal variation at Byrd is shown, but these data may apply only to the two auroral conjugate stations and to periods of low solar activity. Up to the present time, only two cases of coincident satellite and ground station abrupt commencements were observed. These were detected readily only by the midlatitude stations, possibly because the two events occurred when these stations were on the side of the earth facing the solar wind. It is possible that nighttime coincidences will appear chiefly at the two auroral stations. (auth)

6189 AURORAL PHENOMENA IN AN INTEGRAL-INVARIANT COORDINATE SYSTEM. Waite, C. W. (Univ. of Saskatchewan, Saskatoon). Can. J. Phys., 43: 2319-30(Dec. 1965).

Isochasms of auroral phenomena, when plotted in geomagnetic dipole coordinates, are approximately circular and centered on the poles. However, a significant longitude dependence remains. The B, L and R, λ integral-invariant coordinate systems, originated by McIlwain, proved successful in ordering satellite measurements of the radiation belts. The spatial occurrence of aurora is compared with isolines of L, but the R, λ system appears better suited to such plots. The evidence for a close relation between auroral absorption and electron precipitation from the radiation belts is reviewed, and in accordance with this relation it is shown that the R, λ coordinate system provides a convenient longitude-independent representation of the northern auroral absorption zone. (auth)

6190 A COMPARISON OF THE IONIZATION LEVEL IN THE F REGION IN THE ANTARCTIC AND ARCTIC. Yudovich, L. A. (Siberian Inst. of Terrestrial Magnetism, Ionosphere and Radio-Wave Propagation). Geomagnetizm i Aeronomiya, 5: 307-11(1965). (In Russian).

The diurnal f_0F_2 variations at geographically and geomagnetically conjugate stations at high latitudes are examined. An explanation is given for the difference in f_0F_2 values at a number of stations in the northern and southern hemispheres. (tr-auth)

6191 QUIET SOLAR-DIURNAL VARIATIONS OF THE GEOMAGNETIC FIELD DURING THE IGY. I. RELATIONSHIP BETWEEN S_q VARIATIONS AND IONOSPHERIC PARAMETERS. Fatkullin, M. N.; Fel'dshtein, Ya. I. (Siberian Inst. of Terrestrial Magnetism, Ionosphere and Radio-Wave Propagation). Geomagnetizm i Aeronomiya, 5: 312-21(1965). (In Russian).

The relation between quiet solar-diurnal variations and ionospheric parameters is discussed. A physical justification is given for the method of determining S_q variations by reckoning from magnetic field values at midnight hours. (tr-auth)

6192 A CURRENT SYSTEM OF AN ELEMENTARY GEOMAGNETIC DISTURBANCE IN THE AURORAL ZONE. Asaulenko, L. G.; Pudovkin, M. I. (Siberian Inst. of Terrestrial Magnetism, Ionosphere and Radio-wave Propagation). Geomagnetizm i Aeronomiya, 5: 322-7(1965). (In Russian).

The system of electric currents appearing as a result of a sharp increase in ionospheric conductivity in a limited part of the auroral zone is computed. (tr-auth)

6193 COMPUTATION OF THE CURRENT SYSTEM OF S_d VARIATIONS IN HIGH LATITUDES. Loginov, G. A. Geomagnetizm i Aeronomiya, 5: 328-35(1965). (In Russian).

The system of currents in the ionosphere is studied, taking into consideration the direct and Hall conductivities and assuming the wind system based on bay-shaped disturbances in polar regions as a uniform flow. The ionosphere is assumed to be homogeneous with direct σ_1 and Hall σ_2 conductivities in which an annular zone is formed under the action of ionizing radiation. In the annular zone the corresponding conductivities are σ_1' and σ_2'. Ionospheric currents are determined by solving a system of partial differential equations in which the velocity of ionospheric winds, the intensity of the magnetic field, and the conductivities are known quantities. The results show that an eastward current flows on the diurnal and evening side, and a westward current prevails on the night and morning side. Variations of the horizontal component of the geomagnetic field coincide with the current variations. The general current of the ionosphere consists of two currents: one flows through the polar cap, and the other appears in the middle latitudes. The sum of both currents comprises the general current in the ionosphere. The general current is computed for the quiet and disturbed states of the ionosphere and is found to be 133×10^3 amp for the former and 150×10^3 amp for the latter. (ATD)

6194 A FREQUENCY-DEPENDENCE OF THE COSMIC NOISE LEVEL DURING THE PERIOD OF TYPE-II ANOMALOUS ABSORPTION. Khadzha-Akhmedov, Ch. L. (Arctic and Antarctic Scientific Research Inst., USSR). Geomagnetizm i Aeronomiya, 5: 348-51(1965). (In Russian).

The frequency dependence of the cosmic noise level under type II anomalous radio wave absorption was investigated on the basis of data compiled over a nine-month period (June 1963 to February 1964) at the Dixon Island Observatory. A two-frequency ($f_1 = 35.1$ Mc and $f_2 = 48.3$ Mc) riometer and four-element Yagi antennas comprised the basic equipment. Only those absorptions which were in the 1 to 5-db range at 35.1 Mc were considered. It was shown that the ratio of radio wave absorption at the two frequencies A_1/A_2 is equal to $(f_2/f_1)^n$, where $1 < n < 2$. The ratio and the altitude of the absorbing region were independent of the magnitude of absorption at either frequency. (ATD)

6195 COMPARISON OF DETERMINATIONS OF THE MAGNITUDE OF THE TOTAL VECTOR T FROM ABSOLUTE OBSERVATIONS OF THE ELEMENTS OF THE FIELD AT THE VYSOKAYA DUBRAVA OBSERVATORY WITH THE DATA OF A PM-1 PROTON MAGNETOMETER. Panov, T. N.; Shapiro, V. A. (Inst. of Geophysics at the Ukrainian Branch of the USSR Academy of Sciences). Geomagnetizm i Aeronomiya, 5: 369-71(1965). (In Russian).

Values of the proton precession frequency T measured with a PM-1 proton magnetometer were compared with T observations made with a counter frequency meter at the maximum and minimum in the diurnal variation of the T vector and computed using magnetograms. Errors in the determinations are discussed. A constant difference was found between T magnitudes measured with the magnetometer and values computed from magnetograms and other absolute instruments. The possibility of this difference being due to systematic errors of the proton magnetometer, errors in the observatory instruments, or incorrect values of the reduction corrections is discussed. The difference is probably due to errors in the reduction correction. (M.J.T.)

6196 ROCKET MEASUREMENTS OF ENERGETIC PARTICLES. 2. ELECTRON RESULTS. Mozer, F. S. (Service d'Aeronomie, Verrieres-Le-Buisson, France). J. Geophys. Res., 70: 5709-16(Dec. 1, 1965).

Fluxes, energy spectrums, and angular distributions of electrons with energies greater than 150 kev were measured by five detectors on each of two rockets fired along a magnetic field line near L = 5.6. The flux above 150 kev increased with altitude along the field line to a value near 10^5 electrons/cm^2 sec at an altitude of 400 km. The angular distributions were peaked at a pitch angle near 90° with a width less than the detector entrance aperture of 20°. The flux coming down the field line was about 1% of that mirroring and 3 times that coming up the field line. The energy spectrums were functions of altitude and pitch angle, the e-folding energy varying between about 55 and 280 kev. There were no significant intensity fluctuations on a time scale of several milliseconds to 1 second. Sinusoidal-like intensity fluctuations of a factor of 2 and a period near 19 seconds were observed. The qualitative features of the angular distributions and energy spectrums are explicable in terms of atmospheric diffusion of the electrons. Detailed properties of the 19-second periodicity require that an electron source be essentially on the field line of observation and that at least some of the electrons come directly from the source with insignificant atmospheric diffusion. The data are interpreted in terms of the nonconservation of the adiabatic invariants in the equatorial plane, resulting in the scattering from an equatorial reservoir of electrons observed at low altitudes. The data can also be explained in terms of low-altitude acceleration mechanisms or of the nonconservation of the adiabatic invariants along the entire length of the field line. (auth)

6197 ROCKET MEASUREMENTS OF ENERGETIC PARTICLES. 3. PROTON RESULTS. Mozer, F. S. (Service d'Aeronomie, Verrieres-Le-Buisson, France). J. Geophys. Res., 70: 5717-36(Dec. 1, 1965).

Proton data obtained from the flight of a rocket along the magnetic field line L = 5.6 to an altitude near 400 km are presented. Above the atmosphere, the 25-second-averaged energy spectrum and pitch angular distribution of protons above 160 kev was essentially constant during the 200 seconds of data acquisition while the rocket remained on a single field line, and the total flux decreased by about 30%. The angular distribution depended on proton energy, being sharply peaked at a pitch angle of 90° for protons near 160 kev and isotropic for protons near 750 kev. On a 2.5-second time scale, statistically significant fluctuations in the proton flux coincided with similar-order-of-magnitude variations of the opposite sign in the electron intensity. Fluctuations on a time scale of hundreds of milliseconds were observed in the proton flux at a fixed pitch angle, in the angular distribution, and, perhaps, in the energy spectrum. Analyses of the experimental data from many points of view indicate that the adiabatic invariants of the proton motion are not conserved at low altitudes, owing to processes other than interactions with the atmosphere. The data are explained most simply by a model of the proton acceleration to the observed energies at altitudes below a few thousand kilometers. Acceleration of electrons by the same mechanism is neither prohibited nor required by the present data. (auth)

6198 POSITIVE ION COMPOSITION IN THE MAGNETOIONOSPHERE OBTAINED FROM THE OGO-A SATELLITE. Taylor, H. A. Jr.; Brinton, H. C.; Smith, C. R. (Goddard Space Flight Center, Greenbelt, Md.). J. Geophys. Res., 70: 5769-81(Dec. 1, 1965).

First results from the Ogo-A positive ion spectrometer experiment are presented for the period September 23 through December 10, 1964. Thermal hydrogen and helium ion distributions extend from the lowest observations at 1500 km to an altitude of 30,000 km. The density obtained for H^+ at 2000 km is of the order of 10^3 ions cm^{-3}, and the He^+ concentration is 1% of H^+ over most of the altitude range. Whereas the concentration and distribution of H^+ observed at the lower altitudes is in general agreement with theoretical models, the upper altitude profiles show significant departure from predictions based on diffusive equilibrium theory. Evidence is presented indicating that diffusion of ions is controlled by the geomagnetic field and that the ions are distributed in a beltlike region which exhibits a sharp gradient resulting in a "plateau" at its outer boundary, which is characterized by a reduction in both the H^+ and He^+ concentrations by a factor of 10 or more. The ion belt is observed to expand and contract over an altitude range of 8000 to 30,000 km in an inverse relation with the magnetic activity index A_p. There is significant correlation between these results and the knee whistler observations as well as with high-altitude ionization gradients observed from other satellites. Although the data provide some indication of a direct coupling between the lower and upper ionosphere, more data will be required to describe this relation adequately. (auth)

6199 EARLY ELECTROSTATIC PROBE RESULTS FROM EXPLORER 22. Brace, L. H.; Reddy, B. M. (Goddard Space Flight Center, Greenbelt, Md.). J. Geophys. Res., 70: 5783-92(Dec. 1, 1965).

The electrostatic probe experiment on Explorer 22, launched in October 1964, has permitted the concentration and temperature of the electrons at 1000 km to be observed on a global scale. The major features of the ionosphere at this altitude are a maximum concentration at the magnetic equator in the daytime and at night a pair of maximums at 35° north and south. The electron temperature exhibits large variation from day to night at latitudes below 45° but remains high all night at higher latitudes. This behavior is consistent with the heating of the protonosphere by escaping photoelectrons in the daytime, and cooling by electron thermal conduction to the lower atmosphere both day and night. (auth)

6200 TIME AND ALTITUDE DEPENDENCE OF 55-Mev TRAPPED PROTONS, AUGUST 1961 TO JUNE 1964. Filz, Robert C. (Air Force Cambridge Research Labs., Bedford, Mass.); Holeman, Ernest. J. Geophys. Res., 70: 5807-22(Dec. 1, 1965).

Measurements of 55-Mev omnidirectional trapped protons detected in a small region of the South Atlantic by nuclear emulsions flown on recoverable oriented Air Force satellites are reported for the period August 1961 to June 1964 between altitudes of 221 and 736 km. During the period August 1961 to June 1962, the data best fit a flux versus altitude curve $J = 4.99 \times 10^{-11} H^{4.792}$ protons/m^2 sec Mev and is in good agreement with the variation of atmospheric density at these altitudes. H is the altitude over the South Atlantic measured in kilometers, and the time is the total time in orbit. No consistent slow increase of flux with time was observed as would be expected as the result of changes in atmospheric density. A sudden increase in flux was observed after the July 9, 1962, high-altitude nuclear explosion Starfish, which is explained as consistent with a nonadiabatic redistribution of inner-zone protons with an approximate 3.5° pitch angle change for L = 1.4 at the equator. The proton flux decays as expected on the basis of atmospheric ionization losses only, over a 2-year period. The values of the trapped proton average atmospheric density $\bar{\rho}$ that fit the decay are 3×10^7, 7×10^6, 2×10^6, and 1×10^6 atomic electrons per cm^3 for altitudes of 275, 350, 440, and 500 km. (auth)

6201 RELATIVISTIC ELECTRON PRECIPITATION INTO THE MESOSPHERE AT SUBAURORAL LATITUDES. Bailey, D. K. (National Bureau of Standards, Boulder, Colo.); Pomerantz, M. A. J. Geophys. Res., 70: 5823-30 (Dec. 1, 1965).

Ground-based observations of mesospheric effects resulting from the influx of energetic particles in high latitudes following the solar flare of February 5, 1965, besides detecting a small solar proton event have displayed some previously unobserved effects. In particular the analysis of ionospheric forward scatter observations in conjunction with riometer data has revealed the occurrence on Febru-

ary 8, 1965, of an absorption event at subauroral latitudes having extreme characteristics. The collected evidence indicates that this event was produced by precipitation of relativistic electrons. It is concluded that a mesospheric destination accounts for the Mev electrons that are known to disappear from the outer radiation zone during periods of geomagnetic disturbance. (auth)

6202 DETERMINATION OF THE ELECTRON DISTRIBUTION IN THE MAGNETOSPHERE USING HYDROMAGNETIC WHISTLERS. Watanabe, Tomiya (Univ. of British Columbia, Vancouver). J. Geophys. Res., 70: 5839-48(Dec. 1, 1965).

As in the case of atmospheric whistlers the electron-density distribution in the magnetosphere can be inferred from the dispersion characteristics of a hydromagnetic wave propagating between hemispheres along a line of force of the earth's magnetic field. Two methods are investigated in this paper, one of which is similar to that developed by Smith and Carpenter and also by Brice for atmospheric whistlers and is found to be more convenient and accurate than the other. The errors involved in this method are investigated by working out a typical example. The two main sources of error are the lack of precision in scaling group bounce periods and the uncertainty in the model taken for the electron distribution in the magnetosphere. If the errors in scaling group bounce periods are ±5%, the equatorial crossing point of the guiding magnetic line of force is determined within an error of ±3% and the electron number density at that point can be determined within a factor of about 2. The errors due to the second source are comparable to those due to the first. The errors arising from the dipole field assumption made in this paper are estimated also; they seem to be comparable with the errors due to the other two sources of error. (auth)

6203 TIME DELAYS BETWEEN THE INTENSITY VARIATIONS OF THE 3914 A AND 5577 A SPECTRAL LINES IN ARTIFICIAL AURORAS. Daniels, G. M.; Newman, P. (Air Force Cambridge Research Labs., Bedford, Mass.). J. Geophys. Res., 70: 5861-5(Dec. 1, 1965).

Time delays between the intensity variations of 3914 and 5577 Å spectral lines were observed in artificial auroras generated by high-altitude nuclear explosions. An Omholt analysis of the intensity records indicated that the excitation ratio of these lines was constant for the first 1.5 seconds of the auroras. The 5577 Å line lagged the spectral emission in the 6500 Å to 6570 Å region in a similar manner. (auth)

6204 AURORAL-ZONE PEARL PULSATIONS. McPherron, R. L.; Ward, S. H. (Univ. of California, Berkeley). J. Geophys. Res., 70: 5867-82(Dec. 1, 1965).

An analysis was made of Pc 1 band micropulsations observed in the auroral zone during one solar rotation at Flin Flon, Manitoba, August-September 1964. The Pc 1 band micropulsations were subdivided into pearl pulsations (PP), impulsive activity (IMP), and short irregular pulsations (SIP); this discussion is concerned primarily with PP. It was observed: there is no correlation of PP with electron precipitation indicated by bremsstrahlung recorded at balloon altitude; PP type activity occurs at the time of a sudden commencement and can have an hourly repetition of occurrence for 5 or 6 hours thereafter; the K_p and A_p indices are too coarse for adequate representation of geomagnetically disturbed times when studying the dependence of PP occurrence on geomagnetic activity; there may be a slight increase of PP period with increase in K; PP have higher amplitudes when K values are higher; Pc 3, 4 band activity may be used as a good predictor for PP occurrence, since, for days rated as disturbed by Pc 3, 4 activity, there is an inverse correlation between PP and Pc 3, 4. For days rates as quiet by Pc 3, 4 activity, PP occur at any time during the daylight hours; PP are distributed throughout the daylight hours on quiet days, whereas they tend to appear only within an hour or two of 1800 LMT on disturbed days. These observations can be interpreted in terms of a hydromagnetic wave packet origin for PP with the occurrence of PP dependent on triggering mechanism; amplification mechanism; guiding along field lines; transmission through the ionosphere. (auth)

6205 SECULAR VARIATIONS OF THE COSMIC-RAY-PRODUCED ^{14}C IN THE ATMOSPHERE AND THEIR INTERPRETATIONS. Suess, Hans E. (Univ. of California, San Diego, La Jolla). J. Geophys. Res., 70: 5937-52(Dec. 1, 1965).

The carbon-14 content of about 150 wood samples, dated by dendrochronology, was measured. The wood samples of known age used in this investigation cover the past 2000 years. Some were supplied by Dr. Huber of the dendrochronological laboratory at Munich, and some by the Arizona Tree-Ring Laboratory. Wood from European oak, American fir, Hitchcock, and sequoia was used for the measurements. The measurements show that the ^{14}C has not been entirely constant in the past but has varied by several per cent. Two types of variations can be recognized: those that occurred on a time scale of the order of 100 years; those with a time constant of more than 1000 years. Type 1 changes occur only in the atmospheric ^{14}C reservoir; they show correlations with average sunspot numbers; they are caused by changes in the cosmic-ray intensity, which determines the production rate of ^{14}C. Type 2 changes involve the total ^{14}C inventory, including the oceans; their causes cannot yet be established conclusively. The empirical relationship between conventional radiocarbon dates and the true ages of wood samples is graphically shown for the past 2000 years. (auth)

6206 GEOMAGNETIC AND SOLAR DATA. Lincoln, J. Virginia (ed.) (Environmental Science Services Administration, Boulder, Colo.). J. Geophys. Res., 70: 5953-5 (Dec. 1, 1965).

Data for the principal magnetic storm including activities and ranges are presented for April to June, 1965. Also selected geomagnetic and solar data including 3-hr range indices and provisional sunspot numbers are given for July, 1965. (J.F.P.)

6207 AN INTERPRETATION OF TRANSVERSE WHISTLERS. Kimura, I. (Stanford Univ., Calif.); Smith, R. L.; Brice, Niel M. J. Geophys. Res., 70: 5961-6 (Dec. 1, 1965).

The whistlers with anomalous dispersion reported by Carpenter and Dunckel (J. Geophys. Res. 70(15): 3781-6 (1965)) are interpreted as follows: The constant dispersion, independent of latitude, arises from QL propagation in a field-aligned duct. The time delay, which is approximately independent of frequency, arises from subsequent QT propagation. It varies linearly with latitude because the length of the QT-ray path varies linearly with latitude. Since, as was previously pointed out, transverse propagation is possible only when ion effects are included, these whistlers, by providing evidence of transverse propagation, implicitly provide evidence of the importance of ion effects on propagation. (J.F.P.)

6208 THE DYNAMICS OF THE GEOMAGNETIC TRAP. I. Pletnev, V. D.; Skuridin, G. A.; Chesalin, L. S. Kosm. Issled., 3: 408-25(May-June 1965). (In Russian).

Basic experimental data and theoretical concepts pertaining to geophysical phenomena occurring in the near-earth region of outer space are examined. It is demonstrated that such phenomena as magnetic storms, polar auroras, the radiation belts, and the confined magnetosphere of the earth should be studied from a single standpoint, since they are closely interrelated. The complex of these geophysical phenomena is referred to as the dynamics of the geomagnetic trap. An examination is presented of experimental data and certain problems of a general theoretical nature, associated with the dynamics of the geomagnetic trap. (tr-auth)

6209 THE EFFECTS OF THE AMERICAN HIGH-ALTITUDE EXPLOSION OF 9 JULY 1962 IN THE UPPER

ATMOSPHERE. Gal'perin, Yu. I. Kosm. Issled., 3: 426-32(May-June 1965). (In Russian).

An analysis of measurements obtained from the Kosmos-5 satellite during the early stages of the existence of an artificial radiation belt and later measurements of intensities and rates of decrease from the Kosmos-5, Elektron-1, and Elektron-3 satellites enabled the distribution of intensities for the hard electrons injected into the magnetosphere during the explosion to be constructed all the way to L ~ 2.3. The integration of this distribution with respect to volume shows that the total quantity of injected electrons captured in the belt during the first hour after the explosion, exhibiting an invariant coordinate $h_{min} \gtrsim 300$ km, amounted to about $1.5 \cdot 10^{25}$; the number of electrons with energies of $E \gtrsim 1.5$ Mev was $4 \cdot 10^{24}$. For a mean capture efficiency for isotropic injection of ~0.5, in order to inject the indicated quantity of hard electrons by means of β decays, the products of approximately 10^{25} fissions had to rise to great altitudes, where the artificial radiation belt was formed. The calculation of the intensity and the time dependence of the γ emissions of these fission fragments, rising to great altitudes, shows that they correspond exactly to the intensity and time dependence of the appearance of the γ pulses recorded by the Kosmos-5 satellite during the explosion. This indicates that no later than 3 seconds after the explosion the fragments of approximately 10^{25} fissions appeared above the horizon for the Kosmos-5 satellite, i.e., at altitudes of $\gtrsim$1200 km, and there γ and β emissions, respectively, produced a γ pulse and an artificial belt of hard electrons. The upper limit of the total number W of fissions was estimated for the Starfish explosion on the basis of counting-rate measurements with a Geiger counter aboard the Kosmos-5 satellite during its closest approach to Johnston Island within ~20 minutes after the explosion, yielding $W \lesssim 2 \cdot 10^{26}$. (tr-auth)

6210 PRELIMINARY RESULTS OF DETERMINING PARTICLE CONCENTRATION AND ATMOSPHERIC DENSITY ON 18 JUNE 1963. Mikhnevich, V. V.; Golubev, E. N.; Parfianovich, Yu. N. Kosm. Issled., 3: 457-68(May-June 1965). (In Russian).

Analyses of the results are presented for manometer determinations of atmospheric densities and particle concentrations at altitudes between 120 and 360 km made on 18 June 1963. The vehicle used as a high-altitude automatic geophysical station. An analysis of the dependence of the formulas used to determine particle concentrations and densities on temperature showed that the faster the instruments moved, the more accurate the readings became. The effect of manometer sensitivity on the readings is analyzed. The error in the determination of the orientation angle between the apparatus and the vector of the flux velocity was about 3°. It was found that at an altitude of over 200 km, atmospheric density diminishes with diminution in solar activity, but below this altitude the effect of the solar activity is inconsequential. (ATD)

6211 MEASUREMENTS OF SOLAR L_α RADIATION ABSORPTION IN THE EARTH'S UPPER ATMOSPHERE. Katyushina, V. V. Kosm. Issled., 3: 496-9(May-June 1965). (In Russian).

The solar L_α intensity and its variations with altitude were measured to 500 km on June 6 and 18, 1963, using ionization chambers filled with nitric oxide. The L_α absorption coefficient in the upper atmosphere was determined from the data. Discrepancies in the results are discussed in terms of possible variations in the molecular-oxygen concentration or in the overall density. (M.J.T.)

6212 APPLICATION OF THEORETICAL MAGNETOHYDRODYNAMICS TO GEOPHYSICS [Thesis]. Mauersberger, P. Berlin, Humboldt Univ., 1964. 204p. $2.00 Gmelin, AED-DISS. 64-477.

A continuum theory of a plasma is applied to geological problems. Approximate methods for the solution of the hydrodynamic equations are discussed. A specific equation for the plasma in the earth's core is given. (Gmelin Inst.)

Gravitation, Quantum Mechanics, and Relativity Theory

Refer also to abstract 5974.

6213 (ANL-7065) NOTES ON AXIOMS FOR QUANTUM MECHANICS. MacLaren, M. D. (Argonne National Lab., Ill.). July 1965. Contract W-31-109-eng-38. 21p. Dep. mn; CFSTI $1.00 cy, $0.50 mn.

A mathematical survey is presented of the basic foundations of nonrelativistic quantum mechanics. The aim of the investigation is the generation of a precise and elegant set of axioms for nonrelativistic quantum mechanics. 24 references. (T.F.H.)

6214 (INR-610/VI/PH) THE MOMENTUM-INVARIANTS AND THE LORENTZ-COVARIANT FORM OF PHYSICAL LAWS. Chylinski, Z. (Institute of Nuclear Research, Warsaw (Poland)). Feb. 1965. 54p. Dep.

It is shown that motion laws formulated in terms of the momentum-invariants, as e.g. in the theory of dispersion relations, do not imply their Lorentz-covariant structure. The momentum-invariants turn out to be also the objects of another geometry—called the Phase-geometry—which is not isomorphic mathematically with the Lorentz geometry. The Lorentz geometry is a special case of the Phase geometry and remains valid in the "actual" reality of any measuring procedure. (auth)

6215 (NP-15614) SOLUTION OF SCATTERING AND BOUND STATE PROBLEMS BY CONSTRUCTION OF APPROXIMATE DYNAMICAL SYMMETRIES. Technical Report No. 460. Fivel, Daniel I. (Maryland Univ., College Park. Dept. of Physics and Astronomy). May 1965. 60p.

It is shown that it is possible, for essentially all interesting potentials, to find a sequence of approximate dynamical symmetries with the property that the sequence of approximate solutions to the bound state and scattering problems obtained therefrom converge rapidly to the exact solution. The method used is a quantum mechanical analogue of a method first described for classical systems by H. Poincaré. (M.O.W.)

6216 (ORNL-3877) FORTRAN PROGRAMS FOR THE CLEBSCH-GORDAN AND RACAH COEFFICIENTS AND THE NINE-j SYMBOL. Tamura, Taro (Oak Ridge National Lab., Tenn.). Nov. 1965. Contract W-7405-eng-26. 13p. Dep. mn; CFSTI $1.00 cy, $0.50 mn.

FORTRAN programs for the Clebsch-Gordan and Racah coefficients and 9-j symbol are presented. They are written in a way rather compact and easy to understand. Optimization of the speed of computation was made in these routines. These routines allow for treating the case in which the arguments of these coefficients are very large, and thus can be used, for example, in the analysis of the nuclear reactions of heavy and high energy projectiles. (auth)

6217 CONSTRUCTION OF A COMPLETE ORTHOGONAL SYSTEM FOR THE QUANTUM-MECHANICAL THREE-BODY PROBLEM. Zickendraht, Werner (Univ., Marburg, Ger.). Ann. Phys. (N. Y.), 35: 18-41(Oct. 1965).

A coordinate system with simple symmetry properties is described which is suitable for the treatment of the quantum-mechanical three-body problem. The Schrödinger equation for spinless particles is transformed to these coordinates and the orbital angular momentum is separated out, reducing the Schrödinger equation to a system of coupled differential equations involving only three internal coordinates. A special interaction for the three-body system is introduced, for which the system of coupled differential equations can be solved. The solutions form a complete orthogonal system of functions for the internal degrees of freedom. Explicit solutions are given for orbital angular momenta 0, 1, 2. The usefulness of the method is demonstrated for the groundstate of the Helium atom. (auth)

6218 ON THE DIMENSIONALITY OF THE REAL WORLD. Penney, R. (Ford Motor Co., Dearborn, Mich.). J. Math. Phys. (N. Y.), 6: 1607-11(Nov. 1965).

The strength of systems of field equations is defined following a procedure due to Einstein. For an arbitrary dimension number, the strength of Einstein's field equations and of Maxwell's equations are calculated, and it is shown that only in four dimensions do the two systems of field equations determine their respective fields equally strongly. In addition, in four dimensions, Weyl's equation exhibits the same strength as the Einstein or Maxwell fields. The results are used to show that a necessary condition for a unified field-theoretic description of gravity and electromagnetism is that the world be four dimensional. If one also demands that the neutrino field be determined as strongly as the Einstein and Maxwell fields, one must have a two-component neutrino, rather than a four-component neutrino. (auth)

6219 CONTRIBUTIONS TO THE QUANTIZATION PROBLEM IN GENERAL RELATIVITY. Boardman, John (Brooklyn Coll.). J. Math. Phys. (N. Y.), 6: 1696-1701 (Nov. 1965).

It is possible to quantize most classical field theories by identifying the group of canonical transformations which maintain the covariance properties with a group of unitary transformation in Hilbert space which has the same commutator algebra. The commutators among the canonical field variables are equal to the Dirac delta function times a factor which may be zero. But in the general theory of relativity the classical group of the canonical transformations which maintain the covariance properties of the theory has an invariance subgroup. The ambiguities thus introduced by the usual process of quantization can be avoided by the use of the Dirac quantization procedure for theories with constraints. An analogy is established between classical Dirac brackets and commutators, and an intrinsic coordinate system is fixed. This choice of local intrinsic coordinate conditions leads to commutators among the canonical field variables of the general theory of relativity which depend upon the Dirac delta function and its first seven derivatives. (auth)

6220 ON THE STRUCTURE OF THE FINITE PARTS OF THE GENERATING FUNCTIONAL OF PROPAGATORS IN QUANTUMELECTRODYNAMICS. Le Gaillard, Y.; Visconti, A. (Univ. D'Aix, Marseille). J. Math. Phys. (N. Y.), 6: 1774-85(Nov. 1965).

The structure of the finite and divergent parts of propagators in quantum electrodynamics is investigated, starting from their generating functional. A renormalizability condition is expressed by means of a set of recursion formulas between the finite parts of radiative corrections of the generating functional; this condition is the algebraic formulation of Salam's rule for the extraction of finite parts from divergent integrals. The former sets of equations should finally allow the actual computation of the radiative correction of higher orders. (auth)

6221 NEW VARIATIONAL SCHEME FOR FINDING THE EXCITED STATES OF ONE-DIMENSIONAL SYSTEMS. More, Richard M. (Univ. of California, San Diego, La Jolla). J. Math. Phys. (N. Y.), 6: 1804-5(Nov. 1965).

A new relaxation-variation scheme for solving one-dimensional Schrödinger equations is described. The method approximates the nth eigenvalue and eigenfunction directly, without requiring approximations to the lower eigenfunctions. It is applicable to any one-dimensional Sturm-Liouville system. (auth)

6222 NOTE ON THE DYNAMICS OF GRAVITATIONAL SOURCES. Newman, Ezra T.; Unti, T. W. J. (Univ. of Pittsburgh). J. Math. Phys. (N. Y.), 6: 1806-11(Nov. 1965).

Multipole structure for the sources of the gravitational field is considered in the full (axially symmetric) nonlinear gravitational theory. Definitions proposed recently by Janis and Newman for the mass of the source, its linear momentum, dipole moment, and its spin or angular momentum are examined. These definitions are contrasted with those given by other authors. The advantages of the new definitions are discussed, and the manner in which they enter into the dynamics of the system is studied. Some transformation properties of these multiple moments are considered. (auth)

6223 DIRAC EQUATION WITHOUT DIRAC MATRICES. Loinger, A.; Sparzani, A. (Univ., Pavia, Italy. Istituto Nazionale di Fisica Nucleare, Pavia, Italy). Nuovo Cimento (10), 39: 1140-5(Oct. 16, 1965).

The Dirac theory of the relativistic electron is reformulated—without any reference to spinor formalisms—exploiting the properties of one of the concrete representations of the homogeneous Lorentz group, which are generated by differential operators acting in the space of the functions of six Eulerian angles. (auth)

6224 SOME PROPERTIES OF THE QUANTUM LINEARIZED EINSTEIN FIELD. Deser, S.; Trubatch, J.; Trubatch, S. (Brandeis Univ., Waltham, Mass.). Nuovo Cimento (10), 39: 1159-65(Oct. 16, 1965).

Some aspects of the quantized linear approximation to Einstein theory are examined, in view of their relevance to the full theory's quantization. In contrast to the otherwise similar Maxwell field case, it is seen that the Lorentz-invariance requirements on the time-translation and Lorentz-rotation generators P^0, J^{0i} are not expressible in terms of simple local commutation relations for the energy density with itself. This is in agreement with the expectation that such local relations apply only to fields of spin one or lower. It is also shown that the physical requirement— $P_\mu P^\mu \geq 0$ is fulfilled in the linearized theory. (auth)

6225 CLASSICAL DYNAMICS AND THE SCHROEDINGER THEORY. Liebowitz, B. Nuovo Cimento (10), 39: 1201-7(Oct. 16, 1965).

On the basis of a classical construct called orbital density, the Schrödinger equations are derived from the Hamilton-Jacobi equation. The results are compared to previous work by Dirac and by Gryzinski. (M.O.W.)

6226 DISPROOF OF SENITZKY'S "FUNDAMENTAL THEOREM IN QUANTUM OPTICS." Glassgold, A. E. (New York Univ., New York); Holliday, Dennis. Phys. Rev. Lett., 15: 741-2(Nov. 8, 1965).

It is pointed out that the fundamental theorem enunciated by Senitzky (Phys. Rev. Letters 15: 233(1965), that all field sources on which the effect of the detector of some field property is negligible may be treated as classical sources in the interaction under consideration, is incorrect. The proof of this theorem and its application to quantum optics is based on the incorrect assumption that, once two systems no longer interact, a measurement involving one system cannot influence the statistical properties of the other system, thus ignoring the correlations which can be established between two systems through their past interaction. The result of this theorem contradicts the fact that a field can be excited to an arbitrary quantum statistical state by a source which can then be decoupled from the field before any measurements are performed. (J.F.P.)

6227 SYMMETRY VIOLATING TRIAL WAVE FUNCTIONS. Zeh, H. D. (California Inst. of Tech., Pasadena). Z. Phys., 188: 361-73(1965). (TID-22167).

A variational procedure using trial wave functions projected on to symmetry eigenstates is investigated. In the individual particle model it leads to generalized self-consistent single-particle equations being dependent on the symmetry eigenvalue. A perturbation expansion appropriate for the case of strong symmetry violations is described. Model independent expressions for the moment of inertia and the decoupling parameter are derived by applying the method to rotational symmetry. (auth)

Low Temperature Physics

Refer also to abstracts 5569 and 5614.

6228 THE SUPERCONDUCTING BEHAVIOR OF SEVERAL COMPLEX CARBIDES AND NITRIDES. Toth,

L. E.; Jeitschko, W.; Yen, C. M. (Univ. of Minnesota, Minneapolis). J. Less-Common Metals, 10: 29-32(Jan. 1966).

The superconducting behavior of several complex transition metal carbide and nitride phases was determined. For a representative sampling of a large group of isotypic H-phases no superconducting transitions were observed to 1.1°K. The β-Mn nitride Nb_3Al_2N was found to be superconducting at 1.3°K confirming a previous result that the filled and ordered β-Mn crystal structure is favorable for superconductivity. (auth)

6229 HYDRODYNAMICAL EQUATIONS FOR THE SUPERFLUID FERMI LIQUID AND THE TWO-PARTICLE GREEN FUNCTIONS. [PART] I. Galasiewicz, Zygmunt M. (Joint Inst. for Nuclear Research, Dubna, USSR). Nucl. Phys., 76: 145-66(1966).

The hydrodynamical equations for a system of identical Fermi particles with pairing forces (in the system there is a condensate of the coupled pairs) are obtained. In the case of small deviations from thermodynamical equilibrium, using the connection between the variations of the mean values (which are found from the linearized hydrodynamical equations) and the Green functions, the expressions for the poles of the two-particle Green functions are obtained. They describe elementary excitations of two kinds i.e., the quanta of first and second sound. In the computations, the method proposed by Bogolyubov for obtaining the one-particle Green functions for the superfluid Bose systems is applied. (auth)

6230 EFFECTS OF TURBULENCE IN He II THERMAL COUNTERFLOW. Tough, J. T.; McCormick, W. D.; Dash, J. G. (Univ. of Washington, Seattle). Phys. Rev., 140: A1524-8(Nov. 29, 1965).

Measurement of the damping of small-amplitude transverse vibrations of a fine wire was used to investigate thermal counterflow of He II in wide channels of rectangular cross section. Below a critical heat current, the damping is independent of the current, and is dictated by laminar viscous flow of normal fluid. At higher heat currents, the damping increases above the subcritical value, and the excess damping was studied as a function of parameters of the apparatus and liquid. The dependence of the magnitude of the critical heat current on temperature and channel width is described by a critical Reynolds number $R_c = \rho V_{nc} d/\eta \cong 1200$, where V_{nc} is the normal fluid velocity corresponding to the critical heat current, d is the channel width, η is the normal fluid viscosity, and ρ is the total density. R_c is independent of wire diameter and vibration frequency. The excess damping was found to fit a single empirical expression over a wide range of experimental parameters. An outstanding characteristic of the supercritical damping force is its dependence on the Reynolds number as $(R-R_c)^{1/2}$. (auth)

6231 ANOMALOUS THERMAL PROPERTIES OF LIQUID HELIUM I AND II AND THEIR CONNECTION. Goldstein, Louis (Los Alamos Scientific Lab., N. Mex.). Phys. Rev., 140: A1547-63(Nov. 29, 1965). (LA-DC-7225).

A method of determination of the lambda line through simultaneous measurements of the state coordinates and the finite temperature coefficient of the pressure along the transformation line is elaborated. The first derivative thermal property variations were studied throughout the thermally normal and anomalous regions of ^{4}He II and ^{4}He I. For the first-temperature-derivative equilibrium properties, the lambda phenomenon appears as a transformation from a region of anomalous derivative properties of ^{4}He II into a similar region of the same anomalous properties as ^{4}He I. The lambda line is thus a common boundary of the anomalous region of ^{4}He II, limited at the lower temperatures by the locus of pressure minima of the entropy, and of the anomalous region of ^{4}He I, limited on the high-temperature side by the locus of pressure maxima. In between the two pressure loci of the entropy, these regions of ^{4}He II and ^{4}He I exhibit the fundamental anomaly associated with entropy generation on isothermal compression. A tentative interpretation of the persistence of the latter fundamental equilibrium anomaly in ^{4}He I, in terms of the two-fluid model, requires the presence of superfluid atoms in ^{4}He I. This in turn raises the possibility that reversible transport phenomena, including the propagation of thermal waves, persist in some form beyond the lambda line. Of the higher order derivative thermal properties studied here, the most remarkable one is the hitherto ignored pressure anomaly of the isothermal compressibility in ^{4}He II, at the approaches of the lambda line. This refers to the increase of the compressibility on isothermal pressure increase, for which a tentative interpretation will be advanced on the basis of the decrease of the exchange-energy density accompanying the generation of normal atoms on isothermal pressure increase. Finally, a possible approach toward the theory of the lambda line and of the high-temperature boundary of the anomalous region of ^{4}He I is outlined in the free-energy-temperature diagram. A plausible experimental justification for this approach is indicated through the observation of the pressure anomaly of the compressibility at temperatures beyond those of the physically observable lambda line. (auth)

6232 DEPENDENCE OF THE CRITICAL CURRENTS IN SUPERCONDUCTING FILMS ON APPLIED MAGNETIC FIELD AND TEMPERATURE. Mydosh, J. A.; Meissner, Hans (Stevens Inst. of Tech., Hoboken, N. J.). Phys. Rev., 140: A1568-80(Nov. 29, 1965).

Measurements of critical currents i_c were performed on planar and cylindrical films of tin of 650 to 2000 Å thickness. Both pulsed currents (80-nsec duration) and d-c currents with stabilizing network were used. Close agreement was obtained for the d-c data in the temperature dependence and approximate agreement in the magnitude of the critical current when compared with Bardeen's calculation as long as the stabilizing network was effective. The pulse measurements deviate from theory and from the d-c data for temperatures $T/T_c < 0.9$. Oscilloscope pictures of the transitions indicate that this deviation towards lower currents is not caused by usual Joule heating. This and other similar work with pulsed currents and fields would indicate that an entirely new mechanism is responsible for the discrepancy in fast-pulsed critical currents. Critical-current measurements were also taken with the superposition of external magnetic fields H_e. The whole range from the critical current in zero field to the critical field as measured with a current of 100 μA was covered. When the data are plotted as log i_c versus H_e, they form a series of similar curves as the temperature is lowered. If adjusted for a match at $H_e = 0$, these curves closely agree with the theoretical predictions of Ginzburg. (auth)

6233 EQUIVALENCE OF DIFFERENT PAIR-BREAKING MECHANISMS IN SUPERCONDUCTORS. Maki, Kazumi; Fulde, Peter (Univ. of California, Berkeley). Phys. Rev., 140: A1586-92(Nov. 29, 1965).

Paramagnetic impurities in a superconductor and a magnetic field parallel to a thin superconducting film with short electronic mean free path are known to have similar effects on many physical quantities. By investigating the properties of vertex functions and their renormalization factors necessary and sufficient conditions were derived for such a physical quantity to be equally affected by the two pair-breaking mechanisms. It is found that different expressions are obtained in the two theories only for those quantities which involve s-wave, spin-triplet vertices with momentum transfer $q \leq (l\xi_0)^{-1/2}$, where l is the electron mean free path and ξ_0 is the coherence distance. With the help of those results different response functions are analyzed and it is shown that the spin susceptibility is the only one of the quantities usually considered which satisfies the above requirements and hence gives different results for the field and paramagnetic-impurity cases. (auth)

6234 PRESSURE DEPENDENCE OF THE SUPERCONDUCTING TRANSITION TEMPERATURE OF URANIUM. Smith, T. F. (Univ. of California, San Diego, La Jolla); Gardner, W. E. Phys. Rev., 140: A1620-3(Nov. 29, 1965).

The superconducting transition temperature T_c of uranium was observed to increase from 1.0 to 2.3°K on the application of a pressure of 10 kbar. From this result the possibility that T_c will increase with isotopic mass was suggested. (auth)

6235 MACROSCOPIC QUANTUM INTERFERENCE IN SUPERCONDUCTORS. Jaklevic, R. C.; Lambe, J.; Mercereau, J. E.; Silver, A. H. (Ford Motor Co., Dearborn, Mich.). Phys. Rev., 140: A1628-37(Nov. 29, 1965).

The Josephson effect allows supercurrents to flow through thin tunnel barriers separating two superconductors. The d-c critical current depends directly on the quantum phase difference of the superconducting wave function on the two sides of the barrier. An experimental study is made of interference phenomena in multiply connected superconductors utilizing Josephson tunneling. The results are a striking confirmation of the extensive phase coherence of the superconducting state. London's theory is used in conjunction with Josephson's prediction to explain the observations. Modulation of the maximum supercurrent flow through junction-pair devices was measured in an applied magnetic field and showed periodicities resulting from quantum wave interference. These interference "fringes" were found to occur even when the magnetic flux is confined to a region not accessible to the superconductor. Another experiment allows the measurement of an interference directly attributable to phase modulation by the superconducting electron-drift velocity. These results offer a direct verification of long-range quantum behavior in the superconducting state and further demonstrate the validity and usefulness of Josephson tunneling methods. (auth)

6236 UPPER CRITICAL FIELDS OF Nb–Ti ALLOYS: EVIDENCE FOR THE INFLUENCE OF PAULI PARAMAGNETISM. Shapira, Y.; Neuringer, L. J. (Massachusetts Inst. of Tech., Cambridge). Phys. Rev., 140: A1638-44 (Nov. 29, 1965).

Resistivity, flow-resistance, and ultrasonic-attenuation measurements were carried out on Nb–37 at. % Ti and Nb–56 at. % Ti in d-c magnetic fields up to 150 kG. The transition temperatures and the dependence of the upper critical field on temperature were measured by the resistive method. The transition temperatures are: T_c = 9.2 ± 0.2°K for Nb–37 at. % Ti and T_c = 9.0 ± 0.2°K for Nb–56 at. % Ti. Flow-resistance measurements gave the following values for the Ginzburg-Landau-Abrikosov-Gor'kov upper critical field at T = 0: 111 ± 7 kG for Nb–37 at. % Ti and 188 ± 9 kG for Nb–56 at. % Ti. Changes in the ultrasonic attenuation were observed near the upper critical field. The data support the view that the Pauli paramagnetism plays a role in determining the upper critical field. However, the effect of the Pauli paramagnetism is found to be smaller than predicted by Maki. (auth)

6237 THEORY OF A SUPERFLUID FERMI LIQUID. I. GENERAL FORMALISM AND STATIC PROPERTIES. Leggett, A. J. (Univ. of Illinois, Urbana). Phys. Rev., 140: A1869-88(Dec. 13, 1965).

The microscopic theory of a superfluid Fermi liquid at finite temperature is developed for the case of a pure system with S-wave pairing and is applied to the calculation of the static properties. As a function of $\theta \equiv T/T_c$, these properties are determined entirely by the Landau parameters F_0, F_1, Z_0, etc., characterizing quasiparticle interactions in the normal phase. In particular the spin susceptibility χ and the density of the normal component ρ_n are given by $\chi(\theta)/\chi(1) = (1 + \frac{1}{4}Z_0)\, f(\theta)/[1 + \frac{1}{4}Z_0 f(\theta)]$, $\rho_n/\rho = (1 + \frac{1}{3}F_1)\, f(\theta)/[1 + \frac{1}{3}F_1 f(\theta)]$, where the universal function $f(\theta) \equiv -[\nu(0)]^{-1}\Sigma_p (dn/dE_p)$ is the "effective density of states near the Fermi surface" relative to its value $\nu(0)$ in the normal phase. Thus the often-quoted expression $\rho_n = \frac{1}{3}\Sigma_p p^2(dn/dE_p)$ is valid for an interacting system only in the limit $T \to 0$. A simple phenomenological theory of "Fermi-liquid" effects on χ and ρ_n is developed for arbitrary conditions (including the presence of impurities and pairing with $l \neq 0$); it is found that under most circumstances explicit expressions for χ and ρ_n may be obtained which involve only the Landau parameters and a suitably generalized effective density of states. The theory should apply to the possible superfluid phase of He^3 and to most superconductors. It is suggested that the Knight shift in nontransition-metal superconductors should display some "Fermi-liquid" effects. The weak-field d-c penetration depth $\lambda(T)$ is shown to be insensitive to such effects both in the Pippard limit and near T_c; however, in a London superconductor at lower temperatures the correction to $\lambda(T)$ should be observable and yield a direct estimate of F_1. (auth)

6238 THEORY OF THE ANISOTROPIC ENERGY GAP IN SUPERCONDUCTING LEAD. Bennett, Alan J. (Univ. of Chicago). Phys. Rev., 140: A1902-20(Dec. 13, 1965).

The energy gap of a model anisotropic superconductor is considered. This model calculation forms the basis of a more realistic theoretical consideration of the energy gap of superconducting Pb, one in which the phonon density of states is the principal source of gap anisotropy. The effect of energy-band structure, important only near Brillouin-zone boundaries, is included as a perturbation. The phonon density of states is calculated from the experimental dispersion curves and singularities — present in the special density of states entering the superconductivity problem — are discussed. The phonon density of states and the isotropic gap solution obtained by previous workers are used to calculate the anisotropic part of the energy gap. The double gap, 2Δ, is found to have an absolute maximum of 2.86 mev in the [100] direction, and an absolute minimum of 2.55 mev in the [110] direction. Ten other maxima, minima, and saddle points are listed. The effect of the energy-gap anisotropy on electron-tunneling, electromagnetic-absorption, and acoustic-attenuation experiments is predicted. (auth)

6239 SPHERICAL IMPURITY IN AN INFINITE SUPERCONDUCTOR. Fetter, Alexander L. (Univ. of California, Berkeley). Phys. Rev., 140: A1921-36(Dec. 13, 1965).

The modifications in a superconducting medium due to a single, spherically symmetric, nonmagnetic impurity are examined using the BCS theory of superconductivity. The energy spectrum of quasiparticles has both a discrete portion (bound states) and a continuous portion (scattering states). In the scattering region ($E > \Delta$), a given energy corresponds to two distinct momentum states, one above and one below the Fermi level. The calculation of the S matrix for the impurity scattering is thus a problem of two coupled channels. The electron density $n(r)$ and the order parameter $\Delta(r)$ far from the impurity are evaluated asymptotically in terms of the eigenphase shifts and mixing parameter of the two channels. Two soluble models for the impurity are considered. With a hard-sphere, long-range spatial oscillations are found in $\Delta(r)$ as well as in $n(r)$. With a delta-shell potential, a resonant enhancement occurs in the scattering of quasiparticles with momentum near the Fermi momentum. Both the spatial oscillations and the resonant enhancement are expected to appear for more general impurity potentials. (auth)

6240 EXACT SOLUTIONS OF THE SUPERCONDUCTING SURFACE SHEATH. Fink, H. J.; Kessinger, R. D. (Atomics International, Canoga Park, Calif.). Phys. Rev., 140: A1937-44(Dec. 13, 1965).

The exact solutions of the superconducting surface sheath of a semi-infinite superconducting half-space for various values of the Ginzburg-Landau parameter κ were obtained as a function of the applied magnetic field between the critical fields H_c and H_{c3} (for $0.417 < \kappa < 0.707$; type I) and between H_{c2} and H_{c3} (for $0.707 < \kappa < \infty$; type II). For type-II superconductors, the solutions were also extended into the mixed state well below H_{c2}. The order parameter, the supercurrents, the internal magnetic field, the vector potential, the thickness of the surface sheath, and the magnetization per unit volume for a "thick" film were determined. These quantities vary strongly with applied magnetic field for $\kappa < 3$. In order to obtain these solutions, a boundary condition was derived which relates the absolute value of the order parameter at the surface to the

phase of the order parameter and the value of the vector potential at the surface. Two supercurrents of equal magnitude, but opposite direction, flow near the surface for magnetic fields above H_c (type I) or H_{c2} (type II). Below H_{c2}, these currents are slightly different owing to the bulk solution and give rise to a small net surface current. (auth)

6241 GAPLESS HIGH-CURRENT SUPERCONDUCTIVITY. Parmenter, R. H. (Radio Corp. of America, Princeton, N. J.). Phys. Rev., 140: A1952-6(Dec. 13, 1965).

The idea of gaplessness, already familiar in several areas of superconductivity, is considered in connection with high-current superconductivity. A calculation is made of the critical temperature T_c at which a normal metal with zero current becomes thermodynamically unstable against decay into a high-current superconducting phase. It is pointed out that at T_c all the various suggested forms of high-current electron-electron interaction, both retarded and nonretarded, are equivalent, so that a calculation of T_c does not suffer from ambiguity of choice of interaction. It is found that a transition temperature exists when the Bardeen, Cooper, and Schrieffer (BCS) parameter $N(0)V_0 \geq 0.43$ [assuming $N(0)V_{c0} = 0.1$]. In fact, for $0.43 < N(0)V_0 < 0.63$, two values of T_c exist, since at sufficiently low temperatures, the normal phase is thermodynamically stable against high-current superconductivity. When $N(0)V_0 = 0.43$, $T_c = 0.259\hbar\omega/k_B$. At T = 0, a separate calculation is made of the $N(0)V_0$ required to obtain high-current superconductivity with a finite thermal energy gap $2(\epsilon_0 - p_F v_0)$. This calculation, using a nonretarded interaction, includes the correction of an algebraic error in the 1959 paper by Parmenter. The result, $N(0)V_0 \geq 0.70$, is in close agreement with the recent work of Hone, who made use of a retarded interaction in calculating that one must have $N(0)V_0 \geq 0.67$ in order to get finite-thermal-gap high-current superconductivity. This suggests that retardation effects are not crucial in determining the occurrence or nonoccurrence of high-current superconductivity. It is pointed out that experimental measurements of Morin and Maita have suggested that some transition-metal superconductors have large enough values of $N(0)V_0$ for both the gapless form and the finite-thermal-gap form of high-current superconductivity to occur. Either form, if it exists, will exhibit the same form of electrical instability that is known to occur under exceptional conditions in conventional low-current superconductivity. (auth)

6242 BOUNDARY CONDITIONS AND QUANTUM EFFECTS IN THIN SUPERCONDUCTING FILMS. Paskin, Arthur (Brookhaven National Lab., Upton, N. Y.); Singh, A. D. Phys. Rev., 140: A1965-7(Dec. 13, 1965). (BNL-9361).

Earlier calculations of quantum effects in thin superconducting films were based on the assumption that the wave functions of the "Cooper pairs" vanish at the surface of the film. The experimental confirmation of recent calculations of surface superconductivity indicate that the condition of no net electron flow normal to the surface is a valid approximation. This condition suggests that the gradient of the single-electron functions should also vanish at the surface. The present calculation follows closely the work of Thompson and Blatt except that the boundary condition that the wave function vanish at the surface is replaced by the boundary condition that its gradient vanish at the surface. The main results are: the chemical potential decreases with decreasing film thickness, and the superconducting energy gap increases with decreasing film thickness. These results differ from Thompson and Blatt's work in that the chemical potential now has the opposite thickness dependence and the energy-gap parameter increases more rapidly with decreasing film thickness. (auth)

6243 CRITICAL STATE OF THE SUPERCONDUCTING SURFACE SHEATH. Fink, H. J.; Barnes, L. J. (Atomics International Div., North American Aviation, Inc., Canoga Park, Calif.). Phys. Rev. Lett., 15: 792-5(Nov. 15, 1965).

When a long superconducting cylinder is placed into an axial magnetic field whose value is between the upper critical field and the surface nucleation field, then the surface is in the superconducting state, and the core of the cylinder is in the normal state provided the thickness of the surface sheath is small compared to the radius of the cylinder. Although the metal is singly connected, the superconducting surface is multiply connected. It is shown that a persistent current can be induced in the surface sheath and that its magnetic moment can be either diamagnetic or paramagnetic according to whether the magnetic field is increased or decreased, respectively. It is found that these currents are size dependent and have an appreciable effect on the magnetization for Ginzburg-Landau values of order unity and for applied magnetic fields close to the upper critical field. It is also shown for a cylinder that the induced magnetization per unit volume is always considerably larger than the inherent diamagnetic magnetization per unit volume of the surface sheath, in its lowest energy state, although the induced surface current is always considerably smaller than the inherent surface currents provided the radius of the cylinder is very large compared to the penetration depth. (J.F.P.)

6244 MAGNETIC COUPLING BETWEEN TWO ADJACENT TYPE-II SUPERCONDUCTORS. Giaever, Ivar (General Electric Research and Development Center, Schenectady, N. Y.). Phys. Rev. Lett., 15: 825-7(Nov. 22, 1965).

An experiment is presented which shows that it is permissible to interpret literally the voltage drop along a type-II superconductor as arising from the motion of flux. The experimental arrangement is shown. An Sn film (primary) is evaporated onto a microscope glass slide, and a thin film of SiO_2 is evaporated over the primary film. Finally a second Sn film (secondary) is evaporated over the SiO_2 layer. Thus the measured resistance between the two metals approaches infinity. The experiment consists of passing a d-c current along the primary film and measuring the d-c voltage developed both in the primary and in the secondary films. When both films are normal, or when the secondary film is in the normal state and the primary is in the superconducting state, no voltage can be detected in the secondary loop. As soon as both films are superconducting, a d-c voltage is seen in the secondary loop as well as in the primary circuit. This behavior is displayed for three different temperatures. The experiment is consistent with Maxwell's equations, and the result is explained on the basis of a simple model. (J.F.P.)

6245 LOW-TEMPERATURE HEAT CAPACITY OF LIQUID ^{3}He. Abel, W. R.; Anderson, A. C.; Black, W. C.; Wheatley, J. C. (Univ. of Illinois, Urbana). Phys. Rev. Lett., 15: 875-8(Dec. 6, 1965). (COO-1198-308).

An experiment is reported in which it is possible to eliminate the effects of the calorimeter background on the heat capacity measurement of helium-3. Heat capacity data for pure helium-3 only were obtained down to 6m°K for a pressure of 0.28 atm and down to 4m°K for a pressure of 27 atm. The main results of these heat capacity measurements are given, and are considered preferable to previous results in considering the behavior of helium-3 at very low temperatures. The experimental arrangements are described. The results of these experiments are shown for helium-3 and for mixtures of ^{3}He and cerium magnesium nitrate. It is concluded that even in the temperature region where the diffusion coefficient obeys the temperature dependence, the value of heat capacity continues to rise, though the effect is not great down to the lowest temperatures measured. A linear plot is used to extrapolate the heat capacity, divided by nRT, to zero, and the limiting values and effective masses are found and given. No strange behavior suggestive of a superfluid transition was observed. (J.F.P.)

6246 QUANTUM TRANSITIONS AND LOSS IN MULTIPLY CONNECTED SUPERCONDUCTORS. Silver, A. H.; Zimmerman, J. E. (Ford Motor Co., Dearborn, Mich.). Phys. Rev. Lett., 15: 888-91(Dec. 6, 1965).

The observation of quantized flux flow across superconducting weak links is reported. This is accomplished by

incorporating the weak link into a macroscopic superconducting ring and making use of the quantum behavior of this multiply connected superconductor. The quantized flux flow corresponds to direct transitions between the allowed states of the ring. Within this model a criterion is offered for the appearance of a fundamental resistive effect associated with the passage of flux across superconducting elements. This criterion was experimentally verified by measuring the current and voltage across a superconducting weak link or point contact in an otherwise macroscopic superconducting niobium ring. Thus an elementary experiment was performed on the dynamics of the quantized fluxoid which is pertinent to the recent discussions on voltages and resistance in superconductors. These experiments indicate the existence of discrete states for the multiply connected superconductor. The selection rule $\Delta k = \pm 1$ is rigorously obeyed in the current range specified, and the critical condition for the appearance of resistance in the superconducting ring is given. This resistance is of a fundamental nature related to the trapping of flux and a change of state of the superconductor. (J.F.P.)

6247 COEXISTENCE OF ANTIFERROMAGNETISM AND SUPERCONDUCTIVITY. Finnemore, D. K.; Hopkins, D. C.; Palmer, P. E. (Ames Lab., Ames, Iowa). Phys. Rev. Lett., 15: 891-3(Dec. 6, 1965). (IS-1272).

Magnetization data is presented for LaGd alloys which indicate that the ordering in low applied fields is not ferromagnetic but is of a helical or other antiferromagnetic structure. The measurements were made by pulling a spherical sample through a uniform magnetic field between two counter-wound 16,400-turn coils. Superconducting and antiferromagnetic transition temperature curves and constant field magnetization curves are given for these alloys. The data presented indicate that antiferromagnetism and superconductivity coexist in lanthanum-0.8 at.% gadolinium near 0.4°K. (J.F.P.)

6248 ENTROPY TRANSPORT BETWEEN TWO SUPERCONDUCTORS BY ELECTRON TUNNELING. Maki, Kazumi; Griffin, Allan (Univ. of California, San Diego, La Jolla). Phys. Rev. Lett., 15: 921-3(Dec. 13, 1965).

Some preliminary calculations of the tunneling heat current are reported. It is found that the thermal resistance depends very much on whether the metals are in the superconducting or normal phases. In addition there is an oscillatory heat flux due to fluctuations in the quasiparticle tunneling between two superconductors. It is also found that the change in chemical potential due to the temperature difference can give rise to the a-c and d-c Josephson supercurrents. But the calculations show that no entropy is carried by these currents, which is in agreement with expectations. It is assumed that the heat energy carried by the electrons is transferred by a tunneling process through the interface barrier. For this purpose an effective tunneling hamiltonian is used. The metals are assumed to be simple BCS superconductors. (J.F.P.)

6249 DIRECT MEASUREMENT OF THE SIZE OF CHARGED QUANTIZED VORTEX RINGS IN He II. Gamota, G.; Sanders, T. M. Jr. (Univ. of Michigan, Ann Arbor). Phys. Rev. Lett., 15: 949-51(Dec. 20, 1965).

A direct measurement was made of the size of charged quantized vortex rings in liquid helium-4 at about 0.3°K. The method consisted of studying the current-voltage characteristics of a tetrode tube, in which the size of holes in the last grid was varied. The data indicate a cutoff voltage which is determined by the size of the grid openings and implies that the size of these vortex rings can be correctly calculated by classical hydrodynamics. The dependence of the radius of the ring on the energy of charged complexes at temperatures below about 0.6°K was studied. The apparatus is described and some typical current-voltage curves are shown. Plots of the square root of the ratio of vortex transmission coefficient to the geometrical transmission coefficient for the small grids are given. The cutoff energy is shown versus the grid size. (J.F.P.)

6250 MAGNETIC PROPERTIES OF SUPERCONDUCTING THIN FILMS IN THE NONLOCAL REGIME. Thompson, R. S.; Baratoff, A. (Harvard Univ., Cambridge, Mass.). Phys. Rev. Lett., 15: 971-4(Dec. 20, 1965).

Near the transition temperature the Ginzburg-Landau-Gor'kov theory determines the critical field, and in very dirty superconducting films the energy spectrum has been found for all temperatures and fields. Using the same thermodynamic Green's function techniques and assuming the order parameter to be constant, the results are extended to the nonlocal regime, thus encompassing common experimental situations characterized by significant deviations from the thickness dependence predicted by local theories. Previous analyses of relevant data near the transition temperature had no firm microscopic basis. In the case of very dirty superconducting films the restrictions $l \ll d \ll (\xi_0 l)^{1/2}$ precluded any meaningful comparison of the original theory with experiment. These obstacles are removed in this extension. (J.F.P.)

6251 THE STRUCTURE OF A VORTEX LINE AND THE LOWER CRITICAL FIELD IN SUPERCONDUCTING ALLOYS. Neumann, L.; Tewordt, L. (Univ., Hamburg). Z. Physik, 189: 55-66(1966).

The structure of an isolated vortex line, and the lower critical field H_{c1}, is calculated by means of the generalized Ginzburg-Landau (GL) theory for arbitrary values of the GL-parameter $\kappa(\geq 1/\sqrt{2})$ and the mean free path l at temperatures T in the vicinity of T_c. The free energy functional including the corrections of order $[1 - (T/T_c)]$ to the GL-functional is derived exactly. The corresponding Euler-Lagrange equations determining the zero-order (GL) contributions and the corrections of order $[1 - (T/T_c)]$ to the order parameter, $f(r)$, and the superfluid velocity, $v(r)$, are solved numerically. The shapes of the first-order corrections of $f(r)$, $v(r)$, and the magnetic field, $h(r)$, are found to depend markedly, for a given value of κ, on a second parameter, $\alpha = 0.882(\xi_0/l)$ (where ξ_0 is the BCS-coherence-distance). The deviations from the GL-solutions become largest for $h(r)$ at parameter values $\kappa \approx 1$ and $\alpha \approx 0$ (the deviation of $h(0)$ is about 6% at $T = 0.9\ T_c$ for $\kappa = 1$ and $\alpha = 0$). The ratio H_{c1}/H_c (where the thermodynamic critical field H_c has the BCS-temperature-dependence) is found to increase slightly in the clean limit ($\alpha = 0$), and to decrease slightly in the dirty limit ($\alpha = \infty$) as T decreases (the variation of H_{c1}/H_c is always less than 3% for arbitrary values of κ and α as T decreases from T_c to $0.9\ T_c$). (auth)

Neutron Physics

See *also* REACTOR TECHNOLOGY — Criticality Studies

Refer also to abstracts 5935, 5936, 6334, 6671, and 6672.

6252 (AD-617880) ENERGY-DEPENDENT NEUTRON TRANSPORT THEORY IN PLANE GEOMETRY. II. EIGENFUNCTIONS AND FULL-RANGE COMPLETENESS. Leonard, A.; Ferziger, Joel H. (RAND Corp., Santa Monica, Calif.). June 1965. 40p. (P-3166(RAND)). CFSTI $2.00 cy, $0.50 mn.

An earlier treatment of the energy-dependent transport equation was extended to include the case in which cross sections are functions of energy. The technique again consists of finding solutions to the homogeneous transport equation after expanding in terms of a complete set of functions in the energy variable. The full-range completeness theorem for these eigenfunctions requires the solution of a coupled set of singular integral equations. This solution is effected by a generalization of a trick used by Case and is applied to the problem for the infinite medium Green's function. Numerical results are given for a heavy gas model. (TAB)

6253 (AD-617882) ENERGY-DEPENDENT NEUTRON TRANSPORT THEORY IN PLANE GEOMETRY. III. HALF-RANGE COMPLETENESS AND HALF-SPACE PROBLEMS. Leonard, A.; Ferziger, Joel H. (RAND Corp., Santa Monica, Calif.). June 1965. 35p. (P-3167(RAND)). CFSTI $2.00 cy, $0.50 mn.

A set of elementary solutions to the energy-dependent Boltzmann equation, which was previously derived, is shown to possess a half-range completeness property allowing the exact solution to energy-dependent half-space problems and the reduction of finite slab problems to rapidly convergent Fredholm equations. Results follow in analogy with Case's work on the one-velocity transport equation except that a system of singular integral equations is encountered, giving rise to the Hilbert problems for matrices. It is shown that the methods of Muskhelishvili and Vekua are applicable to this matrix problem and lead to the consideration of a class of Fredholm equations to obtain the solution. The explicit form the Fredholm equation for the present problem is derived by extending the analysis of the scalar Hilbert problem to the matrix case. Applications of the completeness proof are made to the albedo and Milne problems for a half-space. (auth)

6254 (AEEW-M-503) REQUESTS FOR THE EVALUATION AND COMPILATION OF DATA FOR THE U.K. NUCLEAR DATA LIBRARY, JANUARY 1965. Freemantle, R. G. (Atomic Energy Establishment, Winfrith (England)). Mar. 1965. 7p. Dep. mn.

The requests and priorities for the compilation of evaluated data for the U. K. Nuclear Data Library are listed and information on evaluation work now in progress is provided. For completeness, the current content of the library is included. (auth)

6255 (AERE-R-5016) MULTIPLE SCATTERING IN PLANE SAMPLES: APPLICATION TO SCATTERING OF THERMAL NEUTRONS. Cocking, S. J.; Heard, C. R. T. (Atomic Energy Research Establishment, Harwell (England)). Oct. 1965. 22p. Dep.; BIS $0.90; HMSO 4s. 6d.

A formulation of multiple scattered intensity in terms of orders of scattering is extended and evaluated for anisotropic, elastic scattering by plane samples. The intensities of once- and twice-scattered components are calculated explicitly, and further components are estimated. Examples of the application to measurements of the scattering of low-energy neutrons by samples of liquid and of solid lead are given. (auth)

6256 (CONF-650217) PULSED HIGH INTENSITY FISSION NEUTRON SOURCES. Proceedings of a Symposium, USAEC, Washington, D. C., February 1965. Kolstad, G. A.; Zartman, I. F. (Division of Research (AEC), Washington, D. C. Division of Reactor Development and Technology (AEC), Washington, D. C.). 152p. Dep. mn; CFSTI $1.75 cy, $1.00 mn.

Eleven papers are included; separate abstracts have been prepared for 9. The remaining two papers were previously abstracted in NSA, see 19: 29174 and 45674 (T.F.H.)

For abstracts of individual papers see: 5569, 5726, 5935, 5936, 6257–6259, 6671, and 6672.

6257 (CONF-650217, pp 11-24) SUB-CRITICAL NEUTRON AMPLIFIER SYSTEMS. Fluharty, R. G. (Phillips Petroleum Co., Idaho Falls, Idaho).

A review is given of the performance of subcritical exponential piles bombarded by beams from high-intensity accelerators as pulsed neutron sources. A Pu pile is proposed that could yield equivalent thermal-neutron source strengths of 10^{16} to 10^{17} neutrons/cm^2 · sec. (T.F.H.)

6258 (CONF-650217, pp 82-101) INELASTIC SCATTERING WITH PULSED NEUTRON SOURCES. Brugger, R. M. (Phillips Petroleum Co., Idaho Falls, Idaho).

Diffraction and time-of-flight methods of slow-neutron inelastic scattering, used to measure the dynamic properties of matter, are outlined. The experimental versatility of the methods is shown. (T.F.H.)

6259 (CONF-650217, pp 111-23) USE OF POLARIZED BEAMS. Sailor, V. L. (Brookhaven National Lab., Upton, N. Y.).

Methods are reviewed for polarizing neutron beams in the milli-ev to 10-kev energy range. Uses of these beams for magnetic studies, nuclear studies, and investigations of the fundamental properties of the neutron are discussed. (T.F.H.)

6260 (CONF-651101-43) REVIEW OF EXPERIMENTAL DETERMINATIONS OF NEUTRON SPECTRA. Slovacek, R. E. (Knolls Atomic Power Lab., Schenectady, N. Y.). Nov. 17, 1965. Contract W-31-109-eng-52. 20p. Dep. mn; CFSTI $1.00 cy, $0.50 mn.

From 13th Conference on Remote Systems Technology, Washington, D. C.

A review is presented of several integral and differential experimental methods for measuring neutron spectra below 10 ev in various media. The advantages, disadvantages, and regimes of usefulness of the different methods are noted. 18 references. (T.F.H.)

6261 (LA-3415) COMPUTATION OF FAST NEUTRON PENETRATION IN AIR BY THE "Sn-METHOD" WITH SPECIAL EMPHASIS ON THE USE OF "MULTITABLE-MULTIGROUP CROSS SECTION SETS." Sandmeier, H. A.; Hansen, G. E.; Lazarus, R. B.; Howerton, R. J. (Los Alamos Scientific Lab., Univ. of California, N. Mex.). Aug. 1965. Contract W-7405-eng-36. 66p. Dep. mn; CFSTI $3.00 cy, $0.75 mn.

Much theoretical work was done earlier to represent the angular dependence in the scattering source term of the Boltzmann equation by means of Legendre or other series expansions. However, relatively little work has been done to feed this information into present day Sn codes. The Sn-transport codes at LASL allow a representation of anisotropy in the scattering-source term by means of multitable cross section sets. A formalism is developed to generate these sets. The numerical evaluation of Sn cross section entries for these multitable sets was computerized. Deep penetration calculations (3000 meters) of high energy neutrons in homogeneous air are presented. These calculations used recently evaluated basic cross section data for nitrogen and oxygen from the LRL-LASL Library (Howerton tape). The variations in the neutron flux due to different approximations are discussed as are also the expected variations in the flux due to inaccuracies in cross section data. (auth)

6262 (NP-15633) A DESCRIPTION OF NEUTRON GENERATOR BEAM SORTERS. Technical Bulletin No. 106. Hollister, Herb (Kaman Nuclear, Colorado Springs, Colo.). [nd]. 5p.

The operating characteristics of a crossed-field beam sorter for use in a drift-tube neutron generator are shown. The characteristic curves are given for atomic and molecular D ions and molecular T ions. (T.F.H.)

6263 (NP-15635) NEUTRON FLUXES AVAILABLE FROM KAMAN NUCLEAR NEUTRON GENERATORS. Technical Bulletin No. 102. Wood, D. E. (Kaman Nuclear, Colorado Springs, Colo.). June 11, 1963. 5p.

The neutron yields, neutron fluxes, and angular flux distributions are measured for two models of drift-tube neutron generators. The flux from each model that can be delivered through a 1-cm^2 target sample is measured. (T.F.H.)

6264 (WAPD-T-1849) TRANSPORT SYNTHESIS. Davis, James A.; Kaplan, Stanley (Bettis Atomic Power Lab., Pittsburgh, Pa.). Sept. 1965. Contract AT(11-1)-Gen-14. 15p. (CONF-651101-45). Dep. mn; CFSTI $1.00 cy, $0.50 mn.

From 13th Conference on Remote Systems Technology, Washington, D. C.

A FORTRAN program (TRANSY) is developed to obtain synthesized solutions to the S_2 or S_4 equations for a monoenergetic x-y problem. The TRANSY synthesis is based on the discrete-ordinate method. The purpose of the synthesis is to investigate the feasibility of synthesizing solutions to high-order approximations to the transport equation. (T.F.H.)

6265 INTERNATIONAL COMPARISON OF NEUTRON SOURCES. Andreev, O. L.; Silin, Yu. S.; Stukov, G. M.;

Fominykh, V. I.; Shchebolev, V. T.; Yaritsyna, I. A. At. Energ. (USSR), 19: 181-3(Aug. 1965). (In Russian).

The relative measurements of the Canadian Ra–α–Be neutron source were carried out considering the neutron distribution in open geometry and using a long counter which could turn the source at any required angle. With the source axis of rotation coinciding with the cylinder axis, the asymmetry was 1% and with the source axis turned to the side of the surface it was 1.5%. The relative measurements for the source indicated 3.25 neutrons/sec. (R.V.J.)

6266 RESONANCE NEUTRON-MOLECULE INTERACTIONS. Ivanov, G. K.; Sayasov, Yu. S. At. Energ. (USSR), 19: 183-4(Aug. 1965). (In Russian).

Cross sections of neutron resonance scattering and absorption by nuclei in molecules were estimated considering that the molecules are free. The obtained formulas hold for molecular gases. However, they also can be used for molecular liquids and crystals, in the case, in which the molecular interactions described by delayed rotation frequencies are smaller in comparison to the molecular oscillation frequencies. Ordinarily such conditions are observed in heavy molecules. The energy dependence of the total cross section was computed for chloride molecules with resonance parameters $\Gamma = 0.8$ ev and $E_0 = 4300$ ev (Γ is the resonance level width and E_0 is the resonance energy). (R.V.J.)

6267 USE OF P_n APPROXIMATION FOR DETERMINATION OF NEUTRON DISTRIBUTION IN AN ABSORBING ROD. Sergeev, I. V. At. Energ. (USSR), 19: 346-9(Oct. 1965). (In Russian).

A system of nonlinear differential equations describing the distribution of neutrons in an absorbing rod in the P_n approximation is transformed into a system of more detailed integral equations for study. A method of solution is presented, based on the use of successive approximations. (tr-auth)

6268 CHOICE OF COLLIMATORS FOR NEUTRON DIFFRACTION. Sakamoto, Masanobu; Kunitomi, Nobuhiko; Motohashi, Haruhiko; Minakawa, Nobuaki (Japan Atomic Energy Research Inst., Tokyo). Jap. J. Appl. Phys., 4: 911-14(Nov. 1965).

The effect of collimators on Bragg peaks was investigated experimentally, in order to obtain a high intensity and good resolution for neutron diffraction measurements of a powder sample. The results showed that, in a rather small scattering angle, the angular divergence of the second collimator must be larger than that of the first and the third collimator, because the focusing effect makes the second collimator insensitive to the width of diffracted neutrons. (auth)

6269 NEUTRON SPECTRA FROM Am–α–Be AND Ra–α–Be SOURCES. Thompson, M. N.; Taylor, J. M. (Univ., Melbourne). Nucl. Instrum. Methods, 37: 305-8 (Nov. 1965).

The neutron energy spectra obtained from the sources Am-α-Be and Ra-α-Be are measured, using a proton recoil spectrometer with γ-ray discrimination. (auth)

6270 DETERMINATION OF DIFFUSION CONSTANTS D(E;T) AND $\overline{Dv}$(T) OF THERMAL NEUTRONS IN H_2O, PHENYLENE, $ZrH_{1.92}$ AND D_2O BY MEASUREMENT OF THE SCATTERING ANGULAR DISTRIBUTION $4\pi/\sigma \cdot d\sigma/d\Omega$. PART I. H_2O. Lemmel, Hans-Dietrich (Technische Hochschule, Munich). Nukleonik, 7: 265-80(July 1965). (In German).

The scattering angular distribution $4\pi/\sigma \cdot d\sigma/d\Omega$ (θ;E;T) in liquid water at temperatures between 0 and 200°C and neutron energies between 0.0225 and 0.105 ev was measured. The temperature dependence was shown as very small. The mean scattering cosine $\mu = \cos\theta$ was compared with earlier measurements and the theory of Nelkin according to Kiefhaber, in which small systematic deviations occur. From the relations between the differential scattering cross section $d\sigma/d\Omega$ and the Egelstaff scattering function an expression is obtained on the temperature behavior of the scattering function. As an important fundamental for the multigroup calculations, the diffusion constant D(E;T) was obtained from μ as function of the neutron energy and the water temperature. It can be assumed proportional to $\sqrt{E}$ for E = 0.2 up to 0.075 ev and T = 0 to 200°C. The diffusion constant $\overline{Dv}$ averaged over the Maxwell spectrum, which is essential for the flux calculation of the thermal groups, was calculated as function of the moderator temperature and the neutron temperature. In the temperature range between 0 and 200°C only small deviations from the direct measurements of $\overline{Dv}$ are seen. The value at 20°C ($Dv = 35{,}300 \pm 300$ cm^2/sec) agrees especially well with direct measurements on pulsed neutron sources. Various theoretical calculations differ by 3 to 6%. The corrections which must be considered in the evaluation of the counting rate are described in detail. Systematic errors in the scattering angular distribution can be kept very small: correction of the scattering on the probe vessel, for the second order of the lead crystal monochromator, and for the multiple scattering are described. A multiple scattering corrector is given that, in contrast to the known vineyard method, approximates the scattering cross section not isotropically but anisotropically and is usable in water probes to layer thickness up to $\Sigma d = 0.6$. (tr-auth)

6271 DETERMINATION OF THE DIFFUSION CONSTANTS D(E_0,T) AND $\overline{Dv}$(T) OF THERMAL NEUTRONS IN H_2O, PHENYLENE, $ZrH_{1.92}$, AND D_2O BY MEASUREMENT OF SCATTERING ANGULAR DISTRIBUTIONS. II. ZIRCONIUM HYDRIDE AND HEAVY WATER. Kornbichler, Siegfried (Technische Hochschule, Munich). Nukleonik, 7: 281-6(July 1965). (In German).

Neutrons with energies E = 0.0225, 0.044, 0.071, and 0.105 ev were scattered on thin layers of heavy water and polycrystalline zirconium hydride $ZrH_{1.92}$. The temperatures T of the scattering samples were 293 and 453°K. From the measured intensity distributions with respect to the scattering angle, the differential cross section $d\sigma/d\Omega$ (E,T,θ), the mean scattering cosine μ, the diffusion constant D(E,T) and the diffusion constant $\overline{Dv}$ averaged over a thermal neutron spectrum were calculated. The slight temperature dependence of the differential scattering cross section and of the average scattering cosine makes possible the calculation of the mean diffusion constants in the temperature range from about 290 to 250°K. The agreement of the measured values of the diffusion constant $\overline{Dv}$ with other integral measurements using pulsed sources and poisoning methods is very good in a broad temperature range. At room temperature, for D_2O a value for 2.9×10^5 cm^2/sec^{-1} is obtained and for $ZrH_{1.92}$ a value of 0.386×10^5 cm^2/sec^{-1}. The measured diffraction pattern can be explained qualitatively using a simple model. In the predominantly coherent scattering of heavy water the elastic interference scattering produces three pronounced maxima in the scattering angular distribution; also in the predominantly incoherent scattering of zirconium hydride numerous Bragg reflexes are found as a result of the coherent scattering on zirconia. (tr-auth)

6272 SCATTERING OF SLOW NEUTRONS AT THE PROTONS IN PHENYLS AND WATER VAPOR [Thesis]. Hofmeyr, C. Munich, Tech. Univ., 1964. 75p. $2.00 Gmelin, AED-DISS. 64-836.

Monochromatic neutrons were scattered by thin samples of benzene, diphenyl, and terphenyl at various temperatures. The relative differential scattering cross section is determined from measurements of the angular distribution of scattered neutrons. Values for the average scattering cosine and for the diffusion constant are given. (Gmelin Inst.)

Nuclear Properties and Reactions

Refer also to abstracts 5715, 5759, 5794, 6034, 6556, and 6659.

6273 (AD-617398) MU CAPTURE IN OXYGEN [Thesis]. Cohen, R. C. (Nevis Labs., Columbia Univ., Irvington-on-Hudson, N. Y.). Apr. 1965. Contract Nonr26672. 80p. (CU-236; NEVIS-130). CFSTI $3.00 cy, $0.75 mn.

By measuring the μ induced ^{16}N beta radioactivity and the low energy gamma transitions in this nucleus, estimates were obtained of the absolute capture rates for μ^- stopping in oxygen and producing ^{16}N in three of the lowest lying states. The results are: $\mu^- + {}^{16}O$ (O+) to ^{16}N (2(–), ground state) + ν = 6,300 ± 700/sec to $^{16*}N$ (O(–), 120 kev) + ν = 1,100 ± 200/sec to $^{16*}N$ (1(–), 392 kev) + ν 1,730 ± 100/sec. Within the limits noted in the text, the rate to the O(–) state indicates the value for the pseudoscalar coupling constant lies between $10g_A$ and $26g_A$. (auth)

6274 (AD–619061) THE POLARIZATION OF 45 Mev PROTONS BY COMPLEX NUCLEI. Cahill, Thomas A. (California Univ., Los Angeles. Dept. of Physics). July 1965. Contract Nonr23344. 82p. CFSTI $3.00 cy, $0.75 mn.

Studies on beam generation, spurious asymmetries, detectors and electronics, rotation of polarization, calibration of polarization, and targets and background are reported. (TAB)

6275 (AD–619534) ELECTRON SCATTERING EXPERIMENTS; MEASUREMENT OF TRANSMISSION OF 8.3-Mev NEUTRONS PRODUCED BY A VAN DE GRAAFF GENERATOR; MAGNETIZATION CURVE OF HOLMIUM. Periodic Status Report, March 15–June 30, 1965. Little, W. A. (Stanford Univ., Calif. Dept. of Physics). Contract Nonr22586. 4p. CFSTI $1.00 cy, $0.50 mn.

Two electron scattering experiments were performed with polarized ^{165}Ho nuclei. A measurement of the transmission of 8.3-Mev neutrons produced by the Van de Graaff generator was attempted. The change of transmission from a polarized to an unpolarized system was found to be less than a few per cent. The magnetization curve of holmium was measured at 4.2°K and fields up to 40 kG. (TAB)

6276 (AD–619576) LINEAR ELECTRON ACCELERATOR PROJECT. Status Report, November 1, 1964–January 31, 1965. (Stanford Univ., Calif. High-Energy Physics Lab.). Feb. 1965. Contract Nonr22567. 36p. (HEPL–362). CFSTI $2.00 cy, $0.50 mn.

Research with Mark II and Mark III continued with both accelerators operating reliably. The colliding beams experiment achieved a major breakthrough in that wide angle electron-electron scattering events were observed with a high signal-to-background ratio. The number of observed events corresponded within a factor of two to the number expected from the experimentally measured beam parameters. The beam switchyard for the new target area was completed to the extent that preliminary runs can be made. The electron scattering program on Mark II recently included a study of elastic scattering at 180°. The measurements extend into a region of lower momentum transfer than was conveniently available on Mark II. The elastic scattering of electrons by deuterons at large angles where magnetic scattering dominates, showed an effect, which could be the result of meson currents. The effect was first observed using the 180 degrees scattering apparatus at Mark II. A more pronounced effect using Mark III at momentum transfers of about 500 Mev/c was observed. (auth)

6277 (AD–619952) RECENT HIGH ENERGY ELECTRON INVESTIGATIONS AT STANFORD UNIVERSITY. Buchanan, C. D.; Collard, H.; Crannell, C.; Clark, B. C.; Ravenhall, D. G. (Stanford Univ., Calif. High-Energy Physics Lab.). June 21, 1965. Contract Nonr22567. 45p. (HEPL–383(Rev.)). CFSTI $2.00 cy, $0.50 mn.

Recent developments in high energy electron physics at Stanford are summarized. The following topics are discussed: nucleon form factors; deuteron form factors; coincidence studies of elastic scattering; inelastic continuum studies; nuclear physics; ^{40}Ca and ^{44}Ca investigations; study of the inelastic continuum in ^3He; magnetic octupole moments in light nuclei; and shower studies at 900 Mev. (TAB)

6278 (AD–623877) PROGRAMS FOR COLLECTIVE NUCLEAR MODEL CALCULATIONS IN DEFORMED EVEN-EVEN NUCLEI. Davidson, J. P. (Naval Radiological Defense Lab., San Francisco, Calif.). Sept. 8, 1965. 72p. (USNRDL-TR–901). CFSTI $3.00 cy, $0.75 mn.

After an outline of current collective model theories of deformed, even-even nuclei, both for positive parity states (quadrupole deformation) and for negative parity states (octupole deformation), a series of FORTRAN II computer programs necessary to calculate relevant physical quantities from these models is discussed. First, programs are given which can be used to calculate eigenvectors and eigenvalues of the allowed angular momenta for rigid rotators of either deformation. Then programs are given with which the reduced matrix elements for electric quadrupole transitions can be calculated. These programs use the eigenvectors calculated by the previous set. Finally, programs are given which can be used to calculate the effect of deformation vibrations on the energy levels and the transition ratios. A number of graphs of the complete transition ratios for E2 transitions within positive parity and within negative parity bands are included. (auth)

6279 (AI–65-225) TUNGSTEN RESONANCE INTEGRALS AND DOPPLER COEFFICIENTS. Quarterly Progress Report No. 1, July–September 1965. Carpenter, S. G.; Otter, J. M.; Paschall, R. K.; Royden, H. N. (Atomics International, Canoga Park, Calif.). Oct. 29, 1965. Contract NAS 3-7982. 21p. (NASA-CR–54769).

Axial flux and source traverses were made in the central void in the SGR-CA, the expected cosine shapes being obtained. Reactivity measurements under cadmium were made on a number of samples, including natural tungsten, gold, lead, depleted uranium, aluminum, stainless steel, and lavite. The results indicate that a sensitivity of better than 0.01 cents is obtained for a single reactivity measurement taking 100 sec. This sensitivity is adequate for the resonance-integral measurements, and can readily be improved as required for Doppler measurements by taking data over a longer period of time. Calculated reactivities are consistently higher than those measured; however, the ratios of various calculated worths agree reasonably well with the corresponding ratios of experimental worths. The use of real and adjoint fluxes calculated with the cadmium sleeve taken into account should improve agreement with experiment. These results also indicate that reactivity effects associated with scattering and structural materials are negligible. Measurements with and without cadmium end caps have demonstrated that end effects are quite small. (auth)

6280 (ANL–6925, pp 249-51) NUCLEAR CONSTANTS. Stupegia, Donald C.; Tevebaugh, A. D. (Argonne National Lab., Ill.).

Data are presented on cross sections for production of 0.741-Mev level ^{93}Nb produced by neutron inelastic scattering at energies up to 1.2 Mev. Radiative capture cross sections are reported for ^{158}Gd and ^{170}Er as function of neutron energies at 4 kev to 2 Mev. Preparation of Pu and U irradiation samples is reported. (J.R.D.)

6281 (CEA-R-2807) CONTRIBUTION A L'ETUDE DES REACTIONS (d,p) ET (d,α) SUR ^{16}O ET ^{11}B DE 200 kev A 1 Mev [Theses]. (Contribution to the Study of (d,p) and (d,α) Reactions on ^{16}O and ^{11}B From 200 kev to 1 Mev [Thesis]). Longequeue, Nicole (Commissariat a l'Energie Atomique, Grenoble (France). Centre d'Etudes Nucleaires). 1965. 56p. Dep. mn.

Submitted to Grenoble Univ. (France). Faculte des Sciences.

The reactions $^{16}O(d,\alpha_0)$, (d,p_0), (d,p_1), and $^{11}B(d,\alpha_0)$, (d,α_2), (d,p_0) were studied from 200 kev to 1 Mev. The interpretation (d,α) reactions by the compound nucleus theory has shown the presence of ^{18}F levels (7.94-Mev, 1+; 8.09-Mev, 1+) and of ^{13}C level (19-Mev, $^3/_2\pm$ or $^5/_2-$). The interpretation of $^{16}O(d,p_1)$ and $^{11}B(d,p_0)$ reactions at energies lower than 400 kev was given by a theory of Coulomb stripping. (auth)

6282 (CERN–64-13(Vol.4), pp 97-136) MAGNETIC MOMENT EXPERIMENTS. Combe, J. C. (European Organization for Nuclear Research, Geneva (Switzerland)).

A brief introduction to magnetic moments is presented. The measurement of magnetic moments is discussed. A discussion of nuclear magnetic resonance methods is presented. Methods using a polarized beam and the precession of the polarization in a constant magnetic field are discussed. (M.O.W.)

6283 (CERN–64-13(Vol.4), pp 137-86) HYPERNUCLEI. Burhop, E. H. S. (London Univ. (England). University Coll.).

Various aspects of hypernuclei are discussed. Among these are: production, detection, identification, decay modes, lifetime, spin, and excited states. Also included are discussions on decay modes of the Λ hyperon, binding energies of Λ hyperons in hypernuclei, the Λ-N interaction, observation of a double hypernucleus, parity of the K^- meson, the decay of a bound Λ hyperon, and hypernuclei as an aid in nuclear physics studies. (M.O.W.)

6284 (GEMP–392) OPERATING INSTRUCTIONS FOR THE FORTRAN IV VERSION OF PROGRAM GAMMA-P (NMP 468). Robertson, C. S.; Edwards, M. R. (General Electric Co., Cincinnati, Ohio. Nuclear Materials and Propulsion Operation). Nov. 23, 1965. Contract AT(40-1)-2847. 20p. Dep. mn; CFSTI $1.00 cy, $0.50 mn.

Program GAMMA-P (production cross sections for gamma rays) was converted to the FORTRAN IV coding system. The changes in input and dimensions of variables required by this conversion are described. (M.O.W.)

6285 (INP–414/PL) OBLICZANIE NIEKTORYCH ZALEZNOSCI KINEMATYCZNYCH W REAKCJACH JADROWYCH PROGRAMY DLA MASZYNY CYFROWEJ UMC-1. (Calculations of Some Kinematical Relations in the Nuclear Reactions Programs for the Digital Computer UMC-1). Pytkowicz, Gustaw (Institute of Nuclear Physics, Krakow (Poland)). July 1965. 30p. Dep.

Descriptions and instructions for practical use of programs for the digital computer UMC-1, when calculating kinetic energy in the lab system as a function of an angle, an angle in the cms system as a function of an angle in the lab system, an angle in the lab system as a function of an angle in the cms system, and a coefficient G converting a cross section from the lab system to the system for a product of a two-body nuclear reaction, are presented. (auth)

6286 (ISS–65/10) SULL'USO DEL METODO DI MONTECARLO PER RISOLVERE I PROBLEMI DI INTERPOLAZIONE. (On the Use of the Monte Carlo Method to Solve Problems of Interpolation). Cortellessa, G.; Farchi, G. (Istituto Superiore di Sanita', Rome (Italy). Laboratori di Fisica). Apr. 15, 1965. 33p. Dep. mn.

A method is proposed to fit experimental data to a theoretical curve with parameters to be determined. The parameters of the fit are extracted at random within intervals wide enough to include the solution. The fit is considered good enough if a choice of parameters satisfies a proper statistical test. A program in FORTRAN IV language is written for the IBM 7040 computer. (auth)

6287 (JINR-P–2373) STATISTICHESKII ANALIZ VZAIMODEISTVIYA π^--MEZONOV S ENERGIEI 17 Gev S TYAZHELYMI YADRAMI FOTOEMULSII. (Statistical Analysis of 17 Gev Pion Interaction with Heavy Emulsion Nuclei). Artykov, I. Z.; Barashenkov, V. S.; Eliseev, S. M. (Joint Inst. for Nuclear Research, Dubna (USSR). Lab. of Theoretical Physics). 1965. 10p. Dep. mn.

The results of calculations of intranuclear cascades made by the Monte Carlo method are compared with experiment. Experiment and theory agree. (auth)

6288 (KAPL–3113) THE INDEPENDENT YIELDS OF ^{86}Rb, ^{132}Cs, ^{134}Cs, AND ^{136}Cs IN THE THERMAL NEUTRON FISSION OF ^{235}U. McHugh, J. A. (Knolls Atomic Power Lab., Schenectady, N. Y.). Sept. 30, 1965. Contract W-31-109-eng-52. 8p. Dep. mn; CFSTI $1.00 cy, $0.50 mn.

The independent yields for the shielded nuclides of rubidium and cesium in the thermal neutron fission of ^{235}U were measured by use of high-sensitivity mass-spectrometric methods. The following yields were determined: ^{86}Rb, 2.40×10^{-5}%; ^{132}Cs, $<1.5 \times 10^{-7}$%; ^{134}Cs, 8.9×10^{-6}%; and ^{136}Cs, 5.94×10^{-3}%. (auth)

6289 (KN–63-10(R)) DETERMINATION OF NEUTRON YIELDS BY THE MEASUREMENT OF POSITRONS FROM THE ^{63}Cu(n,2n)^{62}Cu REACTION. Hoffman, John R. (Kaman Nuclear, Colorado Springs, Colo.). Jan. 11, 1963. 9p.

A simple method for the measurement of 14 Mev neutrons is described. The methods consists of irradiating copper foils and obtaining a ^{63}Cu(n,2n)^{62}Cu reaction. The ^{62}Cu decays with positron emission and a half life of 9.73 minutes. These positrons are measured directly with a thin-window beta counter. This method provides results as soon as 90 seconds after the end of irradiation. The method suffers from the fact that an instantaneous reading of the neutron pulse shape is not obtainable. (auth)

6290 (LA–3380) A TABLE OF BINDING ENERGIES AND PARTICLE SEPARATION ENERGIES FROM A MASS LAW. Seeger, Philip A. (Los Alamos Scientific Lab., Univ. of California, N. Mex.). Sept. 1, 1965. Contract W-7405-eng-36. 106p. Dep. mn; CFSTI $4.00 cy, $1.00 mn.

A table of approximately 10,000 masses for nuclei with $22 \leq Z \leq 120$ and $22 \leq N \leq 184$ is presented. The mass law used is one developed for application to the astrophysical problem of nucleosynthesis by rapid neutron capture. (auth)

6291 (NAA-SR-Memo–11538) THE TRIX-1 CODE, AN IMPROVED ANALYTIC CALCULATION OF RESONANCE INTEGRALS. Otter, J. M. (Atomics International, Canoga Park, Calif.). July 26, 1965. Contract AT(11-1)-Gen-8. 54p. Dep. mn; CFSTI $3.00 cy, $0.50 mn.

TRIX-1 is a FORTRAN code which calculates multigroup, Doppler-broadened effective resonance integrals and cross sections and their temperature coefficients for a heterogeneous or homogeneous resonance absorber. Using basic resonance parameters, geometry, and concentrations, the code combines resolved resonance, unresolved resonance, and 1/v and negative energy resonance calculations. The code is designed for convenient use in comparing theory and experiment, as well as in multigroup reactor calculations. The short running time makes the code desirable for use in survey calculations. The theory is based on the single-level Breit-Wigner line shape with no overlapping of neighboring resonances. Analytic approximations based on the work of Chernick and Vernon and Goldstein and Cohen are used. Detailed descriptions of the theory are given. Situations in which the theory can be deficient are pointed out. The logical flow of the program is shown together with descriptions of the input and output formats. Sample cases are appended. (auth)

6292 (NP–15601) ZAKHVAT OSTANOVIVSHIKHSYA π^--MESONOV LEGKIMI YADRAMI. (Capture of Stopped π^- Mesons by Light Nuclei). Kolybasov, V. M. (Gosudarstvennyi Komitet po Ispol'zovaniyu Atomnoi Energii SSSR, Moscow. Institut Teoreticheskoi i Eksperimental'noi Fiziki). 1965. 36p. Dep. mn.

Capture of stopped mesons (π^-) by light nuclei of α-particle type (^{12}C,^{16}O) with the emission of fast protons, neutrons, deuterons and tritons is considered. Relative yields and energy spectra of the final particles are calculated. It is shown that experimental data are in agreement with the assumption about predominant role of the α-particle pole graph. (auth)

6293 (NP–15603) PRIMENENIYA EFFEKTA MESSBAUERA I VOZMUSHCHENNYKH UGLOVYKH KORRELYATSII V YADERNOI FIZIKE. (Applications of the Moessbauer Effect and the Perturbed Angular Correlation Method in Nuclear Physics). Klyucharev, V. A. (Akademiya Nauk Ukrainskoi SSR, Kharkov. Fiziko-Tekhnicheskii Institut). 1965. 22p. Dep. mn.

The nuclear cascade general representation allows one to compare the possibilities of the Mössbauer experiments and the angular correlation method and to point out the features of the information obtainable with these methods. It is shown that the higher energy resolution connected with

the perturbed angular correlation method allows one to measure the short-lived nuclear states splitting, even if the distance between m-substates is less than the natural linewidth. Experimental results on magnetic dipole and electric quadrupole moments of the short-lived excited nuclear states are summarized. Nuclear information perturbations due to interactions between the nuclear spin and the extranuclear fields and the possible experiments on the interference effects (such as "reorientation" in Coulomb exitation) are discussed. (auth)

6294 (NP–15617) CONTRIBUTION A L'ETUDE DES HYPERNOYAUX LOURDS [THESES]. (Contribution to the Study of Heavy Hypernuclei [Thesis]). Lemonne, J. (Brussels Univ. (Belgium)). 1965. 202p. Dep. mn.

Some general concepts relative to hypernuclei are introduced and a brief description is given of the experimental techniques used for their study. The history of the detection of heavy hyperfragments is traced and the principal experimental data leading to the detection of these hyperfragments are analyzed. The experimental results obtained in the present study on the interactions of K^- mesons with emulsion nuclei are reported. The interaction of K^- mesons at rest and in flight (50 to 400, 500, 1300, and 1500 Mev/c) are studied simultaneously. Some of the most important aspects of the mechanism for the production of heavy hypernuclei are studied. The relative contribution of cascade and nuclear evaporation processes to the transfer of momentum to the observable heavy hyperfragments is determined. The interactions of Λ^0 that can be deduced from the study of heavy hypernuclei are discussed. It is shown that the analysis of non-meson decays of heavy hypernuclei can furnish information on the charge dependence of the initial nucleon and on the cross section of the weak reaction $\Lambda^0 + N \rightarrow N + N$. The results obtained are placed within the general framework of the study of heavy hypernuclei. (J.S.R.)

6295 (NP–15647) EXPERIMENTAL AND THEORETICAL INVESTIGATIONS ON LIGHT NUCLEI [Thesis]. Glaudemans, P. W. M. (Groningen Rijksuniversiteit (Netherlands)). [1964]. 96p. Dep. mn.

The shell model is used to investigate quantitatively the nuclei in the range $^{29}Si-^{40}Ca$. An inert ^{28}Si core is assumed with a two-particle interaction of the outer nucleons in the $2s_{\frac{1}{2}}$ and $1d_{\frac{3}{2}}$ shells. Mixing of all possible configurations in these shells is taken into account. The interaction matrix elements are reduced to linear expressions in 17 parameters (i.e., 15 two-particle interactions and 2 binding energies to the core). The methods used are discussed. The numerical results are presented. The values of the two-particle interactions in the $2s_{\frac{1}{2}}$ $1d_{\frac{3}{2}}$ shell and the binding energies to the ^{28}Si core of $2s_{\frac{1}{2}}$ and $1d_{\frac{3}{2}}$ particles are derived from experimental level energies. The calculated energies, spins and configurations of about 400 levels are listed. With the nuclear wave functions obtained, the spectroscopic factors for stripping reactions are calculated and, where possible, compared with the experimental data. The gamma-ray spectra at six $^{23}Na(p,\gamma)^{24}Mg$ resonances in the $E_p = 300$–750 kev region were investigated with scintillation spectrometers. From single spectra, coincidence spectra and sum-coincidence spectra the gamma-ray branchings of the resonance levels and of eighteen lower ^{24}Mg levels were obtained. At most resonances a 1.63 Mev gamma ray was observed, from which the relative intensity of the $^{23}Na(p,\alpha_1)^{20}Ne$ decay could be found. Thick target gamma-ray yields were measured from which the resonance strengths were obtained. Gamma-ray angular distributions and γ-γ angular correlations were measured at six $^{23}Na(p,\gamma)^{24}Mg$ resonances in the $E_p = 300$–800 kev region. Analysis of these data with an electronic computer yields spin and parity assignments: $J^\pi = 2^{(+)}$, $1^{(+)}$, 2^-, 3^+, $3^{(+)}$, and 2^+ to the resonances at $E_p = 308$, 511, 591, 676, 738, and 743 kev, respectively. The even parities in brackets are regarded as very probable. In each of these cases odd parity would imply the existence of an M2 transition with a strength of at least 0.5 Weisskopf units. The same measurements give $J^\pi = 2^+$ for the ^{24}Mg level at $E_x = 7.35$ Mev. Single spectra and γ-γ coincidence spectra measured at the weak $E_p = 251$ and 374 kev resonances yield the resonance branching ratios. The gamma-ray yield from the reaction $^{32}S(p,\gamma)^{34}Cl$ was measured in the range $E_p = 300$–1300 kev. Twenty-two resonances were observed with resonance strengths $(2J_r + 1)\Gamma_p\Gamma\gamma/T$ between 0.01 and 1.0 ev. From single and coincidence spectra with scintillation spectrometers the gamma-ray branchings of the resonance levels and of nineteen lower levels in ^{34}Cl were obtained. The decay of the levels of ^{34}Cl below 2.5 Mev is compared with spin predictions from the shell model. (M.O.W.)

6296 (ORNL–3858(Vol.1), pp 1-12) NUCLEAR AND REACTOR PHYSICS. (Oak Ridge National Lab., Tenn.).

Summaries of 19 papers on various aspects of nuclear and reactor physics are presented. Aspects of deuteron, neutron, and proton reactions with several different nuclei are discussed. Also several of the discussions deal with stripping reactions. (M.O.W.)

6297 (ORNL–3858(Vol.2), pp 82-90) EXPERIMENTAL STUDIES FOR HIGH-ENERGY RADIATION SHIELDING. (Oak Ridge National Lab., Tenn.).

Summaries of 7 shielding experiments are presented. The experiments deal with neutron and proton reactions with various targets and the yields from these irradiations. (M.O.W.)

6298 (PPAD–2137-566) NUCLEAR CHEMISTRY RESEARCH AT PRINCETON UNIVERSITY, 1964–1965. Annual Progress Report. Kaufman, S. B.; Naumann, R. A.; Thomas, T. D. (Princeton–Pennsylvania Accelerator, Princeton, N. J.). Aug. 25, 1965. Contract AT(30-1)-2137. 49p. Dep. mn; CFSTI $2.00 cy, $0.50 mn.

Results of studies on nuclear properties as revealed by high resolution electron and gamma spectroscopy are reported. Investigations of fission processes and high-energy nuclear- or meson-induced reactions are described. (J.R.D.)

6299 (PUC–1965-158) NUCLEAR SPINS AND MOMENTS OF ^{43}Sc AND ^{45}Ti [Thesis]. Cornwell, Robert G. (Princeton Univ., N. J. Palmer Physical Lab.). Mar. 1965. Contract AT(30-1)-937. 169p. Dep. mn; CFSTI $5.00 cy, $1.00 mn.

The nuclear spins and hyperfine structure intervals of scandium-43 and titanium-45 were measured by the atomic beam magnetic resonance method. The ^{43}Sc measurements were made in the $J = \frac{5}{2}$ atomic state of scandium and the ^{45}Ti measurements were primarily made in the $J = 3$ atomic state of titanium. From the known hyperfine interaction constants and nuclear moments of ^{45}Sc and ^{47}Ti the nuclear magnetic dipole and electric quadrupole moments were calculated. Various nuclear shell model spin and moment calculations are compared with the experimental results. The measured spins were generally expected, however various moment calculations predict differing moments. The calculations of McCullen, et. al., for the magnetic moment of ^{43}Sc agree well with experiment, but no nuclear shell model calculations predict the magnetic moment of ^{45}Ti with accuracy. The comparison of electric quadrupole moment predictions with the experimental results is less informative, partly due to the large uncertainty in the measured quadrupole moment of ^{43}Sc. (auth)

6300 (SGAE-PH–29/1965) DIE PROMPTE UND VERZOEGERTE GAMMASTRAHLUNG BEI DER KERNSPALTUNG. (Prompt and Delayed Gamma Rays in Nuclear Fission). Axmann, Hans Peter; Weinzierl, Peter (Oesterreichische Studiengesellschaft fuer Atomenergie G.m.b.H., Seibersdorf). [1965]. 23p.

A survey is given of the experimental investigations of γ radiations in nuclear fission from its discovery up to the present. The results were discussed and their significance was considered. A new type of nuclear spectroscopy was reported. (tr-auth)

6301 (TID–22165) ISOMERIC CROSS SECTION RATIOS FOR THE ^{46}Sc, ^{134}Cs, AND ^{188}Re ISOMERS [Thesis]. Special Report Number 54. Simons, Gale Gene (Kansas

State Univ., Manhattan. Engineering Experiment Station). 1962. Contract AT(40-1)-3356. 139p. Dep. mn; CFSTI $4.00 cy, $1.00 mn.

Isomeric cross section ratios were studied using (n,γ) reactions produced by reactor neutron bombardment. Isomeric pairs were produced by these reactions on scandium-45, cesium-133, and rhenium-188. Irradiation of scandium oxide and cesium oxide produced Sc-46, 46m, and Cs-134, 134m only. But since rhenium contains Re-185 and -187, a mixture of Re-186 (excessive activity was avoided) and 188 and 188m were produced. Cross section ratios were determined for three ranges of neutron energies: RSR, epicadmium, and thermal. After irradiation the samples were each counted. The decay, irradiation, and live-counting times are given. The data obtained were analyzed using IBM computers. The experimentally determined isomeric cross section ratios were then matched with the corresponding theoretically calculated ratios for the three isomeric pairs. (J.F.P.)

6302 (TID–22384) RECOIL-FREE SCATTERING OF GAMMA-RAYS. Final Technical Report, March 1, 1962–June 30, 1965. Major, John K.; Kalvius, G. Michael; Robinson, Berol L. (Western Reserve Univ., Cleveland, Ohio). Contract AT(11-1)-1146. 6p. Dep. mn; CFSTI $1.00 cy, $0.50 mn.

During this period, instrumentation for experiments on the Mössbauer effect was begun and completed, and recoil-free scattering studied. Brief discussions of work on instrumentation, resonant scattering, and nonresonant scattering are presented. (M.O.W.)

6303 (TID–22393) THE E2 INTERNAL-CONVERSION PROCESS IN ^{152}Gd AND ^{154}Gd AND THE BETA-GAMMA DIRECTIONAL CORRELATION IN THE DECAY OF ^{154}Eu [Thesis]. Zganjar, Edward Francis (Vanderbilt Univ., Nashville, Tenn.). Jan, 1966. Contract AT-40-1-GEN-33. 164p. Dep. mn; CFSTI $5.00 cy, $1.00 mn.

A description of the internal conversion process is presented. The difference between the "static" and "dynamic" effects of nuclear size was pointed out. Theoretical estimates based upon the no-penetration model of Rose and the surface current model of Sliv and Band indicate that the conversion process of E2 transitions is quite insensitive to the static and dynamic effects of nuclear size. Penetration effects are expected to be important only if the transition is highly retarded. Evidence was presented, however, which showed that the E2 conversion process in deformed nuclei did not agree with theoretical predictions. Angular correlations and particle parameters were discussed. It was shown that the measurement of particle parameters can provide a more sensitive test of the conversion process than the conversion coefficient. The presently accepted theory of first-forbidden beta decay was described. It was shown that those transitions which deviate from the ξ-approximation are of greatest interest and that the 1855-kev 1FNU transition in ^{154}Eu was expected to fall into this category. The expressions for the shape, comparative half-life, and beta-gamma directional correlation, which represent corrections to the ξ-approximation for a $3^-(\beta)2^+(\gamma)0^+$ transition, were presented. The "cancellation" and "selection rule" effects were discussed and the distinction between "K-forbiddennes" and "j-forbiddennes" was set forth. Descriptions of the experimental apparatus, experimental procedures, and methods of data analysis were presented. Contained therein are discussions concerning the calibration of the lens spectrometer, the corrections for finite angle, and attenuation effects in directional correlations. Measurements of the K-, L-, and M'-particle parameters of the 123-kev, E2 transition in ^{154}Gd and the K-particle parameter of the 344-kev, E2 transition in ^{152}Gd are described. These nuclei lie at the edge of the deformed region where ^{152}Gd is just outside (spherical) and ^{154}Gd is inside (deformed). (M.O.W.)

6304 (TID–22401) EXCHANGE CURRENTS IN THE DEUTERON [Thesis]. Adler, Ronald John (Stanford Linear Accelerator Center, Stanford Univ., Calif.). June 1965. Contract AT(04-3)-400. 151p. Dep. mn; CFSTI $5.00 cy, $1.00 mn.

The electromagnetic structure of the deuteron is studied by field-theoretic methods. The effects of mesonic exchange currents on the deuteron parameters are investigated, using the impulse approximation. The relation of this approach to the dispersion-theoretic, relativistic approach to the analysis of the deuteron structure is discussed. (T.F.H.)

6305 (UCRL–11784) DECAY SCHEMES OF ODD-ODD EINSTEINIUM ISOTOPES [Thesis]. McHarris, William Charles (Lawrence Radiation Lab., Univ. of California, Berkeley). July 1965. Contract W-7405-eng-48. 191p. Dep. mn; CFSTI $5.00 cy, $1.00 mn.

The radiations from the heavy odd-odd, alpha-emitting isotopes, ^{254}Es and ^{252}Es, were studied and interpreted in light of the Bohr-Mottelson unified theory of deformed nuclei and the accompanying Nilsson wave functions. The study was based on their alpha-particle spectra, which were obtained both with Si alpha detectors and with a high-resolution, double-focussing magnetic spectrograph. Complementing these were gamma-ray spectra obtained with NaI scintillators and Ge gamma detectors conversion-electron spectra obtained with Si electron detectors and precision permanent-magnet spectrographs, and various time-to-height and delayed-coincidence spectra. Levels in the daughter nuclei were grouped into rotational bands, and the experimental properties of these were compared with predictions based on couplings of the odd-nucleon states found in neighboring odd-mass nuclei. Agreement was found to be excellent, indicating that the odd proton and odd neutron in these odd-odd states move with considerable independence of each other. The decay scheme of ^{254}Es was worked out in detail, indicating that the 6.437-Mev, favored alpha group populates a $K\pi I = 7 + 7$ level at 85.5 kev above the ground state of ^{250}Bk. A cascade of three electromagnetic transitions is required to de-excite this level to the 2–2 ground state: a 7-kev E2, with a half-life of 213 μsec, that leads to a 4 + 5 level at 78.1 kev above ground, a fast 42.6-kev M1-E2 rotational transition to the 4 + 4 level at 35.5 kev, and branching transitions, mostly a 35.5-kev M2, that give the 4 + 4 level a 29 μsec half-life and connect it with the ground state. Many subsidiary bands and levels were also studied and assigned. To explain the distortions found for many of the bands in ^{250}Bk and ^{248}Bk, the nuclear Coriolis interaction was invoked. This was developed from the model of a particle coupled to a rigid rotor, and semi-quantitative calculations were made that explained the experimental data quite adequately. (auth)

6306 (UCRL–16217) ENERGY DEPENDENCE OF THE POLARIZATION IN p-^{16}O ELASTIC SCATTERING BETWEEN 21 AND 53 Mev. Boschitz, E. T.; Chabre, M.; Conzett, H. E.; Slobodrian, R. J. (Lawrence Radiation Lab., Univ. of California, Berkeley). Aug. 1965. Contract W-7405-eng-48. 8p. (CONF-650928–13). Dep. mn; CFSTI $1.00 cy, $0.50 mn.

From International Conference on Polarization Phenomena of Nucleons, Karlsruhe.

The polarization resulting from the elastic scattering of 21- to 53-Mev polarized proton beams by ^{16}O is measured at seven discrete energies. The differential cross section is also measured at two of these energies. It is concluded that the optical model fits the experimental data fairly well for the proton–^{16}O elastic scattering in this energy range. (T.F.H.)

6307 (UCRL–16439) APPLICATIONS OF SMALL COMPUTERS IN NUCLEAR SPECTROSCOPY. Robinson, Lloyd (Lawrence Radiation Lab., Univ. of California, Berkeley). Oct. 15, 1965. Contract W-7405-eng-48. 8p. (CONF-651001–13). Dep. mn; CFSTI $1.00 cy, $0.50 mn.

From IEEE Nuclear Science Symposium, San Francisco.

Two data-acquisition systems are described; both built around small digital computers and designed for use in nuclear spectroscopy. The computers are used for storage of data, graph plotting, control of hardware devices and CRT displays, and for routine arithmetical operations required in the preliminary analysis of experimental data.

Both computer systems can be easily operated by relatively inexperienced personnel. Most routine operations can be controlled with simple multiposition selector switches, although more specialized operations are carried out with a question-and-answer routine on the typewriter. Operations involving CRT display can be initiated with the light pen. With this procedure, routine operation of the computer requires little more training than is needed to operate a pulse-height analyzer. (auth)

6308 (ANL-Trans-243) SHELL EFFECTS IN NUCLEAR FISSION. Geilikman, B. T. Translated by Elmar K. Wilip (Argonne National Lab., Ill.), from report IAE-818, 4p. Dep. mn; CFSTI $1.00 cy, $0.50 mn; JCL $1.10 fs, $0.80 mf.

It is shown that several singularities in the fission process (e.g., the dependence of the fission fragments' excitation energy and kinetic energy on the fission-fragment mass ratio) can be explained by the liquid-drop model, if the shell effects in the fragments prior to the scission of the neck of the fissioning nucleus are considered. It is also shown that the liquid-drop and shell models are not incompatible for the analysis of fission. (T.F.H.)

6309 (ANL-Trans-245) PHOTOFISSION OF EVEN-EVEN NUCLEI NEAR THE THRESHOLD. Rabotnov, N. S.; Smirenkin, G. N.; Soldatov, A. S.; Usachev, L. N.; Kapitsa, S. P.; Tsipenyuk, Yu. M. Translated by Elmar K. Wilip (Argonne National Lab., Ill.), from Phys. Chem. Fission, Proc. Symp., Salsburg, 1965, 135-56(1965). 28p. Dep. mn; CFSTI $2.00 cy, $0.50 mn; JCL $2.60 fs, $1.04 mf.

No quadrupole component in the angular distribution of photofission fragments of ^{238}U at energies between 6 and 10 Mev could be found. A quadrupole component is detected in the gamma energy range of 5 to 6 Mev, in agreement with theoretical concepts that follow from the model of fission channels. The analysis of the relative contribution of the quadrupole, dipole, and isotropic components of the angular fragment distribution indicates a previously theoretically predicted structure of fission channels. (auth)

6310 THE $^{93}Nb(d,t)^{92}Nb$ REACTION. Hamburger, E. W. (Universidade de Sao Paulo, Brazil). Anais Acad. Brasil. Cienc., 36: 399-402(1964).

An experiment on the $^{93}Nb(d,t)^{92}Nb$ reaction at 15 Mev incident energy is described and compared to a recent similar experiment at 11 Mev and to a (p,d) experiment at 22 Mev. The three experiments show the same six levels in the final nucleus ^{92}Nb, corresponding to the $(\pi g_{9/2})$ $(\nu d_{5/2})$ configuration. (auth)

6311 COUPLING BETWEEN THE ENERGY GAP AND SINGLE PARTICLE ENERGY. Kobe, Donald H. (Uppsala Univ.). Ann. Phys. (N. Y.), 35: 42-52(Oct. 1965).

The Principle of Compensation of Dangerous Diagrams is applied to second order which, when combined with the quasi-particle self-energy to second order, gives a set of two nonlinear integral equations coupling the energy gap and the single particle energy. These equations are solved for a singlet state shell type interaction. (auth)

6312 PROJECTION OPERATORS FOR REARRANGEMENT COLLISIONS. Coz, Marcel (Massachusetts Inst. of Tech., Cambridge). Ann. Phys. (N. Y.), 35: 53-66 (Oct. 1965). (MIT-2098-143).

As in Mittleman's recent paper a system of equations which describes the scattering of a system into a rearranged channel is derived. Instead of defining a projection operator into the open channel subspace, elementary projectors into each open channel are defined; this definition leads to more simplified equations than those obtained by Mittleman. Discussion of the existence of these elementary projectors is given. (auth)

6313 FISSION NEUTRONS OF EXCITED NUCLEI. Eismont, V. P. At. Energ. (USSR), 19: 113-16(Aug. 1965). (In Russian).

The required time for fragment acceleration to an assigned rate was calculated and correlated to the excited nucleus lifetime computed in relation to the neutron emissions. The obtained data led to the assumption that during nuclear fission at ~20 Mev energy and over, a certain portion of neutrons (increasing with the excitation) are emitted until the fragment reaches the maximum acceleration point. This consideration eliminates certain existing contradictions and indicates that in the case of high excitation, the method for determining the number of neutrons as a function of the fragment mass on the basis of fragment energy correlations may be obsolete. (tr-auth)

6314 PROMPT FISSION GAMMA-RAY QUANTA. Zommer, V. P.; Savel'ev, A. E.; Prokof'ev, A. I. At. Energ. (USSR), 19: 116-19(Aug. 1965). (In Russian).

The spectrum of prompt γ quanta of ^{235}U fission by thermal neutrons was precisely computed using the basic assumptions of the statistical theory of neutron and γ-quantum emissions from excited nuclei. The shape of the spectrum coincided approximately with the experimentally derived spectrum. However, the estimated total γ quantum energy ($\leq$ 6.2 Mev) was much lower than the experimental (8 to 9 Mev) energy. It was concluded that the divergence may be eliminated by taking into account, in the computation of residual excitation, the rarity of nuclear fragment levels near the ground state (0 to 2 Mev). (R.V.J.)

6315 RELATIVE ABUNDANCES OF DELAYED NEUTRON GROUPS FROM PHOTOFISSION OF ^{238}U. Nikotin, O. P.; Petrzhak, K. A. At. Energ. (USSR), 19: 185(Aug. 1965). (In Russian).

Relative yields of delayed neutrons in ^{238}U fission by bremsstrahlung at energies of 10 to 15 Mev were studied using 15 × 10 × 3 mm uranium plate irradiated inside of a betatron. The results of 700 irradiations revealed six groups of delayed neutrons with half life periods 55.0 ± 2.0, 21.0 ± 0.6, 5.4 ± 0.3, 2.2 ± 0.2, 0.7 ± 0.2, and 0.18 ± 0.03 sec; the relative yields from these groups at 14.0 Mev were 0.020 ± 0.001, 0.158 ± 0.008, 0.142 ± 0.012, 0.340 ± 0.014, 0.180 ± 0.010, and 0.160 ± 0.020, respectively. Corrections made for detector efficiency as a function of the neutron energies are discussed. (R.V.J.)

6316 DELAYED GAMMA RAYS FROM ^{235}U FISSION. Popeko, L. A.; Val'skii, G. V.; Kaminker, D. M.; Petrov, G. A. At. Energ. (USSR), 19: 186-8(Aug. 1965). (In Russian).

An electron device with a fast-slow coincidence scheme was used for recording delayed γ emission of fragments at 10 to 70 nsec and energy range of 30 to 500 kev. About 200 μg of ^{235}U was coated on a 20 $\mu g/cm^2$ Al_2O_3 plate. The target was placed into a vacuum chamber with neutron beam emitted from a VVR-M reactor. The tabulated data on the yield of delayed γ quanta showed 4.6 ± 0.5 number of quanta for 100 fissions for heavy fragments and 9.1 ± 1 for light fragments. (R.V.J.)

6317 THE ANGULAR DISTRIBUTION OF 5.6-Mev GAMMA RAYS FROM THE CAPTURE BY ^{124}Sn OF 62-ev NEUTRONS. McNeill, K. G.; McConnell, D. B.; Firk, F. W. K. (Atomic Energy Research Establishment, Harwell, England). Can. J. Phys., 43: 2156-61(Dec. 1965).

Angular distribution measurements were made on the near-ground-state gamma-ray transitions from the state in ^{125}Sn excited by the capture by ^{124}Sn of 62-ev neutrons. The distribution is essentially isotropic. In conjunction with other evidence, it is concluded that the capturing state is a p $\frac{1}{2}$ state. (auth)

6318 GAMMA-RAY TRANSITIONS IN ^{15}O AND ^{15}N. Alexander, T. K.; Litherland, A. E.; Broude, C. (Atomic Energy of Canada Ltd., Chalk River, Ont.). Can. J. Phys., 43: 2310-18(Dec. 1965). (AECL-2364).

The gamma rays from the first two excited states of ^{15}O and ^{15}N populated by the $^{14}N + d$, $T(^{16}O,\alpha\gamma)^{15}N$, and $^{16}O(^3He,\alpha\gamma)^{15}O$ reactions were observed with a Ge(Li) spectrometer. The measured energy separations are 50 ± 5 kev for the ^{15}O doublet and 28.5 ± 3 kev for the ^{15}N doublet. The difference between the 5.24-Mev gamma ray from ^{15}O and the 5.27-Mev gamma ray from ^{15}N is 29 ± 1 kev. From Doppler-shift and broadening measurements of the energies of the gamma rays from the $T(^{16}O,\alpha\gamma)^{15}N$ and $^{16}O(^3He,\alpha\gamma)^{15}O$ reactions, information on the mean lifetimes

of the states was obtained. The mean lifetimes of the 5.30 and 5.27-Mev states of ^{15}N are $4.3 \pm 1.8 \times 10^{-14}$ sec and $>10^{-12}$ sec respectively. The mean lifetimes of the 5.19- and 5.24-Mev states of ^{15}O are $<3 \times 10^{-13}$ sec and $>10^{-12}$ sec respectively. (auth)

6319 EXCITATION CURVE OF THE (n,2n) REACTION ON ^{63}Cu FROM 16.59 TO 17.71 Mev. Bardolle, Gerard; Cabe, Jean; Laurat, Michel (Commissariat a l'Energie Atomique, Montrouge, France). Compt. Rend., 261: 1266-8(Aug. 2, 1965). (In French).

The utilization of a Van de Graaff beam at 2 Mev made it possible to measure the excitation curve of the reaction $^{63}Cu(n,2n)$. The curve obtained has a structure of weak amplitude and a length of the order of 50 kev. (tr-auth)

6320 EVIDENCE OF TWO-BODY INTERACTIONS IN THE REACTION $^{9}Be(n,2n)$ AT 14 Mev. Bouchez, Robert; Perrin, Claude; Giorni, Alain, Darves-Blanc, Robert (Univ., Grenoble, France). Compt. Rend., 261: 1269-72 (Aug. 2, 1965). (In French).

The analysis of 1700 events corresponding to the reaction $^{9}Be(n,2n)$ at 14 Mev shows that the reaction proceeds by the inelastic scattering $^{9}Be(n,n')$ followed by the disintegration of the $^{9*}Be$ excited level to the 0^+ or 2^+ state of ^{8}Be. The excited levels of ^{9}Be thus observed are: 6.76, 7.94, and 9.1 Mev. (tr-auth)

6321 STUDY OF THE α EMISSION OF ^{230}Pa. Briand, Jean-Pierre; Chevallier, Pierre (Univ., Paris). Compt. Rend., 261: 2629-32(Oct. 4, 1965). (In French).

The α emission of ^{230}Pa(T = 17.7 days) was studied. The branching ratio found was 3.1×10^{-5}. Three fine structure rays were observed and their identification is briefly discussed. (tr-auth)

6322 GAMMA-GAMMA ANGULAR CORRELATION IN ^{125}Sn. Nigam, A. K.; Bhattacharyya, R. (Saha Inst. of Nuclear Phys., Calcutta). Indian J. Phys., 39: 215-18 (May 1965).

Spin assignment to the 2.23, 1.98, 1.88, 1.41 and 1.07 Mev of ^{125}Sb was made from directional angular correlation measurements. (auth)

6323 COHERENT SCATTERING CROSS-SECTIONS OF ^{60}Co AND ^{137}Cs GAMMA RAYS. Narasimha Murty, V. A.; Rama Rao, J.; Lakshminarayana, V.; Jnanananda, Swami (Andhra Univ., Waltair, India). Indian J. Pure Appl. Phys., 3: 366-9(Oct. 1965).

Total coherent scattering cross-sections at photon energies 1.332 and 0.662 Mev were determined in three heavy elements (Pb, Pt and Ta) and two light elements (Sn and Zr) at various angles of scattering between 20 and 90°. The results were compared with two sets of theoretical data, one involving the Rayleigh scattering amplitudes as computed from the form-factor theory and the other derived from the exact formalism developed by Brown and coworkers [Brown, G. E., Woodward, J. B. & Peierls, R. E., Proc. roy. Soc., 227A (1954), 51]. For heavy elements and large momentum transfers, good agreement is noticed with the latter theory. For low momentum transfers and light elements, form-factor values are more accurate. These trends are discussed and explained. (auth)

6324 RESONANT SCATTERING OF GAMMA QUANTA BY ^{140}Ce NUCLEI. Begzhanov, R. B.; Islamov, A. A. (Inst. of Nuclear Physics, Academy of Sciences, USSR). Izv. Akad. Nauk Uz. SSR, Ser. Fiz.-Mat. Nauk, No. 1, 67-71(1965). (In Russian).

Sources of ^{140}La were prepared by exposure of liquid and solid La samples to a 1.8×10^{13} n/cm^2 sec neutron beam. The lifetime of the 1597-kev first excited state of ^{140}Ce was measured by self-absorption of the resonant radiation from ^{140}La. The lifetime was found to be $(2.15 \pm 0.80) \times 10^{13}$ sec, in good agreement with data obtained previously by the Coulomb excitation method and with an empirical formula given by Grodzins. (M.J.T.)

6325 ANGULAR DISTRIBUTION OF SHOWER PARTICLES IN COLLISIONS BETWEEN 24-Gev PROTONS AND NUCLEONS AND PHOTOEMULSION NUCLEI. Abduzhamilov, Sh.; Belen'kii, V. M.; Chernova, L. P.; Chernov, G. M. (Inst. of Nuclear Physics, Academy of Sciences, USSR). Izv. Akad. Nauk Uz. SSR, Ser. Fiz.-Mat. Nauk, No. 1, 98-104(1965). (In Russian).

General characteristics of the distributions of the lateral and azimuthal angles of the secondary particles generated by protons colliding with nucleons and nuclei in emulsion were studied. A set of G-5 plates with 600 μ emulsion was irradiated in the CERN accelerator with 24-Bev protons. The lateral angular distribution, as measured by the quantity $x = \log|\tan \Theta|$, was found to be nearly normal for both proton and nucleon collisions and for collisions with heavy particles. A theoretical estimate of the probability density of x, starting from a maxwellian distribution of the particle cms momenta, was made, and an analytic expression was obtained for the mathematical expectation in terms of integrals that have no divergences and can be readily evaluated numerically. A previously developed high-sensitivity procedure was used to investigate the distribution of the azimuthal angles in showers generated by cosmic-ray particles; no correlations were observed other than those due to the momentum conservation law. A comparison of the distribution with respect to x for pions from pN collisions with the theoretical calculations indicates that the angular distribution remains anisotropic at very large multiplicities. (ATD)

6326 $^{14}N(^{3}He,\alpha)^{13}N$ ANGULAR DISTRIBUTION LEADING TO THE GROUND STATE IN ^{13}N. Ali, M. M.; Gupta, H. M. Sen (Dacca Univ., Pakistan). J. Nat. Sci. Math., 5: 25-8(Apr. 1965).

Angular distribution of α particles arising from (He-3, α) reaction in ^{14}N leading to the ground state in ^{13}N is obtained at 25.7 and 27.0 Mev in the cms range of angles 16–65°. The distribution is analyzed in terms of plane wave Born approximation direct interaction model with l = 1 and interaction radius R = 6.0 fm. (auth)

6327 DISINTEGRATION OF ^{134}Cs. Huc, J. M.; Foucher, R. (Faculte des Sciences, Orsay, France). J. Phys. (Paris), 26: 390-8(July 1965). (In French).

A partial scheme is given for the excited levels of ^{134}Ba, following a detailed analysis of the sum-coincidence γ spectra. (auth)

6328 141-Mev POLARIZED PROTON BEAM OF THE ORSAY SYNCHROCYCLOTRON. APPLICATION IN THE MEASUREMENT OF POLARIZATION IN p-^{12}C AND p-d ELASTIC SCATTERING. Poulet, M.; Michalowicz, A.; Le Guen, Y.; Kuroda, K.; Cronenberger, D.; Coignet, G. (Institut du Radium, Orsay, France). J. Phys. (Paris), 26: 399-402(July 1965). (In French).

The polarized proton beam from the Orsay synchrocyclotron is described. The protons have an energy of 141 ± 2 Mev and 61.6 ± 2.5 % polarization. Polarization in p–^{12}C and p–d elastic scattering was measured in the angular range 10 to 25° lab for carbon and 23 to 160° cms for deuterium. The results are compared with previous values and with theoretical calculations for deuterium. (auth)

6329 CALCULATION OF PROTON POLARIZATION IN p-d ELASTIC SCATTERING AT 150 Mev. Benoist-Gueutal, P.; Gomez-Gimeno, F. (Institut du Radium, Orsay, France). J. Phys. (Paris), 26: 403-5(July 1965). (In French).

The proton cross section and polarization are calculated in the impulse approximation for direct scattering and in the Born approximation for exchange scattering. Comparison with experimental values points out the shortcomings of the Born approximation. The calculation of a second order correction is proposed. (auth)

6330 REACTION (p,2p) ON SOME ISOTOPES OF TITANIUM. Cohen, J. P.; Albouy, G.; Poffe, N. (Institut du Radium, Orsay, France). J. Phys. (Paris), 26: 427-9 (July 1965). (In French).

The reaction (p,2p) on the titanium isotopes 49, 48, and 47 at 155 Mev was studied by measuring the radioactivity of the residual nucleus. Cross sections for these reactions were found to be 11.8 ± 2.65, 26.6 ± 5.5, and 21.5 ± 9.4 mb

respectively. The difference between the first two values is large, in spite of relative errors. An attempt was made to localize the 1 d $\frac{5}{2}$ subshell energy levels in titanium nuclei, using Benioff's formalism. It seems that the excitation energy of the 1 d $\frac{5}{2}$ proton hole state in ^{47}Sc could be estimated at 9.1 ± 1.3 Mev. (auth)

6331 INVESTIGATION OF ROTATION LEVELS IN ODD-ODD NUCLEUS ^{234m}Pa. Foucher, R.; Lagrange, J. M.; Rahmouni, O.; Sergolle, H. (Laboratoire Joliot-Curie de Physique Nucleaire, Orsay, France). J. Phys. (Paris), 26: 430-2(July 1965). (In French).

The γ spectrum of ^{234m}Pa (UX2) was examined from the β decay of ^{234}Th. New γ transitions between 115 and 185 kev were observed. (auth)

6332 DYNAMIC NUCLEAR STRUCTURE EFFECTS IN INTERNAL CONVERSION. Berenyi, Denes (Nuclear Research Inst., Hungarian Academy of Sciences, Debrecen). Magyar Fiz. Foly., 13: 251-72(1965). (In Hungarian).

Basic theoretical studies on dynamic nuclear structure effects in internal conversion are reviewed, mentioning those of Church and Weneser, Green and Rose, the M1-transition studies by Reiner, Kisslinger, and Grechikhin, and the E1-transition studies by Nilsson and Rassmussen. Borisoglebskii's investigations on higher forbidden electric and magnetic transitions, which give a quantum-mechanical treatment of the escape probability of conversion electrons, are considered. Magnetic and electric multipole transitions and electric monopole transitions are discussed. Results of previous experimental studies on E2 transitions, dynamic nuclear structure arising from internal conversion, and E0 transitions are presented. 88 references. (M.J.T.)

6333 KINEMATIC RELATIONS IN REACTIONS OF THE FORM A + B → C + D + E. Ohlsen, G. G. (Australian National Univ., Canberra). Nucl. Instrum. Methods, 37: 240-8(Nov. 1965).

The kinematic and phase space formulas that are relevant to nuclear reactions in which three final particles are produced are summarized. Detection of one or of two of the final particles is considered. A FORTRAN II program (KINEM) making use of these formulas is included. (auth)

6334 STUDY OF d-d REACTIONS IN SELF TARGETS WITH COATINGS. Philipp, G.; Hofmann, A. (Univ., Erlangen-Nuremberg). Nucl. Instrum. Methods, 37: 313-17 (Nov. 1965). (In German).

Several metals with thin evaporated layers are bombarded by 200-kev deuterons. The neutron yield of the reaction ^{2}H(d,n)^{3}He + 3.26 Mev in these self-regenerating targets, is measured for different metals and as a function of the thickness of the evaporated metal layer. The results can be understood by means of simple concepts of diffusion theory. (auth)

6335 USE OF A LIQUID HELIUM SCINTILLATION COUNTER IN A SEARCH FOR EXCITED STATES OF ^{5}He BY ELASTIC SCATTERING OF 22- TO 29-Mev NEUTRONS. Benenson, R. E. (Columbia Univ., New York); Lightbody, D. B.; Sayres, A.; Stephens, W. E. Nucl. Instrum. Methods, 37: 340-4(Nov. 1965).

The elastic scattering of neutrons by ^{4}He is measured at neutron energies of 22 to 29 Mev. Pulse-height distributions of recoil alpha particles are measured in a liquid-He scintillation detector, and are used as an approximate method for determining the angular distributions of the scattered neutrons. No narrow resonances indicative of energy levels of ^{5}He are found above a previously reported level at 22.15 Mev. Means for increasing the resolution of the experiment are discussed. (T.F.H.)

6336 CONDITION FOR MAXIMUM SINGLE-LINE MOESSBAUER ABSORPTION. Shimony, U. (Massachusetts Inst. of Tech., Cambridge). Nucl. Instrum. Methods, 37: 350-2(Nov. 1965).

The absorber thickness for Moessbauer studies at which optimum resonance absorption and re-emission occurs is found analytically, for the case of a single resonant energy level. (T.F.H.)

6337 EFFECTIVE NUCLEON-NUCLEON INTERACTIONS IN THE Y, Zr, Nb, Mo AND Tc ISOTOPES. Vervier, J. (Centre d'Etude de l'Energie Nucleaire, Mol, Belg.). Nucl. Phys., 75: 17-78(1965).

The energy levels of the Nb, Mo, and Tc isotopes with a neutron number N between 50 and 56 are first calculated under the assumptions that their protons and neutrons outside Z = 40 and N = 50 are in the $1g_{\frac{9}{2}}$ and $2d_{\frac{5}{2}}$ orbits, respectively, and that the effective nucleon-nucleon interactions are given by the experimental spectra of ^{92}Mo, ^{92}Zr, and ^{92}Nb. Good agreement with experiment is generally achieved for energy level positions, spectroscopic factors for direct reactions, magnetic and quadrupole moments, M1 and E2 transition probabilities. In order to introduce the influence of the $2p_{\frac{1}{2}}$ proton orbit in this mass region, the nuclei with 39 ≦ Z ≦ 43 and N = 50 are then investigated and the effective proton-proton interaction in the $2p_{\frac{1}{2}}$ and $1g_{\frac{9}{2}}$ orbits is determined; the low-lying levels of these isotopes and five E2 transition probabilities in ^{90}Zr and ^{92}Mo are accurately reproduced by these calculations. Using the latter interaction together with effective neutron-neutron and proton-neutron interactions whose validity has been tested earlier, the Y, Zr, and Nb isotopes with 51 ≦ N ≦ 56 are then studied taking thoroughly into account the influence of the $2p_{\frac{1}{2}}$ and $1g_{\frac{9}{2}}$ proton orbits, and assuming as before that the neutron outside N = 50 are in the $2d_{\frac{5}{2}}$ orbit. Satisfactory agreement is again generally obtained. Comparison with the previous calculations shows the ability of the effective nucleon-nucleon interactions to absorb the influence of configuration mixings and justifies their use to correlate a large number of experimental data in widely different fields. (auth)

6338 ACTIVATION CROSS SECTIONS FOR REACTIONS OF Rh AND Ru WITH 14.7 Mev NEUTRONS. Gray, Peter R.; Zander, Arlen R.; Ebrey, Thomas G. (Phillips Petroleum Co., Bartlesville, Okla.). Nucl. Phys., 75: 215-25(1965).

The cross sections for 12 reactions of rhodium and ruthenium isotopes with 14.7 Mev neutrons were measured. The reactions studied and results obtained are: ^{103}Rh(n,n'α)^{99m}Tc, 150 ± 30 μb; ^{103}Rh(n,^{3}He)^{101}Tc, <400 nb; ^{103}Rh(n,2p)^{102}Tc, <3.0 μb; ^{96}Ru(n,p)^{96}Tc, 170 ± 30 mb; ^{96}Ru(n,2n)^{95}Ru, ≈2.6 ± 0.3 b; ^{99}Ru(n,p)^{99m}Tc + ^{100}Ru(n,d) ^{99m}Tc, <16 ± 4.0 mb; ^{101}Ru(n,p)^{101}Tc + ^{102}Ru(n,d) ^{101}Tc, 36 ± 3.0 mb; ^{102}Ru(n,p)^{102}Tc, $6.7^{+2.5}_{-2.0}$ mb; ^{104}Ru(n,p)^{104}Tc, 7.2 ± 1.0 mb; ^{104}Ru(n,γ)^{105}Ru, 2.5 ± 0.5 mb; ^{104}Ru(n,2n)^{103}Ru, 2.5 ± 0.5 mb; ^{104}Ru(n,α)^{101}Mo, 2.6 ± 1.0 mb. The results are compared with theoretical predictions and certain cross section correlation studies. (auth)

6339 THE ELASTIC AND INELASTIC SCATTERING OF 30.3 Mev PROTONS BY Si. Cole, Robert K. (Univ. of Southern California, Los Angeles); Waddell, Charles N.; Dittman, Roger R.; Sandhu, Harbhajan S. Nucl. Phys., 75: 241-54(1965).

The differential cross sections for the scattering of 30.3-Mev protons by the ground state and the first excited state of Si were measured from 15 to 50° in the center of mass. The elastic scattering was analyzed using the diffuse-surface optical model of the nucleus. Both the elastic and inelastic scattering angular distributions were analyzed using the generalized (coupled-channel) optical model of Buck. The inelastic scattering angular distribution is also compared to distorted-wave calculations. (auth)

6340 APPLICATION OF THE QUASI-PARTICLE METHOD TO ^{63}Cu. Beres, William P. (Massachusetts Inst. of Tech., Cambridge). Nucl. Phys., 75: 255-96 (1965). (MIT-2098-116).

The wave functions generated by (i) the quasi-boson plus quasi-proton scheme and (ii) the two quasi-neutron plus quasi-proton scheme are used to study electric transition rates and inelastic alpha scattering cross sections in ^{63}Cu. This nucleus was chosen as a test case for these two methods because of readily available and fairly complete experimental data. Scheme (ii) gives many more low-lying states than scheme (i); however, in both schemes a "quartet" of

spins $\frac{1}{2}^-$, $\frac{3}{2}^-$, $\frac{5}{2}^-$, and $\frac{7}{2}^-$ appears with strong electric transitions and large inelastic alpha scattering cross sections that also obey the well-known parity phase rules for excitation by alpha particles. Such states are identified with the "collective" levels observed experimentally for ^{63}Cu. It is found that scheme (i) is far superior to scheme (ii) as regards agreement between calculation and experiment for negative parity levels. In the case of positive parity levels, however, scheme (i) turns out to be unsuitable and scheme (ii) is used. In this case eight positive parity levels of a collective nature are produced. Comparison with observed energies and excitation cross sections in alpha particle scattering is made in all cases where such experimental data are available. Sum rules for electric quadrupole transitions are also compared with experiment. (auth)

6341 T = 2 STATES IN ^{16}O. Covello, A.; Sartoris, G. (Rutgers Univ., New Brunswick, N. J.). Nucl. Phys., 75: 297-304(1965).

The T = 2 states in ^{16}O are calculated as two-particle, two-hole excitations using various finite range forces. In addition to well-behaved forces a hard-core potential is considered. The comparison with experiment shows that the best agreement is obtained with a Yukawa-Rosenfeld force. (auth)

6342 T = 2 LEVELS IN ^{16}O. Leonardi, R.; Loncke, P.; Pradal, J. (Institut de Physique Nucleaire, Orsay, France). Nucl. Phys., 75: 305-8(1965).

After recent experimental evidence of T = 2 levels in ^{16}O, a second RPA calculation (two particles–two holes excitations) was carried out to account for these levels. The diagonalization process covers all the $(2\hbar\omega)$ configurations. Results depend essentially on the exchange mixture of the potential. Fairly good agreement with experiment is reached with a Rosenfeld-Yukawa potential. (auth)

6343 VARIATIONAL PRINCIPLE AND COMPENSATION METHOD IN PAIRING INTERACTION. Rho, M. (Institut de Physique Nucleaire, Orsay, France. CEN, Saclay, France). Nucl. Phys., 75: 309-20(1965).

The connection between the variational principle and the Bogolyubov compensation principle in the treatment of the nuclear pairing interaction is examined. It is found that to the second order of perturbation theory, one can write down an expression for the ground state energy, whose stationarity condition is equivalent to the compensation equation determining the "energy gap" and the "occupation factors". To higher orders (greater than second order), this in general does not hold, but under certain conditions one may derive the compensation equation from the stationarity of the ground state energy. (auth)

6344 SELF-CONSISTENT THEORY OF BOUNDED ROTATIONAL SPECTRA. I. TWO-DIMENSIONAL ROTATOR. Dreizler, R. M.; Klein, A. (Univ. of Pennsylvania, Philadelphia). Nucl. Phys., 75: 321-43(1965).

The effect of an upper bound of the spectrum for rotational motion of a set of particles confined to move in a plane is studied by means of the generalized Hartree-Fock approximation (GHFA) without pairing. The results can be expressed as corrections to the wave functions and the collective energies of the A-nucleon and (A ± 1)-nucleon systems of the previously considered unbounded case. Full self-consistency of the basic equations in the bounded case is assured under the same restrictions that limited the general accuracy of the method for the unbounded spectrum. A detailed quantitative discussion of the collective energies of the A-nucleon system shows results that are interesting enough to warrant an investigation of the full three-dimensional problem. (auth)

6345 VIBRATIONS, STRENGTH FUNCTIONS AND INTERMEDIATE STRUCTURE. Lande, A.; Brown, G. E. (Princeton Univ., N. J.). Nucl. Phys., 75: 344-52(1965). (PUC-1965-159).

The strength functions for single-particle states in ^{59}Ni are calculated in a simple model which couples the $p_{\frac{3}{2}}$, $f_{\frac{5}{2}}$, $p_{\frac{1}{2}}$, $g_{\frac{9}{2}}$, $d_{\frac{5}{2}}$, $s_{\frac{1}{2}}$, and $d_{\frac{3}{2}}$ neutron states with various numbers of 2^+ and 3^- core vibrations. The coupling splits the single-particle strength into many states. The neutron energies are taken from the experiments of Fulmer, McCarthy, Cohen, and Middleton, and the properties of the core are determined by the energies of the lowest 2^+ and 3^- states in ^{58}Ni. The only parameters which appear are the magnitudes of the $\lambda = 2$, 3 multipole terms of the particle-core interaction. The general complexity of the strength function is roughly that observed by Fulmer et al. (auth)

6346 SCATTERED NEUTRONS AND GAMMA RAYS FROM THE ^{16}O(n,n′γ)^{16}O REACTION AT E_n = 14.1 Mev. McDonald, W. J.; Robson, J. M.; Malcolm, R. (Univ. of Ottawa). Nucl. Phys., 75: 353-70(1965).

Excitation of levels in ^{16}O at 0, 6.1, 7, 8.9, and 11 Mev by 14.1-Mev neutron scattering was observed by using time-of-flight techniques to detect the scattered neutrons and de-excitation gamma rays. Differential cross sections were obtained for the scattered neutron groups. The elastic data were fitted using an optical model with reasonable well parameters, and the inelastic data corresponding to Q = 6.1 Mev were compared with theoretical predictions for direct excitation of a collective octupole state at 6.13 Mev. For the gamma rays, energy, yield and angular distribution measurements were carried out, and a coincidence technique was used to observe cascade gamma ray events. From the information obtained, a set of excitation cross sections for the inelastic scattering process was deduced which was in good agreement with the neutron scattering data. (auth)

6347 DETERMINATION OF INTENSITIES AND MULTIPOLARITIES OF HIGH-ENERGY γ-TRANSITIONS ACCOMPANYING THE DECAY OF ^{182}Ta. Dzelepov, B. S. (Mendeleev Research Inst. for Metrology, Leningrad); Vitman, V. D.; Voinova, N. A. Nucl. Phys., 75: 371-80(1965).

The ^{182}Ta γ-transition intensities with energies above 900 kev were measured accurately on the elotron of the USSR Mendeleyev Research Institute. Metal Ta activated by neutrons in the reactor of the Ioffe Physical-Technical Institute was used as the source. A total of 20 γ transitions was observed. Multipolarities and in some cases percentages of different multipoles were determined for them. The multipolarities of 1342, 1372, 1386, 1410, (1435), and 1453 kev γ-transitions were determined for the first time. The ^{182}W level scheme is discussed. From the analysis of the reduced transition probabilities the following quantum characteristics are assigned to the ^{182}W excited levels K, I^π: $2,2^+$(1222); $0,2^+$(1258); $2,2^-$(1289); $2,3^+$(1331); $(1),2^+$(1410); $I^\pi = 3^-$(1372); 2^-(1435). The data do not contradict the values $I^\pi = 4^-$ for the 1488- and 1554-kev levels and $I^\pi = 4^+$ for the 1443-kev level. (auth)

6348 ROTATIONAL BANDS OF WELL-DEFORMED NUCLEI STUDIED FROM GAMMA RAYS FOLLOWING (α,xn) REACTIONS. Morinaga, H. (Instituut voor Kernphysisch Onderzoek, Amsterdam). Nucl. Phys., 75: 385-95(1965).

Ground state collective bands at the beginning and the middle of the well deformed region around the rare-earth nuclei were obtained up to 8^+ or 10^+ states from the observation of low-energy γ rays following the (α,4n) or (α,2n) reactions on even isotopes of rare-earth elements. Energy spectra for N ≧ 92 show typical rotational characteristics. The softness of the nucleus, that is, the rate of change of the moment of inertia with increasing angular momentum are found to be systematically and substantially higher at the more neutron-deficient side, while the values of the moment of inertia are more or less constant throughout the region. However, nuclei with N = 90, seem to be more deformable than those with larger neutron numbers. (auth)

6349 ELASTIC SCATTERING OF PHOTONS IN THE REGION OF THE GIANT RESONANCE. De Botton, N.; Miller, J.; Schuhl, C.; Tamas, G.; Tzara, C. (Centre d'Etudes Nucleaires, Saclay, France). Nucl. Phys., 75: 396-400(1965). (In French).

The study of photon scattering in the region of the giant resonance for Pb and Bi was undertaken using the Saclay photon monochromator. The analysis of the results shows that Pb and Bi scatter identically in spite of the different ground state spins and low energy nuclear levels. The limit set to the dipole-quadrupole interference is in agreement with what could be expected from predicted values. (auth)

6350 EVEN PARITY STATES OF ^{16}O AND ^{17}O. Brown, G. E. (Princeton Univ., N. J.); Green, A. M. Nucl. Phys., 75: 401-17(1965).

The low-lying even-parity spectrum of ^{16}O and ^{17}O is described by mixing the usual states in the spherical shell model with deformed states obtained by exciting particles out of a deformed core. (auth)

6351 STUDY OF THE REACTION $^6Li + T = 2\alpha + n$ AT LOW INCIDENT ENERGIES. Laugier, J. P. (Centre d'Etudes Nucleaires, Saclay, France); Marquez, L.; Saunier, N.; Rey, J. Nucl. Phys., 75: 418-22(1965). (In French).

The energy spectra of α particles coming from the reaction $^6Li + T = 2\alpha + n$ were studied at incident energies of 0.65, 0.81, and 0.97 Mev. These spectra show a peak at one fifth of the available energy. The results can be explained if one assumes that ^6Li and T form a molecule whose break-up gives the observed peak. (auth)

6352 STRIPPING REACTIONS BELOW THE COULOMB BARRIER. Zeh, H. D. (California Inst. of Tech., Pasadena). Nucl. Phys., 75: 423-32(1965).

A computational method for the analysis of stripping and pick-up reactions in the energy range below the Coulomb barrier is described. The method takes account of finite range effects and of the Coulomb polarization of the incoming or outgoing composite particle. (auth)

6353 EXCITATION OF COLLECTIVE LEVELS OF SPHERICAL NUCLEI IN β-DECAY AND IN STRIPPING. Yakimets, V. V. (Inst. of Nuclear Physics, Academy of Sciences, Novosibirsk, Siberian SSR). Nucl. Phys., 75: 433-40(1965).

The excitation of the vibrational levels of the spherical odd nucleus in the β-decay of the even nucleus is considered in terms of the generalized model of the nucleus. A relative probability for the transition from the state 1^- of the parent nucleus to the states 0^+ and 2^+ of the daughter nucleus is obtained. Results of the theoretical investigation are compared with experimental data. Stripping on the odd neutron nucleus is also considered. (auth)

6354 STUDY OF NUCLEI OF MEDIUM MASS BY INELASTIC SCATTERING OF 155 Mev PROTONS. I. INELASTIC SCATTERING ON ^{23}Na, ^{27}Al, ^{28}Si, ^{31}P, ^{32}S, ^{39}K, AND ^{40}Ca. Liu, M.; Jacmart, J. C.; Ricci, R. A.; Riou, M.; Ruhla, C. (Laboratoire de Physique Nucleaire, Orsay, France). Nucl. Phys., 75: 481-514(1966). (In French).

The differential cross sections from 8 to 35° of 155 Mev protons on ^{23}Na, ^{27}Al, ^{28}Si, ^{31}P, ^{32}S, ^{39}K, and ^{40}Ca nuclei were measured. Scattered protons were analyzed with a magnetic spectrometer with 0.5% overall resolution. Most of the observed levels are of a collective character corresponding to E2 or E3 excitation. By using the plane wave impulse approximation, the reduced transition probabilities were deduced. Comparisons are given with other experimental results and with rotational model and core particle coupling predictions. (auth)

6355 SHAPE OF NEUTRON YIELD FROM THE $^7Li(p,n)^7Be$ REACTION NEAR THRESHOLD AND THRESHOLD ENERGY DETERMINATION. Palmer, D. W.; Mourad, W. G.; Donhowe, J. M.; Nielsen, K. E.; Nickles, R. J. (Univ. of Wisconsin, Madison). Nucl. Phys., 75: 515-28 (1966). (COO-7-0360).

Thick-target experimental yield data from the $^7Li(p,n)^7Be$ threshold reaction are compared to yield curves computed by Monte Carlo techniques. A good fit is obtained which indicates that the yield rises faster above threshold than is expected when discrete energy losses experienced by protons in the target are ignored. Threshold energies determined by extrapolation of two-thirds power yield data are shown to be more than 150 ev below the true threshold. A table of the calculated, relative yield is included for use in locating threshold on experimental data. (auth)

6356 ENERGY DISTRIBUTION OF $^7Li(p,n)^7Be$ NEUTRONS NEAR THRESHOLD. Palmer, D. W. (Univ. of Wisconsin, Madison). Nucl. Phys., 75: 529-38(1966). (COO-7-0358).

Energy distributions were calculated for $^7Li(p,n)^7Be$ neutrons for targets up to 1900 Å thick at 0, 45, 90, 135, and 180°. The distributions are affected in several ways when account is taken of the discrete nature of energy losses experienced by protons in the target. Peaks and long tails appear on the distributions, and the neutron intensity in any direction is seldom equal to the intensity predicted when continuous energy losses are assumed for the protons. (auth)

6357 THE DISINTEGRATION OF Ar BY 13.0 - 20.2 Mev NEUTRONS. Mathur, Suresh C.; Morgan, I. L. (Texas Nuclear Corp., Austin). Nucl. Phys., 75: 561-73 (1966).

The disintegration of argon by neutrons in the energy range 13.0 to 20.2 Mev was studied by the activation technique and with an argon filled noble gas scintillation spectrometer. In the activation experiment, the (n, α) reaction in ^{40}Ar is compared with the (n, p) reaction in ^{37}Cl, both resulting in delayed activity from ^{37}S. The excitation functions were obtained for both of these reactions in the neutron energy range 13.0 to 20.2 Mev. The cross sections for the disintegration of argon with the emission of alpha particles were measured with the gas scintillation spectrometer. The reaction cross sections were also calculated on the basis of compound nucleus theory, and comparisons were made between the results of the experiment and theory. (auth)

6358 DEVIATION FROM THE STATISTICAL SHAPE OF THE $3/2^+ - 1/2^- \beta^-$ TRANSITION IN THE DECAY OF ^{199}Au. Lehmann, J. (CEN-SCK, Mol, Belgium). Nucl. Phys., 75: 574-6(1966).

The spectrum shape factor of the 460-kev beta transition of ^{199}Au was found to deviate from the statistical shape by $-30\% \pm 10\%$ $(mc^2)^{-1}$. The end point energy was measured to be 460 kev ± 6 kev. (auth)

6359 FRESNEL AND FRAUNHOFER DIFFRACTION IN NUCLEAR PROCESSES. Frahn, W. E. (Univ. of Cape Town). Nucl. Phys., 75: 577-91(1966).

Angular distributions for elastic scattering and direct reactions of nuclear particles often have an oscillatory structure which is the analogue of Fraunhofer diffraction by a perfectly absorbing obstacle. It is shown that strong Coulomb interaction changes the diffraction pattern from the Fraunhofer type to the Fresnel type. Several features observed in the differential scattering and reaction cross sections of heavy charged particles are identified as Fresnel diffraction effects. (auth)

6360 ALPHAS FROM THE DEUTERON BOMBARDMENT OF ^9Be AND ^{12}C. Hazzard, E. T. (Haverford Coll., Haverford, Pa.); Ajzenberg-Selove, F.; Hewka, P. V. Nucl. Phys., 75: 592-8(1966).

A thin ^9Be layer deposited on a carbon foil was bombarded by 11 Mev deuterons. The outgoing α particles were analyzed in a Browne-Buechner spectrograph. The widths of the ^7Li states at 4.63 and 7.48 Mev excited in the $^9Be(d,\alpha)^7Li$ reaction were determined to be 93 ± 25 and 80 ± 20 kev, respectively. No evidence was seen for the ^7Li state at ≈5.5 Mev suggested in several experiments. Attempts to observe the excited states at $E_x \approx 8.6$, 9.7, and 12.5 Mev reported in photonuclear work and the new $T = 3/2$ state at $E_x = 11.13$ Mev observed in the $^9Be(p, ^3He)^7Li$ reaction were unsuccessful. The $J^\pi = 0^+$, $T = 1$ state at 1.74 Mev in ^{10}B was not observed in the $^{12}C(d, \alpha)^{10}B$ reaction. Upper limits to the intensities of the alpha-particle groups to this state are about 3% of the intensities of the groups to its $J^\pi = 1^+$, $T = 0$ neighbors at $E_x = 0.72$ and 2.15 Mev. (auth)

6361 ISOBARIC STATES EXCITED IN (p,n) REACTIONS AT 30 AND 50 Mev. Batty, C. J.; Gilmore, R. S.; Stafford, G. H. (Rutherford High Energy Lab., Chilton, England). Nucl. Phys., 75: 599-608(1966).

Measurements were made of the neutron energy spectra from (p, n) reactions on a wide range of elements at 30 and 50 Mev. The Q values for the isobaric analog states were measured and are compared with calculated values for the Coulomb energy difference. Cross sections were also measured and show a marked variation with atomic weight of the target nucleus and incident proton energy. This variation is discussed in terms of a simple model and the results compared with calculations made using the optical model including an isobaric spin dependent term. (auth)

6362 A DWBA ANALYSIS OF $^{12}C(d,p\gamma)^{13}C$ WITH MEASURED OPTICAL MODEL PARAMETERS. Gerke, D. G.; Tilley, D. R.; Fletcher, N. R.; Williamson, R. M. (Duke Univ., Durham, N. C.). Nucl. Phys., 75: 609-31 (1966).

The reaction $^{12}C(d,p\gamma)^{13}C_{3.68,3.85}$ was studied at deuteron bombarding energies of 2.80, 3.23, and 3.70 Mev. Angular distributions were measured for the stripping reactions and for the $^{12}C(d,d)^{12}C$ and $^{13}C(p,p)^{13}C$ elastic scattering. Distorted wave Born approximation calculations were made with the use of optical model potentials which fit the measured elastic scattering, and the results were compared with the stripping angular distributions and previously measured (d,pγ) angular correlation parameters. The spectroscopic factors obtained agree with the values known from higher energy data. Reasonable fits to the angular distributions and qualitative fits to the angular correlation parameters over most of the angular range were obtained. The optical-model parameters do not vary smoothly with energy, but those which fit the measured elastic scattering agree well with those giving the best stripping fits. (auth)

6363 THE SELF-CONSISTENT FIELD AND THE STUDY OF GROUND STATES OF CLOSED SHELL LIGHT NUCLEI. Abgrall, Y.; Monsonego, G. (Centre de Recherches Nucleaires, Strasbourg). Nucl. Phys., 75: 632-40(1966). (In French).

An approximate Hartree-Fock self-consistent field calculation is carried out for the ground state of the light closed shell nuclei ^{4}He, ^{16}O, and ^{40}Ca. By starting with an assumed nucleon-nucleon interaction $v(r_i - r_j)$, the effective Hartree-Fock fields $w(r_i)$ and the single particle energies are derived. A central two-body exchange force is chosen and a hard core, introduced in a phenomenological way, is treated by the Moszkowski-Scott separation method. The individual particle trial wave functions, which are combinations of harmonic oscillator wave functions, are determined by a variational principle. For certain interactions containing a hard core, the binding energies, the rms radii, and the charge distributions are well explained for ^{16}O and ^{40}Ca. Furthermore, the single particle spectrum calculated for ^{16}O is close to the experimental one. The Hartree-Fock fields for 1S and 1P nucleons are given, and the average shape agrees with the results that would be obtained from the scattering of nucleons by nuclei. (auth)

6364 EVAPORATION OF CHARGED PARTICLES FROM HEAVY NUCLEI. Lefort, Marc; Da Silveira, Rui (Univ., Paris). Nucl. Phys., 75: 641-54(1966). (In French).

The statistical model was applied to the de-excitation process on heavy nuclides produced from Bi and Au targets bombarded by 60 to 155 Mev protons. The de-excitation steps consisting of neutron and charged-particle emission were analyzed by the Monte-Carlo method. It was shown that the estimation of the cross section for the inverse process below the Coulomb barrier should be as accurate as possible, in order to account for the rather large probability for charged particle emission, because of the level density amplification properties. Calculations are accordingly in good agreement with experimental data on (i) the energy location for alpha particle evaporation spectra, (ii) the total evaporation cross sections from Au nuclides, (iii) the cross sections for Po isotopes produced through (p, xn) reactions from Bi targets, when the usual parameters $r_0 = 1.3$ fm, $a = 15$ A are adopted and the distribution for residual excited nuclei after prompt cascades given by Metropolis et al. is assumed. (auth)

6365 ELASTIC PHOTOPRODUCTION OF NEUTRAL PIONS FROM ^{4}He. Ananthanarayanan, K. (MATSCIENCE, Madras). Nucl. Phys., 75: 687-90(1966).

The elastic photoproduction of neutral pions from ^{4}He is studied in the impulse approximation using the amplitudes of Chew et al. for the photoproduction of pions from single nucleons. A Gaussian wave function is chosen for the spatial part of the ground state of ^{4}He, and numerical evaluation of the differential cross section is made in the center-of-momentum system for an incoming photon energy of 300 Mev, and agreement with the available experimental data found for two values of the root mean square radius of the ^{4}He nucleus. (auth)

6366 VIBRATIONAL STATES OF DEFORMED NUCLEI POPULATED BY THE (p,2n) REACTION. Graetzer, R.; Hagemann, G. B.; Hagemann, K. A.; Elbek, B. (Univ. of Copenhagen). Nucl. Phys., 76: 1-44(1966).

Spectra of prompt internal conversion electrons with energies up to 2 Mev were obtained from targets of ^{159}Tb, ^{165}Ho, ^{169}Tm, ^{175}Lu and ^{181}Ta bombarded with 12-Mev protons. Gamma-electron coincidence spectra were also measured. Most of the observed lines in the region around 1 Mev were ascribed to decays from vibrational bands populated by the (p,2n) reaction. Quadrupole vibrations with K = 2 were found in ^{158}Dy (945 kev), ^{164}Er (857 kev) and ^{168}Yb (986 kev). Bands with K = 0 were found in ^{158}Dy (991 kev), ^{164}Er (1238 kev), ^{168}Yb (1156, 1197 and 1543 kev), ^{174}Hf (827 kev) and ^{180}W (908 kev). The K = 0 assignment was made on the basis of an E0 component in the decay. The rotational bands were populated up to levels with spin six or more. The spacing of energy levels in the vibrational bands indicates an increase in the moment of inertia as a function of the spin similar to that of the ground-state bands. In the gamma bands there is also a small relative displacement of even and odd spin levels. Mixing of the excited and ground-state bands was calculated from the E2 branching ratios, but accounts for only a small fraction of the energy depression in the ground state rotational bands. (auth)

6367 THE $^{39}K(^3He,\alpha)^{38}K$ AND THE $^{39}K(^3He,^3He)^{39}K$ REACTIONS. Blau, L. M. (Univ. of Rochester, N. Y.); Alford, W. Parker; Cline, D.; Gove, H. E. Nucl. Phys., 76: 45-57(1966). (UR-875-90)

Angular distributions of the $^{39}K(^3He,\alpha)^{38}K$ reaction leading to the ground state and the first four excited states of ^{38}K were measured over an angular range from 10 to 90° at incident energies of 9.00 and 11.00 Mev. The elastic scattering of ^{3}He from ^{32}K was also measured at 9.00 Mev, and an optical model analysis of the results was made. At each energy, the angular distributions leading to all five levels of ^{38}K are similar in shape and are in reasonable agreement with the predictions of a zero range DW analysis. The angular distribution of alpha particles for the reactions leading to the ground ($J = 3^+$, $T = 0$) state and first excited (0^+ 1) state are characteristic of pure d-wave pickup. The reactions leading to the second (1^+ 0), third (1^+ 0), and fourth (2^+ 1) excited states proceed primarily by d-wave with a small admixture of s-wave for the picked-up neutron. The measured spectroscopic factors are in reasonable agreement with the predictions of two theoretical models, one of which considers only $1d_{\frac{3}{2}}$ and $2s_{\frac{1}{2}}$ holes in the closed ^{40}Ca core while the other also includes $1d_{\frac{5}{2}}$ hole configurations. (auth)

6368 THE PERIPHERAL MODEL AND ITS APPLICATION TO THE PHOTODISINTEGRATION OF ^{6}Li. Ferroni, S.; Mosconi, B.; Piragino, G.; Wataghin, V. (Univ., Turin. Istituto Nazionale di Fisica Nucleare, Turin). Nucl. Phys., 76: 58-64(1966).

A field theory model is applied to the photodisintegration

of ^{6}Li into three bodies. The results are compared to the experimental cross section in the energy range extending from threshold to about 50 Mev. The energy spectrum of emitted deuterons is predicted and is compared to some preliminary data. (auth)

6369 (d,α) REACTIONS ON LIGHT NUCLEI. Jahr, R.; Kayser, K.; Kostka, A.; Wurm, J. P. (Max-Planck-Institut fuer Kernphysik, Heidelberg). Nucl. Phys., 76: 79-96(1966). (In German).

The analyzed beam from the Heidelberg Cyclotron was used to investigate (d,α) reactions on ^{24}Mg, ^{25}Mg and ^{28}Si targets at incident beam energies between 11.45 and 12.1 Mev. Angular distributions of alpha particles corresponding to the excitation of the lowest six to ten levels of the residual nuclei were measured in the range between 15 and 165°. The data suggest a mixed direct and compound nucleus interaction mechanism. The latter seems to be predominant in the ^{25}Mg(d,α) reaction. The angular distributions have been analyzed by double pick-up theory where feasible. The (2I + 1) rule was observed to hold for ^{25}Mg(d,α) and to a lower degree of accuracy for ^{28}Si(d,α). From the viewpoint of this rule, it is suggested that the well-known 2.07-Mev level in ^{26}Al is a doublet state as proposed earlier. The integrated cross-sections of various alpha groups from the (d,α) reactions on ^{9}Be, ^{14}N, ^{16}O, ^{31}P and ^{32}S were also measured. A pronounced odd-even effect was observed not only for the transitions to the ground states but also for the transitions to the excited states up to about 3 Mev. (auth)

6370 SPECTRAL FORM OF (0 → 0)-β TRANSITIONS WITH PARITY CHANGE: ^{144}Ce, ^{144}Pr, AND ^{166}Ho. Daniel, H.; Kaschl, G. Th. (Max-Planck-Institut fuer Kernphysik, Heidelberg). Nucl. Phys., 76: 97-117(1966). (In German).

The beta spectra of ^{144}Ce, ^{144}Pr and ^{166}Ho were measured with the Heidelberg double-lens spectrometer. Shape factors were obtained for the 0 → 0 transitions with parity change. The maximum energies of the ^{144}Ce and ^{144}Pr ground-state transitions were found to be 315.6 ± 1.5 and 3000 ± 4 kev, respectively. The spectral shapes show definite deviations from statistical shapes. The measured half life of ^{166}Ho is 26.74 ± 0.05 h. The maximum energies of the beta groups are 1857 ± 3 kev (51%), 1776 ± 4 kev (48%), 427 ± 6 kev (0.7%) and 214 ± 9 kev (0.2%). The spectral shape of the ground-state transition deviates from the statistical shape. The data of this work do not support the concept of a partially conserved axial-vector current as suggested by Tadic. By an analysis of the spectral shape and electron polarization data of ^{144}Pr, a new upper limit was found for the pseudoscalar and induced pseudoscalar coupling constants in nuclear beta decay: $|C_P/C_A| < 5$, $|C_{P'}/C_A| < 5$. (auth)

6371 CONFIGURATIONS OF THREE α PARTICLES IN ^{12}C. Darriulat, P. (CEN, Saclay, France). Nucl. Phys., 76: 118-22(1966). (In French).

A variational approach is given to the problem of three alpha particles interacting through the l dependent potential describing the elastic scattering of alpha particles by helium. The result is consistent with the 7.656-Mev state being the lowest alpha particle parentage state in ^{12}C. (auth)

6372 CROSS SECTIONS FOR PRODUCTION OF ^{149}Tb FROM Au BY HIGH-ENERGY PROTONS. Franz, E. M.; Friedlander, G. (Brookhaven National Lab., Upton, N. Y.). Nucl. Phys., 76: 123-8(1966). (BNL-9454).

Cross sections for the production of the alpha emitter ^{149}Tb (4.12 h) from gold with protons between 0.6 and 30 Bev were measured. Some difficulties of earlier determinations were avoided by use of chemically separated, "weightless" sources for the alpha measurements. A beta-active tracer (^{160}Tb) was used for yield determinations. The excitation function obtained is compared with previous results. The individual cross sections reported are believed to be accurate to 4 to 6%. (auth)

6373 ELASTIC AND INELASTIC SCATTERING OF PROTONS BY ^{18}O. Stevens, J.; Lutz, H. F.; Eccles, S. F. (Univ. of California, Livermore). Nucl. Phys., 76: 129-44 (1966). (UCRL-12152).

Differential cross sections for elastic and inelastic scattering of protons by ^{18}O were obtained. Excitation curves from 7.89 to 16.28 Mev exhibit a large resonance at 10.5 Mev. Angular distributions were obtained at 11 values of the incident energy. The elastic angular distributions were fitted with the optical model, and the inelastic scattering angular distributions were analyzed with both the distorted-wave Born approximation and the Tamm-Dancoff approximation. The analysis indicates a value of $\beta = 0.34$. (auth)

6374 ELECTROMAGNETIC TRANSITIONS IN ^{181}Ta. Alexander, P.; Ryde, H.; Seltzer, E. (California Inst. of Tech., Pasadena). Nucl. Phys., 76: 167-76(1966).

Electromagnetic transitions in ^{181}Ta were studied from the beta decay of 45-day ^{181}Hf. The gamma radiation was investigated with a 4-mm Ge(Li) detector. Internal conversion lines were examined using a high resolution $\sqrt{2}\pi$ beta-ray spectrometer. A careful search for transitions reported in the literature to depopulate levels at 699, 958 and 963 kev gave a negative result. From a measurement of the L subshell ratios for the 136.86-kev transition, it is concluded that this transition is almost pure M1 with an (1 ± 4%) admixture of E2. This is in agreement with the expectations from the measured half life of the 618.9-kev level and supports the $^{3}/_{2}^{+}$ assignment of this level. A 618.9-kev ground-state transition was observed as a weak K conversion line. A measurement of the energy difference between the 482 kev and the 476-kev K conversion lines gave 6.25 ± 0.02 kev in agreement with the measured energy of the suggested first excited state in ^{181}Ta. (auth)

6375 RADIAL INTEGRALS FOR RELATIVISTIC COULOMB FUNCTIONS. Alder, Kurt; Schucan, Thomas H. (Univ. of Basel). Nucl. Phys., 76: 177-80(1966).

Relativistic Coulomb integrals which occur in inelastic electron scattering can be expressed in closed analytic form in the limit of vanishing energy loss. A method of calculation is presented which is based on elementary properties of the confluent hypergeometric functions such as their differential equation, recurrence relations, and asymptotic behavior for large arguments. (auth)

6376 INTENSITIES OF ALPHA SPECTRA FOR THE PARITY-UNFAVOURED TRANSITIONS IN SPHERICAL NUCLEI. Chaudhury, Manujendra L. (Univ. of Ottawa). Nucl. Phys., 76: 181-95(1966).

The relative intensities of alpha spectra for the parity-unfavored transitions in spherical nuclei are calculated by using a Coulomb barrier superposed by a non-local alpha-nuclear interaction. It is further assumed that this alpha-nuclear interaction is of an effective space-exchange character due to the Majorana part of the interactions between the nucleons of the alpha particle and the residual nucleus. The proportion of the exchange potential in the mixture is fixed by normalization. However, for the same order of agreement of normalized value of the proportion parameter varies from 40 to 45% depending on the values of the range of non-locality. The latter are chosen within reasonable limits of the value suggested by the considerations of the effective nucleon mass. With these assumptions, the calculated values of the intensity ratios are in good agreement with experiment, being in most cases within 25% of the observed values. On the other hand, the relative intensities calculated on the basis of a pure Coulomb barrier or on other static barrier hypotheses often show much larger deviations from the observed data and are anomalous. (auth)

6377 THE NEUTRON CROSS SECTIONS OF THORIUM AND THE ANALYSIS OF THE RESONANCES UP TO 1 kev. Asghar, M.; Chaffey, C. M.; Moxon, M. C.; Pattenden, N. J.; Rae, E. R.; Uttley, C. A. (Atomic Energy Research Establishment, Harwell, Eng.). Nucl. Phys., 76: 196-222(1966).

The neutron total, capture and scattering cross sections of thorium were measured in the neutron energy range from about 15 ev to 1 kev by the time-of-flight method. The neutron and radiation widths of the larger resonances were determined by combining the data from the three types of measurement. The small but significant fluctuation observed in the radiation widths about a mean value of 21.5

Mev is discussed. The value of the infinite dilution resonance integral (79 ± 4 b) calculated from these resonance parameters is in agreement with recent measurements. (auth)

6378 THE $\frac{3}{2} \rightarrow \frac{1}{2}$ HOLE TRANSITIONS IN MASS 15. Lopes, J. S.; Haeusser, O.; Rose, H. J.; Poletti, A. R.; Thomas, M. F. (Oxford Univ.). Nucl. Phys., 76: 223-31(1966).

The mixing ratios of the $\frac{3}{2}^- \rightarrow \frac{1}{2}^-$, 6.15- and 6.33-Mev transitions in ^{15}O and ^{15}N were measured. The results were $x(^{15}O) = 0.17 \pm 0.01$ or -2.7 ± 0.1 and $x(^{15}N) = -0.13 \pm 0.02$ or -1.3 ± 0.1; it is suggested that the smaller values are the ones to be accepted. The sign of $x(^{15}N)$ is opposite to the one calculated from the independent particle model; it is concluded that these $\frac{3}{2}^-$ states in ^{15}O and ^{15}N are strongly collective in character. (auth)

6379 NUCLEAR EQUATION OF STATE FROM INELASTIC NEUTRON SCATTERING SPECTRA. Malyshev, A. V.; Shubin, Yu. N. (Inst. of Physics and Energetics, Obninsk, USSR). Nucl. Phys., 76: 232-40(1966).

Information about the nuclear equation of state can be derived from an appropriate analysis of the inelastic neutron scattering spectra measured at different energies of incident neutrons. It is shown that at least two corrections must be taken into account: at relatively low energies there may be an appreciable difference between the "nuclear" temperature derived from the evaporation spectra and the thermodynamic temperature which enters into the nuclear equation of state and at sufficiently high excitation energies the possibility of evaporation of several neutrons should be taken into account. Available experimental data on nuclear temperatures for Fe, Cd, Cu, Sn, Ta, W, Au and Bi in an energy range from 2.5 to 15 Mev are analyzed. It is shown that the dependence of thermodynamic temperature on excitation energy is described satisfactorily by the Fermi gas model if the above corrections are introduced. (auth)

6380 NUCLEAR RESONANT SCATTERING OF BREMSSTRAHLUNG FROM LOW-LYING LEVELS IN ^{27}Al, ^{31}P AND ^{35}Cl. Hough, J. H.; Mouton, W. L. (Univ. of the Witwatersrand, Johannesburg). Nucl. Phys., 76: 248-56(1966).

A 1.4 Mev electron accelerator was used as a source of bremsstrahlung to determine the widths and hence the mean lifetimes τ for ground state transitions of the 1.01 Mev level in ^{27}Al and the first excited states of ^{31}P and ^{35}Cl. Only self-absorption measurements were performed. The object of the work was mainly to resolve discrepancies existing between results obtained by other workers. The following results were obtained: 1.01 Mev level in ^{27}Al: $\tau = 0.5^{+0.5}_{-0.2}$ psec, 1.26 Mev level in ^{31}P: $\tau = 0.73^{+0.13}_{-0.12}$ psec, and 1.22 Mev level in ^{35}Cl: $\tau = 0.13^{+0.03}_{-0.02}$ psec. Extensive measurements to observe resonant scattering from a new level in ^{31}P at an energy of 450 kev yielded negative results. (auth)

6381 SPECTRAL SHAPES AND A BETA-GAMMA DIRECTIONAL CORRELATION IN THE BETA DECAY OF $^{172}Tm(J^\pi = 2^-)$. Hansen, P. G. (Research Establishment Riso, Roskilde, Denmark); Nielsen, H. L.; Wilsky, K.; Agarwal, Y. K.; Baba, C. V. K.; Bhattacherjee, S. K. Nucl. Phys., 76: 257-67(1966).

The isotope ^{172}Tm populates the 0^+, 2^+, and 4^+ states of the ^{172}Yb ground-state rotational band directly in beta decay. The shapes and intensities of the three beta groups were measured by means of a six-gap magnetic spectrometer operated in coincidence with a NaI(Tl) crystal. The experimental shape factor plots are taken relative to the ^{90}Y shape factor measured in the same circumstances, and it is concluded that on this basis the shapes of all three ^{172}Tm beta groups agree with the theoretical shape for a first-forbidden unique transition. The directional correlation for the $2^-(\beta)2^+(\gamma)0^+$ cascade was measured at six energies from 1010 to 1550 kev and these results too are consistent with the assumption that the $2^- \rightarrow 2^+$ beta transition is purely of tensor rank 2. The data for the $2^- \rightarrow 2^+$ transition are analyzed on the basis of the modified B_{ij} approximation, which defines parameters X and Y corresponding to the relative contributions of tensor ranks 0 and 1 respectively. The shape measurement provides the limit $X^2 + Y^2 \leq 0.10$, whereas the angular correlation measurement gives $Y = 1.64X + (0.02 \pm 0.03)$. The reduced transition probabilities $(f_1t)^{-1}$ can therefore be compared with the theoretical intensity rules for $\lambda = 2$, which predict the ratios 0.70 : 1 : 0.05 for the branches to the 0^+, 2^+, and 4^+ states. The experimental result is $(0.63 \pm 0.19) : 1 : (0.046 \pm 0.007)$. (auth)

6382 HOLE-PARTICLE MODEL IN NUCLEI HAVING ONE NUCLEON MORE THAN CLOSED SHELLS APPLICATION TO THE ^{17}O NUCLEUS. Quesne, C. (Univ. Libre, Brussels). Nucl. Phys., 76: 268-88(1966).

The hole-particle model is extended to nuclei having one nucleon more than closed shells. A diagonalization is carried out on ^{17}O using ls coupling and a zero-range interaction, independent of spin and isospin variables and similar to that used in ^{16}O. The effect of varying the single-particle energies and eliminating the spurious states corresponding to the center-of-mass motion is studied. The results are compared with previous calculations and with the predictions of the core-excitation model. The influence of the E3 collective transition in ^{16}O is estimated by computing some E3 transition strengths in ^{17}O. (auth)

6383 THE FEYNMAN GRAPH TREATMENT OF THE INITIAL AND FINAL STATE INTERACTIONS IN DIRECT NUCLEAR REACTIONS. Dolinsky, E. I.; Blokhintsev, L. D.; Mukhamedzhanov, A. M. (Moscow State Univ.). Nucl. Phys., 76: 289-307(1966).

A method is proposed for calculating the amplitude M(s,t) of the direct nuclear reaction $1 + 2 \rightarrow 3 + 4$ taking into account the interactions in the initial and final states (the method of summing diagrams). The amplitude M(s,t) is based on the initial Born amplitude B(s,t) which is described by one or several non-relativistic Feynman graphs and which does not take into account the interaction effects in the initial and final states. The method of summing diagrams is compared with the method of distorted waves and the dispersion method. The analytical properties of the amplitudes M(s,t) in the variables s and t are discussed in detail. (auth)

6384 ANGULAR CORRELATIONS IN THE DECAY OF ^{127}Xe. Leisi, H. J. (Franklin Inst., Swarthmore, Pa.). Nucl. Phys., 76: 308-20(1966). (TID-22155).

Gamma-gamma directional correlations in the decay of ^{127}Xe were measured in different source environments. With an aluminum foil source the anisotropies of the 172–203 kev, 145–58 kev, and 172–58 kev correlations in ^{127}I were found to be $[W(\pi) - W(\frac{1}{2}\pi)]/W(\frac{1}{2}\pi) = +0.377 \pm 0.007$, -0.180 ± 0.043, and $+0.24 \pm 0.12$, respectively. With a gaseous source of ^{127}Xe the anisotropy of the 145–58 kev correlation was observed to be reduced by 0.090 ± 0.026. This reduction is interpreted as indicating a perturbation of the correlation due to hyperfine interaction following K capture. A review of all the available information on the 145–58 kev cascade allows the anisotropy of the unperturbed correlation to be predicted. Comparison with the measured anisotropy suggests that this correlation is perturbed even in the metallic environment. This observation led us to reanalyze the conversion electron-gamma correlation data of Geiger on the 172–203 kev cascade. From this analysis, for which we made use of internal conversion results and the measured anisotropy of the γ-γ correlation, it is concluded that the K conversion particle parameters of Biedenharn and Rose, as modified by Church et al., are compatible with all the measurements, even in the presence of a perturbation. Unambiguous spin values for the 203 kev level ($\frac{3}{2}$) and the 375 kev level ($\frac{1}{2}$) and a positive sign for the mixing amplitude of the 203 kev transition emerge from the analysis, irrespective of perturbations of the angular correlations. The mixing amplitude of the 172 kev transition, however, may not be inferred from presently available data. (auth)

6385 STATES WITH v = 0 AND v = 1 SENIORITY IN Ni ISOTOPES. Auerbach, N. (Weizmann Inst. of

Science, Rehovoth, Israel). Nucl. Phys., 76: 321-35 (1966).

The spectra of the Ni isotopes are considered in the framework of the shell model. The total energies of the $J = 0^+$ ground and first excited states of the even-mass isotopes and the lowest $J = \frac{1}{2}^-$, $\frac{3}{2}^-$, and $\frac{5}{2}^-$ of the odd-mass isotopes are calculated. It is found that these energy levels are accurately reproduced by an effective interaction in states with seniority v = 0 and v = 1 of configurations with neutrons in the $2p_{\frac{3}{2}}$, $2p_{\frac{1}{2}}$, and $1f_{\frac{5}{2}}$ orbits. (auth)

6386 E2/M1 MIXING RATIOS AND K CONVERSION COEFFICIENTS IN ODD-MASS ROTATIONAL NUCLEI. Ashery, D.; Blaugrund, A. E.; Kalish, R. (Weizmann Inst. of Science, Rehovoth, Israel). Nucl. Phys., 76: 336-46(1966).

The E2/M1 mixing ratios and K conversion coefficients of the first two rotational transitions in ^{155}Gd, ^{159}Tb, ^{167}Er, ^{173}Yb, ^{175}Lu, ^{179}Hf, ^{181}Ta, ^{185}Re, and ^{187}Re were measured. The mixing ratios are determined from angular distributions of gamma rays following Coulomb excitation of the second rotational level. Events belonging only to the decay by cascade of the second rotational level were selected by a coincidence circuit. The same experimental arrangement was used for determination of K conversion coefficients from x-ray and gamma intensity ratios. The agreement between the experimental values of the mixing ratios and the predictions of the rotational model is fair except in the case of ^{179}Hf. The agreement between the experimental and theoretical values of the K conversion coefficients is good. In addition E2/M1 mixing ratios of the 99 and the 141 kev transitions in ^{195}Pt were determined. (auth)

6387 THE ROLE OF IDENTITY OF COLLIDING NUCLEI IN NEUTRON TUNNELLING TRANSFER. Dalidchik, F. I.; Sayasov, Yu. S. (Inst. for Chemical Physics, Moscow). Nucl. Phys., 76: 347-52(1966).

A formula is derived for the differential cross section of neutron tunneling transfer valid under any assumptions about the potentials of interaction of a neutron with the nuclear core and the spins of the initial and final states of the nuclei. It is shown that the form of exchange term oscillations essentially depends on the variation of the orbital momentum of relative motion connected with the variation of the nuclear spin states. (auth)

6388 THE LEVEL SCHEME OF ^{231}Th. Gaeta, R.; Vigon, M. A. (Junta de Energia Nuclear, Madrid). Nucl. Phys., 76: 353-61(1966).

A study of the ^{231}Th excited levels from the alpha decay of ^{235}U is carried out. The alpha-particle spectrum was measured by means of a semiconductor counter spectrometer with an effective resolution of 18 kev. Nineteen new lines were identified. The gamma-ray spectrum was measured with thin samples of ^{235}U, which were free from decay products and in such geometrical conditions that most of the interference effects were eliminated. From the experimental data a new decay scheme was proposed, where new rotational terms, belonging to the Nilsson states $\frac{5}{2}^+$ (633), $\frac{1}{2}^+$ (631), $\frac{3}{2}^+$ (631) $\frac{5}{2}^+$ (622), $\frac{5}{2}^-$ (752) $\frac{3}{2}^-$ (761) and $\frac{7}{2}^-$ (743), were identified. (auth)

6389 ^{9}Be(^{3}He,α) REACTIONS TO THE 16.63 AND 16.92 Mev STATES OF ^{8}Be. Sullivan, D. J.; Treacy, P. B. (Australian National Univ., Canberra). Nucl. Phys., 76: 369-76(1966).

Coincidences were observed between successively-emitted α-particles from the ^{9}Be(^{3}He,α)^{8}Be(α) reaction at a laboratory bombarding energy of 3 Mev. The reaction was shown to proceed predominantly by successive transitions via states in ^{8}Be. The observed angular correlations were interpreted to show that the spins and parities of the 16.63 and 16.92 Mev states of ^{8}Be are both 2^+. (auth)

6390 PHOTONEUTRONS FROM ^{9}Be. Thompson, M. N.; Taylor, J. M. (Univ., Melbourne). Nucl. Phys., 76: 377-84(1966).

A measurement of the photoneutron spectrum from ^{9}Be was made using a knock-on proton spectrometer consisting of a stilbene crystal, and incorporating pulse shape discrimination. The resulting spectrum is interpreted in terms of states in ^{9}Be and confirms the existence of several doubtful levels and postulates the presence of at least one new level. (auth)

6391 BETA GAMMA CIRCULAR POLARIZATION CORRELATION IN ^{46}Sc. Mitra, S. K.; Padhi, H. C. (Tata Inst. of Fundamental Research, Bombay). Nucl. Phys., 76: 385-90(1966).

The β-γ circular polarization correlation in the decay of ^{46}Sc was measured by means of forward Compton scattering. In addition to usual corrections that are applied to the data, the effect of transmission through the central lead stopper and scattering from coils etc. were investigated. The effect of different source backings was also studied. The value of the asymmetry parameter A in the β-γ circular polarization correlation was found to be $A = 0.13 \pm 0.02$. This implies a ratio $X = -0.064 \pm 0.030$ between Fermi and Gamow-Teller contributions. (auth)

6392 DETERMINATION OF SPIN AND THE RESONANCE PARAMETERS FOR ^{197}Au +n at 10 TO 1000 ev. Julien, J.; de Barros, S.; Bianchi, G.; Gorge, C.; Huynh, V. D.; Le Poittevin, G.; Morgenstern, J.; Netter, F.; Samour, C.; Vastel, R. (Centre d'Etudes Nucleaires de Saclay, France). Nucl. Phys., 76: 391-432(1966).

Experiments on gold were performed with the Saclay linear accelerator using the time-of-flight method. Resonance parameters are given for 63 resonances in the energy range 10 to 1000 ev. Spin assignment methods are described and discussed. The J value is found for 40 resonances in combining total capture and transmission experiments. A convenient relation is used to take into account interference effects between resonances of the same spin. The strength function value is dependent upon the spin value $S_{0(J=2)} = 2.2\ S_{0(J=1)}$. The total radiation width Γ_γ is practically constant from resonance to resonance within experimental errors. Statistical properties of levels are considered and correlation coefficients are calculated. (auth)

6393 SHELL MODEL CALCULATIONS OF ft VALUES IN THE $2s_{\frac{1}{2}}$ AND $1d_{\frac{5}{2}}$ SHELLS. Engelbertink, G. A. P.; Brussaard, P. J. (Rijksuniversiteit, Utrecht). Nucl. Phys., 76: 442-8(1966).

The ft values of allowed beta transitions between even parity states in the region between ^{29}Si and ^{40}Ca are computed with the use of wave functions that were calculated earlier in a j-j-coupling model with configuration interaction taken into account. On the whole, there is good agreement between theoretical and experimental log ft values (the average absolute difference amounts to 0.5), with the exception of the decays of ^{32}Si and ^{32}P. The results are applied in a calculation of (i) the cross section of ^{37}Cl for solar neutrinos, (ii) the half life of ^{37}Ca and (iii) the Gamow-Teller matrix element for ^{35}Ar decay. (auth)

6394 L-SPACE LOCALIZATION IN DEUTERON STRIPPING REACTIONS. Hooper, M. B. (Univ. of Manchester, Eng.). Nucl. Phys., 76: 449-74(1966).

Demonstration is given of the way in which the DWBA treatment of deuteron stripping causes the reaction amplitude to be dominated by the contributions from a restricted range of combinations of partial waves in the entrance and exit channels. The consequences of this are examined: in particular, an interpretation may be given of the form of the associated polarization parameters for zero angular momentum transfer reactions. (auth)

6395 A SPIN-SPIN PART OF THE LOW-ENERGY NUCLEAR OPTICAL POTENTIAL. Khan, M. Z. Rahman (Muslim Univ., Aligarh, India). Nucl. Phys., 76: 475-8 (1966).

A phenomenological interaction was previously introduced between the spins of the incident nucleon and the target nucleus in the optical potential. However, due to the inavailability of suitable data the parameters of this potential remained undetermined. An upper limit is placed on the strength of this potential by considering a certain observed difference between the low-energy nuclear data of even and odd mass nuclei. (auth)

6396 GAMMA-GAMMA ANGULAR CORRELATIONS IN ^{147}Eu TO ^{147}Sm DECAY. Goworek, Tomasz; Skorzynski, Zbigniew; Wawryszczuk, Jan (Univ. of Curie-Sklodowska, Lublin). Nukleonika, 10: 527-9(1965).

Gamma directional correlation measurements were made in ^{147}Eu decay in order to obtain more data on higher levels of the ^{147}Sm nucleus. An energy level diagram is shown. The measurements were performed using a fast-slow coincidence circuit with a resolving time of 48 nsec. (M.C.G.)

6397 GAMMA INTENSITIES IN THE DECAY OF ^{187}W. Bashandy, E.; Migahed, M.; El-Sayad, G. M.; El-Aassar, M. R. (Atomic Energy Establishment, Cairo). Nuovo Cimento (10), 39: 1017-31(Oct. 16, 1965).

A study of the relative intensities of the γ rays from the decay of ^{187}W to ^{187}Re was performed using the external conversion method. The photoelectrons from uranium converter are analyzed in a double-focusing β spectrometer. Twenty nine γ transitions in the energy region of ~200 kev to one Mev were observed, and their energies and intensities were measured. A modification of the previously reported scheme of levels is proposed. (auth)

6398 STRONGLY EXCITED LEVELS OF ^{39}Ca IN THE ^{40}Ca(^{3}He,α)^{39}Ca REACTION. Yagi, K.; Ishimatsu, T.; Ejiri, H.; Tohei, T.; Ohmura, H.; Nakajima, Y.; Nakagawa, T. (Tokyo Univ.). Nuovo Cimento (10), 39: 1045-50 (Oct. 16, 1965).

Angular distributions of the α-particle groups in the ^{40}Ca(^{3}He,α)^{39}Ca reaction were measured at $E_L(^3He)$ = 24.4 Mev by the use of a broad range magnetic spectrograph. Alpha particle groups corresponding to excitation energies in ^{39}Ca of 0, 2.47 ± 0.03, 2.80 ± 0.03, 3.03 ± 0.05, 3.95 ± 0.03, 4.02 ± 0.03, 5.07 ± 0.05, 5.40 ± 0.05, 5.70 ± 0.1, and 6.05 ± 0.05 Mev were observed. The DWBA analysis shows that the ground state and the first excited (2.47) state consist mainly of a $(1d_{3/2})^{-1}$- and a $(2s)^{-1}$-neutron hole state, respectively. The $(1d_{3/2})^{-1}$ hole state is considered to split into the 5.07, 5.40, and 6.05 Mev levels with nearly equal fractions. The angular distribution corresponding to the 2.80 Mev level suggests an l = 3 neutron pickup, which is due to the configuration mixing with $1f_{7/2}$ neutron shell in the ground state of ^{40}Ca. (auth)

6399 PHOTOPROTONS FROM Mg. Manuzio, G.; Ricco, G.; Sanzone, M. (Istituto Nazionale di Fisica Nucleare, Genoa). Nuovo Cimento (10), 39: 1057-60(Oct. 16, 1965).

Photoprotons from Mg at maximum bremsstrahlung energy 31 Mev were measured. The results were compared with particle-hole calculations. The agreement is quite satisfactory in the lower-energy zone of the spectrum but the large enhancement of the oscillator strengths predicted by theory in the two high-energy 1^- levels, was not observed. (auth)

6400 LEVEL STRUCTURE OF ^{48}Ca. Peterson, R. J. (Univ. of Washington, Seattle). Phys. Rev., 140: B1479-82 (Dec. 20, 1965).

The elastic and inelastic scattering of 42-Mev alpha particles from ^{48}Ca was studied. The resulting elastic differential cross section was compared to a parametrized phase-shift analysis, and inelastic angular distributions were generated using an adiabatic method. Comparison with experiment allowed the determination of spins, parities, and transition rates for nine excited states of ^{48}Ca. The low-lying states (energies in Mev) and their spins and parities are 3.83 (2^+), 5.15 (3^-), 6.34 (1^-), 4.29 (4^+ or 5^-), 5.37 (3^-), 6.75 (2^+), 4.51 (3^-), 5.73 (2^+), 7.75 (3^-). Several other states were excited but can not be assigned unambiguous quantum numbers. The spectrum of ^{48}Ca is compared with that of ^{40}Ca, and the differences are discussed. (auth)

6401 HYPERFINE-STRUCTURE SEPARATION, NUCLEAR MAGNETIC MOMENT, AND HYPERFINE-STRUCTURE ANOMALY OF ^{131}Cs. Worley, Richard D.; Ehlers, Vernon J.; Nierenberg, William A.; Shugart, Howard A. (Univ. of California, Berkeley). Phys. Rev., 140: B1483-7(Dec. 20, 1965). (UCRL-12365).

The atomic-beam magnetic-resonance method was used to obtain the hyperfine-structure separation $\Delta\nu$, the nuclear magnetic dipole moment μ_I, and the hyperfine-structure anomaly Δ of ^{131}Cs. Independent values of μ_I and $\Delta\nu$ were obtained by observing one of the $\Delta F = \pm 1$ doublets in a field-independent region. The results of the measurements, made in the $^2S_{1/2}$ electronic ground state, are $\Delta\nu$ = 13181.375 (2) Mc/sec, μ_I(uncorr) = +3.517 (2) nm, and $^{131}\Delta^{133} = -0.45$ (5)%. Possible nuclear ground states for ^{131}Cs are discussed. (auth)

6402 DECAY OF ^{111}Pd AND ^{111m}Pd. Pandharipande, V. R.; Singru, R. M.; Sharma, R. P. (Tata Inst. of Fundamental Research, Bombay). Phys. Rev., 140: B1488-96 (Dec. 20, 1965).

The decay of 22-min ^{111}Pd and 5.5-hr ^{111m}Pd was studied using scintillation-spectrometer and coincidence techniques. The 22-min activity was studied in equilibrium with ^{111m}Pd and also independently, and it was observed to emit gamma rays of energies 70, 160, 280, 385, 400, 500, 560, 630, 750, 830, 960, 1130, 1380, and 1440 kev. Gamma rays of energies 1080, 1250, 1640, 1690, and 1900 kev were observed only in the decay of 5.5-hr activity. The beta spectrum of both the activities extends up to 2110 kev. From the beta-gamma and gamma-gamma cascade relations, a decay scheme with levels in ^{111}Ag at 70, 120, 280, 385, 470, 560, 1015, 1220, 1515, 1640, 1760, 1810, 1850, and 1970 kev was proposed. Possible spins and parities for these levels are discussed. (auth)

6403 DECAY OF ^{158}Eu. Schima, F.; Katoh, Toshio (Indiana Univ., Bloomington). Phys. Rev., 140: B1496-1500(Dec. 20, 1965).

The beta decay of ^{158}Eu to levels in ^{158}Gd was studied by means of scintillation crystals, beta-gamma, and gamma-gamma coincidence techniques. The sources of the 46 ± 1 min ^{158}Eu activities were obtained from the ^{158}Gd(n,p)^{158}Eu reaction. As observed in singles and coincidence spectra, the following gamma transitions were identified: 79.5, 182, 520, 610, 750, 820, composite 950, 1110, 1190, 1260, 1330, 1960, and 2180 kev. The composite 950-, 1110-, and 1190-kev gamma transitions were observed in coincidence with beta particles of kinetic energy greater than 900 kev. Beta-gamma coincidence experiments yielded the maximum energies of the principal inner beta branches as 2520 ± 120, 1950 ± 230, and 1115 ± 90 kev. The ground-state energy difference between ^{158}Eu and ^{158}Gd was determined as 3450 ± 150 kev, based on these data. The transition data are shown to be consistent with a decay scheme based on previously proposed levels. (auth)

6404 QUALITATIVE ASPECTS OF NEUTRON-NUCLEAR INTERACTIONS AND THE OPTICAL MODEL. Franco, Victor (Massachusetts Inst. of Tech., Cambridge). Phys. Rev., 140: B1501-12(Dec. 20, 1965). (MIT-2098-160).

The appearance of broad maxima and minima in the energy dependence of neutron-nuclear total and scattering cross sections below 100 Mev is given a simple explanation. Within the framework of the Glauber diffraction approximation, the general conditions for the occurrence of these maxima and minima are obtained in terms of an integral, over impact parameters, involving a phase-shift function. A modification of the approximation is used so that the formalism may be applied below 100 Mev. The assumption that the average phase difference between that portion of the neutron wave which traverses the nucleus and that which does not is equal to an integral multiple of π at cross-section maxima and minima is shown to be incorrect. The approximations are illustrated with some optical-model calculations which indicate that the positions of the maxima and minima shift to higher energies with increasing target mass number. Some numerical calculations using the Schroedinger equation with square-well and Woods-Saxon potentials are compared with cross sections calculated from the approximation. Near the maxima, appreciable contributions come from a number of partial cross sections. The appearance of these maxima implies neither a resonance in any single partial wave nor a maximum in any single partial cross section. A brief consideration of

the energy dependence in the total, absorption, and scattering cross sections separately, reveals that the principal qualitative features of the total cross section are manifest in the scattering cross section. (auth)

6405 OXYGEN-13. McPherson, R.; Esterlung, R. A.; Poskanzer, A. M.; Reeder, P. L. (Brookhaven National Lab., Upton, N. Y.). Phys. Rev., 140: B1513-16(Dec. 20, 1965). (BNL–9399).

Oxygen-13, a beta-delayed proton emitter, was produced by the reaction $^{14}N(p,2n)^{13}O$ with 50-Mev protons. Two delayed-proton groups were observed originating from levels in ^{13}N at 8.90 and 9.48 Mev. The half life of ^{13}O was determined to be 8.7 ± 0.4 msec. The beta-decay energy was estimated to be 17.5 ± 0.2 Mev on the basis of this half life and the known log ft values for the mirror nucleus. (auth)

6406 DECAY OF ^{105}Rh. Pierson, William R. (Ford Motor Co., Dearborn, Mich.). Phys. Rev., 140: B1516-28(Dec. 20, 1965).

The beta decay of ^{105}Rh ($t_{\frac{1}{2}}$ = 35.4 ± 0.1 h) was studied by beta and gamma spectrometry, with 4π beta counting (supported by other methods) for finding absolute intensities. Gamma transitions (kev), with intensities including internal conversion, are 306.3 ± 0.3 (5.4%), 319.3 ± 0.3 (19.4%), 442.7 ± 0.5 (0.04%), and a (38.77 ± 0.07)–(280.5 ± 0.4) cascade (0.17%). The energy separation between the 306.3- and 319.3-kev gammas is 12.97 ± 0.10 kev. From Pd K x-ray intensities, α_K are 5.8 ± 0.6, 0.020 ± 0.004, and 0.012 ± 0.001 for gammas 38.77, 280.5, and (306.3, 319.3) kev, respectively. Several gammas reported by earlier investigators are absent. Population of known ^{105}Pd levels at 344 and 489 kev does not occur to an observable extent. The ^{105}Rh beta maximum is 550 ± 54 kev; there is no gamma coincident with it. Betas with maxima 249 ± 17 and 133 ± 15 kev are coincident with the main gamma group (280.5, 306.3, 319.3 kev) and the 442.7-kev gamma, respectively. The Pd K x ray is coincident with betas of end point roughly 250 kev. There is no evidence for any ^{105}Pd levels below 280 kev, and certainly there are no levels below ~200 kev reached directly by beta transitions. Beta transitions to the indicated 280.5-kev level do not occur (≤0.03%). Inferring spin and parity assignments from these data, it is concluded that the decay of ^{105}Rh ($\frac{7}{2}$+, Q_β = 567 ± 20 kev) takes place by beta transitions to ^{105}Pd levels at 0 ($\frac{5}{2}$+, 75%), 306 (probably $\frac{7}{2}$+, 5.4%), 319 ($\frac{5}{2}$+, 19.5%), and 443 ($\frac{3}{2}$+ or $\frac{5}{2}$+, 0.04%) kev; and, via a gamma transition from the 319-kev level, to a level at 280 kev ($\frac{3}{2}$+). The results are discussed in terms of the spherical-potential shell model with phonon states, and the spheroidal-potential (Nilsson) model with rotational states. The Nilsson model gives a better account of the findings than might have been expected, although neither model is completely successful. (auth)

6407 INTENSITY OF THE E3 TRANSITION IN ^{38}Ar. Robinson, Berol L. (Oak Ridge National Lab., Tenn. Western Reserve Univ., Cleveland). Phys. Rev., 140: B1529-32(Dec. 20, 1965). (ORNL-P-1415).

The gamma rays emitted in the decay of ^{38}Cl were studied using a scintillation pair spectrometer. Three gamma lines were found. The transitions in the well-known E1-E2 cascade at 1598 ± 5 and 2166 ± 5 kev, respectively, have an intensity ratio of (0.85 ± 0.03) : 1 in the pair spectrometer. The cross-over E3 transition was also observed with an intensity of (4.9 ± 0.7) × 10^{-4} per 2166-kev gamma ray or (2.5 ± 0.4) × 10^{-4} per disintegration. The E3/E1 branching ratio from the second excited state of ^{38}Ar is (5.8 ± 0.8) × 10^{-4}, about 2300 times the single-particle estimate. The octupole vibrational character of the 3–level is discussed. (auth)

6408 ANGULAR DISTRIBUTIONS OF THE FAST-NEUTRON-INDUCED GAMMA RAYS FROM CALCIUM. Tucker, W. E. (Texas Nuclear Corp., Austin). Phys. Rev., 140: B1541-8(Dec. 20, 1965). (TID–22111).

An investigation was made of the neutron-induced gamma rays from natural calcium for incident neutron energies in the range from 3.5 to 5.0 Mev. Gamma rays which result from the (n,n′γ), (n,p′γ), and (n,α′γ) reactions in ^{40}Ca and from the (n,n′γ) reaction in ^{44}Ca are observed. The 90° differential gamma production cross sections are presented for gamma rays with energies of 0.51, 0.768, 1.158, 3.730, and 3.900 Mev. The angular distributions of the 0.768-, 3.730-, and 3.900-Mev gamma rays are also given at incident neutron energies of 4.2, 4.4, and 5.0 Mev. The experimental data are well described by the Satchler formalism. (auth)

6409 EMISSION OF ^{8}Li FRAGMENTS FROM Cu, Ag, AND Au IRRADIATED BY HIGH-ENERGY PROTONS. Katcoff, S. (Brookhaven National Lab., Upton, N. Y.); Baker, E. W.; Porile, N. T. Phys. Rev., 140: B1549-56 (Dec. 20, 1965). (BNL–9386).

Thin targets of Cu, Ag, and Au were irradiated in a scattering chamber with 2-Bev protons, and the ^{8}Li fragments emitted at various angles were collected in nuclear emulsions. Data were also obtained for ^{8}Li produced in emulsion irradiated directly by 1- to 3-Bev protons. Results are presented on the energy spectra of ^{8}Li, on the angular distributions, and on the emission cross sections. These are compared with the results of a detailed Monte Carlo calculation in which it was assumed that the ^{8}Li fragments are evaporated from the excited nuclei remaining after the prompt cascade. There is rough agreement between experiment and calculation for the cross sections, for the peak energies in the spectra, and for some of the spectral shapes. However, the experimental angular distributions are more strongly forward-peaked, and the experimental energy spectra in the forward direction are considerably broader than the calculated spectra. Either a substantial fraction of the fragments is emitted by a process other than evaporation, or the emission is by a mechanism intermediate between evaporation and fast fragmentation. (auth)

6410 ANGULAR CORRELATION MEASUREMENTS ON THE ^{25}Mg(d,pγ)^{26}Mg REACTION. Horoshko, R. N.; Weinberg, R. B.; Lidofsky, L. J.; Mitchell, G. E. (Columbia Univ., New York). Phys. Rev., 140: B1557-62 (Dec. 20, 1965).

Angular correlations were measured for the ^{25}Mg(d,pγ)^{26}Mg reaction at deuteron energies of 3.00 and 5.22 Mev. Correlations were measured at six proton angles for each energy for the following reactions: (d,p$_1$γ$_{1.81}$), (d,p$_2$γ$_{1.13}$), (d,p$_2$γ$_{1.81}$). These data are compared with calculations performed using the distorted-wave Born approximation. The present experiment is consistent with previous results on the ^{25}Mg(d,p)^{26}Mg reaction, where it was noted that a mixture of l values was necessary in order to fit the data. (auth)

6411 STUDY OF THE ^{203}Tl(n$_{th}$,γ)^{204}Tl REACTION. Prestwich, W. V.; Hughes, L. B.; Kennett, T. J.; Fiedler, H. J. (McMaster Univ., Hamilton, Ont.). Phys. Rev., 140: B1562-6(Dec. 20, 1965).

The gamma spectrum following the capture of thermal neutrons in natural thallium was observed with a lithium-drifted germanium detector. The energies and approximate intensities of 42 transitions in the energy range 4 to 6.6 Mev were determined. From these transitions, a level scheme and neutron-separation energy of ^{204}Tl were obtained. Several transitions in the low-energy region were also observed, and a decay scheme was constructed on the basis of energy considerations. (auth)

6412 SPECTROSCOPY OF THE LOWER EXCITED STATES OF ^{59}Co. Blair, A. G.; Armstrong, D. D. (Los Alamos Scientific Lab., N. Mex.). Phys. Rev., 140: B1567-9(Dec. 20, 1965).

The low-lying states of ^{59}Co were investigated by means of the (^{3}He,d) reaction on ^{58}Fe, using an incident beam whose energy was 22 Mev. In addition to strong l = 3 transitions to the $\frac{7}{2}^-$ ground state and a group of states centered at 2.08 Mev, strong l = 1 transitions to the first, third, and fourth excited states were observed. From these results and the results of previous experiments, the first and third excited states can each be assigned spin and parity of $\frac{3}{2}^-$. These assignments are consistent with the

results from a study of the $^{60}Ni(d,^3He)^{59}Co$ reaction. The present results are in agreement with previous assignments of either $1/2^-$ or $3/2^-$ for the fourth excited state, but can not distinguish between these values. Spectroscopic factors for these transitions were obtained from a comparison of the experimental data with the predictions of a distorted-wave calculation. (auth)

6413 CHARGE DISTRIBUTIONS OF ^{40}Ca AND ^{44}Ca FROM 250-Mev ELECTRON SCATTERING. Hofstadter, R. (Stanford Univ., Calif.); Noeldeke, G. K.; van Oostrum, K. J.; Suelzle, L. R.; Yearian, M. R.; Clark, B. C.; Herman, R.; Ravenhall, D. G. Phys. Rev. Lett., 15: 758-61 (Nov. 8, 1965).

New information is reported on differences between the charge distributions of ^{40}Ca and ^{44}Ca, obtained by means of elastic scattering of 250-Mev electrons. Agreement was reached with the recent result by the muonic-atom method, that the equivalent radius increases by only about 0.8%, compared with the $A^{1/3}$ prediction of 3.2%. It is also found that this 0.8% increase of the radius arises from a 2.2% increase in the half-radius of the charge distribution, together with a 1.6% decrease in the skin thickness. The comparative experiment was carried out on ^{40}Ca and ^{44}Ca by alternating the targets and measuring the cross sections for both isotopes under the same experimental conditions by an improved technique. An example of the spectra of scattered electrons observed with each isotope is shown. The elastic peak is considered and the quantity $D_{expt} = [\sigma(40) - \sigma(44)]/[\sigma(40) + \sigma(44)]$ is formed by inserting the appropriate elastic cross sections for the two calcium isotopes. The isotopic difference of electron scattering from ^{40}Ca and ^{44}Ca at 250 Mev is given. (J.F.P.)

6414 SCATTERING MEASUREMENTS ON NEUTRON RESONANCES IN ^{239}Pu. Sauter, G. D.; Bowman, C. D. (Univ. of California, Livermore). Phys. Rev. Lett., 15: 761-5(Nov. 8, 1965). (UCRL-14200).

Epithermal neutron resonance scattering measurements were made on ^{239}Pu using the electron linear accelerator as a pulsed neutron source for a time-of-flight experiment. Total spin values were obtained for as many resonances of ^{239}Pu as possible. Confirmation was given to the predictions of Bohr and Wheeler that the total spin and average fission width are correlated. The method used was that of the bright line technique which eliminates the fission neutrons and capture gamma rays. From these measurements J values were assigned to 15 levels (14.3, 15.5, 32.3, 35.3, 47.6, 52.6, and 75.2 ev) not previously determined by Fraser and Schwartz (Nucl. Phys. 30: 269 (1962)), and values for three levels (14.7, 22.2, and 44.5 ev) which disagree with their reported values. Also values of $g\Gamma_n^2/\Gamma$ were determined for two other resonances (50.0 and 85.6 ev) but no total spin assignments were made for them. The experimental arrangement and the analysis of data are described. (J.F.P.)

6415 STATIC QUADRUPOLE MOMENT OF THE FIRST EXCITED 2^+ STATE OF ^{114}Cd. Tamura, Taro (Oak Ridge National Lab., Tenn.); Udagawa, Takeshi. Phys. Rev. Lett., 15: 765-7(Nov. 8, 1965).

It is shown that it is not impossible to predict a large static quadrupole moment of the first excited 2^+ state of ^{114}Cd within the framework of the vibrational model. Previous theoretical values of this static quadrupole modes are also listed as well as the models from which they were calculated. (J.F.P.)

6416 INTERPRETATION OF HIGHER ROTATIONAL STATES OF DEFORMED NUCLEI AND FOUNDATIONS OF THE SELF-CONSISTENT CRANKING MODEL. Dreizler, Reiner; Klein, Abraham (Univ. of Pennsylvania, Philadelphia). Phys. Rev. Lett., 15: 893-6(Dec. 6, 1965).

Due to the empirical success of the equations $E(I) = \frac{1}{2}\omega^2(g_0 + 3C\omega^2 + 5D\omega^4 + 4F\omega^5 + \ldots)$ and $[I(I+1)]^{1/2} = \omega(g_0 + 2C\omega^2 + 3D\omega^4 + 4F\omega^5 + \ldots)$ which define the excitation energy through the intermediary of the angular velocity ω, it appears essential to understand more deeply the basis for their validity. The questions of whether they imply any specific mechanism or mechanisms and preclude others and that of the quantum mechanical meaning of the angular velocity parameter ω are investigated. A solution is outlined for these problems within the framework of the generalized Hartree-Fock approximation. In particular it is shown that these equations do not in any way discriminate among mechanisms. Also a quantum mechanical identification of the parameter ω is obtained. (J.F.P.)

6417 SHELL-MODEL STUDY OF THE CALCIUM ISOTOPES. Raz, B. James (State Univ. of New York, Stony Brook. Argonne National Lab., Ill.); Soga, Michi Phys. Rev. Lett., 15: 924-7(Dec. 13, 1965).

In this calculation only two single-particle levels, the $1f_{7/2}$ level and the $2p_{3/2}$ levels were included, and the four calcium isotopes, calcium-42 through calcium-45, were examined. Harmonic-oscillator wave functions were used throughout and only the T = 1 part of the two-particle residual interaction was used since only neutrons outside a closed shell were considered. The central potential was broken into two parts: V_{11}, which is the T = 1, S = 1 part of the interaction, and V_R, which is the T = 1, S = 0 part of the interaction that remains. The theoretical predictions for levels with known spin are listed for the four isotopes, and the experimental energy spectra are given: Good agreement was found. (J.F.P.)

6418 CROSS SECTIONS FOR THE GROUND- AND EXCITED-STATE NEUTRON GROUPS IN THE REACTION $^{16}O(\gamma,n)^{15}O$. Caldwell, J. T.; Bramblett, R. L.; Berman, B. L.; Harvey, R. R.; Fultz, S. C. (Univ. of California, Livermore). Phys. Rev. Lett., 15: 976-9(Dec. 20, 1965). (UCRL-12375).

Monoenergetic photons from the annihilation in flight of fast positrons from the electron linac, covering the range 17 to 28 Mev with a resolution of about 200 kev were used in the experiment on cross sections for the neutron groups in the reaction studied. Four ring ratios from a neutron spectrometer consisting of BF_3-rings obtained for a water sample over the range 17 to 28 Mev are shown and discussed. The cross sections are presented for the ground- and excited-state transitions. The total (γ,n) cross section is obtained at each energy from the sum of all the rings. The experiment supports a basic feature of the particle-hole description of ^{16}O in the giant-resonance region from 21.5 to 26 Mev in that only the ground state and 6.16-Mev, $3/2^-$ excited-state transitions occur with appreciable strength. Also, the shape of this excited state cross section near threshold is consistent with the dominant emission of l = 2 neutrons, as predicted by particle-hole calculations. (J.F.P.)

6419 PROJECTED HARTREE-FOCK SPECTRA IN LIGHT NUCLEI. Bassichis, W. H.; Giraud, B.; Ripka, G. (Centre d'Etudes Nucleaires de Saclay, Gif-sur-Yvette, France). Phys. Rev. Lett., 15: 980-2(Dec. 20, 1965).

It is shown that the Hartree-Fock theory, together with angular-momentum projection, is a useful approximation to the configuration-mixing calculations. The calculated overlap function is shown for neon-20, and the calculated and experimental energies of levels arising from various configurations for neon-20, fluorine-19, fluorine-18, and oxygen-18 are also shown. It is emphasized that the energies are binding energies relative to oxygen-16 and not simply relative excitation energies within a band. It concluded that with a simple Rosenfeld force and a single interaction strength, over 20 levels arising from seven different types of configurations were accounted for satisfactorily. Thus configuration-mixing calculations are well approximated by projecting angular momentum from the Hartree-Fock Slater determinant and using the same force as in the configuration-mixing calculations. (J.F.P.)

6420 HALF-LIFE OF ^{51}Cr. Marais, P. G.; Haasbroek, F. J.; Karsten, J. H. M. (Fruit and Food Tech. Research Inst., Stellenbosch, S. Africa). S. African J. Agr. Sci., 7: 881-4(1964).

Various previous half life values and their accuracy are discussed. To determine a more accurate value, ^{51}Cr was prepared by the reaction $^{50}Cr(n,\gamma)^{51}Cr$ and was used as sodium chromate in isotonic saline. A small aliquot of the

solution was applied to a piece of filter paper which was wrapped around a Perspex rod and fitted into the well of a well-type scintillation counter. The initial counting rate of the sample was ~200,000 cpm. The decay of ^{51}Cr was followed for 165 days and 127 readings were recorded. On each occasion a sufficient number of pulses were recorded to give a standard deviation of not more than 0.2%. The half life obtained was 27.701 ± 0.006 days. (TCO)

6421 ENERGY DEPENDENCE OF MEAN KINETIC ENERGY OF HEAVY NUCLEUS FISSION FRAGMENTS. Okolovich, V. N. Vestn. Akad. Nauk Kaz. SSR, No. 7, 58-62(July 1965). (In Russian).

A review is given of experimental data on the energy dependence of the mean kinetic energy of heavy nucleus fission fragments. Three characteristic energy regions of fissioning nuclei were analyzed: pre-threshold, near threshold, and above barrier fissions. The included diagrams show characteristic irregularities of the dependence on neutron energies in ^{233}U and ^{235}U. The results of the analysis indicated that the energy dependence of the mean kinetic energy of various fission fragments from 0 to ~25 Mev is not in agreement with Fowler hypothesis either at low or high above threshold fission energy. (R.V.J.)

6422 A STUDY OF (d,p) STRIPPING EFFECT ON INTERMEDIATE NUCLEI. [PART] III. Bochin, V. P.; Zherebtsova, K. I.; Komarov, V. A.; Krasnov, L. V.; Litvin, V. F.; Nemilov, Yu. A. Vestn. Leningr. Univ., No. 10, Ser. Fiz. Khim., No. 1, 34-51(1965). (In Russian).

The energy spectra and angular distributions of protons from the (d,p) reactions on targets of enriched ^{58}Fe, ^{58}Ni, ^{60}Ni, ^{61}Ni, ^{62}Ni, ^{64}Ni, ^{64}Zn, ^{66}Zn, ^{67}Zn, ^{68}Zn, and ^{70}Zn were studied with the application of a multi-angle magnetic analyzer. Altogether 245 levels of final nuclei were studied, including 59 new ones. The l and O^2 values were obtained for 160 levels, including 33 new ones. The isobar-spin constant for the nuclear optical potential was estimated by the shift of a single-particle neutron levels after the addition of two neutrons. In the domain A ≈ 64 the considerable number of proton groups with mixed angular distribution $l_n = 0 + l_n = 2$ was observed. A sharp increase of the cross section of stripping for even-even final nuclei was noted which, apparently, corresponds to the breaking of the neutron pair. The absolute cross sections of the formation of the first excited states of even-even nuclei showed correlation with reduced probability of transition in Coulomb excitation. (auth)

6423 α-DECAY AND NUCLEAR STRUCTURE IN THE REGION OF ^{208}Pb. Baktybaev, K. B.; Bukat, G. M. (Ioffe Inst. of Physics and Tech., Leningrad). Yadern. Fiz., 2: 585-95(Oct. 1965). (In Russian).

The α-decay relative reduced widths of nuclei in the region of ^{208}Pb are calculated taking the dynamics of inner motion into account. The results of calculations are compared with experimental data. (auth)

6424 SUM RULES AND TWO-NUCLEON CORRELATIONS IN NUCLEI. Sitenko, A. G.; Simenog, I. V. (Inst. of Physics, Academy of Sciences, Ukrainian SSR). Yadern. Fiz., 2: 603-14(Oct. 1965). (In Russian).

The inelastic scattering of fast electrons by nuclei and two-particle correlations in nuclei are considered. A general relation between the inelastic scattering cross section and the two-particle correlation function for nucleons in a nucleus is obtained. The spectral distributions of two-particle correlation functions are calculated on the basis of the shell model. The double magic nuclei ^4He, ^{16}O, and ^{40}Ca are considered as examples. Sum rules for the correlation functions are obtained. The influence of the motion of the center of inertia on the correlation functions is considered in the case of ^4He. (auth)

6425 THE GREEN FUNCTION METHOD IN A SIMPLE NUCLEAR MODEL. Belyaev, S. T.; Zelevinskii, V. G. Yadern. Fiz., 2: 615-34(Oct. 1965). (In Russian).

A simple model of a spherical nucleus is considered: nucleons on a single isolated level with a large momentum $j \gg 1$, interacting with quadrupole phonons. The purpose is to check the efficiency of the Green function method and the Fermi-liquid theory, for finite systems with low-energy collective excitations. The system of equations for the Green functions is approximately closed using relations of the Ward type. Green functions, vertex parts, and the probabilities of electromagnetic transitions are found. The obtained results are inconsistent with the usual assumptions of the Fermi-liquid theory. (auth)

6426 EFFECTS OF RESONANCE MODES ON CHANNEL COUPLING IN NUCLEAR REACTIONS. Balashov, V. V.; Doleshal, P.; Korenman, G. Ya.; Korotkikh, V. L.; Fetisov, V. N. (Moscow State Univ.). Yadern. Fiz., 2: 643-56(Oct. 1965). (In Russian).

An approximate version of the unified theory of nuclear reactions is formulated, making it possible to connect the general equations in this theory with a model description of the many-particle properties of nuclear structure. Applications of the theory to the elastic and inelastic scattering of nucleons and to the photoeffect are considered. (auth)

6427 CONCERNING THE SPECTRUM OF γ RAYS IN THE (n,γ) REACTION. Kosorukov, A. L.; Strutinskii, V. M. Yadern. Fiz., 2: 657-62(Oct. 1965). (In Russian).

Some results of the calculations of γ-ray spectra from excited nuclei are described. As compared with the previous studies more complete analysis is given of the role of different factors involved in calculations such as the gap energy and lower levels spectrum. (auth)

6428 ENERGY AND INTENSITY MEASUREMENTS OF THE GAMMA RADIATION EMITTED BY ^{182}W AND ^{183}W DURING THE DECAY OF ^{182}Ta AND ^{183}Ta. Gruber, U.; Koch, R.; Maier, B. P.; Schult, O. W. B. (Technische Hochschule, Munich; Daenische Atomenergiekommission, Risoe, Denmark). Z. Naturforsch., 20a: 929-38(July 1965). (In German).

A total of 17 γ-lines were measured in the decay of ^{182}Ta and 31 γ-transitions were observed during the decay of ^{183}Ta using the Risö bent crystal spectrometer. The consistency of the energies found was tested by means of the combination principle. The best set of states was determined for the level scheme of ^{182}W and ^{183}W. Some discrepancies between earlier intensity measurements are removed. (auth)

6429 MEASUREMENT OF THE MOESSBAUER-LAMB FACTORS IN THE NUCLEAR RESONANCE SCATTERING ON ^{197}Au. Speth, J.; Stanek, F. W. (Technische Hochschule, Munich). Z. Naturforsch., 20a: 1175-80(Sept. 1965). (In German).

A combined scattering-absorption experiment was described in which the influence of Lamb-Moessbauer factor f' on the resonance scattering was investigated on the 77.4-kev ground state transition of ^{197}Au. In a theoretical consideration the effect of the mean lattice oscillation time τ_m in comparison with the reciprocal level width $1/\Gamma$ of the excited level on which it was scattered. Both limiting cases $\tau_m \gg 1/\gamma$ and $\tau_m \ll 1/\gamma$ were considered. The first occurs in the Rayleigh scattering of x radiation and was indicated as a fast process and the second case, a so-called slow process, was assumed for the nuclear resonance scattering investigated. For the fast process the contribution f' is linear but for the slow process it is proportional to f'^2. If the resonantly scattered component is used as a secondary source for an absorption experiment, then an 84.5% absorption can be expected for a linear contribution of f'. For a quadratic contribution only 14% was obtained. The present measurements gave an absorption of 15.8 ± 4.2% which confirms satisfactorily that the slow process to be expected occurs. (tr-auth)

6430 A NONLOCAL NUCLEAR SINGLE PARTICLE POTENTIAL AND CHARGE INDEPENDENCE OF SHORT-RANGE FORCES. Meldner, H.; Suessmann, G.; Ulrici, W. (Univ., Frankfurt am Main). Z. Naturforsch., 20a: 1217-19(Sept. 1965).

Some results obtained in an attempt to determine a nuclear single particle potential of the Hartree-Fock type that contains isospin-dependent terms with the same parameters for both kinds of nucleons are reported. An

attempt was made to find the average potential parameters for the calculation of ground state energies. The unified potential obtained appears to be compatible with the available scattering data. (J.S.R.)

6431 ON THE RELATION BETWEEN EXPERIMENTALLY OBSERVED SINGLE PARTICLE ENERGIES AND LEVELS OF THE EXTREME SINGLE PARTICLE MODEL. Meldner, H.; Suessmann, G. (Univ., Frankfurt am Main). Z. Naturforsch., 20a: 1219-21(Sept. 1965).

Some possible reasons for which deviations of the order of 1 Mev and compressions of observed levels may be explained without using the assumption of the anomalous effective mass near the Fermi level are reported. (J.S.R.)

6432 Z DEPENDANCE OF BREMSSTRAHLUNG OF ELECTRONS BETWEEN 2.5 AND 4.0 Mev. Bourgoignie, R. J.; Vanhuyse, V. J.; Creten, W. L. (Univ., Ghent). Z. Phys., 188: 303-25(1965).

The Z-dependence of the high frequency part of the bremsstrahlung spectrum in the forward direction is investigated with a 4.3 Mev electron linear accelerator for electron kinetic energies ranging from 2.5 to 4.0 Mev. Thin beryllium, carbon, aluminum, titanium, copper, zirconium, silver and gold foils were used as targets. The relative photon yields are measured by counting the number of neutrons from the $^{9}Be(\gamma,n)^{8}Be$ reaction, the neutrons being detected by a long counter. An adequate correction factor to the bremsstrahlung yield for multiple scattering of the electrons before radiating is presented and checked at 3.5 Mev with a number of Al foils ranging in thickness from 0.27×10^{-3} to 1.61×10^{-3} radiation lengths. The results are compared with five different theoretical expressions for the bremsstrahlung cross section. The presence of electron-electron bremsstrahlung is very clear. For each used theoretical cross section the amount of photons due to this effect was determined supposing the theoretical nuclear cross section be exact for low Z elements. It is found that theoretical yields obtained with the Elwert corrected Born approximation formulas agree with experiment for all used elements except for gold. The experimental results for gold as compared with the Born approximation formulas are in agreement with the curves given by Koch and Motz. (auth)

6433 ON THE VALIDITY OF THE QUASI-PARTICLE APPROXIMATION IN NUCLEAR PHYSICS. Werner, E.; Mueller, D.; Emrich, K. (Univ., Heidelberg). Z. Phys., 188: 385-96(1965).

The validity of the quasi-particle approximation for the two-point function in nuclear physics is tested by means of one-particle strengths taken from (d,p) reactions. It is found that in general the quasi-particle approximation is not justified. (auth)

6434 NUCLEON-NUCLEUS SCATTERING AND SHELL MODEL. Meldner, Heiner (Univ., Frankfurt am Main). Z. Physik, 189: 10-22(1966).

Nucleon-nucleus scattering is treated in a shell model picture, i.e., the existence of a selfconsistent nuclear single-particle potential is assumed to represent the dominating part of the nucleon-nucleus interaction. For this case of reasonable splitting into effective one-body and many-body interactions the S-matrix is calculated by the formal methods of Gell-Mann, Goldberger, Watson et al., yielding a factorization into a unitary term which exhibits the potential resonances times a nuclear structure term containing reduced transition matrix elements. Some approximations are discussed for this matrix of transition probabilities due to residual many-body interactions. In order to test the applicability of the present form for the nucleon-nucleus S-matrix, a simplified one-parameter model for this reduced transition matrix is proposed. One application is the analysis of elastic neutron scattering on spherical nuclei in the medium Mev region. Some numerical examples show this form to be comparable with successful optical model calculations. An advantage of the present method is the possibility of determining realistic shell model potentials, especially their nonlocality and other nuclear structure information. The formalism is used in a rather specific problem, although it is more generally applicable and appears to be a reasonable approximation of the nuclear scattering problem. (auth)

6435 NUCLEAR STRUCTURE STUDIES IN THE NICKEL ISOTOPES WITH (d,p) AND (d,t) REACTIONS [Thesis]. Fulmer, Richard Harry. Pittsburgh, Univ. of Pittsburgh, 1964. 126p.

The levels of ^{57}Ni, ^{59}Ni, ^{60}Ni, ^{61}Ni, ^{62}Ni, ^{63}Ni, and ^{65}Ni are studied with (d,p) and/or (d,t) reactions. l values are assigned to the levels on the basis of angular distributions analyzed with distorted wave Born approximation (DWBA) calculations. The J-spins of many levels are indicated by their energies, l values, and (d,p)/(d,t) cross section ratios. J-spins of $l = 1$ levels are also indicated by the shape of both the (d,p) and (d,t) angular distributions: $p_{3/2}$ and $p_{1/2}$ neutron transfers lead to angular distributions of markedly different shape at large scattering angles. The difference in relative cross sections is about a factor of three at angles near 125°. From this information, essentially all levels in the odd isotopes up to or beyond 1 Mev binding energy are assigned to a shell model state and, with the aid of DWBA calculations, their spectroscopic factors are measured. These results are used to determine the degree of filling and the "center of gravity" of the shell model states in the $28 < N < 50$ shell. In the $^{58}Ni(d,p)^{59}Ni$ and $^{60}Ni(d,p)^{61}Ni$ reactions, a sufficiently large fraction of the $l = 2$ levels are observed to locate the $d_{5/2}$ and $d_{3/2}$ single-particle states at 6.0 and 9.3 Mev respectively in ^{59}Ni, and at 5.0 and 8.4 Mev respectively in ^{61}Ni. A relation between neutron-reduced width, Γ_n^0, and the stripping spectroscopic factor, S, is derived, and checked experimentally with two levels observed in both experiments; the agreement is satisfactory. Plots of neutron strength function vs. energy are obtained containing both neutron and stripping data, and subjected to the requirements of $\Sigma S = 1$ and width = 2W (where W is the depth of the imaginary potential in optical model). The results give the location of the $3s_{1/2}$ states as 7.3 Mev in ^{59}Ni and 6.0 Mev in ^{61}Ni. The distribution of levels belonging to each single-particle state is found to have approximately the width 2W expected from giant resonance theory, except that the $g_{9/2}$ states tend to be concentrated into single nuclear levels. (Dissertation Abstr.)

6436 MEASUREMENT OF SOME NUCLEAR PARAMETERS IN THE RADIOACTIVE DECAY OF ^{133}Ba, ^{115}Cd, AND ^{197}Pt [Thesis]. Bornemeier, Dwight Daniel. Manhattan, Kan., Kansas State Univ., 1965. 95p.

The radiations emitted by radioactive cadmium (115), cadmium (115m), barium (133), and platinum (197) were studied with the aid of scintillation (NaI(Tl)) and solid state detectors used in conjunction with multichannel analyzers. From the orbital electron-capture decay of barium (133) the gamma-ray intensity of the possible 54-kev transition in ^{133}Cs was measured in a singles absorber experiment and with a coincidence experiment. Results of the singles absorber experiment measurement indicate the ratio of any real 54-kev radiation to that of the 81-79 kev peak to be $2.89 \times 10^{-3} \pm 1.08 \times 10^{-3}$. An analysis of the coincidence experiment yields for this ratio $7.68 \times 10^{-3} \pm 1.38 \times 10^{-3}$ for a calculation that does not use measured or computed internal conversion coefficients. It is concluded that an upper limit for the ratio of the intensity of the 54-kev gamma-ray transition to that of the 81-79 kev transitions is 1 per cent. The K-shell internal conversion coefficient of the 191-kev transition in ^{197}Au was measured as $\alpha_k = 1.59 \pm 0.07$. From the theoretical internal conversion coefficients this measurement implies an E0-M1 mixture with the E0 component dominating. On the basis of a spin and parity of $1/2+$ for the 77-kev level this leads to a $1/2+$ assignment for the 268-kev level, which is in disagreement with a currently accepted model for the ^{197}Au nucleus. The recently reported gamma-ray transitions at 202 and 155 kev in the de-excitation of ^{197}Au following the beta decay of ^{197}Pt were shown to be associated with the de-excitation of ^{199}Au,

which is also present in unpurified sources produced by neutron irradiation of platinum. Gamma rays emitted in the de-excitation of ^{115}In via the beta decay of ^{115}Cd (2.3 days) and ^{115m}Cd (43 days) were confirmed at or near 34, 230, 260-263, 335, 490, 529, 935, 1129, and 1290 kev. The K-shell internal conversion coefficient of the 34-kev transition has been measured as $\alpha_K = 3.43 \pm 0.12$, which, when compared with the theoretical internal conversion coefficient, shows the transition to be E1 in character. Hence, either the 825 or 858 level must have positive parity. On the basis of intensities the 858 level was assigned as $d_{\frac{3}{2}}$. The previously reported and confirmed 656-883 kev cascade in ^{115}In from the decay of ^{115m}Cd was shown to be due to ^{110m}Ag present as an impurity in aged sources of ^{115m}Cd. (Dissertation Abstr.)

6437 INELASTIC SCATTERING OF 14 Mev NEUTRONS TO LOW LYING STATES OF LEAD, THALLIUM, TUNGSTEN AND TANTALUM [Thesis]. Pearlstein, Solomon. Troy, N. Y., Rensselaer Polytechnic Inst., 1964. 127p.

The energy spectra of neutrons inelastically scattered to low lying levels of lead and thallium, which are representative of spherical nuclei, and tungsten and tantalum, which are representative of strongly deformed nuclei, are investigated. Cross sections were obtained for excitation energies up to about 8 Mev. The integrated inelastic cross sections in this energy range varied from 12 ± 3 mb per sterad for tungsten to 17 ± 3 mb per sterad for lead. Discrete levels at about 2.5 Mev were noted in lead and tungsten and at 6.5 Mev in tungsten and tantalum. The experimental data indicated that the inelastic spectra observed were direct excitations of collective levels and had an intensity that lay considerably above the high energy tail resulting from compound nucleus evaporation. (Dissertation Abstr.)

6438 GAMMA RADIATIONS FROM THE PROTON CAPTURE OF ^{25}Mg [Thesis]. Neher, Dean Royce. Lawrence, Kan., Univ. of Kansas, 1964. 163p.

Monoenergetic protons were allowed to strike thin ^{25}Mg targets. The gamma radiation from the resulting ^{26}Al nucleus was then analyzed by standard scintillation techniques. The yield curve was obtained for proton energies ranging between 920 kev and 1.8 Mev. Three peaks that had been reported as single resonances at about 1.310, 1.748, and 1.768 Mev were each resolved into two components. Four weak resonances and a relatively strong resonance at 1.701 Mev were observed that had not been previously reported. In addition, a few previously reported resonances were not observed. Twenty resonances that are sufficiently intense and isolated from adjacent resonances were selected for study. At each of these resonances three pulse height spectra were obtained. Where feasible, coincidence measurements were also made. From these data a decay scheme containing the predominant transitions at each of the twenty resonances was constructed. The observed transition probabilities were used in conjunction with data from previous elastic scattering experiments to propose tentative spin and parity assignments of 3^- and 3^+ to the compound levels at $E_x = 7.35$ and 7.41 Mev respectively. The existence of two levels at 2.07 Mev was confirmed. One member of the pair decays by a cascade through the 1.06-Mev level; the other decays to the 420-kev level in 75% of the transitions and directly to the ground state in 25% of the transitions. At the 2.36-Mev level a 1.94-Mev gamma ray occurs in 60% and a 1.30-Mev gamma ray in 40% of the decays. The observed decay of the 2.66-Mev level is to the 1.06-Mev level. The transition from the 3.16-Mev level to the 0.42-Mev level was found to occur in at least 80% of the decays of the 3.16-Mev level. At the 5.13-Mev level the transitions to the 3.16-Mev level and the 2.08-Mev level occur with about equal probability. Proposed modes of decay for seven additional intermediate energy levels are proposed. (Dissertation Abstr.)

6439 POLARIZATION IN THE ELASTIC SCATTERING OF PROTONS FROM CARBON AND NITROGEN [Thesis]. Steben, John David. Urbana, Ill., Univ. of Illinois, 1965. 199p.

The polarization of protons elastically scattered from nitrogen and carbon was measured using double scattering techniques. The polarization was determined for nitrogen at a scattering angle of $48^\circ_{c.m.}$ in the proton energy interval 7.6 to 11.8 Mev. The polarization from carbon was determined for protons in the energy interval 12.6 to 13.6 Mev. Polarization angular distributions as well as excitation functions were obtained in this energy interval. The polarization resulting from elastic proton scattering with nitrogen targets has a constant value of -0.58 ± 0.10 in the incident proton energy interval 8.2 to 11.7 Mev. The polarization from carbon varied markedly with energy at most scattering angles. Throughout the angular range 20° to 140°, polarization measurements from carbon covered the range of energies from 12.8 to 13.4 Mev. In addition, angular distribution data $P(\theta)$ were obtained separately for the proton energy ranges 12.8 to 13.1 Mev and 13.1 to 13.4 Mev. The separate $P(\theta)$ curves differ significantly for $\theta > 90^\circ$. The experimental method involved double scattering, with the second scattering taking place in a 45° polarimeter. Both carbon and nitrogen targets were used as the second scatterer. The polarization analyzing properties of the polarimeter were measured for the carbon (nitrogen) analyzing targets, by first scattering 8.6 (13.5) Mev protons from carbon at 70°_{lab} (50°_{lab}) to obtain a highly polarized beam. The nitrogen data were taken in this manner. The $P(\theta,E)$ data described for ^{12}C(p,p) near 13 Mev were then obtained using the carbon first target as the polarization to be measured. The present polarimeter, when used with a nitrogen target and solid state detectors, has an overall resolution of 3% and a constant polarization (analyzing power) of 0.6 ± 0.1 for protons of 9 to 12.5 Mev. (Dissertation Abstr.)

6440 DIRECT (n,p) REACTION ON ^{58}Ni AND ^{60}Ni [Thesis]. Malanify, John Joseph. Troy, N. Y., Rensselear Polytechnic Inst., 1964. 115p.

Measurements of the energy and angular distributions of emitted protons from ^{58}Ni(n,p)^{58}Co and ^{60}Ni(n,p)^{60}Co were made with 14-Mev incident neutrons in an attempt to determine the character of the direct proton emission process in these reactions. A $\Delta E - E$ counter telescope with a surface barrier detector for proton energy measurement was used. Protons with energies greater than 8 Mev were studied with improved energy resolution and statistics as compared with previous measurements. The data indicate that the protons are predominately forward peaked, with the energy distributions displaying some gross structure. An interpretation of the results of the experiment is made in terms of a knock-out model for the direct (n,p) reaction process. Since for an appreciable proton energy range the proton comes from the filled $f_{\frac{7}{2}}$ shell, the spectra are characterized by the single-particle states populated by the captured neutrons. The location, angular momentum, and strength of these levels are determined from (d,p) reaction data. This information makes possible a test of the knock-out model. It appears that this model satisfactorily predicts the essential features of the experimental results. (Dissertation Abstr.)

6441 A ROTATION-VIBRATION MODEL FOR ODD-A ATOMIC NUCLEI [Thesis]. Roesser, James Royal. Troy, N. Y., Rensselaer Polytechnic Inst., 1964. 125p.

A collective model calculation is made for odd-A nuclei, which combines the rotational model of Chi and Davidson with the β vibrational model of Davydov and Chaban. The even-even core, which consists of all nucleons except the last odd nucleon, is allowed to undergo collective rotations and vibrations. This core may have a deformation β and an asymmetry γ. The last odd particle is coupled to the core by means of its motion through the shell model potential set up by the core. The eigenvalue equation cannot be exactly separated into rotational and vibrational parts. Thus a perturbation approach is used. The variable β is expanded about an equilibrium value β_I. The zeroth order solution is obtained by substituting β_I for β everywhere in the equation. The perturbation corrections account for the differences between using an average moment of inertia and potential (containing β_I), and the actual values of these

functions. The model is applied to ^{21}Ne, ^{21}Na, and ^{23}Na. The low-lying energy levels and the electromagnetic matrix elements are calculated. All three of these nuclei were examined by Chi and Davidson with the pure rotational model. In general the present work provides a small correction on this previous work. (Dissertation Abstr.)

6442 THE ELASTIC SCATTERING OF LITHIUM BY LITHIUM [Thesis]. Pinsonneault, Lawrence Lee. Minneapolis, Univ. of Minnesota, 1965. 99p.

The ^6Li on ^6Li and the ^7Li on ^7Li elastic scattering cross sections were measured. Angular distributions ranged from 90° cms forward to near 40° cms at 5° cms intervals. Complete angular distributions were obtained for both ^6Li on ^6Li and ^7Li on ^7Li at cms energies of 2.0, 2.1, 2.2, 2.3, 2.4, 2.5, 2.625, 2.75, 2.875, 3.0, and 3.25 Mev. Complete angular distributions were also obtained for ^6Li on ^6Li at cms energies of 1.6, 1.7, 1.8, 1.9, and 3.5 Mev. These angular distributions were normalized to Mott scattering at energies equal to about one half the height of the Coulomb barrier. The results were analyzed using the rounded cutoff Blair model. The parameters were highly correlated, but were consistent with an r_0 of 1.60×10^{-13} cms for ^6Li and with an r_0 of 1.65×10^{-13} cms for ^7Li. These Blair model r_0's are consistent with Blair model r_0's obtained in other heavy ion studies. The results were also analyzed using the continuum model of Blatt and Weisskopf. This analysis led to an r_0 of 1.38×10^{-13} cms for ^6Li and one of 1.52×10^{-13} cms for ^7Li. These continuum model r_0's also agree with other heavy ion continuum model r_0's. The total reaction cross sections predicted by the continuum model were also obtained. The raw data were analyzed using the method of nonlinear least squares, which converged uniformly due to Levenberg's modification. The Li^+ beams were stripped by a carbon film stripper in the acceleration column to obtain Li^{2+} and Li^{3+}. In this way beams of 7-Mev energy could be obtained even though the accelerator potential did not exceed 3.8 million volts. (Dissertation Abstr.)

Plasma Physics and Thermonuclear Processes

See also Fluid Physics and Thermodynamics

Refer also to abstracts 5633, 5683, and 5988.

6443 (AD-617383) NON-EQUILIBRIUM RADIATION. Technical Information Series (Revised Ed.). Kulander, J. L. (General Electric Co., Philadelphia, Pa. Missile and Space Div.). June 1965. 123p. (R64SD41). CFSTI $4.00 cy, $1.00 mn.

The criteria specifying the conditions for which a gas will be in a state of local thermodynamic equilibrium are discussed for both collisionally and radiatively controlled transition processes. Particular emphasis is given to the radiation field in a gas where the particle translational distribution functions are Maxwellian. A microscopic formulation of the transfer equation and solution for the source function is presented for a general n level atom where the first resonance line is optically non-thin. Specific solutions are given for a 3-level atomic model. The calculation of the radiative and collisional cross-sections and transition rates is discussed. The bound-bound and bound-free rates are calculated for the lower lying states of N I-VII assuming equilibrium distribution functions for temperatures between 10,000 and 1,000,000°K. The electron densities and temperatures for which the various collisional and radiative rates are balanced are presented as an indication of situations where the gas (N) will not be in a state of local thermodynamic equilibrium. (auth)

6444 (AD-617553) INTERACTION BETWEEN MAGNETIC FIELD AND FLOW FIELD FOR PLASMAS OF INFINITE CONDUCTIVITY. Cap, Ferdinand; Kerer, Gerold (Innsbruck Univ. (Austria)). Oct. 15, 1964. Contract AF61(052)-675. 8p. (SR-17; AFOSR-65-0933). CFSTI $1.00 cy, $0.50 mn.

Assuming that the boundary curve of a two-dimensional steady flow is given analytically and that the magnetic field in the whole flow domain is vertical to the flow velocity it is possible to calculate the magnetic field at the boundary. (TAB)

6445 (AD-617619) REFLECTION OF ELECTROMAGNETIC WAVES FROM INHOMOGENEOUS PLASMA. Liu, Chao Han; Wetzel, Lewis (Brown Univ., Providence, R. I. Div. of Engineering). June 1965. Contract AF19(628)-2498. 85p. (AFCRL-65-334). CFSTI $3.00 cy, $0.75 mn.

Reflections of electromagnetic waves and signals from an inhomogeneous, lossy, dispersive, anisotropic medium are discussed. Discussion is mainly confined to one dimensional stratified medium and high frequency waves. The medium can be either a dielectric or plasma region. Reflection of a monochromatic electromagnetic wave from a stratified medium was considered. To determine whether the weak reflections of order 1/K come from the bulk effect of inhomogeneity of the medium or from the discontinuities of the gradients of the refractive index, a straightforward field analysis was used in which the behavior of the refractive index in the neighborhood of a gradient discontinuity is controlled by adjustable parameters. An integral equation was derived from the wave equation and from it, a variational expression was obtained for the correction term to the WKB approximation result for the reflection coefficient. The reflection of a turned-on sine signal from a plasma medium was also considered. In the plasma, the electron density varies linearly in one direction. Complex integration was used to calculate the reflected signal. (TAB)

6446 (AD-617696) THE HELICAL INSTABILITY PRODUCED IN GASEOUS MAGNETOPLASMAS BY THE GYRO-INTERACTION OF MICROWAVES. Cherrington, B. E.; Goldstein, L. (Illinois Univ., Urbana. Gaseous Electronics Lab.). June 1965. Contract AF19(628)-2391. 175p. (AFCRL-65-257). CFSTI $5.00 cy, $1.00 mn.

The non-uniform absorption of gyro-resonant microwave energy by an electron gas was used to produce the helical instability in gaseous magnetoplasmas. This helical instability was examined both theoretically and experimentally. Stability criteria for the existence of the helix and the dependence of the properties of the helix on the plasma parameters were derived from the two-fluid magnetohydrodynamic equations for electrons and ions. The experimental examination of the instability was accomplished by the development of a suitable diagnostic procedure using low power (50 microwatt), non-resonant microwave sensing signals. The detailed examination of the properties of the helical instability verified the theoretical predictions. Where it was possible to measure the properties of the plasma discharge exactly, such as helix rotational frequency and discharge tube radius, excellent quantitative agreement between theory and experiment was found. Where it was only possible to estimate the plasma parameters, such as electron temperature and longitudinal gradients, good qualitative agreement between theory and experiment was found. (auth)

6447 (AD-618693) AN INVESTIGATION OF A RADIO FREQUENCY GENERATED CYLINDRICAL PLASMA WITH ALKALI METAL INJECTION [Thesis]. Cheatham, Daniel Washington Jr. (Air Force Inst. of Tech., Wright-Patterson AFB, Ohio. School of Engineering). 1965. 193p. (TR-65-2). CFSTI $5.00 cy, $1.25 mn.

The thermochemical and electrical properties of a moderate temperature cylindrical plasma column were studied. The column consisted of a mixture of a low ionization potential alkali metal and a carrier gas heated by a radio frequency field to elevated temperatures and thus partially ionized. Studies were made to produce a suitable experimental model, analyze such a plasma theoretically, and measure the properties of the laboratory plasma for comparison with theory. The effect of low ionization potential seeding on plasma properties was of primary concern as

was the applicability of various diagnostic techniques to this type plasma. (TAB)

6448 (AD–619045) INVESTIGATION OF THE DYNAMICS OF IONIZED MEDIA (PLASMAS). Final Technical Report. Brittin, Wesley E.; Chappell, Willard R. (Physics, Engineering, Chemistry Corp., Boulder, Colo.). May 1965. Contract AF33(615)-1334. 133p. CFSTI $4.00 cy, $1.00 mn.

A theory of transport phenomena in a nearly homogeneous system of interacting electrons and photons was developed. A hierarchy of equations was derived which couples the various particle and photon distribution functions. The hierarchy was truncated in a physically intuitive way so that a closed set of equations was obtained. The truncated set of equations was then solved in various orders of approximation making use of the well-known Bogoliubov assumption concerning the rates of relaxation of correlations and distributions. There results a set of coupled equations for the particle and photon distributions. Terms in the resulting equations correspond to various physical processes such as shielded electron-electron scattering, bremsstrahlung, Thomson scattering, etc. (auth)

6449 (AD–619370) HIGH-DENSITY PLASMAS. Status Report. Creedon, John E. (Army Electronics Command, Fort Monmouth, N. J.). July 1965. 17p. (ECOM–2603). CFSTI $1.00 cy, $0.50 mn.

The resistivity of high-density plasmas for use in high-current switches is being studied. Consideration is given to the plasma drop and its dependence on current. Data obtained from tests conducted on two diodes at peak current ranges from approximately 12,500 to 75,000 amperes at hydrogen gas pressures of 0.5, 1.0, and 5.0 millimeters are discussed. (auth)

6450 (AD–619527) MECHANISM AND DYNAMICS OF COAXIAL PLASMA ACCELERATION. Final Technical Report, October 1, 1963–September 30, 1964. Bostick, Winston H. (Stevens Inst. of Tech., Hoboken, N. J. Dept. of Physics). July 1965. Contract AF-AFOSR465-64. 11p. (SIT-P161; AFOSR–65-1532). CFSTI $1.00 cy, $0.50 mn.

The character of the current sheet that separates a plasma from a magnetic field was explored. One configuration of this current sheet is that formed by the flow of plasma over the dipole magnetic field produced by a loop coil inserted in the vacuum system. Magnetic field probes and electric field probes showed that this current sheet exhibits turbulence in the form of plasma vortices. The correlation of this plasma behavior with that of the solar wind on the geomagnetic field is being studied. The character of turbulence in the current sheet of the plasma coaxial acceleration was studied. The mechanism of plasma propulsion in the small two-wire and coaxial button guns was investigated. (auth)

6451 (AD–619668) NEUTRON ECONOMY IN FUSION REACTOR BLANKET ASSEMBLIES [Thesis]. Impink, Albert J. Jr. (Massachusetts Inst. of Tech., Cambridge. Research Lab. of Electronics). June 22, 1965. Contract DA36039AMC03200E. 263p. (TR–434). CFSTI $6.00 cy, $1.25 mn.

The conceptual design of a blanket assembly for a hypothesized fusion power reactor is considered from the point of view of neutron economy. Containment of a steady-state thermonuclear plasma composed of equal parts of deuterium and tritium in a cylindrical configuration is assumed. Requirements and limitations imposed on the blanket by the plasma and by other components of the reactor system were analyzed, and the conceptual arrangement of a suitable blanket utilizing a refractory metal first wall and fused-salt cooling is presented. Neutron transport and scattering models were compared in terms of applicability to the present problem. Calculated tritium breeding ratios and neutron-induced reaction rates in a variety of permutations on the basic blanket configuration are summarized and compared. It is shown that the proposed blanket design is adequate from the point of view of neutron economy. A reasonable degree of flexibility for satisfying other requirements imposed on the blanket is indicated when suitable combinations of nuclides are exploited. Consideration is given also to several shielding configurations and to the potential merits of various materials, including certain fissile nuclides, not treated in this study. (auth)

6452 (AD–619669) THERMAL AND CHEMICAL ASPECTS OF THE THERMONUCLEAR BLANKET PROBLEM [Thesis]. Homeyer, William G. (Massachusetts Inst. of Tech., Cambridge. Research Lab. of Electronics). June 29, 1965. Contract DA36 039AMC03200E. 120p. (TR–435). CFSTI $4.00 cy, $0.75 mn.

A theoretical study was made of the blanket that must surround a thermonuclear plasma to provide energy conversion and removal, neutron and gamma-ray shielding, and regeneration of the tritium burned in the D-T reaction. Power distributions and heat transfer were calculated and materials problems analyzed for blanket assemblies that are capable of tritium regeneration. The blanket arrangement chosen as a model consisted of a molybdenum vacuum wall in the form of a long cylindrical shell, cooled by fused Li_2BeF_4 and surrounded by an annulus, 55 cm thick, consisting of fused Li_2BeF_4 and graphite to channel the flow of coolant. Nuclear heating was calculated on a digital computer for neutron flux distributions calculated by Impink. In vacuum walls of 1, 2, and 3 cm of molybdenum, 16, 25, and 31%, respectively, of the D-T neutron energy are absorbed. The total heat liberated in the inner blanket is 17.5 Mev per fusion. The absorption of secondary gamma rays accounts for half of the total heating and almost all of the heating of the vacuum wall. Heat transfer and thermal stress limit the thermonuclear power to 400-500 watts/cm^2 of neutron energy incident on the molybdenum first wall, which is 2 cm thick. (TAB)

6453 (AD–619670) STUDY OF A THERMONUCLEAR REACTOR BLANKET WITH FISSILE NUCLIDES [Thesis]. Lontai, Laszlo N. (Massachusetts Inst. of Tech., Cambridge. Research Lab. of Electronics). July 6, 1965. Contract DA36039AMC03200E. 106p. (TR–436). CFSTI $4.00 cy, $0.75 mn.

The use of fissile nuclides in a fusion power reactor heat-extraction blanket was investigated from the point of view of tritium regeneration and power production. The existence of a stable, steady-state D-T plasma in a cylindrical configuration is postulated. Nuclear reaction rates were analyzed with the aid of theoretical methods and multigroup, multiregion computer codes. Nuclear heating rates were calculated. Optimization studies of several blanket configurations showed that a blanket with a thin Mo first wall, a narrow, fused $(LiF)_2BeF_2$ first-wall coolant region, and about 50 cm 21% C and 79% fused $(LiF\text{-}BeF_2\text{-}UF_4)$ primary attenuator region with 17 to 27 mole % $^{238}UF_4$ and about 50% ^6Li enrichment is feasible and practical. The calculated tritium regeneration is adequate. The total heat recovery is approximately twice that in a nonfissile blanket; approximately 90% of the heat is liberated in the primary attenuator region. The heating rate in the first wall and in the coolant region is independent of the UF_4 salt composition. The thermonuclear power limit is about 5 Mw/m^2 of neutron energy incident on the first wall. The performance of blankets with a UF_4 fused-salt coolant region was found to be marginal; fissioning metallic first-wall configurations are not feasible. (auth)

6454 (AD–619671) FUSION REACTOR BLANKET EXPERIMENT [Thesis]. Spangler, Patrick S. (Massachusetts Inst. of Tech., Cambridge. Research Lab. of Electronics). July 13, 1965. Contract DA36039AMC-03200E. 180p. (TR–437). CFSTI $5.00 cy, $1.00 mn.

The behavior of 1 to 14 Mev neutrons was measured in cylinders, 46 cm in dia and 38 cm thick, to evaluate previous theoretical calculations on neutron economy and tritium production in proposed fusion reactor blankets. The cylinders were constructed from 0.5-in. graphite slabs and 1-in. layers of solid lithium-beryllium fluoride salt encased in aluminum pans. The neutron spectrum

was measured with a series of threshold detectors: $^{238}U(n,f)$, $^{31}P(n,p)$, $^{56}Fe(n,p)$, $^{127}I(n,2n)$, and $^{19}F(n,2n)$. The spectra in the graphite assemblies are characterized by a sharp peak near 14 Mev, with a smaller, broader peak at 3 Mev. Farther from the source, the 14-Mev peak is attenuated more than the 3-Mev peak. Adding 3-cm Mo to the base of the assembly shifts the 3-Mev peak to lower energies and increases its size at the expense of the 14-Mev peak, because of the $^{92}Mo(n,2n)$ reaction. Addition of lithium-beryllium fluoride has no effect, because of the similarity in the scattering properties of the salt and the graphite. The removal of neutrons through the $^{6}Li(n,t)$ reaction was not observed, because of the small size of the assembly and the low (1 to 3%) isotopic content of ^{6}Li in the salt. Preliminary measurements indicated the feasibility of directly measuring the tritium produced in the assemblies by the $^{6}Li(n,t)$ and $^{7}Li(n,tn)$ reactions. (auth)

6455 (AD–619672) GAMMA-RAY SPECTRA IN FUSION BLANKET MOCK-UPS [Thesis]. Petrie, Lester M. Jr. (Massachusetts Inst. of Tech., Cambridge. Research Lab. of Electronics). July 2, 1965. Contract DA36039AMC03200E. 111p. (TR–438). CFSTI $4.00 cy, $0.75 mn.

Gamma spectra were measured in cylinders, 18 in. in dia and 15 to 16 in. thick, to evaluate previous theoretical calculations of gamma spectra in proposed fusion reactor blankets. The cylinders were constructed of 0.5-in. graphite slabs and 1-in. thick layers of lithium beryllium fluoride salt mixture contained in aluminum pans. Molybdenum plates were used to approximate first walls, 0 to 1.25 inches thick. The cylinders were irradiated by 14-Mev neutrons produced by bombarding a tritium target with a beam of deuterons from a 150-kilovolt Cockcroft-Walton accelerator. The target was positioned on the center line of the cylinder, 5.25 inches from its base. The gamma spectra were measured by collimating a beam of gamma rays leaking out of the side of the blanket mock-up and by using a sodium iodide scintillation crystal as a detector. The gamma spectra from the graphite assemblies are characterized by a large peak at 4.43 Mev, a smaller peak at 6.87 Mev, and a still smaller peak at 4.95 Mev. The spectra in the salt assemblies are characterized by large peaks at 6.63 Mev and 5.13 Mev, and several smaller peaks. The relative magnitudes of these peaks at different depths in the assemblies are in agreement with previous theoretical calculations. (auth)

6456 (AD–619888) RADIATION BY A UNIFORMLY ROTATING LINE CHARGE IN A PLASMA. Gianzero, Stanley C. Jr. (Polytechnic Inst. of Brooklyn, N. Y. Dept. of Aerospace Engineering and Applied Mechanics). June 1965. Contracts Nonr83938; Nonr83934. 77p. (PIBAL–873). CFSTI $3.00 cy, $0.75 mn.

A theoretical investigation was made on the radiation produced by a linear distribution of electric charge executing circular motion both inside and outside a cylindrical plasma column. The analysis includes the effects of compressibility and anisotropy of the plasma on the radiation characteristics of the charge distribution. In the incompressible isotropic case, a dipole resonance phenomenon was exhibited for the first harmonic of the angular frequency of rotation of the charge when the charge moved at non-relativistic velocities. If the charge moved at extremely small velocities, the resonance became a singularity. The influence of compressibility on these radiation characteristics is discussed and is shown to be negligible. In the case of the presence of a magnetic field, i.e., for an anisotropic plasma, the dipole resonance was shifted Moreover, a multipole resonance was possible for a sufficiently higher order harmonic. In a frequency range just above this multipole resonance, Cherenkov radiation contributed to the existent bremsstrahlung radiation for a single harmonic in the neighborhood of the singularity of the index of refraction. Thereafter, the radiation contributions of the remaining harmonics was negligible. (auth)

6457 (AD–622876) AN EXPERIMENTAL STUDY OF NONLINEAR PLASMA-WAVE INTERACTION. Scientific Report No. 1. Taylor, W. C. (Stanford Research Inst., Menlo Park, Calif.). Aug. 1965. Contract AF19(628)-4800. 39p. (AFCRL–65–654). CFSTI $2.00 cy, $0.50 mn.

A study was made of the effect of pulsed L-band radiation from a slot antenna upon a layer of hot ionized air passing over the slot, and of the resulting time-resolved radiated power received by a monitoring antenna well beyond the plasma layer. The plasma layers were produced by an r-f plasma jet and were nonuniform in electron density and collision frequency, similar to those expected in hypersonic flight through densities ranging between 10^{-4} and 10^{-3} atmospheres. The plasma frequency at the maximum was varied between about one-tenth and twice critical. Measurements were made of the r-f power thresholds required for producing perceptible electron heating and perceptible additional attenuation produced by r-f induced changes in the plasma conductivity. At low pressures, the electron heating thresholds were found to be considerably lower than required to produce new electrons in the hot gas, and about two orders of magnitude lower than required for breakdown in cold air at the same pressure. The thresholds for additional attenuation over the pressure range were about 8 db below the usual breakdown levels in cold air. The variation with pressure of power transmitted through the resulting plasma corroborates earlier experiments with discharges in cold air in a waveguide, showing a monotonic decrease as pressure decreases when the input power is much higher than the threshold required for nonlinear interaction. (auth)

6458 (CLM-R–44) THE EFFECT OF A FINITE TEMPERATURE ON THE ELECTRON CYCLOTRON RESONANCE INSTABILITY. Cordey, J. G. (Culham Lab., United Kingdom Atomic Energy Authority, Abingdon (England)). June 1965. 14p. Dep. mn; BIS $0.60; HMSO 3s.

The effect of Landau damping on the electron cyclotron resonance instability is investigated for a Burt-Harris type model of a confined plasma cylinder. The axis of the cylindrical shell of plasma lies along a uniform magnetic field. The plasma is assumed to consist of three groups of particles, a group of electrons which move in concentric Larmor orbits about the axis of the cylinder, another group of electrons with no component of velocity perpendicular to the magnetic field and a group of ions also with no component of velocity perpendicular to the magnetic field. A dispersion relation is then deduced, for electrostatic perturbations of this system. Analytical and numerical results are presented for the stability criteria and growth rates of the instability. (auth)

6459 (CNIE-PE–1) INTRODUCTORY COURSE ON MOTION OF CHARGED PARTICLES IN STATIC MAGNETIC FIELDS. Roederer, J. G. (Comision Nacional de Investigaciones Espaciales, Buenos Aires (Argentina)). July 1964. 41p. Dep. mn.

Several topics are reviewed, including motion of particles in static homogeneous magnetic fields, motion in homogeneous fields with external forces, motion in inhomogeneous fields having various geometries, adiabatic invariants, flux relations for trapped particles in a stationary state, effects of scattering on trapped-particle flux, geometric characteristics and particle trapping in pure dipole magnetic fields, and particle trapping in perturbed dipole fields. The effects of temporal field variations are touched upon lightly. (T.F.H.)

6460 (GA–6594) GENERAL ATOMIC TOROIDAL MULTIPOLE CONFINEMENT EXPERIMENT. Ohkawa, T.; Schupp, A. A. Jr.; Voorhies, H. G.; Yoshikawa, M. (General Atomic, San Diego, Calif. John Jay Hopkins Lab. for Pure and Applied Science). July 30, 1965. 15p. (CONF-650935–45).

From 2nd International Conference on Plasma Physics and Controlled Nuclear Fusion Research, Culham, Eng.

Confinement of plasma is studied in the General Atomic toroidal octopole machine. The magnetic field is produced by four current carrying rings supported inside a contoured conductor. The rings are energized by a transformer core linking the machine. The major radius of the machine is

63.5 cm with an aspect ratio of 5. The magnetic field on the minor axis is zero and increases to 3500 gauss at the wall between the rings. After crowbarring, the field decays in 5 milliseconds to its half value. The MHD stability calculation was carried out and the stability is assured up to the plasma pressure of 10^{16} ev/cc. Hydrogen plasmas from either a coaxial gun or a pinch gun with ion energies of 50–2000 ev and with densities of 10^{14}/cc are successfully injected through a port located at the outer conductor wall. After the injection, plasma spreads azimuthally, filling the machine. Electric probes, magnetic probes, and calorimetric probes were used extensively. Optical spectrometers and particle detectors are also used. The initial plasma density of 10^{13}/cc decays with a time constant of 1000 μsec. The electron temperature is about 10 ev and decays more slowly than the density. The ion temperature decays more quickly in about 200 μsec. No electric or magnetic fluctuations were observed on any of the probes. The decay of plasma energy is probably due to charge exchange reactions between hot ions and cold gas produced at the wall surfaces during injection. (auth)

6461 (GA–6646) COLLISIONAL INTERCHANGE INSTABILITIES IN SHEAR AND $\int d\ell/B$ STABILIZED SYSTEMS. Coppi, Bruno; Rosenbluth, Marshall N. (General Atomic, San Diego, Calif. John Jay Hopkins Lab. for Pure and Applied Science). Aug. 23, 1965. 34p. (CONF-650935-46).

From 2nd International Conference on Plasma Physics and Controlled Nuclear Fusion Research, Culham, Eng.

The stability analysis of systems possessing shear or $\int d\ell/B$ stabilization, or both, is performed starting from the Vlasov equation with a Krook collision operator and including the relevant microscopic effects. (auth)

6462 (GA–6650) KINETIC THEORY OF PARTICLES AND WAVES. Rostoker, N.; Matsuda, S. (General Atomic, San Diego, Calif. John Jay Hopkins Lab. for Pure and Applied Science). Aug. 16, 1965. 11p. (CONF-650935–47).

From 2nd International Conference on Plasma Physics and Controlled Nuclear Fusion Research, Culham, Eng.

The classical many-body problem is discussed in terms of a cluster expansion. The ordering of the cluster expansion is motivated by considerations of particle discreteness or mode-coupling. In either case the expansion parameter is potential energy/kinetic energy, so that expansions are the same. The plasma behaves like a collection of statistically independent quasi-particles for all calculations up to first order in the expansion parameter. This approach is generalized to second and higher orders. In addition to a further renormalization of the quasi-particles, statistically independent quasi-pairs emerge. Applications are made to a thermal equilibrium plasma, the kinetic equation for a spatially homogeneous stable plasma, and finally to an unstable plasma. Some corrections to the theory of weak turbulence from discrete particle effects are also discussed. (auth)

6463 (JUL–264-PP) ARBEITSBERICHTE DER THEORETISCHEN UND EXPERIMENTELLEN GRUPPEN FUER DAS JAHR 1964. (Report of the Theoretical and Experimental Groups for the Year, 1964). Vogelbruch, K. (comp.) (Kernforschungsanlage, Juelich (West Germany). Institut fuer Plasmaphysik). Apr. 1965. 108p. Dep. mn.

In 1964 a large θ-pinch research installation for the compression of a plasma in a linear geometry with approximately homogeneous magnetic field was completed and put in operation. The magnetic field has a magnitude of 100,000 gauss maximum and a half period of 17 μsec. Later a smaller magnetic compression experiment in cusp geometry was completed also with initial magnetic field, preheating, and compression field and which used the crowbar for prolongation of the maintenance field. For study of the preheating phase an experiment was undertaken. During the year the following results were obtained: with the 600 kjoule/20 kv compression experiment the ignition of the discharge, the preheating, and the compression up to 45 kgauss in hydrogen at initial densities of 0.03 up to 0.20 torr were investigated optically and spectroscopically. Drifts of the plasma were observed which can be partially reduced by a compensation of the field by means of specially formed coil gaps. Measurements with a differential interferometer showed at higher initial pressure the occurrence of flute instabilities and turbulence. Investigations on the effect of preheating and the field curvature on the stable operating range are in process. On a smaller θ-pinch (5 kj/25kv) measurements on the synchronization of the plasma in the compression, the ionization of the external volume, and the drift of the plasma column were carried out using a streak camera and a mack interferometer in the pressure range from 0.02 up to 0.05 torr of hydrogen. Significant flute instabilities were observed at higher densities. Measurements on the cusp compression experiment showed plasma temperature of 20 to 70 ev at a maximum field of 50 kgauss. On the moving wave accelerator, plasma pulses with a maximum velocity up to 1.1×10^8 cm/sec were observed and the radial and angular distribution of the ion energies in the plasma beam were measured with a newly developed ion spectrometer. The following theoretical studies were concluded: existence and unambiguity in the one dimensional Vlasov equation, particle acceleration in time linearly varying axial fields under consideration of the electrical space charge field, motion processes in a linear plasma accelerator, adiabatic invariants in particle motion in one dimensional spatially strongly changing fields, and Lie elements in free algebras and fast-positive operators. Investigations were continued on the Stark effect in static electric fields, on the theory of the boundary layer between plasma and magnetic field, and on the position of irreversible thermodynamics. Investigations were undertaken on the kinetic theory of plasmas in radiation fields, non-adiabatic particle orbits in the θ-pinch with anti-parallel fields, and the calculations of one-dimensional pulsed magnetic fields in the presence of coil geometry. The improvements made in diagnostic instrumentation are summarized. (tr-auth)

6464 (NASA-TN-D–3121) EFFECTS OF METASTABLE ATOMS ON VOLUME ION PRODUCTION IN A TENUOUS HELIUM PLASMA. Sovie, Ronald J.; Dugan, John V. Jr. (National Aeronautics and Space Administration, Cleveland, Ohio. Lewis Research Center). Nov. 1965. 33p. CFSTI $2.00 cy, $0.50 mn.

The semiclassical Gryzinski method was used to theoretically calculate the excitation and ionization cross sections for interactions between electrons and metastable 2^1S and 2^3S states of helium. These cross sections were used to calculate the effect of electron-metastable atom interactions on volume ion production processes in a steady-state tenuous helium plasma. The effects of neutral-metastable atom collisions were also considered. Experimentally obtained excitation functions were used for ground-state excitations and a Maxwellian distribution of free electron energies was assumed. Including the metastable atom interactions in the calculated volume ion production cost (defined as the net energy required for each ion produced) yielded a surprisingly small effect. Instead of the anticipated substantial reduction, the ion production cost was reduced by only about 12 percent at an electron kinetic temperature of 6 electron volts. Reductions in cost were obtained for electron kinetic temperatures up to 20 electron volts, and slight increases for higher temperatures. The unexpectedly high ion production costs occurred because the cross sections for the allowed excitations $2^1S \rightarrow 2^1P$, $2^3S \rightarrow 2^3P$ are very much greater than the ionization cross sections for the metastable states. The volume ion production cost, ion production rate and power consumed in ion production are presented as functions of electron kinetic temperature. The electron-metastable atom inelastic cross sections are also given as functions of electron energy. (auth)

6465 (RISO–105) AN ATTEMPT TO DETECT MICROINSTABILITIES IN COLLIDING PLASMAS. Jensen, V. O. (Atomenergikommissionen, Risoe (Denmark). Forsoegsinstitut). Aug. 1965. 17p. Dep. mn.

An experimental attempt is made to detect microinstabilities in colliding hydrogen plasmas. The colliding plasmas are produced by two coaxial guns facing each

other. The gas for the guns is supplied by two fast-acting valves. The characteristic plasma velocity is 50 cm/μs and the characteristic density 10^{15} to 10^{16} ions/cm^3. It is predicted that microinstabilities of the counter-streaming type should have a polarizing effect on the hydrogen spectral lines. In a measurement with 2% accuracy no polarization is found, and it is thus concluded that less than 0.3 ppm of the translational energy of the plasmas is converted into electrostatic energy in unstable waves. (auth)

6466 (SIT-2813-33) PROPERTIES OF ALKALI-METAL MAGNETOPLASMAS RELATED TO "ENHANCED DIFFUSION." Rogers, Kenneth C.; Wolf, Neil (Stevens Inst. of Tech., Hoboken, N. J. Dept. of Physics). Aug. 1965. · Contract AT(30-1)-2813. 18p. (SIT-172; CONF-650806-18). Dep. mn; CFSTI $1.00 cy, $0.50 mn.

From 7th International Conference on Phenomena in Ionized Gases, Belgrade.

Evidence for enhanced diffusion was found in thermally ionized alkali-metal plasma columns ("Q" machines). The radial density profile decay length is found not to be a monotonic function of axial magnetic field strength. The effect is similar to the "enhanced diffusion" observed in PIG and r-f discharges. In the experiments, a sudden onset of increased cross-field plasma transport arises from a beam-plasma interaction. The beam is a tenuous 10^6 electrons cm^{-3} hollow cylindrical shell of plate heating electrons (1.6 kev) which leak into the plasma at the edge of the hot end plates. The beam-plasma interaction gives rise to low frequency, 10–75 kc, plasma potential fluctuations. The frequency of these fluctuations is approximately that associated with the plasma column universal instability modes. Enhanced diffusion disappeared when the electron beam was suppressed or when the plasma column was terminated by electron dominated sheaths even in the presence of the beam. Observations tend to support the recent conclusions of Brifford, et al., that enhanced diffusion can arise from the coupling of energy into a plasma column mode by a weak beam of unthermalized electrons flowing along the magnetic field. (auth)

6467 (ORNL-tr-870) INTERACTION OF ION BEAMS WITH PLASMA LEADING TO "TWO-BEAM" INSTABILITIES. Gabovich, M. D.; Kirichenko, G. S. Translated for Oak Ridge National Lab., Tenn., from Paper No. CN-21/222 Presented at the IAEA Conference on Plasma Physics and Controlled Fusion Research, Sept. 6-10, 1965, Culham, England. 18p. Dep. mn; CFSTI $1.00 cy, $0.50 mn; JCL $1,60 fs, $0.80 mf.

Experimental data are presented that demonstrate the production of two-beam instabilities by the bombardment of plasma by ion beams, as well as by the interactions of two parallel interpenetrating ion beams having different velocities. The first case is illustrated by Ar-plasma–Ar-ion-beam interactions, and the second by K-ion-beam–K-ion-beam interactions. The utilization of these results for heating plasma is discussed. (T.F.H.)

6468 (ORNL-tr-871) THE HEATING OF PLASMA UNDER THE CONDITIONS OF BEAM INSTABILITY. Demirkhanov, R.; Gevorkov, A.; Popov, A.; Khorasanov, G. Translated for Oak Ridge National Lab., Tenn., from Paper CN-21/194 Presented at the IAEA Conference on Plasma Physics and Controlled Fusion Research, Sept. 6–10, 1965, Culham, England. 15p. Dep. mn; CFSTI $1.00 cy, $0.50 mn; JCL $1.60 fs, $0.80 mf.

An experimental investigation of plasma heating by injection of electron beams into the plasma volume from an external source is reported. The electron energy varies between 1 and 4 kev. The effects of impurities in the interaction volume are also studied. The studies are carried out using magnetically confined H_2 and He plasmas. The maximum plasma electron temperatures produced by this interaction are measured spectroscopically to be between 500 and 600 kev. (T.F.H.)

6469 (UCRL-Trans-1256(L)) THE HEATING AND CONFINEMENT OF PLASMA IN THE MAGNETIC WELL OF DECA-2. Biguet, A.; Blanc, P.; Gravier, R.; Lecoustey, Luc, H.; Renaud, C.; Tachon, J.; Veron, D. Translated for Univ. of California Lawrence Radiation Lab., Livermore), from paper presented at Second Conference on Plasma Physics and Controlled Nuclear Fusion Research, Culham, England, September 6–10, 1965. 36p. Dep. mn; JCL $3.60 fs, $1.28 mf.

A deuterium plasma jet, produced by an induction gun, is guided and decelerated adiabatically by an increasing longitudinal static magnetic field. A fraction of the plasma is captured between a barrier and a pulsed magnetic door, then compressed adiabatically between two mirrors. The superposing of a pulsed quadrupole field permits creation of a magnetic-well configuration. The lifetime of the hot plasma (with a mean energy of 1 kev) is 50 μs in the configuration with simple mirrors (where flute instabilities are observed), 200 μs in the magnetic-well configuration. The density of the plasma—determined by microwave interferometry, near-ultraviolet spectroscopy, or attenuation of a neutral-atom beam—lies between 10^{13} and 3×10^{14} cm^{-3}. On the other hand, the deduced density of the emission of fast neutral atoms by the plasma (the latter being assumed lost solely through charge exchange) is clearly lower, of the order of 10^{10} cm^{-3}. The total experimental results do not exclude the hypothesis that the lifetime of the plasma is limited by the diffusion in the loss cone. (auth)

6470 PHYSICAL PROPERTY DISTRIBUTIONS IN A LOW-PRESSURE CROSSED-FIELD PLASMA ACCELERATOR. Duclos, Donald P.; Wu, Y. C. Lin; Denison, M. Richard; Ziemer, Richard W. (Electro-Optical Systems, Inc., Pasadena, Calif.). AIAA (Amer. Inst. Aeron. Astronaut.) J., 3: 2026-32(Nov. 1965).

The physical phenomena that occur in a steady crossed-field accelerator were studied both experimentally and analytically. Experiments were conducted on a crossed-field accelerator of conventional design employing a single electrode pair and operated with argon at a channel static pressure of about 1-mm Hg and a magnetic field of up to 5000 gauss. Measurements of the current distribution over the anode and cathode surfaces and the potential and electron temperature distributions between the anode and cathode were obtained. An approximate theoretical analysis of the accelerator was developed which accounts for Hall effects, ion slip, viscosity, and elevated electron temperature. From this analysis, the potential, current density, and electron and atom temperature distributions were calculated. The calculations agreed reasonably well with the measurements except in the region near the electrode surfaces. As expected, at large values of the Hall parameter, the current distribution was found to be unsuitable for producing a high accelerator efficiency. (auth)

6471 DETERMINATION OF PLASMA DENSITY BY LASER INTERFEROMETRIC AND CONTINUUM RADIATION INTENSITY MEASUREMENTS. Boornard, A.; Nicastro, L. J.; Vollmer, James (Radio Corp. of America, Camden, N. J.). Appl. Phys. Lett., 7: 258-60(Nov. 15, 1965).

Helium–neon laser interferometers in which interference of infrared radiation is detected by an accompanying change in intensity of visible radiation were used to measure the electron density of gas discharge plasmas. The technique and results obtained are discussed. (M.O.W.)

6472 TURBULENT MIXING IN A LABORATORY PLASMA. Granatstein, V. L.; Buchsbaum, S. J. (Bell Telephone Labs., Inc., Murray Hill, N. J.). Appl. Phys. Lett., 7: 285-7(Nov. 15, 1965).

Plasma fluctuations were examined in the presence of a turbulent gas flow in a laboratory discharge. It is found that the behavior of the energy-containing eddies corresponds to that expected for a turbulent mixing process. The results are discussed. (M.O.W.)

6473 ON CLASSICAL HEAT TRANSFER IN TOROIDAL PLASMA COLUMN. Shafranov, V. D. At. Energ. (USSR), 19: 120-5(Aug. 1965). (In Russian).

In toroidal equilibrium plasma configurations, the thermal flux drift induces redistribution of plasma temperature along the magnetic surfaces. Compensation of the tempera-

ture gradient by a longitudinal "non-magnetized" thermal flux results in a certain effective thermal flux across magnetic surfaces. This additional toroidal flux was larger than the magnetized flux which is used for determining the plasma heat losses in the cylindrical geometry. An effective toroidal coefficient for heat transfer in plasma was found for smooth toroidal systems Tokomak and stellarator types with figure eight configurations. Equations were derived for the distribution of electric potential related to the above mentioned redistribution. (tr-auth)

6474 INTERACTION OF MODULATED BEAM WITH PLASMA. Fainberg, Ya. B.; Shapiro, V. D. At. Energ. (USSR), 19: 336-42(Oct. 1965). (In Russian).

The excitation of longitudinal waves in the interaction of a modulated electron beam with a plasma is studied. The conditions for the occurrence of instability are found, and the frequency spectrum and the increments of growth of the oscillations are obtained. (tr-auth)

6475 THE POSITIVE ARGON COLUMN IN LONG TUBES. Wojaczek, Karl; Rademacher, Karl (Physikalisch-Technisches Institut, Berlin). Beitr. Plasmaphys., 5: 331-41(1965). (In German).

The electron temperatures and the potential gradients determined in homogeneous positive columns of argon low-pressure discharges in a long tube (R = 6 cm) can be understood with respect to their absolute values and also with respect to their dependence on the discharge current intensity when it is considered that the elastic and inelastic electron collisions limit significant deviations from a Maxwell distribution of the electron velocities in the high electron energy range. (tr-auth)

6476 DETERMINATION OF THE SPACE DISTRIBUTION OF THE ELECTRON TEMPERATURE AND DENSITY IN STATIONARY LAYERS OF A HYDROGEN DISCHARGE USING MICROWAVE MEASUREMENTS. Heymann, P.; Prinzler, H.; Stirand, O. (Heinrich-Hertz-Institut, Berlin; Inst. of Physics, Prague). Beitr. Plasmaphys., 5: 343-58(1965). (In German).

The standing layers characteristic of low-pressure flow discharge in pure hydrogen were investigated using the microwave method at $\Lambda = 20$ cm wave lengths. From the attenuation, detuning and noise temperature of a flat resonator in whose axis the discharge is found, the concentration of the electrons, their collision frequency, and the temperature were determined. The evaluation requires the numerical solution of an integral equation of the first type whose core is the field distribution function of the resonator. In the cathode direction the electron temperature is displaced by approximately 0.25 striation periods ($\varphi \leq \pi/2$) with respect to the concentration. The measurement results permit, on the basis of a simple model, the role of individual elementary processes effective in the striated hydrogen discharge to be evaluated. (tr-auth)

6477 SINGULARITIES OF THE KINETIC DISPERSION EQUATION. Bachmann, P.; Wallis, G. (Heinrich-Hertz-Institut, Berlin). Beitr. Plasmaphys., 5: 359-70(1965). (In German).

Starting from the general expressions for the dielectric tensor and its special form in case of perpendicular propagation some problems of cycloharmonic resonances and of the gaps found by Gross and others are discussed. This concerns the problem of finding complete solutions of the linearized Vlasov equations. The dispersion equation is solved numerically in quasistatic approximation for several plasma parameters. (auth)

6478 SWIFTLY INDUCED ARGON PLASMAS IN INDUCTIVE HYDRODYNAMIC SHOCK WAVES TUBES. Rothhardt, Ludwig (Institut fuer Magnetohydrodynamik, Berlin). Beitr. Plasmaphys., 5: 377-80(1965). (In German).

The producibility of rapidly moved argon plasmas and their dynamics in the inductive hydrodynamic shock wave tube was investigated by means of time resolving photography of the luminescence phenomena at the source and in the guide tube. At argon pressures of 10^{-2} to 5 torr, propagation velocities of more than 5 Mach were obtained; at 0.1 torr, the first collision wave in the plasma moves at over 20 Mach. At the upper limiting pressure, the pulsing behavior of the gases compressed in the source begins to aggravate the effective production of collision waves in the guide tube. (tr-auth)

6479 EXPANDED KINETIC THEORY OF PLASMAS IN ROTATING MAGNETIC FIELDS AND ELECTROMAGNETIC SUPPLEMENTARY FIELDS. Vojta, Guenter; Kirsten, Thomas (Statistische Physik, Leipzig; Karl-Marx-Univ., Leipzig). Beitr. Plasmaphys., 5: 405-23 (1965). (In German).

The behavior of a Lorentz plasma in a spatially homogeneous rotating magnetic field, a constant magnetic field parallel to the rotation axis, the induced electric field and an external alternating electric field (of the same frequency) is treated within the framework of kinetic theory. The Boltzmann equation with collision integral is solved using a Fourier expansion. The tensors of electrical conductivity, diffusion and thermal diffusion are calculated and then discussed by means of the Onsager-Casimir reciprocity relations and the Kronig-Kramers relations. A generalized version of the Kronig-Kramers relations is given. Finally, the case of a spatially rotating magnetic field with arbitrarily space dependent phase (helical field) is treated. (auth)

6480 DETERMINATION OF ELECTRON AND ION DENSITIES AND TEMPERATURES IN XENON HIGH-PRESSURE PLASMA FROM THE ELECTRON AND ION COLLISION BROADENING OF STRONG EFFECT-SENSITIVE XENON LINES. Pranoto, Soemarmo; Schulz, Paul (Technische Hochschule, Karlsruhe, Ger.). Beitr. Plasmaphys., 5: 455-60(1965). (In German).

Electron densities and temperature were determined in the plasma column of a Xe high-pressure discharge from the electron and ion collision widths of the Xe lines 4624 and 4671 Å and compared with values that were obtained from the carrier collision widths of the mercury line 5770 Å in the same plasma when a slight addition of mercury was made to the Xe gas. The measurements were made at a pressure of 22 atm at current intensities of 15 to 30 amp. The electron concentrations are approximately 3.7×10^{16} cm^{-3} at 15 amp to 7.0×10^{16} cm^{-3} at 30 amp. The temperatures varied from 7340 to 7800°K. (tr-auth)

6481 FINITE AND INFINITE H-PLANE BIFURCATION OF A WAVE GUIDE WITH ANISOTROPIC PLASMA MEDIUM. Lee, W. W.; Lo, Y. T.; Mittra, R. (Univ. of Illinois, Urbana). Can. J. Phys., 43: 2123-35(Dec. 1965).

The problem of H-plane bifurcation in a parallel-plate wave-guide filled with homogeneous, anisotropic, incompressible plasma is considered. The static magnetic field is assumed to be along the edge of the septum. By using the Wiener–Hopf technique, the complete field solutions are obtained for both semi-infinite and finite bifurcations. (auth)

6482 ABOUT A DIFFUSIVE SPREADING OF INHOMOGENEITIES IN A WEAKLY-IONIZED PLASMA (IONOSPHERE). Gurevich, A. V.; Tsedilina, E. E. (Lebedev Inst. of Physics, Moscow and Siberian Inst. of Terrestrial Magnetism, Ionosphere and Radio-Wave Propagation). Geomagnetizm i Aeronomiya, 5: 251-9 (1965). (In Russian).

The effect of a vortex electric field on the spreading of inhomogeneities in weakly ionized plasma in a magnetic field is examined. A dispersion equation is obtained, and its roots, describing the process of spreading, are determined. It is shown that under general conditions the diffusive spreading of inhomogeneities is described by the fourth-order equation of ambipolar diffusion. (tr-auth)

6483 ABOUT A FORCE ACTING ON A BODY IN A PLASMA. Gurevich, A. V. (Lebedev Inst. of Physics, Moscow). Geomagnetizm i Aeronomiya, 5: 347-8(1965). (In Russian).

Ion recombination on the surface of a charged body in a plasma is considered qualitatively. A formula is derived for the total momentum imparted to the body by an ion recombining at the surface and rebounding from it. It is

shown that the momentum transferred depends on the recombination probability and on the surface potential of the body. Effects in a rarefied plasma associated with nonuniformity of the body surface or of the electric potential on the surface are discussed. The example of a cylinder with nonuniform surface in a plasma is considered, and force equations are derived for mirror scattering of ions on the surface. (M.J.T.)

6484 ELECTROMAGNETIC WAVE CONFLUENCE IN COLD MAGNETOACTIVE PLASMA. Kropotkin, A. P.; Pustovalov, V. V. (Lebedev Inst. of Physics, Moscow). Izv. Vyssh. Ucheb. Zaved., Radiofiz., 8: 886-92(1965). (In Russian).

On the basis of equations describing the nonlinear electromagnetic wave interaction in the cold magnetoactive plasma the combinational high-frequency wave scattering by the normal oscillations of the plasma is studied. (auth)

6485 SURFACE IMPEDANCE OF NONHOMOGENEOUS PLASMA WITH SHARPLY VARYING PARAMETERS. Permyakov, V. A.; Solodukhov, V. V. (Moscow Inst. of Power Engineering). Izv. Vyssh. Ucheb. Zaved., Radiofiz., 8: 893-8(1965). (In Russian).

A strong skin-effect in the nonhomogeneous plasma layer was studied in the linear approximation. The surface impedances of the nonhomogeneous plasma are represented as inverse power series of a large parameter, i.e., the gradient of permittivity. The large gradients of permittivity permit the reduction of the problem of diffraction on a radially nonhomogeneous sphere to a plane one. (auth)

6486 ON TWO DETECTION MECHANISMS IN GAS DISCHARGE PLASMA. Kononenko, K. I. (Kharkov State Univ.). Izv. Vyssh. Ucheb. Zaved., Radiofiz., 8: 972-6 (1965). (In Russian).

The detection effect in the glow discharge plasma is investigated. The dependence of the detector current upon the uhf power is obtained for the positive column and for the dark Faraday region of the discharge. The experiments in millimeter band are proved to be in good agreement with the theory. (auth)

6487 ELECTROSTATIC INSTABILITY OF A PLASMA WITH DISCONTINUOUS VELOCITY DISTRIBUTION. Brambilla, M. (EURATOM-CNEN, Frascati, Italy). Nuovo Cimento (10), 39: 1174-7(Oct. 16, 1965).

An investigation of a collision free, completely ionized plasma, whose ion distribution function F(V) has a jump in velocity space, is presented. An analysis of the discontinuity in F(V) is presented on the basis that it is the limit of a continuous function whose gradient becomes infinite at the jump velocity. (M.O.W.)

6488 AN ABLATION-TYPE PLASMA GENERATOR. Frind, Gerhard (General Electric Co., Philadelphia). J. Spacecraft Rockets, 2: 458-60(May-June 1965).

A plasma generator is described which uses solid ablating walls for the arcing chamber; this design allows the plasma jet to be discharged at a location different from that of the electrodes, thus keeping a low contamination level. A diagram of the generator layout is presented and discussed. The current-voltage characteristics for various generator parameters are given. The relation between measured current-voltage characteristics and erosion rates and the energy balance and axis temperature of the arc is considered briefly. (M.J.T.)

6489 A "SPARK-PLUG" STARTER FOR ARC PLASMA GENERATORS. Barr, T. A. Jr.; Mayo, R. F. (Army Missile Command, Redstone Arsenal, Ala.). J. Spacecraft Rockets, 2: 808-10(Sept.-Oct. 1965).

An arc starter is described which provides accurate simultaneous starting of two or more arc-type plasma generators under a wide range of pressures. Starter control and power supply are discussed. Results of starter performance tests are given, including the regions of spontaneous arc ignition, starter controlled ignition, and no ignition on a potential vs ambient pressure map. Circuit diagrams for the starting system and for the performance characteristics test are presented. (M.J.T.)

6490 THOMSON SCATTERING MEASUREMENTS OF MAGNETIC ANNULAR SHOCK TUBE PLASMAS. Patrick, Richard M. (Avco-Everett Research Lab., Everett, Mass.). Phys. Fluids, 8: 1985-94(Nov. 1965).

Measurements of Thomson scattering from the plasma electrons created by high speed shock waves in a magnetic annular shock tube were used to determine the electron density behind shock waves and some preliminary measurements of the electron velocity distribution. A Q-switched ruby laser furnished the light beam which was scattered by the plasma electrons. A rotating quartz prism furnished the Q-switching of the optical cavity for the ruby laser, and rather long Q-switched pulses were obtained (between 10^{-7} and 10^{-6} sec duration). The power level during the Q-switched pulse was between 30 and 100 mw. Rayleigh scattering from an air sample at various pressures was used to calibrate the power output of the laser and gave for all of the tests a simultaneous measure of the laser output power, while the Thomson scattering was being measured. The measurements of the electron density using the Thomson scattering and the plasma continuum intensities agreed within the scatter of the data. The electron temperature measurements obtained with the Thomson scattering showed that the electron temperature increased with increasing shock speed for a given initial condition. (auth)

6491 TRAVELING WAVE INTERACTION AND WAVE GROWTH IN A DENSE PLASMA. Messerle, Hugo K. (Cornell Univ., Ithaca, N. Y.). Phys. Fluids, 8: 1995-2005(Nov. 1965).

Traveling wave interaction for one-dimensional flow is analyzed using small-perturbation theory. This permits a separate treatment of the two major fluctuations, i.e., the harmonic response due to the imposed magnetic wave and the transient response to natural disturbances in the presence of the magnetic wave. No interaction takes place when both wave and plasma velocity are equal. The interaction increases as the relative velocity increases, and there are definite resonance peaks for the harmonic fluctuations at the relative sound speeds. The resonance is normally damped; however, the perturbation of the electrical parameters such as the electrical conductivity can have a destabilizing effect. Transient disturbances which travel at the relative magneto acoustic speed are normally damped when moving along the wave. However, as the relative speed is raised, these disturbance waves can be made to grow. Stability criteria are established, defining regions of instability for the relative speed. It is shown that the electric conductivity and the Hall factor are primarily responsible for instability due to their critical dependence on the fluctuating thermodynamic quantities in magnetohydrodynamic converters. (auth)

6492 HYDROMAGNETIC EIGENMODES IN MULTIPOLE FIELDS. Carovillano, R. L. (Boston Coll., Chestnut Hill, Mass.); McClay, J. F. Phys. Fluids, 8: 2006-13 (Nov. 1965).

A formalism is developed providing an exact analytical procedure for determining linearized hydromagnetic wave phenomena in a perfectly conducting plasma permeated by a static magnetic multipole field. All perturbations are harmonically represented by scalar and vector spherical harmonics. The vector wave equation for the perturbed electric field is then reduced to a set of coupled equations in the radial variable alone. Different harmonic modes are coupled because the vector wave equation is not simply separable in spherical coordinates (or any other known system of coordinates). The physical significance of operative couplings derives from parity and angular momentum conservation requirements. It is shown that the radial equations are generally soluble in principle. (auth)

6493 UNSTABLE PRECESSION UNDER THE INFLUENCE OF DRAG FORCES. Furth, H. P. (Univ. of California, Livermore). Phys. Fluids, 8: 2020-5(Nov. 1965). (UCRL-12309).

Coherent precession of plasma particles in ∇B is generally subjected to drag forces associated with viscous or

resistive energy dissipation in background plasma. The dissipated energy can be supplied by continual displacement of the processing entity along $-\nabla B$. Precession in mirror machines therefore tends to be unstable against drag, while the converse is true for minimum-B geometries. A heuristic mechanical model is first described. The precession of the E-layer is next shown to be drag-unstable if one uses the "super-particle model," which does not allow for a finite spread in particle precession frequencies. Similar results are obtained for ordinary mirror-machine plasmas in the two limits that are ordinarily considered stable by virtue of the high-density and low-density finite-Larmor-radius conditions. (auth)

6494 STATISTICAL THEORY OF NONADIABATIC MAGNETIC TRAPS. Robson, A. E.; Taylor, J. B. (United Kingdom Atomic Energy Authority, Abingdon, Eng.). Phys. Fluids, 8: 2026-31(Nov. 1965). (CLM-P-77).

The trapping and containment of particles injected into a nonadiabatic magnetic mirror trap are considered. The results of numerical orbit calculations are compared with a statistical theory which is shown to give essentially identical results. This statistical theory leads to simple expressions for the mean containment time and the mean density of trapped particles. These results indicate that the most significant factors in the nonadiabatic trapping process are the width of the acceptance cone (i.e., the solid angle in velocity within which the injected particles have a finite chance of capture) and the angular spread of the input beam. Optimum trapping requires that these two quantities be appropriately matched. When this is done the density approaches a limiting value (which is generally below the usually quoted "Liouville limit") and the buildup time is a minimum. Provided this matching can be achieved, there appears to be no special merit in using resonant nonadiabatic traps over any other form. (auth)

6495 CUSP COMPRESSION EXPERIMENTS. Allen, T. K.; Spalding, I. J. (United Kingdom Atomic Energy Authority, Abingdon, Eng.). Phys. Fluids, 8: 2032-46 (Nov. 1965).

A shock-heated plasma of density 3.5×10^{15} cm^{-3} and temperature 4×10^4°K is compressed by a rising cusp field which reaches 34 kG between the coils in 15 μsec. Time resolved measurements of electron density and temperature, plasma radius and hole size (at the ring cusp) are described and compared with the predictions of a simple hydrodynamic model in which the primary loss is by classical diffusion across field lines. The agreement between theory and experiment is within a factor of two and strengthens evidence provided by framing pictures that the plasma is stably confined for times of the order 10 μsec, with peak densities and temperature of 2×10^{16} cm^{-3} and 16×10^4°K, respectively. (auth)

6496 ADIABATIC CONTAINMENT OF CHARGED PARTICLES IN COMBINED MIRROR-MULTIPOLE CUSP MAGNETIC FIELDS. Siambis, J. G.; Trivelpiece, A. W. (Univ. of California, Berkeley). Phys. Fluids, 8: 2047-58(Nov. 1965).

Properties of combined mirror-multiple cusp magnetic fields and the motion of charged particles in such fields are presented for the cases of mirror-quadrupole and mirror-hexapole fields. The two methods used to study the motion numerically are: the adiabatic motion in terms of the magnetic moment and longitudinal invariant of the particle; and the guiding center motion. The regions of stable containment in these field configurations are determined by means of the adiabatic motion. The guiding center motion is used to determine when the simpler method of the adiabatic motion is valid. For weakly stabilized field configurations, the adiabatic motion is valid; however, for strongly stabilized field configurations, the guiding motion shows that the adiabatic description has a very limited range of validity. In addition, the effects of shear and torsion of the field on the guiding center motion are shown. (auth)

6497 SCATTERING OF A TEST-PARTICLE BY ENHANCED PLASMA FLUCTUATIONS. Tidman, Derek A., Eviatar, Aharon (Univ. of Maryland, College Park). Phys. Fluids, 8: 2059-65(Nov. 1965).

The scattering of a test-particle by enhanced electric field fluctuations in a plasma containing nonthermal electrons is considered, together with some characteristic times for wave-particle scattering in such a plasma. The calculations are based on the Balescu-Lenard equation. (auth)

6498 EXCITATION OF PLASMA RESONANCES BY A SMALL PULSED DIPOLE. Deering, W. D.; Fejer, J. A. (Southwest Center for Advanced Studies, Dallas). Phys. Fluids, 8: 2066-79(Nov. 1965).

The space and time dependence of decaying resonant oscillations excited in a collisionless plasma by an infinitesimally small pulsed dipole is determined in absence and in presence of an external magnetic field. Oscillations near the plasma frequency, the hybrid frequencies, and harmonics of the electron cyclotron frequency are treated. At a fixed time and at a short distance from the source, the field of the oscillations is nearly uniform. At longer distances the amplitude of the oscillations is proportional to some power of the distance, which in the presence of an external magnetic field is greater than unity and varies for different resonances. The phase of the oscillations also varies with the distance, and this probably explains the complicated interference effects observed with large satellite-borne antennas in the ionosphere. At very long distances the amplitude of the oscillations decreases after reaching a maximum. At the point of excitation the amplitude decreases as some inverse power of the time; at other fixed positions the amplitude at first grows then decreases as a higher inverse power of the time, and eventually the region of uniform decaying field near the point of excitation expands to include the position considered. (auth)

6499 COLLISIONAL DAMPING OF TRANSVERSE PLASMA OSCILLATIONS. Buti, B. (National Physical Lab., New Delhi, India); Jain, R. K. Phys. Fluids, 8: 2080-7(Nov. 1965).

The effect of Coulomb collisions on the transverse electron oscillations in a fully ionized hot plasma is studied by means of the Fokker-Planck equation. The damping coefficient for the electron-ion collisions γ_i turns out to be much greater than the one for the electron-electron collisions γ_e. To first order in electron-collision frequency, these are given by, $\gamma_i = [\nu_e/3(2\pi)^{1/2}][\omega_p^2/(c^2k^2 + \omega_p^2)] \cdot [1 + (2.075k^2v_0^2)/(c^2k^2 + \omega_p^2) - k^2v_0^2\omega_p^2/(c^2k^2 + \omega_p^2)^2]$, $\gamma_e = (41/16)[\nu_e/3\pi^{1/2}][\omega_p^2/(c^2k^2 + \omega_p^2)][k^2v_0^2/(c^2k^2 + \omega_p^2)]$, where v_0 and ω_p are the electron thermal speed and the plasma frequency, respectively. (auth)

6500 SMALL AMPLITUDE WAVE PROPAGATION IN HOT IONIZED GASES. Khosla, P. K.; Murgai, M. P. (Defence Science Lab., Delhi). Phys. Fluids, 8: 2087-96 (Nov. 1965).

Radiative transfer effects on both the forced and the free small-amplitude wave propagation problem in an ordinary as well as an ionized gas were investigated. The results predict an additional radiation induced mode. For an ionized medium, in the presence of a magnetic field, there are the Alfvén wave, adiabatic and isothermal magnetosonic, fast and slow waves. These investigations also show that the skin depth for the waves is proportional to the mean free path of the radiation and the lifetime to the time taken by a sound wave to travel a distance equal to the wavelength or radiation mean free path. The magnetic field seems to support the propagation of some modes, but oppose that of the radiation induced wave in an ionized medium. (auth)

6501 EXPERIMENTAL STUDY OF SHOCK WAVE FORMATION IN AN ALMOST COLLISION-FREE PLASMA. Goldenbaum, G.; Hintz, E. (Univ. of Maryland, College Park). Phys. Fluids, 8: 2111-12(Nov. 1965).

An experimental arrangement similar to the theta pinch experiments was used for the generation of the shock waves studied. Measurements were concerned with two problems. First, the plasma was investigated shortly before the magnetic compression pulse is applied. At this time the radial

temperature distribution was determined by measuring the ratio of the H_β to the continuum intensity, and the electron density was obtained from the measured half-width of H_δ. Second, a study was made of the shock wave formation by measuring the radial magnetic field profile as a function of time by means of a small probe. When the rising axial magnetic field is applied at the boundary of the plasma, cylindrically converging compression waves are generated. This phenomenon is described, and radial magnetic-field profiles at various times are shown. (J.F.P.)

6502 DIFFUSION APPROXIMATION FOR A PHOTON GAS INTERACTING WITH A PLASMA VIA THE COMPTON EFFECT. Weymann, R. (Univ. of Arizona, Tucson). Phys. Fluids, 8: 2112-14(Nov. 1965).

A simple explicit expression is given for the following problem: the time development of the energy spectrum of a low-energy homogeneous, isotropic photon gas interacting solely through the Compton effect with a low-density, low-temperature electron gas with a Maxwellian distribution. Also it is pointed out that under these idealized conditions the equilibrium distribution of the photons will not, in general, be the Planck function because the photon number is conserved. (J.F.P.)

6503 LOW-FREQUENCY ELECTRONIC OSCILLATIONS IN PLASMA BEAM INTERACTION. Rolland, P. (Centre d'Etudes Nucleaires de Saclay, Gif-sur-Yvette, France). Phys. Fluids, 8: 2114-15(Nov. 1965).

It is pointed out that when the inequality, $1 < V^2/a^2 < 1 + (N_b/N_p)$, where V is the monoenergetic electron beam velocity, a is the dispersion relation for the longitudinal electrostatic electronic waves, N_b is the density of the monoenergetic electron beam, and N_p is the density of a Maxwellian collision-free plasma, is satisfied, the dispersion relation for the longitudinal electrostatic electronic waves gives certain information. This information includes the high-frequency branches, and also a low-frequency loop passing through the origin, indicating the existence of electronic oscillations below the plasma frequency. (J.F.P.)

6504 EQUILIBRIUM STATISTICAL MECHANICS OF A TWO-COMPONENT PLASMA. Lamb, G. L. Jr. (United Aircraft Corp., East Hartford, Conn.). Phys. Rev., 140: A1529-34(Nov. 29, 1965).

The equilibrium statistical mechanics of an electron-ion plasma is developed in terms of the Wigner distribution function. This provides a convenient means of including the necessarily quantum nature of the electron-ion interaction at small distances. As an application of the theory, corrections to the Debye-Hückel limiting law for the thermodynamic properties of a two-component plasma are discussed. (auth)

6505 OBSERVATION OF A NEW TYPE OF INSTABILITY IN A THERMAL PLASMA. Porkolab, M.; Kino, G. S. (Stanford Univ., Calif.). Phys. Rev. Lett., 15: 752-5(Nov. 8, 1965).

The observation of an instability which occurs without axial electron drift in a thermally ionized potassium plasma and which may possibly be related to that observed in the Stellarator is reported. The r-f fields are only strong where there is a radial gradient of density within the plasma. Both a one- and a two-ended potassium plasma were used. The various instabilities are described, and a plot of the experimentally measured frequency variation with respect to magnetic field is given. It is observed that the frequency increases with magnetic field unlike the universal instability. Phase measurements indicate m = 1 type flutelike instability propagating in the direction of ion rotation. A collisionless pressure theory in Cartesian coordinates is used to predict the properties of this mode. It can be shown that there is a possible resistive instability, also predicted previously, but because the density is so low, this resistive instability would be extremely weak. Therefore, such an explanation of the effect is not considered satisfactory. (J.F.P.)

6506 RADIATION AND ABSORPTION VIA MODE CONVERSION IN AN INHOMOGENEOUS COLLISION-FREE PLASMA. Stix, Thomas H. (Princeton Univ., N. J.). Phys. Rev. Lett., 15: 878-82(Dec. 6, 1965). (MATT-393).

An outline is given for the small-amplitude wave theory for the conversion of a fast electromagnetic plasma wave into a very slow electrostatic mode (or vice versa) via the process of propagation across a mildly inhomogeneous plasma (e.g., density change of 2 : 1). The mode conversion is illustrated for wave propagation across a magnetic field into a plasma of increasing or decreasing density. The actual conversion takes place in the vicinity of the surface along which the density value satisfies the condition for a hybrid resonance. It is seen that such conversion can be made the basis for an advantageous scheme for ion heating in a plasma at the lower hybrid resonance frequency. At the upper hybrid resonance frequency, such conversion can explain the transferal of wave energy from an extremely short wavelength electrostatic Berstein mode into a long-wavelength electromagnetic mode, thus accounting for the observability of Landauer radiation by detectors placed well outside the plasma. (J.F.P.)

6507 CONSTRUCTION AND CALIBRATION TECHNIQUES OF HIGH FREQUENCY MAGNETIC PROBES. Phillips, R. C.; Turner, E. B. (Aerospace Corp., El Segundo, Calif.). Rev. Sci. Instrum., 36: 1822-5(Dec. 1965).

The construction and calibration of the high-frequency magnetic probes used to measure the transient magnetic fields in a linear pinch device are described. A simple and reliable calibration technique, using conventional laboratory electronic equipment, was developed to measure the absolute sensitivity of magnetic probes in the frequency range of 1 to 50 Mc. Factors affecting the frequency response of magnetic probes are considered, and high-frequency design and construction are discussed. A double probe which measures two magnetic field components simultaneously is described. The use of these probes is briefly mentioned. (auth)

6508 HIGH FREQUENCY INDUCTANCE OF A TORUS. Malmberg, J. H.; Rosenbluth, M. N. (General Dynamics Corp., San Diego, Calif.). Rev. Sci. Instrum., 36: 1886-7 (Dec. 1965). (GA–6395).

A formula for the h-f inductance of tori is presented, together with some numerical results for aspect ratios of 1.1 to 10.0. (D.C.W.)

6509 MINIATURE ROGOWSKI COIL PROBES FOR DIRECT MEASUREMENT OF CURRENT DENSITY DISTRIBUTIONS IN TRANSIENT PLASMAS. Wright, Edward S.; Jahn, Robert G. (Princeton Univ., N. J.). Rev. Sci. Instrum., 36: 1891-2(Dec. 1965).

The measurement of current density distributions in transient plasmas by observation of the emf induced in a Rogowski coil by the flux changes is briefly discussed. (D.C.W.)

6510 ONE DIMENSIONAL FLOW OF A PLASMA WITH AN EXTERNAL MAGNETIC FIELD. Ghoshal, Sudhanshu Kumar (Jadavpur Univ., Calcutta). Z. Angew. Math. Phys., 16: 537-8(1965).

The solution of the one-dimensional flow of a plasma in the presence of a magnetic field perpendicular to the direction of flow is obtained, assuming $P_r = \frac{3}{4}$, c_p is constant, and $T = T(u)$. (M.J.T.)

6511 PLASMA WAVES IN INHOMOGENEOUS MEDIUM. Volland, Hans (Univ., Bonn). Z. Naturforsch., 20a: 1143-9(Sept. 1965). (In German).

The propagation of plane plasma waves in an anisotropic and inhomogeneous medium consisting of many random plasma components was investigated using the linearized magnetohydrodynamic equations. The development of the equation system leads to a system of homogeneous differential equations of the first order, whose general solution is the matrizant. It describes the coupling of the differing characteristic wave forms within the inhomogeneous medium. If the plasma can be approximated by a random number of thin homogeneous layers, solution forms arise which are suitable for numerical calculation on a digital computer. The energy balance for all forward and backward characteristic waves was derived. For a 2-component gas consisting of ions and electrons and with perpendicular

incidence of the waves the solutions forms are given explicitly. (tr-auth)

6512 SUPPLEMENTARY CALCULATIONS FOR REFLECTED COLLISION WAVES IN THERMAL PLASMAS. Artmann, J. (DVL-Institut fuer Plasmadynamik, Stuttgart). Z. Naturforsch., 20a: 1213-16(Sept. 1965). (In German).

The results of supplementary calculations of the plasma parameters with respect to ideal perpendicularly reflected shock waves in helium and argon are given. The excitation energies can be neglected for strong shock waves. (J.S.R.)

6513 GATE VALVES FOR ULTRA-HIGH VACUUM SYSTEMS (Engineering Materials). (Lawrence Radiation Lab., Univ. of California, Livermore). (CAPE-1266).

32 drawings.

The gate valves necessary for optimum operation of vacuum systems were developed for use in an ultra-high vacuum system. All parts of the valve including the gate seal were constructed of inorganic materials and capable of operating through a temperature range of 77 to 700°K. The valve provides isolation of selected parts of the vacuum pumping system as required for optimum operation. The valves were used in the ALICE device in which neutral H atoms are injected at 20,000 ev into a plasma. The ALICE is the third component in the magnetic mirror program. (For details, see TID-4100). (M.C.G.)

6514 ALICE "C" TRAPPING MIRROR COILS (Engineering Materials). (Lawrence Radiation Lab., Univ. of California, Livermore). (CAPE-1265).

19 drawings.

Trapping mirror coils used with the ALICE device were constructed with 360 turns of 0.340 sq hollow Cu conductor with dacron insulation sleeving and vacuum impregnated with epoxy resin. They operate at liquid-nitrogen temperature with a conductor current of 5,000 amps. A special two-in-hand conductor winding technique permits all hydraulic connections to be at the outside of the coil while holding the length of a single hydraulic run to ~210 ft. The coil terminal region is solidly constructed and epoxy impregnated with the main coil body for exceptional strength and rigidity. Neutral H atoms are injected into the ALICE device at 20,000 ev. The ALICE device is used in studying stable confinement in thermonuclear research. (For details, see TID-4100). (M.C.G.)

6515 PROCESS FOR PRODUCING INTENSE MAGNETIC FIELDS FOR THE PURPOSE OF CONFINING A PLASMA. Linhart, Jiri George. U. S. Patent 3,214,342. Oct. 26, 1965. Priority date July 5, 1960, Belgium.

A process and device are described for producing a magnetic field of several megagauss for the purpose of confining a plasma to enable fusion reactions to take place. The apparatus includes a cylindrical enclosure having a wall made of a material permeable to gases and a circular base equipped with a plurality of circular electrical-discharge devices that are concentric with the axis of the enclosure and capable of producing trains of electrical discharges of several tens of kilovolts. The gas is introduced into the highly evacuated cylindrical enclosure immediately after a central column of plasma has been produced in it, and the gas is subjected to a series of electrical discharges co-axial with the central column of plasma causing the gas to assume the shape of a centripetally moving annular column that compresses the field confining the central column of plasma. (B.L.M.)

Shielding

Refer also to abstracts 5673, 5751, 6297, and 6626.

6516 (AD-617524) THE BARRIER ATTENUATION INTRODUCED BY A VERTICAL WALL. Final Technical Report. McDonnell, C.; Velletri, J. V.; Starbird, A. W.; Batter, J. F. (Conesco, Cambridge, Mass.). Sept. 1, 1964. Contract DA18020ENG3096. 62p. (PSDC-TR-15). CFSTI $3.00 cy, $0.75 mn.

A series of tests designed to evaluate the attenuation introduced by a vertical wall adjacent to a horizontal field of contamination is described. The variation of the resultant attenuation with height was found to agree well with theory. Actual attenuation values measured were higher than those theoretically predicted by an amount equivalent to approximately eight percent of the wall thickness. (auth)

6517 (CONF-651101-41) INFINITE MEDIUM SPECTRUM-WEIGHTED GROUP CONSTANTS FOR GAMMA HEATING CALCULATIONS. Dudley, T. E.; Mendelson, M. R. (Knolls Atomic Power Lab., Schenectady, N. Y.). [1965]. Contract W-31-109-eng-52. 35p. Dep. mn; CFSTI $2.00 cy, $0.50 mn.

From 13th Conference on Remote Systems Technology, Washington, D. C.

A numerical solution of the infinite medium gamma ray slowing down equation is presented. Using this solution, a comparison was made to previous calculations for lead, copper, water, zirconium, aluminum, iron, and nickel. It was shown that the spectrum $Ee^{-1.1E}$, while a rather good representation of the equilibrium energy spectrum in a large fuel region, was not a particularly good representation of the equilibrium energy spectrum in large metal region. The effects upon the group constants of weighting with respect to the fission spectrum instead of the appropriate equilibrium spectrum are investigated. Subsequently, the effects upon gamma heating rates are considered. (M.O.W.)

6518 (NAA-SR-Memo-11516) THE OPEX SHIELD OPTIMIZATION CODE. Bernick, R. L. (Atomics International, Canoga Park, Calif.). July 13, 1965. Contract AT(11-1)-Gen-8. 39p. Dep. mn; CFSTI $2.00 cy, $0.50 mn.

The OPEX code uses the method of steepest descent to minimize laminated shield weight subject to the constraint of a constant dose rate at a detector point. The dose rate is approximated by an exponential fit to data obtained from experiments or analytical calculations. A Fortran listing of the code and a sample problem are included. (auth)

6519 (ORNL-3858(Vol.1), pp 20-41) REACTOR SHIELDING. (Oak Ridge National Lab., Tenn.).

Summaries of 26 papers on reactor shielding research are presented. The papers deal primarily with neutron and gamma transport, albedos, and distributions for concrete. (M.O.W.)

6520 (ORNL-3858(Vol.1), pp 42-6) RADIATION SHIELDING INFORMATION CENTER. (Oak Ridge National Lab., Tenn.).

Summaries of 10 papers on radiation shielding carried out at ORNL during the past 2 years are presented. The papers deal with neutron and gamma shielding. (M.O.W.)

6521 (ORNL-3858(Vol.2), pp 73-81) THEORETICAL STUDIES OF HIGH-ENERGY RADIATION SHIELDING. (Oak Ridge National Lab., Tenn.).

Summaries of 19 theoretical studies on high-energy radiation shielding are presented. The summaries deal primarily with nuclear cascade calculations. (M.O.W.)

6522 (UCRL-12411) FINITE DIFFERENCE METHODS FOR NONLINEAR RADIATION TRANSPORT. Campbell, Philip M. (Lawrence Radiation Lab., Univ. of California, Livermore). Aug. 20, 1965. Contract W-7405-eng-48. 23p. Dep. mn; CFSTI $2.00 cy, $0.50 mn.

A formulation is given of the nonlinear, frequency-dependent transport problem in one dimension, assuming local thermodynamic equilibrium. Equivalent representations of the angular distribution are discussed, including the treatment of discontinuities. A method for the combination of transport and diffusion based on the equivalence of the angular representations is presented. The performance of this method is illustrated in a variety of sample calculations. (auth)

6523 ON THE LINEAR ATTENUATION COEFFICIENT OF ^{60}Co AND ^{137}Cs γ-EMISSION BY ALLOYS. Kutovoi, V. I.; Stetsenko, V. I. At. Energ. (USSR), 19: 203(Aug. 1965). (In Russian).

Experimental graphs are given of the linear attenuation coefficient of ^{60}Co and ^{137}Cs gamma radiation as a function of the content of lead in Pb–Bi and Pb–Sn alloys. (R.V.J.)

6524 ATTENUATION OF REACTOR RADIATIONS IN SERPENTINE SAND. Vasil'ev, G. A.; Veselkin, A. P.; Egorov, Yu. A.; Moiseev, G. G.; Pankrat'ev, Yu. V. At. Energ. (USSR), 19: 354-9(Oct. 1965). (In Russian).

Results are presented of an experimental study of the attenuation of reactor radiation in serpentine sand having a specific weight of 1.62 g/cm^3. The sand investigated contained about 11.5% chemically associated water, separating at temperatures above 450°C. Measurements were carried out of the attenuation of fluxes of fast and thermal neutrons, the attenuation of the dose rate of neutrons and gamma radiation, and the spectra of fast neutrons in serpentine sand. The fast-neutron relaxation lengths calculated on the basis of the experimental data are compared with relaxation lengths of fast neutrons in boron carbide, serpentine concrete, and iron-ore concentrate. (tr-auth)

6525 BACK-SCATTERING OF GAMMA RAYS FROM SPHERICAL SURFACES. Andryushin, N. F.; Bulatov, B. P. At. Energ. (USSR), 19: 392-3(Oct. 1965). (In Russian).

The energy build-up factors for the reflection of ^{60}Co and ^{137}Cs gamma rays from convex and concave hemispherical water surfaces were measured. Results are presented of build-up factor as a function of hemisphere radius for h = 0, where h is the height of the detector above the surface of the scatterer, and for various values of h for a 20-cm radius, for both sources. (M.J.T.)

6526 ANGULAR DISTRIBUTION INTENSITIES OF GAMMA RAYS SCATTERED IN LEAD AND WATER. Shirkin, L. M. At. Energ. (USSR), 19: 394-5(Oct. 1965). (In Russian).

The angular distribution of the intensity of scattered gamma radiation in lead and water was calculated by the Monte Carlo method. A plane monodirectional source with energy 4.0 Mev in a barrier geometry was considered. The lead barrier was 14 free path lengths thick, and the water barrier, 16. Results are presented for path lengths of about 3, 13, and 14 in lead and about 3, 14, and 16 in water. The constant of angular distribution of gamma quanta with energy 1.0 Mev in lead was also calculated, and results were correlated with previous data. (M.J.T.)

6527 ANGULAR DISTRIBUTION OF GAMMA RAYS EMITTED BY A POINT SOURCE AND SCATTERED IN SHIELDING. Larichev, A. V. At. Energ. (USSR), 19: 395-6(Oct. 1965). (In Russian).

Experiments were carried out to determine values of the constant θ_0', occurring in the empirical formula for the angular distribution of intensity I_θ of radiation scattered in an element of a solid angle, θ: $I_\theta = a'e^{-\theta/\theta_0'}$. The angular and energy distributions were measured for 0.145- to 1.25-Mev gamma rays in aluminum and for 0.411- and 1.25-Mev gamma rays in lead. Values of θ_0', calculated from the data, are presented as functions of energy. (M.J.T.)

6528 ANGULAR DISTRIBUTIONS OF NEUTRON DOSES NEAR GROUND-AIR BOUNDARIES. Goryachev, V. V. At. Energ. (USSR), 19: 396-7(Oct. 1965). (In Russian).

A previously developed equation for the function of the angular distribution of neutron doses from a point isotropic fission source in an infinite air medium for distances exceeding the mean free path is modified to take into account scattering off an air-earth interface. Equations are derived for the distribution function treating the earth as an absolutely black surface and taking into account corrections due to the neutron albedo, where the correction factor is a function of the total macroscopic neutron cross sections of the soil, the hydrogen contained in the soil, and the angle of incidence with respect to the interface. Results are given of calculations of the coefficient correcting the fraction of total neutron dose in a given solid angle as a function of the angle between the detector-source direction and the earth's surface, for an absolutely black surface, for water, and for soils of various compositions characterized by their H content. (M.J.T.)

6529 SPECTRAL DISTRIBUTION OF GAMMA RAYS FROM ^{60}Co POINT SOURCE SCREENED WITH ALUMINIUM LAYER IN ATMOSPHERE NEAR THE GROUND. Ionov, V. A. At. Energ. (USSR), 19: 397-400(Oct. 1965). (In Russian).

An isotropic detector was situated obliquely above the ^{60}Co source, which was at a fixed distance from the ground and covered with an Al layer. Energy spectra of the gamma radiation scattered in air were measured for different source-detector and detector-ground distances and different Al thicknesses. Results normalized to the intensity of direct rays are presented. Data were correlated with the data from previous works for the gamma spectra in air from an infinite plane isotropic source by integration of the distribution function for a point source with zero Al shielding thickness. Gamma spectra of a vertical rod were obtained by integration of the point-source spectra, in order to calculate energy distributions from thick sources of finite dimensions. (M.J.T.)

6530 SINGLE SCATTERING STREAMING OF GAMMA-RAYS THROUGH CYLINDRICAL DUCTS. Tsuruo, Akira; Shindo, Mitsuo; Kawabata, Masahiro (Tokyo Univ.). J. Nucl. Sci.Technol. (Tokyo), 2: 325-30(Sept. 1965).

An exact equation, for use in the calculation of the γ-ray streaming after single scatterings in a cylindrical duct, and its approximate formula, are presented. The dose of single scatterings at the exit of a cylindrical duct from a disk source at the entrance can be approximated by $D = \{4\pi/(n+1)\}S_a k_1 E_0 Q(L/R_0)^{-2}$ for $s_0 \leq L/R_0 \leq s_1$ and $D = \{4\pi/(n+1)\}S_a k_2 E_0 Q(L/R_0)^{-3}$ for $s_1 \leq L/R_0 \leq 60$, where D = dose at the exit of the duct, S_a = source strength, n = a parameter of the angular distribution of the source, E_0 = energy of the source photons, Q = conversion factor, R_0 = radius and L = duct length. The coefficients k_1 and k_2, as well as the constants s_0 and s_1 vary with source energy and wall materials. The values for lead, iron, concrete, tin, magnetite concrete, graphite and water are given in graphical representation for an energy range from 0.5 to 10 Mev. A study is made of the distribution of the arrival probabilities of photons, corresponding to the positions of scattering points for the photons from the source to the duct exit. It was found that the effective scatterings contributing to the flux at the exit occur mainly in the shallow part of the duct wall, near its surface. (auth)

Solid State Physics

See also CHEMISTRY — Inorganic and Physical Chemistry
METALS, CERAMICS, AND OTHER MATERIALS — Properties and Structure

Refer also to abstracts 5527 and 5883.

6531 (AD-623530) RESEARCH TO INVESTIGATE THE MICROSTRUCTURE OF THE INTERNAL MAGNETIC FIELD IN SELECTED MAGNETIC MATERIALS. Final Report. Graham, C. D. Jr.; Becker, J. J.; Jacobs, I. S. (Research Lab., General Electric Co., Schenectady, N. Y.). Sept. 1965. Contract AF33(615)-1490. 72p. (AFML-TR-65-253). CFSTI $3.00 cy, $0.75 mn.

Three major areas were investigated during this period. The magnetization of a gadolinium single crystal was measured over a range of fields and temperatures. The magnetic behavior in the vicinity of the Curie temperature was analyzed and found to be in reasonable agreement with recent theoretical predictions based on the Heisenberg model. The method of solid-state electrolysis was applied to the purification of Gd, with encouraging preliminary results. Improved metallographic techniques for Gd and other rare earths were developed. A number of compounds were prepared, and some magnetic measurements were made on $Fe_{2-x}Ge$ and Fe_2B. A relatively simple vibrating-sample magnetometer was constructed for use in this program. A variety of experimental and theoretical work was carried out on selected antiferromagnetic compounds. The

low-temperature parallel susceptibilities of FeF_2 and Cr_2O_3 were accounted for by the single-ion Van Vleck susceptibility mechanism. EuTe and $CoCl_2$ were shown to have nonlinear transverse susceptibilities, and this effect was shown to arise primarily from the field-dependence of the zero-point spin wave contribution to the free energy. Careful measurements of the magnetization of metamagnetic $FeCl_2$ were made. Hysteresis was observed in the metamagnetic transitions of $FeCl_2$ and $FeBr_2$, and analysis of this problem leads to the conclusion that hysteretic behavior should be expected in all transitions of this type at least under ideal conditions. The high-field measurements on $CoCl_2$ showed an anomalously high saturation moment per Co^{2+} ion, and this was explained by an exchange-enhanced g-shift. A study of the field dependence of the far infrared absorption of $CoCl_2$ revealed the second of the two expected nondegenerate antiferromagnetic resonance modes. Each shows the predicted functional dependence on applied field. (auth)

6532 (CALT-221-13) ENERGY LEVEL DIAGRAMS OF OXIDES OF MAGNESIUM, ALUMINUM AND SILICON. Das Gupta, K. (California Inst. of Tech., Pasadena. W. M. Keck Lab. of Engineering Materials). Oct. 1965. Contract AT(04-3)-221. 8p. Dep. mn; CFSTI $1.00 cy, $0.50 mn.

The distribution of the occupied and unoccupied electron levels of MgO, Al_2O_3, and SiO_2 in solid state was determined by the method of soft x-ray emission and absorption spectroscopy. From the relative positions of the valence emission band and the absorption edge it was concluded that the 2s and 2p wave functions of oxygen ions overlap in these oxides. Tentative energy level diagrams are illustrated showing the allowed and forbidden zones. (P.C.H.)

6533 (NVO-1163-60) STUDIES OF THE PROPERTIES OF THE EQUATION OF STATE FOR SOLIDS. (Beers (Roland F.), Inc., Alexandria, Va.). Oct. 14, 1965. Contract AT(29-2)-1163. 119p. Dep. mn; CFSTI $4.00 cy, $0.75 mn.

Data relating to the equation of state for solids were obtained in an extensive literary survey. Two populations of materials were used. They are: elements (for a study of basic behavior of simple substances) and geologic materials (those that are to be used in hydrodynamic computations). The equations of state used in the computations for the Hugoniot relations are the Murnaghan equation and the linear velocity relation $D = SU + C$. Constants were determined for both formulas for each of the materials listed. From the Hugoniots obtained, Gruneisen ratios were calculated at various compression ratios by three different methods. Results of the computations are tabulated. These are followed by listings of input data. Programs used in the computations are listed. (M.O.W.)

6534 (SC-DC-65-1843) EFFECT OF ASSUMED ELECTRONIC CONFIGURATION ON THE ELECTRONIC BAND STRUCTURE OF NICKEL. Snow, E. C.; Waber, J. T. (Los Alamos Scientific Lab., Univ. of California, N. Mex.); Switendick, A. C. (Sandia Corp., Albuquerque, N. Mex.). Nov. 1, 1965. Contract AT(29-1)-789. 10p. (CONF-651106-4). Dep. mn; CFSTI $1.00 cy, $0.50 mn.

From Conference on Magnetism and Magnetic Materials, San Francisco.

The electronic band structure of nickel is computed by the APW method by using the atomic Dirac-Slater wave functions of the free nickel atom in five configurations of the general type $3d^{10-x}4s^x$. Movement of the d and sp bands relative to each other occurs as a function of x, the assumed number of holes in the d-states. It is shown that if there is a significant difference between the number of s-like electrons in the spin-up and spin-down bands when a magnetic field is applied, the topology of the two Fermi surfaces will be different. (auth)

6535 CONTRIBUTION TO THE THEORY OF SCATTERING OF FAST CHARGED PARTICLES IN CRYSTALS. Lenchenko, V. M.; Pugacheva, T. S. (Inst. of Nuclear Physics, Academy of Sciences, USSR). Izv. Akad. Nauk Uz. SSR, Ser. Fiz.-Mat. Nauk, No. 1, 48-56(1965). (In Russian).

Scattering of charged particles by the atoms of a crystal is considered. Earlier investigations were made under the assumption that for fast particles such collisions can be regarded as pair collisions with free atoms, and effects connected with the interaction of the atoms in the lattice can be neglected. It is shown that the pair-collision approximation is valid only for short-range collisions, when the energy transferred to the atom is sufficiently large. In the case of long-range glancing collisions, the momentum is transferred not to a single atom but to the entire lattice as a whole, so that the scattering is accompanied by emission of one or several phonons, or without change of energy at all (Mössbauer scattering). The cross section for the scattering of a fast charged particle in a crystal lattice is derived in general form, and the relative contributions made to the energy losses by single-phonon and multiphonon processes are estimated. Collisions accompanied by formation of defects and by excitation of localized oscillations are also considered. It is pointed out that the proposed method makes it possible to separate the collision region in which the energy losses go to phonon excitation. (ATD)

6536 EFFECT OF GAMMA IRRADIATION ON THE FLUORESCENCE YIELD OF RUBY. Starodubtsev, S. V.; Yunusov, M. (Inst. of Nuclear Physics, Academy of Sciences, USSR). Izv. Akad. Nauk Uz. SSR, Ser. Fiz.-Mat. Nauk, No. 1, 111-12(1965). (In Russian).

The results of an electronically measured relative change in the fluorescence of γ-irradiated light-pink ruby containing $\sim 0.09\%$ chromium are reported. The results show that the intensity of luminescence of ruby decreases after irradiation. The shape of the intensity vs wavelength curve remains practically unchanged at all doses. It is therefore concluded that the color centers produced upon γ irradiation of the ruby do not contribute to its luminescence, and possibly contribute to its quenching. The appearance of such centers is attributed to contaminations which produce local defects in the ruby crystal, in addition to the defects produced by the γ rays themselves. (ATD)

6537 X-RAY INDUCED PHOTOLUMINESCENCE SPECTRA FROM NaI(Tl) AND CsI(Tl) IN THE TEMPERATURE RANGE FROM 283 deg K TO 5 deg K. Takemoto, Shigeo (Defence Academy, Yokosuka, Japan); Kondo, Makoto. J. Phys. Soc. Jap., 20: 1576-9(Sept. 1965).

The emission spectra from NaI(Tl) excited by x rays at the temperature of liquid hydrogen showed the peaks at approximately 616, 546, 437, 379, 332, 299 and 285 mμ. The 332 mμ band is predominant at only the temperatures of liquid hydrogen and liquid helium, and is thought to arise from the Tl dimers, consisting of a pair of Tl^+ ions substitutionally displacing two alkali ions in the nearest neighbour ⟨110⟩ direction). Tl dimer becomes an effective luminescent emission center at very low temperature. The emission spectra from CsI(Tl) excited by x rays at the temperature of liquid helium showed a superposition of 595, 537 and 474 mμ bands. The luminescence being weaker at lower temperature than at the room temperature, it shows no band in the ultraviolet region. The temperature dependence of the emission spectra from NaI(Tl) and CsI(Tl) excited by x rays are reported. (auth)

6538 TEMPERATURE DEPENDENCE OF FLOW STRESS IN GAMMA-RAY IRRADIATED SODIUM CHLORIDE CRYSTALS. Okada, Touichi; Suita, Tokuo (Osaka Univ.). J. Phys. Soc. Jap., 20: 1591-6(Sept. 1965).

The mechanisms of radiation hardening in sodium chloride crystals were studied by examining the stress-strain curves and the temperature dependence of the flow stress. It was found that the flow stress of pure crystal is far more temperature insensitive than those which were doped with Ca^{2+} ions both before and after irradiation. The experimental results were compared with the Fleischer's theory of the temperature dependence of the flow stress and a qualitative agreement was obtained for both crystals in the temperature range from 77 to 300°K. Possible mechanisms of the radiation hardening were discussed on the basis of the present results. (auth)

6539 SEARCH FOR THE X-RAY RAMAN EFFECT. Weiss, R. J. (Army Materials Research Agency, Watertown, Mass.). Phys. Rev., 140: A1867-8(Dec. 13, 1965).

A Philips fluorescence spectrometer was used to search for the x-ray Raman line reported by Das Gupta. The search was made on graphite, beryllium, LiF, and boron nitride both under the original conditions employed by Das Gupta on graphite and under the conditions in which Bragg reflections occur. No x-ray Raman line was seen in spite of the increased sensitivity of the scintillation counting vis à vis the film detection employed by Das Gupta. (auth)

6540 MOESSBAUER EFFECT IN MOLECULAR IODINE CRYSTALS. Pasternak, M., Simopoulos, A., Hazony, Y. (Israel Atomic Energy Commission, Yavne). Phys. Rev., 140: A1892-6(Dec. 13, 1965).

The Mössbauer effect of the 26.8-kev transition in ^{129}I was studied in molecular iodine crystals. From the quadrupole splitting of the transitions the ratio $Q_{26.8}/Q_{gnd}$, the quadrupole coupling e^2qQ_{gnd}, and the isomer shift are derived. The sign of the quadrupole coupling shows that the sign of the iodine field gradient is positive. From the isomer shift of I_2 and from those of alkali iodides, a linear dependence of the isomer shift on the number of p holes is derived. The intensities of the peaks give a strong indication of an angular dependence of the recoilless fraction $f(\theta)$. The Θ_D of the I_2 crystal, as well as that of the KI crystal, are derived from the temperature dependence of the recoilless fraction. (auth)

6541 MAGNETIC STRUCTURES OF METALLIC ERBIUM. Cable, J. W.; Wollan, E. O.; Koehler, W. C.; Wilkinson, M. K. (Oak Ridge National Lab., Tenn.). Phys. Rev., 140: A1896-1902(Dec. 13, 1965). (ORNL-P-1311).

Single-crystal neutron-diffraction data were obtained for metallic erbium at sample temperatures from 4.2 to 298°K. Three distinct regions of long-range magnetic order were observed. In the high-temperature region (52–80°K), the ordered moments are confined to the c-axis direction and are sinusoidally modulated with a modulation wavelength of $3.5C_0$. The amplitude of this modulation saturates at 52°K with $\mu_z(\max) = 7.6\mu_B/Er^{3+}$. Below 52°K the basal-plane component of the moment begins to order, and a third-order modulation along the c axis is observed. These effects are interpreted on the basis of a squared elliptical spiral with its major axis tilted relative to the crystal c axis. However, the structural details in this region are obscured by a temperature variation of the modulation wavelength and by the incommensurability of the modulation and the lattice. In the low-temperature region (4.2–20°K), a ferromagnetic spiral structure is indicated. At saturation, the ferromagnetic c-axis component is $7.9\mu_B/Er^{3+}$, and the spiral basal-plane component is $4.3\mu_B/Er^{3+}$. The total ordered moment is then the free-ion value of $9.0\mu_B/Er^{3+}$. (auth)

6542 ANISOTROPIC SPIN-LATTICE RELAXATION RATES OF SOME RARE-EARTH-DOPED LANTHANUM TRICHLORIDES. Mikkelson, R. C.; Stapleton, H. J. (Univ. of Illinois, Urbana). Phys. Rev., 140: A1968-82 (Dec. 13, 1965).

The temperature dependence and the angular anisotropy of the spin-lattice relaxation rate $1/T_1$ of cerium, praseodymium, neodymium, samarium, terbium, and erbium in single crystals of anhydrous lanthanum trichloride were measured. The experiments were performed at X-band frequencies using pulse-saturation techniques on samples containing ≤2 at. % rare-earth doping for temperatures between 1.65 and 4.2°K. Angular measurements at constant temperature were made for magnetic-field orientations between 0 and 90° with respect to the crystal c axis. The results are interpreted as involving an angular-dependent direct process and isotropic Orback and Raman mechanisms. These results are compared with theoretically predicted rates obtained from computer calculations, which are based upon Orbach's approach and require a knowledge of the static crystal-field parameters. Since rare-earth trichlorides have been the object of much optical investigation, these parameters are available for all ions we treat except cerium. Except for this ion, most of the predicted relaxation rates agree with experiments to within a factor of 5 or less, and for all ions the form of the angular anisotropy is followed almost exactly. Theoretical treatments which involve the mixing of excited-state wave functions into the ground magnetic doublet through the anisotropic Zeeman interaction are required to explain the observed angular dependence. One of the ions, praseodymium, exhibits a phonon-limited direct-process relaxation rate which is interesting because the apparent hot-phonon equilibration time is about 80 nsec and corresponds to an equilibration path length of only 160 μ. After neutron bombardment the bottlenecked relaxation rate changed and the equilibration time was apparently reduced to 53 nsec. Prior irradiation of this same sample with 100-kev x rays produced no observable change in the relaxation time. No dependence upon crystal size was observed for the phonon bottleneck in Pr^{3+}-doped $LaCl_3$. (auth)

6543 EFFECT OF PRESSURE ON THE HYPERFINE STRUCTURE OF F CENTERS IN LiF. Blum, Haywood (Massachusetts Inst. of Tech., Cambridge. Brookhaven National Lab., Upton, N. Y.). Phys. Rev., 140: A1998-9(Dec. 13, 1965). (BNL–9113).

An electron-spin-resonance study at room temperature has been performed on F centers in LiF at hydrostatic pressures up to 4 kbar. An average value for the variation of the hyperfine constants with pressure is found to be $a^{-1}\partial a/\partial P = (2.4 \pm 1.1) \times 10^{-6}$ bar^{-1}. This result, when taken with the bulk compressibility of LiF, and the behavior with pressure of the optical transitions of F centers in alkali halides, gives moderately good agreement with the point-ion model of Gourary and Adrian. (auth)

6544 INVESTIGATION OF THE PARAMAGNETIC NEUTRON SCATTERING FROM METALLIC PALLADIUM. Cable, J. W.; Wollan, E. O. (Oak Ridge National Lab., Tenn.). Phys. Rev., 140: A2003-4(Dec. 13, 1965). (ORNL-P-1512).

Neutron paramagnetic scattering measurements were made for metallic palladium at sample temperatures of 15, 77, and 298°K. Within experimental error, the paramagnetic scattering cross section is the same for these temperatures and is only about 5 mb/sr atom. It is concluded that the Pd $4d^9$ spin states exist for a time short relative to the time of passage of a neutron over an atom ($\sim 10^{-13}$ sec for a 1-Å neutron). (auth)

6545 ISOTOPE EFFECTS INDUCED BY LOCAL MODES IN THE U BAND. Baldini, G. (Univ. of Rochester, N. Y.); Mulazzi, E.; Terzi, N. Phys. Rev., 140: A2094-2101(Dec. 13, 1965).

The experimental investigation in the temperature range from 4 to 400°K of the ultraviolet U band in KCl, KBr, and RbCl crystals containing H^- and D^- ions has revealed the following isotope effects: the half-width of the U_H band is from 4 to 8% larger than that of the U_D band, and the U_H band occurs at energies ~0.02 ev smaller than those of the U_D band. In order to describe these results, the method of moments, in the harmonic and Condon approximations, was applied. From the symmetry of the defect, it is shown that only the vibrational modes which transform according to the Γ_{15}^- representation of the full cubic point group can be responsible for the isotope effects; these modes are just those active in the infrared. It is found that during optical transitions, allowed in dipole approximation, the Γ_{15}^- modes suffer, via the electron-phonon interaction, only a frequency shift, and that only the local mode has to be taken into account in order to predict the observed isotope effects, since the contribution coming from the Γ_{15}^- continuum is negligible. Finally, the local-mode frequency of the excited U center has been estimated. (auth)

6546 MAGNETIC STRUCTURE OF $MnSO_4$. Will, G. (Army Electronics Labs., Fort Monmouth, N. J. Brookhaven National Lab., Upton, N. Y.); Frazer, B. C.; Shirane, G.; Cox, D. E.; Brown, P. J. Phys. Rev., 140: A2139-42 (Dec. 13, 1965). (BNL–9359).

The magnetic structure of $MnSO_4$ was determined from a powder neutron-diffraction study. It consists of a cycloidal spiral arrangement related to the simple $CrVO_4$ type of magnetic structure, in which ferromagnetic (001) sheets are coupled antiparallel to adjacent sheets. The propagation vector of the spiral is directed along the a axis, with a periodicity of 30 Å (about 6a), and the spiral spin components lie in the ab plane. The moment of each Mn^{2+} ions is $4.8_{\mu B}$, and the cone half-angle is about 78°. (auth)

6547 MAGNETOSTRICTION OF ERBIUM SINGLE CRYSTALS. Rhyne, J. J.; Legvold, S. (Ames Lab., Ames, Iowa). Phys. Rev., 140: A2143-50(Dec. 13, 1965). (IS–1198).

The magnetostriction of Er single crystals was measured from 300 to 10°K in applied fields up to 30 kgauss. In contrast to the other rare earths, the magnetostriction of Er is dominated by field-induced modifications of the exchange energy. The exchange magnetostriction which results from the application of a c-axis field was determined in the quasi-antiphase-domain and modulated-moment temperature regions. Below 20°K, application of a field in the basal plane produced a sharp change in strain at 18 kgauss. This is presumed to arise from a breakdown of the conical ferromagnetic structure into a conical fan state. The second-order anisotropic basal-plane magnetostriction constant was measured. Negative values were found above 55°K in accordance with theoretical predictions. Below 18°K, anomalously small and positive values were obtained. The temperature dependence of the a-, b-, and c-axis strains in zero field and in a 30-kgauss field was evaluated. (auth)

6548 PLASMA RADIATION FROM THIN SILVER FOILS EXCITED BY LIGHT. Brambring, J.; Raether, H. (Univ., Hamburg). Phys. Rev. Lett., 15: 882-3(Dec. 6, 1965).

An experiment in silver is described in which a radiative plasma mode is excited by electromagnetic radiation. Since the radiative plasma oscillation consists of electrons vibrating perpendicular to the surface, a light emission is expected with an intensity peak as in the electron experiment, if the electric field of the exciting radiation has a component normal to the foil. The emitted radiation is polarized, its electric field vector vibrates in the plane given by the foil normal and the direction of observation, and it shows the angular dependence of intensity calculated by Ferrell. Experiments verify these properties. Such an experiment is described in which the excitation of the plasma mode is observed by its emitted radiation. Recorder traces of the photon emission from a silver foil at room temperature are given. (J.F.P.)

6549 NUCLEAR MAGNETIC RESONANCE IN THE PURE QUADRUPOLE REGIME. Segel, S. L.; Barnes, R. G. (Ames Lab., Ames, Iowa). Phys. Rev. Lett., 15: 886-8(Dec. 6, 1965). (IS–1254).

The feasibility and value of observing an unconventional NMR in polycrystalline samples at roughly twice the Larmor frequency despite the condition that the Larmor frequency is less than the quadrupole frequency are reported. Such double Larmor frequencies were observed for a number of spin-$^3/_2$ nuclei in cases where the field gradient is axially symmetric. The cases of copper-65 in cuprous oxide and chlorine-35 in potassium hexachlororhenate are shown. In both cases, the solid straight line is drawn for the transition frequency equal to twice the Larmor frequency. A wide-line NMR spectrometer was used, providing resonance frequencies in the range 2-16 Mc. The quadrupole couplings and effective γ values were determined by fitting the exact expression for the frequency to the measured frequency-versus-field behavior of the resonance. (J.F.P.)

6550 PREFERENTIAL EMISSION PHENOMENA IN THE AFTERGLOW OF X-IRRADIATED ALKALINE-EARTH FLUORIDES DOPED WITH RARE EARTHS. Makovsky, J. (Hebrew Univ., Jerusalem). Phys. Rev. Lett., 15: 953-5 (Dec. 20, 1965).

The afterglow spectra and their dependence on some parameters are studied. These effects are studied in detail for the system $Gd^{3+}:CaF_2$. The analysis is the basis for the interpretation of the reported phenomena in the afterglow. Some of the implications of these phenomena are pointed out. The afterglow spectra of $Gd^{3+}:CaF_2$ were photographed between 2400 and 3400 Å using a dual-grating spectrograph. The samples were single crystals of different growth conditions and concentrations. As a result of these variations, their optical spectra consisted of different combinations of site spectra. Transitions were observed from the various Stark components of certain levels. A spectrogram is shown of the $^6P_{\frac{7}{2}} \rightarrow {}^8S_{\frac{7}{2}}$ transitions in the afterglows of the x irradiated crystal. Well-resolved spectral components belonging to the different sites were studied. A model of traps is discussed in relation to the phenomenon of preferential emissions in the afterglow. (J.F.P.)

6551 THE MOLECULAR DESIGNING OF MATERIALS AND DEVICES. Von Hippel, Arthur R. (ed.). Cambridge, Mass., The M.I.T. Press, 1965. 281p. $25.00.

The molecular designing of materials and devices is discussed under the following topics: predictions by a priori theory, building from atoms, competitive structures and phase transitions, properties imparted by d electrons, magnetic ordering in Heisenberg magnets, phase transitions in condensed systems, defects in ionic and metal crystals, deformation and fracture of solids, structure in living systems, magnetization process, conduction and diffusion in ionic crystals, luminescence in solids, photoconducting phosphors, electrons and holes in semiconductors, electrons in metallic systems, avalanches and gas breakdown, electric discharges and excited species, space-charge-limited currents, conduction and breakdown, the living cell, studies of cell division with a polarizing microscope, mutual substitution of networks and materials, new combinations of physical phenomena in device design, principles of energy conversion, energy-conversion devices, and sensory coding in the nervous system. (F.J.H.)

REACTOR TECHNOLOGY

General

Refer also to abstract 5834.

6552 (ANL–6925, pp 187-233) REACTOR SAFETY. Baker, L.; Tevebaugh, A. D. (Argonne National Lab., Ill.).

Results are reported from investigations of high-temperature reactions of Zr wire, stainless steel-clad UO_2, Zircaloy-2-clad UO_2 with steam. Reactions of Mo with high-temperature steam were also investigated along with those of Re, W, Nb, and Ta. Studies of laser-heated metal–water reactions are described. Experiments in TREAT concerning the behavior of unclad UO_2 under simulated excursion conditions are also described. The magnitude of possible water hammer occurrences in metal–water autoclave experiments was evaluated. Calculation results on metal–water reactions during reactor coolant-loss accidents are included along with results of studies on cladding and fuel reactions with coolants, and radiation effects on U ignition. (J.R.D.)

6553 (ANL–6925, pp 255-63) STUDIES AND EVALUATIONS. Mecham, W. J.; Seefeldt, W. B.; Trice, V. G.; Levenson, M. (Argonne National Lab., Ill.).

Economic studies of fuels and reprocessing methods for fast reactors are described. Results of studies concerning reprocessing fast reactor Pu fuels are included. Data and information are presented on fuel burnup effects on cast-throughput relations, shipping and inventory costs, and fuel inventory costs. (J.R.D.)

6554 (ANL–7092) CATALOG OF NUCLEAR REACTOR CONCEPTS. PART I. HOMOGENEOUS AND QUASI-HOMOGENEOUS REACTORS. SECTION III. REACTORS FUELED WITH MOLTEN-SALT SOLUTIONS. Teeter, Charles E.; Lecky, James A.; Martens, John H. (Argonne National Lab., Ill.). Sept. 1965. Contract W-31-109-eng-38. 59p. Dep. mn; CFSTI $3.00 cy, $0.75 mn.

Data are tabulated for homogeneous and quasi-homogeneous molten-salt-fueled reactors. The development and state-of-the-art of this type of reactor is discussed. Data are given for 48 one-region and 7 two-region reactors. 76 references. (T.F.H.)

6555 (ANL–7105) REACTOR DEVELOPMENT PROGRAM PROGRESS REPORT, SEPTEMBER 1965. (Argonne National Lab., Ill.). Oct. 20, 1965. Contract W-31-109-eng-38. 93p. Dep. mn; CFSTI $3.00 cy, $0.75 mn.

Separate abstracts were prepared for the four included sections describing research on liquid-metal-cooled reactors, general reactor technology, advanced systems research and development, and nuclear safety. (M.O.W.)

For abstracts of individual sections see: 6556, 6576, 6600, and 6665.

6556 (ANL–7105, pp 36-58) GENERAL REACTOR TECHNOLOGY. (Argonne National Lab., Ill.).

Brief discussions are presented on experimental reactor and nuclear physics, theoretical reactor physics, high-temperature materials, other reactor fuels and materials development, engineering development, chemical separations, sodium coolant chemistry, and plutonium recycle reactors. (M.O.W.)

6557 (ANL–7115) REACTOR DEVELOPMENT PROGRAM PROGRESS REPORT, OCTOBER 1965. (Argonne National Lab., Ill.). Nov. 23, 1965. Contract W-31-109-eng-38. 93p. Dep. mn; CFSTI $3.00 cy, $0.75 mn.

Separate abstracts were prepared for the four included sections. (M.O.W.)

For abstracts of individual sections see: 6558, 6559, 6601, and 6666.

6558 (ANL–7115, pp 42-67) GENERAL REACTOR TECHNOLOGY. (Argonne National Lab., Ill.).

Various research in the areas of experimental reactor and nuclear physics, theoretical reactor physics, high-temperature materials studies, other reactor fuels and materials development, engineering development, chemical separations, sodium coolant chemistry, and the plutonium recycle program is discussed. (M.O.W.)

6559 (ANL–7115, pp 78-83) NUCLEAR SAFETY. (Argonne National Lab., Ill.).

Brief discussions of research progress during this period are presented for reactor kinetics, TREAT, and chemical and associated energy-transfer problems in reactor safety. (M.O.W.)

6560 (BMI-X–10145) AN EVALUATION OF THE APPLICABILITY OF EXISTING DATA TO THE ANALYTICAL DESCRIPTION OF A NUCLEAR-REACTOR ACCIDENT. Quarterly Progress Report for July–September 1965. Sunderman, Duane N.; Morrison, David L.; Gieseke, James A.; Ritzman, Robert L.; Walters, Craig T. (Battelle Memorial Inst., Columbus, Ohio). Oct. 1, 1965. Contract W-7405-eng-92. 35p. (EURAEC–1497). Dep. mn; CFSTI $2.00 cy, $0.50 mn.

Work Performed under United States–Euratom Joint Research and Development Program.

Analyses of LOFT (Loss of Fluid Test) accidents using the NURLOC digital code are in preparation, and preliminary results are shown. Experimental data on fission-product release from urania are used in a simplified release model, which is used in conjunction with an adiabatic-heat-transfer model for the reactor core in parametric-variation analysis of several variables occurring in the release expression. Analyses of the physical form of released fission products are carried out, in order to determine the transport of fission products in vapors, particles, aerosols, and on surfaces of the containment vessel. The analyses are restricted to loss-of-coolant accidents in boiling-water and pressurized-water reactors. (T.F.H.)

6561 (FTI–2) NOISE IN NUCLEAR REACTOR SYSTEMS. A Literature Survey. Nystroem, Anders (Aktiebolaget Atomenergi, Stockholm (Sweden)). Oct. 1965. 59p. Dep. mn.

An annotated bibliography consisting of 107 references to material on noise in nuclear-reactor systems is presented. The whole environment is included as a noise source. Subject and author indexes are included. (T.F.H.)

6562 (NAA-SR-Memo–11369) NAA PROGRAM DESCRIPTION. CAVORT (CALCULATIONS FOR VOID FORMATION IN REACTOR TRANSIENTS). Medeiros, Katharine W. (Atomics International, Canoga Park, Calif.). May 1965. Contract AT(11-1)-Gen-8. 123p. Dep. mn; CFSTI $4.00 cy, $0.75 mn.

A code is described that calibrates digitized oscillogram data from in-pile capsule nuclear transient heating experiments, calculates reactor energy release and average surface temperature, and provides both tabulated and CRT graphic records of answers obtained. Provision is made on an optional basis for calculating fuel-specimen heat content, specific energy release, and relative specific energy release for special capsule experiments conducted without coolant. Raw data other than oscillogram type may be processed by the use of correlated calibration factors and choice of options. (auth)

6563 (TID–3525(Rev.5)(Suppl.2)) REACTOR SAFETY. A Literature Search. Smith, Richard J. (comp.) (Division of Technical Information Extension (AEC), Oak Ridge, Tenn.). Aug. 1965. 70p. Dep. mn; CFSTI $3.00 cy, $0.75 mn.

A total of 671 references to unclassified reports is pre-

sented on reactor systems, materials, and operation designed to provide maximum-safety for the reactor, reactor personnel, and environs. Information is included concerning incidents and conditions of operation considered hazardous. Author, reactor, and report number-availability indexes are provided. (auth)

6564 SELF-EXCITED VIBRATION OF NUCLEAR REACTOR FUEL CHANNELS WITH WATER COOLING. Kacprzynski, Jerzy; Adamska, Hanna. Nukleonika, 10: 443-52(1965). (In Polish).

An attempt was made to explain the self-excited vibration of nuclear reactor fuel channels on the basis of hydro-flutter. The fuel channel was in the form of a very long tube fixed vertically with water flowing both outside and inside. It was assumed that the mean flow velocity is uniform and constant and that a small unsteady perturbation described by the velocity potential is superimposed. The equation of vibration of the channel treated as a beam submerged in a flowing fluid was derived and solved by the Galerkin method. The influence of the directions and the magnitudes of the internal flow velocities on the regions of instabilities was examined. A numerical example solved on the Elliott-803 B computer, showed that self-excited vibration of nuclear reactor fuel channels may be explained on the basis of hydro-flutter. (auth)

Auxiliaries and Components

Refer also to abstract 5881.

6565 (CEND-3336-251) DEVELOPMENT AND TESTING OF A TEMPERATURE TRANSIENT METHOD FOR PERFORMING IN-PILE THERMAL CONDUCTANCE TESTING. Progress Report, July 1-September 30, 1965. Burdg, C. E.; Christopher, S. S. (Combustion Engineering, Inc., Windsor, Conn. Nuclear Div.). Oct. 1965. Contract AT(30-1)-3336. 20p. (EURAEC-1510). Dep. mn; CFSTI $1.00 cy, $0.50 mn.

Work Performed under United States-Euratom Joint Research and Development Program.

The concept investigated is one whereby measurement of the transient temperature response at the surface of an operating fuel element, following a reactor power change, will yield thermal conductance values. This two-phase investigation consists first of out-of-pile demonstrations of feasibility followed by in-pile confirmation of the method. Concurrent mathematical analyses of the thermal model will provide the bases for data interpretation, as well as guides for the design of the experimental portions of the program. Installation of a lowpass filter in the cladding thermocouple signal path has resulted in significant improvement in the signal/noise ratio. Tests of a ZrO_2 element, using square wave cyclic input, have yielded anomalous results. The phase shift of the cladding temperature response with regard to the input signal appears to be different at different locations along the length of the element, by an amount not fully explained by recognizable uncertainties in measurement. However, the fuel was of low density (72% of theoretical) and inhomogeneities or cracks may be responsible for this anomalous behavior. (auth)

6566 (EURAEC-1382) DEVELOPMENT PROGRAM ON THE APPLICATION OF STEAM-WATER SPRAY TO REACTOR COOLING. CAN 3 Final Report, December 15, 1961-August 31, 1964. (Centro Informazioni Studi Esperienze, Milan (Italy)). Oct. 1964. Contract 056-62-1-RDI. 54p. (EUR-2345; CISE-R-136). Dep. mn; CFSTI $3.00 cy, $0.50 mn.

Work Performed under United States-Euratom Joint Research and Development Program.

The CAN-3 research programs concerned a development work linked with features of a possible reactor design and with reactor conditions more closely than the previous CAN-1 and CAN-2 programs. Experimental work was mainly devoted to the field of heat transfer, hydrodynamics and in-pile experiments for corrosion of structural materials and for water chemistry. Fundamental aspects and results of work done in these fields are reported. (auth)

6567 (HW-SA-3600) TECHNIQUE FOR OPTIMIZING THE COMPOSITION OF REGENERATING NEUTRON FLUX MONITORS. Bunch, W. L. (General Electric Co., Richland, Wash. Hanford Atomic Products Operation). Oct. 5, 1964. Contract AT)45-1)-1350. 21p. (CONF-654-96). Dep. mn; CFSTI $1.00 cy, $0.50 mn.

From American Nuclear Society Meeting, San Francisco, Nov.-Dec. 1964.

The development of a technique to determine the optimum composition of regenerating material for any specific application encompassed three steps. The first step was the development and computer programming of the relations to calculate the initial isotopic composition as a function of the germane parameters. Parameters of primary concern are the cross sections of the isotopes being considered and the maximum variation in sensitivity which is to be permitted during the "useful" lifetime of the detector. The second step was to measure effective cross sections in a typical reactor environment. It was assumed the cross section notation of Westcott would be applicable. The isotope ratio technique was exploited to measure the neutron spectral parameters because the incremental exposures received in the facility made the usual radioactivity techniques impractical. Using the experimental spectral parameters, the computer program was employed to calculate the optimum initial composition of regenerating detectors for that environment. The third step was to irradiate samples with approximately the optimum calculated composition and to compare the actual behavior with the predicted results. It is concluded the technique provides regenerating material whose behavior is predictable within the accuracy limitations imposed by the available cross section information. (auth)

6568 ELECTROPHORETIC FILTER FOR PURIFYING REACTOR WATER. Ganzha, V. D.; Egorov, A. I.; Kaminker, D. M.; Kolyadin, A. B.; Konoplev, K. A.; Saikov, Yu. P.; Sharov, V. T. At. Energ. (USSR), 19: 350-4(Oct. 1965). (In Russian).

The hardly soluble hydrate of aluminum oxide is formed as a result of corrosion in the water of the primary loop of the reactor of the A. F. Ioffe Institute of Physics and Technology. An electrophoretic filter, made specially for water purification, allowed the coolant of the primary loop of the reactor to be completely clarified. The filter has a total volume of 10.7 liters and a low hydraulic resistance and is easy to maintain. The effective transmission through the filter is 0.5 m^3/hr. The power consumed is 0.3 kv. (tr-auth)

6569 IMPROVEMENTS IN OR RELATING TO CONTROL ROD MECHANISMS FOR NUCLEAR REACTORS. Gruel, Jean; Fresnes, Batiment K.; Jullien, Georges (to Commissariat a l'Energie Atomique). British Patent 1,009,166. Nov. 10, 1965. Priority date Oct. 5, 1965, France.

A control rod mechanism for a reactor comprises a tube made up of the following parts: a neutron absorbant member; a piston connected to the absorbant member at its upper extremity; a gas reservoir connected to a control system for displacing the piston longitudinally within the tube; and an electromagnet disposed adjacent to the gas reservoir to insure retention of the piston on the lower face of the reservoir to close an opening in the reservoir. De-energization of the electromagnet releases the piston and allows the neutron absorbant material to fall. The release and fall are assisted by the pressure of the compressed gas on the piston. (B.L.M.)

6570 IMPROVEMENTS RELATING TO NUCLEAR REACTOR FUELLING ARRANGEMENTS. (to Atomic Energy of Canada Ltd.). British Patent 1,009,381. Nov. 10, 1965. Priority date Mar. 5, 1962, United States.

A ram mechanism is provided for a reactor loading machine that is reliable and at the same time permits a high degree of flexibility in the performance of its neces-

sary functions. The mechanism can be extended to enter a fuel tube to ram a fuel bundle home or to control the outward movement of a used bundle at the unloading end of the tube and can cooperate with the novel tube plug design to release the tube plug, withdraw the plug into the magazine, and finally return the plug to the tube again locking it in place. (B.L.M.)

6571 IMPROVEMENTS RELATING TO NUCLEAR REACTOR FUELLING ARRANGEMENTS. (to Atomic Energy of Canada Ltd.). British Patent 1,009,382. Nov. 10, 1965. Priority date June 22, 1962, Canada.

A sensing and stop mechanism for accurately locating the position of the end of a fuel bundle in a row of fuel bundles extending from a reactor tube into a fuelling machine acting as an unloading machine is patented. The sensing and stop mechanism mounted on the fuelling machine project into a passageway that terminates in a snout for clamping on to the end of the reactor tube to position the passageway as a coaxial continuation of the tube. Means are provided for urging the sensor into a projecting position to bear resiliently against the side of a fuel bundle, and sensing means sense the movement of the sensor into a gap between the outer peripheries of abutting ends of adjacent fuel bundles. The stop is actuated by the sensing means to arrest movement of the row of fuel bundles extending from the stop into the reactor tube. In response to a signal from the sensor and stop mechanism, the fuel bundle can be deflected along the passageway away from the reactor tube for subsequent disposal. (B.L.M.)

6572 IMPROVEMENTS RELATING TO NUCLEAR REACTOR FUELLING ARRANGEMENTS. (to Atomic Energy of Canada Ltd.). British Patent 1,009,383. Nov. 10, 1965. Priority date June 22, 1962, Canada.

In a fuelling machine for a reactor having fuel elements in bundles in the reactor tubes a gimbal means is provided for mounting a snout onto the projecting end of the reactor tube for pivotal displacement of the snout about two mutually perpendicular axes both perpendicular to the axial direction of the snout. Means are provided for moving the snout in an axial direction towards a selected tube and for sensing and automatically correcting pivotal displacement of the snout about each of the axes resulting from contact between the snout and tube. (B.L.M.)

6573 IMPROVEMENTS RELATING TO NUCLEAR REACTOR FUELLING ARRANGEMENTS. (to Atomic Energy of Canada Ltd.). British Patent 1,009,384. Nov. 10, 1965. Priority date Oct. 10, 1962, Canada.

In a fuelling machine for a nuclear reactor having a snout for clamping onto a projecting end of a reactor tube to form a communicating continuation of the tube, means are provided for producing an auxiliary stream of liquid coolant to flow from the machine into the tube to inhibit flow of coolant from the tube into the machine. (B.L.M.)

6574 SUPPORT FOR SAMPLES TO BE SUBJECTED TO RADIATIONS. Hermann, Horst (to European Atomic Energy Community). Canadian Patent 713,681. July 13, 1965. Priority date July 20, 1961, Belgium.

The support is intended for use in nuclear reactors which have channels adapted to receive fuel elements and also to serve as experimentation channels. Some fuel elements are provided with a radiation channel adapted to receive the samples to be activated. The support consists of a tube closed at the end adapted to receive the sample to be irradiated. There are also ancillary elements for positioning and heating of the sample and for directing the flow of the coolant. The support for the sample and fuel element therefore, constitutes a structural unit. (F.S.A.)

6575 NUCLEAR REACTOR CONTROL MEANS. Robbins, Thomas R. (to U. S. Atomic Energy Commission). U. S. Patent 3,219,535. Nov. 23, 1965.

A nuclear reactor is described which is made up of cylindrical assemblies having an outer annular fixed core containing fissionable material and an inner movable core also containing fissionable material. An annular safety element containing a material of high neutron capture cross-section is disposed for longitudinal movement between the fixed and movable core sections. Both core sections contain fertile material in addition to fissionable material. The fertile materials are disposed at opposite ends of the fixed and movable core sections, the boundary between the fertile and fissionable slanting inwardly in the direction of the fertile material. The movable sections can be used to control neutron leakage between sections and, hence, control the reactor. (AEC)

Criticality Studies

6576 (ANL–7105, pp 72-84) NUCLEAR SAFETY. (Argonne National Lab., Ill.).

Brief discussion of research work for the purpose of nuclear safety are presented. Included are discussions on the equation of state for fast reactor accidents, transients with Th-U fuel, remotely controlled camera state for hot cell examinations, fast neutron hodoscope, fast reactor safety, TREAT operations, and metal-water reactions. (M.O.W.)

6577 (BNWL–149, pp 22-35) ENGINEERING PHYSICS. (Battelle-Northwest, Richland, Wash. Pacific Northwest Lab.).

Brief discussions of 4 papers are presented. These include; comparison of theoretical and experimental resonance absorption in ^{240}Pu, physics analysis of a U-Al polyethylene system, and a preliminary analysis of some Pu-Al polyethylene experiments in the PCTR. (M.O.W.)

6578 (BNWL–149, pp 45-7) HEAVY MODERATOR REACTOR PHYSICS. (Battelle-Northwest, Richland, Wash. Pacific Northwest Lab.).

A series of experiments with hydrogen-moderated plutonium systems was performed in the PCTR. The boron concentration required to reduce the infinite multiplication factor to unity was measured for various ^{240}Pu concentrations, fuel plate thicknesses, and moderator-to-fuel ratios. A summary of these experiments is presented. (M.O.W.)

6579 (BNWL–149, pp 48-56) CRITICAL MASS PHYSICS. (Battelle-Northwest, Richland, Wash. Pacific Northwest Lab.).

Three separate papers are presented along with their results. Foil activation studies in two plutonium critical systems, Monte Carlo calculated values for the critical mass of ^{238}Pu as a function of hydrogen to fuel atomic ratios and ^{239}Pu enrichment, and resonance absorber admixed in the moderator of heterogeneous arrays are the presented papers. (M.O.W.)

6580 (CEA-R–2702) CONSTANTE DE DECROISSANCE DE LA DENSITE NEUTRONIQUE DANS UN RESEAU NON-MULTIPLICATEUR DE DIMENSIONS FINIES. (Neutron Density Decay Constant in a Non-Multiplying Lattice of Finite Size). Deniz, Valentine-C. (Commissariat a l'Energie Atomique, Cadarache (France). Centre d'Etudes Nucleares). July 1965. 45p. Dep. mn.

A general theory, using the integral transport method, is presented for obtaining the neutron density decay constant in a finite non-multiplying lattice. The theory is applied to obtain the expression for the diffusion coefficient. The case of a homogeneous medium with 1/v absorption and of finite size in all directions is treated in detail, assuming an isotropic scattering law. The decay constant is obtained up to the B^6 term. The expressions for the diffusion coefficient and for the diffusion cooling coefficient are the same as those obtained for a slab geometry by NELKIN, using the expansion in spherical harmonics of the Fourier transform in the spatial variable. Furthermore, explicit forms are obtained for the flux and the current. It is shown that the deviation of the actual flux from a Maxwellian is the flux generated in the medium, extended to infinity and deprived of its absorbing power, by various sources, each of which has a zero integral over all velocities. The study of the current permits the generalization

of Fick's law. An independent integral method, valid for homogeneous media, is also presented. (auth)

6581 (CEA-R-2872) METHODE DE MONTE-CARLO—CODES POUR L'ETUDE DES PROBLEMES DE CRITICITE (IBM 7094). (Monte Carlo Method—Codes for the Study of Criticality Problems (on IBM 7094)). Moreau, Jean; Rabot, Hubert; Robin, Claude (Commissariat a l'Energie Atomique, Saclay (France). Centre d'Etudes Nucleaires). Oct. 1965. 76p. Dep. mn.

The two codes are presented which allow one to determine the multiplication constant of media containing fissionable materials under numerous and divided forms. They are based on the Monte-Carlo method. The first code applies to x, y, z, geometries. The volume to be studied should be divisible into parallelepipeds, the media within each parallelepiped being limited by non-secant surfaces. The second code is intended for r, θ, z geometries. The results include an analysis of collisions in each medium. Applications and examples with informations on time and accuracy are given. (auth)

6582 (EUR-2461.f) ETUDE PARAMETRIQUE DES REACTEURS A EAU NATURELLE. I. ETUDE PHYSIQUE DES REACTEURS A EAU LEGERE. II. EVOLUTION DU COMBUSTIBLE. III. ELEMENTS D'OPTIMISATION. (Study of Parameters of Light-Water Reactors. I. Physics of Light-Water Reactors. II. Fuel Behavior. III. Optimization Factors). Elkouby, A. (Commissariat a l'Energie Atomique, Saclay (France). Centre d'Etudes Nucleaires). 1965. 302p. Dep. mn.

A three part study of light-water reactor parameters is presented. Part I, relating to the physics of the non-irradiated core, contains a detailed description of the calculation methods together with a study of the influences of the parameters. Part II contains a study of the fuel behavior for various charging plans. The following items were determined in each case: the isotope composition of the spent fuel, fuel consumption as a function of power generated, and core life as a function of the initial enrichment. Within the framework of an optimization study, part III centers on the fuel cycle. It is shown that the irradiation ceiling for a given reactivity depends only to a slight extent on rod radius and reactor size, so that curves can be plotted, representing the enrichment necessary for the fresh fuel as a function of the moderating ratio for a given burn-up and specified charging plan. (M.O.W.)

6583 (JAERI-1091) EXPANDA. THE ONE-DIMENSIONAL DIFFUSION EQUATION CODE FOR FAST REACTORS. Katsuragi, Satoru; Suzuki, Tomoo (Japan Atomic Energy Research Inst., Tokyo). Apr. 1965. 10p. Dep. mn.

The code EXPANDA was developed from the code WANDA-6. EXPANDA can treat the criticality calculation of fast reactors by many group 1 dimensional diffusion model. The maximum number of groups is assumed 20. The inelastic scattering of neutrons was not included in the code WANDA. However EXPANDA can treat the inelastic scattering. The maximum number of mesh points and regions are 101 and 10 respectively. The criticality search is done by searching the critical thickness of some of multiplicative regions. When one intends to do parametric survey, it is very tedious to prepare a large number of input data. The code PREPANDA was prepared. The code can prepare the required data for EXPANDA automatically. The code LTFR was prepared in order to make the library tape used with PREPANDA. These three codes are described. (auth)

6584 (LA-DC-7248) CRITERIA AND EVALUATION FOR THE STORAGE OF FISSILE MATERIAL IN A LARGE AND VARIED REACTOR RESEARCH AND DEVELOPMENT PROGRAM. Smith, David R. (Los Alamos Scientific Lab., Univ. of California, N. Mex.). [nd]. Contract W-7405-eng-36. 13p. (SM-70-50; CONF-651103-13). Dep. mn; CFSTI $1.00 cy, $0.50 mn.

From IAEA Symposium on Criticality Control of Fissile Materials, Stockholm.

Due to the large amounts of plutonium and uranium stored at LASL, criticality studies were made for stored arrays. Critical masses of air-spaced arrays of 10.5, 15.7, 20.9, and 26.2 Kg cylinders of 93% enriched uranium are presented. Critical masses are given for spheres with core densities reduced by the fraction ρ/ρ_0; water reflected U(93) metal, $U(93)O_2$, $U(93)F_6$, and unreflected U(93) metal. (M.O.W.)

6585 (NAA-SR-Memo-10941) SCAP—IN IBM 7094 CODE FOR THE SPECTRAL ANALYSIS OF PULSED-NEUTRON DECAY DATA. De Juren, J. A.; Paschall, R. K.; Vaughan, E. U. (Atomics International, Canoga Park, Calif.). Mar. 5, 1965. Contract AT-11-1-GEN-8. 38p. Dep. mn; CFSTI $2.00 cy, $0.50 mn.

An IBM 7094 Fortran II code was written to perform the calculations for the spectral correction analysis of pulsed-neutron decay data. The theory of this new approach and the mechanics of using the code are described. The parameters $v\Sigma_a$, D_o and γ (heat transfer coefficient between moderator and neutron spectrum) are obtained as well as their errors. Also the variation in velocity as a function of buckling is calculated. (auth)

6586 (NAA-SR-Memo-11313) MEASUREMENTS OF THERMAL UTILIZATION (f) AND δ^{25} IN SGR URANIUM MONOCARBIDE LATTICES. Stewart, T. E. (Atomics International, Canoga Park, Calif.) June 10, 1965. Contract AT-11-1-GEN-8. 124p. Dep. mn; CFSTI $4.00 cy, $0.75 mn.

Measurements of thermal utilization (f) and δ^{25} were made for a series of graphite moderated, sodium cooled, UC fueled critical assembly lattices. Three triangular pitches (9, 11 and 12 in.) were used; several configurations of fuel and control channels were studied at each pitch. The thermal utilization was measured by the recently developed two foil technique; a fully enriched U-Al alloy foil was used to determine the absorptions in U-235, and nickel-manganese 1/v detectors were used to determine the absorption in the U-238 and all other materials of the lattices. This technique greatly reduces the overall error in the measurement of the thermal utilization compared to the more conventional one detector foil technique which introduces uncertainties associated with the assumed neutron temperatures. The values of the thermal utilization determined in this experiment agree with the theoretical (calculated) values within 1 – 1.1% and hence causes a similar uncertainty in the multiplication factors. The values of δ^{25} determined agree with the calculated values for the 11-in. lattice and are 6% smaller than the calculated values for the 9 and 12-in. lattices. (auth)

6587 (NASA-TN-D-3097) CRITICAL MASS STUDIES WITH NASA ZERO POWER REACTOR II. I. CLEAN HOMOGENEOUS CONFIGURATIONS. Fix, Thomas A.; Hueller, Robert A; Ford, C. Hubbard; Alger, Donald L. (National Aeronautics and Space Administration, Cleveland, Ohio. Lewis Research Center). Nov. 1965. 20p. CFSTI $1.00 cy, $0.50.

The NASA Zero Power Reactor II (ZPR-II) was used to determine experimentally the critical masses for more than a tenfold range of highly enriched (93.2 percent ^{235}U) aqueous uranyl fluoride fuel concentrations in clean cylindrical geometries. The ZPR-II reactor tank permits the assembly of cylindrical cores 76.2 centimeters (30 in.) in diameter and with lengths (heights) up to 90 centimeters either bare or radially reflected by about 15 centimeters (6 in.) of water. The specific range of fuel concentrations was from hydrogen to uranium-235 atom ratios of about 150 (167 g ^{235}U/liter of fuel solution) to 1650 (15 g ^{235}U/liter). In addition to the critical masses, data are presented on the temperature coefficient of reactivity and the incremental reactivity worth at criticality for a similar range of concentrations. Some of the physical properties for the fuel concentrations are presented. A brief description of the ZPR-II and the experimental procedures used are also included. (auth)

6588 (ORNL-3858(Vol.1), pp 13-19) CRITICAL EXPERIMENTS. (Oak Ridge National Lab., Tenn.).

Summaries of 14 various critical experiments are presented. Experiments were carried out with uranyl fluorides,

uranium-metal, uranium-molybdenum, and uranyl nitrate solutions. In addition, criticality studies of various reactor lattices are reported. (M.O.W.)

6589 PILE-NEUTRON BURNUP CROSS SECTION OF ^{149}Pm AND SAMARIUM POISONING. Kaminker, D. M.; Nikitin, A. M.; Petrov, Yu. V. At. Energ. (USSR), 19: 188-90(Aug. 1965). (In Russian).

Pile-neutron burnup cross section of ^{149}Pm and samarium poisoning was measured on the basis of accumulation of ^{150}Pm produced by ^{149}Pm irradiated by a thermal neutron flux. Radioactive ^{149}Pm was produced by ^{148}Nd from ^{148}Nd $(n,\gamma)^{149}$Nd $\rightarrow$ ^{149}Pm reaction. The obtained ^{149}Pm was irradiated by a flux of 10^{14} neutrons cm^{-2} sec^{-1} in the VVR-M reactor. Data on the burnup of promethium enables one to determine the samarium poisoning appearing after a prolonged reactor inactivity $y \equiv (\langle\sigma_a^{Sm}\phi\rangle N_{Pm}/\langle\sigma_a^{F}\phi\rangle N_F)$ where N_{Pm} and N_F are the number of promethium nuclei and fuel per unit volume at the moment of reactor shutdown. The samarium poisoning y as a function of fuel burnup Z at various fluxes ϕ is plotted. The results showed that with large ϕ and Z the poisoning is dangerous because it prevents the startup in a reactor due to the reactivity storage. This concerns mainly reactors operating with thermal neutrons. In reactors with fast or intermediate neutrons the samarium poisoning is negligible. (R.V.J.)

6590 XENON OSCILLATIONS IN NUCLEAR REACTORS. Bacherikov, I. P. At. Energ. (USSR), 19: 389-90(Oct. 1965). (In Russian).

A method is presented for calculating local deviations in the neutron flux distribution due to disturbances in the equilibrium of the ^{135}Xe concentration from changes in the power level or in the neutron field from shifting control rods. Expressions for the harmonics of the deviation of the neutron distribution from its final equilibrium value are set up and are solved numerically for a specific case by the method of successive approximation. (M.J.T.)

6591 MEASUREMENT OF THE ASYMPTOTIC NEUTRON SPECTRUM IN A MULTIPLYING MEDIUM [Thesis]. Slovacek, Rudolf Edward. Troy, N. Y., Rensselaer Polytechnic Inst., 1964. 239p.

Asymptotic (in time) low energy neutron spectra were measured for three multiplying assemblies containing ^{235}U. The first multiplying medium (MM1) consists of an array of 1.3 mil thick ^{235}U fuel strips in water. The MM1 fuel-water region forms a cube about 25 cm on edge. The second assembly (MM2) is similar in construction to MM1 but is a slab only about 6 cm thick. The third assembly (MM3) consists of a homogeneous dispersion of uranium oxide in paraffin and is 30 cm × 30 cm × 10 cm. The calculated k_{eff} is 0.76, 0.15, and 0.14 for MM1, MM2 and MM3 respectively. The time to establish an asymptotic spectrum is observed to be about 50 μsec for a pure water slab 5 cm thick and is about the same for the two thin slab assemblies (MM2 and MM3). For the large assembly an asymptotic distribution is attained 110 μsec after the source pulse. The reentrant hole perturbation on the asymptotic spectrum is measured to be less than 5% for a two-inch-diameter hole to the center of a three-inch-thick polyethylene slab. The intensity decreases by a factor of two and the dieaway time decreases by 2% with the two inch diameter hole perturbation. The measured asymptotic spectrum in a large non-crystalline pure moderator is fitted well with a Maxwellian distribution at the ambient temperature. Steady state calculational techniques are employed to calculate the spectrum by using the poison removal method to reduce the time dependent problem to a stationary one. Better agreement is obtained between spectrum calculation and measurement if the measured decay constant is used to determine the reduced medium absorption instead of a calculated decay constant. In the energy range from 0.625 to 3 ev, the scalar spectrum exhibits significant chemical binding effects. The Nelkin kernel constants in Corngold's spectrum calculation give a good fit to the data for the two water moderated assemblies. The Goldman polyethylene parameters yield a reasonably good fit for the paraffin moderated assembly. In the range below 0.625 the data are fitted better with a bound kernel calculation where significant differences appear between the free atom and bound calculations. (Dissertation Abstr.)

Design and Feasibility

6592 SELF-LIMITING RADIANT NUCLEAR BOILER AND SUPERHEATER. Huntington, Morgan G. (to RNB Corp.). U. S. Patent 3,210,253. Oct. 5, 1965. Filed Nov. 14, 1963.

A heterogeneous dual-moderated (graphite-light water) reactor is patented, and a method of operating and controlling the reactor is described. The moderator of the reactor comprises a plurality of separate moderator graphite blocks assembled in a block shaped pile such that the water and fuel passages are completely separate and continuous through the pile of blocks. The fissionable elements are disposed in a geometric pattern in the fuel passages without completely filling the fuel passages. The fuel elements are capable of operating at a surface temperature above 3000°F. The reactor is capable of furnishing high pressure uncontaminated super-heated steam principally by radiant heat transfer between fuel elements and moderator and between moderator and coolant in coolant tubes. (B.L.M.)

6593 METHOD OF CONSTRUCTING A NUCLEAR REACTOR CORE FROM GRAPHITE BLOCKS. Wood, William George Edgar; Thomas, Peter Barrington (to AEI-John Thompson Nuclear Energy Co., Ltd.). U. S. Patent 3,213,530. Oct. 26, 1965. Priority date Oct. 9, 1957, Great Britain.

A method of constructing a gas cooled reactor core consists of arranging a number of graphite blocks in vertical stacks and horizontal layers to form a central compensation zone in which compensation is made for Wigner growth. An uncompensated zone extends annularly around the compensated zone at least in the upper part of the reactor. The uncompensated zone is so arranged that the overall increase in the horizontal dimension due to Wigner growth increases substantially progressively in successive layers of the graphite blocks. With such an arrangment, the growth of the core increases progressively so that distortion of fuel channels and control rod channels is minimized. (B.L.M.)

Fuels

Refer also to abstract 6023.

6594 (D-910092-4) THEORETICAL INVESTIGATION OF THE OPACITY OF HEAVY-ATOM GASES. Krascella, N. L. (United Aircraft Corp., East Hartford, Conn. Research Labs.). Sept. 1965. Contract NASw-847. 52p.

A theoretical investigation was conducted to determine the composition, spectral absorption coefficients, and Rosseland mean opacity of gaseous nuclear fuel and tungsten using a semi-empirical heavy-atom analytical model in order to obtain information applicable to gaseous nuclear rockets. The characteristics of the nuclear fuel were determined for a range of values of each of the following parameters which must be assumed in using the heavy-atom model; ionization potentials, energy level spacings, total oscillator strengths, and the ratio of partition functions for successive ionization species. Included in these ranges of values were calculated ionization potentials and partition function ratios. The greatest changes in Rosseland mean opacity at a given pressure and temperature resulted from the calculated changes in fuel ionization potentials. The Rosseland mean opacity of gaseous tungsten was calculated on the basis of completely overlapped lines and for finite-width spectral lines due to the presence of specified values of hydrogen partial pressure. (auth)

6595 (EURAEC-1421) APPLICATION OF THE VAPOTRON EFFECT ON BOILING LIGHT WATER REACTORS. Quarterly Report No. 11, October-December 1964. (Compagnie Francaise Thomson-Houston, Paris). Con-

tract 034-63-11-TEEC. 54p. Dep. mn; CFSTI $3.00 cy, $0.50 mn.

Work Performed under United States–Euratom Joint Research and Development Program.

Results from the thermal testing of fuel elements of boiling water reactors are presented. The number of fins on the fuel elements tested were 18, 24, 36, 72, and 108. (M.O.W.)

6596 (GEST–2049) RESEARCH PROGRAM FOR THE LONG TERM TESTING OF CYLINDRICAL DIODES AND THE IRRADIATION OF FUEL AND INSULATORS. Seventh Quarterly Progress Report, December 18, 1964–March 17, 1965. (General Electric Co., Pleasanton, Calif. Special Purpose Nuclear Systems Operation). Apr. 18, 1965. Contract NAS 3-2544. 77p. (NASA-CR–54656).

The experimental and analytical work in nuclear thermionics being performed by the Special Purpose Nuclear Systems Operation of the GE Company for NASA is presented. Information from the literature, information generated under the contract, and information generated by the contractor in other studies, some of which were conducted under other contracts with the government, are included. (M.O.W.)

6597 STUDY OF THE DOSE RATE FIELD WITH A γ SOURCE OF SPENT REACTOR FUEL ELEMENTS. Drozdov, V. E.; Zakharova, I. M.; Dobrovol'skii, S. P. At. Energ. (USSR), 19; 367-71(Oct. 1965). (In Russian).

Experiments were carried out to determine the distribution of activity along the length of a fuel element of the RFT reactor. It was shown that the activity distribution is satisfactorily described by a cosine function, and that the formulas used for calculating the dose-rate field of a radiator with even distribution of activity along the length are inapplicable for fuel elements (the error is 23% for the RFT and 32% for the first nuclear power station). Experimental and theoretical studies were made of the dose-rate fields from a single fuel element and a hollow cylindrical emitter of 18 fuel elements of the RFT. A working formula is obtained for calculation of the dose-rate field from spent fuel elements. It is shown that for the calculation of the dose-rate field within a hollow cylindrical emitter of fuel elements of finite diameter the activity can be considered distributed according to a cosine law along the surface of an infinitely thin cylinder with radius equal to the arithmetic average of the minimum and maximum radii of the emitter. (tr-auth)

6598 THERMOELECTRIC NUCLEAR FUEL ELEMENTS. Danko, Joseph C.; Tower, Stephen N.; Thomas, Garland L. (to Westinghouse Electric Corp.). U. S. Patent 3,214,295. Oct. 26, 1965. Filed Nov. 1, 1962.

A thermoelectric nuclear fuel element of the plate, rod, or tube type includes at least one thermoelectric portion disposed within cladding means. The cladding material is in good thermal relation to the thermoelectric portion so as to form a cold thermoelectric circuit junction for it. If only one thermoelectric portion is provided in the element, this portion is characterized as being fissile or fissionable. If more than one thermoelectric portion is provided in the fuel element, the thermoelectric portions are of alternating semi-conductive type in series circuit relation; and at least one of the protons can have both thermoelectric and fissile properties while the other(s) can be characterized with only thermoelectric properties or with both fissile and thermoelectric properties. With more than one thermoelectric portion, a metallic member connected to adjacent portions provides the hot junction for each thermoelectric portion; while with a single thermoelectric portion, the hot metallic member is extended to the exterior in electrically insulative relation through outer cladding means. (B.L.M.)

Power and Power-Breeder Reactors

Refer also to abstract 5568.

6599 (AES–5) AGESTA KRAFTVAERMEVERK. SAMMANSTAELLNING AV TEKNISKA DATA, BESKRIVNINGAR M. M. FOER REAKTORDELEN. (Agesta Power Heating Plant. Compilation of Technical Data. Description for the Reactor Components). Lilliehoeok, B. (Aktiebolaget Atomenergi, Stockholm (Sweden)). Dec. 1964. 336p. Dep. mn.

The technical data for the reactor components of the Agesta Power Heating Plant are compiled. These include site location, reactor placement, reactor shell, reactor frame, the primary, secondary, and tertiary systems, the heavy water auxiliary system, cooling system, gas system, control elements, fuel handling, the forced cooling system, the residual effect cooling, ventilation system, waste processing, construction control, electric power supply, staff organization, and legal structure. (J.S.R.)

6600 (ANL–7105, pp 1-35) LIQUID-METAL-COOLED REACTORS. (Argonne National Lab., Ill.).

Operation of the EBR-II is described. Results from the surveillance program to determine the condition of the EBR-II Mark I fuel are presented. Further developments in the FARET reactor are reported. These developments include; mockup for cell handling operations, shielding windows, penetration of tank cover for cable take-up and support, modeling studies, in-core instrumentation, fuel assembly sodium flow test loop, and FARET criticals (ZPR-3). Fast reactor fuel development is discussed in terms of metallic fuels, jacket materials, carbide fuel elements, corrosion, irradiation testing, and zero power reactors. Fuel processing developments are discussed. (M.O.W.)

6601 (ANL–7115, pp 1-41) LIQUID-METAL-COOLED REACTORS. (Argonne National Lab., Ill.).

Research progress on the ANL Liquid-Metal-Cooled Reactor program is reported. Various aspects of research on the EBR-II, FARET, general fast reactor physics, general fast reactor fuel development, and general fast reactor fuel reprocessing development are discussed. (M.O.W.)

6602 (BNWL-SA–346) FAST REACTOR SAFETY CONSIDERATIONS RELATED TO FUEL MACROSTRUCTURE. Peterson, R. E.; Goldsmith, S. (Battelle-Northwest, Richland, Wash. Pacific Northwest Lab.). Oct. 6, 1965. Contract AT(45-1)-1830. 19p. (CONF-651009–3). Dep. mn; CFSTI $1.00 cy, $0.50 mn.

From Conference on Safety, Fuels and Core Design in Large Fast Power Reactors, Argonne, Ill.

Reactor fuel design is discussed in terms of achieving maximum safety characteristics for a given reactor design. The transient response of the fuel to very fast burst whether it be entirely thermal or thermo-elastic, depends upon such macroscopic properties as density, homogeneity, thermal conductivity, specific heat, and elastic modulus. Recent work relating macroscopic fuel properties to fast reactor safety when the reactor undergoes a prompt burst accident is summarized. (M.O.W.)

6603 (GA–4165) ADVANCED BERYLLIUM OXIDE CONCEPTS. Progress Report, January 1–March 31, 1963. (General Atomic, San Diego, Calif. John Jay Hopkins Lab. for Pure and Applied Science). May 24, 1963. Contract AT(04-3)-187. 68p. Dep. mn; CFSTI $3.00 cy, $0.75 mn.

Progress in engineering, materials, and physics studies of the feasibility of using $BeO-PuO_2$ and $BeO-ThO_2-UO_2$ fuel bodies is reported. (W.L.G.)

6604 (GA–5842) EXPERIMENTAL BERYLLIUM OXIDE REACTOR PROGRAM. Quarterly Progress Report for the Period Ending September 30, 1964. (General Atomic, San Diego, Calif. John Jay Hopkins Lab. for Pure and Applied Science). Oct. 31, 1964. Contract AT(04-3)-187. 27p. Dep. mn; CFSTI $2.00 cy, $0.50 mn.

Room temperature mechanical testing of the tipping reflector pneumatic actuator mechanism was completed. Mechanical performance was found to be generally excellent, except for some difficulty with seal rings when resetting the actuator and a condition in which the actuator

plunger was damaged by the locking balls. The total helium leakage past the actuator piston was determined. Fuel pin tests are continuing with some deviations noted in length and straightness of pins. No cladding failures were noted at the end of 69 cycles. Preliminary design of the core top support structure continues, with emphasis on its removal and replacement, its compatibility with the handling machine, and its support requirements imposed by the tipping reflector elements. Forty-two fuel elements were completed, with the remaining two to be completed after delivery of special BeO blocks. Performance testing of the scram system in the prototype drive mechanism was completed after a total of 26 scrams. Scram performance was found to be affected by loop pressure; and as a result of malfunctions, some of the system components were returned to the vendor for rework. Insertion times required by core physics were achieved. Performance requirements for the remote viewing system were established; design of the system is continuing. Instrumentation was installed on the core support grid, rework of the failed fuel detection system (FFDS) manifolds was completed, a control rod drive auxiliary test panel was built, and a simplified spot-welding procedure was substituted for an arc-welding procedure for the attachment of thermocouple clips to the pressure vessel. Thermocouples for post-heat treatment of field welds were fabricated and shipped to the site. The electrostatic precipitator for the FFDS was received. Work on the pressure vessel included replacing heli-coil inserts with threaded bushings to avoid difficulties during installation of studs. The hydrostatic test was performed and the vessel was leak-tested. Also materials from several areas on the pressure vessel were impact-tested. (auth)

6605 (GAMD–6673) OPTIMIZATION STATUS REPORT. Freudiger, F. S.; Schultz, G. M. (General Atomic, San Diego, Calif. John Jay Hopkins Lab. for Pure and Applied Science). Aug. 27, 1965. Contract AT(04-3)-167. 35p. Dep. mn; CFSTI $2.00 cy, $0.50 mn.

Optimization of nuclear power plant design is discussed. A detailed and precise statement of the optimization problem, a definition of terms, and a description of the factors influencing the cost of a nuclear power plant are presented. A discussion of a statistical approach to the problem is also presented, and the computer program (GAOP) is described. Possible future improvements in the optimization study are discussed. (M.O.W.)

6606 (GEAP–4962) DEVELOPMENT PROGRAM ON THE GARIGLIANO NUCLEAR REACTOR. Quarterly Report No. 12. Howard, C. L. (General Electric Co., San Jose, Calif. Atomic Power Equipment Dept.). Oct. 1, 1965. Contract AT(04-3)-189. 79p. (EURAEC–1498). Dep. mn; CFSTI $3.00 cy, $0.75 mn.

Work Performed under United States–Euratom Joint Research and Development Program.

The "program acceptance test" for the on-line computer was completed September 12, and the system is now in normal operation. Test of the computer at conditions simulating the stability tests were satisfactorily completed. The instrumented fuel assembly probes and flowmeters were calibrated and shipped to the Garigliano site. Cable installation and hookup are over half completed. Final assembly of the in-core flux detectors and movable chamber drive units is in progress. The equipment and procedures for the fuel gamma scan are ready for the measurements, which are scheduled for October 2 to 9, 1965. Reactor power shape was held constant for the month prior to the shutdown to provide a clear basis for evaluating the results. Operation was with one pump, all control rods out except four notches on the center rod, and power of 121 decreasing to 116 Mw(e). Preparations for the stability and plant system tests are essentially complete, including safeguards data, installation of the control rod oscillator, preparation of test procedures, and calculation of reactor control rod patterns and thermal-hydraulic limits for the test conditions. The reactor was shut down on October 24 for a scheduled 7-week outage. Planned work includes replacement of stainless steel fuel channels with Zircaloy, fuel cleaning, maintenance, turbine inspection, and preparations for the stability and plant systems tests. These tests are scheduled for November and December. (auth)

6607 (GEAP–4965) PLUTONIUM SUBCRITICAL EXPERIMENT PROGRAM. Fifth Quarterly Report, July 1–September 30, 1965. Carver, J. G. (General Electric Co., San Jose, Calif. Atomic Power Equipment Dept.). Oct. 1, 1965. Contract AT(04-3)-189. 15p. (EURAEC–1495). Dep. mn; CFSTI $1.00 cy, $0.50 mn.

Work Performed under United States–Euratom Joint Research and Development Program.

A summary of progress on the Plutonium Subcritical Experiment Program is presented. Brief discussions on development of the pressurized water system, fuel rod procurement, counting equipment, and fission rate calibration measurements are presented. In addition, some lattice parameter calculations are given. (M.O.W.)

6608 (HIT–3459-7) ANALYSIS OF ZERO POWER EXPERIMENTS FOR SM-1 CORE III. (Hittman Associates, Inc., Baltimore, Md.). Dec. 1964. Contract AT(30-1)-3459. 11p. (HIT–158). Dep. mn; CFSTI $1.00 cy, $0.50 mn.

A comparison of theoretical predictions was made with the results of a critical experimental program. For criticality measurements, the control rod positions are predicted to within 1% Δk. For reactivity measurements, the total rod bank work, individual control rod worth, and shutdown margin fall within the experimental accuracy. A difference between theory and experiment in regard to the value of temperature coefficient between 70 and 140°F is attributed to uncertainties in the measurement. These results indicate that the analytic method can be used with confidence to predict SM-1A Core III nuclear characteristics. (auth)

6609 (HIT–3534-1) ADDENDUM TO SM-1A HAZARDS SUMMARY REPORT FOR CORE III. (Hittman Associates, Inc., Baltimore, Md.). June 30, 1965. Contract AT(30-1)-3534, 88p. (HIT–165). Dep. mn; CFSTI $3.00 cy, $0.75 mn.

The safety of operation of the SM-1A reactor plant with Core III was analyzed and is presented. This core contains an identical number of stationary fuel and moveable control-fuel assemblies as used in the previous cores. However, the fuel and burnable poison loadings were increased with a resultant increase in core life. A summary of Core III and SM-1A plant data is presented in tabular form. Nuclear and thermal-hydraulic analyses of the "as-built" core were performed and the results are summarized. A zero power nuclear experiment was performed on Core III. A core loading procedure was established based on the experimental data and is presented. Reactivity insertion accidents caused by control assembly withdrawal at the maximum possible rate and by the introduction of cold water into the reactor vessel were analyzed. Loss of coolant flow accidents were analyzed for both a free rotating and locked primary coolant pump impeller. (M.O.W.)

6610 (HW–79287) FUEL CONSERVATION INDEXES FOR THERMAL REACTORS. Eschbach, E. A.; Kanninen, M. F.; Neef, W. I. (General Electric Co., Richland, Wash. Hanford Atomic Products Operation). July 1964. Contract AT(45-1)-1350. 61p. Dep. mn; CFSTI $3.00 cy, $0.75 mn.

An attempt is made to analyze the various factors involved in uranium conservation, and to derive a general set of indexes to measure the conservation efficiency of various reactors. A 7090 program listing in FORTRAN II is appended. (auth)

6611 (HW-SA–3669) THE EFFECT OF EARLY INTRODUCTION OF BREEDER REACTORS ON URANIUM RESOURCE CONSERVATION. Neef, W. I. (General Electric Co., Richland, Wash. Hanford Atomic Products Operation). Nov. 25, 1964. Contract AT(45-1)-1350. 25p. (CONF-654–97). Dep. mn; CFSTI $1.00 cy, $0.50 mn.

From American Nuclear Society Meeting, San Francisco, Nov.–Dec. 1964.

Uranium conservation is considered with respect to future development of breeder reactors. Economic aspects of electricity production for the next 100 years are discussed. (M.O.W.)

6612 (INR–622/IX/R) ENERGETYCZNE REAKTORY MAGNOXOWE PO III KONFERENCJI GENEWSKIEJ. (Magnox Power Reactors after the Third Geneva Conference). Lopuszynski, Jerzy (Institute of Nuclear Research, Warsaw (Poland)). 1965. 60p. Dep.

Present and future trends in the development of Magnox Power Reactors are discussed. (M.O.W.)

6613 (LA-DC–7475) NUCLEAR DESIGN OF MPBE. Hannum, W. H. (Los Alamos Scientific Lab., Univ. of California, N. Mex.). [1965]. Contract W-7405-eng-36. 18p. (CONF-651009–8). Dep. mn; CFSTI $1.00 cy, $0.50 mn.

From Conference on Safety, Fuels and Core Design in Large Fast Power Reactors, Argonne, Ill.

The design of a Molten Plutonium Burnup Experiment (MPBE) which will be used to determine the properties of a molten plutonium fuel during and after high burnup is presented. The calculated reactivity and reactivity swing for various control configurations are given. (M.O.W.)

6614 (LA-DC–7476) EFFECT OF FISSION GAS BUBBLES ON THE RESPONSE OF MOLTEN FUEL REACTORS TO FAST TRANSIENTS. Carmichael, B. M. (Los Alamos Scientific Lab., Univ. of California, N. Mex.). [nd]. Contract W-7405-eng-36. 12p. (CONF-651009–7). Dep. mn; CFSTI $1.00 cy, $0.50 mn.

From Conference on Safety, Fuels and Core Design in Large Fast Power Reactors, Argonne, Ill.

To evaluate the effects of the fission product gas bubbles on fast transients, a first approximation to the equation of state of the medium consisting of a mixture of liquid fuel and bubbles is considered. The adiabatic case was considered only; i.e., it is assumed no heat is lost from the liquid, either to the bubbles or to the external environment of the capsule. Results of this study are presented. (M.O.W.)

6615 (NAA-SR–10888(Rev.)) RECOMMENDATIONS FOR STANDARDIZATION AND IMPROVEMENT OF PHA PROCEDURES AT PNPF. Mandel, H. (Atomics International, Canoga Park, Calif.). Aug. 27, 1965. Contract AT(11-1)-Gen-8. 17p. Dep. mn; CFSTI $1.00 cy, $0.50 mn.

Recommendations are made for improvement and standardization of PHA procedures for routine use at the PNPF site. These are: use of base-line corrections for specific isotopes, standardization of the number of channels counted per photopeak, improvement of counting statistics for ^{24}Na and ^{38}Cl, a new and improved procedure for calculating effective power levels for various isotopes, and use of gross counting of coolant samples by PHA on a daily basis. (auth)

6616 (NAA-SR-Memo–11324) LARGE SGR CALANDRIA VESSEL STAYED HEAD STUDY. Kniley, D. J. (Atomics International, Canoga Park, Calif.). Apr. 21, 1965. Contract AT-11-1-GEN-8. 80p. Dep. mn; CFSTI $3.00 cy, $0.75 mn.

A limited experimental stress analysis was conducted on a typical section of the calandria vessel upper stayed head. Interior and peripheral sections of the head were incorporated into the test fixture to permit determination of stress and deflection characteristics at the peripheral and interior locations. Due to time limitations, only a minimum of testing was possible. No elevated temperature testing was performed and testing was limited to the test section corresponding to a typical interior region. Data were obtained from electric resistance strain gages placed at strategic locations on ligament regions and in regions of stress raisers such as at the cruciform to head attachment weld. The major observation that can be made, based on the data obtained from the tests performed, is that head flexibility is definitely evident between hanger attachment cruciforms and process channel attachment openings. Two basic core conditions were investigated. Calandria head pressure differentials representing an internal pressure greater than the pressure resulting from the sodium pool; and an internal pressure less than that resulting from the sodium pool. For normal core operating conditions, primary plus secondary stresses were within the allowable limits of 13,500 psi ($3\ S_m$) as specified in Section III of the ASME Boiler and Pressure Vessel Code for long term service at 1200°F. For the loss in core pressure condition, the localized or peak stresses at notches such as the toe of a hanger attachment cruciform were within the allowable limit of 54,000 psi (S_a) for approximately 100 total cycles (3.3 per year) at 1200°F (just prior to shutdown). For this same case, the maximum ligament stress of 9900 psi falls within the allowable limit of 13,500 psi ($3\ S_m$) at 1200°F and well within the 46,000 psi ($3\ S_m$) the lower temperature of 650°F. It should be noted that in the event of loss of internal pressure within the core, the temperature of the core is reduced in steps from approximately 1200 to 650°F at the rate of 100°F per hour. The deflection curves show a definite nonplanar behavior of the specimen. This is to be expected with the specimen edge restraint present. Head curvatures were slightly more severe than would be expected from a flat interior prototype region. The loads applied during this test program do not include thermal or dynamic stressing or secondary mechanical loading from such sources as process channel attachment rotations. It is therefore difficult to formulate a conclusion on the integrity of the interior head region based on the results obtained from these limited tests. However, for the loadings investigated, the design should be adequate. (auth)

6617 (NAA-SR-Memo–11339) ANALYSIS OF PROCESS CONTROL IN AN SGR 200 Mwe PROTOTYPE PLANT. Bonyhady, K. A. (Atomics International, Canoga Park, Calif.). June 26, 1965. Contract AT(11-1)-Gen-8. 23p. Dep. mn; CFSTI $1.00 cy, $0.50 mn.

The throttle temperature control methods of a steam turbine when the steam cycle includes a once-through, subcritical pressure steam generator in an SGR type system are studied. The effect of a feedwater preheater with approximately constant temperature output to the once-through steam generator is available. The parameters for a steam dump system are studied. (auth)

6618 (NAA-SR-Memo–11415) LARGE SGR CALANDRIA VESSEL PERIPHERAL HANGER TEST. Kniley, D. J. (Atomics International, Canoga Park, Calif.). May 14, 1965. Contract AT(11-1)-Gen-8. 21p. Dep. mn; CFSTI $1.00 cy, $0.50 mn.

Results of a very limited ambient temperature experimental stress survey indicate two areas of high stress in the attachment welds. At the upper and lower attachment weld extremities, stresses were measured that were 13.5 and 3.9 times, respectively, the nominal stress in the vessel wall. At the design hanger load of 8700 lb, the peak attachment weld stress (upper extremity) was found to be 4100 psi. Stresses in the straight portion of the rectangular bar section of the hanger bracket were approximately 18500 psi tensile along the inner (towards center of calandria) edge, and 11100 psi compressive along the outer edge. The experimentally determined bending moment in the bracket was found to be 9860 in./lb compared to a theoretical value of 15200 in./lb. The bending moment in the load transducer just above the bracket was found to be 2490 in./lb. This would correspond to a location at the lower end of the hanger rod. (auth)

6619 (NAA-SR-Memo–11416) LARGE SGR PROCESS TUBE-GRAPHITE LOG STRUCTURAL INTERACTION STUDY. Kniley, D. J. (Atomics International, Canoga Park, Calif.). Apr. 28, 1965. Contract AT(11-1)-Gen-8. 31p. Dep. mn; CFSTI $2.00 cy, $0.50 mn.

Using available data on the behavior of graphite subjected to irradiation of high temperatures and a predicted shrinkage saturation level, a total axial log bowing of 0.91 inch was calculated. This coupled with transverse or radial shrinkage of 0.23 inch, results in a total effective diametral reduction of 1.14 inch, which must be resisted by the pro-

cess tube. This distortion produces at the log ends localized contact stresses of $\sigma 1 = 13700$ and $\sigma 2 = 16900$, based on extrapolation of experimental data for a 0.25 inch effective diametral expansion. Log fracture was found to occur at a minimum bow level of $1\frac{1}{32}$ inch and in a previous test program from a diametral expansion of 1.44 inch. Conclusions on log or process tube integrity are impractical due to the limited amount of information available on graphite behavior under irradiation at elevated temperatures. (auth)

6620 (NAA-SR-Memo-11458) SGR TEMPERATURE TRANSIENTS. Cappel, H. H. (Atomics International, Canoga Park, Calif.). June 16, 1965. Contract AT(11-1)-Gen-8. 56p. Dep. mn; CFSTI $3.00 cy, $0.50 mn.

A summary of reactor transients investigated for the design and evaluation study of the 200 Mwe LSGR is presented. The transients considered are those resulting from accident conditions, and comprised of the "classical" reactor accidents as well as some which are new and unique to this reactor system. Each accident was analyzed for transient temperature and flow conditions at various critical points in the primary system. A parallel study was concerned with transients in the low-pressure system of the primary loop. The studies were conducted with the computer codes "SCRATCH 1" and "SCRATCH 2". The codes were developed purposely for this analysis and their mathematical analogies are described in detail. (auth)

6621 (NAA-SR-Memo-11556) RELIABILITY TEST OF AN SRE-PEP MODERATOR ELEMENT. Phelps, R. D.; Brindley, J. H. (Atomics International, Canoga Park, Calif.). Aug. 2, 1965. Contract AT(11-1)-Gen-8. 7p. Dep. mn; CFSTI $1.00 cy, $0.50 mn.

An SRE-PEP moderator element, chosen at random from the production run, was thermally cycled 74 times over temperature ranging from 475 to 1325°F. Temperature gradients between 575 and 675°F were imposed along the length of the element, with differential pressures ranging from 2.5 to 9.0 psi maintained across the element cladding. At the end of the 10th cycle, 22nd cycle, and 74th cycle, the element was removed from the furnace for inspection. In each case the condition of the element was satisfactory; only minor dimensional changes were observed, no anomalies were noted, and the element was fully integral following an environmental exposure equivalent to approximately 58 years of reactor operation. (auth)

6622 (NYO-3250-2) USE OF HYDRAULIC MODELS IN NUCLEAR REACTOR DESIGN. Hetsroni, G. (Connecticut Yankee Atomic Power Co., Haddam). Oct. 1965. Contract AT(30-1)-3250. 105p. Dep. mn; CFSTI $4.00 cy, $0.75 mn.

Experimental studies are conducted on a scaled hydraulic model of the Connecticut Yankee Reactor. Various configurations are tested and compared with regard to pressure drop owing to different components and with regard to the distribution of the flow at the inlet to the core. Based on these studies the geometry of the Connecticut Yankee Reactor vessel internals is determined, and the pressure drops in the vessel are estimated. In addition, the flow distribution in the thermal shield annuli and in the lower plenum is studied. (auth)

6623 (TID-22206) GARIGLIANO NUCLEAR POWER PLANT. Operation Report for the 2nd Quarter of 1965. Technical Report, June 30, 1965. (Ente Nazionale per l'Energia Elettrica, Rome (Italy)). 15p. Dep. mn; CFSTI $1.00 cy, $0.50 mn.

The operations, maintenance, and core performance of the Garigliano Power Reactor are reviewed. Plant chemistry control, liquid and gaseous waste disposal, and health physics operation routines are tabulated. (T.F.H.)

6624 (TID-22425) CONSULTING SERVICES ON THE ADVANCED BONUS CORE BOILER-SUPERHEATER FUEL ELEMENT WELDMENTS. Final Report. McDonald, J. Jr.; Norris, E. B.; Watson, P. D.; Speirs, K. K. (Southwest Research Inst., San Antonio, Tex.). Sept. 20, 1965. Contract AT(40-1)-3154. 176p. Dep. mn; CFSTI $5.00 cy, $1.00 mn.

The development and optimization of welding procedures, and the determination of tensile and fatigue data for the produced weldments, are reviewed for several types of welds in Inconel 600 and 625 and Incoloy 800. The weld configurations studied include welds of steam tubes to tube sheets, welds of boiler clad to tube sheets, and tube-to-tube welds. The techniques developed are intended for use in an advanced BONUS core configuration. (T.F.H.)

6625 (TID-22434) GARIGLIANO NUCLEAR POWER PLANT. Operation Report for the 3rd Quarter of 1965. Technical Report, September 30, 1965. (Ente Nazionale per l'Energia Elettrica, Rome (Italy)). 10p. Dep. mn; CFSTI $1.00 cy, $0.50 mn.

The operation, core performance, maintenance, and plant chemistry activities of the Garigliano power reactor are reviewed. (T.F.H.)

6626 (UNC-5118) SHIELD SMALL SOURCE EXPERIMENTS. Report No. 2. Schamberger, R.; Celnik, J. (United Nuclear Corp., White Plains, N. Y. Development Div.). May 6, 1965. Contract AT(30-1)-3078; Subcontract No. 1. 118p. Dep. mn; CFSTI $4.00 cy, $0.75 mn. For Allison Div., General Motors Corp., Indianapolis, Ind.

MCR shield design analytical techniques and cross sections were tested by comparing calculations with measurements for experiments emphasizing the secondary gamma-ray production in specific test materials. Measurements were made with a gamma-ray spectrometer behind a configuration consisting of a layer of gamma-ray shielding material (the test sample) adjacent to a small Po–Be neutron source, followed by neutron and gamma-ray shielding material to reduce extraneous detector response. Calculations of spectrometer response for samples of lead, tungsten, and titanium hydride were performed with a three-dimensional Monte Carlo code, derived from the one-dimensional Monte Carlo codes used in the MCR preliminary design shield analysis. The calculations generally gave very satisfactory predictions of the measurements, the agreement being within twice the uncertainty in the experiment. Differences between the measured and calculated responses indicated that some of the cross sections used, particularly for lead, were low and should be revised. (auth)

6627 (WAPD-PWR-TE-141) EVALUATION OF CORE THERMAL DATA, PWR CORE 1 SEED 3 SECOND HALF SEED LIFE. PART A. REACTIVITY LIFETIME THERMAL PERFORMANCE, DLCS-36201. PART B. CORE THERMOCOUPLE CALIBRATION, DLCS-24301. Period Covered: March 1962–November 1962. Smeltzer, Paul (Bettis Atomic Power Lab., West Mifflin, Pa.). Aug. 1964. Contract AT-11-1-GEN-14. 105p. Dep. mn; CFSTI $4.00 ct, $0.75 mn.

I. Thirty-five fuel assemblies installed in the Shippingport PWR were instrumented and monitored throughout the Seed 3 operation of Core 1. The measured portion of total core power generated in each of the 35 assemblies was compared with that calculated using TNT depletion sequence. The measured trend in power of the Group II, III, and IV seeds follows that of the calculations. The average measured seed region fraction of total core power varied from three percent below to 7.5 percent above the calculated values for the first and second half of seed life respectively. A positive bias in the data during the second half of seed life accounts for the relatively higher seed power share for that period of operation. II. Data obtained from five thermocouple calibrations performed over Seed 3 life are presented. These data were used to correct the as-read core temperatures acquired by the Data Acquisition System. A comparative evaluation of the calibrations indicates that a significant shift, in excess of 1.0°F was found to have occurred in seven thermocouples between the March 1962 and May 1962 calibration tests. A shift of similar magnitude was observed in six thermocouples between May and July of 1962. Fifty-three thermocouples were considered operable after the July 1963 calibration. (auth)

6628 (WAPD-PWR-TE-201) PWR REACTOR PLANT CONTAINER LEAK RATE TEST, DLCS 57201.

Johnson, R. M. (Bettis Atomic Power Lab., West Mifflin, Pa.). Aug. 6, 1965. Contract AT-11-1-GEN-14. 19p. Dep. mn; CFSTI $1.00 cy, $0.50 mn.

An evaluation of the Shippingport PWR container leak rate data obtained prior to Core 2 criticality is presented. The container leak rate was in the order of 0.0120 to 0.0137% of container volume per day as determined by the internal reference vessel method. A superimposed leak rate equal to the test allowable value of 0.065% of container volume per day was used to verify the accuracy of the test instrumentation. (auth)

6629 (WCAP-3269-24) THE SAXTON CHEMICAL SHIM EXPERIMENT. Weisman, J.; Bartnoff, S. (Westinghouse Electric Corp., Pittsburgh, Pa. Atomic Power Div.). July 1965. Contract AT(30-1)-3269. 98p. Dep. mn; CFSTI $3.00 cy, $0.75 mn.

An extensive program to demonstrate the feasibility of operation with chemical shim control was conducted at the Saxton reactor. Boric acid remained in the core continuously from May 23, 1963, to January 20, 1964. After a brief period of non-borated operation, chemical shim operation resumed on March 6 and continued until April 20 when the reactor was shutdown temporarily for replacement of experimental fuel rods. Total average core burnup was then 6330 Mwd/MTU, of which 4521 Mwd/MTU was incurred during chemical shim operation. Peak burnup was 15,600 Mwd/MTU. The experimental data indicate no significant boron accumulation on the core surface at power and no decrease in core lifetime. The data also indicate that alkali addition for pH control is satisfactory in both pure water and the chemical shim solution; moreover, the expected hot channel factors were achieved. (auth)

6630 (WCAP-3269-46) IN-CORE INSTRUMENTATION FOR THE SAN ONOFRE NUCLEAR GENERATING STATION. Leggett III, W. D. (Westinghouse Electric Corp., Pittsburgh, Pa. Atomic Power Div.). Mar. 1965. Contract AT(30-1)-3269. 80p. Dep. mn; CFSTI $3.00 cy, $0.75 mn.

In-core instrumentation for the San Onofre Nuclear Generating Station consists of thirty Aeroball flux monitoring channels and thirty-five fuel assembly outlet thermocouples. The instrumentation, relevant plant characteristics, and complementary ex-core instruments are described. The bases for the choice of instruments and instrument locations are discussed. The procedure for data reduction is delineated and the anticipated accuracy of the system is stated. (auth)

6631 (YAEC-1005) AN EVALUATION OF THE YANKEE VAPOR CONTAINER LEAKAGE MONITORING SYSTEM. DeVincentis, J. (Yankee Atomic Electric Co., Boston, Mass.). Feb. 15, 1965. 21p. Dep. mn; CFSTI $1.00 cy, $0.50 mn.

A long-term (9 mo.) series of tests of the leakage-monitoring system of the Yankee Reactor vapor container is reported. The sensitivity, reliability, and operational concept of the leakage monitor are discussed. (T.F.H.)

6632 (AEC-tr-6628) APPLICATION OF DIFFERENT METHODS OF NON-DESTRUCTIVE TESTING TO FUEL ELEMENTS OF THE ORGEL TYPE. Bonnet, P.; Jansen, J. Translated from IAEA preprint SM-63/23, paper presented at the Symposium on Non-Destructive Testing in Nuclear Technology, Bucharest, Roumania, May 17–21, 1965. 46p. Dep. mn; JCL $4.60 fs, $1.58 mf.

Non-destructive tests on Orgel fuel elements were made. A comparative description of different methods for the detection of defects is presented. The methods considered are ultrasonics, radiography, Foucault currents, visual inspection, and dimensional metrology. (M.O.W.)

6633 (AECL-2286) PROBLEMS OF DEFECTOSCOPIC EXAMINATION OF STRUCTURAL MATERIALS FOR THE REACTOR OF THE FIRST CZECHOSLOVAKIAN ATOMIC POWER STATION. Radislav, Philip. Translated for Atomic Energy of Canada, Ltd., Chalk River, Ont., from Paper SM-63/11 Presented at the Symposium on Non-Destructive Testing, Bucharest, May 17–21, 1965. 14p. Dep.; AECL $0.50.

Defectoscopy of complicated and simple components using beta particles, x radiation, and ultrasonics is discussed, with particular reference to the applications of defectoscopy to the reactor components in the First Czechoslovakian Atomic Power Station. (T.F.H.)

6634 DYNAMIC CHARACTERISTICS OF FIRST REACTOR OF I. V. KURCHATOV BELOYARSK NUCLEAR POWER STATION. Emel'yanov, I. Ya.; Gavrilov, P. A.; Seliverstov, B. N. At. Energ. (USSR), 19: 131-7(Aug. 1965). (In Russian).

Studies of nonstationary processes in Beloyarsk nuclear power plant carried out using an analog computer and practical control devices are described. The investigation revealed dynamic characteristics of the power unit and permitted selection of optimum parameter adjustment for basic station controls. Theoretical reactor characteristics were correlated with the experimental results obtained during actual operations. (tr-auth)

6635 HALDEN—FROM RESEARCH AND ENGINEERING DEVELOPMENT TO FUEL TESTING. Jansen, E. (OECD Halden Reactor Project, Norway). Atompraxis, 11: 520-3(Sept.-Oct. 1965).

The Halden Reactor Project is discussed. The HBWR proved to be an extremely flexible tool for producing data and experience of considerable importance for larger power reactor projects. The programs gradually changed from fundamental physics and dynamics research to specific engineering experiments and development. The present program includes test fuel element irradiation, development of in-core instruments, and chemistry and physics experiments. Test fuels from the UK, Sweden, Germany, Italy, and Norway are being irradiated. This program calls for steady power operation at 17 Mw for extended periods. The steam produced is delivered to a nearby paper pulp factory at a rate of 20 tons per hour. An experimental program is being prepared, which includes experiments under superheat conditions. (auth)

6636 OPERATING EXPERIENCE WITH THE HBWR ON ITS SECOND FUEL CHARGE. Jamne, E. (OECD Halden Reactor Project, Norway). Atompraxis, 11: 523-7 (Sept.-Oct. 1965).

The HBWR was taken critical for the first time on its second fuel charge in March 1962. High-power operation started in October 1962. Experiments were carried out at variable power levels up to 25 Mw. By June 1st, 1965 the reactor had been on pressure for about 13500 hr mainly at 28.5 atm. The integrated power was 5000 Mwd or about 3600 Mwd/ton UO_2; 84000 tons of process steam has been delivered to the adjacent paper pulp factory since in July 1964. The losses of heavy water were gradually reduced, mainly due to improvements of the leakage control. Some heavy water was lost during incidents. There was no essential heavy water leakage or degradation over the heat exchangers. No standard fuel element failed, however, there were four failures of test elements. A number of modifications to the circuits and the plant control and instrumentation were made, and this improved the utilization factor of the plant. The activity levels in the containers did not cause significant operational or maintenance problems. (auth)

6637 DYNAMIC RESEARCH AND IN-CORE INSTRUMENTATION AT HBWR. Ager-Hanssen, H. (OECD Halden Reactor Project, Norway). Atompraxis, 11: 528-32(Sept.-Oct. 1965).

Research on the dynamic characteristics of heavy-water boiling reactors and development and application of in-core instrumentation to high-power-density operation are important program objectives of the international OECD Halden Reactor Project. Dynamic studies were performed on the HBWR operating with two different fuel charges. The necessary experimental techniques were first developed in connection with the operation on a low-power aluminum-clad natural uranium metallic fuel charge. When these techniques were applied to the reactor operating on an enriched uranium dioxide fuel charge at relatively high coolant power densities, it was observed that heavy-water boiling reactors may become unstable as a

result of flash boiling of moderator between coolant channels. A theoretical model was developed, which makes it possible to select the proper design parameters to avoid this problem. The in-core instrument development program was originally initiated in support of the dynamic studies. The program was broadened in scope to include the application of such instruments to fuel elements operating at high heat ratings and coolant power densities. It was successfully demonstrated that by the application of in-core instrumentation it is possible to reduce considerably the large conservative safety factors applied in present designs to preclude fuel element overheating. (auth)

6638 WATER CHEMISTRY RESEARCH AT HBWR. Rose, R. (OECD Halden Reactor Project, Norway). Atompraxis, 11: 532-6(Sept.-Oct. 1965).

Water chemistry experiments were carried out at the HBWR to study the influence of various reactor operating parameters such as power level, pressure, and subcooling on radiolytic gas formation, and to investigate the feasibility of suppressing the radiolysis by deuterium addition. An additional objective was to study the feasibility of maintaining a high pH in the steam and water by the addition of ammonia. The distribution of ^{16}N between steam and water was measured. Increased power, subcooling, and decreased pressure, i.e., conditions facilitating the transfer of gases to the steam, increased the heavy water decomposition. Radiolytic gas formation could be suppressed effectively by the addition of deuterium. The ammonia experiments showed that a high pH can be maintained in the steam and water and that the formation of nitrates can be prevented by keeping up the deuterium concentration in the moderator. The ^{16}N measurements showed that additions of deuterium and ammonia increase the ^{16}N fraction entering the steam phase. (auth)

6639 COOLANT PURIFICATION AND COOLANT CHEMISTRY FOR THE "DRAGON" HIGH TEMPERATURE GAS COOLED REACTOR. Roemberg, E.; Everett, M. R. (OECD High Temperature Reactor Project, Dorset, Eng.). Atompraxis, 11: 539-44(Sept.-Oct. 1965).

The coolant requirements for the Dragon Reactor Experiment are surveyed. The fission-product content of the coolant is limited from the safety point of view. Chemical impurities above certain levels lead to excessive graphite corrosion and carbon deposition reactions. Maximum permissible levels were specified for safe reactor operation. In order to control and maintain those levels a continuous stream of helium at a rate of 28.2 kg/hr is withdrawn from the reactor's primary circuit via channels inside the fuel elements. The purification process ensures that after purification the helium is non-active and chemically inert. (auth)

6640 DRAGON AND FUTURE GAS COOLED THERMAL REACTORS. Rennie, C. A. (OECD High Temperature Reactor Project, Dorset, Eng.). Atompraxis, 11: 544-6(Sept.-Oct. 1965).

The current status of high temperature reactors is reviewed, and the main features and advantages of this type of reactor are discussed. (auth)

6641 SPECIAL GRAPHITES FOR THE DRAGON REACTOR CORE. Graham, L. W.; Price, M. S. T. (OECD High Temperature Reactor Project, Dorset, Eng.). Atompraxis, 11: 549-54(Sept.-Oct. 1965).

Various methods of containing gaseous fission products in a high-temperature reactor were exploited in the Dragon project. For the first charge a graphite of extremely low permeability was developed for the fuel element. A special base stock was impregnated with a furan resin. Subsequent charges of fuel elements are being made from special graphites where the gaseous fission products are prevented from leaking into the primary circuit by an inward flow of helium through the pores of the graphite. The problems posed by the development of these graphites resulted in a considerably increased understanding of the structure of porous media. (auth)

6642 THE CONTAINMENT OF HELIUM IN THE PRIMARY CIRCUIT OF THE DRAGON REACTOR. Wade, F.; Woodley, H. J. (OECD High Temperature Reactor Project, Dorset, Eng.). Atompraxis, 11: 554-61(Sept.-Oct. 1965).

Due to the possibility of the Dragon reactor primary circuit containing radioactive gas and the fact that continual replacement of helium would be expensive, an unusually high standard of leak tightness was demanded. A considerable amount of work was carried out to determine the effectiveness of various types of sealing systems proposed for the reactor. It was decided that all large demountable joints such as those on the pressure vessel and heat exchangers should be made using flanges with concentric grooved sealing features and silver gaskets. Welding was used for pipe joints wherever possible. However, a limited number of small-bore pipe couplings were used. Most of the valves in the circuit use a plug and seat combination of a hard 90° plug in conjunction with a relatively soft sharp edged seat. There were two major leak tests during construction, one at room temperature and one at 220°C. During both tests the highest total leakage rate was in the order of 1×10^{-2} atmospheric cc/sec. This was mostly from one faulty cable penetration. Further tests after criticality revealed no significant change in the leak tightness of all flanges, welds, etc. (auth)

6643 PRESENT STATUS OF THE DEVELOPMENT OF FAST REACTORS IN FRANCE. An, Shigehiro; Nomoto, Shoji (Tokyo Univ.). Nippon Genshiryoku Gakkaishi., 7: 570-8(1965).

The present status of the development of fast reactors in France is described. The importance of the fast reactor program in the French electric power program, organization and management of the French fast reactor project, process of past development of the RAPSODIE and the main results of its mock-up test, and future fast reactor programs ("Filière Réacteurs Rapides") are discussed. Studies for a prototype reactor (PHENIX) and a 1,000-Mw(e) power reactor and experiments with the zero-power reactor MASURCA and the fast neutron source reactor HARMONIE are described. (auth)

6644 ECONOMIC POWER FROM GAS-COOLED REACTORS. Marsham, T. N.; Thorn, J. D. (United Kingdom Atomic Energy Authority, Windscale, Eng.). Nucleonics, 23: No. 11, 39-44(Nov. 1965).

The development of a fully economic design for the advanced gas-cooled reactor was achieved by retaining the many satisfactory design and operational features evolved during the first program. But the fuel was altered to stainless-steel clad, slightly enriched uranium oxide pellets, allowing much higher operating temperatures and greater output per unit volume of core and pressure vessel. Several new design improvements are discussed. The design philosophy and the optimizing of the station design are discussed including the effects of high temperatures, high power density, and fuel-cycle efficiency. The advanced gas-cooled reactor's economic prospects are also considered. Present generating costs will not exceed 5.25 mills/kwh, and will fall by at least 12% over the next few years for reactors in the 600-Mw(e) range. A further 10% reduction should be realized at double this output. (J.F.P.)

6645 REACTOR BUILDING /EGCR/ (Engineering Materials). (Oak Ridge Operations Office (AEC), Tenn.). (CAPE-974).

224 drawings.

The multistoried building housing the Experimental Gas Cooled Reactor (EGCR) is fabricated of reinforced concrete and structural steel. It is enclosed by a cylindrical steel plate containment shell 114 ft in dia with a hemispherical dome and a torospherical bottom head. The shell extends ~68 ft below grade level to 147 ft above grade level. The shell contains the reactor, biological shield and shield cooling equipment, 2 steam generators, 2 reactor coolant blowers and drives, reactor coolant piping, shafts for fuel loading and spent fuel discharge, charge and service machines, gas purification equipment, burst slug detection

equipment, and heating and ventilating equipment. The reactor building is serviced by a multipurpose passenger and freight elevator, an enclosed stairway, an emergency escape chute, bridgecrane, and air locks. Encircling the reactor containment shell just below grade level is space for experimenters' cells 24 ft wide, 15 ft deep, and 300 ft long. The 7,000 ft^2 area can be subdivided into eight pressure-tight compartments. (For details, see TID-4100). (M.C.G.)

6646 CHARGE MACHINE /EGCR/ (Engineering Materials). (Oak Ridge Operations Office (AEC), Tenn.). (CAPE–975).

91 drawings.

The charge machine, located beneath the reactor, is used for refueling and coolant-flow adjustment operations while the Experimental Gas Cooled Reactor (EGCR) is in operation. It consists of a shielded ram; fuel ram with flow orifice adjustment; fuel transfer tube; and a storage machine contained in a pressure vessel 36 ft 10 in. long, 8 ft 6 in. OD, and constructed of SA 212 Grade B alloy. The pressure vessel is designed for an operating temperature of 510°F and an operating pressure of 350 psi. The machine, supported on a crane for maneuvering to and from the reactor, is positioned to within $\frac{1}{32}$ in. by two transits. The equipment is remotely operated from a console in the charge and service machine control room located in the reactor containment shell. (For details, see TID-4100). (M.C.G.)

6647 HEAT EXTRACTION SYSTEM FOR A NUCLEAR REACTOR. Fortescue, Peter (to General Dynamics Corp.). U. S. Patent 3,210,254. Oct. 5, 1965. Filed Feb. 10, 1961.

A self-sustaining heat extraction system is described for use with gas cooled reactors. The system includes a concentric turbine-compressor unit having integrally connected turbine and compressor blades that effect the circulation of gas coolant through a closed system. The turbocirculator is efficient, free-running, and eliminates the need for external drive means. The system is not limited to use with nuclear reactors, but is applicable to any system having concentric ducting systems through which it is desirable to circulate a fluidized medium without the need of externally powered apparatus. (B.L.M.)

Process Heat Reactors

6648 (HPR–64) HBWR QUARTERLY PROGRESS REPORT, JULY–SEPTEMBER 1965. (Institutt for Atomenergi, Halden (Norway). OECD Halden Reaktor Prosjekt). Oct. 1965. 121p. Dep. mn.

Operations; reactor-dynamics and thermal-hydraulics studies; and the development of in-pile loops, tubular-fuel test sections, thermocouples, neutron and gamma detectors, fuel-elongation detectors, flowmeters, and analytical equipment for water chemistry for the Halden Boiling Reactor are described and outlined. (T.F.H.)

6649 METHOD OF CALCULATION OF WATER AND POWER COSTS FOR NUCLEAR DESALINATION PLANTS. Koryakin, Yu. I.; Loginov, A. A.; Chernyaev, V. A.; Zakharov, I. I. At. Energ. (USSR), 19: 138-43(Aug. 1965). (In Russia).

A method is given for determining the economic aspects of dual-purpose installations enabling an accurate separate estimate of the costs of power generation and fresh water production. The effect of the basic parameters of the installation on the cost of fresh water was analyzed. Economic indices are given for dual-purpose installations used with various types and various heat capacity reactors. (tr-auth)

6650 FRESH WATER BY NUCLEAR POWER. Kronberger, Hans. New Sci., 28: 31-3(Oct. 7, 1965).

Flash distillation, using steam from an AGR, as a method for desalination of sea water is discussed. An advanced gas-cooled reactor and multistage flash distillation plant designed to yield 400 Mw of electricity and 60 million gallons of fresh water daily is described. (M.C.G.)

6651 NUCLEAR REACTOR OPERATIONAL IN A WELL BORE. Natland, Manley L. (to Richfield Oil Corp.). U. S. Patent 3,214,343. Oct. 26, 1965. Filed Jan. 3, 1958.

A reactor of the fast type suitable for use in oil recovery methods and that can be activated and controlled from the earth's surface is patented. The reactor may be operated in either of the following ways: the reactor may be positioned adjacent to the oil bearing formation and the heat released as a result of the self-sustained reaction results in a lowering of the viscosity of the petroleum to render it more flowable either into the heated well or into an adjacent output well, or the reactor can provide a nuclear explosion to simultaneously create high temperatures in the oil bearing zone and to pressurize the formation. (B.L.M.)

Propulsion and Space

See also ENGINEERING — Space Propulsion

Refer also to abstract 6678.

6652 (D–910091-5) EXPERIMENTAL INVESTIGATION OF THE EFFECT OF PERIPHERAL-WALL INJECTION TECHNIQUE ON TURBULENCE IN AN AIR VORTEX TUBE. McFarlin, David J. (United Aircraft Corp., East Hartford, Conn. Research Labs.). Sept. 1965. Contract NASw-847. 48p.

Experiments were conducted to investigate the effect of the peripheral-wall injection technique used to drive an air vortex on the level of turbulence in the vortex. Two injection configurations were tested in separate 10-in.-dia vortex tubes. In both tubes, a controlled quantity of air was removed through ports located at the centers of the two end walls or was injected through a porous tube located on the centerline of the vortex; air was also removed through perforated plates in the peripheral wall. Hot-wire-anemometer measurements of tangential velocity profiles and root-mean-square velocity fluctuations were made near the peripheral wall at three circumferential stations at one axial location (the axial midplane). The results indicated that the interior region of low-turbulence flow was larger for a 2144-port configuration than for a single-slot configuration. (auth)

6653 (D–910091-7) EXPERIMENTAL INVESTIGATION OF PERIPHERAL-WALL INJECTION TECHNIQUES IN A WATER VORTEX TUBE. Travers, Arthur (United Aircraft Corp., East Hartford, Conn. Research Labs.). Sept. 1965. Contract NASw-847. 50p.

An experimental investigation was conducted to determine the effects of the peripheral-wall injection technique used to drive a water vortex on the structure and thickness of the turbulent mixing region near the peripheral wall and on the flow patterns in the primary-flow region outside the peripheral and end-wall boundary layers. Three 10-in.-dia lucite vortex tubes having three different peripheral-wall injection configurations were tested. In most tests, a controllable quantity of fluid was removed through one or more perforated screens in the peripheral wall and the remainder of the fluid was removed through 0.938-in.-dia thru-flow ports located at the centers of the two end walls. However, a few tests were conducted in which no fluid was removed through the thru-flow ports; instead, fluid was injected through a 1.0-in.-dia porous tube located along the centerline of the vortex tube. Microflash photographs of dye patterns were taken through one of the end walls to observe the characteristics of the turbulent mixing region, and time-exposure photographs of dye patterns were taken through the side wall to observe the characteristics of the primary-flow region. Tangential velocity profiles in the primary-flow region were obtained by means of a photographic particle-trace method using small, neutrally buoyant polystyrene spheres. The results indicate that the volume of low-turbulence flow in the primary-flow region was considerably larger for 2144-port injection configuration than for the single-slot and four-slot injection configurations. (auth)

6654 (IDO–17076) SAFETY ANALYSIS REPORT SNAPTRAN 2/10A-1 AND -2 SAFETY TESTS. Neal, W. J. (ed.) (Phillips Petroleum Co. Idaho Falls, Idaho. Atomic Energy Div.). Oct. 1965. Contract AT(10-1)-205. 159p. Dep. mn; CFSTI $5.00 cy, $1.00 mn.

The results of safety analyses performed on the SNAPTRAN 2/10A-1 and SNAPTRAN 2/10A-2 reactors are presented. These reactors will be utilized to experimentally investigate the transient power behavior of a SNAP 10A/2 reactor in both the nondestructive and destructive region. Also included are descriptions of the test program, the reactor test packages, and the test site and facilities. Calculations are presented to indicate the analytical techniques used to determine the transient behavior of the reactor for various reactivity additions and to determine the radiation doses to be expected for various conditions. The calculations show that an unplanned destructive excursion with an energy release of 220 Mw-sec yields a maximum off-site dose of 6.3×10^{-2} rem to a child's thyroid due to inhalation of the released fission products. From the results of the analysis, it was concluded that the SNAPTRAN 2/10A-1 and SNAPTRAN 2/10A-2 test programs can be carried out without undue hazard to the general public. (auth)

6655 (NAA-SR–7088) THE FINAL REPORT ON THE SNAP 2 EXPERIMENTAL REACTOR (SER) OPERATION AND TEST PROGRAM. Beall, J. P.; Hulin, M. W. (eds.) (Atomics International, Canoga Park, Calif.). Apr. 30, 1962. Contract AT-11-1-GEN-8. 74p. Dep. mn; CFSTI $3.00 cy, $0.75 mn.

The operating history of the SNAP 2 Experimental Reactor (SER) is presented from initial fuel loading until final disassembly and removal of fuel. The results of the testing program are also presented. The total energy generated during the life of the reactor was 224,650 kwh. This is equivalent to approximately 6 months of full-power operation. The methods used to obtain the reactor parameters are also described. The experimental data obtained were generally in excellent agreement with calculated values. The principal comparisons are tabulated. (auth)

6656 (NAA-SR-Memo–11333) CALIBRATION OF S10A RADIATION DETECTION SYSTEMS. Lowenson, J.; Chesavage, A. (Atomics International, Canoga Park, Calif.). May 19, 1965. Contract AT(11-1)-Gen-8. 36p. Dep. mn; CFSTI $2.00 cy, $0.50 mn.

The high level neutron and gamma systems were calibrated such that the calculated flux rates will result in a mid-scale reading. The same setting was intended for the low level neutron system, but during system calibration the output from two systems was consistently a factor of 4 low. The discrepancy is believed to be due to improper setting of the discriminator which was inaccessible for adjustment. It appears that the low level neutron system, as is, will provide usable data. From the calibration data of the four high level neutron systems the responses of the two HLNS's on FS-4 and FS-5 were calculated. (auth)

6657 (NAA-SR-Memo–11417) PERFORMANCE OF A THERMOELECTRIC CONVERTER WITH LEAKAGE CURRENT. Smith, A. K. (Atomics International, Canoga Park, Calif.). June 7, 1965. Contract AT(11-1)-Gen-8. 17p. Dep. mn; CFSTI $1.00 cy, $0.50 mn.

Expressions relating converter insulation resistance to converter internal resistance, load voltage, and leakage current are derived. Analysis of on line flight test data indicates that converter conductance was increasing at a linear and essentially constant rate of 2.04 millimhos per day subsequent to 651 hours after launch. The performance of the system was calculated on the basis of the following: converter insulation conductance continues to increase at a constant rate equal to that experienced to date and converter open circuit voltage and internal resistance data may be extrapolated on the basis of FS-3 system performance. (M.O.W.)

6658 (NAA-SR-Memo–11436) POST ASSEMBLY ELECTRICAL CHECKOUT OF 10FS-3 IN BUILDING 013. Klinkner, K. C. (Atomics International, Canoga Park, Calif.). June 11, 1965. Contract AT(11-1)-Gen-8. 90p. Dep. mn; CFSTI $3.00 cy, $0.75 mn.

The post-assembly electrical checkout of the SNAP 10A flight system 10FS-3 is reported. Test results, deviations, and recommendations are presented. (auth)

6659 (NAA-SR-Memo–11473) FISSION PRODUCT CROSS SECTIONS AS A FUNCTION OF EXPOSURE FOR USE WITH SIZZLE. Birney, K. R.; Simon, N. K. (Atomics International, Canoga Park, Calif.). June 11, 1965. Contract AT(11-1)-Gen-8. 16p. Dep. mn; CFSTI $1.00 cy, $0.50 mn.

A set of 16-energy-group fission-product cross sections suitable for use with the SIZZLE code is compiled. The cross sections represent the latest known data available in the open literature. Fission product reactivity worth is calculated for the SNAP 10A at 40 kwt years exposure. A value of –10.5 cents is determined for the reactivity worth, including axial distribution effects. Twenty-three-group microscopic cross sections are presented, which may be used to generate fission product cross sections for any assembly. (auth)

6660 (NAA-SR-Memo–11514) MATEDIR. A CODE TO CALCULATE THE DESIGN POINTS OF A MANNED, DIRECT-RADIATING, THERMOELECTRIC SYSTEM. Bramblett, Elizabeth L. (Atomics International, Canoga Park, Calif.). July 9, 1965. Contract AT(11-1)-Gen-8. 91p. Dep. mn; CFSTI $3.00 cy, $0.75 mn.

MATEDIR is written in FORTRAN II for use on the IBM 7090/7094 with the FORTRAN II Monitor FIB III. A twelve-parameter survey is conducted, and the minimal weight systems are both tabularized and described in detail. (M.O.W.)

6661 (NAA-SR-Memo–11603) FLIGHT-2. A DATA REDUCTION PROGRAM FOR SNAP 10A TRANSIENT FLIGHT TEST DATA. Hammond, E. J. (Atomics International, Canoga Park, Calif.). Aug. 26, 1965. Contract AT(11-1)-Gen-8. 44p. Dep. mn; CFSTI $2.00 cy, $0.50 mn.

FLIGHT-2 is a data reduction and analysis program for SNAP 10A transient FLIGHT test data. The purpose of the FLIGHT-2 computer code is to: permit rapid analysis and evaluation of the performance of the SNAP 10A system during its orbital flight and to facilitate reporting of the experimental results to project management. (auth)

6662 (NASA-TN-D–2951) WHEEL-FLOW GASEOUS-CORE REACTOR CONCEPT. Evvard, John C. (National Aeronautics and Space Administration, Cleveland, Ohio. Lewis Research Center). Nov. 1965. 12p. CFSTI $1.00 cy, $0.50 mn.

The wheel-flow gaseous-core reactor concept employs a cylindrical or toroidal core of hot fissioning uranium or plutonium fuel. This core is surrounded by a rotating annular region of propellant that enters and leaves the reactor tangentially. If the two flows rotate together as a wheel, no shear will occur at the interface between the propellant and the fuel. Hence, the fuel loss due to the mixing processes associated with shear would be minimized. Several reactor geometries employing or modifying the wheel-flow concept are suggested. These range from the basic cylindrical shape to toroidal geometries employing rotation about the jet axis to establish a radially outward centrifugal force. The stability problems in the flows and the possible use of magnetic fields and electric currents for damping of instabilities are briefly discussed. (auth)

6663 A TRANSPIRATION-COOLED NOZZLE AS APPLIED TO A GAS-CORE NUCLEAR PROPULSION SYSTEM. Kramer, E. L.; Gronich, S. (Douglas Aircraft Co., Inc., Santa Monica, Calif.). J. Spacecraft Rockets, 2: 345-53(May-June 1965).

The use of mass injection through a porous wall as a cooling technique for axisymmetric nozzles is investigated. The effect of homogeneous mass injection on the heat transfer in a turbulent, compressible boundary layer is analyzed, using an integral-momentum approach. Approximate formulations of the gaseous thermal radiative and recombination energy contributions are included in the

analysis. Coolant requirements are determined for a conical nozzle associated with a 10^6 lb-thrust gas-core system operating at a 300-atm chamber pressure. Hydrogen is assumed to be used for the propellant and coolant. Chamber temperatures range from 7500 to 20,000°R, and wall temperatures range from 2000 to 3000°R. The degradation of specific impulse, which is a result of expelling the coolant at a lower total temperature than that in the chamber, is found to be as high as 9% at 20,000°R for a wall temperature of 2000°R. (auth)

6664 INTERNAL VS EXTERNAL MOUNTING OF NUCLEAR POWERPLANTS FOR DEEP SUBMERSIBLES. Luchter, Stephen (Aerojet-General Nucleonics, San Ramon, Calif.). J. Spacecraft Rockets, 2: 992-4(Nov.-Dec. 1965).

The relative weights and volumes of external and internal power plants utilizing nuclear reactors as the energy source are evaluated. A gas-cooled closed Brayton cycle plant with a floodable fast reactor was chosen for the analysis. Expressions for the weight and volume of the plant components—reactor, recuperator, precooler, turbomachinery, and miscellaneous parts—are given in terms of power level and diameter. The weight and volume of the hull-mounted plant are found to be significantly greater than those of the pod-mounted plant, for the same power level. (M.J.T.)

Research and Test Reactors

Refer also to abstracts 5715 and 6257.

6665 (ANL-7105, pp 59-71) ADVANCED SYSTEMS RESEARCH AND DEVELOPMENT. (Argonne National Lab., Ill.).

Further developments in the AARR are reported. Brief discussions are presented on critical experiments, theoretical analyses of the critical facility reactors, heat transfer, fuel and material development, development of reactor components, and primary system and components. Brief discussions are presented on MHD and energy conversion systems. (M.O.W.)

6666 (ANL-7115, pp 68-77) ADVANCED SYSTEMS RESEARCH AND DEVELOPMENT. (Argonne National Lab., Ill.).

Brief discussions of research work during this period are presented for the AARR, very large fast breeder reactor for desalination, and two energy conversion systems. (M.O.W.)

6667 (BNL-9686) NUCLEAR REACTOR'S COOLING WATER IS CONSERVED BY RECHARGING AT 15 MGD/ACRE. Wichman, Sven H.; Ahlers, Gordon K. (Brookhaven National Lab., Upton, N. Y.). [nd]. Contract AT-30-2-GEN-16. 5p. Dep. mn; CFSTI $1.00 cy, $0.50 mn.

Elementary well water recycling method has cooled the Medical Research Reactor at BNL for five years without disturbing the natural groundwater balance. Frequent alternation of the twin recharge basins minimizes biological growth problems. Multiple safeguards eliminate groundwater contamination possibilities. The design and performance of the cooling system are discussed. (M.O.W.)

6668 (BNWL-149, pp 5-21) LIGHT MODERATOR REACTOR PHYSICS. (Battelle-Northwest, Richland, Wash. Pacific Northwest Lab.).

Summaries of several water moderated experiments with 1.8 wt % Pu–Al fuel in the PRCF are presented. In addition, abstracts of papers written on the PuO_2–UO_2 experiment in the EBWR and the HTLTR driver fuel design analysis are presented. (M.O.W.)

6669 (BNWL-149, pp 36-44) HIGH TEMPERATURE REACTOR PHYSICS. (Battelle-Northwest, Richland, Wash. Pacific Northwest Lab.).

Summaries of 2 papers on high temperature reactor physics are presented. The papers treat spherical and slab geometry solutions to a two-region boundary value problem giving temperature increase during an exponential power rise and neutron pulsing possibilities in HTLTR. (M.O.W.)

6670 (CEA-R-2864) ETUDE DE QUELQUES DISPOSITIFS DE RADIOPROTECTION EN SERVICE AUPRES DES PILES PISCINES. (A Study of Some Radioprotection Apparatuses Used Near Swimming-Pool Reactors). de Robien, Emmanuel; de Choudens, Henri; Delpuech, Jacques (Commissariat a l'Energie Atomique, Grenoble (France). Centre d'Etudes Nucleaires). Oct. 1965. 22p. Dep. mn.

Various problems of radioprotection concerning swimming-pool reactors in Grenoble are discussed. The liberations of radioactive iodine were measured with activated charcoal cartridges that surround a scintillator connected with a monocanal selector. Finally the control of reactor safety rod fall in case of a radioactive accident was secured by a chain whose detector is a chamber immersed in the swimming-pool, which offers in the particular case of the hot thickness swimming-pool reactor a double advantage: first it enables regulation of the hot thickness, second freedom of transistory radiations which appear in the reactor hall as the experimental apparatuses are taken out of the core. (M.O.W.)

6671 (CONF-650217, pp 1-10) FAST REACTORS—SINGLE PULSES. Wimett, Thomas (Los Alamos Scientific Lab., Univ. of California, N. Mex.).

A discussion is presented of the characteristics of several fast-burst reactors, with regard to their use as pulsed neutron sources. The problems involved in moderating the neutron pulses are noted. Design improvements for these reactors are considered. The reactors specifically considered include Fran, Super Kukla, Godiva, Godiva II, Molly-G, and HPRR. (T.F.H.)

6672 (CONF-650217, pp 25-35) FAST REACTORS REPETITIVELY PULSED BY MECHANICAL MEANS, SUCH AS MOTION OF FUELS (IBR) OR REFLECTOR (SORA). Kouts, Herbert (Brookhaven National Lab., Upton, N. Y.).

The design features and experimental usefulness of the IBR and SORA type concepts are outlined and compared. (T.F.H.)

6673 (DP-988) CONTROL OF THE DISSOLVED GASES IN THE MODERATOR OF THE HEAVY WATER COMPONENTS TEST REACTOR. Arnett, L. M.; Olson, H. P. (Du Pont de Nemours (E. I.) and Co., Aiken, S. C. Savannah River Lab.). Nov. 1965. Contract AT(07-2)-1. 31p. Dep. mn; CFSTI $2.00 cy, $0.50 mn.

Unexpected variations in the nuclear reactivity during the initial mode of hydraulic operation in the Heavy Water Components Test Reactor were traced to the appearance and disappearance of helium bubbles in the moderator. Three mechanisms, aspiration, entrainment, and supersaturation, were each identified, and mechanical and procedural modifications were installed to eliminate the void formation. The investigation of the mechanism for supersaturation of the moderator is of general interest because the problem could arise in other reactors that are pressurized with an inert gas. (auth)

6674 (KFK-332) DAS VERHALTEN SCHNELLER NULLEISTUNGSREAKTOREN BEI REAKTIVITAETSSTOERUNGEN. (The Behavior of Zero-Power Reactors in Reactivity Perturbations). Engelmann, P. (Kernforschungszentrum, Karlsruhe (West Germany). Institut fuer Angewandte Reaktorphysik). May 1965. 66p. Dep. mn.

Model calculations were made on the dynamic behavior of fast zero-power reactors of the SNEAK type. A brief description was given of the installation and the reactor system investigated. Fast and slow reactivity perturbations were treated. Results were summarized. (J.S.R.)

6675 (LFEN-26) TRES ANOS DE OPERACAO DO REACTOR PORTUGUES DE INVESTIGACAO. (Three Years of Operation of the Experimental Portuguese Reactor). Ramalho, Antonio Joaquim Goncalves (Laboratorio de Fisica e Engenharia Nucleares, Junta de Energia Nuclear, Sacavem (Portugal)). 1964. 13p. (CONF-640711-3). Dep. mn.

From 27th Portugo-Spanish Conference on Progress in Sciences, Bilbao, Spain.

A short description of the "Reactor Português de Investigação" (RPI) and its utilization is presented. The more relevant abnormalities that occurred in the installation are described together with a more detailed discussion of the tests performed on the control rods before and after its installation in the reactor. It is shown that the effect produced by the movement of some control rods in regions close to the lower limit is reversed and that this situation can be attributed to an insufficient compactness of the B_4C. (auth)

6676 (NAA-SR-11234) SUPPLEMENT TO SRE SAFETY ANALYSIS REPORT. A Plan for Use of a Fast-Reactor Fuel Test Section in the SRE. (Atomics International, Canoga Park, Calif.). May 3, 1965. Contract AT(11-1)-Gen-8. 78p. Dep. mn; CFSTI $3.00 cy, $0.75 mn.

Modifications in the Sodium Reactor Experiment (SRE) are described, consisting of the replacement of the central seven moderator elements by a fast-fuel test section. This test section is designed to provide a fast-flux trap in the center of the reactor, in order to make possible material testing in a representative fast-reactor environment. The possible effects of this test section on the safety and containment of SRE are evaluated. The SRE building and containment are described. SRE kinetics before and after test-section installation are calculated. Credible and "noncredible" accidents in the modified SRE are evaluated, along with their attendant containment requirements. Means for meeting these increased containment requirements and for environmental control are developed. (T.F.H.)

6677 (NAA-SR-11528) CAPABILITIES OF THE 1 Mw SHIELD TEST AND IRRADIATION REACTOR. Golliher, K. G.; Randen, K. G. (Atomics International, Canoga Park, Calif.). Nov. 10, 1965. Contract AT-11-1-GEN-8. 21p. Dep. mn; CFSTI $2.00 cy, $0.50 mn.

The plant facility and layout for STIR are outlined. STIR is designed to provide a flexible neutron and gamma source for experimental work on shield development, for irradiation-damage studies on electronics, and for the nuclear qualification testing of SNAP components. The irradiation capabilities of STIR are shown in graphic and tabular form. (T.F.H.)

6678 (NAA-SR-Memo-11374) POST-IRRADIATION EXAMINATION OF TREAT CAPSULES NO. 5 THROUGH 9. Miller, K. J. (Atomics International, Canoga Park, Calif.). May 11, 1965. Contract AT(11-1)-Gen-8. 25p. Dep. mn; CFSTI $1.00 cy, $0.50 mn.

Five TREAT (Transient Reactor Tests) capsules were designed to measure the diffusion coefficients of hydrogen in uranium-zirconium hydride fuel at high temperatures. A second objective was to examine the capsules after irradiation. The capsules, each of which contained a thin wafer of SNAP 10A fuel, were irradiated at approximately 1000 Mw for 40 to 50 millisecond duration. Visual examination, metallography, and fuel burnup analyses were performed on the fuel from the five capsules. The fuel was in powdered or granulated form after irradiation. Metallography indicated that the fuel irradiation temperatures were high enough to melt the fuel. The wide range in fuel grain sizes appeared to reflect different cooling rates of the fuel particles. (auth)

6679 (NP-15645) NEUTRON FLUENCE MEASUREMENTS FOR THE SECOND TEST AT THE PULSTAR REACTOR. De Pangher, J.; Pearson, E. B.; Smith, E. A. (Lockheed Missiles and Space Co., Palo Alto, Calif.). June 7, 1965. 17p.

Neutron fluence measurements were made at the Pulstar reactor, in a series of tests in support of irradiations made on circuit boards. Dosimetry with Ni foils was used, with an accuracy of 30%. No perturbation run was found to be necessary when only light well-spaced circuit boards are being irradiated. (auth)

6680 (ORNL-TM-1319) CAPSULE TEMPERATURE CONTROL BY He–N_2 GAS COMPOSITION IN A THIN ANNULUS. Abbatiello, A. A. (Oak Ridge National Lab., Tenn.). Nov. 15, 1965. Contract W-7405-eng-26. 15p. Dep. mn; CFSTI $1.00 cy, $0.50 mn.

Data obtained from the first set of 1300°F EGCR-ORR prototype diameter capsules (0.008 in. gas gap) were used to determine the relative effectiveness of parallel gas-metal heat conductive paths. To meet requirements for 1600°F capsules a 0.012 in. gas gap was specified using thermal conductivities of a He–N_2 gas mixture with an allowance for the metal path conductivity. Experimental data from this second set of ORR capsules confirmed the acceptability of the methods used. The He–N_2 conductivity range is adequate to compensate for momentary perturbations in thermal conductivities attributed to thermal separation in the gas mixture when changing its composition. A set of curves for He–N_2 gas mixture conductivities is included, and also the methods used to determine the gas gap required. (auth)

6681 (SGAE-PH-18/1965) VERGLEICH DER ABBRANDBESTIMMUNGEN MITTELS SONDENAKTIVIERUNG UND GAMMA-SPEKTROSKOPIE FUR EIN MTR-ELEMENT. (Comparison of Consumption Determination with Sound Activation and Gamma Spectroscopy for an MTR Element). Buba, L.; Hick, H.; Rumpold, K. (Oesterreichische Studiengesellschaft fuer Atomenergie G.m.b.H., Vienna). 1965. 48p. Dep. mn.

In December, 1963 a partial element of the ASTRA reactor with neutron probes was prepared and irradiated. Later the probes were removed, their activity measured, and the burnup of the elements were calculated. The element was then stored until December, 1964 and then the burnup was determined from a γ spectroscopic measurement with a semiconductor Compton spectrometer. The results of the two measurements were compared and discussed. (tr-auth)

6682 (SGAE-R-1/1965) MESSUNG DER ASTRA-UEBERTRAGUNGSFUNKTION. A. KONSTRUKTION EINES REAKTIVITAETSOSZILLATORS. B. VERSUCHSDURCHFUEHRUNG UND MESSRESULTATE. (Measurement of the ASTRA-Transfer Function. A. Construction of a Reactivity Scintillator. B. Testing and Measurement Results). Nedelik, A. (Oesterreichische Studiengesellschaft fuer Atomenergie G.m.b.H., Seibersdorf). 1965. 32p. Dep.

In the design of the reactivity scintillator the measurement methods used for the experimental determination of the frequency path in a reactor are described. The fundamentals of the construction are then discussed and the actual construction itself is given. The studies made on the measurement of the transfer function of the ASTRA were reported and the measurement results are shown graphically. (J.S.R.)

6683 R.I.T.M.O. REACTOR TO SUPPORT R.T.M. PROGRAM. Ovazza, Mario. Comit. Naz. Energia Nucl., Notiz., 11: 17-24(July 1965). (In Italian).

The R.I.T.M.O. reactor, a zero-power critical assembly designed to support the R.T.M. reactor, is described. The advantages of a critical system are discussed and a general description of the R.I.T.M.O. reactor is given. The support structure of the reactor, the fuel elements, the irradiation devices, the Be reflector, the control rods, and the rotating control cylinders are considered. The general characteristics of the reactor are tabulated. (J.S.R.)

6684 DISPERSION-TYPE FUEL ELEMENT FOR "EWA" REACTOR. Rutkowski, Wladyslaw; Szteke, Witold; Wieczorkowski, Mariusz. Nukleonika, 10: 503-12 (1965). (In Polish).

In connection with investigations on dispersion-type fuels for experimental and university reactors, the technology of EK-10 elements with UO_2–Mg dispersion cores was studied. Investigation and production data for these fuel rods are presented. (auth)

GENERAL AND MISCELLANEOUS

Refer also to abstracts 5811 and 5812.

6685 (COO–1198-296) ISOTOPIC EFFECTS IN THE LATTICE CONSTANT, THERMAL EXPANSION, AND ISOTHERMAL COMPRESSIBILITY OF NEON SINGLE CRYSTALS. Batchelder, David Neville (Illinois Univ., Urbana). July 1965. Contract AT(11-1)-1198. 118p. Dep. mn; CFSTI $4.00 cy, $0.75 mn.

Single crystals of natural neon and neon of isotopic mass 22 were grown by directional solidification from the liquid. The lattice constant and thermal expansion of these crystals were determined over the range 2.5 to 24.5°K with much greater accuracy than previously reported. The lattice constants extrapolated to 0°K were found to be 4.45453 kX for natural neon and 4.44676 kX for neon-22 with a possible error of ±0.00008 kX. The thermal expansion of neon-22 was slightly larger than that of natural neon crystals. Hydrostatic measurements of the isothermal compressibility of natural neon between 4.2 and 20°K gave an improved value of 0.90×10^{-10} cm^2 $dyne^{-1}$ at 4.2°K, and above 4.2°K, less accurate values which are the first to be reported. The accurate measurements were made possible by the construction of a single-crystal, back-reflection x-ray camera. Contrary to the traditional procedure of mounting the crystal on a small goniometer, the x-ray camera and source were mounted on a very large goniometer. The temperature and pressure of the crystals could then be controlled to ±0.01°K and ±0.5 psi respectively, with the x-ray camera external to the hostile environment (2.5 to 24.5°K and 0 to 120 psi). The results were used to obtain improved values of several thermodynamic functions for neon and neon-22. (P.C.H.)

6686 (NVO–98-12) BUOY DYNAMICS STUDY. Final Report. Byrne, John T. (National Marine Consultants, Anaheim, Calif.). Oct. 1965. Contract AT(26-1)-98. 45p. Dep. mn; CFSTI $2.00 cy, $0.75 mn.

A simple physical analogy, consisting of a spring-mass combination with viscous damping, was proposed for analysis of the motions of the Type I Buoy System. Confirmation of the adequacy and accuracy attainable with this approach was obtained by independent analysis of the data from DOT #2. The average value of the principal period of oscillations measured in these tests after installation varied from 11.5 to 12.5 seconds; the calculated value for the linearized analog falls between 11.8 and 12.4 seconds. The respective damping ratios are 0.041 (determined from the DOT #2) and 0.013 (calculation). The non-linearities due to viscous damping are quite apparent in the results of DOT #2. This is further explored in an analysis of the launching transient, where the vertical amplitudes of oscillation approached 24 feet. For this case, the natural period was about 12.6 seconds and the damping ratio had a value of 0.097. A re-linearization of the damping term in the analytical approach over the velocity range attained in the motion of 24 feet, yielded a value of 0.030, differing by a factor of 3 from that observed experimentally. It is noted, that for both large and small motions, the present analytical approach underestimates the damping ratio by this amount. (auth)

6687 (NYO–3453-1) DISPLACEMENT AND EXCHANGE REACTIONS INVOLVING ORGANOMETALLIC COMPOUNDS. Final Report. Kuivila, Henry G. (State Univ. of New York, Albany). Oct. 15, 1965. Contract AT(30-1)-3453. 18p. Dep. mn; CFSTI $1.00 cy, $0.50 mn.

A study of the protonolysis of allyltins was extended to include examination of kinetic isotope effects, determination of activation parameters, and the effects of metal ions on rate. The results on activation parameters indicated a very large compensation effect between enthalpies and entropies of activation. For the effects of substitution on tin the trend can be interpreted in terms of decreasing solvation with increased bulk of substituents on the tin atom accompanied by an increase in the enthalpy of activation in the same direction. Solvent kinetic isotope effects showed quite convincingly that the proton transfer occurs in the rate determining step of the reaction. Metal ion catalysis was found to compete less well with the protonolysis reaction than it does in the protodeboronation of areneboronic acids previously reported. (P.C.H.)

6688 (Y-DA–1014) EFFECTS OF TEMPERATURE ON MACHINING OPERATIONS. Smith, H. F. Jr. (Union Carbide Corp., Oak Ridge, Tenn. Y-12 Plant). Sept. 24, 1965. Contract W-7405-eng-26. 15p. Dep. mn; CFSTI $1.00 cy, $0.50 mn.

The results on a program to determine the effects of temperature on current production equipment indicated that inadequate attention is being given to this variable by many machine tool and gage manufacturers and users. Sources of temperature errors are discussed. (P.C.H.)

6689 (Y-KE–191) OPTICAL APPLICATIONS IN DIMENSIONAL GAGING. Whitten, L. G. (Union Carbide Corp., Oak Ridge, Tenn. Y-12 Plant). Sept. 15, 1965. Contract W-7405-eng-26. 19p. Dep. mn; CFSTI $1.00 cy, $0.50 mn.

The use of optics in the fields of length, straightness, and surface finish is discussed. Both advantages and disadvantages for optics are listed. However, it was concluded that the use of optics in these fields are unparalleled by any other method. (P.C.H.)

6690 (Y-NA–14) NEW DEVELOPMENTS IN CLOSE TOLERANCE MACHINING. Broome, F. H. (Union Carbide Corp., Oak Ridge, Tenn. Y-12 Plant). Sept. 14, 1965. Contract W-7405-eng-26. 10p. Dep. mn; CFSTI $1.00 cy, $0.50 mn.

Discussion is presented on: meaning of close-tolerance machining; use of the technique at Y-12, factors that affect the ability to machine and inspect to close tolerances; and developments obtained towards realizing a truly close-tolerance manufacturing capability. (P.C.H.)

6691 (JPRS–32985) TRANSLATIONS ON COMMUNIST CHINA'S SCIENCE AND TECHNOLOGY NO. 244. Translated from K'o Hsueh T'ung Pao, No. 6, 526-32(Dec. 1964); No. 10, 862-9; 923-5; 933-5(Oct. 1965). 51p. (TT-65-33562). CFSTI $3.00 cy, $0.50 mn.

Five articles are included; a separate abstract was prepared for one. The remaining 4 articles include information on: development of cybernetics; First National Meeting of Engineering Thermal Physics; formation of the second maximum in the cloud graph; and studies on organophosphorus compounds. (P.C.H.)

For an abstract of the individual paper see: 5304.

6692 HYDROSTATIC PRESS. Stisser, Eugene A. (to U. S. Atomic Energy Commission). U. S. Patent 3,219,736. Nov. 23, 1965.

A method is given for applying hydrostatic pressure to compress a body at a high temperature by rapidly cooling a molten metal encasing the body. The body is centrally located within a spherical shell filled with powdered metal which has a substantially greater coefficient of thermal expansion and a lower melting point than the body, and the assembly is heated to melt the powdered metal. The molten powdered metal is rapidly cooled over the entire periphery thereof producing a thermally contracting shell thereby subjecting the molten metal surrounding the body which is centrally located therein to intense compressive forces while this body is still at a very high temperature. (AEC)

6693 SWITCH ACTUATOR MECHANISM. Yerkovich, S. (to U. S. Atomic Energy Commission). U. S. Patent 3,219,776. Nov. 23, 1965.

An improved snap-action switch of simple, inexpensive design is described, which provides a substantially fool-

proof structure. The switch includes a plunger with a sleeve thereon which is normally held in a desired position by spring detent means. Spring biased contacts are associated with the sleeve so that when the plunger moves the sleeve past the detent on the spring means, a snap action or quick movement of the sleeve occurs instantly opening or closing the contacts, depending upon the direction of plunger movement. (AEC)

CORPORATE AUTHOR INDEX

This index contains entries for this period for all report literature and, in addition, for certain published literature items for which it is felt that a corporate approach is especially desirable, e.g., symposia, conference proceedings, and meetings.

Each entry under a corporate author is a shortened version of the title of the publication, followed by the NSA volume and abstract number. Report numbers are given in parentheses.

The phrase "Progress report" is abbreviated as "Prog. rpt.," permitting a more rapid and complete alphabetical arrangement of the titles without changing the location of the progress report titles in relation to the other titles.

A

ADVISORY GROUP FOR AERONAUTICAL RESEARCH AND DEVELOPMENT, PARIS (FRANCE).
Handbook on properties of niobium, molybdenum, tantalum, tungsten and some of their alloys, 20: 5874 (AGARDograph-94)

AIR FORCE CAMBRIDGE RESEARCH LABS., L. G. HANSCOM FIELD, MASS.
Study of vertically incident cosmic-ray trajectories using sixth-degree simulations of geomagnetic field, 20: 6005 (AD-623632)

AIR FORCE INST. OF TECH., WRIGHT-PATTERSON AFB, OHIO. SCHOOL OF ENGINEERING.
Radio frequency generated cylindrical plasma with alkali metal injection, 20: 6447 (AD-618693)

AKADEMIYA NAUK SSSR, NOVOSIBIRSK. INSTITUT YADERNOI FIZIKI.
Some selection rules for annihilation of polarized fermions, 20: 6040 (NP-15602)

AKADEMIYA NAUK UKRAINSKOI SSR, KHARKOV. FIZIKO-TEKHNICHESKII INSTITUT.
Applications of Moessbauer effect and perturbed angular correlation method in nuclear physics, 20: 6293 (NP-15603)
Evolutionary conditions of oblique and conical shock waves and of transonic flows, 20: 6160 (NP-15604)

AKTIEBOLAGET ATOMENERGI, STOCKHOLM (SWEDEN).
Agesta power heating plant, 20: 6599 (AES-5)
Experimental study of natural circulation in loop with parallel flow test sections, 20: 5620 (AE-200)
Mixed convection heat transfer on outside of vertical cylinder, 20: 5619 (AE-199)
Noise in nuclear reactor systems, 20: 6561 (FTI-2)

ALLISON DIV., GENERAL MOTORS CORP., INDIANAPOLIS, IND.
Shield small source experiments, 20: 6626 (UNC-5118)

AMES LAB., IOWA STATE UNIV. OF SCIENCE AND TECH.
Measurement of piezoresistance in semiconductors, 20: 5883 (IS-1268)

ARGONNE NATIONAL LAB., ILL.
Calorimetry, 20: 5523 (ANL-6925, pp 175-85)
Advanced systems research and development, 20: 6665 (ANL-7105, pp 59-71)
Advanced systems research and development, 20: 6666 (ANL-7115, pp 68-77)
Analytical research and development, 20: 5493 (ANL-6925, pp 253-4)
Catalog of nuclear reactor concepts. I., 20: 6554(ANL-7092)
Compact pyrochemical processes, 20: 5594 (ANL-6925, pp 21-106)
Energy conversion, 20: 6024 (ANL-6925, pp 235-47)
Fuel cycle applications of volatility and fluidization techniques, 20: 5595 (ANL-6925, pp 107-64)
General reactor technology, 20: 6556 (ANL-7105, pp 36-58)
General reactor technology, 20: 6558 (ANL-7115, pp 42-67)
High temperature reactor materials development, 20: 5875 (ANL-6925, pp 165-74)
Investigation of instabilities encountered during heat transfer to supercritical fluid, 20: 5622 (ANL-7032)
Liquid-metal-cooled reactors, 20: 6600 (ANL-7105, pp 1-35)
Liquid-metal-cooled reactors, 20: 6601 (ANL-7115, pp 1-41)
Molecular orbital density comparisons of H_2, Li_2, B_2, C_2, N_2, O_2, and F_2, 20: 5524 (ANL-7076)
Notes on axioms for quantum mechanics, 20: 6213 (ANL-7065)
Nuclear constants, 20: 6280 (ANL-6925, pp 249-51)
Nuclear safety, 20: 6559 (ANL-7115, pp 77-83)
Nuclear safety, 20: 6576 (ANL-7105, pp 72-84)
Phase studies on U–20 wt % Pu–Fs alloys, 20: 5876 (ANL-6974)
Prog. rpt. on chemical engineering, 7–12/64, 20: 5492 (ANL-6925)
Prog. rpt. on reactor development, 9/65, 20: 6555 (ANL-7105)
Prog. rpt. on reactor development, 10/65, 20: 6557 (ANL-7115)
Radiation damage, 20: 5569 (CONF-650217, pp 108-10)
Reactor safety, 20: 6552 (ANL-6925, pp 187-233)
Studies and evaluations, 20: 6553 (ANL-6925, pp 255-63)
Thermodynamic study of urania–uranium system, 20: 5877 (ANL-7048)

ARMY ELECTRONICS COMMAND, FORT MONMOUTH, N. J.
High-density plasmas, 20: 6449 (AD-619370)

ATOMENERGIKOMMISSIONEN, RISOE (DENMARK). FORSOEGSINSTITUT.
Attempt to detect microinstabilities in colliding plasmas, 20: 6465 (RISO-105)
Environmental radioactivity in Denmark in 1964, 20: 5651 (RISO-107)
Prog. rpt. on metallurgy, annual, 4/64–3/65, 20: 5838 (RISO-110)

ATOMIC ENERGY COMMISSION, WASHINGTON, D. C.
Conference on pulsed high intensity fission neutron sources, USAEC, Washington, 2/65, 20: 6256 (CONF-650217)
Fast reactors repetitively pulsed by mechanical means, such as motion of fuels (IBR) or reflector (SORA), 20: 6672 (CONF-650217, pp 25-35)
Fast reactors—single pulses, 20: 6671 (CONF-650217, pp 1-10)
Inelastic scattering with pulsed neutron sources, 20: 6258 (CONF-650217, pp 82-101)
PHERMEX—high current linac, 20: 5936 (CONF-650217, pp 77-81)
Radiation damage, 20: 5569 (CONF-650217, pp 108-10)
Some aspects of neutron diffraction and elastic scattering using pulsed and steady neutron sources, 20: 5726 (CONF-650217, pp 102-7)
Subcritical neutron amplifier systems, 20: 6257 (CONF-650217, pp 11-24)
Thermal neutron facility for LAMPF, 20: 5935 (CONF-650217, pp 73-6)
Use of polarized beams, 20: 6259 (CONF-650217, pp 111-23)

ATOMIC ENERGY ESTABLISHMENT, TROMBAY (INDIA). ANALYTICAL DIV.
Activation analysis through addition of "standard" and solvent extraction, 20: 5494 (AEET-217)

ATOMIC ENERGY ESTABLISHMENT, TROMBAY (INDIA). HEALTH PHYSICS DIV.
Measurements of radioactive fallout in individual rain showers at Bombay, 20: 5661 (AEET-215)

ATOMIC ENERGY ESTABLISHMENT, TROMBAY (INDIA). NUCLEAR PHYSICS DIV.
Nuclear data measuring facilities in India, 20: 5715 (AEET-227)

ATOMIC ENERGY ESTABLISHMENT, WINFRITH (ENGLAND).
Evaluation and compilation of data for U.K. Nuclear Data Library, 1/65, 20: 6254 (AEEW-M-503)
Irradiation testing of pulse fission chamber design, 20: 5807 (AEEW-M-493)
Neutron activation of titanium and its influence on ionization chamber design, 20: 5716 (AEEW-M-470)
Results of RCIO ionization chamber development, 20: 5717 (AEEW-M-508)
Stability of laminar flow of liquid between parallel planes, 20: 5621 (AEEW-R-416)

ATOMIC ENERGY OF CANADA LTD., CHALK RIVER (ONTARIO).

General purpose sub-assemblies, 20: 5680 (ELI-91)
Prog. rpt. on physics, 4–6/65, 20: 5928 (PR-P-66)

ATOMIC ENERGY RESEARCH ESTABLISHMENT, HARWELL (ENGLAND).
Low-voltage diffuse discharge in atmospheric-pressure helium with small additions of potassium, 20: 6159 (AERE-M-1597)
Multiple scattering in plane samples, 20: 6255 (AERE-R-5016)
n = 4 levels of N^V by electron impact, computed with Coulomb-Born approximation, 20: 5982 (AERE-R-5061)

ATOMICS INTERNATIONAL, CANOGA PARK, CALIF.
Analysis of process control in SGR 200 Mwe prototype plant, 20: 6617 (NAA-SR-Memo-11339)
Calibration of S10A radiation detection systems, 20: 6656 (NAA-SR-Memo-11333)
Capabilities of 1 Mw shield test and irradiation reactor, 20: 6677 (NAA-SR-11528)
Evaluation of inclusions found by radiographic inspection in sap tubing, 20: 5630 (NAA-SR-Memo-11562)
Fission product cross sections as function of exposure for use with ZIZZLE, 20: 6659 (NAA-SR-Memo-11473)
FLIGHT-2. A data reduction program for SNAP 10A transient flight test data, 20: 6661 (NAA-SR-Memo-11603)
Large SGR calandria vessel stayed head study, 20: 6616 (NAA-SR-Memo-11324)
Large SGR calandria vessel peripheral hanger test, 20: 6618 (NAA-SR-Memo-11415)
Large SRG process tube-graphite log structural interaction study, 20: 6619 (NAA-SR-Memo-11416)
MATEDIR. Code to calculate design points of manned, direct-radiating, thermoelectric system, 20: 6660 (NAA-SR-Memo-11514)
Measurements of thermal utilization (f) and δ^{25} in SGR uranium monocarbide lattices, 20: 6586 (NAA-SR-Memo-11313)
NAA program description. CAVORT, 20: 6562 (NAA-SR-Memo-11369)
OPEX shield optimization code, 20: 6518 (NAA-SR-Memo-11516)
Performance of thermoelectric converter with leakage current, 20: 6657 (NAA-SR-Memo-11417)
Plan for use of fast-reactor fuel test section in SRE, 20: 6676 (NAA-SR-11234)
Post assembly electrical checkout of 10FS-3 in building 013, 20: 6658 (NAA-SR-Memo-11436)
Post-irradiation examination of TREAT capsules No. 5 through 9, 20: 6678 (NAA-SR-Memo-11374)
Prog. rpt. on W resonance integrals and Doppler coefficients, 7–9/65, 20: 6279 (AI-65-225)
Recommendations for standardization and improvement of PHA procedures at PNPF, 20: 6615 (NAA-SR-10888(Rev.))
Reliability test of an SRE-PEP moderator element, 20: 6621 (NAA-SR-Memo-11556)
SCAP—in IBM 7094 code for spectral analysis of pulsed-neutron decay data, 20: 6585 (NAA-SR-Memo-10941)
SGR temperature transients, 20: 6620 (NAA-SR-Memo-11453)
SNAP 2 Experimental Reactor (SER) operation and test program, 20: 6655 (NAA-SR-7038)
TRIX-1 code, improved analytic calculation of resonance integrals, 20: 6291 (NAA-SR-Memo-11538)

AUSTRALIAN ATOMIC ENERGY COMMISSION RESEARCH ESTABLISHMENT, LUCAS HEIGHTS.
Expansion of a function in terms of Chebyshev polynomials using the IBM 7040, 20: 5828 (AAEC/TM-293)

B

BABES-BOLYAI UNIV., CLUJ (ROMANIA).
Utilization of tracers and of intense radiation sources in chemical research, 20: 5590 (NP-15543, pp 5-26)

BATTELLE MEMORIAL INST., COLUMBUS, OHIO.
Prog. rpt. on analytical description of nuclear-reactor accident, 7–9/65, 20: 6560 (BMI-X-10145)
Tungsten powder metallurgy, 20: 5836 (NASA-SP-5035)

BATTELLE MEMORIAL INST., GENEVA (SWITZERLAND).
Prog. rpt. on mechanical properties of metals subjected to mechanical stress at elevated temperature and neutron irradiation, 3/65, 20: 5880 (EURAEC-1310)
Prog. rpt. on mechanical properties of metals subjected to mechanical stress and neutron irradiation, 10/65, 20: 5913 (EURAEC-1488)

BATTELLE-NORTHWEST, RICHLAND, WASH. PACIFIC NORTHWEST LAB.
Critical mass physics, 20: 6579 (BNWL-149, pp 49-56)
Engineering physics, 20: 6577 (BNWL-149, pp 22-35)
Fast reactor safety considerations related to fuel macrostructure, 20: 6602 (BNWL-SA-346)
Gamma radiation dosimetry of ^{137}Cs in sheep evaluated with thermoluminescent dosimeters, 20: 5285 (BNWL-SA-172)
Heavy moderator reactor physics, 20: 6578 (BNWL-149, pp 45-7)
High temperature reactor physics, 20: 6669 (BNWL-149, pp 36-44)
High temperature creep machine for in-cell operation, 20: 5611 (BNWL-137)
Light moderator reactor physics, 20: 6668 (BNWL-149, pp 5-21)
Prog. rpt. on physics research, 4–6/65, 20: 5923 (BNWL-149)

BEERS (ROLAND F.), INC., ALEXANDRIA, VA.
Studies of properties of the equation of state for solids, 20: 6533 (NYO-1163-60)

BETTIS ATOMIC POWER LAB., PITTSBURGH, PA.
Angular values between crystallographic planes in zirconium as used in transmission electron microscopy, 20: 5898 (WAPD-TM-519)
Computer control and data processing for isotopic mass spectrometers, 20: 5684 (WAPD-T-1770)
Transport synthesis, 20: 6264 (WAPD-T-1849)

BETTIS ATOMIC POWER LAB., WEST MIFFLIN, PA.
Container leak rate test, PWR reactor plant, 20: 6628 (WAPD-PWR-TE-201)
Evaluation of core thermal data, PWR Core 1 Seed 3 second half seed life, Part A, 20: 6627 (WAPD-PWR-TE-141)

BROOKHAVEN NATIONAL LAB., UPTON, N. Y.
Alternating gradient synchrotron conversion summary, 20: 5932 (BNL-9662)
Chemical considerations in fast reactor safety, 20: 5878 (BNL-9667)
Fast reactors repetitively pulsed by mechanical means, such as motion of fuels (IBR) or reflector (SORA), 20: 6672 (CONF-650217, pp 25-35)
Genetic recombination in pneumococcus, 20: 5229 (BNL-9407)
Hyperon nonleptonic decays, 20: 6032 (BNL-9666)
$K^0_2 \rightarrow \pi^+ \pi^- \pi^0$ decay, 20: 6031 (BNL-9613)
Multiturn beam extraction in AG synchrotrons, 20: 5931 (BNL-9352)
Nuclear reactor's cooling water is conserved by recharging at 15 mgd/acre, 20: 6667 (BNL-9686)
Possibility of chemonuclear reactors producing ozone for water treatment, 20: 5568 (BNL-9664)
Strong interactions at high energy, 20: 6101 (BNL-9652)
Use of polarized beams, 20: 6259 (CONF-650217, pp 111-23)
Use of vidicons in on-line measuring machines at BNL, 20: 5718 (BNL-9634)

BROWN UNIV., PROVIDENCE, R. I. DIV. OF ENGINEERING.
Reflection of electromagnetic waves from inhomogeneous plasma, 20: 6445 (AD-617619)

BRUSSELS UNIV. (BELGIUM).
Contribution to study of heavy hypernuclei, 20: 6294 (NP-15617)

C

CALIFORNIA INST. OF TECH., PASADENA. W. M. KECK LAB. OF ENGINEERING MATERIALS.
Energy level diagrams of oxides of magnesium, aluminum and silicon, 20: 6532 (CALT-221-13)

CALIFORNIA UNIV., BERKELEY.
Proposed balloon borne system for interactions above 10^{11} ev, 20: 5724 (CONF-640919, pp II13-23)

CALIFORNIA UNIV., LOS ANGELES. DEPT. OF PHYSICS.
Polarization of 45 Mev protons by complex nuclei, 20: 6274 (AD-619061)

CALIFORNIA UNIV., LOS ANGELES. LAB OF NUCLEAR MEDICINE AND RADIATION BIOLOGY.
FORTRAN IV program for evaluation of post-irradiation survival times, 20: 5300 (UCLA-12-573)

CASE INST. OF TECH., CLEVELAND, OHIO.
Conference on interaction between cosmic rays and high energy physics, Case Inst. of Tech., Cleveland, Ohio, 9/64, 20: 6006 (CONF-640919)
Cosmic ray fluxes and possible experiments, 20: 6009 (CONF-640919, pp III-13)
Cosmic ray muon interactions at 5–50 Bev, 20: 6007 (CONF-640919, pp 143-8)
Experiment to detect basic triplets, 20: 6010 (CONF-640919, pp II23-7)
Gamma-ray induced showers, 20: 6013 (CONF-640919, pp IV17-33)
Magnetic cloud chamber system to study interactions up to 10^{12} ev, 20: 5722 (CONF-640919, pp I2-43)
Neutrino and muon measurements 10,000 ft. underground, 20: 6008 (CONF-640919, pp I48-54)
Prog. rpt. on hydromagnetic shocks, final, 4/15/60–10/31/64, 20: 6158 (AD-619999)
Proposed balloon borne system for interactions above 10^{11} ev, 20: 5724 (CONF-640919, pp II13-23)
Proposed system to study interactions at 300 Bev, 20: 5725 (CONF-640919, pp II27-30)
Proposed 600 m^3 detector for muons and neutrinos, 20: 5723 (CONF-640919, pp I55-65)
Relevance of cosmic ray experiments to astrophysics, 20: 6012 (CONF-640919, pp III1-23)
Theorist's comments, 20: 6011 (CONF-640919, pp II30-3)

CENTRALNE LABORATORIUM OCHRONY RADIOLOGICZNEJ, WARSAW

(POLAND).
Silicon surface-barrier detectors for alpha radiation dosimetry, 20: 5721 (CLOR/IBJ-II-37/D)
CENTRE D'ETUDE DE L'ENERGIE NUCLEAIRE, BRUSSELS (BELGIUM).
Prog. rpt. on in-pile corrosion of nuclear materials, final, 3/1/62–3/31/64, 20: 5852 (EURAEC-1522)
CENTRE D'ETUDE DE L'ENERGIE NUCLEAIRE, MOL (BELGIUM).
Prog. rpt. on in-pile corrosion of nuclear materials, final, 3/1/62–3/31/64, 20: 5852 (EURAEC-1522)
Prog. rpt. on physical properties of UO_2 single crystals, 11/64–3/65, 20: 5882 (EURAEC-1454)
CENTRE NATIONAL DE RECHERCHES METALLURGIQUES, LIEGE (BELGIUM).
Prog. rpt. on embrittlement by plastic fatigue in reactor vessels, 4–6/65, 20: 5881 (EURAEC-1441)
CENTRE NATIONAL D'ETUDES DES TELECOMMUNICATIONS (FRANCE).
Study of VLF radiation by use of Nike-Cajun rocket, 20: 6180 (AD-619250)
CENTRO INFORMAZIONI STUDI ESPERIENZE, MILAN (ITALY).
Large scale experiments on heat transfer and hydrodynamics with steam-water mixtures, 20: 5623 (EURAEC-1325)
Prog. rpt. on application of steam-water spray to reactor cooling, final, 12/61–8/64, 20: 6566 (EURAEC-1382)
CHICAGO UNIV., ILL.
Magnetic cloud chamber system to study interactions up to 10^{12} ev, 20: 5722 (CONF-640919, pp I2-43)
CLEARINGHOUSE FOR FEDERAL SCIENTIFIC AND TECHNICAL INFORMATION, SPRINGFIELD, VA.
Bibliography on Be, 20: 5840 (SB-413(Suppl.1))
CLEREMONT-FERRAND UNIV. (FRANCE). FACULTE DES SCIENCES.
Cherenkov telescope for study of cosmic radiation measurements at ground level, 20: 6014 (NP-15380)
COLORADO STATE UNIV., FORT COLLINS.
Behavior of jet streams in potential fallout situations, 20: 5644 (COO-1340-2, pp 110-21)
Case study of mass transport from stratosphere to troposphere, not associated with surface fallout, 20: 5649 (COO-1340-2, pp 54-83)
Development of computer programs for computation of Montgomery stream functions and plotting of thermodynamic diagrams, 20: 5645 (COO-1340-2, pp 122-45)
Heavy ^{131}I fallout over midwestern United States, May 1962, 20: 5648 (COO-1340-2, pp 1-53)
Prog. rpt. on radioactive fallout, 9/65, 20: 5647 (COO-1340-2)
Relation of tropopause-level index changes to radioactive fallout fluctuations, 20: 5650 (COO-1340-2, pp 84-109)
COLORADO UNIV., BOULDER.
Prog. rpt. on system for solar flare prediction, semiannual, 1/6/65, 20: 5967 (AD-619740)
COLORADO UNIV., BOULDER. DEPT. OF PHYSICS.
Quantum mechanics of $(p\text{-}\mu\text{-}p)^+$ molecular ion, 20: 5980 (AD-617522)
COLUMBIA UNIV., NEW YORK.
Experiment to detect basic triplets, 20: 6010 (CONF-640919, pp II23-7)
COLUMBIA UNIV., NEW YORK. PLASMA LAB.
Magnetohydrodynamics of oscillating dielectric sphere, 20: 6161 (NP-15630)
COLUMBIA UNIV., NEW YORK. RADIOLOGICAL RESEARCH LAB.
Mouse phantom depth dose studies, 20: 5286 (CONF-650616-16)
COMBUSTION ENGINEERING, INC., WINDSOR, CONN. NUCLEAR DIV.
Prog. rpt. on in-pile thermal conductance testing, 7–9/65, 20: 6565 (CEND-3336-251)
COMISSAO NACIONAL DE ENERGIA NUCLEAR DE BRASIL, RIO DE JANEIRO.
Reconnaissance for uranium in northeast coastal Brazil, 20: 5659 (RME-4545(Rev.))
COMISION NACIONAL DE INVESTIGACIONES ESPACIALES, BUENOS AIRES (ARGENTINA).
Motion of charged particles in static magnetic fields, 20: 6459 (CNIE-PE-1)
COMMISSARIAT A L'ENERGIE ATOMIQUE, CADARACHE (FRANCE). CENTRE D'ETUDES NUCLEAIRES.
Neutron density decay constant in nonmultiplying lattice of finite size, 20: 6580 (CEA-R-2702)
COMMISSARIAT A L'ENERGIE ATOMIQUE, FONTENAY-AUX-ROSES (FRANCE). CENTRE D'ETUDES NUCLEAIRES.
Recording of fission fragments occurring in insulators, 20: 5719 (CEA-R-2846)
COMMISSARIAT A L'ENERGIE ATOMIQUE, GRENOBLE (FRANCE). CENTRE D'ETUDES NUCLEAIRES.
Contribution to study of (d,p) and (d,α) reactions on ^{16}O and ^{11}B from 200 kev to 1 Mev, 20: 6281 (CEA-R-2807)
Study of some radioprotection apparatuses used near swimming-pool reactors, 20: 6670 (CEA-R-2864)
COMMISSARIAT A L'ENERGIE ATOMIQUE, SACLAY (FRANCE).
CENTRE D'ETUDES NUCLEAIRES.
Calculations of ψ, ϕ, and of their derivatives, 20: 5829 (CEA-R-2824)
Monte Carlo method—codes for the study of criticality problems (on IBM 7094), 20: 6581 (CEA-R-2872)
Study of hyperon-antihyperon production in antiproton-proton collision at 4 Bev/c, 20: 6033 (CEA-R-2798)
Study of parameters of light-water reactors. I., II., III., 20: 6582 (EUR-2461.f)
COMPAGNIE FRANCAISE THOMSON-HOUSTON, PARIS.
Prog. rpt. on application of vapotron effect on boiling light water reactors, 10–12/64, 20: 6595 (EURAEC-1421)
CONESCO, CAMBRIDGE, MASS.
Barrier attenuation introduced by vertical wall, 20: 6516 (AD-617524)
CONNECTICUT YANKEE ATOMIC POWER CO., HADDAM.
Use of hydraulic models in nuclear reactor design, 20: 6622 (NYO-3250-2)
CORNELL AERONAUTICAL LAB., INC., BUFFALO, N. Y.
Prog. rpt. on Project Aurora III, final, 2/12/62–6/15/65. I. and II., 20: 6182 (AD-619447)
CULHAM LAB., UNITED KINGDOM ATOMIC ENERGY AUTHORITY, ABINGDON (ENGLAND).
Effect of finite temperature on electron cyclotron resonance instability, 20: 6458 (CLM-R-44)

D

DEUTSCHES ELEKTRONEN-SYNCHROTRON, HAMBURG (WEST GERMANY).
Photoproduction of pion and nucleon resonances at energies up to 5.5 Bev, 20: 6037 (DESY-65/11)
DIVISION OF BIOLOGY AND MEDICINE (AEC), WASHINGTON, D. C.
Freshwater research, 20: 5245 (TID-13358(2nd Rev.), pp 89-126)
Offsite ecological research, 20: 5243 (TID-13358(2nd Rev.))
Terrestrial research, 20: 5244 (TID-13358(2nd Rev.), pp 3-88)
DIVISION OF BIOLOGY AND MEDICINE (AEC). WASHINGTON, D. C. FALLOUT STUDIES BRANCH.
Natural environmental radioactivity, 20: 5668 (WASH-1061)
DIVISION OF RAW MATERIALS (AEC), WASHINGTON, D. C.
Reconnaissance for uranium in northeast coastal Brazil, 20: 5659 (RME-4545(Rev.))
DIVISION OF REACTOR DEVELOPMENT (AEC), WASHINGTON, D. C.
Conference on pulsed high intensity fission neutron sources, USAEC, Washington, 2/65, 20: 6256 (CONF-650217)
Fast reactors repetitively pulsed by mechanical means, such as motion of fuels (IBR) or reflector (SORA), 20: 6672 (CONF-650217, pp 25-35)
Fast reactors—single pulses, 20: 6671 (CONF-650217, pp 1-10)
Inelastic scattering with pulsed neutron sources, 20: 6258 (CONF-650217, pp 82-101)
PHERMEX—high current linac, 20: 5936 (CONF-650217, pp 77-81)
Radiation damage, 20: 5569 (CONF-650217, pp 108-10)
Some aspects of neutron diffraction and elastic scattering using pulsed and steady neutron sources, 20: 5726 (CONF-650217, pp 102-7)
Subcritical neutron amplifier systems, 20: 6257 (CONF-650217, pp 11-24)
Thermal neutron facility for LAMPF, 20: 5935 (CONF-650217, pp 73-6)
Use of polarized beams, 20: 6259 (CONF-650217, pp 111-23)
DIVISION OF RESEARCH (AEC), WASHINGTON, D. C.
Conference on pulsed high intensity fission neutron sources, USAEC, Washington, 2/65, 20: 6256 (CONF-650217)
Fast reactors repetitively pulsed by mechanical means, such as motion of fuels (IBR) or reflector (SORA), 20: 6672 (CONF-650217, pp 25-35)
Fast reactors—single pulses, 20: 6671 (CONF-650217, pp 1-10)
Inelastic scattering with pulsed neutron sources, 20: 6258 (CONF-650217, pp 82-101)
PHERMEX—high current linac, 20: 5936 (CONF-650217, pp 77-81)
Radiation damage, 20: 5569 (CONF-650217, pp 108-10)
Some aspects of neutron diffraction and elastic scattering using pulsed and steady neutron sources, 20: 5726 (CONF-650217, pp 102-7)
Subcritical neutron amplifier systems, 20: 6257 (CONF-650217, pp 11-24)
Thermal neutron facility for LAMPF, 20: 5935 (CONF-650217, pp 73-6)
Use of polarized beams, 20: 6259 (CONF-650217, pp 111-23)
DIVISION OF TECHNICAL INFORMATION EXTENSION, (AEC), OAK RIDGE, TENN.
Bibliography on reactor safety, 20: 6563 (TID-3525(Rev.5) (Suppl.2))
Engineering materials list, 11/65, 20: 5608 (TID-4102(1st Rev.))
DU PONT DE NEMOURS (E. I.) & CO., AIKEN, S. C. SAVANNAH RIVER LAB.
Automated analysis of lithium solutions, 20: 5496 (DP-985)
Control of dissolved gases in moderator of heavy water components test reactor, 20: 6673 (DP-988)
Isolating americium and curium from $Al(NO_3)_3$–$NaNO_3$–HNO_3 solutions

by batch extraction with tributyl phosphate, 20: 5495 (DP-972)
Production of transplutonium elements at Savannah River, 20: 5822 (DP-1000)

E

ENGLISH STEEL CORP. LTD., SHEFFIELD (ENGLAND). GROUP RESEARCH LABS.
Prog. rpt. on Garigliano nuclear power plant operation, 9/30/65, 20: 6625 (TID-22434)
ENTE NAZIONALE PER L'ENERGIA ELETTRICA, ROME (ITALY).
Prog. rpt. on Garigliano nuclear power plant, 6/30/65, 20: 6623 (TID-22206)
EUROPEAN ATOMIC ENERGY COMMUNITY.
Linear inequalities on total ordered linear integer ring, 20: 5831 (EUR-1919.f)
Study of parameters of light-water reactors. I., II., III., 20: 6582 (EUR-2461.f)
EUROPEAN ATOMIC ENERGY COMMUNITY, ISPRA (ITALY). EUROPEAN SCIENTIFIC DATA PROCESSING CENTER.
Linear inequalities on total ordered linear integer ring, 20: 5831 (EUR-1919.f)
EUROPEAN ATOMIC ENERGY COMMUNITY, ISPRA (ITALY). JOINT NUCLEAR RESEARCH CENTER.
Linear inequalities on total ordered linear integer ring, 20: 5831 (EUR-1919.f)
EUROPEAN ORGANIZATION FOR NUCLEAR RESEARCH, GENEVA (SWITZERLAND).
Conference on 1964 CERN Easter School, Yugoslavia, 5/64, 20: 6034 (CERN-64-13(Vol.4))
Disc-loaded deflecting waveguide-computations, 20: 5934 (CERN-65-37)
Estimate of induced radioactivity in accelerators, 20: 5933 (CERN-65-34)
High-energy neutrino interactions, 20: 6036 (CERN-64-13(Vol.4), pp 51-95)
Hypernuclei, 20: 6283 (CERN-64-13(Vol.4), pp 137-86)
Liouville theorem and general problem of stability, 20: 5830 (CERN-65-38)
Magnetic moment experiments, 20: 6282 (CERN-64-13(Vol.4), pp 97-136)
Sonic spark chamber system, 20: 5720 (CERN-65-33)
Weak interactions of strange particles, 20: 6035 (CERN-64-13(Vol.4), pp 1-49)

F

FLORIDA UNIV., GAINESVILLE. ENGINEERING AND INDUSTRIAL EXPERIMENT STATION.
Alloys in Nb–Al–Ti system, 20: 5896 (TID-22388)

G

GENERAL ATOMIC, SAN DIEGO, CALIF. JOHN JAY HOPKINS LAB. FOR PURE AND APPLIED SCIENCE.
Collisional interchange instabilities in shear and $\int d\ell/B$ stabilized systems, 20: 6461 (GA-6646)
General atomic toroidal multipole confinement experiment, 20: 6460 (GA-6594)
Kinetic theory of particles and waves, 20: 6462 (GA-6650)
Optimization status report, 20: 6605 (GAMD-6673)
Prog. rpt. on advanced BeO concepts, 1–3/63, 20: 6603 (GA-4165)
Prog. rpt. on EBOR program, 7–9/64, 20: 6604 (GA-5842)
STMGEN—computer code for design of steam generator, 20: 5606 (GAMD-6675)
STMGEN—computer code for design of steam generator, 20: 5607 (GAMD-6675(Suppl.))
GENERAL ELECTRIC CO., CINCINNATI, OHIO. AIRCRAFT NUCLEAR PROPULSION DEPT.
Alloys in Nb–Al–Ti system, 20: 5896 (TID-22388)
GENERAL ELECTRIC CO., CINCINNATI, OHIO. NUCLEAR MATERIALS AND PROPULSION OPERATION.
Operating instructions for FORTRAN IV version of program gamma-p (NMP 468), 20: 6284 (GEMP-392)
GENERAL ELECTRIC CO., PHILADELPHIA, PA. MISSILE AND SPACE DIV.
Fundamentals of MHD flow, 20: 6156 (AD-617562)
Nonequilibrium radiation, 20: 6443 (AD-617383)
Solar flare hazards: predictability, 20: 5966 (AD-618905)
Thermal integration of electrical power and life support systems for manned space stations, 20: 5820 (NASA-CR-316)
GENERAL ELECTRIC CO., PLEASANTON, CALIF. SPECIAL PURPOSE NUCLEAR SYSTEMS OPERATION.
Prog. rpt. on testing of cylindrical diodes and irradiation of fuel and insulators, 12/18/64–3/17/65, 20: 6596 (GEST-2049)
Prog. rpt. on thermionic conversion of heat to electricity, 3/64–6/65, 20: 6023 (AD-619379)
GENERAL ELECTRIC CO., RICHLAND, WASH. HANFORD ATOMIC PRODUCTS OPERATION.
Effect of early introduction of breeder reactors on uranium resource conservation, 20: 6611 (HW-SA-3669)
Fuel conservation indexes for thermal reactors, 20: 6610 (HW-79287)
Prog. rpt. on continuous electrowinning of Pu metal, 4/65, 20: 5839 (RL-SEP-244(Del.))
Technique for optimizing composition of regenerating neutron flux monitors, 20: 6567 (HW-SA-3600)
GENERAL ELECTRIC CO., SAN JOSE, CALIF. ATOMIC POWER EQUIPMENT DEPT.
Prog. rpt. on high performance UO_2 program, 4–6/65, 20: 5914 (GEAP-3771-17)
Prog. rpt. on Garigliano Nuclear Reactor, 10/65, 20: 6606 (GEAP-4962)
Prog. rpt. on Pu subcritical experiment program, 7–9/65, 20: 6607 (GEAP-4965)
GEOLOGICAL SURVEY, WASHINGTON, D. C.
Perched groundwater in zeolitized-bedded tuff, Rainier Mesa and vicinity, Nevada Test Site, Nevada, 20: 5643 (TEI-862)
GHENT RIJKSUNIVERSITEIT (BELGIUM).
Prog. rpt. on stainless steel plating of very thick steels, 4–6/65, 20: 5862 (EURAEC-1481)
GORDON MCKAY LAB. OF APPLIED SCIENCE, HARVARD UNIV., CAMBRIDGE, MASS.
Prog. rpt. on interaction of solid metal and liquid alloys, final, 9/65, 20: 5895 (TID-22271)
GOSUDARSTVENNYI KOMITET PO ISPOL'ZOVANIYU ATOMNOI ENERGII SSSR, MOSCOW. INSTITUT TEORETICHESKOI I EKSPERIMENTAL'NOI FIZIKI.
At what distances does interaction at high energies occur?, 20: 6108 (NP-15600)
Capture of stopped π^- mesons by light nuclei, 20: 6292 (NP-15601)
Large scintillation counters and counters for operation in magnetic fields, 20: 5736 (NP-15597)
Measurement of relationship of proton pulse in ITEF, 20: 5941 (NP-15598)
Study of charged particle beams by means of pick-up electrodes, 20: 5686 (NP-tr-1313)
GRENOBLE UNIV. (FRANCE).
Contribution to study of (d,p) and (d,α) reactions on ^{16}O and ^{11}B from 200 kev to 1 Mev, 20: 6281 (CEA-R-2807)
GRONINGEN RIJKSUNIVERSITEIT (NETHERLANDS).
Experimental and theoretical investigations on light nuclei, 20: 6295 (NP-15647)

H

HARVARD UNIV., CAMBRIDGE, MASS. DIV. OF ENGINEERING AND APPLIED PHYSICS.
Three fluid model ionosphere, 20: 6179 (AD-618911)
HEBREW UNIV., JERUSALEM (ISRAEL). DEPT. OF PHYSICS.
X-ray excitation of second positive and first bands of nitrogen, 20: 6181 (AD-619288)
HITTMAN ASSOCIATES, INC., BALTIMORE, MD.
Addendum to SM-1A hazards summary report for Core III., 20: 6609 (HIT-3534-1)
Analysis of zero power experiments for SM-1 Core III., 20: 6608 (HIT-3459-7)

I

ILLINOIS UNIV., CHAMPAIGN. PHYSICS RESEARCH LAB.
Synchrotron resonator for Illinois 300-Mev betatron, 20: 5942 (NP-15615)
ILLINOIS UNIV., URBANA.
Isotopic effects in lattice constant, thermal expansion, and isothermal compressibility of neon single crystals, 20: 6685 (COO-1198-296)
ILLINOIS UNIV., URBANA. GASEOUS ELECTRONICS LAB.
Helical instability produced in gaseous magnetoplasmas by gyro-interaction of microwaves, 20: 6446 (AD-617696)
INNSBRUCK UNIV. (AUSTRIA).
Interaction between magnetic field and flow field for plasmas of infinite conductivity, 20: 6444 (AD-617553)
MHD characteristics and dispersion relation for finite electrical conductivity, 20: 6157 (AD-617898)
INSTITUTE OF MATHEMATICAL SCIENCE, MADRAS (INDIA).
Mass sum rules, symmetries and dispersion relations, 20: 6109 (NP-15638)
INSTITUTE OF NUCLEAR PHYSICS, KRAKOW (POLAND).
Calculations of some kinematical relations in nuclear reactions programs for digital computer UMC-1, 20: 6286 (INP-414/PL)
INSTITUTE OF NUCLEAR RESEARCH, WARSAW (POLAND).
A general characteristic of the π^--proton inelastic collisions at 10 Bev/c,

20: 6038 (INR-646/VI/PH)
Magnet power reactors after the third Geneva conference, 20: 6612 (INR-622/IX/R)
Momentum-invariants and lorentz-covariant form of physical laws, 20: 6214 (INR-610/VI/PH)
Reduction possibilities of some errors in β-activity measurements by solid angle method, 20: 5729 (INR-617/XIX/D)
Silicon surface-barrier detectors for alpha radiation dosimetry, 20: 5721 (CLOR/IBJ-II-37/D)

INSTITUTT FOR ATOMENERGI, HALDEN (NORWAY). OECD HALDEN REAKTOR PROSJEKT.
Prog. rpt. on HBWR, 7–9/65, 20: 6648 (HPR-64)

INSTITUTUL DE FIZICA ATOMICA, ACADEMIA R. P. R., BUCHAREST (ROMANIA).
Use of radioactive tracers in hydrology in Rumania, 20: 5657 (NP-15543, pp 47-58)

INTERNATIONAL ATOMIC ENERGY AGENCY, VIENNA (AUSTRIA).
Advances in insect population control by sterile-male technique, 20: 5815 (STI/DOC/10/44)

INTERNATIONAL BUSINESS MACHINES CORP., OWEGO, N. Y. FSD SPACE GUIDANCE CENTER.
Neutron and gamma sensitivities of dynamic detectors, 20: 5728 (IBM-65-825-1487)

INTERNATIONAL CENTRE FOR THEORETICAL PHYSICS, TRIESTE (ITALY).
Coupling of non-compact group representations, 20: 6102 (IC/65/79)
Degenerate representations of compact and non-compact unitary groups, 20: 6103 (IC/65/80)
Spin extension of unitary groups, 20: 6104 (IC/65/81)

ISRAEL ATOMIC ENERGY COMMISSION, YAVNE. SOREQ NUCLEAR RESEARCH CENTER.
Reactions of hydrated electron, 20: 5525 (IA-1041)

ISTITUTO SUPERIORE DI SANITA', ROME (ITALY). LABORATORI DI FISICA.
Activities and duties of physics laboratory of Istituto Superiore di Sanita, 20: 5924 (ISS-65/19)
Two channel problem and inelastic unitarity condition in eigenstates of total angular momentum, 20: 6105 (ISS-65/14)
Use of Montecarlo method to solve problems of interpolation, 20: 6286 (ISS-65/10)

J

JAPAN ATOMIC ENERGY RESEARCH INST., TOKYO.
EXPANDA. One-dimensional diffusion equation code for fast reactors, 20: 6583 (JAERI-1091)

JOHNS HOPKINS UNIV., BALTIMORE, MD.
Atomic energy levels, 20: 5984 (NYO-2543-1)

JOINT INST. FOR NUCLEAR RESEARCH, DUBNA (USSR). LAB OF HIGH ENERGY.
Analog wire spark chamber system for measurements of particle moments and angles, 20: 5730 (JINR-E-2366)

JOINT INST. FOR NUCLEAR RESEARCH, DUBNA (USSR). LAB. OF NEUTRON PHYSICS.
Inaccuracies of amplitude-to-time converters, 20: 5731 (JINR-P-2394)

JOINT INST. FOR NUCLEAR RESEARCH, DUBNA (USSR). LAB OF NUCLEAR REACTIONS.
Effect of geometry of cyclotron center upon starting motion of heavy ions (median plane), 20: 5948 (ANL-Trans-246)

JOINT INST. FOR NUCLEAR RESEARCH, DUBNA (USSR). LAB OF THEORETICAL PHYSICS.
Broken symmetry SU(6) and electromagnetic properties of baryons, 20: 6107 (JINR-P-2401)
Method of constructing certain classes of solutions for Chew-Low type equations, 20: 6106 (JINR-P-2369)
Statistical analysis of 17 Bev pion interaction with heavy emulsion nuclei, 20: 6287 (JINR-P-2373)

K

KAMAN NUCLEAR, COLORADO SPRINGS, COLO.
Boron interference in fast-neutron activation analysis for oxygen, 20: 5498 (NP-15636)
Description of neutron generator beam sorters, 20: 6262 (NP-15633)
Determination of neutron yields by measurement of positrons from $^{63}Cu(n,2n)^{62}Cu$ reaction, 20: 6289 (KN-63-10(R))
Neutron fluxes available from Kaman nuclear neutron generators, 20: 6263 (NP-15635)
Selected references for neutron activation analysis, 20: 5499 (NP-15637)

KANSAS ENGINEERING EXPERIMENT STATION, MANHATTAN.
Isomeric cross section ratios for ^{46}Sc, ^{134}Cs, and ^{188}Re isomers, 20: 6301 (TID-22165)

KERNFORSCHUNGSANLAGE, JUELICH (WEST GERMANY). INSTITUT FUER PLASMAPHYSIK.
Report of theoretical and experimental groups for the year, 1964, 20: 6463 (JUL-264-PP)

KERNFORSCHUNGSANLAGE, JUELICH (WEST GERMANY). INSTITUT FUER RADIOCHEMIE.
Chemistry of nucleogenic carbon atoms, 20: 5570 (JUL-228-RC)

KERNFORSCHUNGSZENTRUM, KARLSRUHE (WEST GERMANY). INSTITUT FUER ANGEWANDTE REAKTORPHYSIK.
Behavior of zero-power reactors in reactivity perturbations, 20: 6674 (KFK-332)

KERNFORSCHUNGSZENTRUM, KARLSRUHE (WEST GERMANY). INSTITUT FUER EXPERIMENTELLE KERNPHYSIK.
High-frequency structure for proton linear accelerator, 20: 5937 (KFK-346)
Pulse shape discrimination in half-life determination for study of (γ,α) reactions, 20: 5732 (KFK-335)

KERNFORSCHUNGSZENTRUM, KARLSRUHE (WEST GERMANY). INSTITUT FUER RADIOCHEMIE.
Determination of frequency of plutonium isotopes, 20: 5497 (KFK-339)
PHOTOMETERPROG 4—IBM-7070 program for calculation of stability constants from spectrophotometric measurements, 20: 5526 (KFK-250)

KNOLLS ATOMIC POWER LAB., SCHENECTADY, N. Y.
Independent yields of ^{86}Rb, ^{132}Cs, ^{134}Cs, and ^{136}Cs in thermal neutron fission of ^{235}U, 20: 6288 (KAPL-3113)
Infinite medium spectrum-weighted group constants for gamma heating calculations, 20: 6517 (CONF-651101-41)
Numerical methods for solution of complex gamma spectra, 20: 5727 (CONF-651101-46)
Review of experimental determinations of neutron spectra, 20: 6260 (CONF-651101-43)

L

LABORATORIO DE FISICA E ENGENHARIA NUCLEARES, JUNTA DE ENERGIA NUCLEAR, SACAVEM (PORTUGAL).
Construction and utilization of small-dimension fission chambers, 20: 5734 (LFEN-NI-19)
Three years of operation of experimental Portuguese reactor, 20: 6675 (LFEN-26)

LAWRENCE RADIATION LAB., UNIV. OF CALIFORNIA, BERKELEY.
Amplitude-independent nanosecond timing discriminator for fast photomultipliers, 20: 5744 (UCRL-16227)
Applications of small computers in nuclear spectroscopy, 20: 6307 (UCRL-16439)
Decay schemes of odd-odd einsteinium isotopes, 20: 6305 (UCRL-11784)
Energy dependence of polarization in p-^{16}O elastic scattering between 21 and 53 Mev, 20: 6306 (UCRL-16217)
Inelastic π^- p interactions at 3.3 Bev/c and 3.9 Bev/c, 20: 6041 (UCRL-11942)
Measurement of N^{*-}–N^{*++} mass difference, 20: 6042 (UCRL-16189)
New radiation problems associated with 200-Bev accelerator, 20: 5945 (UCRL-16464)

LAWRENCE RADIATION LAB., UNIV. OF CALIFORNIA, LIVERMORE.
Ambient storage effects and mounting problems of very large volume Ge lid detectors, 20: 5741 (UCRL-14263)
Computer program to find ionization cross sections, 20: 5986 (UCRL-14402-T)
Effect of radially inhomogeneous plasma on microwave interferometer measurements, 20: 5683 (UCRL-14438)
Finite difference methods for nonlinear radiation transport, 20: 6522 (UCRL-12411)
One-dimensional eulerian hydrodynamics difference equations, 20: 6162 (UCRL-12238-T)
Prog. rpt. on hazards control, 4–6/65, 20: 5742 (UCRL-14351)
Response function and sensitivity of double-diffused silicon detectors in high γ-dose rate fields, 20: 5743 (UCRL-14405)

LIEGE UNIV. (BELGIUM). INSTITUT DE CHIMIE.
Mass spectrometry study of diphenyl pyrolysis, 20: 5563 (EUR-2482.f)

LINCOLN LAB., MASSACHUSETTS INST. OF TECH., LEXINGTON.
Analysis of radiation effects in telemetry circuits, 20: 5806 (AD-619387)
Proposed electronic systems for LES radiation experiment (September 1964), 20: 6184 (AD-619977)

LOCKHEED–GEORGIA CO., MARIETTA.
Components irradiation test No. 13.2N2501 transistors TI 551 diodes, and various types of thermistors, 20: 5808 (N65-35081)

LOCKHEED MISSILES AND SPACE CO., PALO ALTO, CALIF.
Neutron fluence measurements for second test at Pulstar reactor, 20: 6679 (NP-15645)

LONDON UNIV. (ENGLAND). UNIVERSITY COLL.
Hypernuclei, 20: 6283 (CERN-64-13(Vol.4), pp 137-86)

LOS ALAMOS SCIENTIFIC LAB., UNIV. OF CALIFORNIA, N. MEX.
Analysis of proton linear accelerator RF system and application to RF phase control, 20: 5938 (LA-3372)

Area radiation monitor system with logarithmic indication and audiovisual warning, 20: 5733 (LA-DC-6790)
Behavior of some delta-stabilized plutonium–gallium alloys at high pressures, 20: 5884 (LA-2312)
Computation of fast neutron penetration in air by "Sn-method", 20: 6261 (LA-3415)
Effect of assumed electronic configuration on electronic band structure of nickel, 20: 6534 (SC-DC-65-1843)
Effect of fission gas bubbles on response of molten fuel reactors to fast transients, 20: 6614 (LA-DC-7476)
Fast reactors—single pulses, 20: 6671 (CONF-650217, pp 1-10)
LASL tandem accelerator facility data system, 20: 5939 (LA-DC-7267)
Nuclear design of MPBE, 20: 6613 (LA-DC-7475)
PHERMEX—high current linac, 20: 5936 (CONF-650217, pp 77-81)
Radiation and shielding design factors for Los Alamos meson physics facility, 20: 5940 (LA-DC-7522)
Storage of fissile material in large and varied reactor research and development program, 20: 6584 (LA-DC-7248)
Table of binding energies and particle separation energies from mass law, 20: 6290 (LA-3380)
Thermal neutron facility for LAMPF, 20: 5935 (CONF-650217, pp 73-6)
Thermal neutron spectra from underground nuclear explosion, 20: 5609 (LA-3403)

LYON UNIV. (FRANCE). FACULTE DES SCIENCES.
Effects of non-lethal doses of x rays on exploring and feeding behavior of larvae of Drosophila melanogaster meig, 20: 5295 (NP-15559)

LYON UNIV. (FRANCE). INSTITUT DE PHYSIQUE NUCLEAIRE.
Circular spark chambers with electric localization at low energies, 20: 5735 (LYCEN-6523)

M

MARYLAND UNIV., COLLEGE PARK. DEPT. OF PHYSICS AND ASTRONOMY.
Solution of scattering and bound state problems by construction of approximate dynamical symmetries, 20: 6215 (NP-15614)

MASSACHUSETTS INST. OF TECH., CAMBRIDGE.
Some aspects of neutron diffraction and elastic scattering using pulsed and steady neutron sources, 20: 5726 (CONF-650217, pp 102-7)
X-ray excitation of second positive and first bands of nitrogen, 20: 6181 (AD-619288)

MASSACHUSETTS INST. OF TECH., CAMBRIDGE. DEPT. OF MECHANICAL ENGINEERING.
Survey and evaluation of techniques to augment convective heat transfer, 20: 5618 (AD-619511)

MASSACHUSETTS INST. OF TECH., CAMBRIDGE. DIV. OF SPONSORED RESEARCH.
Momentum flux in two-phase flow, 20: 5624 (MIT-3496-1)

MASSACHUSETTS INST. OF TECH., CAMBRIDGE. RESEARCH LAB. OF ELECTRONICS.
Fusion reactor blanket experiment, 20: 6454 (AD-619671)
Gamma-ray spectra in fusion blanket mock-ups, 20: 6455 (AD-619672)
Neutron economy in fusion reactor blanket assemblies, 20: 6451 (AD-619668)
Study of thermonuclear reactor blanket with fissile nuclides, 20: 6453 (AD-619670)
Thermal and chemical aspects of thermonuclear blanket problem, 20: 6452 (AD-619669)

MAX-PLANCK-INSTITUT FUER BIOPHYSIK, FRANKFURT AM MAIN (WEST GERMANY).
Bibliography on radiation effects on living tissues and organisms, No. 21, 4/65, 20: 5284 (AED-C-04-21)

MAX-PLANCK-INSTITUT FUER KERNPHYSIK, HEIDELBERG (WEST GERMANY).
Position finding counter for Buechner magnet, 20: 5747 (NP-tr-1302)

MICHIGAN UNIV., ANN ARBOR. DEPT. OF PHYSICS.
Quantum mechanics of $(p\text{-}\mu\text{-}p)^+$ molecular ion, 20: 5980 (AD-617522)

MIDWESTERN UNIVERSITIES RESEARCH ASSN., STOUGHTON, WIS.
High speed digital dynamic field measuring system, 20: 5682 (MURA-716)

MOUND LAB., MIAMISBURG, OHIO.
General method of determining total time integral of transients in linear systems, 20: 5681 (MLM-1288)

N

NATIONAL AERONAUTICS AND SPACE ADMINISTRATION, CLEVELAND, OHIO. LEWIS RESEARCH CENTER.
Critical mass studies with NASA Zero Power Reactor II. I. Clean homogeneous configurations, 20: 6587 (NASA-TN-D-3097)
Effects of metastable atoms on volume ion production in tenuous helium plasma, 20: 6464 (NASA-TN-D-3121)
Summary of thermophysical properties of potassium, 20: 5886 (NASA-TN-D-3120)
Wheel-flow gaseous-core reactor concept, 20: 6662 (NASA-TN-D-2951)

NATIONAL AERONAUTICS AND SPACE ADMINISTRATION, WASHINGTON, D. C.
Plasma jet technology, 20: 5633 (NASA-SP-5033)

NATIONAL BUREAU OF STANDARDS, WASHINGTON, D. C.
Bibliography on high temperature chemistry and physics of materials in condensed state, 20: 5527 (NP-15646)

NATIONAL LEAD CO. OF OHIO, CINCINNATI.
Effects of various fabrication variables on texture gradients in uranium fuel cores, 20: 5863 (NLCO-945)
Plasma spraying of protective coatings, 20: 5837 (NLCO-966)
Study of as-cast and heat-treated uranium-base dilute-carbon alloys by optical and electron microscopy, 20: 5887 (NLCO-953)
Thorium and its MPC's, 20: 5662 (NLCO-962)

NATIONAL MARINE CONSULTANTS, ANAHEIM, CALIF.
Prog. rpt. on buoy dynamics, final, 10/65, 20: 6686 (NVO-98-12)

NATIONAL RADIATION LAB., CHRISTCHURCH (NEW ZEALAND).
Prog. rpt. on fallout in New Zealand, 4–6/65, 20: 5664 (NP-15639)

NAVAL RADIOLOGICAL DEFENSE LAB., SAN FRANCISCO, CALIF.
Homograft response and hemagglutinin production by sensitized thymectomized irradiated adult mice, 20: 5408 (USNRDL-TR-920)
Humoral factor in radiation-induced motivation, 20: 5303 (USNRDL-TR-925)
Nuclear track registration in dosimeter glasses for neutron dosimetry in mixed radiation fields, 20: 5713 (AD-623384)
Programs for collective nuclear model calculations in deformed even-even nuclei, 20: 6278 (AD-623877)
Response of LiF to neutrons and charged particles, 20: 5572 (USNRDL-TR-909)

NERATOOM, N. V., THE HAGUE (NETHERLANDS).
Prog. rpt. on stainless steel plating of very thick steels, 4–6/65, 20: 5862 (EURAEC-1481)

NEVIS LABS., COLUMBIA UNIV., IRVINGTON-ON-HUDSON, N. Y.
μ Capture in oxygen, 19: 6273 (AD-617398)

NEW MEXICO UNIV., ALBUQUERQUE. DEPT. OF CHEMISTRY.
Prog. rpt. on electrochemistry of some transition metals and lanthanides dissolved in molten alkali metaphosphate, 7/64–6/65, 20: 5529 (SC-DC-65-1706)

NEW YORK UNIV., N. Y. RADIATION AND SOLID STATE LAB.
Prog. rpt. on energy transfer during transient nuclear pulses, semiannual, 5–10/64, 20: 5805 (AD-617782)

NORSK HYDRO'S INST. FOR CANCER RESEARCH, OSLO.
Prog. rpt. on cancer research, annual, 1963–64, 20: 5296 (NP-15585)

NOTRE DAME UNIV., IND. DEPT. OF BIOLOGY.
Effects of gamma radiation on electrical properties of muscle, 20: 5293 (COO-205-55, Paper 2)
Gamma-ray effects on mechanical activity of mammalian muscle preparation, 20: 5292 (COO-205-55, Paper 1)
Influence of environmental conditions on radiation sensitivity of Nitella flexilis, 20: 5294 (COO-205-55, Paper 3)
Prog. rpt. on [radiobiology], 1965, 20: 5291 (COO-205-55)

NUCLEAR MATERIALS AND EQUIPMENT CORP., APOLLO, PA.
Effect of PuO_2 content on sintering behavior of mechanically mixed UO_2–PuO_2, 20: 5889 (NUMEC-2389-8)
Thermal expansion of coprecipitated $(U,Pu)O_2$ powders by x-ray diffraction techniques, 20: 5890 (NUMEC-2389-9)

O

OAK RIDGE GASEOUS DIFFUSION PLANT, TENN.
Nucleon-meson cascade in iron initiated by 1- and 3-Bev protons, 20: 5927 (ORNL-P-1733)

OAK RIDGE NATIONAL LAB., TENN.
Acid leaching of products from fluidized-bed combustion of graphite-base reactor fuels and Hf–O_2 disintegration of stainless steel- and zirconium-clad oxide fuels, 20: 5500 (ORNL-3876)
Capsule temperature control by He–N_2 gas composition in thin annulus, 20: 6680 (ORNL-TM-1319)
Critical experiments, 20: 6588 (ORNL-3858(Vol.1), pp 13-19)
Effect of ionizing radiation on coalescence rates in liquid-liquid systems, 20: 5571 (ORNL-TM-1283)
Effects of time delay simulation methods upon stability and time response of simulated systems, 20: 5834 (ORNL-TM-1323)
Experiment S-4, radiation of blood, 20: 5297 (ORNL-P-1734)
Experimental studies for high-energy radiation shielding, 20: 6297 (ORNL-3858(Vol.2), pp 82-90)
FORTRAN programs for Clebsch-Gordan and Racah coefficients and the nine-j symbol, 20: 6216 (ORNL-3877)
Fourier analysis of uniform random number generators, 20: 5833 (ORNL-3866)
Interaction of thermal electrons with polarizable and polar molecules, 20: 5985 (ORNL-TM-1262)

Laboratory preparation of uranium nitride microspheres by sol-gel technique, 20: 5864 (ORNL-3879)
Mathematics and computer programs, 20: 5832 (ORNL-3858(Vol.1), pp 47-53)
Nuclear and reactor physics, 20: 6296 (ORNL-3858(Vol.1), pp 1-12)
Nucleon-meson cascade in iron initiated by 1- and 3-Bev protons, 20: 5927 (ORNL-P-1733)
Prog. rpt. on neutron physics, annual, 8/65, 20: 5925 (ORNL-3858 (Vol.1))
Prog. rpt. on neutron physics, annual, 8/65, 20: 5926 (ORNL-3858 (Vol.2))
Properties and prospects of thoria-base nuclear fuels, 20: 5915 (ORNL-P-1724)
Purification of zirconium tetrafluoride, 20: 5528 (ORNL-TM-1292)
Radiation detector studies. I., 20: 5737 (ORNL-3858(Vol.1), pp 59-64)
Radiation detector studies. II., 20: 5738 (ORNL-3858(Vol.2), pp 91-3)
Radiation shielding information center, 20: 6520 (ORNL-3858(Vol.1), pp 42-6)
Reactor shielding, 20: 6519 (ORNL-3858(Vol.1), pp 20-41)
Standard surface for fission product deposition experiments, 20: 5665 (ORNL-TM-1304)
Theoretical studies of high-energy radiation shielding, 20: 6521 (ORNL-3858(Vol.2), pp 73-81)
Urethane manipulator gauntlets, 20: 5612 (ORNL-TM-1326)

OESTERREICHISCHE STUDIENGESELLSCHAFT FUER ATOMENERGIE G.M.B.H., SEIBERSDORF.
Measurement of ASTRA-transfer function, 20: 6682 (SGAE-R-1/1965)
Prompt and delayed gamma rays in nuclear fission, 20: 6300 (SGAE-PH-29/1965)

OESTERREICHISCHE STUDIENGESELLSCHAFT FUER ATOMENERGIE G.M.B.H., SEIBERSDORF. INSTITUT FUER CHEMIE.
^{99m}Tc generator using Fe_2O_3 as sorbent for ^{99}Mo, 20: 5591 (SGAE-CH-18/1965)

OESTERREICHISCHE STUDIENGESELLSCHAFT FUER ATOMENERGIE G.M.B.H., VIENNA.
Comparison of consumption determination with sound activation and gamma spectroscopy for MTR element, 20: 6681 (SGAE-PH-18/1965)

P

PARIS UNIV. (FRANCE). INSTITUT DE DROIT COMPARE.
Application of sanitary standards in matter of radiological protection, 20: 5663 (NP-15451)

PARIS UNIV., ORSAY (FRANCE). FACULTE DES SCIENCES.
Study of hyperon-antihyperon production in antiproton-proton collision at 4 Bev/c, 20: 6033 (CEA-R-2798)

PENNSYLVANIA STATE UNIV., UNIVERSITY PARK. DEPT. OF BIOPHYSICS.
Prog. rpt. on reactions of bacterial cells to foreign nucleic acids, 12/62–10/65, 20: 5299 (TID-22187)

PENNSYLVANIA STATE UNIV., UNIVERSITY PARK. IONSPHERE RESEARCH LAB.
Electron densities in D region of ionosphere from low frequency signal strength measurements in rockets, 20: 6185 (AFCRL-65-620)

PHILIPPINE ATOMIC ENERGY COMMISSION, MANILA.
Bibliography on ^{198}Au, 20: 5811 (PAEC(A)IN-653)
Radioisotopes in pharmacy, 20: 5812 (PAEC(A)IN-654)

PHILLIPS PETROLEUM CO., IDAHO FALLS, IDAHO.
Inelastic scattering with pulsed neutron sources, 20: 6258 (CONF-650217, pp 82-101)
Subcritical neutron amplifier systems, 20: 6257 (CONF-650217, pp 11-24)

PHILLIPS PETROLEUM CO. IDAHO FALLS, IDAHO., ATOMIC ENERGY DIV.
SNAPTRAN 2/10A-1 and -2 safety tests, 20: 6654 (IDO-17076)

PHYSICS, ENGINEERING, CHEMISTRY CORP., BOULDER, COLO.
Dynamics of ionized media (plasmas), 20: 6448 (AD-619045)

POLYTECHNIC INST. OF BROOKLYN, N. Y. DEPT. OF AEROSPACE ENGINEERING AND APPLIED MECHANICS.
Radiation by uniformly rotating line charge in plasma, 20: 6456 (AD-619888)

POLYTECHNIC INST. OF BROOKLYN, N. Y. MICROWAVE RESEARCH INST.
Diffraction and scattering of electromagnetic waves in anisotropic media, 20: 5922 (AD-618689)

PRATT AND WHITNEY AIRCRAFT, MIDDLETOWN, CONN. CONNECTICUT ADVANCED NUCLEAR ENGINEERING LAB.
Columbium-1 zirconium alloy forced convection lithium slave loop test LCCDB-1, 20: 5853 (TIM-898)
Fission gas migration studies in uranium carbide, 20: 5892 (PWAC-476)
Thermal conductivity and electrical resistivity of uranium monocarbide, 20: 5893 (PWAC-480)

PRINCETON–PENNSYLVANIA ACCELERATOR, PRINCETON, N. J.
Prog. rpt. on nuclear chemistry, annual, 1964–65, 20: 6298 (PPAD-2137-566)

PRINCETON UNIV., N. J. PALMER PHYSICAL LAB.
Nuclear spins and moments of ^{43}Sc and ^{48}Ti, 20: 6299 (PUC-1965-158)

R

RADIATION DYNAMICS, INC., WESTBURY, N. Y.
Prog. rpt. on design and construction of bakeable sputtering apparatus, 11/60–12/63, 20: 5981 (AD-620002)

RAND CORP., SANTA MONICA, CALIF.
Energy-dependent neutron transport theory in plane geometry. II., 20: 6252 (AD-617880)
Energy-dependent neutron transport theory in plane geometry. III., 20: 6253 (AD-617882)

REACTOR GROUP, UNITED KINGDOM ATOMIC ENERGY AUTHORITY, RISLEY (ENGLAND).
Thermal resistance of pressed contacts, 20: 5625 (TRG-Report-1013)

RENSSELAER POLYTECHNIC INST., TROY, N. Y. DEPT. OF MATERIALS ENGINEERING.
Prog. rpt. on metallurgical studies of Zr and Th and of alloying behavior of rare earth-transition metal systems, final, 11/65, 20: 5891 (NYO-2159-1)

RESEARCH LAB., GENERAL ELECTRIC CO., SCHENECTADY, N. Y.
Microstructure of internal magnetic field in selected magnetic materials, 20: 6531 (AD-623530)

ROCHESTER UNIV., N. Y. ATOMIC ENERGY PROJECT.
Chemical toxicity, 20: 5251 (UR-668, pp 123-49)
Molecular and cellular level studies, 20: 5250 (UR-668, pp 110-16)
Prog. rpt., annual, 1964, 20: 5236 (UR-668)
Radiation effects—general, 20: 5301 (UR-668, pp 1-54)
Radiation instruments, 20: 5745 (UR-668, pp 117-23)
Toxicity of radioelements, 20: 5237 (UR-668, pp 55-109)
Unique applications of radioisotopes, 20: 5436 (UR-668, pp 149-60)
Work for other agencies, 20: 5302 (UR-668, pp 161-6)

RUMANIAN COMMITTEE FOR NUCLEAR ENERGY, BUCHAREST.
Investigations and practical applications of radioprotection in Rumania, 1958–1964, 20: 5425 (NP-15543, pp 77-82)
Investigations in medicine carried out in Rumania with aid of radioisotopes, 1958–1964, 20: 5435 (NP-15543, pp 59-75)
Peaceful uses of radioisotopes in the Rumanian People's Republic, 1958–1964, 20: 5810 (NP-15543)
Use of radioactive tracers in hydrology in Rumania, 20: 5657 (NP-1543, pp 47-58)
Use of tracers and of intense radiation sources in industrial processes, 20: 5814 (NP-15543, pp 27-45)
Utilization of ionizing radiation and radioactive isotopes in agriculture and forestry investigations in Rumania, 1958–1964, 20: 5235 (NP-15543, pp 83-90)
Utilization of tracers and of intense radiation sources in chemical research, 20: 5590 (NP-15543, pp 5-26)

S

SANDIA CORP., ALBUQUERQUE, N. MEX.
Absorptivities of complexes from variation and mole ratio methods for complex determinations, 20: 5530 (SC-RR-65-625)
Effect of assumed electronic configuration on electronic band structure of nickel, 20: 6534 (SC-DC-65-1843)

SHEFFIELD UNIV. (ENGLAND). DEPT. OF APPLIED MATHEMATICS.
Power series solution of F2 layer diffusion equation, 20: 6183 (AD-619821)

SOLID STATE RADIATIONS, INC., LOS ANGELES, CALIF.
Neutron detection and spectroscopy with semiconductor detectors, 20: 5714 (AD-623722)
Oxide passivation of semiconductor detectors, 20: 5740 (TID-22407)

SOUDOMETAL, S. A., BRUSSELS (BELGIUM).
Prog. rpt. on stainless steel plating of very thick steels, 4–6/65, 20: 5862 (EURAEC-1481)

SOUTHWEST RESEARCH INST., SAN ANTONIO, TEX.
Advanced BONUS core boiler-superheater fuel element weldments, 20: 6624 (TID-22425)
Nondestructive testing of plastic fatigue pressure vessels, 20: 5894 (SWRI-1228-3-3)
Prog. rpt. on liquid-metal lubricated journal bearings, 8–10/65, 20: 5613 (SWRI-1228-8-16)

STANFORD LINEAR ACCELERATOR CENTER, STANFORD UNIV., CALIF.
Exchange currents in deuteron, 20: 6304 (TID-22401)
General first- and second-order theory of beam transport optics, 20: 5944 (SLAC-PUB-132)
Prog. rpt. on two-mile accelerator project, 4–6/65, 20: 5943 (SLAC-48)
Streamer chamber development, 20: 5739 (SLAC-PUB-140)

STANFORD RESEARCH INST., MENLO PARK, CALIF.
Experimental study of nonlinear plasma-wave interaction, 20: 6457 (AD-622876)
STANFORD UNIV., CALIF. DEPT. OF PHYSICS.
Prog. rpt. on electron scattering experiments, 3/15–6/30/65, 20: 6275 (AD-619534)
STANFORD UNIV., CALIF. HIGH-ENERGY PHYSICS LAB.
Prog. rpt. on linear electron accelerator project, 11/64–1/65, 20: 6276 (AD-619576)
Recent high energy electron investigations at Stanford University, 20: 6277 (AD-619952)
STATE UNIV. OF NEW YORK, ALBANY.
Prog. rpt. on displacement and exchange reactions involving organometallic compounds, final, 10/65, 20: 6687 (NYO-3453-1)
STEVENS INST. OF TECH., HOBOKEN, N. J. DEPT. OF PHYSICS.
Prog. rpt. on mechanism and dynamics of coaxial plasma acceleration, final, 10/63–9/64, 20: 6450 (AD-619527)
Properties of alkali-metal magnetoplasmas related to "enhanced diffusion", 20: 6466 (SIT-2813-33)

T

TENNESSEE UNIV., KNOXVILLE.
Effects of time delay simulation methods upon stability and time response of simulated systems, 20: 5834 (ORNL-TM-1323)
TOKYO UNIV. (JAPAN).
Low temperature resistivity of yttrium-based alloys containing small amounts of rare earth metals, 20: 5888 (NP-15592)
Remark on 30 Bev jet showers, 20: 6039 (INSJ-90)
TRW EQUIPMENT LABS., THOMPSON RAMO WOOLDRIDGE INC., CLEVELAND, OHIO.
Prog. rpt. on generation of long time creep data on refractory alloys at elevated temperatures, 6/26–9/26/65, 20: 5885 (NAS-CR-54773)

U

UNION CARBIDE CORP., OAK RIDGE, TENN. Y-12 PLANT.
Effects of temperature on machining operations, 20: 6688 (Y-DA-1014)
New developments in close tolerance machining, 20: 6690 (Y-NA-14)
Optical applications in dimensional gaging, 20: 6689 (Y-KE-191)
UNION CARBIDE CORP., PARMA, OHIO. CARBON PRODUCTS DIV.
Prog. rpt. on effects of neutron damage on properties of pyrolytic and single crystal graphite, semiannual, 1–6/65, 20: 5897 (TID-22420)
UNITED AIRCRAFT CORP., EAST HARTFORD, CONN. RESEARCH LABS.
Effect of peripheral-wall injection technique on turbulence in air vortex tube, 20: 6652 (D-910091-5)
Experimental refractive indices and theoretical small-particle spectral properties of selected metals, 20: 5879 (D-910092-6)
Peripheral-wall injection techniques in water vortex tube, 20: 6653 (D-910091-7)
Theoretical investigation of lowest five ionization potentials of uranium, 20: 5983 (D-910099-2)
Theoretical investigation of opacity of heavy-atom gases, 20: 6594 (D-910092-4)
UNITED NUCLEAR CORP., NEW HAVEN, CONN. FUELS DIV.
Nuclear aspects of accidental criticality at Wood River Junction, Rhode Island, July 24, 1964, 20: 5666 (TID-21995)
UNITED NUCLEAR CORP., WHITE PLAINS, N. Y. DEVELOPMENT DIV.
Shield small source experiments, 20: 6626 (UNC-5118)
UNITED STATES–EURATOM JOINT RESEARCH AND DEVELOPMENT PROGRAM.
Prog. rpt. on high performance UO_2 program, 4–6/65, 20: 5914 (GEAP-3771-17)
Prog. rpt. on embrittlement by plastic fatigue in reactor vessels, 4–6/65, 20: 5881 (EURAEC-1441)
Prog. rpt. on mechanical properties of metals subjected to mechanical stress and neutron irradiation, 10/65, 20: 5913 (EURAEC-1488)
Prog. rpt. on application of steam-water spray to reactor cooling, final, 12/61–8/64, 20: 6566 (EURAEC-1382)
Prog. rpt. on application of vapotron effect on boiling light water reactors, 10–12/64, 20: 6595 (EURAEC-1421)
Prog. rpt. on Garigliano Nuclear Reactor, 10/65, 20: 6606 (GEAP-4962)
Prog. rpt. on Garigliano nuclear power plant operation, 9/30/65, 20: 6625 (TID-22434)
Prog. rpt. on in-pile corrosion of nuclear materials, final, 3/1/62–3/31/64, 20: 5852 (EURAEC-1522)
Prog. rpt. on mechanical properties of metals subjected to mechanical stress at elevated temperature and neutron irradiation, 3/65, 20: 5880 (EURAEC-1310)
Prog. rpt. on physical properties of UO_2 single crystals, 11/64–3/65, 20: 5882 (EURAEC-1454)
Large scale experiments on heat transfer and hydrodynamics with steam-water mixtures, 20: 5623 (EURAEC-1325)
Prog. rpt. on analytical description of nuclear-reactor accident, 7–9/65, 20: 6560 (BMI-X-10145)
Prog. rpt. on in-pile thermal conductance testing, 7–9/65, 20: 6565 (CEND-3336-251)
Prog. rpt. on Pu subcritical experiment program, 7–9/65, 20: 6607 (GEAP-4965)
Prog. rpt. on stainless steel plating of very thick steels, 4–6/65, 20: 5862 (EURAEC-1481)
UPPSALA UNIV. (SWEDEN).
Study of atmospheric effects on cosmic ray records from plastic scintillation monitors at uppsala, 20: 6004 (AD-619508)
USAF RADIATION LAB., UNIV. OF CHICAGO, ILL.
Dose reduction factor for radiation lethality in mice as function of dose of mercaptoethylamine, 20: 5407 (AD-623599, pp 37-44)
Effect of x-radiation on hexobarbital metabolizing enzyme system of liver microsomes, 20: 5283 (AD-623599, pp 16-27)
Influence of sublethal doses of x-radiation on synthesis of hepatic microsomal enzymes, 20: 5282 (AD-623599, pp 1-15)
Modification of a hyperbaric oxygen chamber for use in hypobaric oxygen exposure studies, 20: 5228 (AD-623599, pp 28-36)
Prog. rpt. on radiobiology, 10/65, 20: 5281 (AD-623599)
USTAV JADERNEHO VYZKUMU, CESKOSLOVENSKA AKADEMIE VED, REZ.
Calcium-activated barium sulfate as sorbent of radiostrontium. III., 20: 5531 (UJV-1382/65)
Initial trajectories of ions leaving an open cyclotron ion source at non-zero initial conditions, 20: 5946 (UJV-1408/65)
UTAH UNIV., SALT LAKE CITY. RADIOBIOLOGY DIV.
Bioassay of influence of cortisol in bones of growing rabbits, 20: 5234 (COO-119-232, pp 122-52)
Comparison of two methods of analyzing hematological data from ^{90}Sr injected beagles, 20: 5290 (COO-119-232, pp 165-89)
Correlation of bone strength with radiation dose from internal emitters and bone resorption, 20: 5289 (COO-119-232, pp 88-98)
Dental eruption pattern of beagle, 20: 5232 (COO-119-232, pp 68-73)
Determination of half-periods of dog serum proteins using ^{35}S-L-methionine, 20: 5249 (COO-119-232, pp 203-18)
Effect of EDTA on excretion of ^{90}Sr and ^{90}Y, 20: 5248 (COO-119-232, pp 200-2)
Injection tables, 20: 5287 (COO-119-232, pp 5-64)
Pilot study of effect of cortisol on $Na_3CaDTPA$ enhanced excretion of ^{239}Pu in beagles, 20: 5247 (COO-119-232, pp 188-99)
Prog. rpt. on radiobiology, annual, 64, 20: 5230 (COO-119-232)
Studies of trabecular bone in beagles and humans, 20: 5233 (COO-119-232, pp 99-121)
Use of therapy in experimental animals, 20: 5231 (COO-119-232, pp 65-7)
^{228}Th induced fractures in beagles, 20: 5288 (COO-119-232, pp 74-87)
UTRECHT RIJKSUNIVERSITEIT (NETHERLANDS).
Development and investigation of photon counter and measurement of optical excitation functions of helium, 20: 5748 (UCRL-trans-1266(L))

V

VANDERBILT UNIV., NASHVILLE, TENN.
E2 internal-conversion process in ^{152}Gd and ^{154}Gd and beta-gamma directional correlation in decay of ^{154}Eu, 20: 6303 (TID-22393)
Interaction of thermal electrons with polarizable and polar molecules, 20: 5985 (ORNL-TM-1262)
VIRGINIA UNIV., CHARLOTTESVILLE. DEPT. OF PHYSICS.
X-ray astronomy, 20: 5968 (NP-15626)

W

WASHINGTON STATE UNIV., PULLMAN.
Prog. rpt. on radiosensitivity of plants, annual, 11/64–10/65, 20: 5298 (RLO-353-4)
WASHINGTON UNIV., SEATTLE.
Cosmic ray muon interactions at 5–50 Bev, 20: 6007 (CONF-640919, pp 143-8)
WEATHER BUREAU RESEARCH STATION, LAS VEGAS, NEV.
Weather and surface radiation prediction activities for Salmon Event—Project Dribble, 20: 5667 (VUF-1020)
WESTERN RESERVE UNIV., CLEVELAND, OHIO.
Prog. rpt. on recoil-free scattering of gamma-rays, final, 3/62–6/65, 20: 6302 (TID-22384)
WESTINGHOUSE ELECTRIC CORP., PITTSBURGH, PA. ATOMIC POWER DIV.
In-core instrumentation for San Onofre nuclear generating station, 20: 6630 (WCAP-3269-46)
New Zircaloy end closure weld joint configuration, 20: 5865 (WCAP-3269-37)
Saxton chemical shim experiment, 20: 6629 (WCAP-3269-24)

Y

YALE UNIV., NEW HAVEN, CONN.
$K_1^0 \to \pi^+\pi^-\pi^0$ decay, 20: 6031 (BNL-9613)
YANKEE ATOMIC ELECTRIC CO., BOSTON, MASS.
Evaluation of Yankee vapor container leakage monitoring system, 20: 6631 (YAEC-1005)

Z

ZENTRALINSTITUT FUER KERNPHYSIK, ROSSENDORF BEI DRESDEN (EAST GERMANY).
Liquid scintillator for slow neutrons, 20: 5746 (ZFK-RN-18)

PERSONAL AUTHOR INDEX

Each entry after an author's name is a shortened version of the title of the report or article, followed by the *NSA* volume and abstract number. Report numbers are given in parentheses.

The phrase "Progress report" is abbreviated as "Prog. rpt.," permitting a more rapid and complete alphabetical arrangement of the titles without changing the location of the progress report titles in relation to the other titles.

Because of problems involving the mechanical preparation of this index, all accent marks are omitted. The following changes in spelling have been introduced to reduce some of the confusion which might result from omitting the accents:

ä	becomes	ae
ö		oe
ø		oe
ü		ue (except in transliterated Chinese names)

A

AARKROG, A., Environmental radioactivity in Denmark in 1964, 20: 5651 (RISO-107)

ABBATIELLO, A. A., Capsule temperature control by He–N_2 gas composition in thin annulus, 20: 6680 (ORNL-TM-1319)

ABBATTISTA, N., Operative definition of threshold of tunnel diode switching circuits, 20: 5700

ABBE, W. J., Modification of Regge-pole representation, 20: 6062

ABDULLAEV, R. S., Investigation of fraction of energy transferred to soft component by particles interacting with carbon nuclei, 20: 6017

ABDUZHAMILOV, Sh., Angular distribution of shower particles in collisions between 24-Bev protons and nucleons and photoemulsion nuclei, 20: 6325

ABEL, W. R., Low-temperature heat capacity of liquid ^{3}He, 20: 6245

ABERTH, W., Perturbation induced in elastic scattering by crossing of molecular states, 20: 5996

ABGRALL, Y., Self-consistent field and study of ground states of closed shell light nuclei, 20: 6363

ABUBACKER, K. M., Spectrophotometric and potentiometric studies of system containing UO_2^{++}, $C_2O_4^{--}$ and H_2O_2, 20: 5549

ACKERMANN, R. J., Thermodynamic study of uranic–uranium system, 20: 5877 (ANL-7048)

ADAM, Geza, Effect of ionizing radiation on iron metabolism of body, 20: 5354

ADAM, W. E., Dosimetry in radiotherapeutic practice, 20: 5478

ADAMSKA, Hanna, Selfexcited vibration of nuclear reactor fuel channels with water cooling, 20: 6564

ADLER, Ronald John, Exchange currents in deuteron, 20: 6304 (TID-22401)

ADLOFF, J. P., Extraction of francium by organic solvents, 20: 5601

AFONSO, Luis Amoral, Construction and utilization of small-dimension fission chambers, 20: 5734 (LFEN-NI-19)

AFRA, Danes, Effect of x-ray on phosphorus metabolism of glioma cultures, 20: 5255

AGARWAL, Y. K., Spectral shapes and beta–gamma directional correlation in beta decay of ^{172}Tm($J^{\pi} = 2^-$), 20: 6381

AGENO, M., Activities and duties of physics laboratory of Istituto Superiore di Sanita, 20: 5924 (ISS-65/19)

AGER-HANSSEN, H., Dynamic research and in-core instrumentation at HBWR, 20: 6637

AHLERS, Gordon K., Nuclear reactor's cooling water is conserved by recharging at 15 MGD/ACRE, 20: 6667 (BNL-9686)

AHNSTROEM, G., Energy transfer in relation to water-content in solid proteins, 20: 5270

AJZENBERG-SELOVE, F., Alphas from deuteron bombardment of ^{9}Be and ^{12}C, 20: 6360

AKHABABYAN, N., Daily variations of hard component intensity of cosmic radiations for 1960–1963, 20: 6016

AKS, S. O., Analytic properties of elastic unitarity integral, 20: 6114

ALASIA, A. M., Determination of ^{90}Sr in deciduous teeth, 20: 5655

ALBOUY, G., Reaction (p,2p) on some isotopes of titanium, 20: 6330

ALBRIGHT, C. H., Baryon resonance production by neutrinos and relativistic generalizations of SU(6), 20: 6065

ALDER, Kurt, Radial integrals for relativistic coulomb functions, 20: 6375

ALEKSANDROVA, N. B., Unsaturated higher fatty acids of "free lipid" fraction from leaves of irradiated plants, 20: 5265

ALEKSANDROWICZ, Julian, Environment and leukemia morbidity. III., 20: 5674

ALEXANDER, Leslie I., Treatment of antral carcinoma with radioactive iridium, 20: 5458

ALEXANDER, P., Electromagnetic transitions in ^{181}Ta, 20: 6374

ALEXANDER, T. K., Gamma-ray transitions in ^{15}O and ^{15}N, 20: 6318

ALFORD, W. Parker, ^{39}K(^{3}He,α)^{38}K and ^{39}K(^{3}He,^{3}He)^{39}K reactions, 20: 6367

ALGER, Donald L., Critical mass studies with NASA Zero Power Reactor II. I. Clean homogeneous configurations, 20: 6587 (NASA-TN-D-3097)

ALI, M. M., ^{14}N(^{3}He,α)^{13}N angular distribution leading to the ground state in ^{13}N, 20: 6326

ALIAN, A., Activation analysis through addition of "standard" and solvent extraction, 20: 5494 (AEET-217)

ALLEN, T. K., Cusp compression experiments, 20: 6495

ALLKOFER, O. C., Spectrum of muons, protons, and electrons at 5200 m altitude, 20: 6021

ALSMILLER, R. G. Jr., Nucleon-meson cascade in iron initiated by 1 and 3-Bev protons, 20: 5927 (ORNL-P-1733)

ALTHAUS, William A., Study of as-cast and heat-treated uranium-base dilute carbon alloys by optical and electron microscopy, 20: 5887 (NLCO-953)

ALVAREZ, L., Proposed balloon borne system for interactions above 10^{11} ev, 20: 5724 (CONF-640919, pp II13-23)

ALY, H. H., Test of N/D method in potential scattering, 20: 6129

AMALDI, U. Jr., Two channel problem and inelastic unitarity condition in Eigen-states of total angular momentum, 20: 6105 (ISS-65/14)

AMDUR, I., Differences in spherical intermolecular potentials of hydrogen and deuterium, 20: 5541

AN, Shigehiro, Status of development of fast reactors in France, 20: 6643

ANANTHANARAYANAN, K., Elastic photoproduction of neutral pions from ^{4}He, 20: 6365

ANBAR, M., Reactions of hydrated electron, 20: 5525 (IA-1041)

ANDEEN, Gerry B., Momentum flux in two-phase flow, 20: 5624 (MIT-3496-1)

ANDERSEN, A. J., Uptake by plants of radiostrontium from contaminated soils, 20: 5257

ANDERSON, A. C., Low-temperature heat capacity of liquid ^{3}He, 20: 6245

ANDERSON, Robert E., Life span in normal and irradiated hamsters, 20: 5330

ANDO, Norio, Studies on chemical protection against radiation injuries in cultured L-strain cells in vitro. I., 20: 5418

ANDO, Norio, Studies on chemical protection against radiation injuries in cultured L-strain cells in vitro. II., 20: 5419

ANDREEFF, Alexander, Liquid scintillator for slow neutrons, 20: 5746 (ZFK-RN-18)

ANDREEV, O. L., International comparison of neutron sources, 20: 6265

ANDREEVSKII, A. A., Alkali metals boiling heat transfer, 20: 5627

ANDRYUSHIN, N. F., Back-scattering of gamma rays from spherical surfaces, 20: 6525

ANGUS, W., Dental eruption pattern of beagle, 20: 5232 (COO-119-232, pp 68-73)

ANISOVICH, V. V., Influence of strong interactions between final state

π-mesons on probability ratio of $K \to 3\pi$ decays, 20: 6086

ANTAKOV, I. I., Use of impulse magnetic fields in devices with trochoidal electron beams, 20: 5929

ANTILL, J. E., Electrochemical aspects of hydrolysis of UC-10% Fe, 20: 5857

ANTONOV, I. N., Dependence of heat conductivity of sodium on concentration of oxides, 20: 5901

ANTUNES, Caio Antonio, Experience with vitamin B_{12} in case of alopecia following deep radiotherapy (x-rays), 20: 5484

ARCHAMBEAU, John O., Mammalian radiation lethality. A disturbance in cellular kinetics, 20: 5405

ARIFOV, U. A., Detection of secondary-electron currents by scintillation counter, 20: 5757

ARMANTROUT, Guy, Ambient storage effects and mounting problems of very large volume Ge lid detectors, 20: 5741 (UCRL-14263)

ARMSTRONG, D. D., Spectroscopy of lower excited states of ^{59}Co, 20: 6412

ARNDT, Rudolf, Space potential determination using glow probes, 20: 6164

ARNETT, L. M., Control of dissolved gases in moderator of heavy water components test reactor, 20: 6673 (DP-988)

ARNOLD, J. S., Studies of trabecular bone in beagles and humans, 20: 5233 (COO-119-232, pp 99-121)

ARTMANN, J., Supplementary calculations for reflected collision waves in thermal plasmas, 20: 6512

ARTYKOV, I. Z., Statistical analysis of 17 Bev pion interaction with heavy emulsion nuclei, 20: 6287 (JINR-P-2373)

ARTYUKHIN, P. I., Extraction of carrier free ^{57}Co from irradiated targets, 20: 5602

ASAULENKO, L. G., Current system of elementary geomagnetic disturbance in the aurora zone, 20: 6192

ASGHAR, M., Neutron cross sections of thorium and analysis of resonances up to 1 kev, 20: 6377

ASHERY, D., E2/M1 mixing ratios and K conversion coefficients in odd-mass rotational nuclei, 20: 6386

ASLANOV, G. A., Arsenate method for iodometric determination of yttrium in presence of aluminum, 20: 5506

ATHERTON, D. R., Effect of EDTA on the excretion of ^{90}Sr and ^{90}Y, 20: 5248 (COO-119-232, pp 200-2)

ATHERTON, D. R., Pilot study of effect of cortisol on $Na_3CaDTPA$ enhanced excretion of ^{239}Pu in beagle, 20: 5247 (COO-119-232, pp 188-99)

ATKINSON, D., Solution of singular N/D equations. I., 20: 6130

ATKINSON, D., Solutions of singular N/D equations. II., 20: 6131

ATKINSON III, Reilly, Radiative corrections for coincidence electron scattering, 20: 6093

AUBURN, R. P., Transplantation site preradiation and rejection patterns, 20: 5344

AUERBACH, N., States with $v = 0$ and $v = 1$ seniority in Ni isotopes, 20: 6385

AXMANN, Hans Peter, Prompt and delayed gamma rays in nuclear fission, 20: 6300 (SGAE-PH-29/1965)

AZHIPA, Ye. I., Influence of low doses of internal irradiation of some aspects of water, mineral, and nitrous metabolism in animals. II., 20: 5381

AZIMOV, S. A., Investigation of fraction of energy transferred to soft component by particles interacting with carbon nuclei, 20: 6017

B

BABA, C. V. K., Spectral shapes and beta–gamma directional correlation in beta decay of $^{172}Tm(J^{\pi} = 2^-)$, 20: 6381

BABAEV, Z. R., Broken symmetry SU(6) and electromagnetic properties of baryons, 20: 6107 (JINR-P-2401)

BABAEVA, E. P., Lithium, cesium, and lanthanum fluoride systems, 20: 5558

BABICKY, A., Generalized response of calcified mammalian tissues to local injury, 20: 5370

BABOIAN, R., Electrochemical studies on zirconium and hafnium in molten LiCl–KCl eutectic, 20: 5543

BACHERIKOV, I. P., Xenon oscillations in nuclear reactors, 20: 6590

BACHMANN, P., Singularities of kinetic dispersion equation, 20: 6477

BACHOFER, C. S., Alterations in muscle activity during gamma-irradiation, 20: 5375

BADIER, S., Baryon-antibaryon pair production in SU_6 symmetry, 20: 6133

BAILEY, D. K., Relativistic electron precipitation into mesosphere at subauroral latitudes, 20: 6201

BAILEY, R. A., Electrochemical studies on zirconium and hafnium in molten LiCl–KCl eutectic, 20: 5543

BAINBRIDGE, A. E., Determination of natural tritium, 20: 5517

BAKAI, A. S., Leakage of particles from storage rings due to random variations in amplitude and frequency of compensating field, 20: 5949

BAKER, E. W., Emission of ^8Li fragments from Cu, Ag, and Au irradiated by high-energy protons, 20: 6409

BAKER, L., Reactor safety, 20: 6552 (ANL-6925, pp 187-233)

BAKTYBAEV, K. B., α-Decay and nuclear structure in region of ^{208}Pb, 20: 6423

BALANDIN, A. A., Kinetic parameters of dehydrogenization and dehydration of isopropyl alcohol and dehydrogenization of tetralin on praseodymium oxide, 20: 5567

BALASHOV, V. V., Effects of resonance modes on channel coupling in nuclear reactions, 20: 6426

BALDINI, G., Isotope effects induced by local modes in U band, 20: 6545

BALLAND, J. C., Considerations on noise of input stage of pulse amplifier, 20: 5697

BANKS, D. E., Transplantation site preradiation and rejection patterns, 20: 5344

BAQUE, P., Zirconium–copper alloys resistant to oxidation by carbon dioxide at high temperature, 20: 5860

BARACH, J. P., Flow modes in electric shock tubes, 20: 6173

BARASHENKOV, V. S., Statistical analysis of 17 Bev pion interaction with heavy emulsion nuclei, 20: 6287 (JINR-P-2373)

BARATOFF, A., Magnetic properties of superconducting thin films in nonlocal regime, 20: 6250

BARATZ, R. A., Oxygen uptake of three life stages of Tenebrio molitor prior and subsequent to massive doses of low energy x-rays, 20: 5314

BARB, Danile, Physical properties of nickel–chromium trioxide catalyst for hydrogen–deuterium isotopic exchange reaction, 20: 5534

BARBIER, M., Estimate of induced radioactivity in accelerators, 20: 5933 (CERN-65-34)

BARDOLLE, Gerard, Excitation curve of (n,2n) reaction on ^{63}Cu from 16.59 to 17.71 Mev, 20: 6319

BARGER, V., Analysis of total cross-section differences at high energy, 20: 6082

BARISH, J., Nucleon-meson cascade in iron initiated by 1 and 3-Bev protons, 20: 5927 (ORNL-P-1733)

BARKER, F. B., Computer control and data processing for isotopic mass spectrometers, 20: 5684 (WAPD-T-1770)

BARMORE, Willis L., Compressive creep of beryllium oxide–uranium dioxide mixtures, 20: 5904

BARNES, L. J., Critical state of superconducting surface sheath, 20: 6243

BARNES, R. G., Nuclear magnetic resonance in pure quadrupole regime, 20: 6549

BARNES, V., $K_2^0 \to \pi^+\pi^-\pi^0$ decay, 20: 6031 (BNL-9613)

BARNETT, Gleanroy W., Method of compensating radiation gage for unwanted changes in measured material, 20: 5712

BARNETT, P. G., Stability of laminar flow of liquid between parallel planes, 20: 5621 (AEEW-R-416)

BARR, T. A. Jr., "Spark-plug" starter for arc plasma generators, 20: 6489

BARSUKOV, K. A., Transient radiation at anisotropic conductive plane, 20: 6043

BARTH, V. D., Tungsten powder metallurgy, 20: 5836 (NASA-SP-5035)

BARTKE, Jerzy, A general characteristic of the π^--proton inelastic collisions at 10 Bev/c, 20: 6038 (INR-646/VI/PH)

BARTNOFF, S., Saxton chemical shim experiment, 20: 6629 (WCAP-3269-24)

BARUA, A. K., Ionization cross-sections of atoms and molecules by electron impact, 20: 5989

BASHANDY, E., Gamma intensities in decay of ^{187}W, 20: 6397

BASSICHIS, W. H., Projected Hartree-Fock spectra in light nuclei, 20: 6419

BATABYAL, A. K., Ionization cross-sections of atoms and molecules by electron impact, 20: 5989

BATCHELDER, David Neville, Isotopic effects in lattice constant, thermal expansion, and isothermal compressibility of neon single crystals, 20: 6685 (COO-1198-296)

BATTER, J. F., Barrier attenuation introduced by vertical wall, 20: 6516 (AD-617524)

BATTY, C. J., Isobaric states excited in (p,n) reactions at 30 and 50 Mev, 20: 6361

BAUER, B., ^{99m}Tc generator using Fe_2O_3 as sorbent for ^{99}Mo, 20: 5591 (SGAE-CH-18/1965)

BAUER, Donald deForest, Textbook of elementary radiography for students and technicians, 20: 5489

BAUER, W., High-frequency structure for proton linear accelerator, 20: 5937 (KFK-346)

BAXTER, R. G., Power series solution of F2 layer diffusion equation, 20: 6183 (AD-619821)

BAYATYAN, G. L., Large scintillation counters and counters for operation in magnetic fields, 20: 5736 (NP-15597)

BEALL, J. P., SNAP 2 experimental reactor (SER) operation and test program, 20: 6655 (NAA-SR-7088)

BEARDEN, J. A., Atomic energy levels, 20: 5984 (NYO-2543-1)

BECHERER, G., Simple method for preparing x-ray filters of strontium metal, 20: 5692

BECKER, J. J., Microstructure of internal magnetic field in selected magnetic materials, 20: 6531 (AD-623530)

BECKER, K., Nuclear track registration in dosimeter glasses for neutron dosimetry in mixed radiation fields, 20: 5713 (AD-623384)
BECKER, L. E., Safety factors in urethrography, 20: 5459
BEGEMANN, F., Rare gas measurements on iron meteorites and their inclusions, 20: 5977
BEGZHANOV, R. B., Resonant scattering of gamma quanta by ^{140}Ce nuclei, 20: 6324
BEHREND, H. J., Search for heavy electron by electron-proton coincidence measurements, 20: 6078
BELEN'KII, V. M., Angular distribution of shower particles in collisions between 24-Bev protons and nucleons and photoemulsion nuclei, 20: 6325
BELL, J. S., $\bar{U}_{12}$, its 143 moments, its little group $U_6 \times U_6$ and its irregular couplings, 20: 6132
BELL, M., Disc-loaded deflecting waveguide-computations, 20: 5934 (CERN-65-37)
BELLER, Morris, Possibility of chemonuclear reactors producing ozone for water treatment, 20: 5568 (BNL-9664)
BELLETTINI, G., Sonic spark chamber system, 20: 5720 (CERN-65-33)
BELOV, V. P., Resonance Ξ_{1820} and unitary symmetry, 20: 6091
BELYAEV, S. T., Green function method in simple nuclear model, 20: 6425
BENASSI, Enrico, Radiotherapy of polycythemia, 20: 5483
BENDER, Michael A., Experimental S-4, radiation of blood, 20: 5297 (ORNL-P-1734)
BENEDEK-LAZAR, Magda, Response of hybrid and inbred maize to radiation of radioactive $^{32}PO_4$, 20: 5305
BENEDICT, Andrzej, Potentiometric determination of rare earths (e.g., erbium), 20: 5519
BENENSON, R. E., Search for excited states of ^5He, 20: 6335
BENES, Jaroslav, Rapid separation of barium from mixture of fission products, 20: 5603
BENEVENTANO, Thomas C., Treatment of antral carcinoma with radioactive iridium, 20: 5458
BENNETT, Alan J., Theory of anisotropic energy gap in superconducting lead, 20: 6238
BENOIST-GUEUTAL, P., Calculation of proton polarization in p-d elastic scattering at 150 Mev, 20: 6329
BENSON, Richard E., USAF whole body gamma spectrometry, 20: 5427
BENSTED, J. P. M., Carcinogenic effects of ^{241}Am and ^{239}Pu in rat, 20: 5321
BENTLE, G. G., Brittle and plastic behavior of hot-pressed BeO, 20: 5902
BEN-ZEEV, Nehama, Viability of heterozygotes for induced mutations in Drosophila melanogaster. I., 20: 5358
BERAK, L., Calcium-activated barium sulfate as sorbent of radiostrontium. III., 20: 5531 (UJV-1382/65)
BERENYI, Denes, Dynamic nuclear structure effects in internal conversion, 20: 6332
BERES, William P., Application of quasi-particle method to ^{63}Cu, 20: 6340
BERGERON, Michel, Radioautographic detection of proteins synthesized from leucine-^3H in mitochondria, 20: 5254
BERGLES, Arthur E., Survey and evaluation of techniques to augment convective heat transfer, 20: 5618 (AD-619511)
BERLANDI, Francis J., Electrochemical preparation of thin metal films as standards on pyrolytic graphite, 20: 5503
BERMAN, B. L., Cross sections for ground- and excited-state neutron groups in reaction $^{16}O(\gamma,n)^{15}O$, 20: 6418
BERNDT, A. F., Growth of large grains in gallium-stabilized delta-plutonium alloy, 20: 5907
BERNESCUT, R., Response function and sensitivity of double-diffused silicon detectors in high γ-dose rate fields, 20: 5743 (UCRL-14405)
BERNICK, R. L., OPEX shield optimization code, 20: 6518 (NAA-SR-Memo-11516)
BERTOLACCINI, M., Fast coincidence system for low energy γ-ray spectroscopy, 20: 5770
BESSIS, M., Positive and negative chemotaxis as observed after destruction of cell by uv or laser microbeams, 20: 5396
BETEV, B., Daily variations of hard component intensity of cosmic radiations for 1960–1963, 20: 6016
BETZ, E. H., Influence of cystamine on immunization phenomena after whole-body irradiation, 20: 5413
BETZ, J. M., Method for low-level gamma radioactivity measurement, 20: 5432
BEWLEY, David K., Increased sensitivity of in vitro murine leukemia cells to fractionated x-rays and fast neutrons, 20: 5361
BHAKAR, B. S., Relativistic corrections to triton binding energy, 20: 6084
BHATNAGAR, Prem Lata, X-irradiation of pupae of house fly Musca domestica L. and adult survival, 20: 5331
BHATNAGAR, V. S., Measurements of radioactive fallout in individual rain showers at Bombay, 20: 5661 (AEET-215)
BHATTACHARYYA, A., Mixed convection heat transfer on outside of vertical cylinder, 20: 5619 (AE-199)
BHATTACHARYYA, R., Gamma-gamma angular correlation in ^{125}Sn, 20: 6322
BHATTACHERJEE, S. K., Spectral shapes and beta–gamma directional correlation in beta decay of $^{172}Tm(J^\pi = 2^-)$, 20: 6381
BIALAS, A., Bremsstrahlung theory for multiple production of mesons, 20: 6053
BIANCASTELLI, R., Two channel problem and inelastic unitarity condition in Eigen-states of total angular momentum, 20: 6105 (ISS-65/14)
BIANCHI, E., Radioresistance in guinea pigs after subsequent lethal dose of x-rays, 20: 5356
BIANCHI, G., Determination of spin and resonance parameters for $^{197}Au + n$ at 10 to 1000 ev, 20: 6392
BIEKER, Richard J., Study of as-cast and heat-treated uranium-base dilute-carbon alloys by optical and electron microscopy, 20: 5887 (NLCO-953)
BIENKOWSKI, Andrzej, Electronic collimation of α particles in gridded ionization chamber, 20: 5782
BIGUET, A., Heating and confinement of plasma in magnetic well of deca-2, 20: 6469 (UCRL-Trans-1256(L))
BILLEN, D., Reorientation of chromosome replication after exposure to ultraviolet light of Escherichia coli, 20: 5349
BILLINGS, Donald E., Prog. rpt. on system for solar flare prediction, semiannual, 1/6/65, 20: 5967 (AD-619740)
BINSACK, Joseph H., Proposed electronic systems for LES radiation experiment (September 1964), 20: 6184 (AD-619977)
BIRCANIN, Ljubisa, Radioactive source production at Boris Kidric Institute, 20: 5813 (JPRS-32260)
BIRDSALL, D. H., Bakeable, pulsed gas valve for plasma physics experiments, 20: 5642
BIRGER, N. G., Measurement of relationship of proton pulse in ITEF, 20: 5941 (NP-15598)
BIRNEY, K. R., Fission product cross sections as function of exposure for use with SIZZLE, 20: 6659 (NAA-SR-Memo-11473)
BLACK, W. C., Low-temperature heat capacity of liquid ^3He, 20: 6245
BLACKWELL, C. E., Gamma-ray evaluation of diagnostic shielding barriers, 20: 5677
BLACKWOOD, E. L., Bioassay of influence of cortisol in bones of growing rabbits, 20: 5234 (COO-119-232, pp 122-52)
BLAEDEL, W. J., Continuous back-titrations with direct readout, 20: 5502
BLAIR, A. G., Spectroscopy of lower excited states of ^{58}Co, 20: 6412
BLANC, P., Heating and confinement of plasma in magnetic well of deca-2, 20: 6469 (UCRL-Trans-1256(L))
BLANKENSHIP, J. L., Elimination of undesirable undershoot in operation and testing of nuclear pulse amplifiers, 20: 5707
BLAU, L. M., $^{39}K(^3He,\alpha)^{38}K$ and $^{39}K(^3He,^3He)^{39}K$ reactions, 20: 6367
BLAUGRUND, A. E., E2/M1 mixing ratios and K conversion coefficients in odd-mass rotational nuclei, 20: 6386
BLECKERMAN, S. S., Columbium-1 zirconium alloy forced convection lithium slave loop test LCCDB-1, 20: 5853 (TIM-898)
BLEIBERG, Ilse, Reversion by erythropoietin of suppression of erythroid clones caused by transfusion-induced polycythemia, 20: 5242
BLEWITT, T. H., Radiation damage, 20: 5569 (CONF-650217, pp 108-10)
BLINOV, V. A., Use of gamma-gamma coincidence spectrometer with summation of pulse amplitudes for analysis of a mixture of radioactive isotopes, 20: 5753
BLIXT, Stig, Linkage studies in pisum. I., 20: 5238
BLOKHINA, V. D., Influence of irradiation on lipids of mitochondria of liver cells, 20: 5379
BLOKHINTSEV, L. D., Feynman graph treatment of initial and final state interactions in direct nuclear reactions, 20: 6383
BLOMEYER, Walter, Method of welding together sheathing tubes of nuclear fuel or breeder elements with their end closures, 20: 5868
BLUEMEL, G., Concluding word to current remarks of P. Koeppe, 20: 5399
BLUEMEL, G., Thorotrast problem, 20: 5398
BLUM, Heywood, Effect of pressure on hyperfine structure of F centers in LiF, 20: 6543
BOARDMAN, John, Contributions to quantization problem in general relativity, 20: 6219
BOBACK, M. W., Thorium and its MPC's, 20: 5662 (NLCO-962)
BOCHIN, V. P., Study of (d,p) stripping effect on intermediate nuclei. III., 20: 6422
BOCKRATH, R. D. Jr., Evidence for mutagenic local effect accompanying decay of incorporated tritium in Escherichia coli, 20: 5350
BOCLET, Daniel, Method of and apparatus for recording pulse spectra, 20: 5797
BODINE, J. E., Remote operating gas pycnometer, 20: 5708
BOGANOV, A. G., Polymorphism of rare-earth sesquioxides, 20: 5536
BOGDANOV, V. S., Reduction of carbon dioxide by hydrogen under effect of fast electrons, 20: 5574
BOLING, M. E., Resistance of micrococcus radiodurans to ultraviolet radiation. II., 20: 5266
BOND, J. B., Plasma jet technology, 20: 5633 (NASA-SP-5033)
BOND, Victor P., Mammalian radiation lethality. A disturbance in cellular kinetics, 20: 5405
BONNET, Georges, Theoretical study of extraction of periodic signal in noise by accumulation of data, 20: 5695
BONNET, P., Application of different methods of non-destructive testing

to fuel elements of ORGEL type, 20: 6632 (AEC-tr-6628)
BONYHADY, K. A., Analysis of process control in SGR 200 Mwe prototype plant, 20: 6617 (NAA-SR-Memo-11339)
BOORNARD, A., Determination of plasma density by laser interferometric and continuum radiation intensity measurements, 20: 6471
BOOZ, G., Influence of cystamine on immunization phenomena after whole-body irradiation, 20: 5413
BORISENKOV, E. P., Structural characteristics of fields of outgoing radiation according to data of artificial satellites Tiros II and Tiros III and their interpretation, 20: 6019
BORISHANSKII, V. M., Alkali metals boiling heat transfer, 20: 5627
BORISOV, V. S., Measurement of relationship of proton pulse in ITEF, 20: 5941 (NP-15598)
BORISOVA, I. G., Unsaturated higher fatty acids of "free lipid" fraction from leaves of irradiated plants, 20: 5265
BORNEMEIER, Dwight Daniel, Decay of ^{133}Ba, ^{115}Cd, and ^{197}Pt, 20: 6436
BORREANI, G., Longitudinal polarization of low-energy muons from $K^+_{\mu 3}$ decay, 20: 6075
BOSCHITZ, E. T., Energy dependence of polarization in p-^{16}O elastic scattering between 21 and 53 Mev, 20: 6306 (UCRL-16217)
BOSE, Asoke, Histochemical studies in irradiated chick embryos, 20: 5306
BOSE, S., Radiosensitivity in cyclic phases of mouse fibrosarcoma cells in vitro, 20: 5362
BOSE, Sudesh, Calculation of s-wave nucleon-nucleon scattering parameters in I = 0, S = 1 state by N/D method, 20: 6049
BOSTICK, Winston H., Prog. rpt. on mechanism and dynamics of coaxial plasma acceleration, final, 10/63–9/64, 20: 6450 (AD-619527)
BOTHIN, W., Photoproduction of pion and nucleon resonances at energies up to 5.5 Bev, 20: 6037 (DESY-65/11)
BOUCHEZ, Robert, Evidence of two-body interactions in reaction ^{9}Be(n,2n) at 14 Mev, 20: 6320
BOUCHIAT, C., Baryon-antibaryon pair production in SU_6 symmetry, 20: 6133
BOURDON, P. A., Columbium-1 zirconium alloy forced convection lithium slave loop test LCCDB-1, 20: 5853 (TIM-898)
BOURGOIGNIE, R. J., Z dependance of bremsstrahlung of electrons between 2.5 and 4.0 Mev, 20: 6432
BOUZOU, Monique, Method for oxidation of Pu(III) to Pu(IV) in a basic solution, 20: 5561
BOWMAN, C. D., Scattering measurements on neutron resonances in ^{239}Pu, 20: 6414
BOYARSKI, A., Streamer chamber development, 20: 5739 (SLAC-PUB-140)
BOYLE, James A., Clinical studies with gamma camera, 20: 5467
BOZZO, S. R., Formulation and testing of compartmental model for calcium metabolism in man, 20: 5260
BRACE, L. H., Early electrostatic probe results from Explorer 22, 20: 6199
BRADHURST, D. H., Electrochemical model for oxidation of zirconium, 20: 5858
BRADLEY, D. J., Ionoluminescence of MgO and Zn_2SiO_4 : Mn, 20: 5573
BRADLEY, Robert F., Pituitary ablation in treatment of diabetic retinopathy, 20: 5468
BRALL, U., Photoproduction of pion and nucleon resonances at energies up to 5.5 Bev, 20: 6037 (DESY-65/11)
BRAMBILLA, M., Electrostatic instability of plasma with discontinuous velocity distribution, 20: 6487
BRAMBLETT, Elizabeth L., MATEDIR. Code to calculate design points of manned, direct-radiating, thermoelectric system, 20: 6660 (NAA-SR-Memo-11514)
BRAMBLETT, R. L., Cross sections for ground- and excited-state neutron groups in reaction ^{16}O(γ,n)^{15}O, 20: 6418
BRAMBRING, J., Plasma radiation from thin silver foils excited by light, 20: 6548
BRAMLAGE, William J., Response of botrytis cinerea to gamma radiation, 20: 5371
BRASSE, F. W., Search for heavy electron by electron-proton coincidence measurements, 20: 6078
BREGER, A. H., Method for computing efficiency coefficient of radiation apparatus with plane gamma sources, 20: 5750
BREGER, A. Kh., About absorption of gamma ray energy by point sources in macrosystems, 20: 5751
BREGER, A. Kh., Air-exchange calculation in rooms for high-power gamma units, 20: 5670
BRENNER, R., General purpose analog pulse height computer, 20: 5835
BRESLAVETS, L. P., Changes in process of cell division and nucleus structure under the influence of irradiation and radiotoxins, 20: 5390
BRETT, J., Diffusion-controlled oxidation of several lanthanides, 20: 5859
BRIAND, Jean-Pierre, Study of α emission of ^{230}Pa, 20: 6321
BRICE, Niel M., Interpretation of transverse whistlers, 20: 6207
BRILLA, G., Effect of x-rays on thrombocyte containing clotted blood plasma, 20: 5365
BRINDLEY, J. H., Reliability test of an SRE-PEP moderator element, 20: 6621 (NAA-SR-Memo-11556)
BRINKLEY, Diana, Clinical trial of radiosensitizers, 20: 5437
BRINTON, H. C., Positive ion composition in magnetoionosphere, 20: 6198
BRITTIN, Wesley E., Dynamics of ionized media (plasmas), 20: 6448 (AD-619045)
BRODA, E., Mechanism of uptake of trace elements by plant roots, 20: 5258
BROHEE, H., Effects of x-radiation and nicotinamide on respiration of rat thymocytes, 20: 5340
BROIDO, Michael M., Complete unitarity equations for pion-pion scattering, 20: 6044
BROMLEY, R. G., Studies of trabecular bone in beagles and humans, 20: 5233 (COO-119-232, pp 99-121)
BROOME, F. H., New developments in close tolerance machining, 20: 6690 (Y-NA-14)
BROUDE, C., Gamma-ray transitions in ^{15}O and ^{15}N, 20: 6318
BROWN, G. E., Even parity states of ^{16}O and ^{17}O, 20: 6350
BROWN, G. E., Vibrations, strength functions and intermediate structure, 20: 6345
BROWN, Karl L., General first- and second-order theory of beam transport optics, 20: 5944 (SLAC-PUB-132)
BROWN, P. J., Magnetic structure of $MnSO_4$, 20: 6546
BROWNING, W. E., Jr., Standard surface for fission product deposition experiments, 20: 5665 (ORNL-TM-1304)
BRUENGER, F. W., Determination of half-periods of dog serum proteins using ^{35}S-L-methionine, 20: 5249 (COO-119-232, pp 203-18)
BRUENGER, F. W., Pilot study of effect of cortisol on $Na_3CaDTPA$ enhanced excretion of ^{239}Pu in beagle, 20: 5247 (COO-119-232, pp 188-99)
BRUGGER, R. M., Inelastic scattering with pulsed neutron sources, 20: 6258 (CONF-650217, pp 82-101)
BRUMBERG, I. Ye., Ultra-violet fluorescence of frog blood cells on cooling, 20: 5318
BRUNSON, Glenn S., Construction and utilization of small-dimension fission chambers, 20: 5734 (LFEN-NI-19)
BRUNST, V. V., Spinal cord in irradiated tail of young axolotl (Siredon mexicanum), 20: 5312
BRUSSAARD, P. J., Shell model calculations of ft values in $2s_{1\ 2}$ and $1d_{3\ 2}$ shells, 20: 6393
BRUZZESE, E., Influence of x rays on take of skin homografts, 20: 5335
BUBA, L., Comparison of consumption determination with sound activation and gamma spectroscopy for MTR element, 20: 6681 (SGAE-PH-18/1965)
BUCHANAN, C. D., Recent high energy electron investigations at Stanford University, 20: 6277 (AD-619952)
BUCHSBAUM, S. J., Turbulent mixing in laboratory plasma, 20: 6472
BUCHWALD, Nathaniel A., Adaptive responses to ionizing radiation, 20: 5319
BUDNITSKAYA, E. V., Unsaturated higher fatty acids of "free lipid" fraction from leaves of irradiated plants, 20: 5265
BUGG, W. M., Search for neutral scalar meson, 20: 6079
BUKAT, G. M., α-Decay and nuclear structure in region of ^{208}Pb, 20: 6423
BUKHALOVA, G. A., Lithium, cesium, and lanthanum fluoride systems, 20: 5558
BUKOWIECKI, B., Silicon surface-barrier detectors for alpha radiation dosimetry, 20: 5721 (CLOR/IBJ-II-37/D)
BULATOV, B. P., Back-scattering of gamma rays from spherical surfaces, 20: 6525
BULBULIAN, S., ^{99m}Tc generator using Fe_2O_3 as sorbent for ^{99}Mo, 20: 5591 (SGAE-CH-18/1965)
BULOS, F., Streamer chamber development, 20: 5739 (SLAC-PUB-140)
BUNCH, W. L., Technique for optimizing composition of regenerating neutron flux monitors, 20: 6567 (HW-SA-3600)
BURDG, C. E., Prog. rpt. on in-pile thermal conductance testing, 7–9/65, 20: 6565 (CEND-3336-251)
BURFORD, A. O., Lockwood—the wood of the future, 20: 5818
BURGGRAAF, R., Studies of trabecular bone in beagles and humans, 20: 5233 (COO-119-232, pp 99-121)
BURHOP, E. H. S., Hypernuclei, 20: 6283 (CERN-64-13(Vol.4), pp 137-86)
BURHOP, E. H. S., Location and analysis of neutrino interactions in photographic emulsion, 20: 6052
BURKE, Gerald, Radioactive iodine treatment of intractable angina pectoris, 20: 5460
BURLESON, G. R., Polarization of Λ^0 particle produced from protons in carbon nuclei by 1.17-Bev/c negative pions, 20: 6071
BURNER, Alvin M., USAF whole body gamma spectrometry, 20: 5427
BURNHAM, John B. Jr., Process for making nuclear fuel element, 20: 5873
BURR, A. F., Atomic energy levels, 20: 5984 (NYO-2543-1)
BURTE, B., Positive and negative chemotaxis as observed after destruction of cell by uv or laser microbeams, 20: 5396
BURTON, R. A., Prog. rpt. on liquid-metal lubricated journal bearings, 8–10/65, 20: 5613(R) (SWRI-1228-8-16)
BURWELL, W. G., Experimental refractive indices and theoretical small-particle spectral properties of selected metals, 20: 5879 (D-910092-6)
BUSH, G. E., High speed digital dynamic field measuring system,

20: 5682 (MURA-716)
BUSSOLATI, C., Fast coincidence system for low energy γ-ray spectroscopy, 20: 5770
BUSZA, W., Location and analysis of neutrino interactions in photographic emulsion, 20: 6052
BUTI, B., Collisional damping of transverse plasma oscillations, 20: 6499
BUTRA, F. P., Temperature and neutron irradiation effects on plastic deformation of alpha uranium single crystals, 20: 5916
BUTTLAR, H. v., Tritium concentration of German river waters, 20: 5654
BUZZI, G., Health protection against dangers of ionizing radiation, 20: 5433
BYCHKOVSKAYA, I. B., Absence of "oxygen after-effects" in Calandria granaris during hibernation induced with low temperature, 20: 5385
BYKHOVSKII, A. V., Radiation protection of personnel during uranium ore mining, 20: 5428
BYRNE, John T., Prog. rpt. on buoy dynamics, final, 10/65, 20: 6686 (NVO-98-12)
BYSHEVA, G. K., Measurement of relationship of proton pulse in ITEF, 20: 5941 (NP-15598)

C

CABE, Jean, Excitation curve of (n,2n) reaction on ^{63}Cu from 16.59 to 17.71 Mev, 20: 6319
CABLE, J. W., Magnetic structures of metallic erbium, 20: 6541
CABLE, J. W., Paramagnetic neutron scattering from metallic palladium, 20: 6544
CACCIARI, Alberto, Method for production of uranium, 20: 5870
CACHIN, Y., Surgery of larynx and hypopharynx after radiotherapy, 20: 5463
CAFORIO, A., Longitudinal polarization of low-energy muons from $K^+_{\mu 3}$ decay, 20: 6075
CAHILL, Thomas A., Polarization of 45 Mev protons by complex nuclei, 20: 6274 (AD-619061)
CALDWELL, J. T., Cross sections for ground- and excited-state neutron groups in reaction $^{16}O(\gamma,n)^{15}O$, 20: 6418
CALDWELL, William L., Increased sensitivity of in vitro murine leukemia cells to fractionated x-rays and fast neutrons, 20: 5361
CALOGERO, F., Integral expressions for difference between contiguous Dirac phase shifts, 20: 6126
CALOGERO, F., Integral expressions for arbitrary phase shift differences, 20: 6127
CAMBEL, Ali Bulent, Laminar and turbulent magnetohydrodynamic free jet, 20: 6175
CAMERON, A., Relevance of cosmic ray experiments to astrophysics, 20: 6012 (CONF-640919,pp III1-23)
CAMERON, J. F., Survey of systems for concentration and low background counting of tritium in water, 20: 5521
CAMION, P., Linear inequalities on total ordered linear integer ring, 20: 5831 (EUR-1919.f)
CAMPBELL, Philip M., Finite difference methods for nonlinear radiation transport, 20: 6522 (UCRL-12411)
CAMPISI, L. S., Solid-solid interactions. II., 20: 5545
CAP, Ferdinand, Interaction between magnetic field and flow field for plasmas of infinite conductivity, 20: 6444 (AD-617553)
CAPLAN, H. S., Calibration of radioactive gas monitors, 20: 5774
CAPP, M. Paul, Radiation problems in children with heart disease, 20: 5455
CAPPEL, H. H., SGR temperature transients, 20: 6620 (NAA-SR-Memo-11458)
CAPPELLANI, F., Germanium compensation by Li-drift in boiling liquids for p-i-n-diode construction, 20: 5702
CARLSON, O. N., Electrotransport of interstitial atoms in yttrium, 20: 5599
CARLSSON, Carl, Integral absorbed doses in roentgen diagnostic procedures. II., 20: 5440
CARMICHAEL, B. M., Effect of fission gas bubbles on response of molten fuel reactors to fast transients, 20: 6614 (LA-DC-7476)
CARNAHAN, W. H., Threshold Regge poles for coupled channels, 20: 6118
CARNIGLIA, S. C., Petch relation in single-phase oxide ceramics, 20: 5903
CAROVILLANO, R. L., Hydromagnetic eigenmodes in multipole fields, 20: 6492
CARPENTER, S. G., Prog. rpt. on W resonance integrals and Doppler coefficients, 7–9/65, 20: 6279 (AI-65-225)
CARPER, H. J., Prog. rpt. on liquid-metal lubricated journal bearings, 8–10/65, 20: 5613(R) (SWRI-1228-8-16)
CARVER, J. G., Prog. rpt. on Pu subcritical experiment program, 7–9/65, 20: 6607 (GEAP-4965)
CASEY, Albert, Effect of radiation on audition and conditioned responses in spanish goat, 20: 5369
CASTLEMAN, A. W. Jr., Chemical considerations in fast reactor safety, 20: 5878 (BNL-9667)
CATARA, F., Bound-state wavefunctions of nonlocal solvable potential, 20: 6119
CATINOT, Liliane, Suppression of diarrhea provoked in rat by fatal dose of x rays, 20: 5411
CATON, Roy D. Jr., Prog. rpt. on electrochemistry of some transition metals and lanthanides dissolved in molten alkali metaphosphate, 7/64–6/65, 20: 5529(R) (SC-DC-65-1706)
CAVINA PRATESI, A., Behavior of enterochromaffin cells of intestine of hedgehog irradiated during hibernation, 20: 5377
CELANDER, D. R., Utilization of inorganic radioselenium for biosynthetic labeling of tracer proteins, 20: 5262
CELANDER, Evelyn, Utilization of inorganic radioselenium for biosynthetic labeling of tracer proteins, 20: 5262
CELNIK, J., Shield small source experiments, 20: 6626 (UNC-5118)
CERMAK V., Induction of synthesis of phase and colicin in culture medium irradiated by uv rays, 20: 5279
CERVINI, A., Radiosensitivity of different meiotic stages of oocytes in parthenogenetic diploid artemia salina leach, 20: 5359
CHABRE, M., Energy dependence of polarization in p-^{16}O elastic scattering, 20: 6306 (UCRL-16217)
CHAFFEY, C. M., Neutron cross sections of thorium and analysis of resonances up to 1 kev, 20: 6377
CHALMERS, Bruce, Interaction of solid metal and liquid alloys, 20: 5895 (TID-22271)
CHANDRASEKHARAIAH, M. S., Thermodynamic study of urania–uranium system, 20: 5877 (ANL-7048)
CHANG, Chi-yo, Enhancement of functional activity of pars intermedia following ^{60}Co irradiation in toad, 20: 5394
CHANG, Yi-hsiang, Anisotropic hyperfine interaction of shallow donor electron with ^{29}Si nucleus, 20: 6001
CHAPPELL, Willard R., Dynamics of ionized media (plasmas), 20: 6448 (AD-619045)
CHARAKHCHYAN, A. N., Diffusion of solar cosmic ray protons in interplanetary space, 20: 5970
CHARAKHCHYAN, A. N., Energy spectrum of protons and α particles of cosmic ray flares on the sun, 20: 5969
CHARAKHCHYAN, T. N., Diffusion of solar cosmic ray protons in interplanetary space, 20: 5970
CHARAKHCHYAN, T. N., Energy spectrum of protons and α particles of cosmic ray flares on the sun, 20: 5969
CHAUDHURY, Manujendra L., Intensities of alpha spectra for parity-unfavoured transitions in spherical nuclei, 20: 6376
CHEATHAM, Daniel Washington Jr., Radio frequency generated cylindrical plasma with alkali metal injection, 20: 6447 (AD-618693)
CHEN, I-feng, Comparison of radiation sensitivity of chromosome in white blood cells of human beings, monkeys, and rabbits, 20: 5304 (JPRS-32985, pp 45-50)
CHEN, Joseph C. Y., Set of coupled second-order differential equations, 20: 6120
CHENG, L. J., Recovery of electrical properties in 45-Mev-electron-irradiated n-type Si, 20: 5920
CHERNOV, G. M., Angular distribution of shower particles in collisions between 24-Bev protons and nucleons and photoemulsion nuclei, 20: 6325
CHERNOVA, L. P., Angular distribution of shower particles in collisions between 24-Bev protons and nucleons and photoemulsion nuclei, 20: 6325
CHERNYAEV, V. A., Method of calculation of water and power costs for nuclear desalination plants, 20: 6649
CHERRINGTON, B. E., Helical instability produced in gaseous magneto-plasmas by gyro-interaction of microwaves, 20: 6446 (AD-617696)
CHESALIN, L. S., Dynamics of geomagnetic trap. I., 20: 7208
CHESAVAGE, A., Calibration of S10A radiation detection systems, 20: 6656 (NAA-SR-Memo-11333)
CHESLER, R. B., Analysis of gamma-ray circular polarization with transmission magnets, 20: 5764
CHESNOKOV, N. I., Radiation protection of personnel during uranium ore mining, 20: 5428
CHESTER, Conrad V., Effect of ionizing radiation on coalescence rates in liquid-liquid systems, 20: 5571 (ORNL-TM-1283)
CHEVALLIER, Pierre, Study of α emission of ^{230}Pa, 20: 6321
CHILD, Edward T., Method for preparing radioactive hydrocarbons, 20: 5593(P)
CHIR, B., Carcinogenic effects of ^{241}Am and ^{239}Pu in rat, 20: 5321
CHOHAN, A. S., Suitability of proportional counter as charged particle spectrometer and study of reaction $^{10}B(d,p)^{11}B$, 20: 5759
CHOU, Hsien-ting, Comparison of radiation sensitivity of chromosome in white blood cells of human beings, monkeys, and rabbits, 20: 5304 (JPRS-32985, pp 45-50)
CHRISTENSEN, W. R., ^{238}Th induced fractures in beagles, 20: 5288 (COO-119-232, pp 74-87)
CHRISTOPHER, S. S., Prog. rpt. on in-pile thermal conductance testing, 7–9/65, 20: 6565 (CEND-3336-251)
CHRISTOPHOROU, L. G., Interaction of thermal electrons with polarizable and polar molecules, 20: 5985 (ORNL-TM-1262)
CHUBURKOV, Yu. T., Production of ^{242}Pu and ^{242}Cm by irradiating ^{241}Am

with neutrons, 20: 5823 (ORNL-tr-892)
CHWASZCZEWSKA, J., Silicon surface-barrier detectors for alpha radiation dosimetry, 20: 5721 (CLOR/IBJ-II-37/D)
CHYLINSKI, Z., Momentum-invariants and Lorentz-covariant form of physical laws, 20: 6214 (INR-610/VI/PH)
CHYZEWSKI, Adam, Radiometric measurements of diffusion rate of ferric ions in solutions, 20: 5556
CIABOTTI, Arnaldo, Late complications in subjects treated with radioactive iodine, 20: 5469
CIBOIS, E., Influence of irradiation on some carbon or low-alloy steels, 20: 5921
CLARIDGE, R. F. C., Production of trapped radicals from alkyl halides in organic glasses, 20: 5577
CLARK, B. C., Charge distributions of ^{40}Ca and ^{44}Ca from 250-Mev electron scattering, 20: 6413
CLARK, B. C., Recent high energy electron investigations at Stanford University, 20: 6277 (AD-619952)
CLARK, George, Gamma-ray induced showers, 20: 6013 (CONF-640919, pp IV17-33)
CLARKE, David O., Correlation of bone strength with radiation dose from internal emitters and bone resorption, 20: 5289 (COO-119-232, pp 88-98)
CLARKE, E. M., Electron–H-atom elastic-scattering resonances, 20: 5999
CLAYTON, C. G., Examples of recent developments in use of radioactive isotopes in British industry, 20: 5817
CLEMMESEN, J., Statistical studies in etiology of malignant neoplasms. I., 20: 5307
CLINE, D., ^{39}K(^{3}He,α)^{38}K and ^{39}K(^{3}He,^{3}He)^{39}K reactions, 20: 6367
CLINTON, S. D., Laboratory preparation of uranium nitride microspheres by sol–gel technique, 20: 5864 (ORNL-3879)
CLOUGH, W. R., Prog. rpt. on metallurgical studies of Zr and Th and of alloying behavior of rare earth-transition metal systems, final, 11/65, 20: 5891 (NYO-2159-1)
CLUFF, Leighton E., Effect of endotoxin upon susceptibility to infection: role of granulocyte, 20: 5315
COCCONI, G., Sonic spark chamber system, 20: 5720 (CERN-65-33)
COCHRAN, D. R. F., Radiation and shielding design factors for Los Alamos meson physics facility, 20: 5940 (LA-DC-7522)
COCKING, S. J., Multiple scattering in plane samples, 20: 6253 (AERE-R-5016)
COE, Harold H., Summary of thermophysical properties of potassium, 20: 5886 (NASA-TN-D-3120)
COGLIATI, Guido, Method for production of uranium, 20: 5870
COHEN, J. P., Reaction (p,2p) on some isotopes of titanium, 20: 6330
COHEN, R. C., μ Capture in oxygen, 20: 6273 (AD-617398)
COHN, H. O., Search for neutral scalar meson, 20: 6079
COHN, S. H., Formulation and testing of compartmental model for calcium metabolism in man, 20: 5260
COIGNET, G., 141-Mev polarized proton beam of Orsay synchrocyclotron, 20: 6328
COLE, L. J., Homograft response and hemagglutinin production by sensitized thymectomized irradiated adult mice, 20: 5408 (USNRDL-TR-920)
COLE, Robert K., Elastic and inelastic scattering of 30.3 Mev protons by Si, 20: 6339
COLEMAN, C. E., Fracture characteristics of hydrided α-zirconium, 20: 5905
COLI, M., Operative definition of threshold of tunnel diode switching circuits, 20: 5700
COLICHMAN, Eugene L., Preparation of radiation-cured elastomeric rocket propellants, 20: 5588(P)
COLLARD, H., Recent high energy electron investigations at Stanford University, 20: 6277 (AD-619952)
COLLIER, Richard E., Irradiation therapy of the larynx, 20: 5486
COLLIN, J. E., Mass spectrometry study of diphenyl pyrolysis, 20: 5563 (EUR-2482.f)
COLVETT, Robert, Alternating gradient synchrotron conversion summary, 20: 5932 (BNL-9662)
COMBE, J. C., Magnetic moment experiments, 20: 6282 (CERN-64-13 (Vol.4), pp 97-136)
COMSTOCK, Craig, Three fluid model ionosphere, 20: 6179 (AD-618911)
CONDO, G. T., Search for neutral scalar meson, 20: 6079
CONEYBEAR, J. Frank, Electric propulsion possibilities using steam space 20: 5639
CONGDON, C. C., Spleen weight as measure of marrow cell growth in irradiated mice, 20: 5372
CONSTANTINIDES, C., Formulation and testing of compartmental model for calcium metabolism in man, 20: 5260
CONTOGOURIS, A. P., Solutions of singular N/D equations. II., 20: 6131
CONTOGOURIS, A. P., Solution of singular N/D equations. I., 20: 6130
CONZETT, H. E., Energy dependence of polarization in p-^{16}O elastic scattering between 21 and 53 Mev, 20: 6306 (UCRL-16217)
COOK, H. D., Computer control and data processing for isotopic mass spectrometers, 20: 5684 (WAPD-T-1770)
COOK, Merlin M., Study of as-cast and heat-treated uranium-base dilute-carbon alloys by optical and electron microscopy, 20: 5887 (NLCO-953)
COOKE-YARBOROUGH, Ion chamber dosimeter for nuclear radiations, 20: 5803
COOPER, A., Estimate of induced radioactivity in accelerators, 20: 5933 (CERN-65-34)
COPPI, Bruno, Collisional interchange instabilities in shear and $\int dl/B$ stabilized systems, 20: 6461 (GA-6646)
CORDEY, J. G., Effect of finite temperature on electron cyclotron resonance instability, 20: 6458 (CLM-R-44)
CORELLI, J. C., Recovery of electrical properties in 45-Mev-electron-irradiated n-type Si, 20: 5920
CORNELIUS, Archie Junior, Investigation of instabilities encountered during heat transfer to supercritical fluid, 20: 5622 (ANL-7032)
CORNILLE, Henri, Singular logarithmic potentials in coordinate space, 20: 6121
CORNWELL, Robert G., Nuclear spins and moments of ^{43}Sc and ^{45}Ti, 20: 6299 (PUC-1965-158)
CORRIGAN, S. J. B., Dissociation of molecular hydrogen by electron impact, 20: 5579
CORTELLESSA, G., Use of Monte Carlo method to solve programs of interpolation, 20: 6286 (ISS-65/10)
COSTACHEL, O., Investigations and practical applications of radioprotection in Rumania, 1958–1964), 20: 5425 (NP-15543, pp 77-82)
COUCHMAN III, C., Cavitation damage resistance of materials in liquid sodium, 20: 5861
COUEY, H. Melvin, Response of botrytis cinerea to gamma radiation, 20: 5371
COVA, S., Fast coincidence system for low energy γ-ray spectroscopy, 20: 5770
COVELLO, A., T = 2 states in ^{18}O, 20: 6341
COVER, Arthur, Direct radiochemical determination of ^{210}Pb in bone, 20: 5504
COVEYOU, R. R., Fourier analysis of uniform random number generators, 20: 5833 (ORNL-3866)
COX, D. E., Magnetic structure of $MnSO_4$, 20: 6546
COZ, Marcel, Projection operators for rearrangement collisions, 20: 6312
CRAMER, Frank B., Preparation of radiation-cured elastomeric rocket propellants, 20: 5588(P)
CRAMER, J., Different effect of bromouracildesoxyriboside and iodouracil-desoxyriboside in irradiation of herpes simplex-virus with uv light, 20: 5363
CRANNELL, C., Recent high energy electron investigations at Stanford University, 20: 6277 (AD-619952)
CREEDON, John E., High-density plasmas, 20: 6449 (AD-619370)
CRETEN, W. L., Z dependance of bremsstrahlung of electrons between 2.5 and 4.0 Mev, 20: 6432
CREWS, Quintous E. Jr., Combined use of 5-fluorouracil and 2-Mev radiation in advanced solid tumors in man, 20: 5452
CRONENBERGER, D., 141-Mev polarized proton beam of Orsay synchrocyclotron, 20: 6328
CROPPER, Wendell P., Apparatus for x-ray determination of metal in hydrocarbon fuel, 20: 5522(P)
CROUTHAMEL, C. E., Energy conversion, 20: 6024 (ANL-6925, pp 235-47)
CRUMP, M. Dominique, Effects of gamma radiation on electrical properties of muscle, 20: 5293 (COO-205-55, Paper 2)
CSAKANY, Antal, Semiconductor-type nuclear radiation detectors and spectrometers, 20: 5763
CSAKY, Laszlo, Effect of x-ray on phosphorus metabolism of glioma cultures, 20: 5255
CUEER, Pierre, Detection of products of fission and of fragmentation of metals under effect of 3-Bev protons, 20: 5756
CURLEY, E. K., Electron–H-atom elastic-scattering resonances, 20: 5999
CUSYNIN, V. I., Effect of electric field on radiolysis of liquid hydrocarbons, 20: 5575

D

DAKE, S., Remark on 30 Bev jet showers, 20: 6039 (INSJ-90)
DAKHNO, L. G., Influence of strong interactions between final state π-mesons on probability ratio of $K \to 3\pi$ decays, 20: 6086
D'ALELIO, Gaetano, Isobutylene-diene copolymerization by low temperature irradiation, 20: 5589(P)
DALIDCHIK, F. I., Role of identity of colliding nuclei in neutron tunnelling transfer, 20: 6387
DALLEY, V. M., Radiation therapy in relation to malignant tumors of temporal bone, 20: 5474
DANA, Jiri, Fast amplitude discriminator, 20: 5694
DANDEU, Yves, Calculations of ψ, ϕ, and of their derivatives, 20: 5829 (CEA-R-2824)
D'ANGELO, Nicolo, Ion-electron recombination, 20: 5994
DANIEL, H., Spectral form of $(0 \to 0)$-β transitions with parity change:

^{144}Ce, ^{144}Pr, and ^{166}Ho, 20: 6370
DANIEL, R. R., Electron component of primary cosmic radiation at energies ≳15 Bev, 20: 6022
DANIELS, G. M., Time delays between intensity variations of 3914 A and 5577 A spectral lines in artificial auroras, 20: 6203
DANIELSON, G. C., Measurement of piezoresistance in semiconductors, 20: 5883 (IS-1268)
DANKO, Joseph C., Thermoelectric nuclear fuel elements, 20: 6598
DARRAH, James G., Process for making nuclear fuel element, 20: 5873
DARRAS, R., Zirconium–copper alloys resistant to oxidation by carbon dioxide at high temperature, 20: 5860
DARRIULAT, P., Configurations of three α particles in ^{12}C, 20: 6371
DARVES-BLANC, Robert, Evidence of two-body interactions in reaction ^{9}Be(n,2n) at 14 Mev, 20: 6320
DAS GUPTA, K., Energy level diagrams of oxides of magnesium, aluminum and silicon, 20: 6532 (CALT-221-13)
DASH, J. G., Effects of turbulence in He II thermal counterflow, 20: 6230
DA SILVEIRA, Rui, Evaporation of charged particles from heavy nuclei, 20: 6364
DAUER, M., X-irradiation of pupae of house fly Musca domestica L. and adult survival, 20: 5331
DAVIDSON, J. P., Programs for collective nuclear model calculations in deformed even-even nuclei, 20: 6278 (AD-623877)
DAVIS, D. H., Location and analysis of neutrino interactions in photographic emulsion, 20: 6052
DAVIS, James A., Transport synthesis, 20: 6264 (WAPD-T-1849)
DAVIS, M. E., Standard surface for fission product deposition experiments, 20: 5665 (ORNL-TM-1304)
DAYTON, R. W., Reactor materials, 20: 5842
DAYTON, R. W., Reactor materials, 20: 5847
DE BAR, Roger, One-dimensional eulerian hydrodynamics difference equations, 20: 6162 (UCRL-12238-T)
DE BARROS, S., Determination of spin and resonance parameters for ^{197}Au + n at 10 to 1000 ev, 20: 6392
DEBEAUVAIS, Monique, Comparison of registration of tracks of heavy ions in ionographic emulsions and in various solid materials, 20: 5755
DEBEAUVAIS, Monique, Detection of products of fission and of fragmentation of metals under effect of 3-Bev protons, 20: 5756
DEBERDEEVA, R. Yu., Determination of TBP, kerosene, and synthol, 20: 5516
DE BOTTON, N., Elastic scattering of photons in region of giant resonance, 20: 6349
DE CHOUDENS, Henri, Study of some radioprotection apparatuses used near swimming-pool reactors, 20: 6670 (CEA-R-2864)
DE CRESCENTE, M. A., Fission gas migration studies in uranium carbide, 20: 5892 (PWAC-476)
DE CRESCENTE, M. A., Thermal conductivity and electrical resistivity of uranium monocarbide, 20: 5893 (PWAC-480)
DEDEKIND, Kendra, Studies of trabecular bone in beagles and humans, 20: 5233 (COO-119-232, pp 99-121)
DEDOV, V. B., Production of ^{242}Pu and ^{242}Cm by irradiating ^{241}Am with neutrons, 20: 5823 (ORNL-tr-892)
DEERING, W. D., Excitation of plasma resonances by small pulsed dipole, 20: 6498
DEGENHARDT, K. H., Clefts of lips, jaws and palate induced in mice by means of x-rays, 20: 5337
DEGENHARDT, K. H., Median jaw and tooth fusion induced by x irradiation in mouse, 20: 5395
DEGENHARDT, K. H., Significance of experimental malformations of head region, 20: 5316
DEHNE, H.-C., Inelastic multiple pion production in antiproton–proton interactions for 3.6 Bev/c, 20: 6097
DE JUREN, J. A., SCAP—in IBM 7094 code for spectral analysis of pulsed-neutron decay data, 20: 6585 (NAA-SR-Memo-10941)
DEKABAN, Anatole, Persisting clone of cells with abnormal chromosome in woman previously irradiated, 20: 5351
DE LEONE, Ruggero, Method for production of uranium, 20: 5870
DELPUECH, Jacques, Study of some radioprotection apparatuses used near swimming-pool reactors, 20: 6670 (CEA-R-2864)
DEL VECCHIO, V., Determination of ^{90}Sr in deciduous teeth, 20: 5655
DE MARIA, G., Mass-spectrometric study of yttrium–carbon system, 20: 5540
DEME, Sandor, Semiconductor-type nuclear radiation detectors and spectrometers, 20: 5763
DEMIRKHANOV, R., Heating of plasma under conditions of beam instability, 20: 6468 (ORNL-tr-871)
DEMKOV, Yu. N., Density matrix for system of noninteracting fermions, 20: 6147
DEMKOV, Yu. N., Ground-state energy of He, 20: 5987 (ANL-Trans-248)
DEMMIG, F., Invariant Lagrange formalism and conservation principles, 20: 6155
DENISON, M. Richard, Physical property distributions in low-pressure crossed-field plasma accelerator, 20: 6470
DENIZ, Valentine-C., Neutron density decay constant in non-multiplying lattice of finite size, 20: 6580 (CEA-R-2702)
DENNIS, P. R., Plasma jet technology, 20: 5633 (NASA-SP-5033)
DE PANGHER, J., Neutron fluence measurements for second test at Pulstar Reactor, 20: 6679 (NP-15645)
DEPTULA, Czeslaw, Solvent extraction of inorganic compounds, 20: 5600
DE ROBIEN, Emmanuel, Study of some radioprotection apparatuses used near swimming-pool reactors, 20: 6670 (CEA-R-2864)
DEROITE, Andre, Method for oxidation of Pu(III) to Pu(IV) in basic solution, 20: 5561
DESER, S., Some properties of quantum linearized Einstein field, 20: 6224
DESHCHEREVSKII, V. I., Effect of D_2O on vital staining and heat stability of skeletal muscles of frog, 20: 5317
DESHPANDE, N. G., Vertex-function poles and bootstrap condition in field theory, 20: 6138
DESSAUER, G., Production of transplutonium elements at Savannah River, 20: 5822 (DP-1000)
DE VINCENTIS, J., Evaluation of Yankee vapor container leakage monitoring system, 20: 6631 (YAEC-1005)
DE VOMECOURT, Annick, Suppression of diarrhea provoked in rat by fatal dose of x rays, 20: 5411
DE VRIES, M. J., Biochemical and morphological changes in lymphatic tissues after partial-body irradiation, 20: 5341
DE WAARD, H., Optical method for absolute velocity calibration of Moessbauer spectrometers, 20: 5786
DEWING, Stephen B., Radiotherapy of benign disease, 20: 5490
DIACONESCU, A., Use of tracers and of intense radiation sources in industrial processes, 20: 5814 (NP-15543, pp 27-45)
DIAMOND, J. J., Bibliography on high temperature chemistry and physics of materials in condensed state, 20: 5527 (NP-15646)
DICE, D. T., Urethane manipulator gauntlets, 20: 5612 (ORNL-TM-1326)
DICKINSON, J. G., Range of protons in human skullbone, 20: 5475
DIDDENS, A. N., Sonic spark chamber system, 20: 5720 (CERN-65-33)
DIEBOLD, R., Streamer chamber development, 20: 5739 (SLAC-PUB-140)
DIENSTBIER, Zdenek, New metabolic and hematologic aspects in pathophysiology of postirradiation changes, 20: 5308
DIETHELM, L., Radiotherapy of cancer, 20: 5442
DIETZ, Leonard A., Basic properties of electron multiplier ion detection and pulse counting methods in mass spectrometry, 20: 5706
DIMCHEV, Teodor, Low-background beta scintillation counting method, 20: 5783
DIMITRIU, Aurora, Action of radiomimetic compounds (nitrogen mustard) on protein macromolecules, 20: 5423
DISTENFELD, Carl, Alternating gradient synchrotron conversion summary, 20: 5932 (BNL-9662)
DI TORO, M., Bound-state wavefunctions of nonlocal solvable potential, 20: 6119
DITTMAN, Roger R., Elastic and inelastic scattering of 30.3 Mev protons by Si, 20: 6339
DMITRIEV, V. N., Use of gamma-gamma coincidence spectrometer with summation of pulse amplitudes for analysis of a mixture of radioactive isotopes, 20: 5753
DOBROVOL'SKII, S. P., Study of dose rate field with γ source of spent reactor fuel elements, 20: 6597
DOCKUM, N. L., Bioassay of influence of cortisol in bones of growing rabbits, 20: 5234 (COO-119-232, pp 122-52)
DOCKUM, N. L., Studies of trabecular bone in beagles and humans, 20: 5233 (COO-119-232, pp 99-121)
DOERING, D. A., STMGEN—computer code for design of steam generator, 20: 5606 (GAMD-6675)
DOLESHAL, P., Effects on resonance modes on channel coupling in nuclear reactions, 20: 6426
DOLINSKY, E. I., Feynman graph treatment of initial and final state interactions in direct nuclear reactions, 20: 6383
DOMAREVA, O. P., Role of vegetative nervous system in transfering remote radiation effects, 20: 5421
DONDRAT'EV, K. Ye., Structural characteristics of fields of outgoing radiation according to data of artificial satellites Tiros II and Tiros III and their interpretation, 20: 6019
DONHOWE, J. M., Shape of neutron yield from ^{7}Li(p,n)^{7}Be reaction near threshold, 20: 6355
DORABIALSKA, Alicja, Radiometric measurements of diffusion rate of ferric ions in solutions, 20: 5556
DORONIN, P., Structural characteristics of fields of outgoing radiation according to data of artificial satellites Tiros II and Tiros III and their interpretation, 20: 6019
DOUGHERTY, Jean H., Comparison of two methods of analyzing hematological data from ^{90}Sr injected beagles, 20: 5290 (COO-119-232, pp 165-89)
DOUGHERTY, T. F., Pilot study of effect of cortisol on $Na_3CaDTPA$ enhanced excretion of ^{239}Pu in beagle, 20: 5247 (COO-119-232, pp 188-99)
DOUGHERTY, Thomas F., Prog. rpt. on radiobiology, annual, 1964, 20: 5230 (COO-119-232)

DOUGLAS, D. A., Properties and prospects of thoria-base nuclear fuels, 20: 5915 (ORNL-P-1724)
DOULL, John, Modification of a hyperbaric oxygen chamber for use in hypobaric oxygen exposure studies, 20: 5228 (AD-623599, pp 28-36)
DOYLE, William P., Method for preparing radioactive hydrocarbons, 20: 5593(P)
DRAGT, A. J., Relativistic three-particle SU_3 states, 20: 6113
DRALEY, J. E., Electrochemical model for oxidation of zirconium, 20: 5858
DREIZLER, R. M., Self-consistent theory of bounded rotational spectra. I., 20: 6344
DREIZLER, Reiner, Interpretation of higher rotational states of deformed nuclei, 20: 6416
DREXLER, Guenter, Solid body dosimetry in radiotherapy, 20: 5479
DRIESCHNER, M., Further search for $Y_0^*(1405)$ production by K- at rest in emulsion, 20: 6051
DROZ, BERNARD, Radioautographic detection of proteins synthesized from leucine-^{3}H in mitochondria, 20: 5254
DROZDOV, V. E., Study of dose rate field with γ source of spent reactor fuel elements, 20: 6597
DU BOIS, Kenneth P., Effect of x-radiation on hexobarbital metabolizing enzyme system of liver microsomes, 20: 5283 (AD-623599, pp 16-27)
DU BOIS, Kenneth P., Influence of sublethal doses of x-radiation on synthesis of hepatic microsomal enzymes, 20: 5282 (AD-623599, pp 1-15)
DUBROVSKII, V. A., Propagation of weak disturbances in MHD, 20: 6170
DUC, Dao-wong, Classifications of meson resonances with higher spins in SU(6) symmetry theory, 20: 6151
DUCLOS, Donald P., Physical property distributions in low-pressure crossed-field plasma accelerator, 20: 6470
DUCROS, Georges, Method of and apparatus for recording pulse spectra, 20: 5797
DUDLEY, T. E., Infinite medium spectrum-weighted group constants for gamma heating calculations, 20: 6517 (CONF-651101-41)
DUFAURE, Jean-Pierre, Early destruction of gonads of viviparous lizard embryo by irradiation, 20: 5324
DUGAN, John V. Jr., Effects of metastable atoms on volume ion production in tenuous helium plasma, 20: 6464 (NASA-TN-D-3121)
DUGGELBY, J. C., Plastic scintillator as airborne gamma radiation detector, 20: 5761
DUNCAN, R., New Zircaloy end closure weld joint configuration, 20: 5865 (WCAP-3269-37)
DURAND, Pierre, Cherenkov telescope for study of cosmic radiation measurements at ground level, 20: 6014 (NP-15380)
DUSTAN, G. G., Tagging oriental fruit moth with radioactive phosphorus, 20: 5246
DUTHIE, Richard E. C., Engineering materials list, 11/65, 20: 5608 (TID-4102(1st Rev.))
DYMNIKOV, A. D., Spherical aberration of compound quadrupole lenses and systems, 20: 5696
DZANTIEV, B. G., Development of hot synthesis methods for ^{35}S labeled biologically active substances. III., 20: 5586
DZELEPOV, B. S., Determination of intensities and multipolarities of high-energy γ-transitions accompanying decay of ^{182}Ta, 20: 6347
DZYONYAR, Janos, Iodine storage in thyroid gland of human fetus, 20: 5259

E

EBEL, M. E., Cross section for production of possible bound cascade-nucleon system, 20: 6073
EBERLE, Siegfried Helmut, PHOTOMETERPROG 4—an IBM-7070 program for calculation of stability constants from spectrophotometric measurements, 20: 5526 (KFK-250)
EBERT, Wilhelm, Investigations on electric arcs in gravitationless state, 20: 6163
EBREY, Thomas G., Activation cross sections for reactions of Rh and Ru with 14.7 Mev neutrons, 20: 6338
ECCLES, S. F., Elastic and inelastic scattering of protons by ^{18}O, 20: 6373
EDMUND, Harry, Ion chamber dosimeter for nuclear radiations, 20: 5803
EDWARDS, M. R., Operating instruction for FORTRAN IV version of program gamma-P (NMP 468), 20: 6284 (GEMP-392)
EDWARDS, R. K., High temperature reactor materials development, 20: 5875 (ANL-6925, pp 165-74)
EGOROV, A. I., Electrophoretic filter for purifying reactor water, 20: 6568
EGOROV, Yu. A., Attenuation of reactor radiations in serpentine sand, 20: 6524
EHLERS, Vernon J., Hyperfine-structure anomaly of ^{131}Cs, 20: 6401
EICK, Harry A., Samarium borides. Tetraboride–hexaboride conversion, 20: 5551
EISENSTADT, Melvin M., Beam source for molecular and atomic hydrogen, 20: 6000
EISMONT, V. P., Fission neutrons of excited nuclei, 20: 6313
EJIRI, H., Strongly excited levels of ^{39}Ca in ^{40}Ca(^{3}He,α)^{39}Ca reaction, 20: 6398
EKLIND, O., Experimental study of natural circulation in loop with parallel flow test sections, 20: 5620 (AE-200)
EKSTROEM, L., Study of atmospheric effects on cosmic ray records from plastic scintillation monitors at Uppsala, 20: 6004 (AD-619508)
EL-AASSAR, M. R., Gamma intensities in decay of ^{187}W, 20: 6397
ELAD, E., Preamplifier with 0.7 kev resolution for semiconductor radiation detectors, 20: 5772
ELBEK, B., Vibrational states of deformed nuclei populated by (p,2n) reaction, 20: 6366
ELISEEV, S. M., Statistical analysis of 17 Bev pion interaction with heavy emulsion nuclei, 20: 6287 (JINR-P-2373)
ELKINA, N. I., Activity of deamination of adenosine and adenylic acid in tissues of irradiated rabbits, 20: 5380
ELKOUBY, A., Study of parameters of light-water reactors. I., II., III., 20: 6582 (EUR-2461.f)
ELLINGTON, H. I., Low-voltage diffuse discharge in atmospheric-pressure helium with small additions of potassium, 20: 6159 (AERE-M-1597)
ELLIOTT, R. O., Behavior of some delta-stabilized plutonium–gallium alloys at high pressures, 20: 5884 (LA-2312)
EL-SAYAD, G. M., Gamma intensities in decay of ^{187}W, 20: 6397
ELSTON, D. L., Plasma spraying of protective coatings, 20: 5837 (NLCO-966)
EL'TEKOV, V. A., About absorption of gamma ray energy by point sources in macrosystems, 20: 5751
ELYUTIN, V. P., Viscosity of liquid zirconium, 20: 5899 (JPRS-32341, pp 1-7)
EMEL'YANOV, I. Ya., Dynamic characteristics of first reactor of I. V. Kurchatov Beloyarsk Nuclear Power Station, 20: 6634
EMERY, F. E., Average energy expended per ionized electron-hole pair in silicon and germanium as function of temperature, 20: 5784
EMRICH, D., Results of radioiodine treatment of thyroid cancer, 20: 5488
EMRICH, K., Validity of quasi-particle approximation in nuclear physics, 20: 6433
ENDEBROCK, R. W., Reactor materials, 20: 5842
ENDEBROCK, R. W., Reactor materials, 20: 5847
ENGELBERTINK, G. A. P., Shell model calculations of ft values in $2s_{1/2}$ and $1d_{3/2}$ shells, 20: 6393
ENGELKE, M. J., Area radiation monitor system with logarithmic indication and audiovisual warning, 20: 5733 (LA-DC-6790)
ENGELMANN, P., Behavior of zero-power reactors in reactivity perturbations, 20: 6674 (KFK-332)
ENGELS, E. Jr., Measurement of proton-proton triple scattering at 430 Mev, 20: 6056
ENGLER, J., Search for heavy electron by electron-proton coincidence measurements, 20: 6078
ENGSTROM, L. L., Gamma-ray evaluation of diagnostic shielding barriers, 20: 5677
ERICKSON, Deane G., Fate of gamma-irradiated Schistosoma mansoni cercariae in mice, 20: 5313
ERMAKOV, S. V., Thermionic emission of hexaborides of samarium and gadolinium, 20: 5532(T) (K-Trans-10)
ERMAKOV, V. A., Production of ^{242}Pu and ^{242}Cm by irradiating ^{241}Am with neutrons, 20: 5823 (ORNL-tr-892)
ESCH, Harald E., Influence of environmental conditions on radiation sensitivity of Nitella flexilis, 20: 5294 (COO-205-55, Paper 3)
ESCHBACH, E. A., Fuel conservation indexes for thermal reactors, 20: 6610 (HW-79287)
ESCHELBACHER, H., High frequency structure for proton linear accelerator, 20: 5937 (KFK-346)
ESTERLUNG, R. A., Oxygen-13, 20: 6405
EVERETT, M. R., Coolant purification and coolant chemistry for "Dragon" high temperature gas cooled reactor, 20: 6639
EVIATAR, Aharon, Scattering of test-particle by enhanced plasma fluctuations, 20: 6497
EVKINA, Z. F., Temperature and neutron irradiation effects on plastic deformation of alpha uranium single crystals, 20: 5916
EVVARD, John C., Wheel-flow gaseous-core reactor concept, 20: 6662 (NASA-TN-D-2951)

F

FABER, Mogens, Antioxidants and lipoperoxides in organs of irradiated rats, 20: 5339
FABJAN, C. W., Study of semiconductor surface barrier detectors at 4.2°K, 20: 5790
FAGER, Charles A., Pituitary ablation in treatment of diabetic retinopathy, 20: 5468
FAINBERG, Ya. B., Interaction of modulated beam with plasma, 20: 6474
FAIRHURST, William, Manufacture of nuclear reactor fuel elements, 20: 5871
FAIRSTEIN, E., Nuclear pulse amplifiers—fundamentals and design

practice. Part 3., 20: 5780
FALK, Raphael, Viability of heterozygotes for induced mutations in Drosophila melanogaster. I., 20: 5358
FARBER, Milton, Thermodynamic and physical properties of beryllium compounds. VIII., 20: 5554
FARCHI, G., Use of Monte Carlo method to solve problems of interpolation, 20: 6286 (ISS-65/10)
FARZINE, K., Tritium concentration of German river waters, 20: 5654
FATKULLIN, M. N., Quiet solar-diurnal variations of geomagnetic field during IGY. I., 20: 6191
FAVUZZI, E., Influence of x rays on take of skin homografts, 20: 5335
FAYARD, Christian, Study of vlf radiation by use of Nike-Cajun rocket, 20: 6180 (AD-619250)
FAYYAZUDDIN, Two types of baryons in broken $(SU_3)_L \otimes (SU_3)_R$ symmetry, 20: 6070
FEDER, H. M., Calorimetry, 20: 5523(R) (ANL-6925, pp 175-85)
FEDER, H. M., High temperature reactor materials development, 20: 5875 (ANL-6925, pp 165-74)
FEDOROVA, G. V., Entrance of ^{14}C into spawn and grubs of autumn spawning fishes, 20: 5261
FEDOROVA, T. T., Urinary secretion of thymidine following whole-body exposure of rats to various doses of x radiation, 20: 5382
FEIT, J., Secondary protons from cosmic-ray collisions in space, 20: 5973
FEJER, J. A., Excitation of plasma resonances by small pulsed dipole, 20: 6498
FELDMAN, Jerome M., Radioactive iodine treatment of intractable angina pectoris, 20: 5460
FELDMAN, Michael, Reversion by erythropoietin of suppression of erythroid clones caused by transfusion-induced polycythemia, 20: 5242
FEL'DSHTEIN, Ye. I., Quiet solar-diurnal variations of geomagnetic field during IGY. I., 20: 6191
FENYVES, E., Physical fundamentals of nuclear radiation measurements, 20: 5795
FERBEL, T., $K_2^0 \rightarrow \pi^+\pi^-\pi^0$ decay, 20: 6031 (BNL-9613)
FERRARI, Sergio, Method for production of uranium, 20: 5870
FERRIS, L. M., Acid leaching of products from fluidized-bed combustion of graphite-base reactor fuels and $HF-O_2$ disintegration of stainless steel- and zirconium-clad oxide fuels, 20: 5500 (ORNL-3876)
FERRONI, S., Peripheral model and its application to photodisintegration of ^6Li, 20: 6368
FERTIK, S. M., Low-inductance capacitors, 20: 5688 (UCRL-Trans-1273(L))
FERZIGER, Joel H., Energy-dependent neutron transport theory in plane geometry. II., 20: 6252 (AD-617880)
FERZIGER, Joel H., Energy-dependeat neutron transport theory in plane geometry. III., 20: 6253 (AD-617882)
FETISOV, V. N., Effects of resonance modes on channel coupling in nuclear reactions, 20: 6426
FETTER, Alexander L., Spherical impurity in infinite superconductor, 20: 6239
FIEDLER, H. J., Study of $^{203}Tl(n_{th},\gamma)^{204}Tl$ reaction, 20: 6411
FIKIORIS, John G., Electromagnetic field inside current-carrying region, 20: 5930
FILIPPOVA, H. F., Changes in process of cell division and nucleus structure under the influence of irradiation and radiotoxins, 20: 5390
FILYASHINA, G. A., Influence of low doses of internal irradiation of some aspects of water, mineral, and nitrous metabolism in animals. II., 20: 5381
FILZ, Robert C., Time and altitude depeadence of 55-Mev trapped protons, Aug. 1961 to June 1964, 20: 6200
FINDENEGG, G., Mechanism of uptake of trace elements by plant roots, 20: 5258
FINDLAY, J. A., Average volumetric concentration in two-phase flow systems, 20: 5629
FINK, H. J., Critical state of superconducting surface sheath, 20: 6243
FINK, H. J., Exact solutions of superconducting surface sheath, 20: 6240
FINK, Uwe, High resolution measurements on infrared absorption spectrum of HBr, 20: 5550
FINK, William J., Neoplasms of liver following injection of thorotrast, 20: 5311
FINNEMORE, D. K., Coexistence of antiferromagnetism and superconductivity, 20: 6247
FINNEY, H. M. A., Ionoluminescence of MgO and Zn_2SiO_4 : Mn, 20: 5573
FIRK, F. W. K., Capture by ^{124}Sn of 62-ev neutrons, 20: 6317
FISCHER, K., Measurement of pion electron scattering cross section for 16 Bev/c pions, 20: 6098
FISHER, George Phillip, Experimental investigation of K_{23}^0 decay, 20: 6095
FISHOVA, T. Ye., Spherical aberration of compound quadrupole lenses and systems, 20: 5696
FIVEL, Daniel I., Solution of scattering and bound state problems by construction of approximate dynamical symmetries, 20: 6215 (NP-15614)
FLATO, M., Connection between external and internal symmetries, 20: 6142
FLEROV, G. N., Extraction of heavy ion beam from cyclotron with azimuthal variation of magnetic field, 20: 5947 (ANL-Trans-241)
FLETCHER, N. R., DWBA analysis of $^{12}C(d,p\gamma)^{13}C$ with measured optical model parameters, 20: 6362
FLIEDNER, Theodor M., Mammalian radiation lethality. A disturbance in cellular kinetics, 20: 5405
FLOOD, Walter A., Prog. rpt. on Project Aurora III, final, 2/12/62–6/15/65. I. and II., 20: 6182(R) (AD-619447)
FLUHARTY, R. G., Sub-critical neutron amplifier systems, 20: 6257 (CONF-650217, pp 11-24)
FLUKE, Donald J., Radiation indication of subunit of lactic dehydrogenase, 20: 5276
FOLSOM, T. R., Method for low-level gamma radioactivity measurement, 20: 5432
FOMINYKH, V. I., International comparison of neutron sources, 20: 6265
FORBES, Robert S., Foldable fallout shelter, 20: 5632(P)
FORBES, V. M., Second maximum of cosmic-ray star frequency under lead, 20: 6015
FORD, C. Hobbard, Critical mass studies with NASA Zero Power Reactor II. I. Clean homogeneous configurations, 20: 6587 (NASA-TN-D-3097)
FORSAITH, Ann L, Spintharicon: new approach to radiation imaging, 20: 5461
FORTESCUE, Peter, Heat extraction system for nuclear reactor, 20: 6647
FORYS, Mechislav, Measurements of ^{14}C radioactivity in organic compounds, 20: 5511
FOUCHER, R., Disintegration of ^{134}Cs, 20: 6327
FOUCHER, R., Investigation of rotation levels in odd-odd nucleus ^{234m}Pa, 20: 6331
FOX, John Dana, Deuteron Compton effect, 20: 6094
FOX, Thomas A., Critical mass studies with NASA Zero Power Reactor II. I. Clean homogeneous configurations, 20: 6587 (NASA-TN-D-3097)
FRADKIN, D. M., Integral expressions for difference between contiguous Dirac phase shifts, 20: 6126
FRADKIN, D. M., Integral expressions for arbitrary phase shift differences, 20: 6127
FRAENKEL, George K., Electron spin resonance studies of deuterium isotope effects, 20: 5566
FRAHN, W. E., Fresnel and Fraunhofer diffraction in nuclear processes, 20: 6359
FRANCAVIGLIA, S., Two channel problem and inelastic unitarity condition in Eigen-states of total angular momentum, 20: 6105 (ISS-65/14)
FRANCO, L., Health protection against dangers of ionizing radiation, 20: 5433
FRANCO, Victor, Qualitative aspects of neutron-nuclear interactions and optical model, 20: 6404
FRANKE, H. G., Spread times of discharges in self-quenching counters. V., 20: 5789
FRANTSEVICH, I. N., Oxidation of binary alloys, 20: 5854 (JPRS-32341, pp 8-16)
FRANZ, E. M., Cross sections for production of ^{149}Tb from Au by high-energy protons, 20: 6372
FRANZEN, W., Spin polarization of slow electrons by elastic resonance scattering from neon, 20: 5998
FRANZINETTI, C., High-energy neutrino interactions, 20: 6036 (CERN-64-13(Vol.4), pp 51-95)
FRAZER, B. C., Magnetic structure of $MnSO_4$, 20: 6546
FREEMANTLE, R. G., Evaluation and compilation of data for U. K. Nuclear Data Library, 1/65, 20: 6254 (AEEW-M-503)
FRENCH, Francis W., Radiation shielding requirements for manned satellites, 20: 5673
FRESNES, Botiment K., Improvements in or relating to control rod mechanisms for nuclear reactors, 20: 6569
FREUDIGER, F. S., Optimization status report, 20: 6605 (GAMD-6673)
FREUND, Peter G. O., Relation between πp, pp, and $\bar{p}p$ scattering at high energies, 20: 6081
FRIED, H. M., Green functions of Thirring model, 20: 6128
FRIEDEL, Helmut, MHD characteristics and dispersion relation for finite electrical conductivity, 20: 6157 (AD-617898)
FRIEDLANDER, G., Cross sections for production of ^{149}Tb from Au by high-energy protons, 20: 6372
FRIND, Gerhard, Ablation-type plasma generator, 20: 6488
FRONTEAU, J., Liouville theorem and general problem of stability, 20: 5830 (CERN-65-38)
FUCHS, N., Extension of theorem of Streater, 20: 6141
FUFAEVA, O. L., Temperature and neutron irradiation effects on plastic deformation, 20: 5916
FULDE, Peter, Equivalence of different pair-breaking mechanisms in superconductors, 20: 6233
FULKERSON, William, Catalytic activation of Vycor glass for H_2–D_2 exchange reaction by beta irradiation, 20: 5578
FULMER, Richard Harry, Nuclear structure studies in nickel isotopes with

(d,p) and (d,t) reactions, 20: 6435
FULTZ, S. C., Cross sections for ground- and excited-state neutron groups in reaction $^{16}O(\gamma,n)^{15}O$, 20: 6418
FUMAGALLI, W., Germanium compensation by Li-drift in boiling liquids for p-i-n-diode construction, 20: 5702
FURNICA, Gheorghe, Action of radiomimetic compounds (nitrogen mustard) on protein macromolecules, 20: 5423
FURTH, H. P., Unstable precession under influence of drag forces, 20: 6493
FUSSELL, E. M., Dispersal studies on radioactive-tagged culex quinquefasciatus say, 20: 5240

G

GABELMAN, John W., Reconnaissance for uranium in northeast coastal Brazil, 20: 5659 (RME-4545(Rev.))
GABOVICH, M. D., Interaction of ion beams with plasma leading to "two-beam" instabilities, 20: 6467 (ORNL-tr-870)
GADDY, Rufus H., Automated analysis of lithium solutions, 20: 5496 (DP-985)
GAETA, R., Level scheme of ^{231}Th, 20: 6388
GAL, D., Investigations on AgI catalyst surface structure by isotope exchange reactions, 20: 5544
GALAKTIONOV, Yu. V., Large scintillation counters and counters for operation in magnetic fields, 20: 5736 (NP-15597)
GALAMBOS, John T., Cancer diagnosis by radioisotopic scanning, 20: 5450
GALASIEWICZ, Zygmunt M., Hydrodynamical equations for superfluid Fermi liquid and two-particle Green functions. I., 20: 6229
GALIBA, I., Investigations on AgI catalyst surface structure by isotope exchange reactions, 20: 5544
GAL'PERIN, Yu. I., Effects of American high-altitude explosion of 9 July 1962 in upper atmosphere, 20: 6209
GALSTER, S., Search for heavy electron by electron-proton coincidence measurements, 20: 6078
GAMOTA, G., Direct measurement of size of charged quantized vortex rings in He II, 20: 6249
GANSSAUGE, E., Search for heavy electron by electron-proton coincidence measurements, 20: 6078
GANZHA, V. D., Electrophoretic filter for purifying reactor water, 20: 6568
GARBER, W. F., Method for low-level gamma radioactivity measurement, 20: 5432
GARCIA, John, Adaptive responses to ionizing radiation, 20: 5319
GARDINER, T., LASL tandem accelerator facility data system, 20: 5939 (LA-DC-7267)
GARDNER, W. E., Pressure dependence of superconducting transition temperature of uranium, 20: 6234
GARELLI, C. M., Longitudinal polarization of low-energy muons from $K^+_{\mu 3}$ decay, 20: 6075
GASPAR, E., Use of radioactive tracers in hydrology in Rumania, 20: 5657 (NP-15543, pp 47-58)
GATES, D. W., Plasma jet technology, 20: 5633 (NAA-SP-5033)
GATTO, R., Classification of higher boson resonances, 20: 6134
GATTO, R., Kinetic supermultiplets of $\bar{U}(12)$, 20: 6058
GAUTIER, Lucienne, Calculations of ψ, ϕ, and of their derivatives, 20: 5829 (CEA-R-2824)
GAVRILOV, P. A., Dynamic characteristics of first reactor of I. V. Kurchatov Beloyarsk Nuclear Power Station, 20: 6634
GAYNOR, Allen J., Viscosity of NaK 78 at low temperatures, 20: 5908
GEHM, Helmut, Pulse shape discrimination in half-life determination for study of (γ,α) reactions, 20: 5732 (KFK-335)
GEIGER, J., Energy losses of fast electrons in nitrogen, 20: 5542
GEILIKMAN, B. T., Shell effects in nuclear fission, 20: 6308 (ANL-Trans-243)
GELFAND, N., Search for neutral scalar meson, 20: 6079
GELMAN, Harry, Alternative formulations of scattering in model field theories, 20: 6116
GENGOZIAN, Nazareth, Spleen cells of heterologous radiation chimeras cultivated in diffusion chambers, 20: 5397
GENNARELLI, L., Means of protection from fallout of nuclear and thermonuclear explosions, 20: 5416
GENS, T. A., Laboratory preparation of uranium nitride microspheres by sol–gel technique, 20: 5864 (ORNL-3879)
GENTILE, P. S., Solid-solid interactions. II., 20: 5545
GERKE, D. G., DWBA analysis of $^{12}C(d,p\gamma)^{13}C$ with measured optical model parameters, 20: 6362
GERSH, Michael E., Improved separation of isotopic hydrogens by gas chromatography, 20: 5824
GERSTEIN, I. S., Vertex-function poles and bootstrap condition in field theory, 20: 6138
GETMANTSEV, G. G., Expected anisotropy of nonthermal cosmic radio emission at low frequencies, 20: 6020
GEVORKOV, A., Heating of plasma under conditions of beam instability, 20: 6468 (ORNL-tr-871)
GFOELLER, D., Experimental studies of Cerenkov radiation in optically single axis crystals, 20: 5792
GHIRINGHELLI, F., Behavior of enterochromaffin cells of intestine of hedgehog irradiated during hibernation, 20: 5377
GHOSE, A. M., Photoelectric cross sections of gamma rays for heavy elements, 20: 5990
GHOSHAL, Sudhanshu Kumar, One dimensional flow of plasma with an external magnetic field, 20: 6510
GIAEVER, Ivar, Magnetic coupling between two adjacent type-II superconductors, 20: 6244
GIANZERO, Stanley C. Jr., Radiation by uniformly rotating line charge in plasma, 20: 6456 (AD-619888)
GIAVELLI, S., Radiosensitivity of different meiotic stages of oocytes in parthenogenetic diploid artemia salina leach, 20: 5359
GIDAL, G., Longitudinal polarization of low-energy muons from $K^+_{\mu 3}$ decay, 20: 6075
GIESEKE, James A., Prog. rpt. on analytical description of nuclear-reactor accident, 7–9/65, 20: 6560 (BMI-X-10145)
GILBERT, E. N., Extraction of carrier free ^{57}Co from irradiated targets, 20: 5602
GILBERT, R. P., Analytic properties of elastic unitarity integral, 20: 6114
GILBERT, William S., New radiation problems associated with 200-Bev accelerator, 20: 5945 (UCRL-16464)
GILEVA, E. A., Influence of ^{60}Co γ irradiation on growth of chlorella cultures, 20: 5389
GILMORE, R. S., Isobaric states excited in (p,n) reactions at 30 and 50 Mev, 20: 6361
GINOZA, William, Prog. rpt. on reactions of bacterial cells to foreign nucleic acids, 12/62–10/65, 20: 5299 (TID-22187)
GINSBERG, D. M., Evidence that initial ultraviolet lethal damage in Escherchia coli strain 15 is independent of growth phase, 20: 5347
GINSBERG, D. M., Radiation sensitivity and growth characteristics of E. coli strain 15, 20: 5348
GIORNI, Alain, Evidence of two-body interactions in reaction $^9Be(n,2n)$ at 14 Mev, 20: 6320
GIRAUD, B., Projected Hartree-Fock spectra in light nuclei, 20: 6419
GLADITZ, B., Breakdown in low pressure region, 20: 6167
GLASSGOLD, A. E., Disproof of Senitzky's fundamental theorem in quantum optics, 20: 6226
GLAUDEMANS, P. W. M., Experimental and theoretical investigations on light nuclei, 20: 6295 (NP-15647)
GLAVIND, John, Antioxidants and lipoperoxides in organs of irradiated rats, 20: 5339
GLUSHKOVA, V. B., Polymorphism of rare-earth sesquioxides, 20: 5536
GOBLE, R. L., Cross section for production of possible bound cascade-nucleon system, 20: 6073
GOLDBERG, M., Momentum dependence of S matrix for many-particle processes, 20: 6061
GOLDENBAUM, G., Shock wave formation in an almost collisionfree plasma, 20: 6501
GOL'DIN, L. L., Measurement of relationship of proton pulse in ITEF, 20: 5941 (NP-15598)
GOL'DIN, L. L., Study of charged particle beams by means of pick-up electrodes, 20: 5686 (NP-tr-1313)
GOLDSCHMIDT, H. J., Tungsten-rich end of tungsten–beryllium system, 20: 5906
GOLDSMITH, S., Fast reactor safety considerations related to fuel macrostructure, 20: 6602 (BNWL-SA-346)
GOLDSTEIN, L., Helical instability produced in gaseous magnetoplasmas by gyro-interaction of microwaves, 20: 6446 (AD-617696)
GOLDSTEIN, Louis, Anomalous thermal properties of liquid helium I and II and their connection, 20: 6231
GOLDSTEIN, N., Response of LiF to neutrons and charged particles, 20: 5572 (USNRDL-TR-909)
GOLENKO, O. D., Fluorimetric investigation of second luminescence of lymphocytes of lymphatic glands in irradiated rats, 20: 5383
GOLLIHER, K. G., Capabilities of 1 Mw shield test and irradiation reactor, 20: 6677 (NAA-SR-11528)
GOLUBEV, E. N., Preliminary results of determining particle concentration and atmospheric density on 18 June 1963, 20: 6210
GOLUTVIN, L. A., Analogue wire spark chamber system for measurements of particle momenta and angles, 20: 5730 (JINR-E-2366)
GOMEZ-GIMENO, F., Calculation of proton polarization in p-d elastic scattering at 150 Mev, 20: 6329
GOOCH, P. Carolyn, Experimental S-4, radiation of blood, 20: 5297 (ORNL-P-1734)
GOOD, R. C. Jr., Solar flare hazards: predictability, 20: 5966 (AD-618905)
GOODINGS, A., Irradiation testing of pulse fission chamber design, 20: 5807 (AEEW-M-493)
GOODINGS, A., Neutron activation of titanium and its influence on ionization chamber design, 20: 5716 (AEEW-M-470)

GOODINGS, A., Results of RCIO ionization chamber development, 20: 5717 (AEEW-M-508)
GOODMAN, Jean Wright, Spleen weight as measure of marrow cell growth in irradiated mice, 20: 5372
GOODMAN, L. J., Mouse phantom depth dose studies, 20: 5286 (CONF-650616-16)
GORDON, G. E., Computer analysis of beta-ray and conversion-electron spectra, 20: 5768
GORE, J. V., High field air-cored betatron, 20: 5961
GORGE, C., Determination of spin and resonance parameters for $^{197}Au + n$ at 10 to 1000 ev, 20: 6392
GORYACHEV, V. V., Angular distributions of neutron doses near ground-air boundaries, 20: 6528
GOTTSCHALK, B., Proton-proton bremsstrahlung at 158 Mev, 20: 6046
GOTTSCHALK, W., Radiation sensitivity in genus triticum, 20: 5403
GOUANERE, Michel, Circular spark chambers with electric localization at low energies, 20: 5735 (LYCEN-6523)
GOUPIL, Jean, Method of and apparatus for recording pulse spectra, 20: 5797
GOVE, H. E., $^{39}K(^3He,\alpha)^{38}K$ and $^{39}K(^3He,^3He)^{39}K$ reactions, 20: 6367
GOVORUN, R. D., Changes of serum protein fractions in blood of rats irradiated with 660-Mev protons, 20: 5378
GOWOREK, Tomasz, Gamma-gamma angular correlations in ^{147}Eu to ^{147}Sm decay, 20: 6396
GRAETZER, R., Vibrational states of deformed nuclei populated by (p,2n) reaction, 20: 6366
GRAHAM, C. D. Jr., Microstructure of internal magnetic field in selected magnetic materials, 20: 6531 (AD-623530)
GRAHAM, Gene P., Underwater radiographic exposure device, 20: 5631(P)
GRAHAM, L. W., Special graphites for Dragon Reactor Core, 20: 6641
GRAHAM, R. H., Solid state radiation detection system with low noise amplification, 20: 5804
GRANATSTEIN, V. L., Turbulent mixing in laboratory plasma, 20: 6472
GRAVIER, R., Heating and confinement of plasma in magnetic well of deca-2, 20: 6469 (UCRL-Trans-1256(L))
GRAY, Peter R., Activation cross sections for reactions of Rh and Ru with 14.7 Mev neutrons, 20: 6338
GRECO, G., Influence of x rays on take of skin homografts, 20: 5335
GREEN, A. M., Even parity states of ^{16}O and ^{17}O, 20: 6350
GREENBAUM, Michael A., Thermodynamic and physical properties of beryllium compounds. VIII., 20: 5554
GREENING, J. R., Medical physics in Edinburgh, 20: 5239
GRIBOV, V. N., At what distances does interaction at high energies occur?, 20: 6108 (NP-15600)
GRIBOV, V. N., What is the range of high energy interactions?, 20: 6153
GRIFFIN, Allen, Entropy transport between two superconductors by electron tunneling, 20: 6248
GRIFFITH, Peter, Momentum flux in two-phase flow, 20: 5624 (MIT-3496-1)
GRIFFITHS, W., Radiation inactivation of potato phosphorylase, 20: 5275
GRIGGS, D. T., Probing earth with nuclear explosions, 20: 5610
GRIMSHAW, J. D. C., ^{137}Cs body burdens in Toronto, 20: 5671
GRISSOM, J. T., Single crystal Compton spectroscopic techniques, 20: 5775
GRONICH, S., Transpiration-cooled nozzle as applied to gas-core nuclear propulsion system, 20: 6663
GROVE, E. L., Viscosity of NaK 78 at low temperatures, 20: 5908
GRUBER, U., Energy and intensity measurements of gamma radiation emitted by ^{182}W and ^{183}W during decay of ^{182}Ta and ^{183}Ta, 20: 6428
GRUEL, Jean, Improvements in or relating to control rod mechanisms for nuclear reactors, 20: 6569
GSCHNEIDNER, K. A. Jr., Behavior of some delta-stabilized plutonium–gallium alloys at high pressures, 20: 5884 (LA-2312)
GUBLER, W., Statistical oscillations of infrared radiation of high-pressure, high-current Ar discharge. II., 20: 6177
GUIDO, M., Mass-spectrometric study of yttrium–carbon system, 20: 5540
GUIDONI, P., $K_2^0 \rightarrow \pi^+\pi^-\pi^0$ decay, 20: 6031 (BNL-9613)
GUILLERMIN, Jean, Calculations of ψ, ϕ, and of their derivatives, 20: 5829 (CEA-R-2824)
GUNSCHMANN, K., Equipment for indicating, recording and controlling oscillations of axis of rotation and speed of rotor of gas centrifuge, 20: 5685 (K-Trans-5)
GUON, J., Remote operating gas pycnometer, 20: 5708
GUPTA, H. M. Sen, $^{14}N(^3He,\alpha)^{13}N$ angular distribution leading to the ground state in ^{13}N, 20: 6326
GUPTA, R., Spin polarization of slow electrons by elastic resonance scattering from neon, 20: 5998
GUPTA, V. K., Relativistic corrections to triton binding energy, 20: 6084
GUREVICH, A. V., Diffusive spreading of inhomogeneities in weakly-ionized plasma, 20: 6482
GUREVICH, A. V., Force acting on a body in a plasma, 20: 6483
GUSMANO, E. A., Formulation and testing of compartmental model for calcium metabolism in man, 20: 5260
GVOZDEV, B. A., Production of ^{242}Pu and ^{242}Cm by irradiation ^{241}Am with neutrons, 20: 5823 (ORNL-tr-892)

H

HAASBROEK, F. J., Half-life of ^{51}Cr, 20: 6420
HADJIANTONIOU, A., Interaction of thermal electrons with polarizable and polar molecules, 20: 5985 (ORNL-TM-1262)
HAEUSSER, O., $\frac{3}{2} \rightarrow \frac{1}{2}$ Hole transitions in mass 15, 20: 6378
HAEUSSERMANN, W., Power from radioisotopes, 20: 5821
HAGEMANN, G. B., Vibrational states of deformed nuclei populated by (p,2n) reaction, 20: 6366
HAGEMANN, K. A., Vibrational states of deformed nuclei populated by (p,2n) reaction, 20: 6366
HAGEN, Nancy S., FORTRAN IV program for evaluation of post-irradiation survival times, 20: 5300 (UCLA-12-573)
HAHN, H., Design of deflector for rf beam separator at Brookhaven AGS, 20: 5960
HAHN, J., Nuclear pulse amplifiers—fundamentals and design practice. Part 3., 20: 5780
HAHN, Richard G., Thorium dioxide infusions to demonstrate malignant lesions in the liver, 20: 5465
HAIMAN, O., Physical fundamentals of nuclear radiation measurements, 20: 5795
HAINS, F. D., Stability diagrams for magnetogasdynamic channel flow, 20: 6174
HAKEN, H., Quantum noise operators for N-level system, 20: 6002
HALAMA, H. J., Design of deflector for rf beam separator at Brookhaven AGS, 20: 5960
HALLER, Kurt, Alternative formulations of scattering in model field theories, 20: 6116
HALLEWELL, V. A., Comprehensive safety shutter and collimator coupling for Philips x-ray tube shield PW 1016, 20: 5693
HALPERN, M. B., S-matrix theory and higher order corrections to weak interactions, 20: 6057
HALTEMAN, E. K., Thermal expansion of coprecipitated (U, Pu)O_2 powders by x-ray diffraction techniques, 20: 5890 (NUMEC-2389-9)
HAM, W. M., Tungsten-rich end of tungsten–beryllium system, 20: 5906
HAMBURGER, E. W., $^{93}Nb(d,t)^{92}Nb$ reaction, 20: 6310
HAMMOND, E. J., FLIGHT-2. A data reduction program for SNAP 10A transient flight test data, 20: 6661 (NAA-SR-Memo-11603)
HANDLER, R., Measurement of proton-proton triple scattering at 430 Mev, 20: 6056
HANNA, R. C., Differential ion chamber for beam energy measurement, 20: 5778
HANNUM, W. H., Nuclear design of MPBE, 20: 6613 (LA-DC-7475)
HANSEN, G. E., Computation of fast neutron penetration in air by "Sn-method", 20: 6261 (LA-3415)
HANSEN, Gordon E., Thermal neutron spectra from underground nuclear explosion, 20: 5609 (LA-3403)
HANSEN, Kent F., Radiation shielding requirements for manned satellites, 20: 5673
HANSEN, Lis, Antioxidants and lipoperoxides in organs of irradiated rats, 20: 5339
HANSEN, P. G., Spectral shapes and beta–gamma directional correlation in beta decay of $^{172}Tm(J^\pi = 2^-)$, 20: 6381
HANSON, K. L., Thermal integration of electrical power and life support systems for manned space stations, 20: 5820 (NASA-CR-316)
HANTZSCHE, E., Light from fall space, 20: 6166
HARA, Yasuo, Single-resonance productions and double-resonance productions, 20: 6069
HARAN-GHERA, Nechama, Effects of ionizing radiation on growth and regeneration of intrarenal thymus grafts in mice, 20: 5376
HARARI, H., Experimental tests of broken $\bar{U}(12)$ and approximate $U(6) \times U(6)$, 20: 6066
HARARI, H., Noncollinear diagrams and Johnson-Treiman relations, 20: 6143
HARDIE, D., Characteristics of hydrided α-zirconium, 20: 5905
HARLAN, James R., Synchrotron resonator for Illinois 300-Mev betatron, 20: 5942 (NP-15615)
HARRISON, J. E., ^{137}Cs body burdens in Toronto, 20: 5671
HARTLE, James B., Variational principle for hydrostatic equilibrium of relativistic, rotating fluid, 20: 5974
HARTWIG, G., Search for heavy electron by electron-proton coincidence measurements, 20: 6078
HARVEY, R. R., Cross sections for ground- and excited-state neutron groups in reaction $^{16}O(\gamma,n)^{15}O$, 20: 6418
HARZDORF, C., Titration of fluoride with uranium (IV), 20: 5520
HASEGAWA, A. T., Dose reduction factor for radiation lethality in mice as function of dose of mercaptoethylamine, 20: 5407 (AD-623599, pp 37-44)
HASEGAWA, Akira, Studies on quality and test method of radiopharmaceuticals. I., 20: 5515
HASEGAWA, S., Remark on 30 Bev jet showers, 20: 6039 (INSJ-90)
HASLAM, R., Bioassay of influence of cortisol in bones of growing rabbits,

20: 5234 (COO-119-232, pp 122-52)
HATUDA, Zin'itiro, Deterimining U and Th content in rocks by radioactive measurements. I., 20: 5513
HAWKER, P. A. E., Expansion of a function in terms of Chebyshev polynomials using the I.B.M. 7040, 20: 5828 (AAEC/TM-293)
HAWLEY, R., Electrode protrusions produced by electron beam bombardment, 20: 5809
HAYBITTLE, J. L., Clinical trial of radiosensitizers, 20: 5437
HAYES, B. A., Thermal conductivity and electrical resistivity of uranium monocarbide, 20: 5893 (PWAC-480)
HAYNIE, Thomas P., Radioisotope photoscans in nuclear medicine, 20: 5487
HAZEN, Wayne C., Recovery of metal values from aqueous solution by solvent extraction with organo phosphorus extractant, 20: 5605(P)
HAZONY, Y., Moessbauer effect in molecular iodine crystals, 20: 6540
HAZZARD, E. T., Alphas from deuteron bombardment of ^{9}Be and ^{12}C, 20: 6360
HEAL, Thomas, John, Manufacture of nuclear reactor fuel elements, 20: 5872
HEARD, C. R. T., Multiple scattering in plane samples, 20: 6255 (AERE-R-5016)
HEATHERTON, R. C., Thorium and its MPC's, 20: 5662 (NLCO-962)
HEISTAD, G. T., Effect of whole brain ^{60}Co gamma irradiation on cortical arousal in burro, 20: 5329
HELTON, D. M., Laboratory preparation of uranium nitride microspheres by sol-gel technique, 20: 5864 (ORNL-3879)
HENKEL, R. L., Area radiation monitor system with logarithmic indication and audiovisual warning, 20: 5733 (LA-DC-6790)
HENRICKSON, Angus V., Recovery of metal values from aqueous solution by solvent extraction with organo phosphorus extractant, 20: 5606(P)
HENRY, Hugh E., Isolating americium and curium from $Al(NO_3)_3$–$NaNO_3$–HNO_3 solutions by batch extraction with tributyl phosphate, 20: 5495 (DP-972)
HENRY, P. E., Effects of various fabrication variables on texture gradients in uranium fuel cores, 20: 5863 (NLCO-945)
HENSCHKE, U. K., ^{131}Cs seeds for permanent implants, 20: 5482
HEPP, Klaus, One-particle singularities of S-matrix in quantum field theory, 20: 6122
HERBST, Arthur L., Hyperthyroidism during pregnancy, 20: 5470
HERBST, L. J., Position finding counter for Buechner magnet, 20: 5747 (NP-tr-1302)
HERCZEG, P., General form of the time-reversal non-invariant internucleon potential, 20: 6047
HEREWARD, H. G., Disc-loaded deflecting waveguide-computations, 20: 5934 (CERN-65-37)
HERMAN, R., Charge distributions of ^{40}Ca and ^{44}Ca from 250-Mev electron scattering, 20: 6413
HERMS, G., Simple method for preparing x-ray filters of strontium metal, 20: 5692
HERNADY, Tibor, Radiobiological role of hydrogen–peroxide–catalase system, 20: 5271
HERSH, Charles K., Viscosity of NaK 78 at low temperatures, 20: 5908
HERVE, A., Phantoms for radiotherapeutic measurements, 20: 5481
HESSON, J. C., Energy conversion, 20: 6024 (ANL-6925, pp 235-47)
HETSRONI, G., Use of hydraulic models in nuclear reactor design, 20: 6622 (NYO-3250-2)
HEWITT, R., Reorientation of chromosome replication after exposure to ultraviolet light of Escherichia coli, 20: 5349
HEWKA, P. V., Alphas from deuteron bombardment of ^{9}Be and ^{12}C, 20: 6360
HEYMANN, P., Space distribution of electron temperature and density in stationary layers of hydrogen discharge, 20: 6476
HICK, H., Comparison of consumption determination with sound activation and gamma spectroscopy for MTR element, 20: 6681 (SGAE-PH-18/1965)
HIEBERT, R. D., Area radiation monitor system with logarithmic indication and audiovisual warning, 20: 5733 (LA-DC-6790)
HILL, D. L., Electrochemical studies on zirconium and hafnium in molten LiCl–KCl eutectic, 20: 5543
HILL, R. D., Evidence for quarks from baryon resonances?, 20: 6135
HILL, Walter S., Procedure for improving gamma scintillography, 20: 5447
HINE, Jack, Catalysis of α-H exchange. I., 20: 5565
HINTENBERGER, H., Isotopic composition and site of light primordial rare gases in stone meteorites, 20: 5975
HINTZ, E., Shock wave formation in an almost collisionfree plasma, 20: 6501
HIROSE, Y., Properties and prospects of thoria-base nuclear fuels, 20: 5915 (ORNL-P-1724)
HLAVATY, V., Adaptation of organism during fractionated x-ray treatment, 20: 5364
HOBSON, J. P., Total pressure measurements below 10^{-10} torr with non-magnetic ionization gages, 20: 5641
HOCHACHKA, Peter W., Radiation indication of subunit of lactic dehydrogenase, 20: 5276
HOCKWIN, Otto, Effect of x irradiation on metabolic activity of lens as related to age, 20: 5333
HODGES, T. A., Differential ion chamber for beam energy measurement, 20: 5778
HODGSON, John R., Thorium dioxide infusions to demonstrate malignant lesions in the liver, 20: 5465
HOFFMAN, John R., Determination of neutron yields by measurement of positrons from $^{63}Cu(n,2n)^{62}Cu$ reaction, 20: 6289 (KN-63-10(R))
HOFMANN, A., Study of d-d reactions in self targets with coatings, 20: 6334
HOFMEYR, C., Scattering of slow neutrons at protons in phenyls and water vapor, 20: 6272
HOFSTADTER, R., Charge distributions of ^{40}Ca and ^{44}Ca from 250-Mev electron scattering, 20: 6413
HOLEMAN, Ernest, Time and altitude dependence of 55-Mev trapped protons, Aug. 1961 to June 1964, 20: 6200
HOLLIDAY, Dennis, Disproof of Senitzky's fundamental theorem in quantum optics, 20: 6226
HOLLISTER, Herb, Description of neutron generator beam sorters, 20: 6262 (NP-15633)
HOLROYD, Richard A., Radical yields in radiolysis of hydrocarbons. II., 20: 5576
HOLSTI, L. R., Megavoltage therapy, 20: 5453
HOMEYER, William G., Thermal and chemical aspects of thermonuclear blanket problem, 20: 6452 (AD-619669)
HOOPER, M. B., L-space localization in deuteron stripping reactions, 20: 6394
HOPKINS, D. C., Coexistence of antiferromagnetism and superconductivity, 20: 6247
HORIE, Kenyo, Experimental osteogenic sarcoma, 20: 5334
HOROSHKO, R. N., Angular correlation measurements on $^{25}Mg(d,p\gamma)^{26}Mg$ reaction, 20: 6410
HORROCKS, Donald L., Remote opening of metal containers with laser beam, 20: 5669
HORST, Hermann, Support for samples to be subjected to radiations, 20: 6574
HORWITZ, Norman H., Spintharicon: new approach to radiation imaging, 20: 5461
HOUGH, J. H., Nuclear resonant scattering of bremsstrahlung from low-lying levels in ^{27}Al, ^{31}P, and ^{35}Cl, 20: 6380
HOUSTON, James G., Catalysis of α-H exchange. I., 20: 5565
HOUSTON, M. D., Effect of PuO_2 content on sintering behavior of mechanically mixed UO_2–PuO_2, 20: 5889 (NUMEC-2389-8)
HOWARD, C. L., Prog. rpt. on Garigliano nuclear reactor, 10/65, 20: 6606 (GEAP-4962)
HOWARD, H. C., Analytic properties of elastic unitarity integral, 20: 6114
HOWERTON, R. J., Computation of fast neutron penetration in air by "Sn-method", 20: 6261 (LA-3415)
HRDA, A., Initial trajectories of ions leaving an open cyclotron ion source at non zero initial conditions, 20: 5946 (UJV-1408/65)
HSU, Y. C., Prog. rpt. on liquid-metal lubricated journal bearings, 20: 5613 8–10/65, 20: 5613 (SWRI-1228-8-16)
HUBAY, Charles, Transplantation site preradiation and rejection patterns, 20: 5344
HUBBARD, W. N., Calorimetry, 20: 5523(R) (ANL-6925, pp 175-85)
HUC, J. M., Disintegration of ^{134}Cs, 20: 6327
HUDGENS, J. E., Computer control and data processing for isotopic mass spectrometers, 20: 5684 (WAPD-T-1770)
HUDGINS, Philip T., Injury of small intestine following irradiation for gynecologic cancer, 20: 5392
HUENE, D. R., Formulation and testing of compartmental model for calcium metabolism in man, 20: 5260
HUG, Otto, Cytological aspects of radiotherapy, 20: 5477
HUGHES, L. B., Study of $^{203}Tl(n_{th},\gamma)^{204}Tl$ reaction, 20: 6411
HUKE, Kazuo, Pole face windings in todai AG electron synchrotron, 20: 5952
HULIN, M. W., SNAP 2 experimental reactor (SER) operation and test program, 20: 6655 (NAA-SR-7088)
HULL, C. D., Adaptive responses to ionizing radiation, 20: 5319
HULTSCHIG, H., Search for heavy electron by electron-proton coincidence measurements, 20: 6078
HUMPHREY, W., Proposed balloon borne system for interactions above 10^{11} ev, 20: 5724 (CONF-640919, pp II13-23)
HUNDSTAD, Richard L., Magnetohydrodynamic generator, 20: 6030
HUNT, E. L., Humoral factor in radiation-induced motivation, 20: 5303 (USNRDL-TR-925)
HUNTER, Norvell W., Activity of phosphomonoesterases of stylonychia pustulata following ultraviolet irradiation, 20: 5272
HUNTINGTON, Morgan G., Self-limiting radiant nuclear boiler and superheater, 20: 6592
HUNZIKER, F., Metabolism of Noveril: ^{14}C labeling and synthesis of metabolites, 20: 5564
HURST, G. S., Interaction of thermal electrons with polarizable and polar molecules, 20: 5985 (ORNL-TM-1262)

HUSSAIN, S. A., Suitability of proportional counter as charged particle spectrometer and study of reaction $^{10}B(d,p)^{11}B$, 20: 5759
HUYNH, V. D., Determination of spin and resonance parameters for $^{197}Au + n$ at 10 to 1000 ev, 20: 6392
HWA, Rudolph C., Bootstrap algebra for mesons, 20: 6060
HYODO, Yasuko, Development of intestinal damage after x-irradiation of goldfish, 20: 5374

I

IBARAKI, Y., Energy dependence of quantameter. I., 20: 5765
ICE, C. H., Production of transplutonium elements at Savannah River, 20: 5822 (DP-1000)
IMAM, M., Radiation sensitivity in genus triticum, 20: 5403
IMINOV, I., Contribution to theory of semiconductor counters for ionizing particles, 20: 5758
IMPINK, Albert J. Jr., Neutron economy in fusion reactor blanket assemblies, 20: 6451 (AD-619668)
INDREASH, G., Effect of geometry of cyclotron center upon starting motion of heavy ions (median plane), 20: 5948 (ANL-Trans-246)
IOANID, G., Use of tracers and of intense radiation sources in industrial processes, 20: 5814 (NP-15543, pp 27-45)
IOFFE, B. L., At what distances does interaction at high energies occur?, 20: 6108 (NP-15600)
IOFFE, B. L., What is the range of high energy interactions?, 20: 6153
IONOV, V. A., Spectral distribution of gamma rays from ^{60}Co point source screened with aluminium layer in atmosphere near ground, 20: 6529
IORGULESCU, Adriana, γ-spectrometric analyses of 1963 atmospheric fallout samples, 20: 5652
ISHIKAWA, Tomokiyo, Radiation control at National Institute of Radiological Sciences, 20: 5672
ISHIMATSU, T., Strongly excited levels of ^{39}Ca in $^{40}Ca(^3He,\alpha)^{39}Ca$ reaction, 20: 6398
ISLAMOV, A. A., Resonant scattering of gamma quanta by ^{140}Ce nuclei, 20: 6324
ISRAEL, H. I., Radiation and shielding design factors for Los Alamos meson physics facility, 20: 5940 (LA-DC-7522)
IVANOV, G. K., Resonance neutron-molecule interactions, 20: 6266
IVANOV, N. F., Measurements of ion beam phase volume in linear accelerator injector, 20: 5956
IWAO, S., Spin and unitary spin independence in SU(8) symmetry, 20: 6110
IZENSTARK, Joseph L., Cancer diagnosis by radioisotopic scanning, 20: 5450
IZRAEL', Yu. A., Gamma radiation spectrum from artificial model of radioactive fallout, 20: 5653

J

JACKSON, J., Theorist's comments, 20: 6011
JACKSON, J. D., Comparison of some $SU(6)_W$ predictions on collinear processes with experiment, 20: 6144
JACMART, J. C., Study of nuclei of medium mass by inelastic scattering of 155 Mev protons. I., 20: 6354
JACOBI, Guenter, Effect of x rays on chloroplast reactions and protective effect of ascorbate, 20: 5402
JACOBS, I. S., Microstructure of internal magnetic field in selected magnetic materials, 20: 6531 (AD-623530)
JACOBS, J. A., Geomagnetic micropulsation results from Byrd station and Great Whale River, 20: 6188
JAGGER, J., Evidence that initial ultraviolet lethal damage in Escherchia coli strain 15 is independent of growth phase, 20: 5347
JAGGER, J., Radiation sensitivity and growth characteristics of E. coli strain 15, 20: 5348
JAGOSZ, Ryszard, Potentiometric determination of rare earths (e.g., erbium), 20: 5519
JAHN, Robert G., Direct measurement of current density distributions in transient plasmas, 20: 6509
JAHR, R., (d,α) Reactions on light nuclei, 20: 6369
JAIN, R. K., Collisional damping of transverse plasma oscillations, 20: 6499
JAKLEVIC, R. C., Macroscopic quantum interference in superconductors, 20: 6235
JAMESON, Robert A., Analysis of proton linear accelerator rf system and application to rf phase control, 20: 5938 (LA-3372)
JAMMET, Henri, Application of sanitary standards in matter of radiological protection, 20: 5663 (NP-15451)
JAMNE, E., Operating experience with HBWR on its second fuel charge, 20: 6636
JANICKI, Kazimierz, Environment and leukemia morbidity. III., 20: 5674
JANSEN, E., Halden—from research and engineering development to fuel testing, 20: 6635
JANSEN, J., Application of different methods of non-destructive testing to fuel elements of ORGEL type, 20: 6632 (AEC-tr-6628)
JARLSKOG, Cecilia, Determination of coupling constants in muon decay from experiments, 20: 6048
JARVIS, Timothy Robert, Linear electron accelerator, 20: 5964
JEE, W. S. S., Bioassay of influence of cortisol in bones of growing rabbits, 20: 5234 (COO-119-232, pp 122-52)
JEE, W. S. S., Studies of trabecular bone in beagles and humans, 20: 5233 (COO-119-232, pp 99-121)
JEE, W. S. S., ^{238}Th induced fractures in beagles, 20: 5288 (COO-119-232, pp 74-87)
JEE, Webster S. S., Correlation of bone strength with radiation dose from internal emitters and bone resorption, 20: 5289 (COO-119-232, pp 88-98)
JEFFERSON, Sidney, Package irradiation systems, 20: 5617(P)
JEITSCHKO, W., Superconducting behavior of several complex carbides and nitrides, 20: 6228
JENGO, R., SU_6, SU_6W and meson photoproduction, 20: 6055
JENKINS, Samuel G. Jr., Hormonal and isotope measures in thyroid carcinoma, 20: 5444
JENNINGS, H. K., Area radiation monitor system with logarithmic indication and audiovisual warning, 20: 5733 (LA-DC-6790)
JENSEN, James H., Catalysis of α-H exchange. I., 20: 5565
JENSEN, V. O., Attempt to detect microinstabilities in colliding plasmas, 20: 6465 (RISO-105)
JESSEPH, J. E., Formulation and testing of compartmental model for calcium metabolism in man, 20: 5260
JNANANANDA, Swami, Coherent scattering cross-sections of ^{60}Co and ^{137}Cs gamma rays, 20: 6323
JOHNSON, Marvin J., Optimum operation of recording count rate meters for radioactive paper chromatograms, 20: 5508
JOHNSON, R. M., Container leak rate test, PWR reactor plant, 20: 6628 (WAPD-PWR-TE-201)
JOHNSTON, Herbert Charles, Manufacture of motor vehicles for additional protection from radiation hazards, 20: 5679
JONES, C. H., Cancer of middle ear; technique of radiation treatment, 20: 5448
JONES, L., Proposed system to study interactions at 300 Bev, 20: 5725 (CONF-640919, pp II27-30)
JONKE, A. A., Fuel cycle applications of volatility and fluidization techniques, 20: 5595(R) (ANL-6926, pp 107-64)
JORDAN, K. C., General method of determining total time integral of transients in linear systems, 20: 5681 (MLM-1288)
JORDAN, Pierre, Simultaneous gas-proportional counting of ^3H and ^{14}C, 20: 5779
JUETTNER, B., Nature of pre-breakdown current in high vacuum, 20: 6169
JULIEN, J., Determination of spin and resonance parameters for $^{197}Au + n$ at 10 to 1000 ev, 20: 6392
JULLIEN, Georges, Improvements in or relating to control rod mechanisms for nuclear reactors, 20: 6569
JUPITER, C., Response function and sensitivity of double-diffused silicon detectors in high γ-dose rate fields, 20: 5743 (UCRL-14405)

K

KACPRZYNSKI, Jerzy, Selfexcited vibration of nuclear reactor fuel channels with water cooling, 20: 6564
KAERCHER, Gerald C., Instrumented probe for fast clearance measurement, 20: 5703
KAHN, M. Z. Rahman, Spin-spin part of low-energy nuclear optical potential, 20: 6395
KAINDL, K., International project on irradiation of fruits and fruit juices, 20: 5816
KAISER, W., Potassium analysis of amphoterite chondrites and their K–Ar age, 20: 5979
KAJIKAWA, R., Electron-photon beam monitoring with image amplifying plate, 20: 5773
KALISH, R., E2/M1 mixing ratios and K conversion coefficients in odd-mass rotational nuclei, 20: 6386
KALLMANN, Hartmut P., Prog. rpt. on energy transfer during transient nuclear pulses, semiannual, 5–10/64, 20: 5805 (AD-617782)
KALMUS, P. I. P., Polarization of Λ^0 particle produced from protons in carbon nuclei by 1.17-Bev/c negative pions, 20: 6071
KALVIUS, G. Michael, Prog. rpt. on recoil-free scattering of gamma-rays, final, 3/62–6/65, 20: 6302 (TID-22384)
KAMINKAR, D. M., Electrophoretic filter for purifying reactor water, 20: 6568
KAMINKER, D. M., Delayed gamma rays from ^{235}U fission, 20: 6316
KAMINKER, D. M., Pile-neutron burnup cross section of ^{149}Pm and samarium poisoning, 20: 6589
KAMM, W., Development of computer programs for computation of Montgomery stream functions and plotting of thermodynamic diagrams, 20: 5645(R) (COO-1340-2, pp 122-45)
KANG, Kyungsik, Theory of low-energy $\pi\omega$ scattering, 20: 6068
KANNINEN, M. F., Fuel conservation indexes for thermal reactors, 20: 6610 (HW-79287)

KANTELE, J., Versatile routing system for multichannel analyzers, 20: 5769
KAPIL, Rajendra, Effects of non-lethal doses of x rays on exploring and feeding behavior of larvae of Drosophila melanogaster meig, 20: 5295
KAPITSA, S. P., Photofission of even-even nuclei near threshold, 20: 6309 (ANL-Trans-245)
KAPLAN, Alan L., Injury of small intestine following irradiation for gynecologic cancer, 20: 5392
KAPLAN, Henry S., Radiotherapy for cancer, 20: 5451
KAPLAN, M. H., Design and performance of ion-engine systems, 20: 5638
KAPLAN, Stanley, Transport synthesis, 20: 6264 (WAPD-T-1849)
KARPLUS, Martin, Electron spin resonance studies of deuterium isotope effects, 20: 5566
KARSTEN, J. H. M., Half-life of ^{51}Cr, 20: 6420
KASCHL, G. Th., Spectral form of $(0 \rightarrow 0)$-β transitions with parity change: ^{144}Ce, ^{144}Pr, and ^{166}Ho, 20: 6370
KASYMOV, A., Changes in process of cell division and nucleus structure under the influence of irradiation and radiotoxins, 20: 5390
KATCOFF, S., Emission of ^{8}Li fragments from Cu, Ag, and Au irradiated by high-energy protons, 20: 6409
KATO, Hidemasa, Activation analysis of Mn in Fe, 20: 5514
KATOH, Toshio, Decay of ^{158}Eu, 20: 6403
KATSUHARA, Ryo, Studies on chemical protectors against radiation injury. I., 20: 5410
KATSURAGI, Setoru, EXPANDA. One-dimensional diffusion equation code for fast reactors, 20: 6583 (JAERI-1091)
KATYUSHINA, V. V., Measurements of solar L_α radiation absorption in earth's upper atmosphere, 20: 6211
KATZ, Joseph, Synthesis and metabolism of glucose-3-^{3}H and glucose-4-^{3}H, 20: 5252
KATZ, O. M., Angular values between crystallographic planes in zirconium as used in transmission electron microscopy, 20: 5898 (WAPD-TM-519)
KAUFMAN, S. B., Prog. rpt. on nuclear chemistry, annual, 1964–65, 20: 6298 (PPAD-2137-566)
KAUS, P., Modification of Regge-pole representation, 20: 6062
KAVLAKOV, Shr., Daily variations of hard component intensity of cosmic radiations for 1960–1963, 20: 6016
KAWABATA, Masahiro, Single scattering streaming of gamma-rays through cylindrical ducts, 20: 6530
KAWAMURA, T., Remark on 30 Bev jet showers, 20: 6039 (INSJ-90)
KAWARABAYASHI, K., Current commutation relations and meson-meson scattering, 20: 6077
KAWASAKI, Sunao, Pole face windings in todai AG electron synchrotron, 20: 5952
KAYSER, K., (d,α) Reactions on light nuclei, 20: 6369
KAZANSKII, V. B., Nature of surface radiation-induced defects in irradiated silicagel. I., 20: 5584
KAZES, E., Solution of integral equation in V-θ scattering, 20: 6123
KEEGAN, M. R., High temperature creep machine for in-cell operation, 20: 5611 (BNWL-137)
KELLER, H. L., Film dosimetry in radiotherapy, 20: 5480
KELLER, J. C., Advances in insect population control by sterile-male technique, 20: 5815 (STI/DOC/10/44)
KELLIHER, Maurice Grodon, Microwave linear accelerator, 20: 5965
KELLY, T. M., Positron lifetimes in low-temperature helium gas, 20: 5997
KENAWY, M., Study of semiconductor surface barrier detectors at 4.2°K, 20: 5790
KENDALL, P. C., Power series solution of F2 layer diffusion equation, 20: 6183 (AD-619821)
KENNETT, T. J., Study of $^{203}(n_{th},\gamma)^{204}Tl$ reaction, 20: 6411
KERER, Gerold, Interaction between magnetic field and flow field for plasmas of infinite conductivity, 20: 6444 (AD-617553)
KERNAHAN, D. A., Review of literature on burns and trauma, September 1963 to August 1964, 20: 5415
KERTESZ, Laszlo, Iodine storage in thyroid gland of human fetus, 20: 5259
KESSINGER, R. D., Exact solutions of superconducting surface sheath, 20: 6240
KEUFFEL, Jack, Proposed 600 m^3 detector for muons and neutrinos, 20: 5723 (CONF-640919, pp 155-65)
KHALIKOV, A. Kh., Detection of secondary-electron currents by scintillation counter, 20: 5757
KHALISI, Faisal, Some regularities of changes in plants after γ irradiation, 20: 5388
KHANTADZE, A. G., Kochin's problems in MHD, 20: 6172
KHANTADZE, A. G., Movement of medium with finite conductivity in presence of mass forces and planar magnetic field, 20: 6171
KHEIFETS, M. I., On limitations in density of interacting currents in colliding ultrarelativistic beams, 20: 5950
KHODZHA-AKHMEDOV, Ch. L., Frequency-dependence of cosmic noise level during anomalous absorption of type II, 20: 6194
KHORASANOV, G., Heating of plasma under conditions of beam instability, 20: 6468 (ORNL-tr-871)
KHOSLA, P. K., Small amplitude wave propagation in hot ionized gases, 20: 6500
KHRIPLOVICH, I. B., Some selection rules for annihilation of polarized fermions, 20: 6040 (NP-15602)
KHRULEV, V. V., Optimum wavelength and spectral interval measurements of distributed cosmic radiation polarization, 20: 6018
KIDO, Yasumasa, Studies on quality and test method of radiopharmaceuticals. I., 20: 5515
KIKUCHI, K., Electron-photon beam monitoring with image amplifying plate, 20: 5773
KIM, Sedong, Measurement of N^{*-}–N^{*++} mass difference, 20: 6042 (UCRL-16189)
KIM, Young S., Polarization of Λ^0 particle produced from protons in carbon nuclei by 1.17-Bev/c negative pions, 20: 6071
KIMBALL, R. F., Induction of reparable permutational damage in paramecium aurelia by alkylating agent triethylene melamine, 20: 5417
KIMELDORF, D. J., Humoral factor in radiation-induced motivation, 20: 5303 (USNRDL-TR-925)
KIMURA, I., Interpretation of transverse whistlers, 20: 6207
KINCL, F. A., Bioassay of influence of cortisol in bones of growing rabbits, 20: 5234 (COO-119-232, pp 122-52)
KIND, Wolfgang, Theory of a glow light of low-pressure discharge, 20: 6165
KINO, G. S., New type of instability in thermal plasma, 20: 6505
KINOSHITA, Florence, Influence of sublethal doses of x-radiation on synthesis of hepatic microsomal enzymes, 20: 5282 (AD-623599, pp 1-15)
KINSEY, V. EVERETT, Studies on crystalline lens. XI., 20: 5256
KIRICENKO, G. S., Interaction of ion beams with plasma leading to "two-beam" instabilities, 20: 6467 (ORNL-tr-870)
KIRIN, I. S., Production of unusual rare earth phthalocyanines, 20: 5560
KIRSTEN, Thomas, Expanded kinetic theory of plasmas in rotating magnetic fields and electromagnetic supplementary fields, 20: 6479
KISELEV, V. G., Reduction of carbon dioxide by hydrogen under effect of fast electrons, 20: 5574
KISELEVA, N. N., Development of hot synthesis methods for ^{35}S labeled biologically active substances. III., 20: 5586
KLAUDER, John R., Rotationally symmetric model field theories, 20: 6117
KLEIN, A., Self-consistent theory of bounded rotational spectra. I., 20: 6344
KLEIN, Abraham, Interpretation of higher rotational states of deformed nuclei, 20: 6416
KLEIN, George W., Radical yields in radiolysis of hydrocarbons. II., 20: 5576
KLEMENT, Alfred W. Jr., Natural environmental radioactivity, 20: 5668 (WASH-1061)
KLIMOV, V. G., Use of impulse magnetic fields in devices with trochoidal electron beams, 20: 5929
KLINKNER, K. C., Post assembly electrical checkout of 10FS-3 in building 013, 20: 6658 (NAA-SR-Memo-11436)
KLOEPPEL, P., Measurement of proton-proton triple scattering at 430 Mev, 20: 6056
KLOEPPER, R. M., Neutron and gamma sensitivities of dynamic detectors, 20: 5728 (IBM-65-825-1487)
KLOUWEN, H. M., Biochemical and morphological changes in lymphatic tissues after partial-body irradiation, 20: 5341
KLYUCHAREV, V. A., Applications of Moessbauer effect and perturbed angular correlation method in nuclear physics, 20: 6293 (NP-15603)
KNIEFEL, R. M., Brittle and plastic behavior of hot-pressed BeO, 20: 5902
KNILEY, D. J., Large SGR calandria vessel stayed head study, 20: 6616 (NAA-SR-Memo-11324)
KNILEY, D. J., Large SGR calandria vessel peripheral hanger test, 20: 6618 (NAA-SR-Memo-11415)
KNILEY, D. J., Large SGR process tube-graphite log structural interaction study, 20: 6619 (NAA-SR-Memo-11416)
KNOCH, W., Separation of some fission products and actinides on paper treated with liquid anion exchanger, 20: 5509
KOBE, Donald H., Coupling between energy gap and single particle energy, 20: 6311
KOCH, Guenter, Determination of uranium and free acid in organic solutions of long-chain ammonium nitrates, 20: 5518
KOCH, R., Energy and intensity measurements of gamma radiation emitted by ^{182}W and ^{183}W during decay of ^{182}Ta and ^{183}Ta, 20: 6428
KOEHLER, A. M., Range of protons in human skullbone, 20: 5475
KOEHLER, D. R., Single crystal Compton spectroscopic techniques, 20: 5775
KOEHLER, W. C., Magnetic structures of metallic erbium, 20: 6541
KOELLING, R. A., Adaptive responses to ionizing radiation, 20: 5319
KOEPPE, P., Remarks on work "on thorotrast problem" of G. Bluemel, R. Lehner, and W. Zaunbauer, 20: 5400
KOEVER, G., Effects of x radiation and different substances on permeability characteristics of red cells, 20: 5342
KOGA, Kohachiro, Influences of estrogen on radiosensitivity of cervical cancer, 20: 5472

KOGAN, V. I., Detection of secondary-electron currents by scintillation counter, 20: 5757
KOHONEN, T., Versatile routing system for multichannel analyzers, 20: 5769
KOLAR, J., Generalized response of calcified mammalian tissues to local injury, 20: 5370
KOLOTOV, O. S., Recording of short pulses of electron current from betatron injector, 20: 5958
KOLSTAD, G. A., Conference on pulsed high intensity fission neutron sources, USAEC, Washington, 20: 6256 (CONF-650217)
KOLYADIN, A. B., Electrophoretic filter for purifying reactor water, 20: 6568
KOLYBASOV, V. M., Capture of stopped π^- mesons by light nuclei, 20: 6292 (NP-15601)
KOMAROV, I. V., Density matrix for system of noninteracting fermions, 20: 6147
KOMAROV, V. A., Study of (d,p) stripping effect on intermediate nuclei. III., 20: 6422
KONDO, Makoto, X-ray induced photoluminescence spectra from NaI(Tl) and CsI(Tl), 20: 6537
KONDO, Sohei, Experiment S-4, radiation of blood, 20: 5297 (ORNL-P-1734)
KONONENKO, K. I., Two detection mechanisms in gas discharge plasma, 20: 6486
KONOPLEV, K. A., Electrophoretic filter for purifying reactor water, 20: 6568
KONOTOP, V. V., Low-inductance capacitors, 20: 5688 (UCRL-Trans-1273(L))
KONOVALOV, E. A., Application of polyethylene pipes in dosimetric lines for air control, 20: 5752
KONZAK, C. F., Prog. rpt. on radiosensitivity of plants, annual, 11/64–10/65, 20: 5298 (RLO-353-4)
KORENMAN, G. Ya., Effects of resonance modes on channel coupling in nuclear reactions, 20: 6426
KORNBICHLER, Siegfried, Diffusion constants of thermal neutrons in H_2O, phenylene, $ZrH_{1.92}$, and D_2O. II., 20: 6271
KORNIYENKO, I. A., Effect of D_2O on vital staining and heat stability of skeletal muscles of frog, 20: 5317
KOROBEINIKOV, I. A., Temperature and neutron irradiation effects on plastic deformation of alpha uranium single crystals, 20: 5916
KOROTKIKH, V. L., Effects of resonance modes on channel coupling in nuclear reactions, 20: 6426
KOROTKOV, M. M., Measurement of relationship of proton pulse in ITEF, 20: 5941 (NP-15598)
KORYAKIN, Yu. I., Method of calculation of water and power costs for nuclear desalination plants, 20: 6649
KOSORUKOV, A. L., Concerning spectrum of γ rays in (n,γ) reaction, 20: 6427
KOSTKA, A., (d,α) Reactions on light nuclei, 20: 6369
KOTTMEIER, H. L., Diagnosis and treatment of ovarian malignancies, 20: 5446
KOUTS, Herbert, Fast reactors repetitively pulsed by mechanical means, such as motion of fuels (IBR) or reflector (SORA), 20: 6672 (CONF-650217, pp 25-35)
KOWALSKI, K. L., Off-shell equations for two-particle scattering, 20: 6139
KOZLOV, F. A., Dependence of heat conductivity of sodium on concentration of oxides, 20: 5901
KOZLOV, I. G., Experimental investigation of electrostatic charged particle energy analyzer properties, 20: 5691
KOZYREV, A. P., Alkali metals boiling heat transfer, 20: 5627
KRAAK, W., Electrophoretic separation of some actinide and lanthanide elements, 20: 5598
KRACHT, U., Data logging used on proton linear accelerator, 20: 5953
KRAFT, E., Spectrum of muons, protons, and electrons at 5200 m altitude, 20: 6021
KRAMASZ, J. G. Jr., Multichannel spectrometer for analysis of pulsed ion sources, 20: 5698
KRAMER, E. L., Transpiration-cooled nozzle as applied to gas-core nuclear propulsion system, 20: 6663
KRASCELLA, N. L., Experimental refractive indices and theoretical small-particle spectral properties of selected metals, 20: 5879 (D-910092-6)
KRASCELLA, N. L., Theoretical investigation of opacity of heavy-atom gases, 20: 6594 (D-910092-4)
KRASNOV, L. V., Study of (d,p) stripping effect on intermediate nuclei. III., 20: 6422
KRAUS, K., Uncertainty between angle and angular momentum, 20: 6154
KRAUS, Kurt A., Ion exchange procedures. VII., 20: 5597
KRIMIGIS, S. M., Impulsive emission of ≈ 40-kev electrons from the sun, 20: 5971
KRISE, George M., Effect of radiation on audition and conditioned responses in spanish goat, 20: 5369
KRISTOFF, J., Stabilization of lithium-drifted silicon surface-barrier detectors, 20: 5767
KROEGER, Henry R., Electric propulsion possibilities using steam space power, 20: 5639
KRONBERGER, Hans, Fresh water by nuclear power, 20: 6650
KROPOTKIN, A. P., Electromagnetic wave confluence in cold magnetoactive plasma, 20: 6484
KRUECKEMEYER, K., Renal carcinoma as thorotrast injury, 20: 5332
KRUGER, Owen L., Phase studies on U–20w/o Pu–Fs alloys, 20: 5876 (ANL-6974)
KUBOTA, Masayuki, Studies on chemical protectors against radiation injury. I., 20: 5410
KUCHEROV, R. Ya., Cascade theory for multicomponent isotope separation, 20: 5825
KUCHOWICZ, Bronislaw, Proposal of experiment with artificial neutrino source, 20: 6050
KUCKUCK, R. W., Response function and sensitivity of double-diffused silicon detectors in high γ-dose rate fields, 20: 5743 (UCRL-14405)
KUHNKE, E., Effect of x-rays on thrombocyte containing clotted blood plasma, 20: 5365
KUIVILA, Henry G., Prog. rpt. on displacement and exchange reactions involving organometallic compounds, final, 10/65, 20: 6687 (NYO-3453-1)
KUKULA, F., Iron determination in antimony by activation analysis, 20: 5507
KULAKOV, B. A., Analogue wire spark chamber system for measurements of particle momenta and angles, 20: 5730 (JINR-E-2366)
KULANDER, J. L., Non-equilibrium radiation, 20: 6443 (AD-617383)
KULT, K., Initial trajectories of ions leaving an open cyclotron ion source at non zero initial conditions, 20: 5946 (UJV-1408/65)
KUNITOMI, Nobuhiko, Choice of collimators for neutron diffraction, 20: 6268
KUNTZE, M., High-frequency structure for proton linear accelerator, 20: 5937 (KFK-346)
KURASHOV, A. A., Light pencil, 20: 5690
KURODA, K., 141-Mev polarized proton beam of Orsay synchrocyclotron, 20: 6328
KURODA, P. K., Strontium isotopes: global circulation after Chinese nuclear explosion of 14 May 1965, 20: 5656
KURTEPOV, M. M., Corrosion of austenitic stainless steel during evaporation of radioactive solution, 20: 5856
KUTOVOI, V. I., Linear attenuation coefficient of ^{60}Co and ^{137}Cs γ-emission by alloys, 20: 6523
KUZMIAK, M., Initial trajectories of ions leaving an open cyclotron ion source at non zero initial conditions, 20: 5946 (UJV-1408/65)
KUZNETSOV, M. I., Use of gamma-gamma coincidence spectrometer with summation of pulse amplitudes for analysis of a mixture of radioactive isotopes, 20: 5753

L

LA BRECQUE, G. C., Advances in insect population control by sterile-male technique, 20: 5815 (STI/DOC/10/55)
LACKS, Sanford, Genetic recombination in pneumococcus, 20: 5229 (BNL-9407)
LADU, M., Background current in dielectric liquid ionization chambers, 20: 5771
LAESSIG, R. H., Continuous back-titrations with direct readout, 20: 5502
LAFONTAINE, A., Radionuclides in food, 20: 5431
LAGRANGE, J. M., Investigation of rotation levels in odd-odd nucleus ^{234m}Pa, 20: 6331
LAHR, H., Separation of some fission products and actinides on paper treated with liquid anion exchanger, 20: 5509
LAIHO, R., Superconducting magnet using double Helmholtz coils, 20: 5614
LAKSHMINARAYANA, V., Coherent scattering cross-sections of ^{60}Co and ^{137}Cs gamma rays, 20: 6323
LAL, M., Step annealing in radiation damage in solids, 20: 5580
LALANNE, C. M., Surgery of larynx and hypopharynx after radiotherapy, 20: 5463
LAMB, G. L. Jr., Equilibrium statistical mechanics of two-component plasma, 20: 6504
LAMBE, J., Macroscopic quantum interference in superconductors, 20: 6235
LAMERTON, Leonard F., Increased sensitivity of in vitro murine leukemia cells to fractionated x-rays and fast neutrons, 20: 5361
LAMPE, Laszlo, Iodine storage in thyroid gland of human fetus, 20: 5259
LANDAHL, H. D., Dose reduction factor for radiation lethality in mice as function of dose of mercaptoethylamine, 20: 5407 (AD-623599, pp 37-44)
LANDE, A., Vibrations, strength functions and intermediate structure, 20: 6345
LANDSBERG, L. G., Large scintillation counters and counters for operation in magnetic fields, 20: 5736 (NP-15597)
LANG, H. J., Area radiation monitor system with logarithmic indication and audiovisual warning, 20: 5733 (LA-DC-6790)
LANGE-HESSE, G., Oscillation of ionization ionosphere in median latitudes, 20: 6187
LANZOLA, E., Determination of ^{90}Sr in deciduous teeth, 20: 5655
LAPIDUS, I. Richard, Radiative τ decays and σ meson, 20: 6067

LARICHEV, A. V., Angular distribution of gamma rays emitted by a point source and scattered in shielding, 20: 6527
LARSEN, R. P., Analytical research and development, 20: 5493 (ANL-6925, pp 253-4)
LATZKOVITS, L., Investigations on AgI catalyst surface structure by isotope exchange reactions, 20: 5544
LAUBERT, Roman, Prog. rpt. on design and construction of bakeable sputtering apparatus, 11/60–12/63, 20: 5981 (AD-620002)
LAUGIER, J. P., Reaction $^{6}Li + T = 2\alpha + n$ at low incident energies, 20: 6351
LAURAT, Michel, Excitation curve of (n,2n) reaction on ^{63}Cu from 16.59 to 17.71 Mev, 20: 6319
LAUTZENHEISER, Clarence E., Nondestructive testing of plastic fatigue pressure vessels, 20: 5894 (SWRI-1228-3-3)
LAWLER, Ronald G., Electron spin resonance studies of deuterium isotope effects, 20: 5566
LAWRENCE, D. C., ^{131}Cs seeds for permanent implants, 20: 5482
LAWRENCE, D. Dennis, PLANE WAVE—computer program to find ionization cross sections, 20: 5986 (UCRL-14402-T)
LAYZER, Arthur, Vertex theory of many-fermion systems, 20: 6111
LAZARD, Bertrand, Method for bithermal isotopic enrichment of ammonia with deuterium, 20: 5827
LAZARUS, R. B., Computation of fast neutron penetration in air by "Sn-method", 20: 6261 (LA-3415)
LEBEDEV, A. I., Magnetic polarizability of π and K mesons, 20: 6090
LEBEDEV, I. A., Production of ^{242}Pu and ^{242}Cm by irradiating ^{241}Am with neutrons, 20: 5823 (ORNL-tr-892)
LEBEDEV, L. M., Temperature and neutron irradiation effects on plastic deformation of alpha uranium single crystals, 20: 5916
LECKY, James A., Catalog of nuclear reactor concepts. I., 20: 6554 (ANL-7092)
LECOUSTEY, Luc H., Heating and confinement of plasma in magnetic well of deca-2, 20: 6469 (UCRL-Trans-1256(L))
LEDERMAN, M., Cancer of middle ear; technique of radiation treatment, 20: 5448
LEE, W. W., Finite and infinite H-plane bifurcation of wave guide with anisotropic plasma medium, 20: 6481
LEFEVRE, Harlen W., Amplitude-independent nanosecond timing discriminator for fast photomultipliers, 20: 5744 (UCRL-16227)
LEFORT, Marc, Evaporation of charged particles from heavy nuclei, 20: 6364
LE GAILLARD, Y., Generating functional of propagators in quantum electrodynamics, 20: 6220
LEGGETT, A. J., Theory of superfluid Fermi liquid. I., 20: 6237
LEGGETT III, W. D., In-core instrumentation for San Onofre nuclear generating station, 20: 6630 (WCAP-3269-46)
LE GUEN, Y., 141-Mev polarized proton beam of Orsay synchrocyclotron, 20: 6328
LEGVOLD, S., Magnetostriction of erbium single crystals, 20: 6547
LEHMANN, J., Deviation from statistical shape of $\frac{1}{2}^{+}-\frac{1}{2}^{-}$ β^{-} transition in decay of ^{199}Au, 20: 6358
LEHNER, R., Concluding word to current remarks of P. Koeppe, 20: 5399
LEHNER, R., Thorotrast problem, 20: 5398
LEISI, H. J., Angular correlations in decay of ^{127}Xe, 20: 6384
LEITCH, James L., FORTRAN IV program for evaluation of post-irradiation survival times, 20: 5300 (UCLA-12-573)
LEITNER, J., Momentum dependence of S matrix for many-particle processes, 20: 6061
LELAND, Thomas W. Jr., Catalytic activation of Vycor glass for H_2-D_2 exchange reaction by beta irradiation, 20: 5578
LEMAIRE, J., Influence of irradiation on some carbon or low-alloy steels, 20: 5921
LEMMEL, Hans-Dietrich, Diffusion constants of thermal neutrons in H_2O, phenylene, $ZrH_{1.92}$ and D_2O. I., 20: 6270
LEMOINE, J., Contribution to study of heavy hypernuclei, 20: 6294 (NP-15617)
LENCHENKO, V. M., Contribution to theory of semiconductor counters for ionizing particles, 20: 5758
LENCHENKO, V. M., Theory of scattering of fast charged particles in crystals, 20: 6535
LEONARD, A., Energy-dependent neutron transport theory in plane geometry. II., 20: 6252 (AD-617880)
LEONARD, A., Energy-dependent neutron transport theory in plane geometry. III., 20: 6253 (AD-617882)
LEONARDI, R., T = 2 levels in ^{16}O, 20: 6342
LE POITTEVIN, G., Determination of spin and resonance parameters for $^{197}Au + n$ at 10 to 1000 ev, 20: 6392
LERAT, Jean-Marie, Method for bithermal isotopic enrichment of ammonia with deuterium, 20: 5827
LESSMANN, H. D., Renal carcinoma as thorotrast injury, 20: 5332
LEVENSON, M., Studies and evaluations, 20: 6553 (ANL-6925, pp 255-63)
LEVIN, J., LASL tandem accelerator facility data system, 20: 5939 (LA-DC-7267)
LEVIS, Angelo Gino, Radiomimetic effects of nitrogen mustard on multiplication of mammalian cells cultured in vitro, 20: 5323
LEWIS, B. A., n = 4 Levels of N^{V} by electron impact, computed with Coulomb-Born approximation, 20: 5982 (AERE-R-5061)
LEWIS, George C. Jr., Gynecologists' retreat from cancer therapy, 20: 5473
LIANG, George Hsueh-lee, Effect of x-rays in red clover Trifolium pratense L., 20: 5491
LIBINSON, R. E., Activity of deamination of adenosine and adenylic acid in tissues of irradiated rabbits, 20: 5380
LICHTIN, Norman N., Radiolysis of methanol and methanolic solutions. IV., 20: 5581
LIDOFSKY, L. J., Angular correlation measurements on $^{25}Mg(d,p\gamma)^{26}Mg$ reaction, 20: 6410
LIEBERMAN, M. L., Scandium–yttrium–hydrogen system, 20: 5909
LIEBOWITZ, B., Classical dynamics and Schroedinger theory, 20: 6225
LIGHTBODY, D. B., Search for excited states of ^{5}He, 20: 6335
LILLEGRAVEN, A. L., Systematic arc calibration method for body radioactivity measurement, 20: 5426
LILLIEHOEOK, B., Agesta Power Heating Plant, 20: 6599 (AES-5)
LINCOLN, J. Virginia, Geomagnetic and solar data, 20: 6206
LINDENBAUM, S. J., Strong interactions at high energy, 20: 6101 (BNL-9652)
LINETSKII, V. Ya., Low-inductance capacitors, 20: 5688 (UCRL-Trans-1273(L))
LINHART, Jiri George, Process for producing intense magnetic fields for purpose of confining plasma, 20: 6515
LIN'KOV, R. V., Use of impulse magnetic fields in devices with trochoidal electron beams, 20: 5929
LIPKIN, H. J., Experimental tests of broken $\bar{U}(12)$ and approximate $U(6) \times U(6)$, 20: 6066
LIPKIN, H. J., Noncollinear diagrams and Johnson-Treiman relations, 20: 6143
LIPPERT, J., Environmental radioactivity in Denmark in 1964, 20: 5651 (RISO-107)
LIRON, Meir, Reversion by erythropoetin of suppression of erythroid clones caused by transfusion-induced polycythemia, 20: 5242
LITHERLAND, A. E., Gamma-ray transitions in ^{15}O and ^{16}N, 20: 6318
LITTLE, W. A., Prog. rpt. on electron scattering experiments, 3/15–6/30/65, 20: 6275 (AD-619534)
LITVIN, V. F., Study of (d,p) stripping effect on intermediate nuclei. III., 20: 6422
LIU, Chao Han, Reflection of electromagnetic waves from inhomogeneous plasma, 20: 6445 (AD-617619)
LIU, L. S., Baryon resonance production by neutrinos and relativistic generalizations of SU(6), 20: 6065
LIU, M., Study of nuclei of medium mass by inelastic scattering of 155 Mev protons. I., 20: 6354
LIUZZO, Joseph A., Physiological changes induced by gamma irradiation of bacteria from shrimp, 20: 5346
LO, Liew-fu, Selection rules in nonleptonic decays of strange particles, 20: 6085
LO, Y. T., Finite and infinite H-plane bifurcation of wave guide with anisotropic plasma medium, 20: 6481
LOBANOV, Yu. N., Recording of short pulses of electron current from betatron injector, 20: 5958
LOBOV, G. A., CP-parity violation in decay of polarized neutrons, 20: 6087
LOFSTROM, James E., Spinthariscon: new approach to radiation imaging, 20: 5461
LOGINOV, A. A., Method of calculation of water and power costs for nuclear desalination plants, 20: 6649
LOGINOV, G. A., Computation of current system of S_d variations in high latitudes, 20: 6193
LOINGER, A., Dirac equation without Dirac matrices, 20: 6223
LOISELEUR, Jean, Suppression of diarrhea provoked in rat by fatal dose of x rays, 20: 5411
LOKEN, Merle K., ^{99m}Tc compounds for visualization of body organs, 20: 5456
LONCKE, P., T = 2 levels in ^{16}O, 20: 6342
LONGEQUEUE, Nicole, Contribution to study of (d,p) and (d,α) reactions on ^{16}O and ^{11}B from 200 kev to 1 Mev, 20: 6281 (CEA-R-2807)
LONTAI, Laszlo N., Study of thermonuclear reactor blanket with fissile nuclides, 20: 6453 (AD-619670)
LOPES, J. S., $\frac{5}{2}^{+} + \frac{1}{2}$ Hole transitions in mass 15, 20: 6378
LOPUSZYNSKI, Jerzy, Magnox power reactors after the Third Geneva Conference, 20: 6612 (INR-622/IX/R)
LORENTS, D. C., Perturbation induced in elastic scattering by crossing of molecular states, 20: 5996
LORIERS, H., Zirconium–copper alloys resistant to oxidation by carbon dioxide at high temperature, 20: 5860
LOW, W., X-ray excitation of second positive and first bands of nitrogen, 20: 6181 (AD-619288)
LOWE, M., Studies of trabecular bone in beagles and humans, 20: 5233

(COO-119-232, pp 99-121)
LOWENSON, J., Calibration of S10A radiation detection systems, 20: 6656 (NAA-SR-Memo-11333)
LUCHTER, Stephen, Internal vs external mounting of nuclear powerplants for deep submersibles, 20: 6664
LUETJENS, G., Search for neutral scalar meson, 20: 6079
LUKASH, N. I., Decrease in resistance of mice to blastomogenetic effect of urethan after their generalized treatment with small doses of γ-rays, 20: 5328
LUTZ, H. F., Elastic and inelastic scattering of protons by ^{18}O, 20: 6373
LYONS, M. F., Prog. rpt. on high performance UO_2 program, 4–7/65, 20: 5914 (GEAP-3771-17)

M

MAC LAREN, M. D., Notes on axioms for quantum mechanics, 20: 6213 (ANL-7065)
MAC PHERSON, R. D., Fourier analysis of uniform random number generators, 20: 5833 (ORNL-3866)
MACUR, George, Viscosity of NaK 78 at low temperatures, 20: 5908
MACZKA, D., Electromagnetic isotope separator at Lublin, 20: 5826
MAEDER, Paul F., High-efficiency A.C. MHD apparatus, 20: 6028
MAENTYSALO, E., Superconducting magnet using double Helmholtz coils, 20: 5614
MAGERU, Victor, Correlation between radon concentration at ground level and certain meteorological parameters, 20: 5646
MAHLMAN, J. D., Case study of mass transport from stratosphere to troposphere, not associated with surface fallout, 20: 5649(R) (COO-1340-2, pp 54-83)
MAHLMAN, J. D., Development of computer programs for computation of Montgomery stream functions and plotting of thermodynamic diagrams, 20: 5645(R) (COO-1340-2, pp 122-45)
MAHLMAN, J. D., Heavy ^{131}I fallout over midwestern United States, May 1962, 20: 5648(R) (COO-1340-2, pp 1-53)
MAHLMAN, J. D., Relation of tropopause-level index changes to radioactive fallout fluctuations, 20: 5650(R) (COO-1340-2, pp 84-109)
MAIANI, L., Classification of higher boson resonances, 20: 6134
MAIANI, L., Kinetic supermultiplets of $\bar{U}(12)$, 20: 6058
MAIER, B. P., Energy and intensity measurements of gamma radiation emitted by ^{182}W and ^{183}W during decay of ^{182}Ta and ^{183}Ta, 20: 6428
MAITLAND, A., Electrode protrusions produced by electron beam bombardment, 20: 5809
MAJOR, John K., Prog. rpt. on recoil-free scattering of gamma-rays, final, 3/62–6/65, 20: 6302 (TID-22384)
MAKASHEV, Yu. A., Production of unusual rare earth phthalocyanines, 20: 5560
MAKHLIS, F. A., Method for computing efficiency coefficient of radiation apparatus with plane gamma sources, 20: 5750
MAKI, Kazumi, Entropy transport between two superconductors by electron tunneling, 20: 6248
MAKI, Kazumi, Equivalence of different pair-breaking mechanisms in superconductors, 20: 6233
MAKITA, Motoo, Experimental osteogenic sarcoma, 20: 5334
MAKOVSKY, J., Afterglow of x-irradiated alkaline-earth fluorides doped with rare earths, 20: 6550
MALANIFY, John Joseph, Direct (n,p) reaction on ^{58}Ni and ^{60}Ni, 20: 6440
MALASPINA, L., Mass-spectrometric study of yttrium–carbon system, 20: 5540
MALCOLM, R., Scattered neutrons and gamma rays from $^{16}O(n,n\gamma)^{16}O$ reaction at $E_n = 14.1$ Mev, 20: 6346
MALLAMS, John T., Irradiation therapy of the larynx, 20: 5486
MALMBERG, J. H., High frequency inductance of torus, 20: 6508
MALYHIN, V. M., Biological dose of ^{90}Sr internal irradiation of man, 20: 5429
MALYSHEV, A. V., Nuclear equation of state from inelastic neutron scattering spectra, 20: 6379
MAMEDOV, T. G., Some regularities of changes in plants after γ irradiation, 20: 5388
MANCHETTE, M., New apparatus for increased protection in televised radioscope, 20: 5464
MANDEL, H., Recommendations for standardization and improvement of PHA procedures at PNPF, 20: 6615 (NAA-SR-10888(Rev.))
MANFRASS, Peter, Liquid scintillator for slow neutrons, 20: 5746 (ZFK-RN-18)
MANGIALAJO, M., Indirect method for monitoring 2.5 Mev neutrons, produced by 150 kv accelerator, 20: 5777
MANGIARACINA, Richard S., Zero-field electron magnetic resonance of irradiated glycine peptides, 20: 5273
MANI, H. S., T violation and electromagnetic interactions, 20: 6059
MANKO, V. I., Possible use of groups B_3, C_3 and D_3 for classification of elementary particles, 20: 6149
MANTEIFEL, V. M., Fluorimetric investigation of second luminescence of lymphocytes of lymphatic glands in irradiated rats, 20: 5383
MANUZIO, G., Photoprotons from Mg, 20: 6399
MARAIS, P. G., Half-life of ^{51}Cr, 20: 6420
MARCHI, R. P., Perturbation induced in elastic scattering by crossing of molecular states, 20: 5996
MARK, Harry B. Jr., Electrochemical preparation of thin metal films as standards on pyrolytic graphite, 20: 5503
MARQUEZ, L., Reaction $^6Li + T = 2\alpha + n$ at low incident energies, 20: 6351
MARSHAM, T. N., Economic power from gas-cooled reactors, 20: 6644
MARTENEY, P. J., Experimental refractive indices and theoretical small-particle spectral properties of selected metals, 20: 5879 (D-910092-6)
MARTENS, John H., Catalog of nuclear reactor concepts. I., 20: 6554 (ANL-7092)
MARTIN, J. A., Neutron and gamma sensitivities of dynamic detectors, 20: 5728 (IBM-65-825-1487)
MARTUSOV, E. T., Measurement of relationship of proton pulse in ITEF, 20: 5941 (NP-15598)
MARTYNOVA, T. T., Influence of irradiation on lipids of mitochondria of liver cells, 20: 5379
MASAIKA, A., Electron-photon beam monitoring with image amplifying plate, 20: 5773
MASLOV, V. I., Action of low irradiation doses and incorporated natural radioactive elements on spermatogenesis of Microtus oeconomus under natural conditions, 20: 5387
MASLOVA, K. I., Action of low irradiation doses and incorporated natural radioactive elements on spermatogenesis of Microtus oeconomus under natural conditions, 20: 5387
MASON, E. A., Differences in spherical intermolecular potentials of hydrogen and deuterium, 20: 5541
MATHE, Georges, Hematopoietic cell grafts and their applications, 20: 5420
MATHISEN, R. P., Experimental study of natural circulation in loop with parallel flow test sections, 20: 5620 (AE-200)
MATHUR, Suresh C., Disintegration of Ar by 13.0–20.2 Mev neutrons, 20: 6357
MATINYAN, S. G., Hadronic decays of baryons in broken SU(6)-symmetry, 20: 6152
MATSUDA, S., Kinetic theory of particles and waves, 20: 6462 (GA-6650)
MATSUNANGA, Sakuro, Alternating current magnetohydrodynamic generator, 20: 6026
MAUERSBERGER, P., Application of theoretical magnetohydrodynamics to geophysics, 20: 6212
MAURAKH, M. A., Viscosity of liquid zirconium, 20: 5899 (JPRS-32341, pp 1-7)
MAYER, E. G., Several cases of radiation injury, 20: 5241
MAYNEORD, M. V., Background radiations and their origins, 20: 5409
MAYO, R. F., "Spark-plug" starter for arc plasma generators, 20: 6489
MC CLAY, J. F., Hydromagnetic eigenmodes in multipole fields, 20: 6492
MC CLELLAN, R. O., Gamma radiation dosimetry of ^{137}Cs in sheep evaluated with thermoluminescent dosimeters, 20: 5285 (BNWL-SA-172)
MC CLURE, J. A., Spin correlations in photoproduction of vector mesons, 20: 6076
MC CONNELL, D. B., Capture by ^{124}Sn of 62-ev neutrons, 20: 6317
MC CORMICK, W. D., Effects of turbulence in He II thermal counterflow, 20: 6230
MC CRACKEN, K. G., Study of vertically incident cosmic-ray trajectories using sixth-degree simulations of geomagnetic field, 20: 6005 (AD-623632)
MC CULLOCH, R. D., Search for neutral scalar meson, 20: 6079
MC DONALD, J. Jr., Advanced BONUS core boiler-superheater fuel element weldments, 20: 6624 (TID-22425)
MC DONALD, W. J., Scattered neutrons and gamma rays from $^{16}O(n,n\gamma)^{16}O$ reaction at $E_n = 14.1$ Mev, 20: 6346
MC DONNELL, C., Barrier attenuation introduced by vertical wall, 20: 6516 (AD-617524)
MC FARLIN, David J., Effect of peripheral-wall injection technique on turbulence in air vortex tube, 20: 6652 (D-910091-5)
MCGIRR, Edward M, Clinical studies with gamma camera, 20: 5467
MC GLINN, W. D., Current commutation relations and meson-meson scattering, 20: 6077
MC GOWAN, J. William, Electron–H-atom elastic-scattering resonances, 20: 5999
MC HARRIS, William Charles, Decay schemes of odd-odd Einsteinium isotopes, 20: 6305 (UCRL-11784)
MC HUGH, J. A., Independent yields of ^{86}Rb, ^{132}Cs, ^{134}Cs, and ^{136}Cs in thermal neutron fission of ^{235}U, 20: 6288 (KAPL-3113)
MC INTIRE, H. O., Tungsten powder metallurgy, 20: 5836 (NASA-SP-5035)
MC KEE, D. W., Kinetics of methane–deuterium exchange over noble metal alloys, 20: 5557
MC NEILL, K. G., Capture by ^{124}Sn of 62-ev neutrons, 20: 6317
MC NEILL, K. G., Scintillation spectra from point sources in scattering medium, 20: 5760
MC NEILL, K. G., ^{137}Cs body burdens in Toronto, 20: 5671

MC PHERRON, R. L., Auroral-zone pearl pulsations, 20: 6204

MC PHERSON, A. I., Second maximum of cosmic-ray star frequency under lead, 20: 6015

MC PHERSON, R., Oxygen-13, 20: 6405

MC WILLIAMS, Paul, Radiosensitivity, circadian rhythmicity, and radiobiology, 20: 5336

MDZEWSKI, B., Influence of occupational exposure to chemical agents and x-rays on leucocyte alkaline phosphatase activity, 20: 5269

MECHAM, W. J., Studies and evaluations, 20: 6553 (ANL-6925, pp 255-63)

MEDEIROS, Katherine W., NAA program description. CAVORT, 20: 6562 (NAA-SR-Memo-11369)

MEERS, J. T., Prog. rpt. on effects of neutron damage on properties of pyrolytic and single crystal graphite, semiannual, 1–6/65, 20: 5897 (TID-22420)

MEISSNER, Hans, Dependence of critical currents in superconducting films on applied magnetic field and temperature, 20: 6232

MELDNER, H., Nonlocal nuclear single particle potential and charge independence of short-range forces, 20: 6430

MELDNER, H., Relation between experimentally observed single particle energies and levels of extreme single particle model, 20: 6431

MELDNER, Heiner, Nucleon-nucleus scattering and shell model, 20: 6434

MELE, A., γ-radiolysis of ethylene sensitized by "inert" gases, 20: 5582

MELZER, W., Position finding counter for Buechner magnet, 20: 5747 (NP-tr-1302)

MENDELSON, M. R., Infinite medium spectrum-weighted group constants for gamma heating calculations, 20: 6517 (CONF-651101-41)

MERCEREAU, J. E., Macroscopic quantum interference in superconductors, 20: 6235

MERRIHUE, Craig, Origin of anomalous ^{129}Xe in meteorites, 20: 5978

MESHCHERYAKOV, V. A., Method of constructing certain classes of solutions for Chew-Low type equations, 20: 6106 (JINR-P-2369)

MESSERLE, Hugo K., Traveling wave interaction and wave growth in dense plasma, 20: 6491

MEYER, R. J., Analytical research and development, 20: 5493 (ANL-6925, pp 253-4)

MEYER, Wolfgang, Method for fabrication of compact uranium dioxide particles of predetermined grain size, 20: 5869

MICAL, R., Studies of trabecular bone in beagles and humans, 20: 5233 20: 5233 (COO-119-232, pp 99-121)

MICHALOWICZ, A., 141-Mev polarized proton beam of Orsay synchrocyclotron, 20: 6328

MICHELS, H. H., Theoretical investigation of lowest five ionization potentials of uranium, 20: 5983 (D-910099-2)

MICHELSON, Donna C., Ion exchange procedures. VII., 20: 5597

MICKELSEN, William R., Ion propulsion systems for spacecraft, 20: 5637

MIGAHED, M., Gamma intensities in decay of ^{187}W, 20: 6397

MIKHAILOV, B. M., Reduction of carbon dioxide by hydrogen under effect of fast electrons, 20: 5574

MIKHAILOVA, L. F., Urinary secretion of thymidine following whole-body exposure of rats to various doses of x radiation, 20: 5382

MIKHNEVICH, V. V., Preliminary results of determining particle concentration and atmospheric density on 18 June 1963, 20: 6210

MIKKELSON, R. C., Anisotropic spin-lattice relaxation rates of some rare-earth-doped lanthanum trichlorides, 20: 6542

MIKOLAJ, Peter J., Comparison of two methods of analyzing hematological data from ^{90}Sr injected beagles, 20: 5290 (COO-119-232, pp 165-89)

MILCU, S. M., Investigations in medicine carried out in Rumania with aid of radioisotopes, 1958–1964, 20: 5435 (NP-15543, pp 59-75)

MILFORD, S. N., Secondary protons from cosmic-ray collisions in space, 20: 5973

MILLER, J., Elastic scattering of photons in region of giant resonance, 20: 6349

MILLER, J. F. A. P., Etiology and pathogenesis of mouse leukemia, 20: 5309

MILLER, K. J., Post-irradiation examination of treat capsules No. 5 through 9, 20: 6678 (NAA-SR-Memo-11374)

MILTENYI, Laszlo, Effect of ionizing radiation on iron metabolism of body, 20: 5354

MINAKAWA, Nobuaki, Choice of collimators for neutron diffraction, 20: 6258

MINC, Stefan, Solvent extraction of inorganic compounds, 20: 5600

MINENKO, V. P., Cascade theory for multicomponent isotope separation, 20: 5825

MIRMAN, R., Hermitian mass operators in certain combined invariance theories, 20: 6136

MISHCHENKO, Yu. A., Nature of surface radiation-induced defects in irradiated silicagel. I., 20: 5584

MITANI, Shichiro, Method for preparation of liquid scintillator in vacuum, 20: 5785

MITCHELL, G. E., Angular correlation measurements on $^{25}Mg(d,p\gamma)^{26}Mg$ reaction, 20: 6410

MITCHELL, J. S., Clinical trial of radiosensitizers, 20: 5437

MITRA, A. N., Relativistic corrections to triton binding energy, 20: 6084

MITRA, S. K., Beta gamma circular polarization correlation in ^{46}Sc, 20: 6391

MITSCHERLICH, H., Equipment for indicating, recording and controlling oscillations of axis of rotation and speed of rotor of gas centrifuge, 20: 5685 (K-Trans-5)

MITTRA, R., Finite and infinite H-plane bifurcation of wave guide with anisotropic plasma medium, 20: 6481

MIYAKE, Y., Strontium isotopes: global circulation after Chinese nuclear explosion of 14 May 1965, 20: 5656

MIZUSHINA, Tomoyuki, Neutron surface moisture gage for determining moisture contents of building materials, 20: 5819

MOEHRUNG, Rolf, Circuit arrangement for Geiger-Mueller counting tube, 20: 5801

MOERTEL, Charles G., Thorium dioxide infusions to demonstrate malignant lesions in the liver, 20: 5465

MOFFAT, J. W., Higher symmetries and neutron-proton magnetic-moment ratio, 20: 6074

MOHAN, Gyan, T violation and electromagnetic interactions, 20: 6059

MOHANRAO, G. J., Method for low-level gamma radioactivity measurement, 20: 5432

MOHINDRA, V. K., Scintillation spectra from point sources in scattering medium, 20: 5760

MOISEEV, A. A., Biological dose of ^{90}Sr internal irradiation of man, 20: 5429

MOISEEV, G. G., Attenuation of reactor radiations in serpentine sand, 20: 6524

MOLANDER, David W., Lymphosarcoma: choice of treatment and end-results in 567 patients, 20: 5485

MOLINARI, Vincenzo, Resistance to physical and chemical agents of entamoeba histolytica, 20: 5366

MOLITOR, J. H., Design and performance of ion-engine systems, 20: 5638

MONAGHAN, Ralph, Radioactivity well logging apparatus utilizing scintillation detector, 20: 5658(P)

MONNIN, Michael, Comparison of registration of tracks of heavy ions in ionographic emulsions and in various solid materials, 20: 5755

MONSONEGO, G., Self-consistent field and study of ground states of closed shell light nuclei, 20: 6363

MONTALVO, Rafael, Irradiation of estrone and derivatives in acetic acid, 20: 5274

MOOS, W. S., Oxygen uptake of three life stages of Tenebrio molitor prior and subsequent to massive doses of low energy x-rays, 20: 5314

MORE, Richard M., New variational scheme for finding excited states of one-dimensional systems, 20: 6221

MOREAU, Jean, Monte Carlo Method—codes for the study of criticality problems (on IBM 7094), 20: 6581 (CEA-R-2872)

MORGAN, I. L., Disintegration of Ar by 13.0–20.2 Mev neutrons, 20: 6357

MORGENSTERN, J., Determination of spin and resonance parameters for $^{197}Au + n$ at 10 to 1000 ev, 20: 6392

MORINAGA, H., Rotational bands of well-deformed nuclei, 20: 6348

MORIYAMA, Hideo, Studies on x-agent. XXIV., 20: 5587

MORK, Kjell, Radiative corrections. I., 20: 6072

MORRISON, David L., Prog. rpt. on analytical description of nuclear-reactor accident, 7–9/65, 20: 6560 (BMI-X-10145)

MORRISON, Ian Hugh, Manufacture of nuclear reactor fuel elements, 20: 5872

MORTON, Harmon L., Survey and evaluation of techniques to augment convective heat transfer, 20: 5618 (AD-619511)

MORTON, P. L., Longitudinal space-charge effects in standing wave linacs, 20: 5962

MORY, Jean, Recording of fission fragments occurring in insulators, 20: 5719 (CEA-R-2846)

MOSCONI, B., Peripheral model and its application to photodisintegration of ^6Li, 20: 6368

MOSKALEV, P. N., Production of unusual rare earth phthalocyanines, 20: 5560

MOTOHASHI, Haruhiko, Choice of collimators for neutron diffraction, 20: 6268

MOTZ, Henry T., PHERMEX—high current linac, 20: 5936 (CONF-650217, pp 77-81)

MOTZ, Henry T., Thermal neutron facility for LAMPF, 20: 5935 (CONF-650217, pp 73-6)

MOTZ, Robin O., Magnetohydrodynamics of oscillating dielectric sphere, 20: 6161 (NP-15630)

MOTZFELD, V., Simple method for preparing x-ray filters of strontium metal, 20: 5692

MOULD, R. F., Cancer of middle ear; technique of radiation treatment, 20: 5448

MOURAD, W. G., Shape of neutron yield from $^7Li(p,n)^7Be$ reaction near threshold, 20: 6355

MOURAVIEFF, N., Study of charged particle beams by means of pick-up electrodes, 20: 5686 (NP-tr-1313)

MOUSTACCHI, E., Induction by physical and chemical agents of mutations for radioresistance in Saccharomyces cerevisiae, 20: 5360

MOUTON, W. L., Nuclear resonant scattering of bremsstrahlung from low-lying levels in ^{27}Al, ^{31}P, and ^{35}Cl, 20: 6380
MOXON, M. C., Neutron cross sections of thorium and analysis of resonances up to 1 kev, 20: 6377
MOZER, F. S., Rocket measurements of energetic particles. II., 20: 6196
MOZER, F. S., Rocket measurements of energetic particles. III., 20: 6197
MUAN, Arnulf, Stability of zircon in temperature range 1180 deg to 1366 deg C, 20: 5537
MUARMATSU, Mitsuo, Desorption of carrier-free ^{60}Co, ^{144}Ce, and ^{147}Pm from charcoal surfaces, 20: 5675
MUCSI, Otto, Effect of ionizing radiation on iron metabolism of body, 20: 5354
MUELLER, Andreas J., Time period of mutation induction after treating soaked seeds of arabidopsis with N-nitroso-N-methylurea, 20: 5357
MUELLER, D., Validity of quasi-particle approximation in nuclear physics, 20: 6433
MUELLER, D. W., Radiation and shielding design factors for Los Alamos meson physics facility, 20: 5940 (LA-DC-7522)
MUELLER, H. J. W., Test of N/D method in potential scattering, 20: 6129
MUELLER, Norbert, Method for fabrication of compact uranium dioxide particles of predetermined grain size, 20: 5869
MUELLER, Robert A., Critical mass studies with NASA Zero Power Reactor II. I. Clean homogeneous configurations, 20: 6587 (NASA-TN-D-3097)
MUENICH, J., Calcium-activated barium sulfate as sorbent of radio-strontium. III., 20: 5531 (UJV-1382/65)
MUETTERTIES, E. L., Chelate chemistry. III., 20: 5538
MUGGLETON, A. H. F., Etching cell for semiconductor counters, 20: 5776
MUJU, B., Separation of some fission products and actinides on paper treated with liquid anion exchanger, 20: 5509
MUKHAMEDZHANOV, A. M., Feynman graph treatment of initial and final state interactions in direct nuclear reactions, 20: 6383
MULAZZI, E., Isotope effects induced by local modes in U band, 20: 6545
MULDERS, Julien, Catalysis of α-H exchange. I., 20: 5565
MULHOLLAND, John H., Effect of endotoxin upon susceptibility to infection: role of granulocyte, 20: 5315
MUMINOV, V. A., Ion source with longitudinal magnetic field, 20: 5951
MURAMATSU, Mitsuo, Removal of radioactive isotopes from cotton cloths, 20: 5676
MURATA, Y., Electron-photon beam monitoring with image amplifying plate, 20: 5773
MURGAI, M. P., Small amplitude wave propagation in hot ionized gases, 20: 6500
MURPHY, R. J., Comprehensive safety shutter and collimator coupling for Philips x-ray tube shield PW 1016, 20: 5693
MURPHY, Walter, Is reirradiation of recurrent cervical carcinoma of any value?, 20: 5457
MUSHRAN, S. P., Conductive and potentiometric study of interaction between sodium succinate and thorium chloride, 20: 5555
MYDOSH, J. A., Dependence of critical currents in superconducting films on applied magnetic field and temperature, 20: 6232

N

NAITOH, P., Effect of whole brain ^{60}Co gamma irradiation on cortical arousal in burro, 20: 5329
NAKACHE, F. R., Nuclear aspects of accidental criticality at Wood River Junction, Rhode Island, July 24, 1964, 20: 5666 (TID-21995)
NAKAGAWA, T., Strongly excited levels of ^{39}Ca in $^{40}Ca(^3He,\alpha)^{39}Ca$ reaction, 20: 6398
NAKAJIMA, Y., Strongly excited levels of ^{39}Ca in $^{40}Ca(^3He,\alpha)^{39}Ca$ reaction, 20: 6398
NARASIMHA MURTY, V. A., Coherent scattering cross-sections of ^{60}Co and ^{137}Cs gamma rays, 20: 6323
NARYSHKINA, L. G., Transient radiation at anisotropic conductive plane, 20: 6043
NATALI, S., Longitudinal polarization of low-energy muons from $K^+_{\mu 3}$ decay, 20: 6075
NATH, P., Modification of Regge-pole representation, 20: 6062
NATLAND, Manley L., Nuclear reactor operational in well bore, 20: 6651
NAUMANN, R. A., Prog. rpt. on nuclear chemistry, annual, 1964–65, 20: 6298 (PPAD-2137-566)
NEAL, Thomas E., Electrochemical preparation of thin metal films as standards on pyrolytic graphite, 20: 5503
NEAL, W. J., SNAPTRAN 2/10A-1 and -2 safety tests, 20: 6654 (IDO-17076)
NEARY, G. J., Chromosome aberrations and theory of RBE. 1., 20: 5343
NEBEKER, H., ^{228}Th induced fractures in beagles, 20: 5288 (COO-119-232, pp 74-87)
NEDDERMEYER, Seth, Cosmic ray muon interactions at 5–50 Bev, 20: 6007
NEDELIK, A., Measurement of ASTRA-transfer function. A and B, 20: 6682 (SGAE-R-1/1965)
NEEF, W. I., Effect of early introduction of breeder reactors on uranium resource conservation, 20: 6611 (HW-SA-3669)
NEEF, W. I., Fuel conservation indexes for thermal reactors, 20: 6610 (HW-79287)
NEHER, Dean Royce, Gamma radiations from proton capture of ^{25}Mg, 20: 6438
NEIDINGER, J. W., Oxygen uptake of three life stages of Tenebrio molitor prior and subsequent to massive doses of low energy x-rays, 20: 5314
NEIGAUZ, M. G., Ground-state energy of He, 20: 5987 (ANL-Trans-248)
NEKOZYREV, A. F., Gamma radiation spectrum from artificial model of radioactive fallout, 20: 5653
NEKRASOVA, I. V., Radioprotective activity of cystamine in process of irradiation of cells of Ehrlich's ascitic carcinoma in vitro, 20: 5412
NELSON, Frederick, Ion exchange procedures. VII., 20: 5597
NEMILOV, Yu. A., Study of (d,p) stripping effect on intermediate nuclei. III., 20: 6422
NEMODA, Djordje, Radioactive source production at Boris Kidric Institute, 20: 5813 (JPRS-32260)
NEMODRUK, A. A., Determination of TBP, kerosene, and synthol, 20: 5516
NEMOTO, J., Strontium isotopes: global circulation after Chinese nuclear explosion of 14 May 1965, 20: 5656
NESS, Norman F., Quasi-stationary corotating structure in interplanetary medium, 20: 5972
NETTER, F., Determination of spin and resonance parameters for ^{197}Au + n at 10 to 1000 ev, 20: 6392
NETTLESHIP, Anderson, Neoplasms of liver following injection of thorotrast, 20: 5311
NEURINGER, L. J., Upper critical fields of Nb–Ti alloys, 20: 6236
NEWMAN, Ezra T., Dynamics of gravitational sources, 20: 6222
NEWMAN, P., Time delays between intensity variations of 3914 A and 5577 A spectral lines in artificial auroras, 20: 6203
NEWMANN, L., Structure of vortex line and lower critical field in superconducting alloys, 20: 6251
NICASTRO, L. J., Determination of plasma density by laser interferometric and continuum radiation intensity measurements, 20: 6471
NICKLES, R. J., Shape of neutron yield from $^7Li(p,n)^7Be$ reaction near threshold, 20: 6355
NICULA, Ai, Electron spin resonance of copper(II) and manganese(II) ions in polycrystalline substances, 20: 5533
NIEH, H. T., Renormalization effects and Cabibbo angle, 20: 6140
NIELSEN, H. L., Spectral shapes and beta–gamma directional correlation in beta decay of $^{172}Tm(J^\pi = 2^-)$, 20: 6381
NIELSEN, K. E., Shape of neutron yield from $^7Li(p,n)^7Be$ reaction near threshold, 20: 6355
NIERENBERG, William A., Hyperfine-structure anomaly of ^{131}Cs, 20: 6401
NIEWIAROWICZ, A., Effect of gamma irradiation on content of free amino acids in meat, 20: 5278
NIGAM, A. K., Gamma-gamma angular correlation in ^{128}Sn, 20: 6322
NIGAM, B. P., Energy-level shift for atoms with point nuclei due to higher order vacuum polarization, 20: 5995
NIKITIN, A. M., Pile-neutron burnup cross section of ^{149}Pm and samarium poisoning, 20: 6589
NIKOLAEV, P. V., Gamma radiation spectrum from artificial model of radioactive fallout, 20: 5653
NIKOLSKAYA, E. B., Method for determining inactivation of alkaline phosphatase solutions under influence of ionizing radiation, 20: 5277
NIKOTIN, O. P., Relative abundances of delayed neutron groups from photofission of ^{238}U, 20: 6315
NILAN, Robert A., Prog. rpt. on radiosensitivity of plants, annual, 11/64–10/65, 20: 5298 (RLO-353-4)
NILSSON, Agnar, Suppression of ^{90}Sr-induced development of bone tumors by infection with bacillus calmette-guerin (BCG), 20: 5373
NISHIMURA, Susumu, Determining U and Th content in rocks by radioactive measurements. I., 20: 5513
NOELDEKE, G. K., Charge distributions of ^{40}Ca and ^{44}Ca from 250-Mev electron scattering, 20: 6413
NOGUCHI, Shun, Removal of radioactive isotopes from cotton cloths, 20: 5676
NOMOTO, Shoji, Status of development of fast reactors in France, 20: 6643
NORRIS, E. B., Advanced BONUS core boiler-superheater fuel element weldments, 20: 6624 (TID-22425)
NOVAK, Arthur F., Physiological changes induced by gamma irradiation of bacteria from shrimp, 20: 5346
NOVOZHILOV, Yu. V., Inhomogeneous group $P(SU_6)$ in elementary particles theory, 20: 6145
NOWLIN, C. H., Elimination of undesirable undershoot in operation and testing of nuclear pulse amplifiers, 20: 5707
NYMAN, D. H., High temperature creep machine for in-cell operation, 20: 5611 (BNWL-137)
NYMAN, J. C., Vacuum sealing technique for photomultiplier tubes, 20: 5787

NYSTROEM, Anders, Noise in nuclear reactor systems, 20: 6561 (FTI-2)

O

OBERMAN, B., "Melanosebaceous formation" of golden hamster. IV., 20: 5322
OCHINSKAYA, G. K., Absence of "oxygen after-effects" in Calandria granaria during hibernation induced with low temperature, 20: 5385
ODIAN, A., Streamer chamber development, 20: 5739 (SLAC-PUB-140)
ODORICO, R., SU_6, SU_6W and meson photoproduction, 20: 6055
OGANESYAN, Yu. Ts., Extraction of heavy ion beam from cyclotron with azimuthal variation of magnetic field, 20: 5947 (ANL-Trans-241)
OHATA, I., Remark on 30 Bev jet showers, 20: 6039 (INSJ-90)
OHKAWA, T., General atomic toroidal multipole confinement experiment, 20: 6460 (GA-6594)
OHLSEN, G. G., Kinematic relations in reactions of form A + B → C + D + E, 20: 6333
OHMURA, H., Strongly excited levels of ^{39}Ca in $^{40}Ca(^3He,\alpha)^{39}Ca$ reaction, 20: 6398
OKADA, Touichi, Temperature dependence of flow stress in gamma-ray irradiated sodium chloride crystals, 20: 6538
OKAJIMA, Nobuo, Neutron surface moisture gage for determining moisture contents of building materials, 20: 5819
OKOLOVICH, V. N., Energy dependence of mean kinetic energy of heavy nucleus fission fragments, 20: 6421
OKUN', L. B., Shadow universe and neutrino experiment, 20: 6045
OLDHAM, William J. B. Jr., Calculations of energy and angular distribution of electrons ejected from helium by protons, 20: 5993
OLIVIE, Ginette, Calculations of ψ, ϕ, and of their derivatives, 20: 5829 (CEA-R-2824)
OLSEN, A. R., Properties and prospects of thoria-base nuclear fuels, 20: 5915 (ORNL-P-1724)
OLSEN, Haakon, Radiative corrections. I., 20: 6072
OLSON, H. P., Control of dissolved gases in moderator of heavy water components test reactor, 20: 6673 (DP-988)
OLSSON, M., Analysis of total cross-section differences at high energy, 20: 6082
ONCESCU, M., Use of radioactive tracers in hydrology in Rumania, 20: 5657 (NP-15543, pp 47-58)
ONEDA, S., K_{e3} decay and universality in Cabibbo's theory of leptonic decays, 20: 6080
OPIE, William Robert, Production of pure Ti and Zr by electrolysis, 20: 5604(P)
OPPENHEIM, I., Differences in spherical intermolecular potentials of hydrogen and deuterium, 20: 5541
ORE, V., Influence of ionizing radiation from radioactive cobalt on certain biochemical processes in peas, 20: 5280
ORLYANSKAYA, R. L., Changes of serum protein fractions in blood of rats irradiated with 660-Mev protons, 20: 5378
ORTEGO, Jesse R., Physiological changes induced by gamma irradiation of bacteria from shrimp, 20: 5346
OTTE, William K. Jr., Radioisotope photoscans in nuclear medicine, 20: 5487
OTTER, J. M., Prog. rpt. on W resonance integrals and Doppler coefficients, 7–9/65, 20: 6279 (AI-65-225)
OTTER, J. M., TRIX-1 code, improved analytic calculation of resonance integrals, 20: 6291 (NAA-SR-Memo-11538)
OVAZZA, Mario, R.I.T.M.O. reactor to support R.T.M. program, 20: 6683
OVERBECK, W. P., Production of transplutonium elements at Savannah River, 20: 5822 (DP-1000)
OZERYANAYA, I. N., Corrosion of zirconium in alkaline metal chloride melt, 20: 5855 (JPRS-32341, pp 24-31)

P

PAAP, W., Equipment for indicating, recording and controlling oscillations of axis of rotation and speed of rotor of gas centrifuge, 20: 5685 (K-Trans-5)
PACK, George T., Lymphosarcoma: choice of treatment and end-results in 567 patients, 20: 5485
PADHI, H. C., Beta gamma circular polarization correlation in ^{46}Sc, 20: 6391
PAGELS, Heinz, Approximate solution to multichannel ND^{-1} equations, 20: 6063
PAL, Y., Cosmic ray fluxes and possible experiments, 20: 6009
PALE, P. N., Determination of TBP, kerosene, and synthol, 20: 5516
PALMER, D. W., Energy distribution of $^7Li(p,n)^7Be$ neutrons near threshold, 20: 6356
PALMER, D. W., Shape of neutron yield from $^7Li(p,n)^7Be$ reaction near threshold, 20: 6355
PALMER, P. E., Coexistence of antiferromagnetism and superconductivity, 20: 6247
PALMIN, W. W., Effect of gamma irradiation on content of free amino acids in meat, 20: 5278
PALYI, Iren, Effect of x-ray on phosphorus metabolism of glioma cultures, 20: 5255
PANDE, L. K., T violation and electromagnetic interactions, 20: 6059
PANDEY, R. C., Nuclear quadrupole moment of 482 kev level of ^{181}Ta, 20: 5794
PANDHARIPANDE, V. R., Decay of ^{111}Pd and ^{111m}Pd, 20: 6402
PANKRAT'EV, Yu. V., Attenuation of reactor radiations in serpentine sand, 20: 6524
PANOV, T. N., Comparison of determinations of total vector T with data of PM-1 proton magnetometer, 20: 6195
PANY, Johannes E., Calcium nutrition and radiostrontium injury, 20: 5263
PAPADICHEV, V. A., Measurements of index of magnetic field loss in charged particle accelerator, 20: 5959
PAPIROV, I. I., Beryllium aging, 20: 5900
PARAMONOV, V. V., Light pencil, 20: 5690
PARFIANOVICH, Yu. N., Preliminary results of determining particle concentration and atmospheric density on 18 June 1963, 20: 6210
PARIISKII, G. B., Nature of surface radiation-induced defects in irradiated silicagel. I., 20: 5584
PARMENTER, R. H., Gapless high-current superconductivity, 20: 6241
PASCHALL, R. K., Prog. rpt. on W resonance integrals and Doppler coefficients, 7–9/65, 20: 6279 (AI-65-225)
PASCHALL, R. K., SCAP—in IBM 7094 code for spectral analysis of pulsed-neutron decay data, 20: 6585 (NAA-SR-Memo-10941)
PASHEK, G. M., Model study of protective characteristics of some radioprotectors, 20: 5422
PASKANZER, A. M., Oxygen-13, 20: 6405
PASKIN, Arthur, Boundary conditions and quantum effects in thin superconducting films, 20: 6242
PASTERNAK, M., Moessbauer effect in molecular iodine crystals, 20: 6540
PATIL, Sharadchandra H., Bootstrap algebra for mesons, 20: 6060
PATRIARCA, G., Influence of x rays on take of skin homografts, 20: 5335
PATRICK, Richard M., Thomson scattering measurements of magnetic annular shock tube plasmas, 20: 6490
PATTENDEN, N. J., Neutron cross sections of thorium and analysis of resonances up to 1 kev, 20: 6377
PAUL, T. M., Studies of inhibition of intestinal absorption of radioactive strontium, 20: 5253
PAULING, P. J., Comprehensive safety shutter and collimator coupling for Philips x-ray tube shield PW 1016, 20: 5693
PAULL, P. R., Neutron activation of titanium and its influence on ionization chamber design, 20: 5716 (AEEW-M-470)
PAWELSKI, S., Influence of occupational exposure to chemical agents and x-rays on leucocyte alkaline phosphatase activity, 20: 5269
PAWLOWSKI, Zdzislaw, Electronic collimation of α particles in gridded ionization chamber, 20: 5782
PEAKALL, K. A., Electrochemical aspects of hydrolysis of UC-10% Fe, 20: 5857
PEARLMAN, M., Mouse phantom depth dose studies, 20: 5286 (CONF-650616-16)
PEARLSTEIN, Solomon, Inelastic scattering of 14 Mev neutrons to low lying states of lead, thallium, tungsten and tantalum, 20: 6437
PEARSON, E. B., Neutron fluence measurements for second test at Pulstar Reactor, 20: 6679 (NP-15645)
PELLICCIONI, M., Background current in dielectric liquid ionization chambers, 20: 5771
PELTIER, Marcel, Thorium oxides and mixed thorium oxides and method, 20: 5562(P)
PEN'KOV, I. A., Viscosity of liquid zirconium, 20: 5899 (JPRS-32341, pp 1-7)
PENNEY, R., Dimensionality of real world, 20: 6218
PERELOMOV, A. M., Casimir operators for unitary group, 20: 6125
PERELOMOV, A. M., Geometrical method for reducing groups SU(4) and SU(3) with respect to subgroups SU(2) ⊗ SU(2) and O(3), 20: 6150
PEREPELKIN, S. R., Dynamics of gastric secretion and riboflavin in blood during radiation sickness, 20: 5384
PERKINS, M. A., Stabilization of lithium-drifted silicon surface-barrier detectors, 20: 5767
PERKINS, Roger A., Status of coated refractory metals, 20: 5910
PERMYAKOV, V. A., Surface impedance of nonhomogeneous plasma with sharply varying parameters, 20: 6485
PERRET, R. P., Power from radioisotopes, 20: 5821
PERRIN, Claude, Evidence of two-body interactions in reaction $^9Be(n,2n)$ at 14 Mev, 20: 6320
PERRY, Harold, Automation of radiation treatment planning. V., 20: 5449
PERSKY, Lester, Transplantation site preradiation and rejection patterns, 20: 5344
PERSON, S., Evidence for mutagenic local effect accompanying decay of incorporated tritium in Escherichia coli, 20: 5250
PESCE, B., Mass-spectrometric study of yttrium–carbon system, 20: 5540
PESCHKE, Fritz, Pulse counting fission ionization chamber, 20: 5800
PETERLONGO, G., Large scale experiments on heat transfer and hydrodynamics with steam-water mixtures, 20: 5623 (EURAEC-1325)

PETERSON, D. T., Electrotransport of interstitial atoms in yttrium, 20: 5599
PETERSON, R. E., Fast reactor safety considerations related to fuel macrostructure, 20: 6602 (BNWL-SA-346)
PETERSON, R. J., Level structure of ^{48}Ca, 20: 6400
PETRIE, Lester M. Jr., Gamma-ray spectra in fusion blanket mock-ups, 20: 6455 (AD-619672)
PETROV, G. A., Delayed gamma rays from ^{235}U fission, 20: 6316
PETROV, Yu. V., Pile-neutron burnup cross section of ^{149}Pm and samarium poisoning, 20: 6589
PETROW, Henry G., Direct radiochemical determination of ^{210}Pb in bone, 20: 5504
PETRUNKIN, V. A., Magnetic polarizability of π and K mesons, 20: 6090
PETRZHAK, K. A., Relative abundances of delayed neutron groups from photofission of ^{238}U, 20: 6315
PETUSHKOV, A. A., Air-exchange calculation in rooms for high-power gamma units, 20: 5670
PFEIFFER, E. W., Mandan milk mystery, 20: 5678
PFOHL, Raymond, Comparison of registration of tracks of heavy ions in ionographic emulsions and in various solid materials, 20: 5755
PHELPS, R. D., Reliability test of an SRE-PEP moderator element, 20: 6621 (NAA-SR-Memo-11556)
PHILIPP, G., Study of d-d reactions in self targets with coatings, 20: 6334
PHILIPPS, Georg R., Dissociation of reticulocyte ribosomes, 20: 5264
PHILLIPS, G. O., Radiation inactivation of potato phosphorylase, 20: 5275
PHILLIPS, Harold O., Ion exchange procedures. VII., 20: 5597
PHILLIPS, R. C., Construction and calibration techniques of high frequency magnetic probes, 20: 6507
PHILLIPSON, Paul, Quantum mechanics of (p-μ-p)$^+$ molecular ion, 20: 5980 (AD-617522)
PIERQUIN, B., Beta therapy of hemangiomas with artificial radioisotopes, 20: 5443
PIERSON, Mary B., Alterations in muscle activity during gamma-irradiation, 20: 5375
PIERSON, Mary Brendan, Gamma-ray effects on mechanical activity of mammalian muscle preparation, 20: 5292 (COO-205-55, Paper 1)
PIERSON, William R., Decay of ^{105}Rh, 20: 6406
PIGNERET, J., Considerations on noise of input stage of pulse amplifier, 20: 5697
PINAJIAN, J. J., Production of ^{242}Pu and ^{242}Cm by irradiating ^{241}Am with neutrons, 20: 5823 (ORNL-tr-892)
PINCHINAT, Antonio Michael, Recurrent intercrossing coupled with neutron irradiation, 20: 5406
PING, D. E., Bakeable, pulsed gas valve for plasma physics experiments, 20: 5642
PINSONNEAULT, Lawrence Lee, Elastic scattering of lithium by lithium, 20: 6442
PIRAGINO, G., Peripheral model and its application to photodisintegration of ^{6}Li, 20: 6368
PISAREVSKII, A. N., Model study of protective characteristics of some radioprotectors, 20: 5422
PISTORIUS, Elfriede, Photosynthetic reactions in uv-irradiated chloroplasts, 20: 5401
PLANTAMURA, V. L., Operative definition of threshold of tunnel diode switching circuits, 20: 5700
PLETNEV, V. D., Dynamics of geomagnetic trap. I., 20: 6208
PLEWA, Stanislaw, Environment and leukemia morbidity. III., 20: 5674
PLOSHCHANSKII, L. M., Application of polyethylene pipes in dosimetric lines for air control, 20: 5752
POFFE, N., Reaction (p,2p) on some isotopes of titanium, 20: 6330
POLETTI, A. R., $\frac{5}{2} \rightarrow \frac{1}{2}$ Hole transitions in mass 15, 20: 6378
POLOVIN, R. V., Evolutionary conditions of oblique and conical shock waves and of transonic flows, 20: 6160 (NP-15604)
POLYACHENOK, O. G., Enthalpy of formation of lanthanum and praseodymium fluorides, 20: 5559
POLYAK, Yu. V., Investigation of fraction of energy transferred to soft component by particles interacting with carbon nuclei, 20: 6017
POMERANCHUK, I. Ya., At what distances does interaction at high energies occur?, 20: 6108 (NP-15600)
POMERANCHUK, I. Ya., Shadow universe and neutrino experiment, 20: 6045
POMERANCHUK, I. Ya., What is the range of high energy interactions?, 20: 6153
POMORSKI, J., Electromagnetic isotope separator at Lublin, 20: 5826
PON, W. G., Multichannel spectrometer for analysis of pulsed ion sources, 20: 5698
PONDROM, Lee G., Measurement of proton-proton triple scattering at 430 Mev, 20: 6056
POPECKO, L. A., Delayed gamma rays from ^{235}U fission, 20: 6316
POPOV, A., Heating of plasma under conditions of beam instability, 20: 6468 (ORNL-tr-871)
POPOV, V. M., Casimir operators for unitary group, 20: 6125
POPOV, V. S., Geometrical method for reducing groups SU(4) and SU(3) with respect to subgroups SU(2) $\otimes$ SU(2) and O(3), 20: 6150
POPOVA, L., Daily variations of hard component intensity of cosmic radiations for 1960–1963, 20: 6016
POPP, Raymond A., Spleen weight as measure of marrow cell growth in irradiated mice, 20: 5372
PORILE, N. T., Emission of ^{8}Li fragments from Cu, Ag, and Au irradiated by high-energy protons, 20: 6409
PORKOLAB, M., New type of instability in thermal plasma, 20: 6505
POULET, M., 141-Mev polarized proton beam of Orsay synchrocyclotron, 20: 6328
POWELL, B. M., Phonons in disordered niobium–molybdenum alloys, 20: 5911
PRADAC, J., Adaptation of organism during fractionated x-ray treatment, 20: 5364
PRADAL, J., T = 2 levels in ^{16}O, 20: 6342
PRANOTO, Soemarno, Electron and ion densities and temperatures in xenon high-pressure plasma, 20: 6480
PRASAD, N. S. Krishna, Solid state studies on ammonium uranyl peroxy oxalates, 20: 5546
PRASAD, N. S. Krishna, Spectrophotometric and potentiometric studies of system containing UO_2^{++} $C_2O_4^{--}$ and H_2O_2, 20: 5549
PRASLICKA, M., Influence of irradiation upon resistance against diphtheria intoxication in rats, 20: 5391
PREDAZZI, Enrico, Singular logarithmic potentials in coordinate space, 20: 6121
PREISER, H. S., Cavitation damage resistance of materials in liquid sodium, 20: 5861
PREPARATA, G., Classification of higher boson resonances, 20: 6134
PREPARATA, G., Kinetic supermultiplets of $\bar{U}(12)$, 20: 6058
PRESS, Frank, Probing earth with nuclear explosions, 20: 5610
PRESTON, W. M., Range of protons in human skullbone, 20: 5475
PRESTWICH, W. V., Study of ^{203}Tl$(n_{th},\gamma)^{204}$Tl reaction, 20: 6411
PRIADCENCU, Al, Utilization of ionizing radiation and radioactive isotopes in agriculture and forestry investigations in Rumania, 1958–1964, 20: 5235 (NP-15543, pp 83-90)
PRICE, M. S. T., Special graphites for Dragon Reactor Core, 20: 6641
PRICE, W. C., Inactivation and denaturation of plant viruses, 20: 5310
PRIKHOD'KO, V. I., Inaccuracies of amplitude-to-time converters, 20: 5731 (JINR-P-2394)
PRINZLER, H., Space distribution of electron temperature and density in stationary layers of hydrogen discharge, 20: 6476
PROBERT, S. D., Thermal resistance of pressed contacts, 20: 5625 (TRG-Report-1013)
PROKOF'EV, A. I., Prompt fission gamma-ray quanta, 20: 6314
PRONIN, V. A., Extraction of carrier free ^{57}Co from irradiated targets, 20: 5602
PUDOVKIN, M. I., Current system of elementary geomagnetic disturbance in aurora zone, 20: 6192
PUDWITZ, K. R., Renal carcinoma as thorotrast injury, 20: 5332
PUEHLHOFER, F., Position finding counter for Buechner magnet, 20: 5747 (NP-tr-1302)
PUGACHEVA, T. S., Theory of scattering of fast charged particles in crystals, 20: 6535
PUSTOVALOV, V. V., Electromagnetic wave confluence in cold magneto-active plasma, 20: 6484
PUTILIN, M. A., Alkali metals boiling heat transfer, 20: 5627
PYTKOWICZ, Gustaw, Calculations of some kinematical relations in nuclear reactions programs for digital computer UMC-1, 20: 6285 (INP-414/PL)

Q

QUAZI, A. H., Influence of sample volume on weak β-counting efficiency in liquid scintillation counting, 20: 5510
QUESNE, C., Hole-particle model in nuclei having one nucleon more than closed shells, 20: 6382
QUIVY, R., Absolute measurement of Compton scattering cross section in lead, 20: 5991

R

RABOT, Hubert, Monte Carlo method—codes for the study of criticality problems (on IBM 7094), 20: 6581 (CEA-R-2872)
RABOTNOV, N. S., Photofission of even-even nuclei near threshold, 20: 6309 (ANL-Trans-245)
RABSON, T. A., Average energy expended per ionized electron-hole pair in silicon and germanium as function of temperature, 20: 5784
RACZKA, R., Degenerate representations of compact and noncompact unitary groups, 20: 6103 (IC/65/80)
RADEMACHER, Karl, Positive argon column in long tubes, 20: 6475
RADISLAV, Philip, Defectoscopic examination of structural materials for reactor, 20: 6633 (AECL-2286)
RAE, E. R., Neutron cross sections of thorium and analysis of resonances up to 1 kev, 20: 6377
RAETHER, H., Plasma radiation from thin silver foils excited by light,

20: 6548
RAHAT, Aaa, Viability of heterozygotes for induced mutations in Drosophila melanogaster. I., 20: 5358
RAHMOUNI, O., Investigation of rotation levels in odd-odd nucleus ^{234m}Pa, 20: 6331
RAINEY, W. T. Jr., Purification of zirconium tetrafluoride, 20: 5528 (ORNL-TM-1292)
RAJKOVA, Jarmila, Scintillation counter for measurement of beta radioactivity of low concentration in liquids, 20: 5798
RAMALHO, Antonio Joaquim Goncalves, Three years of operation of experimental Portuguese reactor, 20: 6675 (LFEN-26)
RAMA RAO, J., Coherent scattering cross-sections of ^{60}Co and ^{137}Cs gamma rays, 20: 6323
RAMETTE, R. W., Thermodynamics of iodine solubility and triiodide ion formation in water and in deuterium oxide, 20: 5539
RAMPACHER, H., Fundamentals of dynamics in nonlinear spin theory of elementary particles, 20: 6112
RANADE, S. S., Radiosensitivity in cyclic phases of mouse fibrosarcoma cells in vitro, 20: 5362
RANADIVE, K. J., Radiosensitivity in cyclic phases of mouse fibrosarcoma cells in vitro, 20: 5362
RAND, R. E., Upper limit to electric dipole moment of electron, 20: 6064
RANDEN, K. G., Capabilities of 1 Mw shield test and irradiation reactor, 20: 6677 (NAA-SR-11528)
RANK, D. H., High resolution measurements on infrared absorption spectrum of HBr, 20: 5550
RASHID, M. A., Two types of baryons in broken $(SU_3)_L \otimes (SU_3)_R$ symmetry, 20: 6070
RAUCH, H., Study of semiconductor surface barrier detectors at 4.2°K, 20: 5790
RAUH, E. G., Thermodynamic study of urania–uranium system, 20: 5877 (ANL-7048)
RAVENHALL, D. G., Charge distributions of ^{40}Ca and ^{44}Ca from 250-Mev electron scattering, 20: 6413
RAVENHALL, D. G., Recent high energy electron investigations at Stanford University, 20: 6277 (AD-619952)
RAVETTA, R., Large scale experiments on heat transfer and hydrodynamics with steam-water mixtures, 20: 5623 (EURAEC-1325)
RAZ, B. James, Shell-model study of calcium isotopes, 20: 6417
RAZBITNOI, V. M., Production of ^{242}Pu and ^{242}Cm by irradiating ^{241}Am with neutrons, 20: 5823 (ORNL-tr-892)
RAZIN, V. A., Optimum wavelength and spectral interval measurements of distributed cosmic radiation polarization, 20: 6018
READER, Paul D., Ion propulsion systems for spacecraft, 20: 5637
REDDY, B. M., Early electrostatic probe results from Explorer 22, 20: 6199
REDDY, D. V. N., Studies on crystalline lens. XI., 20: 5256
REDHEAD, P. A., Total pressure measurements below 10^{-10} torr with nonmagnetic ionization gages, 20: 5641
REEDER, P. L., Oxygen-13, 20: 6405
REES, Searle B., Pituitary ablation in treatment of diabetic retinopathy, 20: 5468
REHFELD, C. E., ^{226}Th induced fractures in beagles, 20: 5288 (COO-119-232, pp 74-87)
REIMANN, G., Photoproduction of pion and nucleon resonances at energies up to 5.5 Bev, 20: 6037 (DESY-65/11)
REINES, F., Neutrino and muon measurements 10,000 ft underground, 20: 6008
REINHARDT, D., Different effect of bromouracildesoxyriboside and iodouracildesoxyriboside in irradiation of herpes simplex-virus with uv light, 20: 5363
REINHARDT, Johann, Determination of frequency of plutonium isotopes, 20: 5497 (KFK-339)
REITEMEIER, Richard J., Thorium dioxide infusions to demonstrate malignant lesions in the liver, 20: 5465
REITER, E. R., Case study of mass transport from stratosphere to troposphere, not associated with surface fallout, 20: 5649(R) (COO-1340-2, pp 54-83)
REITER, E. R., Heavy ^{131}I fallout over midwestern United States, May 1962, 20: 5648(R) (COO-1340-2, pp 1-53)
REITER, Elmer R., Behavior of jet streams in potential fallout situations, 20: 5644(R) (COO-1340-2, pp 110-21)
RENARD, Claude, Study of vlf radiation by use of Nike-Cajun rocket, 20: 6180 (AD-619250)
RENAUD, C., Heating and confinement of plasma in magnetic well of deca-2, 20: 6469 (UCRL-Trans-1256(L))
RENNIE, C. A., Dragon and future gas cooled thermal reactors, 20: 6640
RESTELLI, G., Germanium compensation by Li-drift in boiling liquids for p-i-n-diode construction, 20: 5702
REVEL, Daniel, Study of hyperon-antihyperon production in antiproton-proton collision at 4 Bev/c, 20: 6033 (CEA-R-2798)
REVESZ, Laszlo, Suppression of ^{90}Sr-induced development of bone tumors by infection with bacillus calmette-guerin (BCG), 20: 5373
REY, J., Reaction ^{6}Li + T = 2α + n at low incident energies, 20: 6351
REZLESCU, Nicolae, Correlation between radon concentration at ground level and certain meteorological parameters, 20: 5646
RHINES, Frederick N., Alloys in Nb–Al–Ti system, 20: 5896 (TID-22388)
RHO, M., Variational principle and compensation method in pairing interaction, 20: 6343
RHYNE, J. J., Magnetostriction of erbium single crystals, 20: 6547
RIAZUDDIN, Two types of baryons in broken $(SU_3)_L \otimes (SU_3)_R$ symmetry, 20: 6070
RICCI, R. A., Study of nuclei of medium mass by inelastic scattering of 155 Mev protons. I., 20: 6354
RICCO, G., Photoprotons from Mg, 20: 6399
RICE, J., Study of charged particle beams by means of pick-up electrodes, 20: 5686 (NP-tr-1313)
RICHARD, J., Surgery of larynx and hypopharynx after radiotherapy, 20: 5463
RICHARDS, Albert G., Sources of x radiation in dental office, 20: 5430
RICHHARIA, A. K., Induced partial male-sterile and multipistillate dwarf plant in tetraploid rice by x-ray treatment, 20: 5393
RICHTER, B., Streamer chamber development, 20: 5739 (SLAC-PUB-140)
RICHTER, P., Absorption and scattering in β activity measurement of samples, 20: 5791
RIDGWAY, N. W., Expansion of a function in terms of Chebyshev polynomials using the I.B.M. 7040, 20: 5828 (AAEC/TM-293)
RIMSHAW, S. J., Production of ^{242}Pu and ^{242}Cm by irradiating ^{241}Am with neutrons, 20: 5823 (ORNL-tr-892)
RINAUDO, G., Longitudinal polarization of low-energy muons from $K^+_{\mu 3}$ decay, 20: 6075
RIOU, M., Study of nuclei of medium mass by inelastic scattering of 155 Mev protons. I., 20: 6354
RIPAN, R., Utilization of tracers and of intense radiation sources in chemical research, 20: 5590 (NP-15543, pp 5-26)
RIPKA, G., Projected Hartree-Fock spectra in light nuclei, 20: 6419
RITTENHOUSE, L. E., Experiments on Faraday-type MHD accelerator with series-connected electrodes, 20: 6025
RITTER, W., Clefts of lips, jaws and palate induced in mice by means of x-rays, 20: 5337
RITTER, W., Dental fusions induced in mouse by x irradiation. II., 20: 5327
RITTER, W., Development of secondary palate, 20: 5326
RITTER, W., Median jaw and tooth fusion induced by x irradiation in mouse, 20: 5395
RITZMAN, Robert L., Prog. rpt. on analytical description of nuclear-reactor accident, 7–9/65, 20: 6560 (BMI-X-10145)
RIVA, V., Large scale experiments on heat transfer and hydrodynamics with steam-water mixtures, 20: 5623 (EURAEC-1325)
RIVIERE, M. R., "Melanosebaceous formation" of golden hamster. IV., 20: 5322
RIXON, R. H., Effects of freezing on radiation sensitivity of rat thymocytes, 20: 5414
ROBBINS, Thomas R., Nuclear reactor control means, 20: 6575
ROBERTS, A., Polarization of Λ^0 particle produced from protons in carbon nuclei by 1.17-Bev/c negative pions, 20: 6071
ROBERTS, P. J., Lockwood—the wood of the future, 20: 5818
ROBERTSHAW, F. C., Neutron-irradiation effects on Nb-modified 80 Ni–20 Cr alloy, 20: 5917
ROBERTSON, C. S., Operating instructions for FORTRAN IV version of program gamma-P (NMP 468), 20: 6284 (GEMP-392)
ROBERTSON, D. S., Multiturn beam extraction in Ag synchrotrons, 20: 5931 (BNL-9352)
ROBERTSON, G. B., Comprehensive safety shutter and collimator coupling for Philips x-ray tube shield PW 1016, 20: 5693
ROBIN, Claude, Monte Carlo method—codes for the study of criticality problems (on IBM 7094), 20: 6581 (CEA-R-2872)
ROBINSON, A. W., Changing pattern of obstetric radiology, 20: 5476
ROBINSON, Berol L., Intensity of E3 transition in ^{38}Ar, 20: 6407
ROBINSON, Berol L., Prog. rpt. on recoil-free scattering of gamma-rays, final, 3/62–6/65, 20: 6302 (TID-22384)
ROBINSON, Lloyd, Applications of small computers in nuclear spectroscopy, 20: 6307 (UCRL-16439)
ROBSON, A. E., Statistical theory of nonadiabatic magnetic traps, 20: 6494
ROBSON, J. M., Scattered neutrons and gamma rays from ^{16}O(n,nγ)^{16}O reaction at E_n = 14.1 Mev, 20: 6346
ROCCELLA, M., Background current in dielectric liquid ionization chambers, 20: 5771
ROCHE, Franck, Calculations of ψ, ϕ, and of their derivatives, 20: 5829 (CEA-R-2824)
ROCKSTEIN, M., X-irradiation of pupae of house fly Musca domestica L. and adult survival, 20: 5331
ROEDERER, J. G., Motion of charged particles in static magnetic fields, 20: 6459 (CNIE-PE-1)
ROELLIG, L. O., Positron lifetimes in low-temperature helium gas, 20: 5997

ROEMBERG, E., Coolant purification and coolant chemistry for "Dragon" high temperature gas cooled reactor, 20: 6639
ROESSER, James Royal, Rotation-vibration model for odd-a atomic nuclei, 20: 6441
ROGERS, Kenneth C., Properties of alkali–metal magnetoplasmas related to "enhanced diffusion," 20: 6466 (SIT-2813-33)
ROGERS, P. C., Computer analysis of beta-ray and conversion-electron spectra, 20: 5768
ROGNSTAD, Robert, Synthesis and metabolism of glucose-3-^{3}H and glucose-4-^{3}H, 20: 5252
ROHRLICH, F., Momentum dependence of S matrix for many-particle processes, 20: 6061
ROLLAND, P., Low-frequency electronic oscillations in plasma beam interaction, 20: 6503
ROMAN, J., Silicon surface-barrier detectors for alpha radiation dosimetry, 20: 5721 (CLOR/IBJ-II-37/D)
ROMANOV, V. A., Autofocusing ion source for electrostatic accelerators, 20: 5957
ROMANOWSKI, T. A., Polarization of Λ^0 particle produced from protons in carbon nuclei by 1.17-Bev/c negative pions, 20: 6071
ROMBAU, Paul, Thorium oxides and mixed thorium oxides and method, 20: 5562(P)
ROMERO, Jacob B., Radioisotope propulsion, 20: 5634
ROPER, T. J., Technique for scanning posterior fossa, 20: 5462
ROSCISZEWSKI, Jan, Rocket motor with electrical acceleration in throat, 20: 5636
ROSE, H. J., $\frac{1}{2} \rightarrow \frac{1}{2}$ Hole transitions in mass 15, 20: 6378
ROSE, R., Water chemistry research at HBWR, 20: 6638
ROSEN, C.-G., Energy transfer in relation to water-content in solid proteins, 20: 5270
ROSEN, Erik, Stability of zircon in temperature range 1180 deg to 1366 deg C, 20: 5537
ROSENBLATT, Leon S., Comparison of two methods of analyzing hematological data from ^{90}Sr injected beagles, 20: 5290 (COO-119-232, pp 165-89)
ROSENBLUM, M., Use of vidicons in on-line measuring machines at BNL, 20: 5718 (BNL-9634)
ROSENBLUTH, M. N., High frequency inductance of torus, 20: 6508
ROSENBLUTH, Marshall N., Collisional interchange instabilities in shear and $\int dl/B$ stabilized systems, 20: 6461 (GA-6646)
ROSTOKER, N., Kinetic theory of particles and waves, 20: 6462 (GA-6650)
ROSTRON, Robert Walther, Production of metastable Hg atoms by charge exchange, 20: 6003
ROSZKOWSKI, S., Influence of occupational exposure to chemical agents and x-rays on leucocyte alkaline phosphatase activity, 20: 5269
ROTH, J., Thermal expansion of coprecipitated (U, Pu)O_2 powders by x-ray diffraction techniques, 20: 5890 (NUMEC-2389-9)
ROTH, R., Measurement of proton-proton triple scattering at 430 Mev, 20: 6056
ROTHE, Heinz J., Crossing symmetric Regge representation for invariant scattering amplitude, 20: 6115
ROTHHARDT, Ludwig, Swiftly induced argon plasmas in inductive hydrodynamic shock waves tubes, 20: 6478
ROYDEN, H. N., Prog. rpt. on W resonance integrals and Doppler coefficients, 7–9/65. 20: 6279 (AI-65-225)
ROZE, K. K., Radiobiological effects of gamma rays on potatoes, 20: 5404
RUBIERA, L., Large scale experiments on heat transfer and hydrodynamics with steam-water mixtures, 20: 5623 (EURAEC-1325)
RUBY, L., Multichannel spectrometer for analysis of pulsed ion sources, 20: 5698
RUDAKOV, V. S., Hypervirial relations for distorted Coulomb field, 20: 6146
RUEGG, H., $\tilde{U}_{12}$, its 143 momenta, its little group $U_6 \times U_6$ and its irregular couplings, 20: 6132
RUGE, I., Particle counting by cascade production in solids especially in Si p-n layers, 20: 5793
RUHLA, C., Study of nuclei of medium mass by inelastic scattering of 155 Mev protons. I., 20: 6354
RUIJGROK, T., Bremsstrahlung theory for multiple production of mesons, 20: 6053
RULF, Benjamin, Diffraction and scattering of electromagnetic waves in anisotropic media, 20: 5922 (AD-618689)
RUMPOLD, K., Comparison of consumption determination with sound activation and gamma spectroscopy for MTR element, 20: 6681 (SGAE-PH-18/1965)
RUNDO, J., Systematic arc calibration method for body radioactivity measurement, 20: 5426
RUPRECHT, Manfred, Method for fabrication of compact uranium dioxide particles of predetermined grain size, 20: 5869
RUTKOWSKI, Wladyslaw, Dispersion-type fuel element for "EWA" reactor, 20: 6684
RYDE, H., Electromagnetic transitions in ^{181}Ta, 20: 6374
RYLOV, Yu. A., Theory of ionization calorimeter, 20: 5788
RYZHOV, N. V., Continuous centralized control of individual radiation doses, 20: 5749

S

SADASIVAN, S., Measurements of radioactive fallout in individual rain showers at Bombay, 20: 5661 (AEET-215)
SAFFOURI, Mohammad Hussein, Bound states in system of two vector mesons, 20: 6092
SAIKOV, Yu. P., Electrophoretic filter for purifying reactor water, 20: 6568
SAILOR, V. L., Use of polarized beams, 20: 6259 (CONF-650217, pp 111-23)
SAKAMOTO, Masanobu, Choice of collimators for neutron diffraction, 20: 6268
SAKKA, Masatoshi, Incidence of leukemia in patients with breast cancer treated by radiotherapy, 20: 5471
SAKURAI, Junji, New glasses for low background counting, 20: 5585
SALAM, Abdus, Coupling of noncompact group representations, 20: 6102 (IC/65/79)
SALGADO, Jose Francisco, Construction and utilization of small-dimension fission chambers, 20: 5734 (LFEN-NI-19)
SALMON, Robert J., ^{99m}Tc compounds for visualization of body organs, 20: 5456
SAMARANAYAKE, V. K., New determination of pion-nucleon coupling constant and s-wave scattering lengths, 20: 6083
SAMIOS, N. P., Hyperon non-leptonic decays, 20: 6032 (BNL-9666)
SAMOILOVA, K. A., Influence of short-wave uv-light on sensitivity of infusoria to inhibitors of breathing and glycolysis, 20: 5386
SAMOUR, C., Determination of spin and resonance parameters for ^{197}Au + n at 10 to 1000 ev, 20: 6392
SAMS, Alice, Long term effects of 2000 r of x rays on bone marrow of mouse tibia, 20: 5320
SAMUELI, J.-J., Considerations on noise of input stage of pulse amplifier, 20: 5697
SANDERS, T. M. Jr., Direct measurement of size of charged quantized vortex rings in He II, 20: 6249
SANDFORD, R. W. Jr., Thermodynamics of iodine solubility and triiodide ion formation in water and in deuterium oxide, 20: 5539
SANDHU, Harbhajan S., Elastic and inelastic scattering of 30.3 Mev protons by Si, 20: 6339
SANDMEIER, H. A., Computation of fast neutron penetration in air by "Sn-method", 20: 6251 (LA-3415)
SANDMEIER, Henry A., Thermal neutron spectra from underground nuclear explosion, 20 5609 (LA-3403)
SANDRI, R., Nuclear-thermal vs. chemical drives for super-orbital velocities, 20: 5635
SANNIKOV, S. S., Creation of muons by electrons in Coulomb field of nucleus, 20: 6089
SANTHANAM, T. S., Spin extension of unitary groups, 20: 6104 (IC/65/81)
SANZONE, M., Photoprotons from Mg, 20: 6399
SARAZIN, A., Considerations on noise of input stage of pulse amplifier, 20: 5697
SARTORIS, G., T = 2 states in ^{16}O, 20: 6341
SATO, Kazuto, Experimental osteogenic sarcoma, 20: 5334
SAUNIER, N., Reaction ^{6}Li + T = 2α + n at low incident energies, 20: 6351
SAUTER, G. D., Scattering measurements on neutron resonances in ^{239}Pu, 20: 6414
SAVEL'EV, A. E., Prompt fission gamma-ray quanta, 20: 6314
SAVEL'EV, G. G., Effect of additives on certain physico-chemical properties, 20: 5583
SAVICH, A. P., Gross-linkages and locally denatured areas induced in double-strand DNA by ultraviolet light, 20: 5268
SAWADA, K., Variation ground-state energy of Bose system, 20: 6137
SAWICKI, Aleksander, Fast universal diode-transistor logic circuit and some of its uses, 20: 5704
SAWYER, J. C., Prog. rpt. on generation of long time creep data on refractory alloys at elevated temperatures, 6/26–9/26/65, 20: 5885 (NAS-CR-54773)
SAYASOV, Yu. S., Resonance neutron-molecule interactions, 20: 6266
SAYASOV, Yu. S., Role of identity of colliding nuclei in neutron tunnelling transfer, 20: 6387
SAYRES, A., Search for excited states of ^{5}He, 20: 6335
SAZHIN, N. P., Interaction between hafnium tetrafluoride and ammonium fluoride in aqueous solution, 20: 5535
SCHAMBERGER, R., Shield small source experiments, 20: 6626 (UNC-5118)
SCHARMANN, Artur, Solid body dosimetry in radiotherapy, 20: 5479
SCHENCK, G. F., Columbium-1 zirconium alloy forced convection lithium slave loop test LCCDB-1, 20: 5853 (TIM-898)
SCHERAGA, Harold A., Near-infrared study of hydrogen bonding in water and deuterium oxide, 20: 5552
SCHIMA, F., Decay of ^{158}Eu, 20: 6403

SCHINDLER, O., Metabolism of Noveril: ^{14}C labeling and synthesis of metabolites, 20: 5564
SCHIRREN, C. G., Genetic irradiation burden of patients in dermatological x ray therapy, 20: 5445
SCHMIDT, F. A., Electrotransport of interstitial atoms in yttrium, 20: 5599
SCHMIDT, Paul W., Small angle x-ray scattering study of colloidal thorium oxide, 20: 5553
SCHNEIDER, H., Properties of Ξ hyperons, 20: 6099
SCHNEIDER, Herman, Effect of radially inhomogeneous plasma on microwave interferometer measurements, 20: 5683 (UCRL-14438)
SCHNEIDERMAN, S. B., Theoretical investigation of lowest five ionization potentials of uranium, 20: 5983 (D-910099-2)
SCHOFFENIELS, E., Effects of x radiation and different substances on permeability characteristics of red cells, 20: 5342
SCHOPPER, H., Search for heavy electron by electron-proton coincidence measurements, 20: 6078
SCHOTT, E., Oscillation of ionization in ionosphere in median latitudes, 20: 6187
SCHRIER, Eugene E., Near-infrared study of hydrogen bonding in water and deuterium oxide, 20: 5552
SCHUCAN, Thomas H., Radial integrals for relativistic coulomb functions, 20: 6375
SCHUHL, C., Elastic scattering of photons in region of giant resonance, 20: 6349
SCHULT, O. W. B., Energy and intensity measurements of gamma radiation emitted by ^{182}W and ^{183}W during decay of ^{182}Ta and ^{183}Ta, 20: 6428
SCHULTZ, G. M., Optimization status report, 20: 6605 (GAMD-6673)
SCHULTZ, G. M., STMGEN—computer code for design of steam generator, 20: 5606 (GAMD-6675)
SCHULTZ, G. M., STMGEN. Computer code for design of steam generator, 20: 5607 (GAMD-6675(Suppl.))
SCHULTZ, Vincent, Offsite ecological research, 20: 5243 (TID-13358 (2nd Rev.))
SCHULZ, Paul, Electron and ion densities and temperatures in xenon high-pressure plasma, 20: 6480
SCHULZ, Paul, Multi-cathode discharges in xenon-hydrogen mixture, 20: 6168
SCHUMANN, Thomas G., Inelastic π^-p interactions at 3.3 Bev/c and 3.9 Bev/c, 20: 6041 (UCRL-11942)
SCHUNICHT, B. F., Numerical methods for solution of complex gamma spectra, 20: 5727 (CONF-651101-46)
SCHUPP, A. A. Jr., General atomic toroidal multipole confinement experiment, 20: 6460 (GA-6594)
SCHWARTZ, F. L., Correlation of sound generation and heat transfer in boiling, 20: 5628
SCHWARTZ, M., Experiment to detect basic triplets, 20: 6010
SCOTT, J. L., Properties and prospects of thoria-base nuclear fuels, 20: 5915 (ORNL-P-1724)
SEEFELDT, W. B., Studies and evaluations, 20: 6553 (ANL-6925, pp 255-63)
SEEGER, Philip A., Table of binding energies and particle separation energies from mass law, 20: 6290 (LA-3380)
SEGEL, S. L., Nuclear magnetic resonance in pure quadrupole regime, 20: 6549
SEIGLE, L., Diffusion-controlled oxidation of several lanthanides, 20: 5859
SEINO, Hideaki, Activation analysis of Mn in Fe, 20: 5514
SEKIGUCHI, Morimasa, Bibliography of hematopoietic tissue transplantation, 20: 5424
SELENKOW, Herbert A., Hyperthyroidism during pregnancy, 20: 5470
SELESNEV, A. F., Model study of protective characteristics of some radioprotectors, 20: 5422
SELIGA, T. A., Electron densities in D region of ionosphere from low frequency signal strength measurements in rockets, 20: 6185 (AFCRL-65-620)
SELIVERSTOV, B. N., Dynamic characteristics of first reactor of I. V. Kurchatov Beloyarsk Nuclear Power Station, 20: 6634
SELLECK, E. G., Fission gas migration studies in uranium carbide, 20: 5892 (PWAC-476)
SELLERI, F., Virtual nucleon effects, 20: 6054
SELTZER, E., Electromagnetic transitions in ^{181}Ta, 20: 6374
SENYUKOV, R. V., Ground-state energy of He, 20: 5987 (ANL-Trans-248)
SERBINOV, A. N., Autofocusing ion source for electrostatic accelerators, 20: 5957
SERGEEV, I. V., Use of P_n approximation for determination of neutron distribution in an absorbing rod, 20: 6267
SERGOLLE, H., Investigation of rotation levels in odd-odd nucleus ^{234m}Pa, 20: 6331
SETAELAE, Kai, Dose planning in radiotherapy, 20: 5439
SETLOW, Jane K., Resistance of micrococcus radiodurans to ultraviolet radiation. II., 20: 5266
SHABESTARI, L., Dental eruption pattern of beagle, 20: 5232 (COO-119-232, pp 68-73)
SHAFRANOV, V. D., Classical heat transfer in toroidal plasma column, 20: 6473
SHAKHTAKHTINSKII, G. B., Arsenate method for iodometric determination of yttrium in presence of aluminum, 20: 5506
SHALAEV, I. L., Radiation protection of personnel during uranium ore mining, 20: 5428
SHAMOV, V. P., Biological dose of ^{90}Sr internal irradiation of man, 20: 5429
SHAPIRA, Y., Upper critical fields of Nb–Ti alloys, 20: 6236
SHAPIRO, Mathew M., Nuclear aspects of accidental criticality at Wood River Junction, Rhode Island, July 24, 1964, 20: 5666 (TID-21995)
SHAPIRO, V. A., Comparison of determinations of total vector T with data of PM-1 proton magnetometer, 20: 6195
SHAPIRO, V. D., Interaction of modulated beam with plasma, 20: 6474
SHAPIRO, V. D., On limitations in density of interacting currents in colliding ultrarelativistic beams, 20: 5950
SHAPOVALOV, A. S., Experimental investigation of electrostatic charged particle energy analyzer properties, 20: 5691
SHARMA, R. P., Decay of ^{111}Pd and ^{111m}Pd, 20: 6402
SHAROV, V. T., Electrophoretic filter for purifying reactor water, 20: 6568
SHARP, David H., Variational principle for hydrostatic equilibrium of relativistic, rotating fluid, 20: 5974
SHATZKES, M., Neutron and gamma sensitivities of dynamic detectors, 20: 5728 (IBM-65-825-1487)
SHCHEBOLEV, V. T., International comparison of neutron sources, 20: 6265
SHCHEPOCHKIN, B. V., Interaction between hafnium tetrafluoride and ammonium fluoride in aqueous solution, 20: 5535
SHEA, M. A., Study of vertically incident cosmic-ray trajectories using sixth-degree simulations of geomagnetic field, 20: 6005 (AD-623632)
SHEARIN, P. E., Recovery of pure and alloyed aluminum in stages I and II after 2-Mev electron irradiation, 20: 5918
SHEER, Charles, Fluid transpiration plasma jet, 20: 6178(P)
SHEKHTER, V. M., Resonance Ξ_{1820} and unitary symmetry, 20: 6091
SHELAEV, I. A., Effect of geometry of cyclotron center upon starting motion of heavy ions (median plane), 20: 5948 (ANL-Trans-246)
SHERMAN, Arthur, Fundamentals of MHD flow, 20: 6156 (AD-617562)
SHIBATA, Shinkichi, New glasses for low background counting, 20: 5585
SHIMONY, U., Condition for maximum single-line Moessbauer absorption, 20: 6336
SHINDO, Mitsuo, Single scattering streaming of gamma-rays through cylindrical ducts, 20: 6530
SHIRANE, G., Magnetic structure of $MnSO_4$, 20: 6546
SHIRKIN, L. M., Angular distribution of gamma rays scattered in lead and water, 20: 6526
SHISHKOV, A. V., Development of hot synthesis methods for ^{35}S labeled biologically active substances. III., 20: 5586
SHLAER, W. J., Proton-proton bremsstrahlung at 158 Mev, 20: 6046
SHNEIDERMAN, L. L., Alkali metals boiling heat transfer, 20: 5627
SHORIN, S. N., Heat transfer and frictional resistance of high-temperature gas flow, 20: 5626(T) (NP-tr-1300)
SHUBIN, Yu. N., Nuclear equation of state from inelastic neutron scattering spectra, 20: 6379
SHUGART, Howard A., Hyperfine-structure anomaly of ^{131}Cs, 20: 6401
SHULL, C. G., Some aspects of neutron diffraction and elastic scattering using pulsed and steady neutron sources, 20: 5726 (CONF-650217, pp 102-7)
SIAMBIS, J. G., Adiabatic containment of charged particles in combined mirror-multipole cusp magnetic fields, 20: 6496
SIDORENKO, Z. S., Measurement of relationship of proton pulse in ITEF, 20: 5941 (NP-15598)
SIEDENTOPF, H., Scintillation of terrestrial radiation, 20: 6186(T) (UCRL-Trans-1269(L))
SIEGFRIED, W., Prog. rpt. on mechanical properties of metals subjected to 20: 5880 (EURAEC-1310)
SIEGFRIED, W., Prog. rpt. on mechanical properties of metals subjected to mechanical stress and neutron irradiation, 10/65, 20: 5913 (EURAEC-1488)
SILER, L. G., Correlation of sound generation and heat transfer in boiling, 20: 5628
SILIN, Yu. S., International comparison of neutron sources, 20: 6265
SILL, Claude W., Radiochemical determination of ^{210}Pb in mill products and biological materials, 20: 5505
SILVER, A. H., Macroscopic quantum interference in superconductors, 20: 6235
SILVER, A. H., Quantum transitions and loss in multiply connected superconductors, 20: 6246
SIMAR, L. J., Influence of cystamine on immunization phenomena after whole-body irradiation, 20: 5413
SIMENOG, I. V., Sum rules and two-nucleon correlations in nuclei, 20: 6424
SIMKOVA, M., Iron determination in antimony by activation analysis, 20: 5507
SIMMONS, Eric, Modification of a hyperbaric oxygen chamber for use in

hypobaric oxygen exposure studies, 20: 5228 (AD-623599, pp 28-36)
SIMON, Albert, Glove box for decontamination and dismantling of radioactively contaminated containers, 20: 5711
SIMON, N. K., Fission product cross sections as function of exposure for use with SIZZLE, 20: 6659 (NAA-SR-Memo-11473)
SIMONS, E. M., Reactor materials, 20: 5842
SIMONS, E. M., Reactor materials, 20: 5847
SIMONS, Gale Gene, Isomeric cross section ratios for ^{46}Sc, ^{134}Cs, and ^{188}Re isomers, 20: 6301 (TID-22165)
SIMOPOULOS, A., Moessbauer effect in molecular iodine crystals, 20: 6540
SINGER, Ralph M., Transient magnetohydrodynamic flow and heat transfer, 20: 6176
SINGH, A. D., Boundary conditions and quantum effects in thin superconducting films, 20: 6242
SINGRU, R. M., Decay of ^{111}Pd and ^{111m}Pd, 20: 6402
SITE, A. Delle, γ-radiolysis of ethylene sensitized by "inert" gases, 20: 5582
SITENKO, A. G., Sum rules and two-nucleon correlations in nuclei, 20: 6424
SIUDA, Andrzej, Separation of some inorganic and phenyl phorphorus compounds, 20: 5512
SIVKOV, Yu. P., Measurements of ion beam phase volume in linear accelerator injector, 20: 5956
SJAARDA, John R., Life span in normal and irradiated hamsters, 20: 5330
SKARSGARD, H. M., High field air-cored betatron, 20: 5961
SKATKIN, V. M., Continuous centralized control of individual radiation doses, 20: 5749
SKORYNA, Stanley C., Studies of inhibition of intestinal absorption of radioactive strontium, 20: 5253
SKORZYNSKI, Zbigniew, Gamma-gamma angular correlations in ^{147}Eu to ^{147}Sm decay, 20: 6396
SKURIDIN, G. A., Dynamics of geomagnetic trap. I., 20: 6208
SKURIDIN, G. A., Propagation of weak disturbances in MHD, 20: 6170
SKURIDIN, G. A., Theory of ionization calorimeter, 20: 5788
SLOBODRIAN, R. J., Energy dependence of polarization in p-^{16}O elastic scattering between 21 and 53 Mev, 20: 6306 (UCRL-16217)
SLOVACEK, R. E., Review of experimental determinations of neutron spectra, 20: 6260 (CONF-651101-43)
SLOVACEK, Rudolf Edward, Measurement of asymptotic neutron spectrum in multiplying medium, 20: 6591
SMARDA, J., Induction of synthesis of phage and colicin in culture medium irradiated by uv rays, 20: 5279
SMART, D. F., Study of vertically incident cosmic-ray trajectories using sixth-degree simulations of geomagnetic field, 20: 6005 (AD-623632)
SMELTZER, Paul, Evaluation of core thermal data, PWR Core 1 Seed 3 second half seed life. Parts A and B, 3–11/62, 20: 6627 (WAPD-PWR-TE-141)
SMIRENKIN, G. N., Photofission of even-even nuclei near threshold, 20: 6309 (ANL-Trans-245)
SMIRNOV, M. V., Corrosion of zirconium in alkaline metal chloride melt, 20: 5855 (JPRS-32341, pp 24-31)
SMIT, Christiaan, Development and investigation of photon counter and measurement of optical excitation functions of helium, 20: 5748 (UCRL-Trans-1266(L))
SMITH, A. K., Performance of thermoelectric converter with leakage current, 20: 6657 (NAA-SR-Memo-11417)
SMITH, C. R., Plasma jet technology, 20: 5633 (NASA-SP-5033)
SMITH, C. R., Positive ion composition in magnetoionosphere, 20: 6198
SMITH, David C., Laminar and turbulent magnetohydrodynamic free jet, 20: 6175
SMITH, David R., Storage of fissile material in large and varied reactor research and development program, 20: 6584 (LA-DC-7248)
SMITH, E. A., Neutron fluence measurements for second test at Pulstar Reactor, 20: 6679 (NP-15645)
SMITH, F. T., Perturbation induced in elastic scattering by crossing of molecular states, 20: 5996
SMITH, H. F. Jr., Effects of temperature on machining operations, 20: 6688 (Y-DA-1014)
SMITH, R. L., Interpretation of transverse whistlers, 20: 6207
SMITH, Richard J., Bibliography on reactor safety, 20: 6563 (TID-3525 (Rev.5)(Suppl.2))
SMITH, T. F., Pressure dependence of superconducting transition temperature of uranium, 20: 6234
SMEAD, C. J. Jr., Recovery of pure and alloyed aluminum in stages I and II after 2-Mev electron irradiation, 20: 5918
SNOW, E. C., Effect of assumed electronic configuration on electronic band structure of nickel, 20: 6534 (SC-DC-65-1843)
SOA, E. A., Systematic investigations into electrostatic immersion objectives, 20: 5687 (UCRL-Trans-1237(L))
SOBELS, F. H., Frequencies of recessive lethals and translocations produced by irradiation in N_2 or O_2, 20: 5338
SOBENIN, N. P., Resonance method for adjusting circular Iris waveguides in linear accelerators, 20: 5955
SOBKOWSKI, J., Oxidation reduction potential of U(IV)–U(VI) system. III., 20: 5548
SOBOL', N. V., Air-exchange calculation in rooms for high-power gamma units, 20: 5670
SOGA, Michi, Shell-model study of calcium isotopes, 20: 6417
SOINE, T. S., Prog. rpt. on continuous electrowinning of Pu metal, 4/65, 20: 5839 (RL-SEP-244(Del.))
SOJKA, Bohumil, Fast amplitude discriminator, 20: 5694
SOLDATOV, A. S., Photofission of even-even nuclei near threshold, 20: 6309 (ANL-Trans-245)
SOLNYSHKOV, A. I., Measurements of ion beam phase volume in linear accelerator injector, 20: 5956
SOLODUKHOV, V. V., Surface impedance of nonhomogeneous plasma with sharply varying parameters, 20: 6485
SOLOV'EV, V. A., Application of polyethylene pipes in dosimetric lines for air control, 20: 5752
SORANTIN, H., ^{99m}Tc generator using Fe_2O_3 as sorbent for ^{99}Mo, 20: 5591 (SGAE-CH-18/1965)
SOTA, Susumu, Leukemogenesis of mouse leukemia by x irradiation. II., 20: 5367
SOTA, Susumu, Leukemogenesis of mouse leukemia by x irradiation. III., 20: 5368
SOVIE, Ronald J., Effects of metastable atoms on volume ion production in tenuous helium plasma, 20: 6464 (NASA-TN-D-3121)
SOWBY, F. D., Carcinogenic effects of ^{241}Am and ^{239}Pu in rat, 20: 5321
SPACH, Madison S., Radiation problems in children with heart disease, 20: 5455
SPALDING, I. J., Cusp compression experiments, 20: 6495
SPALDING, J. F., Radiosensitivity, circadian rhythmicity, and radiobiology, 20: 5336
SPANGLER, Patrick S., Fusion reactor blanket experiment, 20: 6454 (AD-619671)
SPANIO, Luigi, Radiomimetic effects of nitrogen mustard on multiplication of mammalian cells cultured in vitro, 20: 5323
SPARZANI, A., Dirac equation without Dirac matrices, 20: 6223
SPEIRS, K. K., Advanced BONUS core boiler-superheater fuel element weldments, 20: 6624 (TID-22425)
SPETH, J., Measurement of Moessbauer-Lamb factors in nuclear resonance scattering on ^{197}Au, 20: 6429
SPIEGELHALTER, Fritz, Multi-cathode discharges in xenon-hydrogen mixture, 20: 6168
SPURRELL, F. A., Effect of whole brain ^{60}Co gamma irradiation on cortical arousal in burro, 20: 5329
SRIVASTAVA, B. N., Ionization cross-sections of atoms and molecules by electron impact, 20: 5989
SRIVASTAVA, Y. N., Modification of Regge-pole representation, 20: 6062
STAFFORD, G. H., Isobaric states excited in (p,n) reactions at 30 and 50 Mev, 20: 6361
STAHLHOFEN, W., Bibliography on radiation effects on living tissues and organisms. No. 21, 4/65, 20: 5284 (AED-C-04-21)
STANEK, F. W., Measurement of Moessbauer-Lamb factors in nuclear resonance scattering on ^{197}Au, 20: 6429
STANLEY, A. G., Analysis of radiation effects in telemetry circuits, 20: 5806 (AD-619387)
STAPLETON, H. J., Anisotropic spin-lattice relaxation rates of some rare-earth-doped lanthanum trichlorides, 20: 6542
STARBIRD, A. W., Barrier attenuation introduced by vertical wall, 20: 6516 (AD-617524)
STARODUBTSEV, S. V., Effect of gamma irradiation on fluorescence yield of ruby, 20: 6536
STARODUBTSEV, S. V., Ion source with longitudinal magnetic field, 20: 5951
STAROVOITOV, V. S., Continuous centralized control of individual radiation doses, 20: 5749
STEBEN, John David, Polarization in elastic scattering of protons from carbon and nitrogen, 20: 6439
STEIGERWALD, E. A., Prog. rpt. on generation of long time creep data on refractory alloys at elevated temperatures, 6/26–9/26/65, 20: 5885 (NAS-CR-54773)
STEINBERG, Meyer, Possibility of chemonuclear reactors producing ozone for water treatment, 20: 5568 (BNL-9664)
STEJSKAL, R., Iron determination in antimony by activation analysis, 20: 5507
STEPHENS, S. A., Electron component of primary cosmic radiation at energies ≈15 Bev, 20: 6022
STEPHENS, W. E., Search for excited states of ^{5}He, 20: 6335
STERLING, Theodor D. Automation of radiation treatment planning. V., 20: 5449
STERNHEIMER, D., Connection between external and internal symmetries, 20: 6142
STETSENKO, V. I., Linear attenuation coefficient of ^{60}Co and ^{137}Cs γ-emission by alloys, 20: 6523
STEVENS, J., Elastic and inelastic scattering of protons by ^{18}O, 20: 6373

STEVENS, W., Determination of half-periods of dog serum proteins using ^{35}S-L-methionine, 20: 5249 (COO-119-232, pp 203-18)
STEWART, T. E., Measurements of thermal utilization (f) and δ^{25} in SGR uranium monocarbide lattices, 20: 6586 (NAA-SR-Memo-11313)
STICKEL, W., Energy losses of fast electrons in nitrogen, 20: 5542
STIRAND, O., Space distribution of electron temperature and density in stationary layers of hydrogen discharge, 20: 6476
STISSER, Eugene A., Hydrostatic press, 20: 6692
STIX, Thomas H., Radiation and absorption via mode conversion in inhomogeneous collision-free plasma, 20: 6506
STJERNSWAERD, Jan, Suppression of ^{90}Sr-induced development of bone tumors by infection with bacillus calmette-guerin (BCG), 20: 5373
STOECKLIN, Gerhard, Chemistry of nucleogenic carbon atoms, 20: 5570 (JUL-228-RC)
STOVER, B. J., Determination of half-periods of dog serum proteins using ^{35}S-L-methionine, 20: 5249 (COO-119-232, pp 203-18)
STOVER, B. J., Pilot study of effect of cortisol on $Na_3CaDTPA$ enhanced excretion of ^{239}Pu in beagle, 20: 5247 (COO-119-232, pp 188-99)
STRATHDEE, J., Coupling of noncompact group representations, 20: 6102 (IC/65/79)
STRAUSS, M. G., General purpose analog pulse height computer, 20: 5835
STROMATT, R. W., Formation of uranyl(VI) from uranium dioxide and chlorine in molten alkali chlorides, 20: 5547
STRUTINSKII, V. M., Concerning spectrum of γ rays in (n,γ) reaction, 20: 6427
STRUTT, M. J. O., Statistical oscillations of infrared radiation of high pressure, high-current Ar discharge. II., 20: 6177
STUDIER, Martin H., Remote opening of metal containers with laser beam, 20: 5669
STUKIN, E. D., Gamma radiation spectrum from artificial model of radioactive fallout, 20: 5653
STUKOV, G. M., International comparison of neutron sources, 20: 6265
STUMPF, H., Fundamentals of dynamics in nonlinear spin theory of elementary particles, 20: 6112
STUPEGIA, Donald C., Nuclear constants, 20: 6280 (ANL-6925, pp 249-51)
STURGEON, George D., Samarium borides. Tetraboride–hexaboride conversion, 20: 5551
SUCHER, J., K_{e3} decay and universality in Cabibbo's theory of leptonic decays, 20: 6080
SUELZLE, L. R., Charge distributions of ^{40}Ca and ^{44}Ca from 250-Mev electron scattering, 20: 6413
SUESS, Hans E., Secular variations of cosmic-ray-produced ^{14}C in atmosphere, 20: 6205
SUESSMANN, G., Nonlocal nuclear single particle potential and charge independence of short-range forces, 20: 6430
SUESSMANN, G., Relation between experimentally observed single particle energies and levels of extreme single particle model, 20: 6431
SUGAWARA, Tadashi, Low temperature resistivity of yttrium-based alloys containing small amounts of rare earth metals, 20: 5888 (NP-15592)
SUGIMORI, Hajime, Influences of estrogen on radiosensitivity of cervical cancer, 20: 5472
SUGIYAMA, H., Energy dependence of quantameter. I., 20: 5765
SUGIYAMA, H., Energy dependence of quantameter. II., 20: 5766
SUGIYAMA, S., Energy dependence of quantameter. II., 20: 5766
SUITA, Tokuo, Temperature dependence of flow stress in gamma-ray irradiated sodium chloride crystals, 20: 6538
SULLIVAN, D. J., ^{9}Be(^{3}He,α) reactions to 16.63 and 16.92 Mev states of ^{8}Be, 20: 6389
SUN, Kuan H., Discriminating radiation detector for determining given radiation in presence of other radiations, 20: 5802
SUNDBOM, Lennart, Dose planning for irradiation of thorax with ^{60}Co in fixed-beam teletherapy, 20: 5438
SUNDERMAN, Donn N., Prog. rpt. on analytical description of nuclear-reactor accident, 7–9/65, 20: 6560 (BMI-X-10145)
SUZUKI, Tomoo, EXPANDA. One-dimensional diffusion equation code for fast reactors, 20: 6583 (JAERI-1091)
SVANSTROM, Kjell Ake, Production of pure Ti and Zr by electrolysis, 20: 5604(P)
SWITENDICK, A. C., Effect of assumed electronic configuration on electronic band structure of nickel, 20: 6534 (SC-DC-65-1843)
SYRE, R., Handbook on properties of niobium, molybdenum, tantalum, tungsten and some of their alloys, 20: 5874 (AGARDograph-94)
SYROMYATNIKOV, N. G., Use of ^{234}U/^{238}U isotopic ratio for interpretation of uranium anomaly, 20: 5660
SZLAVY, Laszlo Pal, Radiobiological role of hydrogen–peroxide–catalase system, 20: 5271
SZTEKE, Witold, Dispersion-type fuel element for "EWA" reactor, 20: 6684

T

TACCONI, F. A., Large scale experiments on heat transfer and hydrodynamics with steam-water mixtures, 20: 5623 (EURAEC-1325)
TACHON, J., Heating and confinement of plasma in magnetic well of deca-2, 20: 6469 (UCRL-Trans-1256(L))
TAIRA, Kazumasa, Studies on chemical protectors against radiation injury. I., 20: 5410
TAKADA, Kazuo, Removal of radioactive isotopes from cotton cloths, 20: 5676
TAKEMOTO, SHIGEO, X-ray induced photoluminescence spectra from NaI(Tl) and CsI(Tl), 20: 6537
TAKIGUCHI, Yoji, Influences of estrogen on radiosensitivity of cervical cancer, 20: 5472
TAL'ROSE, V. L., Effect of electric field on radiolysis of liquid hydrocarbons, 20: 5575
TAMAS, G., Elastic scattering of photons in region of giant resonance, 20: 6349
TAMURA, Taro, FORTRAN programs for Clebsch-Gordan and Racah coefficients and the nine-j symbol, 20: 6216 (ORNL-3877)
TAMURA, Taro, Static quadrupole moment of first excited 2^+ state of ^{114}Cd, 20: 6415
TANAKA, Hisao, Influences of estrogen on radiosensitivity of cervical cancer, 20: 5472
TANAKA, Y., Effects of freezing on radiation sensitivity of rat thymocytes, 20: 5414
TANG, I. N., Chemical considerations in fast reactor safety, 20: 5878 (BNL-9667)
TANNIOU, J., Action of x rays on cellular metabolism, using Warburg technique, 20: 5352
TASKINEN, P. J., Megavoltage therapy, 20: 5453
TAUSNER, Menasha J., Radiative τ decays and σ meson, 20: 6067
TAYLOR, A. Jeanne, n = 4 Levels of N^V by electron impact, computed with Coulomb-Born approximation, 20: 5982 (AERE-R-5061)
TAYLOR, D. M., Carcinogenic effects of ^{241}Am and ^{239}Pu in rat, 20: 5321
TAYLOR, G. N., Dental eruption pattern of beagle, 20: 5232 (COO-119-232, pp 68-73)
TAYLOR, G. N., Pilot study of effect of cortisol on $Na_3CaDTPA$ enhanced excretion of ^{239}Pu in beagle, 20: 5247 (COO-119-232, pp 188-99)
TAYLOR, G. N., Use of therapy in experimental animals, 20: 5231 (COO-119-232, pp 65-7)
TAYLOR, G. N., ^{238}Th induced fractures in beagles, 20: 5288 (COO-119-232, pp 74-87)
TAYLOR, H. A. Jr., Positive ion composition in magnetoionosphere, 20: 6198
TAYLOR, J. B., Statistical theory of nonadiabatic magnetic traps, 20: 6494
TAYLOR, J. Mi, Neutron spectra from Am–α–Be and Ra–α–Be sources, 20: 6269
TAYLOR, J. M., Photoneutrons from ^{9}Be, 20: 6390
TAYLOR, W. C., Experimental study of nonlinear plasma-wave interaction, 20: 6457 (AD-622876)
TAYSUM, David H., Correlation of bone strength with radiation dose from internal emitters and bone resorption, 20: 5289 (COO-119-232, pp 88-98)
TEETER, Charles E., Catalog of nuclear reactor concepts. I., 20: 6554 (ANL-7092)
TEGGE, Renate, Bioassay of influence of cortisol in bones of growing rabbits, 20: 5234 (COO-119-232, pp 122-52)
TELANDER, Gerald T., ^{99m}Tc compounds for visualization of body organs, 20: 5456
TEMPELMEYER, K. E., Experiments on Faraday-type MHD accelerator with series-connected electrodes, 20: 6025
TEMPLE, Paul Arthur, Measurement of piezoresistance in semiconductors, 20: 5883 (IS-1268)
TEODORU, V., Stabilization of acceleration intensity of U-120 cyclotron, 20: 5954
TEPLITZ, Vigdor Louis, Higher resonances in pion-nucleon scattering, 20: 6096
TERANAKA, M., Remark on 30 Bev jet showers, 20: 6039 (INSJ-90)
TERENT'EV, B. M., About absorption of gamma rav energy by point sources in macrosystems, 20: 5751
TERENT'EV, I. A., Inhomogeneous group $P(SU_6)$ in elementary particles theory, 20: 6145
TER-ORGANES'YANTS, A. A., Heat transfer and frictional resistance of high-temperature gas flow, 20: 5626(T) (NP-tr-1300)
TERZI, N., Isotope effects induced by local modes in U band, 20: 6545
TEVEBAUGH, A. D., Energy conversion, 20: 6024 (ANL-6925, pp 235-47)
TEVEBAUGH, A. D., Nuclear constants, 20: 6280 (ANL-6925, pp 249-51)
TEVEBAUGH, A. D., Reactor safety, 20: 6552 (ANL-6925, pp 187-233)
TEWORDT, L., Structure of vortex line and lower critical field in superconducting alloys, 20: 6251
THIRUVENGADAM, A., Cavitation damage resistance of materials in liquid sodium, 20: 5861
THOMAS, Colin G. Jr., Hormonal and isotope measures in thyroid carcinoma, 20: 5444
THOMAS, Garland L., Thermoelectric nuclear fuel elements, 20: 6598
THOMAS, M. F., $\frac{1}{2} \rightarrow \frac{1}{2}$ Hole transitions in mass 15, 20: 6378
THOMAS, Mary R., Near-infrared study of hydrogen bonding in water and

deuterium oxide, 20: 5552
THOMAS, Peter Barrington, Method of constructing nuclear reactor core from graphite blocks, 20: 6593
THOMAS, Robert G., USAF whole body gamma spectrometry, 20: 5427
THOMAS, T. D., Prog. rpt. on nuclear chemistry, annual, 1964–65, 20: 6298 (PPAD-2137-566)
THOMAS, T. R., Thermal resistance of pressed contacts, 20: 5625 (TRG-Report-1013)
THOMPSON, M. N., Neutron spectra from Am–α–Be and Ra–α–Be sources, 20: 6269
THOMPSON, M. N., Photoneutrons from ^{9}Be, 20: 6390
THOMPSON, R. S., Magnetic properties of superconducting thin films in nonlocal regime, 20: 6250
THOMPSON, R. W., Magnetic cloud chamber system to study interactions up to 10^{12} ev, 20: 5722 (CONF-640919, 12-43)
THOMSON, John A., Clinical studies with gamma camera, 20: 5467
THORDARSON, William, Perched ground water in zeolitized-bedded tuff, Ranier Mesa and vicinity, Nevada Test Site, Nevada, 20: 5643 (TEI-862)
THORN, J. D., Economic power from gas-cooled reactors, 20: 6644
THOURSON, Thomas L., Apparatus for x-ray determination of metal in hydrocarbon fuel, 20: 5522(P)
TIDMAN, Derek A., Scattering of test-particle by enhanced plasma fluctuations, 20: 6497
TIETZ, T., Mott polarization effect in scattering of fast electrons on Thomas-Fermi and Hartree-Fock atoms, 20: 5992
TILLEY, D. R., DWBA analysis of ^{12}C(d,pγ)^{13}C with measured optical model parameters, 20: 6362
TIMOFEEVA, N. A., Influence of ^{60}Co γ irradiation on growth of chlorella cultures, 20: 5389
TIMOFEEV-RESOVSKII, N. V., Influence of ^{60}Co γ irradiation on growth of chlorella cultures, 20: 5389
TISHIN, V. G., Inaccuracies of amplitude-to-time converters, 20: 5731 (JINR-P-2394)
TOCHILIN, E., Response of LiF to neutrons and charged particles, 20: 5572 (USNRDL-TR-909)
TOHEI, T., Strongly excited levels of ^{39}Ca in ^{40}Ca(^{3}He,α)^{39}Ca reaction, 20: 6398
TOLSTOPYATOVA, A. A., Kinetic parameters of dehydrogenization and dehydration of isopropyl alcohol and dehydrogenization of tetralin on praseodymium oxide, 20: 5567
TOMIMASU, T., Energy dependence of quantameter. I., 20: 5765
TOMIMASU, T., Energy dependence of quantameter. II., 20: 5766
TORRETTA, Alessandro, Radiotherapy of polycythemia, 20: 5483
TOTH, Geza, Effect of x-ray on phosphorus metabolism of glioma cultures, 20: 5255
TOTH, L. E., Superconducting behavior of several complex carbides and nitrides, 20: 6228
TOUGH, J. T., Effects of turbulence in He II thermal counterflow, 20: 6230
TOWER, Stephen N., Thermoelectric nuclear fuel elements, 20: 6598
TRAIBEL, Jorge, Procedure for improving gamma scintillography, 20: 5447
TRAVERS, Arthur, Peripheral-wall injection techniques in water vortex tube, 20: 6653 (D-910091-7)
TREACY, P. B., ^{9}Be(^{3}He,α) reactions to 16.63 and 16.92 Mev states of ^{8}Be, 20: 6389
TREBST, Achim, Photosynthetic reactions in uv-irradiated chloroplasts, 20: 5401
TRICE, V. G., Studies and evaluations, 20: 6553 (ANL-6925, pp 255-63)
TRIVELPIECE, A. W., Adiabatic containment of charged particles in combined mirror-multipole cusp magnetic fields, 20: 6496
TRUBATCH, J., Some properties of quantum linearized Einstein field, 20: 6224
TRUBATCH, S., Some properties of quantum linearized Einstein field, 20: 6224
TRUKHLYAEV, P. S., Production of ^{242}Pu and ^{242}Cm by irradiating ^{241}Am with neutrons, 20: 5823 (ORNL-tr-892)
TSAREV, B. M., Thermionic emission of hexaborides of samarium and gadolinium, 20: 5532(T) (K-Trans-10)
TSEDILINA, E. E., Diffusive spreading of inhomogeneities in weakly-ionized plasma, 20: 6482
TSIPENYUK, Yu. M., Photofission of even-even nuclei near threshold, 20: 6309 (ANL-Trans-245)
TSUANG, Ling-tsu, Enhancement of functional activity of pars intermedia following ^{60}Co irradiation in toad, 20: 5394
TSUKERMAN, I. S., Theory of leptonic baryon decays, 20: 6088
TSURUO, Akira, Single scattering streaming of gamma-rays through cylindrical ducts, 20: 6530
TSYGANOV, E. N., Analogue wire spark chamber system for measurements of particle momenta and angles, 20: 5730 (JINR-E-2366)
TU, Pham Qui, Classifications of meson resonances with higher spins in SU(6) symmetry theory, 20: 6151
TUCKER, W. E., Angular distributions of fast-neutron-induced gamma rays from calcium, 20: 6408
TUDWAY, Robert C., Radiotherapy, 20: 5466
TULINOVA, N. I., Recording of short pulses of electron current from betatron injector, 20: 5958
TUMANOV, G. K., Measurement of relationship of proton pulse in ITEF, 20: 5941 (NP-15598)
TURNER, E. B., Construction and calibration techniques of high frequency magnetic probes, 20: 6507
TURNER, Grenville, Origin of anomalous ^{129}Xe in meteorites, 20: 5978
TUZZOLINO, A. J., Stabilization of lithium-drifted silicon surface-barrier detectors, 20: 5767
TYAN, M. L., Homograft response and hemagglutinin production by sensitized thymectomized irradiated adult mice, 20: 5408 (USNRDL-TR-920)
TYUTIN, I. V., Ademollo-Gatto theorem for arbitrary SU(3) representation, 20: 6148
TZARA, C., Elastic scattering of photons in region of giant resonance, 20: 6349

U

UDAGAWA, Takeshi, Static quadrupole moment of first excited 2^{+} state of ^{114}Cd, 20: 6415
ULLMANN, J. W., Properties and prospects of thoria-base nuclear fuels, 20: 5915 (ORNL-P-1724)
ULLRICH, Horst, Pulse shape discrimination in half-life determination for study of (γ,α) reactions, 20: 5732 (KFK-335)
ULRICI, W., Nonlocal nuclear single particle potential and charge independence of short-range forces, 20: 6430
UNTI, T. W. J., Dynamics of gravitational sources, 20: 6222
UPADHYA, Y. D., Conductometric and potentiometric study of interaction between sodium succinate and thorium chloride, 20: 5555
URAKUBO, Goro, Studies on quality and test method of radiopharmaceuticals. I., 20: 5515
URBANEK, E., Influence of irradiation upon resistance against diphtherial intoxication in rats, 20: 5391
URSO, Paul, Spleen cells of heterologous radiation chimeras cultivated in diffusion chambers, 20: 5397
USACHEV, L. N., Photofission of even-even nuclei near threshold, 20: 6309 (ANL-Trans-245)
UTTLEY, C. A., Neutron cross sections of thorium and analysis of resonances up to 1 kev, 20: 6377

V

VALOV, P. V., Extraction of carrier free ^{57}Co from irradiated targets, 20: 5602
VAL'SKII, G. V., Delayed gamma rays from ^{235}U fission, 20: 6316
VAN ALLEN, J. A., Impulsive emission of ≈ 40-kev electrons from the sun, 20: 5971
VAN BEKKUM, D. W., Biochemical and morphological changes in lymphatic tissues after partial-body irradiation, 20: 5341
VAN DER PLAATS, G. J., Medical x-ray technique: principles and applications, 20: 5434
VANDERVOORT, Richard R., Compressive creep of beryllium oxide–uranium dioxide mixtures, 20: 5904
VANDERVORT, P. S., Evaluation of inclusions found by radiographic inspection in sap tubing, 20: 5630 (NAA-SR-Memo-11562)
VAN DRUNEN, C. J., Electrochemical model for oxidation of zirconium, 20: 5858
VAN HOVE, L., Weak interactions of strange particles, 20: 6035 (CERN-64-13(Vol.4), pp 1-49)
VANHUYSE, V. J., Z dependance of bremsstrahlung of electrons between 2.5 and 4.0 Mev, 20: 6432
VAN OOSTRUM, K. J., Charge distributions of ^{40}Ca and ^{44}Ca from 250-Mev electron scattering, 20: 6413
VAN WIJNGAARDEN, A., Ionoluminescence of MgO and Zn_2SiO_4 : Mn, 20: 5573
VASIL'EV, G. A., Attenuation of reactor radiations in serpentine sand, 20: 6524
VASKU, J., Influence of irradiation upon resistance against diphtherial intoxication in rats, 20: 5391
VASSOS, Basil H., Electrochemical preparation of thin metal films as standards on pyrolytic graphite, 20: 5503
VASTEL, R., Determination of spin and resonance parameters for ^{197}Au + n at 10 to 1000 ev, 20: 6392
VAUGHN, E. U., SCAP—in IBM 7094 code for spectral analysis of pulsed-neutron decay data, 20: 6585 (NAA-SR-Memo-10941)
VELIEV, B. S., Arsenate method for iodometric determination of yttrium in presence of aluminum, 20: 5506
VELLETRI, J. V., Barrier attenuation introduced by vertical wall, 20: 6516 (AD-617524)
VENKATESAN, K., Mass sum rules, symmetries and dispersion relations, 20: 6109 (NP-15638)
VERKHOVSKAYA, I. N., Action of low irradiation doses and incorporated

natural radioactive elements on spermatogenesis of Microtus oeconomus under natural conditions, 20: 5387
VERMILLION, R. E., Flow modes in electric shock tubes, 20: 6173
VERON, D., Heating and confinement of plasma in magnetic well of deca-2, 20: 6469 (UCRL-Trans-1256(L))
VERONESI, G., Health protection against dangers of ionizing radiation, 20: 5433
VERVIER, J., Effective nucleon-nucleon interactions in Y, Zr, Nb, Mo, and Tc isotopes, 20: 6337
VERWEIJ, H., Tunnel diode cascade circuit, 20: 5699
VESELKIN, A. P., Attenuation of reactor radiations in serpentine sand, 20: 6524
VIBLYI, N. I., Creation of muons by electrons in Coulomb field of nucleus, 20: 6089
VIGON, M. A., Level scheme of ^{231}Th, 20: 6388
VILAR BONET, J., Thorotrast disease, 20: 5355
VILCSEK, E., Isotopic composition and site of light primordial rare gases in stone meteorites, 20: 5975
VILLA, F., Streamer chamber development, 20: 5739 (SLAC-PUB-140)
VILLANI, M., Longitudinal polarization of low-energy muons from $K^+_{\mu 3}$ decay, 20: 6075
VISCONTI, A., Generating functional of propagators in quantum electrodynamics, 20: 6220
VITMAN, V. D., Determination of intensities and multipolarities of high-energy γ-transitions accompanying decay of ^{182}Ta, 20: 6347
VOBECKY, Miloslev, Rapid separation of barium from mixture of fission products, 20: 5603
VOCI, Vincenzo, Old and new methods of radiation therapy of carcinoma of bladder, 20: 5454
VOGELBRUCH, K., Report of theoretical and experimental groups for the year, 1964, 20: 6463 (JUL-264-PP)
VOINOVA, N. A., Determination of intensities and multipolarities of high-energy γ-transitions accompanying decay of ^{182}Ta, 20: 6347
VOISIN, J., Unitary representations of Galilei group. II., 20: 6124
VOJTA, Guenter, Expanded kinetic theory of plasmas in rotating magnetic fields and electromagnetic supplementary fields, 20: 6479
VOLKOV, V. V., Production of ^{242}Pu and ^{242}Cm by irradiating ^{241}Am with neutrons, 20: 5823 (ORNL-tr-892)
VOLLAND, Hans, Plasma waves in inhomogeneous medium, 20: 6511
VOLLMER, James, Determination of plasma density by laser interferometric and continuum radiation intensity measurements, 20: 6471
VOLODIN, V. P., Corrosion of zirconium in alkaline metal chloride melt, 20: 5855 (JPRS-32341, pp 24-31)
VON HIPPEL, Arthur R., Molecular designing of materials and devices, 20: 6551
VOOK, Frederick L., Thermal conductivity of electron-irradiated silicon, 20: 5919
VOORHIES, H. G., General atomic toroidal multipole confinement experiment, 20: 6460 (GA-6594)
VOYTOVICH, R. F., Oxidation of binary alloys, 20: 5854 (JPRS-32341, pp 8-16)
VULETICH, T., Multichannel spectrometer for analysis of pulsed ion sources, 20: 5698
VYALOV, G. N., Extraction of heavy ion beam from cyclotron with azimuthal variation of magnetic field, 20: 5947 (ANL-Trans-241)

W

WABER, J. T., Effect of assumed electronic configuration on electronic band structure of nickel, 20: 6534 (SC-DC-65-1843)
WACHSMANN, F., Dosimetry in radiotherapeutic practice, 20: 5478
WACKER, A., Different effect of bromouracildesoxyriboside and iodouracildesoxyriboside in irradiation of herpes simplex-virus with uv light, 20: 5363
WADA, W. W., Current commutation relations and meson-meson scattering, 20: 6077
WADACHI, Yoshiki, Desorption of carrier-free ^{60}Co, ^{144}Ce, and ^{147}Pm from charcoal surfaces, 20: 5675
WADACHI, Yoshiki, Removal of radioactive isotopes from cotton cloths, 20: 5676
WADDELL, Charles N., Elastic and inelastic scattering of 30.3 Mev protons by Si, 20: 6339
WADE, F., Containment of helium in primary circuit of the Dragon Reactor, 20: 6642
WAELISCHMILLER, Hans, Improvements in or relating to master-slave manipulators, 20: 5616(P)
WAENKE, H., Isotopic composition and site of light primordial rare gases in stone meteorites, 20: 5975
WAENKE, H., Solar wind as source of primordial rare gases in stone meteorites, 20: 5976
WAGNER, F., Fundamentals of dynamics in nonlinear spin theory of elementary particles, 20: 6112
WAHL, Arnold C., Molecular orbital density comparisons of H_2, Li_2, B_2, C_2, N_2, O_2, and F_2, 20: 5524 (ANL-7076)
WAHLBECK, P. G., Scandium–yttrium–hydrogen system, 20: 5909
WAITE, C. W., Auroral phenomena in integral-invariant coordinate system, 20: 6189
WALDRON, R. A., Development and investigation of photon counter and measurement of optical excitation functions of helium, 20: 5748 (UCRL-Trans-1266(L))
WALDRON-EDWARD, D., Studies of inhibition of intestinal absorption of radioactive strontium, 20: 5253
WALFORD, Roy L., Life span in normal and irradiated hamsters, 20: 5330
WALL, John A., Injury of small intestine following irradiation for gynecologic cancer, 20: 5392
WALLIS, G., Singularities of kinetic dispersion equation, 20: 6477
WALS, G. D., Electrophoretic separation of some actinide and lanthanide elements, 20: 5598
WALSH, M. L., Calibration of radioactive gas monitors, 20: 5774
WALTERS, Craig T., Prog. rpt. on analytical description of nuclear-reactor accident, 7–9/65, 20: 6560 (BMI-X-10145)
WANG, An-chu, Comparison of radiation sensitivity of chromosome in white blood cells of human beings, monkeys, and rabbits, 20: 5304 (JPRS-32985, pp 45-50)
WANG, K. H., Proton-proton bremsstrahlung at 158 Mev, 20: 6046
WARD, S. H., Auroral-zone pearl pulsations, 20: 6204
WATAGHIN, V., Peripheral model and its application to photodisintegration of ^{6}Li, 20: 6368
WATANABE, Tomiya, Determination of electron distribution in magnetosphere using hydromagnetic whistlers, 20: 6202
WATSON, C. R., Gamma radiation dosimetry of ^{137}Cs in sheep evaluated with thermoluminescent dosimeters, 20: 5285 (BNWL-SA-172)
WATSON, P. D., Advanced BONUS core boiler-superheater fuel element weldments, 20: 6624 (TID-22425)
WATSON, T. A., Irradiation in management of tumours of head and neck, 20: 5441
WATTS, F. C., Gamma-ray evaluation of diagnostic shielding barriers, 20: 5677
WAWRYSZCZUK, Jan, Gamma-gamma angular correlations in ^{147}Eu to ^{147}Sm decay, 20: 6396
WAWRZYCZEK, Wiktor, Potentiometric determination of rare earths (e.g., erbium), 20: 5519
WAY, Stewart, Magnetohydrodynamic generator apparatus, 20: 6029
WAY, Stewart, Magnetohydrodynamic generator, 20: 6030
WEAR, James O., Absorptivities of complexes from variation and mole ratio methods for complex determinations, 20: 5530 (SC-RR-65-625)
WEAVER, D. L., Spin correlations in photoproduction of vector mesons, 20: 6076
WEBB, John, Improvements relating to handling equipment for radioactive charges, 20: 5615(P)
WEIDLICH, W., Quantum noise operators for N-level system, 20: 6002
WEIHER, Justine, Thermodynamic and physical properties of beryllium compounds. VIII., 20: 5554
WEINBERG, R. B., Angular correlation measurements on ^{25}Mg(d,pγ)^{26}Mg reaction, 20: 6410
WEINKAM, James J., Automation of radiation treatment planning. V., 20: 5449
WEINZIERL, Peter, Prompt and delayed gamma rays in nuclear fission, 20: 6300 (SGAE-PH-29/1965)
WEISMAN, J., Saxton chemical shim experiment, 20: 6629 (WCAP-3269-24)
WEISS, R. J., Search for x-ray Raman effect, 20: 6539
WEISS, Rene, Reading and charging instrument for dosimeters, 20: 5799
WERBROUCK, A. E., Longitudinal polarization of low-energy muons from $K^+_{\mu 3}$ decay, 20: 6075
WERNER, E., Validity of quasi-particle approximation in nuclear physics, 20: 6433
WESSEL, W. Roy, Quantum mechanics of $(p\text{-}\mu\text{-}p)^+$ molecular ion, 20: 5980 (AD-617522)
WETZEL, Lewis, Reflection of electromagnetic waves from inhomogeneous plasma, 20: 6445 (AD-617619)
WEYMANN, R., Diffusion approximation for photon gas interacting with plasma via Compton effect, 20: 6502
WHEATLEY, J. C., Low-temperature heat capacity of liquid ^{3}He, 20: 6245
WHEELER, Owen H., Irradiation of estrone and derivatives in acetic acid, 20: 5274
WHITFIELD, J. F., Effects of x-radiation and nicotinamide on respiration of rat thymocytes, 20: 5340
WHITING, Allen R., Nondestructive testing of plastic fatigue pressure vessels, 20: 5894 (SWRI-1228-3-3)
WHITTEN, L. G., Optical applications in dimensional gaging, 20: 6689 (Y-KE-191)
WICHMAN, Sven H., Nuclear reactor's cooling water is conserved by recharging at 15 MGD/ACRE, 20: 6667 (BNL-9686)
WICHRZYCKA, E., Influence of occupational exposure to chemical agents and x-rays on leucocyte alkaline phosphatase activity, 20: 5269
WICKER, C. D., Urethane manipulator gauntlets, 20: 5612 (ORNL-TM-1326)

WIEBER, Donald L., Amplitude-independent nanosecond timing discriminator for fast photomultipliers, 20: 5744 (UCRL-16227)
WIECZOREK, L. W., Light from fall space, 20: 6166
WIECZORKOWSKI, Mariusz, Dispersion-type fuel element for "EWA" reactor, 20: 6684
WIGGINS, T. A., High resolution measurements on infrared absorption spectrum of HBr, 20: 5550
WILCOX, John M., Quasi-stationary corotating structure in interplanetary medium, 20: 5972
WILHELM, Johannes, Theory of a glow light of low-pressure discharge, 20: 6165
WILIP, Elmar K., Effect of geometry of cyclotron center upon starting motion of heavy ions (median plane), 20: 5948 (ANL-Trans-246)
WILIP, Elmar K., Extraction of heavy ion beam from cyclotron with azimuthal variation of magnetic field, 20: 5947 (ANL-Trans-241)
WILIP, Elmar K., Ground-state energy of He, 20: 5987 (ANL-Trans-248)
WILIP, Elmar K., Photofission of even-even nuclei near threshold, 20: 6309 (ANL-Trans-245)
WILIP, Elmar K., Shell effects in nuclear fission, 20: 6308 (ANL-Trans-243)
WILKINSON, M. K., Magnetic structures of metallic erbium, 20: 6541
WILL, G., Magnetic structure of $MnSO_4$, 20: 6546
WILLARD, J. E., Production of trapped radicals from alkyl halides in organic glasses, 20: 5577
WILLIAMS, J. A., High temperature creep machine for in-cell operation, 20: 5611 (BNWL-137)
WILLIAMSON, H. A., Theoretical investigation of lowest five ionization potentials of uranium, 20: 5983 (D-910099-2)
WILLIAMSON, R. M., DWBA analysis of $^{12}C(d,p\gamma)^{13}C$ with measured optical model parameters, 20: 6362
WILLIS, Conrad P., Radiochemical determination of ^{210}Pb in mill products and biological materials, 20: 5505
WILSKY, K., Spectral shapes and beta–gamma directional correlation in beta decay of $^{172}Tm(I^{\pi} = 2^-)$, 20: 6381
WILSON, D. R., Experiments on Faraday-type MHD accelerator with series-connected electrodes, 20: 6025
WILSON, Judith W., Radiolysis of methanol and methanolic solutions. IV., 20: 5581
WILSON, Raphael, Prog. rpt. on radiobiology, 196, 20: 5291 (COO-205-55)
WIMETT, Thomas, Fast reactors—single pulses, 20: 6671 (CONF-650217, pp 1-10)
WINBORN, Claude D., Irradiation therapy of the larynx, 20: 5486
WINDLE, D. W., Power series solution of F2 layer diffusion equation, 20: 6183 (AD-619821)
WINGATE, C. L., Response of LiF to neutrons and charged particles, 20: 5572 (USNRDL-TR-909)
WISE, Benjamin N., Effects of ultraviolet microbeam irradiation on morphogenesis in euplotes, 20: 5345
WISSHAK, F., Scintillation of terrestrial radiation, 20: 6186(T) (UCRL-Trans-1269(L))
WITCOFSKI, R. L., Gamma-ray evaluation of diagnostic shielding barriers, 20: 5677
WITCOFSKI, Richard L., Technique for scanning posterior fossa, 20: 5462
WOHLFAHRT, H.-D., Tritium concentration of German river waters, 20: 5654
WOJACZEK, Karl, Positive argon column in long tubes, 20: 6475
WOJTOWICZ, Stefan, Detection of low β-activity with G-M detector, 20: 5781
WOLF, G., π–p interactions at 4 Bev/c, 20: 6100
WOLF, Neil, Properties of alkali–metal magnetoplasmas related to "enhanced diffusion," 20: 6466 (SIT-2813-33)
WOLF, Peter, Determination of frequency of plutonium isotopes, 20: 5497 (KFK-339)
WOLLAN, E. O., Magnetic structures of metallic erbium, 20: 6541
WOLLAN, E. O., Paramagnetic neutron scattering from metallic palladium, 20: 6544
WOOD, D. E., Boron interference in fast-neutron activation analysis for oxygen, 20: 5498 (NP-15636)
WOOD, D. E., Neutron fluxes available from Kaman nuclear neutron generators, 20: 6263 (NP-15635)
WOOD, Donald E., Selected references for neutron activation analysis, 20: 5499 (NP-15637)
WOOD, William George Edgar, Method of constructing nuclear reactor core from graphite blocks, 20: 6593
WOODLEY, H. J., Containment of helium in primary circuit of the Dragon Reactor, 20: 6642
WOODS, A. D. B., Phonons in disordered niobium–molybdenum alloys, 20: 5911
WOOLCOCK, W. S., New determination of pion-nucleon coupling constant and s-wave scattering lengths, 20: 6083
WORLEY, Richard D., Hyperfine-structure anomaly of ^{131}Cs, 20: 6401
WRIGHT, C. M., Chelate chemistry. III., 20: 5538
WRIGHT, C. S., Geomagnetic micropulsation results from Byrd Station and Great Whale River, 20: 6188
WRIGHT, Edward S., Direct measurement of current density distributions in transient plasmas, 20: 6509
WRIGHT, S. C., Measurement of proton-proton triple scattering at 430 Mev, 20: 6056
WRIGHT, Wister Cordell, Effects of time delay simulation methods upon stability and time response of simulated systems, 20: 5834 (ORNL-TM-1323)
WU, Y. C. Lin, Physical property distributions in low-pressure crossed-field plasma accelerator, 20: 6470
WURM, J. P., (d,α) Reactions on light nuclei, 20: 6369
WUTTIG, Manfred, Neutron diffraction of ordered $PtMn_3$, 20: 5912

Y

YAGI, K., Strongly excited levels of ^{39}Ca in $^{40}Ca(^3He,\alpha)^{39}Ca$ reaction, 20: 6398
YAGODIN, G. A., Interaction between hafnium tetrafluoride and ammonium fluoride in aqueous solution, 20: 5535
YAJIMA, N., Remark on 30 Bev jet showers, 20: 6039 (INSJ-90)
YAKIMETS, V. V., Excitation of collective levels of spherical nuclei in β-decay and in stripping, 20: 6353
YAKOVLEV, G. N., Production of ^{242}Pu and ^{242}Cm by irradiating ^{241}Am with neutrons, 20: 5823 (ORNL-tr-892)
YAM, Kai-Ming, Effect of x-radiation on hexobarbital metabolizing enzyme system of liver microsomes, 20: 5283 (AD-623599, pp 16-27)
YAMADA, Mamoru, Influences of estrogen on radiosensitivity of cervical cancer, 20: 5472
YAMAKOSHI, Kozuo, New glasses for low background counting, 20: 5585
YAMAMOTO, Moriyuki, Neutron surface moisture gage for determining moisture contents of building materials, 20: 5819
YAMAOKA, Yoshito, Removal of radioactive isotopes from cotton cloths, 20: 5676
YANO, Syukuro, Alternating current magnetohydrodynamic generator, 20: 6026
YARITSYNA, I. A., International comparison of neutron sources, 20: 6265
YAVOR, S. Ya., Spherical aberration of compound quadrupole lenses and systems, 20: 5696
YEARIAN, M. R., Charge distributions of ^{40}Ca and ^{44}Ca from 250-Mev electron scattering, 20: 6413
YEATTS, L. B. Jr., Purification of zirconium tetrafluoride, 20: 5528 (ORNL-TM-1292)
YEN, C. M., Superconducting behavior of several complex carbides and nitrides, 20: 6228
YEN, J. T., Electrostatic probe performance as influenced by its magnetogasdynamic boundary layer, 20: 5689
YERKOVICH, S., Switch actuator mechanism, 20: 6693
YGUERABIDE, Juan, Generation and detection of subnanosecond light pulses, 20: 5705
YOKOI, K., Remark on 30 Bev jet showers, 20: 6039 (INSJ-90)
YOSHIKAWA, M., General atomic toroidal multipole confinement experiment, 20: 6460 (GA-6594)
YOUDALE, T., Effects of x-radiation and nicotinamide on respiration of rat thymocytes, 20: 5340
YU, Chi-chuan, Kinetic parameters of dehydrogenization and dehydration of isopropyl alcohol and dehydrogenization of tetralin on praseodymium oxide, 20: 5567
YUDOVICH, L. A., Comparison of ionization level in F2 region in Antarctic and Arctic, 20: 6190
YUNUSOV, M., Effect of gamma irradiation on fluorescence yield of ruby, 20: 6536

Z

ZAEHRINGER, J., Potassium analysis of amphoterite chondrites and their K–Ar age, 20: 5979
ZAKHAROV, I. I., Method of calculation of water and power costs for nuclear desalination plants, 20: 6649
ZAKHAROV, V. I., Ademollo-Gatto theorem for arbitrary SU(3) representation, 20: 6148
ZAKHAROV, Yu. A., Effect of additives on certain physico-chemical properties of silver oxalate. V., 20: 5583
ZAKHAROVA, I. M., Study of dose rate field with γ source of spent reactor fuel elements, 20: 6597
ZAKOVSKY, J., Several cases of radiation injury, 20: 5241
ZAMIRALOV, V. S., Broken symmetry SU(6) and electromagnetic properties of baryons, 20: 6107 (JINR-P-2401)
ZANDER, Arlen R., Activation cross sections for reactions of Rh and Ru with 14.7 Mev neutrons, 20: 6338
ZANEVSKY, Yu. V., Analogue wire spark chamber system for measurements of particle momenta and angles, 20: 5730 (JINR-E-2366)
ZARTMAN, I. F., Conference on pulsed high intensity fission neutron sources, USAEC, Washington, 20: 6256 (CONF-650217)
ZATZICK, M. R., Neutron detection and spectroscopy with semiconductor

detectors, 20: 5714 (AD-623722)
ZATZICK, M. R., Response function and sensitivity of double-diffused silicon detectors in high γ-dose rate fields, 20: 5743 (UCRL-14405)
ZAUNBAUER, W., Concluding word to current remarks of P. Koeppe, 20: 5399
ZAUNBAUER, W., Thorotrast problem, 20: 5398
ZAVIL'GEL'SKII, G. B., Gross-linkages and locally denatured areas induced in double-strand DNA by ultraviolet light, 20: 5268
ZEH, H. D., Stripping reactions below coulomb barrier, 20: 6352
ZEH, H. D., Symmetry violating trial wave functions, 20: 6227
ZEL'DOVICH, O. Ya., Large scintillation counters and counters for operation in magnetic fields, 20: 5736 (NP-15597)
ZELEVINSKII, V. G., Green function method in simple nuclear model, 20: 6425
ZGANJAR, Edward Francis, E2 internal-conversion process in ^{152}Gd and ^{154}Gd and beta–gamma directional correlation in decay of ^{154}Eu, 20: 6303 (TID-22393)
ZHARKOV, Yu. A., Urinary secretion of thymidine following whole-body exposure of rats to various doses of x radiation, 20: 5382
ZHARNOVETSKI, K. I., Reduction possibilities of some errors in β-activity measurements by solid angle method, 20: 5729 (INR-617/XIX/D)
ZHEREBTSOVA, K. I., Study of (d,p) stripping effect on intermediate nuclei. III., 20: 6422
ZHERNOV, V. S., Continuous centralized control of individual radiation doses, 20: 5749
ZHOKHOV, K. A., Alkali metals boiling heat transfer, 20: 5627
ZICKENDRAHT, Werner, Construction of complete orthogonal system for quantum-mechanical three-body problem, 20: 6217
ZIEMER, Richard W., Physical property distributions in low-pressure crossed-field plasma accelerator, 20: 6470
ZIMERING, S., Prog. rpt. on mechanical properties of metals subjected to mechanical stress at elevated temperature and neutron irradiation, 3/65, 20: 5880 (EURAEC-1310)
ZIMERING, S., Prog. rpt. on mechanical properties of metals subjected to mechanical stress and neutron irradiation, 10/65, 20: 5913 (EURAEC-1488)
ZIMMERMAN, E. L., Neutron detection and spectroscopy with semiconductor detectors, 20: 5714 (AD-623722)
ZIMMERMAN, J. E., Quantum transitions and loss in multiply connected superconductors, 20: 6246
ZIOCK, K., Impedance matched delay-line clip, 20: 5701
ZIOCK, Klaus, X-ray astronomy, 20: 5968 (NP-15626)
ZLOTOWSKI, Izrail, Measurements of ^{14}C radioactivity in organic compounds, 20: 5511
ZOGRAFOV, D., Fibrinolysis in whole-body irradiation of rabbits, 20: 5325
ZOLTAN, Laszlo, Effect of x-ray on phosphorus metabolism of glioma cultures, 20: 5255
ZOMMER, V. P., Prompt fission gamma-ray quanta, 20: 6314
ZOTIKOV, A. A., Microfluorometric examination of radiation injuries of macronucleus of tetrahymena Pyriformis infusoria, 20: 5267
ZUBER, N., Average volumetric concentration in two-phase flow systems, 20: 5629
ZUK, W., Electromagnetic isotope separator at Lublin, 20: 5826
ZVEREV, B. V., Resonance method for adjusting circular iris waveguides in linear accelerators, 20: 5955

SUBJECT INDEX

Main entries in this index are generally specific materials, things, and processes. These are followed by modifiers that describe the properties of, and processes applied to, the main entries.

The number preceding the colon is the *NSA* volume number, and the number following is the abstract number. The designation (R) following the abstract number indicates that the abstract is of a progress report; (P) indicates a patent; and (T) indicates a translation. Abstracts for reports other than progress reports carry no letter designation. References to report numbers, where appropriate, are included after the abstract number of the citation. Published literature (journal article or book) is identifiable by the absence of a report number.

The user should bear in mind that the ideas presented in the original literature, rather than key words, have been indexed. The indexers have tried to select what seemed the most probable and logical place to look for typical information. Since it is not possible to anticipate where a user would look for information, numerous cross references are included in cumulative indexes to assist him in his search.

Experience in using an index of this type will be the best guide in obtaining the desired information, and a consideration of synonymous or closely related terms will prove valuable.

Information must be so indexed as to be of the greatest use to the greatest number of users. This requires that a topic be indexed to headings that most specifically describe it and not ordinarily to the headings that describe its ultimate use, nor to the general class headings that include the specific headings. For example, information on the treatment of thyroid disease with I-131 would be indexed under Thyroid Gland and under Iodine Isotopes I-131, but not necessarily under Radiotherapy. A study of the effects of x radiation on hair would be indexed under both X Radiation and Hair. However, the information would not be indexed under the experimental animal, e.g., Rats, unless the report discusses the effects on rat hair as compared with the effect on the hair of other animals.

The broad, general class headings are used only for general information or for comprehensive reports or articles.

Subject Heading Styles

Generally, the direct form of subject entry is used rather than inverted headings, e.g., Amino Acids rather than Acids, Amino; Helium Isotopes He-4 rather than Helium—isotopes He-4 or Helium—He-4 isotopes. Note, however, that in some cases parenthetic modifying terms or inverted headings of the form Neutrons, Fast are used in preference to a direct entry that would result in the scattering of information. Organic compounds are usually entered in the index in the inverted form so that substituted compounds can be listed near the parent compound; e.g., Benzene, Bromo- rather than Bromobenzene. In general, the style of nomenclature used is that of Chemical Abstracts, except that some items listed in that publication as subheadings are elevated to form part of the main heading; e.g., Butyric Acid, Methyl Ester rather than Butyric Acid—methyl ester.

Alphabetization

Main headings are alphabetized word-by-word. A parenthetic qualifier following a main heading is disregarded in alphabetizing unless there are two or more headings identical except for the parenthetic qualifier, in which case the qualifier determines the order. Headings involving Greek letters are arranged as if the names of the letters were spelled out.

Examples:

M-Capture
  see Electron Capture
Magnesium
Magnesium Alloys
Manganese Fluorides
Manganese(II) Fluorides
Mesons
Mesons (π)
Mesons (ρ)
3-Pentanol, 2,4-Dimethyl-
2-Pentanol, 2-Methyl-
2-Pentanol, 4-Methyl-

Nomenclature of Inorganic Compounds

Inorganic compounds are indexed in the direct form, listing cations in the order of increasing valence in the case of polycationic salts of varying valence and in alphabetic order for polycationic salts in which all cations have the same valence; e.g., Sodium Aluminum Silicates and Potassium Sodium Sulfates.

Multicomponent Alloys and Other Systems

Multicomponent alloys, except well-known trade names are indexed under a main heading in the form "element alloy" for each element in the alloy. The modifier begins with element symbols for each component arranged alphabetically as if the English name for the element were spelled out.

Example: Copper-Gold Alloy is indexed
  Copper Alloys
    Cu-Au...
  Gold Alloys
    Cu-Au...

Well-known alloys such as Zircaloy-2 are indexed directly to the trade name; cross references referring from each component of the alloy to the entry for the trade name appear in cumulative indexes.

Multicomponent systems of non-metallic elements are indexed in a manner similar to alloys except the main heading used contains the word "Systems" in place of "Alloys."

Example: Silicon–Tungsten Systems are indexed
  Silicon Systems
    Si-W...
  Tungsten Systems
    Si-W...

Multicompound systems and mixtures of compounds are indexed under the main heading for each component com-

pound; the modifiers begin with an alphabetical listing of compound formulas.

Example: Lead Titanate–Lead Zirconate is indexed
Lead Titanates
$PbTiO_3$-$PbZrO_3$...
Lead Zirconates
$PbTiO_3$-$PbZrO_3$...

A mixed system of compounds and elements is indexed using a combined form of the above conventions, e.g., a dispersion of copper and alumina would be indexed

Aluminum Oxides
Al_2O_3-Cu...
Copper Systems
Al_2O_3-Cu..

Physical States and Configurations of Materials

Specification of the physical state, if other than normal, or geometric configuration of the material is included in the modifying phrase, i.e., liquid metals would be indexed to the metal with "liquid" in the modifier, and carbon crucibles would be indexed to Carbon with "crucibles" appropriately placed in the modifier and also to Crucibles if appropriate.

Modifying Phrases

The modifiers appearing under a main heading are written specifically to describe the relation of the item being indexed to that main heading. The modifier, therefore, will generally contain more useful information about that relation than will a title or a phrase written to be used under every main heading assigned to the item. Effort is exerted to begin the modifier with the word judged to be of greatest use to the greatest number of users; this, however, does not obviate the need to consider all modifiers under the main heading(s) of interest.

Modifiers are usually intended to form a meaningful phrase when combined with the main heading. Some are intended to be read following the main heading, e.g., the entry Hydrogen—sorption by charcoal is read "hydrogen sorption by charcoal"; however, as a result of placing the important word first, many modifiers must be arranged for smooth reading, e.g., Formaldehyde—yields in radiolysis of ethyl ether, effects of deuterium on is read "effects of deuterium on formaldehyde yields in radiolysis of ethyl ether" and Uranium—crystal structure of, effect of cooling rate on allotropic transformations in is read "effect of cooling rate on allotropic transformations in crystal structure of uranium." Prepositions are sometimes omitted if no ambiguity results.

Special characters are added to modifiers in the field of physics; if the modifier does not establish the experimental or theoretical character of a reference, a symbol (E), (T), or (E/T) is placed immediately after the modifying phrase and before the journal reference number. The value of this identification has been established by the American Institute of Physics.

A

A-286 ALLOY
radiation effects on stress rupture of, fast and thermal neutron, 20: 5851
radiation effects on creep properties of, thermal-neutron, 20: 5846
ABDOMEN
radiosensitivity of rat, x, 20: 5319
ABSTRACTS
on atom and electron collisions, 20: 5988(T) (JPRS-32421)
on plasma jet technology, 20: 5633 (NASA-SP-5033)
ACCELERATORS
beam transport optics for, first and second order, (T), 20: 5944 (SLAC-PUB-132)
magnetic field loss in charged-particle, device for measuring index of, 20: 5959
particle leakage from storage-ring, due to amplitude variations and frequency of compensating field, (T), 20: 5949
performance with exponential piles as targets, as pulsed neutron sources, (E), 20: 6257 (CONF-650217, pp 11-24)
power supplies for, engineering drawings of double pulser in, 20: 5963
radioactivity in, estimate of induced, (E/T), 20: 5933 (CERN-65-34)
ACETATES, FLUORO-
radiosensitivity effects on paramecium, uv, 20: 5386
ACETIC ACID, (ETHYLENEDIAMINE)TETRA-
analytical use in determination of selected metal ions by potentiometric titration, 20: 5502
effects on fission tracks in glasses, 20: 5713 (AD-623384)
ACETIC ACID, (ETHYLENEDIAMINE)TETRA-, AMMONIUM SALTS
effects on excretion of strontium-90 by dogs, 20: 5248(R) (COO-119-232, pp 200-2)
effects on excretion of yttrium-90 by dogs, 20: 5248(R) (COO-119-232, pp 200-2)
ACETONE
uses as medium for drifting lithium into germanium, (E), 20: 5702
ACETYLENE
yields in pyrolysis of diphenyl at 375 to 1375°K, 20: 5563 (EUR-2482.f)
yields in recoil carbon-11 atom reactions on alicyclic and aliphatic hydrocarbons, 20: 5570 (JUL-228-RC)
ACID PHOSPHATES
effects on uptake of strontium-89 from contaminated soil, by barley, 20: 5257
ACRIFLAVINE
effects on Saccharomyces radiosensitivity, mutagenic, 20: 5360
ACTINIDES
diffusion in pyrolytic carbon, 20: 5843
separation by electrophoresis, 20: 5598
ACTINIUM
separation from francium by solvent extraction using 4-*sec*-butyl-2-*α*-methylbenzylphenol, 20: 5601
ACTINIUM ISOTOPES Ac-228
content in Thorotrast of, 20: 5398
ACTIVATION ANALYSIS
bibliography on neutron, 20: 5499 (NP-15637)
chemical yield correction in, method for avoiding, 20: 5494 (AEET-217)
competing reactions in neutron, 20: 5514
ACTIVATION DETECTORS
description of, using copper-62 beta activity from (n,2n) reactions with copper-63 for detecting fast neutrons, (E), 20: 6289 (KN-63-10(R))
ADENOSINEPHOSPHORIC ACIDS
radioinduced deamination in rabbit tissues of, γ, 20: 5380
AERIAL SURVEYING
equipment for gamma, design of plastic-scintillator, 20: 5761
AEROSOL GENERATORS
design and performance of electrostatic, 20: 5237(R) (UR-668, pp 55-109)
AEROSOLS
generator for, electrostatic, 20: 5237(R) (UR-668, pp 55-109)
AGE
radiosensitivity effects of, on metabolism in lens of cattle and guinea pigs, x, 20: 5333
radiosensitivity effects on leukemogenesis in mice, 20: 5367
AGING
radiation effects on, of hamsters, 20: 5330
AGRICULTURE
radiation and radioisotopes in Rumanian, 20: 5235 (NP-15543, pp 83-90)
AIR
corrosive effects on uranium–10 molybdenum, electroplating with nickel for prevention of, 20: 5867
electric arcs in gravitationless state in, 20: 6163
flow of peripherally injected, in vortex tubes, 20: 6652 (D-910091-5)
monitoring for radioactivity, performance of polyethylene tubes in equipment for, 20: 5752
neutron penetration in, Sn-method for calculating, 20: 6261 (LA-3415)
processing aboard space vehicles, using electric-power plants, (E/T), 20: 5820 (NASA-CR-316)
reactions with beryllium at 100 to 1500°C, 20: 5844
reactions with beryllium at 500 to 900°C, 20: 5844
reactions with niobium–tungsten alloys at 900 to 1300°C, effects of niobium content on, 20: 5851
air–water, momentum flux measurement by impulse method for flow of, 20: 5624 (MIT-3496-1)
ALBUMINS
energy transfer in, effects of water content on, 20: 5270
radiation effects on content in rat blood serum, proton, 20: 5378
ALGINATES
sodium, effects on strontium-89 uptake by bones, 20: 5253
ALKALI METAL IONS
transport in yeast, mechanisms of, 20: 5251(R) (UR-668, pp 123-49)
ALKALI METALS
critical temperature of, equipment for measurement of, 20: 5594(R) (ANL-6925, pp 21-106)
diffusion of plasma of, in Q machines, 20: 6466 (SIT-2813-33)
effects on electric and thermochemical properties of plasma, (E/T), 20: 6447 (AD-618693)
separation by ion exchange, 20: 5597
ALKENES
radioinduced polymerization with isobutylene at low temperature, 20: 5589(P)
ALLOYS
critical field and vortex line structure in superconducting, lower, (T), 20: 6251
interactions in liquid and solid, morphology of, 20: 5895(R) (TID-22271)
ALPHA DECAY
transitions in spherical nuclei, (T), 20: 6376
ALPHA PARTICLES
activity of, in Thorotrast, 20: 5399
angular and energy distributions from beryllium-9 and carbon-12 (d,*α*) reactions at 11 Mev, (E), 20: 6360
collimation in gridded ionization chamber, electronic, 20: 5782
content in Thorotrast of, 20: 5400
detection and discrimination by semiconductor counters, (E), 20: 5732 (KFK-335)
detection in nuclear emulsions and solids, 20: 5755
detection of, surface barrier detectors for, 20: 5790
detection using lithium-drifted germanium and silicon detectors, 20: 5784
dose of, from deposited Thorotrast, 20: 5398
dosimetry of, performance of silicon surface-barrier detectors for, 20: 5721 (CLOR/IBJ-II-37/D)
dosimetry of, performance of lithium fluoride thermoluminescent detector for, 20: 5572 (USNRDL-TR-909)
effects of, from deposited Thorotrast, pathological, 20: 5398
effects of, from deposited Thorotrast, pathological, 20: 5400
effects of, from injected Thorotrast, pathological, 20: 5355
effects on coalescence rates in liquid-liquid systems, mechanism of, 20: 5571 (ORNL-TM-1283)
effects on plant viruses, biological, 20: 5310
effects on plutonium hexafluoride decomposition, 20: 5595(R) (ANL-6925, pp 107-64)
emission in uranium-235 decay, thorium-231 level scheme from, (E), 20: 6388
energy spectra from solar flares, 20: 5969
energy spectra from proton reactions with bismuth-209 and gold-197 at 60 to 155 Mev, (T), 20: 6364
interactions with alpha particles in carbon-12, three-body, (T), 20: 6371
interactions with nucleons in spherical nuclei, (T), 20: 6376
reactions (*α*,*γ*) with carbon at 58 Mev, spectra from, (E), 20: 6297(R) (ORNL-3858(Vol.2), pp 82-90)
reactions (*α*,xnγ) with rare earth nuclei at 27 to 52 Mev, gamma spectra from, (E), 20: 6348
scattering by calcium-48 at 42 Mev, elastic and inelastic, (E), 20: 6400
ALPHA SOURCES
inhalation by animals and man, effects of, 20: 5237(R) (UR-668, pp 55-109)
ALUMINUM
coating with rare earths, electrolytic, 20: 5867
combustion in water, effects of pellet size on consumption time of, 20: 5846
combustion with fluorine, products and yields from, 20: 5523(R) (ANL-6925, pp 175-85)
determination by potentiometric titration using EDTA, equipment for, 20: 5502
effects on hot hardness of zirconium oxides, 20: 5846
effects on oxidation resistance of beryllium–niobium and beryllium–zirconium alloys, 20: 5844

electron reactions at 2.5 to 4.0 Mev, bremsstrahlung spectra from, (E), 20: 6432
gamma heating in, calculations for, (E/T), 20: 6517 (CONF-651101-41)
gamma scattering at 0.145 to 1.25 Mev in, angular distributions of, (E), 20: 6527
gamma shielding in air near ground, point-source, (E), 20: 6529
performance as coatings for self-regenerating deuterium targets, (E/T), 20: 6334
powder particle size separation techniques, 20: 5839(R) (RISO-110)
proton reactions (p,n) at 30 and 50 Mev, isobaric-state excitation in, (E/T), 20: 6361
radiation effects on in-pile corrosion of, by aqueous solutions, 20: 5852(R) (EURAEC-1522)
radiation effects on electric conductivity of, stage I and II recovery from electron, 20: 5918
reactions with uranio, 20: 5843
reactions with U_3O_8, 20: 5848
reactions with water, mechanisms of laser-induced, 20: 6552(R) (ANL-6925, pp 187-233)
reactivity worth calculation of, 20: 6279(R) (AI-65-225)
sintering in air and argon, effects of sintering temperature on density of, 20: 5839(R) (RISO-110)
welding of aluminum alloy 1100 to parameters for electron-beam, 20: 5867

ALUMINUM ALLOYS
analysis for yttrium, arsenate method for iodometric, 20: 5506
coating type 6061, with nickel, 20: 5866
corrosion by water at low temperatures of type 1100, methods of inhibiting, 20: 5846
radiation effects on corrosion of type 1100, by Santowax OM at 500 to 700°F, fast-neutron, 20: 5846
radiation effects on properties of type 6061, fast- and thermal-neutron, 20: 5846
welding of aluminum to type 1100, parameters for electron-beam, 20: 5867
welding parameters for type 6061, electron-beam, 20: 5867
Al–Cu, radiation effects on electric conductivity of, state I and II recovery from electron, 20: 5918
Al–Cu–Ni, embrittlement of hydrogenated, solute-induced, 20: 5846
Al–Fe–U, hot hardness and microstructure, effects of chromium or silicon additions on, 20: 5848
Al–Fe–U, microstructure, effects of heat treatments on, 20: 5848
Al–Fe–U, phase studies, 20: 5843
Al–Ge, radiation effects on electric conductivity of, stage I and II recovery from electron, 20: 5918
Al–Li, precipitation of helium in irradiated, effects of density and defect distribution on, 20: 5848
Al–Mg, separation of lanthanum from, by fused chloride extraction, 20: 5594(R) (ANL-6925, pp 21-106)
Al–Mo, phase studies, 20: 5846
Al–Mo–Ti–V, phase studies, 20: 5851
Al–Nb, oxidation, 20: 5896 (TID-22388)
Al–Nb, phase studies on, 20: 5896 (TID-22388)
Al–Nb–Ti, oxidation, 20: 5896 (TID-22388)
Al–Nb–Ti, phase studies on, 20: 5896 (TID-22388)
Al–Pu, criticality, 20: 6668(R) (BNWL-149, pp 5-21)
Al–Sn–Ti, performance for ionization chamber construction, 20: 5716 (AEEW-M-470)
Al–Th, properties of Th_2Al, 20: 5848
Al–Ti, oxidation, 20: 5896 (TID-22388)
Al–Ti, phase studies on, 20: 5896 (TID-22388)
Al–U, fabrication by roll bonding of, fuel plates clad with aluminum, 20: 5866
Al–U, phase studies at 600 to 1200°C of high-uranium, 20: 5848
Al–U, processing for uranium recovery by fluoride volatility, 20: 5595(R) (ANL-6925, pp 107-64)
Al–Zn, radiation effects on electric conductivity of, stage I and II recovery from electron, 20: 5918
Al–Zr, diffusion in, inter-, 20: 5851

ALUMINUM BORIDES
tensile properties of sintered, 20: 5845

ALUMINUM COMPOUNDS
analysis for yttrium, arsenate method for iodometric, 20: 5506

ALUMINUM ISOTOPES Al-26
energy levels, (E), 20: 6438

ALUMINUM ISOTOPES Al-27
bremsstrahlung resonant scattering at 1.0 to 1.3 Mev, energy level lifetimes from, (E), 20: 6380
gamma reactions with, alpha and proton yields from, (E), 20: 5732 (KFK-335)
proton inelastic scattering at 155 Mev, cross sections and energy levels from, (E), 20: 6354

ALUMINUM NITRATES
$Al(NO_3)_3$–HNO_3–$NaNO_3$, separation of americium-243 and curium-244 from, using TBP, 20: 5495 (DP-972)

ALUMINUM OXIDES
densification during vacuum hot-pressing, mechanism of, 20: 5851
effects on fluid-bed fluorination of plutonium–uranium oxides, 20: 5595(R) (ANL-6925, pp 107-64)
energy levels of, 20: 6532 (CALT-221-13)
fracture of, Petch equation for grain size effect in, 20: 5903
radiation effects on insulating properties of, 20: 6596(R) (GEST-2049)
Al_2O_3–Gd_2O_3, fabrication of control-rod elements of, 20: 5845

ALUMINUM SYSTEMS
Al–C–Cr, superconductivity of Cr_2AlC, 20: 6228
Al–CdO, stability of hot-pressed powder compacts of, at 500 and 600°C, 20: 5838(R) (RISO-110)
Al–C–Mo, superconductivity of Mo_3Al_2C, 20: 6228
Al–C–V, superconductivity of V_2AlC, 20: 6228
Al–H_2O, gamma heating in, calculations for, (E/T), 20: 6517 (CONF-651101-41)
Al–Nb–N, superconductivity of Nb_3Al_2N, 20: 6228
Al–polyethylene–U, neutron multiplication in borated, 20: 6577(R) (BNWL-149, pp 22-35)
Al–Pu–polyethylene, neutron multiplication in borated, 20: 6577(R) (BNWL-149, pp 22-35)
Al–Pu–polyethylene, neutron multiplication in borated, 20: 6578(R) (BNWL-149, pp 45-7)
Al–ThO_2, fabrication of powder-compacted slugs of, 20: 5866
Al–UO_2, fabrication of powder-compacted slugs of, 20: 5866
Al–U_3Si, properties of dispersions of, 20: 5843

AMERICIUM
separation from curium and plutonium, (E), 20: 5823(T) (ORNL-tr-892)
separation from other actinides and rare earths by electrophoresis, 20: 5598

AMERICIUM ALLOYS
Am–Pu, phase studies, 20: 5848

AMERICIUM ISOTOPES Am-241
effects on rat bones, tumorigenic, 20: 5321
neutron reactions (n,γ) with, separation of daughters from, (E), 20: 5823 (ORNL-tr-892)

AMERICIUM ISOTOPES Am-243
production at Savannah River, program for, 20: 5822 (DP-1000)
separation from aluminum nitrate–sodium nitrate–nitric acid solutions using TBP, 20: 5495 (DP-972)

AMINES
effects of tertiary, on deuterium exchange between isobutyraldehyde and water, 20: 5565

AMINO ACIDS
radiation effects on content of free, in stored beef muscle, γ, 20: 5278

AMMONIA
effects on radiolysis of heavy water in boiling reactors, 20: 6638
D–H–NH_3, bithermal isotopic exchange in, 20: 5827(P)

AMMONIUM CARBONATES
$(NH_4)_2CO_3$–1-butanol–dioxane, use in paper chromatography of compounds labeled with iodine-125 and iodine-131, 20: 5515
$(NH_4)_2CO_3$–1-butanol–ethanol, use in paper chromatography of compounds labeled with iodine-125 and iodine-131, 20: 5515

AMMONIUM COMPOUNDS, QUATERNARY
analysis for nitric acid and uranium by potentiometric titration, 20: 5518

AMMONIUM FLUORIDES
reactions with hafnium fluorides in aqueous solution, 20: 5535

AMMONIUM OXALATES
analytical uses for potentiometric determination of rare earths, 20: 5519

AMMONIUM URANYL OXALATES
peroxy-, spectra of, infrared, 20: 5546
peroxy-, stability of, potentiometric and spectrometric studies of, 20: 5549

AMOEBA
radiation effects on *Entamoeba histolytica* in water supplies and sewage, 20: 5366

AMPLIFIERS
design, 20: 5780
design and performance of, (E), 20: 5680 (ELI-91)
design of high-resolution transistorized pre-, (E), 20: 5772
design of low-noise bootstrapped-cascade 20-dB, (E), 20: 5697
design of pre-, for boron-trifluoride proportional detectors, (E), 20: 5680 (ELI-91)
pulse shaping in charge-sensitive, 20: 5707

ANEMIA
radioinduced, Thorotrast, 20: 5353

ANILINE
effects on activity of leukocyte alkaline phosphatase, toxicity, 20: 5269

ANIMAL CARE
of dog experimental colonies, 20: 5231(R) (COO-119-232, pp 65-7)

ANIMAL CELLS
growth of tumorous, in tissue culture, 20: 5296(R) (NP-15585)

molecular structure, 20: 6551
radiation effects on virulence of *Herpes simplex* viruses in HeLa, 20: 5363
radiation effects on tumorous, cytological, 20: 5477
radiation effects on mouse leukemic, x, 20: 5368
radiation injuries in cultured, protective effects of cysteine and MEA on, 20: 5418
radiation injuries in cultured, protective effects of aminoethylisothiuronium, 20: 5419
radiosensitivity of isolated rat thymocytes, effects of freezing on, 20: 5414
radiosensitivity of neoplastic, 20: 5477
radiosensitivity of fibrosarcoma, in mice, 20: 5362
radiosensitivity of hedgehog intestinal, effects of hibernation on x, 20: 5377

ANIMAL RESPIRATION
effects of nicotinamide on, in thymocytes, 20: 5340
of hypobaric oxygen, design of exposure chamber for mice, 20: 5228(R) (AD-623599, pp 28-36)
radiation effects on, in rat thymocytes in culture, 20: 5340
radiation effects on, in kidney sections, x, 20: 5352

ANIMALS
ecology of aquatic, research programs of AEC, 1965, 20: 5245 (TID-13358(2nd Rev.), pp 89-126)
ecology of terrestrial, research programs of AEC, 1965, 20: 5244 (TID-13358(2nd Rev.), pp 3-88)
effects of inhaled urania dust on, 20: 5251(R) (UR-668, pp 123-49)
effects of microwaves on, 20: 5302(R) (UR-668, pp 161-6)
metabolism of mercury-203-labeled neohydrin in, 20: 5251(R) (UR-668, pp 123-49)
radiation effects on life span of, computer program for evaluation of, 20: 5300 (UCLA-12-573)
radiation injuries of, therapy of acute, x, 20: 5301(R) (UR-668, pp 1-54)

ANIONS
reactions with hydrated electrons, review on, 20: 5525 (IA-1041)

ANOXIA
radiosensitivity effects on insects, x, 20: 5385
radiosensitivity effects in Drosophila, x, 20: 5338

ANTIBARYONS
production of, SU(6) analysis of, 20: 6133

ANTIBODIES
effects of ϵ-aminocaproic acid on iodine-131-labeled, in rats, 20: 5436(R) (UR-668, pp 149-60)
effects on membrane defects in erythrocytes, 20: 5251(R) (UR-668, pp 123-49)
preparation of iodine-131-labeled, 20: 5436(R) (UR-668, pp 149-60)
preparation of tissue-specific, for tumor therapy, 20: 5436(R) (UR-668, pp 149-60)
recovery of labeled, from rats, 20: 5436(R) (UR-668, pp 149-60)
use of labeled, for detection of venous thrombi in dogs, 20: 5436(R) (UR-668, pp 149-60)

ANTIFERROMAGNETIC MATERIALS
magnetic properties of, 20: 6531 (AD-623530)

ANTIGENS
formation of, in spleen cells of heterologous radiation chimeras in culture, 20: 5397

ANTIHYPERONS
production in antiproton-proton interactions at 4 Bev/c, (E), 20: 6033 (CEA-R-2798)

ANTIMONY
analysis for iron, activation, 20: 5507
diffusion from irradiated cerium-cobalt-plutonium alloy to sodium at 550°C, 20: 5848

ANTIMONY ISOTOPES Sb-125
energy levels of, spin of, (E), 20: 6322

ANTIPROTONS
interactions with protons at 4 Bev/c, hyperon pair production in, (E), 20: 6033 (CEA-R-2798)
interactions with protons at high energies, M(12) invariance and universality for, (T), 20: 6081
interactions with protons, baryon pair production in, (T), 20: 6133
interactions with protons at 3.6 Bev/c, meson (π) production in inelastic, (E), 20: 6097

APATITES
crystal structure, 20: 5237(R) (UR-668, pp 55-109)

ARGININE
radiosensitivity effects on *Escherichia coli*, γ and uv, 20: 5348

ARGON
argon ion beam reactions with plasma of, 20: 6467(T) (ORNL-tr-870)
effects on radiolysis of ethylene, 20: 5582
electric arcs in gravitationless state in, 20: 6163
electron reactions with, ionization cross sections for, (E/T), 20: 5989
electron temperature in positive-column low-pressure discharges in, 20: 6475
helium ion elastic scattering by, molecular state crossing for perturbation induced in, (E), 20: 5996
infrared radiation of high-pressure high-current discharge in, statistical oscillations of, (E/T), 20: 6177
production of plasma of, in inductive hydrodynamic shock tubes, 20: 6478
purification for glove boxes, equipment for, 20: 5594(R) (ANL-6925, pp 21-106)
separation from nitrogen using titanium sponges, 20: 5594(R) (ANL-6925, pp 21-106)
shock-wave reflection in thermal plasma of, (T), 20: 6512

ARGON IONS
reactions of beams of, with argon plasma, (E), 20: 6467(T) (ORNL-tr-870)

ARGON ISOTOPES
content in iron meteorites, (E), 20: 5977

ARGON ISOTOPES Ar-35
beta decay of, Gamow-Teller matrix element for, (T), 20: 6393
beta decay of, shell model calculations of ft values in, (T), 20: 6393

ARGON ISOTOPES Ar-37
beta decay of, shell model calculations of ft values in, (T), 20: 6393

ARGON ISOTOPES Ar-38
energy level transitions in, intensity of E3, (E), 20: 6407

ARGON ISOTOPES Ar-40
mesons (π^-) reactions (π^-,π^-pa) at 500 to 1100 Mev, cross sections of, (E), 20: 6298(R) (PPAD-2137-566)
neutron reactions (n,α) at 13.0 to 20.2 Mev, cross sections for, (E/T), 20: 6357

ARGONNE ADVANCED RESEARCH REACTOR
development, 20: 6666(R) (ANL-7115, pp 68-77)
energy conversion system for, development of MHD, 20: 6665(R) (ANL-7105, pp 59-71)
heat transfer in, 20: 6665(R) (ANL-7105, pp 59-71)
pressure vessel stress analysis, 20: 6666(R) (ANL-7115, pp 68-77)

ARGONNE FAST REACTOR EXPERIMENT TEST
core design for, reference, 20: 6601(R) (ANL-7115, pp 1-41)
development, 20: 6600(R) (ANL-7105, pp 1-35)
experimental facilities for, development of, 20: 6600(R) (ANL-7105, pp 1-35)
safety analysis of reference core, 20: 6601(R) (ANL-7115, pp 1-41)

ARGONNE RESEARCH REACTOR
fuel element burnup in, ceramic and metallic, 20: 6558(R) (ANL-7115, pp 42-67)

ARMY REACTORS (SL-1)
accident at, pressure of water-hammer produced in, 20: 6552(R) (ANL-6925, pp 187-233)

ARMY REACTORS (SM-1)
criticality studies, core III, (E/T), 20: 6608 (HIT-3459-7)
hazards summary for 1A core III, 20: 6609 (HIT-3534-1)

ASCORBIC ACID
effects on photosynthetic reactions in irradiated chloroplasts, x, 20: 5402

ASTRONOMY
review of x-ray, 20: 5968 (NP-15626)

ASTROPHYSICS
cosmic-ray experiments for studies in, 20: 6012 (CONF-640919, pp III1-23)

ATMOSPHERE
carbon-14 content in, secular variations of cosmic-ray produced, (T), 20: 6205
densities and particle concentrations at 120 to 360 km, 20: 6210
light emission in, spectra of x-ray induced, (E), 20: 6181 (AD-619288)
light propagation in terrestrial, scintillation of, 20: 6186(T) (UCRL-Trans-1269(L))
monitoring for total beta and gamma activity in, New Zealand, April-June 1965, 20: 5664(R) (NP-15639)
Montgomery stream function of, 20: 5645(R) (COO-1340-2, pp 122-45)
neutron absorbed dose in, near ground-air interface, (T), 20: 6528
nitrogen-13 and oxygen-15 monitoring in, from electron linacs, 20: 5774
radiation absorption in upper, solar L_α, (E), 20: 6211
radiation emission to interplanetary space, (E), 20: 6019
radioactivity of, in Kansas and Missouri, 1962, 20: 5648(R) (COO-1340-2, pp 1-53)
radioactivity of, natural, bibliography on, 20: 5668 (WASH-1061)
radon content at ground level in, effects of meteorological conditions on, 20: 5646
thermodynamics of, computer analysis of, 20: 5645(R) (COO-1340-2, pp 122-45)

ATMOSPHERE EXPOSURE CHAMBERS
design and performance of, for hypobaric oxygen exposure of mice, 20: 5228(R) (AD-623599, pp 28-36)
design and testing of inert gas, 20: 5594(R) (ANL-6925, pp 21-106)

ATMOSPHERES
container for inert, for fused salt studies, 20: 5529(R) (SC-DC-65-1706)
ATOMIC BEAMS
production of hydrogen, ion source for, 20: 6000
ATOMIC ENERGY COMMISSION
research programs on freshwater ecology, 1965, 20: 5245 (TID-13358 (2nd Rev.), pp 89-126)
research programs on terrestrial ecology, 1965, 20: 5244 (TID-13358 (2nd Rev.), pp 3-88)
ATOMIC ENERGY, LEGAL ASPECTS
radiation injuries, 20: 5241
ATOMS
book: *The Molecular Designing of Materials and Devices*, 20: 6551
electron scattering on, Mott polarization effect in fast, 20: 5992
energy levels of, tabulations of, 20: 5984 (NYO-2543-1)
energy-level shifts in hydrogen, from vacuum polarization, (T), 20: 5995
interactions with electrons, conference on, 20: 5988(T) (JPRS-32421)
ionization cross sections for, computer program for calculating, 20: 5986 (UCRL-14402-T)
quantum noise operators for one electron n-level, subjected to fluctuating forces or heatbath, 20: 6002
AUDITORY ORGANS
radiosensitivity of, in goats, γ, 20: 5369
radiotherapy of ear cancer, 20: 5474
radiotherapy of tumors in, techniques for, 20: 5448
AURORAL STORMS
occurrence of, integral-invariant coordinate system for spatial, 20: 6189
AUSTRALIA
calcium and strontium-90 uptake by population in, 1962, 20: 5263

B

BACTERIA
genetic recombination in Pneumococcus, 20: 5229 (BNL-9407)
identification of radioresistant populations of, from fresh Gulf shrimp, 20: 5346
infections induced by staphylococci, in rabbit skin, 20: 5315
radiation effects on optimum growth temperature of radioresistant, γ, 20: 5346
radiation effects on *Micrococcus radiodurans*, uv, 20: 5266
radiosensitivity of, from shrimp, γ, 20: 5346
BACTERIOPHAGES
induced in *E. coli* by uv irradiated culture media, 20: 5279
metabolism of nucleic acids by, 20: 5250(R) (UR-668, pp 110-16)
radiation effects on bacterial reactions to, target theory for γ and x, 20: 5299(R) (TID-22187)
radioinduced cross-linking and denaturation of double-strand desoxyribonucleic acid from, uv, 20: 5268
BARBITURIC ACIDS
metabolism in rats of, effects of mercaptoethylamine and magnesium on, 20: 5283(R) (AD-623599, pp 16-27)
BARIUM
diffusion in spherical uranium dicarbide particles, coefficient for, 20: 5848
separation from other fission products by precipitation as sulfate, 20: 5603
BARIUM ISOTOPES Ba-133
decay of, gamma transitions from, 20: 6436
BARIUM ISOTOPES Ba-134
energy levels of, from cesium-134 decay, (E), 20: 6327
BARIUM SULFATES
sorptive properties of calcium-activated, for radiostrontium, 20: 5531 (UJV-1382/65)
BARLEY
radiation effects on seed of, effects of dimethyl sulfoxide and nitric oxide on oxygen effect in 20: 5298(R) (RLO-353-4)
uptake of radioisotopes by roots of, mechanisms for, 20: 5258
uptake of strontium-89 from soil by, 20: 5257
BARRIERS
radiation attenuation by vertical, (E/T), 20: 6516 (AD-617524)
BARYONS
decay in broken SU(6) symmetry, S-wave amplitudes in hadronic, 20: 6152
detection of basic triplets in cosmic radiation, experiment for, 20: 6010 (CONF-640919, pp II23-7)
electromagnetic structure in broken SU(6), 20: 6107 (JINR-P-2401)
interactions with mesons, Muskhelishvili method for amplitude of $V-\theta$, 20: 6123
interactions with mesons, non-compact group representation of, 20: 6102 (IC/65/79)
production of, SU(6) analysis of, 20: 6133
symmetry for, subgroup of SU(8), (T), 20: 6110
symmetry of, representation mixing in broken $(SU_3)_L \oplus (SU_3)_R$, (T), 20: 6070
BARYONS, RESONANCE
decays and identification of Ξ (1820), in unitary multiplet model, 20: 6091
mass difference of N^{*-} and N^{*++}, (E/T), 20: 6042 (UCRL-16189)
photoproduction of N^* (1238) on protons at 0.3 to 5.5 Bev, (E/T), 20: 6037 (DESY-65/11)
production in neutrino-nucleon interactions, (T), 20: 6065
production of hyperon (Ξ^-)-neutron, in deuteron-meson (K^-) interactions, (T), 20: 6073
production of Y_0^* (1405) by meson (K^-) capture at rest in emulsions, (E), 20: 6051
properties of, evidence for quarks from, 20: 6135
proton in meson (π^-)-proton interactions at 3.3 and 3.9 Bev/c, (E/T), 20: 6041 (UCRL-11942)
BEANS
irradiated lipids from, effects on wheat development and growth of, 20: 5265(T)
radiation effects with recurrent intercrossing on genetic variability in, neutrons, 20: 5406
radiation effects on growth of seedlings of, γ, 20: 5388
radiation effects on free lipid content in leaves of, x, 20: 5265(T)
BEARINGS
testing for EBR-II fuel cycle facility, 20: 5594(R) (ANL-6925, pp 21-106)
BEHAVIOR
radiation effects on chemotactic, in Euglena and leukocytes, 20: 5396
radiation effects on adaptive responses of rats, x, 20: 5319
radiation effects on conditioned behavior in burros, γ, 20: 5329
radiation effects on conditioned reflex in goats, γ, 20: 5369
BENZENE
effects on activity of leukocyte alkaline phosphatase, toxicity, 20: 5269
effects on induction of leukopenia in rabbits, 20: 5315
electron reaction with, cross sections for momentum transfer and drift velocities in, 20: 5985 (ORNL-TM-1262)
electron reactions with, ionization cross sections for, (E/T), 20: 5989
electron reactions in ethylene mixture, cross sections for momentum transfer and drift velocities in, 20: 5985 (ORNL-TM-1262)
neutron scattering by, cross sections for slow, 20: 6272
yields in pyrolysis of diphenyl at 375 to 1375°K, 20: 5563 (EUR-2482.f)
benzene–H_2O, radiation effects on coalescence rates in liquid, 20: 5571 (ORNL-TM-1283)
benzene–ethanol–H_2O, use in paper chromatography of compounds labeled with iodine-125 and iodine-131, 20: 5515
BENZENE, BROMO-
electron reactions in ethylene mixture, cross sections for momentum transfer and drift velocities in, 20: 5985 (ORNL-TM-1262)
BENZENE, CHLORO-
electron reactions in ethylene mixture, cross sections for momentum transfer and drift velocities in, 20: 5985 (ORNL-TM-1262)
BENZENE, DICHLORO-
electron reactions in ethylene mixture, cross sections for momentum transfer and drift velocities in, 20: 5985 (ORNL-TM-1262)
BENZOIC ACID, p-AMINO-
radiation chemistry of solutions of, 20: 5296(R) (NP-15585)
BENZOPHENANTHRENES
effects on rats, carcinogenic, 20: 5334
BERKELIUM ISOTOPES Bk-248
energy levels of, distortions in, (E/T), 20: 6305 (UCRL-11784)
BERKELIUM ISOTOPES Bk-250
energy levels of, distortions in, (E/T), 20: 6305 (UCRL-11784)
BERYLLIUM
aging of, method for, 20: 5900
analysis for impurities, methods for, 20: 5849
bibliography on, 20: 5840 (SB-413(Suppl.1))
casting techniques, 20: 5844
coating with nickel, electroless, 20: 5867
corrosion by water, 20: 6666(R) (ANL-7115, pp 68-77)
corrosion by water at 100 and 120°C, 20: 5844
deformation properties of single-crystal, effects of iron and silicon additions on, 20: 5844
deposition of electroless nickel coatings on, 20: 5849
diffusion in molybdenum, 20: 5846
ductility of, techniques for increasing, 20: 5849
electron reactions at 2.5 to 4.0 Mev, bremsstrahlung spectra from, (E), 20: 6432
fabrication by vacuum hot pressing, 20: 5849
handling of, bibliography on, 20: 5840 (SB-413(Suppl.1))
machining of, surface damage due to, 20: 5849
mechanical properties of, effects of purification on, 20: 5849
oxidation by air at 500 to 900°C, 20: 5844
plasticity at 400 to 600°C, method for increasing, 20: 5900
proton reactions at 0.54 to 1.47 Bev, neutron yields from, (E), 20: 5928(R) (PR-P-66)
radiation effects on density and tensile properties of, fast neutron,

20: 5849
reactions with air, carbon monoxide, nitrogen, and oxygen at 1000 to 1500°C, 20: 5844
tensile properties at −195 to 200°C of extruded, 20: 5844
x-ray Raman effect in, search for, (E), 20: 6539
BERYLLIUM ALLOYS
bibliography on, 20: 5840 (SB-413(Suppl.1))
Be–Cu, welding parameters, electron-beam, 20: 5867
Be–Nb, oxidation resistance of, effects of aluminum, nickel, silicon, and tantalum additions on, 20: 5844
Be–Th, properties of $ThBe_{13}$, 20: 5848
Be–U, hardness of splat-cooled, effects of heat treatments on, 20: 5866
Be–W, phase studies at 1000 to 2100°C, 20: 5906
Be–Zr, corrosion by borated water at 600°F, 20: 5846
Be–Zr, oxidation resistance of, effects of aluminum, nickel, silicon, and tantalum additions on, 20: 5844
BERYLLIUM COMPOUNDS
bibliography on, 20: 5840 (SB-413(Suppl.1))
BERYLLIUM ISOTOPES
bibliography on, 20: 5840 (SB-413(Suppl.1))
BERYLLIUM ISOTOPES Be-8
energy levels from beryllium-9(He-3,α) reactions at 3.0 Mev, spin and parities of, (E), 20: 6389
BERYLLIUM ISOTOPES Be-9
deuteron reactions (d,α) at 11.8 and 12.0 Mev, (E), 20: 6369
deuteron reactions (d,α) at 11 Mev, alpha spectra from, (E), 20: 6360
energy levels, (E), 20: 6320
gamma reactions (γ,n) at 3 to 17 Mev, energy levels from, (E), 20: 6390
helium-3 reactions (He-3,α) at 3 Mev, beryllium-8 level spins and parities from, (E), 20: 6389
neutron reactions (n,2n) at 14 Mev, excitation and decay mechanisms of, (E), 20: 6320
BERYLLIUM OXIDE REACTOR EXPERIMENT
development and operation, July–Sept. 1964, 20: 6604(R) (GA-5842)
development, Jan.–Mar. 1963, 20: 6603(R) (GA-4165)
BERYLLIUM OXIDES
corrosive effects on rhenium to 3000°K, 20: 5554
diffusion in, effects of density on self-, 20: 5844
fracture of, Petch equation for grain size effect in, 20: 5903
plastic flow and fracture mechanisms of hot-pressed, at −196 to 1800°C, 20: 5902
properties for skull reclamation process crucibles, 20: 5594(R) (ANL-6925, pp 21-106)
radioinduced swelling of, equation for, 20: 5844
reactions with chloride flux products of fissium–plutonium–uranium slagging, 20: 5594(R) (ANL-6925, pp 21-106)
stabilization of high-temperature beta-phase, 20: 5849
thermodynamic properties of, at 2273 to 2863°K, 20: 5554
BeO–UO_2, creep at 1375 to 1540°C, effects of grain size and stress on, 20: 5904
BETA DECAY
energy level excitation of spherical nuclei in, collective, (T), 20: 6353
BETA PARTICLES
content in atmosphere and on ground in New Zealand, 1965, 20: 5664(R) (NP-15639)
detection and measurement in man of, whole-body, 20: 5426
detection and measurement of, scintillation sandwich counting method for, 20: 5783
detection and measurement of, scintillation counter for, 20: 5798(P)
detection and measurement of soft, evaluation of instruments for, 20: 5754
detection and measurement of, effects of cosmic radiation on performance of G-M tube in, 20: 5781
detection and measurement by scintillation counting, effects of sample volume on efficiency of, 20: 5510
detection of, performance of end window counters for, 20: 5791
detection of, surface barrier detectors for, 20: 5790
effects in rats, carcinogenic, 20: 5296(R) (NP-15585)
effects of, from therapeutic doses of iodine-131, pathological, 20: 5469
effects on catalytic activation of hydrogen–deuterium exchange in Vycor reactor vessels, 20: 5578
effects on *Escherichia coli* of, from incorporated tritium, mutagenic, 20: 5350
effects on growth of corn seedlings of, in contaminated soil, 20: 5305
effects on hematopoietic system of dogs of, from deposited strontium-90, 20: 5290(R) (COO-119-232, pp 165-89)
effects on intractable angina pectoris, therapeutic, 20: 5460
effects on mechanical strength of bone of, from deposited radioisotopes, 20: 5289(R) (COO-119-232, pp 88-98)
effects on metabolism of electrolytes and nitrogen in dogs of, from injected sodium-24, 20: 5381
effects on polycythemia, therapeutic, 20: 5483
effects on rats, carcinogenic, 20: 5334
effects on reproduction of Drosophila, 20: 5296(R) (NP-15585)
effects on Saccharomyces radiosensitivity, mutagenic, 20: 5360
effects on white blood cells during manned space flight, 20: 5297 (ORNL-P-1734)
polarization correlation with gamma radiation in scandium-46 decay, (E), 20: 6391
reactions with sodium nitrate crystals, Cherenkov radiation detection in, 20: 5792
use for pituitary ablation, for treatment of diabetic retinopathy, 20: 5468
BETA SOURCES
use for therapy of hemangiomas in children, 20: 5443
BETA SPECTROMETERS
data from low-resolution, computer analysis of, (T), 20: 5768
description of, at installations in India, 20: 5715 (AEET-227)
BETA SPECTROSCOPY
computer analysis of low-resolution beta and conversion-electron spectra, (T), 20: 5768
errors in solid-angle, reduction of, 20: 5729 (INR-617/XIX/D)
BETATRONS
beam injector for, recording of electron current pulses from, 20: 5958
cavity resonator for 300-Mev, fabrication of synchrotron, 20: 5942 (NP-15615)
magnet coils for air-core, design of, 20: 5961
BIBLIOGRAPHIES
on beryllium, 20: 5840 (SB-413(Suppl.1))
on burns and trauma, 20: 5415
on characteristics of molten-salt-fueled homogeneous reactors, 20: 6554 (ANL-7092)
on chemistry of recoil carbon-11 atoms, 20: 5570 (JUL-228-RC)
on ecology of aquatic animals and plants, 20: 5245 (TID-13358(2nd Rev.), pp 89-126)
on ecology of terrestrial animals and plants, 20: 5244 (TID-13358 (2nd Rev.), pp 3-88)
on fabrication and properties of molybdenum, niobium, tantalum, tungsten, and their alloys, 20: 5874 (AGARDograph-94)
on gold-198, 20: 5811 (PAEC(A)IN-653)
on hematopoietic tissue transplantation, 20: 5424
on high-temperature chemistry and physics of materials in condensed state, 20: 5527 (NP-15646)
on living organisms and tissues, 20: 5284 (AED-C-04-21)
on mathematical axioms for quantum mechanics, (T), 20: 6213 (ANL-7065)
on natural environmental radioactivity, 20: 5668 (WASH-1061)
on neutron activation analysis, 20: 5499 (NP-15637)
on neutron spectroscopy below 10 ev, (E), 20: 6260 (CONF-651101-43)
on noise in nuclear-reactor systems, 20: 6561 (FTI-2)
on plasma jet technology, 20: 5633 (NASA-SP-5033)
on radioisotopes in pharmacy, 20: 5812 (PAEC(A)IN-654)
on reactions of hydrated electrons, 20: 5525 (IA-1041)
on reactor materials papers presented at Third Conference on Atomic Energy at Geneva, 20: 5842
on reactor safety, 20: 6563 (TID-3525(Rev.5)(Suppl.2))
on techniques to augment convective heat transfer, 20: 5618 (AD-619511)
on thermophysical properties of potassium, 20: 5886 (NASA-TN-D-3120)
on tungsten powder metallurgy, 20: 5836 (NASA-SP-5035)
BINDING ENERGY
data tabulation for nuclei $22 \leq Z \leq 120$, 20: 6290 (LA-3280)
BIOLOGICAL MATERIALS
radioactivity of, natural, bibliography on, 20: 5668 (WASH-1061)
radiosensitivity of, effects of water content, 20: 5270
BIOLOGICAL MODELS
of calcium metabolism in man, using computer calculations, 20: 5260
BIOSYNTHESIS
of selenium-75-labeled blood proteins, 20: 5262
BIPHENYL
neutron scattering by, cross sections for slow, 20: 6272
pyrolysis of deuterated and normal, mass spectrometric study of, 20: 5563 (EUR-2482.f)
BISMUTH
corrosive effects on iron and steel at 850 to 1000°C, 20: 6024(R) (ANL-6925(p.235-47))
gamma elastic scattering in giant resonance region, cross sections for, (E), 20: 6349
separation from lead by solvent extraction using dithizone, 20: 5505
BISMUTH ALLOYS
Bi–Li, spectra in lithium halides, absorption, 20: 6024(R) (ANL-6925 (p.235-47))
Bi–Na, solubility of intermetallic compound in, in fused halide salts, 20: 6024(R) (ANL-6925(p.235-47))
Bi–Pb, gamma attenuation coefficient in shielding of, (E), 20: 6523
BISMUTH ISOTOPES Bi-209
proton reactions at 60 to 155 Mev, charged-particle and neutron emission

in, (T), 20: 6364
BISMUTH ISOTOPES Bi-210
alpha decay widths and nuclear structure, (T), 20: 6423
BLADDER
radiotherapy of cancer in, advantages of mega- and supervoltage for, 20: 5451
radiotherapy of cancers of, 20: 5454
BLOOD
analysis for lead-210, radiochemical, 20: 5505
exchange reactions with bone, mechanisms of, 20: 5237(R) (UR-668, pp 55-109)
incorporation of selenium-75 into proteins of, 20: 5262
radiation effects on riboflavin content in dog, x, 20: 5384
radiation effects on, chemical, 20: 5308
specific activity of, in radiocalcium-injected dog, 20: 5237(R) (UR-668, pp 55-109)
BLOOD CELLS
radiation damage in, effects of membranes on, 20: 5251(R) (UR-668, pp 123-49)
radiation effects on human, 20: 5301(R) (UR-668, pp 1-54)
BLOOD COAGULATION
effects of fibrin and fibrinase on, tracer study, 20: 5262
radiation effects on, 20: 5308
radiation effects on, in rabbits, x, 20: 5325
radiation effects on, x, 20: 5365
tracer study of venous, use of labeled antibodies for, 20: 5436(R) (UR-668, pp 149-60)
BLOOD PICTURE
radiation effects on, in rabbits, x, 20: 5325
radiation effects on rabbit, fractionated doses of x, 20: 5364
radiation effects on, from deposited strontium-90 in dogs, B, 20: 5290(R) (COO-119-232, pp 165-89)
BLOOD PLASMA
radiation effects on, x, 20: 5365
BLOOD PLATELETS
counting precursor megakaryocytes of, membrane filter methods for, 20: 5301(R) (UR-668, pp 1-54)
dissociation of ribosomes of, 20: 5264
radiation effects on, effects of suspension media on x, 20: 5365
BLOOD PRESSURE
effects of alpha-methyldopa and hydrochlorothiazide on, 20: 5237(R) (UR-668, pp 55-109)
radiation effects on rat, x, 20: 5301(R) (UR-668, pp 1-54)
BLOOD SERUM
from irradiated rabbits, therapeutic effects for radioinduced diarrhea in rats, 20: 5411
metabolism of proteins in, tracer study in dogs, 20: 5249(R) (COO-119-232, pp 203-18)
radiation effects on protein fractions in, proton, 20: 5378
BLOOD VOLUME
determination using tanned erythrocytes, 20: 5301(R) (UR-668, pp 1-54)
BOILERS
design of, computer program for, 20: 5606 (GAMD-6675)
design of, computer program for, 20: 5607 (GAMD-6675(Suppl.))
BOILING
heat transfer and sound intensity correlation in, 20: 5628
BOILING REACTORS
accidents in, analysis of coolant-loss, (T), 20: 6560(R) (BMI-X-10145)
component and instrumentation development for, 20: 6648(R) (HPR-64)
dynamics of heavy-water, research on, 20: 6637
fuel elements of, thermal testing of finned vapotron, 20: 6595(R) (EURAEC-1421)
BONE FRACTURES
radioinduced, by injected thorium-228 in dogs, 20: 5288(R) (COO-119-232, pp 74-87)
BONE MARROW
erythropoietic activity of transplants of, in mouse spleen, 20: 5242
megakaryocyte counts in normal dog, 20: 5301(R) (UR-668, pp 1-54)
radiation effects on rat, β, 20: 5296(R) (NP-15585)
radiation effects on mouse, x, 20: 5320
radiation effects on mouse immunity to transplants of, methods for assaying x, 20: 5372
BONE TUMORS
chemically induced in rats, 20: 5334
radioinduced in rats, 20: 5334
BONES
analysis for thorium, methods for, 20: 5237(R) (UR-668, pp 55-109)
analysis of ash of, for lead-210, radiochemical, 20: 5504
analysis of ash of, for lead-210, radiochemical, 20: 5505
calcification of, effects of calcium-phosphorus ratio on, 20: 5237(R) (UR-668, pp 55-109)
effects of cortisol on growth and atrophy of compact and spongy, in rabbits, 20: 5234(R) (COO-119-232, pp 122-52)
exchange reactions with blood, mechanisms of, 20: 5237(R) (UR-668, pp 55-109)
osteoid content of vertebral, effects of age in dogs and man, 20: 5233(R) (COO-119-232, pp 99-121)
proton attenuation by skull, 20: 5475
radiation effects on mineral metabolism in rat, effects of denervation on x, 20: 5370
radiation effects on mechanical strength of, from deposited radioisotopes, 20: 5289(R) (COO-119-232, pp 88-98)
radioisotope tumors in rat, americium-241 and plutonium-239, 20: 5321
strontium-89 uptake by, effects of sodium alginates on, 20: 5253
strontium-90 uptake by human, effects of dietary calcium on, 20: 5263
BORIC ACID
corrosive effects on selected alloys at 600°F, 20: 5846
performance as neutron absorber, for control of Saxton Power Reactor, 20: 6629 (WCAP-3269-24)
BORON
effects on activation determination of oxygen, 20: 5498 (NP-15636)
effects on ductility of molybdenum, 20: 5851
molecular structure of, orbital density in, 20: 5524 (ANL-7076)
BORON CARBIDES
thermal conductivity at 500 and 1000°F of powdered, 20: 5850
B_4C–Cu, fabrication as shutdown control rods, 20: 5850
B_4C–graphite, radiation effects on properties of, in-reactor, 20: 5845
BORON FLUORIDES
use as catalyst in preparation of radioactive hydrocarbons, 20: 5593(P)
BORON ISOTOPES B-8
meson (π^-) capture by, yields and energy spectra from, (E/T), 20: 6292 (NP-15601)
BORON ISOTOPES B-10
deuteron reactions (d,p) at 5.1 and 6.07 Mev, differential cross section for, (E), 20: 5759
energy levels from carbon-12 (d,α) reactions at 11 Mev, (E), 20: 6360
BORON ISOTOPES B-11
deuteron reactions (d,α) and (d,p) at 0.2 to 1 Mev, analysis of, (T), 20: 6281 (CEA-R-2807)
BORON NITRIDES
x-ray Raman effect in, search for, (E), 20: 6539
BN–$MoSi_2$–ZrB_2, mechanical properties of composites of, 20: 5845
BORON SYSTEMS
B–C, phase studies, 20: 5851
BOSONS
detection of basic triplets in cosmic radiation, experiment for, 20: 6010 (CONF-640919, pp II23-7)
detection of intermediate W, using corona-spike G-M counters and Cherenkov detectors, 20: 5723 (CONF-640919, pp 155-65)
interactions in system of, ground-state energy for repulsive, (T), 20: 6137
interactions of spin-zero, threshold Regge poles in coupled-channel, 20: 6118
interactions with fermions, model field theory for amplitudes of, 20: 6116
production of intermediate vector, (T), 20: 6036 (CERN-64-13(Vol.4), pp 51-95)
BRAIN
scanning techniques for posterior fossa of, angled detector probe for, 20: 5462
uptake of technetium-99-labeled albumins and colloids by, for visualization by external scanning, 20: 5456
BRAZIL (BAIA)
uranium reconnaissance in, 20: 5659 (RME-4545(Rev.))
BREASTS
radiotherapy of tumors of, leukemia incidence after, 20: 5471
BREEDER REACTORS
economics for uranium conservation, 20: 6611 (HW-SA-3669)
fuel burnup experiment for fast, design of molten plutonium, 20: 6613 (LA-DC-7475)
BREMSSTRAHLUNG
angular distributions from proton-proton interactions at 158 Mev, (E), 20: 6046
detection and measurement at 0.2 to 50 Mev, using quantometers, 20: 5765
detection and measurement at 5 to 35 Mev, using quantometers, 20: 5766
production in plasma by uniformly rotating line charge, 20: 6456 (AD-619888)
reactions (γ,p) with magnesium-24, spectra from, (E), 20: 6399
reactions with nuclear Coulomb field, radiative corrections to pair production in, (T), 20: 6072
reactions with uranium-238 at 10 to 15 Mev, delayed neutron yields from fission, (E), 20: 6315
scattering by aluminum-27, chlorine-35, and phosphorus-31 at 1.0 to 3.0 Mev, energy level lifetimes from resonant, (E), 20: 6380
spectra from electron reactions with nuclei, Z dependence on, (E), 20: 6432

BROMINE ISOTOPES Br-79
effects on infrared spectra of hydrobromic acid, 20: 5550
BROMINE ISOTOPES Br-81
effects on infrared spectra of hydrobromic acid, 20: 5550
BROOKHAVEN ALTERNATING-GRADIENT SYNCHROTRON
beam deflectors for, design using iris-loaded waveguides, 20: 5960
beam extraction in, multiturn, (T), 20: 5931 (BNL-9352)
modification for high intensity, reasons for, 20: 5932 (BNL-9662)
BROOKHAVEN MEDICAL REACTOR
cooling system for, well water recycling, 20: 6667 (BNL-9686)
BUBBLE CHAMBERS
data analysis for, computer program for, 20: 6099
BUILDING MATERIALS
moisture content of, neutron gage for determining, 20: 5819
BUOYS
kinetics of submerged, in sea, 20: 6686(R) (NVO-98-12)
BURROS
radiation effects on cortical arousal in, γ, 20: 5329
BUTANE
electron reaction with, cross sections for momentum transfer and drift velocities in, 20: 5985 (ORNL-TM-1262)
electron reactions with, ionization cross sections for, (E/T), 20: 5989
reactions with recoil carbon-11 atoms, mechanism and products of, 20: 5570 (JUL-228-RC)
BUTANE, 1-CHLORO-
reactions with electrons in organic glasses, yields of free radicals from, 20: 5577
BUTANE, 2-CHLORO-
reactions with electrons in organic glasses, yields of free radicals from, 20: 5577
BUTANE, 2-METHYL-
radiolysis of, tracer studies of radical yields in, 20: 5576
1-BUTANOL
$(NH_4)_2CO_3$–1-butanol–dioxane, use in paper chromatography of compounds labeled with iodine-125 and iodine-131, 20: 5515
$(NH_4)_2CO_3$–1-butanol–ethanol, use in paper chromatography of compounds labeled with iodine-125 and iodine-131, 20: 5515
BUTENYNE
yields in pyrolysis of diphenyl at 375 to 1375°K, 20: 5563 (EUR-2482.f)
BUTYL PHOSPHATES
effects on determination of uranium as thiocyanate, 20: 5516
solvent properties for americium-243 and curium-244, 20: 5495 (DP-972)
BUTYRIC ACID
uptake of, by rabbit eye lens in culture, 20: 5256

C

CADMIUM
effects on hydrochloric acid cleavage of organotin compounds in methanol–water, 20: 6687(R) (NYO-3453-1)
CADMIUM ALLOYS
Cd–In–Ag, corrosion by borated water at 600°F, 20: 5846
Cd–In–Ag, properties as control rod material, effects of palladium, platinum, and tin additions on, 20: 5850
Cd–Mg, separation of uranium from, by fused chloride extraction, 20: 5594(R) (ANL-6925, pp 21-106)
Cd–Mg, solvent properties for uranium, 20: 5594(R) (ANL-6925, pp 21-106)
Cd–Mg–Pu–Zn, stability in mild steel and stainless steel containers at 600°C, 20: 5594(R) (ANL-6925, pp 21-106)
Cd–Mg–U–Zn, corrosive effects with chloride flux on carbon steel, Croloy, and stainless steel at 600 to 650°C, 20: 5594(R) (ANL-6925, pp 21-106)
Cd–Mg–U–Zn, phase studies, 20: 5594(R) (ANL-6925, pp 21-106)
Cd–Nd, thermodynamic properties of liquid, 20: 5594(R) (ANL-6925, pp 21-106)
Cd–rare earth, eutectic temperatures of, 20: 5594(R) (ANL-6925, pp 21-106)
CADMIUM IONS
effects on photolysis and radiolysis of silver oxalate, 20: 5583
CADMIUM ISOTOPES Cd-114
nuclear quadrupole moments of first excited 2+ state, (T), 20: 6415
CADMIUM ISOTOPES Cd-115
decay of, gamma transitions from, 20: 6436
CADMIUM OXIDES
Al–CdO, stability of hot-pressed powder compacts of, at 500 and 600°C, 20: 5838(R) (RISO-110)
CADMIUM SYSTEMS
Cd–C–Ti, superconductivity of Ti_2CdC, 20: 6228
CALCIFICATION
effects of fluoride and magnesium on *in vitro*, 20: 5237(R) (UR-668, pp 55-109)
CALCIUM
determination in soft tissue, methods for, 20: 5237(R) (UR-668, pp 55-109)
metabolism in chickens, effects of vitamin D on, 20: 5237(R) (UR-668, pp 55-109)
metabolism in man, computer model for calculation of, 20: 5260
neutron reactions at 3.5 to 5.0 Mev, gamma production in, (E), 20: 6408
radiation effects on content in dog blood, β and γ, 20: 5381
uptake by Austrian population, 1962, 20: 5263
uptake by human bones, effects on strontium-90 uptake of, 20: 5263
CALCIUM CARBONATES
effects on uptake of strontium-89 from contaminated soil, by barley, 20: 5257
CALCIUM FLUORIDES
radioinduced luminescence in gadolinium-ion doped, preferential emission in afterglow of x, (E), 20: 6550
CALCIUM ISOTOPES Ca-37
beta decay of, half life for, (T), 20: 6393
beta decay of, shell model calculations of ft values in, (T), 20: 6393
CALCIUM ISOTOPES Ca-39
beta decay of, shell model calculations of ft values in, (T), 20: 6393
energy levels of, strongly excited, (E), 20: 6398
CALCIUM ISOTOPES Ca-40
electron inelastic scattering by, two-nucleon correlation functions and cross sections for, (T), 20: 6424
electron scattering at 250 Mev, charge distributions from, (E), 20: 6413
Hartree-Fock fields and single-particle energies for ground state of, (T), 20: 6363
helium-3 reactions (He-3,α) at 24.4 Mev, angular distributions from, (E), 20: 6398
neutron inelastic scattering at 3.5 to 5.0 Mev, gamma production in, (E), 20: 6408
proton inelastic scattering at 155 Mev, cross sections and energy levels from, (E), 20: 6354
transfer by dog renal tissue, 20: 5237(R) (UR-668, pp 55-109)
CALCIUM ISOTOPES Ca-42
energy levels of, shell-model study of, (T), 20: 6417
CALCIUM ISOTOPES Ca-43
energy levels of, shell-model study of, (T), 20: 6417
CALCIUM ISOTOPES Ca-44
electron scattering at 250 Mev, charge distributions from, (E), 20: 6413
energy levels of, shell-model study of, (T), 20: 6417
neutron inelastic scattering at 3.5 to 5.0 Mev, gamma production in, (E), 20: 6408
CALCIUM ISOTOPES Ca-45
energy levels of, shell-model study of, (T), 20: 6417
exchange between blood and tissues in rats, 20: 5237(R) (UR-668, pp 55-109)
metabolism in rat bones of, effects of nerve supply on, 20: 5370
radiation effects on metabolism of, in rat bones, x, 20: 5370
specific activity in blood and urine of injected, in dogs, 20: 5237(R) (UR-668, pp 55-109)
transfer by dog renal tissue, 20: 5237(R) (UR-668, pp 55-109)
CALCIUM ISOTOPES Ca-47
metabolism in man of, kinetics of, 20: 5260
CALCIUM ISOTOPES Ca-48
alpha elastic and inelastic scattering at 42 Mev, (E), 20: 6400
energy level structure, (E), 20: 6400
CALCIUM OXIDES
effects on properties of zirconia at high temperatures, 20: 5851
CALCIUM PHOSPHATES
crystal structure, 20: 5237(R) (UR-668, pp 55-109)
effects on bone calcification, 20: 5237(R) (UR-668, pp 55-109)
CALCIUM SYSTEMS
Ca–O–W, phase studies, 20: 5851
CALDER HALL REACTORS
design for economic power, 20: 6644
CALIFORNIUM
separation from molten magnesium–zinc alloys by fused chloride extraction, 20: 5594(R) (ANL-6925, pp 21-106)
CALIFORNIUM ISOTOPES Cf-252
fission of, electron spectra from, (E), 20: 6298(R) (PPAD-2137-566)
fission of, time distribution of x rays from, (E), 20: 6298(R) (PPAD-2137-566)
fission of, xenon isotopes from, (E), 20: 6298(R) (PPAD-2137-566)
neutron fission of prompt gamma rays from thermal, 20: 6314
CALORIMETERS
accuracy at ionization, for high-energy cosmic particles, 20: 5788
design of fluorine-flow, 20: 5523(R) (ANL-6925, pp 175-85)
design of 1500- and 2500°C drop, 20: 5523(R) (ANL-6925, pp 175-85)
CANADA

fallout monitoring, 1963 and 1964, 20: 5415
radiation protection program, 20: 5415
CAPROIC ACID
ε-amino-, effects on fibrinolysis of rat plasma clots, 20: 5436 (UR-668, pp 149-60)
CARBAMIC ACID, ETHYL ESTER
fabrication of manipulator gauntlets of, 20: 5612 (ORNL-TM-1326)
radiation effects on tumorogenic action of, in mouse lungs, γ, 20: 5328
CARBIDES
binding energy of Group IIIA, 20: 5540
CARBOHYDRATES
radiation effects on bacterial metabolism of, γ, 20: 5346
CARBON
alpha reactions (α,γ) at 58 Mev, spectra from, (E), 20: 6297(R) (ORNL-3858(Vol.2), pp 82-90)
determination in sodium, methods for, 20: 5594(R) (ANL-6925, pp 21-106)
diffusion in yttrium at 1235 to 1460°C in electric field, 20: 5599
diffusion of actinides in pyrolytic, 20: 5843
effects on mechanical properties of tungsten of interstitial impurities of, 20: 5846
effects on properties of uranium for use as reactor fuel core, 20: 5887 (NLCO-953)
electron reactions at 2.5 to 4.0 Mev, bremsstrahlung spectra from, (E), 20: 6432
molecular structure of, orbital density in, 20: 5524 (ANL-7076)
performance of coatings of pyrolytic, on carbide and oxide fuels, irradiation, 20: 5843
preparation of coatings of pyrolytic, 20: 5843
proton elastic scattering at 12.6 to 13.6 Mev, polarization in, 20: 6439
proton reactions (p,γ) at 16 to 56 Mev, spectra from, (E), 20: 6297(R) (ORNL-3858(Vol.2), pp 82-90)
solubility in sodium, 20: 5594(R) (ANL-6925, pp 21-106)
structure of coatings of pyrolytic, 20: 5848
yields in pyrolysis of diphenyl at 375 to 1375°K, 20: 5563 (EUR-2482.f)
CARBON DIOXIDES
electric arcs in gravitationless state in, 20: 6163
electron reaction with, cross sections for momentum transfer and drift velocities in, 20: 5985 (ORNL-TM-1262)
electron reactions with, ionization cross sections for, (E/T), 20: 5989
performance in fission chambers, 20: 5734 (LFEN-NI-19)
processing aboard space vehicles, using electric-power plants, (E/T), 20: 5820 (NASA-CR-316)
radiation effects on reduction of, by hydrogen, 20: 5574
reactions with zirconium, copper–zirconium, and copper–molybdenum–zirconium at 600 and 700°C, 20: 5860
CARBON ISOTOPES C-11
recoil reactions with alicyclic and aliphatic hydrocarbons, methylamine, and oxygen, 20: 5570 (JUL-228-RC)
CARBON ISOTOPES C-12
alpha-particle interactions in, three-body, (T), 20: 6371
deuteron reactions (d,d) and (d,pγ) at 2.8 to 3.7 Mev, angular distributions from, (E/T), 20: 6362
deuteron reactions (d,α) at 11 Mev, alpha spectra from, (E), 20: 6360
electron scattering at 100 Mev, electron electric dipole moment from, (E), 20: 6064
meson (π⁻) capture by yields and energy spectra from, (E/T), 20: 6292 (NP-15601)
oxygen-16 reactions (O-16,αγ) with, magnesium-24 levels from, (E), 20: 5928(R) (PR-P-66)
proton elastic scattering at 141 Mev, polarization in, (E), 20: 6328
CARBON ISOTOPES C-13
energy levels, (T), 20: 6281 (CEA-R-2807)
proton elastic scattering at 1.5 to 2.4 Mev, angular distributions from, (E/T), 20: 6362
CARBON ISOTOPES C-14
activity measurements of, by gas-proportional counting, 20: 5779
content in atmosphere, secular variations of cosmic-ray produced, (T), 20: 6205
determination by beta scintillation counting, effects of sample volume on efficiency of, 20: 5510
determination in organic compounds, design and operation of G-M counter for, 20: 5511
incorporation in fish eggs, 20: 5261
incorporation in 5-methyl-10-β-dimethylaminoethyl-10,11-dihydro-11-oxo-5H-dibenzo-1,4-diazepine (Noveril), 20: 5564
CARBON MONOXIDES
electron reactions with, ionization cross sections for, (E/T), 20: 5989
reactions with beryllium at 100 to 1500°C, 20: 5844
CARBON STEEL
corrosion by bismuth at 1000°C, 20: 6024(R) (ANL-6925(p.235-47))
corrosion by cadmium–magnesium–uranium–zinc alloys with chloride flux at 600 to 650°C, 20: 5594(R) (ANL-6925, pp 21-106)
radiation effects on corrosion of ASTM-A-7, by Santowax OM at 500 to 700°F, fast-neutron, 20: 5846
radiation effects on mechanical properties of, fast-neutron, 20: 5921
CARBON SYSTEMS
Al–C–Cr, superconductivity of Cr_2AlC, 20: 6228
Al–C–Mo, superconductivity of Mo_3Al_2C, 20: 6228
Al–C–V, superconductivity of V_2AlC, 20: 6228
B–C, phase studies, 20: 5851
C–Cr–Ga, superconductivity of Cr_2GaC, 20: 6228
Cd–C–Ti, superconductivity of Ti_2CdC, 20: 6228
C–Hf, phase studies, 20: 5851
C–Hf–In, superconductivity of Hf_2InC, 20: 6228
C–In–Nb, superconductivity of Nb_2InC, 20: 6228
C–In–Zr, superconductivity of Zr_2InC, 20: 6228
C–Mo–Ti–Zr, microstructure and tensile properties of, effects of composition, heat treatment, and processing on, 20: 5846
C–Mo–U, phase studies, 20: 5843
C–Nb–Sn, superconductivity of Nb_2SnC, 20: 6228
C–Nb–W–Zr, bonding of D-43, method for diffusion, 20: 5867
C–Nb–W–Zr, electric conductivity to 1500°C of D-43, 20: 5851
C–Nb–W–Zr, emissivity to 1500°C of D-43, total hemispherical, 20: 5851
C–Nb–W–Zr, mechanical properties of D-43, effects of protective coatings and welding on, 20: 5866
C–Nb–W–Zr, weld stability in D-43, 20: 5866
C–Nb–W–Zr, welding parameters for D-43, electron-beam, 20: 5867
C–Nb–Zr, corrosion by lithium in niobium–1–zirconium alloy forced-convection loop, 20: 5853 (TID-898)
C–Ni–Th, phase studies, 20: 5848
C–Pb–Ti, superconductivity of Ti_2PbC, 20: 6228
C–Pu–U, preparation techniques, 20: 5843
C–Pu–U, properties, 20: 5843
C–Ta, phase studies, 20: 5851
C–Ta–U, phase studies, 20: 5843
C–U, properties for use as reactor fuel cores, 20: 5887 (NLCO-953)
CARCINOGENESIS
prognostic factors for clinical evaluation of, 20: 5296(R) (NP-15585)
CARCINOGENS
sarcoma induction in rats by chemical, 20: 5334
CARCINOMAS
localization of, use of iodine-131-labeled fibrinogen in rat, 20: 5436(R) (UR-668, pp 149-60)
radiography of gastrointestinal, using Thorotrast, 20: 5465
radioinduced in liver following radiography of liver and spleen Thorotrast, 20: 5311
radioinduced renal, by deposited Thorotrast, 20: 5332
radiosensitivity of cervical, effects of estradiol on, 20: 5472
radiotherapy of antral, iridium-192 gamma, 20: 5458
radiotherapy of bronchial, sensitizing effects of inhaled oxygen or Synkayvite, 20: 5437
radiotherapy of cervical, advantages of mega- and supervoltage for, 20: 5451
radiotherapy of cervical, 20: 5457
radiotherapy of cervical, effects of estrogen treatment on, 20: 5472
radiotherapy of gynecologic, intestinal injury from electron and radium, 20: 5392
radiotherapy of laryngeal, 20: 5486
radiotherapy of ovarian, recovery rate of, 20: 5446
radiotherapy of thyroid, evaluation of iodine-131, 20: 5444
CASCADE SHOWERS
production in shielding materials, (T), 20: 6521(R) (ORNL-3858 (Vol.2), pp 73-81)
production in solids, particle counting by, 20: 5793
CATALASES
radiation effects on hydrogen peroxide systems of, 20: 5271
CATIONS
reactions with hydrated electrons, review on, 20: 5525 (IA-1041)
CATTLE
radiation effects on metabolism in lens of, effects of age, x, 20: 5333
CAVITY RESONATORS
fabrication and testing for 300-Mev betatrons, 20: 5942 (NP-15615)
CELLULOSE ACETATES
ion tracks in, registration mechanisms of heavy, 20: 5755
CERAMIC CRUCIBLES
performance in uranium distillation from magnesium–zinc alloys, 20: 5594(R) (ANL-6925, pp 21-106)
reactions of beryllia, with products of fuel alloy halide slagging, 20: 5594(R) (ANL-6925, pp 21-106)
CERAMIC MATERIALS
joining to metals using pressure at high temperatures, 20: 5866
preparation of high-purity, by decomposition of organometallic compounds, 20: 5851
tensile properties of, method for testing, 20: 5846

CERIUM
deposition on aluminum, copper, and stainless steel, electrolytic, 20: 5867
determination by potentiometric titration using EDTA, equipment for, 20: 5502
determination in mixtures of actinides and fission products by paper chromatography, 20: 5509
reactions in chloride slagging of fissium–plutonium–uranium alloys, 20: 5594(R) (ANL-6925, pp 21-106)
separation from actinides and other rare earths by electrophoresis, 20: 5598
sorption on charcoal powders, effects of sodium dodecyl sulfate and water on, 20: 5675
CERIUM ALLOYS
Ce–Co–Cu–Fe–Ni–Pu, phase studies, 20: 5848
Ce–Co–Pu, casting technique, 20: 5848
Ce–Co–Pu, diffusion of fission products from irradiated, to sodium at 550°C, 20: 5848
Ce–Co–Pu, viscosity, effects of composition and temperature on, 20: 5848
Ce–Mn, phase studies at 500 to 800°C of cerium-rich, 20: 5851
Ce–Y, electric conductivity at low temperatures, 20: 5888 (NP-15592)
CERIUM IONS
spin-lattice relaxation rates in single crystals of anhydrous lanthanum trichloride, (E), 20: 6542
CERIUM ISOTOPES Ce-132
preparation, (E), 20: 6298(R) (PPAD-2137-566)
CERIUM ISOTOPES Ce-133
preparation, (E), 20: 6298(R) (PPAD-2137-566)
CERIUM ISOTOPES Ce-134
preparation, (E), 20: 6298(R) (PPAD-2137-566)
CERIUM ISOTOPES Ce-137
content in man in Toronto, 20: 5671
preparation, (E), 20: 6298(R) (PPAD-2137-566)
CERIUM ISOTOPES Ce-140
energy levels of, lifetime of first-excited, (E), 20: 6324
CERIUM ISOTOPES Ce-144
beta transitions in, with parity change, (E), 20: 6370
distribution in urania fuel rods irradiated with gross central melting, 20: 5914(R) (GEAP-3771-17)
CERIUM OXIDES
CeO_2–UO_2, effects of cerium dioxide content on sintering behavior of mechanically mixed, 20: 5889 (NUMEC-2389-8)
CERMETS
processing clad, by destructive oxidation and fluorination, 20: 5595(R) (ANL-6925, pp 107-64)
CESIUM
corrosive effects on niobium, zirconium, and niobium–1 zirconium at 1600, 1800, and 2500°F, 20: 5846
corrosive effects on refractory metals and alloys at 2500 to 3400°F, 20: 5851
diffusion from irradiated cerium–cobalt–plutonium alloy to sodium at 550° C, 20: 5848
plasma seeding with, 20: 6030(P)
stability of plasma of, with discontinuous velocity distribution, (T), 20: 6487
CESIUM FLUORIDES
CsF–LaF_3–LiF, phase diagram, 20: 5558
CESIUM IODIDES
radioinduced photoluminescence spectra of thallium-activated, x, (E), 20: 6537
CESIUM ISOTOPES Cs-131
absorption by metal planchets, 20: 5482
nuclear magnetic moment and hyperfine structure, (E), 20: 6401
use in therapy, advantages of, 20: 5482
CESIUM ISOTOPES Cs-132
yields from uranium-235 thermal fission, (E), 20: 6288 (KAPL-3113)
CESIUM ISOTOPES Cs-133
energy level transitions in, from barium-133, 20: 6436
neutron reactions (n,γ) with, isomeric cross sections for, (E/T), 20: 6301 (TID-22165)
CESIUM ISOTOPES Cs-134
beta decay of, gamma spectra from, (E), 20: 6327
production of isomeric pairs of, in cesium-133 (n,γ) reactions, (E/T), 20: 6301 (TID-22165)
yields from uranium-235 thermal fission, (E), 20: 6288 (KAPL-3113)
CESIUM ISOTOPES Cs-136
yields from uranium-235 thermal fission, (E), 20: 6288 (KAPL-3113)
CESIUM ISOTOPES Cs-137
content in fallout, 1963, 20: 5652
content in food, in Denmark, 20: 5651 (RISO-107)
content in individual rain showers at Bombay, 20: 5661 (AEET-215)
content in man, in Denmark, 20: 5651 (RISO-107)
content in milk in New Zealand, 1965, 20: 5664(R) (NP-15639)
distribution in urania fuel rods irradiated with gross central melting, 20: 5914(R) (GEAP-3771-17)
dosimetry in sheep, use of thermoluminescent detector for, 20: 5285 (BNWL-SA-172)
CESIUM ISOTOPES Cs-144
use for evaluation of shielding barriers, 20: 5677
CHARCOAL
sorption of cerium, cobalt, and promethium on powdered, effects of water and sodium dodecyl sulfate on, 20: 5675
CHARGED PARTICLE BEAMS
density of ultrarelativistic colliding, limitations in, (T), 20: 5950
diagnostics of, probe design for, (E), 20: 5686(T) (NP-tr-1313)
leakage from storage rings, due to amplitude and frequency variations of compensating field, (T), 20: 5949
motion in electromagnetic fields, effects of image and space charges on, 20: 5928(R) (PR-P-66)
trajectories of polarized, from cyclotron ion sources, (T), 20: 5946 (UJV-1408/65)
CHARGED PARTICLES
containment by mirror-multipole cusp fields, (T), 20: 6496
density distribution in ionosphere, three-fluid model for, (T), 20: 6179 (AD-618911)
detection and momentum-measurement on, using spark chamber arrays, (E), 20: 5730 (JINR-E-2366)
detection of heavy, surface-barrier p-n semiconductor counters for, (T), 20: 5758
energy of performance of electrostatic analyzer for, 20: 5691
motion and trapping in static magnetic fields, (T), 20: 6459 (CNIE-PE-1)
motion in plasma under influence of drag forces, precession, (T), 20: 6493
radiation emission at anisotropic conductive plane, 20: 6043
reactions with nuclei, Fraunhofer and Fresnel diffraction in, (T), 20: 6359
scattering by nuclei, radial relativistic Coulomb integrals for, (T), 20: 6375
scattering by plasma electric field fluctuations, (T), 20: 6497
scattering in crystals, cross sections for, (T), 20: 6535
scattering on distorted Coulomb potential, hypervirial relations for, (T), 20: 6146
trapping and containment by magnetic mirrors, statistical theory for, (T), 20: 6494
trapping in geomagnetic fields, dynamics of, 20: 6208
CHEMICAL ANALYSIS
instruments for, for water chemistry control in Halden boiling reactor, (E), 20: 6648(R) (HPR-64)
standards for use in, preparation of thin metal films on pyrolytic graphite as, 20: 5503
CHEMICAL ENGINEERING
research programs on, ANL summary of, for July–Dec. 1964, 20: 5492(R) (ANL-6925)
CHEMICAL RADIATION DETECTORS
performance for gamma rays, 20: 5751
CHEMOTHERAPY
use for lymphosarcoma treatment, 20: 5485
CHERENKOV DETECTORS
design of coincidence, for cosmic ray intensity measurements, 20: 6014 (NP-15380)
performance in cosmic meson (μ) and neutrino detector, 20: 5723 (CONF-640919, pp 155-65)
CHERENKOV RADIATION
detection in optically single axis crystals, method for, 20: 5792
production in plasma by uniformly rotating line charge, 20: 6456 (AD-619888)
CHICKENS
calcium–vitamin D metabolism in, 20: 5237(R) (UR-668, pp 55-109)
radiation effects on development of embryos of, from exposed eggs, x, 20: 5306
CHIMERAS
immune reactions in tissue transplants from mouse-rat radiation, 20: 5397
CHLORELLA
radiation effects on growth of, γ, 20: 5389
CHLORIDES
neutron resonance absorption and scattering by molecules of, cross sections for, (T), 20: 6266
CHLORINE
reactions with uranium dioxide in molten alkali chlorides, thermodynamics of, 20: 5547
CHLORINE ISOTOPES Cl-32
beta decay of, shell model calculations of ft values in, (T), 20: 6393
CHLORINE ISOTOPES Cl-33
beta decay of, shell model calculations of ft values in, (T), 20: 6393
CHLORINE ISOTOPES Cl-34

beta decay of, shell model calculations of ft values in, (T), 20: 6393
energy levels of, gamma branching in, (E/T), 20: 6295 (NP-15647)

CHLORINE ISOTOPES Cl-35
bremsstrahlung resonant scattering at 1.0 to 1.3 Mev, energy level lifetimes from, (E), 20: 6380
nuclear magnetic resonance in potassium hexachlorohenate, 20: 6549

CHLORINE ISOTOPES Cl-36
uptake of, by rabbit eye lens in culture, 20: 5256

CHLORINE ISOTOPES Cl-37
neutrino reactions (ν,β) with, cross section for, (T), 20: 6393
neutron reactions (n,p) at 13.0 to 20.2 Mev, cross sections for, (E/T), 20: 6357

CHLORINE ISOTOPES Cl-38
beta decay, (E), 20: 6407
content in PNPF coolant, monitoring standardization for determining, 20: 6615 (NAA-SR-10888(Rev.))

CHLOROFORM
uses as medium for drifting lithium into germanium, (E), 20: 5702

CHLOROPLASTS
radiation effects on photosynthetic reactions in isolated, uv, 20: 5401
radiation effects on photosynthetic reactions in isolated, x, 20: 5402

CHOLANTHRENE, 3-METHYL-
effects on rats, carcinogenic, 20: 5334

CHROMATES
preparation of radioactive, for medical use, 20: 5592(P)

CHROMATOGRAPHIC SEPARATIONS
performance for separating americium isotopes, curium-242, and plutonium-242, (E), 20: 5823(T) (ORNL-tr-892)

CHROMATOGRAPHY
scanning radioactive paper in, optimum operation of rate meter for, 20: 5508

CHROMIUM
compatibility with plutonium-uranium carbides, 20: 6600(R) (ANL-7105, pp 1-35)
determination by potentiometric titration using EDTA, equipment for, 20: 5502
diffusion in niobium, inter-, 20: 5846
effects on hot hardness of zirconium oxides, 20: 5846
effects on hot hardness and microstructure of aluminum–iron–uranium alloy, 20: 5848
proton reactions at 3 Bev, fission and fragmentation products from, (E), 20: 5756

CHROMIUM ALLOYS
Cr–Fe–Mo–Ni, corrosion of Hastelloy X-280, by helium–water system at 1700, 1900, and 2100°F, 20: 5846
Cr–Fe–Mo–Ni, oxidation at 2050°F of Hastelloy X-280, 20: 5851
Cr–Gd–Fe, properties as control-rod material, 20: 5845
Cr–Gd–Fe, tensile properties of, effects of gadolinium content on, 20: 5845
Cr–Nb, precipitation of $NbCr_2$ in, cellular, 20: 5846
Cr–Nb–Ti–V, properties as cladding materials, 20: 5846
Cr–Ni–Nb, radiation effects on stress-rupture properties of, neutron, 20: 5917
Cr–Re, internal friction, effects of nitrogen on, 20: 5851
Cr–Ta, thermochemical properties of Cr_2Ta Laves phase, 20: 5851
Cr–Ti–V, corrosion by flowing sodium at 650°C, effects of chromium content on, 20: 5851
Cr–Ti–V, creep rate of, 20: 6601(R) (ANL-7115, pp 1-41)
Cr–Ti–V, elastic properties, 20: 6556(R) (ANL-7105, pp 36-58)
Cr–U, phase transformation in, kinetics of beta-alpha, 20: 5843
Cr–Zircaloy-2, corrosion cracking by iodine at 350°C, stress-, 20: 5914(R) (GEAP-3771-17)

CHROMIUM COMPOUNDS
preparation of high specific activity, 20: 5592(P)

CHROMIUM ISOTOPES
incorporation in compounds, 20: 5592(P)

CHROMIUM ISOTOPES Cr-51
half life, (E), 20: 6420

CHROMIUM OXIDES
magnetic properties of, 20: 6531 (AD-623530)
CrO_3–Ni, properties for use as catalyst for hydrogen–deuterium exchange, 20: 5534

CHROMIUM STEEL
corrosion by cadmium–magnesium–uranium–zinc alloys with chloride flux at 600 to 650°C, 20: 5594(R) (ANL-6925, pp 21-106)
corrosion by potassium–sodium at 1425°F of Croloy 9M, effects of oxygen on, 20: 5851
design stress for Croloy 2¼ in sodium environment, 20: 5851
mechanical properties of Croloy 2¼, effects of sodium at 1100°F on, 20: 5846
oxidation by air at 600°C, 20: 5594(R) (ANL-6925, pp 21-106)
Cr–Mo, radiation effects on corrosion of AISI 4130, by Santowax OM at 500 to 700°F, fast-neutron, 20: 5846
Cr–Mo–Ni–Nb–V, development as HY-180/210 steel, 20: 5851

CHROMIUM SYSTEMS
Al–C–Cr, superconductivity of Cr_2AlC, 20: 6228
C–Cr–Ga, superconductivity of Cr_2GaC, 20: 6228

CHROMOSOMES
aberrations in man following skin radiotherapy, genetic effects of, 20: 5351
radiation effects on replication in *E. coli*, uv, 20: 5349
radiation effects on human, during space flight, 20: 5297 (ORNL-P-1734)
radioinduced aberrations of, in root cells grown in irradiated nutrient solution, 20: 5390
radioinduced aberrations in Drosophila, x, 20: 5338
radioinduced aberrations of, 20: 5343
radioinduced mutations in Drosophila, x, 20: 5358
radiosensitivity of, in leukocytes in humans, monkeys, and rabbits, 20: 5304(T) (JPRS-32985, pp 45-50)

CIRCUITS
design and performance of bistable and monostable, (E), 20: 5680 (ELI-91)
design for correcting output of time-to-pulse height converter, 20: 5796
design for Geiger-Mueller tubes, 20: 5801(P)
design of delay-line clipping, with source termination, (E), 20: 5701
design of ratemeter-pump, (E), 20: 5680 (ELI-91)
design of tunnel-diode cascade, (E), 20: 5699
development and uses of fast universal diode-transistor logic, 20: 5704
radiation effects on, measurement in Pulstar reactor, 20: 6679 (NP-15645)
radiation effects on telemetry, in LES satellites, 20: 5806 (AD-619387)
thresholds for tunnel-diode switching, (E), 20: 5700
transients in linear, total time integrals of, (T), 20: 5681 (MLM-1288)

CIVILIAN DEFENSE
protection of population from fallout from thermonuclear explosions, 20: 5416
vehicle design for, shielded, 20: 5679(P)

CLOUD CHAMBERS
design of magnetic, for cosmic-particle interactions to 10^{12} ev, 20: 5722 (CONF-640919, pp 12-43)

COATINGS
development of corrosion-protection, for heat-resisting metals, 20: 5851

COAXIAL CABLES
radiation response in, method for reduction of, 20: 5805(R) (AD-617782)

COBALT
deposition on pyrolytic graphite for use as analytical standard, electro-, 20: 5503
neutron absorption integrals for, infinite-dilution, (E), 20: 6558(R) (ANL-7115, pp 42-67)
optical properties of small particles of, (T), 20: 5879 (D-910092-6)
proton reactions at 450 Mev, secondary proton spectra from, (E), 20: 6297(R) (ORNL-3858(Vol.2), pp 82-90)
separation from iron and manganese by solvent extraction, 20: 5602
sorption on charcoal powders, effects of sodium dodecyl sulfate and water on, 20: 5675

COBALT ALLOYS
Ce–Co–Cu–Fe–Ni–Pu, phase studies, 20: 5848
Ce–Co–Pu, casting technique, 20: 5848
Ce–Co–Pu, diffusion of fission products from irradiated, to sodium at 550°C, 20: 5848
Ce–Co–Pu, viscosity, effects of composition and temperature on, 20: 5848
Co–Ta, oxidation kinetics at 500 to 900°C, 20: 5854(T) (JPRS-32341, pp 8-16)
Co–W, oxidation kinetics at 500 to 900°C, 20: 5854(T) (JPRS-32341, pp 8-16)
Co–Zr, oxidation kinetics at 500 to 900°C, 20: 5854(T) (JPRS-32341, pp 8-16)

COBALT(II) CHLORIDES
magnetic properties of, 20: 6531 (AD-623530)

COBALT ISOTOPES Co-59
energy levels, (E), 20: 6412

COBALT ISOTOPES Co-60
depth dose planning for therapeutic use of, 20: 5449
preparation, packaging, and standardization of, 20: 5813(T) (JPRS-32260)
separation from cotton cloth soiled with oily materials, 20: 5676

COBALT SYSTEMS
Co–O–W, phase studies, 20: 5851
Co–ZrB_2, oxidation kinetics at 500 to 1000°C, 20: 5845

COCKCROFT-WALTON ACCELERATORS
description of, at installations in India, 20: 5715 (AEET-227)

COINCIDENCE COUNTERS
design for nuclear quadrupole moment determinations, 20: 5794
design for x-ray astronomy, 20: 5968 (NP-15626)
design of Cherenkov, for cosmic radiation, 20: 6014 (NP-15380)

design of fast, for low-energy gamma spectroscopy, (E), 20: 5770
development for Cherenkov radiation, 20: 5792
performance of summing, in isotope mixture analysis, 20: 5753
COLICINS
induced in *E. coli* by uv irradiated culture media, 20: 5279
COLLAGEN
radiation effects on ratio of soluble to insoluble, in hamster skin, x, 20: 5330
COLLIMATORS
design for x-ray tube shield, 20: 5693
effects on Bragg peaks in neutron diffraction, 20: 6268
COLLOIDS
effects of x agent on kaolin, 20: 5587
COLORADO
fallout monitoring, 1963, 20: 5649(R) (COO-1340-2, pp 54-83)
COMPLEXES
reactions of physiological, with yttrium, 20: 5237(R) (UR-668, pp 55-109)
sorptive properties of, mole ratio and variation methods for determining, 20: 5530 (SC-RR-65-625)
stability constants for, computer program for calculation of, from spectrophotometric measurements, 20: 5526 (KFK-250)
COMPUTER PROGRAMS
CLEB, NINEJ, and RAC7, for Clebsch-Gordon, 9-J, and Racah coefficients, FORTRAN for CDC 1604, 20: 6216 (ORNL-3877)
development, 20: 5832(R) (ORNL-3858(Vol.I), pp 47-58)
development for analysis of bubble chamber films, 20: 6099
EXPANDA, for fast reactor criticality, 20: 6583 (JAERI-1091)
FLIGHT-2, for SNAP-10A flight test data reduction and analysis, FORTRAN II, 20: 6661 (NAA-SR-Memo-11603)
for calculation and illustration of contour diagrams of molecular orbital densities of molecules, on CDC-3600, 20: 5524 (ANL-7076)
for collective nuclear model calculations on deformed even-even nuclei, FORTRAN II for IBM 704, 20: 6278 (AD-623877)
for evaluation of post-irradiation survival times in animals, FORTRAN IV for, 20: 5300 (UCLA-12-573)
for expanding functions in terms of Chebyshev polynomials, for IBM 7040, 20: 5828 (AAEC/TM-293)
for fuel conservation efficiencies of thermal reactors, FORTRAN II for IBM 7090, 20: 6610 (HW-79287)
for least-squares regression analysis of complex gamma spectra, 20: 5727 (CONF-651101-46)
for meteorological Montgomery stream functions, for IBM 1620, 20: 5645(R) (COO-1340-2, pp 122-45)
for Monte-Carlo fitting of experimental data to theoretical curves, FORTRAN IV for IBM 7040, 20: 6286 (ISS-65/10)
for neutron multiplication factor calculations, for IBM 7094, 20: 6581 (CEA-R-2872)
for nuclear heating transients in in-pile fuel samples, 20: 6562 (NAA-SR-Memo-11369)
for thermodynamic data on atmosphere, IBM 1620, 20: 5645(R) (COO-1340-2, pp 122-45)
GAMMA-P, for gamma production cross sections, FORTRAN IV for IBM 7094, 20: 6284 (GEMP-392)
KINEM, for kinematics of nuclear reactions having three-particle final states, FORTRAN II, 20: 6333
KURIE, for analysis of low-resolution beta and conversion-electron spectra, (T), 20: 5768
LTFR, for fast reactor criticality, 20: 6583 (JAERI-1091)
MATEDIR, for design of manned, direct-radiating, thermoelectric systems, FORTRAN II for IBM 7090/94, 20: 6660 (NAA-SR-Memo-11514)
NIH-OMR-SAAM, for calculation of calcium metabolism in man, 20: 5260
NURLOC, for coolant-loss accidents in LOFT, (T), 20: 6560(R) (BMI-X-10145)
OPEX, for shield optimization, FORTRAN, 20: 6518 (NAA-SR-Memo-11516)
PHOTOMETERPROG 4, for calculation of stability constants from spectrophotometric measurements, FORTRAN for IBM-7070, 20: 5526 (KFK-250)
PLANE WAVE, for ionization cross sections, for Univac Larc, 20: 5986 (UCRL-14402-T)
PREPANDA, for fast reactor criticality, 20: 6583 (JAERI-1091)
SCAP, for spectral analysis of pulsed neutron decay data, FORTRAN II for IBM 7094, 20: 6585 (NAA-SR-Memo-10941)
SCRATCH-1 and -2, for SGR transient analysis, 20: 6620 (NAA-SR-Memo-11458)
SIZZLE, for fission-product reactivity worths in reactors, 20: 6659 (NAA-SR-Memo-11473)
STMGEN, for steam generator designing, for IBM 7044, 20: 5606 (GAMD-6675)
STMGEN, for steam generator designing, for IBM 7044, 20: 5607 (GAMD-6675(Suppl.))
TRANSY, for S2 and S4 transport calculations, FORTRAN, 20: 6264 (WAPD-T-1849)
TRIX-1, for neutron resonance integrals, FORTRAN, 20: 6291 (NAA-SR-Memo-11538)
COMPUTERS
design of analog, for pulse-height data reduction, 20: 5835
number generators for, Fourier analysis of random, 20: 5833 (ORNL-3866)
performance of digital, for logging data from proton linacs, (E), 20: 5953
programming from ordered integer rings, linear, 20: 5831 (EUR-1919.f)
use for analysis of thermodynamic data on atmosphere, 20: 5645(R) (COO-1340-2, pp 122-45)
use for high gradient time variant magnetic field measurement, 20: 5682 (MURA-716)
use for tandem Van De Graaff data processing, 20: 5939 (LA-DC-7267)
use in nuclear spectroscopy, 20: 6307 (UCRL-16439)
use of UMC-1, for kinematic relations in nuclear reactions, 20: 6285 (INP-414/PL)
uses for analysis of small-angle proton scattering at high energies, 20: 5720 (CERN-65-33)
uses for system simulation, time-delay models for, 20: 5834 (ORNL-TM-1323)
uses with vidicons and digital scanners for particle-track analysis, (E), 20: 5718 (BNL-9634)
CONCRETES
gamma scattering by duct in, streaming in, (T), 20: 6530
moisture content of, neutron gage for determining, 20: 5819
neutron albedo from, accuracy of Monte Carlo method for calculating, 20: 6519(R) (ORNL-3858(Vol.1), pp 20-41)
neutron scattering in rectangular ducts of, (E/T), 20: 6519(R) (ORNL-3858(Vol.1), pp 20-41)
neutron slowing down in, albedo and capture-gamma dose rates for, 20: 6519(R) (ORNL-3858(Vol.1), pp 20-41)
CONNECTICUT YANKEE POWER REACTOR
hydraulic design of, models for, (E), 20: 6622 (NYO-3250-2)
CONVECTION
augmenting of, evaluation of methods for, 20: 5618 (AD-619511)
CONVECTION (FORCED)
heat transfer in, from vertical cylinder in square channel, 20: 5619 (AE-199)
CONVERSION ELECTRONS
computer analysis of low-resolution beta and conversion-electron spectra, (T), 20: 5768
CONVEYERS
design for package irradiation, 20: 5617(P)
COPPER
coating with rare earths, electrolytic, 20: 5867
deposition on pyrolytic graphite for use as analytical standard, electro-, 20: 5503
deposition on Zircaloy-2 to prevent hydrogen absorption, electrolytic, 20: 5867
determination by potentiometric titration using EDTA, equipment for, 20: 5502
diffusion into Nimonic-75 and type V2A stainless steel at 900°C, 20: 5850
effects on hydrochloric acid cleavage of organotin compounds in methanol–water, 20: 6687(R) (NYO-3453-1)
electron reactions at 2.5 to 4.0 Mev, bremsstrahlung spectra from, (E), 20: 6432
gamma heating in, calculations for, (E/T), 20: 6517 (CONF-651101-41)
proton reactions (p,n) at 30 and 50 Mev, isobaric-state excitation in, (E/T), 20: 6361
proton reactions at 2 Bev, lithium-8 production in, (E), 20: 6409
radiation effects on electrodes of, correlation of high-vacuum breakdown with electron, 20: 5809
welding parameters, electron-beam, 20: 5867
COPPER ALLOYS
Al–Cu, radiation effects on electric conductivity of, stage I and II recovery from electron, 20: 5918
Al–Cu–Ni, embrittlement of hydrogenated, solute-induced, 20: 5846
Be–Cu, welding parameters, electron-beam, 20: 5867
Ce–Co–Cu–Fe–Ni–Pu, phase studies, 20: 5848
Cu–Mo–Zr, oxidation resistance of, in carbon dioxide at 600 and 700°C, 20: 5860
Cu–Nb–Zr, alloy element distribution in bulk metal and oxide film on, 20: 5851
Cu–Pu, crystal structure of $PuCu_4$, 20: 5843
Cu–Zr, oxidation resistance of, in carbon dioxide at 600 and 700°C, 20: 5860
COPPER IONS
electron spin resonance of divalent, 20: 5533
COPPER ISOTOPES Cu-62
uses of neutron-activated, as fast-neutron detectors, (E), 20: 6289 (KN-63-10(R))
COPPER ISOTOPES Cu-63

energy levels of, quasi-particle method for, (T), 20: 6340
neutron capture by, neutrino emission following, 20: 6050
neutron reactions (n,2n) with, uses of resultant copper-62 beta activity as neutron detector, (E), 20: 6289 (KN-63-10(R))
neutron reactions (n,2n) at 16.59 to 17.71 Mev, excitation curve for, (E), 20: 6319

COPPER ISOTOPES Cu-64
neutrino emission by, 20: 6050

COPPER ISOTOPES Cu-65
nuclear magnetic resonance in cuprous oxide, in pure quadrupole regime, (E), 20: 6549

COPPER OXIDES
copper-65 NMR in, in pure quadrupole regime, (E), 20: 6549

COPPER SYSTEMS
B_4C–Cu, fabrication as shutdown control rods, 20: 5850

CORROSION LOOPS
effects of sample location in, on corrosion rate, 20: 5846
testing of niobium–zirconium alloy forced-convection lithium, 20: 5853 (TIN-898)

CORROSION-RESISTANT ALLOYS
creep property measurements on, mathematical system for extrapolation of, 20: 5880(R) (EURAEC-1310)

CORTICOSTEROIDS
effects on bone growth and atrophy in compact and spongy bones of rabbits, effects of drug dose, 20: 5234(R) (COO-119-232, pp 122-52)
effects on plutonium-239 excretion by dogs, 20: 5247(R) (COO-119-232, pp 188-99)

COSMIC ELECTRONS
energy spectra and flux of primary, at energies above 15 Bev, (E), 20: 6022
energy spectra at 5200 m above sea level, 20: 6021

COSMIC MESONS
fluxes of K, in atmosphere, possible experiments using, 20: 6009 (CONF-640919, pp I11-13)
intensity variations in 1960 to 1963, solar-diurnal, 20: 6016

COSMIC MESONS (μ)
detection of neutrino-produced, 10,000 ft underground, 20: 6008 (CONF-640919, pp I48-54)
detection using corona-spike G-M counters and Cherenkov detectors, 20: 5723 (CONF-640919, pp 155-65)
energy spectra at 5200 m above sea level, 20: 6021
fluxes in atmosphere, possible experiments using, 20: 6009 (CONF-640919, pp I11-13)
interactions with electrons and nuclei at 5 to 50 Bev, (E), 20: 6007 (CONF-640919, pp I43-8)

COSMIC MESONS (π)
fluxes in atmosphere, possible experiments using, 20: 6009 (CONF-640919, pp I11-13)

COSMIC NEUTRINOS
detection using corona-spike G-M counters and Cherenkov detectors, 20: 5723 (CONF-640919, pp 155-65)
detection 10,000 ft underground, 20: 6008 (CONF-640919, pp I48-54)
fluxes in atmosphere, possible experiments using, 20: 6009 (CONF-640919, pp I11-13)
fluxes of, for studies of astrophysical phenomena, 20: 6012 (CONF-640919, pp III1-23)

COSMIC NUCLEONS
fluxes in atmosphere, possible experiments using, 20: 6009 (CONF-640919, pp I11-13)

COSMIC PARTICLES
conference on high-energy interactions of, 20: 6006 (CONF-640919)
detection of basic triplets in, experiment for, 20: 6010 (CONF-640919, pp II23-7)
energy of primary, ionization calorimeter for determining, 20: 5788
interactions above 100 Bev, balloon-borne system for investigating, 20: 5724 (CONF-640919, pp II13-23)
interactions at 300 Bev, proposed system for investigating, 20: 5725 (CONF-640919, pp II27-30)
interactions to 10^{12} ev, magnetic cloud chamber for study of, 20: 5722 (BNL-640919, pp 12-43)
interactions with nucleons at 24 Bev, angular distributions from, (E), 20: 6325
measurements of, high-energy physics experiments using, 20: 6009 (CONF-640919, pp I11-13)
reactions with carbon, electron-photon yield from, (E), 20: 6017
reactions with emulsion nuclei at 24 Bev, angular distributions from, 20: 6325
trapping in geomagnetic fields, dynamics of, 20: 6208

COSMIC PHOTONS
interactions at high energies, electromagnetic showers from, (E), 20: 6013 (CONF-640919, pp IV17-33)

COSMIC PROTONS
energy spectra at 5200 m above sea level, 20: 6021
interaction with interstellar matter, low-energy secondary proton intensity from, (T), 20: 5973

COSMIC RADIATION
absorption of r-f, in interstellar ionized gases, (T), 20: 6020
conference on high-energy interactions of, 20: 6006 (CONF-640919)
detection and measurement of, atmospheric effects on scintillation, 20: 6004 (AD-619508)
detection and measurement for astrophysical studies, 20: 6012 (CONF-640919, pp III1-23)
distribution of field of, reflected from earth's atmosphere, (E), 20: 6019
effects of x agent on kaolin colloids, 20: 5587
effects on background counting rate of G-M counters, 20: 5781
energy spectra of primary, at 10^{14} to 10^{16} ev, (E), 20: 6013 (CONF-640919, pp IV17-33)
frequency dependence of noise level of, during type-II anomalous absorption, 20: 6194
intensity of, Cherenkov telescope for measuring ground-level, 20: 6014 (NP-15380)
magnetic field corotating structure effects on intensity of, interplanetary, (E), 20: 5972
measurements of, limitations in high-energy physics using, 20: 6011 (CONF-640919, pp II30-3)
polarization of, optimum wavelength and spectra interval measurements of, 20: 6018
reactions with carbon, electron-photon yield from, (E), 20: 6017
trajectories and cutoff rigidities for, data tabulations on, 20: 6005 (AD-623632)
transmission through lead, second maximum in, (E), 20: 6015

COSMIC SHOWERS
detection of electromagnetic high-energy, (E), 20: 6013 (CONF-640919, pp IV17-33)

COSMOLOGY
dimensionality of real world, comparitive strength of systems of field equations for four, 20: 6218

CREEP
measurements of, mathematical system for extrapolation of, 20: 5880(R) (EURAEC-1310)
testing to 1300°C by remote operation, design of machine for, 20: 5611 (BNWL-137)

CRITICAL ASSEMBLIES
critical masses of enriched uranium arrays, 20: 6584 (LA-DC-7248)
design of RITMO, to support Italian RTM reactor program, 20: 6683
neutron spectra in, measurement of asymptotic, 20: 6591
neutron transport in plutonium, foil activation studies of, 20: 6579(R) (BNWL-149, pp 48-56)
performance of fast-burst, as pulsed neutron sources, (E), 20: 6671 (CONF-650217, pp 1-10)
reactivity worth calculations in ZPR type, 20: 6601(R) (ANL-7115, pp 1-41)

CRITICALITY STUDIES
of enriched uranium arrays, 20: 6584 (LA-DC-7248)
of plutonium enriched, water moderated power reactors, 20: 6607(R) (GEAP-4965)
of Wood River Junction accident, 20: 5666 (TID-21995)
research, (E), 20: 6588(R) (ORNL-3858(Vol.1), pp 13-19)

CROSS SECTIONS
calculation of ionization, computer program for, 20: 5986 (UCRL-14402-T)

CROTON OIL
effects on rats, carcinogenic, 20: 5334

CRUCIBLES
development for skull reclamation process, 20: 5594(R) (ANL-6925, pp 21-106)
testing for skull reclamation processes, 20: 5594(R) (ANL-6925, pp 21-106)

CRUSTACEA
radiation effects on meiotic stages in oocytes of Artemia, x, 20: 5359
radioresistant bacterial populations in shrimp, physiological effects of γ-irradiation on, 20: 5346

CRYSTALS
charged-particle scattering in, cross sections for, (T), 20: 6535
chemistry and physics of, bibliography on high-temperature, 20: 5527 (NP-15646)
interactions in, morphology of, 20: 5895(R) (TID-22271)
molecular structure, 20: 6551

CURIUM
separation from neutron-irradiated americium, (E), 20: 5823(T) (ORNL-tr-892)
separation from other actinides and rare earths by electrophoresis, 20: 5598

CURIUM COMPOUNDS
chemical properties of solid, (E), 20: 5823(T) (ORNL-tr-892)

CURIUM ISOTOPES Cm-244

production at Savannah River, program for, 20: 5822 (DP-1000)
separation from aluminum nitrate–sodium nitrate–nitric acid solutions using TBP, 20: 5495 (DP-972)
CURIUM OXALATES
chemical properties, (E), 20: 5823(T) (ORNL-tr-892)
CURIUM OXIDES
chemical properties, (E), 20: 5823(T) (ORNL-tr-892)
CUTTING TOOLS
design of chemical saw for cutting irradiated uranium rods, 20: 5839(R) (RISO-110)
CYCLOHEXANE
electron reactions in ethylene mixture, cross sections for momentum transfer and drift velocities in, 20: 5985 (ORNL-TM-1262)
cyclohexane–4-*sec*-butyl-2-α-methylbenzylphenol, solvent properties for francium, 20: 5601
CYCLOHEXANES
electron reactions with, ionization cross sections for, (E/T), 20: 5989
CYCLOPENTANE
radiolysis of, tracer studies of radical yields in, 20: 5576
CYCLOPROPANE
reactions with recoil carbon-11 atoms, mechanism and products of, 20: 5570 (JUL-228-RC)
CYCLOTRONS
beam dynamics in, effect of center geometry on, 20: 5948(T) (ANL-Trans-246)
beam extraction system for heavy ion, 20: 5947(T) (ANL-Trans-241)
description of, at installations in India, 20: 5715 (AEET-227)
ion trajectories in, from polarized-ion sources, (T), 20: 5946 (UJV-1408/65)
voltage stabilization of U-120, 20: 5954
CYLINDERS
heat transfer from vertical, in square channel, 20: 5619 (AE-199)
CYSTEINE
radiosensitivity effects on animal cells in tissue culture, 20: 5418
CYTOCHROME C
metabolism in yeast, factors affecting, 20: 5251(R) (UR-668, pp 123-49)
CYTOLOGY
book: *Mammalian Radiation Lethality*, 20: 5405
of radiation effects on Euplotes, 20: 5345

D

DATA RECORDING SYSTEMS
design for use with multichannel analyzers, (E), 20: 5769
design of data-logging and analog-to-digital-converter systems, (E), 20: 5953
development for continuous centralized recording of individual radiation doses, 20: 5749
development for isotopic mass spectrometers, 20: 5684 (WAPD-T-1770)
DATA TABULATIONS
characteristics of molten-salt-fueled homogeneous reactors, 20: 6554 (ANL-7092)
cosmic ray trajectories and cutoff rigidities, 20: 6005 (AD-623632)
energy levels of atoms, 20: 5984 (NYO-2543-1)
fabrication and properties of molybdenum, niobium, tantalum, tungsten, and their alloys, 20: 5874 (AGARDograph-94)
geomagnetic and solar activity parameters for 1965, 20: 6206
Hugoniot constants and Grueneisen ratios for equation of state of solids, 20: 6533 (NVO-1163-60)
neutron cross section requests at U.K. Nuclear Data Library, 20: 6254 (AEEW-M-503)
nuclear binding and particle separation energies for nuclei $22 \leq Z \leq 120$, 20: 6290 (LA-3280)
DEAMINASES
radiation effects on activity of adenosinedeaminase in rabbit tissues, γ, 20: 5380
radiation effects on activity of adenylic acid deaminase in rabbit tissues, γ, 20: 5380
DECANE
electron reactions in ethylene mixture, cross sections for momentum transfer and drift velocities in, 20: 5985 (ORNL-TM-1262)
decane–$UO_2(NO_3)_2$, radiation effects on coalescence rates in liquid, 20: 5571 (ORNL-TM-1283)
DECONTAMINATING SOLUTIONS
effectiveness of sodium dodecyl sulfate solutions as, 20: 5675
efficiency of, for cotton cloth, 20: 5676
DECONTAMINATION
equipment for containers, glove box, 20: 5711(P)
procedures for uranium mines, 20: 5428
DEHYDROGENASES
radiation effects on activity of, electrons, 20: 5276
DELAY LINES
clipping circuits for, design of impedance-matched, (E), 20: 5701
DENMARK
fallout monitoring, 1964, 20: 5651 (RISO-107)
DENSITOMETERS
development of radiometric, 20: 5817
DEUTERIUM
deuteron reactions with, use of (d,p) for monitoring (d,n), (E), 20: 5777
deuteron reactions (d,n) with, in self-regenerating metal targets, (E/T), 20: 6334
effects on ESR studies of aromatic radicals, 20: 5566
effects on heavy water cleavage of organotin compounds, 20: 6687(R) (NYO-3453-1)
effects on radiolysis of heavy water in boiling reactors, 20: 6638
exchange between hydrogen and water vapor, properties of chromium trioxide–nickel catalyst for, 20: 5534
exchange with hydrogen in methane over palladium–ruthenium alloys, 20: 5557
intermolecular potentials of, comparison with hydrogen, 20: 5541
photon elastic scattering by, cross sections for, (E), 20: 6094
proton elastic scattering at 141 Mev, polarization in, (E), 20: 6328
proton elastic scattering at 150 Mev, cross sections and polarization in, (T), 20: 6329
radioinduced catalytic activation of exchange with hydrogen in Vycor glass vessels, 20: 5578
separation from hydrogen, tritium, and their compounds by gas chromatography, 20: 5824
DEUTERIUM HYDRIDES
separation from deuterium, hydrogen, and tritium and other of their compounds by gas chromatography, 20: 5824
DEUTERIUM IONS
motion of beams of, in crossed-field beam sorters, (E), 20: 6262 (NP-15633)
DEUTERIUM SYSTEMS
D–H–NH_3, bithermal isotopic exchange in, 20: 5827(P)
DEUTERIUM TRITIDES
separation from deuterium, hydrogen, and tritium and other of their compounds by gas chromatography, 20: 5824
DEUTERONS
effects on plant viruses, biological, 20: 5310
electromagnetic structure of, field-theoretical analysis of, 20: 6304 (TID-22401)
electron scattering by, form factors from, (E/T), 20: 6304 (TID-22401)
form factors of, review of Stanford research on, 20: 6277 (AD-619952)
interactions with mesons (K^-), hyperon (Ξ⁻)-neutron resonance production in, (T), 20: 6073
interactions with mesons (π^+) at 3.29 Bev/c, neutral scalar meson production from, (E), 20: 6079
interactions with electrons, radiative corrections for, (T), 20: 6093
interactions with deuterons at 3.64 Bev/c, N^{8-} and N^{8++} production in (E/T), 20: 6042 (UCRL-16189)
interactions with electrons, elastic, 20: 6276(R) (AD-619576)
reactions (d,α) with beryllium-9, nitrogen-14, oxygen-16, phosphorus-31, and sulfur-32 at 11.8 and 12.0 Mev, (E), 20: 6369
reactions (d,α) and (d,p) with boron-11 and oxygen-16 at 0.2 to 1 Mev, analysis of, (T), 20: 6281 (CEA-R-2807)
reactions (d,α) with beryllium-9 and carbon-12 at 11 Mev, alpha spectra from, (E), 20: 6360
reactions (d,α) with magnesium-24, magnesium-25, and silicon-28 at 11.45 and 12.10 Mev, (E), 20: 6369
reactions (d,d) and (d,pγ) with carbon-12 at 2.8 to 3.7 Mev, angular distributions from, (E/T), 20: 6362
reactions (d,n) with deuterium in self-regenerating metal targets, (E/T), 20: 6334
reactions (d,pγ) with magnesium-25 at 3.00 and 5.22 Mev, angular correlations in, (E), 20: 6410
reactions (d,pγ) with nitrogen-14, gamma spectra from, (E), 20: 5928(R) (PR-P-66)
reactions (d,p) and (d,t) with nickel isotopes, nuclear structure studies using, 20: 6435
reactions (d,p) with boron-10 at 5.1 and 6.07 Mev, differential cross section for, (E), 20: 5759
reactions (d,p) with iron-58 and nickel and zinc isotopes, angular distributions and energy spectra of, (E), 20: 6422
reactions (d,t) at 15 Mev, energy levels from, (E), 20: 6310
reactions with deuterium, use of (d,p) for monitoring (d,n), (E), 20: 5777
reactions with nitrogen-14, oxygen-15 gamma transitions from, (E), 20: 6318
reactions with nuclei, L-space localization in stripping, 20: 6394
yields from meson (π^-) capture by nuclei, (E/T), 20: 6292 (NP-15601)
DIABETES
radioinduced pituitary ablation for treatment of retinopathy resulting from, 20: 5468
DIALYSIS

use of fluoridated water in hemo-, 20: 5237(R) (UR-668, pp 55-109)
DIARRHEA
radioinduced in rats, therapeutic effects of serum from irradiated rabbit, 20: 5411
DIELECTRICS
electromagnetic wave reflection from inhomogeneous, signal from, (T), 20: 6445 (AD-617619)
DIET
calcium content in human, effects on strontium-90 uptake by bones of, 20: 5263
effects of rachitogenic, on response of growing bones to cortisol, 20: 5234(R) (COO-119-232, pp 122-52)
DIFFERENTIAL EQUATIONS
Liouville theorem for, general forms of, 20: 5830 (CERN-65-38)
solutions of set of coupled second-order, for many-body problems, 20: 6120
transients in linear systems, total time integrals of, (T), 20: 5681 (MLM-1288)
DIFFRACTION
problems of electromagnetic wave, in anisotropic media, (T), 20: 5922 (AD-618689)
DIODES
fabrication of compensated p-i-n germanium, (E), 20: 5702
radiation effects on transistor, gamma and neutron, 20: 5808 (N65-35081)
thresholds for tunnel, in switching circuits, (E), 20: 5700
uses of low- and high-peak-current tunnel, in cascade circuits, (E), 20: 5699
DIOXANE
radioinduced scintillation in, effects of radioprotective compounds on γ, 20: 5422
$(NH_4)_2CO_3$–1-butanol–dioxane, use in paper chromatography of compounds labeled with iodine-125 and iodine-131, 20: 5515
DIRECT ENERGY CONVERSION DEVICES
development, 20: 6551
DISASTERS
analysis of Wood River Junction criticality incident, 20: 5666 (TID-21995)
DISCONNECTS
design for collimator and shutters of x-ray tubes, 20: 5693
DISEASES
radiodiagnosis of thyroid, gamma camera for, 20: 5467
DITHIZONE
solvent properties for bismuth and lead, 20: 5505
DOGS
care of experimental colony of, 20: 5231(R) (COO-119-232, pp 65-7)
dental eruption pattern of beagles, 20: 5232(R) (COO-119-232, pp 68-73)
effects of injected radium-226 on, long-term pathological, 20: 5287(R) (COO-119-232, pp 5-64)
effects of injected radium-228 on, long-term pathological, 20: 5287(R) (COO-119-232, pp 5-64)
effects of injected strontium-90 on, long-term pathological, 20: 5287(R) (COO-119-232, pp 5-64)
erythropoiesis in, effects of acute bleeding on, 20: 5301(R) (UR-668, pp 1-54)
excretion of plutonium-239 by, effects of cortisol on, 20: 5247(R) (COO-119-232, pp 188-99)
excretion of strontium-90 by, effects of EDTA, 20: 5248(R) (COO-119-232, pp 200-2)
excretion of yttrium-90 by, effects of EDTA, 20: 5248(R) (COO-119-232, pp 200-2)
immune reactions to renal transplants in, effects of irradiating transplantation site on, 20: 5344
metabolism of proteins in blood serum of, tracer study, 20: 5249(R) (COO-119-232, pp 203-18)
metabolism of selenium-75 in, 20: 5262
osteoid content of vertebral bones of, effects of age, 20: 5233(R) (COO-119-232, pp 99-121)
radiation effects on gastric secretion and blood riboflavin content in, x, 20: 5384
radiation effects on metabolism of electrolytes and nitrogen in, from injected sodium-24, β and γ, 20: 5381
radiation effects on mechanical strength of bones of, from deposited radioisotopes, 20: 5289(R) (COO-119-232, pp 88-98)
radiation effects on cardiopulmonary system of, x, 20: 5301(R) (UR-668, pp 1-54)
radiation effects on exercise tolerance of, x, 20: 5301(R) (UR-668, pp 1-54)
radiation effects on, late manifestations of acute, x, 20: 5301(R) (UR-668, pp 1-54)
radiation effects on erythropoiesis in, x, 20: 5301(R) (UR-668, pp 1-54)
radiation effects on renal functions of, x, 20: 5301(R) (UR-668, pp 1-54)
radiation effects on, effects of trauma, x, 20: 5302(R) (UR-668, pp 161-6)
radiation effects on reproductive fitness of, x, 20: 5301(R) (UR-668, pp 1-54)
radioinduced bone fractures in, after thorium-228 injection, 20: 5288(R) (COO-119-232, pp 74-87)
radioinduced myocardial necrosis in, x, 20: 5301(R) (UR-668, pp 1-54)
DOSIMETERS
charging and reading instrument for, design of, 20: 5799(P)
cleaning technique for silver metaphosphate, 20: 5742(R) (UCRL-14351)
design and performance of silver-activated glass, for gamma and x radiation, 20: 5745(R) (UR-668, pp 117-23)
design of ion chamber type, with aural warning, 20: 5803(P)
development of stimulated luminescence, 20: 5742(R) (UCRL-14351)
development with transmitters for continuous centralized recording of individual doses, 20: 5749
efficiency of gamma, method for calculating, 20: 5750
performance of silver-activated metaphosphate glasses for neutron, 20: 5713 (AD-623384)
performance of silicon surface-barrier, for alpha particles, 20: 5721 (CLOR/IBJ-II-37/D)
performance of solid-state, for fission fragments and neutrons, 20: 5719 (CEA-R-2846)
DROSOPHILA
radiation effects on behavior of larvae of, 20: 5295 (NP-15559)
radiation effects on reproduction in, 20: 5296(R) (NP-15585)
radiation effects on, genetic, x, 20: 5338
radioinduced mutations in, x, 20: 5358
DRUGS
effects of α-methyldopa and hydrochlorothioazide, on blood pressure, 20: 5237(R) (UR-668, pp 55-109)
labeling of Noveril with carbon-14, 20: 5564
DUSTS
analysis for lead-210, radiochemical, 20: 5505
DYSPROSIUM
alpha reactions (α,x$n\gamma$) at 27 to 52 Mev, gamma spectra from, (E), 20: 6348
oxidation of, kinetics of high-temperature, 20: 5859
DYSPROSIUM ALLOYS
Dy–Au, oxidation of, kinetics of high-temperature, 20: 5859
Dy–Y, electric conductivity at low temperatures, 20: 5888 (NP-15592)
Dy–Zr, metallurgical properties and phase studies on, 20: 5891(R) (NYO-2159-1)
DYSPROSIUM ISOTOPES Dy-158
energy levels, (E), 20: 6366
DYSPROSIUM OXIDES
phase transformations in, at 50 to 1500°C, 20: 5536
reactions with Hastelloy-X at 1850°F, 20: 5850

E

EARTH
cosmic radiation reflection from atmosphere of, satellite measurements of, 20: 6019
structure of, use of nuclear explosions for determining internal, 20: 5610
ECOLOGY
of insects, tracer studies, 20: 5815 (STI/DOC/10/44)
oriental fruit moth, tracer study, 20: 5246
research programs of AEC on freshwater, 1965, 20: 5245 (TID-13358 (2nd Rev.), pp 89-126)
research programs of AEC on terrestrial, 1965, 20: 5244 (TID-13358 (2nd Rev.), pp 3-88)
EGGS
incorporation of carbon-14 in fish, 20: 5261
radiation effects on development of chick embryos from, x, 20: 5306
EINSTEINIUM ISOTOPES E_{s}-252
decay scheme for, analysis of, (E/T), 20: 6305 (UCRL-11784)
EINSTEINIUM ISOTOPES E_{s}-254
decay scheme for, analysis of, (E/T), 20: 6305 (UCRL-11784)
ELECTRIC ARCS
energy transfer to fluid streams, 20: 6178(P)
plasma generation by, performance of spark-plug starter for, (E), 20: 6489
plasma production by, in chamber with ablating walls, (E), 20: 6488
properties in air, argon, carbon dioxide, and nitrogen, in gravitationless state, 20: 6163
properties of high-pressure high-current argon, (E/T), 20: 6177
ELECTRIC CELLS
properties of lithium-tellurium system, 20: 6666(R) (ANL-7115, pp 68-77)
ELECTRIC CHARGES
radiation production by uniformly rotating, in plasma, 20: 6456 (AD-619888)
ELECTRIC CONDENSERS
description of low-inductance high-voltage, (E), 20: 5688(T) (UCRL-Trans-1273(L))

radiation response in, method for reduction of, 20: 5805(R) (AD-617782)
ELECTRIC CONDUCTIVITY
magnetohydrodynamic characteristics and dispersion relation for finite, (T), 20: 6157 (AD-617898)
ELECTRIC CURRENTS
distributions in transient plasma, measurement using Rogowski coils, 20: 6509
generation of a-c, design of magnetohydrodynamic generator for, 20: 6026(P)
ELECTRIC DISCHARGE
current in high vacuum, 20: 6169
properties of high-current low-voltage, in potassium-seeded helium, (E/T), 20: 6159 (AERE-M-1597)
properties of, in low-pressure region in gases, 20: 6167
ELECTRIC FIELDS
effects of vortex, on diffusion of inhomogeneities in weakly-ionized plasma, (T), 20: 6482
effects on charged-particle scattering in plasma, (T), 20: 6497
effects on radiolysis of liquid hydrocarbons, 20: 5575
ELECTRIC INSULATORS
development for nuclear thermionic generating system, (E), 20: 6023(R) (AD-619379)
development for radiation protection of coaxial cables and electric condensers, 20: 5805(R) (AD-617782)
performance in fission fragment and neutron dosimetry, 20: 5719 (CEA-R-2846)
ELECTRIC POWER
generation by nuclear thermionic system, research on, (E), 20: 6023(R) (AD-619379)
generation of, use of radioisotopes as heat source for, 20: 5821
ELECTRIC PROBES
design and performance for charged-particle beam diagnostics, (E), 20: 5686(T) (NP-tr-1313)
design and performance for space potential determination in neon glow discharges, 20: 6164
performance of electrostatic, effects of MGD boundary layer on, (T), 20: 5689
ELECTRICITY
production of, economics of, 20: 6611 (HW-SA-3669)
transients in linear systems, total time integrals of, (T), 20: 5681 (MLM-1288)
ELECTROCHEMISTRY
cell development and performance for continuous plutonium electrowinning, 20: 5839(R) (RL-SEP-244(Del.))
ELECTRODES
design and performance of, for use in electric probes, (E), 20: 5686(T) (NP-tr-1313)
mechanisms of lithium hydride cell, kinetic, 20: 6024(R) (ANL-6925, pp 235-47)
radiation effects on surfaces of copper correlation of high-vacuum breakdown with electron, 20: 5809
ELECTROLUMINESCENCE
performance of electroluminescent image intensifiers for monitoring electron and gamma beams, (E), 20: 5773
ELECTROLYSIS
performance for titanium and zirconium production, 20: 5604(P)
ELECTROLYTES
radiation effects on metabolism in dogs of, β and γ, 20: 5381
transport in rabbit lens in culture of, tracer study, 20: 5256
ELECTROLYTIC CELLS
development of regenerative bimetallic and lithium hydride, 20: 6024(R) (ANL-6925, pp 235-47)
regeneration of bismuth–sodium, liquid-vapor relations in, 20: 6024(R) (ANL-6925(p.235-47))
ELECTROLYTIC SEPARATION PROCESSES
development of, for titanium and zirconium, 20: 5604(P)
ELECTROMAGNETIC FIELDS
charged particle beams in, effects of image and space charges on, (T), 20: 5928(R) (PR-P-66)
intensity inside current-carrying region, (T), 20: 5930
ELECTROMAGNETIC LENSES
aberration in compound quadrupole, analysis of spherical, (T), 20: 5696
beam transport in, first- and second-order theory of, 20: 5944 (SLAC-PUB-132)
ELECTROMAGNETIC WAVES
absorption and emission in inhomogeneous collision-free plasma via mode conversion, (T), 20: 6506
diffraction and scattering of, in anisotropic media, (T), 20: 5922 (AD-618689)
dispersion relations for, magnetohydrodynamics of finite conductivity in, 20: 6157 (AD-617898)
interactions in cold magnetoactive plasma, 20: 6484
interactions with plasma, nonlinear, (E), 20: 6457 (AD-622876)
reaction with silver foils, plasma radiation from, 20: 6548
reflection from inhomogeneous plasma, signal from, (T), 20: 6445 (AD-617619)
ELECTROMAGNETISM
field equations for, dimensionality of real world from strength of, 20: 6218
ELECTRON BEAMS
current pulses from betatron injector, recording of, 20: 5958
density of ultrarelativistic colliding, limitations in, (T), 20: 5950
effects on activity of dry dehydrogeneses, chemical, 20: 5276
effects on copper electrode surfaces, correlation with high-vacuum breakdown of, 20: 5809
effects on parametria, intestinal injuries from, 20: 5392
interactions Maxwellian collision-free plasma, low-frequency electronic oscillations from, (T), 20: 6503
interactions with plasma, wave excitation in, (T), 20: 6474
interactions with electromagnetic waves in oscillators, use of pulsed magnetic fields with, 20: 5929
leakage from storage rings, due to amplitude and frequency variations of compensating field, (T), 20: 5949
monitoring low-intensity 600-Mev, using electroluminescent image intensifier, (E), 20: 5773
reactions with alkali-metal magnetoplasma, enhanced diffusion from, 20: 6466 (SIT-2813-33)
reactions with helium gas, optical excitation functions for, (E/T), 20: 5748(T) (UCRL-Trans-1266(L))
use for radiotherapy of tumors, 20: 5453
ELECTRON LENSES
image properties of three-electrode, 20: 5687(T) (UCRL-Trans-1237(L))
ELECTRON MICROSCOPY
development of staining methods for biological, 20: 5250(R) (UR-668, pp 110-16)
ELECTRON MULTIPLIER TUBES
use for ion detection in mass spectrometers, 20: 5706
ELECTRON PAIRS
production by bremsstrahlung in nuclear Coulomb field, radiative corrections to, (T), 20: 6072
ELECTRON TUBES
beam-wave interactions in, use of pulsed magnetic fields with resonant, 20: 5929
plasma electric conductivity in, for switching circuits, 20: 6449 (AD-619370)
ELECTRONIC EQUIPMENT
design and performance of general-purpose, (E), 20: 5680 (ELI-91)
design for electron detection by Lincoln Experimental Satellite, 20: 6184 (AD-619977)
design of delay-line clipping circuits having source termination, (E), 20: 5701
design of routing system for multichannel analyzers, (E), 20: 5769
design using tunnel-diode cascade circuits, (E), 20: 5699
performance for signal analysis in noise background by data accumulation, (T), 20: 5695
transients in linear, total time integrals of, (T), 20: 5681 (MLM-1288)
ELECTRONICS
review of research at University of Edinburgh on, 20: 5239
ELECTRONS
acceleration using betatron magnetic fields, 20: 5961
angular distributions, energy spectra, and fluxes of 150-kev, along magnetic field line near L = 5.6, (E), 20: 6196
cyclotron resonance instability in plasma, effect of Landau damping on, (T), 20: 6458 (CLM-R-44)
density and temperature in standing layers of hydrogen discharge, (E), 20: 6476
density and temperature in high-pressure xenon plasma, 20: 6480
density and temperature in ionosphere, (E), 20: 6199
density and velocity behind shock waves in plasma, laser beam diagnostics of, (E), 20: 6490
density distribution in auroral echoes, 20: 6182(R) (AD-619447)
density in ionospheric D region, techniques for measuring, (E), 20: 6185 (AFCRL-65-620)
density in plasma, measurement using laser interferometers, 20: 6471
detection and discrimination by semiconductor counters, (E), 20: 5732 (KFK-335)
detection and measurement of, Lincoln Experimental Satellite equipment for, 20: 6184 (AD-619977)
detection of secondary, scintillation detector for, 20: 5757
detection using lithium-drifted germanium and silicon detectors, 20: 5784
Dirac theory for relativistic, formalism of, 20: 6223
distribution in magnetosphere, from hydromagnetic wave dispersion characteristics, (T), 20: 6202
distributions in earth's magnetic field, diffusion equations for, 20: 6183 (AD-619821)
dosimetry of therapeutic, use of photographic film detectors for, 20: 5480

effects on carbon dioxide reduction by hydrogen, 20: 5574
effects on cyclopentane, isopentane, and neopentane, 20: 5576
effects on electric conductivity of aluminum and aluminum alloys, stage I and II recovery from, 20: 5918
effects on liquid hydrocarbons in presence of electric field, 20: 5575
effects on silicon, annealing of, 20: 5920
effects on thermal conductivity of single crystals of silicon, (E), 20: 5919
electric dipole moment at high momentum transfers, (E), 20: 6064
emission of δ rays in ion track formation in nuclear emulsions and solids, 20: 5755
emission of 40-kev, from sun, (E), 20: 5971
energy losses in nitrogen, 20: 5542
injection into artificial radiation belt, from Starfish explosion, 20: 6209
interactions with atoms, conference on, 20: 5988(T) (JPRS-32421)
interactions with deuterons and protons, radiative corrections for, (T), 20: 6093
interactions with mesons (π) at 16 Bev/c, cross sections for, (E), 20: 6098
interactions with plasma, heating effects in, 20: 6468(T) (ORNL-tr-871)
interactions with cosmic mesons (μ) at 5 to 50 Bev, (E), 20: 6007 (CONF-640919, pp I43-8)
interactions with photons in plasma, transport phenomena in, (T), 20: 6448 (AD-619045)
interactions with polarized positrons, selection rules for annihilation, (T), 20: 6040 (NP-15602)
interactions with protons at 4 Bev, heavy electron production from, (E), 20: 6078
interactions with electrons, effects of beam parameters on, 20: 6276(R) (AD-619576)
interactions with deuterons, elastic, 20: 6276(R) (AD-619576)
magnetic moment of free, g-factor for, 20: 6282 (CERN-64-13(Vol.4), pp 97-136)
precipitation of relativistic, in mesosphere at subauroral latitudes, (E), 20: 6201
production in cosmic-ray reactions in carbon, (E), 20: 6017
quantum noise operators for one, in n-level system subjected to fluctuating forces or heatbath, 20: 6002
reactions (e,e'p) with nuclei, Monte Carlo analysis of, 20: 6286 (ISS-65/10)
reactions at high energies, review of Stanford research on, 20: 6277 (AD-619952)
reactions of hydrated, with inorganic and organic compounds, 20: 5525 (IA-1041)
reactions with alkyl halides in organic glasses, free radical production in, 20: 5577
reactions with atoms and molecules, ionization cross sections for, (E/T), 20: 5989
reactions with molecular hydrogen, dissociation in, 20: 5579
reactions with nonpolar and polar molecules, cross sections for momentum transfer and drift velocities in, 20: 5985 (ORNL-TM-1262)
reactions with nuclear Coulomb field, cross sections for meson (μ^-) production in, (T), 20: 6089
reactions with nuclei at 2.5 to 4.0 Mev, bremsstrahlung spectra from, (E), 20: 6432
reactions with silicon-29, anisotropic hyperfine, (T), 20: 6001
recombination by two-body collisions in ion field, (T), 20: 5994
scattering by calcium-40 and -44 at 250 Mev, charge distributions from, (E), 20: 6413
scattering by carbon-12 at 100 Mev, electron electric dipole moment from, (E), 20: 6064
scattering by deuterons, form factors from, (E/T), 20: 6304 (TID-22401)
scattering by helium-3, inelastic continuum in, 20: 6277 (AD-619952)
scattering by hydrogen, resonance structure from elastic, (E), 20: 5999
scattering by neon, spin polarization from elastic, (T), 20: 5998
scattering by nitrogen, excitation of nitrogen(V) ions in, (T), 20: 5982 (AERE-R-5061)
scattering by nuclei, radial relativistic Coulomb integrals for, (T), 20: 6375
scattering by nuclei, two-nucleon correlation functions and cross sections for inelastic, (T), 20: 6424
scattering by polarized holmium-165, 20: 6275(R) (AD-619534)
scattering by targets in linear accelerator, review of research on, 20: 6276(R) (AD-619576)
scattering of, coincidence studies of elastic, 20: 6277 (AD-619952)
scattering on atoms, Mott polarization effect in fast, 20: 5992
spectra of californium-252 fission-induced, (E), 20: 6298(R) (PPAD-2137-566)
spectra of radioisotope decay-induced, (E), 20: 6298(R) (PPAD-2137-566)
temperature in positive-column low-pressure argon discharges, 20: 6475
tunneling in superconductors, entropy transport from, (T), 20: 6248

ELECTROSTATIC ANALYZERS
performance, 20: 5691

ELECTROSTATIC GENERATORS
ion source for, autofocusing, 20: 5957
performance for polymer aerosols, 20: 5237(R) (UR-668, pp 55-109)

ELECTROSTATIC LENSES
image properties of three-electrode, 20: 5687(T) (UCRL-Trans-1237(L))

ELECTROSTATIC PRECIPITATORS
performance for dust-sampling, 20: 5237(R) (UR-668, pp 55-109)

ELEMENTARY PARTICLES
angular momenta of, effects of angle on, 20: 6154
conference on cosmic-ray physics for high-energy interactions of, 20: 6006 (CONF-640919)
decay of, renormalization of semileptonic weak coupling constants for, (T), 20: 6140
decays of hadrons, SU(3) in renormalization of vector constants of weak, 20: 6148
detection of basic triplets in cosmic radiation, experiment for, 20: 6010 (CONF-640919, pp II23-7)
field theory of, bootstrap condition in, 20: 6138
interactions above 100 Bev, balloon-borne system for investigating, 20: 5724 (CONF-640919, pp II13-23)
interactions and properties of, 20: 6034 (CERN-64-13(Vol.4))
interactions at high energy, range of, (T), 20: 6153
interactions at 300 Bev in cosmic radiation, proposed system for investigating, 20: 5725 (CONF-640919, pp II27-30)
interactions in axiomatic field theory, review of strong, 20: 6101 (BNL-9652)
interactions in coordinate space, singular logarithmic potentials of, 20: 6121
interactions in nonlocal solvable potential, wave functions for bound-state, 20: 6119
interactions of strongly interacting, T violation in electromagnetic, (T), 20: 6059
interactions of three relativistic, SU(3) classification of bound-state, 20: 6113
interactions of, crossing symmetric Regge representation for invariant amplitude of, 20: 6115
interactions of, higher-order corrections to, (T), 20: 6057
interactions of, momentum dependence of S matrix for many-body, 20: 6061
interactions of, off-shell equations for two-body, (T), 20: 6139
interactions of, quantum field theory for one-particle singularities of S-matrix in, 20: 6122
interactions of, review of weak, 20: 6035 (CERN-64-13(Vol.4), pp 1-49)
interactions of, singular N/D equations for, 20: 6131
interactions of, solution of singular N/D equations for, 20: 6130
interactions of, threshold Regge poles in coupled many-channel, 20: 6118
interactions to 10^{12} ev, magnetic cloud chamber for study in cosmic radiation, 20: 5722 (CONF-640919, pp 12-43)
kinematics of system of two, unitary representations of Galilei group for, 20: 6124
mass operators in combined invariance theories for, Hermitian, 20: 6136
model for, Green functions of Thirring, 20: 6128
motion of, momentum invariants and Lorentz covariant forms for, 20: 6214 (INR-610/VI/PB)
properties of quarks, baryon resonance analogies with, 20: 6135
properties of, field-theoretic dispersion relations, mass sum rules, and symmetries, 20: 6109 (NP-15638)
representations in compact and non-compact unitary groups, degeneracy effects on, 20: 6103 (IC/65/80)
representations using non-compact groups, 20: 6102 (IC/65/79)
scattering amplitudes for, Regge-pole representation of, (T), 20: 6062
scattering amplitudes for, approximate solution of N/D equations for multichannel, (T), 20: 6063
symmetries, (E), 20: 6074
symmetries for, Casimir operators for unitary groups in, (T), 20: 6125(T)
symmetries for, connection between external and internal, (T), 20: 6142
symmetries of noncollinear diagrams and the Johnson-Treiman relations for, 20: 6143
symmetries of, testing of broken $\bar{U}(12)$ and approximate $U(6) \times U(6)$, (T), 20: 6066
symmetry for, comparison of $SU(6)_W$ predictions on collinear processes with experiment, (T), 20: 6144
symmetry for, extension of theorem on broken, (T), 20: 6141
symmetry for, $P(SU_6)$, (T), 20: 6145
symmetry for, spin and unitary spin independence in SU(8), (T), 20: 6110
symmetry group for, formalism and properties of $\bar{U}(12)$, 20: 6132
symmetry groups for, spin extension of unitary, 20: 6104 (IC/65/81)
symmetry model for, irreducible representations of B(3), C(3), and D(3) groups for, 20: 6149
symmetry models for, isotopic and spin content of multiplets in SU(4) and SU(3), 20: 6150

symmetry theory Ū(12), multiplet structure of broken, 20: 6058
theory of, dynamics in nonlinear spin, 20: 6112
ELEMENTS
equation of state of, properties of, 20: 6533 (NVO-1163-60)
EMBRYOS
development of *Rana nigromaculata* tadpoles, effects of irradiated pituitary extract from *Bufo bufo* on hypothalectomized, 20: 5394
radiation effects on skeletal development in mouse, x, 20: 5395
radiation effects on development of chick, from exposed eggs, 20: 5306
radiation effects on skeletal development in mouse, x, 20: 5316
radiation effects on gonads of viviparous lizard, x, 20: 5324
radiation effects on skeletal development of mouse, x, 20: 5326
radiation effects on skeletal development in mouse, x, 20: 5327
radiation effects on skeletal development in mouse, x, 20: 5337
strontium-90 toxicity in rat, 20: 5237(R) (UR-668, pp 55-109)
ENERGY
transfer from electric arcs to fluid streams, 20: 6178(P)
transfer in solid proteins of, effects of water content on, 20: 5270
ENGINEERING
systems analysis using analog simulation, 20: 5834 (ORNL-TM-1323)
ENGINEERING TEST REACTOR
experimental facilities for, capsule temperature control in, 20: 6680 (ORNL-TM-1319)
ENZYMES
content of potassium–sodium ATPase, in intestinal epithelium, 20: 5251(R) (UR-668, pp 123-49)
radiation effects on activity of, in gastric juice of dogs, x, 20: 5384
radiation effects on activity of phosphomonoesterases in protozoa, uv, 20: 5272
radiation effects on synthesis of hematic microsomal, in rats, x, 20: 5282(R) (AD-623599, pp 1-15)
radiation effects on synthesis of hepatic microsomal, in rats, x, 20: 5283(R) (AD-623599, pp 16-27)
radiation effects on activity of, in rabbit tissues, γ, 20: 5380
synthesis of hepatic microsomal, effects of age on, in rats, 20: 5283(R) (AD-623599, pp 16-27)
EPITHELIUM
content of potassium–sodium ATPase in intestinal, 20: 5251(R) (UR-668, pp 123-49)
metabolism of thymidine by intestinal, effects of temperature in fish, tracer study, 20: 5374
EQUATION OF STATE
determination of nuclear, from neutron inelastic scattering spectra, (T), 20: 6379
properties of, for elements and geologic materials, 20: 6533 (NVO-1163-60)
EQUIPMENT AND PROCEDURES
design of creep machine for testing to 1300°C by remote operation, 20: 5611 (BNWL-137)
for skull reclamation process, 20: 5594(R) (ANL-6925, pp 21-106)
ERBIUM
alpha reactions (α,xnγ) at 27 to 52 Mev, gamma spectra from, (E), 20: 6348
determination using ammonium oxalate by potentiometric titration, 20: 5519
magnetic structure, (E), 20: 6541
magnetostriction of single crystals of, from 10 to 300°K, (E), 20: 6547
ERBIUM ALLOYS
Er–Th, metallurgical properties and phase studies on, 20: 5891(R) (NYO-2159-1)
Er–Y, electric conductivity at low temperatures, 20: 5888 (NP-15592)
Er–Zr, metallurgical properties and phase studies on, 20: 5891(R) (NYO-2159-1)
ERBIUM IONS
spin-lattice relaxation rates in single crystals of anhydrous lanthanum trichloride, (E), 20: 6542
ERBIUM ISOTOPES Er-160
energy levels of, rotational, (E), 20: 6348
ERBIUM ISOTOPES Er-162
energy levels of, rotational, (E), 20: 6348
ERBIUM ISOTOPES Er-164
energy levels, (E), 20: 6366
energy levels of, rotational, (E), 20: 6348
ERBIUM ISOTOPES Er-166
energy levels of, rotational, (E), 20: 6348
ERBIUM ISOTOPES Er-167
energy level transitions in, E2/M1 mixing ratios and K conversion coefficients in rotational, (E), 20: 6386
ERBIUM ISOTOPES Er-170
neutron capture cross sections at 4 kev to 2 Mev, (E), 20: 6280(R) (ANL-6925(p.249-51)
ERBIUM OXIDES
phase transformations in, at 50 to 1500°C, 20: 5536
ERBIUM PHTHALOCYANINES
preparation and spectra of, 20: 5560
ERYTHROCYTES
fluorescence intensity in frog, effects of temperature on uv, 20: 5318
lysis of human, mechanisms of antibody-induced, 20: 5251(R) (UR-668, pp 123-49)
radiation effects on permeability of, effects of cysteamine and sodium cyanide on, x, 20: 5342
regulation of, role of erythropoietin, 20: 5242
use of tanned, in cell volume determinations, 20: 5301(R) (UR-668, pp 1-54)
ERYTHROPOIESIS
effects of acute bleeding on dog, 20: 5301(R) (UR-668, pp 1-54)
radiation effects on dog, x, 20: 5301(R) (UR-668, pp 1-54)
ERYTHROPOIETIN
effects on erythropoiesis of, 20: 5242
ESCHERICHIA COLI
colicin and phage induction by uv irradiated culture media in, 20: 5279
photoreactivation of uv-induced injuries in, 20: 5347
photosensitivity of, effects of arginine and uracil on, 20: 5348
radiation effects on chromosome replication in, uv, 20: 5349
radiation effects from incorporated tritium in, mutagenic, β, 20: 5350
radiation injuries of, uv, 20: 5347
radiosensitivity of, effects of arginine and uracil on γ and uv, 20: 5348
ESTRADIOL
radiosensitivity effects of, on cervical carcinomas, 20: 5472
ETHANE
electron reactions with, ionization cross sections for, (E/T), 20: 5989
ethane–O, reactions with recoil carbon-11 atoms, 20: 5570 (JUL-228-RC)
ETHANE, BROMO-
reactions with electrons in organic glasses, yields of free radicals from, 20: 5577
ETHANE, CHLORO-
reactions with electrons in organic glasses, yields of free radicals from, 20: 5577
ETHANE, IODO-
reactions with electrons in organic glasses, yields of free radicals from, 20: 5577
ETHANETHIOL, 2-AMINO-
effects on metabolism of hexobarbital in rats, 20: 5283(R) (AD-623599, pp 16-27)
effects on oxygen tension of spleen in mice, 20: 5407(R) (AD-623599, pp 37-44)
effects on radioinduced permeability of erythrocytes, 20: 5342
effects on sulfhydryl content in mouse spleen, 20: 5407(R) (AD-623599, pp 37-44)
radiosensitivity effects of, in mice, 20: 5407(R) (AD-623599, pp 37-44)
radiosensitivity effects of, on homogenates of Ehrlich ascitic tumor cells, 20: 5412
radiosensitivity effects of, on tissue homogenates of mouse liver, muscle, spleen, and thymus, 20: 5412
radiosensitivity effects on animal cells in tissue culture, 20: 5418
ETHANOL
benzene–ethanol–H_2O, use in paper chromatography of compounds labeled with iodine-125 and iodine-131, 20: 5515
$(NH_4)_2CO_3$–1-butanol–ethanol, use in paper chromatography of compounds labeled with iodine-125 and iodine-131, 20: 5515
ETHER, BIS(CHLOROETHYL)
solvent properties for cobalt, iron, and manganese, 20: 5602
ETHYLAMINE, 2,2'-DITHIOBIS-
effects on immune reactions in irradiated mice, 20: 5413
ETHYLENE
electron reaction with, cross sections for momentum transfer and drift velocities in, 20: 5985 (ORNL-TM-1262)
electron reactions with, ionization cross sections for, (E/T), 20: 5989
radiolysis of, effects of inert gases on, 20: 5582
yields in recoil carbon-11 atom reactions on alicyclic and aliphatic hydrocarbons, 20: 5570 (JUL-228-RC)
ETHYLENE OXIDE
effects on peas, mutagenic, 20: 5238
ETHYLENE POLYMERS
performance of tubes of, in equipment for air monitoring, 20: 5752
Al–polyethylene–U, neutron multiplication in borated, 20: 6577(R) (BNWL-149, pp 22-35)
Al–Pu–polyethylene, neutron multiplication in borated, 20: 6577(R) (BNWL-149, pp 22-35)
Al–Pu–polyethylene, neutron multiplication in borated, 20: 6578(R) (BNWL-149, pp 45-7)
ETHYLENIMINE
effects on peas, mutagenic, 20: 5238
EUGLENA
radiation effects on, laser and uv, 20: 5396
EUROPIUM

diffusion from irradiated cerium–cobalt–plutonium alloy to sodium at 550°C, 20: 5848
separation from actinides and other rare earths by electrophoresis, 20: 5598
EUROPIUM BORIDES
thermionic emission of, on iridium and tungsten substrates, (E), 20: 5532(T) (K-Trans-10)
EUROPIUM ISOTOPES Eu-147
decay of, γ-γ angular correlations in, 20: 6396
EUROPIUM ISOTOPES Eu-152
beta decay of, conversion coefficients from, (E), 20: 6303 (TID-22393)
EUROPIUM ISOTOPES Eu-154
beta decay of, β-γ directional correlation and conversion coefficients from, (E), 20: 6303 (TID-22393)
EUROPIUM ISOTOPES Eu-156
beta decay of, γ-γ coincidences from, (E), 20: 5928(R) (PR-P-66)
EUROPIUM ISOTOPES Eu-158
beta decay, (E), 20: 6403
EUROPIUM OXIDES
phase transformations in, at 50 to 1500°C, 20: 5536
EXCRETORY SYSTEMS
radiography of, radiation hazards to patient and personnel during, 20: 5459
EXPERIMENTAL BREEDER REACTOR-II
development and operation, 20: 6600(R) (ANL-7105, pp 1-35)
development, Oct. 1965, 20: 6601(R) (ANL-7115, pp 1-41)
fuel burnup in, analysis of, 20: 6600(R) (ANL-7105, pp 1-35)
fuel cycle facility of, operations summary for, 20: 5594(R) (ANL-6925, pp 21-106)
fuel element burnup in, ceramic and metallic, 20: 6558(R) (ANL-7115, pp 42-67)
fuel processing development for, 20: 6601(R) (ANL-7115, pp 1-41)
fuel rod burnup testing, 20: 6601(R) (ANL-7115, pp 1-41)
EXPERIMENTAL GAS COOLED REACTOR
housing for, engineering drawings of, 20: 6645
loading machine for, engineering drawings of, 20: 6646
moderator irradiation stability, graphite, 20: 5849
EXPONENTIAL PILES
performance of accelerator-beam-driven, as pulsed neutron sources, (E), 20: 6257 (CONF-650217, pp 11-24)
EXTRACTION APPARATUS
design of high-temperature metal-salt, 20: 5594(R) (ANL-6925, pp 21-106)
EYES
electrolyte transport in rabbit lens in tissue culture, tracer study, 20: 5256
physiology of, role of epithelium and capsule in transport of electrolytes in lens cultures, 20: 5256
radiation effects on mitosis in cornea of mouse, effects of head shielding on x, 20: 5421
radiation effects on mitosis in cornea of mouse, effects of ganglionic blocking drugs, x, 20: 5421
radiation effects on metabolism in lens of, effects of age in cattle and guinea pigs, x, 20: 5333

F

FALLOUT
age estimation of, by determination of barium, 20: 5603
deposition of, meteorological factors affecting, 20: 5678
effects on radioactivity of foods, 20: 5431
from stratosphere of, meteorological factors in, 20: 5649(R) (COO-1340-2, pp 54-83)
gamma spectra from simulated, 20: 5653
gamma spectra of, 1963, 20: 5652
monitoring in atmosphere, milk, and rain water in New Zealand, 1965, 20: 5664(R) (NP-15639)
monitoring in Canada, 1963 and 1964, 20: 5415
monitoring in Denmark, 1964, 20: 5651 (RISO-107)
monitoring in Great Britain, 1963 and 1964, 20: 5415
monitoring in Kansas, 1962, 20: 5648(R) (COO-1340-2, pp 1-53)
monitoring in Missouri, 1962, 20: 5648(R) (COO-1340-2, pp 1-53)
monitoring in U. S., 1963, 20: 5649(R) (COO-1340-2, pp 54-83)
monitoring of, in Italy by strontium-90 content of deciduous teeth collected in 1962, 20: 5655
monitoring, cesium-137, ruthenium-106, and zirconium-95 in rain water in Bombay, 1963, 20: 5661 (AEET-215)
performance of fast-burst, as pulsed neutron sources, (E), 20: 6671 (CONF-650217, pp 1-10)
protection against, design of motor vehicles for, 20: 5679(P)
protection against, testing vertical wall barrier for, 20: 6516 (AD-617524)
protection of populations against, from thermonuclear explosion, 20: 5416
seasonal and short-period variations in, effects of cyclonic activity on, 20: 5650(R) (COO-1340-2, pp 84-109)
transport mechanisms for stratospheric, 20: 5650(R) (COO-1340-2, pp 84-109)
transport of stratospheric, to troposphere, meteorological factors in, 20: 5649(R) (COO-1340-2, pp 54-83)
FAST REACTORS
breeding and fuel element processing for, pyrochemical batch-extraction, 20: 6600(R) (ANL-7105, pp 1-35)
cost factors of metal-fueled, 20: 6553(R) (ANL-6925, pp 255-63)
criticality of, computer programs for calculating, 20: 6583 (JAERI-1091)
design for use in oil wells, 20: 6651(P)
development in France, review of, 20: 6643
fuel burnup experiment for breeder, design of molten plutonium, 20: 6613 (LA-DC-7475)
fuel development for, 20: 6600(R) (ANL-7105, pp 1-35)
fuel development for, 20: 6601(R) (ANL-7115, pp 1-41)
fuel processing development for, 20: 6601(R) (ANL-7115, pp 1-41)
fuels for, preparation methods of, 20: 5594(R) (ANL-6925, pp 21-106)
kinetics of SNEAK, 20: 6674 (KFK-332)
kinetics of zero-power, 20: 6674 (KFK-332)
macrostructure for, safety aspects of, 20: 6602 (BNWL-SA-346)
performance of accelerator-beam-driven exponential, as pulsed neutron sources, (E), 20: 6257 (CONF-650217, pp 11-24)
performance of mechanically pulsed neutron-burst-producing, (E), 20: 6672 (CONF-650217, pp 25-35)
safety studies on, 20: 6552(R) (ANL-6925, pp 187-233)
FECES
analysis for lead-210, radiochemical, 20: 5505
processing aboard space vehicles, using electric-power plants, (E/T), 20: 5820 (NASA-CR-316)
FERMIONS
density matrix for system of non-interacting, (T), 20: 6147
interactions in many-body systems of, vertex theory of, 20: 6111
interactions of spin-½, threshold Regge poles in coupled-channel, 20: 6118
interactions with bosons, model field theory for amplitudes of, 20: 6116
superfluidity of liquids of, (T), 20: 6237
symmetry groups for, spin extension of unitary, 20: 6104 (IC/65/81)
theory of superfluid liquids of, 20: 6229
FERRITIN
radiation effects on metabolism of injected, in rats, 20: 5354
FERROMAGNETIC MATERIALS
magnetic properties of, 20: 6531 (AD-623530)
FETUSES
iodine-131 uptake by human, effects of age on, 20: 5259
radiosensitivity of human, x, 20: 5476
FIBRIN
radioinduced lysis of, in rabbits, x, 20: 5325
FIBRINOGEN
effects of ϵ-aminocaproic acid on rat-blood, 20: 5436(R) (UR-668, pp 149-60)
effects of ϵ-aminocaproic acid on iodine-131-labeled, in rats, 20: 5436(R) (UR-668, pp 149-60)
localization of iodine-131-labeled, mechanisms in rat tumors, 20: 5436(R) (UR-668, pp 149-60)
localization of iodine-131-labeled in rat carcinomas, methods of, 20: 5436(R) (UR-668, pp 149-60)
FIELD THEORY
elementary particle strong interactions in axiomatic, review, 20: 6101 (BNL-9652)
elementary particle dynamics in, 20: 6112
elementary particle dispersion relations, mass sum rules, and symmetries in, 20: 6109 (NP-15638)
elementary-particle bootstrap theory in, 20: 6138
formalism of conservation principles and Lagrange invariance in quantized, 20: 6155
formulation of unified electromagnetic-gravitational, dimensionality of real world from, 20: 6218
properties of quantum linearized Einstein, (T), 20: 6224
properties of rotationally symmetric Euclidean-invariant nonrelativistic model scalar, 20: 6117
quantization in general-relativity, Dirac procedure for, 20: 6219
S-matrix in quantum, one-particle singularities of, 20: 6122
scattering amplitude in quantum, analytic properties of unitarity integral for elastic, 20: 6114
scattering amplitudes in model, boson-fermion, 20: 6116
scattering amplitudes in, effects of S-matrix unitarity on inelastic, (T), 20: 6105 (ISS-65/14)
solutions of Chew-Low equations in, with finite numbers of poles, 20: 6106 (JINR-P-2369)
Thirring model in, Green functions of, 20: 6128

FILMS
critical currents in superconducting, applied magnetic field and temperature dependence of, (E), 20: 6232
magnetic properties of superconducting, in nonlocal regime, (T), 20: 6250
quantum effects in thin superconducting, (T), 20: 6242
FILTERS
design and performance of electrophoretic, for reactor water,. 20: 6568
FILTRATION
of hydrolyzed plutonium hexafluoride, 20: 5595(R) (ANL-6925, pp 107-64)
FISH
incorporation of carbon-14 in eggs of, 20: 5261
radiation effects on metabolism of thymidine in intestinal epithelium of, 20: 5374
radiation injuries of, effects of temperature on, 20: 5374
FISSION
gamma emission in, review, 20: 6300 (SGAE-PH-29/1965)
spectra from, liquid-drop model with shell effects for energy and mass, (T), 20: 6308(T) (ANL-Trans-243)
FISSION CHAMBERS
design and performance of miniature, 20: 5734 (LFEN-NI-19)
design of pulse counting, 20: 5800(P)
development of regenerating, for in-pile flux measurements, 20: 6567 (HW-SA-3600)
performance for in-pile gamma and neutron detection, (E), 20: 5728 (IBM-65-825-1487)
radiation effects testing of pulse-operating, (E), 20: 5807 (AEEW-M-493)
FISSION FRAGMENTS
angular distributions from photofission of even-even nuclei, (E), 20: 6309(T) (ANL-Trans-245)
detection in nuclear emulsions and solids, 20: 5755
dosimetry of, performance of insulators for, 20: 5719 (CEA-R-2846)
effects on coalescence rates in liquid-liquid systems, mechanism of, 20: 5571 (ORNL-TM-1283)
ionizing effects in carbon dioxide, propane, and nitrogen, 20: 5734 (LFEN-NI-19)
kinetic energy of uranium-233 and -235, (T), 20: 6421
neutron emission by excited, (T), 20: 6313
FISSION PRODUCTS
deposition of, recommendation of standard surface for studies on, 20: 5665 (ORNL-TM-1304)
diffusion from hydrided uranium–zirconium, 20: 5844
diffusion from urania fuel rods of cored pellets or vibratory compacted powders, gaseous, 20: 5914(R) (GEAP-3771-17)
diffusion from urania cored pellet fuels at 1530 and 1680°C, gaseous, 20: 5914(R) (GEAP-3771-17)
diffusion gas from urania single crystals, 20: 5843
diffusion in urania, effects of density on gaseous, 20: 5848
distribution in irradiated urania, relation of microstructure and, 20: 5848
distribution in urania fuel rods irradiated with gross central melting, 20: 5914(R) (GEAP-3771-17)
neutron cross sections of, for use in SIZZLE code, 20: 6659 (NAA-SR-Memo-11473)
reactor criticality effects of gas bubble, in LAMPRE, 20: 6614 (LA-DC-7476)
separation from fast reactor blankets and fuels, methods for, 20: 6553(R) (ANL-6925, pp 255-63)
separation from uranium by skull reclamation process, flowsheets for, 20: 5594(R) (ANL-6925, pp 21-106)
separation of barium from, by precipitation as sulfate, 20: 5603
FISSIUM
fissium–Pu–U, burnup studies, 20: 6600(R) (ANL-7105, pp 1-35)
fissium–Pu–U, chloride slagging of, reactions of cerium and zirconium in, 20: 5594(R) (ANL-6925, pp 21-106)
fissium–Pu–U, phase studies on, 20: 5876 (ANL-6974)
fissium–Pu–U–Zr, phase studies on, 20: 5876 (ANL-6974)
fissium–Pu–U, reactions with vanadium–20 titanium at 550 to 700°C, 20: 5843
FLOWMETERS
development for use in boiling reactors, (E), 20: 6648(R) (HPR-64)
FLUID FLOW
dynamics of, in natural circulation loops, 20: 5620 (AE-200)
equations of MHD, for finite—conductivity medium with mass forces, 20: 6171
equations of rotational MHD, in planar-magnetic and gravitational fields, 20: 6172
heat transfer stability in, above critical point, (T), 20: 5622 (ANL-7032)
magnetohydrodynamic, from oscillating dielectric sphere, (T), 20: 6161 (NP-15630)
magnetohydrodynamic, heat transfer in transient, (T), 20: 6176
measurement of, use of radioisotopes for, 20: 5817
momentum flux measurement in two-phase, 20: 5624 (MIT-3496-1)
propagation of weak disturbances in MHD, (T), 20: 6170
properties of magnetohydrodynamic, 20: 6156 (AD-617562)
volumetric concentration in two-phase, equations for average, 20: 5629
FLUID FLOW (LAMINAR)
stability of, between parallel planes, 20: 5621 (AEEW-R-416)
FLUID FLOW (TURBULENT)
characteristics of three-dimensional motions of air, 20: 5645(R) (COO-1340-2, pp 122-45)
measurement in vortex tubes, 20: 6652 (D-910091-5)
measurement in vortex tubes, 20: 6653 (D-910091-7)
FLUID FUEL REACTORS
characteristics of molten-salt-fueled homogeneous, catalog, 20: 6554 (ANL-7092)
FLUIDIZATION
combustion of graphite-base reactor fuels, acid leaching of products from, 20: 5500 (ORNL-3876)
FLUIDS
equilibrium of relativistic rotating, variational principle for, (T), 20: 5974
FLUORESCENCE
intensity in frog blood cells, effects of temperature on uv, 20: 5318
FLUORIDE VOLATILITY PROCESSES
development and testing of, for plutonium and uranium recovery, 20: 5595(R) (ANL-6925, pp 107-64)
equipment and procedures for uranium recovery from irradiated fuels by, 20: 5595(R) (ANL-6925, pp 107-64)
flowsheets for spent plutonia–urania fuels, 20: 5595(R) (ANL-6925, pp 107-64)
materials corrosion, testing of, 20: 5595(R) (ANL-6925, pp 107-64)
FLUORIDES
effects on *in vitro* calcification, 20: 5237(R) (UR-668, pp 55-109)
formation energies and mechanisms, studies of, 20: 5523(R) (ANL-6925, pp 175-85)
toxicology of, 20: 5251(R) (UR-668, pp 123-49)
FLUORINE
corrosive effects on nickel-200 in volatility environments, 20: 5595(R) (ANL-6925, pp 107-64)
molecular structure of, orbital density in, 20: 5524 (ANL-7076)
reactions with aluminum, magnesium, rare earths, and yttrium, 20: 5523(R) (ORNL-6925, pp 175-85)
reactions with phosphorus, kinetics of, 20: 5523(R) (ORNL-6925, pp 175-85)
reactions with silicon carbide, kinetics of, 20: 5523(R) (ORNL-6925, pp 175-85)
reactions with tantalum diboride, kinetics of, 20: 5523(R) (ORNL-6925, pp 175-85)
use as oxidant in enthalpy determinations, 20: 5523(R) (ORNL-6925, pp 175-85)
FLUORINE ISOTOPES F-18
energy levels, (T), 20: 6281 (CEA-R-2807)
energy levels of, projected Hartree-Fock spectra for, (T), 20: 6419
FLUORINE ISOTOPES F-19
energy level transitions in, E3, (T), 20: 5928(R) (PR-P-66)
energy levels of, projected Hartree-Fock spectra for, (T), 20: 6419
FOOD
processing aboard space vehicles, using electric-power plants, (E/T), 20: 5820 (NASA-CR-316)
radiation effects on wholesomeness of fruits and fruit juices, 20: 5816
radiation preservation of fruit juices, 20: 5816
radioactivity in, of Great Britain, 20: 5409
radioactivity in, natural, fallout, and induced, 20: 5431
FORMALDEHYDE
effects on activity of leukocyte alkaline phosphatase, toxicity, 20: 5269
yields from radiolysis of methanol, 20: 5581
FRANCE
reactor development in, review of fast, 20: 6643
FRANCIUM
separation from actinium by solvent extraction using 4-*sec*-butyl-2-α-methylbenzylphenol, 20: 5601
seperation from sodium hydroxide solutions by solvent extraction using 4-*sec*-butyl-2-α-methylbenzylphenol, 20: 5601
FREE RADICALS
production of trapped, from alkyl halides in organic glasses by dissociative electron attachment and photodissociation, 20: 5577
radioinduced, in glycine peptides, ESR spectra of, 20: 5273
radioinduced, in rat tissues, γ, 20: 5339
reactions with hydrated electrons, review on, 20: 5525 (IA-1041)
yields from radiolysis of hydrocarbons, tracer studies of, 20: 5576
FROGS
development of *Rana nigromaculata* hypothalectomized tadpoles, effects of irradiated *Bufo bufo* pituitary extract on, 20: 5394
fluorescence intensity in blood cells of, effects of temperature on uv, 20: 5318
radiation effects on pituitary gland of *Bufo bufo*, 20: 5394

radiation effects on mechanical activity of muscles of, γ, 20: 5292(R) (COO-205-55, Paper 1)
radiation effects on electrical activity of excised muscles of, γ, 20: 5293(R) (COO-205-55, Paper 2)
uptake of neutral red in muscles of, effects of heavy water on, 20: 5317
FRUITS
juices of, radiation effects on wholesomeness of, 20: 5816
radiation effects on Botrytis infections in grapes, γ, 20: 5371
radiation effects on wholesomeness of, 20: 5816
FURNACES
design for alkali metal critical temperature determination, 20: 5594(R) (ANL-6925, pp 21-106)
design for injection casting of fuels, 20: 5594(R) (ANL-6925, pp 21-106)
development for skull reclamation process, 20: 5594(R) (ANL-6925, pp 21-106)
FUSED SALTS
precipitation of plutonium carbide and uranium carbide from, 20: 5594(R) (ANL-6925, pp 21-106)
separations in, ion exchange materials for, 20: 5594(R) (ANL-6925, pp 21-106)

G

GADOLINIUM
combustion with fluorine, products and yields from, 20: 5523(R) (ANL-6925, pp 175-85)
magnetic properties of, 20: 6531 (AD-623530)
oxidation of, kinetics of high-temperature, 20: 5859
separation from actinides and other rare earths by electrophoresis, 20: 5598
GADOLINIUM ALLOYS
Cr–Gd–Fe, properties as control-rod material, 20: 5845
Cr–Gd–Fe, tensile properties of, effects of gadolinium content on, 20: 5845
Ga–Au, oxidation of, kinetics of high-temperature, 20: 5859
Gd–La, antiferromagnetism and superconductivity coexistence in, (E), 20: 6247
Gd–Th, metallurgical properties and phase studies on, 20: 5891(R) (NYO-2159-1)
Gd–Y, electric conductivity at low temperatures, 20: 5888 (NP-15592)
Gd–Zr, metallurgical properties and phase studies on, 20: 5891(R) (NYO-2159-1)
GADOLINIUM BORIDES
thermionic emission of, on iridium and tungsten substrates, (E), 20: 5532(T) (K-Trans-10)
GADOLINIUM IONS
radioinduced luminescence in calcium fluorides doped with, preferential emission in afterglow of x, (E), 20: 6550
GADOLINIUM ISOTOPES Gd-152
conversion coefficients for E2 transitions in, (E), 20: 6303 (TID-22393)
energy levels of, rotational, (E), 20: 6348
GADOLINIUM ISOTOPES Gd-154
conversion coefficients for E2 transitions in, (E), 20: 6303 (TID-22393)
GADOLINIUM ISOTOPES Gd-155
energy level transitions in, E2/M1 mixing ratios and K conversion coefficients in rotational, (E), 20: 6386
GADOLINIUM ISOTOPES Gd-156
energy levels of, parity and spin of, (E), 20: 5928(R) (PR-P-66)
energy levels of, rotational, (E), 20: 6348
GADOLINIUM ISOTOPES Gd-158
energy levels, (E), 20: 6403
neutron capture cross sections at 5 kev to 2 Mev, (E), 20: 6280(R) (ANL-6925(p.249-51))
GADOLINIUM OXIDES
phase transformations in, at 50 to 1500°C, 20: 5536
Al_2O_3–Gd_2O_3, fabrication of control-rod elements of, 20: 5845
GAGES
uses of optical, dimensional, 20: 6689 (Y-KE-191)
GALLIUM ALLOYS
Ga–Pu, effects of pressure on properties and transformation of delta-stabilized, 20: 5884 (LA-2312)
Ga–Pu, grain growth in, strain-anneal technique for, 20: 5907
GALLIUM SYSTEMS
C–Cr–Ga, superconductivity of Cr_2GaC, 20: 6228
GAMMA CAMERAS
use in medical scanning, 20: 5467
GAMMA RADIATION
absorption by mice, phantom study, 20: 5286 (CONF-650616-16)
absorption in macrosystems from point sources, 20: 5751
angular correlations in xenon-127 decay, (E), 20: 6384
angular distribution in europium-147 decay, 20: 6396
attenuation in lead alloy shields, (E), 20: 6523
attenuation of reactor, in serpentine sand, (E), 20: 6524
content in atmosphere and on ground in New Zealand, 1965, 20: 5664(R) (NP-15639)
detection and measurement in man of, 20: 5427
detection and measurement of, from radioisotopes deposited in glands or organs, by external scanning, 20: 5447
detection and measurement in spark chambers, imaging method for radiodiagnostic, 20: 5461
detection and measurement of in-pile, detectors for, (E), 20: 5728 (IBM-65-825-1487)
detection and measurement of, performance of plastic scintillator for aerial, 20: 5761
detection and measurement of, triple-coincidence counters for, (E), 20: 5770
detection and measurement of low-intensity beams of, using electro-luminescent image intensifiers, (E), 20: 5773
detection and measurement at high dose rates, using p-i-n silicon detectors, (E), 20: 5743 (UCRL-14405)
detection and measurement of, in fallout, 1963, 20: 5652
detection of, audio-visual warning system for, 20: 5733 (LA-DC-6790)
dose from Wood River Junction criticality accident, 20: 5666 (TID-21995)
dose rate distribution from spent fuel elements, (E/T), 20: 6597
dosimetry of cesium-137 in sheep, use of thermoluminescent detector for, 20: 5285 (BNWL-SA-172)
dosimetry of fixed teletherapy beams, for irradiation of thoracic tumors, 20: 5438
dosimetry of therapeutic, use of photographic film detectors for, 20: 5480
dosimetry of therapeutic doses, use of phantoms for, 20: 5481
dosimetry of, method for, 20: 5750
effects of in-pile, on SNAP 10A fuels, (E), 20: 6678 (NAA-SR-Memo-11374)
effects of, from therapeutic doses of iodine-131, pathological, 20: 5469
effects on antioxidant content of rat tissues, 20: 5339
effects on antral carcinomas, therapeutic, 20: 5458
effects on auditory response of goats, 20: 5369
effects on bacterial reactions to phages and viruses, target theory for, 20: 5299(R) (TID-22187)
effects on Botrytis infections in grapes, 20: 5371
effects on cells in pea seedling roots, morphological, 20: 5390
effects on conditioned reflex of goats, 20: 5369
effects on cortical arousal in burros, 20: 5329
effects on electrical activity of excised frog muscles, 20: 5293(R) (COO-205-55, Paper 2)
effects on electrical potential of frog muscle membranes, 20: 5293(R) (COO-205-55, Paper 2)
effects on electrical properties of plant cells, 20: 5294(R) (COO-205-55, Paper 3)
effects on enzyme activity in rabbit tissues, γ, 20: 5380
effects on *Escherichia coli* growth, effects of arginine and uracil on, 20: 5348
effects on ethylene in presence of inert gases, 20: 5582
effects on fibrosarcoma cell line in mice, 20: 5362
effects on fluorescence of light pink rubies, 20: 6536
effects on free amino acid content in beef muscle, 20: 5278
effects on growth of bean and pea seedlings, 20: 5388
effects on growth of chlorella, 20: 5389
effects on hormone content of pituitary gland of toad *Bufo bufo*, 20: 5394
effects on in-pile corrosion of nuclear materials by aqueous solutions, 20: 5852(R) (EURAEC-1522)
effects on incidence of urethan-induced tumors in mouse lungs, 20: 5328
effects on life span of mice, computer program for evaluation of, 20: 5300 (UCLA-12-573)
effects on lipid binding by mitochondria, isolated from rabbit liver, 20: 5379
effects on lipoperoxide content of rat tissues, 20: 5339
effects on man, protective effects of bone marrow grafts, 20: 5420
effects on materials at cryogenic temperatures, measurement in reactors, (E), 20: 5569 (CONF-650217, pp 108-10)
effects on mechanical activity of muscle preparations from frogs and rats, 20: 5292(R) (COO-205-55, Paper 1)
effects on mechanical strength of bone of, from deposited radioisotopes, 20: 5289(R) (COO-119-232, pp 88-98)
effects on metabolism of electrolytes and nitrogen in dogs of, from injected sodium-24, 20: 5381
effects on mice, protective effects of AET, 20: 5410
effects on mice, protective effects of aminothiazoline salts, 20: 5410
effects on muscle activity of rats, 20: 5375
effects on organic glasses containing alkyl halides, 20: 5577
effects on phosphatase activity in aqueous solutions, dose effects, 20: 5277
effects on phosphorylase, inactivating, 20: 5275

effects on plant viruses, biological, 20: 5310
effects on polycythemia, therapeutic, 20: 5483
effects on potato tubers, 20: 5404
effects on pulse fission chambers, (E), 20: 5807 (AEEW-M-493)
effects on rat immunity to diphtheria toxins, 20: 5391
effects on scintillation in dioxane, effects of radioprotective compounds on, 20: 5422
effects on sodium chloride crystals, temperature dependence of flow stress in, 20: 6538
effects on storage life of potatoes, 20: 5404
effects on subsequent pharyngo-laryngectomy, 20: 5463
effects on sugar content in peas, 20: 5280
effects on thermistors and transistors, 20: 5808 (N65-35081)
effects on viability of *Schistosoma mansoni* cercariae in mice, 20: 5313
emission in fission, review, 20: 6300 (SGAE-PH-29/1965)
emission in proton capture by magnesium-25, 20: 6438
emission of delayed, from uranium-235 fission, (E), 20: 6316
energy spectra from point source shielded with aluminum layer, in air near ground, (E/T), 20: 6529
energy spectra from (n,γ) reactions, (T), 20: 6427
energy spectra from simulated fallout, 20: 5653
interactions with protons at 0.3 to 5.5 Bev, resonances from, (E/T), 20: 6037 (DESY-65/11)
measurement in dogs using silver-activated glass rods, 20: 5745(R) (UR-668, pp 117-23)
phantom depth dose studies on mice, 20: 5286 (CONF-650616-16)
polarization correlation with beta particles in scandium-46 decay, (E), 20: 6391
polarization measurements on, using iron transmission magnets, 20: 5764
production cross sections for, computer program for calculating, 20: 6284 (GEMP-392)
reactions (γ,n) with beryllium-9 at 3 to 17 Mev, energy levels from, 20: 6390
reactions (γ,n) with oxygen-16 at 17 to 28 Mev, cross sections for, (E), 20: 6418
reactions (γ,π^0) with helium-4 at 300 Mev, impulse approximation for, (T), 20: 6365
reactions with aluminum-27, alpha and proton yields from, (E), 20: 5732 (KFK-335)
reactions with even-even nuclei below 10 Mev, fission fragment angular distributions from, (E), 20: 6309(T) (ANL-Trans-245)
reactions with lead and mercury, cross sections for photoelectric, (E), 20: 5990
reactions with media surrounding high-power gamma facility, explosive gas yields from, 20: 5670
scattering by bismuth and lead in giant resonance region, cross sections for, (E), 20: 6349
scattering by cylindrical duct, streaming in, (T), 20: 6530
scattering by lead at 662 kev, cross section for Compton, (E), 20: 5991
scattering by lead, platinum, tantalum, tin, and zirconium at 0.662 and 1.332 Mev, cross sections for, (E/T), 20: 6323
scattering from spherical water surfaces at 0.7 and 1.25 Mev, back-, (E), 20: 6525
scattering in aluminum at 0.145 to 1.25 Mev, angular distributions of, (E), 20: 6527
scattering in lead at 1.0 and 4.0 Mev, intensity angular distribution of, (T), 20: 6526
scattering in lead at 0.411 to 1.25 Mev, angular distributions of, (E), 20: 6527
scattering in water at 4.0 Mev, intensity angular distribution of, (T), 20: 6526
scattering on gold-197, Moessbauer-Lamb factors in resonant, (E), 20: 6429
shielding studies, 20: 6520(R) (ORNL-3858(Vol.1), pp 42-6)
transport in reactors, group constants and heating calculations for, (T), 20: 6517 (CONF-651101-41)
use for radiotherapy of tumors, 20: 5453
use for therapy of tumors of head and neck, 20: 5441
use for therapy of bladder cancers, 20: 5454
use for therapy of cervical carcinomas, effects of estradiol, 20: 5472
use for therapy of ear cancers, 20: 5474
use for therapy of carcinomas of larynx, 20: 5486
use in radiodiagnosis, Spintharicon spark chamber imager for, 20: 5461

GAMMA SHIELDING
dose rates behind, (E/T), 20: 6626 (UNC-5118)

GAMMA SOURCES
analysis of mixed summing γ-γ coincidence spectrometer for, 20: 5753
depth dose planning for therapeutic use of, 20: 5449
dose calculations for heterogeneous, 20: 6597
dosimetry of plane, method for, 20: 5750
energy spectra from aluminum-shielded, in air near ground, (E/T), 20: 6529
preparation, packaging, and standardization of, 20: 5813(T) (JPRS-32260)
radioinduced explosive gases in air around high-power, ventilation calculations for, 20: 5670
spectra from point, in scattering medium, 20: 5760
use of cesium-131 seeds as, for radiotherapy, 20: 5482

GAMMA SPECTRA
measurement in thermonuclear reactor blanket mockups, 20: 6455 (AD-619672)

GAMMA SPECTROMETERS
design of triple-coincidence, (E), 20: 5770
design of, for whole-body counting of man, 20: 5427
performance of one-crystal Compton, (E/T), 20: 5775
performance of summing coincidence, for analysis of radioisotope mixtures, 20: 5753
velocity calibration of Mössbauer, optical method for, 20: 5786

GAMMA SPECTROSCOPY
coincidence circuits for triple, (E), 20: 5770
data analysis from, using least-squares regression computer code, 20: 5727 (CONF-651101-46)
methods development, 20: 6300 (SGAE-PH-29/1965)
methods for one-crystal Compton, 20: 5775

GANGLIONIC BLOCKING DRUGS
radiosensitivity effects of, in mice, x, 20: 5421

GARIGLIANO POWER REACTOR
core power distributions for, 20: 6606(R) (GEAP-4962)
development, 20: 6606(R) (GEAP-4962)
operation, 20: 6625(R) (TID-22434)
operations, (E), 20: 6623(R) (TID-22206)

GAS CENTRIFUGES
control equipment design for, 20: 5685(T) (K-Trans-5)

GAS COOLED REACTORS
components and materials of First Czechoslovakian Atomic Power Station, defectoscopic inspection of, 20: 6633(T) (AECL-2286)
cooling system for, design of self-sustaining, 20: 6647(P)
design for economic power, 20: 6644
development of high-temperature, 20: 6640
development of Magnox fueled, review of, 20: 6612 (INR-622/IX/R)
moderator structure for, design of graphite-block, 20: 6593(P)
use for power production and desalination, 20: 6650

GAS FLOW
determination in electric shock tubes, (E), 20: 6173
heat transfer and frictional resistance of high-temperature, measurements of, 20: 5626(T) (NP-tr-1300)
magnetohydrodynamic, field effects on stability of channel, (T), 20: 6174

GASEOUS FUEL REACTORS
development of wheel-flow, for rocket propulsion, 20: 6662 (NASA-TN-D-2951)
fuel injection techniques for, analysis of vortex, 20: 6652 (D-910091-5)
fuel injection techniques for, analysis of vortex, 20: 6653 (D-910091-7)
fuel opacity in, (T), 20: 6594 (D-910092-4)
nozzle cooling in rocket, transpiration, 20: 6663

GASES
content in meteorites, solar wind source for, 20: 5976
electric breakdown in low-pressure region in, 20: 6167
energy transfer to, from electric arcs, 20: 6178(P)
excitation functions for, photon counter for measurement of optical, 20: 5748(T) (UCRL-Trans-1266(L))
ionization of a stream of, device for, 20: 5640(P)
opacity of heavy-atom, (T), 20: 6594 (D-910092-4)
transition processes in, thermodynamic equilibrium for collisionally and radiatively controlled, 20: 6443 (AD-617383)

GASTRIC JUICE
radiation effects on secretion of, in dogs, x, 20: 5384
radiation effects on enzyme activity of, in dogs, x, 20: 5384

GASTROINTESTINAL TRACT
radiography of carcinomas in, using Thorotrast, 20: 5465
radiostrontium absorption in human, effects of calcium on, 20: 5263

GEIGER-MUELLER TUBES
circuitry for, design of, 20: 5801(P)
electric discharges in self-quenching, spread times of, (T), 20: 5789
glass for, development and evaluation of, 20: 5585
performance in corona-spike mode, in cosmic meson (μ) and neutrino detector, 20: 5723 (CONF-640919, pp 155-65)

GENES
linkage and mapping of chlorophyll-deficiency, in peas, 20: 5238
radiosensitivity effects of, in wheat, 20: 5403

GENETICS
radiation effects with recurrent intercrossing on variability in Phaseolus, neutrons, 20: 5406
recombination frequencies in Pneumococcus, 20: 5229 (BNL-9407)

GEOLOGY
equation of state of geologic materials, properties of, 20: 6533 (NVO-1163-60)

GEOMAGNETIC FIELDS
effects on helium and hydrogen ion diffusion in magnetosphere, (E), 20: 6198
electron angular distributions, energy spectra, and fluxes along lines near L = 5.6, (E), 20: 6196
electron densities in auroral echoes in, 20: 6182(R) (AD-619447)
electron density distributions in, diffusion equations for, 20: 6183 (AD-619821)
intensity variations of, correlation of ionospheric parameters and quiet solar-diurnal, 20: 6191
intensity variations in, ionospheric current systems at high latitudes from solar-diurnal, (T), 20: 6193
intensity variations of, measurements using absolute determinations and proton magnetometer, 20: 6195
kinetics of, as charged-particle trap, 20: 6208
magnetic field corotating structure effects on activity in, interplanetary, (E), 20: 5972
oscillations from near-conjugate stations, micropulsation, 20: 6188
perturbations in, auroral-zone electric current system from, (T), 20: 6192
proton angular distribution, energy spectra, and flux along lines near L = 5.6, (E), 20: 6197
pulsation properties in auroral-zone, pearl, (E), 20: 6204
GEOMAGNETIC STORMS
commencements of micropulsation, from near-conjugate stations, 20: 6188
data for principle, for 1965, 20: 6206
GEOPHYSICS
plasma description in, MHD equation for, (T), 20: 6212
GERMANIUM
fabrication of lithium-drift compensated p-i-n diodes of, (E), 20: 5702
piezoelectric properties of n-type, at 50 to 300°K, (E), 20: 5883 (IS-1263)
properties of large lithium-drifted detectors of, mounting and storage, 20: 5741 (UCRL-14263)
GERMANIUM ALLOYS
Al–Ge, radiation effects on electric conductivity of, stage I and II recovery from electron, 20: 5918
GERMANY
tritium distributions in Main and Rhine Rivers, 20: 5654
GLANDS
radiation effects on sebaceous, in hamsters, x, 20: 5322
GLASS
development for use in G-M and scintillation counters, 20: 5585
fission product track density in, techniques for evaluating, 20: 5713 (AD-623384)
free radical production from alkyl halides in organic, 20: 5577
radioinduced catalytic activation of Vycor, for hydrogen–deuterium exchange, 20: 5578
GLOBULIN
radiation effects on content in rat blood serum, proton, 20: 5378
GLOVE BOXES
design for equipment decontamination, 20: 5711(P)
GLOW DISCHARGES
cathode fall of, light density distribution in, 20: 6166
electric potential in neon, performance of probes for determination of space, 20: 6164
theory of low-pressure, 20: 6165
GLUCOSE
preparation of tritium-labeled in 3 and 4 positions, 20: 5252
GLYCINE
radioinduced free radicals in peptides of, 20: 5273
GLYCOGEN
radiation effects on content of, in developing chick embryos, x, 20: 5306
GOATS
radiation effects on auditory response of, γ, 20: 5369
radiation effects on conditioned reflex of, γ, 20: 5369
GOLD
deposition on pyrolytic graphite for use as analytical standard, electro-, 20: 5503
electron reactions at 2.5 to 4.0 Mev, bremsstrahlung spectra from, (E), 20: 6432
neutron absorption integrals for, infinite-dilution, (E), 20: 6558(R) (ANL-7115, pp 42-67)
performance as coatings for self-regenerating deuterium targets, (E/T), 20: 6334
proton reactions (p,n) at 30 and 50 Mev, isobaric-state excitation in, (E/T), 20: 6361
proton reactions at 3 Bev, fission and fragmentation products from, (E), 20: 5756
proton reactions at 2 Bev, lithium-8 production in, (E), 20: 6409
reactivity worth calculation of, 20: 6279(R) (AI-65-225)
GOLD ALLOYS
Au–La, oxidation of, kinetics of high-temperature, 20: 5859
Au–Nd, oxidation of, kinetics of high-temperature, 20: 5859
Au–Sm, oxidation of, kinetics of high-temperature, 20: 5859
Au–Tb, oxidation of, kinetics of high-temperature, 20: 5859
Au–Y, oxidation of, kinetics of high-temperature, 20: 5859
Au–Yb, oxidation of, kinetics of high-temperature, 20: 5859
Dy–Au, oxidation of, kinetics of high-temperature, 20: 5859
Ga–Au, oxidation of, kinetics of high-temperature, 20: 5859
GOLD COUPLES
Au/U, contact potential difference, 20: 5843
GOLD ISOTOPES Au-189
half life, (E), 20: 6298(R) (PPAD-2137-566)
GOLD ISOTOPES Au-190
energy levels and half life, (E), 20: 6298(R) (PPAD-2137-566)
GOLD ISOTOPES Au-197
energy levels, 20: 6436
gamma resonance scattering on, Moessbauer-Lamb factors in, (E), 20: 6429
neutron reactions (n,γ) with gold-198 spin and resonance parameters from, (E), 20: 6392
proton reactions (p,n) at 2.8 Bev, cross sections for production of mercury isotopes in, (E), 20: 6298(R) (PPAD-2137-566)
proton reactions at 0.6 to 30 Bev, terbium-149 production in, (E), 20: 6372
proton reactions at 60 to 155 Mev, charged-particle and neutron emission in, (T), 20: 6364
GOLD ISOTOPES Au-198
energy levels from neutron reactions (n,γ) with gold-197, spins and parameters of resonance, (E), 20: 6392
uses of, bibliography on, 20: 5811 (PAEC(A)IN-653)
GOLD ISOTOPES Au-199
beta decay of, spectrum shape factor in, (E), 20: 6358
GONADS
radiation dose to, from radiotherapy of skin diseases, x, 20: 5445
radiation effects on, of embryos of viviparous lizards, x, 20: 5324
radiosensitivity of male, of field mice, 20: 5387
radiotherapy combined with surgery for cancer of ovarian, recovery rate of, 20: 5446
radiotherapy for cancer of ovarian, recovery rate of, 20: 5446
GRAPHITE
coating of pyrolytic, with thin metal films for use as analytical standards, 20: 5503
coating of, equipment and procedure for plasma-spray, 20: 5837 (NLCO-966)
development for Dragon reactor core, 20: 6641
diffusion of nickel, radium, silver, thorium, and uranium in pyrolytic, 20: 5846
diffusion of uranium in S-700 and ZTA, 20: 5846
dimensional stability of, effects on reactor process tubes, 20: 6619 (NAA-SR-Memo-11416)
fabrication of high-density bodies of, by gas-pressure bonding, 20: 5867
gamma scattering by duct in, streaming in, (T), 20: 6530
mechanical properties of pyrolytic and single-crystal, 20: 5897(R) (TID-22420)
oxidation inhibitors for, study of, 20: 5844
oxidation protection coating for, properties of iridium for, 20: 5849
radiation effects on stability of moderator, in EGCR, 20: 5849
radioinduced defects in, studies on, 20: 5844
reactions with thoria and urania, 20: 5843
thermal conductivity at 1000°F of boronated, 20: 5850
x-ray Raman effect in, search for, (E), 20: 6539
B_4C–graphite, radiation effects on properties of, in-reactor, 20: 5845
GRAPHITE MODERATED REACTORS
design using combined light water moderation, 20: 6592(P)
moderator structure for, 20: 6593(P)
power output control systems for 200-Mw(e) sodium-cooled, 20: 6617 (NAA-SR-Memo-11339)
GRASS
preparation for radioactivity measurements, 20: 5742(R) (UCRL-14351)
GRAVITATION
field equations for, dimensionality of real world from strength of, 20: 6218
field properties of, quantum linearized Einstein, (T), 20: 6224
quantization in general-relativity theory of, Dirac procedure for, 20: 6219
sources of field of, multipole structure for, 20: 6222
GREAT BRITAIN
fallout monitoring, 1963 and 1964, 20: 5415
radiation dose to population of, from diagnostic radiography, 20: 5409
radioactivity in food in, 20: 5409
radioactivity in water supplies in, 20: 5409
GROUND
fallout deposition on, New Zealand, April–June 1965, 20: 5664(R) (NP-15639)
GROUND WATERS
discharge, movement, and occurrence of perched, in tuffaceous rocks, Rainier Mesa, Nevada Test Site, 20: 5643 (TEI-862)

radioactivity of, natural, bibliography on, 20: 5668 (WASH-1061)
use in reactor cooling systems, recycling in, 20: 6667 (BNL-9686)
GUINEA PIGS
radiation effects on metabolism in lens of, effects of age, x, 20: 5333
radiation effects on, effects of pre-irradiation before lethal x, 20: 5356

H

HAFNIUM
effects on mechanical properties of tungsten of alloying additions of, 20: 5851
electrochemical properties in molten chloride eutectic, 20: 5543
oxidation rate of coarse-grained, anisotropy of, 20: 5850
phase transformations in, effects of nitrogen and oxygen on alpha-beta, 20: 5850
radiation effects on tensile properties of, fast neutron, 20: 5850
refractive index of gaseous, (E/T), 20: 5879 (D-910092-6)
HAFNIUM ALLOYS
Hf–Nb–W–Y, welding parameters for C-129Y, electron-beam, 20: 5867
Hf–Sn, tin solubility in, 20: 5845
Hf–Ta, properties as oxidation-resistant coatings for refractory metals, 20: 5846
Hf–Ta–W, bonding of T-111, method for diffusion, 20: 5867
Hf–Ta–W, corrosion by lithium in niobium–1–zirconium alloy forced-convection loop, 20: 5853 (TIM-898)
Hf–Ta–W, corrosion by cesium vapor and liquid lithium at 2500 to 3400°F of T-111, 20: 5851
Hf–Ta–W, creep tests on T-111 and T-222 at 3200°F, 20: 5885(R) (NAS-CR-54773)
Hf–Ta–W, electric conductivity to 1500°C of T-111, 20: 5851
Hf–Ta–W, emissivity to 1500°C of T-111, total hemispherical, 20: 5851
Hf–Ta–W, welding parameters for T-111, electron-beam, 20: 5867
HAFNIUM CARBIDES
tensile properties and thermal expansion of, effects of carbon content on, 20: 5850
HAFNIUM COMPLEXES
with tropolone, preparation, properties, and structure, 20: 5538
HAFNIUM FLUORIDES
reactions with ammonium fluorides in aqueous solution, 20: 5535
HAFNIUM ISOTOPES Hf-170
energy levels of, rotational, (E), 20: 6348
HAFNIUM ISOTOPES Hf-172
energy levels of, rotational, (E), 20: 6348
HAFNIUM ISOTOPES Hf-174
energy levels, (E), 20: 6366
energy levels of, rotational, (E), 20: 6348
HAFNIUM ISOTOPES Hf-176
energy levels of, rotational, (E), 20: 6348
HAFNIUM ISOTOPES Hf-178
energy levels of, rotational, (E), 20: 6348
HAFNIUM ISOTOPES Hf-179
energy level transitions in, E2/M1 mixing ratios and K conversion coefficients in rotational, (E), 20: 6386
HAFNIUM ISOTOPES Hf-181
beta decay, (E), 20: 6374
HAFNIUM ISOTOPES Hf-182
beta decay, (E), 20: 6298(R) (PPAD-2137-566)
HAFNIUM SYSTEMS
C–Hf, phase studies, 20: 5851
C–Hf–In, superconductivity of Hf_2InC, 20: 6228
Hf–In–N, superconductivity of Hf_2InN, 20: 6228
HAIR
radiation effects on growth of, after therapeutic doses to head, x, 20: 5484
HALDEN BOILING REACTOR
coolant chemistry, 20: 6638
development and research program at, review of, 20: 6635
instrumentation development for, in-core, 20: 6637
operation of, with second fuel charge, 20: 6636
operations and uses, (E), 20: 6648(R) (HPR-64)
HAMSTERS
radiation effects on sebaceous glands in, x, 20: 5322
radiation effects on life span of, x, 20: 5330
radiation effects on collagen content of skin of, x, 20: 5330
HANDBOOKS AND MANUALS
on fabrication and properties of molybdenum, niobium, tantalum, tungsten, and their alloys, 20: 5874 (AGARDograph-94)
HASTELLOY C
corrosion by helium–water system at 1700, 1900, and 2100°F, 20: 5846
HASTELLOY X
compatibility with plutonium-uranium carbides, 20: 6600(R) (ANL-7105, pp 1-35)
corrosion by helium–water system at 1700, 1900, and 2100°F, 20: 5846
radiation effects on stress rupture of, fast and thermal neutron, 20: 5851
reactions with dysprosium oxides at 1850°F, 20: 5850
HAWAIIAN ISLANDS
mosquito control and distributions in, 20: 5240
HAYNES 25 ALLOY
carburization and oxidation at 2050°F, 20: 5851
HEAD
proton attenuation by skull bones, 20: 5475
radiation effects on osseous development of, in mouse embryos, x, 20: 5316
radiotherapy of tumors of, 20: 5441
HEALTH PHYSICS
gamma field calculation for heterogeneous sources, 20: 6597
permissible limits for thorium, inconsistencies in regulations on, 20: 5662 (NLCO-962)
program at National Institute of Radiological Sciences in Chiba, Japan, 20: 5672
HEART
diseases of, radiation dose to children from radiographic diagnosis of congenital, 20: 5455
radiotherapy of intractable angina pectoris, iodine-131, 20: 5460
HEAT
conversion to electricity by nuclear thermionic system, research on, (E), 20: 6023(R) (AD-619379)
HEAT-RESISTING ALLOYS
chemistry and physics of, bibliography on high-temperature, 20: 5527 (NP-15646)
contamination by residual gases in vacuums below 10^{-6} torr, 20: 5846
corrosion-protection coatings for, development of, 20: 5851
creep property measurements on, mathematical system for extrapolation of, 20: 5880(R) (EURAEC-1310)
welding of, facility for, 20: 5867
welding of, solid-state, 20: 5867
welding parameters, electron-beam, 20: 5867
HEAT TRANSFER
correlation with momentum transfer in high-temperature gas flow, 20: 5626(T) (NP-tr-1300)
from vertical cylinder in square channel, 20: 5619 (AE-199)
in boiling potassium and sodium, 20: 5627
in steam-water flow in round vertical tubes, 20: 5623 (EURAEC-1325)
in steam–water mixtures, 20: 6566(R) (EURAEC-1382)
in toroidal plasma column, 20: 6473
sound generation in boiling, 20: 5628
stability of, in flows of supercritical fluids, (T), 20: 5622 (ANL-7032)
transients in linear systems, total time integrals of, (T), 20: 5681 (MLM-1288)
HEAVY WATER REACTORS
components and materials of First Czechoslovakian Atomic Power Station, defectoscopic inspection of, 20: 6633(T) (AECL-2286)
dynamics of boiling, research on, 20: 6637
HELIUM
chemistry of reactor coolant, 20: 6639
containment of high-temperature circulating, system for, 20: 6642
diffusion in uranium carbide, method for studying, 20: 5892 (PWAC-476)
effects on radiolysis of ethylene, 20: 5582
electron reactions with, ionization cross sections for, (E/T), 20: 5989
energy levels of, energy calculations for ground-state, (T), 20: 5987(T) (ANL-Trans-248)
energy levels of, three-body problem for ground, (T), 20: 6217
excitation functions for, photon counter for measurement of optical, 20: 5748(T) (UCRL-Trans-1266(L))
glow discharges in, properties of low-pressure, (E/T), 20: 6165
heating of plasma of, by electron bombardment, 20: 6468(T) (ORNL-tr-871)
helium ion elastic scattering by, molecular state crossing for perturbation induced in, (E), 20: 5996
ion production in tenuous plasma of, effects of metastable atoms on, (T), 20: 6464 (NASA-TN-D-3121)
positron annihilation spectra in low temperature gaseous, (E), 20: 5997
precipitation in irradiated aluminum–lithium alloy, effects of density and defect distribution on, 20: 5848
proton reactions at 50 to 150 kev, electron angular distributions and energies from, (T), 20: 5993
shock-wave reflection in thermal plasma of, (T), 20: 6512
solubility in uranio, 20: 5843
stability of liquid II, in thermal counterflow, (E), 6230
thermal properties of liquid I and II, correlation of, (T), 20: 6231
HELIUM IONS
diffusion in magnetosphere, geomagnetic field effects on, (E), 20: 6198
distributions in magnetosphere, whistler correlations with, (E), 20: 6198
scattering by argon, helium, and neon, molecular state crossing for perturbation induced in elastic, (E), 20: 5996
HELIUM ISOTOPES

content in iron meteorites, (E), 20: 5977
HELIUM ISOTOPES He-3
content in bronzite chondrites, ratio to helium-4, (E), 20: 5975
electron scattering by, inelastic continuum in, 20: 6277 (AD-619952)
reactions (He-3,α) with potassium-39 at 9.0 and 11.0 Mev, angular distributions for, (E/T), 20: 6367
reactions (He-3,α) with beryllium-9 at 3 Mev, beryllium-8 level spins and parities from, (E), 20: 6389
reactions (He-3,α) with calcium-40 at 24.4 Mev, angular distributions from, (E), 20: 6398
reactions (He-3,$\alpha\gamma$) with oxygen-16, oxygen-15 gamma transitions from, (E), 20: 6318
reactions (He-3,α) with nitrogen-14 at 25.7 and 27.0 Mev, angular distributions from, (E), 20: 6326
reactions (He-3,d) with iron-58 at 22 Mev, cobalt-59 energy levels from, (E), 20: 6412
scattering by potassium-39 at 9.0 Mev, elastic, (E/T), 20: 6367
thermal capacity of low-temperature liquid, (E), 20: 6245
HELIUM ISOTOPES He-4
content in bronzite chondrites, ratio to helium-3 and neon-20, (E), 20: 5975
electron inelastic scattering by, two-nucleon correlation functions and cross sections for, (T), 20: 6424
gamma reactions (γ,π^0) at 300 Mev, impulse approximation for, (T), 20: 6365
Hartree-Fock fields and single-particle energies for ground state of, (T), 20: 6363
neutron elastic scattering at 22 to 29 Mev, helium-5 energy levels from, (E), 20: 6335
vortex rings in liquid II, size of charge quantized, (T), 20: 6249
HELIUM ISOTOPES He-5
energy levels at 16.6 to 26.6 Mev, (E), 20: 6335
HELIUM SYSTEMS
He–H_2O, corrosive effects on nickel-base alloys at 1700, 1900, and 2100°F, 20: 5846
He-K, electric discharge in, at low voltage and high current, (E/T), 20: 6159 (AERE-M-1597)
He–N, performance for irradiation capsule temperature control, 20: 6680 (ORNL-TM-1319)
HEMAGGLUTININS
radiation effects on production of, by thymectomized mice, 20: 5408 (USNRDL-TR-920)
HEMATOLOGY
statistical analysis of data, 20: 5290(R) (COO-119-232, pp 165-89)
HEMATOPOIETIC SYSTEM
effects of nitrogen mustards on mouse, pathological, 20: 5296(R) (NP-15585)
radiation effects on rabbit, fractionated doses of x, 20: 5364
radiation effects on, from deposited strontium-90 in dogs, B, 20: 5290(R) (COO-119-232, pp 165-89)
tissue transplants from, bibliography, 20: 5424
HEPTANE
electron reactions in ethylene mixture, cross sections for momentum transfer and drift velocities in, 20: 5985 (ORNL-TM-1262)
heptane–$UO_2(NO_3)_2$, radiation effects on coalescence rates in liquid, 20: 5571 (ORNL-TM-1283)
heptane–LiCl, radiation effects on coalescence rates in liquid, 20: 5571 (ORNL-TM-1283)
HETEROCYCLIC COMPOUNDS
reactions with hydrated electrons, review on, 20: 5525 (IA-1041)
HETEROGENEOUS REACTORS
design of dual moderated, 20: 6592(P)
neutron resonance absorption in, (T), 20: 6579(R) (BNWL-149, pp 48-56)
HEXANE
electron reactions with, ionization cross sections for, (E/T), 20: 5989
electron reactions in ethylene mixture, cross sections for momentum transfer and drift velocities in, 20: 5985 (ORNL-TM-1262)
uses as medium for drifting lithium into germanium, (E), 20: 5702
hexane–$LiNO_3$, radiation effects on coalescence rates in liquid, 20: 5571 (ORNL-TM-1283)
hexane–$UO_2(NO_3)_2$, radiation effects on coalescence rates in liquid, 20: 5571 (ORNL-TM-1283)
HIBERNATION
radiosensitivity effects of low-temperature-induced, in grain weevils, 20: 5385
radiosensitivity effects of, on intestinal cells of hedgehog, x, 20: 5377
HIGH-ALTITUDE EXPLOSIONS
electron injection into artificial radiation belt from Starfish, 20: 6209
spectral lines from artificial auroras produced by, intensity variations of, (E), 20: 6203
HIGH TEMPERATURE GAS COOLED REACTOR EXPERIMENT
coolant chemistry for, 20: 6639
cooling system leak tightness for, testing of, 20: 6642
moderator development for, graphite, 20: 6641
HIGH TEMPERATURE LATTICE TEST REACTOR
neutron pulsing possibilities of, (T), 20: 6669(R) (BNWL-149, pp 36-44)
power increase in, boundary value solution for heat conduction from, (T), 20: 6669(R) (BNWL-149, pp 36-44)
HIGH TEMPERATURE SEPARATION PROCESSES
development for recovery of fertile and fissionable materials, 20: 5594(R) (ANL-6925, pp 21-106)
equipment for EBR-II fuel cycle processes performance of, 20: 5594(R) (ANL-6925, pp 21-106)
flowsheets for fast reactor fuel alloys, 20: 6553(R) (ANL-6925, pp 255-63)
flowsheets for fast reactor metal fuels, 20: 5493(R) (ANL-6925, pp 253-4)
HILSCH TUBES
injection techniques for, analysis of peripheral-wall, 20: 6652 (D-910091-5)
injection techniques for, analysis of peripheral-wall, 20: 6653 (D-910091-7)
HIPPURIC ACID, o-IODO-, SODIUM SALTS
analysis of iodine-125- or iodine-131-labeled, for impurities by paper chromatography, 20: 5515
HOLMIUM
combustion with fluorine, products and yields from, 20: 5523(R) (ANL-6925, pp 175-85)
magnetization, 20: 6275(R) (AD-619534)
HOLMIUM ALLOYS
Ho–Th, metallurgical properties and phase studies on, 20: 5891(R) (NYO-2159-1)
Ho–Y, electric conductivity at low temperatures, 20: 5888 (NP-15592)
Ho–Zr, metallurgical properties and phase studies on, 20: 5891(R) (NYO-2159-1)
HOLMIUM ISOTOPES Ho-163
half life, (E), 20: 6298(R) (PPAD-2137-566)
HOLMIUM ISOTOPES Ho-165
electron scattering by polarized, 20: 6275(R) (AD-619534)
neutron transmission at 8.3 Mev by polarized, 20: 6275(R) (AD-619534)
proton reactions (p,2n) at 12 Mev, erbium-164 levels from, (E), 20: 6366
HOLMIUM ISOTOPES Ho-166
beta transitions in, with parity change, (E), 20: 6370
HOLMIUM OXIDES
phase transformations in, at 50 to 1500°C, 20: 5536
HOMOGENEOUS REACTORS
characteristics of molten-salt-fueled, catalog, 20: 6554 (ANL-7092)
HORMONES
radiation effects on estrone, x, 20: 5274
HOSPITALS
radiation protection of personnel, 20: 5433
HYDROAROMATIC COMPLEXES
electron spin resonance spectra of radicals in, effects of deuterium on, 20: 5566
HYDROBROMIC ACID
spectra of, effects of bromine-79 and bromine-81 on infrared, 20: 5550
HYDROCARBONS
analysis for lead, apparatus for radiometric, 20: 5522(P)
preparation of tritium-containing, 20: 5593(P)
radiolysis of liquid, effects of electric field on electron, 20: 5575
reactions with recoil carbon-11 atoms, mechanism and products of, 20: 5570 (JUL-228-RC)
HYDROCHLORIC ACID
electron reactions with, ionization cross sections for, (E/T), 20: 5989
reactions with organotin compounds, rate constants for, 20: 6687(R) (NYO-3453-1)
reactions with organotin compounds, effects of metal ions on, 20: 6687(R) (NYO-3453-1)
reactions with stainless steel in air-fluidized beds, 20: 5595(R) (ANL-6925, pp 107-64)
HYDRODYNAMICS
equations for one-dimensional, Eulerian difference, 20: 6162 (UCRL-12238-T)
HYDROFLUORIC ACID
effects on fission tracks in glasses, 20: 5713 (AD-623384)
HF–O, effects of acid leaching on uranium in alumina fluidized bed, 20: 5500 (ORNL-3876)
HF–O, effects on stainless steel, oxidizing, 20: 5595(R) (ANL-6925, pp 107-64)
HYDROGEN
deuterium exchange with water vapor, properties of chromium trioxide–nickel catalyst for, 20: 5534
distribution in zirconium alloys during hydrogenation and oxidation, 20: 5851
effects on creep properties of SAP 930, 20: 5838 (RISO-110)

effects on critical resolved shear stress of zirconium, 20: 5851
effects on solute-induced brittleness of fcc alloys and steel, 20: 5846
effects on tensile properties of Zircaloy-2, on neutron effects, 20: 5851
electron density and temperature in standing layers of low-pressure discharges in, (E), 20: 6476
electron elastic scattering by, resonance structure from, (E), 20: 5999
energy-level shifts in atomic, from vacuum polarization, (T), 20: 5995
heating of plasma of, by electron bombardment, 20: 6468(T) (ORNL-tr-871)
intermolecular potentials of, comparison with deuterium, 20: 5541
isotope effects on uv spectra of potassium bromide, potassium chloride, and rubidium chloride, 20: 6545
molecular structure of, orbital density in, 20: 5524 (ANL-7076)
production of atomic and molecular beams of, ion source for, 20: 6000
radiation effects on carbon dioxide reduction by, 20: 5574
radioinduced catalytic activation of exchange with deuterium in Vycor glass vessels, 20: 5578
radioinduced dissociation of molecular, electron, 20: 5579
radioinduced formation of, in water shielding of high-power gamma facility, 20: 5670
separation from deuterium, tritium, and their compounds by gas chromatography, 20: 5824
separation from uranium, 20: 5843
solubility in zirconium–2.5 niobium alloy, terminal, 20: 5849
sorption by radioinduced color centers in silica gel, 20: 5584
sorption by SAP 895 sintered aluminum products from Progil OM2 terphenyl at 400 and 450°C, 20: 5838(R) (RISO-110)
sorption by Zircaloy-2, electroplating with copper for prevention of, 20: 5867
stability of colliding plasmas of, (E/T), 20: 6465 (RISO-105)
yields in pyrolysis of diphenyl at 375 to 1375°K, 20: 5563 (EUR-2482.f)

HYDROGEN IONS
diffusion in magnetosphere, geomagnetic field effects on, (E), 20: 6198
distributions in magnetosphere, whistler correlations with, (E), 20: 6198
energies and wave functions of molecular mesic, (T), 20: 5980 (AD-617522)
production in oscillating-discharge source in longitudinal magnetic field, (E), 20: 5951

HYDROGEN ISOTOPES
separation by gas chromatography, 20: 5824

HYDROGEN PEROXIDES
radiation effects on catalase systems of, 20: 5271
reactions with uranyl ions in presence of oxalate ions, 20: 5549
yields from radiolysis of methanol, effects of water on, 20: 5581

HYDROGEN SULFIDES
electron reactions with, ionization cross sections for, (E/T), 20: 5989
radioprotective effects of, in biological systems, 20: 5296(R) (NP-15585)

HYDROGEN SYSTEMS
D–H–NH_3, bithermal isotopic exchange, in, 20: 5827(P)
H–Ir–Li, phase studies, 20: 5849
H–Li–Rh, phase studies, 20: 5849
H–Sc–Y, phase studies, 20: 5909
H–U, diffusivity, (T), 20: 5983 (D-910099-2)
H–Xe, electric discharges in, multi-cathode, 20: 6168

HYDROGEN TRITIDES
separation from deuterium, hydrogen, and tritium and other of their compounds by gas chromatography, 20: 5824

HYDROLYSIS
of plutonium hexafluoride, equipment for airborne, 20: 5595(R) (ANL-6925, pp 107-64)

HYDROMAGNETIC WAVES
propagation in plasma in magnetic multipole field eigenmodes for, (T), 20: 6492
use in electron distribution diagnostics in magnetosphere, (T), 20: 6202

HYPERFRAGMENTS
production and properties of, review of, (E/T), 20: 6283 (CERN-64-13 (Vol.4), pp 137-86)
production in meson (K⁻) reactions with emulsion nuclei at 50 to 1500 Mev/c, (E), 20: 6294 (NP-15617)
production of double, (T), 20: 6283 (CERN-64-13(Vol.4), pp 137-86)

HYPERONS
decay of, angular, energy, and polarization correlations for leptonic, (T), 20: 6088
magnetic moments for, measurement of, 20: 6282 (CERN-64-13(Vol.4), pp 97-136)
production in antiproton-proton interactions at 4 Bev/c, (E), 20: 6033 (CEA-R-2798)

HYPERONS (Λ)
binding energies in hypernuclei, (T), 20: 6283 (CERN-64-13(Vol.4), pp 137-86)
decay modes, (T), 20: 6283 (CERN-64-13(Vol.4), pp 137-86)
decay of, review of nonleptonic, 20: 6032 (BNL-9666)
interactions with nucleons, (T), 20: 6283 (CERN-64-13(Vol.4), pp 137-86)

HYPERONS (Λ^0)
production in meson (π^-)-proton interactions in carbon, polarization in, (E), 20: 6071

HYPERONS (Ω^-)
decay of, review of nonleptonic, 20: 6032 (BNL-9666)

HYPERONS (Σ^-)
decay of, review of nonleptonic, 20: 6032 (BNL-9666)

HYPERONS (Σ^0)
decay of, review of nonleptonic, 20: 6032 (BNL-9666)

HYPERONS (Σ^+)
decay in broken SU(6) symmetry, S-wave amplitudes in hadronic, 20: 6152
decay of, review of nonleptonic, 20: 6032 (BNL-9666)

HYPERONS (Ξ)
properties, (E), 20: 6099

HYPERONS (Ξ^-)
decay of, review of nonleptonic, 20: 6032 (BNL-9666)

HYPERONS ($\bar{\Xi}^0$)
decay of, review of nonleptonic, 20: 6032 (BNL-9666)

HYPERTHYROIDISM
radiotherapy during therapy, hazards of radioiodine for, 20: 5470
radiotherapy using iodine-131, late pathological effects of, 20: 5469

I

ICE
hydrogen bonding in, infrared spectral study of, 20: 5552

ICE-d_2
hydrogen bonding in, infrared spectral study of, 20: 5552

IMAGE BRIGHTNESS INTENSIFIERS
performance of electroluminescent, for electron and gamma beam monitoring, 20: 5773

IMIDAZOLE
effects on deuterium exchange between isobutyraldehyde and water, 20: 5565

IMMUNE REACTIONS
effects of irradiating transplantation site on, to renal transplants in dogs, 20: 5344
in spleen cultures from heterologous radiation chimeras, 20: 5397
in x irradiated mice, effects of cystamine on, 20: 5413
of mice, to γ irradiated *Schistosoma mansoni* cercariae, 20: 5313
radiation effects on, in thymectomized mice, 20: 5408 (USNRDL-TR-920)
radiation effects on, in mice, 20: 5413
radiation effects on, to bone marrow grafts in man, 20: 5420
radiation effects on, to skin homografts in rats, x, 20: 5335
radiation effects on marrow transplant, methods for assay in mice of x, 20: 5372
to bacillus infection, effects on development of strontium-90-induced bone tumors in mice, 20: 5373
to hematopoietic tissue transplants, bibliography, 20: 5424

IMMUNITY
radiation effects on rat, to diphtheria toxins, γ, 20: 5391

IMPACT SHOCK
calculation of water-hammer, in TREAT experiments, 20: 6552(R) (ANL-6925, pp 187-233)

IN-PILE LOOPS
development of, for Halden boiling reactor, (E), 20: 6648(R) (HPR-64)
uses of cryogenic, for basic radiation-damage studies, (E), 20: 5569 (CONF-650217, pp 108-10)

INCOLOY
compatibility with uranio and Zircaloy-2 at 475 to 1200°C, 20: 5914(R) (GEAP-3771-17)
corrosion of type 800, by steam at 705°C, 20: 5846
radiation effects on mechanical properties of type 800, fast neutron, 20: 5851
welding techniques for 800, (E), 20: 6624 (TID-22425)

INCONEL
corrosion by borated water at 600°F, 20: 5846
corrosion of type 600, by helium–water system at 1700, 1900, and 2100°F, 20: 5846
erosion of 600, by liquid sodium, 20: 5861
radiation effects on mechanical properties of types 600, 625, and 718, fast neutron, 20: 5851
welding techniques for 600 and 625, (E), 20: 6624 (TID-22425)

INCONEL X
corrosion by borated water at 600° F, 20: 5846

INDIA
fallout monitoring, radioactivity from cesium-137, ruthenium-106, and zirconium-95 in rain water in Bombay, 1963, 20: 5661 (AEET-215)

INDIUM
determination by potentiometric titration using EDTA, equipment for, 20: 5502

neutron absorption integrals for, infinite-dilution, (E), 20: 6558(R) (ANL-7115, pp 42-67)
proton reactions (p,n) at 30 and 50 Mev, isobaric-state excitation in, (E/T), 20: 6361

INDIUM ALLOYS
Cd–In–Ag, corrosion by borated water at 600°F, 20: 5846
Cd–In–Ag, properties as control rod material, effects of palladium, platinum, and tin additions on, 20: 5850

INDIUM COMPLEXES
with tropolone, preparation, properties, and structure, 20: 5538

INDIUM ISOTOPES In-115
energy levels in, from cadmium-115 decay, 20: 6436

INDIUM SYSTEMS
C–Hf–In, superconductivity of Hf_2InC, 20: 6228
C–In–Nb, superconductivity of Nb_2InC, 20: 6228
C–In–Zr, superconductivity of Zr_2InC, 20: 6228
Hf–In–N, superconductivity of Hf_2InN, 20: 6228
In–N–Ti, superconductivity of Ti_2InN, 20: 6228

INDOLE,3-(2-AMINOETHYL)-
radioprotective properties of, 20: 5422

5-INDOLOL, 3-(2-AMINOETHYL)-
radioprotective properties of, 20: 5422

INDUCED RADIOACTIVITY
estimation of, in accelerators, (E/T), 20: 5933 (CERN-65-34)

INFECTIONS
effects of tuberculosis, on development of strontium-90-induced bone tumors in mice of, 20: 5373
in skin of rabbits, effects of leukopenia on, 20: 5315
radiation effects on Botrytis in grapes, γ, 20: 5371

INFORMATION CENTERS
functions of RSIC, library and technical, 20: 6520(R) (ORNL-3858 (Vol.1), pp 42-6)

INFRARED RADIATION
emission from high-pressure high-current argon discharge, statistical oscillations of, (E/T), 20: 6177

INOR-8
corrosion by helium–water system at 1700, 1900, and 2100°F, 20: 5846
corrosion by potassium–sodium at 1425°F, effects of oxygen on, 20: 5851
ductility of, effects of heat treatments on, 20: 5846
tensile properties at 1100, 1300, and 1500°F, 20: 5846

INSECTS
ecology of oriental fruit moth, *Grapholitha molesta*, tracer study, 20: 5246
incorporation of phosphorus-32 into oriental fruit moths, *Grapholitha molesta*, 20: 5246
incorporation of radioisotopes in, for use in ecological studies, 20: 5815 (STI/DOC/10/44)
radiation control of populations of, by sterile-male technique, 20: 5815 (STI/DOC/10/44)
radiation effects on oxygen uptake by *Tenebrio molitor*, 20: 5314
radiation effects on life span of house fly, *Musca domestica*, x, 20: 5331
radiosensitivity of *Calandria granaria*, effects of oxygen concentration and temperature on x, 20: 5385

INSTRUMENTATION
design for gas centrifuge control, 20: 5685(T) (K-Trans-5)
design for reading and charging dosimeters, 20: 5799(P)
design for x-ray astronomy, 20: 5968 (NP-15626)
development for plasma diagnostics, 20: 5633 (NASA-SP-5033)
development of in-core, for San Onofre Power Reactor, 20: 6630 (WCAP-3269-46)

INSTRUMENTS
development for fuel-elongation monitoring in boiling reactors, (E), 20: 6648(R) (HPR-64)
performance for signal analysis in noise background by data accumulation, (T), 20: 5695

INSULIN
preparation of iodine-131-labeled, 20: 5436(R) (UR-668, pp 149-60)
properties of, effects of iodination on biological, electrophoretic, and immunochemical, 20: 5436(R) (UR-668, pp 149-60)

INTERFEROMETERS
plasma effects on microwave, inhomogeneous, (T), 20: 5683 (UCRL-14438)
use of laser, for plasma electron density measurements, 20: 6471

INTERNAL CONVERSION
nuclear structure effects in, review of dynamic, 20: 6332

INTESTINE
radiation effects on, following therapy of gynecologic cancer, electron and radium, 20: 5392
radiation effects on vasculature of, x, 20: 5301(R) (UR-668, pp 1-54)
radiation injuries of goldfish, effects of temperature on, 20: 5374
radiosensitivity of cells of hedgehog, effects of hibernation on x, 20: 5377

INVERTASE
production in yeast, mechanisms of, 20: 5251(R) (UR-668, pp 123-49)

IODIDE IONS
formation in light water and heavy water, 20: 5539

IODIDES
analysis of radioactive, 20: 5436(R) (UR-668, pp 149-60)

IODINE
corrosive effects on zirconium and Zircaloy-2 at 350°C, 20: 5914(R) (GEAP-3771-17)
diffusion from uranium and uranium carbide in helium atmosphere, behavior and chemical state of, 20: 5878 (BNL-9667)
diffusion in spherical uranium dicarbide particles, coefficient for, 20: 5848
iodine-129 Mössbauer effect in molecular crystals of, (E), 20: 6540
solubility in light water and heavy water at 5 to 50°C, 20: 5539

IODINE ISOTOPES I-127
energy levels of, spin of, (E), 20: 6384

IODINE ISOTOPES I-129
decay in meteorites, xenon-129 production from, 20: 5978
Mössbauer effect in molecular crystals of iodine, (E), 20: 6540

IODINE ISOTOPES I-131
content in milk in Kansas and Missouri, 1962, 20: 5648(R) (COO-1340-2, pp 1-53)
effects of therapeutic doses of, pathological, 20: 5469
effects on hyperthyroidism, hazards during pregnancy from therapeutic, 20: 5470
effects on intractable angina pectoris, therapeutic, 20: 5460
effects on thyroid carcinoma, evaluation of therapeutic, 20: 5444
exchange between silver iodide and methyl iodide, effects of surface structure on, 20: 5544
incorporation in insulin, 20: 5436(R) (UR-668, pp 149-60)
metabolism in rats, effects of ε-aminocaproic acid on, 20: 5436(R) (UR-668, pp 149-60)
separation from cotton cloth soiled with oily materials, 20: 5676
uptake by human fetus, effects of age on, 20: 5259
uptake by man of, from contaminated milk, 20: 5237(R) (UR-668, pp 55-109)
uptake by thyroid tumors of, effects of thyrotropic harmones, thyrostatic agents, and surgical thyroidectomy on, 20: 5488
use for therapy of thyroid tumors, 20: 5488
use in cancer therapy, 20: 5436(R) (UR-668, pp 149-60)

ION BEAMS
design and performance of systems using, for orbit control of earth satellites, (E/T), 20: 5638
mass spectra of, analysis using 94-channel mass spectrometer, (E), 20: 5698
motion in crossed-field beam sorters, (E), 20: 6262 (NP-15633)
production in electron-bombardment thrustor systems for spacecraft propulsion, 20: 5637
reactions with magnesium oxides and zinc silicates, luminescence in, 20: 5573
reactions with plasma, heating effects from, (E), 20: 6467(T) (ORNL-tr-870)

ION EXCHANGE MATERIALS
development of, for separations in molten salts, 20: 5594(R) (ANL-6925, pp 21-106)

ION SOURCES
design and performance of oscillating-discharge, (E), 20: 5951
design for production of atomic and molecular hydrogen beams, 20: 6000
design of duoplasmatron, for use in sputtering studies, 20: 5981(R) (AD-620002)
development of autofocusing, for electrostatic accelerators, 20: 5957
extraction from cyclotrons, method for, 20: 5947(T) (ANL-Trans-241)
ion trajectories from polarized, in cyclotrons, (T), 20: 5946 (UJV-1408/65)
mass spectra of, analysis using 94-channel mass spectrometer, (E), 20: 5698

IONIZATION CHAMBERS
alpha collimation in gridded, electronic, 20: 5782
background-current analysis in dielectric-liquid, (E/T), 20: 5771
design characteristics of boron-10-coated, for inpile uses, (E), 20: 5717 (AEEW-M-508)
design for power reactors, material activation analysis for, 20: 5716 (AEEW-M-470)
design for use in radiation protection, 20: 5762
use in aural-warning personnel monitor, 20: 5803(P)
uses of differential, for proton-beam energy measurements at 10 to 200 Mev, (E), 20: 5778

IONOSPHERE
electric-current system in auroral zone of, from geomagnetic disturbance, (T), 20: 6192
electric-current systems in high latitudes, from solar-diurnal variations, (T), 20: 6193

electrodynamic parameters of, correlation with quiet solar-diurnal variations, 20: 6191
electron densities in auroral D and E region, 20: 6182(R) (AD-619447)
electron densities in D region of, techniques for measuring, (E), 20: 6185 (AFCRL-65-620)
electron density in F2 region of, diffusion equations for, 20: 6183 (AD-619821)
electron distribution and temperature in, (E), 20: 6199
ionization frequency variations in E_1, F_1, and F_2 layers of, effects of solar radiation on, 20: 6187
ionization levels in F region, in Antarctic and Arctic, 20: 6190
magnetic field in, equipment for measuring vlf, (E), 20: 6180 (AD-619250)
particle distribution in, three-fluid model for, (T), 20: 6179 (AD-618911)
plasma density fluctuations in, turbulence of, 20: 6472
radio-wave absorption in, cosmic noise level during type-II anomalous, 20: 6194

IONS
density and temperature in high-pressure xenon plasma, 20: 6480
detection in mass spectrometers using electron multiplier tubes, 20: 5706
electron recombination with, by two-electron collisions in field of, (T), 20: 5994
motion in cyclotrons, effect of center geometry on, 20: 5948(T) (ANL-Trans-246)
production in tenuous helium plasma, effects of metastable atoms on, (T), 20: 6464 (NASA-TN-D-3121)
recombination on surface of charged body in plasma, (T), 20: 6483

IRIDIUM
diffusion in tungsten, inter-, 20: 5846
properties as oxidation protection coating for graphite, 20: 5849
properties as substrate for rare-earth–hexaboride thermionic emitters, (E), 20: 5532(T) (K-Trans-10)

IRIDIUM ISOTOPES Ir-192
effects on antral carcinomas, therapeutic, 20: 5458
preparation, packaging, and standardization of, 20: 5813(T) (JPRS-32260)

IRIDIUM SYSTEMS
H–Ir–Li, phase studies, 20: 5849

IRON
analysis for manganese by activation methods, 20: 5514
corrosion by bismuth at 1000°C, 20: 6024(R) (ANL-6925(p.235-47))
determination in antimony, activation, 20: 5507
diffusion in zirconium, 20: 5846
ductility of, mechanism controlling, 20: 5851
effects on rolling properties of uranium, 20: 5866
effects on deformation properties of beryllium single crystals, 20: 5844
effects on hot hardness of zirconium oxides, 20: 5846
erosion by liquid sodium, 20: 5861
gamma heating in, calculations for, (E/T), 20: 6517 (CONF-651101-41)
gamma scattering by duct in, streaming in, (T), 20: 6530
neutron elastic scattering at 7 and 14.5 Mev, shell model for, 20: 6434
optical properties of small particles of, (T), 20: 5879 (D-910092-6)
performance of gold-coated, as self-regenerating deuterium target, (E/T), 20: 6334
proton reactions at 1 and 3 Bev, nucleon-pion cascades from, (T), 20: 5927 (ORNL-P-1733)
radiation effects on metabolism of, in rats, 20: 5354
radiation effects on chemical reactions of oxygen with, fast-neutron, 20: 5846
radiation effects on deformation mechanisms in, neutron, 20: 5851
separation from cobalt by solvent extraction, 20: 5602
welding parameters for Armco, electron-beam, 20: 5867

IRON ALLOYS
Al–Fe–U, hot hardness and microstructure, effects of chromium or silicon additions on, 20: 5848
Al–Fe–U, microstructure, effects of heat treatments on, 20: 5848
Al–Fe–U, phase studies, 20: 5843
Ce–Co–Cu–Fe–Ni–Pu, phase studies, 20: 5848
Cr–Fe–Mo–Ni, corrosion of Hastelloy X-280, by helium–water system at 1700, 1900, and 2100°F, 20: 5846
Cr–Fe–Mo–Ni, oxidation at 2050°F of Hastelloy X-280, 20: 5851
Cr–Gd–Fe, properties as control-rod material, 20: 5845
Cr–Gd–Fe, tensile properties of, effects of gadolinium content on, 20: 5845
Fe–Pu, corrosive effects on tantalum–tungsten–yttrium at 700°C, effects of yttrium content on, 20: 5846
Fe–Pu–U, casting of, centrifugal, 20: 5866
Fe–Ta, oxidation kinetics at 500 to 900°C, 20: 5854(T) (JPRS-32341, pp 8-16)
Fe–Ti, oxidation kinetics at 500 to 900°C, 20: 5854(T) (JPRS-32341, pp 8-16)
Fe–W, oxidation kinetics at 500 to 900°C, 20: 5854(T) (JPRS-32341, pp 8-16)

IRON BORIDES
magnetic properties of, 20: 6531 (AD-623530)

IRON(II) CHLORIDES
magnetic properties of, 20: 6531 (AD-623530)

IRON(II) FLUORIDES
magnetic properties of, 20: 6531 (AD-623530)

IRON IONS
diffusion of trivalent, in acid solutions, tracer studies of, 20: 5556
reduction of trivalent, in uranium and/or vanadium aqueous solutions, 20: 5605(P)

IRON ISOTOPES Fe-58
deuteron reactions (d,p), proton polarization from, (E), 20: 6422
helium-3 reactions (He-3,d) at 22 Mev, cobalt-59 energy levels from, (E), 20: 6412

IRON ISOTOPES Fe-59
uptake by marrow transplants in irradiated mice, 20: 5372

IRON OXIDES
effects on fluid-bed fluorination of plutonium–uranium oxides, 20: 5595(R) (ANL-6925, pp 107-64)

IRON(III) OXIDES
sorptive properties for molybdenum-99 in presence of technetium-99, 20: 5591 (SGAE-CH-18/1965)
Fe_2O_3–La_2O_3–NiO, phase studies, 20: 5851
Fe_2O_3–PuO_2, phase studies, 20: 5843

IRON(II) SULFATES
performance for gamma dosimetry, 20: 5750

IRON SYSTEMS
Fe–H_2O, gamma heating in, calculations for, (E/T), 20: 6517 (CONF-651101-41)
Fe–PuO_2, preparation of fuel dispersions of, 20: 5843
Fe–Si–U, crystal structure of U_2Fe_3Si, 20: 5848
Fe–UC, corrosion resistance to steam and water, 20: 5857
Fe–UN, preparation of fuel dispersions of, 20: 5843
Fe–UO_2, preparation of fuel dispersions of, 20: 5843
Fe–ZrB_2, oxidation kinetics at 500 to 1000°C, 20: 5845

IRRADIATION FACILITIES
conveyor system for package, 20: 5617(P)
radioinduced explosive gases in air around high-power gamma, 20: 5670

ISOBUTYRALDEHYDE
deuterium exchange with water, effects of acids, amines, and oxygen bases on, 20: 5565

ISOTOPE EFFECTS
on electron spin resonance of aromatic radicals, 20: 5566

ISOTOPE SEPARATION METHODS
design of electromagnetic mass separator, (E), 20: 5826
diffusion, equations for multicomponent cascade, 20: 5825

ISOTOPIC EXCHANGE
between hydrogen and water vapor, properties of chromium trioxide–nickel catalyst for, 20: 5534
bithermal, of deuterium between liquid ammonia and hydrogen, 20: 5827(P)
of deuterium between isobutyraldehyde and water, effects of acids, amines, and oxygen bases on, 20: 5565
radioinduced catalytic activation of deuterium–hydrogen, in Vycor glass, 20: 5578

ITALY
fallout monitoring in, by strontium-90 content of deciduous teeth collected in 1962, 20: 5655
radiation protection program of, 20: 5433

J

JAPAN
health physics program at National Institute of Radiological Science in Chiba, 20: 5672
strontium-89 and -90 content in rain at Tokyo four weeks after Chinese nuclear explosion of May 14, 1965, 20: 5656

JAWS
radiation effects on development of, in mouse embryos, x, 20: 5395

JOURNAL BEARINGS
properties of liquid-metal lubricated, 20: 5613 (SWRI-1228-8-16)

K

KANSAS
fallout monitoring at Wichita, 1962, 20: 5648(R) (COO-1340-2, pp 1-53)
fallout monitoring, 1963, 20: 5649(R) (COO-1340-2, pp 54-83)

KAOLINS
effects of x agent on colloids of, 20: 5587

KIDNEYS
immune reactions in dogs to transplants of, effects of irradiating transplantation site on, 20: 5344
iodine-131 uptake by fetal, effects of age on, 20: 5259
metabolism of radioactive phosphate in, effects of parathyroid extract on,

20: 5237(R) (UR-668, pp 55-109)
protein synthesis in mitochondria of, tracer study, 20: 5254
radiation effects on metabolism in tissue sections of rat, x, 20: 5352
radiation effects on growth of thymus transplants in mouse, x, 20: 5376
radioinduced carcinoma of, from deposited Thorotrast, 20: 5332
radiosensitivity of, effects of oxygen on, 20: 5466

KRYPTON
diffusion in spherical uranium dicarbide particles, coefficient for, 20: 5848
diffusion in uranium, effects of heating on coefficient of, 20: 5848
effects on radiolysis of ethylene, 20: 5582
electron reactions with, ionization cross sections for, (E/T), 20: 5989
solubility in molten urania at 2900°C, 20: 5914(R) (GEAP-3771-17)

L

LABORATORIES
design of ORNL high-radiation-level analytical, 20: 5501

LABORATORY EQUIPMENT
design of etching cells for semiconductors, (E), 20: 5776
development analysis of highly radioactive materials, 20: 5501

LANTHANUM
combustion with fluorine, products and yields from, 20: 5523(R) (ANL-6925, pp 175-85)
determination by potentiometric titration using EDTA, equipment for, 20: 5502
determination in mixtures of actinides and fission products by paper chromatography, 20: 5509
oxidation of, kinetics of high-temperature, 20: 5859
separation from molten aluminum–magnesium alloys by fused chloride extraction, 20: 5594(R) (ANL-6925, pp 21-106)

LANTHANUM ALLOYS
Au–La, oxidation of, kinetics of high-temperature, 20: 5859
Gd–La, antiferromagnetism and superconductivity coexistence in, (E), 20: 6247
La–Y, electric conductivity at low temperatures, 20: 5888 (NP-15592)

LANTHANUM BORIDES
thermionic emission of, on iridium and tungsten substrates, (E), 20: 5532(T) (K-Trans-10)

LANTHANUM CHLORIDES
spin-lattice relaxation rates of rare earth ions in single crystals of anhydrous, 20: 6542

LANTHANUM FLUORIDES
enthalpy of formation, 20: 5559
$CsF–LaF_3–LiF$, phase diagram, 20: 5558

LANTHANUM OXIDES
phase transformations in, at 50 to 1500°C, 20: 5536
$Fe_2O_3–La_2O_3–NiO$, phase studies, 20: 5851
$La_2O_3–NiO$, phase studies, 20: 5851

LARVAE
radiation effects on behavior of *D. melanogaster*, 20: 5295 (NP-15559)

LARYNX
effects of preirradiation on surgery of, 20: 5463
radiotherapy of carcinomas of, 20: 5486
radiotherapy of tumors of, 20: 5441

LEAD
cosmic-ray transmission through, second maximum in, (E), 20: 6015
determination in hydrocarbon fuels, apparatus for radiometric, 20: 5522(P)
effects on hydrochloric acid cleavage of organotin compounds in methanol–water, 20: 6687(R) (NYO-3453-1)
energy gap in superconducting, (T), 20: 6238
gamma attenuation coefficient of, (E), 20: 6523
gamma coherent scattering at 0.662 and 1.332 Mev, cross sections for, (E/T), 20: 6323
gamma elastic scattering in giant resonance region, cross sections for, (E), 20: 6349
gamma heating in, calculations for, (E/T), 20: 6517 (CONF-651101-41)
gamma scattering at 662 kev, cross section for Compton, (E), 20: 5991
gamma scattering at 1.0 and 4.0 Mev in barriers of, intensity angular distribution of, (T), 20: 6526
gamma scattering at 0.411 to 1.25 Mev in, angular distributions of, (E), 20: 6527
gamma scattering by duct in, streaming in, (T), 20: 6530
neutron elastic scattering at 7 and 14.5 Mev, shell model for, 20: 6434
neutron inelastic scattering at 14 Mev, cross sections for, 20: 6437
neutron scattering by liquid and solid, distributions from multiple, (E/T), 20: 6255 (AERE-R-5016)
performance as gamma and neutron shielding material, (E/T), 20: 6626 (UNC-5118)
photoelectric cross sections of, gamma, (E), 20: 5990
proton reactions at 0.54 to 1.47 Bev, neutron yields from, (E), 20: 5928(R) (PR-P-66)
reactions with sodium metaphosphate, 20: 5529(R) (SC-DC-65-1706)
reactivity worth calculation of, 20: 6279(R) (AI-65-225)
separation from bismuth by solvent extraction using dithizone, 20: 5505

LEAD ACETATES
proton reactions at 3 Bev, fission and fragmentation products from, (E), 20: 5756

LEAD ALLOYS
Bi–Pb, gamma attenuation coefficient in shielding of, (E), 20: 6523
Pb–Sn, gamma attenuation coefficient in shielding of, (E), 20: 6523

LEAD COMPLEXES
with tropolone, preparation, properties, and structure, 20: 5538

LEAD IONS
effects on photolysis and radiolysis of silver oxalate, 20: 5583

LEAD ISOTOPES Pb-210
determination in bone ash, radiochemical, 20: 5504
determination in mill products and biological materials, radiochemical, 20: 5505

LEAD SYSTEMS
C–Pb–Ti, superconductivity of Ti_2PbC, 20: 6228
Pb–H_2O, gamma heating in, calculations for, (E/T), 20: 6517 (CONF-651101-41)

LEAK DETECTORS
development of radiometric, 20: 5817

LEUCINE
metabolism of, in liver and kidney mitochondria, tracer study, 20: 5254

LEUKEMIA
incidence in population of Poland, effects of environmental radioactivity on, 20: 5674
incidence of, after radiotherapy of breast cancer, 20: 5471
radiation effects on cells of murine, in culture, survival curves for neutron and x, 20: 5361
radioinduced in man, statistical study of etiology of, 20: 5307
radioinduced in mice, effects of age, dose, and sex on rate of, 20: 5367
radioinduced in mice, mechanisms for, 20: 5368
radioinduced, etiology and pathology in mice, 20: 5309
radioinduced, Thorotrast, 20: 5353
radiotherapy of, effects of bone marrow grafts on whole-body response to, 20: 5420

LEUKOCYTES
effects of chemicals on activity of alkaline phosphatase in human, 20: 5269
fluorescence intensity in frog, effects of temperature on uv, 20: 5318
radiation effects on, laser and uv, 20: 5396
radiation effects on activity of alkaline phosphatase in human, x, 20: 5269
radiation effects on content in rabbit blood of, fractionated doses of x, 20: 5364
radiation effects on human, during space flight, 20: 5297 (ORNL-P-1734)
radiosensitivity of chromosomes in human, monkey, and rabbit, 20: 5304(T) (JPRS-32985, pp 45-50)

LEUKOCYTOSIS
mechanisms of, study by transfer of inhaled and injected colloids, 20: 5237(R) (UR-668, pp 55-109)

LEUKOPENIA
effects on bacterial infections of rabbit skin, 20: 5315

LEVEL INDICATORS
design of liquid metal, 20: 5594(R) (ANL-6925, pp 21-106)
development of radiometric, 20: 5817

LIGHT
detection of subnanosecond pulses of, 20: 5705
effects on chemotaxis in Euglena and leukocytes, 20: 5396
effects on oxidation-reduction potential of uranium ions, 20: 5548
emission in atmosphere, spectra of x-ray induced, (E), 20: 6181 (AD-619288)
intensity modulation of terrestrial, atmospheric effects on, 20: 6186(T) (UCRL-Trans-1269(L))

LIGHT SOURCES
design of subnanosecond, 20: 5705
operation of pencil, for programming storage device using cathode-ray tube, 20: 5690

LINEAR ACCELERATORS
accelerating stage structures for proton, design of, (T), 20: 5937 (KFK-348)
beam control system for proton, analysis of r-f, (T), 20: 5938 (LA-3372)
beam duration for electron, method for extending, 20: 5964(P)
beam phase volume parameters in injector, proton, 20: 5956
data logging equipment for proton, (E), 20: 5953
description of 3.5-Mev electron, in India, 20: 5715 (AEET-227)
development, 20: 5965(P)
feasibility of modified PHERMEX as photoneutron source, (E), 20: 5936 (CONF-650217, pp 77-81)
monitoring nitrogen-13 and oxygen-15 from electron, 20: 5774
research with Mark II and Mark III, review of, 20: 6276(R) (AD-619576)

shielding design criteria for 800-Mev proton, 20: 5940 (LA-DC-7522)
space-charge effects in standing-wave, longitudinal, (T), 20: 5962
uses of LAMPF proton, as thermal neutron sources, (E), 20: 5935 (CONF-650217, pp 73-6)
waveguides for, resonance method for adjusting circular-iris, 20: 5955

LINOLEIC ACID
radiation effects on content in bean leaves of, x, 20: 5265(T)

LINOLENIC ACID
radiation effects on content in bean leaves of, x, 20: 5265(T)

LIPIDS
radiation effects on rabbit liver mitochondrial, y, 20: 5379

LIQUID JETS
perturbation solution for laminar and turbulent MHD free, in transverse magnetic field effects, (T), 20: 6175

LIQUID METAL COOLED REACTORS
power output control systems for 200-Mw(e) sodium graphite, 20: 6617 (NAA-SR-Memo-11339)

LIQUIDS
interactions in alloys of, morphology of, 20: 5895(R) (TID-22271)
superfluidity of Fermi, (T), 20: 6237
theory of superfluid Fermi, 20: 6229

LITHIUM
corrosive effects on refractory alloys in niobium–zirconium alloy forced-convection loop, 20: 5853 (TIM-898)
corrosive effects on refractory metals and alloys at 2500 to 3400°F, 20: 5851
determination in radioactive process solutions, automated flame photometric method for, 20: 5496 (DP-985)
diffusion in germanium in boiling liquids, (E), 20: 5702
molecular structure of, orbital density in, 20: 5524 (ANL-7076)

LITHIUM ALLOYS
Al–Li, precipitation of helium in irradiated, effects of density and defect distribution on, 20: 5848
Bi–Li, spectra in lithium halides, absorption, 20: 6024 (ANL-6925 (p.235-47))

LITHIUM BERYLLIUM FLUORIDES
uses in thermonuclear reactors, 20: 6452 (AD-619669)

LITHIUM CHLORIDES
heptane–LiCl, radiation effects on coalescence rates in liquid, 20: 5571 (ORNL-TM-1283)
LiCl–KCl, effects of molten, on reaction of uranium dioxide with chlorine, 20: 5547
LiCl–$MgCl_2$–NaCl, melting points of, effects of composition on, 20: 5594(R) (ANL-6925, pp 21-106)
LiCl–$MgCl_2$–KCl, melting points of, effects of composition on, 20: 5594(R) (ANL-6925, pp 21-106)
LiCl–$MgCl_2$, solvent properties for californium and yttrium, 20: 5594(R) (ANL-6925, pp 21-106)
LiCl–NaCl, effects of molten, on reaction of uranium dioxide with chlorine, 20: 5547

LITHIUM FLUORIDES
color centers in, pressure effects on hyperfine structure of F, (E), 20: 6543
performance as thermoluminescent radiation detector for charged particles and neutrons, 20: 5572 (USNRDL-TR-909)
use in thermoluminescence dosimetry of cesium-137 in sheep, 20: 5285 (BNWL-SA-172)
x-ray Raman effect in, search for, (E), 20: 6539
$CsF–LaF_3–LiF$, phase diagram, 20: 5558

LITHIUM ISOTOPES Li-6
lithium-6 elastic scattering at 1.6 to 3.5 Mev, 20: 6442
neutron reactions (n,t) with, in thermonuclear reactor blankets, 20: 6454 (AD-619671)
photodisintegration, (T), 20: 6368
reactions (Li-6,2α) with tritium at 0.65 to 0.97 Mev, alpha spectra from, (E), 20: 6351

LITHIUM ISOTOPES Li-7
energy levels from beryllium-9 (d,α) reactions at 11 Mev, (E), 20: 6360
lithium-7 elastic scattering at 2.0 to 3.25 Mev, 20: 6442
neutron reactions (n,tn) with, in thermonuclear reactor blankets, 20: 6454 (AD-619671)
proton reactions (p,n) near threshold, neutron yield from, (E/T), 20: 6355
proton reactions (p,n) near threshold, neutron energy spectra from, (T), 20: 6356

LITHIUM ISOTOPES Li-8
production in proton reactions with copper, gold, and silver at 2 Bev, (E), 20: 6409

LITHIUM NITRATES
hexane–$LiNO_3$, radiation effects on coalescence rates in liquid, 20: 5571 (ORNL-TM-1283)

LITHIUM SYSTEMS
H–Ir–Li, phase studies, 20: 5849
H–Li–Rh, phase studies, 20: 5849

LITHIUM TELLURIDES
spectra in lithium halides, absorption, 20: 6024(R) (ANL-6925(p.235-47))

LIVER
iodine-131 uptake by fetal, effects of age on, 20: 5259
protein synthesis in mitochondria of, tracer study, 20: 5254
radiation effects on synthesis of microsomal enzymes in rat, x, 20: 5282(R) (AD-623599, pp 1-15)
radiation effects on synthesis of microsomal enzymes in rat, x, 20: 5283(R) (AD-623599, pp 16-27)
radiation effects on binding of mitochondrial lipids isolated from rat, y, 20: 5379
radiography of metastases in, using Thorotrast, 20: 5465
radioinduced fibrosis in human, Thorotrast, 20: 5353
radioinduced hemangioma in human, following radiography, Thorotrast, 20: 5311
uptake of technetium-99-labeled albumins and colloids by, for visualization by external scanning, 20: 5456

LOOPS
design and performance of molten salt test, 20: 5594(R) (ANL-6925, pp 21-106)
fluid flow in natural-circulation, 20: 5620 (AE-200)

LOS ALAMOS MOLTEN PLUTONIUM REACTOR EXPERIMENTS
fuel burnup determination in, experiment design for, 20: 6613 (LA-DC-7475)
reactivity response to fission gas bubbles, 20: 6614 (LA-DC-7476)

LUMINESCENCE
radiation effects on, of acridine-orange-stained Tetrahymena, x, 20: 5267
radioinduced, in lymphocytes, x, 20: 5383

LUMINESCENT DETECTORS
performance of electroluminescent image intensifiers for monitoring electron and gamma beams, (E), 20: 5773
performance of, for solid body dosimetry for radiotherapy, 20: 5479

LUNGS
radiation effects on incidence of urethan-induced tumors in mouse, y, 20: 5328
uptake of technetium-99-labeled albumins and colloids by, for visualization by external scanning, 20: 5456

LUTETIUM ALLOYS
Lu–Th, metallurgical properties and phase studies on, 20: 5891(R) (NYO-2159-1)
Lu–Y, electric conductivity at low temperatures, 20: 5888 (NP-15592)
Lu–Zr, metallurgical properties and phase studies on, 20: 5891(R) (NYO-2159-1)

LUTETIUM ISOTOPES Lu-175
energy level transitions in, E2/M1 mixing ratios and K conversion coefficients in rotational, (E), 20: 6386
neutron reactions (n,γ) at 0.4 to 3 Mev, cross sections for, (E), 20: 6556(R) (ANL-7105, pp 36-58)
proton reactions (p,2n) at 12 Mev, hafnium-174 levels from, (E), 20: 6366

LUTETIUM PHTHALOCYANINES
preparation and spectra of, 20: 5560

LYMPH CELLS
radiation effects on content in lymph nodes, x, 20: 5296(R) (NP-15585)
radioinduced luminescence of, x, 20: 5383

LYMPH SYSTEM
analysis for deposited Thorotrast in nodes, 20: 5399
chemotherapy of sarcomas of, 20: 5485
fluorescence intensity in frog, effects of temperature on uv, 20: 5318
radiation effects on repopulation by lymphocytes of nodes of, x, 20: 5296(R) (NP-15585)
radiation effects on, biochemical, x, 20: 5341
radiation effects on, morphological, x, 20: 5341
radiation effects on immunological competence in dog, y, 20: 5344
radiotherapy of sarcomas of, 20: 5485
surgery of sarcomas of, 20: 5485

M

MACHINING
developments in close tolerance, 20: 6690 (Y-NA-14)
effects of temperature on operations in, 20: 6688 (Y-DA-1014)

MAGNESIUM
bremsstrahlung reactions (γ,p) at 31 Mev, spectra from, (E), 20: 6399
combustion with fluorine, products and yields from, 20: 5523(R) (ANL-6925, pp 175-85)
diffusion of plutonium in, at 420, 460, and 500°C, 20: 5848
effects on *in vitro* calcification, 20: 5237(R) (UR-668, pp 55-109)
radiation effects on corrosion by Santowax OM at 500 to 700°F, fast-neutron, 20: 5846
reactions with uranium fluorides, 20: 5870(P)

MAGNESIUM ALLOYS

pressing coating of, on reactor fuel, grain-size control in, 20: 5871(P)
pressing coatings of, on fuel elements for operation at 140 to 350°C, 20: 5872(P)
separation from praseodymium by fused chloride extraction, 20: 5594(R) (ANL-6925, pp 21-106)
Al–Mg, separation of lanthanum from, by fused chloride extraction, 20: 5594(R) (ANL-6925, pp 21-106)
Cd–Mg, separation of uranium from, by fused chloride extraction, 20: 5594(R) (ANL-6925, pp 21-106)
Cd–Mg, solvent properties for uranium, 20: 5594(R) (ANL-6925, pp 21-106)
Cd–Mg–Pu–Zn, stability in mild steel and stainless steel containers at 600°C, 20: 5594(R) (ANL-6925, pp 21-106)
Cd–Mg–U–Zn, corrosive effects with chloride flux on carbon steel, Croloy, and stainless steel at 600 to 650°C, 20: 5594(R) (ANL-6925, pp 21-106)
Cd–Mg–U–Zn, phase studies, 20: 5594(R) (ANL-6925, pp 21-106)
Mg–Mn–Zr, diffusion of plutonium in MAGZAN-II and ZR55, at 420, 460, and 500°C, 20: 5848
Mg–Pu, melting points of, effects of composition on, 20: 5594(R) (ANL-6925, pp 21-106)
Mg–Zn, separation of plutonium from, by fused chloride extraction, 20: 5594(R) (ANL-6925, pp 21-106)
Mg–Zn, separation of californium and yttrium from, by fused chloride extraction, 20: 5594(R) (ANL-6925, pp 21-106)

MAGNESIUM CHLORIDES
$LiCl–MgCl_2–NaCl$, melting points of, effects of composition on, 20: 5594(R) (ANL-6925, pp 21-106)
$LiCl–MgCl_2–KCl$, melting points of, effects of composition on, 20: 5594(R) (ANL-6925, pp 21-106)
$LiCl–MgCl_2$, solvent properties for californium and yttrium, 20: 5594(R) (ANL-6925, pp 21-106)
$MgCl_2–KCl–NaCl$, solvent properties for lanthanum, plutonium, and praseodymium, 20: 5594(R) (ANL-6925, pp 21-106)
$MgCl_2–KCl–NaCl$, solvent properties for uranium, 20: 5594(R) (ANL-6925, pp 21-106)

MAGNESIUM ISOTOPES Mg-24
bremsstrahlung reactions (γ,p) at 31 Mev, spectra from, (E), 20: 6399
deuteron reactions (d,α) at 11.45 to 12.10 Mev, (E), 20: 6369
energy levels of, parity and spin, 20: 5928(R) (PR-P-66)
energy levels of, gamma branching in, (E/T), 20: 6295 (NP-15647)

MAGNESIUM ISOTOPES Mg-25
deuteron reactions (d,α) at 11.45 to 12.10 Mev, (E), 20: 6369
deuteron reactions (d,pγ) at 3.00 and 5.22 Mev, angular correlations in, (E), 20: 6410
proton reactions (p,γ) at 920 kev to 1.8 Mev, energy spectra from, (E), 20: 6438

MAGNESIUM ISOTOPES Mg-26
energy levels of, parity and spin of, (E), 20: 6410

MAGNESIUM OXIDES
effects on properties of zirconia at high temperatures, 20: 5851
energy levels of, 20: 6532 (CALT-221-13)
fracture of, Petch equation for grain size effect in, 20: 5903
radioinduced luminescence of, energy variation of ion, 20: 5573

MAGNESIUM SULFIDES
preparation for luminescence dosimeters, 20: 5742(R) (UCRL-14351)

MAGNESIUM SYSTEMS
$Mg–UO_2$, properties in dispersion type fuel elements, 20: 6684

MAGNET COILS
design for magnetic mirror machines, engineering drawings for, 20: 6514
design of air-core betatron, 20: 5961
use of niobium–zirconium superconducting, in double Helmholtz arrangement, 20: 5614

MAGNETIC FIELDS
charged particle containment and motion in static, (T), 20: 6459 (CNIE-PE-1)
configuration in plasma-filled waveguide, bifurcation, (T), 20: 6481
effects of coplanar, on conducting gas channel flow stability, (T), 20: 6174
effects of corotating structure in interplanetary, on cosmic radiation and geomagnetic activity, (E), 20: 5972
effects of multipole, on hydromagnetic eigenmodes in plasma, (T), 20: 6492
effects on critical currents in superconducting films, (E), 20: 6232
effects on erbium single crystals from 10 to 300°K, (E), 20: 6547
effects on laminar and turbulent MHD free jet, perturbation solution for, (T), 20: 6175
effects on scintillation counter operation, 20: 5736 (NP-15597)
effects on small pulsed dipole-induced oscillations in collisionless plasma, (T), 20: 6498
effects on small-amplitude wave propagation in hot plasma, (T), 20: 6500
interactions with plasma of infinite conductivity, (T), 20: 6444 (AD-617553)
loss in charged-particle accelerators, device for measuring index of, 20: 5959
measurement in linear pinch devices, probes for, 20: 6507
measurement of high gradient time variant, digital system for, 20: 5682 (MURA-716)
measurement of ionospheric, equipment for vlf, (E), 20: 6180 (AD-619250)
plasma acceleration by, turbulence in current sheet in, 20: 6450(R) (AD-619527)
plasma compression by cusp, electron density and temperature in shock-heated, (E), 20: 6495
plasma containment in toroidal octopole, (E), 20: 6460 (GA-6594)
plasma kinetics in rotating, 20: 6479
production of megagauss, for plasma confinement, 20: 6515(P)
shock propagation in nonuniform, 20: 6158(R) (AD-619999)
structure of interplanetary, quasi-stationary corotating, 20: 5972
use of pulsed, in devices with trochoidal electron beams, 20: 5929

MAGNETIC MIRROR MACHINES
magnetic coils for ALICE, engineering drawings of trapping, 20: 6514
plasma confinement and heating in DECA-2, 20: 6469(T) (UCRL-Trans-1256(L))
plasma diffusion in Q, enhanced, 20: 6466 (SIT-2813-33)
vacuum system gate valves for ALICE, engineering drawings of, 20: 6513

MAGNETIC MIRRORS
charged particle adiabatic containment by multipole cusp, (T), 20: 6496
charged particle trapping and containment in nonadiabatic, statistical theory for, (T), 20: 6494
plasma containment and motion in, (T), 20: 6459 (CNIE-PE-1)

MAGNETIC PROBES
design for field measurements in linear pinch devices, 20: 6507

MAGNETIC PROPERTIES
of radioinduced free radicals in glycine peptides, 20: 5273

MAGNETITE CONCRETES
gamma scattering by duct in, streaming in, (T), 20: 6530

MAGNETOHYDRODYNAMIC CELLS
design of a-c, 20: 6026(P)
design of high-efficiency a-c, 20: 6028(P)
design of multi-stage, with reheat means, 20: 6029(P)
design using cesium minerals for plasma seeding, 20: 6030(P)
design using helical gas flow, 20: 6027(P)
development for AARR, 20: 6665(R) (ANL-7105, pp 59-71)
performance of Faraday-type, with series connected electrodes, (E), 20: 6025

MAGNETOHYDRODYNAMICS
boundary layer effects on electrostatic probe performance, (T), 20: 5689
electric conductivity in, finite, (T), 20: 6157 (AD-617898)
equations for plasma waves in inhomogeneous medium, 20: 6511
equations of, uses in geophysics, (T), 20: 6212
flow in planar-magnetic and gravitational fields, nonuniform rotational, 20: 6172
flow of conducting incompressible fluid, oscillating dielectric sphere induced, (T), 20: 6161 (NP-15630)
flow of medium with finite conductivity, in presence of mass forces, 20: 6171
fluid flow disturbances in, propagation of weak, (T), 20: 6170
fluid flow in, heat transfer in transient, (T), 20: 6176
fluid flow in, properties and problems of, 20: 6156 (AD-617562)
gas flow in, magnetic field effects on stability of channel, (T), 20: 6174

MAGNETOMETERS
design for ionospheric use, 20: 6180 (AD-619250)
development for high-gradient time-variant fields, 20: 5682 (MURA-716)

MAGNETOSPHERE
electron distribution in, hydromagnetic wave dispersion characteristics for, (T), 20: 6202
ion distributions in, helium and hydrogen, (E), 20: 6198

MAGNETS
description of 9.5-kOe, for production of nuclear orientation, 20: 5715 (AEET-227)
design and fabrication of niobium–zirconium superconducting, 20: 5614
uses of iron transmission, for circular-polarization measurements on gamma radiation, 20: 5764

MAGNOX ALLOYS
development for advanced GCR, review of, 20: 6612 (INR-622/IX/R)

MAIZE
radiation effects on growth of seedlings of, in contaminated soil, β, 20: 5305

MAKROFOL
ion tracks in, registration mechanisms of heavy, 20: 5755
performance as heavy ion detector, 20: 5756

MAMMALS
book: *Mammalian Radiation Lethality*, 20: 5405
radiation effects on adaptive responses of, x, 20: 5319
radiosensitivity of, cyclic variations in, 20: 5336

radiosensitivity of intestinal cells of hedgehog, *Erinaceus europaeus*, effects of hibernation on x, 20: 5377
MAN
calcium-47 metabolism in, kinetics of, 20: 5260
cesium-137 body burden of, in Toronto, 20: 5671
content of thorium-232 daughters in thorotrast-injected, 20: 5237(R) (UR-668, pp 55-109)
metabolism of calcium in, computer model for, 20: 5260
osteoid content of vertebral bones of, effects of age, 20: 5233(R) (COO-119-232, pp 99-121)
radiation dose absorbed by, during diagnostic radiography, x, 20: 5440
radiation dose to children, from radiographic diagnosis of congenital heart disease, 20: 5455
radiation dose to skeleton of, time variation of strontium-90, 20: 5429
radiation effects on white blood cells during space flight, 20: 5297 (ORNL-P-1734)
radiation hazards of diagnostic radiography during pregnancy, 20: 5476
radiation injuries, protective effects of bone marrow grafts, 20: 5420
radioactivity in, calibration of whole-body counting instruments, 20: 5426
radioactivity in, whole-body counting of, 20: 5427
radioinduced leukemia in, statistical study of etiology of, 20: 5307
radioinduced tumors in, statistical study of etiology of, 20: 5307
radiosensitivity of chromosomes in leukocytes in, 20: 5304(T) (JPRS-32985, pp 45-50)
radiotherapy of hemangiomas in children, 20: 5443
uptake of iodine-131 from ingestion of contaminated milk, 20: 5237(R) (UR-668, pp 55-109)
MANGANESE
determination in iron by activation methods, 20: 5514
determination in tissues, spectrochemical method for, 20: 5251(R) (UR-668, pp 123-49)
effects on radioinduced luminescence of zinc silicates, 20: 5573
separation from cobalt by solvent extraction, 20: 5602
MANGANESE ALLOYS
Ce–Mn, phase studies at 500 to 800°C of cerium-rich, 20: 5851
Mg–Mn–Zr, diffusion of plutonium in MAGZAN-II and Zr55, at 420, 460, and 500°C, 20: 5848
Mn–Pt, neutron diffraction by ordered, at 26 and 250°C, 20: 5912
MANGANESE IONS
electron spin resonance of divalent, 20: 5533
MANGANESE ISOTOPES Mn-54
activity and half life of, (E), 20: 5928(R) (PR-P-66)
MANGANESE STEEL
performance for ionization chamber construction, 20: 5716 (AEEW-M-470)
Mn–Mo, radiation effects on mechanical properties of A302B and AMMO2, fast-neutron, 20: 5846
MANGANESE SULFATES
magnetic structure, (E), 20: 6546
MASERS (OPTICAL)
effects on chemotaxis in Euglena and leukocytes, 20: 5396
performance as heat sources for metal–water reaction studies, 20: 6552(R) (ANL-6925, pp 187-233)
use for determining electron density and velocity behind shock waves, (E), 20: 6490
use for remote opening of metal containers, 20: 5669
use with interferometers for plasma density measurements, 20: 6471
MASS SPECTROMETERS
data recording system for isotopic, development of, 20: 5684 (WAPD-T-1770)
description of, at installations in India, 20: 5715 (AEET-227)
design of isotope-separating, (E), 20: 5826
design of 94-channel, for analysis of pulsed ion beams, (E), 20: 5698
ion detection in, using electron multiplier tubes, 20: 5706
MATERIALS TESTING
defectoscopy of components and materials of First Czechoslovakian Atomic Power Station, (E), 20: 6633(T) (AECL-2286)
methods for plastic fatigue of pressure vessels, nondestructive, 20: 5894 (SWRI-1228-3-3)
nondestructive methods for SAP tubing, 20: 5630 (NAA-SR-Memo-11562)
nondestructive radiometric, method of gage compensation for, 20: 5712(P)
MATERIALS TESTING REACTOR
fuel element burnup in, ceramic and metallic, 20: 6558(R) (ANL-7115, pp 42-67)
MATHEMATICS
calculation of ψ, ϕ, and their derivatives, 20: 5829 (CEA-R-2824)
expansion of functions in terms of Chebyshev polynomials, 20: 5828 (AAEC/TM-293)
Liouville theorem for variational analysis, general forms of, 20: 5830 (CERN-65-38)
number generators for, Fourier analysis of random, 20: 5833 (ORNL-3866)
rings of, computer programming from linear ordered, 20: 5831 (EUR-1919.f)
MATTER
energy gap and single particle energy in, coupling between, (T), 20: 6311
neutron resonance integrals for, computer program for calculating, 20: 6291 (NAA-SR-Memo-11538)
radiation transport in, finite difference methods for nonlinear, 20: 6522 (UCRL-12411)
radioinduced damage at low temperatures, facilities for in-pile studies of, (E), 20: 5569 (CONF-650217, pp 108-10)
MEATS
radiation effects on content of free amino acids in beef, γ, 20: 5278
MECHANICS
Liouville theorem in statistical, general forms of, 20: 5830 (CERN-65-38)
MEDICAL PERSONNEL
phosphatase activity in leukocytes of radiological, 20: 5269
radiation dose to dental, during radiography, 20: 5430
radiation hazards to radiological, review, 20: 5434
radiation hazards to urologists, during urethrographic examinations, 20: 5459
radiation protection of, 20: 5433
radiation protection of radiography technicians, 20: 5489
MEIOSIS
radiation effects on stages of, in Artemia oocytes, x, 20: 5359
MELAMINE, TRIETHYLENE-
effects on *Paramecium aurelia*, effects of streptomycin on recovery from mutagenic, 20: 5417
MEMBRANE FILTERS
performance in counting megakaryocytes, 20: 5301(R) (UR-668, pp 1-54)
MEMBRANES
radiation effects on electrical potential of frog muscle, γ, 20: 5293(R) (COO-205-55, Paper 2)
radiation effects on permeability of, in plant cells, 20: 5294(R) (COO-205-55, Paper 3)
radioinduced permeability of erythrocyte, effects of cysteamine and sodium cyanide on, x, 20: 5342
MEMORY DEVICES
operation of computer, using light pencil and cathode-ray tube, 20: 5690
MERCURY
excretion of inhaled volatile, by mercury–salt-injected rats, 20: 5251(R) (UR-668, pp 123-49)
flow of, MHD of oscillating sphere induced, (T), 20: 6161 (NP-15630)
mercury ion reactions with vapors of, production of metastable atoms in, 20: 6003
metabolism of inhaled, in rats, 20: 5251(R) (UR-668, pp 123-49)
photoelectric cross sections of, gamma, (E), 20: 5990
production of metastable atoms of, by charge exchange, 20: 6003
radioinduced emanation from, holdup time of, (E), 20: 6298(R) (PPAD-2137-566)
MERCURY IONS
formation from neutral metastable mercury atoms, 20: 6003
reactions with mercury vapor, production of metastable atoms in, 20: 6003
MERCURY ISOTOPES Hg-189
energy levels and half life, (E), 20: 6298(R) (PPAD-2137-566)
MERCURY ISOTOPES Hg-191
production by proton reactions with gold-197 at 2.3 Bev, cross section for, (E), 20: 6298(R) (PPAD-2137-566)
MERCURY ISOTOPES Hg-192
production by proton reactions with gold-197 at 2.3 Bev, cross section for, (E), 20: 6298(R) (PPAD-2137-566)
MERCURY ISOTOPES Hg-193
decay of, gamma spectra from, (E), 20: 6298(R) (PPAD-2137-566)
production by proton reactions with gold-197 at 2.3 Bev, cross section for, (E), 20: 6298(R) (PPAD-2137-566)
MERCURY ISOTOPES Hg-195
production by proton reactions with gold-197 at 2.3 Bev, cross section for, (E), 20: 6298(R) (PPAD-2137-566)
MERCURY ISOTOPES Hg-197
production by proton reactions with gold-197 at 2.3 Bev, cross section for, (E), 20: 6298(R) (PPAD-2137-566)
MESIC ATOMS
energy-level shifts in hydrogen, from vacuum polarization, (T), 20: 5995
MESIC MOLECULES
energies and wave functions of $(p\mu p)^+$, (T), 20: 5980 (AD-617522)
MESONS
interactions of pseudoscalar and vector, at low energies, (T), 20: 6068
interactions of, solution of singular N/D equations for, 20: 6130
interactions with mesons, current commutation relations for, (T), 20: 6077
interactions with baryons, Muskhelishvili method for amplitude of V–θ, 20: 6123
interactions with nucleons at high energy, total cross section differences for, (T), 20: 6082
interactions with baryons, non-compact group representation of, 20: 6102 (IC/65/79)

photoproduction of vector, spin correlations in, (T), 20: 6076
photoproduction on nucleons, SU(6) and SU(6)W for, 20: 6055
production in nucleon-nucleon interactions, bremsstrahlung theory for multiple, 20: 6053
production of pseudoscalar, in electron-positron annihilations, selection rules for, (T), 20: 6040 (NP-15602)
symmetries of noncollinear diagrams and the Johnson-Treiman relations for, 20: 6143
symmetry for, subgroup of SU(8), (T), 20: 6110
theory of pseudoscalar and vector, bootstrap algebra for, 20: 6060
MESONS, RESONANCE
classification of, supermultiplet for, 20: 6134
production in meson (π^-)-proton interactions at 3.3 and 3.9 Bev/c, (E/T), 20: 6041 (UCRL-11942)
properties of meson (ρ) bound states, (T), 20: 6092
symmetry models for spin-2 SU(6), 20: 6151
MESONS (ϵ)
production in deuteron-meson (π^+) interactions at 3.29 Bev/c, (E), 20: 6079
MESONS (η)
photoproduction on protons at 0.3 to 5.5 Bev, (E/T), 20: 6037 (DESY-65/11)
MESONS (K)
decay of, effect of final-state strong interactions on probability of (3π), (T), 20: 6086
decay of, matrix elements for leptonic, (T), 20: 6035 (CERN-64-13 (Vol.4), pp 1-49)
interactions with nucleons, single and double resonance production in, (T), 20: 6069
interactions with photons, resonance model for magnetic polarizability from, 20: 6090
interactions with protons, hyperon (Ξ) production in, (E), 20: 6099
MESONS (K^-)
capture by emulsion nuclei, production of Y_0^* (1405) in, (E), 20: 6051
interactions with deuterons, hyperon (Ξ^-)-neutron resonance production in, 20: 6073
parity, (T), 20: 6283 (CERN-64-13(Vol.4), pp 137-86)
reactions with emulsion nuclei at 50 to 1500 Mev/c, heavy hypernuclei from, (E), 20: 6294 (NP-15617)
MESONS (K^0)
decay of K_2^0, 3π, (E), 20: 6031 (BNL-9613)
decay of, shadow universe correlations with neutrino experiment, (T), 20: 6045(T)
MESONS (K^+)
decay of, effect of final-state strong interactions on probability of (3π), (T), 20: 6086
MESONS (K_{e3})
decay of, universality in Cabibbo's theory for, (T), 20: 6080
MESONS ($K_{\mu 2}^0$)
decay, (E), 20: 6095
MESONS ($K_{\mu 3}^+$)
decay of, meson (μ^+) polarization in, (E), 20: 6075
MESONS ($K_{\pi 3}$)
decay of, effect of final-state strong interactions on probability of, (T), 20: 6086
decay of, radiative, (T), 20: 6067
MESONS (μ)
decay of, V-A interaction and coupling constants in, (T), 20: 6048
shielding against, at 200-Bev proton synchrotron, (T), 20: 5945 (UCRL-16464)
MESONS (μ^-)
capture by oxygen-16, rate of, (E), 20: 6273 (AD-617398)
interactions with electrons and nuclei at 5 to 50 Bev, (E), 20: 6007 (CONF-640919, pp 143-8)
production by electrons in nuclear Coulomb field, cross sections for, (T), 20: 6089
MESONS (μ^+)
interactions with electrons and nuclei at 5 to 50 Bev, (E), 20: 6007 (CONF-640919, pp 143-8)
magnetic moment of, g-factor for, 20: 6282 (CERN-64-13(Vol.4), pp 97-136)
polarization in decay of mesons ($K_{\mu 3}^+$), (E), 20: 6075
MESONS (ω)
interactions with mesons (π) at low energies, (T), 20: 6068
photoproduction on protons at 0.3 to 5.5 Bev, (E/T), 20: 6037 (DESY-65/11)
production in antiproton-proton inelastic interactions at 3.6 Bev/c, (E), 20: 6097
MESONS (π)
interactions of many-body systems of, SU(4) and SU(3) for isotopic structure of, 20: 6150
interactions with mesons (π), off-the-mass-shell complete-unitarity equations for, 20: 6044
interactions with virtual nucleons, effects on vertex of, (T), 20: 6054
interactions with mesons (ω) at low energies, (T), 20: 6068
interactions with nucleons, single and double resonance production in, (T), 20: 6069
interactions with mesons (π), current commutation relations for, (T), 20: 6077
interactions with protons at high energies, M(12) invariance and universality for, (T), 20: 6081
interactions with photons, resonance model for magnetic polarizability from, 20: 6090
interactions with nucleons, calculation of higher resonance energies in, 20: 6096
interactions with electrons at 16 Bev/c, cross sections for, (E), 20: 6098
interactions with nucleons, solutions of Chew-Low equations for, 20: 6106 (JINR-P-2369)
interactions with nucleons in emulsion, intranuclear cascades from, (E/T), 20: 6287 (JINR-P-2373)
photoproduction on protons at 0.3 to 5.5 Bev, (E/T), 20: 6037 (DESY-65/11)
production in antiproton-proton inelastic interactions at 3.6 Bev/c, (E), 20: 6097
production of nucleon-pion, showers in iron by 1- and 3-Bev protons, (T), 20: 5927 (ORNL-P-1733)
MESONS (π^-)
capture by light nuclei, yields and energy spectra from, (E/T), 20: 6292 (NP-15601)
interactions with protons at 10 Bev/c, analysis of inelastic, (E/T), 20: 6038 (INR-646/VI/PH)
interactions with protons in carbon, hyperon (Λ^0) production in, (E), 20: 6071
interactions with protons, coupling constant and s-wave scattering lengths for elastic, (T), 20: 6083
interactions with protons at 4 Bev/c, cross sections for elastic, (E), 20: 6100
interactions with protons at 3.3 and 3.9 Bev/c, resonances from, (E/T), 20: 6041 (UCRL-11942)
reactions (π^-,π^-pn) with argon-40 at 500 to 1100 Mev, cross sections of, (E), 20: 6298(R) (PPAD-2137-566)
MESONS (π^0)
photoproduction on deuterium, cross sections for, 20: 6094
photoproduction on helium-4 at 300 Mev, impulse approximation for, (T), 20: 6365
MESONS (π^+)
interactions with deuterons at 3.29 Bev/c, neutral scalar meson production from, (E), 20: 6079
interactions with protons, coupling constant and s-wave scattering lengths for elastic, (T), 20: 6083
MESONS (ρ)
bound states in systems of, (T), 20: 6092
photoproduction on protons at 0.3 to 5.5 Bev, (E/T), 20: 6037 (DESY-65/11)
MESOSPHERE
electron precipitation at subauroral latitudes, effects of relativistic, (E), 20: 6201
METABOLISM
determination of skeletal, methods for, 20: 5237(R) (UR-668, pp 55-109)
radiation effects on, 20: 5308
radiation effects on, in lens of cattle and guinea pigs, effects of age, x, 20: 5333
radiation effects on oxidative phosphorylation in rat thymus and spleen, 20: 5341
radiation effects on bacterial, γ, 20: 5346
METAL SPRAYING
equipment and procedure for, plasma, 20: 5837 (NLCO-966)
METALLIC FILTERS
fabrication of strontium, for x-ray absorption, 20: 5692
METALLURGICAL EQUIPMENT
press design, hydrostatic, 20: 6692(P)
METALS
boiling and entrainment mechaniams of, 20: 5594(R) (ANL-6925, pp 21-(ANL-6925, pp 21-106)
creep property measurements on, mathematical system for extrapolation of, 20: 5880(R) (EURAEC-1310)
determination by activation, method for avoiding correction for chemical yield in, 20: 5494 (AEET-217)
fabrication by explosive forming, 20: 5867
joining to ceramics using pressure at high temperatures, 20: 5866
lubricity of liquid, in journal bearings, 20: 5613 (SWRI-1228-8-16)
molecular structure, 20: 6551
METAPHOSPHATES
performance of silver-activated glasses of for neutron dosimetry, 20: 5713 (AD-623384)

METASTASES
radiography of liver, using Thorotrast, 20: 5465
METEORITES
age, origin, and rare-gas loss of, (E), 20: 5979
analysis of bronzite chondrites, for rare gases, (E), 20: 5975
analysis of iron, for argon, helium, and neon isotopes, (E), 20: 5977
gas content of, solar wind source for primordial, 20: 5976
potassium content in amphoterite chondrites, (E), 20: 5979
xenon-129 production in, mechanisms for, 20: 5978
METEOROLOGY
computer analysis of data on Montgomery stream functions and thermodynamics, 20: 5645(R) (COO-1340-2, pp 122-45)
criteria for rapid transport of nuclear debris from stratosphere to troposphere, 20: 5649(R) (COO-1340-2, pp 54-83)
effects on fallout deposition, 20: 5678
jet stream behavior over U. S., 20: 5644(R) (COO-1340-2, pp 110-21)
of North Dakota, 20: 5678
predictions in, for Salmon Event, 20: 5667 (VUF-1020)
tropopause-level cyclogenesis, effects of, on fallout transport from stratosphere, 20: 5650(R) (COO-1340-2, pp 84-109)
METHANE
deuterium exchange with hydrogen in, over palladium–ruthenium alloys at 90 to 170°C, 20: 5557
electron reactions with, ionization cross sections for, (E/T), 20: 5989
reactions with recoil carbon-11 atoms, mechanism and products of, 20: 5570 (JUL-228-RC)
methane–O, reactions with recoil carbon-11 atoms, 20: 5570 (JUL-228-RC)
METHANE, BROMO-
reactions with electrons in organic glasses, yields of free radicals from, 20: 5577
METHANE, CHLORO-
electron reactions with, ionization cross sections for, (E/T), 20: 5989
METHANE, IODO-
iodine-131 exchange with silver iodide, effects of surface structure on, 20: 5544
reactions with electrons in organic glasses, yields of free radicals from, 20: 5577
METHANESULFONIC ACID
effects on red clover, morphological and mutagenic, 20: 5491
METHANOL
radiolysis of, effects of water on yields of hydrogen peroxide from, 20: 5581
uses as medium for drifting lithium into germanium, (E), 20: 5702
methanol–H_2O, use in paper chromatography of compounds labeled with iodine-125 and iodine-131, 20: 5515
METHIONINE
metabolism in blood serum of, tracer study in dogs, 20: 5249(R) (COO-119-232, pp 203-18)
METHYL SULFOXIDE
effects on oxygen effect in irradiated barley seed, 20: 5298(R) (RLO-353-4)
METHYLAMINE
reactions with recoil carbon-11 atoms, mechanism and products of, 20: 5570 (JUL-228-RC)
METHYLTHYMOL BLUE
analytical uses in determination of fluorides by titration using uranium, 20: 5520
METROLOGY
signal analysis in noise background using data accumulation, (T), 20: 5695
use of dimensional, for nondestructive fuel element testing, 20: 6632(T) (AEC-tr-6628)
MICA
ion tracks in, registration mechanisms of heavy, 20: 5755
performance as heavy ion detector, 20: 5756
MICE
effects of injected x irradiated cystamine-treated ascitic cell and normal tissue homogenates on mitotic activity in, 20: 5412
hypobaric oxygen respiration in, design of exposure chamber for, 20: 5228(R) (AD-623599, pp 28-36)
immune reactions in cultured spleen from irradiated, treated with rat bone marrow, 20: 5397
radiation dosimetry of phantom depth dose studies on gamma and neutron, 20: 5286 (CONF-650616-16)
radiation effects on immune reactions in thymectomized, 20: 5408 (USNRDL-TR-920)
radiation effects on spermatogenesis in, living on radioactive soils, 20: 5387
radiation effects on skeletal development of embryos of, x, 20: 5395
radiation effects on immune reactions in, 20: 5413
radiation effects on mitosis in cornea of, x, 20: 5421
radiation effects on viability of *Schistosoma mansoni* cercariae in, γ, 20: 5313
radiation effects on skeletal development in embryos of, x, 20: 5316
radiation effects on bone marrow, x, 20: 5320
radiation effects on skeletal development of embryos of, x, 20: 5326
radiation effects on skeletal development in embryos of, x, 20: 5327
radiation effects on incidence of urethan-induced tumors in lungs of, γ, 20: 5328
radiation effects on skeletal development in embryos of, x, 20: 5337
radiation effects on immune reactions to marrow transplants in, methods for assaying x, 20: 5372
radiation effects on growth of thymus transplants in kidneys of, x, 20: 5376
radiation effects on life span of, computer program for evaluation of, 20: 5300 (UCLA-12-573)
radiation injuries in, protective effects of mercaptoethylamine, 20: 5407(R) (AD-623599, pp 37-44)
radiation injuries in, protective effects of AET against γ, 20: 5410
radiation injuries in, protective effects of 2-aminothiazoline salts against γ, 20: 5410
radioinduced leukemia in, etiology and pathology of, 20: 5309
radioinduced leukemia in, effects of age, dose, and sex on rate of, 20: 5367
radiosensitivity of fibrosarcoma cell line in, 20: 5362
radiosensitivity of, effects of circadian rhythmicity on x, 20: 5336
strontium-90 induced bone tumors in, effects of bacterial infection on incidence of, 20: 5373
MICROÖRGANISMS
radioinduced sensitization of, in food, 20: 5816
MICROSOMES
dissociation of reticulocyte, 20: 5264
properties of subunits of reticulocyte, 20: 5264
radiation effects on synthesis of enzymes in hepatic, x, 20: 5282(R) (AD-623599, pp 1-15)
radiation effects on synthesis of enzymes in hepatic, x, 20: 5283(R) (AD-623599, pp 16-27)
MICROWAVE EQUIPMENT
development for linear accelerators, 20: 5965(P)
magnetic-field-plane bifurcation in waveguide filled with anisotropic plasma, (T), 20: 6481
properties of disc-loaded deflecting waveguides, (T), 20: 5934 (CERN-65-37)
use of iris-loaded waveguides for extending electron beam duration, 20: 5964(P)
waveguides for linear accelerators, resonance method for adjusting circular-iris, 20: 5955
MICROWAVES
effects on animals, 20: 5302(R) (UR-668, pp 161-6)
effects on gaseous magnetoplasma, helical instability, (E/T), 20: 6446 (AD-617696)
MILITARY COMPACT REACTOR
shielding for, design and testing of, (E/T), 20: 6626 (UNC-5118)
MILK
cesium-137 content in Toronto, 20: 5671
iodine-131 content of, in Kansas and Missouri, 1962, 20: 5648(R) (COO-1340-2, pp 1-53)
radioactivity from cesium-137 and strontium-90 in, New Zealand, April–June 1965, 20: 5664(R) (NP-15639)
strontium-90 content of, from Mandan-Minot region of North Dakota, 20: 5678
MINERAL METABOLISM
effects of nerve supply on, in rat bones, tracer study, 20: 5370
radiation effects on, in rat bones, tracer study, 20: 5370
MISSOURI
fallout monitoring at Kansas City, 1962, 20: 5648(R) (COO-1340-2, pp 1-53)
fallout monitoring, 1963, 20: 5649(R) (COO-1340-2, pp 54-83)
MITOCHONDRIA
radiation effects on lipids of, isolated from rabbit liver, γ, 20: 5379
radioinduced changes in, x, 20: 5301(R) (UR-668, pp 1-54)
synthesis of proteins by hepatic and kidney, tracer study, 20: 5254
MITOSIS
chemically-induced inhibition of, in RCP cell strain, nitrogen mustard, 20: 5323
radiation effects on rate in mouse cornea of, effects of ganglionic blocking drugs and head shielding on, 20: 5421
radioinduced inhibitation of, in RCP cell strain, x, 20: 5323
MOLDS
radiation effects on *Botrytis cinerea*, γ, 20: 5371
MOLECULAR BEAMS
production of hydrogen, ion source for, 20: 6000
MOLECULAR STRUCTURE
book: *The Molecular Designing of Materials and Devices*, 20: 6551
orbital density comparisons in, 20: 5524 (ANL-7076)

MOLECULES
neutron resonance absorption and scattering by, cross sections for, (T), 20: 6266
reaction mechanisms of protein macro-, with radiomimetic and radioprotective compounds, 20: 5423
reactions with hydrated electrons, review on, 20: 5525 (IA-1041)
MOLLUSKS
electron reactions with nonpolar and polar, thermal, 20: 5985 (ORNL-TM-1262)
MOLTEN SALT REACTORS
characteristics of homogeneous and quasi-homogeneous, catalog, 20: 6554 (ANL-7092)
MOLYBDENUM
brazing alloys for, development of, 20: 5867
brazing to TZM molybdenum alloy, brazing alloy development for, 20: 5866
coatings on, lifetime and performance of molybdenum silicide, 20: 5910
compatibility with plutonium-uranium carbides, 20: 6600(R) (ANL-7105, pp 1-35)
corrosion by tin at 1000°C, 20: 6024(R) (ANL-6925(p.235-47))
diffusion in molybdenum disulfide, inter-, 20: 5846
diffusion of beryllium in, 20: 5846
dislocation loops in quenched, 20: 5851
dislocation structures in annealed and deformed sheets of, 20: 5846
ductility of, effects of boron on, 20: 5851
ductility of, mechanism controlling, 20: 5851
fabrication and properties of, handbook on, 20: 5874 (AGARDograph-94)
internal friction of annealed and deformed, 20: 5846
oxidation by air at 800°C, effects of phosphide coatings on, 20: 5851
oxidation rates of, effects of dissociation of molecular oxygen on, 20: 5846
properties of single-crystal, relations between, 20: 5851
radiation effects on properties of, combined impurity and neutron, 20: 5851
radiation effects on creep-rupture of, fast neutron, 20: 5851
reactions with steam at 1100 to 1700°C, 20: 6552(R) (ANL-6925, pp 187-233)
reactions with water at 1100 to 1700°C, 20: 5846
refractive index of gaseous, (E/T), 20: 5879 (D-910092-6)
stress relaxation prior to yield point in, 20: 5851
uses in thermonuclear reactors, 20: 6452 (AD-619669)
MOLYBDENUM ALLOYS
coatings on, lifetime and performance of molybdenum silicide, 20: 5910
fabrication and properties of, handbook on, 20: 5874 (AGARDograph-94)
Al–Mo, phase studies, 20: 5846
Al–Mo–Ti–V, phase studies, 20: 5851
Cr–Fe–Mo–Ni, corrosion of Hastelloy X-280, by helium–water system at 1700, 1900, and 2100°F, 20: 5846
Cr–Fe–Mo–Ni, oxidation at 2050°F of Hastelloy X-280, 20: 5851
Cu–Mo–Zr, oxidation resistance of, in carbon dioxide at 600 and 700°C, 20: 5860
Mo–Nb, crystal structure of, phonons in disordered, (E), 20: 5911
Mo–Nb, oxidation by oxygen at 400 to 1200°C, 20: 5851
Mo–Nb–Ta–W–Zr, creep tests on NB132M at 3200°F, 20: 5885(R) (NAS-CR-54773)
Mo–Nb–Ta–W, strain aging of solution-hardened, 20: 5851
Mo–Nb–V–Zr, bonding of B-66, method for diffusion, 20: 5867
Mo–Nb–V–Zr, corrosion by cesium vapor and liquid lithium at 2500 to 3400°F of B-66, 20: 5851
Mo–Nb–V–Zr, weld stability in B-66, 20: 5866
Mo–Nb–V–Zr, welding parameters for B-66, electron-beam, 20: 5867
Mo–Ni–W, mechanical properties, effects of aging temperature and molybdenum and tungsten content on, 20: 5851
Mo–Pu–U, ignition of, effects of molybdenum content on, 20: 5843
Mo–Pu–U, properties of, compressive, thermal expansion, and tensile, 20: 5843
Mo–Re, dislocation structures in annealed and deformed sheets of, 20: 5846
Mo–Re, internal friction of annealed and deformed, 20: 5846
Mo–Re, properties of sigma-phase precipitates in, 20: 5851
Mo–Re–W, fabrication of thin-walled tubing of, 20: 5867
Mo–Ti, bonding to foils of nickel, niobium tantalum, and titanium by vacuum hot-pressing, 20: 5866
Mo–Ti, creep tests on TZC and TZM at 3200°F, 20: 5885(R) (NAS-CR-54773)
Mo–Ti–V, elastic properties, 20: 6556(R) (ANL-7105, pp 36-58)
Mo–Ti–Zr, bonding of TZM, method for diffusion, 20: 5867
Mo–Ti–Zr, brazing molybdenum to TZM, brazing alloy development for, 20: 5866
Mo–Ti–Zr, corrosion by cesium vapor and liquid lithium at 2500 to 3400°F of TZM, 20: 5851
Mo–Ti–Zr, extrusion of TZM, process for, 20: 5867
Mo–U, coating with nickel to prevent stress-corrosion cracking in air, electrolytic, 20: 5867
Mo–U, radioinduced swelling in, reactor, 20: 5848
Mo–W, corrosion by liquid lithium and cesium vapor at 2500 to 3400°F, 20: 5851
Mo–Zr, internal friction of annealed and deformed, 20: 5846
MOLYBDENUM BORIDES
phase studies of molybdenum-rich, 20: 5850
MOLYBDENUM ISOTOPES
determination in irradiated uranium-235, 20: 5493(R) (ANL-6925, pp 253-4)
nucleon interactions in, effective, (T), 20: 6337
MOLYBDENUM ISOTOPES Mo-98
neutron reactions (n,γ) at 0.4 to 3 Mev, cross sections for, (E), 20: 6556(R) (ANL-7105, pp 36-58)
MOLYBDENUM ISOTOPES Mo-99
separation from metastable technetium-99 by sorption on ferric oxide, 20: 5591 (SGAE-CH-18/1965)
MOLYBDENUM OXIDES
preparation of thin films of, 20: 5846
reactions with fluorine, 20: 5595(R) (ANL-6925, pp 107-64)
MOLYBDENUM SILICIDES
performance as coating on molybdenum and molybdenum alloys, 20: 5910
BN–$MoSi_2$–ZrB_2, mechanical properties of composites of, 20: 5845
MOLYBDENUM STEEL
radiation embrittlement, effects of dispersed second phase on fast neutron, 20: 5846
Cr–Mo, radiation effects on corrosion of AISI 4130, by Santowax OM at 500 to 700°F, fast-neutron, 20: 5846
Cr–Mo–Ni–Nb–V, development as HY-180/210 steel, 20: 5851
Mn–Mo, radiation effects on mechanical properties of A302B and AMMO2, fast-neutron, 20: 5846
MOLYBDENUM SULFIDES
diffusion in molybdenum, inter-, 20: 5846
MOLYBDENUM SYSTEMS
Al–C–Mo, superconductivity of Mo_3Al_2C, 20: 6228
C–Mo–Ti–Zr, microstructure and tensile properties of, effects of composition, heat treatment, and processing on, 20: 5846
C–Mo–U, phase studies, 20: 5843
MONKEYS
radiosensitivity of chromosomes in leukocytes in, 20: 5304(T) (JPRS-32985, pp 45-50)
MONTE CARLO METHOD
performance for calculating neutron albedo from concretes, 20: 6519(R) (ORNL-3858(Vol.1), pp 20-41)
performance for fitting experimental data to theoretical curves, 20: 6286 (ISS-65/10)
uses for analysis of intranuclear cascades, (E/T), 20: 6287 (JINR-P-2373)
MOSQUITOES
distribution in Hawaii of Culex, 20: 5240
incorporation of phosphorus-32 in, method for, 20: 5240
MÖSSBAUER EFFECT
absorber thickness optimization for, 20: 6336
measurement of, velocity calibration of spectrometers for, 20: 5786
research, 20: 6302(R) (TID-22384)
use in nuclear physics, 20: 6293 (NP-15603)
MOUTH
radiation effects on development of, in mouse embryos, x, 20: 5326
radiation effects on osseous development of, in mouse embryos, x, 20: 5327
radiation effects on development of, in mouse embryos, x, 20: 5337
MULTIPLICATION FACTOR
calculation of, computer programs for, 20: 6581 (CEA-R-2872)
measurement for borated aluminum-plutonium-polyethylene systems, 20: 6578(R) (BNWL-149, pp 45-7)
measurement for borated aluminum-polyethylene-uranium and aluminum-plutonium-polyethylene systems, 20: 6577(R) (BNWL-149, pp 22-35)
MUSCLES
radiation effects on content of free amino acids in beef, γ, 20: 5278
radiation effects on activity of, γ, 20: 5375
radiation effects on mechanical properties of excised frog and rat, γ, 20: 5292(R) (COO-205-55, Paper 1)
radiation effects on electrical properties of excised frog, γ, 20: 5293(R) (COO-205-55, Paper 2)
uptake of neutral red by frog sartorius, effects of heavy water on, 20: 5317
MUTATIONS
chemically-induced in peas, 20: 5238
chemically-induced in presoaked Arabidopsis seeds, 20: 5357
chemically-induced in Saccharomyces, for radioresistance, 20: 5360
radio- and chemically-induced in red clover, x, 20: 5491
radioinduced in Arabidopsis seeds, x, 20: 5357

radioinduced in Drosophila, x, 20: 5338
radioinduced in Drosophila, x, 20: 5358
radioinduced in Drosophila, 20: 5301(R) (UR-668, pp 1-54)
radioinduced in *Escherichia coli*, β, 20: 5350
radioinduced in peas, x, 20: 5238
radioinduced in rice, x, 20: 5393
radioinduced in Saccharomyces, β, uv, and x, 20: 5360
radioinduced in wheat, x, 20: 5403

N

NAPHTHALENE, 1,2,3,4-TETRAHYDRO-
dehydration and dehydrogenation of, on praseodymium oxide, 20: 5567
1,4-NAPHTHALENEDIOL, 2-METHYL- DIPHOSPHATE, SODIUM SALTS
radiosensitivity effects of, in cancer patients, 20: 5437
NEBRASKA
fallout monitoring, 1963, 20: 5649(R) (COO-1340-2, pp 54-83)
NECK
radiotherapy of tumors of, 20: 5441
NEODYMIUM
alpha reactions (α,xny) at 27 to 52 Mev, gamma spectra from, (E), 20: 6348
oxidation of, kinetics of high-temperature, 20: 5859
NEODYMIUM ALLOYS
Au–Nd, oxidation of, kinetics of high-temperature, 20: 5859
Cd–Nd, thermodynamic properties of liquid, 20: 5594(R) (ANL-6925, pp 21-106)
Nb–Zr, metallurgical properties and phase studies on, 20: 5891(R) (NYO-2159-1)
Nd–Th, metallurgical properties and phase studies on, 20: 5891(R) (NYO-2159-1)
Nd–Y, electric conductivity at low temperatures, 20: 5888 (NP-15592)
NEODYMIUM IONS
spin-lattice relaxation rates in single crystals of anhydrous lanthanum trichloride, (E), 20: 6542
NEODYMIUM OXIDES
hardness and melting point, 20: 5845
phase transformations in, at 50 to 1500°C, 20: 5536
NEODYMIUM PHTHALOCYANINES
preparation and spectra of, 20: 5560
NEON
effects on radiolysis of ethylene, 20: 5582
electron elastic scattering by, spin polarization from, (T), 20: 5998
electron reactions with, ionization cross sections for, (E/T), 20: 5989
glow discharges in, performance of probes for space potential determination in, 20: 6164
helium ion elastic scattering by, molecular state crossing for perturbation induced in, (E), 20: 5996
structure of single crystal, isotope effects in isothermal compressibility, lattice constant, and thermal expansion in, 20: 6685 (COO-1198-296)
NEON ISOTOPES
content in iron meteorites, (E), 20: 5977
NEON ISOTOPES Ne-20
content in bronzite chondrites, ratio to helium-4 and neon-22, (E), 20: 5975
energy levels of, projected Hartree-Fock spectra for, (T), 20: 6419
NEON ISOTOPES Ne-21
nuclear structure of, rotation-vibration model for, 20: 6441
NEON ISOTOPES Ne-22
content in bronzite chondrites, ratio to neon-20, (E), 20: 5975
effects on structure of single crystal, isothermal compressibility, lattice constant, and thermal expansion in neon, 20: 6685 (COO-1198-296)
NEPTUNIUM
determination in mixtures of actinides and fission products by paper chromatography, 20: 5509
NEPTUNIUM COMPLEXES
with phenolphthalein, mole ratio and variation methods for determining sorptive properties of, 20: 5530 (SC-RR-65-625)
NEPTUNIUM FLUORIDES
properties and reactions of, 20: 5595(R) (ANL-6925, pp 107-64)
NEPTUNIUM ISOTOPES Np-237
neutron sensitivity of foil-glass dosimeters of, 20: 5713 (AD-623384)
NERVOUS SYSTEM
radiation effects on adaptive responses of rat, x, 20: 5319
radiation effects on central, γ, 20: 5329
radiation effects on conditioned reflex in goats, γ, 20: 5369
radiation effects on physiology of rat, γ, 20: 5292(R) (COO-205-55, Paper 1)
radiation effects on physiology of frog, γ, 20: 5293(R) (COO-205-55, Paper 2)
radiation effects on physiology of frog, γ, 20: 5292(R) (COO-205-55, Paper 1)
transfer of radiation effects by, in mice, 20: 5421
NEUTRAL RED
uptake by frog sartorius muscle, effects of heavy water on, 20: 5317
NEUTRINOS
emission by copper-63 following neutron capture, 20: 6050
field equations for, dimensionality of real world from strength of, 20: 6218
interactions in emulsions, location and analysis of, (E), 20: 6052
interactions of, review, (T), 20: 6036 (CERN-64-13(Vol.4), pp 51-95)
interactions of, shadow universe concept for, (T), 20: 6045(T)
interactions with nucleons, baryon resonance production in, (T), 20: 6065
production in meson (μ^-) capture by oxygen-16, (E), 20: 6273 (AD-617398)
production of, isotopic sources for, 20: 6050
reactions with chlorine-37, cross sections for, (T), 20: 6393
NEUTRON BEAMS
flux distribution measurements in, from drift-tube neutron generators, (E), 20: 6263 (NP-15635)
monitoring 2.5 Mev, indirect method for, (E), 20: 5777
production and uses of polarized, in mev to 10-kev range, (E), 20: 6259 (CONF-650217, pp 111-23)
NEUTRON CAPTURE CROSS SECTIONS
measurement for erbium-170 and gadolinium-158 at 4 kev to 2 Mev, (E), 20: 6280(R) (ANL-6925(p.249-51))
NEUTRON CROSS SECTIONS
data requests at U.K. Nuclear Data Library, 20: 6254 (AEEW-M-503)
energy dependence of nuclear, (T), 20: 6404
measurement for thorium from 0.015 to 1.00 kev, (E), 20: 6377
NEUTRON-DIFFRACTION ANALYSIS
neutron sources for, pulsed and steady-state sources, (T), 20: 5726 (CONF-650217, pp 102-7)
neutron sources for, use of pulsed thermal, 20: 6258 (CONF-650217, pp 82-101)
NEUTRON DIFFRACTOMETERS
collimators for, 20: 6268
NEUTRON SHIELDING
gamma dose rates behind, (E/T), 20: 6625 (UNC-5118)
NEUTRON SOURCES
beam sorter design for drift-tube, (E), 20: 6262 (NP-15633)
calibration of Canadian radium–beryllium, absolute and relative, 20: 6265
description of polarized, for mev to 10-kev energies, (E), 20: 6259 (CONF-650217, pp 111-23)
description of, using reactions of LAMPF proton beam with moderated targets, (E), 20: 5935 (CONF-650217, pp 73-6)
development of high-intensity pulsed, conference on, 20: 6256 (CONF-650217)
feasibility of use of upgraded PHERMEX linac as photo-, (E), 20: 5936 (CONF-650217, pp 77-81)
flux distributions from drift-tube, (E), 20: 6263 (NP-15635)
neutron production by D-D, indirect monitoring of, (E), 20: 5777
neutron spectra from americium–beryllium and radium–beryllium, (E), 20: 6269
performance of accelerator-bombarded exponential piles as pulsed, (E), 20: 6257 (CONF-650217, pp 11-24)
performance of fast-burst reactors as pulsed, (E), 20: 6671 (CONF-650217, pp 1-10)
performance of mechanically pulsed fast-burst reactors as, 20: 6672 (CONF-650217, pp 25-35)
performance of pulsed and steady, for diffraction and scattering analysis, (T), 20: 5726 (CONF-650217, pp 102-7)
targets for D-D, performance of self-regenerating, (E/T), 20: 6334
use in moisture gage, 20: 5819
uses of in-pile cryogenic, for basic radiation-damage studies, (E), 20: 5569 (CONF-650217, pp 108-10)
uses of pulsed thermal, for inelastic-scattering analysis of matter, (T), 20: 6258 (CONF-650217, pp 82-101)
NEUTRON SPECTRA
calculation of thermal, in bomb debris, 20: 5609 (LA-3403)
NEUTRON SPECTROMETERS
circuit design for time-of-flight, walk-correction, 20: 5796
description of crystal, at installations in India, 20: 5715 (AEET-227)
design of lithium-6 sandwich semiconductor, for epithermal range, (E), 20: 5714 (AD-623722)
development, 20: 5737(R) (ORNL-3858(Vol.I), pp 59-64)
development of epithermal, 20: 5737(R) (ORNL-3858(Vol.I), pp 59-64)
performance with pulsed and steady-state sources, for diffraction and scattering studies, (T), 20: 5726 (CONF-650217, pp 102-7)
resolution of time-of-flight, geometric, 20: 6297(R) (ORNL-3858(Vol.2), pp 82-90)
NEUTRON SPECTROSCOPY

development for pulsed and steady neutron sources, (T), 20: 5726 (CONF-650217, pp 102-7)
methods for, review of differential and integral, (E), 20: 6260 (CONF-651101-43)

NEUTRONS

absorption by moisture in building materials, 20: 5819
absorption by molecules, cross sections for resonance, (T), 20: 6266
absorption by plutonium-240, calculations for resonance, (E/T), 20: 6577(R) (BNWL-149, pp 22-35)
absorption by promethium-149, cross sections for, (E), 20: 6589
absorption by tungsten, resonance integrals and Doppler coefficients for, 20: 6279(R) (AI-65-225)
absorption in heterogeneous assemblies, resonance, (T), 20: 6579(R) (BNWL-149, pp 48-56)
absorption integrals for cobalt, gold, indium, silver, and uranium-238, infinite-dilution, 20: 6558(R) (ANL-7115, pp 42-67)
absorption resonance integrals for, computer program for calculating, 20: 6291 (NAA-SR-Memo-11538)
attenuation of reactor, in serpentine sand, (E), 20: 6524
decay of polarized, CP violation in, 20: 6087
decay of, angular, energy, and polarization correlations for leptonic, (T), 20: 6088
detection and measurement in reactors, using boron-10-coated ionization chambers, (E), 20: 5717 (AEEW-M-508)
detection and measurement of in-pile, detectors for, (E), 20: 5728 (IBM-65-825-1487)
detection of, audio-visual warning system for, 20: 5733 (LA-DC-6790)
detection of, performance of Eastman Type A film for, 20: 5742(R) (UCRL-14351)
diffraction by ordered platinum–manganese alloys at 26 and 250°C, 20: 5912
distribution in absorbing rod, P_n approximation for, 20: 6267
dose from Wood River Junction criticality accident, 20: 5666 (TID-21995)
effects of in-pile, on SNAP 10A fuels, (E), 20: 6678 (NAA-SR-Memo-11374)
effects on alpha-uranium, orientation and Burgers vectors of dislocation loops from, 20: 5848
effects on circuits, measurement in Pulstar reactor, 20: 6679 (NP-15645)
effects on deformation mechanisms in iron, 20: 5851
effects on man, protective effects of bone marrow grafts, 20: 5420
effects on materials at cryogenic temperatures, measurement in reactors, (E), 20: 5569 (CONF-650217, pp 108-10)
effects on mechanical properties of stainless steels under stress, thermodynamic method for evaluating, 20: 5913(R) (EURAEC-1488)
effects on plastic deformation of alpha-uranium monocrystals, 20: 5916
effects on polymerization of monomers in wood, 20: 5818
effects on properties of molybdenum, combined impurity and, 20: 5851
effects on pulse fission chambers, (E), 20: 5807 (AEEW-M-493)
effects on stress-rupture properties of chromium–nickel–niobium alloys, 20: 5917
effects on tensile properties of Zircaloy-2, effects of hydrogen content on, 20: 5851
effects on thermistors and transistors, 20: 5808 (N65-35081)
effects with recurrent intercrossing on genetic variability in Phaseolus, 20: 5406
emission by excited fission nuclei, (T), 20: 6313
energy spectra from lithium-7 (p,n) reactions near threshold, (T), 20: 6356
energy spectra from (p,n) reactions at 30 and 50 Mev, (E/T), 20: 6361
flux decay constants for finite non-multiplying media, (T), 20: 6580 (CEA-R-2702)
flux decay in reactor moderators, computer program for spectral analysis of, 20: 6585 (NAA-SR-Memo-10941)
flux distribution in reactors, xenon oscillation effects on, (T), 20: 6590
flux distribution in cylindrical cells, energy-dependent, (T), 20: 5928(R) (PR-P-66)
flux distributions in air near ground-air interface, (T), 20: 6528
flux monitoring in reactors, development of regenerating detectors for, 20: 6567 (HW-SA-3600)
interactions with neutrons, N^{9-} production in, (E/T), 20: 6042 (UCRL-16189)
magnetic moment, (T), 20: 6074
multiplication in fissionable media, computer programs for calculating, 20: 6581 (CEA-R-2872)
reactions (n,α), (n,γ), and (n,2n) with ruthenium-104 at 14.7 Mev, cross sections for, (E), 20: 6338
reactions (n,α) with argon-40 at 13.0 to 20.2 Mev, cross sections for, (E/T), 20: 6357
reactions (n,d) with ruthenium-100 and -102, cross sections for, (E), 20: 6338
reactions (n,γ) with cesium-133, rhenium-187, and scandium-45, isomeric cross section ratios for, (E/T), 20: 6301 (TID-22165)
reactions (n,γ) with americium-241, separation of daughters from, (E), 20: 5823(T) (ORNL-tr-892)
reactions (n,γ) with lutetium-175 and molybdenum-98 at 0.4 to 3 Mev, cross sections for, (E), 20: 6556(R) (ANL-7105, pp 36-58)
reactions (n,γ) with gold-197, gold-198 resonance parameters and spins from, (E), 20: 6392
reactions (n,γ) with nuclei, gamma spectra from, (T), 20: 6427
reactions (n,p) with nickel isotopes at 14 Mev, angular and energy distributions from direct, (E), 20: 6440
reactions (n,p) with ruthenium-99 and -101 at 14.7 Mev, cross sections for, (E), 20: 6338
reactions (n,p) with ruthenium-102 and -104 at 14.7 Mev, cross sections for, (E), 20: 6338
reactions (n,p) with chlorine-37 at 13.0 to 20.2 Mev, cross sections for, (E/T), 20: 6357
reactions (n,2n) with copper-63 at 16.59 to 17.71 Mev, excitation curve for, (E), 20: 6319
reactions (n,2n) with beryllium-9 at 14 Mev, excitation and decay mechanisms of, (E), 20: 6320
reactions (n,2n), and (n,p) with ruthenium-96 at 14.7 Mev, cross sections for, (E), 20: 6338
reactions (n,2p), (n,He-3), and (n,2p) with rhodium-103 at 14.7 Mev, cross sections for, (E), 20: 6338
reactions and transport in thermonuclear reactor blankets, 20: 6454 (AD-619671)
reactions with calcium at 3.5 to 5.0 Mev, gamma production in, (E), 20: 6408
reactions with fission products, cross-section calculations for SIZZLE code, 20: 6659 (NAA-SR-Memo-11473)
reactions with plutonium-239, Doppler shifts at 300 to 600°K, 20: 6556(R) (ANL-7105, pp 36-58)
reactions with plutonium-239, Doppler contributions to cross sections for, 20: 6558(R) (ANL-7115, pp 42-67)
reactions with uranium-235 in SGR lattices, epicadmium/subcadmium fission ratios for, (E), 20: 6586 (NAA-SR-Memo-11313)
reactions with uranium-233 and -235, fission fragment kinetic energy from, (T), 20: 6421
reactions with uranium-235, delayed gamma emission in fission, (E), 20: 6316
scattering and transport in fusion reactor blanket assemblies, 20: 6451 (AD-619668)
scattering by benzene, diphenyl, and terphenyl, cross sections for low-energy, 20: 6272
scattering by helium-4 at 22 to 29 Mev, helium-5 energy levels from elastic, (E), 20: 6335
scattering by iron and lead at 7 and 14.5 Mev, shell model for elastic, 20: 6434
scattering by lead, tantalum, thallium, and tungsten at 14 Mev, cross sections for inelastic, 20: 6437
scattering by molecules, cross sections for resonance, (T), 20: 6266
scattering by niobium-93, energy levels from inelastic, (E), 20: 6280(R) (ANL-6925, pp 249-51)
scattering by nuclei, errors in optical model analysis of, 20: 6296(R) (ORNL-3858(Vol.1), pp 1-12)
scattering by nuclei, determination of nuclear equation of state by inelastic, (T), 20: 6379
scattering by palladium at 15, 77, and 298°K, paramagnetic, (E), 20: 6544
scattering by plutonium-239, spin values, average fission width, and total spin correlation from resonance, (E), 20: 6414
shielding studies, 20: 6520(R) (ORNL-3858(Vol.1), pp 42-6)
spectra from gamma reactions (y,n) with beryllium-9 at 3 to 17 Mev, energy levels from, (E), 20: 6390
spectra in multiplying media, measurement of asymptotic, 20: 6591
spectroscopy below 10 ev, differential and integral methods for, (E), 20: 6260 (CONF-651101-43)
thermal utilization in SGR uranium carbide lattices, (E), 20: 6586 (NAA-SR-Memo-11313)
transmission by polarized holmium-165 at 8.3-Mev, 20: 6275(R) (AD-619534)
transport in plane geometry, eigenfunctions and full-range completeness for, (T), 20: 6252 (AD-617880)
transport in plane geometry, half-range completeness and half-space problems for, (T), 20: 6253 (AD-617882)
transport in plutonium critical assemblies, foil activation studies of, 20: 6579(R) (BNWL-149, pp 48-56)
transport in reactors, S2 and S4 calculations of, (T), 20: 6264 (WAPD-T-1849)
tunneling transfer in reactions of identical nuclei, 20: 6387
yields from lithium-7 (p,n) reactions near threshold, (E/T), 20: 6355
yields from meson (π^-) capture by nuclei, (E/T), 20: 6292 (NP-15601)

NEUTRONS, DELAYED

yields in uranium-238 photofission, (E), 20: 6315
NEUTRONS, EPITHERMAL
detection and spectroscopy of, using lithium-6 semiconductor detector, (E), 20: 5714 (AD-623722)
slowing down in concretes, albedo and capture-gamma dose rates for, 20: 6519(R) (ORNL-3858(Vol.1), pp 20-41)
NEUTRONS, FAST
attenuation of reactor, in serpentine sand, (E), 20: 6524
detection and measurement of, using copper-62 activation in copper-63, (E), 20: 6289 (KN-63-10(R))
diffusion in fast reactors, computer program for calculating, 20: 6583 (JAERI-1091)
dosimetry of, performance of silver-activated metaphosphate glass for, 20: 5713 (AD-623384)
dosimetry of, performance on insulators for, 20: 5719 (CEA-R-2846)
dosimetry of, performance of lithium fluoride thermoluminescent detector for, 20: 5572 (USNRDL-TR-909)
effects on chemical reactions of iron with oxygen, 20: 5846
effects on corrosion of selected metals by Santowax OM at 500 to 700°F, 20: 5846
effects on creep-rupture of molybdenum, tungsten, and tungsten–25 rhenium alloy, 20: 5851
effects on density and tensile properties of beryllium, 20: 5849
effects on embrittlement of molybdenum steels with dispersed second phase, 20: 5846
effects on in-pile corrosion of nuclear materials by aqueous solutions, 20: 5852(R) (EURAEC-1522)
effects on mechanical properties of A302B and AMMO2 manganese–molybdenum steels, 20: 5846
effects on mechanical properties of Inconel 600, Inconel 625, Inconel 718, and Incoloy 800, 20: 5851
effects on mechanical properties of carbon or low-alloy steel, 20: 5921
effects on murine leukemia cells in vitro, survival curves for, 20: 5361
effects on properties of type 6061 aluminum alloy, 20: 5846
effects on stress rupture of A-286 alloy and Hastelloy X, 20: 5851
effects on tensile properties of SAP 865, 895, and 930, effects of test temperature on, 20: 5839(R) (RISO-110)
effects on tensile properties of hafnium, 20: 5850
reactions (n,γ) with tin-124 at 62 ev, angular distributions from, (E), 20: 6317
scattering by nitrogen-15 at 1 to 12 Mev, cross sections for, (T), 20: 6426
scattering in rectangular concrete ducts, (E/T), 20: 6519(R) (ORNL-3858(Vol.1), pp 20-41)
transport in air, Sn-method for calculating, 20: 6261 (LA-3415)
NEUTRONS, FISSION
absorption by mice, phantom study, 20: 5286 (CONF-650616-16)
emission of, rate and yields for, (T), 20: 6313
phantom depth dose studies on mice, 20: 5286 (CONF-650616-16)
production of high-intensity pulsed beams of, conference on, 20: 6256 (CONF-650217)
NEUTRONS, THERMAL
attenuation of reactor, in serpentine sand, (E), 20: 6524
detection of, discriminating semiconductor device for, 20: 5802(P)
detection of, performance of liquid scintillators for, 20: 5746 (ZFK-RN-18)
dosimetry of, performance of silver-activated metaphosphate glass for, 20: 5713 (AD-623384)
dosimetry of, performance of insulators for, 20: 5719 (CEA-R-2846)
dosimetry of, performance of lithium fluoride thermoluminescent detector for, 20: 5572 (USNRDL-TR-909)
effects on creep properties of A-286 alloy, 20: 5846
effects on in-pile corrosion of nuclear materials by aqueous solutions, 20: 5852(R) (EURAEC-1522)
effects on properties of type 6061 aluminum alloy, 20: 5846
effects on stress rupture of A-286 alloy and Hastelloy X, 20: 5851
production of pulsed beams of, using accelerator-bombarded exponential piles, (E), 20: 6257 (CONF-650217, pp 11-24)
production of, using reactions of LAMPF proton beam with moderated targets, (E), 20: 5935 (CONF-650217, pp 73-6)
reactions (n,γ) with thallium-203, thallium-204 energy levels from, (E), 20: 6411
reactions with californium-252 and uranium-235, prompt gamma rays from, 20: 6314
reactions with uranium-235, fission yields from, (E), 20: 6288 (KAPL-3113)
scattering by concretes, accuracy of Monte Carlo method for calculating albedo from, 20: 6519(R) (ORNL-3858(Vol.1), pp 20-41)
scattering by liquid and solid lead, distributions from multiple, (E/T), 20: 6255 (AERE-R-5016)
scattering by matter, analytic uses of pulsed-beam inelastic, (T), 20: 6258 (CONF-650217, pp 82-101)
scattering by water, angular distributions and diffusion constants from thermal, (E), 20: 6270
scattering by water-d_2 and zirconium hydride, angular distributions and diffusion constants from, (E), 20: 6271
scattering in rectangular concrete ducts, (E/T), 20: 6519(R) (ORNL-3858(Vol.1), pp 20-41)
NEVADA TEST SITE
ground water discharge, movement, and occurrence in tuffaceous rocks of, 20: 5643 (TEI-862)
NICKEL
bonding to molybdenum–titanium alloy and tungsten by vacuum hot-pressing, 20: 5866
corrosion of 200, by fluoride volatility environments, 20: 5595(R) (ANL-6925, pp 107-64)
deposition on aluminum alloy 6061, 20: 5866
deposition on beryllium of coatings of electroless, 20: 5849
deposition on beryllium and niobium–1 zirconium, electroless, 20: 5867
deposition on fast-burst reactor components, electrolytic, 20: 5867
deposition on uranium–10 molybdenum to prevent stress-corrosion cracking in air, electrolytic, 20: 5867
diffusion in pyrolytic graphite, 20: 5846
effects on hot hardness of zirconium oxides, 20: 5846
effects on oxidation resistance of beryllium–niobium and beryllium–zirconium alloys, 20: 5844
electron band structure of, effects of electron configurations on, (T), 20: 6534 (SC-DC-65-1843)
erosion of 201, by liquid sodium, 20: 5861
gamma heating in, calculations for, (E/T), 20: 6517 (CONF-651101-41)
refractive index of gaseous, (E/T), 20: 5879 (D-910092-6)
NICKEL ALLOYS
Al–Cu–Ni, embrittlement of hydrogenated, solute-induced, 20: 5846
Ce–Co–Cu–Fe–Ni–Pu, phase studies, 20: 5848
Cr–Fe–Mo–Ni, corrosion of Hastelloy X-280, by helium–water system at 1700, 1900, and 2100°F, 20: 5846
Cr–Fe–Mo–Ni, oxidation at 2050°F of Hastelloy X-280, 20: 5851
Cr–Ni–Nb, radiation effects on stress-rupture properties of, neutron, 20: 5917
Mo–Ni–W, mechanical properties, effects of aging temperature and molybdenum and tungsten content on, 20: 5851
Ni–W, creep properties at 750 to 1200°C, effects of tungsten content on, 20: 5851
Ni–W, oxidation kinetics at 500 to 900°C, 20: 5854(T) (JPRS-32341, pp 8-16)
Ni–Zr, oxidation kinetics at 500 to 900°C, 20: 5854(T) (JPRS-32341, pp 8-16)
NICKEL ISOTOPES
deuteron reactions (d,p) and (d,t) with, nuclear structure studies using, 20: 6435
energy levels of, shell model calculations of, 20: 6385
NICKEL ISOTOPES Ni-58
deuteron reactions (d,p), proton polarization from, (E), 20: 6422
neutron reactions (n,p) at 14 Mev, angular and energy distributions from direct, (E), 20: 6440
NICKEL ISOTOPES Ni-59
energy levels of, strength functions for single-particle, 20: 6345
NICKEL ISOTOPES Ni-60
deuteron reactions (d,p), proton polarization from, (E), 20: 6422
neutron reactions (n,p) at 14 Mev, angular and energy distributions from direct, (E), 20: 6440
NICKEL ISOTOPES Ni-61
deuteron reactions (d,p), proton polarization from, (E), 20: 6422
NICKEL ISOTOPES Ni-62
deuteron reactions (d,p), proton polarization from, (E), 20: 6422
NICKEL ISOTOPES Ni-64
deuteron reactions (d,p), proton polarization from, (E), 20: 6422
NICKEL OXIDES
Fe_2O_3–La_2O_3–NiO, phase studies, 20: 5851
La_2O_3–NiO, phase studies, 20: 5851
NICKEL STEEL
welding parameters for maraging, electron-beam, 20: 5867
Cr–Mo–Ni–Nb–V, development as HY-180/210 steel, 20: 5851
NICKEL SYSTEMS
C–Ni–Th, phase studies, 20: 5848
CrO_3–Ni, properties for use as catalyst for hydrogen–deuterium exchange, 20: 5534
Ni–H_2O, gamma heating in, calculations for, (E/T), 20: 6517 (CONF-651101-41)
Ni–ThO_2, bonding of Td nickel, method for diffusion, 20: 5867
Ni–ThO_2, recrystallization properties, 20: 5851
Ni–ZrB_2, oxidation kinetics at 500 to 1000°C, 20: 5845
NICOTINAMIDES
effects on respiration in rat thymocytes in culture, 20: 5340
NIMONIC-75
diffusion into copper at 900°C, 20: 5850

NIOBIUM
annealing properties of single-crystal, containing deformation in twins, 20: 5846
bonding to molybdenum–titanium alloy and tungsten by vacuum hot-pressing, 20: 5866
compatibility with plutonium-uranium carbides, 20: 6600(R) (ANL-7105, pp 1-35)
corrosion by cesium at 1600, 1800, and 2500°F, 20: 5846
diffusion in chromium, inter-, 20: 5846
diffusion in, self-, 20: 5846
effects on mechanical properties of tungsten of alloying additions of, 20: 5851
enthalpy, 20: 5851
fabrication and properties of, handbook on, 20: 5874 (AGARDograph-94)
magnetic fluxoid transitions and loss in multiply connected superconductors of, (E/T), 20: 6246
metallurgy of, research on, 20: 5851
oxidation by air at 800°C, effects of phosphide coatings on, 20: 5851
radiation effects on in-pile corrosion of, by aqueous solutions, 20: 5852(R) (EURAEC-1522)
reactions with steam at 1050 to 1500°C, 20: 6552(R) (ANL-6925, pp 187-233)
sorptive properties for nitrogen, oxygen, and nitrogen–oxygen mixtures, 20: 5851
stress relaxation prior to yield point in, 20: 5851

NIOBIUM ALLOYS
coatings on, lifetime and performance of niobium silicide, 20: 5910
fabrication and properties of, handbook on, 20: 5874 (AGARDograph-94)
Al–Nb, oxidation, 20: 5896 (TID-22388)
Al–Nb, phase studies of, 20: 5896 (TID-22388)
Al–Nb–Ti, oxidation, 20: 5896 (TID-22388)
Al–Nb–Ti, phase studies on, 20: 5896 (TID-22388)
Be–Nb, oxidation resistance of, effects of aluminum, nickel, silicon, and tantalum additions on, 20: 5844
Cr–Nb, precipitation of $NbCr_2$ in, cellular, 20: 5846
Cr–Nb–Ti–V, properties as cladding materials, 20: 5846
Cr–Ni–Nb, radiation effects on stress-rupture properties of, neutron, 20: 5917
Cu–Nb–Zr, alloy element distribution in bulk metal and oxide film on, 20: 5851
Hf–Nb–W–Y, welding parameters for C-129Y, electron-beam, 20: 5867
Mo–Nb, crystal structure of, phonons in disordered, (E), 20: 5911
Mo–Nb, oxidation by oxygen at 40 to 1200°C, 20: 5851
Mo–Nb–Ta–W–Zr, creep tests on NB132M at 3200°F, 20: 5885(R) (NAS-CR-54773)
Mo–Nb–Ta–W, strain aging of solution-hardened, 20: 5851
Mo–Nb–V–Zr, bonding of B-66, method for diffusion, 20: 5867
Mo–Nb–V–Zr, corrosion by cesium vapor and liquid lithium at 2500 to 3400°F of B-66, 20: 5851
Mo–Nb–V–Zr, weld stability in B-66, 20: 5866
Mo–Nb–V–Zr, welding parameters for B-66, electron-beam, 20: 5867
Nb–Ru, phase studies, 20: 5851
Nb–Ta–W–Zr, corrosion by lithium in niobium–1–zirconium alloy forced-convection loop, 20: 5853 (TIM-898)
Nb–Ti, oxidation, 20: 5896 (TID-22388)
Nb–Ti, phase studies on, 20: 5896 (TID-22388)
Nb–Ti, superconducting critical fields in, Pauli paramagnetism effects on upper, (E), 20: 6236
Nb–Ti–V, elastic properties, 20: 6556(R) (ANL-7105, pp 36-58)
Nb–Ti–Zr, bonding of D-36, method for diffusion, 20: 5867
Nb–U–Zr, properties of metastable γ-phase, 20: 5843
Nb–W, corrosion by liquid lithium and cesium vapor at 2500 to 3400°F, 20: 5851
Nb–W, oxidation kinetics at 500 to 900°C, 20: 5854(T) (JPRS-32341, pp 8-16)
Nb–W, oxidation by air at 900 to 1300°C, effects of niobium content on, 20: 5851
Nb–W–Zr, creep tests on AS-30 at 3200°F, 20: 5885(R) (NAS-CR-54773)
Nb–Zr, coating with nickel, electroless, 20: 5867
Nb–Zr, corrosion by cesium at 1600, 1800, and 2500°F, 20: 5846
Nb–Zr, electric conductivity to 1500°C, 20: 5851
Nb–Zr, emissivity to 1500°C, total hemispherical, 20: 5851
Nb–Zr, solubility in sodium at 800 to 1380°C, 20: 5846
Nb–Zr, solvent properties for hydrogen, 20: 5849
Nb–Zr, use as loop material for forced-convection corrosion of refractory alloys by lithium, 20: 5853 (TIM-898)
Nb–Zr, use for superconducting magnet coils, 20: 5614

NIOBIUM CARBIDES
enthalpy equations, 20: 5846
thermal expansion at 30 to 2843°C, 20: 5846

NIOBIUM COMPOUNDS
with tropolone, preparation, properties, and structure, 20: 5538

NIOBIUM ISOTOPES
nucleon interactions in, effective, (T), 20: 6337

NIOBIUM ISOTOPES Nb-92
energy levels of, parity and spin of, (E), 20: 6310

NIOBIUM ISOTOPES Nb-93
deuteron reactions (d,t) at 15 Mev, energy levels from, (E), 20: 6310
energy levels of, neutron cross sections for production of 0.741-Mev, (E), 20: 6280(R) (ANL-6925, pp 249-51)
gamma emission at 0.741, 0.809, and 0.958 Mev, (E), 20: 6280(R) (ANL-6925, pp 249-51)

NIOBIUM ISOTOPES Nb-95
content in fallout, 1963, 20: 5652

NIOBIUM OXIDES
Nb_2O_5–WO_3, phase studies, 20: 5846

NIOBIUM SILICIDES
performance as coating on niobium alloys, 20: 5910

NIOBIUM STEEL
Cr–Mo–Ni–Nb–V, development as HY-180/210 steel, 20: 5851

NIOBIUM SYSTEMS
Al–Nb–N, superconductivity of Nb_3Al_2N, 20: 6228
C–In–Nb, superconductivity of Nb_2InC, 20: 6228
C–Nb–Sn, superconductivity of Nb_2SnC, 20: 6228
C–Nb–W–Zr, bonding of D-43, method for diffusion, 20: 5867
C–Nb–W–Zr, electric conductivity to 1500°C of D-43, 20: 5851
C–Nb–W–Zr, emissivity to 1500°C of D-43, total hemispherical, 20: 5851
C–Nb–W–Zr, mechanical properties of D-43, effects of protective coatings and welding on, 20: 5866
C–Nb–W–Zr, weld stability in D-43, 20: 5866
C–Nb–W–Zr, welding parameters for D-43, electron-beam, 20: 5867
C–Nb–Zr, corrosion by lithium in niobium–1–zirconium alloy forced-convection loop, 20: 5853 (TIM-898)
Nb–N, phase studies, 20: 5851

NITRIC ACID
corrosive effects on stainless steel, 20: 5856
determination in solutions of quaternary ammonium nitrates, potentiometric, 20: 5518
$Al(NO_3)_3$–HNO_3–$NaNO_3$, separation of americium-243 and curium-244 from, using TBP, 20: 5495 (DP-972)

NITRO COMPOUNDS
effects on activity of leukocyte alkaline phosphatase, toxicity, 20: 5269

NITROGEN
diffusion in yttrium at 1235 to 1460°C in electric field, 20: 5599
effects on alpha-beta phase transformation in hafnium, 20: 5850
effects on corrosion of Zircaloy-2 powders by steam or water, 20: 5851
effects on internal friction of chromium–35 rhenium alloy, 20: 5851
effects on radiolysis of ethylene, 20: 5582
effects on strain aging and transition temperature in vanadium, 20: 5851
electric arcs in gravitationless state in, 20: 6163
electron energy losses in, 20: 5542
electron reaction with, cross sections for momentum transfer and drift velocities in, 20: 5985 (ORNL-TM-1262)
electron reactions with molecular, ionization cross sections for, (E/T), 20: 5989
electron scattering by, ionization from, (T), 20: 5982 (AERE-R-5061)
molecular structure of, orbital density in, 20: 5524 (ANL-7076)
performance in fission chambers, 20: 5734 (LFEN-NI-19)
proton elastic scattering at 7.6 to 11.8 Mev, polarization in, 20: 6439
radiation effects on metabolism in dogs of, β and γ, 20: 5381
radiosensitivity effects in Drosophila, x, 20: 5338
reactions with beryllium at 1000 to 1500°C, 20: 5844
separation from argon using titanium sponges, 20: 5594(R) (ANL-6925, pp 21-106)
sorption by niobium, 20: 5851
spectra of atmospheric, x-ray excitation of first negative and second positive band, (E), 20: 6181 (AD-619288)

NITROGEN IONS
production of (V), by electron bombardment, (T), 20: 5982 (AERE-R-5061)

NITROGEN ISOTOPES N-13
energy level transitions in, (E), 20: 6405
energy levels of, parity and spin of ground-state, 20: 6326
monitoring airborne, from electron linacs, 20: 5774

NITROGEN ISOTOPES N-14
deuteron reactions (d,α) at 11.8 and 12.0 Mev, (E), 20: 6369
deuteron reactions (d,pγ) with, gamma spectra from, (E), 20: 5928(R) (PR-P-66)
deuteron reactions with, oxygen-15 gamma transitions from, (E), 20: 6318
helium-3 reactions (He-3,α) at 25.7 and 27.0 Mev, angular distributions from, (E), 20: 6326

NITROGEN ISOTOPES N-15
energy level transitions in, mixing ratios for, (E), 20: 6378
energy levels of, lifetime, parity, and spin of, (E), 20: 5928(R) (PR-P-66)

energy levels of, gamma rays from first two excited, (E), 20: 6318
neutron scattering at 1 to 12 Mev, cross sections for, (T), 20: 6426
NITROGEN ISOTOPES N-16
distribution between steam and water in boiling reactors, 20: 6638
NITROGEN MUSTARDS
effects on giant cell formation in RCP cell strain, 20: 5323
effects on hematopoietic system of rats, pathological, 20: 5296(R) (NP-15585)
effects on induction of leukopenia in rabbits, 20: 5315
effects on mitosis in RCP cell strain, 20: 5323
effects on Saccharomyces radiosensitivity, mutagenic, 20: 5360
NITROGEN OXIDES
effects on oxygen effect in irradiated barley seed, 20: 5298(R) (RLO-353-4)
radioinduced formation of, around high-power gamma facility, ventilation calculations for, 20: 5670
radioprotective effects of, in biological systems, 20: 5296(R) (NP-15585)
NITROGEN SYSTEMS
Al–Nb–N, superconductivity of Nb_3Al_2N, 20: 6228
He–N, performance for irradiation capsule temperature control, 20: 6680 (ORNL-TM-1319)
Hf–In–N, superconductivity of Hf_2InN, 20: 6228
In–N–Ti, superconductivity of Ti_2InN, 20: 6228
Nb–N, phase studies, 20: 5851
N–O, sorption by niobium, 20: 5851
NITROUS ACID
effects on Saccharomyces radiosensitivity, mutagenic, 20: 5360
NONANE
electron reactions in ethylene mixture, cross sections for momentum transfer and drift velocities in, 20: 5985 (ORNL-TM-1262)
NORTH DAKOTA
strontium-90 content in milk of Mandan-Minot region of, 20: 5678
NUCLEAR BATTERIES
performance for electric-power and life-support systems on spacecraft, (E/T), 20: 5820 (NASA-CR-316)
NUCLEAR EMULSIONS
ion tracks in, registration mechanisms of heavy, 20: 5755
meson (K⁻) capture at rest, Y_0^* (1405) production in, (E), 20: 6051
meson (π) reactions with nuclei in, intranuclear cascades from, (E/T), 20: 6287 (JINR-P-2373)
neutrino interactions in, location and analysis of, (E), 20: 6052
nucleon-proton interactions at 30 Bev/c in, models for jets from, (E/T), 20: 6039 (INSJ-90)
proton-induced showers at 24 Bev in, angular distributions from, (E), 20: 6325
NUCLEAR ENGINEERING
Engineering Materials List, cumulative indexes for, 20: 5608 (TID-4102 (1st Rev.))
NUCLEAR HEATING PLANTS
design for use in oil wells, 20: 6651(P)
NUCLEAR MAGNETIC MOMENTS
measurement of, review, (E), 20: 6282 (CERN-64-13(Vol.4), pp 97-136)
orientation of, description of 9.5-kOe magnet for, (E), 20: 5715 (AEET-227)
NUCLEAR MODELS
energy levels in single-particle, 20: 6431
Fermi-liquid theory and Green-function method for spherical, 20: 6425
potentials in single-particle, nonlocal, 20: 6430
rotation-vibration, for odd-A nuclei, 20: 6441
theory of self-consistent cranking, for higher rotational states, 20: 6416
NUCLEAR MODELS (COLLECTIVE)
nuclei physical quantity calculations from, computer programs for even-even, 20: 6278 (AD-623877)
NUCLEAR MODELS (DROP)
fission product distributions in, shell effects on, (T), 20: 6308(T) (ANL-Trans-243)
NUCLEAR MODELS (OPTICAL)
potential for spin-spin interaction in nucleon-nuclei reactions, low-energy, (T), 20: 6395
NUCLEAR MODELS (SHELL)
energy level calculations from, $28 < A \leq 40$, 20: 6295 (NP-15647)
fission product distributions in, (T), 20: 6308(T) (ANL-Trans-243)
properties of $28 < N < 50$, 20: 6435
NUCLEAR PHYSICS
Mössbauer effect applications in, 20: 6293 (NP-15603)
research, 20: 6034 (CERN-64-13(Vol.4))
research, (E), 20: 6296(R) (ORNL-3858(Vol.1), pp 1-12)
research, (E/T), 20: 5928(R) (PR-P-66)
review of research at University of Edinburgh on, 20: 5239
NUCLEAR POWER
use in desalination, economic aspects of, 20: 6649
NUCLEAR POWER PLANTS
design of, optimization program for, 20: 6605 (GAMD-6673)
mounting submarine, external vs internal, 20: 6664
NUCLEAR REACTIONS
amplitudes of direct, Feynman graph method for, 20: 6383
deuteron stripping, L-space localization in, 20: 6394
energy level excitation in spherical nuclei in stripping, collective, (T), 20: 6353
kinematics of, computer programs for UMC-1 for, 20: 6285 (INP-414/PL)
kinematics of, having three-particle final states, 20: 6333
neutron tunneling transfer in, 20: 6387
projection operators for rearrangement in, (T), 20: 6312
resonance-mode effects on channel coupling in, (T), 20: 6426
theory of pickup and stripping, below Coulomb barrier, 20: 6352
NUCLEAR SHOWERS
distributions in intranuclear, from 17-Bev mesons, (π), (E/T), 20: 6287 (JINR-P-2373)
distributions in nucleon-pion, in iron from 1- and 3-Bev protons, (T), 20: 5927 (ORNL-P-1733)
NUCLEAR SPECTRA
measurement of, data acquisition systems for, 20: 6307 (UCRL-16439)
NUCLEAR STRUCTURE
effects of dynamic, on internal conversion, review of, 20: 6332
theory of, quasi-particle approximation in, 20: 6433
NUCLEAR THEORY
deuteron electromagnetic structure in, 20: 6304 (TID-22401)
NUCLEI
alpha transitions in spherical, (T), 20: 6376
beta decay of spherical, collective level excitation in, (T), 20: 6353
bremsstrahlung reactions with Coulomb field of, pair production in, (T), 20: 6072
charged-particle reactions and scattering, Fraunhofer and Fresnel diffraction in, (T), 20: 6359
charged-particle scattering by, radial relativistic Coulomb integrals for, (T), 20: 6375
deuteron stripping reactions with, L-space localization in, 20: 6394
electron inelastic scattering by, two-nucleon correlation functions and cross sections for, (T), 20: 6424
electron reactions with Coulomb field of, cross sections for meson (μ^-) production in, (T), 20: 6089
electron reactions (e,e'p) with, Monte Carlo analysis of, 20: 6286 (ISS-65/10)
energy level excitation in spherical, collective, 20: 6353
energy levels for $28 < A \leq 40$, shell model calculations for, 20: 6295 (NP-15647)
energy levels of deformed, cranking model for higher rotational, (T), 20: 6416
energy levels of, self-consistent theory of bounded rotational, 20: 6344
energy spectra from solar flares, 20: 5969
excitations of spherical, Fermi-liquid theory and Green-function method for collective, 20: 6425
fission of, liquid-drop model with shell effects for energy and mass spectra from, (T), 20: 6308(T) (ANL-Trans-243)
fission of, neutron emission from, (T), 20: 6313
internal conversion in, review of dynamic structure effects in, 20: 6332
magnetic moment measurement of, review, 20: 6282 (CERN-64-13(Vol.4), pp 97-136)
magnetic octupole moments in, 20: 6277 (AD-619952)
meson (K⁻) capture by emulsion, production of Y_0^* (1405) in, (E), 20: 6051
meson (K⁻) reactions with emulsion, heavy hypernuclei from, (E), 20: 6294 (NP-15617)
meson (μ) reactions at 5 to 50 Bev, 20: 6007 (CONF-640919, pp 143-8)
meson (π^-) capture by, yields and energy spectra from, (E/T), 20: 6292 (NP-15601)
meson (π) interactions with nucleons in emulsion, intranuclear cascades from, (E/T), 20: 6287 (JINR-P-2373)
neutron cross sections of, energy dependence of, (T), 20: 6404
neutron inelastic scattering by, equation of state from, (T), 20: 6379
neutron reactions (n,γ) with, gamma spectra from, (T), 20: 6427
nuclear binding and particle separation energies for $22 \leq Z \leq 120$, 20: 6290 (LA-3280)
nucleon pairing interactions in, Bogolyubov compensation method and variational principle for, (T), 20: 6343
nucleon reactions with, spin-spin interaction in low-energy optical potential for, (T), 20: 6395
nucleon scattering by, errors in optical model analysis of, 20: 6296(R) (ORNL-3858(Vol.1), pp 1-12)
nucleon scattering by, resonance-mode effects on channel coupling in, (T), 20: 6426
nucleon scattering by, shell model for, 20: 6434
nucleon single-particle potential for, nonlocal, 20: 6430
nucleon-proton interactions at 30 Bev/c in, models for jets from, (E/T), 20: 6039 (INSJ-90)

photon reactions with, resonance-mode effects on channel coupling in, (T), 20: 6426
proton polarization by complex, 45-Mev, (E), 20: 6274 (AD-619061)
proton reactions (p,γ) with 56 ≤ Z ≤ 77 at 10.5 Mev, isomeric transitions in, 20: 5928(R) (PR-P-66)
proton reactions (p,d) with, projection operators for, (T), 20: 6312
proton scattering at 20 Bev, analysis of small-angle, 20: 5720 (CERN-65-33)
reactions of identical, neutron tunneling transfer in, 20: 6387
structure of deformed even-even, computer programs for collective model calculations of, 20: 6278 (AD-623877)

NUCLEI (CELLS)
effects of nitrogen mustard on RCP strain, 20: 5323

NUCLEIC ACIDS
metabolism by bacteriophages, 20: 5250(R) (UR-668, pp 110-16)
radiation effects on content of, in developing chick embryos, x, 20: 5306

NUCLEONS
form factors of, review of Stanford research on, 20: 6277 (AD-619952)
interactions in molybdenum, niobium, technetium, yttrium, and zirconium isotopes, effective, (T), 20: 6337
interactions with protons at 30 Bev/c, models for jets from, (E/T), 20: 6039 (INSJ-90)
interactions with nucleons, time-reversal noninvariant potential for, 20: 6047
interactions with nucleons in I = 0 S = 1 state, N/D method for s-wave, 20: 6049
interactions with nucleons, bremsstrahlung theory of multiple meson production in, 20: 6053
interactions with mesons (π), virtuality effects on, (T), 20: 6054
interactions with photons, SU(6) and SU(6)W for meson production in, 20: 6055
interactions with neutrinos, baryon resonance production in, (T), 20: 6065
interactions with mesons (K) and (π), single and double resonance production in, (T), 20: 6069
interactions with photons, spin correlations in vector meson production in, (T), 20: 6076
interactions with mesons and nucleons at high energy, total cross section differences for, (T), 20: 6082
interactions with mesons (π), calculation of higher resonance energies in, 20: 6096
interactions with alpha particles in spherical nuclei, (T), 20: 6376
interactions with mesons (π), solutions of Chew-Low equations for, 20: 6106 (JINR-P-2369)
interactions with hyperon (Λ), (T), 20: 6283 (CERN-64-13(Vol.4), pp 137-86)
interactions with mesons (π) in emulsion nuclei, intranuclear cascades from, (E/T), 20: 6287 (JINR-P-2373)
interactions with protons at 24 Bev, angular distributions from shower, (E), 20: 6325
magnetic moment ratio of, (T), 20: 6074
pairing interactions in nuclei, Bogolyubov compensation method and variational principle for, (T), 20: 6343
photoproduction of N* (1238) on protons at 0.3 to 5.5 Bev, (E/T), 20: 6037 (DESY-65/11)
potential in nuclei, nonlocal single-particle, 20: 6430
production of nucleon-pion, showers in iron by 1- and 3-Bev protons, (T), 20: 5927 (ORNL-P-1733)
reactions with nuclei, spin-spin interaction in low-energy optical potential for, (T), 20: 6395
scattering by nuclei, resonance-mode effects on channel coupling in, (T), 20: 6426
scattering by nuclei, shell model for, 20: 6434

NUCLEOPROTEINS
radiation effects on Tetrahymena, x, 20: 5267

NUCLEOSIDES
radiosensitivity effects of bromouracildesoxyriboside and iodouracil-desoxyriboside on *Herpes simplex* virus in HeLa cell cultures, 20: 5363

NUCLEOTIDES
reactions with uranyl ions, 20: 5237(R) (UR-668, pp 55-109)

O

OCTANE
electron reactions in ethylene mixture, cross sections for momentum transfer and drift velocities in, 20: 5985 (ORNL-TM-1262)

OLEIC ACID
radiation effects on content in bean leaves of, x, 20: 5265(T)

OOCYTES
radiosensitivity in meiotic stages of Artemia, x, 20: 5359

OPTICAL SYSTEMS
design of split beam comparator for measuring thermal expansions, 20: 5709
evaluation of, for dimensional gaging, 20: 6689 (Y-KE-191)
uses of vidicons with digital scanners for particle-track analysis, (E), 20: 5718 (BNL-9634)

ORES
analysis for lead-210, radiochemical, 20: 5505

ORGANIC COMPOUNDS
analysis for carbon-14, design and operation of G-M counter for, 20: 5511
reactions with hydrated electrons, review on, 20: 5525 (IA-1041)

ORGANISMS
radiation effects on living, bibliography on, 20: 5284 (AED-C-04-21)

ORGEL REACTOR
fuel element testing of, methods for nondestructive, 20: 6632(T) (AEC-tr-6628)

ORNL HIGH FLUX ISOTOPE REACTOR
fuel element acceptance of, development of reactivity test for, 20: 6588(R) (ORNL-3858(Vol.1), pp 13-19)
fuel element handling procedures for, 20: 6588(R) (ORNL-3858 (Vol.1), pp 13-19)

ORNL RESEARCH REACTOR
experimental facilities for, capsule temperature control in, 20: 6680 (ORNL-TM-1319)

OSCILLATORS
design and performance of, (E), 20: 5680 (ELI-91)

OSCILLOGRAPHS
use for scintillation measurement of terrestrial radiation, 20: 6186(T) (UCRL-Trans-1269(L))

OXALATE COMPLEXES
with neptunium, sorptive properties of, methods for determining, 20: 5530 (SC-RR-65-625)

OXIDATION
radiation effects on, in rat tissues, γ, 20: 5339

OXIDES
binding energy of Group IIIA, 20: 5540

OXYGEN
determination by activation, effects of boron on, 20: 5498 (NP-15636)
determination in sodium, neutron activation, 20: 5594(R) (ANL-6925, pp 21-106)
diffusion in uranium dioxide single crystals, (E), 20: 5882(R) (EURAEC-1454)
diffusion in yttrium at 1235 to 1460°C in electric field, 20: 5599
effects on alpha-beta phase transformation in hafnium, 20: 5850
effects on corrosion of Zircaloy-2 powders by steam or water, 20: 5851
effects on critical resolved shear stress of zirconium, 20: 5851
effects on irradiated barley seed, effects of dimethyl sulfoxide and nitric oxide on, 20: 5298(R) (RLO-353-4)
effects on mechanical properties of tungsten of interstitial impurities of, 20: 5846
effects on radiation damage in silicon, 20: 5920
electron reactions with molecular, ionization cross sections for, (E/T), 20: 5989
molecular structure of, orbital density in, 20: 5524 (ANL-7076)
oxidation of niobium–10 molybdenum alloy at 400 to 1200°C, 20: 5851
radiation effects on chemical reactions with iron fast-neutron, 20: 5846
radiosensitivity effects of inhaled, in cancer patients, 20: 5437
radiosensitivity effects in Drosophila, x, 20: 5338
reactions with beryllium at 1000 to 1500°C, 20: 5844
reactions with molybdenum and tungsten, effects of molecular dissociation on rates of, 20: 5846
reactions with recoil carbon-11 atoms, mechanism and products of, 20: 5570 (JUL-228-RC)
sorption by niobium, 20: 5851
uptake by irradiated *Tenebrio molitor*, 20: 5314

OXYGEN IONS
detection in nuclear emulsions and solids, 20: 5755

OXYGEN ISOTOPES O-13
beta decay of delayed proton emission in, (E), 20: 6405

OXYGEN ISOTOPES O-15
energy level transitions in, mixing ratios for, (E), 20: 6378
energy levels of, gamma rays from first two excited, (E), 20: 6318
monitoring airborne, from electron linacs, 20: 5774

OXYGEN ISOTOPES O-16
deuteron reactions (d,α) at 11.8 and 12.0 Mev, (E), 20: 6369
deuteron reactions (d,α) and (d,p) at 0.2 to 1 Mev, analysis of, (T), 20: 6281 (CEA-R-2807)
electron inelastic scattering by, two-nucleon correlation functions and cross sections for, (T), 20: 6424
energy levels, (E), 20: 6346
energy levels of, T = 2, (T), 20: 6341
energy levels of, T = 2, (T), 20: 6342
energy levels of, even parity, (T), 20: 6350
gamma reactions (γ,n) at 17 to 28 Mev, cross sections for, (E), 20: 6418
Hartree-Fock fields and single-particle energies for ground state of, (T),

20: 6363
helium-3 reactions (He-3,αγ) with, oxygen-15 gamma transitions from, (E), 20: 6318
meson (μ⁻) capture by, rate of, (E), 20: 6273 (AD-617398)
meson (π⁻) capture by, yields and energy spectra from, (E/T), 20: 6292 (NP-15601)
neutron inelastic scattering at 14.1 Mev, gamma and neutron angular distributions from, (E), 20: 6346
oxygen-16 reactions (O-16,αγ) with, silicon-28 levels from, (E), 20: 5928(R) (PR-P-66)
proton elastic scattering at 21 to 53 Mev, polarization from, (E), 20: 6306 (UCRL-16217)
reactions (O-16,αγ) with carbon-12, magnesium-24 levels from, (E), 20: 5928(R) (PR-P-66)
reactions (O-16,αγ) with tritium, nitrogen-15 gamma transitions from, (E), 20: 6318

OXYGEN ISOTOPES O-17
energy levels in, hole-particle model for, 20: 6382
energy levels of, even parity, (T), 20: 6350

OXYGEN ISOTOPES O-18
energy levels of, projected Hartree-Fock spectra for, (T), 20: 6419
proton elastic and inelastic scattering at 7.89 to 16.28 Mev, (E), 20: 6373

OXYGEN SYSTEMS
Ca–O–W, phase studies, 20: 5851
Co–O–W, phase studies, 20: 5851
ethane–O, reactions with recoil carbon-11 atoms, 20: 5570 (JUL-228-RC)
HF–O, effects of acid leaching on uranium in alumina fluidized bed, 20: 5500 (ORNL-3876)
HF–O, effects on stainless steel, oxidizing, 20: 5595(R) (ANL-6925, pp 107-64)
methane–O, reactions with recoil carbon-11 atoms, 20: 5570 (JUL-228-RC)
N–O, sorption by niobium, 20: 5851
O–propane, reactions with recoil carbon-11 atoms, 20: 5570 (JUL-228-RC)
O–Sm–W, phase studies, 20: 5851
O–Ta–Ti–Zr, phase studies at 1500°C, 20: 5846
O–Ti–W, phase studies, 20: 5851

OZONE
production for water treatment, feasibility of chemonuclear reactors for, 20: 5568 (BNL-9664)
radioinduced formation of, around high-power gamma facility, ventilation calculations for, 20: 5670

P

PALLADIUM
effects on properties of cadmium–indium–silver alloy as control rod material, 20: 5850
neutron paramagnetic scattering at 15, 77, and 298°K, (E), 20: 6544
performance of aluminum-coated, as self-regenerating deuterium target, (E/T), 20: 6334

PALLADIUM ALLOYS
Pd–Ru, effects on kinetics of deuterium exchange with hydrogen in methane at 90 to 170°K, 20: 5557
Pd–U, phase studies, 20: 5843
Pd–W, phase studies, 20: 5846

PALLADIUM ISOTOPES Pd-103
decay of, electron capture, (E), 20: 6298(R) (PPAD-2137-566)

PALLADIUM ISOTOPES Pd-105
energy levels, (E), 20: 6406

PALLADIUM ISOTOPES Pd-111
decay, (E), 20: 6402

PARAMECIUM
chemically-induced permutational damage in, effects of streptomycin on, 20: 5417
radiation effects on life-span of, effects of metabolic inhibitors on uv, 20: 5386
radioinduced permutational damage in, effects of streptomycin on, x, 20: 5417

PARATHYROID EXTRACTS
effects on metabolism of radiophosphates in kidneys, 20: 5237(R) (UR-668, pp 55-109)

PARATHYROID HORMONES
effects on HeLa cell cultures, 20: 5237(R) (UR-668, pp 55-109)

PARTICLE BEAMS
transport optics for, first and second order, (T), 20: 5944 (SLAC-PUB-132)

PARTICLE TRACKS
analysis in streamer-chamber photographs, 20: 5739 (SLAC-PUB-140)
analysis of small-angle proton scattering at high energies using spark chambers, 20: 5720 (CERN-65-33)
analysis using digitized scanners with vidicon tubes, (E), 20: 5718 (BNL-9634)
determination of heavy-ion, in emulsions and solid materials, 20: 5755
determination of heavy ion, in Makrofol and mica, 20: 5756

PARTICLE TRAJECTORIES
determination of, for polarized particles from cyclotron ion sources, (T), 20: 5946 (UJV-1408/65)

PARTICLES
distribution and residence times in gas-fluidized beds, 20: 5595(R) (ANL-6925, pp 107-64)

PEAS
gene linkage for chlorophyll deficiency in, 20: 5238
radiation effects on growth of seedlings of, γ, 20: 5388
radiation effects on root cells of seedlings, γ, 20: 5390
radiation effects on sugar content in leaves of, γ, 20: 5280

PENTANE, 3-METHYL-
free radical production from alkyl halides in glass of, 20: 5577
radiation effects on alkyl halide-containing glass of, 20: 5577

PENTANES
electron reaction with, cross sections for momentum transfer and drift velocities in, 20: 5985 (ORNL-TM-1262)
electron reactions with, ionization cross sections for, (E/T), 20: 5989
electron reactions in ethylene mixture, cross sections for momentum transfer and drift velocities in, 20: 5985 (ORNL-TM-1262)
reactions with recoil carbon-11 atoms, mechanism and products of, 20: 5570 (JUL-228-RC)
uses as medium for drifting lithium into germanium, (E), 20: 5702

PEPTIDES
radioinduced free radicals in glycine, 20: 5273
synthesis of, role of ribosomes in, tracer study, 20: 5264

PEROXIDES
radiation effects on content of lipid, in rat tissues, 20: 5339

PERSONNEL
phosphatase activity in leukocytes of chemical industry, 20: 5269
radiation dosimetry of, continuous centralized recording of individual, 20: 5749
radiation protection of Rumanian, developments in, 20: 5425 (NP-15543, pp 77-82)
radiation protection of, in uranium mines, 20: 5428

PETROLEUM
recovery of, nuclear reactor operation in bore holes for, 20: 6651(P)
uses as medium for drifting lithium into germanium, (E), 20: 5702

PHANTOMS
materials of, for use in γ or x radiation therapeutic measurements, 20: 5481
use of, for calibration of whole-body radiation counting of man, 20: 5426

PHARMACEUTICALS
analysis of iodine-125- or iodine-131-labeled, for impurities by paper chromatography, 20: 5515

PHARMACOLOGY
of cortisol, bioassay of effects on growing bones, 20: 5234(R) (COO-119-232, pp 122-52)
radioisotopes in, bibliography on, 20: 5812 (PAEC(A)IN-654)

PHARNYX
effects of preirradiation on surgery hypo-, 20: 5463

PHENOL, 4-*sec*-BUTYL-2-α-METHYLBENZYL-
cyclohexane–4-*sec*-butyl-2-α-methylbenzylphenol, solvent properties for francium, 20: 5601

PHENOLPHTHALEIN
complexes with neptunium, sorptive properties of, methods for determining, 20: 5530 (SC-RR-65-625)

PHENOXIDE IONS
effects on deuterium exchange between isobutyraldehyde and water, 20: 5565

PHOSPHATASES
effects of chemicals on activity of leukocyte alkaline, 20: 5269
radiation effects on activity of leukocyte alkaline, x, 20: 5269
radiation effects on content of, in developing chick embryos, x, 20: 5306
radiation inactivation of phosphorylase, γ, 20: 5275
radioinduced inactivation of, in aqueous solutions, γ, 20: 5277

PHOSPHATES
metabolism in kidneys, effect of parathyroid extract on, 20: 5237(R) (UR-668, pp 55-109)

PHOSPHATIDES
radiation effects on phosphorus-32 uptake by gliomas, x, 20: 5255

PHOSPHIDES
properties as oxidation-protection coatings for heat-resisting metals, 20: 5851

PHOSPHINE SULFIDE, TRIS(1-AZIRIDINYL)-
labeling with phosphorus-32 and sulfur-35, recoil, 20: 5586

PHOSPHORIC ACID, ALKYL ESTERS
effects on solvent properties of trioctylamine for sulfuric acid, 20: 5600

PHOSPHORS

photocouductivity of, effects of molecular structure on, 20: 6551
preparation of liquid, in vacuum, 20: 5785
radioinduced photoluminescence spectra of thallium-activated cesium iodide and sodium iodide, x, (E), 20: 6537
PHOSPHORUS
combustion with fluorine, data on, 20: 5523(R) (ANL-6925, pp 175-85)
radiation effects on metabolism of, in glioma cultures, x, 20: 5255
PHOSPHORUS COMPOUNDS
separation by paper electrophoresis and paper chromatography, 20: 5512
PHOSPHORUS ISOTOPES P-29
beta decay of, shell model calculations of ft values in, (T), 20: 6393
PHOSPHORUS ISOTOPES P-30
beta decay of, shell model calculations of ft values in, (T), 20: 6393
PHOSPHORUS ISOTOPES P-31
bremsstrahlung resonant scattering at 1.0 to 1.3 Mev, energy level lifetimes from, (E), 20: 6380
deuteron reactions (d,α) at 11.8 and 12.0 Mev, (E), 20: 6369
proton inelastic scattering at 155 Mev, cross sections and energy levels from, (E), 20: 6354
PHOSPHORUS ISOTOPES P-32
beta decay of, shell model calculations of ft values in, (T), 20: 6393
effects on growth of corn seedlings of, in contaminated soil, 20: 5305
effects on rats, carcinogenic, 20: 5334
incorporation in Culex Sarvae, method for, 20: 5240
incorporation in *tris*(1-aziridinyl)phosphine sulfide by recoil reactions, 20: 5586
incorporation into oriental fruit moths of, 20: 5246
radiation effects on metabolism of, in glioma cultures, x, 20: 5255
separation from cotton cloth soiled with oily materials, 20: 5676
use as beta source for therapy of hemangiomas in children, 20: 5443
use as tracer for Culex control project, 20: 5240
use for therapy of polycythemia, 20: 5483
use in plant and soil studies in Rumania, 20: 5235 (NP-15543, pp 83-90)
PHOSPHORUS ISOTOPES P-33
beta decay of, shell model calculations of ft values in, (T), 20: 6393
PHOSPHORUS ISOTOPES P-34
beta decay of, shell model calculations of ft values in, (T), 20: 6393
PHOSPHORYL CHLORIDES
properties as oxidation inhibitor for graphite, 20: 5844
PHOTOELECTRIC CELLS
performance for electric-power and life-support systems on spacecraft, (E/T), 20: 5820 (NASA-CR-316)
PHOTOGRAPHIC FILM
particle track analysis in, using vidicons with digital scanners, (E), 20: 5718 (BNL-9634)
particle-track analysis in, 20: 5739 (SLAC-PUB-140)
PHOTOGRAPHIC FILM DETECTORS
response of Eastman Type A, to 14 Mev neutrons, 20: 5742(R) (UCRL-14351)
use for dosimetry in radiotherapy, 20: 5480
PHOTOMULTIPLIER TUBES
design and performance for optical excitation measurements of gases, 20: 5748(T) (UCRL-Trans-1266(L))
timing circuit design for, amplitude-independent, 20: 5744 (UCRL-16227)
vacuum seals for, design of, 20: 5787
PHOTON BEAMS
monitoring low-intensity 600-Mev, using electroluminescent image intensifier, (E), 20: 5773
PHOTONS
interactions with nucleons, SU(6) and SU(6)W for meson production in, 20: 6055
interactions with protons, T violation in, (T), 20: 6059
interactions with nucleons, spin correlations in vector meson production in, (T), 20: 6076
interactions with mesons (K) and (π), resonance model for magnetic polarizability from, 20: 6090
interactions with plasma via Compton effect, diffusion approximation for, (T), 20: 6502
interactions with electrons in plasma, dynamics of transport phenomena in, (T), 20: 6448 (AD-619045)
production in cosmic-ray reactions in carbon, (E), 20: 6017
reactions with lithium-6, disintegration, (T), 20: 6368
reactions with nuclei, resonance-mode effects on channel coupling in, (T), 20: 6426
scattering by deuterium, cross sections for elastic, (E), 20: 6094
PHOTOSENSITIVITY
of *Escherichia coli*, 20: 5347
of *Escherichia coli*, 20: 5348
PHOTOSYNTHESIS
radiation effects on, in isolated chloroplasts, uv, 20: 5401
radiation effects on, in isolated chloroplasts, x, 20: 5402
PHYSICAL CONSTANTS TESTING REACTOR
neutron multiplication in, with borated aluminum-plutonium-polyethylene fuels, 20: 6578(R) (BNWL-149, pp 45-7)
PHYSICS
research, 20: 5923(R) (BNWL-149)
research, (E), 20: 5925(R) (ORNL-3858(Vol.I))
research, (E/T), 20: 5926(R) (ORNL-3858(Vol.2))
research in Italy, 20: 5924 (ISS-65/19)
PIEZOELECTRIC EFFECT
measurement in semiconductors, apparatus for, (E), 20: 5883 (IS-1263)
PINCH DEVICES
magnetic field measurements in linear, probes for, 20: 6507
plasma compression in theta, 20: 6463 (JUL-264-PP)
PIPES
heat transfer in steam-water flow in round vertical, 20: 5623 (EURAEC-1325)
momentum flux in air–water and steam–water flow in, measurement of, 20: 5624 (MIT-3496-1)
PIQUA POWER REACTOR
coolant monitoring of, standardization of techniques for, 20: 6615 (NAA-SR-10888(Rev.))
PITUITARY GLAND
radiation effects on hormone content of toad *Bufo bufo*, 20: 5394
radioinduced ablation of, for treatment of diabetic retinopathy, 20: 5468
PITUITARY HORMONES
effects of irradiated *Bufo bufo* on development of hypothalectomized tadpoles of *Rana nigromaculata*, 20: 5394
radiation effects on production and release of, in frogs, 20: 5394
PLACENTA
iodine-131 uptake by human, 20: 5259
uptake of technetium-99-labeled albumins and colloids by, for visualization by external scanning, 20: 5456
PLANT CELLS
effects of radioinduced toxins on, genetic, 20: 5390
molecular structure, 20: 6551
radiation effects on pea seedling root, γ, 20: 5390
radiation effects on electrical properties of *Nitella flexilis*, effects of environment on γ, 20: 5294(R) (COO-205-55, Paper 3)
PLANTS
chemically-induced mutations in Arabidopsis, x, 20: 5357
ecology of aquatic, research programs of AEC, 1965, 20: 5245 (TID-13358(2nd Rev.), pp 89-126)
ecology of terrestrial, research programs of AEC, 1965, 20: 5244 (TID-13358(2nd Rev.), pp 3-88)
radiation effects on red clover, morphological and mutagenic, 20: 5491
radioinduced inactivation of viruses affecting, 20: 5310
radioinduced mutations in Arabidopsis, x, 20: 5357
uptake of radioisotopes by roots of barley, mechanisms of, 20: 5258
uptake of strontium-89 by barley, from contaminated soils, 20: 5257
PLASMA
acceleration of, turbulence in current sheet in coaxial, 20: 6450(R) (AD-619527)
charged particle scattering by electric field fluctuations in, (T), 20: 6497
charged-particle unstable precession under influence of drag forces, (T), 20: 6493
compression in theta pinch devices, 20: 6463 (JUL-264-PP)
containment and heating in DECA-2, 20: 6469(T) (UCRL-Trans-1256(L))
containment in toroidal octopole systems, (E), 20: 6460 (GA-6594)
containment of, production of megagauss magnetic fields for, 20: 6515(P)
current density distributions in transient, measurement using Rogowski coils, 20: 6509
density fluctuations in ionosphere, turbulence of, 20: 6472
diagnostics of column, methods for, (E), 20: 6447 (AD-618693)
diagnostics of glow discharge mechanisms in, 20: 6486
diagnostics of instrumentation development for, 20: 5633 (NASA-SP-5033)
diffusion of inhomogeneities in weakly ionized, effect of vortex electric field on, (T), 20: 6482
effects on microwave interferometer measurements, (T), 20: 5683 (UCRL-14438)
electric conductivity of, in high-current switches, (E), 20: 6449 (AD-619370)
electromagnetic wave absorption and emission via mode conversion in inhomogeneous collision-free, (T), 20: 6506
electromagnetic wave reflection from inhomogeneous, signal from, (T), 20: 6445 (AD-617619)
electromagnetic wave interactions with, nonlinear, (E), 20: 6457 (AD-622876)
electromagnetic wave interactions in cold magnetoactive, 20: 6484
electron and ion densities and temperatures in high-pressure xenon, 20: 6480
electron beam interactions with, low-frequency electronic oscillations from monoenergetic, (T), 20: 6503

electron beam interactions with, heating effects in, 20: 6468(T) (ORNL-tr-871)
electron beam interactions with, wave excitation in, (T), 20: 6474
electron beam reactions with alkali-metal magneto-, enhanced diffusion from, 20: 6466 (SIT-2813-33)
electron cyclotron instability in, effect of Landau damping on, (T), 20: 6458 (CLM-R-44)
electron density and temperature in standing layers of hydrogen discharge, (E), 20: 6476
electron density measurement by laser interferometers, 20: 6471
electron oscillations in hot fully ionized, Coulomb collision effects on transverse, (T), 20: 6499
electron temperature in positive-column argon discharge, 20: 6475
flow in magnetic field, interactions in, (T), 20: 6444 (AD-617553)
flow in transverse magnetic field, one-dimensional, 20: 6510
flow of, properties and problems of MHD, 20: 6156 (AD-617562)
heat transfer in toroidal column of, 20: 6473
heating by bombardment with electron beams, 20: 6468(T) (ORNL-tr-871)
heating by ion beam bombardment, (E), 20: 6467(T) (ORNL-tr-870)
hydromagnetic wave eigenmodes in magnetic multipole fields, (T), 20: 6492
interactions of, microinstabilities from, (E/T), 20: 6465 (RISO-105)
ion production in tenuous helium, effects of metastable atoms on, (T), 20: 6464 (NASA-TN-D-3121)
ion recombination on surface of charged body in, (T), 20: 6483
kinetic dispersion equation for, singularities of, 20: 6477
kinetic theory of, in rotating magnetic fields and electromagnetic fields, 20: 6479
kinetics of stable and unstable, cluster-expansion analysis of, (T), 20: 6462 (GA-6650)
magnetic compression of shock-heated, electron density and temperature in cusp, (E), 20: 6495
magnetic-field-plane bifurcation in waveguide filled with anisotropic, (T), 20: 6481
magnetohydrodynamic equations for geo-, (T), 20: 6212
motion and trapping in static magnetic fields, (T), 20: 6459 (CNIE-PE-1)
oscillations in collisionless, magnetic field effects on small pulsed dipole-induced, (T), 20: 6498
photon gas interactions via Compton effect with, diffusion approximation for, (T), 20: 6502
production of arc, ablation-type, (E), 20: 6488
production of arc, performance of spark-plug starter for, (E), 20: 6489
production of argon, in inductive hydrodynamic shock tubes, 20: 6478
properties in crossed-field accelerators, (E/T), 20: 6470
properties of low-temperature, 20: 5988(T) (JPRS-32421)
properties of radiofrequency generated cylindrical column, electric and thermochemical, (E/T), 20: 6447 (AD-618693)
radiation from silver foils, excited by light, (E), 20: 6548
radiation production in, by uniformly rotating line charge, 20: 6456 (AD-619888)
seeding with cesium minerals, device for, 20: 6030(P)
shock formation in nearly collisionless, (E), 20: 6501
shock propagation in, electron density and velocity behind, (E), 20: 6490
shock-wave reflection in argon and helium thermal, (T), 20: 6512
stability in gaseous magneto-, microwave production of helical, (E/T), 20: 6446 (AD-617696)
stability in thermal potassium, mode without axial electron drift in, (E/T), 20: 6505
stability in traveling wave interaction for one-dimensional flow in, (T), 20: 6491
stability of, analysis of, 20: 6461 (GA-6646)
stability of, with discontinuous velocity distribution, (T), 20: 6487
statistical mechanics of two-component, Wigner distribution function for equilibrium, (T), 20: 6504
surface impedance of nonhomogeneous, (T), 20: 6485
transition processes in, thermodynamic equilibrium for collisionally and radiatively controlled, 20: 6443 (AD-617383)
transport phenomena in nearly homogeneous, dynamics of, (T), 20: 6448 (AD-619045)
turbulence in, mixing, 20: 6472
wave propagation in hot, magnetic field effects on small-amplitude, (T), 20: 6500
wave propagation in inhomogeneous medium, 20: 6511

PLASMA JETS
bibliography on, 20: 5633 (NASA-SP-5033)
kinetics in coaxial, 20: 6450(R) (AD-619527)
performance of Faraday-type, with series connected electrodes, (E), 20: 6025
production of, apparatus for, 20: 6178(P)
production of, device for, 20: 5640(P)
properties of crossed-field, (E/T), 20: 6470
uses of, review, 20: 5633 (NASA-SP-5033)

PLASTICS
radioinduced formation of, in wood, 20: 5818

PLATES
fluid flow between parallel, stability of laminar, 20: 5621 (AEEW-R-416)

PLATINUM
diffusion in tungsten, inter-, 20: 5846
effects on properties of cadmium–indium–silver alloy as control rod material, 20: 5850
gamma coherent scattering at 0.662 and 1.332 Mev, cross sections for, (E/T), 20: 6323
proton reactions (p,n) at 30 and 50 Mev, isobaric-state excitation in, (E/T), 20: 6361
radiation effects on in-pile corrosion of, by aqueous solutions, 20: 5852(R) (EURAEC-1522)

PLATINUM ALLOYS
Mn–Pt, neutron diffraction of ordered, at 26 and 250°C, 20: 5912
Pt–Pu, phase studies, 20: 5848

PLATINUM ISOTOPES Pt-197
decay of, gamma transitions from, 20: 6436

PLUTONIUM
burnup determination of molten, experiment design for, 20: 6613 (LA-DC-7475)
deformation modes in alpha, 20: 5848
determination from abundance of plutonium isotopes, radiochemical, 20: 5497 (KFK-339)
determination in mixtures of actinides and fission products by paper chromatography, 20: 5509
diffusion coefficients at 218.8 and 299.1°C, self-, 20: 5848
diffusion in magnesium and magnesium alloys at 420 to 500°C, 20: 5848
electrowinning of, conditions for continuous, 20: 5839 (RL-SEP-244 (Del.))
monitor design for, alpha, 20: 5742(R) (UCRL-14351)
performance as fuel in accelerator-beam-driven exponential-pile pulsed neutron sources, (E), 20: 6257 (CONF-650217, pp 11-24)
phase transformations in, effects of refining process on, 20: 5843
processing of spent fuels and breeder materials of, pyrochemical batch-extraction, 20: 6600(R) (ANL-7105, pp 1-35)
production at Marcoule, flowsheet of process for, 20: 5596
separation for irradiated fuel elements, 20: 5596
separation from low enrichment fuels, 20: 6558(R) (ANL-7115, pp 42-67)
separation from molten magnesium–zinc alloys by fused chloride extraction, 20: 5594(R) (ANL-6925, pp 21-106)
separation from neutron-irradiated americium, (E), 20: 5823(T) (ORNL-tr-892)
separation from reactor fuel alloys, methods for, 20: 6553(R) (ANL-6925, pp 255-63)
separation from wastes by fluorination, 20: 5595(R) (ANL-6925, pp 107-64)

PLUTONIUM ALLOYS
Al–Pu, criticality, 20: 6668(R) (BNWL-149, pp 5-21)
Am–Pu, phase studies, 20: 5848
Cd–Mg–Pu–Zn, stability in mild steel and stainless steel containers at 600°C, 20: 5594(R) (ANL-6925, pp 21-106)
Ce–Co–Cu–Fe–Ni–Pu, phase studies, 20: 5848
Ce–Co–Pu, casting technique, 20: 5848
Ce–Co–Pu, diffusion of fission products from irradiated, to sodium at 550°C, 20: 5848
Ce–Co–Pu, viscosity, effects of composition and temperature on, 20: 5848
Cu–Pu, crystal structure of $PuCu_4$, 20: 5843
Fe–Pu, corrosive effects on tantalum–tungsten–yttrium at 700°C, effects of yttrium content on, 20: 5846
Fe–Pu–U, casting of, centrifugal, 20: 5866
fissium–Pu–U, burnup studies, 20: 6600(R) (ANL-7105, pp 1-35)
fissium–Pu–U, chloride slagging of, reactions of cerium and zirconium in, 20: 5594(R) (ANL-6925, pp 21-106)
fissium–Pu–U, phase studies on, 20: 5876 (ANL-6974)
fissium–Pu–U–Zr, phase studies on, 20: 5876 (ANL-6974)
fissium–Pu–U, reactions with vanadium–20 titanium at 550 to 700°C, 20: 5843
Ga–Pu, effects of pressure on properties and transformation of delta-stabilized, 20: 5884 (LA-2312)
Ga–Pu, grain growth in, strain-anneal technique for, 20: 5907
Mg–Pu, melting points of, effects of composition on, 20: 5594(R) (ANL-6925, pp 21-106)
Mo–Pu–U, ignition of, effects of molybdenum content on, 20: 5843
Mo–Pu–U, properties of, compressive, thermal expansion, and tensile, 20: 5843
Pt–Pu, phase studies, 20: 5848
Pu–Sc, phase studies, 20: 5843
Pu–Sc, phase studies, 20: 5848
Pu–Th, electric conductivity at 25 to 900°C, 20: 5843
Pu–Th, thermal expansion at 25 to 900°C, 20: 5843

Pu–Ti–U, compressive strength of, 20: 6601(R) (ANL-7115, pp 1-41)
Pu–Ti–U, tensile properties, 20: 6600(R) (ANL-7105, pp 1-35)
Pu–Ti–U, thermal expansion, 20: 5848
Pu–U, ignition properties of, effects of alloying additions on, 20: 5843
Pu–U, processing spent, methods for, 20: 5594(R) (ANL-6925, pp 21-106)
Pu–U–Zr, compressive strength of, 20: 6601(R) (ANL-7115, pp 1-41)
Pu–U–Zr, phase studies, 20: 6600(R) (ANL-7105, pp 1-35)
Pu–U–Zr, tensile properties, 20: 6600(R) (ANL-7105, pp 1-35)
Pu–U–Zr, thermal expansion, 20: 5848

PLUTONIUM CARBIDES
thermal expansion of fuels of, during fast burst accident, 20: 6602 (BNWL-SA-346)
vapor pressure of monocarbide at 1500 to 1565°C, 20: 5843
PuC–UC, compatibility with jacketing materials, 20: 6600(R) (ANL-7105, pp 1-35)
PuC–UC, precipitation from fused salts, methods for, 20: 5594(R) (ANL-6925, pp 21-106)

PLUTONIUM(VI) FLUORIDES
corrosive effects on B120VCA titanium alloy, stress-, 20: 5846
radioinduced decomposition of, factors affecting alpha, 20: 5595(R) (ANL-6925, pp 107-64)
reactions with metal fluorides at 25 to 100°C, 20: 5595(R) (ANL-6925, pp 107-64)
separation from air by hydrolysis, apparatus for, 20: 5595(R) (ANL-6925, pp 107-64)
PuF_6–UF_6, conversion to oxides, equipment for, 20: 5595(R) (ANL-6925, pp 107-64)
PuF_6–UF_6, phase studies, 20: 5595(R) (ANL-6925, pp 107-64)

PLUTONIUM IONS
oxidation of trivalent to tetravalent in basic solution, method for, 20: 5561(P)

PLUTONIUM ISOTOPES
determination of abundance of, in plutonium samples, 20: 5497 (KFK-339)

PLUTONIUM ISOTOPES Pu-238
critical mass of, Monte Carlo calculations for, 20: 6579(R) (BNWL-149, pp 48-56)

PLUTONIUM ISOTOPES Pu-239
distribution in urania fuel rods irradiated with gross central melting, 20: 5914(R) (GEAP-3771-17)
effects on rat bones, tumorigenic, 20: 5321
excretion of deposited, effects of cortisol in dogs, 20: 5247(R) (COO-119-232, pp 188-99)
neutron capture-to-fission ratios in EBR-II, (E), 20: 6280(R) (ANL-6925 (p.249-51))
neutron cross sections for, Doppler contributions to, 20: 6558(R) (ANL-7115, pp 42-67)
neutron Doppler shifts at 300 to 600°K, (T), 20: 6556(R) (ANL-7105, pp 36-58)
neutron resonance scattering by spin values, average fission width, and total spin correlation from, (E), 20: 6414

PLUTONIUM ISOTOPES Pu-240
neutron capture-to-fission ratios in EBR-II, (E), 20: 6280(R) (ANL-6925 (p.249-51))
neutron resonance absorption calculations, (E/T), 20: 6577(R) (BNWL-149, pp 22-35)
photofission below 10 Mev, angular distributions from, (E), 20: 6309(T) (ANL-Trans-245)
properties as oxide fuel in beryllia-moderated reactor, analysis of, 20: 6603(R) (GA-4165)

PLUTONIUM ISOTOPES Pu-242
neutron capture-to-fission ratios in EBR-II, (E), 20: 6280(R) (ANL-6925 (p.249-51))
production at Savannah River, program for, 20: 5822 (DP-1000)

PLUTONIUM NITRIDES
thermal expansion of fuels of, during fast burst accident, 20: 6602 (BNWL-SA-346)
vapor pressure at 1250 and 1550°C, 20: 5848

PLUTONIUM OXIDES
phase studies, 20: 5843

PLUTONIUM(IV) OXIDES
inhalation by animals and man, effects of, 20: 5237(R) (UR-668, pp 55-109)
properties as fuel in beryllium oxide-moderated reactors, 20: 6603(R) (GA-4165)
thermal expansion of fuels of, during fast burst accident, 20: 6602 (BNWL-SA-346)
thermal expansion coefficient at 20 to 1200°C, 20: 5843
Fe_2O_3–PuO_2, phase studies, 20: 5843
Fe–PuO_2, preparation of fuel dispersions of, 20: 5843
PuO_2–UO_2, effects of plutonium dioxide content on sintering behavior of mechanically mixed, 20: 5889 (NUMEC-2389-8)
PuO_2–UO_2, fabrication of fuel rods of, by vibrational compaction, 20: 5867
PuO_2–U_3O_8, fluorination in fluid beds, equipment and procedure for, 20: 5595(R) (ANL-6925, pp 107-64)
PuO_2–UO_2, fluorination in fluidized-beds, equipment and procedures for, 20: 5595(R) (ANL-6925, pp 107-64)
PuO_2–UO_2, processing of irradiated, by fluoride volatility, 20: 5595(R) (ANL-6925, pp 107-64)
PuO_2–UO_2, thermal expansion of coprecipitated powders of, 20: 5890 (NUMEC-2389-9)

PLUTONIUM PHOSPHIDES
hardness of, micro-, 20: 6556(R) (ANL-7105, pp 36-58)
lattice parameters and preparation, 20: 5848

PLUTONIUM RECYCLE TEST REACTOR
criticality studies, 20: 6668(R) (BNWL-149, pp 5-21)

PLUTONIUM SILICIDES
phase studies, 20: 5848

PLUTONIUM SUBCRITICAL EXPERIMENT
development, July–Sept. 1965, 20: 6607(R) (GEAP-4965)

PLUTONIUM SULFIDES
hardness of, micro-, 20: 6556(R) (ANL-7105, pp 36-58)
lattice parameters and preparation, 20: 5848
thermal diffusivity of, 20: 6558(R) (ANL-7115, pp 42-67)
thermal expansion of fuels of, during fast burst accident, 20: 6602 (BNWL-SA-346)

PLUTONIUM SYSTEMS
Al–Pu–polyethylene, neutron multiplication in borated, 20: 6577(R) (BNWL-149, pp 22-35)
Al–Pu–polyethylene, neutron multiplication in borated, 20: 6578(R) (BNWL-149, pp 45-7)
C–Pu–U, preparation techniques, 20: 5843
C–Pu–U, properties, 20: 5843
Pu–UO_2–H_2O, criticality studies, 20: 6607(R) (GEAP-4965)

POLAND
leukemia incidence in population of, effects of environmental radioactivity on, 20: 5674

POLONIUM ISOTOPES
production cross sections in bismuth-209 (p,xn) reactions at 60 to 155 Mev, (T), 20: 6364

POLONIUM ISOTOPES Po-210
alpha decay widths and nuclear structure, (T), 20: 6423
effects on life-span and tumorigenesis in rats, 20: 5237(R) (UR-668, pp 55-109)

POLONIUM ISOTOPES Po-212
alpha decay widths and nuclear structure, (T), 20: 6423

POLYCYTHEMIA
radiotherapy of, 20: 5483
transfusion-induced, effects of erythropoietin on, 20: 5242

POLYSACCHARIDES
effects on lymphosarcomas in rats, 20: 5436(R) (UR-668, pp 149-60)

POPULATIONS
leukemia incidence in, statistical analysis, 20: 5471
leukemia incidence in Polish, effects of environmental radioactivity on, 20: 5674
protection against fallout from thermonuclear explosions, role of shelters for, 20: 5416
radiation control of insect, by sterile-male technique, 20: 5815 (STI/DOC/10/44)
radiation dose of, effects of radiography on, 20: 5415
radiation exposure of, in Great Britain, 20: 5409
radioinduced leukemia in human, statistical study of etiology, 20: 5307
radioinduced tumors in human, statistical study of etiology, 20: 5307

POSITRON BEAMS
density of ultrarelativistic colliding, limitations in, (T), 20: 5950
leakage from storage rings, due to amplitude and frequency variations of compensating field, (T), 20: 5949

POSITRONS
annihilation spectra in low temperature helium gas, (E), 20: 5997
interactions with polarized electrons, selection rules for annihilation, (T), 20: 6040 (NP-15602)

POTASSIUM
boiling heat transfer in, 20: 5627
content in amphoteric chondrites, (E), 20: 5979
stability in thermal plasma of, mode without axial electron drift in, (E/T), 20: 6505
thermodynamic properties of, bibliography on, 20: 5886 (NASA-TN-D-3120)

POTASSIUM ALLOYS
K–Na, corrosive effects on Croloy 9M, INOR-8, and types 316 and 347 stainless steel, 20: 5851
K–Na, thermodynamic properties of liquid, 20: 5594(R) (ANL-6925, pp 21-106)
K–Na, viscosity of, at −10 to 148.9°C, 20: 5908

POTASSIUM BROMIDES

spectra of, deuterium and hydrogen impurity effects on uv, 20: 6545
POTASSIUM CHLORIDES
spectra of, deuterium and hydrogen impurity effects on uv, 20: 6545
KCl–NaCl, corrosive effects on zirconium, 20: 5855(T) (JPRS-32341, pp 24-31)
KCl–NaCl, effects of molten, on reaction of uranium dioxide with chlorine, 20: 5547
LiCl–KCl, effects of molten, on reaction of uranium dioxide with chlorine, 20: 5547
LiCl–$MgCl_2$–KCl, melting points of, effects of composition on, 20: 5594(R) (ANL-6925, pp 21-106)
$MgCl_2$–KCl–NaCl, solvent properties for lanthanum, plutonium, and praseodymium, 20: 5594(R) (ANL-6925, pp 21-106)
$MgCl_2$–KCl–NaCl, solvent properties for uranium, 20: 5594(R) (ANL-6925, pp 21-106)
POTASSIUM CHLORORHENATES
chlorine-35 NMR in, in pure quadrupole regime, (E), 20: 6549
POTASSIUM CYANIDES
radiosensitivity effects on paramecium, uv, 20: 5386
POTASSIUM FLUORIDES
determination by titration using uranium(IV), 20: 5520
POTASSIUM IONS
content in growing yeast cells, 20: 5251(R) (UR-668, pp 123-49)
reactions between parallel interpenetrating beams of, (E), 20: 6467(T) (ORNL-tr-870)
POTASSIUM ISOTOPES K-37
beta decay of, shell model calculations of ft values in, (T), 20: 6393
POTASSIUM ISOTOPES K-38
beta decay of, shell model calculations of ft values in, (T), 20: 6393
POTASSIUM ISOTOPES K-39
helium-3 elastic scattering at 9.0 Mev, (E/T), 20: 6367
helium-3 reactions (He-3,α) at 9.0 and 11.0 Mev, angular distributions for, (E/T), 20: 6367
proton inelastic scattering at 155 Mev, cross sections and energy levels from, (E), 20: 6354
POTASSIUM ISOTOPES K-42
uptake by barley roots, mechanism for, 20: 5258
uptake of, by rabbit eye lens in culture, 20: 5256
use in plant and soil studies in Rumania, 20: 5235 (NP-15543, pp 83-90)
POTASSIUM PHOSPHATES
KPO_3–$NaPO_3$, reference electrode for emf studies in, 20: 5529(R) (SC-DC-65-1706)
POTASSIUM SYSTEMS
He-K, electric discharge in, at low voltage and high current, (E/T), 20: 6159 (AERE-M-1597)
POTATOES
radiation effects on tubers of, γ, 20: 5404
radiation processing of, effects on storage life of, γ, 20: 5404
radioinduced inactivation of phosphorylase activity in, γ, 20: 5275
POTENTIOMETRIC ANALYSIS
equipment for continuous back-titrations with direct readout in, 20: 5502
POWDER METALLURGY
press for, design of hydrostatic, 20: 6692(P)
review on tungsten, 20: 5836 (NASA-SP-5035)
POWDERS
neutron diffraction by, effects of collimators on Bragg peaks in, 20: 6268
POWER REACTORS
components and materials of First Czechoslovakian, defectoscopic inspection of, (E), 20: 6633(T) (AECL-2286)
control system of Beloyarsk, 20: 6634
development of fast, in France, 20: 6643
development of high-temperature gas-cooled, 20: 6640
development of Magnox fueled, review of, 20: 6612 (INR-622/IX/R)
economics of dual-purpose, 20: 6649
fuel conservation efficiencies of thermal, 20: 6610 (HW-79287)
ionization chambers for, activation analysis materials of, 20: 5716 (AEEW-M-470)
kinetics of Beloyarsk, 20: 6634
power output control systems for 200-Mw(e) sodium graphite, 20: 6617 (NAA-SR-Memo-11339)
use for ozone production for water treatment, 20: 5568 (BNL-9664)
POWER SUPPLIES
design of double pulser, engineering drawings for, 20: 5963
PRASEODYMIUM
deposition on aluminum, copper, and stainless steel, electrolytic, 20: 5867
determination by potentiometric titration using EDTA, equipment for, 20: 5502
separation from molten magnesium alloys by fused chloride extraction, 20: 5594(R) (ANL-6925, pp 21-106)
PRASEODYMIUM ALLOYS
Pr–Y, electric conductivity at low temperatures, 20: 5888 (NP-15592)
PRASEODYMIUM FLUORIDES
enthalpy of formation, 20: 5559
PRASEODYMIUM IONS
spin-lattice relaxation rates in single crystals of anhydrous lanthanum trichloride, (E), 20: 6542
PRASEODYMIUM ISOTOPES Pr-144
beta transitions in, with parity change, (E), 20: 6370
use for evaluation of shielding barriers, 20: 5677
PRASEODYMIUM OXIDES
effects on dehydration and dehydrogenation of 2-propanol and tetralin, 20: 5567
PRASEODYMIUM PHTHALOCYANINES
preparation and spectra of, 20: 5560
PRECIPITATION, ATMOSPHERIC
radioactivity of, in Kansas and Missouri, 1962, 20: 5648(R) (COO-1340-2, pp 1-53)
strontium-89 and -90 content in Tokyo, four weeks after Chinese nuclear explosion of May 14, 1965, 20: 5656
PREGNANCY
radiation hazards of diagnostic radiography during, 20: 5476
radiotherapy of hyperthyroidism during, hazards from radioiodine, 20: 5470
PRESSURE
effects on properties and transformation of delta-stabilized gallium–plutonium alloys, 20: 5884 (LA-2312)
PRESSURE DROP
in steam-water flow in round vertical tubes, 20: 5623 (EURAEC-1325)
PRESSURE VESSELS
embrittlement of steel, by plastic fatigue, 20: 5881(R) (EURAEC-1441)
failure by low-cycle plastic fatigue, nondestructive testing techniques for, 20: 5894 (SWRI-1228-3-3)
PRESSURIZED WATER REACTORS
accidents in, analysis of coolant-loss, (T), 20: 6560(R) (BMI-X-10145)
PROCESS HEAT REACTORS
development for desalination, 20: 6650
PROMETHIUM
sorption on charcoal powders, effects of sodium dodecyl sulfate and water on, 20: 5675
PROMETHIUM ISOTOPES Pm-147
determination of, efficiency of beta scintillation sandwich counting method for, 20: 5783
PROMETHIUM ISOTOPES Pm-149
neutron absorption cross section, (E), 20: 6589
PROPANE
electron reaction with, cross sections for momentum transfer and drift velocities in, 20: 5985 (ORNL-TM-1262)
electron reactions in ethylene mixture, cross sections for momentum transfer and drift velocities in, 20: 5985 (ORNL-TM-1262)
performance in fission chambers, 20: 5734 (LFEN-NI-19)
O–propane, reactions with recoil carbon-11 atoms, 20: 5570 (JUL-228-RC)
PROPANE, 1-CHLORO-
reactions with electrons in organic glasses, yields of free radicals from, 20: 5577
PROPANE, 2-CHLORO-
reactions with electrons in organic glasses, yields of free radicals from, 20: 5577
PROPANE, 2,2-DIMETHYL-
radiolysis of, tracer studies of radical yields in, 20: 5576
PROPANE, 2-METHYL-
reactions with recoil carbon-11 atoms, mechanism and products of, 20: 5570 (JUL-228-RC)
2-PROPANETHIOL, 1-AMINO-
radioprotective properties of, 20: 5422
2-PROPANOL
dehydration and dehydrogenation of, on praseodymium oxide, 20: 5567
PROPELLANTS
preparation of radiation-cured elastomeric rocket, 20: 5588(P)
PROPENE
electron reactions with, ionization cross sections for, (E/T), 20: 5989
PROPENE, 2-METHYL-
electron reactions with, ionization cross sections for, (E/T), 20: 5989
radioinduced polymerization with dienes at low temperatures, 20: 5589(P)
PROPORTIONAL DETECTORS
design and performance as proton spectrometer, 20: 5759
design of boron-trifluoride, with preamplifier, (E), 20: 5680 (ELI-91)
performance for carbon-14 and tritium counting, 20: 5779
performance for tritium determinations in river water, 20: 5654
PROPULSION
electric-rocket, flow calculations for combined, 20: 5636
electric-steam, performance of systems for, 20: 5639
ion, orbit control of earth satellites using, (E/T), 20: 5638
ion, performance of electron-bombardment thrustor systems for space, 20: 5637

plasma jet, development of, 20: 5633 (NASA-SP-5033)
systems for space, design and performance of radioisotope, 20: 5634
systems for super-orbital rocket, chemical and nuclear-thermal, 20: 5635
PROPYNE
yields in pyrolysis of diphenyl at 375 to 1375°K, 20: 5563 (EUR-2482.f)
PROTACTINIUM
determination in mixtures of actinides and fission products by paper chromatography, 20: 5509
PROTACTINIUM ISOTOPES Pa-230
alpha decay of, branching ratios for, (E), 20: 6321
PROTACTINIUM ISOTOPES Pa-234
energy levels and gamma spectra of isomeric, rotational, (E), 20: 6331
PROTEINS
energy transfer in, effects of water content on, 20: 5270
incorporation of selenium-75 into blood, biosynthetic, 20: 5262
metabolism in blood serum of, tracer study in dogs, 20: 5249(R) (COO-119-232, pp 203-18)
radiation effects on blood serum, proton, 20: 5378
radiation effects on synthesis and catabolism of, 20: 5301(R) (UR-668, pp 1-54)
reaction mechanisms of macromolecules of, with radiomimetic and radioprotective compounds, 20: 5423
synthesis of, by mitochondria of liver and kidney, trace study, 20: 5254
synthesis of, role of ribosomes in, tracer study, 20: 5264
PROTON BEAMS
acceleration in linacs, design of r-f structures for, (T), 20: 5937 (KFK-348)
acceleration in 200-Bev synchrotron, radiation problems from, (T), 20: 5945 (UCRL-16464)
attenuation in human skull of, 20: 5475
density distribution in phase volume of linac injector, 20: 5956
energy measurements on 10- to 200-Mev, ionization chambers for, (E), 20: 5778
use for pituitary ablation, for treatment of diabetic retinopathy, 20: 5468
PROTON SHIELDING
nuclear showers in steel, from 1- and 3-Bev primaries, (T), 20: 5927 (ORNL-P-1733)
PROTON SPECTROMETERS
design and performance of proportional detectors as, 20: 5759
PROTONS
angular distribution and energy of, from nickel-58 and nickel-60 (n,p) reactions, (E), 20: 6440
angular distribution, energy spectra, and flux along magnetic field line L = 5.6, (E), 20: 6197
attenuation of 1- and 3-Bev, in steel, (T), 20: 5927 (ORNL-P-1733)
density distribution in Van Allen belts, altitude and time dependence of 55-Mev, (E), 20: 6200
detection and discrimination by semiconductor counters, (E), 20: 5732 (KFK-335)
diffusion of solar-flare, in interplanetary space, 20: 5970
effects on blood serum proteins in rats, 20: 5378
effects on coalescence rates in liquid-liquid systems, mechanism of, 20: 5571 (ORNL-TM-1283)
energy spectra from solar flares, 20: 5969
interactions with antiprotons at 4 Bev/c, hyperon pair production in, (E), 20: 6033 (CEA-R-2798)
interactions with gamma rays at 0.3 to 5.5 Bev, resonances from, (E/T), 20: 6037 (DESY-65/11)
interactions with mesons (π^-) at 10 Bev/c, analysis of inelastic, (E/T), 20: 6038 (INR-646/VI/PH)
interactions with nucleons at 30 Bev/c, models for jets from, (E/T), 20: 6039 (INSJ-90)
interactions with protons at 158 Mev, bremsstrahlung and angular distributions from, (E), 20: 6046
interactions with protons at 430 Mev, triple, (E), 20: 6056
interactions with photons, T violation in, (T), 20: 6059
interactions with mesons (π^-) in carbon, hyperon (Λ^0) production in, (E), 20: 6071
interactions with antiprotons, mesons (π), and protons at high energies, relation between, (T), 20: 6081
interactions with mesons (π^-) and (π^+), coupling constant and s-wave scattering lengths for elastic, (T), 20: 6083
interactions with electrons, radiative corrections for, (T), 20: 6093
interactions with antiprotons at 3.6 Bev/c, meson (π) production in inelastic, (E), 20: 6097
interactions with mesons (K), hyperon (Ξ) production in, 20: 6099
interactions with antiprotons, baryon pair production in, (T), 20: 6133
interactions with mesons (π^-) at 3.3 and 3.9 Bev/c, resonances from, (E/T), 20: 6041 (UCRL-11942)
interactions with protons, N^{*++} production in, (E/T), 20: 6042 (UCRL-16189)
interactions with mesons (π^-) at 4 Bev/c, cross sections for elastic, (E), 20: 6100
interactions with electrons at 4 Bev, heavy electron production from, (E), 20: 6078
interactions with nucleons at 24 Bev, angular distributions from, (E), 20: 6325
magnetic moment, (T), 20: 6074
photoproduction on magnesium-24, spectra from, (E), 20: 6399
polarization by complex nuclei at 45 Mev, (E), 20: 6274 (AD-619061)
polarization in (d,p) reactions on iron-58 and nickel and zinc isotopes, angular distributions and energy spectra of, (E), 20: 6422
reactions (p,d) with nuclei, projection operators for, (T), 20: 6312
reactions (p,γ) with carbon at 16 to 56 Mev, spectra from, (E), 20: 6297(R) (ORNL-3858(Vol.2), pp 82-90)
reactions (p,γ) with magnesium-25 at 920 kev to 1.8 Mev, energy spectra from, (E), 20: 6438
reactions (p,γ) with nuclei $56 \leq Z \leq 77$ at 10.5 Mev, isomeric transitions in, 20: 5928(R) (PR-P-66)
reactions (p,γ) with sodium-23 at 300 to 750 kev, gamma branching in, (E/T), 20: 6295 (NP-15647)
reactions (p,γ) with sulfur-33 at 300 to 1300 kev, gamma branching in, (E/T), 20: 6295 (NP-15647)
reactions (p,n) with gold-197 at 2.8 Bev, cross sections for production of mercury isotopes in, (E), 20: 6298(R) (PPAD-2137-566)
reactions (p,n) with lithium-7 near threshold, neutron yield from, (E/T), 20: 6355
reactions (p,n) with lithium-7 near threshold, neutron energy spectra from, (T), 20: 6356
reactions (p,n) with nuclei at 30 and 50 Mev, cross sections and energy spectra from, (E/T), 20: 6361
reactions (p,2n) with holmium-165, lutetium-175, tantalum-181, terbium-159, and thulium-169 at 12 Mev, (E), 20: 6366
reactions (p,2p) with titanium-47, -48, and -49 at 155 Mev, cross sections for, (E), 20: 6330
reactions with bismuth and gold at 60 to 155 Mev, charged-particle and neutron emission in, (T), 20: 6364
reactions with cobalt at 450 Mev, secondary proton spectra from, (E), 20: 6297(R) (ORNL-3858(Vol.2), pp 82-90)
reactions with copper, gold, and silver at 2 Bev, lithium-8 production in, (E), 20: 6409
reactions with emulsion nuclei at 24 Bev, angular distributions from shower, (E), 20: 6325
reactions with gold-197 at 0.6 to 30 Bev, terbium-149 production in, (E), 20: 6372
reactions with heavy nuclei at 3 Bev, fission and fragmentation products from, (E), 20: 5756
reactions with helium at 50 to 150 Mev, electron angular distributions and energies from, (T), 20: 5993
reactions with iron at 1 and 3 Bev, nucleon-pion cascades from, (T), 20: 5927 (ORNL-P-1733)
reactions with nuclei at 0.54 to 1.47 Bev, neutron yields from, (E), 20: 5928(R) (PR-P-66)
reactions with zinc-64 at 12 Mev, energy levels from, 20: 6296(R) (ORNL-3858(Vol.1), pp 1-12)
scattering by carbon and nitrogen, polarization in elastic, 20: 6439
scattering by carbon-12 and deuterium at 141 Mev, polarization in elastic, (E), 20: 6328
scattering by carbon-13 at 1.5 to 2.4 Mev, angular distributions from elastic, (E/T), 20: 6362
scattering by deuterium at 150 Mev, cross sections and polarization in elastic, (T), 20: 6329
scattering by nuclei around 20 Bev, analysis of small-angle, 20: 5720 (CERN-65-33)
scattering by nuclei, errors in optical model analysis of, 20: 6296(R) (ORNL-3858(Vol.1), pp 1-12)
scattering by odd-mass nuclei, level excitation in, (E), 20: 6386
scattering by oxygen-16 at 21 to 53 Mev, polarization from elastic, (E), 20: 6306 (UCRL-16217)
scattering by oxygen-18 at 7.89 to 16.28 Mev, elastic and inelastic, (E), 20: 6373
scattering by silicon-28 at 30.3 Mev, differential cross sections for, (E), 20: 6339
scattering on medium-mass nuclei at 155 Mev, differential cross sections from inelastic, (E), 20: 6354
yields from meson (π^-) capture by nuclei, (E/T), 20: 6292 (NP-15601)
PROTOZOA
radiation effects on luminescence of acridine-orange-stained cells of, x, 20: 5267
radiation effects on enzyme activity in homogenates of *Stylonychia pustulata*, uv, 20: 5272
radiation effects on morphogenesis in Euplotes, uv, 20: 5345
PSEUDOUREA, 2-(2-AMINOETHYL)-2-THIO-
radioprotective properties of, 20: 5422
radiosensitivity effects in mice, γ, 20: 5410
radiosensitivity effects on animal cells in culture, 20: 5419

reaction mechanisms of, with protein macromolecules, 20: 5423
PUERTO RICO POWER REACTOR
fuel element weldments for, engineering analyses of, (E), 20: 6624 (TID-22425)
PULSE ANALYZERS
circuit design for correcting output of time-to-pulse height, 20: 5796
design and performance of discriminators, (E), 20: 5680 (ELI-91)
design for rapid readout, 20: 5797(P)
design of fast-amplitude, 20: 5694
performance for signal analysis in noise background by data accumulation, (T), 20: 5695
performance of multichannel, with routing system, (E), 20: 5769
performance of time-to-amplitude, error analysis for, 20: 5731 (JINR-P-2394)
use in PNPF coolant monitoring, 20: 6615 (NAA-SR-10888(Rev.))
PULSE GENERATORS (ELECTRONICS)
design and operation of ramp, 20: 5710
design for accelerator beam deflecting plates, 20: 5963
PULSE MODIFIERS
design, 20: 5780
PULSES
recording apparatus for, 20: 5797(P)
PUPAE
radiation effects on house fly, *Musca domestica*, x, 20: 5331
PYCNOMETRY
design of remotely operated gas pycnometer, 20: 5708
PYRIDINES
effects on deuterium exchange between isobutyraldehyde and water, 20: 5565

Q

QUALITY CONTROL
radiometric technique for, method of gage compensation in, 20: 5712(P)
QUANTOMETERS
response to bremsstrahlung at 0.2 to 50 Mev, 20: 5765
response to bremsstrahlung at 5 to 35 Mev, 20: 5766
QUANTUM ELECTRODYNAMICS
propagators in, finite parts of generating functional of, 20: 6220
QUANTUM MECHANICS
angular momentum and angle in, uncertainty between, 20: 6154
angular momentum operators in, computer program for calculating, 20: 6216 (ORNL-3877)
axiomatic studies of basic nonrelativistic, (T), 20: 6213 (ANL-7065)
bound state problems in, development of approximate dynamical symmetries for, 20: 6215 (NP-15614)
Dirac equation without Dirac matrices, formalism of, 20: 6223
elementary particle motion in, momentum invariants and Lorentz covariant forms for, 20: 6214 (INR/610/VI/PB)
energy levels in one-dimensional systems, variational method for, excited, 20: 6221
formalism for three-body problem, complete orthogonal system in, (T), 20: 6217
Schroedinger equation in, derivation from orbital density concept, 20: 6225
Senitzky theorem in, disproof of, (T), 20: 6226
wave functions in, symmetry violating trial, 20: 6227

R

RABBITS
blood serum of irradiated, effects on radioinduced diarrhea in rats, 20: 5411
effects of cortisol on bone growth and atrophy in, 20: 5234(R) (COO-119-232, pp 122-52)
infections in skin of, effects of leukopenia on, 20: 5315
radiation effects on blood coagulation in, x, 20: 5325
radiation effects on blood picture in, x, 20: 5325
radiation effects on hematopoietic system of, fractionated doses of x, 20: 5364
radiation effects on binding of mitochondrial liver lipids in, γ, 20: 5379
radiation effects on enzyme activity of various tissues of, γ, 20: 5380
radioinduced fibrinolysis in, x, 20: 5325
radiosensitivity of chromosomes in leukocytes in, 20: 5304(T) (JPRS-32985, pp 45-50)
RACAH COEFFICIENTS
calculation of, computer program for, 20: 6216 (ORNL-3877)
RADIATION
attenuation by vertical barriers, (E/T), 20: 6516 (AD-617524)
book: *The Physical Fundamentals of Nuclear Radiation Measurements* (In German), 20: 5795
carcinogenic effects of, 20: 5466
detection and measurement in man of, calibration of whole-body counting instruments for, 20: 5426
dose distribution during therapy middle ear tumors, technique for, 20: 5448
dosimetry of therapeutic doses of, performance of luminescent and semiconductor detectors for, 20: 5479
effects on barley seed, effects of dimethyl sulfoxide and nitric oxide on oxygen effect in, 20: 5298(R) (RLO-353-4)
effects on catalase-hydrogen peroxide system, 20: 5271
effects on chromosomes of, effects of dose, linear energy transfer, and modifying agents on, 20: 5343
effects on color center formation in silica gel, 20: 5584
effects on growth of tumor cells, 20: 5477
effects on hematopoietic system, 20: 5308
effects on ignition of uranium, 20: 6552(R) (ANL-6925, pp 187-233)
effects on immune reactions to tissue transplants, bibliography, 20: 5424
effects on living organisms and tissues, bibliography on, 20: 5284 (AED-C-04-21)
effects on metabolism, 20: 5308
effects on metabolism of injected ferritin in rats, 20: 5354
effects on metabolism of iron in rats, 20: 5354
effects on methanol and methanolic solutions, 20: 5581
effects on mice, leukemogenic, 20: 5309
effects on properties of thoria-base fuel elements, 20: 5915(R) (ORNL-P-1724)
effects on solids, step annealing of, 20: 5580
effects on spermatogenesis in field mice living on radioactive soils, 20: 5387
effects on telemetry circuits in LES satellites, 20: 5806 (AD-619387)
effects on tumor cells, cytological, 20: 5477
emission by charged particles at anisotropic conductive plane, 20: 6043
surface activity predictions, for Salmon Event, 20: 5667 (VUF-1020)
transport of, finite difference methods for nonlinear, 20: 6522 (UCRL-12411)
use for therapy of gynecological cancers, 20: 5473
use in agriculture and forestry in Rumania, 20: 5235 (NP-15543, pp 83-90)
RADIATION DETECTION INSTRUMENTS
book: *The Physical Fundamentals of Nuclear Radiation Measurements* (In German), 20: 5795
calibration of SNAP-10A, 20: 6656 (NAA-SR-Memo-11333)
calibration of, for monitoring airborne radioactivity, 20: 5774
design for use in radiation protection, 20: 5762
development, 20: 5737(R) (ORNL-3858(Vol.I), pp 59-64)
particle track analysis from, using vidicons with digital scanners, (E), 20: 5718 (BNL-9634)
performance in soft beta measurement, survey of, 20: 5754
performance of end window, for beta, 20: 5791
review of research at University of Edinburgh on, 20: 5239
RADIATION DETECTION INSTRUMENTS (PULSE TYPE)
background counting rate of G-M, effects of cosmic radiation on, 20: 5781
data readout circuit for, 20: 5797(P)
design for cosmic particle interactions above 100 Bev, 20: 5724 (CONF-640919, pp II13-23)
design of boron-trifluoride, with preamplifier, (E), 20: 5680 (ELI-91)
design of cosmic-ray, for interactions at 300 Bev, 20: 5725 (CONF-640919, pp II27-30)
design of G-M, 20: 5801(P)
design of solid-state, with low-noise amplification, 20: 5804(P)
performance of G-M, in determination of carbon-14 in organic compounds, 20: 5511
performance of plastic scintillator, for gamma aerial monitoring, 20: 5761
performance of scintillation, in strong magnetic fields, 20: 5736 (NP-15597)
RADIATION DETECTORS
book: *The Physical Fundamentals of Nuclear Radiation Measurements* (In German), 20: 5795
data analysis from low-resolution measurements of beta and conversion-electron spectra, (T), 20: 5768
design characteristics of boron-10-coated ionization chambers for neutron counting, (E), 20: 5717 (AEEW-M-508)
design of angled probe for use in brain scanning, 20: 5462
development, 20: 5738(R) (ORNL-3853(Vol.2), pp 91-3)
development for gamma and neutron detection in boiling reactors, (E), 20: 6648(R) (HPR-64)
development of regenerating, for neutrons, 20: 6567 (HW-SA-3600)
development with transmitters for continuous centralized recording of individual doses, 20: 5749
performance of Makrofol and mica, for heavy ions, 20: 5756
performance of scanner-type, for *in vivo* radioisotope mapping, 20: 5745(R) (UR-668(p.117-23))
RADIATION INJURIES
book: *Mammalian Radiation Lethality*, 20: 5405
diagnosis of, role of blood studies in, 20: 5308

in goldfish, effects of temperature on, 20: 5374
legal aspects of, 20: 5241
pathology of α, induced by deposited Thorotrast, 20: 5398
pathology of α, induced by deposited Thorotrast, 20: 5400
pathology of, induced by iodine-131 therapy of hyperthyroidism, 20: 5469
pathology of, induced by Thorotrast injections, 20: 5355
protection against, effects of mercaptoethylamine in mice, 20: 5407(R) (AD-623599, pp 37-44)
protection against γ, effects of 2-aminothiazoline salts in mice, 20: 5410
protection against γ, effects of AET in mice, 20: 5410
protection against, effects of cysteine and MEA in cultured cells, x, 20: 5418
protection against, effects of aminoethylisothiuronium, cystamine, and homocysteinethiolactone in cultured cells, x, 20: 5419
protection against, effects of bone marrow grafts in man, 20: 5420
protection against, effects of hematopoietic tissue transplants, bibliography, 20: 5424
recovery from, of mouse bone marrow, 20: 5320

RADIATION MONITORING
equipment design and performance for, portable, 20: 5742(R) (UCRL-14351)
equipment design for plutonium alpha, transistorized, 20: 5742(R) (UCRL-14351)
equipment design for, aural-warning, 20: 5803(P)
instrument calibration for airborne, 20: 5774
system for gamma and neutron, audio-visual warning, 20: 5733 (LA-DC-6790)

RADIATION PROTECTION
apparatus for televised radiography, 20: 5464
developments in, in Rumania, 20: 5425 (NP-15543, pp 77-82)
equipment for, in reactor areas, 20: 6670 (CEA-R-2864)
instrumentation for, 20: 5762
measures for radiological personnel, 20: 5434
measures in uranium mines, 20: 5428
methods for dental personnel during radiography, 20: 5430
of fetuses, during diagnostic radiography during pregnancy, 20: 5476
of radiography technicians, 20: 5489
program in Italy, 20: 5433
program of Canada, 20: 5415
requirements for, at 200-Bev proton synchrotron, (T), 20: 5945 (UCRL-16464)
review of research at University of Edinburgh on, 20: 5239
standards of ICRP for, 20: 5663 (NP-15451)

RADIATION SICKNESS
effects on cortical arousal induced by conditioned stimuli in burros, 20: 5329
effects on gastric secretion, enzyme activity, and blood riboflavin content in dogs, 20: 5384
in rats, therapeutic effects of serum from irradiated rabbits, 20: 5411

RADIATION SOURCES
preparation of isotopic, 20: 5590 (NP-15543, pp 5-26)

RADIATION TARGET CANS
design of reactor, 20: 6574(P)
temperature control by helium-nitrogen gas gap, 20: 6680 (ORNL-TM-1319)

RADIATION TARGETS
performance of self-regenerating deuterium, using coated metals, (E/T), 20: 6334

RADIO WAVES
absorption in ionosphere, cosmic noise level during type-II anomalous, 20: 6194
emission of low-frequency nonthermal cosmic, anisotropy of, (T), 20: 6020

RADIOACTIVE MATERIALS
deposition and retention of inhaled dusts by animals and man, 20: 5237(R) (UR-668, pp 55-109)
handling of, design of equipment for, 20: 5615(P)

RADIOACTIVE WATERS
bibliography on, 20: 5668 (WASH-1061)

RADIOACTIVITY
bibliography on natural environmental, 20: 5668 (WASH-1061)
environmental, effects on leukemia incidence in Poland, 20: 5674
of foods, natural, fallout, and induced, 20: 5431

RADIOAPPLICATORS
design for therapy of antral carcinomas, iridium-192, 20: 5458
use for therapy of bladder cancers, 20: 5454
use for therapy of gynecological cancers, 20: 5473
use for therapy of ear cancers, 20: 5474
use of beta, for therapy of hemangiomas in children, 20: 5443

RADIOBIOLOGY
radiation protection in, in Rumania, 20: 5425 (NP-15543, pp 77-82)

RADIOCHEMISTRY
developments in Rumania, 20: 5590 (NP-15543, pp 5-26)

RADIODIAGNOSIS
device for imaging in, 20: 5461
device for posterior fossa, scanning, 20: 5462
equipment and procedure for gamma imaging in, Spintharicon spark-chamber, 20: 5461
hazards to personnel from, 20: 5434
of lesions of brain, liver, and lungs, use of technetium-99-labeled albumin and colloids and external scanning for, 20: 5456
of tumors, use of labeled compounds and external scanning for, 20: 5450
tracer techniques using external scanning, 20: 5447
use of photoscanning for, review, 20: 5487

RADIOGRAPHY
apparatus for televised, design of, 20: 5464
book: *Textbook of Elementary Radiography for Students and Technicians*, 20: 5489
effects of, on radiation dose of population of Canada, 20: 5415
effects on radiation dose of population of Great Britain, 20: 5415
method for hollow underwater structures, 20: 5631(P)
of heart, radiation dose to children from diagnosis of congenital heart disease, 20: 5455
of tumors, use of Thorotrast for delineation of liver, 20: 5465
radiation dose absorbed during diagnostic, measurements of, 20: 5440
radiation dose from diagnostic, in Great Britain, 20: 5409
radiation hazards to patients and personnel during diagnostic urological, 20: 5459
radiation hazards of diagnostic, during pregnancy, 20: 5476
radiation protection of personnel during diagnostic, 20: 5433
shielding barriers for, diagnostic, gamma source for evaluating, 20: 5677
use in nondestructive fuel element testing, 20: 6632(T) (AEC-tr-6628)
use in nondestructive analysis of inclusions in SAP tubing, 20: 5630 (NAA-SR-Memo-11562)
use of gamma camera for, 20: 5467

RADIOISOTOPES
analysis of mixtures of, summing γ-γ coincidence spectrometer for, 20: 5753
analysis of mixtures of, using least-squares regression analysis of gamma spectra, 20: 5727 (CONF-651101-46)
decay of neutron-deficient, survey on $189 \leq A \leq 200$, (E), 20: 6298(R) (PPAD-2137-566)
distribution of gamma emitting *in vivo*, methods of measuring, 20: 5745(R) (UR-668(p.117-23)
medical use of, review, 20: 5487
methods for storage of, at National Institute of Radiological Sciences in Chiba, Japan, 20: 5672
performance in space propulsion systems, 20: 5634
preparation, 20: 5590 (NP-15543, pp 5-26)
review of research at University of Edinburgh on, 20: 5239
use for electric power generation, 20: 5821
use in British industry, 20: 5817
use in industrial processes, 20: 5814 (NP-15543, pp 27-45)
use in Rumania, 20: 5810 (NP-15543)

RADIOLOGICAL DEFENSE
protection of population against fallout from thermonuclear explosions, 20: 5416

RADIOMETRIC ANALYSIS
data analysis from gamma-, using least-squares regression computer code, 20: 5727 (CONF-651101-46)

RADIOMIMETIC SUBSTANCES
reaction mechanisms of, with protein macromolecules, 20: 5423

RADIOPROTECTIVE COMPOUNDS
effects on radioinduced scintillation in dioxane, 20: 5422
evaluation of 20 aminothiazoline salts in mice, 20: 5410
reaction mechanisms of, with protein macromolecules, 20: 5423
reaction mechanisms of, 20: 5296(R) (NP-15585)
testing of, using liquid scintillator systems, 20: 5422

RADIOSENSITIVITY
circadian rhythmicity of x, in mice, 20: 5336
effects of temperature on phage and virus, 20: 5299(R) (TID-22187)
of carcinomas, effects of estradiol on cervical, 20: 5472
of *Escherichia coli*, γ and uv, 20: 5348
of guinea pigs, effects of pre-irradiation on x, 20: 5356
of thymocytes isolated from rats, effects of freezing on, 20: 5414
of tumors, effects of inhaled oxygen or Synkayvite on, 20: 5437
radiation effects on Saccharomyces, mutagenic β, uv, and x, 20: 5360
variations in mammals, cyclic, 20: 5336

RADIOSTERILIZATION
of foods, effects on radioactivity, 20: 5431
of insects, use for population control, 20: 5815 (STI/DOC/10/44)

RADIOTHERAPY
book: *Radiotherapy of Benign Diseases*, 20: 5490
depth doses for cobalt-60 beam, method for calculating, 20: 5449
hazards to personnel from, 20: 5434
indications for reirradiation of cervical carcinomas, 20: 5457

leukemia incidence after breast cancer, 20: 5471
mega- and supervoltage radiation for, advantages of, 20: 5451
of tumors, criteria for dose fractionation, 20: 5466
of tumors, synergistic effects of 5-fluorouracil, 20: 5452
of tumors, synergistic effects of chemotherapy, 20: 5466
review of research at University of Edinburgh on, 20: 5239
sources for high-energy, 20: 5442
techniques for pharyngo-laryngeal, γ and x, 20: 5463
use of cesium-131 seeds for, advantages of, 20: 5482

RADIUM
diffusion in pyrolytic graphite, 20: 5846
effects on gynecologic carcinoma, intestinal injury from therapeutic, 20: 5392
use for therapy of ear cancers, 20: 5474

RADIUM ISOTOPES Ra-222
alpha decay widths and nuclear structure, (T), 20: 6423

RADIUM ISOTOPES Ra-224
content in Thorotrast of, 20: 5398

RADIUM ISOTOPES Ra-226
effects of deposited, on mechanical strength of bones, 20: 5289(R) (COO-119-232, pp 88-98)
effects of injected, long-term pathological on dogs, 20: 5287(R) (COO-119-232, pp 5-64)

RADIUM ISOTOPES Ra-228
effects of deposited, on mechanical strength of bones, 20: 5289(R) (COO-119-232, pp 88-98)
effects of injected, long-term pathological on dogs, 20: 5287(R) (COO-119-232, pp 5-64)

RADON
content in atmosphere at ground level, effects of meteorological conditions on, 20: 5646
diffusion from soils, effects of meteorological conditions on, 20: 5646
effects of airborne, on mice and rats, 20: 5237(R) (UR-668, pp 55-109)
loss and retention by man, 20: 5237(R) (UR-668, pp 55-109)

RAIN WATER
radioactivity from cesium-137, ruthenium-106, and zirconium-95 in, at Bombay, 20: 5661 (AEET-215)
strontium-89 and -90 content in Tokyo, four weeks after Chinese nuclear explosion of May 14, 1965, 20: 5656
strontium-90 content in, New Zealand, 1965, 20: 5664(R) (NP-15639)

RAINIER MESA QUADRANGLE (NEV.)
ground water discharge, movement, and occurrence in tuffaceous rocks in, 20: 5643 (TEI-862)

RARE EARTH ALLOYS
Cd–rare earth, eutectic temperatures of, 20: 5594(R) (ANL-6925, pp 21-106)

RARE EARTH COMPLEXES
with tropolone, preparation, properties, and structure, 20: 5538

RARE EARTH IONS
spin-lattice relaxation rates in single crystals of anhydrous lanthanum trichloride, (E), 20: 6542

RARE EARTHS
deposition on aluminum, copper, and stainless steel, electrolytic, 20: 5867
determination using ammonium oxalate by potentiometric titration, 20: 5519
effects on allotropic transformation of zirconium, 20: 5891(R) (NYO-2159-1)
effects on metallurgical properties of thorium, 20: 5891(R) (NYO-2159-1)
magnetic properties of, 20: 6531 (AD-623530)
reactions with sodium metaphosphate, 20: 5529(R) (SC-DC-65-1706)
separation by electrophoresis, 20: 5598

RATE METERS
performance in scanning radioactive paper chromatograms, 20: 5508
pump-circuit design for, (E), 20: 5680 (ELI-91)

RATS
calcium exchange in soft tissues of, 20: 5237(R) (UR-668, pp 55-109)
development of, effects of strontium-90 maternal doses on, 20: 5237(R) (UR-668, pp 55-109)
effects of benzopheanthrenes in, carcinogenic, 20: 5334
effects of croton oil in, carcinogenic, 20: 5334
effects of methylcholanthrene in, carcinogenic, 20: 5334
effects of nitrogen mustards on, pathological, 20: 5296(R) (NP-15585)
effects of phosphorus-32 in, carcinogenic, 20: 5334
excretion of inhaled volatile mercury by mercury–salt-injected, 20: 5251(R) (UR-668, pp 123-49)
life-span and tumorigenesis in, effects of polonium-210 on, 20: 5237(R) (UR-668, pp 55-109)
metabolism of hexobarbitol in, effects of mercaptoethylamine and magnesium on, 20: 5283(R) (AD-623599, pp 16-27)
metabolism of inhaled mercury by, 20: 5251(R) (UR-668, pp 123-49)
radiation effects on immunity to diphtheria toxins in, γ, 20: 5391
radiation effects on synthesis of hepatic microsomal enzymes in, x, 20: 5282(R) (AD-623599, pp 1-15)
radiation effects on synthesis of hepatic microsomal enzymes in, x, 20: 5283(R) (AD-623599, pp 16-27)
radiation effects on, carcinogenic, 20: 5296(R) (NP-15585)
radiation effects on motivation in, humoral factor in, 20: 5303 (USNRDL-TR-925)
radiation effects on adaptive responses of, x, 20: 5319
radiation effects on immune reactions to skin homografts in, x, 20: 5335
radiation effects on antioxidant content of tissues of, γ, 20: 5339
radiation effects on lipoperoxide content of tissues of, γ, 20: 5339
radiation effects on, biochemical, x, 20: 5341
radiation effects on, morphological, x, 20: 5341
radiation effects on metabolism in kidney tissue sections of, x, 20: 5352
radiation effects on metabolism of injected ferritin by, 20: 5354
radiation effects on metabolism of iron in, 20: 5354
radiation effects on mineral metabolism in bones of, effects of denervation on x, 20: 5370
radiation effects on muscle activity of, γ, 20: 5375
radiation effects on blood serum proteins, proton, 20: 5378
radiation effects on urinary excretion of thymidine by, x, 20: 5382
radiation effects on mechanical activity of muscles of, γ, 20: 5292(R) (COO-205-55, Paper 1)
radiation effects on nervous responses of, dependence on pre-irradiation cold stresses, 20: 5301(R) (UR-668, pp 1-54)
radiation effects on reproductive fitness of, x, 20: 5301(R) (UR-668, pp 1-54)
radiation effects on hypertension and nephrosclerosis in, x, 20: 5301(R) (UR-668, pp 1-54)
radioinduced diarrhea in, therapeutic effects of serum from irradiated rabbits, 20: 5411
radioinduced hematologic changes in, x, 20: 5301(R) (UR-668, pp 1-54)
radioinduced tumors in bones of, americium-241 and plutonium-239, 20: 5321
respiration in tissue cultures of thymocytes of, 20: 5340
retention of strontium-90 by fetal and newborn, 20: 5237(R) (UR-668, pp 55-109)
synthesis of hepatic microsomal enzymes in, effects of age, 20: 5283(R) (AD-623599, pp 16-27)
tritium uptake from glucose by fatty tissues in, 20: 5252
urania excretion and lung burden in aerosol-exposed, 20: 5251(R) (UR-668, pp 123-49)

REACTOR BREEDING BLANKETS
development of mobile, 20: 5594(R) (ANL-6925, pp 21-106)

REACTOR BREEDING ELEMENTS
processing of fast reactor, pyrochemical batch-extraction, 20: 6600(R) (ANL-7105, pp 1-35)

REACTOR COMPONENTS
inspection by defectoscopic methods, for First Czechoslovakian Atomic Power Station, (E), 20: 6633(T) (AECL-2286)

REACTOR CONTROL RODS
drive mechanism for, gas pressure-electromagnetic, 20: 6569(P)
neutron distribution in absorbing, P_n approximation for, 20: 6267
worth calculations for, central, 20: 6601(R) (ANL-7115, pp 1-41)

REACTOR CONTROL SYSTEMS
design for process control in 200-Mw(e) sodium graphite reactors, 20: 6617 (NAA-SR-Memo-11339)
design using movable core section, 20: 6575(P)

REACTOR COOLANTS
performance and properties of gaseous, comparison of, 20: 6603(R) (GA-4165)

REACTOR COOLING SYSTEMS
coolant sonic velocities in two-phase, sodium, 20: 6559(R) (ANL-7115, pp 77-83)
design of self-sustaining, for gas-cooled reactors, 20: 6647(P)
development of steam–water spray, 20: 6566(R) (EURAEC-1382)
failures of, analysis of coolant-loss accidents from, (T), 20: 6560(R) (BMI-X-10145)
fracture modes in pipes of water-cooled, review of, 20: 5851

REACTOR ENGINEERING
inspection by defectoscopic methods, for First Czechoslovakian Atomic Power Station, (E), 20: 6633(T) (AECL-2286)

REACTOR EXPERIMENTAL FACILITIES
description of ZERLINA pile oscillator, 20: 5715 (AEET-227)
safety analysis of fast-flux test section in SRE, (T), 20: 6676 (NAA-SR-11234)

REACTOR FUEL ALLOYS
processing by fluoride volatility for uranium recovery, 20: 5595(R) (ANL-6925, pp 107-64)
processing spent Pu–U, methods for, 20: 5594(R) (ANL-6925, pp 21-106)
processing spent, methods for, 20: 6553(R) (ANL-6925, pp 255-63)

REACTOR FUEL ELEMENTS
burnup studies, 20: 6558(R) (ANL-7115, pp 42-67)
fabrication of magnesium alloy-clad uranium, grain-size control in,

20: 5871(P)
fabrication of magnesium alloy-clad uranium, for operation at 140 to 350°C, 20: 5872(P)
gamma dose rate distribution from spent, (E/T), 20: 6597
heating transients of, computer analysis of in-pile, 20: 6562 (NAA-SR-Memo-11369)
processing of fast breeder, 20: 6601(R) (ANL-7115, pp 1-41)
processing of irradiated, for plutonium separation, 20: 5596
testing in Halden boiling reactor, (E), 20: 6648(R) (HPR-64)
testing of, methods for nondestructive, 20: 6632(T) (AEC-tr-6628)
thermal conductivity of in-pile, temperature transient method for measuring, 20: 6565(R) (CEND-3336-251)
thermal testing of finned vapotron, 20: 6595(R) (EURAEC-1421)
welding of end seals to, method for, 20: 5868(P)

REACTOR FUEL ELEMENTS (CERAMIC)
burnup studies, 20: 6558(R) (ANL-7115, pp 42-67)
combustion by fluidization, separation of thorium and uranium from, 20: 5500 (ORNL-3876)
design analysis for beryllia-base, 20: 6603(R) (GA-4165)
fabrication of silicon carbide–uranium carbide, process for, 20: 5873(P)
processing of fast reactor, pyrochemical batch-extraction, 20: 6600(R) (ANL-7105, pp 1-35)
processing of irradiated, by fluoride volatility, 20: 5595(R) (ANL-6925, pp 107-64)
radiation effects on thoria-base, 20: 5915(R) (ORNL-P-1724)
reactions with water in TREAT at 2250 to 3300°C, 20: 6552(R) (ANL-6925, pp 187-233)
thermal expansion during fast burst accidents, 20: 6602 (BNWL-SA-346)
wetting by sodium, 20: 5594(R) (ANL-6925, pp 21-106)

REACTOR FUEL ELEMENTS (DISPERSION)
production and testing of magnesium–uranium dioxide, 20: 6684

REACTOR FUEL ELEMENTS (THERMOELECTRIC)
design, 20: 6598(P)
development, 20: 6023(R) (AD-619379)
development and testing of, 20: 6596(R) (GEST-2049)

REACTOR FUEL PINS
dimensional stability of, strain gages for measuring, 20: 5703
reactions of uranium, in TREAT meltdown experiments, 20: 6552(R) (ANL-6925, pp 187-233)

REACTOR FUEL TUBES
properties of carbon–uranium for use as, 20: 5887 (NLCO-953)
texture gradients in uranium, effects of fabrication variables on, 20: 5863 (NLCO-945)
welding of end seals to, method for, 20: 5868(P)

REACTOR FUELS
burnup and conservation in thermal reactors, 20: 6610 (HW-79287)
cycle facility design and operation for EBR-II, 20: 5594(R) (ANL-6925, pp 21-106)
development for fast reactors, 20: 6600(R) (ANL-7105, pp 1-35)
development of paste, 20: 5594(R) (ANL-6925, pp 21-106)
fabrication of compact uranium dioxide particles, method for, 20: 5869(P)
fabrication of processed, equipment and procedures for, 20: 5594(R) (ANL-6925, pp 21-106)
heating transients of, computer analysis of in-pile, 20: 6562 (NAA-SR-Memo-11369)
opacity of gaseous, (T), 20: 6594 (D-910092-4)
processing irradiated EBR-II, 20: 5594(R) (ANL-6925, pp 21-106)
processing of plutonium, costs and methods of, 20: 6553(R) (ANL-6925, pp 255-63)
research on coated-particle, 20: 5848
testing in Halden boiling reactor, (E), 20: 6648(R) (HPR-64)
thermal expansion during fast burst accidents, 20: 6602 (BNWL-SA-346)

REACTOR MATERIALS
inspection by defectoscopic methods, for First Czechoslovakian Atomic Power Station, (E), 20: 6633(T) (AECL-2286)
reactions with sodium, research plans for, 20: 6552(R) (ANL-6925, pp 187-233)
research progress on, *Technical Progress Reviews*, Spring 1965, 20: 5842
research progress on, *Technical Progress Reviews*, Fall 1965, 20: 5847

REACTOR MATRICES
cost analysis of 500-Mw(e) beryllia-moderated, 20: 6603(R) (GA-4165)
design analysis of beryllia-moderated thoria–urania-fueled, 20: 6603(R) (GA-4165)
design analysis of beryllia-moderated plutonium-fueled, 20: 6603(R) (GA-4165)

REACTOR MODERATORS
neutron decay in, computer program for spectral analysis of pulsed, 20: 6585 (NAA-SR-Memo-10941)

REACTOR SAFETY
analysis in coolant-loss accidents in boiling- and pressurized-water reactors, (T), 20: 6560(R) (BMI-X-10145)
bibliography, 20: 6563 (TID-3525(Rev.5)(Suppl.2))
fuel behavior during fast burst accidents, 20: 6602 (BNWL-SA-346)
metal–water reactions in coolant-loss accidents, calculations of, 20: 6552(R) (ANL-6925, pp 187-233)
radioprotection devices used near swimming pool reactors, review of, 20: 6670 (CEA-R-2864)
research, 20: 6559(R) (ANL-7115, pp 77-83)
research programs on, 20: 6552(R) (ANL-6925, pp 187-233)

REACTOR SAFETY EXPERIMENTS
accidents in LOFT, analysis of coolant-loss, (T), 20: 6560(R) (BMI-X-10145)
criticality studies in TREAT, for fast reactor safety, 20: 6576(R) (ANL-7105, pp 72-84)
fuel meltdown studies in TREAT, 20: 6576(R) (ANL-7105, pp 72-84)
metal–water reactions in LOFT, 20: 6552(R) (ANL-6925, pp 187-233)
testing urania and uranium fuels in TREAT, 20: 6552(R) (ANL-6925, pp 187-233)
uses of TREAT for irradiation testing of SNAP-10A fuels, (E), 20: 6678 (NAA-SR-Memo-11374)

REACTOR SHIELD VOIDS
research, 20: 6519(R) (ORNL-3858(Vol.1), pp 20-41)

REACTOR SHIELDING
gamma dose rates behind, (E/T), 20: 6626 (UNC-5118)
gamma heating and transport in, (E/T), 20: 6517 (CONF-651101-41)

REACTOR SIMULATORS
time delay simulation methods for analog, 20: 5834 (ORNL-TM-1323)

REACTOR TUBES
moderator dimensional stability effects on, graphite, 20: 6619 (NAA-SR-Memo-11416)

REACTORS
burnout in, use of sound generation in boiling heat transfer for predicting, 20: 5628
control using movable core sections, 20: 6575(P)
design of fast, for use in oil wells, 20: 6651(P)
development, 20: 6555(R) (ANL-7105)
development, 20: 6557(R) (ANL-7115)
fuel development for, 20: 6556(R) (ANL-7105, pp 36-58)
fuel heating transients in, computer analysis of, 20: 6562 (NAA-SR-Memo-11369)
gamma transport in, group constants and heating calculations for, (T), 20: 6517 (CONF-651101-41)
kinetics of boiling, (E/T), 20: 6648(R) (HPR-64)
loading device for, ram and tube plug design for, 20: 6570(P)
loading machine design for, coolant leak prevention in, 20: 6573(P)
loading machine for, sensing and step mechanism for, 20: 6571(P)
loading machine for, gimbal means for mounting, 20: 6572(P)
neutron detection in, design of boron-10-coated ionization chambers for, (E), 20: 5717 (AEEW-M-508)
neutron flux decay constants for non-multiplying media of, (T), 20: 6580 (CEA-R-2702)
neutron flux distribution in, effects of xenon oscillations on, (T), 20: 6590
neutron flux monitoring in, development of regenerating detectors for, 20: 6567 (HW-SA-3600)
neutron transport in, S2 and S4 calculations of, (T), 20: 6264 (WAPD-T-1849)
reactivity noise in, bibliography, 20: 6561 (FTI-2)
samarium buildup in, (E), 20: 6589
use for ozone production for water treatment, 20: 5568 (BNL-9664)

RECUPLEX PROCESS
criticality incident in, effects on blood cells of exposed operators in, 20: 5301(R) (UR-668, pp 1-54)

REFRACTORY COATINGS
development of metal-reinforced ceramic, 20: 5846
plasma spraying of, equipment and procedure for, 20: 5837 (NLCO-966)

REFRACTORY MATERIALS
crushing of, electrohydraulic, 20: 5846
performance as coatings on metals, 20: 5910
reactions with uranium dioxide, kinetics of, 20: 6023(R) (AD-619379)

RELATIVITY THEORY
field equations for, dimensionality of real world from strength of, 20: 6218
gravitational sources in, multipole structure for, 20: 6222
quantization in general, Dirac procedure for, 20: 6219

REMOTE-CONTROL EQUIPMENT
design for EGCR, engineering drawings of, 20: 6646
design for handling radioactive materials, 20: 5615(P)
design of manipulator, 20: 6556(R) (ANL-7105, pp 36-58)
design of mechanical master-slave, 20: 5616(P)
design of remotely operated gas pycnometer, 20: 5708
development, 20: 5594(R) (ANL-6925, pp 21-106)
development for use with creep machine, 20: 5611 (BNWL-137)
gauntlets for, fabrication of neoprene coated urethan, 20: 5612 (ORNL-TM-1326)

REPTILES
radiation effects on gonads of embryos of viviparous, x, 20: 5324
RESEARCH REACTORS
description and performance of Shield Test and Irradiation Reactor, (E), 20: 6677 (NAA-SR-11528)
description of SORA fast-burst, (E), 20: 6672 (CONF-650217, pp 25-35)
fuel element development for EWA, 20: 6684
kinetics of SNEAK, 20: 6674 (KFK-332)
kinetics of zero-power fast, 20: 6674 (KFK-332)
neutron fluence measurements in Pulstar, 20: 6679 (NP-15645)
oscillator in ZERLINA, description of, 20: 5715 (AEET-227)
performance of mechanically pulsed neutron-burst-producing, (E), 20: 6672 (CONF-650217, pp 25-35)
uses of cryogenic, for basic radiation-damage studies, (E), 20: 5569 (CONF-650217, pp 108-10)
RESISTORS
radiation effects on thermistors, gamma and neutron, 20: 5808 (N65-35081)
RESPIRATORY TRACTS
radiation injuries to, in uranium miners, 20: 5428
RHENIUM
corrosion by beryllium oxide to 3000°K, 20: 5554
corrosion by cesium vapor and liquid lithium at 2500 to 3400°F, 20: 5851
effects on mechanical properties of tungsten of alloying additions of, 20: 5851
electric conductivity to 1500°C, 20: 5851
emissivity to 1500°C, total hemispherical, 20: 5851
reactions with steam at 850 to 1700°C, 20: 6552(R) (ANL-6925, pp 187-233)
RHENIUM ALLOYS
Cr–Re, internal friction, effects of nitrogen on, 20: 5851
Mo–Re, dislocation structures in annealed and deformed sheets of, 20: 5846
Mo–Re, internal friction of annealed and deformed, 20: 5846
Mo–Re, properties of sigma-phase precipitates in, 20: 5851
Mo–Re–W, fabrication of thin-walled tubing of, 20: 5867
Re–W, corrosion by lithium in niobium–zirconium alloy forced-convection loop, 20: 5853 (TIM-898)
Re–W, corrosion by liquid lithium and cesium vapor at 2500 to 3400°F, 20: 5851
Re–W, creep tests at 3200°F on, 20: 5885(R) (NAS-CR-54773)
Re–W, oxidation rate of, effects of rhenium content on, 20: 5846
Re–W, properties of, 20: 6596(R) (GEST-2049)
Re–W, radiation effects on creep-rupture of, fast neutron, 20: 5851
RHENIUM ISOTOPES Re-185
energy level transitions in, E2/M1 mixing ratios and K conversion coefficients in rotational, (E), 20: 6386
RHENIUM ISOTOPES Re-187
energy level transitions in, E2/M1 mixing ratios and K conversion coefficients in rotational, (E), 20: 6386
energy levels, (E), 20: 6397
neutron reactions (n,γ) with, isomeric cross sections for, (E/T), 20: 6301 (TID-22165)
RHENIUM ISOTOPES Re-188
production of isomeric pairs of, in rhenium-187 (n,γ) reactions, (E/T), 20: 6301 (TID-22165)
RHENIUM SYSTEMS
Re–W–UO_2, compatibility of, 20: 6596(R) (GEST-2049)
RHODIUM
diffusion in tungsten, inter-, 20: 5846
RHODIUM ISOTOPES Rh-100
energy levels of, g-factors of 74.8-kev, (E), 20: 6298(R) (PPAD-2137-566)
RHODIUM ISOTOPES Rh-101
decay schemes, (E), 20: 6298(R) (PPAD-2137-566)
RHODIUM ISOTOPES Rh-103
neutron reactions (n,He-3), (n,n′α), and (n,2p) at 14.7 Mev, cross sections for, (E), 20: 6338
RHODIUM ISOTOPES Rh-105
beta decay, (E), 20: 6406
RHODIUM SYSTEMS
H–Li–Rh, phase studies, 20: 5849
RIBONUCLEIC ACID
peptidyl, effects on ribosome dissociation, 20: 5264
radiation effects on phosphorus-32 uptake by gliomas, x, 20: 5255
RIBONUCLEIC ACID, DESOXY-
radiation effects on phosphorus-32 uptake by gliomas, x, 20: 5255
radiation effects on synthesis in *Micrococcus radiodurans* of, uv, 20: 5266
radiation effects on, in fibrosarcoma cell line in mice, 20: 5362
radiation effects on catabolism in rats of, x, 20: 5382
radioinduced cross-linking and denaturation of double-strand, uv, 20: 5268
RICE
radioinduced mutations of, x, 20: 5393
ROCKET MOTOR NOZZLES
cooling of gas-core nuclear, transpiration, (T), 20: 6663
ROCKET MOTORS
design and performance of, with electric acceleration in throat, (T), 20: 5636
ROCKET REACTORS
development of wheel-flow gaseous-core, 20: 6662 (NASA-TN-D-2951)
fuel injection techniques for gaseous-core, analysis of vortex, 20: 6653 (D-910091-7)
fuel injection techniques for gaseous-core, analysis of vortex, 20: 6652 (D-910091-5)
nozzle cooling in gas-core, transpiration, (T), 20: 6663
ROCKETS
propellants for, preparation of radiation-cured elastomeric, 20: 5588(P)
propulsion systems for super-orbital, chemical and nuclear-thermal, 20: 5635
use of NIKE-CAJUN, for vlf radiation measurements in ionosphere, (E), 20: 6180 (AD-619250)
ROCKS
analysis for thorium and uranium by parallel alpha-scintillation and radioscope measurements, 20: 5513
ground water discharge, movement, and occurrence in tuffaceous, Rainier Mesa, Nevada Test Site, 20: 5643 (TEI-862)
RODS
neutron distribution in absorbing, P_n approximation for, 20: 6267
ROOTS
radiation effects on cells in, of pea seedlings, γ, 20: 5390
uptake of radioisotopes by barley, mechanisms of, 20: 5258
uptake of strontium-89 by barley, from contaminated soils, 20: 5257
RUBIDIUM CHLORIDES
spectra of, deuterium and hydrogen impurity effects on uv, 20: 6545
RUBIDIUM ISOTOPES Rb-86
uptake by barley roots, mechanism for, 20: 5258
uptake of, by rabbit eye lens in culture, 20: 5256
use in plant and soil studies in Rumania, 20: 5235 (NP-15543, pp 83-90)
yields from uranium-235 thermal fission, (E), 20: 6288 (KAPL-3113)
RUBIES
radiation effects on fluorescence of pink, gamma, 20: 6536
RUMANIA
radiation protection in, 20: 5425 (NP-15543, pp 77-82)
radioisotope use in, 20: 5810 (NP-15543)
tracer techniques in medicine in, evaluation of, 20: 5435 (NP-15543, pp 59-75)
RUSSIAN REACTORS
control system of Beloyarsk, 20: 6634
description of IBR fast-burst, (E), 20: 6672 (CONF-650217, pp 25-35)
kinetics of Beloyarsk, 20: 6634
RUTHENIUM
determination in mixtures of actinides and fission products by paper chromatography, 20: 5509
diffusion from irradiated cerium–cobalt–plutonium alloy to sodium at 550°C, 20: 5848
diffusion in tungsten, inter-, 20: 5846
RUTHENIUM ALLOYS
Nb–Ru, phase studies, 20: 5851
Pd–Ru, effects on kinetics of deuterium exchange with hydrogen in methane at 90 to 170°K, 20: 5557
RUTHENIUM ISOTOPES
determination in irradiated uranium-235, 20: 5493(R) (ANL-6925, pp 253-4)
RUTHENIUM ISOTOPES Ru-96
neutron reactions (n,2n), and (n,p) at 14.7 Mev, cross sections for, (E), 20: 6338
RUTHENIUM ISOTOPES Ru-99
neutron reactions (n,p) at 14.7 Mev, cross sections for, (E), 20: 6338
RUTHENIUM ISOTOPES Ru-100
neutron reactions (n,d) at 14.7 Mev, cross sections for, (E), 20: 6338
RUTHENIUM ISOTOPES Ru-101
neutron reactions (n,p) at 14.7 Mev, cross sections for, (E), 20: 6338
RUTHENIUM ISOTOPES Ru-102
neutron reactions (n,d) at 14.7 Mev, cross sections for, (E), 20: 6338
neutron reactions (n,p) at 14.7 Mev, cross sections for, (E), 20: 6338
RUTHENIUM ISOTOPES Ru-104
neutron reactions (n,p) at 14.7 Mev, cross sections for, (E), 20: 6338
neutron reactions (n,α), (n,γ), and (n,2n) at 14.7 Mev, cross sections for, (E), 20: 6338
RUTHENIUM ISOTOPES Ru-106
content in individual rain showers at Bombay, 20: 5661 (AEET-215)

S

SACCHARIN
radiation effects on rat aversion to, humoral factor in, 20: 5303 (USNRDL-TR-925)
SAFETY
program at National Institute of Radiological Sciences, Japan, 20: 5672
radiological, program for Salmon Event, 20: 5667 (TID-1020)
standards for radiation protection of ICRP, 20: 5663 (NP-15451)
SALAMANDERS
radiation effects on development of axial skeleton and spinal cord in, x, 20: 5312
SAMARIUM
alpha reactions (α,xny) at 27 to 52 Mev, gamma spectra from, (E), 20: 6348
oxidation of, kinetics of high-temperature, 20: 5859
SAMARIUM ALLOYS
Au–Sm, oxidation of, kinetics of high-temperature, 20: 5859
SAMARIUM BORIDES
preparation and thermodynamic properties, 20: 5551
thermionic emission of, on iridium and tungsten substrates, (E), 20: 5532(T) (K-Trans-10)
SAMARIUM IONS
spin-lattice relaxation rates in single crystals of anhydrous lanthanum trichloride, (E), 20: 6542
SAMARIUM ISOTOPES
buildup in reactors, (E), 20: 6589
SAMARIUM ISOTOPES Sm-147
energy levels, 20: 6396
SAMARIUM ISOTOPES Sm-150
energy levels of, rotational, (E), 20: 6348
SAMARIUM ISOTOPES Sm-152
energy levels of, rotational, (E), 20: 6348
SAMARIUM OXIDES
hardness and melting point, 20: 5845
phase transformations in, at 50 to 1500°C, 20: 5536
SAMARIUM SYSTEMS
O–Sm–W, phase studies, 20: 5851
SAN ONOFRE POWER REACTOR
instrumentation for, in-core, 20: 6630 (WCAP-3269-46)
SANDS
gamma and neutron attenuation in serpentine, reactor, (E), 20: 6524
moisture content of, in mixtures with sugar, neutron gage for determining, 20: 5819
SAP (SINTERED ALUMINUM PRODUCTS)
compatibility with uranium dioxide to 525°C, 20: 5839(R) (RISO-110)
compatibility with uranium carbide to 600°C, 20: 5839(R) (RISO-110)
creep properties of type 930, effects of hydrogen on, 20: 5838(R) (RISO-110)
creep rupture of M-257, M-583, SAP-895 and SAP-915, at 700 to 900°F, 20: 5851
ductility properties at 25 to 500°C, 20: 5839(R) (RISO-110)
hardness of types 865, 895, and 930, 20: 5838(R) (RISO-110)
inclusions in tubing of, size and type of, 20: 5630 (NAA-SR-Memo-11562)
radiation effects on tensile properties of types 865, 895, and 930, effects of test temperature on fast neutron, 20: 5839(R) (RISO-110)
recrystallization, 20: 5839(R) (RISO-110)
rupture life of rods and tubes of type 930, at 500°C, 20: 5838(R) (RISO-110)
rupture life, effects of oxide content on, 20: 5839(R) (RISO-110)
sorptive properties for hydrogen from Progil ON2 terphenyl at 400 and 450°C of type 895, 20: 5838(R) (RISO-110)
tensile properties at 25 and 400°C, effects of oxide content on, 20: 5838(R) (RISO-110)
texture of extruded, 20: 5839(R) (RISO-110)
SARCOMAS
chemically induced osteogenic, in rats, 20: 5334
chemotherapy of lymphosarcomas, 20: 5485
lympho-, effects of lipopolysaccharides on rat, 20: 5436(R) (UR-668, pp 149-60)
radiation effects on immune reactions to transplanted, in mice, 20: 5413
radioinduced osteogenic, in rats, 20: 5334
radioinduced, in rats, 20: 5296(R) (NP-15585)
radiosensitivity of cells of fibro-, in mice, 20: 5362
radiotherapy of lymphosarcomas, 20: 5485
surgery of lymphosarcomas, 20: 5485
SATELLITES
control of earth, design and performance of ion-engine systems for orbit, (E/T), 20: 5638
electron detection and measurement by Lincoln Experimental, equipment for, 20: 6184 (AD-619977)
power plants for manned, efficiency of thermally integrated electric-power/life-support, (E/T), 20: 5820 (NASA-CR-316)
radiation effects on telemetry circuits in, 20: 5806 (AD-619387)
shielding for manned, (T), 20: 5673
SAVANNAH RIVER COMPONENTS TEST REACTOR
moderator of, control of dissolved gases in, 20: 6673 (DP-988)
SAVANNAH RIVER PLANT
transplutonium element production at, 20: 5822 (DP-1000)
SAXTON POWER REACTOR
control of, chemical shim experiment for, 20: 6629 (WCAP-3269-24)
SCALERS
design and performance of fast and slow, (E), 20: 5680 (ELI-91)
design for electron detection by Lincoln Experimental Satellite, 20: 6184 (AD-619977)
SCANDIUM ALLOYS
Pu–Sc, phase studies, 20: 5843
Pu–Sc, phase studies, 20: 5848
SCANDIUM COMPLEXES
with tropolone, preparation, properties, and structure, 20: 5538
SCANDIUM ISOTOPES Sc-43
nuclear moments and spins of, determination, (E/T), 20: 6299 (PUC-1965-158)
SCANDIUM ISOTOPES Sc-45
neutron reactions (n,γ) with, isomeric cross sections for, (E/T), 20: 6301 (TID-22165)
SCANDIUM ISOTOPES Sc-46
beta decay of, β-γ circular polarization correlation in, (E), 20: 6391
production of isomeric pairs of, in scandium-45 (n,γ) reactions, (E/T), 20: 6301 (TID-22165)
SCANDIUM ISOTOPES Sc-47
energy levels from titanium-48 (p,2p) reactions at 155 Mev, (E), 20: 6330
SCANDIUM SYSTEMS
H–Sc–Y, phase studies, 20: 5909
SCATTERING
amplitude of, solution of singular N/D equations for, 20: 6130
amplitudes for inelastic, effects of S-matrix unitarity on, (T), 20: 6105 (ISS-65/14)
amplitudes for multichannel, approximate solution of N/D equations for, (T), 20: 6063
amplitudes for, Regge-pole representation of, (T), 20: 6062
amplitudes in, singular N/D equations for, 20: 6131
amplitudes of boson-fermion, in model field theory, 20: 6116
amplitudes of elastic, analytic properties of unitarity integral of quantum field theory for, 20: 6114
amplitudes of, crossing symmetric Regge representation for invariant, 20: 6115
differential equations in many-body problems in, solutions for set of coupled second-order, 20: 6120
hypervirial relations for distorted Coulomb, (T), 20: 6146
potential, arbitrary phase shift differences in, (T), 20: 6127
potential, contiguous Dirac phase shifts in, (T), 20: 6126
potential, distance determination for high-energy, (T), 20: 6108 (NP-15600)
potential, N/D method in, 20: 6129
potentials in coordinate space, singular logarithmic, 20: 6121
ranges of high-energy, energy variation of, 20: 6153
S-matrix in quantum field theory, one-particle singularities of, 20: 6122
wave functions for bound-state, in nonlocal solvable potential, 20: 6119
SCHISTOSOMA
radiation effects on growth of cercariae of, in mice, γ, 20: 5313
SCINTILLATION
radioinduced in dioxane, effects of radioprotective compounds on γ, 20: 5422
spectra from point sources in scattering medium, 20: 5760
SCINTILLATION DETECTORS
data analysis from low-resolution measurements of beta and conversion-electron spectra, (T), 20: 5768
design for low beta activity in liquids, 20: 5798(P)
design for reactor transfer function measurement, 20: 6682 (SGAE-R-1/1965)
design for use in radiation protection, 20: 5762
design for well logging, 20: 5658(P)
design of liquid, for slow neutrons, 20: 5746 (ZFK-RN-18)
development for beta counting using plastic sandwich phosphors, 20: 5783
efficiency for beta counting, effects of sample volume on, 20: 5510
glass for, development and evaluation of, 20: 5585
medical use of, review, 20: 5487
performance as cosmic-ray monitors, atmospheric effects on, 20: 6004 (AD-619508)
performance for γ point sources in scattering media, 20: 5760
performance for in-pile gamma and neutron detection, (E), 20: 5728 (IBM-65-825-1487)
performance for secondary-electron detection, 20: 5757
performance for triple-coincidence gamma spectroscopy, (E), 20: 5770
performance in magnetic fields, 20: 5736 (NP-15597)
performance of large plastic, for gamma aerial monitoring, 20: 5761

preparation of vacuum-sealed liquid-phosphor, 20: 5785
pulse amplifiers and modifiers for, design of, 20: 5780
use for detection of gamma radiation from isotopes deposited in glands or organs, by external scanning, 20: 5447
uses for Compton spectroscopy of gamma radiation, 20: 5775
uses for detecting helium-5 energy levels from neutron-helium scattering, (E), 20: 6335

SEA WATER
buoy dynamics in, submerged, (T), 20: 6686(R) (NVO-98-12)
desalination of, development of dual purpose nuclear power plants for, 20: 6650
desalination using reactors, economic aspects of, 20: 6649

SEALS AND GLANDS
development of ceramic-to-metal, for nuclear thermionic generating system, 20: 6023(R) (AD-619379)
development of frozen electrolyte–silicone rubber, 20: 6024(R) (ANL-6925(p.235-47))
fabrication of manipulator gauntlets of, 20: 5612 (ORNL-TM-1326)

SEED
analysis for lead-210, radiochemical, 20: 5505
radiation effects on rice, genetic, 20: 5393
radiation effects on wheat, genetic, x, 20: 5403
radiation effects on barley, effects of dimethyl sulfoxide and nitric oxide on oxygen effect in, 20: 5298(R) (RLO-353-4)
radio- and chemically-induced mutations in presoaked Arabidopsis, x, 20: 5357

SEEDLINGS
radiation effects on growth of bean and pea, γ, 20: 5388
radiation effects on cells in roots of pea, γ, 20: 5390
radiation effects on growth of corn, in contaminated soil, β, 20: 5305

SEISMOLOGY
developments in, for using nuclear explosions in determining internal structure of earth, 20: 5610

SELENIUM ISOTOPES Se-75
incorporation into blood proteins, 20: 5262
metabolism in dogs, 20: 5262

SEMICONDUCTOR DETECTORS
charge production in lithium-drifted germanium and silicon, 20: 5784
design and performance of silicon, for particle impact position finding, 20: 5747(T) (NP-tr-1302)
design of discriminating, 20: 5802(P)
design with capability of distinguishing alphas, electrons, and protons, (E), 20: 5732 (KFK-335)
development using cascade production mechanism for particle counting, 20: 5793
etching surfaces of lithium-drifted, cells for, (E), 20: 5776
fabrication of compensated p-i-n germanium-diode, (E), 20: 5702
fabrication of silicon, with plasma-oxidized surfaces, 20: 5740 (TID-22407)
fabrication, operation, and uses of, review of, 20: 5763
performance for in-pile gamma and neutron detection, (E), 20: 5728 (IBM-65-825-1487)
performance for neutron detection and spectroscopy, (E), 20: 5714 (AD-623722)
performance in fission fragment and neutron dosimetry, 20: 5719 (CEA-R-2846)
performance of surface barrier, at 4.2°K, 20: 5790
performance of, for solid body dosimetry for radiotherapy, 20: 5479
preamplifiers for, design of high-resolution transistorized, (E), 20: 5772
properties of large lithium-drifted germanium, mounting and storage, 20: 5741 (UCRL-14263)
response and sensitivity of silicon p-i-n, in high-dose-rate gamma fields, (E), 20: 5743 (UCRL-14405)
response of surface-barrier p-n, to heavy ionizing particles, (T), 20: 5758
stability of lithium-drifted silicon, 20: 5767

SEMICONDUCTORS
etching of, design of cells for, (E), 20: 5776
molecular structure, 20: 6551
oxidation of silicon surfaces in oxygen plasma, (E), 20: 5740 (TID-22407)
performance of silicon surface-barrier for α dosimetry, 20: 5721 (CLOR/IBJ-II-37/D)
piezoelectric properties of, apparatus for measuring, (E), 20: 5883 (IS-1263)

SEPARATION PROCESSES
development for fast reactor breeding and fuel elements, 20: 6600(R) (ANL-7105, pp 1-35)

SEWAGE
flow through treatment plants of, tracer study, 20: 5432
radiation control of *Entamoeba histolytica* in, 20: 5366
radioactivity of, due to fallout, 20: 5432

SEWAGE SYSTEMS
flow through treatment plant, tracer study, 20: 5432

SEX
radiation effects on, of viviparous lizards exposed while embryos, x, 20: 5324
radiosensitivity effects on leukemogenesis in mice, 20: 5367

SHEEP
radiation dosimetry of cesium-137 in, use of thermoluminescent detector for, 20: 5285 (BNWL-SA-172)

SHELTERS
design of foldable, tent-like, 20: 5632(P)
role in radiological defense of, 20: 5416

SHIELDING
design criteria for 800-Mev proton linear accelerators, 20: 5940 (LA-DC-7522)
design for manned space vehicles, (T), 20: 5673
design optimization for laminated, computer program for, 20: 6518 (NAA-SR-Memo-11516)
radiation attenuation by vertical, (E/T), 20: 6516 (AD-617524)
requirements for, at 200-Bev proton synchrotron, (T), 20: 5945 (UCRL-16464)
research, (T), 20: 6521(R) (ORNL-3858(Vol.2), pp 73-81)
research, (E), 20: 6297(R) (ORNL-3858(Vol.2), pp 82-90)
research on gamma and neutron, (E), 20: 6520(R) (ORNL-3858(Vol.1), pp 42-6)

SHIELDING MATERIALS
cascade showers in, (T), 20: 6521(R) (ORNL-3858(Vol.2), pp 73-81)
gamma attenuation in lead alloy, (E), 20: 6523
radiolysis of water, around high-power gamma facility, 20: 5670

SHIPPINGPORT PRESSURIZED WATER REACTOR
containment leak rate testing, 20: 6628 (WAPD-PWR-TE-201)
core thermocouple calibration, 20: 6627 (WAPD-PWR-TE-141)
reactivity lifetime thermal performance, 20: 6627 (WAPD-PWR-TE-141)

SHOCK TUBES
gas flow in electric, modes of, (E), 20: 6173
plasma production in inductive hydrodynamic, argon, 20: 6478

SHOCK WAVES
electron density and velocity behind, laser beam diagnostics of, 20: 6490
production and structure in nearly collisionless plasma, (E), 20: 6501
production of, electromagnetic, 20: 6158(R) (AD-619999)
propagation in argon plasma, 20: 6478
propagation in nonuniform magnetic fields, 20: 6158(R) (AD-619999)
reflection in argon and helium thermal plasmas, (T), 20: 6512
transonic flow around bodies, analysis of, (T), 20: 6160 (NP-15604)

SILICON
effects on deformation properties of beryllium single crystals, 20: 5844
effects on hot hardness and microstructure of aluminum–iron–uranium alloy, 20: 5848
effects on oxidation resistance of beryllium–niobium and beryllium–zirconium alloys, 20: 5844
effects on rolling properties of uranium, 20: 5866
oxidation in oxygen plasma, (E), 20: 5740 (TID-22407)
performance of detectors of, for alpha dosimetry, 20: 5721 (CLOR/IBJ-II-37/D)
performance of lithium-drifted, as surface-barrier detectors, 20: 5767
radiation effects on thermal conductivity of single crystals of, electron, (E), 20: 5919
radioinduced defects in, annealing of electron, 20: 5920

SILICON CARBIDES
combustion with fluorine, data on, 20: 5523(R) (ANL-6925, pp 175-85)
properties for skull reclamation process crucibles, 20: 5594(R) (ANL-6925, pp 21-106)
SiC–UC, fabrication of fuel elements of, process for, 20: 5873(P)

SILICON ISOTOPES Si-27
energy levels from aluminum-27 (p,n) reactions at 30 and 50 Mev, (E), 20: 6361

SILICON ISOTOPES Si-28
deuteron reactions (d,α) at 11.45 to 12.10 Mev, (E), 20: 6369
energy levels of, parity and spin of, (E), 20: 5928(R) (PR-P-66)
proton inelastic scattering at 155 Mev, cross sections and energy levels from, (E), 20: 6354
proton scattering at 30.3 Mev, differential cross sections for, (E), 20: 6339

SILICON ISOTOPES Si-29
electron anisotropic hyperfine interactions with, shallow donor, 20: 6001

SILICON ISOTOPES Si-31
beta decay of, shell model calculations of ft values in, (T), 20: 6393

SILICON ISOTOPES Si-32
beta decay of, shell model calculations of ft values in, (T), 20: 6393

SILICON JUNCTIONS
cascade production in p-n, particle counting by, 20: 5793

SILICON OXIDES
energy levels of, 20: 6532 (CALT-221-13)
radioinduced color centers in colloidal, hydrogen sorption by, 20: 5584
reactions with zirconium oxides, Gibb's free energy of, 20: 5537

SILICON SYSTEMS
Fe–Si–U, crystal structure of U_2Fe_3Si, 20: 5848
SILVER
deposition on pyrolytic graphite for use as analytical standard, electro-, 20: 5503
diffusion in pyrolytic graphite, 20: 5846
effects on hydrochloric acid cleavage of organotin compounds in methanol–water, 20: 6687(R) (NYO-3453-1)
electromagnetic wave reactions with foils of, plasma radiation from, (E), 20: 6548
electron reactions at 2.5 to 4.0 Mev, bremsstrahlung spectra from, (E), 20: 6432
neutron absorption integrals for, infinite-dilution, (E), 20: 6558(R) (ANL-7115, pp 42-67)
proton reactions at 3 Bev, fission and fragmentation products from, (E), 20: 5756
proton reactions (p,n) at 30 and 50 Mev, isobaric-state excitation in, (E/T), 20: 6361
proton reactions at 2 Bev, lithium-8 production in, (E), 20: 6409
SILVER ALLOYS
Cd–In–Ag, corrosion by borated water at 600°F, 20: 5846
Cd–In–Ag, properties as control rod material, effects of palladium, platinum, and tin additions on, 20: 5850
SILVER GLASS
cleaning technique for dosimeters of, 20: 5742(R) (UCRL-14351)
SILVER IODIDES
iodine-131 exchange with methyl iodide, effects of surface structure on, 20: 5544
SILVER ISOTOPES Ag-110
gamma emission from metastable, 20: 6436
SILVER ISOTOPES Ag-111
energy levels, 20: 6402
SILVER OXALATES
photolysis of, effects of cadmium and lead ions on, 20: 5583
radiolysis of, effects of cadmium and lead ions on, 20: 5583
SILVER PHOSPHATES
$Ag–AgPO_3$, development and testing as standard electrode for emf studies in alkali metaphosphates, 20: 5529(R) (SC-DC-65-1706)
SILVER SYSTEMS
$Ag–AgPO_3$, development and testing as standard electrode for emf studies in alkali metaphosphates, 20: 5529(R) (SC-DC-65-1706)
SKELETON
metabolism of, methods of investigating overall, 20: 5237(R) (UR-668, pp 55-109)
radiation dose to human, time variation of strontium-90, 20: 5429
radiation effects on development of, in mouse embryos, x, 20: 5395
radiation effects on development of axial, in salamanders, x, 20: 5312
radiation effects on development of, in mouse embryos, x, 20: 5316
radiation effects on development of, in mouse embryos, x, 20: 5326
radiation effects on development of, in mouse embryos, x, 20: 5327
radiation effects on development of, in mouse embryos, x, 20: 5337
SKIN
infections in rabbit, effects of leukopenia on, 20: 5315
radiation effects on ratio of soluble to insoluble collagen in hamster, x, 20: 5330
radiotherapy of diseases in human, gonadal dose from x, 20: 5445
radiotherapy of human, effects on offspring of chromosomal aberrations following, 20: 5351
SKIN GRAFTING
radiation effects on immune reactions to, in thymectomized mice, 20: 5408 (USNRDL-TR-920)
radiation effects on graft take in rats, x, 20: 5335
SODIUM
analysis for carbon and oxygen, methods for, 20: 5594(R) (ANL-6925, pp 21-106)
boiling heat transfer in, 20: 5627
corrosive effects on binary vanadium alloys, 20: 6601(R) (ANL-7115, pp 1-41)
corrosive effects on vanadium–20 titanium alloy at 650°C, 20: 5846
corrosive effects on stainless steel, effects of corrosion loop location on, 20: 5846
corrosive effects on chromium–titanium–vanadium alloy, effects of chromium content on, 20: 5851
diffusion of fission products into, from irradiated cerium–cobalt–plutonium alloys, 20: 5848
effects on design stress for Croloy 2¼ and type 316 stainless steel, 20: 5851
effects on mechanical properties of Croloy 2¼ at 1100°F, 20: 5846
erosive effects on metals, 20: 5861
flow in reactor cooling systems, sonic velocities in two-phase, 20: 6559(R) (ANL-7115, pp 77-83)
purification of, development of methods for, 20: 5594(R) (ANL-6925, pp 21-106)
radiation effects on content in dog blood, β and γ, 20: 5381
reactions with fast reactor materials, research plans for, 20: 6552(R) (ANL-6925, pp 187-233)
reactions with inert cover gas impurities, 20: 5594(R) (ANL-6925, pp 21-106)
reactions with iodine released from uranium and uranium carbide, 20: 5878 (BNL-9667)
solubility in fused halide salts, 20: 6024(R) (ANL-6925(p.235-47))
solvent properties for carbon, 20: 5594(R) (ANL-6925, pp 21-106)
solvent properties for niobium–1 zirconium at 800 to 1380°C, 20: 5846
thermal conductivity of, dependence of, on oxide concentration, 20: 5901
wetting properties for ceramic fuels, 20: 5594(R) (ANL-6925, pp 21-106)
SODIUM ALLOYS
Bi–Na, solubility of intermetallic compound in, in fused halide salts, 20: 6024(R) (ANL-6925(p.235-47))
K–Na, corrosive effects on Croloy 9M, INOR-8, and types 316 and 347 stainless steel, 20: 5851
K–Na, thermodynamic properties of liquid, 20: 5594(R) (ANL-6925, pp 21-106)
K–Na, viscosity of, at –10 to 148.9°C, 20: 5908
SODIUM CARBONATES
$Na_2CO_3–UO_2(NO_3)_2$, criticality of aqueous solutions of, 20: 5666 (TID-21995)
SODIUM CHLORIDES
corrosive effects on type 304 stainless steel at 90°C, 20: 5846
corrosive effects on type 304 stainless steel, factors controlling, 20: 5851
radioinduced hardening in, temperature dependence of flow stress in y, 20: 6538
KCl–NaCl, corrosive effects on zirconium, 20: 5855(T) (JPRS-32341, pp 24-31)
KCl–NaCl, effects of molten, on reaction of uranium dioxide with chlorine, 20: 5547
$LiCl–MgCl_2–NaCl$, melting points of, effects of composition on, 20: 5594(R) (ANL-6925, pp 21-106)
LiCl–NaCl, effects of molten, on reaction of uranium dioxide with chlorine, 20: 5547
$MgCl_2–KCl–NaCl$, solvent properties for lanthanum, plutonium, and praseodymium, 20: 5594(R) (ANL-6925, pp 21-106)
$MgCl_2–KCl–NaCl$, solvent properties for uranium, 20: 5594(R) (ANL-6925, pp 21-106)
NaCl–NaF–NaI, solvent properties for bismuth–sodium alloys and sodium, 20: 6024(R) (ANL-6925(p.235-47))
SODIUM CYANIDES
effects on radioinduced permeability of erythrocytes, 20: 5342
SODIUM DODECYL SULFATES
solvent properties for cerium, cobalt, and promethium sorbed on charcoal powders, 20: 5675
use for washing radioactively contaminated surfaces, 20: 5675
SODIUM FLUORIDES
NaCl–NaF–NaI, solvent properties for bismuth–sodium alloys and sodium, 20: 6024(R) (ANL-6925(p.235-47))
SODIUM GRAPHITE REACTORS
calandria vessel peripheral hanger tests, 20: 6618 (NAA-SR-Memo-11415)
calandria vessel stayed head study, 20: 6616 (NAA-SR-Memo-11324)
criticality studies in uranium monocarbide lattices of, (E), 20: 6586 (NAA-SR-Memo-11313)
reactivity temperature transients in 200-Mw(e) operation and accidents, analysis of, 20: 6620 (NAA-SR-Memo-11458)
tubes of, moderator dimensional stability effects on, 20: 6619 (NAA-SR-Memo-11416)
SODIUM HYDROXIDES
effects on fission tracks in glasses, 20: 5713 (AD-623384)
separation of francium from, by solvent extraction using 4-*sec*-butyl-2-α-methylbenzylphenol, 20: 5601
SODIUM IODIDES
analysis of iodine-125- or iodine-131-labeled, for impurities by paper chromatography, 20: 5515
radioinduced photoluminescence spectra of thallium-activated, x, (E), 20: 6537
NaCl–NaF–NaI, solvent properties for bismuth–sodium alloys and sodium, 20: 6024(R) (ANL-6925(p.235-47))
SODIUM IONS
content in growing yeast cells, 20: 5251(R) (UR-668, pp 123-49)
SODIUM ISOTOPES Na-21
nuclear structure of, rotation-vibration model for, 20: 6441
SODIUM ISOTOPES Na-22
uptake of, by rabbit eye lens in culture, 20: 5256
SODIUM ISOTOPES Na-23
nuclear structure of, rotation-vibration model for, 20: 6441
proton inelastic scattering at 155 Mev, cross sections and energy levels from, (E), 20: 6354

proton reactions (p,γ) at 300 to 750 kev, gamma branching in, (E/T), 20: 6295 (NP-15647)
SODIUM ISOTOPES Na-24
content in PNPF coolant, monitoring standardization for determining, 20: 6615 (NAA-SR-10888(Rev.))
radiation effects from injected, on metabolism of electrolytes and nitrogen in dogs, 20: 5381
SODIUM NITRATES
beta reactions with, Cherenkov radiation detection in, 20: 5792
$Al(NO_3)_3$–HNO_3–$NaNO_3$, separation of americium-243 and curium-244 from, using TBP, 20: 5495 (DP-972)
SODIUM OXIDES
effects on thermal conductivity of sodium, 20: 5901
SODIUM PHOSPHATES
reactions with rare earths and transition metals, 20: 5529(R) (SC-DC-65-1706)
KPO_3–$NaPO_3$, reference electrode for emf studies in, 20: 5529(R) (SC-DC-65-1706)
SODIUM REACTOR EXPERIMENT
moderator elements for, reliability testing of, 20: 6621 (NAA-SR-Memo-11556)
safety analysis for, with fast-flux test section in center of core, (T), 20: 6676 (NAA-SR-11234)
SOILS
diffusion of radon from, effects of meteorological conditions on, 20: 5646
neutron reflection by surfaces of, absorbed dose in air from, (T), 20: 6528
radioactivity due to radium and uranium in, effects on spermatogenesis in field mice living on, 20: 5387
radioactivity in, effects on growth of corn seedlings in, β, 20: 5305
radioactivity of, natural, bibliography on, 20: 5668 (WASH-1061)
SOLAR BATTERIES
performance for electric-power and life-support systems on spacecraft, (E/T), 20: 5820 (NASA-CR-316)
uses of radioinduced deterioration of, for neutron dosimetry, 20: 6679 (NP-15645)
SOLAR FLARES
alpha and proton energy spectra from, 20: 5969
hazards of, evaluation of, (T), 20: 5966 (AD-618905)
occurrence of, methods for predicting, 20: 5967(R) (AD-619740)
prediction of, 20: 5966 (AD-618905)
protons from, diffusion in interplanetary space of, 20: 5970
SOLAR RADIATION
absorption of L_α, in earth's upper atmosphere, (E) 20: 6211
diffusion of flare, in interplanetary space, 20: 5970
effects on ionization variations in E_1, F_1, and F_2 layers, 20: 6187
emission of 40-kev electron, (E), 20: 5971
energy spectra of alpha and proton, from flares, 20: 5969
reactions with meteorites, gas production from, 20: 5976
SOLIDS
cascade production in, particle counting by, 20: 5793
chemistry and physics of, bibliography on high-temperature, 20: 5527 (NP-15646)
decontamination from radioactive dusts by washing, use of sodium dodecyl sulfate or water, 20: 5675
equation of state of, properties of, 20: 6533 (NVO-1163-60)
interections in, morphology of, 20: 5895(R) (TID-22271)
luminescence, 20: 6551
molecular structure, 20: 6551
radioinduced damage in, step annealing of, 20: 5580
SOLVENT EXTRACTION PROCESSES
design for uranium and/or vanadium in aqueous solutions, 20: 5605(P)
performance for separating americium isotopes, curium-242, and plutonium-242, (E), 20: 5823(T) (ORNL-tr-892)
SOUND
production in boiling, correlation of heat transfer with, 20: 5628
SOUTH DAKOTA
fallout monitoring, 1963, 20: 5649(R) (COO-1340-2, pp 54-83)
SPACE
cosmic proton reactions with matter in interstellar, secondary proton spectra from, (T), 20: 5973
cosmic ray absorption in ionized gases in interstellar, r-f, (T), 20: 6020
SPACE FLIGHT
power plants for electric-power and life-support systems in manned space stations, (E/T), 20: 5820 (NASA-CR-316)
propulsion in, using electric thrusters and steam power plants, 20: 5639
radiation effects on white blood cells of man during, 20: 5297 (ORNL-P-1734)
SPACE VEHICLES
design of nuclear thermoelectric powered, computer program for, 20: 6660 (NAA-SR-Memo-11514)
power plants for manned, efficiency of thermally integrated electric-power/life-support, (E/T), 20: 5820 (NASA-CR-316)
propulsion of, performance of electron-bombardment thrustor systems for, 20: 5637
propulsion systems for, design and performance of radioisotope, 20: 5634
shielding for manned, (T), 20: 5673
SPARK CHAMBERS
design for cosmic particle interactions above 100 Bev, 20: 5724 (CONF-640919, pp II13-23)
design of cosmic-ray, for interactions at 300 Bev, 20: 5725 (CONF-640919, pp II27-30)
development and performance of streamer, 20: 5739 (SLAC-PUB-140)
performance for analysis and location of neutrino interactions in emulsions, 20: 6052
performance of arrays of, for measuring particle momenta, (E), 20: 5730 (JINR-E-2366)
performance of circular, with electric localization, 20: 5735 (LYCEN-6523)
use in gamma radiodiagnosis, 20: 5461
uses of sonic, for analyzing proton scattering below 20 mrad, 20: 5720 (CERN-65-33)
SPECTROMETERS
data analysis from, using multichannel analyzer with routing system, (E), 20: 5769
design of, beam transport optics for, (T), 20: 5944 (SLAC-PUB-132)
focusing of magnetic, using position finding detector, 20: 5745(T) (NP-tr-1302)
SPECTROSCOPY
data acquisition systems for nuclear, computer uses for, 20: 6307 (UCRL-16439)
SPERM
radioinduced mutations in Drosophila, x, 20: 5301(R) (UR-668, pp 1-54)
SPERMATOGENESIS
radiation effects on, in field mice living on radioactive soils, 20: 5387
radiation effects on dog, x, 20: 5301(R) (UR-668, pp 1-54)
SPHERES
fluid flow around oscillating, MHD of, (T), 20: 6161 (NP-15630)
SPINAL CORD
radiation effects on development in salamanders of, x, 20: 5312
SPLEEN
colony formation and weight used as methods for assaying immunity to marrow transplants in mice, 20: 5372
effects of Thorotrast on, pathological, 20: 5355
immune reactions in cultures of heterologous radiation chimeras, 20: 5397
radiation effects on oxidative phosphorylation in nuclei from rat, 20: 5341
SPUTTERING
equipment for studying, design and testing of, 20: 5981(R) (AD-620002)
STAINING
methods for biological electron microscopy, 20: 5250(R) (UR-668, pp 110-16)
STAINLESS STEEL
coating with rare earths, electrolytic, 20: 5867
compatibility of type 304, with plutonium-uranium carbides, 20: 6600(R) (ANL-7105, pp 1-35)
corrosion by bismuth at 850°C, 20: 6024(R) (ANL-6925(p.235-47))
corrosion by boiling nitrates in radioactive waste, 20: 5856
corrosion by borated water at 600°F, 20: 5846
corrosion by cadmium–magnesium–uranium–zinc alloys with chloride flux at 600 to 650°C, 20: 5594(R) (ANL-6925, pp 21-106)
corrosion by potassium–sodium at 1425°F of types 316 and 347, effects of oxygen on, 20: 5851
corrosion by sodium, effects of corrosion loop location on, 20: 5846
corrosion by steam at 400°C and water at 300°C, effects of surface treatments on, 20: 5846
corrosion by steam at 2000°F of type 304, 20: 5851
corrosion by uranyl nitrates and uranyl phosphates, 20: 5846
corrosion cracking by sodium chloride of type 304, factors controlling stress-, 20: 5851
corrosion of type 304, by sodium chloride at 90°C, effects of pH on stress-, 20: 5846
creep properties at 500 to 600°C of type 304, in-reactor, 20: 5851
deposition on thick 1.2 MD07 A and Soudotenax 56 steel plates by welding, 20: 5862(R) (EURAEC-1481)
design stress for type 316, in sodium environment, 20: 5851
diffusion into copper at 900°C of type V2A, 20: 5850
erosion of 316, by liquid sodium, 20: 5861
fatigue detection before crack initiation using ultrasonic techniques, 20: 5867
mechanical properties at high temperatures under stress, thermodynamic method for evaluating, 20: 5913(R) (EURAEC-1488)
oxidation of type-405, by air at 600°C, 20: 5594(R) (ANL-6925, pp 21-106)
performance of low-manganese, for ionization chamber construction,

20: 5716 (AEEW-M-470)
properties for containers of liquefied plutonium alloys with molten salts, 20: 5594(R) (ANL-6925, pp 21-106)
radiation effects on in-pile corrosion of, by aqueous solutions, 20: 5852(R) (EURAEC-1522)
radiation effects on mechanical properties of, thermodynamic method for evaluating, 20: 5913(R) (EURAEC-1488)
radiation effects on corrosion of types 304 and 347, by Santowax OM at 500 to 700°F, fast-neutron, 20: 5846
radiation effects on mechanical properties of type 347, irradiated at 80 to 1500°F, fast-neutron, 20: 5846
radiation effects on ductility of types 304 and 348, effects of irradiation temperature on, 20: 5851
reactions with hydrofluoric acid–oxygen mixtures, 20: 5595(R) (ANL-6925, pp 107-64)
reactions with hydrochloric acid in air-fluidized beds, 20: 5595(R) (ANL-6925, pp 107-64)
reactivity worth calculation of, 20: 6279(R) (AI-65-225)
reactor tubes of, graphite dimensional stability effects on, 20: 6619 (NAA-SR-Memo-11416)
thermal expansion of fuel materials of, during fast burst accident, 20: 6602 (BNWL-SA-346)
use for fission product deposition studies, recommendations for, 20: 5665 (ORNL-TM-1304)
welding parameters for type 304, electron-beam, 20: 5867
stainless steel–UO_2, fabrication by roll bonding of, clad with stainless steel, 20: 5866
stainless steel–UO_2, preparation of fuel plates of, 20: 5843
stainless steel–UO_2, preparation of disperaions of, 20: 5848
stainless steel–UO_2, thermal cycling between 50 and 800°C, 20: 5848

STANDARD ELECTRODES
development and performance for electrochemical studies on metals in molten alkali metaphosphates, 20: 5529(R) (SC-DC-65-1706)

STANFORD LINEAR ACCELERATOR
development, 20: 5943(R) (SLAC-48)

STARS
fluid rotation in, variational principle for hydrostatic equilibrium of relativistic, (T), 20: 5974

STATISTICS
Liouville theorem of statistical mechanics, general forms of, 20: 5830 (CERN-65-38)
use in analysis of data on leukemia incidence in populations, 20: 5471
use in studies of etiology of malignant neoplasms in human populations, 20: 5307

STEAM
corrosive effects on low-alloy and stainless steels, effects of surface treatments on, 20: 5846
corrosive effects on Incoloy 800 at 705°C, 20: 5846
corrosive effects on Zircaloy-2 powders at 750°F, effects of nitrogen and oxygen additions on, 20: 5851
corrosive effects on type 304 stainless steel and Zircaloy-2 at 2000°F, 20: 5851
corrosive effects on Zircaloy-2, effects of heat treatments on, 20: 5846
nitrogen-16 distribution between water and, in boiling reactors, 20: 6638
reactions with cladding materials and urania at high temperatures, 20: 6552(R) (ANL-6925, pp 187-233)
reactions with iodine released from uranium and uranium carbide, 20: 5878 (BNL-9667)
reactions with refractory metals at high temperatures, 20: 6552(R) (ANL-6925, pp 187-233)
reactions with uranium dioxides, effects on oxygen/uranium ratio of, 20: 6559(R) (ANL-7115, pp 77-83)
reactions with uranium at 600 to 1600°C, 20: 5843
steam–H_2O, momentum flux measurement by impulse method for flow of, 20: 5624 (MIT-3496-1)
steam–water, corrosive effects on Zircaloy-2, 20: 6566(R) (EURAEC-1382)
steam–water, heat transfer and pressure drop data for flow in round vertical tubes, 20: 5623 (EURAEC-1325)
steam–water, heat transfer and hydrodynamics in mixtures of, 20: 6566(R) (EURAEC-1382)

STEAM POWER PLANTS
performance with electric thrusters for space propulsion, 20: 5639

STEARIC ACID
radioinduced emanation from, holdup time of, (E), 20: 6298(R) (PPAD-2137-566)

STEEL
corrosion by steam at 400°C and water at 300°C, effects of surface treatments on, 20: 5846
deposition of stainless steel cladding on 1.2 MD07 A and Soudotenax 56, by welding, 20: 5862(R) (EURAEC-1481)
embrittlement of hydrogenated, solute-induced, 20: 5846
embrittlement of pressure vessels of, by plastic fatigue, 20: 5881(R) (EURAEC-1441)
failure by low-cycle plastic fatigue of pressure vessel, nondestructive testing techniques for, 20: 5894 (SWRI-1228-3-3)
fatigue detection before crack initiation using ultrasonic techniques, 20: 5867
properties of type 1020, for containers of liquefied plutonium alloys with molten salts, 20: 5594(R) (ANL-6925, pp 21-106)
radiation effects on mechanical properties of low-alloy, fast-neutron, 20: 5921
welding high-strength low-alloy, development of filler materials and procedures for, 20: 5867

STEROIDS
effects of, on growth of tumor cells in culture, 20: 5296(R) (NP-15585)
radiation chemistry of estrone in acetic acid, x, 20: 5274

STIRRING APPARATUS
development for skull reclamation process, 20: 5594(R) (ANL-6925, pp 21-106)

STOMACH
iodine-131 uptake by fetal, effects of age on, 20: 5259
radiation effects on gastric juice secretion in dog, x, 20: 5384

STRAIN GAGES
design for fuel pin warpage measurements, 20: 5703

STRANGE PARTICLES
decay of, nonleptonic, (T), 20: 6035 (CERN-64-13(Vol.4), pp 1-49)
decay of, selection rules in nonleptonic, (T), 20: 6085
interactions of, weak, (T), 20: 6035 (CERN-64-13(Vol.4), pp 1-49)

STRATOSPHERE
fallout transport from, 20: 5649(R) (COO-1340-2, pp 54-83)
fallout transport from, effects of cyclonic activity in, 20: 5650(R) (COO-1340-2, pp 84-109)

STREPTOMYCIN
effects on permutational damage induced in Paramecium by triethylene melamine, 20: 5417
radiosensitivity effects on permutational damage in Paramecium, x, 20: 5417

STRONTIUM
diffusion from irradiated cerium–cobalt–plutonium alloy to sodium at 550°C, 20: 5848
use in x-ray filters, 20: 5692

STRONTIUM ISOTOPES Sr-85
detection and measurement in man of, whole-body, 20: 5426

STRONTIUM ISOTOPES Sr-89
content in rain at Tokyo four weeks after Chinese nuclear explosion of May 14, 1965, 20: 5656
global circulation following Chinese nuclear explosion of May 14, 1965, 20: 5656
uptake by barley of, from contaminated soils, 20: 5257
uptake by bones, effects of sodium alginate on, 20: 5253

STRONTIUM ISOTOPES Sr-90
beta and conversion-electron spectra, 20: 5768
bone tumors induced in mice by injected, effects of infection on incidence of, 20: 5373
content in bone, in Denmark, 20: 5651 (RISO-107)
content in bones of children in Great Britain, 20: 5415
content in deciduous teeth, 1962, 20: 5655
content in food, in Denmark, 20: 5651 (RISO-107)
content in man of, time variation of radiation dose from, 20: 5429
content in milk and rain water in New Zealand, 1965, 20: 5664(R) (NP-15639)
content in milk of Mandan-Minot region of North Dakota, 20: 5678
content in rain at Tokyo four weeks after Chinese nuclear explosion of May 14, 1965, 20: 5656
determination of, efficiency of beta scintillation sandwich counting method for, 20: 5783
effects of deposited, on mechanical strength of bones, 20: 5289(R) (COO-119-232, pp 88-98)
effects of deposited, on hematopoietic system in dogs, 20: 5290(R) (COO-119-232, pp 165-89)
effects of injected, long-term pathological on dogs, 20: 5287(R) (COO-119-232, pp 5-64)
excretion of deposited, effects of EDTA in dogs, 20: 5248(R) (COO-119-232, pp 200-2)
global circulation following Chinese nuclear explosion of May 14, 1965, 20: 5656
retention by fetal and newborn rats, 20: 5237(R) (UR-668, pp 55-109)
retention in rats, effects of age and dose on, 20: 5237(R) (UR-668, pp 55-109)
sorption by calcium-activated barium sulfate, process limiting, 20: 5531 (UJV-1382/65)
toxicity in rat embryos, 20: 5237(R) (UR-668, pp 55-109)
uptake by human bones, effects of calcium uptake on, 20: 5263
uptake in relationship to calcium uptake by Austrian population, 1962, 20: 5263

use as beta source for therapy of hemangiomas in children, 20: 5443
STRONTIUM SULFIDES
preparation for luminescence dosimeters, 20: 5742(R) (UCRL-14351)
STRUCTURES
radiation attenuation by vertical, (E/T), 20: 6516 (AD-617524)
testing hollow underwater, radiographic method for, 20: 5631(P)
STYRENE POLYMERS
aerosols of, particle size distribution in, 20: 5237(R) (UR-668, pp 55-109)
SUBMARINE POWER PLANTS
mounting of, external vs internal, 20: 6664
SUCCINIC ACID, SODIUM SALTS
reaction with thorium chloride, conductometric and potentiometric study of, 20: 5555
SUGARS
moisture content of, in mixtures with sand, neutron gage for determining, 20: 5819
radiation effects on content in pea leaves of, γ, 20: 5280
SULFUR COMPOUNDS
radioprotective effects of, reaction mechanisms, 20: 5296(R) (NP-15585)
SULFUR IONS
detection in nuclear emulsions and solids, 20: 5755
SULFUR ISOTOPES S-32
deuteron reactions (d,α) at 11.8 and 12.0 Mev, (E), 20: 6369
proton inelastic scattering at 155 Mev, cross sections and energy levels from, (E), 20: 6354
SULFUR ISOTOPES S-33
proton reactions (p,γ) at 300 to 1300 kev, gamma branching in, (E/T), 20: 6295 (NP-15647)
SULFUR ISOTOPES S-35
beta decay of, shell model calculations of ft values in, (T), 20: 6393
determination by beta scintillation counting, effects of sample volume on efficiency of, 20: 5510
incorporation in *tris*(1-aziridinyl)phosphine sulfide by recoil reactions, 20: 5586
metabolism in rat bones of, effects of nerve supply on, 20: 5370
radiation effects on metabolism of, in rat bones, x, 20: 5370
SULFURIC ACID
solubility in mixtures of alkyl esters of phosphoric acid and trioctylamine, 20: 5600
SUN
activity data for July 1965, 20: 6206
SUPERCONDUCTIVITY
theory of high-current gapless, 20: 6241
SUPERCONDUCTORS
critical currents in films of, applied magnetic field and temperature dependence of, (E), 20: 6232
critical field and vortex line structure in alloy, lower, (T), 20: 6251
critical fields in niobium-titanium alloy, Pauli paramagnetism effects on upper, (E), 20: 6236
currents in surface sheath of, persistent, (T), 20: 6243
electron tunneling in, macroscopic quantum interference in Josephson, (E), 20: 6235
electron tunneling in, entropy transport from, (T), 20: 6248
energy gap in lead, (T), 20: 6238
magnetic coupling between adjacent type-II, (E), 20: 6244
magnetic fluxoid transitions and loss in multiply connected niobium, (E/T), 20: 6246
magnetic properties of gadolinium-lanthanum, antiferro-, (E), 20: 6247
magnetic properties of thin-film, in nonlocal regime, (T), 20: 6250
pair-breaking mechanisms in, equivalence of, (T), 20: 6233
quantum effects in thin film, (T), 20: 6242
surface sheath of, (T), 20: 6240
theory of, containing spherically symmetric nonmagnetic impurities, 20: 6239
transition temperature of uranium, pressure dependence of, (E), 20: 6234
use of niobium–zirconium, as magnet coils, 20: 5614
SUPERFLUIDITY
theory of Fermi liquid, 20: 6229
theory of Fermi liquid, (T), 20: 6237
SURFACE WATERS
analysis for lead-210, radiochemical, 20: 5505
radioactivity of, natural, bibliography on, 20: 5668 (WASH-1061)
tritium distributions in Main and Rhine Rivers in Germany, 20: 5654
SURFACES
decontamination of, by washing using sodium dodecyl sulfate or water, 20: 5675
standard, for fission product deposition studies, 20: 5665 (ORNL-TM-1304)
SURGERY
effects of preirradiation on ovarian cancer, recovery rate of, 20: 5446
effects of preirradiation on pharyngo-larnyngectomy, 20: 5463
of cancers, presurgical irradiation, 20: 5477
use for lymphosarcoma extirpation, 20: 5485
SWEDISH REACTORS (R-3)
design and performance, 20: 6599 (AEE-5)
SWIMMING POOL REACTORS
description and performance of Shield Test and Irradiation Reactor, (E), 20: 6677 (NAA-SR-11528)
fuel burnup calculations for ASTRA, 20: 6681 (SGAE-PH-18/1965)
operation of RPI, 20: 6675 (LFEN-26)
radioprotection devices used near, review of, 20: 6670 (CEA-R-2864)
reactivity transfer function of ASTRA, scintillator for measuring, 20: 6682 (SGAE-R-1/1965)
SWITCHES
properties of high-density plasma, 20. 6449 (AD-619370)
thresholds for tunnel-diode, operational definition of, (E), 20: 5700
trigger mechanism for snap-action, 20: 6693(P)
SYNCHROTRONS
beam momentum measurements in ITEP, proton, 20: 5941 (NP-15598)
magnet pole face windings in Todai AG, 20: 5952
radiation problems in 200-Bev proton, (T), 20: 5945 (UCRL-16464)
SYSTEMS FOR NUCLEAR AUXILIARY POWER
design of nuclear thermoelectric, computer program for, 20: 6660 (NAA-SR-Memo-11514)
SYSTEMS FOR NUCLEAR AUXILIARY POWER (SNAP-2)
operation and testing of, 20: 6655 (NAA-SR-7088)
safety analysis of SNAPTRAN 2/10A-1 and -2 tests, 20: 6654 (IDO-17076)
SYSTEMS FOR NUCLEAR AUXILIARY POWER (SNAP-10)
flight data reduction and analysis of 10A, computer program for, 20: 6661 (NAA-SR-Memo-11603)
flight system 10FS-3 of, post-assembly electrical testing of, 20: 6658 (NAA-SR-Memo-11436)
fuel for 10A, irradiation testing of, (E), 20: 6678 (NAA-SR-Memo-11374)
radiation detection systems for 10A, calibration of, 20: 6656 (NAA-SR-Memo-11333)
reactivity worths of fission products in 10A, computer analysis of, 20: 6659 (NAA-SR-Memo-11473)
safety analysis of SNAPTRAN 2/10A-1 and -2 tests, 20: 6654 (IDO-17076)
thermoelectric converter performance for 10A, leakage current effects on, 20: 6657 (NAA-SR-Memo-11417)

T

TANTALUM
bonding to molybdenum–titanium alloy and tungsten by vacuum hot-pressing, 20: 5866
brazing alloys for, development of, 20: 5867
compatibility with plutonium-uranium carbides, 20: 6600(R) (ANL-7105, pp 1-35)
corrosion by tin at 900 to 1000°C, 20: 6024(R) (ANL-5925(p.235-47))
effects on mechanical properties of tungsten of alloying additions of, 20: 5851
effects on oxidation resistance of beryllium–niobium and beryllium–zirconium alloys, 20: 5844
fabrication and properties of, handbook on, 20: 5874 (AGARDograph-94)
gamma coherent scattering at 0.662 and 1.332 Mev, cross sections for, (E/T), 20: 6323
neutron inelastic scattering at 14 Mev, cross sections for, 20: 6437
oxidation by air at 800°C, effects of phosphide coatings on, 20: 5851
proton reactions (p,n) at 30 and 50 Mev, isobaric-state excitation in, (E/T), 20: 6361
reactions with steam at 950 to 1300°C, 20: 6552(R) (ANL-6925, pp 187-233)
solubility in tin at 600 to 1000°C, equation for, 20: 5851
TANTALUM ALLOYS
fabrication and properties of, handbook on, 20: 5874 (AGARDograph-94)
Co–Ta, oxidation kinetics at 500 to 900°C, 20: 5854(T) (JPRS-32341, pp 8-16)
Cr–Ta, thermochemical properties of Cr_2Ta Laves phase, 20: 5851
Fe–Ta, oxidation kinetics at 500 to 900°C, 20: 5854(T) (JPRS-32341, pp 8-16)
Hf–Ta, properties as oxidation-resistant coatings for refractory metals, 20: 5846
Hf–Ta–W, bonding of T-111, method for diffusion, 20: 5867
Hf–Ta–W, corrosion by lithium in niobium–1–zirconium alloy forced-convection loop, 20: 5853 (TIM-898)
Hf–Ta–W, corrosion by cesium vapor and liquid lithium at 2500 to 3400°F of T-111, 20: 5851
Hf–Ta–W, creep tests on T-111 and T-222 at 3200°F, 20: 5885(R)
TELEVISION EQUIPMENT
uses of vidicons with digital scanners for particle-track analysis, (E), (NAS-CR-54773)
Hf–Ta–W, electric conductivity to 1500°C of T-111, 20: 5851
Hf–Ta–W, emissivity to 1500°C of T-111, total hemispherical, 20: 5851
Hf–Ta–W, welding parameters for T-111, electron-beam, 20: 5867

Mo–Nb–Ta–W–Zr, creep tests on NB132M at 3200°F, 20: 5885(R) (NAS-CR-54773)
Mo–Nb–Ta–W, strain aging of solution-hardened, 20: 5851
Nb–Ta–W–Zr, corrosion by lithium in niobium–1–zirconium alloy forced-convection loop, 20: 5853 (TIM-898)
O–Ta–Ti–Zr, phase studies at 1500°C, 20: 5846
Ta–Ti, oxidation kinetics at 500 to 900°C, 20: 5854(T) (JPRS-32341, pp 8-16)
Ta–Ti–V, elastic properties, 20: 6556(R) (ANL-7105, pp 36-58)
Ta–W, corrosion by cesium vapor and liquid lithium at 2500 to 3400°F, 20: 5851
Ta–W, oxidation kinetics at 500 to 900°C, 20: 5854(T) (JPRS-32341, pp 8-16)
Ta–W, welding parameters, electron-beam, 20: 5867
Ta–W–Y, corrosion by iron–plutonium at 700°C, effects of yttrium content on, 20: 5846
Ta–Zr, oxidation kinetics at 500 to 900°C, 20: 5854(T) (JPRS-32341, pp 8-16)

TANTALUM BORIDES
combustion with fluorine, data on, 20: 5523(R) (ANL-6925, pp 175-85)

TANTALUM CARBIDES
thermal expansion at 30 to 2500°C, 20: 5846
TaC–ZrC, thermal expansion at 30 to 2300°C, effects of composition and hot-pressing direction on, 20: 5846

TANTALUM COMPLEXES
with tropolone, preparation, properties, and structure, 20: 5538

TANTALUM ISOTOPES Ta-181
energy level transitions in, electromagnetic, (E), 20: 6374
energy level transitions in, E2/M1 mixing ratios and K conversion coefficients in rotational, (E), 20: 6386
energy levels of, quadrupole moment determination for, 20: 5794
proton reactions (p,2n) at 12 Mev, tungsten-180 levels from, (E), 20: 6366

TANTALUM ISOTOPES Ta-182
beta decay of, gamma transitions from, (E), 20: 6428
beta decay of, gamma energies and intensities from, (E), 20: 6347

TANTALUM ISOTOPES Ta-183
beta decay of, gamma transitions from, (E), 20: 6428

TANTALUM SYSTEMS
C–Ta, phase studies, 20: 5851
C–Ta–U, phase studies, 20: 5843

TECHNETIUM ISOTOPES
nucleon interactions in, effective, (T), 20: 6337

TECHNETIUM ISOTOPES Tc-99
incorporation into colloids, 20: 5456
incorporation into serum albumin, 20: 5456
preparation of metastable, by using ferric oxide as sorbent for molybdenum-99, 20: 5591 (SGAE-CH-18/1965)

TEETH
eruption pattern of, in beagles, 20: 5232(R) (COO-119-232, pp 68-73)
radiation effects on development of, in mouse embryos, x, 20: 5327
strontium-90 content in deciduous, 1962, 20: 5655

TELEMETERING SYSTEMS
development for continuous centralized recording of individual radiation doses, 20: 5749
radiation effects on circuits in, 20: 5806 (AD-619387) 20: 5718 (BNL-9634)

TELLURIUM
diffusion in spherical uranium dicarbide particles, coefficient for, 20: 5848

TEMPERATURE
effects on machining operations, 20: 6688 (Y-DA-1014)
radiosensitivity effects on insects, x, 20: 5385
radiosensitivity effects of freezing, on isolated rat thymocytes, 20: 5414
radiosensitivity effects of, in goldfish, 20: 5374

TERBIUM
oxidation of, kinetics of high-temperature, 20: 5859
separation from actinides and other rare earths by electrophoresis, 20: 5598

TERBIUM ALLOYS
Au–Tb, oxidation of, kinetics of high-temperature, 20: 5859
Tb–Y, electric conductivity at low temperatures, 20: 5888 (NP-15592)
Tb–Zr, metallurgical properties and phase studies on, 20: 5891(R) (NYO-2159-1)

TERBIUM IONS
spin-lattice relaxation rates in single crystals of anhydrous lanthanum trichloride, (E), 20: 6542

TERBIUM ISOTOPES Tb-149
production in proton reactions with gold-197 at 0.6 to 30 Bev, cross sections for, (E), 20: 6372

TERBIUM ISOTOPES Tb-159
energy level transitions in, E2/M1 mixing ratios and K conversion coefficients in rotational, (E), 20: 6386
proton reactions (p,2n) at 12 Mev, dysprosium-158 levels from, (E), 20: 6366

TERBIUM OXIDES
phase transformations in, at 50 to 1500°C, 20: 5536

TERPHANE
ion tracks in, registration mechanisms of heavy, 20: 5755

TERPHENYL
neutron scattering by, cross sections for slow, 20: 6272
radiation effects on corrosive effects of Santowax OM, on selected metals, fast-neutron, 20: 5846
sorption of hydrogen by SAP 895 sintered aluminum products from Progil OM2, at 400 and 450°C, 20: 5838(R) (RISO-110)

TEXAS
fallout monitoring, 1963, 20: 5649(R) (COO-1340-2, pp 54-83)

TEXTILES
decontamination of cotton, 20: 5676

THALLIUM
neutron inelastic scattering at 14 Mev, cross sections for, 20: 6437

THALLIUM ISOTOPES Tl-194
half life, (E), 20: 6298(R) (PPAD-2137-566)

THALLIUM ISOTOPES Tl-196
decay of, electron spectra from, (E), 20: 6298(R) (PPAD-2137-566)

THALLIUM ISOTOPES Tl-203
neutron reactions (n,γ) with, thallium-204 energy levels from thermal, (E), 20: 6411

THALLIUM ISOTOPES Tl-204
determination of, efficiency of beta scintillation sandwich counting method for, 20: 5783
energy levels, (E), 20: 6411

THERMAL CONDUCTIVITY
measurement in in-pile fuel elements, temperature transient method for, 20: 6565(R) (CEND-3336-251)
review on pressed-contact, (E/T), 20: 5625 (TRG-Report-1013)

THERMAL DIFFUSION
equations for multi-isotope, 20: 5825

THERMAL PROPERTIES
measurement of thermal expansion, optical system for, 20: 5709

THERMAL REACTORS
fuel conservation efficiencies of, 20: 6610 (HW-79287)

THERMIONIC CELLS
development and performance of cylindrical, 20: 6596(R) (GEST-2049)
development of nuclear, (E), 20: 6023(R) (AD-619379)

THERMOCOUPLES
calibration of in-pile, 20: 6627 (WAPD-PWR-TE-141)
development for use in boiling reactors, (E), 20: 6648(R) (HPR-64)

THERMODYNAMICS
of regenerative emf cells, 20: 6024(R) (ANL-6925(p.235-47))

THERMOELECTRIC CELLS
design of nuclear, 20: 6598(P)
performance of SNAP-10A, leakage current effects on, 20: 6657 (NAA-SR-Memo-11417)

THERMOLUMINESCENT DETECTORS
performance of lithium fluoride, for fast and thermal neutrons at 0.26 to 14 Mev, 20: 5572 (USNRDL-TR-909)
use of lithium fluoride, for radiation dosimetry of cesium-137 in sheep, 20: 5285 (BNWL-SA-172)

THERMONUCLEAR EXPLOSIONS
protection against fallout from, 20: 5416

THERMONUCLEAR REACTORS
blanket for, use of fissile nuclides in heat-extraction, 20: 6453 (AD-619670)
blankets of, gamma spectra in, 20: 6455 (AD-619672)
breeding blanket for, heat transfer and power distribution in, 20: 6452 (AD-619669)
breeding blankets for, neutron scattering and transport in, 20: 6451 (AD-619668)
breeding blankets for, neutron economy and tritium production in, 20: 6454 (AD-619671)

THIAZOLINE
amino salts of, radiosensitivity effects in mice, γ, 20: 5410

THICKNESS GAGES
compensation of radiometric, for material composition, 20: 5712(P)
development of radiometric, 20: 5817

THORACIC VISCERA
radiotherapy of tumors of, dosimetry of fixed teletherapy gamma beam, 20: 5438

THORIUM
combustion by fluidization, separation of thorium and uranium from, 20: 5500 (ORNL-3876)
deposition on metals, electrolytic, 20: 5867
determination by potentiometric titration using EDTA, equipment for, 20: 5502
determination in bone, methods for, 20: 5237(R) (UR-668, pp 55-109)

determination in mixtures of actinides and fission products by paper chromatography, 20: 5509
determination in rocks by parallel alpha-scintillation and radioscope measurements, 20: 5513
diffusion in pyrolytic graphite, 20: 5846
neutron cross sections from 0.015 to 1.00 kev, (E), 20: 6377
neutron resonance parameters of, (E), 20: 6377
neutron sensitivity of foil-glass dosimeters of, 20: 5713 (AD-623384)
permissible limits for, inconsistencies in regulations on, 20: 5662 (NLCO-962)
properties of, effects of rare earths on metallurgical, 20: 5891(R) (NYO-2159-1)

THORIUM ALLOYS
Al–Th, properties of Th_3Al, 20: 5848
Be–Th, properties of $ThBe_{13}$, 20: 5848
Er–Th, metallurgical properties and phase studies on, 20: 5891(R) (NYO-2159-1)
Gd–Th, metallurgical properties and phase studies on, 20: 5891(R) (NYO-2159-1)
Ho–Th, metallurgical properties and phase studies on, 20: 5891(R) (NYO-2159-1)
Lu–Th, metallurgical properties and phase studies on, 20: 5891(R) (NYO-2159-1)
Nd–Th, metallurgical properties and phase studies on, 20: 5891(R) (NYO-2159-1)
Pu–Th, electric conductivity at 25 to 900°C, 20: 5843
Pu–Th, thermal expansion at 25 to 900°C, 20: 5843
Th–U, brazing of Zircaloy-2-clad, 20: 5843

THORIUM BORIDES
properties of ThB_4, 20: 5848

THORIUM CARBIDES
electric conductivity discontinuities at 1440 and 1490°C in ThC_2, 20: 5848
properties of ThC and ThC_2, 20: 5848
ThC_2–UC_2, separation of products from fluidized-bed combustion of, by acid leaching, 20: 5500 (ORNL-3876)

THORIUM CHLORIDES
reactions with sodium succinate, conductometric and potentiometric study of, 20: 5555

THORIUM COMPLEXES
with tropolone, preparation, properties, and structure, 20: 5538

THORIUM ISOTOPES Th-228
content in Thorotrast, 20: 5399
content in Thorotrast of, and decay products, 20: 5400
effects of injected, in dogs, pathological, 20: 5288(R) (COO-119-232, pp 74-87)

THORIUM ISOTOPES Th-230
permissible limits for, inconsistencies in regulations on, 20: 5662 (NLCO-962)

THORIUM ISOTOPES Th-231
energy level scheme from uranium-235 alpha decay, (E), 20: 6388

THORIUM ISOTOPES Th-232
content in Thorotrast of, 20: 5398
content in Thorotrast, 20: 5399
content in Thorotrast of, 20: 5400
content of daughters of, in thorotrast-injected humans, 20: 5237(R) (UR-668, pp 55-109)
permissible limits for, inconsistencies in regulations on, 20: 5662 (NLCO-962)
photofission below 10 Mev, angular distributions from, (E), 20: 6309(T) (ANL-Trans-245)

THORIUM ISOTOPES Th-234
beta decay of, gamma spectra from, (E), 20: 6331

THORIUM OXALATES
conversion to thorium oxides having large specific surface area, 20: 5562(P)

THORIUM OXIDES
particle dimensions in colloidal, small-angle x-ray scattering studies of, 20: 5553

THORIUM(IV) OXIDES
alpha activity in Thorotrast, 20: 5399
combustion reactions in alumina fluidized bed, acid leaching separation of uranium from, 20: 5500 (ORNL-3876)
content of thorium-232 in Thorotrast, 20: 5399
content of thorium-228 in Thorotrast, 20: 5399
content of thorium-228 and thorium-232 in Thorotrast, 20: 5400
determination of Thorotrast in ashed lymph nodes, 20: 5399
effects in man following radiography of liver and spleen, carcinogenic, 20: 5311
effects in man, late pathologic, 20: 5353
effects of deposited Thorotrast, photological, 20: 5332
effects of injected Thorotrast, pathological, 20: 5398
effects of injected, pathological, 20: 5355
injection of colloidal in man, production of thorium-232 daughters after, 20: 5237(R) (UR-668, pp 55-109)
preparation and properties of, from thorium oxalate, 20: 5562(P)
preparation by sol-gel process, 20: 5843
radiation effects on properties of, for use as reactor fuels, 20: 5915(R) (ORNL-P-1724)
reactions with graphite, 20: 5843
thermal expansion of fuels of, during fast burst accident, 20: 6602 (BNWL-SA-346)
use in radiography of gastrointestinal carcinoma, 20: 5465
use in radiography of liver metastases, 20: 5465
Al–ThO_2, fabrication of powder-compacted slugs of, 20: 5866
Ni–ThO_2, bonding of TD nickel, method for diffusion, 20: 5867
Ni–ThO_2, recrystallization properties, 20: 5851
ThO_2–UO_2, preparation by sol-gel process, 20: 5843
ThO_2–UO_2, radiation effects on properties of, for use as nuclear fuels, 20: 5915(R) (ORNL-P-1724)
ThO_2–UO_2, separation of products from fluidized-bed combustion of, by acid leaching, 20: 5500 (ORNL-3876)

THORIUM PHOSPHIDES
ThP–UP, melting points, 20: 5848

THORIUM SILICIDES
properties of ThSi and Th_3Si_2, 20: 5848

THORIUM SYSTEMS
C–Ni–Th, phase studies, 20: 5848

THULIUM
separation from actinides and other rare earths by electrophoresis, 20: 5598

THULIUM BORIDES
thermionic emission of, on iridium and tungsten substrates, (E), 20: 5532(T) (K-Trans-10)

THULIUM ISOTOPES Tm-169
proton reactions (p,2n) at 12 Mev, ytterbium-168 levels from, (E), 20: 6366

THULIUM ISOTOPES Tm-172
beta decay of, spectral shapes and β-γ angular correlation in, (E), 20: 6381

THULIUM OXIDES
phase transformations in, at 50 to 1500°C, 20: 5536

THYMIDINE
radiation effects on metabolism in fish intestinal epithelium of, effects at temperatures on, tracer study, 20: 5374
radiation effects on urinary excretion by rats, x, 20: 5382

THYMINES
radioinduced dimerization in *Micrococcus radiodurans* of, uv, 20: 5266

THYMUS GLAND
effects of nicotinamide on respiration in tissue culture of rat, 20: 5340
effects on radiation effects on hemagglutinin production and homograft response in mice, 20: 5408 (USNRDL-TR-920)
radiation effects on respiration in tissue culture of rat, 20: 5340
radiation effects on oxidative phosphorylation in nuclei from rat, 20: 5341
radiation effects on growth of transplants of, in mouse kidney, x, 20: 5376
radioinduced cross-linking and denaturation of double-strand desoxyribonucleic acid from, uv, 20: 5268
radiosensitivity of isolated rat thymocytes, effects of freezing on, 20: 5414

THYROID GLAND
iodine-131 uptake by fetal, effects of age on, 20: 5259
radiation effects on dog, x, 20: 5301(R) (UR-668, pp 1-54)
radiodiagnosis of diseases of human, use of gamma camera for, 20: 5467
radiotherapy of carcinomas of, using iodine-131, evaluation, 20: 5444
radiotherapy of tumors of, use of iodine-131 for, 20: 5488

THYRONINE, TRIIODO-
analysis of iodine-125- or iodine-131-labeled, for impurities by paper chromatography, 20: 5515

TIMING CIRCUITS
design of amplitude-independent, for fast photomultipliers, 20: 5744 (UCRL-16227)

TIN
corrosive effects on molybdenum, tantalum, and tungsten at 900 to 1000°C, 20: 6024(R) (ANL-6925(p.235-47))
effects on properties of cadmium–indium–silver alloy as control rod material, 20: 5850
gamma coherent scattering at 0.662 and 1.332 Mev, cross sections for, (E/T), 20: 6323
gamma scattering by duct in, streaming in, (T), 20: 6530
magnetic coupling between adjacent type-II superconductors of, (E), 20: 6244
proton reactions at 0.54 to 1.47 Bev, neutron yields from, (E), 20: 5928(R) (PR-P-66)
solvent properties for tantalum at 600 to 1000°C, equation for, 20: 5851

superconducting critical currents in films of, magnetic field and temperature dependence of, (E), 20: 6232
TIN ALLOYS
Al–Sn–Ti, performance for ionization chamber construction, 20: 5716 (AEEW-M-470)
Hf–Sn, tin solubility in, 20: 5845
Pb–Sn, gamma attenuation coefficient in shielding of, (E), 20: 6523
TIN COMPLEXES
with tropolone, preparation, properties, and structure, 20: 5538
TIN COMPOUNDS
organic, deuterium isotope effects on water cleavage of, 20: 6687(R) (NYO-3453-1)
organic, effects of metal ions on hydrochloric acid cleavage of, 20: 6687(R) (NYO-3453-1)
organic, preparation of, 20: 6687(R) (NYO-3453-1)
organic, reactions with hydrochloric acid in methanol–water, 20: 6687(R) (NYO-3453-1)
TIN FLUORIDES
reactions with fluorine, 20: 5595(R) (ANL-6925, pp 107-64)
TIN ISOTOPES Sn-124
neutron reactions (n,γ) at 62 ev, angular distributions from, (E), 20: 6317
TIN ISOTOPES Sn-125
beta decay of, γ-γ angular correlations for, (E), 20: 6322
gamma angular distributions from tin-124 (n,γ) reactions, (E), 20: 6317
TIN SYSTEMS
C–Nb–Sn, superconductivity of Nb_2SnC, 20: 6228
TISSUE CULTURES
effects of nitrogen mustard on giant cell formation in RCP strain, 20: 5323
effects of parathyroid hormones on HeLa, 20: 5237(R) (UR-668, pp 55-109)
of eye lens, role of epithelium and capsule on electrolyte transport, tracer study, 20: 5256
of thymocytes, respiration in, 20: 5340
of tumor cells, growth studies in, 20: 5296(R) (NP-15585)
radiation effects on phosphorus metabolism in glioma, tracer study of x, 20: 5255
radiation effects on giant cell formation in RCP strain, x, 20: 5323
radiation effects on virulence of *Herpes simplex* viruses in HeLa, 20: 5363
radiation injuries of cells in, protective effects of cysteine and MEA on, 20: 5418
radiation injuries of cells in, protective effects of aminoethylisothiuronium, 20: 5419
TISSUE HOMOGENATES
radiation effects on mitosis in cystamine-treated mouse, x, 20: 5412
radiation effects on enzyme activity of rabbit, γ, 20: 5380
TISSUE TRANSPLANTS
erythroid, effects of erythropoietin on erythropoiesis in, 20: 5242
hematopoietic, bibliography, 20: 5424
immune reactions in, from mouse-rat radiation chimeras, 20: 5397
immune reactions to dog renal, effects of irradiating transplantation site on, 20: 5344
radiation effects on immune reactions in mice to sarcoma, effects of cystamine on, 20: 5413
radiation effects on immune reactions to bone marrow, in man, 20: 5420
radiation effects on take of skin homografts in rats, x, 20: 5335
radiation effects on growth of thymus, in mouse kidney, x, 20: 5376
TISSUES
analysis for calcium, methods of, 20: 5237(R) (UR-668, pp 55-109)
analysis for lead-210, radiochemical, 20: 5505
analysis for manganese, spectrochemical method for, 20: 5251(R) (UR-668, pp 123-49)
phantoms of, for radiotherapeutic measurements, 20: 5481
radiation effects on living, bibliography on, 20: 5284 (AED-C-04-21)
radiation effects on antioxidant content of rat, γ, 20: 5339
radiation effects on lipoperoxide content of rat, γ, 20: 5339
radiation effects on metabolism in sections of rat kidney, x, 20: 5352
transfer of calcium-40 and calcium-45 by dog renal, 20: 5237(R) (UR-668, pp 55-109)
tritium uptake from glucose by fatty, in rats, 20: 5252
TITANIUM
bonding to molybdenum–titanium alloy and tungsten by vacuum hot-pressing, 20: 5866
electron reactions at 2.5 to 4.0 Mev, bremsstrahlung spectra from, (E), 20: 6432
erosion of 600, by liquid sodium, 20: 5861
optical properties of small particles of, (T), 20: 5879 (D-910092-6)
performance for ionization chamber construction, 20: 5716 (AEEW-M-470)
production by electrolysis, technique for, 20: S604(P)
radiation effects on in-pile corrosion of, by aqueous solutions, 20: 5852(R) (EURAEC-1522)
sorptive properties of hot spongy, for nitrogen, 20: 5594(R) (ANL-6925, pp 21-106)
TITANIUM ALLOYS
corrosion cracking of B120VCA, by plutonium hexafluoride, stress, 20: 5846
Al–Mo–Ti–V, phase studies, 20: 5851
Al–Nb–Ti, oxidation, 20: 5896 (TID-22388)
Al–Nb–Ti, phase studies on, 20: 5896 (TID-22388)
Al–Sn–Ti, performance for ionization chamber construction, 20: 5716 (AEEW-M-470)
Al–Ti, oxidation, 20: 5896 (TID-22388)
Al–Ti, phase studies on, 20: 5896 (TID-22388)
Cr–Nb–Ti–V, properties as cladding materials, 20: 5846
Cr–Ti–V, corrosion by flowing sodium at 650°C, effects of chromium content on, 20: 5851
Cr–Ti–V, creep rate of, 20: 6601(R) (ANL-7115, pp 1-41)
Cr–Ti–V, elastic properties, 20: 6556(R) (ANL-7105, pp 36-58)
Fe–Ti, oxidation kinetics at 500 to 900°C, 20: 5854(T) (JPRS-32341, pp 8-16)
Mo–Ti, bonding to foils of nickel, niobium, tantalum, and titanium by vacuum hot-pressing, 20: 5866
Mo–Ti, creep tests on TZC and TZM at 3200°F, 20: 5885(R) (NAS-CR-54773)
Mo–Ti–V, elastic properties, 20: 6556(R) (ANL-7105, pp 36-58)
Mo–Ti–Zr, bonding of TZM, method for diffusion, 20: 5867
Mo–Ti–Zr, brazing molybdenum to TZM, brazing alloy development for, 20: 5866
Mo–Ti–Zr, corrosion by cesium vapor and liquid lithium at 2500 to 3400°F of TZM, 20: 5851
Mo–Ti–Zr, extrusion of TZM, process for, 20: 5867
Nb–Ti, oxidation, 20: 5896 (TID-22388)
Nb–Ti, phase studies on, 20: 5896 (TID-22388)
Nb–Ti, superconducting critical fields in, Pauli paramagnetism effects on upper, (E), 20: 6236
Nb–Ti–V, elastic properties, 20: 6556(R) (ANL-7105, pp 36-58)
Nb–Ti–Zr, bonding of D-36, method for diffusion, 20: 5867
O–Ta–Ti–Zr, phase studies at 1500°C, 20: 5846
Pu–Ti–U, compressive strength of, 20: 6601(R) (ANL-7115, pp 1-41)
Pu–Ti–U, tensile properties, 20: 6600(R) (ANL-7105, pp 1-35)
Pu–Ti–U, thermal expansion, 20: 5848
Ta–Ti, oxidation kinetics at 500 to 900°C, 20: 5854(T) (JPRS-32341, pp 8-16)
Ta–Ti–V, elastic properties, 20: 6556(R) (ANL-7105, pp 36-58)
Ti–V, compatibility with plutonium-uranium carbides, 20: 6600(R) (ANL-7105, pp 1-35)
Ti–V, corrosion of TV-20, by sodium at 650°C, 20: 5846
Ti–V, reactions with fissium–plutonium–uranium alloy at 550 to 700°C, 20: 5843
Ti–V, removal from fuel elements by chlorination, 20: 5594(R) (ANL-6925, pp 21-106)
Ti–W, oxidation kinetics at 500 to 900°C, 20: 5854(T) (JPRS-32341, pp 8-16)
Ti–Zr, oxidation kinetics at 500 to 900°C, 20: 5854(T) (JPRS-32341, pp 8-16)
TITANIUM COMPLEXES
with tropolone, preparation, properties, and structure, 20: 5538
TITANIUM HYDRIDES
performance as gamma and neutron shielding material, (E/T), 20: 6626 (UNC-5118)
properties as reactor moderator, 20: 5844
TITANIUM ISOTOPES Ti-45
nuclear moments and spins of, determination, (E/T), 20: 6299 (PUC-1965-158)
TITANIUM ISOTOPES Ti-47
proton reactions (p,2p) at 155 Mev, cross sections for, (E), 20: 6330
TITANIUM ISOTOPES Ti-48
proton reactions (p,2p) at 155 Mev, cross sections for, (E), 20: 6330
TITANIUM ISOTOPES Ti-49
proton reactions (p,2p) at 155 Mev, cross sections for, (E), 20: 6330
TITANIUM OXIDES
preparation of high-purity, by fluidized-bed chemical vapor deposition, 20: 5866
TITANIUM SYSTEMS
Cd–C–Ti, superconductivity of Ti_2CdC, 20: 6228
C–Mo–Ti–Zr, microstructure and tensile properties of, effects of composition, heat treatment, and processing on, 20: 5846
C–Pb–Ti, superconductivity of Ti_2PbC, 20: 6228
In–N–Ti, superconductivity of Ti_2InN, 20: 6228
O–Ti–W, phase studies, 20: 5851
TOLUENE
effects on activity of leukocyte alkaline phosphatase, toxicity, 20: 5269
TOLUENE, α-BROMO-
electron reactions in ethylene mixture, cross sections for momentum transfer and drift velocities in, 20: 5985 (ORNL-TM-1262)

TORI
inductance of, h-f, 20: 6508
TOXICOLOGY
of chemicals to activity of leukocyte alkaline phosphatase, 20: 5269
TOXINS
effects of, on growth of tumor cells in culture, 20: 5296(R) (NP-15585)
effects on induction of leukopenia in rabbits, 20: 5315
radiation effects on rat immunity to diphtheria, γ, 20: 5391
radioinduced in nutrient solutions, effects on cells in pea seedling roots, genetic, 20: 5390
TRACER TECHNIQUES
gold-198 in, bibliography on, 20: 5811 (PAEC(A)IN-653)
use in pharmacy, bibliography on, 20: 5812 (PAEC(A)IN-654)
use in Rumania, 20: 5810 (NP-15543)
TRACER TECHNIQUES (AGRICULTURE)
use in Rumania, 20: 5235 (NP-15543, pp 83-90)
TRACER TECHNIQUES (BIOLOGY)
calcium–vitamin D metabolism, 20: 5237(R) (UR-668, pp 55-109)
for insect ecological studies, 20: 5815 (STI/DOC/10/44)
use of selenium-75-labeled blood proteins for, 20: 5262
TRACER TECHNIQUES (CHEMISTRY)
developments in Rumania, 20: 5590 (NP-15543, pp 5-26)
TRACER TECHNIQUES (ENGINEERING)
development in Rumania, 20: 5814 (NP-15543, pp 27-45)
for sewage flow through treatment plants, 20: 5432
TRACER TECHNIQUES (HYDROLOGY)
development in Rumania, 20: 5657 (NP-15543, pp 47-58)
TRACER TECHNIQUES (MEDICINE)
evaluation of, in Rumania, 20: 5435 (NP-15543, pp 59-75)
for calcium metabolism in man, 20: 5260
for cancer diagnosis, 20: 5450
for cancer research, 20: 5436(R) (UR-668, pp 149-60)
for detection of venous thrombi, 20: 5437(R) (UR-668, pp 149-60)
for metabolism of mercurial diuretics, 20: 5251(R) (UR-668, pp 123-49)
use of external scanning for, 20: 5447
use of technetium-99 and external scanning for organ visualization, 20: 5456
TRAMEX PROCESS
analysis of solutions in, for lithium, automated flame photometric method for, 20: 5496 (DP-985)
TRANSISTORS
fabrication of compensated germanium p-i-n diodes, (E), 20: 5702
performance of field-effect, in input stages of preamplifiers, (E), 20: 5772
radiation effects on, gamma and neutron, 20: 5808 (N65-35081)
thresholds for tunnel-diode switching circuits, (E), 20: 5700
use in fast-amplitude discriminator, 20: 5694
use in universal logic circuit, 20: 5704
uses of low- and high-peak-current tunnel diodes in cascade circuits, 20: 5699
TRANSITION METALS
reactions with sodium metaphosphate, 20: 5529(R) (SC-DC-65-1706)
TRANSPLUTONIC ELEMENTS
production at Savannah River, program for, 20: 5822 (DP-1000)
TRIAFOL
ion tracks in, registration mechanisms of heavy, 20: 5755
TRIOCTYLAMINE
solvent properties for sulfuric acid, effects of alkyl esters of phosphoric acid on, 20: 5600
solvent properties for cobalt and manganese, 20: 5602
TRITIUM
activity measurements of, by gas-proportional counting, 20: 5779
determination by beta scintillation counting, effects of sample volume on efficiency of, 20: 5510
determination in Main and Rhine Rivers in Germany, 20: 5654
determination in water, method for, 20: 5517
determination in water, survey of counting systems and concentration methods for, 20: 5521
effects on *Escherichia coli* of incorporated, mutagenic, 20: 5350
incorporation in glucose-3 and -4, enzyme method for, 20: 5252
incorporation in hydrocarbons, 20: 5593(P)
lithium-6 reactions (Li-6,2α) at 0.65 to 0.97 Mev, alpha spectra from, (E), 20: 6351
oxygen-16 reactions (O-16,αγ) with, nitrogen-15 gamma transitions from, (E), 20: 6318
production in thermonuclear reactors, 20: 6452 (AD-619669)
production in thermonuclear reactor blankets by neutron reactions with lithium-6 and lithium-7, 20: 6454 (AD-619671)
separation from deuterium, hydrogen, and their compounds by gas chromatography, 20: 5824
uptake from glucose by fatty tissues in rats, 20: 5252
TRITIUM IONS
motion of beams of, in crossed-field beam sorters, (E), 20: 6262 (NP-15633)
TRITONS
binding energy of, relativistic corrections to, (T), 20: 6084
yields from meson (π−) capture by nuclei, (E/T), 20: 6292 (NP-15601)
TROPOLONES
complexes with selected metals, preparation, properties, and structure, 20: 5538
TROPOSPHERE
fallout transport to, from stratosphere, 20: 5649(R) (COO-1340-2, pp 54-83)
fallout transport to, from stratosphere, effects of cyclonic activity on, 20: 5650(R) (COO-1340-2, pp 84-109)
TUBERCULOSIS
effects of immune reactions induced by, on incidence of radioinduced bone tumors in mice, 20: 5373
TUBES
performance of polyethylene, in equipment for air monitoring, 20: 5752
weld joint design for Zircaloy-4, end closure, 20: 5865 (WCAP-3269-37)
TUMORS
chemotherapy of, synergistic effects of radiotherapy, 20: 5466
etiology of, 20: 5296(R) (NP-15585)
localization of iodine-131-fibrinogen in, mechanisms of, 20: 5436(R) (UR-668, pp 149-60)
radiation effects on, metabolic, 20: 5477
radiation effects on, morphological, 20: 5477
radiation effects on, immunological, 20: 5477
radiation effects on phosphorus metabolism in glioma cultures, x, 20: 5255
radiation effects on induction by urethan of, in mouse lungs, γ, 20: 5328
radiodiagnosis of, use of labeled compounds and external scanning for, 20: 5450
radioinduced bone, americium-241 and plutonium-239, 20: 5321
radioinduced bone, effects of antigenic stimulation on incidence in mice, 20: 5373
radioinduced in man, statistical study of etiology of, 20: 5307
radioinduced in rats, by polonium-210, 20: 5237(R) (UR-668, pp 55-109)
radioinduced, etiology of, 20: 5466
radioinduced, Thorotrast, 20: 5353
radiosensitivity of, effects of various drugs on, 20: 5442
radiotherapy of benign, 20: 5490
radiotherapy of bladder, 20: 5454
radiotherapy of breast, leukemia incidence after, 20: 5471
radiotherapy of ear, 20: 5474
radiotherapy of gynecological, 20: 5473
radiotherapy of head, x, 20: 5484
radiotherapy of head and neck, 20: 5441
radiotherapy of hemangiomas in children, 20: 5443
radiotherapy of middle ear, techniques for, 20: 5448
radiotherapy of thoracic, dosimetry of fixed teletherapy gamma beam, 20: 5438
radiotherapy of thyroid, use of iodine-131 for, 20: 5488
radiotherapy of, dosimetry of x radiation, 20: 5439
radiotherapy of, effects of 5-fluorouracil on, 20: 5452
radiotherapy of, presurgical, 20: 5477
radiotherapy of, synergistic effects of chemotherapy, 20: 5466
radiotherapy of, use of high energy sources for, 20: 5442
radiotherapy of, use of megavoltage sources for, 20: 5453
radiotherapy of, use of fibrin antibodies, and fibrinogen as iodine-131 carriers for, 20: 5436(R) (UR-668, pp 149-60)
surgery of ear, 20: 5474
therapy of malignant, use of tissue-specific antibodies for, 20: 5436(R) (UR-668, pp 149-60)
TUNGSTEN
bonding to foils of nickel, niobium, tantalum, and titanium by vacuum hot-pressing, 20: 5866
compatibility with plutonium-uranium carbides, 20: 6600(R) (ANL-7105, pp 1-35)
corrosion by liquid lithium and cesium vapor at 2500 to 3400°F, 20: 5851
creep tests on, at 3200°F, 20: 5885(R) (NAS-CR-54773)
deposition by pyrolysis of tungsten hexacarbonyl, 20: 5867
deposition of metallic oxidation-protection coatings on, electrolytic, 20: 5867
diffusion in iridium, platinum, rhodium, and ruthenium, inter-, 20: 5846
ductility at low temperatures, effects of dispersed oxides on, 20: 5846
extrusion of sleeves of, 20: 5866
fabrication and properties of, handbook on, 20: 5874 (AGARDograph-94)
mechanical properties, effects of hafnium, niobium, rhenium, and tantalum alloying additions on, 20: 5851
mechanical properties of, effects of carbon and oxygen interstitial impurities on, 20: 5846
metallurgy of, review on powder, 20: 5836 (NASA-SP-5035)
neutron Doppler coefficients and resonance integrals for, 20: 6279(R) (AI-65-225)
neutron inelastic scattering at 14 Mev, cross sections for, 20: 6437

opacity of gaseous, (T), 20: 6594 (D-910092-4)
oxidation by air at 800°C, effects of phosphide coatings on, 20: 5851
oxidation rates of, effects of dissociation of molecular oxygen on, 20: 5846
performance as gamma and neutron shielding material, (E/T), 20: 6626 (UNC-5118)
properties as substrate for rare-earth–hexaboride thermionic emitters, (E), 20: 5532(T) (K-Trans-10)
properties for skull reclamation process crucibles, 20: 5594(R) (ANL-6925, pp 21-106)
properties of vapor-deposited, 20: 5867
radiation effects on creep-rupture of, fast neutron, 20: 5851
radioinduced emanation at 300 and 1300°K, holdup time of, (E), 20: 6298(R) (PPAD-2137-566)
reactions with steam at 1050 to 1700°C, 20: 6552(R) (ANL-6925, pp 187-233)
reactivity worth calculation of, 20: 6279(R) (AI-65-225)
refractive index of gaseous, (E/T), 20: 5879 (D-910092-6)
welding parameters, electron-beam, 20: 5867

TUNGSTEN ALLOYS
creep tests on Sylvania A at 3200°F, 20: 5885(R) (NAS-CR-54773)
fabrication and properties of, handbook on, 20: 5874 (AGARDograph-94)
Be–W, phase studies at 1000 to 2100°C, 20: 5906
Co–W, oxidation kinetics at 500 to 900°C, 20: 5854(T) (JPRS-32341, pp 8-16)
Fe–W, oxidation kinetics at 500 to 900°C, 20: 5854(T) (JPRS-32341, pp 8-16)
Hf–Nb–W–Y, welding parameters for C-129Y, electron-beam, 20: 5867
Hf–Ta–W, bonding of T-111, method for diffusion, 20: 5867
Hf–Ta–W, corrosion by lithium in niobium–1–zirconium alloy forced-convection loop, 20: 5853 (TIM-898)
Hf–Ta–W, corrosion by cesium vapor and liquid lithium at 2500 to 3400°F of T-111, 20: 5851
Hf–Ta–W, creep tests on T-111 and T-222 at 3200°F, 20: 5885(R) (NAS-CR-54773)
Hf–Ta–W, electric conductivity to 1500°C of T-111, 20: 5851
Hf–Ta–W, emissivity to 1500°C of T-111, total hemispherical, 20: 5851
Hf–Ta–W, welding parameters for T-111, electron-beam, 20: 5867
Mo–Nb–Ta–W–Zr, creep tests on NB132M at 3200°F, 20: 5885(R) (NAS-CR-54773)
Mo–Nb–Ta–W, strain aging of solution-hardened, 20: 5851
Mo–Ni–W, mechanical properties, effects of aging temperature and molybdenum and tungsten content on, 20: 5851
Mo–Re–W, fabrication of thin-walled tubing of, 20: 5867
Mo–W, corrosion by liquid lithium and cesium vapor at 2500 to 3400°F, 20: 5851
Nb–Ta–W–Zr, corrosion by lithium in niobium–1–zirconium alloy forced-convection loop, 20: 5853 (TIM-898)
Nb–W, corrosion by liquid lithium and cesium vapor at 2500 to 3400°F, 20: 5851
Nb–W, oxidation kinetics at 500 to 900°C, 20: 5854(T) (JPRS-32341, pp 8-16)
Nb–W, oxidation by air at 900 to 1300°C, effects of niobium content on, 20: 5851
Nb–W–Zr, creep tests on AS-30 at 3200°F, 20: 5885(R) (NAS-CR-54773)
Ni–W, creep properties at 750 to 1200°C, effects of tungsten content on, 20: 5851
Ni–W, oxidation kinetics at 500 to 900°C, 20: 5854(T) (JPRS-32341, pp 8-16)
Pd–W, phase studies, 20: 5846
Re–W, corrosion by lithium in niobium–zirconium alloy forced-convection loop, 20: 5853 (TIM-898)
Re–W, corrosion by liquid lithium and cesium vapor at 2500 to 3400°F, 20: 5851
Re–W, creep tests at 3200°F on, 20: 5885(R) (NAS-CR-54773)
Re–W, oxidation rate of, effects of rhenium content on, 20: 5846
Re–W, properties of, 20: 6596(R) (GEST-2049)
Re–W, radiation effects on creep-rupture of, fast neutron, 20: 5851
Ta–W, corrosion by cesium vapor and liquid lithium at 2500 to 3400°F, 20: 5851
Ta–W, welding parameters, electron-beam, 20: 5867
Ta–W–Y, corrosion by iron–plutonium at 700°C, effects of yttrium content on, 20: 5846
Ti–W, oxidation kinetics at 500 to 900°C, 20: 5854(T) (JPRS-32341, pp 8-16)
W–Zr, oxidation kinetics at 500 to 900°C, 20: 5854(T) (JPRS-32341, pp 8-16)

TUNGSTEN BORIDES
thermionic emission of, on iridium and tungsten substrates, (E), 20: 5532(T) (K-Trans-10)

TUNGSTEN ISOTOPES W-180
energy levels, (E), 20: 6366

TUNGSTEN ISOTOPES W-182
energy levels of, parity and spin of, (E), 20: 6428
energy levels of, parity and spin of, (E), 20: 6347
neutron resonance parameters of, 20: 6279(R) (AI-65-225)

TUNGSTEN ISOTOPES W-183
energy levels of, parity and spin of, (E), 20: 6428
neutron resonance parameters of, 20: 6279(R) (AI-65-225)

TUNGSTEN ISOTOPES W-184
neutron resonance parameters of, 20: 6279(R) (AI-65-225)

TUNGSTEN ISOTOPES W-186
neutron resonance parameters of, 20: 6279(R) (AI-65-225)

TUNGSTEN ISOTOPES W-187
beta decay of, gamma intensities in, (E), 20: 6397

TUNGSTEN OXIDES
Nb_2O_5–WO_3, phase studies, 20: 5846

TUNGSTEN SYSTEMS
Ca–O–W, phase studies, 20: 5851
C–Nb–W–Zr, bonding of D-43, method for diffusion, 20: 5867
C–Nb–W–Zr, electric conductivity to 1500°C of D-43, 20: 5851
C–Nb–W–Zr, emissivity to 1500°C of D-43, total hemispherical, 20: 5851
C–Nb–W–Zr, mechanical properties of D-43, effects of protective coatings and welding on, 20: 5866
C–Nb–W–Zr, weld stability in D-43, 20: 5866
C–Nb–W–Zr, welding parameters for D-43, electron-beam, 20: 5867
Co–O–W, phase studies, 20: 5851
O–Sm–W, phase studies, 20: 5851
O–Ti–W, phase studies, 20: 5851
Re–W–UO_2, compatibility of, 20: 6596(R) (GEST-2049)
W–UO_2, preparation and properties of dispersions of, 20: 5843

TURBINES
design of self-sustained gas, with compressor, for gas-cooled reactors, 20: 6647(P)

U

ULTRASONICS
use in nondestructive fuel element testing, 20: 6632(T) (AEC-tr-6628)
uses for fatigue detection before crack initiation in steels, 20: 5867

ULTRAVIOLET RADIATION
effects on chemotaxis in Euglena and leukocytes, 20: 5396
effects on chromosome replication in *E. coli*, 20: 5349
effects on double-strand desoxyribonucleic acid cross-linkage, 20: 5268
effects on *E. coli* culture media, effects on colicin and phage induction by, 20: 5279
effects on enzyme activity in protozoa homogenates, effects of pH on, 20: 5272
effects on *Escherichia coli*, photoreactivation of, 20: 5347
effects on *Escherichia coli* growth, effects of arginine and uracil on, 20: 5348
effects on fluorescence intensity in frog blood cells, effects of temperature on, 20: 5318
effects on *Herpes simplex* virus in HeLa cell cultures, 20: 5363
effects on life-span of paramecium, effects of metabolic inhibitors on, 20: 5386
effects on *Micrococcus radiodurans*, 20: 5266
effects on morphogenesis in Euplotes, 20: 5345
effects on organic glasses containing alkyl halides, 20: 5577
effects on photosynthetic reactions in isolated chloroplasts, 20: 5401
effects on Saccharomyces radiosensitivity, mutagenic, 20: 5360

UNDERGROUND EXPLOSIONS
neutron spectra in, calculation of thermal, 20: 5609 (LA-3403)
use of nuclear, for determining internal structure of earth, 20: 5610

UNITED STATES
jet stream behavior over, 20: 5644(R) (COO-1340-2, pp 110-21)

URACIL
radiosensitivity effects on *Escherichia coli*, γ and uv, 20: 5348

URACIL, 5-FLUORO-
effects on Saccharomyces radiosensitivity, mutagenic, 20: 5360
radiosensitivity effects of, in tumors, 20: 5452
toxicity in man of, 20: 5452

URANIUM
analytical uses for determination of fluorides by titration, 20: 5520
burnup and conservation in thermal reactors, 20: 6610 (HW-79287)
casting of tubular fuel cores of, 20: 5867
combustion by fluidization, separation of thorium and uranium from, 20: 5500 (ORNL-3876)
creep in, activation energy for, 20: 5843
critical masses of enriched arrays of, 20: 6584 (LA-DC-7248)
cutting of rods of, design of chemical saw for, 20: 5839(R) (RISO-110)
deposition on metals, electrolytic, 20: 5867
determination as thiocyanate, effects of solvents on, 20: 5516
determination in mixtures of actinides and fission products by paper chromatography, 20: 5509

determination in rocks by parallel alpha-scintillation and radioscope measurements, 20: 5513
determination in solutions of quaternary ammonium nitrates, potentiometric, 20: 5518
diffusion coefficients of krypton and xenon in, effects of heating on, 20: 5848
diffusion in pyrolytic, S-700, and ZTA graphite, 20: 5846
diffusion of iodine in helium atmosphere from, behavior and chemical state of, 20: 5878 (BNL-9667)
ductility of, effects of annealing temperature on, 20: 5843
fabrication into magnesium alloy-clad fuel elements for operation at 140 to 350°C, 20: 5872(P)
fabrication into magnesium alloy-clad fuel elements, grain-size control in, 20: 5871(P)
formation in uranin during irradiation at high temperatures, 20: 5843
hydridation in tungsten crucibles, feasibility of, 20: 5594(R) (ANL-6925, pp 21-106)
ionization potentials for, (T), 20: 5983 (D-910099-2)
machining extrusion billet of, electrochemical, 20: 5866
neutron sensitivity of foil-glass dosimeters of, 20: 5713 (AD-623384)
performance of aluminum-coated, as self-regenerating deuterium target, (E/T), 20: 6334
processing of spent fuels and breeder materials of, pyrochemical batch-extraction, 20: 6600(R) (ANL-7105, pp 1-35)
production from uranyl nitrate, 20: 5870(P)
proton reactions (p,n) at 30 and 50 Mev, isobaric-state excitation in, (E/T), 20: 6361
proton reactions at 3 Bev, fission and fragmentation products from, (E), 20: 5756
proton reactions at 0.54 to 1.47 Bev, neutron yields from, (E), 20: 5928(R) (PR-P-66)
radiation and temperature effects on plastic deformation of alpha, neutron, 20: 5916
radiation effects on ignition of, 20: 6552(R) (ANL-6925, pp 187-233)
radioinduced dislocation loops in alpha, orientation and Burgers vectors of neutron, 20: 5848
radioinduced swelling in, effects of alloying additions on, 20: 5848
radioinduced swelling in, effects of texture on, 20: 5848
radioinduced swelling of Harwell model for, 20: 5843
radioinduced swelling of, in-pile, 20: 5848
reactions with steam at 600 to 1600°C, 20: 5843
reactions with water in TREAT meltdown experiments, 20: 6552(R) (ANL-6925, pp 187-233)
reactivity worth calculation of depleted, 20: 6279(R) (AI-65-225)
rolling properties of, effects of iron and silicon on, 20: 5866
separation from aqueous solutions by extraction using organo-phosphorus solutions, 20: 5605(P)
separation from enriched fuel alloys by fluoride volatility, 20: 5595(R) (ANL-6925, pp 107-64)
separation from fission products by skull reclamation process, flow-sheets for, 20: 5594(R) (ANL-6925, pp 21-106)
separation from fused chlorides by liquid metal extraction, 20: 5594(R) (ANL-6925, pp 21-106)
separation from low enrichment fuels, 20: 6558(R) (ANL-7115, pp 42-67)
separation from molten cadmium–magnesium alloys by fused chloride extraction, 20: 5594(R) (ANL-6925, pp 21-106)
separation from reactor fuel alloys, methods for, 20: 6553(R) (ANL-6925, pp 255-63)
separation from skull reclamation fuel alloys by distillation, 20: 5594(R) (ANL-6925, pp 21-106)
separation from spent fuel by selective dissolution, 20: 5594(R) (ANL-6925, pp 21-106)
separation of hydrogen from, 20: 5843
sintering mechanisms, 20: 5848
superconducting transition temperature of pressure dependence of, (E), 20: 6234
texture gradients in fuel cores of, effects of fabrication variables on, 20: 5863 (NLCO-945)
welding parameters, electron-beam, 20: 5867

URANIUM ALLOYS
cracking of, effects of repeated quenching on, 20: 5867
fabrication into magnesium alloy-clad fuel elements for operation at 140 to 350°C, 20: 5872(P)
fabrication into magnesium alloy-clad fuel elements, grain-size control in, 20: 5871(P)
Al–Fe–U, hot hardness and microstructure, effects of chromium or silicon additions on, 20: 5848
Al–Fe–U, microstructure, effects of heat treatments on, 20: 5848
Al–Fe–U, phase studies, 20: 5843
Al–U, fabrication by roll bonding of, fuel plates clad with aluminum, 20: 5866
Al–U, phase studies at 600 to 1200°C of high-uranium, 20: 5848
Al–U, processing for uranium recovery by fluoride volatility, 20: 5595(R) (ANL-6925, pp 107-64)
Be–U, hardness of splat-cooled, effects of heat treatments on, 20: 5866
Cd–Mg–U–Zn, corrosive effects with chloride flux on carbon steel, Croloy, and stainless steel at 600 to 650°C, 20: 5594(R) (ANL-6925, pp 21-106)
Cd–Mg–U–Zn, phase studies, 20: 5594(R) (ANL-6925, pp 21-106)
Cr–U, phase transformation in, kinetics of beta-alpha, 20: 5843
Fe–Pu–U, casting of, centrifugal, 20: 5866
fissium–Pu–U, burnup studies, 20: 6600(R) (ANL-7105, pp 1-35)
fissium–Pu–U, chloride slagging of, reactions of cerium and zirconium in, 20: 5594(R) (ANL-6925, pp 21-106)
fissium–Pu–U, phase studies on, 20: 5876 (ANL-6974)
fissium–Pu–U–Zr, phase studies on, 20: 5876 (ANL-6974)
fissium–Pu–U, reactions with vanadium–20 titanium at 550 to 700°C, 20: 5843
Mo–Pu–U, ignition of, effects of molybdenum content on, 20: 5843
Mo–Pu–U, properties of, compressive, thermal expansion, and tensile, 20: 5843
Mo–U, coating with nickel to prevent stress-corrosion cracking in air, electrolytic, 20: 5867
Mo–U, radioinduced swelling in, reactor, 20: 5848
Nb–U–Zr, properties of metastable γ-phase, 20: 5843
Pd–U, phase studies, 20: 5843
Pu–Ti–U, compressive strength of, 20: 6601(R) (ANL-7115, pp 1-41)
Pu–Ti–U, tensile properties, 20: 6600(R) (ANL-7105, pp 1-35)
Pu–Ti–U, thermal expansion, 20: 5848
Pu–U, ignition properties of, effects of alloying additions on, 20: 5843
Pu–U, processing spent, methods for, 20: 5594(R) (ANL-6925, pp 21-106)
Pu–U–Zr, compressive strength of, 20: 6601(R) (ANL-7115, pp 1-41)
Pu–U–Zr, phase studies, 20: 6600(R) (ANL-7105, pp 1-35)
Pu–U–Zr, tensile properties, 20: 6600(R) (ANL-7105, pp 1-35)
Pu–U–Zr, thermal expansion, 20: 5848
Th–U, brazing of Zircaloy-2-clad, 20: 5843
U–Zircaloy-2, processing for uranium recovery by fluoride volatility, 20: 5595(R) (ANL-6925, pp 107-64)
U–Zr, diffusion of fission gas from hydrided, 20: 5844
U–Zr, phase transformations in, effects of cooling rate on, 20: 5843

URANIUM CARBIDES
compatibility with SAP 930 to 600°C, 20: 5839(R) (RISO-110)
diffusion of helium in, method for studying, 20: 5892 (PWAC-476)
diffusion of iodine in helium atmosphere from, behavior and chemical state of, 20: 5878 (BNL-9667)
fission product diffusion in spherical particles of, 20: 5848
precipitation of dicarbide platelets in monocarbide, 20: 5848
preparation by gas–solid reaction, 20: 5848
preparation processes for, 20: 5594(R) (ANL-6925, pp 21-106)
properties, 20: 5843
thermal conductivity of, effects of nitrogen and oxygen impurities on, 20: 5893 (PWAC-480)
thermal expansion of fuels of, during fast burst accident, 20: 6602 (BNWL-SA-346)
wetting by sodium at 250°C, contact angles in, 20: 5594(R) (ANL-6925, pp 21-106)
Fe–UC, corrosion resistance to steam and water, 20: 5857
PuC–UC, compatibility with jacketing materials, 20: 6600(R) (ANL-7105, pp 1-35)
PuC–UC, precipitation from fused salts, methods for, 20: 5594(R) (ANL-6925, pp 21-106)
SiC–UC, fabrication of fuel elements of, process for, 20: 5873(P)
ThC_2–UC_2, separation of products from fluidized-bed combustion of, by acid leaching, 20: 5500 (ORNL-3876)
UC_2–UO_2, phase studies, 20: 5848
UC–ZrC, ductility at 1800°C, 20: 5848

URANIUM CHLORIDES
preparation by reactions of uranium dioxide with chlorine in molten alkali chlorides, thermodynamics of, 20: 5547

URANIUM COUPLES
Au/U, contact potential difference, 20: 5843

URANIUM DEPOSITS
genesis, deposition, and source of, method for determining, 20: 5660
uranium-234/-238 ratios in, 20: 5660

URANIUM DEPOSITS (BRAZIL)
reconnaissance of northeast coastal, 20: 5659 (RME-4545(Rev.))

URANIUM FLUORIDES
reactions with magnesium, 20: 5870(P)

URANIUM(IV) FLUORIDES
use of uranium-238-enriched, in heat-extraction blanket for thermo-nuclear reactors, 20: 6453 (AD-619670)

URANIUM(VI) FLUORIDES
critical masses of enriched arrays of, 20: 6584 (LA-DC-7248)
PuF_6–UF_6, conversion to oxides, equipment for, 20: 5595(R) (ANL-

6925, pp 107-64)
PuF_6–UF_6, phase studies, 20: 5595(R) (ANL-6925, pp 107-64)
URANIUM HYDRIDES
UH–ZrH, radiation effects on, measurement in TREAT, (E), 20: 6678 (NAA-SR-Memo-11374)
URANIUM IONS
ionization potentials for, (T), 20: 5983 (D-910099-2)
oxidation-reduction potential of, effects of light on, 20: 5548
properties of pentavalent, photoelectrochemical, 20: 5548
URANIUM ISOTOPES U-233
neutron capture-to-fission ratios in EBR-II, (E), 20: 6280(R) (ANL-6925 (p.249-51))
neutron fission of, fragment kinetic energies from, (T), 20: 6421
neutron sensitivity of foil-glass dosimeters of, 20: 5713 (AD-623384)
URANIUM ISOTOPES U-234
content in uranium deposits, ratio to uranium-238, 20: 5660
URANIUM ISOTOPES U-235
alpha decay of, thorium-231 level scheme from, (E), 20: 6388
analysis of irradiated, for cesium and molybdenum, 20: 5493(R) (ANL-6925, pp 253-4)
fission of, yields of molybdenum and ruthenium isotopes from, 20: 5493(R) (ANL-6925, pp 253-4)
neutron capture-to-fission ratios in EBR-II, (E), 20: 6280(R) (ANL-6925 (p.249-51))
neutron capture-to-fission cross sections for, measurement of, 20: 6296(R) (ORNL-3858(Vol.1), pp 1-12)
neutron fission of, yields from thermal, (E), 20: 6288 (KAPL-3113)
neutron fission of, fragment kinetic energies from, (T), 20: 6421
neutron fission of, prompt gamma rays from, thermal, 20: 6314
neutron fission of, delayed gamma emission from, (E), 20: 6316
neutron fission ratio in SGR lattices, epicadmium/subcadmium, (E), 20: 6586 (NAA-SR-Memo-11313)
neutron sensitivity of foil-glass dosimeters of, 20: 5713 (AD-623384)
URANIUM ISOTOPES U-238
content in uranium deposits, ratio to uranium-234, 20: 5660
neutron absorption integrals for, infinite-dilution, (E), 20: 6558(R) (ANL-7115, pp 42-67)
neutron capture-to-fission ratios in EBR-II, (E), 20: 6280(R) (ANL-6925 (p.249-51))
photofission at 10 to 15 Mev, delayed neutron emission from, (E), 20: 6315
photofission below 10 Mev, angular distributions from, (E), 20: 6309(T) (ANL-Trans-245)
use in fusion reactor blankets, 20: 6453 (AD-619670)
URANIUM NITRIDES
preparation from oxide, 20: 5843
preparation of microspheres of, by sol-gel method, 20: 5864 (ORNL-3879)
thermal decomposition pressure of mononitride, 20: 5843
thermal expansion of fuels of, during fast burst accident, 20: 6602 (BNWL-SA-346)
wetting by sodium at 255°C, contact angles in, 20: 5594(R) (ANL-6925, pp 21-106)
Fe–UN, preparation of fuel dispersions of, 20: 5843
URANIUM ORES
mining of, health hazards and protection in, 20: 5428
URANIUM OXIDES
inhalation by animals and man, effects of, 20: 5237(R) (UR-668, pp 55-109)
URANIUM OXIDES (STAINLESS STEEL CLAD)
processing by destructive oxidation and fluorination, 20: 5595(R) (ANL-6925, pp 107-64)
reactions with steam at high temperatures, 20: 6552(R) (ANL-6925, pp 187-233)
URANIUM OXIDES (Zr ALLOY CLAD)
reactions with steam at high temperatures, 20: 6552(R) (ANL-6925, pp 187-233)
URANIUM(IV) OXIDES
combustion reactions in alumina fluidized bed, acid leaching separation of uranium from, 20: 5500 (ORNL-3876)
compatibility with Incoloy and Zircaloy-2 at 475 to 1200°C, 20: 5914(R) (GEAP-3771-17)
compatibility with SAP 930 to 525°C, 20: 5839(R) (RISO-110)
critical masses of enriched arrays of, 20: 6584 (LA-DC-7248)
diffusion of xenon in, at 1000 to 1800°C activation energy for, 20: 5843
diffusion of, fission from single-crystal, 20: 5843
effects of inhaled, five-year study on animals, 20: 5251(R) (UR-668, pp 123-49)
excretion and lung burden in rats exposed to aerosols of, 20: 5251(R) (UR-668, pp 123-49)
fabrication of compact particles of, method for, 20: 5869(P)
fission gas diffusion from cored pellet and vibratory compacted powder fuel rods of, 20: 5914(R) (GEAP-3771-17)
fission gas diffusion from cored pellet fuels of, at 1530 and 1680°C, 20: 5914(R) (GEAP-3771-17)
fission gas diffusion in, effects of density on, 20: 5848
fission product distribution in fuel rods of, irradiated with gross central melting, 20: 5914(R) (GEAP-3771-17)
fission product distribution and related microstructure of irradiated, 20: 5848
formation of uranium in, irradiated at high temperatures, 20: 5843
meltdown of stainless steel- and Zircalloy-2-clad, in TREAT, 20: 6576(R) (ANL-7105, pp 72-84)
microstructure at solid-liquid interface after heat treatment at 2900°C, 20: 5914(R) (GEAP-3771-17)
microstructure of vibratory compacted powders of, effects of heat treatments at 1900, 2000, and 2600°C on, 20: 5914(R) (GEAP-3771-17)
oxygen diffusion in single crystals of, (E), 20: 5882(R) (EURAEC-1454)
performance of fuel rods of, operated with gross central melting to high burnups, 20: 5914(R) (GEAP-3771-17)
physical properties of single crystals of, (E), 20: 5882(R) (EURAEC-1454)
preparation of fuel bodies of, 20: 5843
preparation of pellets and spherical particles of, 20: 5848
preparation of vibratory compactable powders of, 20: 5843
radiation effects on melting point of, 20: 5848
radioinduced lattice defects in, effects of annealing on, 20: 5848
radioinduced swelling of Harwell model for, 20: 5843
reactions with aluminum, 20: 5843
reactions with chlorine in molten alkali chlorides, thermodynamics of, 20: 5547
reactions with graphite, 20: 5843
reactions with refractory materials, kinetics of, 20: 6023(R) (AD-619379)
reactions with water in TREAT at 2250 to 3300°C, 20: 6552(R) (ANL-6925, pp 187-233)
solvent properties of molten, for krypton at 2900°C, 20: 5914(R) (GEAP-3771-17)
solvent properties for helium, 20: 5843
steam effects on oxygen/uranium ratio of, 20: 6559(R) (ANL-7115, pp 77-83)
thermal conductivity, 20: 5848
thermal conductivity of hypostoichiometric, at 400 to 2400°C, 20: 5914(R) (GEAP-3771-17)
thermal expansion of fuels of, during fast burst accident, 20: 6602 (BNWL-SA-346)
thermal expansion of single-crystal, at 300 to 1600°C, 20: 5843
thermodynamic properties of hypostoichiometric, 20: 6558(R) (ANL-7115, pp 42-67)
vapor pressure at 1500 to 2800°K, 20: 5848
wetting by sodium at 210°C, contact angles in, 20: 5594(R) (ANL-6925, pp 21-106)
Al–UO_2, fabrication of powder-compacted slugs of, 20: 5866
BeO–UO_2, creep at 1375 to 1540°C, effects of grain size and stress on, 20: 5904
CeO_2–UO_2, effects of cerium dioxide content on sintering behavior of mechanically mixed, 20: 5889 (NUMEC-2389-8)
Fe–UO_2, preparation of fuel dispersions of, 20: 5843
Mg–UO_2, properties in dispersion type fuel elements, 20: 6684
PuO_2–UO_2, effects of plutonium dioxide content on sintering behavior of mechanically mixed, 20: 5889 (NUMEC-2389-8)
PuO_2–UO_2, fabrication of fuel rods of, by vibrational compaction, 20: 5867
PuO_2–UO_2, fluorination in fluidized-beds, equipment and procedures for, 20: 5595(R) (ANL-6925, pp 107-64)
PuO_2–UO_2, processing of irradiated, by fluoride volatility, 20: 5595(R) (ANL-6925, pp 107-64)
PuO_2–UO_2, thermal expansion of coprecipitated powders of, 20: 5890 (NUMEC-2389-9)
Pu–UO_2–H_2O, criticality studies, 20: 6607(R) (GEAP-4965)
Re–W–UO_2, compatibility of, 20: 6596(R) (GEST-2049)
stainless steel–UO_2, fabrication by roll bonding of, clad with stainless steel, 20: 5866
stainless steel–UO_2, preparation of fuel plates of, 20: 5843
stainless steel–UO_2, preparation of dispersions of, 20: 5848
stainless steel–UO_2, thermal cycling between 50 and 800°C, 20: 5848
ThO_2–UO_2, preparation by sol-gel process, 20: 5843
ThO_2–UO_2, radiation effects on properties of, for use as nuclear fuels, 20: 5915(R) (ORNL-P-1724)
ThO_2–UO_2, separation of products from fluidized-bed combustion of, by acid leaching, 20: 5500 (ORNL-3876)
UC_2–UO_2, phase studies, 20: 5848
U–UO_2, phase diagram and thermodynamics of, 20: 5877 (ANL-7048)
U–UO_2, phase studies, 20: 5875(R) (ANL-6925, pp 165-74)
U–UO_2, thermodynamic properties of, effusion, spectral, and vapor pressure studies of, 20: 5875(R) (ANL-6925, pp 165-74)
W–UO_2, preparation and properties of dispersions of, 20: 5843
URANIUM(IV-VI) OXIDES

reactions with aluminum, 20: 5848
PuO_2–U_3O_8, fluorination in fluid beds, equipment and procedure for, 20: 5595(R) (ANL-6925, pp 107-64)
URANIUM PHOSPHIDES
wetting by sodium at 260°C, contact angles in, 20: 5594(R) (ANL-6925, pp 21-106)
ThP–UP, melting points, 20: 5848
URANIUM SILICIDES
Al–U_3Si, properties of dispersions of, 20: 5843
URANIUM SULFIDES
combustion with fluorine, equipment for testing, 20: 5523(R) (ANL-6925, pp 175-85)
thermal expansion of fuels of, during fast burst accident, 20: 6602 (BNWL-SA-346)
wetting by sodium at 240°C, contact angles in, 20: 5594(R) (ANL-6925, pp 21-106)
URANIUM SYSTEMS
Al–polyethylene–U, neutron multiplication in borated, 20: 6577(R) (BNWL-149, pp 22-35)
C–Mo–U, phase studies, 20: 5843
C–Pu–U, preparation techniques, 20: 5843
C–Pu–U, properties, 20: 5843
C–Ta–U, phase studies, 20: 5843
C–U, properties for use as reactor fuel cores, 20: 5887 (NLCO-953)
Fe–Si–U, crystal structure of U_2Fe_3Si, 20: 5848
H–U, diffusivity, (T), 20: 5983 (D-910099-2)
U–UO_2, phase diagram and thermodynamics of, 20: 5877 (ANL-7048)
U–UO_2, phase studies, 20: 5875(R) (ANL-6925, pp 165-74)
U–UO_2, thermodynamic properties of, effusion, spectral, and vapor pressure studies of, 20: 5875(R) (ANL-6925, pp 165-74)
U–US, phase studies, 20: 5875(R) (ANL-6925(p.165-74))
U–US, phase studies, 20: 5875(R) (ANL-6925(p.165-74))
URANYL FLUORIDES
critical dimensions of enriched arrays of, 20: 6588(R) (ORNL-3858 (Vol.1), pp 13-19)
critical masses and reactivities of enriched aqueous, 20: 6587 (NASA-TN-D-3097)
URANYL IONS
reactions with hydrogen peroxide in presence of oxalate ions, 20: 5549
reactions with nucleotides, 20: 5237(R) (UR-668, pp 55-109)
URANYL NITRATE COMPLEXES
with urea preparation and properties of, 20: 5545
URANYL NITRATES
corrosive effects on austenitic stainless steels, 20: 5846
reduction and fluorination, 20: 5870(P)
decane–$UO_2(NO_3)_2$, radiation effects on coalescence rates in liquid, 20: 5571 (ORNL-TM-1283)
heptane–$UO_2(NO_3)_2$, radiation effects on coalescence rates in liquid, 20: 5571 (ORNL-TM-1283)
hexane–$UO_2(NO_3)_2$, radiation effects on coalescence rates in liquid, 20: 5571 (ORNL-TM-1283)
Na_2CO_3–$UO_2(NO_3)_2$, criticality of aqueous solutions of, 20: 5666 (TID-21995)
URANYL PHOSPHATES
corrosive effects on austenitic stainless steels, 20: 5846
UREA
N-nitroso-N-methyl-, effects on presoaked Arabidopsis seeds, mutagenic, 20: 5357
UREA, [3-(CHLOROMERCURI)-2-METHOXYPROPYL]-
metabolism of mercury-203-labeled, 20: 5251(R) (UR-668, pp 123-49)
UREA COMPLEXES
with uranyl nitrate, preparation and properties of, 20: 5545
URINE
analysis for lead-210, radiochemical, 20: 5505
processing aboard space vehicles, using electric-power plants, (E/T), 20: 5820 (NASA-CR-316)
specific activity of, in radiocalcium-injected dog, 20: 5237(R) (UR-668, pp 55-109)
UTAH
fallout monitoring, 1963, 20: 5649(R) (COO-1340-2, pp 54-83)
UTERUS
radiotherapy of cancer in, advantages of mega- and supervoltage for, 20: 5451
radiotherapy of cancers of, 20: 5473
radiotherapy of carcinomas of, 20: 5457
radiotherapy of carcinomas of, effects of estrogen treatment on, 20: 5472

V

VACUUM
electric breakdown current in high, 20: 6169
VACUUM GAGES
performance below 10^{-10} torr, 20: 5641
VACUUM SEALS
design for photomultiplier tubes, 20: 5787
VACUUM VALVES
design of gate, for ALICE magnetic mirror device, engineering drawings of, 20: 6513
design of pulsed gas, for plasma studies, 20: 5642
VAGINA
radiotherapy of carcinomas of, 20: 5457
VALVES
design for gas injection in plasma studies, 20: 5642
VAN ALLEN RADIATION BELTS
electron injection into artificial, from Starfish explosion, 20: 6209
proton distribution in, altitude and time dependence of 55-Mev, (E), 20: 6200
VAN DE GRAAFF ACCELERATORS
data processing system for tandem, design of, 20: 5939 (LA-DC-7267)
description of, at installations in India, 20: 5715 (AEET-227
radiation monitor system for large, audio-visual warning, 20: 5733 (LA-DC-6790)
VANADIUM
compatibility with plutonium-uranium carbides, 20: 6600(R) (ANL-7105, pp 1-35)
optical properties of small particles of, (T), 20: 5879 (D-910092-6)
proton reactions (p,n) at 30 and 50 Mev, isobaric-state excitation in, (E/T), 20: 6361
separation from aqueous solutions by extraction using organo-phosphorus solutions, 20: 5605(P)
strain aging and transition temperature in, effects of nitrogen on, 20: 5851
VANADIUM ALLOYS
corrosive effects of sodium on binary, 20: 6601(R) (ANL-7115, pp 1-41)
Al–Mo–Ti–V, phase studies, 20: 5851
Cr–Nb–Ti–V, properties as cladding materials, 20: 5846
Cr–Ti–V, corrosion by flowing sodium at 650°C, effects of chromium content on, 20: 5851
Cr–Ti–V, creep rate of, 20: 6601(R) (ANL-7115, pp 1-41)
Cr–Ti–V, elastic properties, 20: 6556(R) (ANL-7105, pp 36-58)
Mo–Nb–V–Zr, bonding of B-66, method for diffusion, 20: 5867
Mo–Nb–V–Zr, corrosion by cesium vapor and liquid lithium at 2500 to 3400°F of B-66, 20: 5851
Mo–Nb–V–Zr, weld stability in B-66, 20: 5866
Mo–Nb–V–Zr, welding parameters for B-66, electron-beam, 20: 5867
Mo–Ti–V, elastic properties, 20: 6556(R) (ANL-7105, pp 36-58)
Nb–Ti–V, elastic properties, 20: 6556(R) (ANL-7105, pp 36-58)
Ta–Ti–V, elastic properties, 20: 6556(R) (ANL-7105, pp 36-58)
Ti–V, compatibility with plutonium-uranium carbides, 20: 6600(R) (ANL-7105, pp 1-35)
Ti–V, corrosion of TV-20, by sodium at 650°C, 20: 5846
Ti–V, reactions with fissium–plutonium–uranium alloy at 550 to 700°C, 20: 5843
Ti–V, removal from fuel elements by chlorination, 20: 5594(R) (ANL-6925, pp 21-106)
VANADIUM COMPLEXES
with tropolone, preparation, properties, and structure, 20: 5538
VANADIUM STEEL
Cr–Mo–Ni–Nb–V, development as HY-180/210 steel, 20: 5851
VANADIUM SYSTEMS
Al–C–V, superconductivity of V_2AlC, 20: 6228
VEHICLES
design of motor, for protection from fallout, 20: 5679(P)
VELA PROJECT
surface radiation and weather prediction activities for Salmon Event, 20: 5667 (VUF-1020)
VESSELS
decontamination and dismantling of radioactively contaminated containers, glove box for, 20: 5711(P)
remote opening of metal, use of lasers for, 20: 5669
VIRUSES
radiation effects on plant, biological, 20: 5310
radiation effects on bacterial reactions to, target theory for γ and x, 20: 5299(R) (TID-22187)
radiosensitivity of *Herpes simplex*, effects of bromouracildesoxyriboside and iodouracildesoxyriboside on, 20: 5363
size measurements for, use of radioinduced inactivation for, 20: 5310
VISCOMETERS
development for fused salts and liquid metals, 20: 5594(R) (ANL-6925, pp 21-106)
VITAMIN B
radiation effects on bacterial metabolism of, y, 20: 5346
VITAMIN B_2
radiation effects on blood content of, in dogs, x, 20: 5384
VITAMIN B_{12}
effects on radioinduced alopecia, 20: 5484

VITAMIN D
effects on calcium metabolism in chickens, 20: 5237(R) (UR-668, pp 55-109)

W

WASTE DISPOSAL
methods at National Institute of Radiological Science in Chiba, Japan, 20: 5672
WASTE PROCESSING
for plutonium recovery, 20: 5595(R) (ANL-6925, pp 107-64)
WASTE SOLUTIONS
analysis for lead-210, radiochemical, 20: 5505
WATER
analysis for tritium, method for, 20: 5517
analysis for tritium, survey of concentration and counting methods for, 20: 5521
corrosive effects on beryllium, 20: 6666(R) (ANL-7115, pp 68-77)
corrosive effects on beryllium at 100 and 120°C, 20: 5844
corrosive effects on type 1100 aluminum alloy, methods of inhibiting, 20: 5846
corrosive effects on low-alloy and stainless steels, effects of surface treatments on, 20: 5846
corrosive effects on Zircaloy-2 powders at 680°F, effects of nitrogen and oxygen additions on, 20: 5851
determination in building materials by neutron absorption, gage for, 20: 5819
deuterium exchange with isobutyraldehyde, effects of acids, amines, and oxygen bases on, 20: 5565
effects on energy transfer in proteins, 20: 5270
effects on yields of hydrogen peroxide from radiolysis of methanol, 20: 5581
flow patterns for peripherally injected, in vortex tubes, 20: 6653 (D-910091-7)
gamma backscattering from spherical surfaces of, at 0.7 and 1.25 Mev, (E), 20: 6525
gamma heating in, calculations for, (E/T), 20: 6517 (CONF-651101-41)
gamma scattering at 4.0 Mev in barriers of, intensity angular distribution of, (T), 20: 6526
gamma scattering by duct in, streaming in, (T), 20: 6530
hydrogen bonding in, infrared spectral study of, 20: 5552
neutron reflection by surfaces of, absorbed dose in air from, (T), 20: 6528
neutron scattering by, angular distributions and diffusion constants from thermal, (E), 20: 6270
nitrogen-16 distribution between steam and, in boiling reactors, 20: 6638
processing aboard space vehicles, using electric-power plants, (E/T), 20: 5820 (NASA-CR-316)
purification of reactor coolant, electrophoretic filter for, 20: 6568
radiolysis of shielding, for high-power gamma facility, 20: 5670
radiosensitivity effects on mutagenesis in Arabidopsis, x, 20: 5357
reactions with hydrated electrons, review on, 20: 5525 (IA-1041)
reactions with molybdenum at 1100 to 1700°C, 20: 5846
reactions with Zircaloy-2 during meltdown experiments, 20: 5843
solvent properties for cerium, cobalt, and promethium sorbed on charcoal powders, 20: 5675
solvent properties for iodine at 5 to 50°C, 20: 5539
use of fluoridated, in hemodialysis, 20: 5237(R) (UR-668, pp 55-109)
air–water, momentum flux measurement by impulse method for flow of, 20: 5624 (MIT-3496-1)
Al–H_2O, gamma heating in, calculations for, (E/T), 20: 6517 (CONF-651101-41)
benzene–ethanol–H_2O, use in paper chromatography of compounds labeled with iodine-125 and iodine-131, 20: 5515
benzene–H_2O, radiation effects on coalescence rates in liquid, 20: 5571 (ORNL-TM-1283)
Fe–H_2O, gamma heating in, calculations for, (E/T), 20: 6517 (CONF-651101-41)
He–H_2O, corrosive effects on nickel-base alloys at 1700, 1900, and 2100°F, 20: 5846
H_2O–Zr, gamma heating in, calculations for, (E/T), 20: 6517 (CONF-651101-41)
methanol–H_2O, use in paper chromatography of compounds labeled with iodine-125 and iodine-131, 20: 5515
Ni–H_2O, gamma heating in, calculations for, (E/T), 20: 6517 (CONF-651101-41)
Pb–H_2O, gamma heating in, calculations for, (E/T), 20: 6517 (CONF-651101-41)
Pu–UO_2–H_2O, criticality studies, 20: 6607(R) (GEAP-4965)
steam–H_2O, momentum flux measurement by impulse method for flow of, 20: 5624 (MIT-3496-1)
steam–water, corrosive effects on Zircaloy-2, 20: 6566(R) (EURAEC-1382)
steam–water, heat transfer and pressure drop data for flow in round vertical tubes, 20: 5623 (EURAEC-1325)
steam–water, heat transfer and hydrodynamics in mixtures of, 20: 6566(R) (EURAEC-1382)
WATER-d_2
effects on neutral red uptake by frog sartorius muscle, 20: 5317
hydrogen bonding in, infrared spectral study of, 20: 5552
neutron scattering by, angular distributions and diffusion constants from thermal, (E), 20: 6271
radiolysis in boiling reactors, effects of ammonia and deuterium on, 20: 6638
solvent properties for iodine at 5 to 50°C, 20: 5539
WATER-t
reaction with hydrocarbons to produce radioactive hydrocarbons, 20: 5593(P)
WATER-t_2
uptake of, by rabbit eye lens in culture, 20: 5256
WATER COOLED REACTORS
coolant purification for, electrophoretic filter for, 20: 6568
cooling system for, development of steam–water spray, 20: 6566(R) (EURAEC-1382)
criticality parameters of, 20: 6582 (EUR-2461.f)
fuel and fuel cycle parameters of, 20: 6582 (EUR-2461.f)
fuel channel vibration in, hydro-flutter theory of self-excited, 20: 6564
WATER MODERATED REACTORS
criticality parameters of, 20: 6582 (EUR-2461.f)
design using combined graphite moderation, 20: 6592(P)
fuel and fuel cycle parameters of, 20: 6582 (EUR-2461.f)
WATER PURIFICATION EQUIPMENT
design and performance of electrophoretic, for reactor coolants, 20: 6568
use of chemonuclear reactors for ozone production, 20: 5568 (BNL-9664)
WATER SUPPLIES
radiation control of *Entamoeba histolytica* in, 20: 5366
radioactivity in, of Great Britain, 20: 5409
WATER VAPOR
deuterium exchange with hydrogen, properties of chromium trioxide–nickel catalyst for, 20: 5534
WATER WAVES
buoy dynamics from, submerged, (T), 20: 6686(R) (NVO-98-12)
WELDED JOINTS
design for Zircaloy-4 tubes, end closure, 20: 5865 (WCAP-3269-37)
WELDING
development of filler materials and procedures for, high-strength low-alloy steels, 20: 5867
method for reactor fuel elements and end enclosures, 20: 5868(P)
refractory metals, facility for, 20: 5867
refractory metals, parameters for electron-beam, 20: 5867
WELDING RODS
cooling resistance-, method for, 20: 5867
WELDS
production methods for, in Incoloy 800 and Inconel 600 and 625, (E), 20: 6624 (TID-22425)
WELL LOGGING
equipment for, scintillation, 20: 5658(P)
WHEAT
effects on development and growth of irradiated bean lipid, 20: 5265(T)
radiation effects on seeds of, genetic, x, 20: 5403
WHISTLERS
propagation of, interpretation of, (T), 20: 6207
use for determining helium and hydrogen ion distribution in magnetosphere, (E), 20: 6198
WIND
prediction of activities of, for Salmon Event, 20: 5667 (VUF-1020)
WOOD
radioinduced polymerization of monomer impregnated, to produce wood-plastic combination, 20: 5818
WYOMING
fallout monitoring, 1963, 20: 5649(R) (COO-1340-2, pp 54-83)

X

X AGENT
effects on kaolin colloids, 20: 5587
X RADIATION
absorption of, fabrication of strontium filters for, 20: 5692
alopecia induced by therapeutic doses to head, effects of vitamin B_{12} on, 20: 5484
dose absorbed by man of, during diagnostic radiography, 20: 5440
dose received by urologist, from retrograde pyelogram examinations, 20: 5459
dose to children of, from radiographic diagnosis of congenital heart disease, 20: 5455

dose to dentists during radiography, 20: 5430
dose to gonads of, from therapy of dermatological diseases in man, 20: 5445
dosimetry of therapeutic doses, use of phantoms for, 20: 5481
dosimetry of, for cancer therapy, 20: 5439
dosimetry of, for therapeutic use, 20: 5478
dosimetry of, for therapy of lymphosarcomas, 20: 5485
effects on activity of alkaline phosphatase in human leukocytes, 20: 5269
effects on adaptive response of rats, 20: 5319
effects on animal cells in tissue culture, protective effects of cysteine and MEA on, 20: 5418
effects on animal cells in tissue culture, protective effects of aminoethylisothiuronium on, 20: 5419
effects on animals and man, 20: 5301(R) (UR-668, pp 1-54)
effects on bacterial reactions to phages and viruses, target theory for, 20: 5299(R) (TID-22187)
effects on behavior of larvae of *D. melanogaster*, 20: 5295 (NP-15559)
effects on blood coagulation in rabbits, 20: 5325
effects on blood coagulation and blood plasma, 20: 5365
effects on blood picture in rabbits, 20: 5325
effects on bone marrow in mice, pathological, 20: 5320
effects on cervical and bladder cancer, mega- and supervoltage *vs.* kilovoltage, 20: 5451
effects on chick embryos from eggs exposed to, 20: 5306
effects on chromosomes in leukocytes in humans, monkeys, and rabbits, 20: 5304(T) (JPRS-32985, pp 45-50)
effects on coaxial cables and electric condensers, method for reduction of, 20: 5805(R) (AD-617782)
effects on collagen in skin of hamsters, 20: 5330
effects on developing fetuses, pathological, 20: 5476
effects on development of axial skeleton and spinal cord in salamanders, 20: 5312
effects on DNA catabolism in rats, 20: 5382
effects on dogs, combined effects of trauma, 20: 5302(R) (UR-668, pp 161-6)
effects on Drosophila, genetic, 20: 5338
effects on Drosophila, genetic, 20: 5358
effects on estrone in acetic acid, chemical, 20: 5274
effects on fibrinolysis in rabbits, whole-body, 20: 5325
effects on free lipid fraction in bean sprouts, biochemical, 20: 5265(T)
effects on gadolinium doped calcium fluoride, preferential emission in afterglow of, (E), 20: 6550
effects on gastric juice secretion and enzyme activity in dogs, 20: 5384
effects on giant cell formation in RCP cell strain, 20: 5323
effects on glycine peptides of, chemical, 20: 5273
effects on gonads of viviparous lizard embryos, biological, 20: 5324
effects on grain weevils, effects of oxygen concentration and temperature, 20: 5385
effects on growth of thymus transplants in mouse kidney, 20: 5376
effects on guinea pigs, effects of pre-irradiation on lethal, 20: 5356
effects on hematopoietic system of rabbits, fractionated exposures, 20: 5364
effects on human chromosomes, aberrant, 20: 5351
effects on immune reactions in thymectomized mice, 20: 5408 (USNRDL-TR-920)
effects on immune reactions in mice, 20: 5413
effects on immune reactions to marrow transplants in mice, methods for assaying, 20: 5372
effects on induction of leukopenia in rabbits, 20: 5315
effects on intestinal cells of hedgehog, effects of hibernation on histologic, 20: 5377
effects on leukemic cells in mice, 20: 5368
effects on life span of hamsters, 20: 5330
effects on life span of house fly, *Musca domestica*, 20: 5331
effects on life span of mice, computer program for evaluation of, 20: 5300 (UCLA-12-573)
effects on luminescence of lymphocytes, 20: 5383
effects on luminescence of thallium-activated cesium iodide and sodium iodide phosphors, (E), 20: 6537
effects on luminescence of acridine-orange-stained Tetrahymena, 20: 5267
effects on man, protective effects of bone marrow grafts, 20: 5420
effects on meiotic stages in Artemia oocytes, 20: 5359
effects on metabolism in lens of cattle and guinea pigs, effects of age, 20: 5333
effects on metabolism in rat kidney tissue sections, 20: 5352
effects on metabolism of calcium and sulfur, tracer study in rat bones, 20: 5370
effects on mice, circadian rhythmicity of, 20: 5336
effects on mice, effects of age, dose, and sex on leukemogenic, 20: 5367
effects on mice, protective effects of mercaptoethylamine, 20: 5407(R) (AD-623599, pp 37-44)
effects on mitosis in mouse cornea, 20: 5421
effects on mitosis in RCP cell strain, 20: 5323
effects on motivation in rats, humoral factor in, 20: 5303 (USNRDL-TR-925)
effects on murine leukemia cells in vitro, survival curves for, 20: 5361
effects on nucleoproteins in Tetrahymena, 20: 5267
effects on oxygen uptake by *Tenebrio molitor*, 20: 5314
effects on *Paramecium aurelia*, effects of streptomycin on recovery from mutagenic, 20: 5417
effects on peas, genetic, 20: 5238
effects on phosphorus metabolism in glioma cultures, 20: 5255
effects on photosynthetic reactions in isolated chloroplasts, 20: 5402
effects on physiological properties of cysteine-treated mouse ascitic cell and normal tissue homogenates, 20: 5412
effects on polycythemia, therapeutic, 20: 5483
effects on presoaked Arabidopsis seeds, mutagenic, 20: 5357
effects on rats, biochemical, 20: 5341
effects on rats, morphological, 20: 5341
effects on rats, pathological, 20: 5411
effects on red clover, morphological and mutagenic, 20: 5491
effects on reproduction, Drosophila, 20: 5296(R) (NP-15585)
effects on respiration in rat thymocytes in culture, 20: 5340
effects on riboflavin content in blood of dogs, 20: 5384
effects on rice seeds, genetic, 20: 5393
effects on Saccharomyces radiosensitivity, mutagenic, 20: 5360
effects on sebaceous glands in hamsters, 20: 5322
effects on skeletal development of mouse embryos, 20: 5395
effects on skeletal development in mouse embryos, 20: 5316
effects on skeletal development of mouse embryos, 20: 5326
effects on skeletal development in mouse embryos, 20: 5327
effects on skeletal development in mouse embryos, 20: 5337
effects on subsequent pharyngo-laryngectomy, 20: 5463
effects on synthesis of hepatic microsomal enzymes in rats, 20: 5282(R) (AD-623599, pp 1-15)
effects on synthesis of hepatic microsomal enzymes in rats, 20: 5283(R) (AD-623599, pp 16-27)
effects on take of skin homografts in rats, 20: 5335
effects on thrombocytes, effects of suspension media on, 20: 5365
effects on thymidine metabolism in intestinal epithelium of goldfish, effects of temperature on, 20: 5374
effects on tumor of head, therapeutic, 20: 5484
effects on urinary excretion of thymidine by rats, 20: 5382
effects on wheat seeds, genetic, 20: 5403
excitation of nitrogen by, spectra of first negative and second positive band, (E), 20: 6181 (AD-619288)
measurement in dogs using silver-activated glass rods, 20: 5745(R) (UR-668, pp 117-23)
production by californium-252 fission, timing of, (E), 20: 6298(R) (PPAD-2137-566)
use for therapy of tumors of head and neck, 20: 5441
use for therapy of bladder cancers, 20: 5454
use for therapy of cervical carcinomas, effects of estradiol, 20: 5472
use for therapy of ear cancers, 20: 5474
use for therapy of carcinomas of larynx, 20: 5486
use in medical diagnosis and therapy, review, 20: 5434
use in therapy of lymphosarcomas, 20: 5485

X-RAY CAMERAS
collimator and shutter coupling for, 20: 5693
filters for, fabrication of strontium, 20: 5692

X-RAY EQUIPMENT
design for use in urethrographic examinations, 20: 5459

X-RAY SHIELDING
evaluation of, for diagnostic radiography, 20: 5677

XENON
diffusion in spherical uranium dicarbide particles, coefficient for, 20: 5848
diffusion in urania single crystals at 1000 to 1800°C, activation energy for, 20: 5843
diffusion in uranium, effects of heating on coefficient of, 20: 5848
effects on radiolysis of ethylene, 20: 5582
electron and ion densities and temperatures in high-pressure plasma of, 20: 6480
electron reactions with, ionization cross sections for, (E/T), 20: 5989

XENON ISOTOPES Xe-127
decay of, gamma angular correlations in, (E), 20: 6384

XENON ISOTOPES Xe-129
production in meteorites, mechanisms for, 20: 5978

XENON ISOTOPES Xe-135
content in reactors, reactivity effects of oscillations in, (T), 20: 6590

XENON ISOTOPES Xe-137
yield from californium-252 fission, (E), 20: 6298(R) (PPAD-2137-566)

XENON ISOTOPES Xe-138
yield from californium-252 fission, (E), 20: 6298(R) (PPAD-2137-566)

XENON ISOTOPES Xe-139
yield from californium-252 fission, (E), 20: 6298(R) (PPAD-2137-566)
XENON ISOTOPES Xe-140
yield from californium-252 fission, (E), 20: 6298(R) (PPAD-2137-566)
XENON ISOTOPES Xe-141
yield from californium-252 fission, (E), 20: 6298(R) (PPAD-2137-566)
XENON ISOTOPES Xe-142
yield from californium-252 fission, (E), 20: 6298(R) (PPAD-2137-566)
XENON ISOTOPES Xe-143
yield from californium-252 fission, (E), 20: 6298(R) (PPAD-2137-566)
XENON SYSTEMS
H–Xe, electric discharges in multi-cathode, 20: 6168
XYLENE
effects on activity of leukocyte alkaline phosphatase, toxicity, 20: 5269
electron reactions in ethylene mixture, cross sections for momentum transfer and drift velocities in, 20: 5985 (ORNL-TM-1262)
uses as medium for drifting lithium into germanium, (E), 20: 5702
XYLENOL ORANGE
analytical uses in determination of fluorides by titration using uranium, 20: 5520

Y

YANKEE POWER REACTOR
vapor container systems of, leakage monitoring in, (E), 20: 6631 (YAEC-1005)
YEASTS
alkali metal ion transport in, mechanisms of, 20: 5251(R) (UR-668, pp 123-49)
content of potassium and sodium in growing, 20: 5251(R) (UR-668, pp 123-49)
invertase production in, mechanisms, 20: 5251(R) (UR-668, pp 123-49)
metabolism of cytochrome *c* in, factors affecting, 20: 5251(R) (UR-668, pp 123-49)
radiation damage in cells of, effects of membranes on, 20: 5251(R) (UR-668, pp 123-49)
radio- and chemically-induced mutations for radioresistance in, β, uv, and x, 20: 5360
YTTERBIUM
alpha reactions (α,xγ) at 27 to 52 Mev, gamma spectra from, (E), 20: 6348
oxidation of, kinetics of high-temperature, 20: 5859
YTTERBIUM ALLOYS
Au–Yb, oxidation of, kinetics of high-temperature, 20: 5859
YTTERBIUM ISOTOPES Yb-166
energy levels of, rotational, (E), 20: 6348
YTTERBIUM ISOTOPES Yb-168
energy levels, (E), 20: 6366
energy levels of, rotational, (E), 20: 6348
YTTERBIUM ISOTOPES Yb-170
energy levels of, rotational, (E), 20: 6348
YTTERBIUM ISOTOPES Yb-172
energy levels of, rotational, (E), 20: 6348
YTTERBIUM ISOTOPES Yb-173
energy level transitions in, E2/M1 mixing ratios and K conversion coefficients in rotational, (E), 20: 6386
YTTERBIUM OXIDES
phase transformations in, at 50 to 1500°C, 20: 5536
YTTRIUM
combustion with fluorine, products and yields from, 20: 5523(R) (ANL-6925, pp 175-85)
determination in mixtures of actinides and fission products by paper chromatography, 20: 5509
determination in presence of aluminum, arsenate method for iodometric, 20: 5506
diffusion of carbon, nitrogen, and oxygen in, at 1235 to 14600°C in electric field, 20: 5599
effects on hot hardness of zirconium oxides, 20: 5846
oxidation of, kinetics of high-temperature, 20: 5859
reactions with physiological ligands, 20: 5237(R) (UR-668, pp 55-109)
separation from molten magnesium–zinc alloys by fused chloride extraction, 20: 5594(R) (ANL-6925, pp 21-106)
separation of interstitial impurities from by electrotransport, 20: 5599
YTTRIUM ALLOYS
Au–Y, oxidation of, kinetics of high-temperature, 20: 5859
Ce–Y, electric conductivity at low temperatures, 20: 5888 (NP-15592)
Dy–Y, electric conductivity at low temperatures, 20: 5888 (NP-15592)
Er–Y, electric conductivity at low temperatures, 20: 5888 (NP-15592)
Gd–Y, electric conductivity at low temperatures, 20: 5888 (NP-15592)
Hf–Nb–W–Y, welding parameters for C-129Y, electron-beam, 20: 5867
Ho–Y, electric conductivity at low temperatures, 20: 5888 (NP-15592)
La–Y, electric conductivity at low temperatures, 20: 5888 (NP-15592)
Lu–Y, electric conductivity at low temperatures, 20: 5888 (NP-15592)
Nd–Y, electric conductivity at low temperatures, 20: 5888 (NP-15592)
Pr–Y, electric conductivity at low temperatures, 20: 5888 (NP-15592)
Ta–W–Y, corrosion by iron–plutonium at 700°C, effects of yttrium content on, 20: 5846
Tb–Y, electric conductivity at low temperatures, 20: 5888 (NP-15592)
Y–Zr, metallurgical properties and phase studies on, 20: 5891(R) (NYO-2159-1)
YTTRIUM CARBIDES
binding energy, 20: 5540
thermodynamic properties, 20: 5540
YTTRIUM COMPLEXES
with tropolone, preparation, properties, and structure, 20: 5538
YTTRIUM HYDRIDES
dissociation pressure, 20: 5844
YTTRIUM ISOTOPES
nucleon interactions in, effective, (T), 20: 6337
YTTRIUM ISOTOPES Y-90
beta and conversion-electron spectra, 20: 5768
determination of, efficiency of beta scintillation sandwich counting method for, 20: 5783
excretion of deposited, effects of EDTA in dogs, 20: 5248(R) (COO-119-232, pp 200-2)
use as beta source for therapy of hemangiomas in children, 20: 5443
use as β source for ablation of pituitary gland, 20: 5468
YTTRIUM OXIDES
phase transformations in, at 50 to 1500°C, 20: 5536
uses for dispersion strengthening of Zircaloy-2, 20: 5851
YTTRIUM SYSTEMS
H–Sc–Y, phase studies, 20: 5909

Z

ZERO POWER REACTOR (MARK II)
criticality studies in, 20: 6587 (NASA-TN-D-3097)
ZINC
determination by potentiometric titration using EDTA, equipment for, 20: 5502
effects on hydrochloric acid cleavage of organotin compounds in methanol–water, 20: 6687(R) (NYO-3453-1)
ZINC ALLOYS
Al–Zn, radiation effects on electric conductivity of, stage I and II recovery from electron, 20: 5918
Cd–Mg–Pu–Zn, stability in mild steel and stainless steel containers at 600°C, 20: 5594(R) (ANL-6925, pp 21-106)
Cd–Mg–U–Zn, corrosive effects with chloride flux on carbon steel, Croloy, and stainless steel at 600 to 650°C, 20: 5594(R) (ANL-6925, pp 21-106)
Cd–Mg–U–Zn, phase studies, 20: 5594(R) (ANL-6925, pp 21-106)
Mg–Zn, separation of plutonium from, by fused chloride extraction, 20: 5594(R) (ANL-6925, pp 21-106)
Mg–Zn, separation of californium and yttrium from, by fused chloride extraction, 20: 5594(R) (ANL-6925, pp 21-106)
ZINC ISOTOPES Zn-64
deuteron reactions (d,p), proton polarization from, (E), 20: 6422
proton reactions at 12 Mev, energy levels from, 20: 6296(R) (ORNL-3858 (Vol.1), pp 1-12)
ZINC ISOTOPES Zn-65
uptake by barley roots, mechanism for, 20: 5258
ZINC ISOTOPES Zn-66
deuteron reactions (d,p), proton polarization from, (E), 20: 6422
ZINC ISOTOPES Zn-67
deuteron reactions (d,p), proton polarization from, (E), 20: 6422
ZINC ISOTOPES Zn-68
deuteron reactions (d,p), proton polarization from, (E), 20: 6422
ZINC ISOTOPES Zn-70
deuteron reactions (d,p), proton polarization from, (E), 20: 6422
ZINC SILICATES
radioinduced luminescence of manganese-doped, energy variation of ion, 20: 5573
ZIRCALOY-2
alloy element distribution in bulk metal and oxide film on, 20: 5851
coating with copper to prevent hydrogen absorption, electrolytic, 20: 5867
compatibility with Incoloy and Zircaloy-2 at 475 to 1200°C, 20: 5914(R) (GEAP-3771-17)
corrosion by borated water at 600°F, 20: 5846
corrosion by reactor environments, effects of preoxidation on nickel-free, 20: 5851
corrosion by steam–water sprays, 20: 6566(R) (EURAEC-1382)
corrosion by steam, effects of heat treatments on, 20: 5846
corrosion by steam at 750°F or water at 680°F, effects of nitrogen and oxygen additions on, 20: 5851
corrosion by steam at 2000°F, 20: 5851
corrosion cracking by iodine at 350°C, stress-, 20: 5914(R) (GEAP-3771-

17)
creep properties at 450 to 750°F, effects of cycling stress and temperature on, 20: 5851
distribution of hydrogen in, during hydrogenation and oxidation, 20: 5851
fracture of, effects of hydride precipitates on mode of, 20: 5849
radiation effects on in-pile corrosion of, by aqueous solutions, 20: 5852(R) (EURAEC-1522)
radiation effects on tensile properties of, effects of hydrogen content on neutron, 20: 5851
reactions with water during meltdown experiments, 20: 5843
strengthening with yttria dispersions, 20: 5851
tensile properties, 20: 5846
tensile properties of hydrided, restoration of, at 100 to 200°C, 20: 5849
Cr–Zircaloy-2, corrosion cracking by iodine at 350°C, stress-, 20: 5914(R) (GEAP-3771-17)
U–Zircaloy-2, processing for uranium recovery by fluoride volatility, 20: 5595(R) (ANL-6925, pp 107-64)

ZIRCALOY-4
weld joint design for tubes of, end closure, 20: 5865 (WCAP-3269-37)

ZIRCONIUM
corrosion by cesium at 1600, 1800, and 2500°F, 20: 5846
corrosion by molten mixture of potassium and sodium chlorides, 20: 5855 (JPRS-32341, pp 24-31)
corrosion cracking by iodine at 350°C, stress-, 20: 5914(R) (GEAP-3771-17)
determination by potentiometric titration using EDTA, equipment for, 20: 5502
determination in mixtures of actinides and fission products by paper chromatography, 20: 5509
diffusion from irradiated cerium–cobalt–plutonium alloy to sodium at 550°C, 20: 5848
diffusion of iron in, 20: 5846
electrochemical properties in molten chloride eutectic, 20: 5543
electron reactions at 2.5 to 4.0 Mev, bremsstrahlung spectra from, (E), 20: 6432
gamma coherent scattering at 0.662 and 1.332 Mev, cross sections for, (E/T), 20: 6323
gamma heating in, calculations for, (E/T), 20: 6517 (CONF-651101-41)
optical properties of small particles of, (T), 20: 5879 (D-910092-6)
oxidation at 700°C, electrochemical model for, 20: 5858
oxidation resistance of, in carbon dioxide at 600 and 700°C, 20: 5860
production by electrolysis, technique for, 20: 5604(P)
proton reactions (p,n) at 30 and 50 Mev, isobaric-state excitation in, (E/T), 20: 6361
radiation effects on in-pile corrosion of, by aqueous solutions, 20: 5852(R) (EURAEC-1522)
reactions in chloride slagging of fissium–plutonium–uranium alloys, 20: 5594(R) (ANL-6925, pp 21-106)
reactions in skull reclamation processes, 20: 5594(R) (ANL-6925, pp 21-106)
reactions with steam at high temperatures, 20: 6552(R) (ANL-6925, pp 187-233)
shear stress of, effects of hydrogen and oxygen on critical resolved, 20: 5851
structure of, angular values between crystallographic planes in, 20: 5898 (WAPD-TM-519)
tensile properties of hydrided alpha-, 20: 5905
transformation of, effects of rare earths on allotropic, 20: 5891(R) (NYO-2159-1)
viscosity of liquid, to 2400°K, 20: 5899(T) (JPRS-32341, pp 1-7)

ZIRCONIUM ALLOYS
distribution of hydrogen in, during hydrogenation and oxidation, 20: 5851
electric potentials across corroding oxides on, measurement of, 20: 5851
Al–Zr, diffusion in, inter-, 20: 5851
Be–Zr, corrosion by borated water at 600°F, 20: 5846
Be–Zr, oxidation resistance of, effects of aluminum, nickel, silicon, and tantalum additions on, 20: 5844
Co–Zr, oxidation kinetics at 500 to 900°C, 20: 5854(R) (JPRS-32341, pp 8-16)
Cu–Mo–Zr, oxidation resistance of, in carbon dioxide at 600 and 700°C, 20: 5860
Cu–Nb–Zr, alloy element distribution in bulk metal and oxide film on, 20: 5851
Cu–Zr, oxidation resistance of, in carbon dioxide at 600 and 700°C, 20: 5860
Dy–Zr, metallurgical properties and phase studies on, 20: 5891(R) (NYO-2159-1)
Er–Zr, metallurgical properties and phase studies on, 20: 5891(R) (NYO-2159-1)
fissium–Pu–U–Zr, phase studies on, 20: 5876 (ANL-6974)
Gd–Zr, metallurgical properties and phase studies on, 20: 5891(R) (NYO-2159-1)
Ho–Zr, metallurgical properties and phase studies on, 20: 5891(R) (NYO-2159-1)
Lu–Zr, metallurgical properties and phase studies on, 20: 5891(R) (NYO-2159-1)
Mg–Mn–Zr, diffusion of plutonium in MAGZAN-II and ZR55, at 420, 460, and 500°C, 20: 5848
Mo–Nb–Ta–W–Zr, creep tests on NB132M at 3200°F, 20: 5885(R) (NAS-CR-54773)
Mo–Nb–V–Zr, bonding of B-66, method for diffusion, 20: 5867
Mo–Nb–V–Zr, corrosion by cesium vapor and liquid lithium at 2500 to 3400°F of B-66, 20: 5851
Mo–Nb–V–Zr, weld stability in B-66, 20: 5866
Mo–Nb–V–Zr, welding parameters for B-66, electron-beam, 20: 5867
Mo–Ti–Zr, bonding of TZM, method for diffusion, 20: 5867
Mo–Ti–Zr, brazing molybdenum to TZM, brazing alloy development for, 20: 5866
Mo–Ti–Zr, corrosion by cesium vapor and liquid lithium at 2500 to 3400°F of TZM, 20: 5851
Mo–Ti–Zr, extrusion of TZM, process for, 20: 5867
Mo–Zr, internal friction of annealed and deformed, 20: 5846
Nb–Ta–W–Zr, corrosion by lithium in niobium–1–zirconium alloy forced-convection loop, 20: 5853 (TIM-898)
Nb–Ti–Zr, bonding of D-36, method for diffusion, 20: 5867
Nb–U–Zr, properties of metastable γ-phase, 20: 5843
Nb–W–Zr, creep tests on AS-30 at 3200°F, 20: 5885(R) (NAS-CR-54773)
Nb–Zr, coating with nickel, electroless, 20: 5867
Nb–Zr, corrosion by cesium at 1600, 1800, and 2500°F, 20: 5846
Nb–Zr, electric conductivity to 1500°C, 20: 5851
Nb–Zr, emissivity to 1500°C, total hemispherical, 20: 5851
Nb–Zr, metallurgical properties and phase studies on, 20: 5891(R) (NYO-2159-1)
Nb–Zr, solubility in sodium at 800 to 1380°C, 20: 5846
Nb–Zr, solvent properties for hydrogen, 20: 5849
Nb–Zr, use as loop material for forced-convection corrosion of refractory alloys by lithium, 20: 5853 (TIM-898)
Nb–Zr, use for superconducting magnet coils, 20: 5614
Ni–Zr, oxidation kinetics at 500 to 900°C, 20: 5454(T) (JPRS-32341, pp 8-16)
O–Ta–Ti–Zr, phase studies at 1500°C, 20: 5846
Pu–U–Zr, compressive strength of, 20: 6601(R) (ANL-7115, pp 1-41)
Pu–U–Zr, phase studies, 20: 6600(R) (ANL-7105, pp 1-35)
Pu–U–Zr, tensile properties, 20: 6600(R) (ANL-7105, pp 1-35)
Pu–U–Zr, thermal expansion, 20: 5848
Ta–Zr, oxidation kinetics at 500 to 900°C, 20: 5854(T) (JPRS-32341, pp 8-16)
Tb–Zr, metallurgical properties and phase studies on, 20: 5891(R) (NYO-2159-1)
Ti–Zr, oxidation kinetics at 500 to 900°C, 20: 5854(T) (JPRS-32341, pp 8-16)
U–Zr, diffusion of fission gas from hydrided, 20: 5844
U–Zr, phase transformations in, effects of cooling rate on, 20: 5843
W–Zr, oxidation kinetics at 500 to 900°C, 20: 5854(T) (JPRS-32341, pp 8-16)
Y–Zr, metallurgical properties and phase studies on, 20: 5891(R) (NYO-2159-1)

ZIRCONIUM BORIDES
oxidation kinetics at 945 to 1256°C, 20: 5845
BN–$MoSi_2$–ZrB_2, mechanical properties of composites of, 20: 5845
Co–ZrB_2, oxidation kinetics at 500 to 1000°C, 20: 5845
Fe–ZrB_2, oxidation kinetics at 500 to 1000°C, 20: 5845
Ni–ZrB_2, oxidation kinetics at 500 to 1000°C, 20: 5845

ZIRCONIUM CARBIDES
oxidation kinetics at 554 to 652°C, 20: 5845
thermal expansion at 30 to 2390°C, 20: 5846
TaC–ZrC, thermal expansion at 30 to 2300°C, effects of composition and hot-pressing direction on, 20: 5846
UC–ZrC, ductility at 1800°C, 20: 5848

ZIRCONIUM COMPLEXES
with tropolone, preparation, properties, and structure, 20: 5538

ZIRCONIUM FLUORIDES
purification by sublimation, 20: 5528 (ORNL-TM-1292)

ZIRCONIUM HYDRIDES
neutron scattering by, angular distributions and diffusion constants from thermal, (E), 20: 6271
phase studies, 20: 5844
preparation, 20: 5844
properties as reactor moderator, 20: 5844
UH–ZrH, radiation effects on, measurement in TREAT, (E), 20: 6678 (NAA-SR-Memo-11374)

ZIRCONIUM ISOTOPES
nucleon interactions in, effective, (T), 20: 6337

ZIRCONIUM ISOTOPES Zr-95
content in fallout, 1963, 20: 5652
content in individual rain showers at Bombay, 20: 5661 (AEET-215)

ZIRCONIUM OXIDES
hardness of, effects of metal additions on hot, 20: 5846
properties at high temperatures, effects of calcia or magnesia on, 20: 5851
reactions with silicon oxides, Gibb's free energy of, 20: 5537
ZIRCONIUM SYSTEMS
C–In–Zr, superconductivity of Zr_2InC, 20: 6228
C–Mo–Ti–Zr, microstructure and tensile properties of, effects of composition, heat treatment, and processing on, 20: 5846
C–Nb–W–Zr, bonding of D-43, method for diffusion, 20: 5867
C–Nb–W–Zr, electric conductivity to 1500°C of D-43, 20: 5851
C–Nb–W–Zr, emissivity to 1500°C of D-43, total hemispherical, 20: 5851
C–Nb–W–Zr, mechanical properties of D-43, effects of protective coatings and welding on, 20: 5866
C–Nb–W–Zr, weld stability in D-43, 20: 5866
C–Nb–W–Zr, welding parameters for D-43, electron-beam, 20: 5867
C–Nb–Zr, corrosion by lithium in niobium–1–zirconium alloy forced-convection loop, 20: 5853 (TID-898)
H_2O–Zr, gamma heating in, calculations for, (E/T), 20: 6517 (CONF-651101-41)
ZIRCONS
stability of, at 1180 to 1366°C, 20: 5537

REPORT NUMBER INDEX

Reports, conference papers and proceedings, numbered translations, and patents abstracted during the period are included in this index. Each item is listed by report number; this is followed by the abstract number and a brief notation regarding public availability. The index entries show which reports are on file in the depository libraries, which reports have been published in open-literature journals (journal citation given), and which reports can be purchased (source and price). Whenever a report is identified by more than one number, cross references from secondary to primary report numbers are cited.

The report number codes apply to AEC reports unless designated otherwise. Non-AEC reports are identified by parenthetical notes after the report codes; e.g., (non-AEC), (British), (Canadian), (French). The note (Misc.) identifies those codes used for both USAEC and non-AEC reports. Patents are listed under the heading "PATENTS"; the country of origin is included in parentheses.

A comprehensive listing of both AEC and non-AEC report codes is contained in TID-8505(5th Rev.), *Report Number Series Used by the Division of Technical Information in Cataloging Reports*. This information is also included in the Cumulative Report Number Index (issued annually).

Public Availability of USAEC Reports

All USAEC reports abstracted in *NSA* are available to the public through one or more of the following sources:

(1) Depository libraries in the United States, in other countries, and in international agencies. A list of these depositories appears on the inside covers of each issue of *NSA*.

(2) Scientific and technical journals or other publications.

(3) Microcard Editions, Inc., in Microcard and micronegative form. Orders and inquiries should be sent to: Accounting and Shipping Department, West Salem, Wisconsin 54669.

(4) Clearinghouse for Federal Scientific and Technical Information, U. S. Department of Commerce, Springfield, Virginia 22151.

(5) Superintendent of Documents, U. S. Government Printing Office, Washington, D. C. 20402.

Public Availability of Non-AEC Reports

U. S. Reports. Many reports of U. S. Government agencies are available to the public from the Clearinghouse for Federal Scientific and Technical Information (CFSTI). This availability is given when known. Such reports should be ordered by AD number or NASA-N number. If availability is not shown, inquiries may be directed to CFSTI. In the case of NP numbers, inquiries should be by title and author.

Non-U. S. Reports. Many reports of atomic energy establishments of other countries are deposited in the libraries listed on the inside covers of each issue of *NSA*.

Additionally, the following have made their reports available as indicated.

AUSTRALIA

Australian Atomic Energy Commission Research Establishment. Available upon request from the Library, Australian Atomic Research Establishment, Private Mail Bag, Sutherland, New South Wales, Australia.

BELGIUM

Centre d'Étude de l'Énergie Nucléaire. Available upon request to individuals and organizations, from the Centre d'Étude de l'Énergie Nucléaire (CEN), 31, Rue Belliard, Bruxelles, Belgium.

CANADA

Atomic Energy of Canada Limited. For sale by the Technical Information Officer, Atomic Energy of Canada Limited, Chalk River, Ontario, Canada. Copies are also deposited in libraries in the United Kingdom.

National Research Council of Canada. Available from the National Research Council of Canada, Ottawa 2, Ontario, Canada.

DENMARK

Atomic Energy Commission Research Establishment, Risø. Available on exchange from the Library, Danish Atomic Energy Commission, Risø, Roskilde, Denmark. Also for sale by Jul. Gjellerup, Booksellers, 87 Sölvgade, København K., Denmark.

Danatom. Available on loan from Research Establishment, Risø, Roskilde, Denmark. Copies are available from Danatom, Aurehøjvej 2, Hellerup, Denmark.

EURATOM

Reports from the Commission of the European Atomic Energy Community are available from: Presses academiques europeennes, 98, chaussee de Charleroi, Brussels 6, Belgium; and Office central de vente des publications des Communautes eurodeennes 2, place de Metz, Luxemburg.

FRANCE

Commissariat à l'Énergie Atomique. Inquiries for reports numbered 1-2199 should be addressed to Commissariat à l'Énergie Atomique, Service Central de Documentation, Centre d'Études Nucléaires de Saclay, Boite Postale No. 2, Gif-sur-Yvette (S. et O.), France. Reports numbered 2200 and above are available from La Documentation Francaise, 16 Rue Lord-Byron, Paris VIII, France.

Service Central de Protection contre les Rayonnements Ionisants. Copies are available from Ministère de la Santé Publique, Service Central de Protection contre les Rayonnements Ionisants, B. P. n° 35–LE VESINET (S. et O.), France.

GERMANY

Deutsches Elektronen-Synchrotron DESY. Copies are available from Deutsches Elektronen-Synchrotron Desy, Dokumentation, 2000 Hamburg-Gr. Flottbek 1, Notkestieg 1, Germany.

Gesellschaft für Kernforschung mbH (KFK). Copies are available from Gesellschaft für Kernforschung mbH, 75 Karlsruhe, Postfach 947, Germany. Copies are also deposited in many national nuclear centers in the world.

Kernforschungsanlage. Copies may be ordered from Zentralbibliothek der Kernforschungsanlage Jülich, Jülich, Bundesrepublik Deutschland.

Hahn-Meitner-Institute für Kernforschung. Available without charge from Hahn-Meitner-Institute für Kernforschung Berlin, Bibliothek, Glienicker Strasse 100, 1 Berlin

39, Germany. Copies are deposited in many national nuclear centers in the world.

Johann-Wolfgang-Goethe Universität, Frankfurt Am Main, Institut für Kernphysik, (IKF). Copies are available from Gmelin Institut, 40-42 Varrentrappstrasse, Frankfurt (Main), West Germany.

ISRAEL

Israel Atomic Energy Commission. Available without charge from Ministry of Defence/Atomic Energy Commission, Soreq Research Establishment, Yavne, Israel. Copies are deposited in libraries in Israel and in other countries.

ITALY

Centro Informazioni Studi Esperienze (CISE). For sale at CISE Press Office, Casella Postale 3986, Milano, Italy. Copies are deposited in libraries in Italy.

Comitato Nazionale per l'Energia Nucleare. Copies are available from Comitato Nazionale per l'Energia Nucleare, Divisione Affari Internazionali e Studi Economici, Ufficio Pubblicazioni, Via Belisario, 15, Roma, Italy.

JAPAN

Japan Atomic Energy Research Institute (JAERI). Available from the Staff Supply Cooperative of Japan Atomic Energy Research Institute (JAERI), 1-1 Tamura-Cho, Shiba, Minato-Ku, Tokyo, Japan. Copies are deposited in depositories in Tokyo, Nagoya, and Osaka.

Nagoya University. Copies are available from Research Information Center, Institute of Plasma Physics, Nagoya University, Nagoya, Japan.

University of Tokyo. Available free of charge from Institute for Nuclear Study, University of Tokyo, Tanashi-Machi, Kitatama-gun, Tokyo, Japan.

NETHERLANDS

Reactor Centrum Nederland. For sale by Reactor Centrum Nederland, 112 Scheveningseweg, 's-Gravenhage, The Netherlands. Copies are deposited in university libraries in Holland and in many national nuclear centers in the world.

NEW ZEALAND

Institute of Nuclear Sciences. Copies are available from Librarian, Institute of Nuclear Sciences, D.S.I.R., Private Bag, Lower Hutt, New Zealand. Copies are deposited in other countries.

NORWAY

Forsvarets Forskningsinstitutt. Copies available from Norwegian Defence Research Establishment, Library, P. O. Box 25, Kjeller, Norway.

Institutt for Atomenergi. "KR" reports are available on an exchange basis from the Library, Institutt for Atomenergi, Box 40, Kjeller, Norway. Other series are not generally available to the public.

Norwegian Reactor School. Copies are available from The Library, Institutt for Atomenergi, P.O. Box 40, Kjeller, Norway.

PAKISTAN

Atomic Energy Center. Copies are available from Atomic Energy Center, P. O. Box 658, Lahore, (West Pakistan).

POLAND

Reports of the Polish nuclear institutes are published by the Nuclear Energy Information Center of the Government Commissioner for Use of Nuclear Energy. Copies are available from Ośrodek Informacji o Energii Jądrowej, Warszawa, PKiN, Poland.

SPAIN

Junta de Energia Nuclear. "JEN" reports are available without charge from Servicio de Documentation, Junta de Energia Nuclear, Ciudad Universitaria, Madrid (3), Spain.

SWEDEN

Aktiebolaget Atomenergi. "AE" reports are for sale from Aktiebolaget Atomenergi, Library Section, Box 43041, Stockholm 43, Sweden. Bibliographies and literature surveys of the VDDIT- series may be obtained from Aktiebolaget Atomenergi, Information Office, Scientific and Technical Information, Box 43041, Stockholm 43, Sweden. Other series are not generally available to the public. Organizations in the atomic energy field may obtain copies from Aktiebolaget Atomenergi. Microcopy of AE reports is available from the International Documentation Centre, Tumba, Sweden.

SWITZERLAND

CERN European Organization for Nuclear Research. Available without charge from CERN European Organization for Nuclear Research, Geneva 23, Switzerland. Copies are deposited in libraries in 13 countries.

Eidgenössisches Institut für Reaktorforschung. "EIR" reports are available from Eidgenössiches Institut für Reaktorforschung, c/o Bibliothek, Würenlingen/Ag, Switzerland.

TURKEY

Turkish Atomic Energy Commission. Copies are available free of charge from T.A.E.C., Çekmece Nuclear Research Center, P. O. Box 1, Airport, Istanbul, Turkey.

UNITED KINGDOM

United Kingdom Atomic Energy Authority. Some reports are for sale in the United States by the British Information Service (BIS), 845 Third Avenue, New York, N. Y. 10022. United Kingdom reports generally may be purchased from Her Majesty's Stationery Office, London. Copies not for sale by Her Majesty's Stationery Office may be purchased in microcopy form from Micro Methods Limited, East Ardsley, Wakefield, Yorks, England. Report copies are deposited in a large number of libraries in England.

Conferences

Published conference proceedings as well as individual unpublished papers from conferences are included in this index. A CONF number is assigned to the conference if published proceedings are received and also if only a single paper is received. The base number used is year-month-sequence. Thus, the number CONF-650101 would indicate that the conference was held in 1965, in January, and that this was the first January 1965 conference so received. This number would be assigned to complete published proceedings, or if individual papers are received, the base number would be extended to include a paper number, i.e., CONF-650101-1. As additional papers are received, they will be assigned consecutive numbers in the series, CONF-650101-1, 2, 3, 4, etc. This numbering system ensures that all papers received from a conference will be associated with that conference in this index.

If published proceedings are received after the receipt of individual papers, the complete proceedings will be abstracted and the abstract number will appear in this index with the base CONF number.

Abbreviations Used in Availability Column

AECL	For sale by Atomic Energy of Canada Ltd., Chalk River, Ontario, Canada.
BIS	For sale by British Information Service, 845 Third Avenue, New York, N. Y. 10022
CFSTI	For sale by the Clearinghouse for Federal Scientific and Technical Information, U.S. Department of Commerce, Spring-

field, Virginia 22151. The symbol "cy" indicates that the format of the item sold may be either a printed document or a photographic reproduction (two-thirds of original size) depending upon the availability of printed stock. The indicated price is for either format. The symbol "mn" is used to indicate that copy is also available in the form of micronegatives (microfiche).

Dep. AEC reports: Full-size copy is on deposit in the depository libraries both inside and outside the United States. These reports are also for sale by Microcard Editions, Inc., Accounting and Shipping Department, West Salem, Wisconsin 54669.

Non-AEC reports: Full-size copy on deposit in the depository libraries in the United States only.

Dep.(mn) Same as for Dep., except copy is in micronegative (microfiche) form.

DSIR For sale by the National Lending Library for Science and Technology (D.S.I.R.), Boston Spa, Yorkshire, England.

DTI Extension Available from the U. S. Atomic Energy Commission, Division of Technical Information Extension, P. O. Box 62, Oak Ridge, Tennessee 37830.

EM Blueprints and microcopy of AEC engineering drawings are available from Clearinghouse for Federal Scientific and Technical Information, U. S. Department of Commerce, Springfield, Virginia 22151. Current prices of the CAPE- packages may be obtained from this address. TID-4100, available from the Division of Technical Information Extension, P. O. Box 62, Oak Ridge, Tennessee 37831, contains information on all the CAPE- packages for sale.

Gmelin Available at a nominal charge and under the AED- number shown from Atomic Energy Documentation Center, Gmelin Institute, 40-42 Varrentrappstrasse Frankfurt (Main), West Germany.

GPO For sale by the Superintendent of Documents, Government Printing Office, Washington, D. C. 20402.

HMSO Her Majesty's Stationery Office, London.

IAEA Available from the International Atomic Energy Agency, Vienna, Austria, and from its sales agencies in various countries throughout the world. A list of these agencies is found in each STI/DOC and STI/PUB publication.

JCL For sale by the Special Libraries Association Translation Center, John Crerar Library, 35 West 33rd Street, Chicago, Illinois 60616.

NAS National Academy of Sciences, National Research Council, Washington, D. C. 20418.

NRC For sale by the National Research Council of Canada, Ottawa, Ontario, Canada.

ORAU Available on interlibrary loan from the Library, Oak Ridge Associated Universities, Post Office Box 117, Oak Ridge, Tennessee 37830.

ORINS See ORAU.

UKAEA, London Available from United Kingdom Atomic Energy Authority, 11 Charles II Street, London, S. W. 1.

UN United Nations Bookshop, United Nations Headquarters, New York, New York.

USGS Available free of charge from the U. S. Geological Survey, Washington, D. C. 20242.

[The symbols "ph," "mf," and "fs" are used to designate that copy is available only in photostat, microfilm, or facsimile form. The symbol **"mn"** is used to designate that copy is available in micronegative (microfiche) form. The symbol **"cy"** is used to designate full size or photographically enlarged copy (two-thirds of original size).]

Report No.	Abstract No.	Availability
AAEC-TM–	**(Australian)**	
293	20-5828	Dep. mn
AD–	**(Misc.)**	
613611	20-6006	See CONF-640919
617383	20-6443	CFSTI $4.00 cy, $1.00 mn
617398	20-6273	CFSTI $3.00 cy, $0.75 mn
617522	20-5980	CFSTI $1.00 cy, $0.50 mn
617524	20-6516	CFSTI $3.00 cy, $0.75 mn
617553	20-6444	CFSTI $1.00 cy, $0.50 mn
617562	20-6156	CFSTI $1.00 cy, $0.50 mn
617619	20-6445	CFSTI $3.00 cy, $0.75 mn
617696	20-6446	CFSTI $5.00 cy, $1.00 mn
617782	20-5805	CFSTI $2.00 cy, $0.50 mn
617880	20-6252	CFSTI $2.00 cy, $0.50 mn
617882	20-6253	CFSTI $2.00 cy, $0.50 mn
617898	20-6157	CFSTI $1.00 cy, $0.50 mn
618689	20-5922	CFSTI $4.00 cy, $1.00 mn
618693	20-6447	CFSTI $5.00 cy, $1.25 mn
618905	20-5966	CFSTI $2.00 cy, $0.50 mn
618911	20-6179	CFSTI $4.00 cy, $1.00 mn
619045	20-6448	CFSTI $4.00 cy, $1.00 mn
619061	20-6274	CFSTI $3.00 cy, $0.75 mn
619250	20-6180	CFSTI $3.00 cy, $0.75 mn
619288	20-6181	CFSTI $1.00 cy, $0.50 mn
619370	20-6449	CFSTI $1.00 cy, $0.50 mn
619379	20-6023	CFSTI $1.00 cy, $0.50 mn
619387	20-5806	CFSTI $2.00 cy, $0.50 mn
619447	20-6182	CFSTI $2.00 cy, $0.50 mn
619508	20-6004	CFSTI $1.00 cy, $0.50 mn
619511	20-5618	CFSTI $4.00 cy, $1.00 mn
619527	20-6450	CFSTI $1.00 cy, $0.50 mn
619534	20-6275	CFSTI $1.00 cy, $0.50 mn
619576	20-6276	CFSTI $2.00 cy, $0.50 mn
619668	20-6451	CFSTI $6.00 cy, $1.25 mn
619669	20-6452	CFSTI $4.00 cy, $0.75 mn
619670	20-6453	CFSTI $4.00 cy, $0.75 mn
619671	20-6454	CFSTI $5.00 cy, $1.00 mn
619672	20-6455	CFSTI $4.00 cy, $0.75 mn
619740	20-5967	CFSTI $1.00 cy, $0.50 mn
619821	20-6183	CFSTI $1.00 cy, $0.50 mn
619888	20-6456	CFSTI $3.00 cy, $0.75 mn
619952	20-6277	CFSTI $2.00 cy, $0.50 mn
619977	20-6184	CFSTI $3.00 cy, $0.75 mn
619999	20-6158	CFSTI $1.00 cy, $0.50 mn
620002	20-5981	CFSTI $3.00 cy, $0.75 mn
622876	20-6457	CFSTI $2.00 cy, $0.50 mn
623384	20-5713	
623530	20-6531	CFSTI $3.00 cy, $0.75 mn
623599	20-5281	
623632	20-6005	CFSTI $7.00 cy, $1.75 mn
623722	20-5714	CFSTI $4.00 cy, $0.75 mn
623877	20-6278	CFSTI $3.00 cy, $0.75 mn
AE–	**(Non-AEC)**	
199	20-5619	Dep. mn
200	20-5620	Dep. mn
AEC-tr–	**(For complete listing see TID-4025)**	
6628	20-6632	Dep. mn; JCL $4.60 fs, $1.58 mf
AECL–	**(Canadian)**	
2286	20-6633	Dep.; AECL $0.50
2294	20-5680	See ELI-91
2364	20-6318	Can. J. Phys., 43: 2310-18(1965)
2501	20-5928	See PR-P-66
AED-C–	**(Non-AEC)**	
04-21	20-5284	Dep. mn
AEET–	**(Indian)**	
215	20-5661	Dep. mn
217	20-5494	Dep. mn
227	20-5715	Dep. mn
AEEW-M–	**(British)**	
470	20-5716	Dep. mn
493	20-5807	Dep. mn
503	20-6254	Dep. mn
508	20-5717	Dep. mn
AEEW-R–	**(British)**	
416	20-5621	Dep. mn
AERE-M–	**(British)**	
1597	20-6159	Dep. mn
AERE-R–	**(British)**	
5016	20-6255	Dep.; BIS $0.90; HMSO 4s. 6d.
5061	20-5982	Dep.; BIS $0.50; HMSO 2s. 6d.
AES–	**(Swedish)**	
5	20-6599	Dep. mn
AFCRL–	**(Non-AEC)**	
65-257	20-6446	See AD-617696
65-334	20-6445	See AD-617619
65-426	20-6158	See AD-619999
65-451	20-6182	See AD-619447
65-563	20-6183	See AD-619821
65-587	20-6004	See AD-619508
65-620	20-6185	CFSTI $4.00 cy, $1.00 mn
65-654	20-6457	See AD-622876
65-705	20-6005	See AD-623632
AFML-TR–	**(Non-AEC)**	
65-253	20-6531	See AD-623530
AFOSR–	**(Misc.)**	
64-1425	20-6156	See AD-617562
65-0933	20-6444	See AD-617553
65-1313	20-6157	See AD-617898
65-1532	20-6450	See AD-619527
AGARDograph–	**(Non-AEC)**	
94	20-5874	Dep. mn
Al–	**(Misc.)**	
65-225	20-6279	
AL-TDR–	**(Non-AEC)**	
64-58	20-5981	See AD-620002
ANL–		
6925	20-5492	Dep. mn; CFSTI $6.00 cy, $1.25 mn
6974	20-5876	Dep. mn; CFSTI $2.00 cy, $0.50 mn
7032	20-5622	Dep. mn; CFSTI $3.00 cy, $0.75 mn
7048	20-5877	Dep. mn; CFSTI $2.00 cy, $0.50 mn
7065	20-6213	Dep. mn; CFSTI $1.00 cy, $0.50 mn
7076	20-5524	Dep. mn; CFSTI $3.00 cy, $0.75 mn
7092	20-6554	Dep. mn; CFSTI $3.00 cy, $0.75 mn
7105	20-6555	Dep. mn; CFSTI $3.00 cy, $0.75 mn
7115	20-6557	Dep. mn; CFSTI $3.00 cy, $0.75 mn
ANL-Trans–		
241	20-5947	Dep. mn; CFSTI $1.00 cy, $0.50 mn; JCL $1.60 fs, $0.80 mf
243	20-6308	Dep. mn; CFSTI $1.00 cy, $0.50 mn; JCL $1.10 fs, $0.80 mf
245	20-6309	Dep. mn; CFSTI $2.00 cy, $0.50 mn; JCL $2.60 fs, $1.04 mf
246	20-5948	Dep. mn; CFSTI $3.00 cy, $0.50 mn; JCL $5.60 fs, $1.91 mf
248	20-5987	Dep. mn; CFSTI $1.00 cy, $0.50 mn; JCL $1.10 fs, $0.80 mf
BMI-X–		
10145	20-6560	Dep. mn; CFSTI $2.00 cy, $0.50 mn
BNL–		
8693	20-5260	Radiat. Res., 26: 319-33(1965)
8707	20-6120	J. Math. Phys. (N. Y.), 6: 1723-9(1965)
9113	20-6543	Phys. Rev., 140: A1998-9(1965)
9306	20-5960	Rev. Sci. Instrum., 36: 1788-96(1965)
9352	20-5931	Dep. mn; CFSTI $1.00 cy, $0.50 mn
9359	20-6546	Phys. Rev., 140: A2139-41(1965)
9361	20-6242	Phys. Rev., 140: A1965-7(1965)
9386	20-6409	Phys. Rev., 140: B1549-56(1965)
9399	20-6405	Phys. Rev., 140: B1513-16(1965)
9407	20-5229	Dep. mn; CFSTI $1.00 cy, $0.50 mn
9454	20-6372	Nucl. Phys., 76: 123-8(1966)
9613	20-6031	Dep. mn; CFSTI $1.00 cy, $0.50 mn
9634	20-5718	Dep. mn; CFSTI $1.00 cy, $0.50 mn
9652	20-6101	Dep. mn; CFSTI $3.00 cy, $0.75 mn

Report No.	Abstract No.	Availability
9662	20-5932	Dep. mn; CFSTI $1.00 cy, $0.50 mn
9664	20-5568	Dep. mn; CFSTI $1.00 cy, $0.50 mn
9666	20-6032	Dep. mn; CFSTI $2.00 cy, $0.50 mn
9667	20-5878	Dep. mn; CFSTI $1.00 cy, $0.50 mn
9686	20-6667	Dep. mn; CFSTI $1.00 cy, $0.50 mn
BNWL–		
137	20-5611	Dep. mn; CFSTI $1.00 cy, $0.50 mn
149	20-5923	Dep. mn; CFSTI $3.00 cy, $0.75 mn
BNWL-SA–		
172	20-5285	Dep. mn; CFSTI $1.00 cy, $0.50 mn
346	20-6602	Dep. mn; CFSTI $1.00 cy, $0.50 mn
CAL-CM–	**(Non-AEC)**	
1677-P-1	20-6182	See AD-619447
CALT–		
51-4	20-5264	Z. Naturforsch., 20b: 930-2(1965)
221-13	20-6532	Dep. mn; CFSTI $1.00 cy, $0.50 mn
CAPE–		
974	20-6645	
975	20-6646	
1215	20-5963	
1264	20-5796	
1265	20-6514	
1266	20-6513	
1314	20-5709	
1315	20-5710	
CEA-R–	**(French)**	
2702	20-6580	Dep. mn
2798	20-6033	Dep. mn
2807	20-6281	Dep. mn
2824	20-5829	Dep. mn
2846	20-5719	Dep. mn
2864	20-6670	Dep. mn
2872	20-6581	Dep. mn
CEND–	**(Misc.)**	
3336-251	20-6565	Dep. mn; CFSTI $1.00 cy, $0.50 mn
CERN–	**(European Organization for Nuclear Research)**	
64-13(Vol.4)	20-6034	Dep. mn
65-33	20-5720	Dep. mn
65-34	20-5933	Dep. mn
65-37	20-5934	Dep. mn
65-38	20-5830	Dep. mn
CISE-R–	**(Italian)**	
122	20-5623	See EURAEC-1325
136	20-6566	See EURAEC-1382
CLM-P–	**(British)**	
77	20-6494	Phys. Fluids, 8: 2026-31(1965)
CLM-R–	**(British)**	
44	20-6458	Dep. mn; BIS $0.60; HMSO 3s.
CLOR-IBJ–	**(Polish)**	
II-37/D	20-5721	Dep.
CNIE-PE–	**(Argentinian)**	
1	20-6459	Dep. mn
CONF-654	**19-2907**	**(American Nuclear Society Meeting,**
	19-6030	**San Francisco, Nov. 30–Dec. 3, 1964) Proceedings**
96	20-6567	See HW-SA-3600
97	20-6611	See HW-SA-3669
CONF-640711–	**(27th Portugo-Spanish Conference on Progress in Sciences, Bilbao, Spain, July 20–24, 1964)**	
3	20-6075	See LFEN-26
4	20-5734	See LFEN-NI-19
CONF-640919	**20-6006**	**(Conference on the Interaction Between Cosmic Rays and High Energy Physics, Cleveland, Sept. 25–26, 1964)**

Report No.	Abstract No.	Availability
CONF-650210–	**(Application of X-Ray Diffraction in the Atomic Energy Field Meeting, Richland, Wash., Feb. 23–24, 1965)**	
4	20-5863	See NLCO-945
CONF-650217	**20-6256**	**(Symposium on Pulsed High Intensity Fission Neutron Sources, Washington, D. C., Feb. 18, 1965)**
CONF-650306	**19-37263**	**(Particle Accelerator Conference, Mar. 10–12, 1965, Washington, D. C.)**
63	20-5733	See LA-DC-6790
CONF-650410–	**(American Physical Society, Washington, D. C., Apr. 26–29, 1965)**	
46	20-5765	Nucl. Instrum. Methods, 37: 194-200(1965)
47	20-5766	Nucl. Instrum. Methods, 37: 201-3(1965)
CONF-650519–	**(13th Annual Conference of American Society of Testing Materials, St. Louis, May 16–21, 1965)**	
7	20-5684	See WAPD-T-1770
CONF-650602–	**(American Nuclear Society 11th Annual Meeting, Gatlinburg, Tenn., June 20–24, 1965)**	
79	20-5887	See NLCO-953
CONF-650616–	**(Health Physics Society, Annual Meeting, Los Angeles, June 14–17, 1965)**	
16	20-5286	Dep. mn; CFSTI $1.00 cy, $0.50 mn
CONF-650652–	**(International C-14 and H-3 Dating Conference, Pullman, Wash., June 7–11, 1965)**	
3	20-5521	Gmelin, AED-CONF-65-158-7
CONF-650662	**20-5988**	**(3rd All-Union Conference on the Physics of Electron and Atom Collisions, Kharkov, U.S.S.R., June 21–28, 1965) See also JPRS-32421**
CONF-650806–	**(7th International Conference on Phenomena in Ionized Gases, Belgrade, Aug. 22–27, 1965)**	
18	20-6466	See SIT-2813-33
CONF-650814–	**(Symposium on Mutational Process, Prague, Aug. 9–11, 1965)**	
2	20-5229	See BNL-9407
CONF-650923–	**(5th International Conference on High Energy Accelerators, Frascati, Italy, Sept. 9–16, 1965)**	
24	20-5944	See SLAC-PUB-132
25	20-5739	See SLAC-PUB-140
CONF-650928–	**(International Conference on Polarization Phenomena of Nucleons, Karlsruhe, Germany, Sept. 6–10, 1965)**	
13	20-6306	See UCRL-16217
CONF-650935–	**(2nd IAEA Conference on Plasma Physics and Controlled Nuclear Fusion Research, Culham, England, Sept. 6–10, 1965)**	
45	20-6460	See GA-6594
46	20-6461	See GA-6646
47	20-6462	See GA-6650
CONF-650945–	**(International Conference on Elementary Particles, Oxford, Sept. 19–25, 1965)**	
3	20-6101	See BNL-9652
CONF-651001–	**(IEEE Nuclear Science Symposium, San Francisco, Oct. 1965)**	
11	20-5741	See UCRL-14263
12	20-5743	See UCRL-14405
13	20-6307	See UCRL-16439
14	20-5744	See UCRL-16227
15	20-5939	See LA-DC-7267
CONF-651008–	**(Annual Bio-Assay Meeting, Albuquerque, N. Mex., Oct. 7–8, 1965)**	
3	20-5662	See NLCO-962
CONF-651009–	**(Conference on Safety, Fuels and Core Design in Large Fast Power Reactors, Argonne, Oct. 11–14, 1965)**	
3	20-6602	See BNWL-SA-346
6	20-5878	See BNL-9667
7	20-6614	See LA-DC-7476

Report No.	Abstract No.	Availability
8	20-6613	See LA-DC-7475
CONF-651027–	**(New Mexico Academy of Science, Albuquerque, Oct. 8, 1965)**	
1	20-5529	See SC-DC-65-1706
CONF-651029–	**(15th Annual National Lead Co. Analytical and Physical Testing Symposium, Hightstown, N. J., Oct. 14–15, 1965)**	
2	20-5837	See NLCO-966
CONF-651039–	**(Conference on Programming for Flying Spot Devices, Columbia, N. Y., Oct. 26–29, 1965)**	
1	20-5718	See BNL-9634
CONF-651041–	**(Nuclear and Engineering Ceramics Conference, Harwell, England, Oct. 25–27, 1965)**	
1	20-5915	See ORNL-P-1724
CONF-651042–	**(Manned Space Flight Experiments Symposium, Gemini Missions 3 and 4, Washington, D. C., Oct. 19, 1965)**	
1	20-5297	See ORNL-P-1734
CONF-651043–	**(Weak Interactions Conference, Argonne, Ill., Oct. 25–27, 1965)**	
1	20-6031	See BNL-9613
2	20-6032	See BNL-9666
CONF-651101	**20-3647**	**(American Nuclear Society, Winter Meeting, Washington, D. C., Nov. 15–18, 1965) (Revised 11–8–65)**
38	20-5927	See ORNL-P-1733
41	20-6517	Dep. mn; CFSTI $2.00 cy, $0.50 mn
42	20-5822	See DP-1000
43	20-6260	Dep. mn; CFSTI $1.00 cy, $0.50 mn
45	20-6264	See WAPD-T-1849
46	20-5727	Dep. mn; CFSTI $2.00 cy, $0.50 mn
CONF-651103–	**(IAEA Symposium on Criticality Control of Fissile Materials, Stockholm, Nov. 1–5, 1965)**	
13	20-6584	See LA-DC-7248
CONF-651106–	**(Conference on Magnetism and Magnetic Materials, San Francisco, Nov. 16–19, 1965)**	
4	20-6534	See SC-DC-65-1843
CONF-651109–	**(1st Symposium on Accelerator Radiation Dosimetry and Experience, Upton, N. Y., Nov. 3–5, 1965)**	
9	20-5932	See BNL-9662
10	20-5945	See UCRL-64
13	20-5940	See LA-DC-7522
COO–		
7-0358	20-6356	Nucl. Phys., 75: 529-38(1966)
7-0360	20-6355	Nucl. Phys., 75: 515-28(1966)
30-102	20-6073	Phys. Rev., 140: B1675-80(1965)
32-108	20-5577	J. Amer. Chem. Soc., 87: 4992-7(1965)
119-232	20-5230	Dep. mn; CFSTI $6.00 cy, $1.25 mn
205-55	20-5291	Dep. mn; CFSTI $5.00 cy, $1.00 mn
264-225	20-6121	J. Math. Phys. (N. Y.), 6: 1730-40(1965)
881-53	20-6056	Phys. Rev., 140: B1533-40(1965)
881-55	20-6082	Phys. Rev. Lett., 15: 930-4(1965)
1029-7	20-5909	J. Phys. Chem., 69: 3973-80(1965)
1198-296	20-6685	Dep. mn; CFSTI $4.00 cy, $0.75 mn
1198-308	20-6245	Phys. Rev. Lett., 15: 875-8(1965)
1261-17	20-6071	Phys. Rev., 140: B1655-60(1965)
1261-21	20-6077	Phys. Rev. Lett., 15: 897-900(1965)
1340-2	20-5647	Dep. mn; CFSTI $4.00 cy, $1.00 mn
CU–	**(Misc.)**	
236	20-6273	See AD-617398
D–	**(Misc.)**	
910091-5	20-6652	
910091-7	20-6653	
910092-4	20-6594	
910092-6	20-5879	
910099-2	20-5983	
DESY–	**(German)**	
65/11	20-6037	Dep. mn
DP–		
972	20-5495	Dep. mn; CFSTI $1.00 cy, $0.50 mn
985	20-5496	Dep. mn; CFSTI $1.00 cy, $0.50 mn
988	20-6673	Dep. mn; CFSTI $2.00 cy, $0.50 mn
1000	20-5822	Dep. mn; CFSTI $1.00 cy, $0.50 mn
DUBNA REPORTS	**(Russian)**	
See JINR (Russian)		
ECOM–	**(Non-AEC)**	
2603	20-6449	See AD-619370
ELI–	**(Canadian)**	
91	20-5680	Dep.; AECL $1.00
ER–	**(Misc.)**	
7899	20-5808	See N65-35081
ESD-TDR–	**(Non-AEC)**	
65-54	20-6184	See AD-619977
65-310	20-5806	See AD-619387
EUR–	**(European Atomic Energy Community)**	
1919.f	20-5831	Dep. mn
2307	20-5623	See EURAEC-1325
2345	20-6566	See EURAEC-1382
2384	20-5882	See EURAEC-1454
2461.f	20-6582	Dep. mn
2482.f	20-5563	Dep. mn
2655	20-5913	See EURAEC-1488
2674	20-5852	See EURAEC-1522
EURAEC–		
1310	20-5880	Dep. mn; CFSTI $3.00 cy, $0.75 mn
1325	20-5623	Dep. mn; CFSTI $3.00 cy, $0.75 mn
1382	20-6566	Dep. mn; CFSTI $3.00 cy, $0.50 mn
1421	20-6595	Dep. mn; CFSTI $3.00 cy, $0.50 mn
1441	20-5881	Dep. mn; CFSTI $1.00 cy, $0.50 mn
1454	20-5882	Dep. mn; CFSTI $2.00 cy, $0.50 mn
1481	20-5862	Dep. mn; CFSTI $2.00 cy, $0.50 mn
1488	20-5913	Dep. mn; CFSTI $1.00 cy, $0.50 mn
1495	20-6607	See GEAP-4965
1497	20-6560	See BMI-X-10145
1498	20-6606	See GEAP-4962
1510	20-6565	See CEND-3336-251
1512	20-5914	See GEAP-3771-17
1522	20-5852	Dep. mn; CFSTI $2.00 cy, $0.50 mn
FTI–	**(Swedish)**	
2	20-6561	Dep. mn
GA–	**(Misc.)**	
4165	20-6603	Dep. mn; CFSTI $3.00 cy, $0.75 mn
5842	20-6604	Dep. mn; CFSTI $2.00 cy, $0.50 mn
6395	20-6508	Rev. Sci. Instrum., 36: 1886-7(1965)
6594	20-6460	
6646	20-6461	
6650	20-6462	
GAMD–	**(Misc.)**	
6673	20-6605	Dep. mn; CFSTI $2.00 cy, $0.50 mn
6675	20-5606	Dep. mn; CFSTI $4.00 cy, $1.00 mn
6675(Suppl.)	20-5607	Dep. mn; CFSTI $2.00 cy, $0.50 mn
GEAP–	**(Misc.)**	
3771-17	20-5914	Dep. mn; CFSTI $3.00 cy, $0.50 mn
4962	20-6606	Dep. mn; CFSTI $3.00 cy, $0.75 mn
4965	20-6607	Dep. mn; CFSTI $1.00 cy, $0.50 mn
GEMP–	**(Misc.)**	
392	20-6284	Dep. mn; CFSTI $1.00 cy, $0.50 mn
GEST–	**(Misc.)**	
2049	20-6596	
HEPL–	**(Misc.)**	
362	20-6276	See AD-619576
383(Rev.)	20-6277	See AD-619952
HIT–		
158	20-6608	See HIT-3459-7
165	20-6609	See HIT-3534-1

Report No.	Abstract No.	Availability
3459-7	20-6608	Dep. mn; CFSTI $1.00 cy, $0.50 mn
3534-1	20-6609	Dep. mn; CFSTI $3.00 cy, $0.75 mn
HPR–	**(Norwegian)**	
64	20-6648	Dep. mn
HW–		
79287	20-6610	Dep. mn; CFSTI $3.00 cy, $0.75 mn
HW-SA–		
3600	20-6567	Dep. mn; CFSTI $1.00 cy, $0.50 mn
3669	20-6611	Dep. mn; CFSTI $1.00 cy, $0.50 mn
IA–	**(Non-AEC)**	
1041	20-5525	Dep. mn
IBJ–	**(Polish)**	
See INR		
IBM–	**(Non-AEC)**	
65-825-1487	20-5728	
IC–	**(Misc.)**	
65/79	20-6102	Dep. mn
65/80	20-6103	Dep. mn
65/81	20-6104	Dep. mn
IDO–		
17076	20-6654	Dep. mn; CFSTI $5.00 cy, $1.00 mn
IFJ–	**(Polish)**	
See INP		
INP–	**(Polish)**	
414/PL	20-6285	Dep.
INR–	**(Non-AEC)**	
610/VI/PH	20-6214	Dep.
617/XIX/D	20-5729	Dep.
622/IX/R	20-6612	Dep.
646/VI/PH	20-6038	Dep.
INSJ–	**(Japanese)**	
90	20-6039	Dep. mn
IS–		
1198	20-6547	Phys. Rev., 140: A2143-50(1965)
1210	20-5599	J. Less-Common Metals, 10: 1-11(1966)
1254	20-6549	Phys. Rev. Lett., 15: 886-8(1965)
1268	20-5883	Dep. mn; CFSTI $2.00 cy, $0.50 mn
1272	20-6247	Phys. Rev. Lett., 15: 891-3(1965)
ISS–	**(Italian)**	
65/10	20-6286	Dep. mn
65/14	20-6105	Dep. mn
65/19	20-5924	Dep. mn
JAERI–	**(Japanese)**	
1091	20-6583	Dep. mn
JINR–	**(Russian)**	
E-2366	20-5730	Dep. mn
P-2369	20-6106	Dep. mn
P-2373	20-6287	Dep. mn
P-2394	20-5731	Dep. mn
P-2401	20-6107	Dep. mn
JNPC-RPWP–	**(British)**	
NF1SG/P35	20-5716	See AEEW-M-470
JPRS–	**(Non-AEC)**	
32260	20-5813	CFSTI $1.00 cy, $0.50 mn
32341	20-5841	CFSTI $2.00 cy, $0.50 mn
32421	20-5988	CFSTI $3.00 cy, $0.75 mn
32985	20-6691	CFSTI $3.00 cy, $0.50 mn
JüL–	**(German)**	
228-RC	20-5570	Dep. mn
264-PP	20-6463	Dep. mn
K-Trans–		
5	20-5685	Dep. mn; JCL $1.10 fs, $0.80 mf
10	20-5532	Dep. mn; CFSTI $1.00 cy, $0.50 mn; JCL $1.10 fs, $0.80 mf
KAPL–		
3113	20-6288	Dep. mn; CFSTI $1.00 cy, $0.50 mn
KFK–	**(German)**	
250	20-5526	Dep. mn
332	20-6674	Dep. mn
335	20-5732	Dep. mn
339	20-5497	Dep. mn
346	20-5937	Dep. mn
KN–	**(Non-AEC)**	
63-10(R)	20-6289	
LA–		
2312	20-5884	Dep. mn; CFSTI $1.00 cy, $0.50 mn
3372	20-5938	Dep. mn; CFSTI $7.00 cy, $1.50 mn
3380	20-6290	Dep. mn; CFSTI $4.00 cy, $1.00 mn
3403	20-5609	Dep. mn; CFSTI $3.00 cy, $0.50 mn
3415	20-6261	Dep. mn; CFSTI $3.00 cy, $0.75 mn
LA-DC–		
6404(Rev.)	20-5336	Health Phys., 11: 647-51(1965)
6790	20-5733	Dep. mn; CFSTI $1.00 cy, $0.50 mn
7248	20-6584	Dep. mn; CFSTI $1.00 cy, $0.50 mn
7267	20-5939	Dep. mn; CFSTI $1.00 cy, $0.50 mn
7475	20-6613	Dep. mn; CFSTI $1.00 cy, $0.50 mn
7476	20-6614	Dep. mn; CFSTI $1.00 cy, $0.50 mn
7522	20-5940	Dep. mn; CFSTI $1.00 cy, $0.50 mn
LFEN–	**(Portuguese)**	
26	20-6675	Dep. mn
LFEN-NI–	**(Portuguese)**	
19	20-5734	Dep. mn
LYCEN–	**(French)**	
6523	20-5735	Dep. mn
MATT–		
393	20-6506	Phys. Rev. Lett., 15: 878-82(1965)
MIT–	**(Misc.)**	
905-36	20-5768	Nucl. Instrum. Methods, 37: 259-64(1965)
2098-116	20-6340	Nucl. Phys., 75: 255-96(1965)
2098-143	20-6312	Ann. Phys. (N. Y.), 35: 53-66(1965)
2098-160	20-6404	Phys. Rev., 140: B1501-12(1965)
3496-1	20-5624	Dep. mn; CFSTI $4.00 cy, $1.00 mn
MLM–		
1288	20-5681	Dep. mn; CFSTI $1.00 cy, $0.50 mn
MURA–	**(Misc.)**	
716	20-5682	Dep. mn; CFSTI $1.00 cy, $0.50 mn
N–	**(Misc.)**	
65-35081	20-5808	CFSTI $3.00 cy, $0.50 mn
NAA-SR–		
7088	20-6655	Dep. mn; CFSTI $3.00 cy, $0.75 mn
10888(Rev.)	20-6615	Dep. mn; CFSTI $1.00 cy, $0.50 mn
11234	20-6676	Dep. mn; CFSTI $3.00 cy, $0.75 mn
11528	20-6677	Dep. mn; CFSTI $2.00 cy, $0.50 mn
NAA-SR-Memo–		
10941	20-6585	Dep. mn; CFSTI $2.00 cy, $0.50 mn
11313	20-6586	Dep. mn; CFSTI $4.00 cy, $0.75 mn
11324	20-6616	Dep. mn; CFSTI $3.00 cy, $0.75 mn
11333	20-6656	Dep. mn; CFSTI $2.00 cy, $0.50 mn
11339	20-6617	Dep. mn; CFSTI $1.00 cy, $0.50 mn
11369	20-6562	Dep. mn; CFSTI $4.00 cy, $0.75 mn
11374	20-6678	Dep. mn; CFSTI $1.00 cy, $0.50 mn
11415	20-6618	Dep. mn; CFSTI $1.00 cy, $0.50 mn
11416	20-6619	Dep. mn; CFSTI $2.00 cy, $0.50 mn
11417	20-6657	Dep. mn; CFSTI $1.00 cy, $0.50 mn
11436	20-6658	Dep. mn; CFSTI $3.00 cy, $0.75 mn
11458	20-6620	Dep. mn; CFSTI $3.00 cy, $0.50 mn
11473	20-6659	Dep. mn; CFSTI $1.00 cy, $0.50 mn
11514	20-6660	Dep. mn; CFSTI $3.00 cy, $0.75 mn
11516	20-6518	Dep. mn; CFSTI $2.00 cy, $0.50 mn

Report No.	Abstract No.	Availability
11538	20-6291	Dep. mn; CFSTI $3.00 cy, $0.50 mn
11556	20-6621	Dep. mn; CFSTI $1.00 cy, $0.50 mn
11562	20-5630	Dep. mn; CFSTI $1.00 cy, $0.50 mn
11603	20-6661	Dep. mn; CFSTI $2.00 cy, $0.50 mn
NAS-CR–	**(Non-AEC)**	
54773	20-5885	CFSTI $4.00 cy, $0.75 mn
NASA-CR–	**(Misc.)**	
316	20-5820	CFSTI $7.00 cy, $1.50 mn
54656	20-6596	See GEST-2049
54769	20-6279	See AI-65-225
64433	20-5808	See N65-35081
NASA-SP–	**(Misc.)**	
5033	20-5633	GPO $1.00
5035	20-5836	GPO $0.35
NASA-TN–	**(Misc.)**	
D-2951	20-6662	CFSTI $1.00 cy, $0.50 mn
D-3097	20-6587	CFSTI $1.00 cy, $0.50 mn
D-3120	20-5886	CFSTI $2.00 cy, $0.50 mn
D-3121	20-6464	CFSTI $2.00 cy, $0.50 mn
NDL-TR–	**(Non-AEC)**	
54	20-5714	See AD-623722
NEVIS–	**(Misc.)**	
130	20-6273	See AD-617398
NLCO–		
945	20-5863	Dep. mn; CFSTI $1.00 cy, $0.50 mn
953	20-5887	Dep. mn; CFSTI $1.00 cy, $0.50 mn
962	20-5662	Dep. mn; CFSTI $1.00 cy, $0.50 mn
966	20-5837	Dep. mn; CFSTI $1.00 cy, $0.50 mn
NP–	**(AEC File No. for Non-AEC Reports)**	
15380	20-6014	Dep. mn
15451	20-5663	Dep. mn
15543	20-5810	Dep. mn
15559	20-5295	Dep. mn
15585	20-5296	Dep. mn
15592	20-5888	Dep. mn
15597	20-5736	Dep. mn
15598	20-5941	Dep. mn
15600	20-6108	Dep. mn
15601	20-6292	Dep. mn
15602	20-6040	Dep. mn
15603	20-6293	Dep. mn
15604	20-6160	Dep. mn
15614	20-6215	
15615	20-5942	
15617	20-6294	Dep. mn
15626	20-5968	
15630	20-6161	
15633	20-6262	
15635	20-6263	
15636	20-5498	
15637	20-5499	
15638	20-6109	Dep. mn
15639	20-5664	Dep. mn
15645	20-6679	
15646	20-5527	
15647	20-6295	Dep. mn
NP-tr–	**(AEC File No. for Non-AEC Translations)**	
1300	20-5626	Dep. mn; CFSTI $1.00 cy, $0.50 mn; JCL $1.60 fs, $0.80 mf
1302	20-5747	Dep. mn; JCL $2.60 fs, $0.83 mf
1313	20-5686	Dep. mn; CFSTI $1.00 cy, $0.50 mn; JCL $1.60 fs, $0.80 mf
NRL–	**(Misc.)**	
F17	20-5664	See NP-15639
NUMEC–		
2389-8	20-5889	Dep. mn; CFSTI $1.00 cy, $0.50 mn
2389-9	20-5890	Dep. mn; CFSTI $3.00 cy, $0.75 mn
NYO–		
98-12	20-6686	Dep. mn; CFSTI $2.00 cy, $0.75 mn
1163-60	20-6533	Dep. mn; CFSTI $4.00 cy, $0.75 mn
2159-1	20-5891	Dep. mn; CFSTI $3.00 cy, $0.75 mn
2262-99	20-6068	Phys. Rev., 140: B1626-42(1965)
2543-1	20-5984	Dep.; CFSTI $6.00 cy, $1.25 mn
3250-2	20-6622	Dep. mn; CFSTI $4.00 cy, $0.75 mn
3399-22	20-6124	J. Math. Phys. (N. Y.), 6: 1822-32(1965)
3453-1	20-6687	Dep. mn; CFSTI $1.00 cy, $0.50 mn
ORNL–		
3858(Vol.1)	20-5925	Dep. mn; CFSTI $3.00 cy, $0.75 mn
3858(Vol.2)	20-5926	Dep. mn; CFSTI $2.00 cy, $0.50 mn
3866	20-5833	Dep. mn; CFSTI $3.00 cy, $0.75 mn
3876	20-5500	Dep. mn; CFSTI $2.00 cy, $0.50 mn
3877	20-6216	Dep. mn; CFSTI $1.00 cy, $0.50 mn
3879	20-5864	Dep. mn; CFSTI $2.00 cy, $0.50 mn
ORNL-P–	**(Misc.)**	
261	20-5553	J. Phys. Chem., 69: 3849-57(1965)
992	20-5266	Biochim. Biophys. Acta, 108: 259-65(1965)
1138	20-5597	J. Chromatog., 20: 107-21(1965)
1214	20-5417	Mutat. Res., 2: 413-25(1965)
1288	20-5372	Proc. Soc. Exp. Biol. Med., 120: 395-8 (1965)
1311	20-6541	Phys. Rev., 140: A1896-1902(1965)
1415	20-6407	Phys. Rev., 140: B1529-32(1965)
1512	20-6544	Phys. Rev., 140: A2003-4(1965)
1585	20-5707	Rev. Sci. Instrum., 36: 1830-9(1965)
1665	20-6079	Phys. Rev. Lett., 15: 906-8(1965)
1719	20-6415	Phys. Rev. Lett., 15: 765-7(1965)
1724	20-5915	Dep. mn; CFSTI $2.00 cy, $0.50 mn
1733	20-5927	Dep. mn; CFSTI $1.00 cy, $0.50 mn
1734	20-5297	Dep. mn; CFSTI $2.00 cy, $0.50 mn
ORNL-TM–		
1262	20-5985	Dep. mn; CFSTI $3.00 cy, $0.75 mn
1283	20-5571	Dep. mn; CFSTI $4.00 cy, $0.75 mn
1292	20-5528	Dep. mn; CFSTI $1.00 cy, $0.50 mn
1304	20-5665	Dep. mn; CFSTI $1.00 cy, $0.50 mn
1319	20-6680	Dep. mn; CFSTI $1.00 cy, $0.50 mn
1323	20-5834	Dep. mn; CFSTI $4.00 cy, $1.00 mn
1326	20-5612	Dep. mn; CFSTI $1.00 cy, $0.50 mn
ORNL-tr–		
870	20-6467	Dep. mn; CFSTI $1.00 cy, $0.50 mn; JCL $1.60 fs, $0.80 mf
871	20-6468	Dep. mn; CFSTI $1.00 cy, $0.50 mn; JCL $1.60 fs, $0.80 mf
892	20-5823	Dep. mn; CFSTI $1.00 cy, $0.50 mn; JCL $2.60 fs, $0.83 mf
P–	**(Misc.)**	
3166(RAND)	20-6252	See AD-617880
3167(RAND)	20-6253	See AD-617882
PAEC(A)IN–	**(Philippines)**	
653	20-5811	Dep. mn
654	20-5812	Dep. mn
PAN–	**(Polish)**	**(This series of reports was terminated in 1965. Subsequent reports are identified by the code INR)**
PATENTS	**(British)**	**(4s. 6d. each, U. K. Patent Office)**
1,009,166	20-6569	
1,009,236	20-5592	
1,009,333	20-5615	
1,009,381	20-6570	
1,009,382	20-6571	
1,009,383	20-6572	
1,009,384	20-6573	
1,009,465	20-5797	
1,009,563	20-5640	
1,009,637	20-5616	
1,009,714	20-6026	
1,009,766	20-6027	
PATENTS	**(Canadian)**	
713,681	20-6574	
PATENTS	**(German)**	
1,197,560	20-5711	

Report No.	Abstract No.	Availability
1,200,963	20-5798	
1,200,966	20-5868	
1,200,972	20-5964	
1,201,320	20-5869	
1,201,321	20-5561	
1,201,567	20-5604	
1,201,921	20-5799	
1,201,922	20-5800	
1,201,923	20-5801	
1,201,929	20-5965	
1,202,505	20-5870	
PATENTS	**(U. S.)**	**($0.25 each, U. S. Patent Office)**
3,201,590	20-5802	
3,210,253	20-6592	
3,210,254	20-6647	
3,210,255	20-5871	
3,210,526	20-5872	
3,210,541	20-5522	
3,210,545	20-5712	
3,212,809	20-5679	
3,213,530	20-6593	
3,213,868	20-5632	
3,214,238	20-5562	
3,214,239	20-5605	
3,214,243	20-5827	
3,214,295	20-6598	
3,214,306	20-5588	
3,214,342	20-6515	
3,214,343	20-6651	
3,214,358	20-5589	
3,214,486	20-5593	
3,214,499	20-5873	
3,214,582	20-5617	
3,214,586	20-5631	
3,214,587	20-5658	
3,214,588	20-5803	
3,214,614	20-6028	
3,214,615	20-6029	
3,214,616	20-6030	
3,214,623	20-6178	
3,219,535	20-6575	
3,219,736	20-6692	
3,219,776	20-6693	
3,219,825	20-5804	
PIBAL–	**(Non-AEC)**	
873	20-6456	See AD-619888
PIBMRI–	**(Non-AEC)**	
1262-65	20-5922	See AD-618689
PPAD–		
2137-566	20-6298	Dep. mn; CFSTI $2.00 cy, $0.50 mn
PR-P–	**(Canadian)**	
66	20-5928	Dep.; AECL $1.50
PSDC-TR–	**(Non-AEC)**	
15	20-6516	See AD-617524
PUC–		
1965-158	20-6299	Dep. mn; CFSTI $5.00 cy, $1.00 mn
1965-159	20-6345	Nucl. Phys., 75: 344-52(1965)
PWAC–	**(Misc.)**	
476	20-5892	Dep. mn; CFSTI $1.00 cy, $0.50 mn
480	20-5893	Dep. mn; CFSTI $1.00 cy, $0.50 mn
R–	**(Misc.)**	
2354	20-5882	See EURAEC-1454
64SD41	20-6443	See AD-617383
65SD31	20-5966	See AD-618905
RISÖ–	**(Danish)**	
105	20-6465	Dep. mn
107	20-5651	Dep. mn
110	20-5838	Dep. mn
RL-SEP–		
244(Del.)	20-5839	Dep. mn; CFSTI $2.00 cy, $0.50 mn
RLO–		
353-4	20-5298	Dep. mn; CFSTI $1.00 cy, $0.50 mn
RME–		
4545(Rev.)	20-5659	Dep. mn; CFSTI $2.00 cy, $0.50 mn
RRL–		
2310-157	20-5576	J. Amer. Chem. Soc., 87: 4983-8(1965)
RS–		
471	20-5613	See SWRI-1228-8-16
SB–	**(Non-AEC)**	
413(Suppl.1)	20-5840	CFSTI Free
SC-DC–		
65-1706	20-5529	Dep. mn; CFSTI $1.00 cy, $0.50 mn
65-1843	20-6534	Dep. mn; CFSTI $1.00 cy, $0.50 mn
SC-RR–		
65-625	20-5530	Dep. mn; CFSTI $1.00 cy, $0.50 mn
SGAE-CH–	**(Austrian)**	
18/1965	20-5591	Dep. mn
SGAE-PH–	**(Austrian)**	
18/1965	20-6681	Dep. mn
29/1965	20-6300	
SGAE-R–	**(Austrian)**	
1/1965	20-6682	Dep.
SIT–	**(Misc.)**	
172	20-6466	See SIT-2813-33
2813-33	20-6466	Dep. mn; CFSTI $1.00 cy, $0.50 mn
P161	20-6450	See AD-619527
SLAC–		
48	20-5943	Dep. mn; CFSTI $4.00 cy, $0.75 mn
SLAC-PUB–		
132	20-5944	Dep. mn; CFSTI $1.00 cy, $0.50 mn
140	20-5739	Dep. mn; CFSTI $2.00 cy, $0.50 mn
SM–	**(Misc.)**	
70-50	20-6584	See LA-DC-7248
SR–	**(Misc.)**	
2	20-6004	See AD-619508
2	20-6183	See AD-619821
17	20-6444	See AD-617553
23	20-6157	See AD-617898
STI-DOC–	**(International Atomic Energy Agency)**	
10/44	20-5815	IAEA US $2.00; S 42,-; 12/-stg; F.Fr. 8,-; DM 6,40
SWRI–		
1228-3-3	20-5894	Dep. mn; CFSTI $4.00 cy, $1.00 mn
1228-8-16	20-5613	Dep. mn; CFSTI $3.00 cy, $0.75 mn
TEI–		
862	20-5643	Dep. mn; CFSTI $3.00 cy, $0.75 mn
TID–		
3525(Rev.5) (Suppl.2)	20-6563	Dep. mn; CFSTI $3.00 cy, $0.75 mn
4102(1st Rev.)	20-5608	Dep.; DTI Extension Free
13358(2nd Rev.)	20-5243	Dep. mn; CFSTI $2.50 cy, $1.00 mn
21961	20-5918	Phys. Rev., 140: A1781-7(1965)
21995	20-5666	Dep. mn; CFSTI $5.00 cy, $1.00 mn
22035	20-5545	J. Inorg. Nucl. Chem., 27: 2291-2300(1965)
22111	20-6408	Phys. Rev., 140: B1541-8(1965)
22155	20-6384	Nucl. Phys., 76: 308-20(1966)
22165	20-6301	Dep. mn; CFSTI $4.00 cy, $1.00 mn
22167	20-6227	Z. Phys., 188: 361-73(1965)
22187	20-5299	Dep. mn; CFSTI $1.00 cy, $0.50 mn
22206	20-6623	Dep. mn; CFSTI $1.00 cy, $0.50 mn
22271	20-5895	Dep. mn; CFSTI $1.00 cy, $0.50 mn
22384	20-6302	Dep. mn; CFSTI $1.00 cy, $0.50 mn
22388	20-5896	Dep. mn; CFSTI $4.00 cy, $1.00 mn
22393	20-6303	Dep. mn; CFSTI $5.00 cy, $1.00 mn

Report No.	Abstract No.	Availability
22401	20-6304	Dep. mn; CFSTI $5.00 cy, $1.00 mn
22407	20-5740	Dep. mn; CFSTI $1.00 cy, $0.50 mn
22420	20-5897	Dep. mn; CFSTI $3.00 cy, $0.75 mn
22425	20-6624	Dep. mn; CFSTI $5.00 cy, $1.00 mn
22434	20-6625	Dep. mn; CFSTI $1.00 cy, $0.50 mn
TIM–	**(Misc.)**	
898	20-5853	Dep. mn; CFSTI $2.00 cy, $0.50 mn
TN–	**(Non-AEC)**	
1965-5	20-6184	See AD-619977
TR–	**(Misc.)**	
434	20-6451	See AD-619668
435	20-6452	See AD-619669
436	20-6453	See AD-619670
437	20-6454	See AD-619671
438	20-6455	See AD-619672
65-2	20-6447	See AD-618693
TRG-Report–	**(British)**	
1013	20-5625	Dep.; BIS $0.90; HMSO 4s. 6d.
TT–	**(Canadian)**	
65-32750	20-5813	See JPRS-32260
65-32831	20-5841	See JPRS-32341
65-32910	20-5988	See JPRS-32421
65-33562	20-6691	See JPRS-32985
U-COL–	**(Misc.)**	
64-16	20-5980	See AD-617522
UCLA–		
12-573	20-5300	Dep. mn; CFSTI $2.00 cy, $0.50 mn
UCRL–		
11784	20-6305	Dep. mn; CFSTI $5.00 cy, $1.00 mn
11790	20-6115	J. Math. Phys. (N. Y.), 6: 1635-42(1965)
11942	20-6041	Dep. mn; CFSTI $4.00 cy, $0.75 mn
12152	20-6373	Nucl. Phys., 76: 129-44(1966)
12238-T	20-6162	Dep. mn; CFSTI $1.00 cy, $0.50 mn
12309	20-6493	Phys. Fluids, 8: 2020-5(1965)
12365	20-6401	Phys. Rev., 140: B1483-7(1965)
12375	20-6418	Phys. Rev. Lett., 15: 976-9(1965)
12411	20-6522	Dep. mn; CFSTI $2.00 cy, $0.50 mn
14150	20-5642	Rev. Sci. Instrum., 36: 1777-8(1965)
14200	20-6414	Phys. Rev. Lett., 15: 761-5(1965)
14263	20-5741	Dep. mn; CFSTI $2.00 cy, $0.50 mn
14351	20-5742	Dep. mn; CFSTI $2.00 cy, $0.50 mn
14402-T	20-5986	Dep. mn; CFSTI $3.00 cy, $0.75 mn
14405	20-5743	Dep. mn; CFSTI $2.00 cy, $0.50 mn
14438	20-5683	Dep. mn; CFSTI $1.00 cy, $0.50 mn
16167	20-5698	Nucl. Instrum. Methods, 37: 293-6(1965)
16189	20-6042	Dep. mn; CFSTI $3.00 cy, $0.75 mn
16217	20-6306	Dep. mn; CFSTI $1.00 cy, $0.50 mn
16227	20-5744	Dep. mn; CFSTI $1.00 cy, $0.50 mn
16390	20-5772	Nucl. Instrum. Methods, 37: 327-9(1965)
16439	20-6307	Dep. mn; CFSTI $1.00 cy, $0.50 mn
16464	20-5945	Dep. mn; CFSTI $1.00 cy, $0.50 mn
UCRL-Trans–		
1237(L)	20-5687	Dep. mn; JCL $7.60 fs, $2.39 mf
1256(L)	20-6469	Dep. mn; JCL $3.60 fs, $1.28 mf
1266(L)	20-5748	Dep. mn; JCL $13.00 fs, $5.87 mf
1269(L)	20-6186	Dep. mn; JCL $2.60 fs, $0.95 mf
1273(L)	20-5688	Dep. mn; CFSTI $1.00 cy, $0.50 mn; JCL $1.60 fs, $0.80 mf
UJV–	**(Czechoslovakian)**	
1382/65	20-5531	Dep. mn
1408/65	20-5946	Dep. mn
UNC–	**(Misc.)**	
5118	20-6626	Dep. mn; CFSTI $4.00 cy, $0.75 mn
UR–		
668	20-5236	Dep. mn; CFSTI $5.00 cy, $1.00 mn
875-90	20-6367	Nucl. Phys., 76: 45-57(1966)
USNRDL-TR–	**(Misc.)**	
901	20-6278	See AD-623877
904	20-5713	See AD-623384
909	20-5572	CFSTI $2.00 cy, $0.50 mn
920	20-5408	CFSTI $1.00 cy, $0.50 mn
925	20-5303	CFSTI $2.00 cy, $0.50 mn
VUF–		
1020	20-5667	Dep. mn; CFSTI $2.00 cy, $0.50 mn
WAPD-PWR–		
TE-141	20-6627	Dep. mn; CFSTI $4.00 cy, $0.75 mn
TE-201	20-6628	Dep. mn; CFSTI $1.00 cy, $0.50 mn
WAPD-T–		
1770	20-5684	Dep. mn; CFSTI $1.00 cy, $0.50 mn
1849	20-6264	Dep. mn; CFSTI $1.00 cy, $0.50 mn
WAPD-TM–	**(Misc.)**	
519	20-5898	Dep. mn; CFSTI $1.00 cy, $0.50 mn
WASH–		
1061	20-5668	Dep. mn; CFSTI $4.00 cy, $1.00 mn
WCAP–	**(Misc.)**	
3269-24	20-6629	Dep. mn; CFSTI $3.00 cy, $0.75 mn
3269-37	20-5865	Dep. mn; CFSTI $1.00 cy, $0.50 mn
3269-46	20-6630	Dep. mn; CFSTI $3.00 cy, $0.75 mn
Y-DA–		
1014	20-6688	Dep. mn; CFSTI $1.00 cy, $0.50 mn
Y-KE–		
191	20-6689	Dep. mn; CFSTI $1.00 cy, $0.50 mn
Y-NA–		
14	20-6690	Dep. mn; CFSTI $1.00 cy, $0.50 mn
YAEC–	**(Misc.)**	
1005	20-6631	Dep. mn; CFSTI $1.00 cy, $0.50 mn
ZFK-RN–	**(German)**	
18	20-5746	Dep. mn

DEPOSITORIES OF USAEC REPORTS

In Countries Other than the U.S.

ARGENTINA
Buenos Aires, Comisión Nacional de Energía Atómica
AUSTRALIA
Canberra, Australian National Library
Sutherland, New South Wales, Australian Atomic Energy Commission
AUSTRIA
Vienna, Zentral Bibliothek der Physikalischen Institute der Universität
BELGIUM
Mol-Donk, Centre d'Etude de l'Energie Nucleaire
BOLIVIA
La Paz, Comisión Nacional de Energiá Nuclear
BRAZIL
Rio de Janeiro, Instituto Brasileiro de Bibliografia e Documentacao
São Paulo, Instituto de Energia Atomica, Cidade Universitaria São Paulo
BURMA
Rangoon, Union of Burma Applied Research Institute, Atomic Energy Center Library
CANADA
Hamilton, McMaster University
Ottawa, National Research Council Library
Vancouver, University of British Columbia
CHILE
Santiago, Instituto de Fisica y Matematicas, Universidad de Chile
CHINA
Hsinchu, Taiwan, Free China, National Tsing Hua University
COLOMBIA
Bogota, Instituto De Asuntos Nucleares
COSTA RICA
San Pedro, University of Costa Rica Library
DENMARK
Risö, Danish Atomic Energy Commission
ECUADOR
Quito, Escuela Politécnica Nacional
EL SALVADOR
San Salvador, Universidad de El Salvador, Biblioteca de Energia Nuclear
FINLAND
Helsinki, Teknillisen Korkeakoulun Kirjasto
FRANCE
Gif-sur-Yvette, Centre d'Etudes Nucléaires de Saclay
Paris, Académie des Sciences
GERMANY
Berlin, Hahn-Meitner-Institut für Kernforschung Berlin
Frankfurt/Main, Gmelin-Institut
Munich, Technische Hochschule, Bibliothek
GHANA
Accra, University College of Ghana
GREECE
Athens, Nuclear Research Center "Democritus"
GUATEMALA
Guatemala, Comisión Nacional de Energía Nuclear
INDIA
Bombay, Department of Atomic Energy
IRAN
Tehran, Tehran University Nuclear Centre
IRAQ
Baghdad, Iraqi Atomic Energy Commission
IRELAND
Dublin, University College
ISRAEL
Rehovoth, Israel Atomic Energy Commission
ITALY
Rome, Centro di Studi Nucleari della Casaccia
Rome, Comitato Nazionale per l'Energia Nucleare
JAPAN
Tokyo, National Diet Library
KOREA
Seoul, Office of Atomic Energy
LEBANON
Beirut, Lebanese National Council for Scientific Research
LUXEMBOURG
Luxembourg, Ministry of Transport and Electricity
MALAYSIA
Kuala Lumpur, University of Malaysia
MEXICO
Mexico, D.F., Comisión Nacional de Energía Nuclear
NETHERLANDS
The Hague, Reactor Centrum Nederland
NEW ZEALAND
Lower Hutt, Institute of Nuclear Sciences
NIGERIA
Ibadan, University of Ibadan
NORWAY
Lillestrøm, Institutt för Atomenergi
PAKISTAN
Lahore, West Pakistan, Atomic Energy Centre
PERU
Lima, Junta de Control de Energia Atomica
PHILIPPINE REPUBLIC
Manila, Philippine Atomic Energy Commission
POLAND
Warsaw, Biura Pelnomocnika Rzadu do Spraw Wykorzystania Energii Jadrowej
PORTUGAL
Sacavem, Junta de Energía Nuclear
REPUBLIC OF SOUTH AFRICA
Pretoria, Atomic Energy Board Library
REPUBLIC OF THE CONGO
Leopoldville, Université Lovanium
SPAIN
Madrid, Junta de Energía Nuclear, Biblioteca Documentación y Publicaciones, Ciudad Universitaria
SWEDEN
Nyköping, Aktiebolaget Atomenergi
SWITZERLAND
Zürich, Eidgenössische Technische Hochschule, Bibliothek
THAILAND
Bangkok, Office of the Thai Atomic Energy Commission, Department of Science
TURKEY
Ankara, Turkish Atomic Energy Commission, Atomic Energy Library
UNITED ARAB REPUBLIC
Cairo, Atomic Energy Commission
UNITED KINGDOM
Birmingham, Central Library
Boston Spa, National Lending Library for Science and Technology
Bristol, Central Library
Kingston upon Hull, Central Library
Liverpool, Central Library
London, Central Library, Acton
London, National Reference Library
London, Science Museum Library, South Kensington
Manchester, Central Library
Newcastle upon Tyne, Central Library
Nottingham, Central Library
Sheffield, Central Library
URUGUAY
Montevideo, Comision Nacional de Energia Atomica
VENEZUELA
Caracas, Instituto Venezolano de Investigaciones Científicas
VIET-NAM
Saigon, Atomic Energy Office
YUGOSLAVIA
Belgrade, Federal Commission for Nuclear Energy

In International Agencies

AUSTRIA
Vienna, International Atomic Energy Agency
BELGIUM
Brussels, La Bibliotheque EURATOM
FRANCE
Paris, European Nuclear Energy Agency, O.E.C.D.
ITALY
Ispra, EURATOM Research Center
SWITZERLAND
Geneva, United Nations Library

UNITED STATES
GOVERNMENT PRINTING OFFICE
DIVISION OF PUBLIC DOCUMENTS
WASHINGTON, D.C. 20402

OFFICIAL BUSINESS

POSTAGE AND FEES PAID
U.S. GOVERNMENT PRINTING OFFICE

TECHNICAL PROGRESS REVIEWS

The Division of Technical Information, U. S. Atomic Energy Commission, also publishes the Technical Progress Reviews, a series of five quarterly journals on nuclear technology. These journals, compiled by specialists and recognized authorities, summarize, evaluate, and reference the progress of development in five important fields.

Isotopes and Radiation Technology P. S. Baker, A. F. Rupp, and associates, Oak Ridge National Laboratory. Reviews AEC-sponsored projects and related significant worldwide developments in radioisotopes and radiation technology.

Nuclear Safety Wm. B. Cottrell, W. H. Jordan, and associates, Oak Ridge National Laboratory. Covers topics relevant to the analysis and control of hazards associated with nuclear reactors and with operations involving fissionable materials and the products of nuclear fission.

Power Reactor Technology Argonne National Laboratory. Reviews research, development, design practices, and operating experiences associated with power reactors, including aerospace applications.

Reactor Fuel Processing Stephen Lawroski and associates, Argonne National Laboratory. Reviews all aspects of the fuel-processing field, including aqueous and nonaqueous processing and waste disposal.

Reactor Materials R. W. Dayton, E. M. Simons, and associates, Battelle Memorial Institute. Covers the properties, behavior, and fabrication processes of materials used in nuclear reactors and associated equipment.

MIAMI UNIVERSITY LIBRARY

Availability

SUBSCRIPTION RATE: The Technical Progress Reviews may be purchased from the Superintendent of Documents, U. S. Government Printing Office, Washington, D. C. 20402, at $2.50 per year for each subscription or $0.70 per issue.

POSTAGE: Postpaid within the United States, Canada, Mexico, and all Central and South American countries except Argentina, Brazil, British and French Guiana, Surinam, and British Honduras. For these Central and South American countries and all other countries, add $0.75 per year or $0.20 per single issue.

REMITTANCE: Payment should be by check, money order, or document coupons and MUST accompany order. Remittances from foreign countries should be made by international money order or draft on an American bank payable to the Superintendent of Documents or by UNESCO book coupons.

V
O
L

2

4

XI